



D.W. van Krevelen ⁺
K. te Nijenhuis

Properties of Polymers

Their Correlation with Chemical Structure;
their Numerical Estimation and Prediction
from Additive Group Contributions

FOURTH
COMPLETELY
REVISED
EDITION

PROPERTIES OF POLYMERS

THEIR CORRELATION WITH CHEMICAL
STRUCTURE; THEIR NUMERICAL
ESTIMATION AND PREDICTION FROM
ADDITIVE GROUP CONTRIBUTIONS

Fourth, completely revised edition

This page intentionally left blank

PROPERTIES OF POLYMERS

**THEIR CORRELATION WITH CHEMICAL
STRUCTURE; THEIR NUMERICAL
ESTIMATION AND PREDICTION FROM
ADDITIVE GROUP CONTRIBUTIONS**

Fourth, completely revised edition

D. W. VAN KREVELEN[†]

*Professor-Emeritus, Delft University of Technology, The Netherlands
and Former President of AKZO Research and Engineering N.V., Arnhem,
The Netherlands*

Revised by

K. TE NIJENHUIS

*Associate Professor-Emeritus, Delft University of Technology, Delft,
The Netherlands*



Amsterdam • Boston • Heidelberg • London • New York • Oxford
Paris • San Diego • San Francisco • Singapore • Sydney • Tokyo

Elsevier
Radarweg 29, PO Box 211, 1000 AE Amsterdam, The Netherlands
Linacre House, Jordan Hill, Oxford OX2 8DP, UK

First edition 1972
Second, completely revised edition 1976
Second impression 1980
Third impression 1986
Fourth impression 1987
Fifth impression 1989
Third, completely revised edition 1990
Second impression 1992
Third impression 1994
Fourth, completely revised edition 2009

Copyright © 2009 Elsevier B.V. All rights reserved

No part of this publication may be reproduced, stored in a retrieval system or transmitted in any form or by any means electronic, mechanical, photocopying, recording or otherwise without the prior written permission of the publisher

Permissions may be sought directly from Elsevier's Science & Technology Rights Department in Oxford, UK: phone (+44) (0) 1865 843830; fax (+44) (0) 1865 853333; email: permissions@elsevier.com. Alternatively you can submit your request online by visiting the Elsevier web site at <http://elsevier.com/locate/permissions>, and selecting *Obtaining permission to use Elsevier material*

Notice

No responsibility is assumed by the publisher for any injury and/or damage to persons or property as a matter of products liability, negligence or otherwise, or from any use or operation of any methods, products, instructions or ideas contained in the material herein.

British Library Cataloguing in Publication Data

A catalogue record for this book is available from the British Library

Library of Congress Cataloging-in-Publication Data

Krevelen, D. W. van (Dirk Willem)

Properties of polymers : their correlation with chemical structure : their numerical estimation and prediction from additive group contributions / by D. W. van Krevelen. – 4th, completely rev. ed. / K. te Nijenhuis.

p. cm.

ISBN 978-0-08-054819-7

1. Polymers—Mechanical properties. I. Nijenhuis, K. te. II. Title.
TA455.P58K74 2009
620.1'9204292—dc22

2008044601

For information on all Elsevier publications
visit our website at books.elsevier.com

Printed and bound in Slovenia

09 10 11 10 9 8 7 6 5 4 3 2 1

Working together to grow
libraries in developing countries

www.elsevier.com | www.bookaid.org | www.sabre.org

ELSEVIER BOOK AID International Sabre Foundation

I stand at the seashore, alone, and start to think. . .

*There are the rushing
waves mountains of molecules
each stupidly minding its own business
trillions apart
yet forming white surf in unison.*

*Ages on ages before
any eyes could see
year after year
thunderously pounding the shore as now.
For whom, for what?
On a dead planet
with no life to entertain.*

*Never at rest
tortured by energy
wasted prodigiously by the sun
poured into space.
A mite makes the sea roar.*

*Deep in the sea
all molecules repeat
the pattern of one another
till complex new ones are formed.
They make others like themselves
and a new dance starts.*

*Growing in size and complexity
living things
masses of atoms
DNA, protein
dancing a pattern ever more intricate.*

*Out of the cradle
onto dry land
here it is
standing:
atoms with consciousness;
matter with curiosity.*

*Stands at the sea,
wonders at wondering: I
a universe of atoms
an atom in the universe.*

Richard P. Feynman (1955)

This page intentionally left blank

FROM THE PREFACE TO THE FIRST EDITION (1972)

This book is intended for those who work on *practical* problems in the field of polymers and who are in need of *orienting numerical information* on polymer properties; for the organic chemist who is faced with the task of synthesizing new polymers and wonders if the structures he wants to realize will actually have the properties he has as a target; for the chemical engineer who is often forced to execute his designs without having enough data at his disposal and who looks in vain for numerical values of the quantities needed under the conditions of the process; for the polymer processor who tries to predict and understand how certain physical parameters will react to changes in process conditions; for the polymer technologist who tries to get a better insight into the interrelations of the many disciplines in his branch; and finally for all students who are interested in the correlation between chemical structure and properties and in the mutual relation of the properties.

With the chemical constitution as the basis, our aim has consistently been to show that each functional group in the molecular structure actually performs a function that is reflected in *all* properties. Ample use has been made of the *empirical fact* that a number of quantities and combinations of quantities have additive properties – within certain limits of precision - so that these quantities can be calculated in a simple manner from empirically derived group contributions or increments. Many readers will be surprised to see how far one can get by setting out from this simple starting point.

Theoretical expositions have purposely been omitted, except where some elucidation is indispensable for a proper understanding of quantities that are less widely known.

It follows that this book has not been written for the polymer scientist proper, notably the polymer physicist and physical chemist, its design being too empirical for him and too much directed to practice. In this book the expert will find no data that are not available elsewhere. Many experts may even have great objections, some of them justified, to the design of this book and its approach.

Unfortunately, the gap between polymer scientists and practitioners is not narrowing but constantly widening. The work in the field of polymer science is becoming increasingly sophisticated, in the experimental as well as in the theoretical disciplines.

This book is meant to be a modest contribution towards narrowing the gap between polymer science and polymer practice. Time will have to show whether this attempt has been successful.

This page intentionally left blank

FROM THE PREFACE TO THE SECOND EDITION (1976)

On its appearance this book was given such a good welcome that a second edition proved to be necessary within four years. For this purpose the book was completely revised, updated and considerably extended. The scope of the chapters dealing with the mechanical and rheological properties was much enlarged, as were the sections discussing polymer solutions. An improved system for the assessment of the transition temperatures was introduced. SI units are used throughout the book.

While the first impression confined itself to the intrinsic properties, the second edition also covers the processing and product properties, if to a limited extent and on a selective basis.

This page intentionally left blank

PREFACE TO THE THIRD EDITION (1990)

Fourteen years passed since the second edition of this book appeared. Since then four new prints were made. As a source of data and for estimations it is now widely used all over the world.

The present Third Edition required a thorough revision and updating, and consequently a certain extension.

The existing subdivision of the book in seven Parts and 27 Chapters remained the same, with one exception: chapter 14. This deals now with a new subject: the Acoustic Properties; its original subject, properties of oriented polymers, is now divided over the chapters 13 and 19.

This page intentionally left blank

INTRODUCTION OF THE PRESENT AUTHOR

In the year 2000, Dr Kostas Marinakis, senior acquisitions editor at Elsevier, asked my father to consider the preparation of a revised edition of his *Properties of Polymers*, the handbook that was first published in 1972 and later revised by him twice, in 1976 and in 1990. The proposal pleased him greatly, as this book was still very dear to him.

The unorthodox, practice oriented set-up which he had chosen for the book, by arranging the research findings according to properties, while giving prominence to predictability of properties on the basis of chemical structures, had been very productive and successful. During his long career as a chemical scholar working in industrial research and management, my father had always dedicated himself to bridging technological practice with scientific research, and to combining the insights of all relevant sub-specialties of science and technology.

His other well-known handbook, *Coal* (Elsevier 1961, 1993: 3rd Edition) - fruit of the first twenty years of his professional career - is another clear example of his comprehensive and nearly encyclopaedic approach. He was very much aware of the fact that he still belonged to the generation of classic science authors who aimed at a broad, systematic, coherent presentation of the subject matter. He once said to me that in the future such handbooks like *Coal* and *Properties of Polymers* would not be written anymore by a single person, assuming that there would still be any need for such books in the digital era. Not without nostalgia, he spoke about the things that he had helped to build up, and that had disappeared under his eyes. The glorious coal research activities of DSM, where he had worked from 1940 till 1959, had completely vanished, and the same was true for the innovative research into polymers of AKZO, his pride from 1960 till his retirement in 1976. His two successful handbooks are the only witnesses of those exciting periods of his scholarly life.

The idea that *Properties of Polymers* would get a new life cycle pleased my father immensely therefore, although he was very much aware that he would not be capable to achieve such a huge task alone at the age of 86 years. So he decided to look for a co-author and consulted some of his professional friends. One of them, Dr. Ger Challa, former professor in polymer chemistry at Groningen University, suggested Dr. Ir. Klaas te Nijenhuis to him as a possible co-author. Te Nijenhuis was at that time associate-professor at Delft University of Technology, where he had specialized in polymers.

Te Nijenhuis and my father got very well together, and they agreed to co-operate as soon as possible in the revision of the book. Te Nijenhuis would retire from the university by the end of 2003, so from then on he would have sufficient time to work on his share of the revision. On the 3rd of September 2001, the joint publishing agreement with Elsevier was signed.

Eight days later, however, on the catastrophic 11th of September, my father was struck by a bad brain haemorrhage from which he did not recover. He died on 27th of October 2001.

In the hard weeks of his suffering, he clung to the few moments of hope and joy. Such a moment was the visit of Klaas te Nijenhuis. They discussed the intended revision of *Properties of Polymers*, and Te Nijenhuis told him that in the mean time he also had signed the contract and he promised my father that the 4th edition would be prepared

by him anyway. In the face of death, my father was utterly happy to know that his book would survive.

Dr. te Nijenhuis has kept his word, and he has even managed to do the enormous job alone - brushing aside the sceptical remark of my father that after him nobody could or would do such a thing alone. I want to express my deep gratitude to Dr. te Nijenhuis, also on behalf of my sister Irene and my brothers Hans and Frits, for his marvellous achievement. May this 4th edition of *Properties of Polymers* find its way to many readers and users!

Laurens van Krevelen, LL M

Bloemendaal, The Netherlands
August 2008

PREFACE TO THE FOURTH EDITION (2008)

Eighteen years have passed since the third edition of this book appeared. Since then it has been reprinted twice and has appeared in a paperback edition (1977). As a source of data and estimations it is still widely used all over the world.

In the early 2000's there was a feeling within "Polymer-The Netherlands" that a revised edition of "PROPERTIES OF POLYMERS" was needed. This was already preceded by a suggestion from Elsevier Science B.V. to Prof. Van Krevelen to consider the preparation of a revised edition of his book. However, because of his age Prof. Van Krevelen did not feel capable of doing all the effort for the preparation of a new edition alone. For that reason he invited me in May 2001 to cooperate in the preparation of the fourth edition. I accepted this honourable invitation hesitantly, knowing that it would be a tremendous amount of work. Our joint discussions with Elsevier Science B.V. resulted in a contract that was signed in the autumn of 2001. Prof. Van Krevelen would support me with his fabulous amount of knowledge and experience. Unfortunately, this was not to be, because on 27th of October of the same year he passed away after a brief illness. I will never forget his radiant face when I told him, visiting him in the hospital on 4th of October, together with his son Laurens, that I also had signed the Elsevier contract. Anyhow, I now had to do the work alone and, indeed, it appeared to be a long and lonesome activity. But the mere thought of his radiant face in all his distress, proved to be a stimulus not only to start, but in particular also to continue this huge task.

The present Fourth Edition has been updated and also, when necessary, extended. However, I did not take the opportunity to change the plan of the book: the existing subdivision of the book in seven parts and 27 Chapters has not been changed. The following shows where small changes were made or where the text was extended greatly.

Part I *General Introduction: A bird's-eye view of polymer science and engineering.* Chapter 1, dealing with approach and objectives of polymer properties, remained almost unchanged. In Chapter 2, where the typology of polymers is discussed, the milestones (Appendix I) are extended and updated, Nobel prize winners concerning Polymers are added and the development of commercial polymers (Appendix II) is updated. In Chapter 3, where the typology of properties is discussed, only small changes and extensions are made.

Part II *Thermophysical properties of polymers.* In Chapters 4 and 5, that deal with volumetric properties and calorimetric properties, respectively, only marginal extensions are made. In Chapter 6, on transition temperatures, more attention is paid to the thermodynamics of the glass-rubber-transition. Moreover, the treatment of the calculation of the melting temperature of polymer families with two functional groups in the repeating units is changed in such a way that the agreement between calculated and experimental melting temperatures is better. In Chapter 7, on cohesive properties and solubility, the solubility parameter is compared with the Flory Huggins interaction parameter. Further, temperature dependence of the solubility parameter and the solubility parameter of solvent mixtures are added. In Chapter 8, on interfacial energy properties,

a correction term in the equations for the surface energy and more refined approaches of surface energy contributions with the aid of Lifschitz-Van der Waals interactions are added. In Chapter 9, on conformation aspects and conformation statistics, the Kuhn length, the persistence length and the worm-like chain are added. More attention is paid to the limiting viscosity number of branched polymers and in particular of polyelectrolytes.

- Part III** *Properties of polymers in fields of force.* In Chapter 10, on optical properties, much more attention is paid to reflection and transmission of light. Chapter 11, on electrical properties, is greatly extended with the relationships between the dielectric constant and (1) polarization and (2) refractive index and with Debye relaxation. Some attention is paid to Thermally Stimulated Discharge (TSD) and electrets. Also electric conductivity, doping of polymers and non-linear optics are greatly extended. In Chapter 12, on magnetic properties, the introduction of magnetism is extended. The introduction of the NMR phenomenon is greatly extended, just as the detection of NMR and the relaxation mechanisms (spin-lattice and spin-spin). Chapter 13, on mechanical properties, still the most important class of polymer properties, is extended greatly, in particular the subchapters Rubber elasticity, Viscoelasticity, Ultimate mechanical properties and Mechanical properties of uniaxially oriented polymers (fibres). In Chapter 14, on acoustic properties, the dependence of sound speed on various parameters is extended.
- Part IV** *Transport properties of polymers.* Chapter 15, on rheological properties of polymer melts, is greatly extended, in particular the subchapters Modes of deformation and definition of viscosity, Newtonian shear viscosity of polymer melts, Non-Newtonian shear viscosity and first normal stress coefficient of polymer melts, Extensional viscosity of polymer melts, Elastic effects in polymer melts and Rheological properties of thermotropic liquid crystalline polymers. Also Chapter 16, on rheological properties of polymer solutions, is extended quite greatly, in particular the subchapters Viscoelastic properties of polymer solutions in steady shear flow, Extensional flow of polymer solutions and Solutions of lyotropic liquid crystalline polymers. In Chapters 17 and 18, on transport of heat and mass, respectively, the introduction of thermal transport and permeability is extended slightly. In Chapter 19, on crystallization and recrystallization, the Avrami equation and the Critical size of crystal nuclei are paid more attention to. The subsection Aspects of structure formation in processing is completely revised. In the subchapter Crystallization phenomena in uniaxial drawing: fibre spinning, several smaller parts are extended.
- Part V** *Properties determining the chemical stability and breakdown of polymers.* In Chapter 20, on thermomechanical properties, some thermodynamics of the reaction from monomer to polymer are added, included the ceiling and floor temperatures of polymerization. Chapters 21 and 22, on thermal decomposition and chemical degradation, respectively, needed only slight extensions.
- Part VI** *Polymer properties as an integral concept.* Chapter 24, on processing properties, is extended slightly. Chapter 25, on mechanical product properties, remained almost unchanged. The three subchapters of Chapter 26, on environmental product properties, are extended quite greatly. Chapter 27 on examples of end use properties remained unchanged.
- Part VII** *Comprehensive tables* Only marginal changes are made.

The *Bibliographies* of the chapters are updated and extended greatly.

I sincerely hope that also this "fourth" edition of "PROPERTIES OF POLYMERS" will find (following the preface to the third edition) "a good acceptance in the polymer world and that it will prove a useful guide and aid to many users", notwithstanding that the present author is not the well-known Prof. D.W. van Krevelen, but somebody who attended many of his various lectures on "PROPERTIES OF POLYMERS" at Delft University of Technology.

K. te Nijenhuis

Dronten, The Netherlands
August, 2008

This page intentionally left blank

ACKNOWLEDGEMENTS

This edition of *PROPERTIES OF POLYMERS* would not have been appeared as such, without the assistance of a number of scientists, each with her or his expertise.

In particular I have to mention Dr.H.Boerstoel (Teijin, Arnhem), Prof. A .D. Gotsis (Crete, Greece), Prof. H. Janeschitz-Kriegl (Linz, Austria), Dr. M. G. Northolt (formerly AKZO, Arnhem), Prof. S. J. Picken (Delft) and Dr. J. Spěváček (Institute for Macromolecular Chemistry, Prague). Their criticism, suggestions, improvements, provisional drafts and extensions are gratefully acknowledged.

Other suggestions, comments and help in any way are, first from former colleagues at Delft University: Dr. T. W. De Loos, Prof. W. J. Mijs, Prof. J. van Turnhout, Prof. J. A. Wesselingh (now at Groningen), Prof. M. Wübbenhorst (now at Leuven, Belgium) and Dr. J. Zuidema and secondly from Dr. J. B. Helms (formerly Shell Amsterdam), Prof. S. Hvilsted (Roskilde, Denmark), Prof. E. W. Meijer (Eindhoven), Prof. R. J. M. Nolte (Nijmegen), Prof. J. W. M. Noordermeer (Enschede and DSM Geleen), Prof. A. J. Schouten (Groningen), Prof. R. P. Sijbesma (Eindhoven), Prof. L. C. M. Struik (Enschede and DSM Geleen), Dr. C. J. M. Van den Heuvel (Teijin, Arnhem), Dr. H. Van der Werff (DSM Geleen) and Prof. W. Van Saarloos (Leiden). Also their help is gratefully acknowledged.

In the preface I already mentioned that rewriting this book would be a long and lonesome activity, but in a family consisting of only two persons this activity is also long and lonesome for the other. I am deeply grateful to my wife Laura that I got the opportunity to do this work and for her stimulus and incredible patience: it has been a very special way to spend together a retirement time.

ACKNOWLEDGEMENTS FOR USE OF ILLUSTRATIONS

Thanks are due to the following publishers for their permission to reproduce in this fourth edition some figures from copyright books and journals:

The American Chemical Society, for Fig. 16.34;
The American Institute of Physics, for Figs. 13.57, 13.58, 14.5,
The American Physical Society for Fig. 11.22;
Carl Hanser Verlag, for Fig. 11.4;
Chapman & Hall, for Figs. 13.31, 13.44, 15.25, 15.47 and 16.21;
Elsevier Science Publishers, for Figs. 13.5, 13.27, 13.42, 13.47–13.53, 13.55, 15.15, 15.24, 16.24 and 16.25
Hüthig and Wepf Verlag, for Fig. 16.5;
IOP Publishing, for Fig. 15.51;
IUPAC Secretariat, for Fig. 16.6;
John Wiley & Sons Ltd., for Figs. 11.17, 11.18, 13.3, 13.24, 13.28, 13.29, 13.41, 13.71, 13.89, 13.90, 13.95, 13.96, 13.98, 13.99, 13.100, 15.30, 16.10, 16.11 and 16.32, and for Schemes 11.1, 11.2 and 11.3;
Oxford University Press, for Figs. 13.5, 13.6 and 13.82;
The Plastics & Rubber Institute, for Figs. 15.40 and 15.41;

The Society of Rheology, for Figs. 15.23, 15.33–15.37, 15.46, 16.16 and 16.18;
Springer Verlag, for Figs. 11.12, 11.13, 11.19, 13.15, 13.39, 13.40, 13.56, 13.72, 13.97, 13.101,
13.103, 13.104, 13.105, 14.3, 14.4, 15.5, 15.12, 15.13, 15.27, 15.29, 15.53, 16.17 and 19.10;
Taylor & Francis Group, for Figs. 6.4, 13.30, 16.33 and 16.35;
Trans Tech Publications, for Fig. 11.20.
Prof. A. D. Gotsis, for Fig. 15.46;
Prof. W. W. Greassley, for Figs. 15.34–15.37, 16.16 and 16.18;
Prof. H. Münstedt, for Fig. 15.23;
Prof. L. C. E. Struik, for Figs. 13.42, 13.47–13.53 and 13.55
Prof. J. Van Turnhout, for Fig. 11.5A;
Prof. M. Wübbenhorst, for Fig. 11.3.

CONTENTS

From the preface to the first edition (1972)	vii
From the preface to the second edition (1976)	ix
Preface to the third edition (1990)	xi
Introduction of the present author	xiii
Preface to the fourth edition (2008)	xv
Acknowledgements	xix

Part I. General introduction: A bird's-eye view of polymer science and engineering

Chapter 1 Polymer properties	3
-------------------------------------	----------

1.1 Approach and objective	3
Bibliography	5

Chapter 2 Typology of polymers	7
---------------------------------------	----------

2.1 Introduction	7
2.2 Polymer structure	8
2.3 Molar mass and molar mass distribution	17
2.4 Phase transitions in polymers	25
2.5 Morphology of solid polymers	29
2.6 Polymeric liquid crystals	34
2.7 Multiple component polymer systems	36
2.8 Relaxation phenomena	38
Appendix I. Milestones in the history of polymer science	40
Appendix II. Chronological development of commercial polymers	44
Bibliography	45

Chapter 3 Typology of properties	49
---	-----------

3.1 The concept "polymer properties"	49
3.2 Physical quantities and their units	52
3.3 Categories of physical quantities	54
3.4 Dimensionless groups of quantities	55
3.5 Types of molar properties	57
3.6 Additive molar functions	60
Bibliography	66

Part II. Thermophysical properties of polymers

Chapter 4 Volumetric properties	71
--	-----------

4.1 Introduction: mass and packing of matter	71
4.2 Fundamental quantities of mass and volume	72
4.3 Standard molar volumes at room temperature (298 K)	76

4.4 Thermal expansion	89
4.5 Isothermal compression - Equations of state	101
Bibliography	107
Chapter 5 Calorimetric properties	109
5.1 Heat capacity	109
5.2 Latent heat of crystallization and fusion (melting)	118
5.3 Enthalpy and entropy	123
Bibliography	127
Chapter 6 Transition temperatures	129
6.1 Introduction	129
6.2 The glass transition temperature	130
6.3 The crystalline melting point	152
6.4 Relationship between glass transition temperature and melting point of polymers	167
6.5 Relationship between T_g , T_m and other transition temperatures	170
6.6 Transitions in thermotropic liquid crystal polymers	172
Appendix I. Rules of thumb for substituting an H-atom by a group X	182
Appendix II. Similarities and differences between \mathbf{Y}_g and \mathbf{Y}_m	183
Bibliography	187
Chapter 7 Cohesive properties and solubility	189
7.1 Introduction	189
7.2 Cohesive energy	190
7.3 Solubility	201
7.4 Internal pressure	222
Bibliography	225
Chapter 8 Interfacial energy properties	229
8.1 Introduction	229
8.2 Surface energy of liquids and melts	230
8.3 Surface energy of solid polymers	234
8.4 General expression for the interfacial tension	239
8.5 Polymer adhesion	242
Bibliography	244
Chapter 9 Limiting viscosity number (intrinsic viscosity) and related properties of very dilute solutions	245
9.1 Introduction	245
9.2 Molecular dimensions of the conformational state	246
9.3 The limiting viscosity number (intrinsic viscosity)	249
9.4 Interrelationships of "limiting" diffusive transport quantities	280
Bibliography	283

Part III. Properties of polymers in fields of force

Chapter 10 Optical properties	287
10.1 Optical properties in general	287
10.2 Light refraction	290
10.3 Reflection and transmission	297
10.4 Birefringence (and optical rotation)	299
10.5 Light scattering	308
10.6 Absorption	313
10.7 Optical appearance properties	313
Bibliography	317
Chapter 11 Electrical properties	319
11.1 Introduction	319
11.2 Dielectric polarisation	319
11.3 Static electrification and conductivity	333
11.4 Ultimate electrical properties	352
Bibliography	352
Chapter 12 Magnetic properties	355
12.1 Magnetic susceptibility (magnetic inductive capacity)	355
12.2 Magnetic resonance	359
Bibliography	380
Chapter 13 Mechanical properties of solid polymers	383
13.1 Introduction	383
13.2 Elastic parameters	383
13.3 Rubber elasticity	401
13.4 Viscoelasticity	405
13.5 Ultimate mechanical properties	453
13.6 Mechanical properties of uniaxially oriented polymers (fibres)	478
Bibliography	500
Chapter 14 Acoustic properties	505
14.1 Introduction	505
14.2 Sound propagation and absorption	506
14.3 Additive molar functions for sound propagation	513
14.4 Sonic absorption	517
Bibliography	521
Part IV. Transport properties of polymers	
Chapter 15 Rheological properties of polymer melts	525
15.1 Introduction	525
15.2 Modes of deformation and definition of viscosity and normal stress coefficients	526
15.3 Newtonian shear viscosity of polymer melts	533
15.4 Non-Newtonian shear viscosity and first normal stress coefficient of polymer melts	545

15.5 Extensional viscosity of polymer melts	564
15.6 Elastic effects in polymer melts	573
15.7 Rheological properties of thermotropic liquid crystalline polymers	581
Appendix I. Flow of polymer melts through narrow tubes and capillaries	591
Appendix II. Analysis of flow in processing operations	592
Bibliography	595
Chapter 16 Rheological properties of polymer solutions	599
16.1 Introduction	599
16.2 Dilute polymer solutions	600
16.3 Concentrated polymer solutions	604
16.4 Viscoelastic properties of polymer solutions in simple shear flow	619
16.5 Extensional flow of polymer solutions	630
16.6 Solutions of lyotropic liquid crystalline polymers	634
Bibliography	643
Chapter 17 Transport of thermal energy	645
17.1 Thermal conductivity	645
17.2 Appendix	651
Bibliography	652
Chapter 18 Properties determining mass transfer in polymeric systems	655
18.1 Introduction	655
18.2 Permeation of simple gases	656
18.3 Permeations of a more complex nature	681
18.4 Dissolution of polymers as a case of permeation	696
Bibliography	701
Chapter 19 Crystallisation and recrystallisation	703
19.1 Crystallinity, nucleation and growth	703
19.2 Spherulitic crystallisation of polymers from the melt	706
19.3 Induced crystallisation of flexible polymeric molecules by pressure and stress	726
19.4 Crystallisation phenomena in uniaxial drawing: fibre spinning	728
Bibliography	743
Part V. Properties determining the chemical stability and breakdown of polymers	
Chapter 20 Thermochemical properties	749
20.1 Thermodynamics and kinetics	749
20.2 Calculation of the free enthalpy of reaction from group contributions	752
20.3 Thermodynamics of free radicals	758
Bibliography	761

Chapter 21 Thermal decomposition	763
21.1 Introduction	763
21.2 Thermal degradation	763
21.3 Char formation	772
21.4 Kinetics of thermal degradation	776
Bibliography	776
Chapter 22 Chemical degradation	779
22.1 Introduction	779
22.2 Degradation under the influence of light	779
22.3 Oxidative degradation	781
22.4 Photo-oxidation	781
22.5 Thermal oxidation	783
22.6 Effects of oxidation degradation	783
22.7 Stabilisation	784
22.8 Hydrolytic degradation	785
22.9 Stress relaxation as a measure of chemical degradation	785
Bibliography	786
Part VI. Polymer properties as an integral concept	
Chapter 23 Intrinsic properties in retrospect	789
23.1 Introduction	789
23.2 Reference values of intrinsic properties expressed as a function of additive quantities	790
23.3 Effect of structural groups on properties	792
23.4 Dependence of intrinsic properties on process variables	792
23.5 Outlook	796
Chapter 24 Processing properties	799
24.1 Classification of processes	799
24.2 Some important processing properties	800
24.3 Implementation of processing research	816
Bibliography	817
Chapter 25 Product properties (I): Mechanical behaviour and failure	819
25.1 Introduction	819
25.2 Failure mechanisms in polymers	820
25.3 Deformation properties	824
25.4 Toughness and endurance	829
25.5 Hardness	836
25.6 Friction and wear	840
25.7 The mechanical shortcomings of homogeneous materials and the need for composites	841
Bibliography	844

Chapter 26 Product properties (II): Environmental behaviour and failure	847
26.1 Introduction	847
26.2 Thermal end use properties	847
26.3 Flammability and combustion of polymers	850
26.4 Environmental decay of polymers	864
Bibliography	872
Chapter 27 An illustrative example of end use properties: Article properties of textile products	875
27.1 Introduction	875
27.2 Aesthetic properties	875
27.3 Use or performance properties	877
27.4 Maintenance or care properties	882
27.5 Integral evaluation of fibre polymers, fibres and yarns by the criteria mentioned (profile method)	884
Bibliography	885
Part VII. Comprehensive tables	
I International system of units (SI)	889
II Survey of conversion factors	891
III Values of some fundamental constants	903
IV Physical constants of the most important solvents	904
V Physical properties of the most important polymers	920
VI Published data of “high performance” polymers	934
VII Code symbols for the most important polymers	938
VIII Trade names and generic names	941
IX Survey of group contributions in additive molar quantities	946
Indexation	
Symbol index	957
Author index	979
Subject index	987

PART

GENERAL INTRODUCTION: A BIRD'S-EYE VIEW OF POLYMER SCIENCE AND ENGINEERING

*"It is the lone worker who makes the first advance in a subject,
the details may be worked out by a team"*

Alexander Fleming, 1881–1955

This page intentionally left blank

CHAPTER 1

Polymer Properties

1.1. APPROACH AND OBJECTIVE

The continuous development of the modern process industries has made it increasingly important to have information about the properties of materials, including many new chemical substances whose physical properties have never been measured experimentally. This is especially true of polymeric substances. The design of manufacturing and processing equipment requires considerable knowledge of the processed materials and related compounds. Also for the application and final use of these materials this knowledge is essential.

In some handbooks, for instance the "Polymer Handbook" (Brandrup et al., 1966, 1975, 1989, 1999), "Physical Constants of Linear Homopolymers" (Lewis, 1968), "International Plastics Handbook for the Technologist, Engineer and User" (Saechtling, 1988), "Polymer Data Handbook" (Mark, 1999) and similar compilations, one finds part of the data required, but in many cases the property needed cannot be obtained from such sources.

The major aim of the present book is twofold:

1. *To correlate the properties of known polymers with their chemical structure*, in other words: *to establish structure–properties relationships*.
2. *To provide methods for the estimation and/or prediction of the more important properties of polymers, in the solid, liquid and dissolved states, in cases where experimental values are not to be found.*

Thus, this book is concerned with predictions. These are usually based on correlations of known information, with interpolation or extrapolation, as required. Reid and Sherwood (1958) distinguished correlations of three different types:

- Purely empirical; on extrapolation these correlations are often unreliable, or even dangerous to use.
- Purely theoretical; these are seldom adequately developed or directly usable.
- Partly empirical but based on theoretical models or concepts; these "semi-empirical" correlations are the most useful and reliable for practical purposes.

Among scientists there is often a tendency to look down upon semi-empirical approaches for the estimation of properties. This is completely unjustified. There are almost no purely theoretical expressions for the properties in which practice is interested.

One of the great triumphs of theoretical physics is the kinetic theory of gases. On the basis of an interaction–potential function, e.g. the Lennard–Jones force function, it is

possible to develop theoretical expressions for all the important properties of gases, such as the $p-v-T$ relationships, viscosity, molecular diffusivity, thermal conductivity and thermal-diffusion coefficient. The predicted variations of these properties with temperature are in excellent agreement with experimental data. But it should be realized that this extremely successful theoretical development has a purely empirical basis, viz. the force function. Except for the simplest cases, there is no sufficiently developed theory for a quantitative description of the forces between molecules. Whereas the theory of gases is relatively advanced, that of solids is less well understood, and the theory of liquids is still less developed.

In the relatively new field of macromolecular matter the semi-empirical approach is mostly necessary, and sometimes even the only possible way.

Fundamental theory is generally too remote from the phenomena, which have to be described. *What is needed in practice is a formulation that is designed to deal directly with the phenomena and makes use of the language of observation.* This is a pragmatic approach that is designed specifically for use; it is a completely non-speculative procedure.

In the low-molecular field Reid et al. (1977) have performed this task in a most admirable way, as far as gases and liquids are concerned. For molecular crystals and glasses Bondi (1968) gave a similar contribution, which partly covers the polymeric field, too.

In the macromolecular field the amount of literature is extremely large. Nevertheless the researcher is often confronted with the problem that neither directly measured properties, nor reliable methods to calculate them, can be found. This is the justification of the present book. The value of estimation and correlation methods largely depends, however, on their simplicity. Complicated methods have to be rejected. This has been one of our guiding principles.

The simplest and yet very successful method is based on the *concept of additive group contributions.*

The underlying idea in this concept is the following: There are thousands of chemical compounds of interest in science and practice; however, the number of structural and functional groups, which constitute all these compounds, is very much smaller. The assumption that a physical property of a compound, e.g. a polymer, is *in some way* determined by a sum of contributions made by the structural and functional groups in the molecule or in the repeating unit of the polymer, forms the basis of a method for estimating and correlating the properties of a very large number of compounds or polymers, in terms of a much smaller number of parameters which characterize the contributions of individual groups. These group contributions are often called *increments*.

Such a group contribution- or increment-method is necessarily an approximation, since the contribution of a given group in one surroundings is not necessarily the same as that in another environment.

The fundamental assumption of the group-contribution technique is *additivity*. This assumption, however, is valid only when the influence of any one group in a molecule or in a structural unit of a polymer is not affected by the nature of the other groups. If there is mutual interaction, it is sometimes possible to find general rules for corrections to be made in such a case of interaction (e.g. conjugation of double bonds or aromatic rings). Every correction or distinction in the contribution of a group, however, means an increase in the number of parameters. As more and more distinctions are made, finely the ultimate group will be recovered, namely the molecule or the structural unit of the polymer itself. Then the advantage of the group-contribution method is completely lost.

So the number of distinct groups must remain reasonably small, but not so small as to neglect significant effects of molecular structure on physical properties. For practical

utility always a compromise must be attained; it is this compromise that determines the potential accuracy of the method.

It is obvious that reliable experimental data are always to be preferred to values obtained by an estimation method. In this respect all the methods proposed in this book have a restricted value.

The first edition of the present book appeared in 1972, i.e. almost 40 years ago. The approach then proposed found a growing number of applications.

That the approach is useful has been demonstrated in a variety of ways in the literature, including a Russian translation of the book and a book by Askadskii and Matvyeyev (1983, in Russian), which is also devoted to the group contribution method and its application in polymer science and engineering. In 2002 the 3rd edition of Bicerano's book "Prediction of Polymer Properties" appeared; it is based on a different way of group contributions; nevertheless in the preface of this edition he mentions: "Much of the information provided by Van Krevelen's classic textbook, "Properties of Polymers" was extremely valuable in our work".

BIBLIOGRAPHY

- Askadskii AA and Matvyeyev Yu I, "Khimicheskoye Stroyeniye i Fizicheskiye Svoistva Polimerov" (Chemical Structure and Physical Properties of Polymers). Nauka, Moskva, 1983.
- Bicerano J, "Prediction of Polymer Properties". Marcel Dekker, New York, 3rd Ed, 2002.
- Bondi A, *Physical Properties of Molecular Crystals, Liquids and Glasses*. Wiley, New York, 1968.
- Brandrup J, Immergut EH and Grulke EA (Eds) "Polymer Handbook". Wiley-Interscience, New York, 1st Ed, 1966; 2nd Ed, 1975; 3rd Ed, 1989; 4th Ed, 1999.
- Lewis OG, "Physical Constants of Linear Homopolymers". Springer, Berlin, New York, 1968.
- Mark JE, "Polymer Data Handbook". Oxford University Press, 1999.
- Reid RC and Sherwood Th K, "The Properties of Gases and Liquids." McGraw-Hill, New York, 1st Ed 1958; 2nd Ed, 1966.
- Reid RC, Prausnitz JM and Sherwood Th K, "The Properties of Gases and Liquids". McGraw-Hill, New York, 3rd Ed, 1977.
- Saechting H, "International Plastics Handbook for the Technologist, Engineer and User". Oxford University Press, New York, 1988.

Encyclopaedic works

- Encyclopaedia of Polymer Science and Engineering*, Editors: Mark HF, Bikales NM, Overberger CG, Menges G and Kroschwitz JL, Wiley, New York, 2nd Ed, 1984–1990.
- Encyclopaedia of Materials Science and Engineering*, 1986–87. Editor in chief: Bever MB, Pergamon Press, Oxford.
- Comprehensive Polymer Science, The Synthesis, Characteristics, Reactions and Applications of Polymers, 8 Volumes. Editors: Allen SG and Bevington JC, Pergamon Press, Oxford, 1989.

This page intentionally left blank

CHAPTER 2

Typology of Polymers

2.1. INTRODUCTION

Macromolecules are giant molecules in which at least a thousand atoms are linked together by covalent bonds. They may be linear, branched chains or three-dimensional networks. Many natural substances, especially the biological construction materials, are macromolecules. Of these, proteins and cellulose are the most important. While cellulose (being made up of β -D-glucose units) has a relatively simple chemical structure, proteins are built up from many amino acids (varying from four to about twenty five), in a fixed sequence. This gives the proteins a very marked identity. In some cases the whole protein macromolecule is one single chemical unit, characterised by the nature and sequence of its amino acids. In contrast with these complex natural macromolecules, many synthetic macromolecules have a relatively simple structure, since they consist of identical *constitutional repeating units (structural units or monomers)*. This is the reason why they are called polymers.

If the basic units are identical we have a *homo-polymer*; if there are more kinds of basic units (e.g. two or three) we have a *copolymer*. In that case the composition of the macromolecule may vary from ordered repetition to random distribution. In this book we confine ourselves to these synthetic macromolecules or polymers.

In essence there are only two really *fundamental* characteristics of polymers: their *chemical structure* and their *molar mass distribution pattern*.

The *chemical structure* (CS) of a polymer comprises:

- a. The nature of the repeating units
- b. The nature of the end groups
- c. The composition of possible branches and cross links
- d. The nature of defects in the structural sequence

The *molecular weight distribution* (MWD) or *molar mass distribution* (MMD) informs us about the average molecular size and describes how regular (or irregular) the molecular size is. The MMD may vary greatly, depending on the method of synthesis of the polymer.

These two fundamental characteristics, CS and MMD, determine all the properties of the polymer. In a direct way they determine the *cohesive forces*, the *packing density* (and potential crystallinity) and the *molecular mobility* (with phase transitions). In a more indirect way they control the *morphology* and the *relaxation phenomena*, i.e. the total behaviour of the polymer.

In the geometrical arrangements of the atoms in a polymer chain two categories can be discerned:

- Arrangements fixed by the chemical bonding, known as configurations. The configuration of a chain cannot be altered unless chemical bonds are broken or reformed. Examples of configurations are *cis*- and *trans*-isomers or D- and L-forms.
- Arrangements arising from rotation about single bonds, known as conformations.

In dilute solutions the molecules are in continuous motion and assume different conformations in rapid succession (random coils). In the solid state many polymers have typical conformations, such as folded chains and helical structures. In polypeptides helical structures containing two or three chains (double and triple helices, respectively) are found.

There have been a lot of quarrels in the early years of the twentieth century about the reality of what now are called *polymers*. It is the great merit of Staudinger (1920) to have proposed, contrary to the prevailing ideas, that rubber and other biological substances, such as starch, cellulose and proteins, are long chains of short repeating units linked by covalent bonds. He also coins the name "macromolecule". Since then it became clear that polymer molecules are "normal" molecules and that only their chainlike nature is "different" and imposes restrictions, but also provides new properties.

In this chapter we shall consider the main aspects of polymer typology, viz. the chemical structure, the MWD, the phase transition temperatures, the morphology, and the relaxation phenomena. Furthermore a short survey will be given on multicomponent polymer systems.

2.2. POLYMER STRUCTURE

The polymer molecule consists of a "skeleton" (which may be a linear or branched chain or a network structure) and peripheral atoms or atom groups.

Polymers of a finite size contain so-called end groups, which do not form part of the repeating structure proper. Their effect on the chemical properties cannot be neglected, but their influence on the physical properties is usually small at degrees of polymerisation as used in practice. Sometimes use is made of these end groups to increase molecular weight (telechelic polymers).

2.2.1. Structural groups

Every polymer structure can be considered as a summation of structural groups. A long chain may consist mainly of bivalent groups, but any bivalent group may also be replaced by a trivalent or tetravalent group, which in turn carries one or two monovalent groups, thus forming again a bivalent "composed" group, e.g.

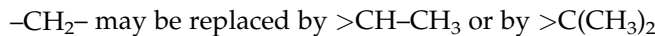


Table 2.1 gives the most important structural groups.

Sometimes it is better to regard a composed unit as one structural group. It is, e.g. often advisable to consider

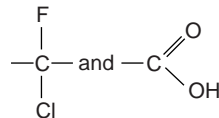


TABLE 2.1 Main structural groups

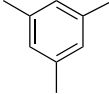
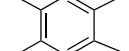
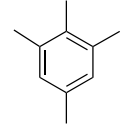
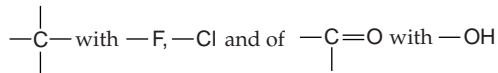
Groups	Monovalent	Bivalent	Trivalent	Tetravalent
1. Hydrocarbon groups	$-\text{CH}_3$ $-\text{CH} = \text{CH}_2$	$-\text{CH}_2-$ $-\text{CH} = \text{CH}-$	$>\text{C}-$ $>\text{CH} = \text{C}-$	$>\text{C}<$ $>\text{C} = \text{C}<$
				
				
				
2. Non-hydrocarbon groups	$-\text{OH}$ $-\text{SH}$ $-\text{NH}_2$ $-\text{F}$ $-\text{Cl}$ $-\text{Br}$ $-\text{I}$ $-\text{C} \equiv \text{N}$	$-\text{O}-$ $-\text{S}-$ $-\text{NH}-$ $\text{O}=\text{C}-$ $\text{O}=\text{S}-$	$-\text{N}<$	$>\text{Si}<$

TABLE 2.1 (continued)

Groups	Monovalent	Bivalent	Trivalent	Tetravalent
3. Composed groups				
	---O---C=			
	---HN---C=			
$-\text{COOH}$	---O---C=O---			$\text{---N=C---NH---C---N=H---}$
	---O---C---NH---			
	---HN---C---NH---			
	---C=O---O---C=			
$-\text{CONH}_2$	$\text{---O---C=O---O---C=O---O---}$			
	$\text{---C(=O)---C_6H_4---C(=O)---N---C=O---}$			

as individual structural groups and not as combinations of



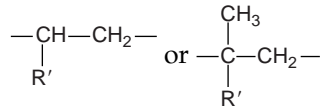
2.2.2. Linear chain polymers

Linear chain polymers can be distinguished into two main classes:

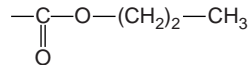
1. *Homochain polymers*, containing only carbon atoms in the main chain. These polymers are normally prepared by *addition* or *chain-reaction polymerisation*.
2. *Heterochain polymers*, which may have other atoms (originating in the monomer functional groups) as part of the chain. These polymers are usually prepared by *Polycondensation* or *step-reaction polymerisation*.

Tables 2.2 and 2.3 give a survey of the principal polymer families belonging to these two classes.

Most of the homochain polymers are built up according to the following schemes (per structural unit):



where R' is a monovalent side group. R' may be composed of several structural groups, e.g.:



Heterochains are usually built up according to the following scheme (per structural unit):



where R' and R'' are bivalent hydrocarbon groups and -AB- is a bivalent group originating from the original monomer functional groups (e.g. -NH-CO- from -NH₂ and -COOH).

2.2.3. Configurations of polymer chains

It may be useful to describe at this point the several *stereoregular* configurations, which are observed in polymer chains. The possible regular structure of *poly- α -olefins* was recognised by Natta et al. (1955), who devised a nomenclature now accepted to describe stereoregular polymers of this type. Fig. 2.1 shows the different possibilities. In general atactic polymers cannot crystallise, but if the pending group is only small, like OH in polyvinylalcohol, crystallisation is also possible.

Polymers of 1,3-dienes containing one residual double bond per repeat unit after polymerisation can contain sequences with different configurations (Fig. 2.2).

For further stereoregular configurations we refer to Corradini (1968).

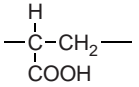
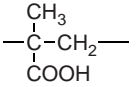
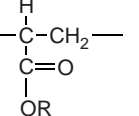
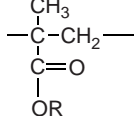
Stereoregularity plays a very important role in the structure of proteins, nucleic acids and other substances of biological importance and also in polypropylene that derives its right for application on its crystallinity.

2.2.4. Copolymers

Copolymers can be distinguished into alternating-, random-, graft-, and block copolymers.

TABLE 2.2 Class of homochain polymers $\left[R' = (CH_2)_n - B \text{ with } B = \begin{array}{c} -CH_3 \\ | \\ -CH(CH_3)_2 \\ | \\ -C(CH_3)_3 \end{array} \right]$

Polymer families	Basic unit	α -Substituted basic unit	Derivatives of basic unit	Derivatives of α -substituted basic unit
Polyolefins	Polyethylene $-CH_2-CH_2-$	Polypropylene $\begin{array}{c} CH_3 \\ \\ -C-CH_2- \\ \\ H \end{array}$	$\begin{array}{c} H \\ \\ -C-CH_2- \\ \\ R \end{array}$	$\begin{array}{c} CH_3 \\ \\ -C-CH_2- \\ \\ R \end{array}$
Polystyrenes	$\begin{array}{c} H \\ \\ -C-CH_2- \\ \\ \text{C}_6\text{H}_4 \end{array}$	$\begin{array}{c} CH_3 \\ \\ -C-CH_2- \\ \\ \text{C}_6\text{H}_4 \end{array}$	$\begin{array}{c} H \\ \\ -C-CH_2- \\ \\ \text{C}_6\text{H}_4 \\ \\ R \end{array}$	$\begin{array}{c} CH_3 \\ \\ -C-CH_2- \\ \\ \text{C}_6\text{H}_4 \\ \\ R \end{array}$
"Polyvinyls"	Poly (vinyl alcohol) $\begin{array}{c} H \\ \\ -C-CH_2- \\ \\ OH \end{array}$		Polyvinyl ethers $\begin{array}{c} H \\ \\ -C-CH_2- \\ \\ O \\ \\ R \end{array}$	
			Polyvinyl esters $\begin{array}{c} H \\ \\ -C-CH_2- \\ \\ O \\ \\ C=O \\ \\ R \end{array}$	

"Polyacrylics"	Poly(acrylic acid) ^a 	Poly(methacrylic acid) ^a 	Polyacrylates 	Polymethacrylates 
Polyacrylamide		Polymethacrylamide	N-substituted Polyacrylamides	N-substituted Polymethacrylamides
"Polyhalo-olefins"	$\begin{array}{c} X_1 \quad X_2 \\ \quad \quad \\ -C-C- \\ \quad \quad \\ X_3 \quad X_4 \end{array}$ X=H,F,Cl,Br,CN			
Polydienes	Polybutadiene $-\text{CH}_2-\text{CH}=\text{CH}-\text{CH}_2-$	Polyisoprene $-\text{CH}_2-\overset{\text{CH}_3}{\underset{ }{\text{C}}}=\text{CH}-\text{CH}_2-$		$-\text{CH}_2-\overset{\text{R}}{\underset{ }{\text{C}}}=\text{CH}-\text{CH}_2-$

*^a Often also polyacrylonitrile and polymethacrylonitrile (-COOH replaced by -CN) are included in this family.

TABLE 2.3 Class of heterochain polymers

Main polymer families	Smallest basic unit (often obtained by ring-opening polymerisation)	Bi-composed basic unit (obtained by condensation Polymerisation)
Polyoxides/ethers/acetals	$-\text{O}-\text{R}-$	$-\text{O}-\text{R}_1-\text{O}-\text{R}_2-$
Polysulphides	$-\text{S}-\text{R}-$	$-\text{S}-\text{R}_1-\text{S}-\text{R}_2-$
Polyesters	$\text{---}\overset{\text{O}}{\underset{\text{O}}{\text{C}}}\text{---R---}$	polylactones $\text{---}\overset{\text{O}}{\underset{\text{O}}{\text{C}}}\text{---R}_1\text{---}\overset{\text{O}}{\underset{\text{O}}{\text{C}}}\text{---R}_2\text{---}\overset{\text{O}}{\underset{\text{O}}{\text{C}}}\text{---}$
Polyamides	$\text{---}\overset{\text{O}}{\underset{\text{O}}{\text{C}}}\text{---R---}$	polylactams $\text{---NH---R}_1\text{---NH---}\overset{\text{O}}{\underset{\text{O}}{\text{C}}}\text{---R}_2\text{---}\overset{\text{O}}{\underset{\text{O}}{\text{C}}}\text{---}$
Polyurethanes	$\text{---}\overset{\text{O}}{\underset{\text{O}}{\text{C}}}\text{---O---R---}$	$\text{---}\overset{\text{O}}{\underset{\text{O}}{\text{C}}}\text{---R}_1\text{---}\overset{\text{O}}{\underset{\text{O}}{\text{C}}}\text{---NH---R}_2\text{---NH---}\overset{\text{O}}{\underset{\text{O}}{\text{C}}}\text{---}$
Polyureas	$\text{---}\overset{\text{O}}{\underset{\text{O}}{\text{C}}}\text{---NH---R---}$	$\text{---NH---R}_1\text{---NH---}\overset{\text{O}}{\underset{\text{O}}{\text{C}}}\text{---NH---R}_2\text{---NH---}\overset{\text{O}}{\underset{\text{O}}{\text{C}}}\text{---}$
Polyimides	$\text{---}\overset{\text{O}}{\underset{\text{O}}{\text{C}}}\text{---N---C---}$	$\text{---R}_1\text{---N---}\overset{\text{O}}{\underset{\text{O}}{\text{C}}}\text{---R}_2\text{---}\overset{\text{O}}{\underset{\text{O}}{\text{C}}}\text{---N---}$
Polyanhydrides	$\text{---}\overset{\text{O}}{\underset{\text{O}}{\text{C}}}\text{---O---C---R---}$	$\text{---}\overset{\text{O}}{\underset{\text{O}}{\text{C}}}\text{---R}_1\text{---}\overset{\text{O}}{\underset{\text{O}}{\text{C}}}\text{---O---C---R}_2\text{---}\overset{\text{O}}{\underset{\text{O}}{\text{C}}}\text{---}$
Polycarbonates	$\text{---}\overset{\text{O}}{\underset{\text{O}}{\text{C}}}\text{---O---R---}$	$\text{---}\overset{\text{O}}{\underset{\text{O}}{\text{C}}}\text{---R}_1\text{---O---}\overset{\text{O}}{\underset{\text{O}}{\text{C}}}\text{---O---R}_2\text{---}\overset{\text{O}}{\underset{\text{O}}{\text{C}}}\text{---}$
Polyimines	$\text{---}\overset{\text{R}_1}{\underset{\text{R}_2}{\text{N}}}\text{---}$	$\text{---}\overset{\text{R}}{\underset{\text{R}}{\text{N}}}\text{---R}_1\text{---N---R}_2\text{---}$
Polysiloxanes	$\text{---}\overset{\text{R}}{\underset{\text{R}}{\text{Si}}}\text{---O---}$	$\text{---}\overset{\text{R}_1}{\underset{\text{R}_2}{\text{Si}}}\text{---O---}\overset{\text{R}_1}{\underset{\text{R}_2}{\text{Si}}}\text{---O---R---}$

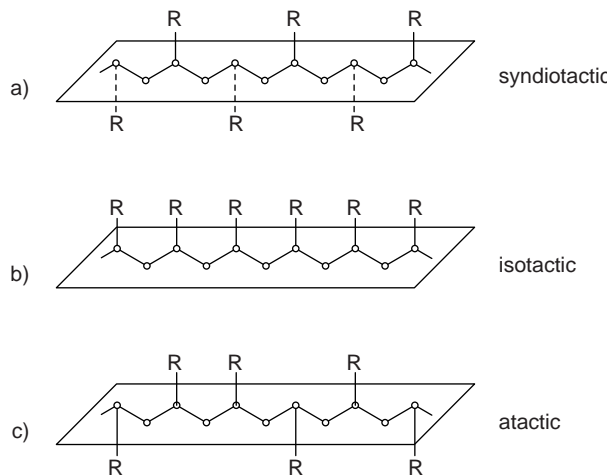


FIG. 2.1 Configurations in vinyl polymers. (The main carbon homochain is depicted in the fully extended planar zigzag conformation. For clarity, hydrogen atoms are omitted.)

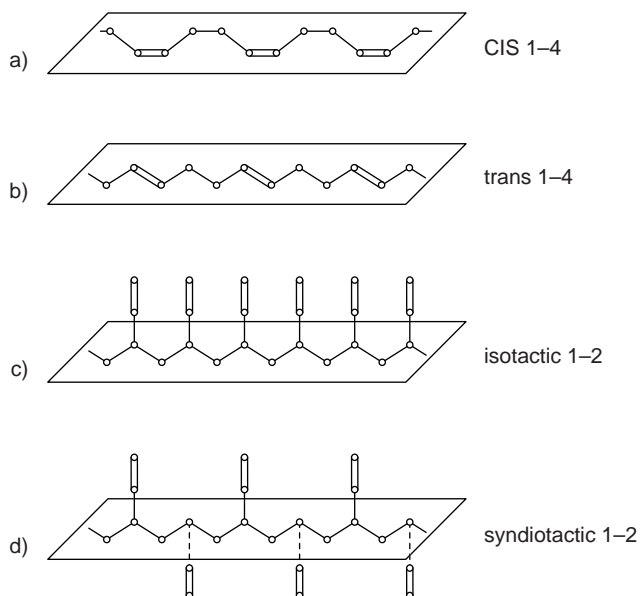


FIG. 2.2 Configurations involving a carbon–carbon double bond.

Alternating copolymers may be considered as homopolymers with a structural unit composed of the two different monomers. Random copolymers are obtained from two or more monomers, which are present simultaneously in one polymerisation reactor. In graft polymerisation a homopolymer is prepared first and in a second step one or two monomers are grafted onto this polymer; the final product consists of a polymeric backbone with side branches. In block copolymerisation one monomer is polymerised, after which another monomer is polymerised on to the living ends of the polymeric chains; the final block copolymer is a linear chain with a sequence of different segments.

All types of copolymer have found industrial application. Some examples are shown in Table 2.4.

TABLE 2.4 Examples of copolymers

Type of copolymers	Examples of commercial systems
Alternating copolymers -A-B-A-B-A-B-	Vinylacetate-maleic anhydride-copolymers Condensation polymers of diamines and diacids
Random copolymers -A-A-A-B-A-B-B-A-A-	Styrene-butadiene rubber Styrene-acrylonitrile rubber Ethylene-vinyl acetate copolymer
Graft copolymers A A A -B-B-B-B-B-B-B-B- A A A	Rubber-styrene graft copolymers (high-impact polystyrene) Acrylonitrile-butadiene-styrene graft copolymer (ABS)
Block copolymers -A-A-A-A-A-B-B-B-B-	Styrene-butadiene diblock copolymers Styrene-butadiene-styrene triblock copolymers Polyurethane multiblock copolymers (elastomeric yarns)

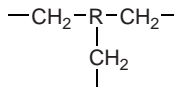
2.2.5. Branched polymers

Polymers obtained by condensation polymerisation of purely bifunctional monomers, must be linear. The chains produced in addition polymerisations may have a number of short or long branches attached at random along their axes. Especially in radical polymerisation, branching is probable and cannot be easily controlled. Branching affects the properties of a polymer in the molten state and in solution. Viscometric, nuclear magnetic resonance (NMR) and infrared absorption (IR) studies provided the most promising methods for the measuring of branching properties of a polymer in the molten state and in solution. Methods for the measurement of chain branching are viscosimetry, NMR, infrared absorption, gel permeation chromatography/size exclusion chromatography (GPC/SEC), size exclusion chromatography/multiangle laser light scattering (SEC/MALLS), etc.

2.2.6. Network polymers

Network polymers are formed either if tri-functional or even tetra-functional monomers are present during the polymerisation reaction or by cross linking of high molecular weight polymers, like vulcanisation of rubber.

A widely used type of network polymers is the formaldehyde resin, in which the following groupings are frequent:



Other network polymers are the so-called unsaturated polyester resins, epoxy resins, polyurethane foams and vulcanised rubbers.

2.3. MOLAR MASS AND MOLAR MASS DISTRIBUTION

Normally a polymeric product will contain molecules having many different chain lengths. These lengths are distributed according to a probability function, which is governed by the mechanism of the polymerisation reaction and by the conditions under which it was carried out.

The processing behaviour and many end-use properties of polymers are influenced not only by the *average molar mass* but also by the width and the shape of the MMD or MWD. The basic reason is that some properties, including tensile and impact strength, are specifically governed by the short molecules; for other properties, like solution viscosity and low shear melt flow, the influence of the middle class of the chains is predominant; yet other properties, such as melt elasticity, are highly dependent on the amount of the longest chains present.

M is the *molar mass* or (*relative molar mass*), as recommended by IUPAC. The older expression, *molecular weight*, is still widely used in the literature and still recognised as an alternative name. Both of them will be used in this book.

Fig. 2.3 shows a MMD curve. In this figure also the characteristic molar mass averages are indicated; their definition is given in Table 2.5.

A MMD curve is reasonably characterised when at least three different molar masses are known, by preference M_n , M_w and M_z .

The most important mass ratios are:

$$Q = \frac{M_w}{M_n} \quad \text{and} \quad Q' = \frac{M_z}{M_w} \quad (2.1)$$

$Q = Q' = 1$ would correspond to a perfectly uniform or *monodisperse* polymer.

Most of the *thermodynamical properties* are dependent on the *number-average molar mass*. Many of these properties can be described by an equation of the type:

$$X = X_\infty - \frac{A}{M_n} \quad (2.2)$$

where X is the property considered, X_∞ is its asymptotic value at very high molar mass, and A is a constant.

For a number of properties in this group, including density, specific heat capacity, refractive index, etc., X attains its limiting value X_∞ already at molar mass below the real macromolecular range. For these properties the configuration of the structural unit alone is the preponderant factor determining the property.

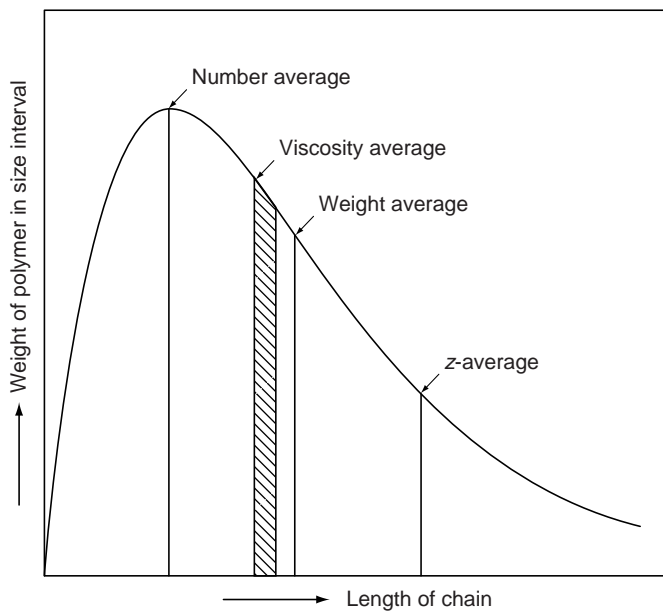


FIG. 2.3 Distribution of molar mass in a polymer with a Schultz–Flory distribution with $M_n:M_w:M_z = 1:2:3$.

TABLE 2.5 Definition of molar mass averages

Average molar mass	Symbol and definition
Number-average molar mass	$M_n = \frac{\sum_i n_i M_i}{\sum_i n_i} = \frac{\sum_i w_i}{\sum_i w_i/M_i} = \frac{W}{N}$
Weight-average molar mass	$M_w = \frac{\sum_i n_i M_i^2}{\sum_i n_i M_i} = \frac{\sum_i w_i M_i}{\sum_i w_i}$
<i>z</i> -Average molar mass	$M_z = \frac{\sum_i n_i M_i^3}{\sum_i n_i M_i^2} = \frac{\sum_i w_i M_i^2}{\sum_i w_i M_i}$
(<i>z</i> + 1)-Average molar mass	$M_{z+1} = \frac{\sum_i n_i M_i^4}{\sum_i n_i M_i^3} = \frac{\sum_i w_i M_i^3}{\sum_i w_i M_i^2}$
Viscosity-average molar mass	$M_v = \left[\frac{\sum_i n_i M_i^{1+a}}{\sum_i n_i} \right]^{1/a} = \left[\frac{\sum_i w_i M_i^a}{\sum_i w_i} \right]^{1/a}$

Where the symbols used have the following meaning: M_i = molar mass of the component molecules of kind i ; n_i = number-fraction of the component molecules i ; w_i = weight-fraction of the component molecules i ; N = total number of moles of all kinds; W = total weight of moles of all kinds; a = exponent of the Mark–Houwink relationship relating intrinsic viscosity to molar mass.

Typical *mechanical properties*, such as tensile strength, vary significantly with molecular weight within the range of the real macromolecules. As Eq. (2.2) applies to these properties (*number-average molar mass* being important), it indicates that the number of chain ends is a preponderant factor.

Bulk properties connected with *large deformations*, such as melt and solution viscosity, are largely determined by the *weight-average molar mass*, i.e. by the mass to be transferred. Branching and cross linking have a very pronounced effect in this case.

Typical viscoelastic properties, such as melt elasticity, depend on the z - and $z + 1$ -*average molar masses*.

2.3.1. Experimental determination of the MM-averages

Table 2.6 gives a survey of the classical methods for the determination of the different averages of the molar mass. For the detailed description we must refer here to the hand- and textbooks.

2.3.2. Determination of the full molar mass distribution

During the last decades several methods for the determination of the complete MMD have been developed. Table 2.7 gives a survey of these methods, the principles of which will be shortly discussed.

Gel-permeation Chromatography (or better: *Size-exclusion chromatography*) is a technique, which separates the molecules according to their dimensions. The separation method involves column chromatography in which the stationary phase is a heteroporous, solvent swollen polymer gel varying in permeability over many orders of magnitude. As the liquid phase, which contains the polymer, passes through the gel, the polymer molecules diffuse into all parts of the gel not mechanically barred to them. The smaller molecules permeate more completely and spend more time in the pores than the larger molecules, which pass through the column more rapidly. The instrument has to be calibrated by means of narrow fractions of known molecular weight (determined by some absolute method).

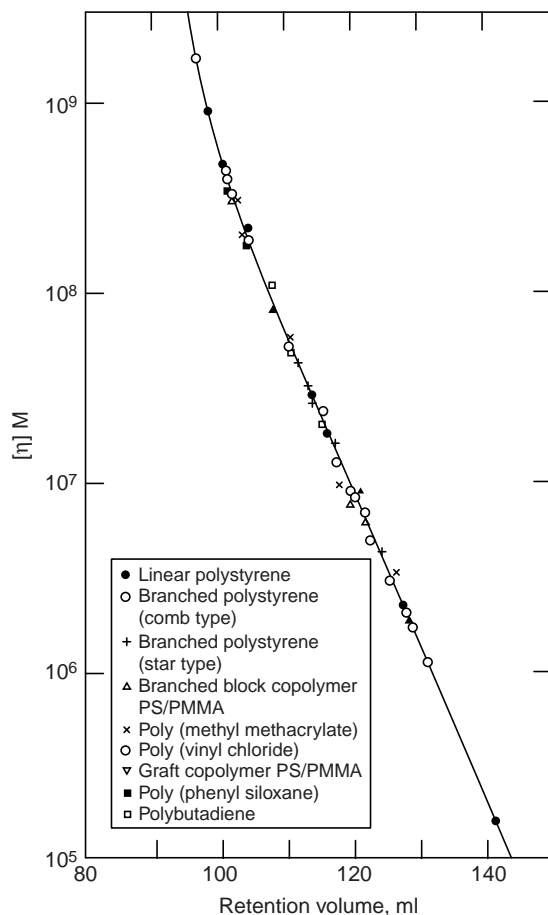
TABLE 2.6 Determination of MM-averages (\overline{M}_x)

Principle of the method	M_x determined	Upper limit of method
I. <i>Chemical analysis</i>		
End-group Analysis	M_n	10^4
Do., with radioactive labelling		10^6
II. <i>Measurement of colligative properties</i>		
Lowering of vapour pressure	M_n	10^4
Ebulliometry and cryoscopy		10^5
Vapour pressure osmometry		10^5
Membrane osmometry		10^6
III. <i>Viscometry of dilute solutions</i>		
Intrinsic viscosity measurement	M_v	10^7
IV. <i>Light Scattering</i>	M_w	
Laser-light scattering (X-Ray- and neutron scattering)		10^7
V. <i>Sedimentation</i>		?
Ultra-centrifuge	M_w, M_z, M_{z+1}	10^7

TABLE 2.7 Methods for determination of the complete MMD

Principle of the method	Upper M_w -limit
<i>I. Chromatographic methods</i>	
Gel-permeation chromatography (GPC)	10^7
<i>II. Light scattering</i>	
Dynamic Laser-light scattering	10^7
<i>III. Field flow fractionation (FFF)</i>	
Sedimentation FFF	10^7
Cross-flow FFF	
Electric FFF	up to particles of $100 \mu\text{m}$ in diameter (colloidal)
Thermal FFF	

Fig. 2.4 gives an example of a calibration curve where the hydrodynamic volume (a quantity directly related to the molar mass, and proportionally denoted by $[\eta]M$), is plotted versus the retention volume (the retention volume is the volume of liquid passed through the column from the middle of the sample injection to the peak maximum, as measured by a suitable detector, e.g. a differential refractometer).

**FIG. 2.4** Example of a universal calibration curve for GPC. From Billmeyer (1984); Courtesy John Wiley & Sons.

Dynamic light scattering (DLS), also called *photon correlation spectroscopy* (PCS) or *laser light scattering* (LLS) is a technique based on the principle that moving objects cause a frequency shift due to the Doppler effect. If a solution of macromolecules with random Brownian motion is illuminated with monochromatic laser light, the scattered light should contain a distribution of frequencies about the incident frequency; the spectral line is virtually broadened. The width of the distribution is related to the MMD.

Since the velocities of the dissolved macromolecules are far less than the velocity of light, the Doppler shift will be extremely small and thus the frequency shifts are very small. The high intensity of the laser source makes it possible, however, to measure weakly scattered light and to observe very small frequency shifts. Like conventional light scattering, DLS can be used successfully to determine the molecular weight, size and shape of macromolecules. Moreover, DLS is such a powerful tool that also the diffusion coefficient can be measured, and that in a more elegant manner than many other classical tools (Sun, 1994, 2004).

The principles and applications of this method were described and discussed by Blagrove (1973), Burchard (1985) and Chu (1985).

Field flow fractionation (FFF) comprises a family of techniques that have demonstrated, over more than two decades, the ability to characterise supra molecular species in a size range spanning many order of magnitude, from macromolecules to micron-sized particles. The discovery of FFF dates back to the late 1960s due to Giddings and Myers (1957–1993).

In the FFF a field or gradient is applied in a direction, perpendicular to the axis of a narrow flow channel. At the same time a solvent is forced steadily through the channel forming a cross-sectional flow profile of parabolic shape. When a polymer sample is injected into the channel, a steady state is soon reached in which the field induced motion and the opposed diffusion are exactly balanced. The continuous size-distribution of the polymer will migrate with a continuous spectrum of velocities and will emerge at the end of the flow channel with a continuous time distribution. When processed through a detector and its associated electronics, the time distribution becomes an elution (retention) spectrum.

This technique and its application were invented and developed by Giddings and Myers (1966–1988). Giddings' review in *Science* (1993) is an excellent description of FFF techniques; see also Schimpf et al. (2000).

Of the many kinds of interactive fields or gradients possible, five principal types have proved the most practical: sedimentation (Sd-FFF), electrical (El-FFF), thermal (Th-FFF), steric (St-FFF) and lateral cross flow (F-FFF). A commercial high-spin-rate sedimentation FFF instrument was developed by Kirkland and Yau, the SF³ technique (1982).

2.3.3. The polydispersity index Q

The width of a MMD curve is characterised by the ratios of averages of the molar mass, combined with one absolute value of in average mass.

Usually the ratio $Q \equiv M_w/M_n$ is applied, in combination with M_w . The term Q is called the *polydispersity index*. Also $(Q-1) = U$ is used, and U is called *non-uniformity index*. The larger the values of Q and U , the broader the MMD. U is directly connected with the standard width of the distribution (σ_n) (Elias, 1971):

$$U = \left(\frac{\sigma_n}{M_n} \right)^2 \quad (2.3)$$

As mentioned already, the numerical value of Q is determined by the reaction mechanism of the polymerisation and by the conditions (p , T , etc.) under which it was carried out.

Table 2.8 gives a survey of the empirical values of index Q for different types of polymerisation.

TABLE 2.8 Values of the polydispersity index $Q (= M_w/M_n)$

Type of polymer	Mechanism of polymerisation	Value of Q
"Living polymers"	Anionic Group-transfer	1.0–1.05
Condensation polymers	Step reaction of bifunctional monomers	~2 in a batch reactor ">>>2 in a continuous reactor
Addition polymers	Radical addition Kationic addition Coordination-pol. by means of metal-organic complexes	1.5–10 2–10 2–30
Branched polymers	Radical addition	2–50
Network polymers	Step reaction in the presence of tri- or tetrafunctional monomers	2–∞ (∞ at gel-point)

2.3.4. The index Q as the key parameter for the full MMD

A crucial question is the following: "is the index Q really the key parameter for the full MMD?" Or, in other words: does a sufficiently universal relationship exist between $Q (=M_w/M_n)$ and the other important ratios M_z/M_w and M_{z+1}/M_z ?

If this question can be answered in the affirmative, then dimensionless relationships where Q is used as the key parameter for the MMD (e.g. in rheological master graphs) will have a general validity. If not – one can hardly expect any generally valid set of master curves (e.g. viscosity versus shear rate) even for one polymer!

Van Krevelen et al. (1977) studied this problem by means of very accurate Gel-permeation experiments on 13 structurally very different polymers; they also compared their results with reliable MMD/GPC-data in the literature. The latter were assembled for six different polymers and were obtained by 10 different authors. The results of Van Krevelen et al. are presented in Table 2.9 those of the other authors are given in Figs. 2.5 and 2.6.

The most important conclusions are the following:

- (1) All reliable data available indicate the approximate relationships given in Table 2.10.
- (2) The spread in the data of Table 2.9 proved to be within the experimental accuracy of the (experimental) MMD determination.
- (3) Within the range of experimental accuracy there is no justification for the use of parameters other than M_w and Q , to characterise the MMD of polymers, on condition that they are unblended.
- (4) This means that any mechanical or rheological property of polymers may be described as a function of M_w and Q , and this for any MMD.
- (5) None of the commonly used theoretical MMDs, such as Gaussian, Log-normal, Lansing-Kraemer, Schulz-Flory, Tung, Poisson, etc., are in exact agreement with the experimental relationships given in Table 2.9.

It should be mentioned that the width of the MMD is also highly dependent on the production process: there are big differences in MMDs by polymer production in continuous or batch reactors.

TABLE 2.9 Experimentally determined molar mass distributions, as obtained from GPC-curves

Polymer	M_n (kg/mol)	M_w (kg/mol)	M_z (kg/mol)	M_{z+1} (kg/mol)	M_w/M_n	M_z/M_w	M_{z+1}/M_z	$M_z M_{z+1}/M_w^2$
1. Polyisobutylene	171	597	1730	5012	3.5	2.9	2.9	24.3
	565	3382	10930	24372	6.0	3.2	2.2	23.3
2. Polystyrene	74	165	304	479	2.2	1.8	1.58	5.3
3. Poly(vinylidene fluoride)	75	191	409	689	2.6	2.1	1.68	7.7
4. Poly(vinyl alcohol)	66	294	941	1846	4.5	3.2	1.96	20.1
5. Poly(vinyl acetate)	217	611	1821	5287	2.8	3.0	2.90	25.8
6. Poly(vinyl pyrrolidon)	10	24	54	100	2.5	2.3	1.85	9.4
7. Poly(methyl methacrylate)	252	481	766	1196	1.9	1.6	1.56	4.0
8. Polyacrylonitrile	38	116	249	405	3.1	2.1	1.63	7.5
9. Polybutadiene	142	443	1076	1745	3.1	2.4	1.6	9.6
10. Poly(2,6-dimethyl-1, 4 -phenylene oxide)	26	56	88	117	2.2	1.6	1.33	3.3
11. Poly(2,6-diphenyl-1, 4 -phenylene oxide)	297	550	875	1319	1.9	1.6	1.51	3.8
12. Poly(ethylene terephthalate)	27	62	116	198	2.3	1.9	1.71	6.0
13. Poly(6-aminohexanoic acid)	50	118	233	371	2.4	2.0	1.59	6.2

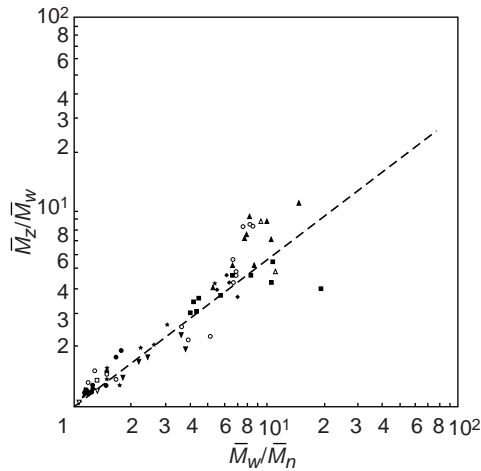


FIG. 2.5 Relation between M_w/M_n and M_z/M_w literature data. (●) PE, Mendelson et al. (1970); (□) EI, Mills (1969); (■) M, Saeda et al. (1971); (Δ) A, Shah and Darby (1976); (▲) A, Wales (1969). PS: (▽) V, Cotton et al. (1974); (▼) V, Chee and Rudin (1974); (◇) Mills (1969); PP: (◆) Thomas (1971). PMMA: (⊕) ED, Mills (1969). PDMS: (○) Mills (1969). BR: (*) Dunlop and Williams (1973).

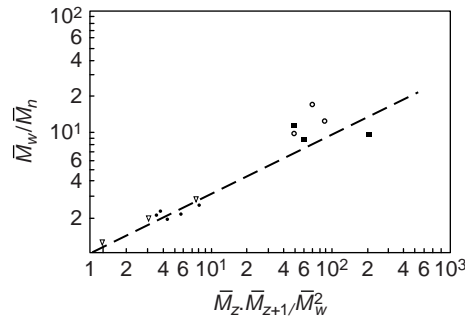


FIG. 2.6 Relation between M_z/M_w and M_zM_{z+1}/M_w^2 , literature data. PE: (○) Graessley and Segal (1970); (■) Shah and Darby (1976). PS: (▽) Graessley and Segal (1970). PVC: (●) Collins and Metzger (1970).

TABLE 2.10 Experimentally determined “Universal Ratios” of MM-averages (data of Van Krevelen et al. 1977)

Ratios of the form: M_x/M_n	$\frac{M_w}{M_n} = Q$	$\frac{M_z}{M_n} \approx Q^{1.75}$	$\frac{M_{z+1}}{M_n} \approx Q^{2.31}$
Ratios of adjacent averages	$\frac{M_w}{M_n} = Q$	$\frac{M_z}{M_w} \approx Q^{0.75}$	$\frac{M_{z+1}}{M_z} \approx Q^{0.56}$
Ratios, being Ratio-products	$\frac{M_zM_{z+1}}{M_n^2} \approx Q^{4.06}$	$\frac{M_zM_{z+1}}{M_nM_w} \approx Q^{3.06}$	$\frac{M_zM_{z+1}}{M_w^2} \approx Q^{2.06}$
Ratios of the form: M_v/M_n	$\frac{M_v}{M_n} \approx Q^{0.6}$	$\frac{M_v}{M_w} \approx Q^{-0.4}$	$\frac{M_v}{M_z} \approx Q^{-1.0}$

2.4. PHASE TRANSITIONS IN POLYMERS

Simple molecules may occur in three states, the solid, the liquid and the gaseous state. The transitions between these phases are sharp and associated with a thermodynamic equilibrium. Under these conditions, phase changes are typical *first-order transitions*, in which a primary thermodynamic function, such as volume or enthalpy, shows a sudden jump.

In the case of polymer molecules the situation is much more complex. Polymers cannot be evaporated since they decompose before boiling. In the solid state a polymer is only exceptionally purely crystalline (so-called single crystals), but generally it is partially or totally amorphous. Furthermore a very high viscosity characterises the liquid state.

It is impossible to understand the properties of polymers without knowledge of the types of transition that occur in such materials. Primarily these transitions and the temperatures, at which they occur, determine nearly all the properties of polymers.

The only “normal” phase state for polymers, known from the physics of small molecules, is the liquid state, though even here polymers show special properties, like viscoelasticity. The typical states of polymers are the *glassy*, the *rubbery* and the *semi-crystalline* state, all of which are thermodynamically metastable.

An interesting classification of phase states is that based on two parameters: the degree of order (long- and short range) and the time dependence of stiffness (long- and short time). Each state can be characterised by a matrix of the following form:

Short-range order (SRO)	Long-range order (LRO)
Short-time stiffness (STS)	Long-time stiffness (LTS)

If “+” means present and “-” means absent, we get the picture shown in Fig. 2.7 for the possible phase states; “ \pm ” means a transition case.

None of the phase states of polymers shows perfect long-range order. The basic difference of a glass and a (super cooled) liquid is the presence of short- and long-time stiffness (and therefore absence of the short-time fluidity) in the glass. The rubbery state, on the other hand, has all the properties of the liquid, except the short-time fluidity.

Fig. 2.7 holds for non-oriented polymers. Orientation in semi-crystalline polymers gives the material a long-range order, which is important for many product properties.

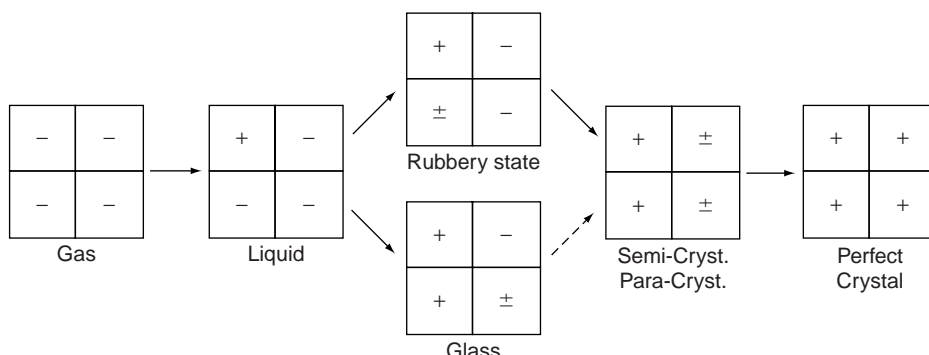


FIG. 2.7 Characterisation of phase states in non-oriented polymers.

2.4.1. Linear thermoplastic amorphous polymers

The situation for amorphous linear polymers is sketched in Fig. 2.8a. If a polymeric glass is heated, it will begin to soften in the neighbourhood of the *glass–rubber transition* temperature (T_g) and become quite rubbery. On further heating the elastic behaviour diminishes, but it is only at temperatures more than 50° above the glass–rubber transition temperature that a shear stress will cause viscous flow to predominate over elastic deformation.

The glass–rubber transition temperature, commonly known as glass transition temperature (T_g), is a phase change *reminiscent* of a thermodynamic *second-order transition*. In the case of a second-order transition a plot of a primary quantity shows an abrupt change in slope, while a plot of a *secondary* quantity (such as expansion coefficient and specific heat) then shows a sudden jump.

In fact T_g is *not* a thermodynamic second-order transition, but is kinetically controlled. The exact position of T_g is determined by the rate of cooling; the slower the cooling process, the lower T_g . Yet, for practical purposes one can say that every polymer is characterised by its own T_g .

If the molar mass is sufficiently high, the glass–rubber transition temperature is almost independent of the molar mass. On the other hand, the very *diffuse rubbery–liquid transition*

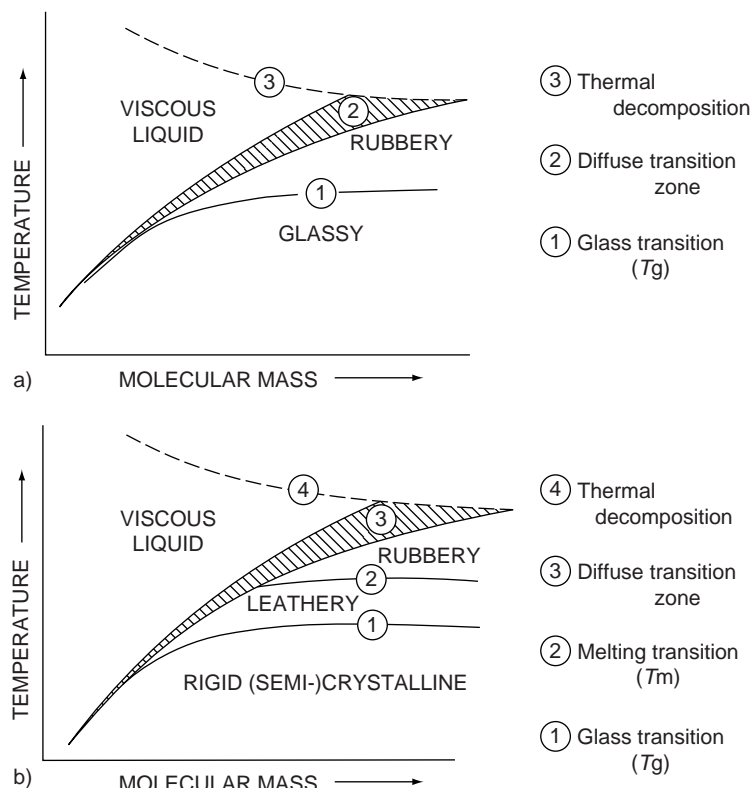


FIG. 2.8 T–M Diagram for polymers. (a) Amorphous polymers; (b) (semi) crystalline polymers.

heavily depends on the molar mass, whilst the decomposition temperature tends to decrease slightly with increasing molar mass.

As is well known, the glass–rubber transition is of considerable importance technologically. The glass transition temperature (T_g) determines the lower use limit of a rubber and the upper use limit of an amorphous thermoplastic material. With increasing molar mass the ease of “forming” (shaping) diminishes.

Below the glass–rubber transition temperature glassy polymers also show other, *secondary transitions*. Their effects are smaller and often less obvious, although they are important to the mechanical behaviour (to diminish brittleness). Secondary transitions can be detected by studies of mechanical damping, by NMR or by electric loss measurements over a range of temperatures.

While the main transition occurs as soon as large segments of the polymer backbone chain are free to move, secondary transitions occur at temperatures where subgroups, side chains, etc., can freely move or oscillate.

2.4.2. Linear thermoplastic semi-crystalline polymers

Many polymers show regions of high order and may be considered (semi-) crystalline. The major factor determining whether a polymer can crystallise is the occurrence of successive units in the chain in a configuration of high geometrical regularity. If the chain elements are small, simple and equal, as in linear polyethylene, crystallinity is highly developed. If, however, the chain elements are complex, containing bulky (side) groups, as in polystyrene, the material can crystallise only if these substituent groups are arranged in an ordered or tactic configuration.

In these cases it is possible to identify a melting temperature (T_m). Above this melting temperature the polymer may be liquid, viscoelastic or rubbery according to its molar mass, but below it, at least in the high molar mass range, it will tend to be leathery and tough down to the glass transition temperature. (The lower-molecular-mass grades will tend to be rather brittle waxes in this zone.)

The crystalline melting point, T_m is (theoretically) the highest temperature at which polymer crystallites can exist. Normally, crystallites in a polymer melt in a certain temperature range.

Secondary crystalline transitions (below T_m) occur if the material transforms from one type of crystal to another. These transitions are, like the melting point, thermodynamic first-order transitions.

Suitable methods for studying the transitions in the crystalline state are X-ray diffraction measurements, differential thermal analysis and optical (birefringence) measurements. The situation for crystalline linear polymers is sketched in Fig. 2.8b. Though in crystalline polymers T_m rather than T_g determines the upper service temperature of plastics and the lower service temperature of rubbers, T_g is still very important. The reason is that between T_m and T_g the polymer is likely to be tough; the best use region of the polymer may therefore be expected at the lower end of the leathery range. This, however, is an oversimplification, since in these polymers other (secondary) transitions occur which may override T_g in importance. Below the glass transition temperature many polymers tend to be brittle, especially if the molecular weight is not very high. Secondary transitions may be responsible if a rigid material is tough rather than brittle.

Fig. 2.9 gives a schematic survey of the influence of the main transition points on some important physical quantities.

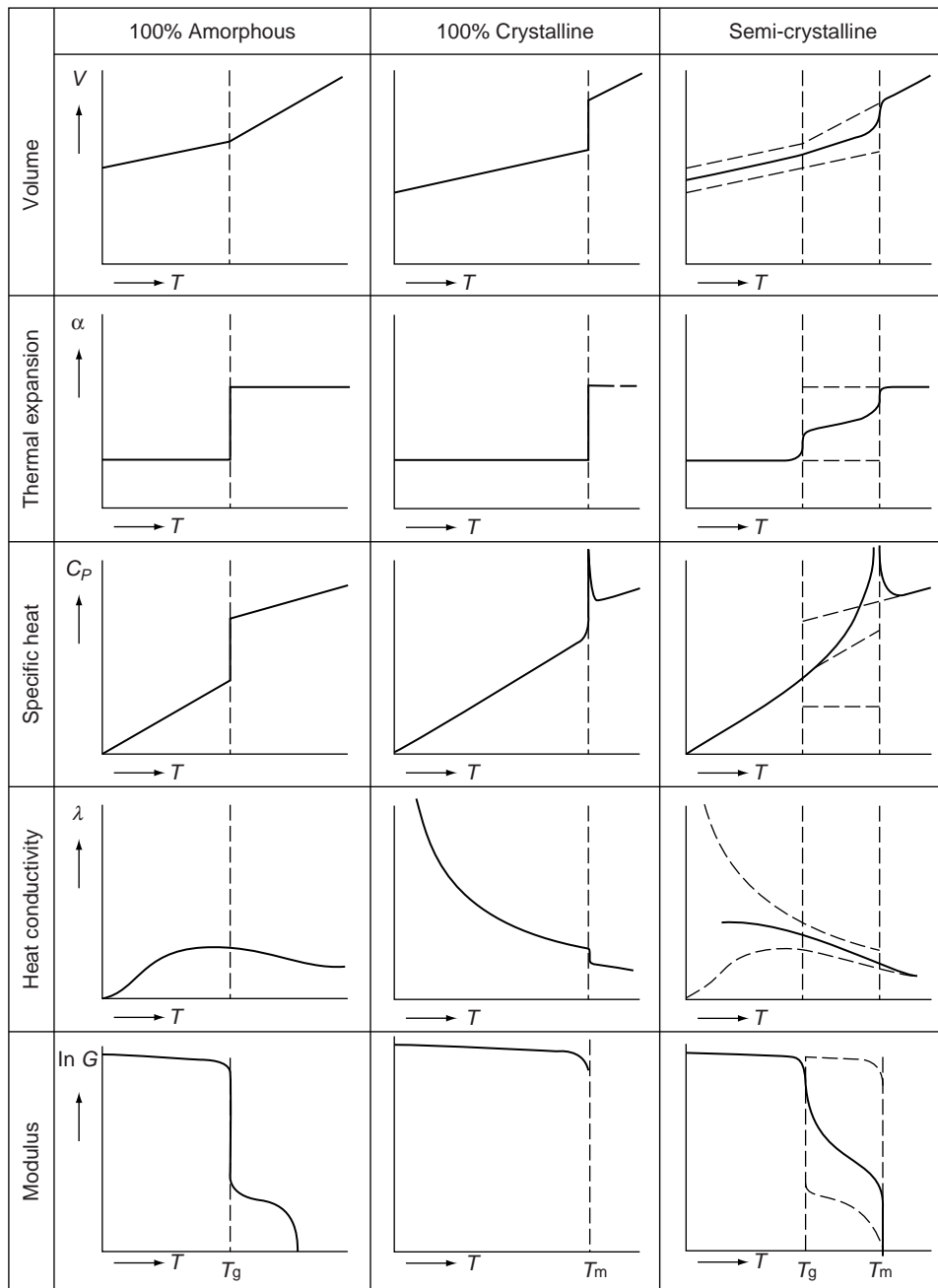


FIG. 2.9 Behaviour of some polymer properties at transition temperatures.

2.4.3. Linear non-thermoplastic polymers

Some polymers, such as cellulose, although linear in structure, have such a strong molecular interaction, mostly due to hydrogen bridges and polar groups that they do not soften or melt. Consequently, the transition temperatures as such are less important to this class of polymers. Normally they are highly crystalline, with a crystalline melting point (far) above the decomposition temperature. Their physical behaviour – except for

the melting – is that of crystalline polymers. Therefore they are suitable raw materials for fibres (via solution spinning).

Many of these polymers are “plasticized” by water, due to the strong influence of water on the molecular interaction. The polymers can therefore be called “*hydroplastics*” in contradistinction to thermoplastics. Moisture may cause a tremendous depression of the glass transition temperature.

2.4.4. Cross-linked polymers

If an amorphous polymer is cross linked, the basic properties are fundamentally changed. In some respects the behaviour at a high degree of cross linking is similar to that at a high degree of crystallinity. (crystallisation can be considered as a physical form of cross linking). The influence of the glass transition temperature becomes less and less pronounced as cross-linking progresses; T_g increases with decreasing molecular weight between cross links.

2.4.5. Classification of polymers on the basis of their mechanical behaviour

On the basis of the general behaviour described in the preceding sections it is possible to develop a classification of polymers for practical use. This is given in Table 2.11. The nomenclature is to agreement with a proposal by Leuchs (1968).

2.5. MORPHOLOGY OF SOLID POLYMERS

As discussed earlier, solid polymers can be distinguished into amorphous and the semi-crystalline categories. Amorphous solid polymers are either in the glassy state, or – with chain cross linking – in the rubbery state. The usual model of the macromolecule in the amorphous state is the “random coil”. Also in polymer melts the “random coil” is the usual model. The fact, however, that melts of semi-crystalline molecules, although very viscous, show rapid crystallisation when cooled, might be an indication that the conformation of a polymer molecule in such a melt is more nearly an irregularly folded molecule than it is a completely random coil.

The traditional model used to explain the properties of the (partly) crystalline polymers is the “fringed micelle model” of Hermann et al. (1930). While the coexistence of small crystallites and amorphous regions in this model is assumed to be such that polymer chains are perfectly ordered over distances corresponding to the dimensions of the crystallites, the same polymer chains include also disordered segments belonging to the amorphous regions, which lead to a composite single-phase structure (Fig. 2.10).

The fringed micelle model gives an extremely simple interpretation of the “degree of crystallinity” in terms of fractions of well-defined crystalline and amorphous regions. Many excellent correlations have evolved from this model through the years, so that it has long been popular.

Later events have made it necessary to re-examine the concept of the polymeric solid state. The most important of these events was the discovery and exploration of polymer single crystals (Schiesinger and Leeper, 1953; Keller, 1957). It had long been believed that single crystals could not be produced from polymer solutions because of the molecular entanglements of the chains. Since 1953 the existence of single crystals has been reported for so many polymers that the phenomenon appears to be quite general. These single crystals are platelets (lamellar structures), about 10 nm thick, in which perfect order exists, as has been shown by electron diffraction patterns. On the other hand, dislocations

TABLE 2.11 Classification of polymers on the basis of mechanical behaviour (nomenclature according to Leuchs, 1968)

Polymer class	General properties	Range of use temperatures	Degree of crystallinity	Degree of cross linking	Example
I. Molliplasts	Elasto-viscous liquids	$T > T_g$	0	0	Polyisobutylene
II. Mollielasts (Elastomers)	Soft and flexible rubbery solids	$T > T_g$	0	Low	Polybutadiene
III. Fibroplasts	Tough, leathery-to-hornlike solids	$T < T_m$ ($T > T_g$)	20–50	0	Polyamide
IV. Fibroelasts	Tough and flexible leathery solids	$T > T_g$ ($T < T_m$)	0	Intermediate	Cross-linked polyethylene
V. Duroplasts	Hard and stiff solids	$T < T_g$	0	0	Polystyrene
	Hard and tough, stiff solids	$T < T_m$	Intermediate to high	0	Poly(4-methyl pentene-1)
VI. Duroelasts	Hard solids	$T < T_g$	0	Intermediate to high	Phenolic resin

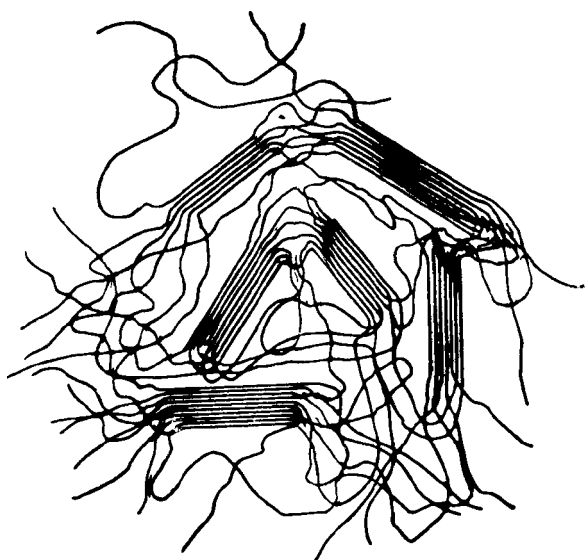


FIG. 2.10 Diagrammatic representation of the fringed micelle model.

exactly analogous to those in metals and low-molecular crystals have been found in these polymeric single crystals.

A second important event was the development by Hosemann (1950) of a theory by which the X-ray patterns are explained in a completely different way, namely, in terms of statistical disorder. In this concept, the *paracrystallinity model* (Fig. 2.11), the so-called amorphous regions appear to be the same as small defect sites. A randomised amorphous phase is not required to explain polymer behaviour. Several phenomena, such as creep, recrystallisation and fracture, are better explained by motions of dislocations (as in solid state physics) than by the traditional fringed micelle model.

These two insights, viz. lamellar, perfectly ordered structures – composed of folded chain molecules – and paracrystallinity, were of preponderant importance in the concept of polymer morphology.

In most solid crystalline polymers spherical aggregates of crystalline material, called *spherulites*, are recognised by their characteristic appearance under the polarising microscope. Electron microscopy of fracture surfaces in spherulites has shown that here, too, lamellar structures persist throughout the body of the spherulites. The latter seem to be the normal results of crystal growth in which the spherulites originating from a nucleus (often a foreign particle) grow at the expense of the non-crystalline melt.

In the present concept of the structure of crystalline polymers there is only room for the fringed micelle model when polymers of low crystallinity are concerned. For polymers of intermediate degrees of crystallinity, a structure involving “paracrystals” and discrete amorphous regions seems probable. For highly crystalline polymers there is no experimental evidence whatsoever of the existence of discrete amorphous regions. Here the fringed micelle model has to be rejected, whereas the paracrystallinity model is acceptable.

It is now generally accepted that the morphology of a polymer depends on the contributions of three different macro-conformations: (a) the random coil or irregularly folded molecule as found in the glassy state, (b) the folded chain, as found in lamellar structures and (c) the extended chain. The fringed micelle (d) may be seen as mixture of (a), (b) and (c) (see Fig. 2.12) with paracrystallinity as an extreme.

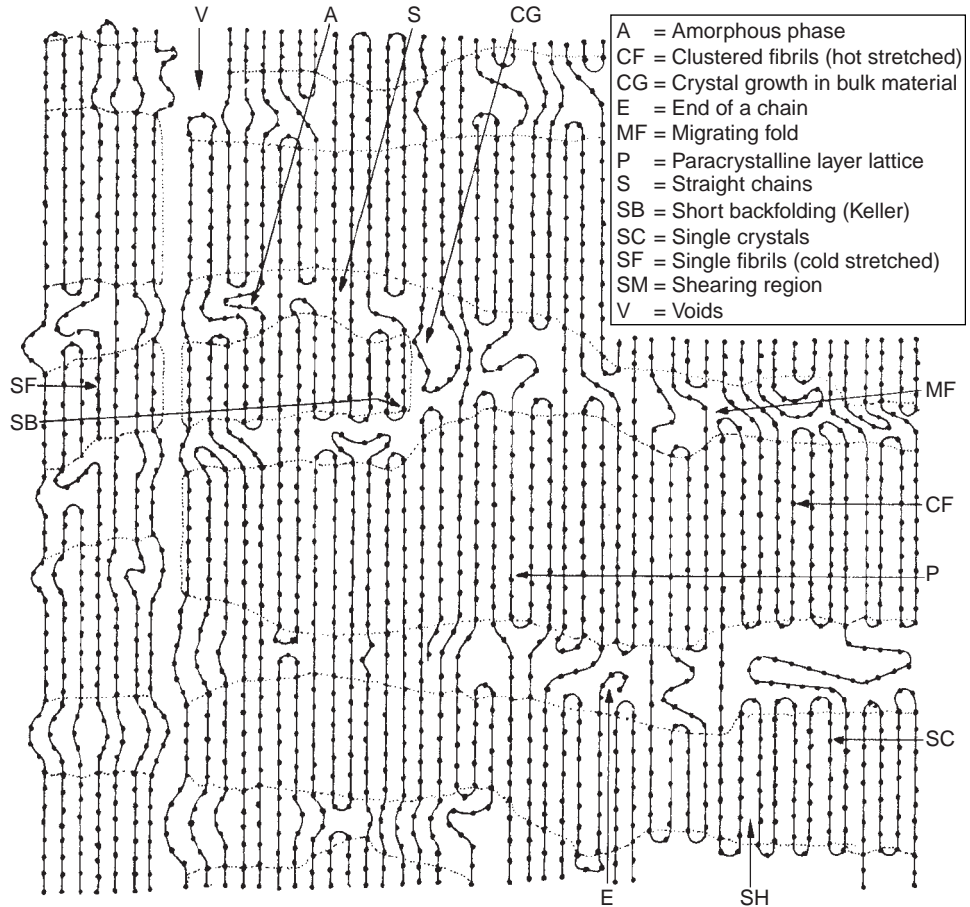


FIG. 2.11 Diagrammatic representation of the paracrystallinity model (after Hosemann, 1962).

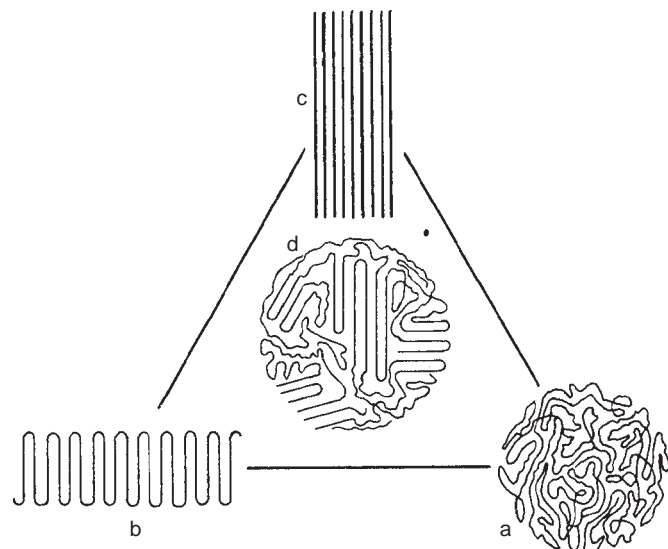


FIG. 2.12 Schematic drawing of the different macro-conformations possible in solid linear macromolecules. (a) Random, glassy; (b) folded chain, lamellar; (c) extended chain equilibrium: (d) fringed micelle, mixture of (a) to (c) (after Wunderlich, 1970).

2.5.1. The amorphous phase in semi-crystalline polymers

In the 1970s a model for semi-crystalline polymers was presented by Struik (1978); it is reproduced here as Fig. 2.13. The main feature of this model is that the crystalline regions disturb the amorphous phase and reduce its segmental mobility. This reduction is at its maximum in the immediate vicinity of the crystallites; at large distances from the crystallites will the properties of the amorphous phase become equal to those of the bulk amorphous material. This model is similar to that of filled rubbers in which the carbon black particles restrict the mobility of parts of the rubbery phase (Smith, 1966).

The main consequence of this reduced mobility is an extension of the glass transition region towards the high temperature side; it will show a lower and an upper value, viz. $T_g(L)$ and $T_g(U)$, the values of the undisturbed amorphous region and that of regions with reduced mobility. By means of this model, Struik could interpret his measurements on volume relaxation (physical ageing) and creep in semi-crystalline materials.

2.5.2. The composite structure of fibres in the oriented state

A few words have to be said about the concept of the composite structure of fibrous material in the oriented state. The basic element in this concept (Peterlin, 1971) is the *micro-fibril*, a very long (some μm) and thin (10–20 nm) structure composed of alternating amorphous layers and crystalline blocks (see Fig. 2.14). The micro-fibrils are formed during the orientation process (mainly in the “necking” zones); the stacked lamellae of the starting material are transformed into densely packed and aligned *bundles* of micro-fibrils, the *fibrils*. During the further phases of the drawing operation the fibrils may be sheared and axially displaced. The shearing of the fibrils displaces the micro-fibrils in the fibre direction and enormously extends the inter-fibrillar tie molecules by some chain unfolding without substantial change of the micro-fibrillar structure. Thus this enhanced volume fraction of *taut tie molecules* connecting the micro-fibrils is responsible for the strength and modulus of the fibrils, in the same way as the *intra-fibrillar tie molecules* between subsequent crystal blocks are responsible for the strength and modulus of the micro-fibril.

There is evidence that by a heat treatment both the crystalline and amorphous regions grow in length and in width, thus forming a definite two-phase system. On the other hand, in cold drawing at high draw ratios the regions become very small and approach the paracrystalline concept.

This picture also illustrates the mechanical behaviour of semi-crystalline polymers and the role of the small percentage of *tie molecules* (see Fig. 2.15).

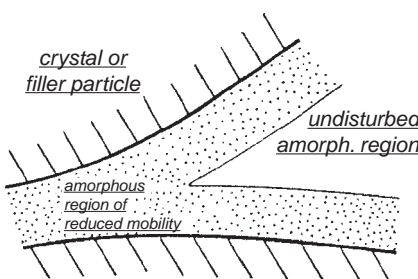


FIG. 2.13 Extended glass transition in semi-crystalline polymers (reproduced from Struik, 1978).

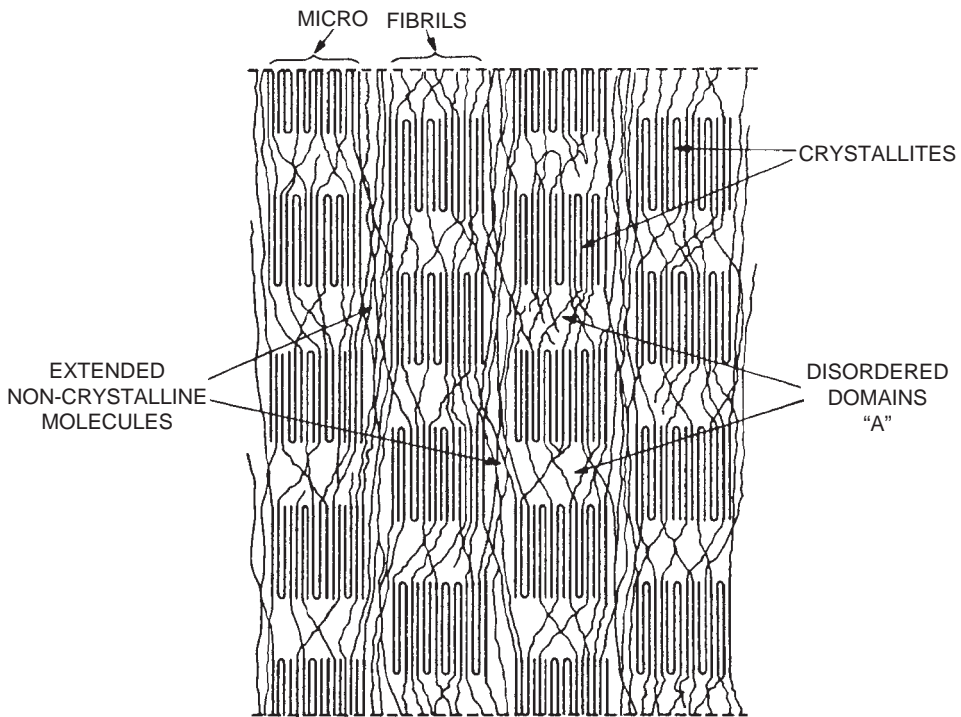


FIG. 2.14 Structural model of a drawn polyester fibre, fibre axis vertical (after Prevorsek and Kwon, 1976; by permission of Marcel Dekker, Inc.).

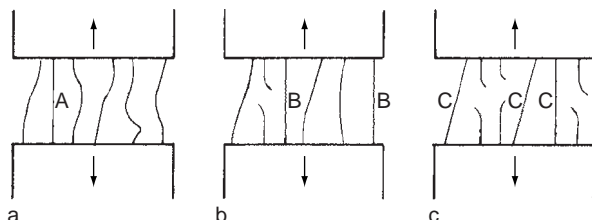


FIG. 2.15 Tie molecules in the “amorphous” layer between subsequent crystal blocks of the micro-fibril. At low strain (a) a single tie molecule (A), at medium strain (b) two tie molecules (B), and at the highest strain (e) three molecules (C) are stretched up to the rupture point (after Peterlin, 1971).

2.6. POLYMERIC LIQUID CRYSTALS

A relatively recent field in polymer science and technology is that of the polymeric liquid crystals. Low molecular liquid crystals have been known for a long time already: they were discovered almost simultaneously by Reinitzer (1888) and Lehmann (1889). These molecules melt in steps, the so-called *mesophases* (phases between the solid crystalline and the isotropic liquid states). All these molecules possess rigid molecular segments, the “*mesogenic*” groups, which is the reason that these molecules may show spontaneous orientation. Thus the melt shows a pronounced anisotropy and one or more thermodynamic phase transitions of the first order.

Different types of mesophases can be distinguished: *nematic* (from Greek “nèma”, thread) with order in one direction; *smectic* (from Greek “smegma”, soap) with a molecular arrangement in layers, so order in two directions; *chiral* or *cholesteric*, with a rotating order (from “kheir”, hand, and from “khōlē” and “stereos”: bile and firm); and a fourth category: the *discotic* with piles of disclike molecules. Fig. 2.16 gives a schematic representation of some of the more than 35 liquid crystalline mesophases (see also Chap. 15).

If monomeric liquid crystals are polymerised, the polymers also show in many cases the liquid-crystalline effects. In addition, their viscosity during flow is unexpectedly low in the anisotropic phase state.

There is no consensus yet as far as the name of these materials is concerned. Some investigators use the name *polymer(ic) liquid crystals* (PLCs), others call them *liquid crystalline polymers* (LCPs) or *mesogenic macromolecules*.

PLCs, which melt without decomposition, are called *thermotropic*; those who decompose on heating before melting but can be dissolved in liquids, are called *lyotropic*.

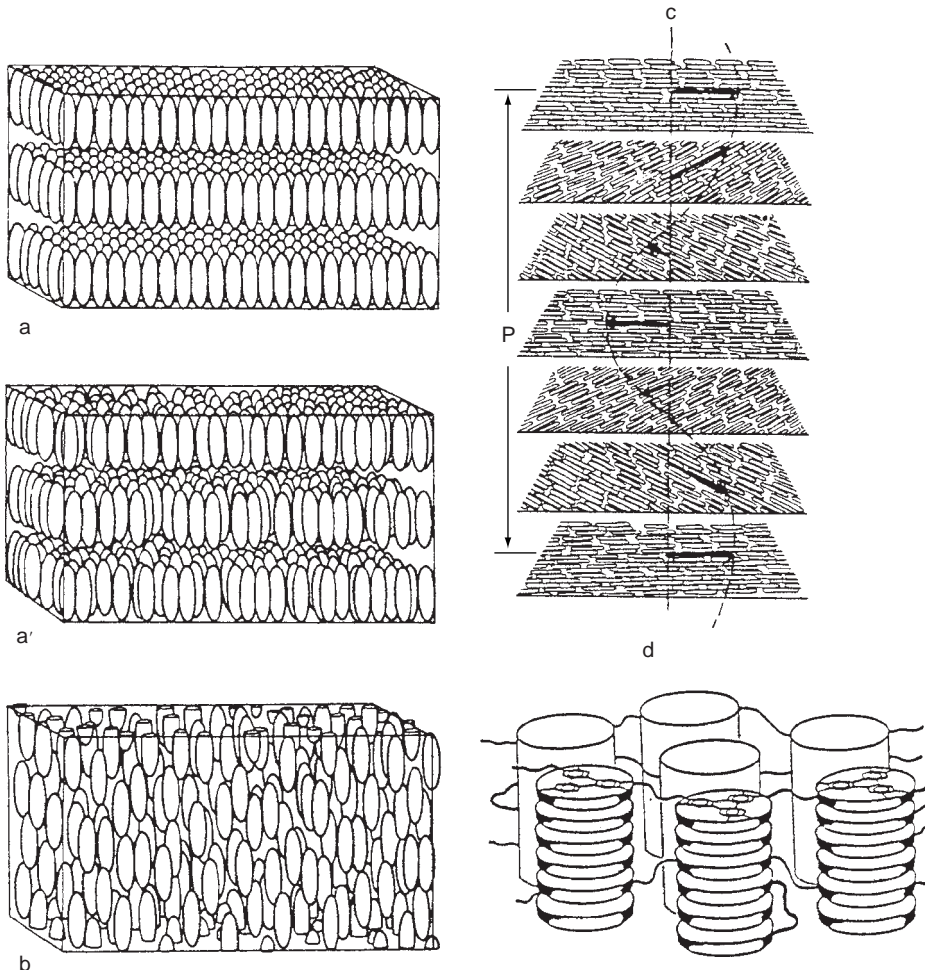
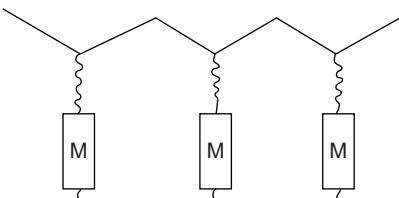
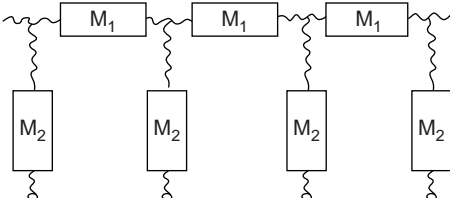


FIG. 2.16 Schematic representation of the four main types of mesophases. Smectic with ordered (a) and unordered (a') arrangement of the molecules in layers; b) nematic; c) cholesteric and d) discotic (from Platé and Shibaev (1987); Courtesy Plenum Press).

SCHEME 2.1 Classification of polymeric liquid crystals^a

Classes of polymeric liquid crystals	General chemical structure of the molecule	Physical behaviour
Mesogenic groups in Main Chain		Thermotropic (e.g. arylates) or lyotropic (e.g. aramids)
Mesogenic groups in SIDE Chains		Usually thermotropic
Mesogenic groups both in Main and Side chains		Usually lyotropic

^a Based on schemes of Finkelmann (1982) and Ringsdorf (1981).

Finally there exists a structural classification on the basis of the position of the mesogenic groups; these may be found *in the main chain*, *in the side chain* or in *both*. Scheme 2.1 gives a representation of this classification. A more elaborate classification was developed by Brostow (1988). A full description of structures and textures of the most important LC phases is given by Demus and Richter (1980). Smectic phases are treated by Gray and Goodby (1984) and discotic phases by Demus (1994). Excellent reviews concerning structure–property–application relations of low and high molecular weight LC materials are presented by Meier et al. (1975), by Prasad and Williams (1991) and by McArdle (1989).

2.7. MULTIPLE COMPONENT POLYMER SYSTEMS

Polymeric materials consisting of more than one component are produced in even larger quantities and their practical importance increases. These materials are usually stronger and/or tougher than one-component systems. In the field of metallurgy this fact has been known for centuries already: metal alloys are often as old as metals themselves. For polymers the same empirical fact proved to be true.

One can distinguish between real *more-component polymeric systems* (Class A), which do not contain anything else than polymeric materials, and *polymer-based systems* (Class B) in which isotropic polymeric materials are present together with either non-polymeric components or with already preformed oriented polymeric components (fibres or filaments).

One can also make a distinction based on the *nature of the blend* of the components. This may be (1) *homogeneous* on a molecular or a microscopic scale or (2) *heterogeneous* on a macroscopic and/or microscopic scale.

SCHEME 2.2 Classification of multiple component polymer systems (based on a less elaborate scheme of Platzer, 1971)

Classes	Subclasses	Subgroups	
		Homogeneous (molecular/micro-scale)	Heterogeneous (micro/macro-scale)
A <i>Multiple component polymeric materials (no other than polymeric components)</i>	A1 <i>Intramolecular blends or copolymers (alternating, random, block-, graft-, network-or cross linked)</i>	A11 <i>(Co)polymers with rigid segments or polymeric liquid crystals (self-reinforcing)</i>	A12 <i>Block-copolymers with large difference in T_g between components Thermoplastic elastomers</i>
	A2 <i>Intermolecular blends or polymer alloys</i>	A21 <i>Homogeneous polymer alloys molecular composites (if one component rigid)</i>	A22 <i>Heterogeneous polymer alloys, e.g. impact resistant materials (rubber particles!)</i>
B <i>Polymer-based systems (often containing non-polymeric components)</i>	B1 <i>Polymers with non-polymeric added materials (functional composites)</i>	B11 <i>Plasticized polymers (containing compatible solvent, e.g. plasticized PVC)</i>	B12 <i>Filled polymers Fillers: carbon black, silica, talc, ZnO</i>
	B2 <i>Reinforced polymers (structural composites)</i>	B21 <i>Blends of polymer with compatible antiplasticizer</i>	B22 <i>Fibre-reinforced Polymer systems (fibre or filament: carbon, glass, steel, textile)</i>

Scheme 2.2 gives an elaborate classification of the multicomponent polymer systems. Basically this scheme is an extension of the more restricted classification given by Platzer (1971).

Scheme 2.2 requires some explanation.

Class A is subdivided into two subclasses: the *intramolecular blends* or *copolymers* (A1) and the *intermolecular blends* (A2) or *Polymeric Alloys*. Both subclasses can be subdivided again on the basis of homogeneity or heterogeneity.

Subclass A1 obtains the so-called *self-reinforcing* polymers viz. the polymeric liquid crystals (reinforcement by orientation in the mesophase followed by quenching below the solidification temperature). Subgroup A12 contains the *thermoplastic elastomers*, block copolymers in which the segments have very different T_g values, giving the possibility of intermolecular segregation and formation of physical networks.

Subgroup A21 are the really homogeneous alloys, in which the components are fully compatible. True compatibility is relatively rare; more often we have quasi- or partial

compatibility. Examples of compatibility are the systems: poly(vinylidene fluoride) with poly(methyl methacrylate); poly(vinylidene fluoride) with poly(ethyl methacrylate); and poly(2,6-dimethylphenylene oxide) with polystyrene. If the blend consists of a compatible rigid component, dispersed with a flexible one at the molecular level, the system is called a *molecular composite* (which must well be distinguished from the traditional composites!). The heterogeneous polymeric alloys form subgroup A22. To this subgroup belong the *impact-resistant polymer systems* (rubber particles in amorphous matrix; however, these may also be based on copolymerisation with dienes).

Polymers blended with non-polymeric additives form subclass B1. It can be distinguished into subgroup B11, the *plasticized or "soft"* PVC and subgroup B12, the *filled polymers*, with fillers such as carbon black, silica, zinc oxide, etc. A filler usually is cheaper than the polymeric main component; it can constitute as much as 40% by weight of the material. Other additives, such as pigments, accelerators, hardeners, stabilisers, flame-retardants, lubricating agents, etc. are used in much lower concentrations (*functional composites*).

Subclass B2 is formed by the so-called *structural composites*, in which an outspoken mechanical reinforcement is given to the polymer. Subgroup B21 consists of blends of polymers with compatible anti-plasticizers; subgroups B22 are the most important: the *fibre-reinforced polymer systems*. The two components, the polymer matrix and the reinforcing fibbers or filaments (glass, ceramic, steel, textile, etc.) perform different functions: the fibrous material carries the load, while the matrix distributes the load; the fibbers act as crack stoppers, the matrix as impact-energy absorber and reinforcement connector. Interfacial bonding is the crucial problem.

The gap between pure polymers and multicomponent polymer systems is not as large as it looks.

In some respects semi-crystalline polymers are similar to filled reinforced systems (crystallites, embedded in amorphous matrix); in the same way highly oriented semi-crystalline polymers are similar to fiber-reinforced systems (micro-fibrils embedded in amorphous matrix).

So paracrystalline polymers are nearly identical with liquid-crystalline polymers, filled with amorphous defect domains. And network polymers or copolymers may be compared with filled materials, cross links playing the same role as sub microscopic filler particles.

It is understandable that the properties of these multicomponent polymer systems are related to those of the homopolymers in a very complex way. In some case, e.g. in random copolymers and homogeneously filled polymer systems, additivity is found for certain properties.

2.8. RELAXATION PHENOMENA

In all non-equilibrium systems relaxation phenomena can be observed. *Relaxation is the time-dependent return to equilibrium (or to a new equilibrium) after a disturbance.*

Relaxation processes are universal. They are found in all branches of physics: mechanical relaxation (stress and strain relaxation, creep), ultrasonic relaxation, dielectric relaxation, luminescence depolarisation, electronic relaxation (fluorescence), etc. Also the chemical reaction might be classified under the relaxation phenomena. It will be readily understood that especially in polymer science this time-dependent behaviour is of particular importance.

The relaxation process is characterised by a driving force and by a rate constant. The driving force is always connected with the surplus of free energy in the non-equilibrium

state. Sometimes the rate is directly proportional to the driving force; in this case the rate process is a first order process (cf. the first order chemical reaction). The reciprocal value of the rate constant is called *relaxation time*, τ .

If P is the driving force, one gets:

$$-\frac{dP}{dt} = \frac{P}{\tau} \quad (2.4)$$

which after integration gives:

$$P(t) = P_0 \exp(-t/\tau) \quad (2.5)$$

The equation shows that relaxation is strong if $t \geq \tau$, whereas practically no relaxation takes place if $t < \tau$. The relaxation time is temperature dependent; it is an exponential function of temperature:

$$\tau = \tau_0 \exp(E_{act}/RT) \quad (2.6)$$

The ratio relaxation time/observation time = τ/t is called the *Deborah number*. It is zero for ideal fluids and infinite for ideal solids.

Frequently, however, relaxation is not a first order process. In that case

$$\frac{P(t)}{P_0} = f(t) \quad (2.7)$$

Often $f(t)$ is approximated by the summation $\sum C_i \exp(-t/\tau_i)$ in which the combination of τ_i -values is called the relaxation time spectrum.

Sometimes the deviation from the equilibrium state is a periodical or cyclic process. If the latter is of the sinusoidal type,

$$P(t) = P_0 \sin(\omega t) \quad (2.8)$$

where ω is the angular frequency, the response R to the driving force P will be:

$$R(t) = R_0 \sin(\omega t - \delta) \quad (2.9)$$

δ is the so-called loss angle, it is defined as the angle over which the response lags behind the driving force due to energy loss. If P is a stress, the response R will be a strain; if P is an electric field strength, R will be the dielectric displacement, etc.

Using the "complex notation", this situation can be described by the equation:

$$P^* = P_0 \exp(i\omega t) \quad (2.10)$$

$$R^* = R_0 \exp[i(\omega t - \delta)] \quad (2.11)$$

So

$$\frac{P^*}{R^*} = \frac{P_0}{R_0} \exp(i\delta) = \frac{P_0}{R_0} (\cos \delta + i \sin \delta) \quad (2.12)$$

If $P/R = S$, where S is the response coefficient

$$S^* = S_0 (\cos \delta + i \sin \delta) = S' + iS'' \quad (2.13)$$

where S^* = the complex response coefficient;

$S' = S_0 \cos \delta$ = real component or storage component;

$S'' = S_0 \sin \delta$ = imaginary component or loss component.

Furthermore it is obvious that:

$$\frac{S''}{S'} = \tan \delta \quad (2.14)$$

$$|S^*| = S_0 = [(S')^2 + (S'')^2]^{1/2} \quad (2.15)$$

From the above equations, one can derive for a system with only one relaxation time τ

$$S'(\omega) = S_0 \frac{\omega^2 \tau^2}{1 + \omega^2 \tau^2} \quad \text{and} \quad S''(\omega) = S_0 \frac{\omega \tau}{1 + \omega^2 \tau^2} \quad (2.16)$$

It follows that S'' shows a maximum when $\omega = 1/\tau$. In general, but not always, $\tan \delta$ shows a maximum, as a function of frequency, which in many cases practically coincides with that of S'' .

Between the static (time-dependent) and the dynamic (frequency-dependent) behaviour the following correlation exists:

$$\tan \delta = \frac{S''}{S'} \approx \frac{\pi}{2} \left(\frac{d \ln R}{d \ln t} \right) \approx -\frac{\pi}{2} \left(\frac{d \ln P}{d \ln t} \right) \quad (2.17)$$

Very important phenomena in polymer behaviour, such as viscoelasticity, stress, strain, volume and enthalpy relaxation, ageing, etc., are characterised by time-dependence of the polymer properties.

APPENDIX I

Milestones in the history of polymer science (Morawetz, 1985, Percec, 2001, Hawker and Wooley, 2005)

1516	Discovery of ca-hu-chu, natural rubber during the second journey of Columbus to the Americas
1769	Development of the first application of ca-hu-chu into a "rubber" by Priestley in the UK
1832	Berzelius coins the term <i>polymer</i> for any compound with a molecular weight that is a multiple of the MW of another compound with the same composition
1839	Discovery of vulcanisation of Natural Rubber with sulphur by Goodyear
1860–1880	Bouchardat's work on natural rubber; he demonstrates the thermal depolymerisation to isoprene and the reverse polymerisation of isoprene
1862	Definitive report on Polyaniline (PANI), but at that time not recognised as a conducting polymer
1863	Berthelot coins the terms <i>dimer</i> , <i>trimer</i> , <i>tetramer</i> , etc.
1872	Von Bayer discovers the acid-catalysed condensation of phenol with formaldehyde
1880–1900	The great inventions of the first man-made fibres by chemical manipulation of natural materials has a great impact on the interest in their chemical nature (1883 De Chardonnet: nitrocellulose)
1890	Frémery and Urban: "copper cellulose"; 1892 Cross and Bevan: viscose process, regenerated cellulose; 1894 Cross and Bevan: cellulose acetate.)
1889	Brown demonstrates the very high "molecular weights" of starch (20,000–30,000 g/mol) by means of cryoscopy

1907	Emil Fischer synthesises polypeptide chains containing as many as 18 amino acid residues
1900–1930	Profound controversial disputes on the nature of polymers: colloidal associates (“micelles”) or giant molecules
1907	Hofmann starts his work on synthetic rubber
1910	Baekeland makes the first synthetic industrial plastic (Bakelite)
1913	X-ray diffraction shows cotton, silk and asbestos to be crystalline products (Nishikawa and Ono, later confirmed by Herzog and Polanyi, 1920)
1913	X-ray diffraction shows cotton, silk and asbestos to be crystalline products (Nishikawa and Ono, later confirmed by Herzog and Polanyi, 1920)
1914–1918	Production of “methyl-rubber” on commercial scale in Germany due to lack of natural rubber during World War I
1920	Staudinger starts his epoch-making work on polymers; he coins the term macromolecule
1925	Svedberg proves unambiguously the existence of macromolecules by means of the ultracentrifuge; he also develops the first precise method for obtaining the molecular weight distribution
1925	Katz demonstrates by X-ray diffraction that natural rubber is amorphous in the relaxed state and crystalline upon stretching
1928	Meyer and Mark show that the crystallographic and the chemical evidence for the chain concept are in agreement
1930	Hermann’s concept of “fringed micelles” formulated (chain molecules pass through crystalline and amorphous regions)
1930	First study of co-polymerisation by Wagner-Jauregg
1930–1936	Early theories of rubber-elasticity (Mark, Meyer, Guth, Kuhn and others)
1930–1937.	Carothers’ famous work proves by means of organic synthesis that polymers are giant, stable molecules. He first proves it by the discovery of neoprene (polychloro-butadiene), then by the condensation polymerisation of amino acids and esters. As a consequence the first fully synthetic textile fibre, nylon, is developed. In Carothers’ group Flory elucidates the mechanisms of radical and condensation polymerisation
1930–1940	Development of polybutadiene, polychloroprene and especially copolymers of butadiene and styrene, as best replacements for natural rubber for tire-applications. Sodium used as catalyst
1934	Ring-opening polycondensation of caprolactam discovered by Schlack
1938/40	Formulation of the well-known Mark–Houwink equation for the viscometric determination of the molecular weight (mass)
1939–1943	Redox- and photo-initiation of free radical polymerisation found (Melville, Logemann, Kern, et al.)
1941	Roche discovers polycondensation of siloxanes
1942	Formulation of the thermodynamics and statistics of the polymer chain in dilute solution by Flory and Huggins
1942–1947	Further development of the theory of rubber elasticity (based on networks) by Flory, James, Guth, et al.
1943	Otto Bayer discovers the polyaddition synthesis of polyurethanes and proves that some form of cross linking is necessary for reversible elasticity
1944	Introduction of two very important physical techniques in polymer science, <i>viz.</i> Light Scattering for molecular weight determination (by Debye) and Infra-red Spectroscopy for structural analysis (by Thompson)

1947	Alfrey and Price develop a semi-quantitative theory of "reactivity-ratios" in co-polymerisation
1948	Theory of <i>emulsion polymerisation</i> developed by Harkins and by Smith and Ewart
1950	Further development of the theory of polymer solutions by Flory and Krigbaum
1951	Sanger develops his <i>sequence analysis</i> for amino acids in proteins
1953	Nobel Prize Chemistry to Hermann Staudinger for contributions to the understanding of macromolecular chemistry
1953	Watson and Crick discover the double <i>helix conformation</i> of DNA, the break-through in bio-polymer science
1953	Synthesis of linear polyethylene and <i>coordinate polymerisation</i> (combination of trialkyl aluminium and titanium chloride as catalyst) by Ziegler
1954	<i>Isotactic and syndiotactic polymerisation</i> (polypropylene and polydienes) discovered by Natta
1955	Williams, Landel and Ferry introduce their famous WLF-equation for describing the temperature dependence of relaxation times as a universal function of T and T_g
1955	<i>Interfacial polycondensation</i> discovered (Morgan)
1956	Szwarc discovers the <i>living polymers</i> by <i>anionic polymerisation</i>
1957	Theory of <i>paracrystallinity</i> developed by Hosemann
1957	Discovery of <i>single crystals</i> of polymers and of <i>folding of chain molecules</i> , leading to a revision of the concept of semi-crystallinity (Keller)
1959–1965	Introduction of <i>new techniques of instrumental analysis</i>
1959	<i>Gel-permeation</i> or Size-exclusion Chromatography (Moore)
1959	<i>Magnetic resonance</i> techniques (ESR and NMR)
1959	<i>Thermo gravimetric analysis</i>
1960	<i>Differential thermal analysis</i>
1960	Discovery of thermoplastic elastomers by block-copolymerisation (rubbery blocks flanked by glassy or crystalline blocks in one chain)
1961	Discovery of <i>oxidative coupling</i> of phenols (Hay)
1963	Nobel Prize Chemistry to Karl Ziegler and Giulio Natta for their discoveries in the field of the chemistry and technology of high polymers (Ziegler–Natta catalysis)
1963	First report on a conducting polymer, viz oxidised iodine doped polypyrrole by D.E. Weiss et al., a polyacetylene derivative
1969–1983	Development of Thermoplastic Vulcanizates, a new class of thermoplastic elastomers by Gessler, Fisher, Coran and Patel.
1970–1985	Development of heat resistant matrix polymers for composites (aromatic polysulphides, -ether ketones, -sulphones and -imides) and of high strength reinforcing polymers (arylates, ther-motropic liquid crystalline polymers)
1970–1985	Further development of sophisticated techniques for instrumental analysis and characterisation (Fourier Transformed IR Spectroscopy; Dynamic Light Scattering; Fourier Transformed NMR Spectroscopy with Cross Polarisation and Magic Angle Spinning; Secondary Ion Mass Spectroscopy; Neutron Scattering Spectroscopy; etc.)
1970–1980	De Gennes' <i>scaling concepts</i> for polymer solutions and melts and the concept of <i>reptation</i> movement of polymer chains in melts
1970–1980	Pennings' discovery of <i>chain extension</i> and <i>shish-kebab</i> formation in stirred solutions of very high MW polyethylene; this eventually led to the ultra-high modulus gel-spinning process of polyethylene

- 1971 Introduction of ring-opening metathesis as a versatile polymerisation technique (ROMP) by Chauvin and Hérisson
- 1974 Nobel Prize Chemistry to Paul J. Flory for his fundamental achievements, both theoretical and experimental, in the physical chemistry of the macromolecules
- 1974 Fully aromatic polyamides developed: Aramids, being lyotropic liquid crystalline polymers of high strength, due to extended molecular chains (Morgan and Kwolek)
- 1978 Introduction of Dendrimers and Hyperbranched Polymers by, e.g. Vögtle, Tomalia and Newkome
- 1982 Discovery of the *group transfer polymerisation* of acrylates, initiated by a complex (trimethylsilylketene acetal); it has the same characteristics as the Ziegler–Natta polymerisation: the polymer “grows like a hair from its root” (the complex) and the polymer has a “living” character with narrow molecular weight distribution; control of end groups- and thus of chain length- is a built-in advantage (Webster)
- 1983 Development of metallocene catalysed polymerisation (Kaminsky)
- 1984 Polyolefin ketone synthesis (the alternating copolymer of ethylene and carbon monoxide; E. Drenth, Shell) later marketed as Carilon by Shell and BP
- 1990 First commercial use of PA6/clay nano-composites for timing belt covers by Toyota, Japan
- 1991 Nobel Prize Physics to Pierre-Gillis de Gennes for discovering that methods developed for studying order phenomena in simple systems can be generalised to more complex forms of matter, in particular to liquid crystals and polymers
- 1991 Report of graphitic carbon nano-tubes by Sumio Iijima of NEC (SWCNT had been reported earlier but remained unnoticed at the time)
- 1992 Synthesis of M5 (PIPD) by Sikkema and Lishinsky (Akzo-Nobel); a fibre was produced in 1993
- 1992 Introduction of supramolecular polymers by Lehn
- 1993 Introduction by Michelin et Cie. of the “Green Tyre”, with a silica-reinforced tread, rather than with carbon black, and using solution-polymerised rather than emulsion-polymerised SBR, for 30% reduced rolling resistance and corresponding energy saving
- 1994/1995 Development of ATRP (Atom Transfer Radical Polymerisation) by Wang, Matyjaszewski and Sawamoto
- 1997 Realisation of synthesis supramolecular polymers with useful material properties by E.W. Meijer and R.P. Sijbesma
- 1998 Development of Radical Addition-Fragmentation Chain Transfer (RAFT) by the Australian Commonwealth Scientific and Industrial Research Organisation (CSIRO)
- 1998 Marketing of Zylon (PBO) fibre by Toyoba
- 2000 Nobel Prize Chemistry to Alan J. Heeger, Alan G. MacDiarmid and Hideki Shirakawa for their discovery and development of conductive polymers (i.e. electro-luminescent conjugated polymers)
- 2002 Melt processable PTFE reported by P. Smith

Nobel prizes related to polymers

- 1953 (Chemistry) Hermann Staudinger for contribution to the understanding of macromolecular chemistry
- 1963 (Chemistry) Karl Ziegler and Giulio Natta for contributions in polymer synthesis (Ziegler–Natta catalysis)

1974	(Chemistry) Paul J. Flory for contributions to theoretical polymer chemistry
1991	(Physics) Pierre-Gillis de Gennes for discovering that methods developed for studying order phenomena in simple systems can be generalised to more complex forms of matter, in particular to liquid crystals and polymers
2000	(Chemistry) to Alan J. Heeger, Alan G. MacDiarmid and Hideki Shirakawa for the discovery and development of conductive polymers

APPENDIX II

Chronological development of commercial polymers

Date	Material
1839/44	Vulcanisation of rubber
1846	Nitration of cellulose
1851	Ebonite (hard rubber)
1868	Celluloid (plasticized cellulose nitrate)
1889	Regenerated cellulosic fibbers
1889	Cellulose nitrate photographic films
1890	Cuprammonia rayon fibres
1892	Viscose rayon fibres
1907	Phenol-formaldehyde resins
1907	Cellulose acetate solutions
1908	Cellulose acetate photographic films
1912	Regenerated cellulose sheet (cellophane)
1923	Cellulose nitrate automobile lacquers
1924	Cellulose acetate fibres
1926	Alkyd polyester
1927	Poly(vinyl chloride) sheets (PVC) wall covering
1927	Cellulose acetate sheet and rods
1929	Polysulfide synthetic elastomer
1929	Urea-formaldehyde resins
1931	Poly(methyl methacrylate) plastics (PMMA)
1931	Polychloroprene elastomer (Neoprene)
1935	Ethylcellulose
1936	Poly(vinyl acetate)
1936	Polyvinyl butyral safety glass
1937	Polystyrene
1937	Styrene–butadiene (Buna-S) and styrene–acrylonitrile (Buna-N) copolymer elastomers
1938	Nylon-66 fibres
1939	Melamine-formaldehyde resins
1940	Isobutylene-isoprene elastomers (butyl rubber)
1941	Low-density polyethylene
1942	Unsaturated polyesters
1943	Fluorocarbon resins (Teflon)
1943	Silicones

(continued)

Appendix II (continued)

Date	Material
1943	Polyurethanes
1943	Butyl rubber
1943	Nylon 6
1947	Epoxy resins
1948	Copolymers of acrylonitrile, butadiene and styrene (ABS)
1950	Polyester fibres
1950	Poly(acrylo nitrile) fibres
1955	Nylon 11
1956	Poly(oxy methylene) (acetals)
1957	High-density (linear) polyethylene
1957	Polypropylene
1957	Polycarbonate
1959	cis-Polybutadiene and polyisoprene elastomers
1960	Ethylene-propylene copolymer elastomers
1962	Polyimide resins
1964	Ionomers
1965	Poly(phenylene oxide)
1965	Polysulphones
1965	Styrene-butadiene block copolymers
1965	Polyester for injection moulding
1965	Nylon 12
1970	Poly(butylene terephthalate); Thermoplastic elastomers
1971	Poly(phenylene sulfide)
1974	Aramids – Aromatic polyamides
1974	Poly(arylether-sulphones)
1976	Aromatic Polyesters (Polyarylates)
1982	Poly(arylether-ketones)
1982	Poly(ether imides)
1983	Polybenzimidazoles
1984	Thermotropic liquid crystal polyesters
1984	Ethylene and carbon monoxide alternating copolymer (PECO)
1990	Polyethylene ultra-high molecular weight
1990	Nylon 4,6
1998	PBO fibre
1992–1993	PIPD fibre
2007	Nylon 4,T

BIBLIOGRAPHY**General references***A. Polymer structure*

Billmeyer FW, "Textbook of Polymer Science", Interscience, New York, 3rd Ed, 1984.

Corradini P, in "The Stereochemistry of Macromolecules" (Ketley AD, Ed), Marcel Dekker, New York, Vol 3, 1968.

Elias HG, "Makromoleküle", Hüthig & Wepf Verlag, Basel, 1971.

Flory PJ, "Principles of Polymer Chemistry", Cornell University Press, Ithaca, NY, 1953.

Staudinger H, "Die Hochmolekularen organischen Verbindungen", Springer, Berlin, 1932; "Arbeitserinnerungen", Hüttig Verlag, Heidelberg, 1961.

B. Molar mass distribution

- Altgelt KH and Segal L (Eds) "Gel Permeation Chromatography", Marcel Dekker, New York, 1971.
 Bark LS and Allen NS (Eds) "Analysis of Polymer Systems", Applied Science Publishers, London, 1982.
 Billingham NC "Molar Mass Measurements in Polymer Science", Halsted Press (Div. of Wiley), New York 1977.
 Chu B "Laser Light Scattering", Academic Press, Orlando, FL, 1974.
 Dawkins JV (Ed) "Developments in Polymer Characterization" 1-5. Elsevier Appl Science Publishers, Barking UK, 1986.
 Janca J (Ed) "Steric Exclusion Liquid Chromatography of Polymers" Marcel Dekker, New York, 1984.
 Peebles LH "Molecular Weight Distributions in Polymers", Wiley-Interscience, New York, 1971.
 Slade PE (Ed) "Polymer Molecular Weights", Marcel Dekker, New York, 1975.
 Tung LH (Ed) "Fractionation of Synthetic Polymers", Marcel Dekkers, New York, 1977.
 Yau WW, Kirkland JJ and Bly DD (Eds) "Modern Size Exclusion Chromatography", Wiley-Interscience, New York, 1979.

C/D. Phase transitions and morphology

- Haward RN (Ed), "The Physics of Glassy Polymers", Applied Science Publishers, London, 1973.
 Hearle JWS, in "Supramolecular Structures in Fibres" (Lindenmeyer PH, Ed), Interscience, New York, 1967, 215-251.
 Holzmüller W and Altenburg K, "Physik der Kunststoffe", Akademie Verlag, Berlin, 1961.
 Jenkins AD (Ed), "Polymer Science", North Holland, Amsterdam, 1972.
 Wunderlich B, "Macromolecular Physics", Academic Press, New York, 3 vols, 1980-1983.

E. Polymer liquid crystals

- Blumstein A (Ed), "Polymer Liquid Crystals", Plenum Press, New York, 1985.
 Ciferri A, Krigbaum WR and Meyer RB (Eds), "Polymer Liquid Crystals", Academic Press, New York, 1982.
 Demus D, "Phase Types, Structures and Chemistry of Liquid Crystals" in Stegemeyer H (Ed) "Liquid Crystals", Steinkopff Verlag, Darmstadt, 1994.
 Demus D and Richter L, "Textures of Liquid Crystals", Deutscher Verlag für Grundstoffsindustrie, Leipzig, 2nd Ed, 1980.
 Gordon M and Platé NA (Eds), "Liquid Crystal Polymers", Advanced Polymer Science, Springer, Berlin/New York, 1984, 59-61.
 Gray GW and Goodbye JWG, "Smectic Liquid Crystals", Leonard Hill, Glasgow, 1984.
 McArdle CB, "Side Chain Liquid Crystal Polymers", Blackie, Glasgow, 1989.
 Meier G, Sackmann E and Grabmaier JG, "Applications of Liquid Crystals", Springer, Berlin, 1975.
 Platé NA and Shibaev VP "Comb-Shaped Polymers and Liquid Crystals" Plenum Press, New York, 1987.
 Prasad PN and Williams DJ, "Introduction to Nonlinear Optical Effects in Molecules and Polymers", Wiley New York, 1991.

F. Multiple-component systems

- Platzer NAJ, "Multicomponent Polymer Systems", Advances in Chemistry Series No 99, American Chemical Society, Washington, 1971.
 Rodriguez F, "Principles of Polymer Systems", McGraw-Hill, New York, 1970.

G. Relaxation phenomena

- Holzmüller W and Altenburg K, "Physik der Kunststoffe", Akademie Verlag, Berlin, 1961.
 Struik L, "Physical Aging of Amorphous Polymers and other Materials", Elsevier, Amsterdam, 1978.
 Tobolski AV, "Properties and Structure of Polymers", Wiley, New York, 1960.

Special references

- Blagrove RJ, J Macromol Sci, (Revs) C 9(1) (1973) 71-90.
 Brostow W, Kunststoffe - German Plastics 78 (1988) 411; Polymer 31 (1990) 979.
 Burchard W, Chimia 39 (1985) 10-18.
 Chee KK and Rudin A, Trans Soc Rheol 18 (1974) 103.
 Chu BJ et al., Polymer 26 (1985) 1401, 1409.
 Collins EA and Metzger AP, Polym Eng Sci 10 (1970) 57.
 Cote JA and Shida MJ, J Appl Polym Sci 17 (1973) 1639.
 Cotton JP et al., Macromolecules 7 (1974) 863.
 Dunlop AN and Williams HL, J Appl Polym Sci 17 (1973) 2945.

- Finkelmann H, Chapter 2 in "Polymer Liquid Crystals", Ciferri A et al (Eds), see General references.
- Giddings JC, Separ Sci 1 (1966) 123; J Chromatogr 125 (1976) 3; Pure Appl Chem 51 (1979) 1459; Chem & Eng News, Oct 10 (1988) 34–45; Science 260 (1993) 1456.
- Giddings JC, Myers MN et al., J Chromatogr 142 (1977) 23; Anal Chem 59 (1987) 1957.
- Gloor WE, J Appl Polym Sci 19 (1975) 273; 22 (1978) 1177; 28 (1983) 795; Polymer 19 (1978) 984.
- Graessley WW and Segal, L, AIChE J 16 (1970) 261.
- Hawker CJ and Wooley KL, "The Convergence of Synthetic Organic and Polymer Chemistries"; Science 209 (2005) 1200.
- Hermann K, Gerngross O and Abitz W, Z physik Chem B 10 (1930) 371.
- Hosemann R, Z Physik 128 (1950) 1, 465; Polym 3 (1962) 349.
- Hosemann R and Bonart R, Kolloid-Z 152 (1957) 53.
- Huggins ML, Natta G, Desreux V and Mark H, J Polym Sci 56 (1962) 153.
- Keller A, Phil Mag (8) 2 (1957) 1171.
- Kirkland JJ and Yau WW Science 218 (1982) 121.
- Krause S, J Macromol Sci, Rev Macromol Chem, C7 (1972) 251.
- Lehmann O, Z phys Chem 4 (1889) 462.
- Leuchs O, "The Classifying of High Polymers", Butterworth, London, 1968.
- McGrew FC, J Chem Educ 35 (1958) 178.
- Mendelson RA, et al., J Polym Sci A-2, 8 (1970) 127.
- Mills NJ, Eur Polym J 5 (1969) 675.
- Morawetz H, "Polymers: the Origins and Growth of Science", Wiley, New York, 1985.
- Natta G et al., J Am Chem Soc 77 (1955) 1708.
- Natta G and Corradini P, J Polym Sci 20 (1956) 251; 39 (1959) 29.
- Percec V (Guest Editor) "Frontiers in Polymer Chemistry", Thematic Issue of Chemical Reviews 101 (2001) Issue 12.
- Peterlin A, J Phys Chem 75 (1971) 3921; J Polym Sci A-2, 7 (1969) 1151; IUPAC Symposium, Helsinki, 1972.
- Prevorsek DC and Kwon YD, J Macromol Sci, Phys B 12 (1976) 453.
- Ringsdorf H and Schneller A, Br Polym J 13 (1981) 43.
- Reinitzer F, Monatsh Chem 9 (1888) 421.
- Saeda S et al., J Appl Polym Sci 15 (1971) 277.
- Schiesinger W and Leeper HM, J Polym Sci 11 (1953) 203.
- Schimpff ME, Caldwell K and Giddings JC, "Field Flow Fractionation Handbook", Wiley New York, 2000.
- Shah BH and Darby R, Polym Eng Sci 16 (1976) 579.
- Smit PPA, Rheol Acta 5 (1966) 277.
- Staudinger H, Ber Deut Chem Ges 53 (1920) 1073.
- Struik LCE, Polymer 28 (1987) 1521 and 1534; Polymer 30 (1989) 799 and 815.
- Sun SF, "Physical Chemistry of Macromolecules", Wiley New York, 1994, 2nd Ed 2004.
- Thomas DP, Polym Eng Sci 11 (1971) 305.
- Van Krevelen DW, Goedhart DJ and Hoftyzer PJ, Polymer 18 (1977) 750.
- Wales JLS, Pure Appl Chem 20 (1969) 331.
- Wunderlich B, Ber Bunsenges 74 (1970) 772.

This page intentionally left blank

CHAPTER 3

Typology of Properties

3.1. THE CONCEPT “POLYMER PROPERTIES”

The properties of materials can always be divided into three distinct, though inseparable, categories: intrinsic properties, processing properties and product or article properties. Fig. 3.1 (Van Krevelen, 1967) gives a survey. It should be emphasised that these three categories of properties are strongly interrelated. Whereas intrinsic properties always refer to a *substance*, product properties refer to an *entity*; they also depend on size and

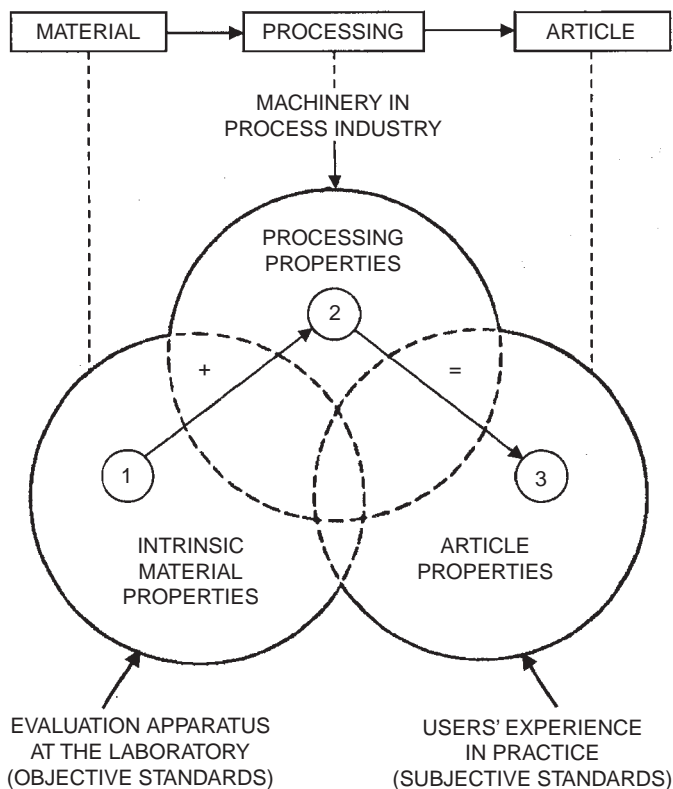


FIG. 3.1 The concept “property”.

shape. One speaks of the conductivity of iron (an intrinsic property) and of the conductance of an iron wire of a certain size (a product property). Processing properties occupy an intermediate position. Here, too, the "form factor" may have an influence.

The *intrinsic properties* lend themselves to almost exact reproducible measurement. The *Processing properties* are *combinations* of some intrinsic properties that determine the possibility of processing materials and the efficacy of this operation. During processing a number of properties are *added*, e.g. form and orientation. It is the combination of certain intrinsic properties and the added properties that constitutes the *product properties*.

A distinctive feature of polymeric materials is that the properties can be influenced decisively by the method of manufacturing and by processing. The sensitivity of polymers to processing conditions is much greater than that of other materials. This is because at a given chemical composition a polymeric material may show considerable differences in physical structure (e.g. orientation, degree and character of crystallinity). The physical structure is very much dependent on processing conditions. Moreover, both chemical composition and physical structure changes with time owing to degradation or relaxation processes.

3.1.1. Intrinsic properties

As the actual material properties are anchored in the chemical and physical structure of the material, all intrinsic properties relate to a material with a distinct processing history. Usually the change in chemical structure during processing is small compared with the change in physical structure.

This poses a typical problem for the determination of intrinsic properties. A specimen prepared for the testing of its mechanical properties, for instance, has gone through a number of processing stages during which the structure may have been altered. Yet it is possible to systematise the sample preparation and the methods of measuring in such a way that an impression is obtained of the intrinsic material properties as such, hence largely unaffected by influences.

3.1.2. Processing properties

Fig. 3.2 presents a survey of processing techniques based on rheological aspects. Practically all polymers are processed via a *melt* or a (rather concentrated) *solution*. In every processing technique four phases may be distinguished, which are often closely connected:

- *Transportation* of the material to the forming section of the processing machine (transport properties important)
- *Conditioning* (mostly by heating) of the material to the forming process (thermal properties important)
- *Forming* proper (rheological properties important)
- *Fixation* of the imposed shape (thermal and rheological properties and especially transfer properties, like thermal conductivity, rate of crystallisation, etc., are important)

In each of these phases the material is subject to changing temperatures, changing external and internal forces and varying retention times, all of which contribute to the ultimate structure. It is this fluctuating character of the conditions in processing which makes it so difficult to choose criteria for the processing properties.

In order to find answers to the problems of processability and to bridge the gap between research data (i.e. the behaviour expected) and the behaviour in practice, usually simulation experiments are carried out. As regards processing, the simulation experiment has to approach actual practice as closely as possible.

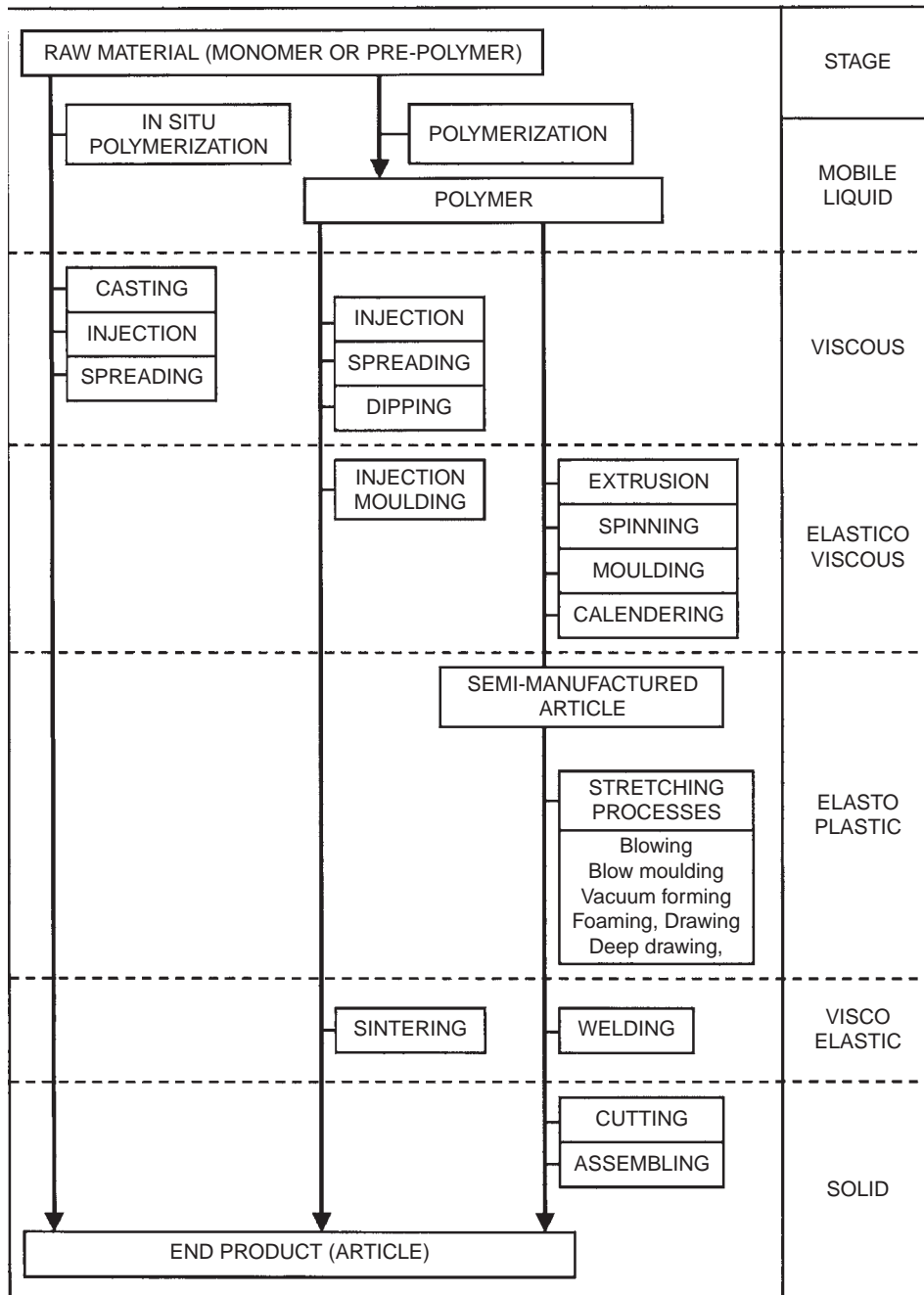


FIG. 3.2 Unit processes and operations.

3.1.3. Product (article) properties

For a product (article) “permanence” may be regarded as the most important aspect, whether this permanence relates to shape (dimensional stability), mechanical properties (tensile and impact strength, fatigue) or environment (resistance to ageing). Not enough is as yet known about the fundamental background of these permanence properties.

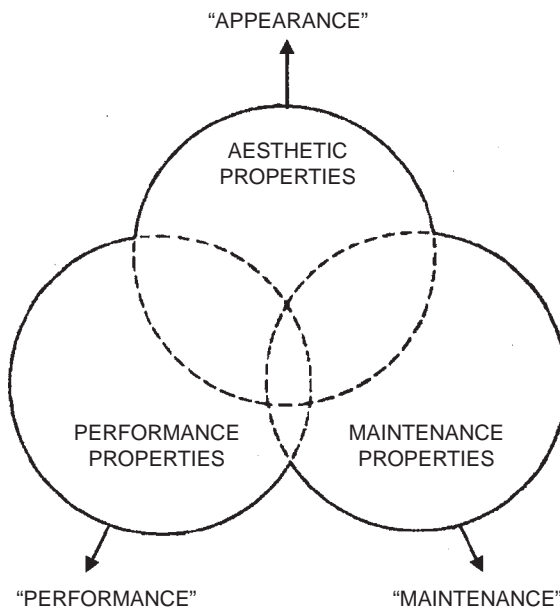


FIG. 3.3 The concept “article properties.”

The article (product) properties can be distinguished into three subgroups (Fig. 3.3):

- Aesthetic properties
- Performance properties
- Maintenance properties

Most of these are extremely subjective and depend on – often as yet unexplored – combinations of intrinsic and added properties. Nearly all the article (product) properties are connected with the *solid* polymeric state.

Since all the article properties depend on choice of materials, processing and application, it may be said that *there are no bad materials as such, but only bad articles (products)*.

Bad products result from the wrong choice of material, poor processing, wrong application and often poor design. What we ultimately need are methods of predicting use properties from intrinsic material properties and processing parameters. *In this book attention will mainly be paid to the intrinsic material properties of polymers.*

3.2. PHYSICAL QUANTITIES AND THEIR UNITS

A property can usually be expressed numerically by a physical quantity or by a combination or a function of physical quantities. The concept “physical quantity” was created by Maxwell (1873). Since then it has obtained a central position in the mathematical formalism of science and technology. In general one may write (Maxwell, 1873):

$$\text{Physical quantity} = \text{numerical value} \times \text{unit}$$

The unit of a physical quantity is in essence a reference quantity in which other quantities of the same kind can be expressed.

A well-organised system of units forms an essential part of the whole system of physical quantities and the equations by which they are interrelated. Many different unit systems have been in use, which has given rise to much confusion and trouble. Here we confine ourselves to two of these units systems.

Among scientists the so-called *dynamic or absolute system* of units has been widely used. It is founded on the three base quantities of mechanics: length, mass and time, with the corresponding units *centimetre*, *gram-mass* and *second*. The derived unit of force is called *dyne* ($= g \text{ cm s}^{-2}$), which is the force that gives the unit mass (g) a unit acceleration (1 cm s^{-2}); the derived unit of energy is called *erg* ($= \text{dyn cm} = g \text{ cm}^2 \text{ s}^{-2}$)¹. Physical and chemical thermodynamics required the introduction of two additional base quantities, viz. the temperature and the amount of substance; as corresponding base units the *Kelvin* (K) and the *gram-molecule* (mol) were introduced. Further complications arise if also the field of electricity is included in this unit system.

Nowadays the so-called *practical unit system* is in general used. It is a really coherent system, which means that no multiplication factors are introduced in the definition of derived units as soon as the base units have been defined. In 1969 this coherent system was recommended by the International Organisation for Standardisation as *International System of Units* (SI = Système International d'Unités) and in 1973 it was accepted as such, according to International Standard ISO 1000.

The International System of Units is founded on seven base quantities (Table 3.1) that cover the whole field of natural science. Again, the system of quantities and equations of mechanics rests on the three base quantities length, mass and time, for which the units *meter*, *kilogram* and *second* are now internationally accepted. The derived unit of force is the *Newton* (N), being the force that gives the unit mass (kg) a unit acceleration (1 m s^{-2}). The derived unit of energy is the *Newton meter* (N m).

Combination of the mechanical system with electric phenomena requires an additional base quantity of an electrical nature. As such the *Ampere* has been chosen as basic unit. The derived unit of electrical energy, the *Joule* (= Volt Ampere second = Watt second) is equal to and identical with the unit of mechanical energy, the N m:

$$1 \text{ N m} = 1 \text{ J} = 1 \text{ VAs} = 1 \text{ Ws}$$

It follows that $1 \text{ N} = 10^5 \text{ dyn}$ and $1 \text{ J} = 10^7 \text{ erg}$

TABLE 3.1 SI base units

Base quantity	Name	Symbol
Length	Meter	m
Mass	Kilogram	kg
Time	Second	s
Electric current	Ampere	A
Thermodynamic Temperature	Kelvin	K
Amount of substance	Mole	mol
Luminous intensity	Candela	cd

¹ Those who were born after 1960 are in general not familiar with this system: they do in general not know the *dyne* and the *erg*.

It is clear that with the definition of the Ampere also the other electrical quantities are defined. Thermodynamics required the introduction of the base quantities temperature and amount of substance, with the *Kelvin* and the *mol* as units. The unit of energy is the *Joule*, so that no conversion factor is involved here either.

Finally in the field of light the base unit *candela* is introduced as unit of luminous intensity.

In the international system every physical quantity is represented by an appropriate symbol (which often is internationally agreed upon), printed in italics. The symbols of the units are printed in normal (straight) type, e.g. a force F is expressed in N.

3.3. CATEGORIES OF PHYSICAL QUANTITIES

Physical quantities may be divided into different categories, according to their nature. The following groups may be distinguished:

1. *Extensive quantities*, which are proportional to the extension of the system considered. Examples are: mass, volume, enthalpy, entropy, etc. When subsystems are combined, the values of the extensive quantities are summed up.
2. *Intensive quantities*, these are independent of the extension of the system, but, as the name suggests, determine an "intensity" or a "quality" of the system. Examples are: temperature, pressure, density, heat capacity, compressibility, field strength, etc. When subsystems are combined, the intensive quantities are "averaged" in accordance with the composition. An intensive quantity may nearly always be regarded as the quotient of two extensive quantities.

$$\text{pressure} = \frac{\text{force}}{\text{area}}$$

$$\text{density} = \frac{\text{mass}}{\text{volume}}$$

$$\text{transition temperature} = \frac{\text{enthalpy difference}}{\text{entropy difference}}$$

3. *Specific quantities*. These, two, are independent of the extension of the system under consideration. They result from extensive quantities when these are related to the unit of mass. So these quantities are also quotients of two extensive quantities and consequently have all the characteristics of intensive quantities. For mixtures the numerical value of these specific quantities is determined by the composition and averaged in accordance with it. Examples:

$$\text{specific volume} = \frac{\text{volume}}{\text{mass}}$$

$$\text{specific heat} = \frac{\text{heat capacity}}{\text{mass}}, \text{etc.}$$

Molar quantities are related to the specific quantities, but now numerically related to one mole as unit of amount of substance. These quantities are, *inter alia*, obtained by multiplication of the specific quantities (related to the unit of mass) by the molar mass. These molar quantities will play an important role in the considerations that are to follow.

Extensive and intensive quantities are characterised in that together they can form parameter couples having the dimensions of an energy. For instance:

Kind of energy	Parameter couple (product)	
	Intensive quantity	Extensive quantity
Mechanical energy	Pressure	Volume
	Tensile stress	Elongation
	Torque	Torsion angle
	Surface tension	Area
Electrical energy	Potential	Charge
Magnetic energy	Field strength	Magnetisation
Thermal energy	Temperature	Entropy

3.4. DIMENSIONLESS GROUPS OF QUANTITIES

Dimensionless groups of quantities or “numerics” occupy a unique position in physics. The magnitude of a numeric is independent of the units in which its component physical properties are measured provided only that these are measured in consistent units. The numerics form a distinct class of entities, which, though being dimensionless, cannot be manipulated as pure numbers. They do not follow the usual rules of addition and multiplication since they have only a meaning if they are related to a specific phenomenon.

The laws of physics may all be expressed as relations between numerics and are in their simplest form when thus expressed. The use of dimensionless expressions is of particular value in dealing with phenomena too complicated for a complete treatment in terms of the fundamental transport equations of mass, energy and angular momentum. Most of the physical problems in the process industry are of this complicated nature and the combination of variables in the form of dimensionless groups can always be regarded as a safe start in the investigation of new problems.

A complete physical law expressed as an equation between numerics is independent of the size of the system. Therefore dimensionless expressions are of great importance in problems of change of scale. When two systems exhibit similarity, one of them, and usually the smaller system, can be regarded as the “model”. Two systems are dynamically similar when the ratio of every pair of forces or rates in one system is the same as the corresponding ratio in the other. The ratio of any pair of forces or rates constitutes a dimensionless quantity. Corresponding dimensionless quantities must have the same numerical value if dynamical similarity holds.

The value of dimensionless groups has long been recognised. As early as 1873, Von Helmholtz derived groups now called the Reynolds and Froude “numbers”, although Weber (1919) was the first to name these numerics.

The standardised notation of numerics is a two-letter abbreviation of the name of the investigator after whom the numeric is named: Xy

3.4.1. Categories of dimensionless groups

Engel (1954, 1958) has divided dimensionless groups into five categories:

1. Those that can be *derived from the fundamental equations of dynamics*. Engel calls these the groups that form the *model laws of dynamic similarity*. This is the most important category in engineering practice; we come back to it later.

Examples of numerics of this group are²:

$$\text{Reynolds' number } (Re) = \frac{\rho v L}{\eta} = \frac{vL}{v} = \frac{\text{transport of angular momentum by convection}}{\text{transport of angular momentum by internal friction}} \quad (3.1)$$

$$\text{Péclet's number } (Pe) = \frac{\rho c_p v L}{\lambda} = \frac{vL}{h} = \frac{\text{heat transport of convection}}{\text{heat transport of conduction}} \quad (3.2)$$

2. Dimensionless ways of expressing an experimental result. This category forming dependent variables, but not model laws, can be derived from the boundary conditions of the model laws.

Examples are:

$$\text{Nusselt's number } (Nu) = \frac{hL}{\lambda} = \frac{\text{heat transport by transfer}}{\text{heat transport by conduction}} \quad (3.3)$$

$$\text{Sherwood's number } (Sh) = \frac{k_m L}{D} = \frac{\text{mass transport by transfer}}{\text{mass transport by diffusion}} \quad (3.4)$$

3. Dimensionless combinations of quantities, which describe the properties of a material (intrinsic numerics). Examples:

$$\text{Lewis' number } (Le) = \frac{\lambda}{\rho c_p D} = \frac{a}{D} = \frac{\text{thermal diffusivity}}{\text{diffusivity}} \quad (3.5)$$

$$\text{Schmidt's number } (Sc) = \frac{\eta}{\rho D} = \frac{v}{D} = \frac{\text{kinematic viscosity}}{\text{diffusivity}} \quad (3.6)$$

$$\text{Prandtl's number } (Pr) = \frac{c_p \eta}{\lambda} = \frac{v}{h} = \frac{\text{kinematic viscosity}}{\text{thermal diffusivity}} = \frac{Pe}{Re} \quad (3.7)$$

$$\text{Stefan number } (Ste) = \frac{\text{sensible heat}}{\text{latent heat of melting}} = \frac{C_p \Delta T}{L} \quad (3.8)$$

4. Ratios of two quantities with the same dimension. These may be:

- 4a. Reduced quantities, i.e. ratios of quantities and chosen standard values:

$$\text{Mach's number } (Ma) = \frac{v}{v_{\text{sound}}} = \frac{\text{velocity}}{\text{velocity of sound}} \quad (3.9)$$

Furthermore: T/T_g , T/T_m , etc.

- 4b. Ratios of forces:

$$\frac{\rho g L}{\Delta p} = \frac{\text{gravitational pressure}}{\text{pressure gradient}} \quad (3.10)$$

$$\frac{\rho g L^2}{\eta v} = \frac{\text{gravitational force}}{\text{viscous force}} \quad (3.11)$$

$$\frac{\eta v}{\gamma} = \frac{\text{viscous force}}{\text{surface tension}} \quad (3.12)$$

² For nomenclature see Scheme 3.2.

$$\frac{\tau}{E} = \frac{\text{shear force}}{\text{elastic force}}, \text{etc.} \quad (3.13)$$

4c. Ratios of characteristic times

$$k_1 t_{\text{res}} = \frac{\text{residence time(in reactor)}}{\text{characteristic reaction time}} \quad (3.14)$$

$$\frac{Dt_{\text{res}}}{L^2} = \frac{\text{residence time}}{\text{characteristic diffusion time}} \quad (3.15)$$

$$\text{Deborah's number}(De) = \frac{\tau}{T} = \frac{\text{natural time of material}}{\text{characteristic time of deformation}} \quad (3.16)$$

$$\text{Weissenberg's number}(We) = \dot{\gamma}\tau = \frac{\text{characteristic time of viscoelastic deformation}}{\text{reciprocal time of deformation}} \quad (3.17)$$

$$\text{Janeschitz-Kriegl's number}(Jk) = \frac{\tau_{\text{th}}}{\tau_{\text{cr}}} = \frac{\text{time needed for thermal equilibration}}{\text{time needed by crystallization process}} \quad (3.18)$$

4d. "Intrinsic" ratios. These are quantities such as:

$$\frac{T_m}{T_g}, \quad \frac{M_w}{M_n}, \text{etc.}$$

4. "*Trivial*" ratios. These are only trivial in the sense that they are simple ratios of quantities with the same dimensions but their effects may be far from trivial. The most important representatives in this category are the *geometric shape factors*, which are often of primary importance.
5. Derived groups, which are simply combinations of the above.

3.4.2. Dimensionless groups derived from the equations of transport

The most important category of dimensionless groups is that of the numerics connected with transport (of mass, energy and angular momentum). Scheme 3.1 shows the three fundamental equations of conservation, written in their simplest form (i.e., one-dimensional). A complete system of numerics can be derived by forming "ratios" of the different terms of these three equations, as was suggested by Klinkenberg and Mooy (1943). This system is reproduced in Scheme 3.2.

3.5. TYPES OF MOLAR PROPERTIES

Polymer properties may (from the molar point of view) be placed in three categories:

1. *Colligative properties*

Per mole of matter these properties have the same value, independent of the special constitution of the substance. The numerical value of the quantity measured experimentally therefore depends on the *number of moles*.

Real colligative properties are only found in ideal gases and ideal solutions. Examples are: osmotic pressure, vapour pressure reduction, boiling-point elevation, freezing-point depression, in other words: the *osmotic properties*.

SCHEME 3.1 The three fundamental equations of conservation

	I	II	III	IV	= 0	V			
Equation of conservation of	Local change	+	Change by convection	+	Change by diffusion	+	Change by production	= 0	Boundary condition
Mass	$\frac{\partial c}{\partial t}$	+	$v \frac{\partial c}{\partial x}$	-	$D \frac{\partial^2 c}{\partial x^2}$	+	r	= 0	Mass transfer = $k_m a \Delta c$
Energy	$c_p \rho \frac{\partial T}{\partial t}$	+	$c_p \rho v \frac{\partial T}{\partial x}$	-	$\lambda \frac{\partial^2 T}{\partial x^2}$	+	\dot{q}	= 0	Heat transfer = $h a \Delta T$
Angular momentum	$\rho \frac{\partial v}{\partial t}$	+	$\rho v \frac{\partial v}{\partial x}$	-	$\eta \frac{\partial^2 v}{\partial x^2}$	+	f	= 0	Shear force = σ_{sh}^a Surface tension force = γl

Corresponding Quantities (per unit of volume)	Unit	Diffusive transport	Production	Boundary transfer
Mass	c	D	r	$k_m a \Delta c$
Energy	$\rho c_p T$	λ	\dot{q}	$h a \Delta T$
Angular momentum	ρv	η	f	σ_{sh}^a or γL^{-1}

Meaning of symbols:
see Scheme 3.2

SCHEME 3.2 System of dimensionless groups (numerics)

Ratio of terms in Scheme 3.1	III/I	IV/I	V/I	II/III	IV/II	V/II	IV/III	V/III	IV/V
Mass	$\frac{Dt}{L^2}$	$\frac{rt}{c}$	$\frac{k_m t}{L}$	$\frac{vl}{D} = Bo$	$\frac{rL}{vc} = Da_I$	$\frac{k_m}{v} = Me$	$\frac{rL^2}{Dc} = Da_{II}$	$\frac{k_m L}{D} = Sh$	$\frac{rL}{k_m c}$
Energy	$\frac{\lambda t}{c_p \rho L^2} = Fo$	$\frac{\dot{q}t}{c_p \rho T}$	$\frac{ht}{c_p \rho L}$	$\frac{c_p \rho v L}{\lambda} = Pe$	$\frac{\dot{q}L}{c_p \rho T v} = Da_{III}$	$\frac{h}{c_p \rho v} = St$	$\frac{\dot{q}L^2}{\lambda T} = Da_{IV}$	$\frac{hL}{\lambda} = Nu$	$\frac{\dot{q}L}{hT}$
Angular momentum	$\frac{\eta t}{\rho L^2}$	$\frac{ft}{\rho v}$	$\frac{\sigma_{sh} t}{\rho v L}$	$\frac{\rho v L}{\eta} = Re$	$\frac{fL}{\rho v^2} = We$	$\frac{\sigma_{sh}}{\rho v^2} = Fa$	$\frac{fL^2}{\eta v} = Po$	$\frac{\sigma_{sh} L}{\eta v} = Bm$	$\frac{fL}{\sigma_{sh}}$

Meaning of symbols	Numerics (see general references)
a = surface per unit of volume	Bm = Bingham
c = concentration	Bo = Bodenstein
c_p = specific heat	Da = Damköhler
D = diffusivity	Fa = Fanning
e = electric charge	Fo = Fourier
E = modulus of elasticity	Me = Merkel
f_{el} = electric field per unit of volume	Nu = Nusselt
g = gravitational acceleration	Pe = Pécelt
h = heat transfer coefficient	Po = Poiseuille
k = reaction rate constant	Re = Reynolds
k_m = mass transfer coefficient	Sh = Sherwood
l = length per unit of volume	St = Stanton
L = characteristic length	We = Weber
p = pressure	
t = time	
T = temperature	
v = velocity	
x = length coordinate	

2. Additive properties

Per mole these properties have a value, which in the ideal case is equal to the sum of values of the constituent atoms. Only the molar mass is strictly additive.

By approximation other quantities are additive as well, such as the molar volume, molar heat capacity, molar heat of combustion and formation, molar refraction, etc.

3. Constitutive properties

These properties are largely determined by the constitution of the molecule, without there being any question of additivity or colligativity. Typical constitutive properties are selective light absorption, magnetic resonance absorption, etc. Often these properties are the "fingerprints" of the substance.

Intramolecular and intermolecular interactions sometimes have a very great influence on colligativity and additivity, and often accentuate constitutive properties. *Our coming considerations will deal in particular with the field of the additive properties and the borderland between the additive and the constitutive properties*

3.6. ADDITIVE MOLAR FUNCTIONS

A powerful tool in the semi-empirical approach in the study of physical properties in general, and of polymer properties in particular, is the use of the *additivity principle*. This principle means that a large number of properties, when expressed per mole of a substance, may be calculated by summation of either atomic, group or bond contributions, where *molar properties are expressed in bold*:

$$\mathbf{F} = \sum_i n_i \mathbf{F}_i \quad (3.19)$$

where \mathbf{F} is a molar property, n_i is the number of contributing components of the type i , and \mathbf{F}_i is the numerical contribution of the component i . Due to their sequential structure, polymers are ideal materials for the application of the additivity principle. End groups play a minor part in general. *Therefore the molar quantities may be expressed per mole of the structural unit.*

Discrepancy between numerical values calculated by means of the additivity principle and experimental values is always caused by interactions.

3.6.1. Additivity and interaction, intrinsically polar concepts, are basic in physical sciences

Chemistry became a real science when the first additivity concept was introduced: the mass of a molecule as the sum of the additive masses \mathbf{A}_i of the composing atoms (based on the law of conservation of mass). But from the beginning it was clear that interaction is the second pillar of chemistry and physics. Additivity is valid as long as interaction is weak or follows simple laws; discrepancies arise when interactions become strong or follow complicated laws.

In the field of polymers two ways of interactions exist. In the first place we have intramolecular interactions. Steric hindrance of backbone groups in their torsional oscillation or of side groups in their rotation is a well-known example; through it the stiffness of the chain is increased. Another example is conjugation of π -electrons ("resonance") between double bonds and/or aromatic ring systems; this also increases the stiffness and thus decreases the flexibility of the chain backbone. The second way is intermolecular interaction; entanglements of long side-chains, precise intermolecular fitting, and physical network formation by hydrogen bonding, are typical examples.

The concept of additivity has proved extremely fruitful for studying the correlation between the chemical constitution of substances and their physical properties. Its usefulness

applies both to individual compounds and to their mixtures, even if these mixtures are of considerable complexity such as mineral oils (Van Nes and Van Westen, 1951) or coals (Van Krevelen, 1961). Properties of homogeneous mixtures can be calculated very accurately by means of additive molar quantities.

Sometimes the discrepancies between numerical values calculated by means of the additivity principle and experimental values form an extremely important key to the disclosure of constitutional effects.

3.6.2. Methods for expressing the additivity within structural units

According to the nature of the structural elements used, three additive methods should be mentioned.

- 1. Use of "atomic" contributions.** If the additivity is perfect, the relevant property of a molecule may be calculated from the contributions of the atoms from which it is composed.

The *molar mass (molar weight)* is an example (the oldest additive molar quantity). This *most simple system of additivity* however, has a restricted value. Accurate comparison of molar properties of related compounds reveals that contributions from the same atoms may have different values according to the nature of their neighbour atoms. The extent to which this effect is observed depends upon the importance of outer valence electrons upon the property concerned.

- 2. Use of "group" contributions.** More sophisticated models start from the basic group contributions and hence have *inbuilt information* on the valence structure associated with a significant proportion of the atoms present. This is the most widely used method.
- 3. Use of "bond" contributions.** A further refinement is associated with bond contributions in which specific differences between various types of carbon–carbon, carbon–oxygen, carbon–nitrogen bonds, etc., are directly included.

The use of atomic contributions is too simplistic in general; the use of bond contributions leads to an impractically large number of different bond types, and so to a very complicated notation.

For practical purposes the method of group contributions is to be preferred.

Discovery of Additive Functions and Derivation of Additive Group Contributions (=Group Increments)

Additive Functions are discovered, sometimes by intuitive vision, sometimes along theoretical lines.

A typical example is the Molar Refraction Function of organic compounds, based on the refractive index n .

In 1858 Gladstone and Dale (1858) found that the product $(n - 1) \cdot M / \rho$, when calculated for series of aliphatic organic compounds with increasing chain lengths grows with a constant increment for the CH_2 -group; they also found that other non-polar groups gave a characteristic increase. This resulted in the *purely empirical* additive function: molar refraction. Later Lorentz and Lorenz (independently of each other, 1880) derived from Maxwell's electromagnetic theory of light another form of the molar refraction:

$$[(n^2 - 1)/(n^2 + 2)]M/\rho \quad (3.20)$$

This more complex form of the refractive index function resulted from *theoretical* studies. In the hands of Eisenlohr and others this additive function became the basis of a system of increments. Many years later Vogel (1948) found that the simplest combination, viz. $n \cdot M$ is also additive, though not temperature independent. Finally Looyenga (1965) showed that

the combination $(n^{2/3} - 1) \cdot M / \rho$ has advantages over the former ones: it is nearly temperature-independent and can be used for pure substances and for homogeneous and heterogeneous mixtures.

So the additive functions must be *discovered*; the values of the *atom group contributions* or *increments* must be *derived*. This derivation of group contributions is relatively easy when the shape of the additive function is known and if sufficient experimental data for a fairly large number of substances are known. The derivation is mostly based on trial and error methods or linear programming; in the latter case the program contains the desired group increments as adjustable parameters. The objective function aims at minimum differences between calculated and experimental molar quantities.

3.6.3. Survey of the additive molar functions

A survey of the Additive Molar Functions (AMFs), which will be discussed in this book, is given in Scheme 3.3. There the names, symbols and definitions are given of the 21 AMFs from which the majority of the physical and physicochemical properties of polymers can be calculated or at least estimated. Scheme 3.3 is at the same time a condensed list of the Nomenclature used.

Seven Classes of Additive Molar Functions can be distinguished, each containing three AMFs:

- I. Those which are "exact" and "fundamental", since they are based on the Mass and on the "hard" Volume of the constituting atom groups; they are completely independent of temperature and time (age) (Chap. 4).
- II. Those, which are connected with Phase Transitions and Phase States and thus are of paramount importance for nearly all properties (Chaps. 4 and 6).
- III. Those connected with the different forms of Internal Energy (Chaps. 5 and 7).
- IV. Those connected with the Interplay between polymers and liquids or gases: solubility, wetting and repulsion (Chaps. 7 and 8); permeability, sorption and diffusivity (Chaps. 9 and 18).
- V. Those connected with Elastic Phenomena and Molecular Mobility: elasto-mechanical properties (Chaps. 13 and 14); viscometric and rheological properties (Chaps. 9, 15 and 16).
- VI. Those connected with Electromagnetic Phenomena (Chaps. 10, 11 and 12).
- VII. Those connected with Thermal Stability and Decomposition (Chaps. 20 and 21).

3.6.4. Calculation of required physical quantities

A Catalog of the (bivalent) group contributions or group increments is given in the comprehensive Table IX of Part VII.

3.6.5. Improvement of the accuracy of estimation

If a molar property can be calculated by means of the additivity principle, the relevant physical quantity can be calculated from the information on chemical structure only. For instance, surface tension follows from:

$$\gamma = \left(\frac{P_S}{V} \right)^4 \quad (3.21)$$

where P_S is the so-called parachor (see Chap. 8); V is the molar volume.

SCHEME 3.3 Additive molar functions (per structural unit)

Class	AMF	Name	Symbol	Formula	Main parameter	
					Name	Symbol
I	1.	Molar mass	\mathbf{M}	$\sum n_i \mathbf{M}_i$	Mass of bivalent structural Group	M_i
	2.	Molar number of backbone atoms	\mathbf{Z}	$\sum n_i \mathbf{Z}_i$	Number of backbone atoms per structural group	Z_i
	3.	Molar Van der Waals volume	\mathbf{V}_W	$\sum n_i \mathbf{V}_{W,i}$	"Hard Volume" per structural group	$V_{W,i}$
II	4.	Molar glass temperature	\mathbf{Y}_g	$\mathbf{M} \cdot T_g$	Glass transition	T_g
	5.	Molar melt transition	\mathbf{Y}_m	$\mathbf{M} \cdot T_m$	Melt transition temperature	T_m
	6.	Molar unit volume	\mathbf{V}	\mathbf{M} / ρ	Density	ρ
III	7.	Molar heat	\mathbf{C}_p	$\mathbf{M} \cdot c_p$	Specific heat capacity	c_p
	8.	Molar melt entropy	$\Delta \mathbf{S}_m$	$\Delta H_m / T_m$	Heat of melting	ΔH_m
	9.	Molar cohesive energy	\mathbf{E}_{coh}	$\mathbf{M} \cdot e_{coh}$	Cohesive energy density	e_{coh}
IV	10.	Molar attraction	\mathbf{F}	$\mathbf{V} \cdot \delta$	Solubility parameter	δ
	11.	Molar parachor	\mathbf{P}_S	$\mathbf{V} \cdot \gamma^{1/4}$	Surface tension	γ
	12.	Molar permachor	Π	$\mathbf{N} \cdot \pi$	Specific permachor (permeability)	π
V	13.	Molar elastic wave velocity	\mathbf{U}	$\mathbf{V} \cdot u^{1/3}$	Sound wave velocity	u
	14.	Molar intrinsic viscosity	\mathbf{J}	$K_\Theta^{1/2} \cdot \mathbf{M} - 4.2 \mathbf{Z}$	Intrinsic viscosity parameter	$K_\Theta^{1/2}$
	15.	Molar viscosity-temperature gradient	\mathbf{H}_η	$\mathbf{M} \cdot E_\eta$	Activation energy of viscous flow	E_η
VI	16.	Molar polarisation	\mathbf{P}	$\mathbf{V} \cdot \frac{\epsilon - 1}{\epsilon + 2}$	Dielectric constant	ϵ
	17.	Molar optical refraction	\mathbf{R}	$\mathbf{V} \cdot (n - 1)$	Index of light refraction	n
	18.	Molar magnetic susceptibility	\mathbf{X}	$\mathbf{M} \cdot \chi$	Magnetic susceptibility	χ
VII	19.	Molar free energy of formation	$\Delta \mathbf{G}_f^\circ$	$\mathbf{A} - \mathbf{B}T$	Heat of formation	A
	20.	Molar thermal decomposition	$\mathbf{Y}_{d,1/2}$	$\mathbf{M} \cdot T_{d,1/2}$	Entropy of formation	B
	21.	Molar char forming tendency	\mathbf{C}_{FT}	$\mathbf{M} \cdot CR / 1200$	Temperature of half-way decomposition	$T_{d,1/2}$
					Char residue in weight-%	CR

(continued)

SCHEME 3.3 (continued)

AMF nr	Symbol	Introduced by	Dimensions used
1	M	Dalton (1801); Berzelius (1810)	g mol^{-1}
2	Z	Weyland (1970)	mol^{-1}
3	V_W	Bondi (1968)	$\text{cm}^3 \text{mol}^{-1}$
4	Y_g	Van Krevelen–Hoftyzer (1976)	K kg mol^{-1}
5	Y_m	Van Krevelen–Hoftyzer (1976)	K kg mol^{-1}
6	V_a	Traube (1895)	$\text{cm}^3 \text{mol}^{-1}$
7a	C_{p,s}	Satoh (1948)	$\text{J mol}^{-1} \text{K}^{-1}$
7b	C_{p,l}	Shaw (1969)	$\text{J mol}^{-1} \text{K}^{-1}$
8	ΔS_m	Bondi (1968)	$\text{J mol}^{-1} \text{K}^{-1}$
9	E_{coh}	Bunn (1955)	kJ mol^{-1}
10	F	Small (1953)	$(\text{J mol}^{-1})^{1/2} (\text{cm}^3 \text{mol}^{-1})^{1/2}$
11	P_s	Sugden (1924)	$(\text{cm}^3 \text{mol}^{-1})^{1/2} (\text{mJ m}^{-2})^{1/4}$
12	Π	Salame (1986)	mol^{-1}
13	U	Rao (1940); Schuyer (1958)	$(\text{cm}^3 \text{mol}^{-1}) (\text{cm s}^{-1})^{1/3}$
14	J	Van Krevelen–Hoftyzer (1967/76)	$K_{\Theta}: (\text{cm}^3 \text{g}^{-1}) (\text{g mol}^{-1})^{1/2}$
15	H_n	Van Krevelen–Hoftyzer (1975)	$(\text{g mol}^{-1}) (\text{J mol}^{-1})^{1/3}$
16	P_{LL}	Mosotti (1850); Clausius (1879)	$\text{m}^3 \text{mol}^{-1} 10^{-6}$
17	R_{GD}	Gladstone–Dale (1858)	$\text{m}^3 \text{mol}^{-1} 10^{-6}$
18	X	Pascal (1923)	$\text{m}^3 \text{mol}^{-1} 10^{-12}$
19	ΔG_f^o = A - BT	Van Krevelen–Chermin (1950)	kJ mol^{-1}
20	Y_{d,1/2}	Van Krevelen (1988)	K kg mol^{-1}
21	C_{FT}	Van Krevelen (1975)	mol^{-1}

The accuracy of such a numerical value is limited, of course, since the additivity of a molar property is never exactly valid. Generally the accuracy is sufficient for practical use.

There are two ways to improve the accuracy of the calculation, viz. by using a "standard property" or by using a "standard substance". We shall explain what is meant by these terms.

1. Method of Standard Properties

Let us assume that the required physical property of a substance, e.g. its surface tension, is unknown, but that another property, e.g. its refractive index, has been measured with great accuracy. Then we can use the latter as a standard property and apply the formula

$$\gamma = \left(\frac{P_S}{R_{LL}} \frac{n^2 - 1}{n^2 + 2} \right)^4 \quad (3.22)$$

The attraction is twofold: first of all Eq. (3.22) has the advantage that the absolute value of the molar volume V , often the least reliable additive quantity, is not used, secondly, Eq. (3.22) can easily be transformed into a dimensionless group, viz.:

$$\frac{\gamma^{1/4}}{(n^2 - 1)/(n^2 + 2)} \frac{R_{LL}}{P_S} = 1 \quad (3.23)$$

with all the advantages of the dimensionless expressions.

2. Method of Standard Substances

This method may be applied if a physical property of the substance in question is unknown, but if the same property has been measured accurately in a related substance. In this case one may use the related substance as a "model" or a "standard" (symbol o) and apply the rule:

$$\frac{\gamma}{\gamma_o} = \left(\frac{P_S}{P_{So}} \frac{V_o}{V} \right)^4 \quad (3.24)$$

Also this equation is dimensionless.

Especially by the possibility of these two refinements, the principle of additivity becomes even more useful for practice and permits us to estimate physical quantities with an accuracy, which could hardly be expected.

3.6.6. Comparison with Huggins' interaction-additivity method

The group additivity methods described in this chapter may be considered a special form of the more general method proposed by Huggins (1969, 1970). The latter method might be called an interaction additivity method. It assumes that a number of properties of a liquid (or a mixture) is equal to the sum of the contributions of every interaction P between the groups present.

In its most general formulation this theory assumes that a property F may be calculated by

$$F = \sum_{i=1}^n \sum_{j=1}^n w_{ij} F_{ij} \quad (3.25)$$

where w_{ij} = a weight factor taking into account the relative importance of the contacts between groups i and j; F_{ij} = the contribution to property F , attributed to a contact between groups i and j; n = the number of groups present.

In the theory of Huggins, the weight factors w are supposed to be proportional to the area of contact between the groups i and j.

For a ditonic system, containing the groups A and B, Eq. (3.25) reduces to:

$$\mathbf{F} = w_{aa}\mathbf{F}_{aa} + w_{bb}\mathbf{F}_{bb} + w_{ab}\mathbf{F}_{ab} \quad (3.26)$$

If the factors w are expressed in fractions of the numbers of moles n_A and n_B :

$$w_{aa} = \frac{n_A^2}{n_A + n_B}, \quad w_{bb} = \frac{n_B^2}{n_A + n_B}, \quad w_{ab} = \frac{2n_A n_B}{n_A + n_B}$$

and if it is assumed that

$$\mathbf{F}_{ab} = \frac{1}{2}\mathbf{F}_{aa} + \frac{1}{2}\mathbf{F}_{bb}$$

then, Eq. (3.26) reduces to:

$$\mathbf{F}_{ab} = n_A\mathbf{F}_{aa} + n_B\mathbf{F}_{bb} \quad (3.27)$$

which is the equation of a group additivity method for a ditonic system.

A ditonic system is defined as a system consisting of a mixture of two different molecules, both containing only one kind of atoms or groups with regard to intermolecular actions, e.g. CCl_4 , where only the chlorine atoms are assumed to be involved in intermolecular actions (see, e.g. Huggins, 1970)

BIBLIOGRAPHY

General references

- Bondi A, "Physical Properties of Molecular Crystals, Liquids and Glasses", Wiley, New York, 1968.
 Bridgman PW, "Dimensional Analysis", Yale University Press, New Haven, 1931.
 Catchpole JP and Fulford G, "Dimensionless Groups", Ind. Eng. Chem. 58 (1966) 46 and 60 (1968) 71.
 Exner O, "Additive Physical Properties, 1. General Relationships and Problems of Statistical Nature", Collection Czechoslov. Chem. Commun., 1966, Vol 31.
 Exner O, "Additive Physical Properties, 2. Molar Volume as an Additive Property", Collection Czechoslov. Chem. Commun., 1967, Vol 32.
 Jerrard HG and McNeill DB, "A Dictionary of Scientific Units, Including Dimensionless Numbers and Scales", Chapman & Hall, London, 1986.
 Langhaar HL, "Dimensional Analysis and Theory of Models" Wiley, New York, 1951.
 Mills J, Cvitas T, Kallay N and Homann K, "Quantities, Units and Symbols in Physical Chemistry", Blackwell Sci Publishers, Oxford, 1988.
 Pallacios J, "Dimensional Analysis", Macmillan, London, 1964.
 Van Krevelen DW, "Coal; Typology, Physics, Chemistry and Constitution", Elsevier, Amsterdam, 1961/1981.
 Van Nes K and Van Westen HA, "Aspects of the Constitution of Mineral Oils", Elsevier, Amsterdam, 1951.

Special references

- Bunn CW, *J. Polym. Sci.* 16 (1955) 323.
 Clausius R, "Die mechanische Wärmetheorie", Braunschweig, 1879, p 62.
 Debye P, *Phys. Z.*, 13 (1912) 97.
 Engel FVA, *The Engineer* 198 (1954) 637; 206 (1958) 479.
 Franklin JL, *Ind. Eng. Chem.*, 41 (1949) 1070.
 Gladstone JH and Dale TP, *Trans. Roy. Soc.*, (London) A 148 (1858) 887; A 153 (1863) 317.
 Huggins ML, *J. Paint Technol.*, 41 (1969) 509; *J. Phys. Chem.*, 74 (1970) 371.
 Klinkenberg A and Mooy HH, *Ned. T. Natuurk.* 10 (1943) 29; *Chem. Eng. Progr.*, 44 (1948) 17.
 Looyenga H, *Mol. Phys.*, 9 (1965) 501; *J. Pol. Sci. Phys. Ed.*, 11 (1973) 1331.
 Lorentz HA, *Wied Ann. Phys.*, 9 (1880) 641.
 Lorenz LV, *Wied Ann. Phys.*, 11 (1880) 70.
 Maxwell JC, "A Treatise on Electricity and Magnetism", Oxford, 1873.

- Mosotti OF, *Mem. di mathem e Fis. Modina*, 24 11 (1850) 49.
- Pascal P, *Rev. Gen. Sci.*, 34 (1923) 388.
- Rao R, *Indian J. Phys.*, 14 (1940) 109.
- Salame M, *Polym. Eng. Sci.*, 26 (1986) 1543.
- Satoh S, *J. Sci. Res. Inst.*, (Tokyo) 43 (1948) 79.
- Schuyer J, *Nature* 181 (1958) 1394; *J. Polym. Sci.*, 36 (1959) 1475.
- Shaw R, *J. Chem. Eng. Data.*, 14 (1969) 461.
- Small PA, *J. Appl. Chem.*, 3 (1953) 71.
- Sugden S, *J. Chem. Soc.*, 125 (1924) 1177; "The Parachor and Valency", George Routledge, London, 1930.
- Traube J, *Ber. Dtsch. Chem. Ges.*, 28 (1895) 2722.
- Van Krevelen DW, "Processing Polymers to Products", International Plastics Congress 1966, 't Raedthuys, Utrecht, 1967, pp 11–19.
- Van Krevelen DW, *Polymer* 16 (1975) 615.
- Van Krevelen DW, (1988), unpublished.
- Van Krevelen DW and Chermin HAG, *Ingenieur* 38 (1950), *Chem. Techn.*, 1; *Chem. Eng. Sci.*, 1 (1951) 66.
- Van Krevelen DW and Hoftyzer PJ, *J. Appl. Polym. Sci.*, 11 (1967) 1409; "Properties of Polymers", 2nd Ed (1976), pp. 180–182.
- Van Krevelen DW and Hoftyzer PJ (1976), "Properties of Polymers", 2nd Ed pp 100 and 113.
- Van Krevelen DW and Hoftyzer PJ, *Z. Angew. Makromol. Chem.*, 52 (1976) 101.
- Vogel A, *Chem. Ind.*, (1950) 358; (1951) 376; (1952) 514; (1953) 19; (1954) 1045.
- Von Helmholtz H, *Monatsber königl Preuss Akad. Wiss.*, (1873) 501.
- Weber M, *Jahrb. Schiffbautechn Ges.*, 20 (1919) 355.
- Weyland HG, Hoftyzer PJ and Van Krevelen DW, *Polymer*, 11 (1970) 79.

This page intentionally left blank

PART

THERMOPHYSICAL PROPERTIES OF POLYMERS

*“Discovery consists of seeing what everybody has seen,
and thinking what nobody has thought”.*

Albert Szent-Gyorgi, 1893–1986

This page intentionally left blank

CHAPTER 4

Volumetric Properties

The volumetric properties are extremely important for nearly every phenomenon or process. The main volumetric properties are:

- (1) *Specific and molar volumes* and the related reciprocals of specific volumes, the *densities*; these quantities are different for the glassy, rubbery and crystalline states
- (2) *Specific and molar thermal expansivities*, again dependent on the physical state
- (3) *Specific and molar melt expansion* for crystalline polymers

It will be shown that the molar volumetric properties can be calculated with a remarkable accuracy from additive group contributions. Furthermore there exist interesting correlations with the Van der Waals volume.

4.1. INTRODUCTION: MASS AND PACKING OF MATTER

Mass and Packing are the most important fundamental properties of matter. Nearly all other properties are eventually determined by these two. Whereas Mass is unambiguously defined and measurable, Packing is by no means a simple property; it is highly influenced by the electronic structure of the atoms, by the type of bonding forces and by structural and spatial variations.

Some properties are directly connected with mass and packing: *density* (or its reciprocal: *specific volume*), *thermal expansibility* and *isothermal compressibility*. Especially the mechanical properties, such as moduli, Poisson ratio, etc., depend on mass and packing. In this chapter we shall discuss the densimetric and volumetric properties of polymers, especially density and its variations as a function of temperature and *pressure*. Density is defined as a ratio:

$$\rho = \frac{\text{molar mass}}{\text{molar volume}}$$

Because of the sequential nature of polymers we may also use the molar mass and volume of the structural unit:

$$\rho = \frac{\mathbf{M}}{\mathbf{V}}$$

The chapter will be divided into the following parts:

1. Fundamental quantities of mass and volume
2. Standard molar volume and density (at room temperature)
3. Thermal expansion
4. Isothermal compression

4.2. FUNDAMENTAL QUANTITIES OF MASS AND VOLUME

4.2.1. Mass and volume of atoms

Molecules are composed of atoms, so that eventually mass and volume of molecules are determined by mass and volume of the atoms. Whereas the mass of molecules is the simple sum of the masses of the composing atoms, the volume of molecules is not just the sum of the atomic volumes.

In Table 4.1 the (molar) masses of the atoms of the elements, normally occurring in polymers, are given in g/mol. Table 4.1 also shows two characteristic spatial dimensions: the Van der Waals radius and the covalent atomic radius.

The Van der Waals radius is determined by the outer electron shell of the atom. If two neutral atoms (in the simplest case atoms of noble gases) approach each other – without reacting chemically – the sum of the Van der Waals radii will be their closest distance.

TABLE 4.1 Fundamental data on atoms

Element	Atomic mass	Covalent atomic Radius (nm)	Van der Waals Radius (nm), according to:		
			Pauling (1940)	Bondi (1968)	Slonimskii et al. (1970)
-H	1.008	0.031	0.120	0.120	0.117
-F	19.00	0.064	0.135	0.147	0.150
-Cl	35.45	0.099	0.180	0.175	0.178
-Br	79.90	0.114	0.195	0.185	
-O-	16.00	0.066	0.136	0.150	0.136
=O	16.00	0.062			
-S-	32.07	0.104	0.185	0.180	
=S	32.07	0.094			
-N<	14.01	0.070	0.157	0.155	0.157
N _{ar}	14.01	0.065			
=N-	14.01	0.063			
≡N	14.01	0.055			
-P<	30.97	0.110	0.190	0.180	
=P-	30.97	0.100			
≡P	30.97	0.093			
>C<	12.01	0.077	0.180	0.170	0.180
C _{ar}	12.01	0.070	0.170		
=C<	12.01	0.067			
≡C-	12.01	0.060			
>Si<	28.09	0.117		0.210	

Similarly, if two molecules approach each other the sum of the van der Waals radii of the outer atoms determines the closest distance of the molecules.

If reaction takes place, however, the combined atomic volumes of the atoms are strongly reduced: now the sum of the adjacent covalent atomic radii determines the inter-atomic distance. The consequence is that the Van der Waals volume of a molecule is much smaller than the sum of the van der Waals volumes of the composing atoms.

4.2.2. Molar mass of polymeric structural units and of structural groups

If the elemental formula of the structural unit of a polymer is known, the molar mass per structural unit can be calculated directly by addition (=summation) of the atomic masses. The molar mass is the oldest Additive Function; it is additive by definition, since it is based on a fundamental law of chemistry: the law of "Conservation of mass".

Since structural units consist of a number of characteristic structural groups, the mass of the structural unit can also be calculated as *sum of the masses of the structural groups*. Table 4.2 gives the masses of the main structural groups in polymers.

4.2.3. Van der Waals volumes of structural units and structural groups

The Van der Waals volume of a molecule may be defined as the space occupied by this molecule, which is impenetrable to other molecules with normal thermal energies (i.e. corresponding with ordinary temperatures). For comparison with other quantities discussed in this chapter, the Van der Waals volume will be expressed in cm^3 per mole of unit structure.

For an approximate calculation, the Van der Waals volume is assumed to be bounded by the outer surface of a number of *interpenetrating* spheres. The radii of the spheres are assumed to be (constant) atomic radii for the elements involved and the distances between the centres of the spheres are the (constant) bond distances.

The contribution of a given atom A with radius R to the Van der Waals volume is then given by

$$V_{W,A} = N_A \left[\frac{4}{3} \pi R^3 - \sum \pi h_i^2 \left(R - \frac{h_i}{3} \right) \right] \quad (4.1)$$

with

$$h_i = R - \frac{l_i}{2} - \frac{R^2}{2l_i} + \frac{r_i^2}{2l_i}$$

where N_A is Avogadro's number, r_i is the radius of atom i, covalently bonded to A, and l_i is the bond distance between the atoms A and i.

According to this definition, the volume contribution $V_{W,A}$ of the atom considered is *not* constant, as its value depends on the nature of the surrounding atoms i.

On the other hand, the volume contribution of structural groups already contains inbuilt information on the influence of the atomic surroundings. As a consequence the Van der Waals volume of the structural units can approximately be calculated as the sum of the Van der Waals volumes of the composing structural groups. Bondi (1964, 1968) was the first to calculate the contributions of about 60 structural groups to V_W . Later Slonimskii et al. (1970) and Askadskii (1987) calculated about 100 values of atomic increments in different surroundings. Since the two approaches used the same method of calculation, and nearly equal basic data on the atomic radii, the calculated values for the structural units are approximately equal. In Table 4.2 also the group increments of V_W are shown, next to those of M . By means of these data the Van der Waals volumes of the Structural Units are easily calculated.

TABLE 4.2 Group increments of mass and Van der Waals volume (bivalent groups)

Group increment	M_i (g/mol)	V_{wi} (cm ³ /mol)	Group increment	M_i (g/mol)	V_{wi} (cm ³ /mol)
$-\text{CH}_2-$	14.03	10.23	$-\text{O}-$	16.00	$\left\{ \begin{array}{l} 5.5 \\ 5.0 \end{array} \right.$
$-\text{CH}(\text{CH}_3)-$	28.05	20.45	$-\text{NH}-$	15.02	(4)
$-\text{CH}(\text{iso-C}_3\text{H}_7)-$	56.11	40.9	$-\text{S}-$	32.06	10.8
$-\text{CH}(\text{ter-C}_4\text{H}_9)-$	70.13	51.1	$-\text{S}-\text{S}-$	64.12	22.7
$-\text{CH}(\text{C}_6\text{H}_5)-$	90.12	52.6	$\begin{array}{c} \text{O} \\ \parallel \\ \text{S} \end{array}$	64.06	20.3
$-\text{CH}(\text{C}_6\text{H}_4-\text{CH}_3)-$	104.14	63.8	$-\text{COO}-$	44.01	15.2
$-\text{CH}(\text{OH})-$	30.03	14.8	$-\text{OCOO}-$	60.01	18.9
$-\text{CH}(\text{OCH}_3)-$	44.05	25.5	$-\text{CONH}-$	43.03	(13)
$-\text{CH}(\text{OCOCH}_3)-$	72.06	37.0	$-\text{OCONH}-$	59.03	(18)
$-\text{CH}(\text{COOCH}_3)-$	72.06	37.0	$-\text{NHCONH}-$	58.04	(18)
$-\text{CH}(\text{CN})-$	39.04	21.5	$-\text{Si}(\text{CH}_3)_2-$	58.15	42.2
$-\text{CHF}-$	32.02	12.5			
$-\text{CHCl}-$	48.48	19.0			
$-\text{C}(\text{CH}_3)_2-$	42.08	30.7		82.14	53.3
$-\text{C}(\text{CH}_3)(\text{C}_6\text{H}_5)-$	104.1	62.8		76.09	43.3
$-\text{C}(\text{CH}_3)$ $(\text{COOCH}_3)-$	86.05	46.7		76.09	43.3
$-\text{CF}_2-$	50.01	14.8		104.14	65.6
$-\text{CFCl}-$	66.47	21.0		228.28	130
$-\text{CCl}_2-$	82.92	27.8		126.18	69.9
$-\text{CH}=\text{CH}-$	26.04	16.9		214.13	94.5
$-\text{CH}=\text{C}(\text{CH}_3)-$	40.06	27.2			
$-\text{CH}=\text{CCl}-$	60.49	25.7			
$-\text{C}\equiv\text{C}-$	24.02	16.1			
$-\overset{\text{O}}{\underset{\parallel}{\text{C}}}-$ $\left\{ \begin{array}{l} \text{al.} \\ \text{ar.} \end{array} \right.$	28.01	$\left\{ \begin{array}{l} 8.5 \\ 11.7 \end{array} \right.$			

(continued)

TABLE 4.2 (continued)

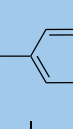
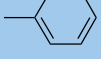
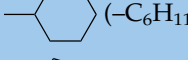
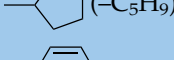
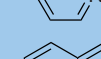
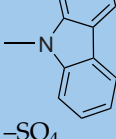
Group increment	M_i (g/mol)	V_{wi} (cm ³ /mol)	Group increment	M_i (g/mol)	V_{wi} (cm ³ /mol)
Group increments of mass and Van der Waals volume (Non-bivalent groups)					
Monovalent			Aromatic ("3/2"-valent)		
-H	1.008	3.44	CH _{ar}	13.02	8.05
-CH ₃	15.03	13.67	C _{ar} (exo)	12.01	5.55
-CH(CH ₃) ₂	43.09	34.1	C _{ar} * (endo)	12.01	4.75
-C(CH ₃) ₃	57.11	44.35	N _{ar} (pyrid)	14.00	5.2
-C≡CH	25.02	19.5	Trivalent		
-C≡N	26.02	14.7	>CH-	13.02	6.8
-OH	17.01	8.0	-CH=C<	25.03	13.5
-SH	33.07	14.8	Tetravalent		
-F	19.00	5.7	-N<	14.01	4.3
-Cl { al	35.45	{ 11.6	Tetravalent		
-Cl { ar	35.45	{ 12.0	>C<	12.01	3.3
-CF ₃	69.01	21.3	=C=	12.01	6.95
-CHCl ₂	83.93	31.3	-C≡	13.02	(8)
-CH ₂ Cl	49.48	21.85		74.08	38.3
-CCl ₃	118.38	38.2		74.08	38.3
-NO ₂	46.01	16.8		28.09	16.6
	77.10	45.85			
	83.15	56.8			
	69.12	46.5			
	78.07	43.0			
	127.2	71.45			
	166.4	88.7			
-SO ₄	96.06	35.1			

TABLE 4.3 Atomic and structural constants for $V^0(0)$ in cm^3/mol

Atomic constants	Atomic constants	Structural constants
H = 6.7	I = 28.3	Triple bond = 15.5
C = 1.1	P = 12.7	Double bond = 8.0
N = 3.6	S = 14.3	3-Membered ring = 4.8
O = 5.0	O (in alcohols) = 3.0	4-Membered ring = 3.2
F = 10.3	N (in amines) = 0.0	5-Membered ring = 1.8
Cl = 19.3		6-Membered ring = 0.6
Br = 22.1		Semipolar double bond = 0.0

4.2.4. Zero point molar volume ($V^0(0)$)

Timmermans (1913) and Mathews (1916) introduced the concept of zero point density based on the extrapolation of densities of crystalline and liquid substances to 0 K. Sugden (1927) and Biltz (1934) developed an additive system for deriving values of $V^0(0)$ from chemical constitution. The zero point volume is closely related to the Van der Waals volume. According to Bondi (1968a) a good approximation is given by the following expression:

$$\frac{V^0(0)}{V_W} = \frac{V_c(0)}{V_W} \approx 1.3 \quad (4.2)$$

For the sake of completeness we give in Table 4.3 Sugden's list of atomic and structural constants (increments) for the zero-volume of liquids (in cm^3/mol)

4.3. STANDARD MOLAR VOLUMES AT ROOM TEMPERATURE (298 K)

4.3.1. Molar volumes of organic liquids at room temperature

The molar volume at room temperature is one of the first physical quantities, for which group contribution methods have been proposed. Atomic contribution methods were derived by Traube (1895) and by Le Bas (1915). A characteristic difference between the two approaches was that Traube added to the sum of atomic contributions for a given compound an additional value called "residual volume" (Ω), so that

$$V_1(298) = \sum_i V_i(298) + \Omega \quad (4.3)$$

Ω is a constant with an average value of $24 \text{ cm}^3/\text{mol}$. The existence of a residual volume has been confirmed by a number of other investigators. As Le Bas disregarded this effect, his values for the atomic contributions are always larger than the corresponding values of Traube, and of little practical value. Nevertheless the method of Le Bas can still be found in a number of textbooks.

In the 1960s Davis and Gottlieb (1963) and Harrison (1965, 1966) improved the method of Traube. It appeared that the atomic contribution of a given element is not constant, but dependent on the nature of the surrounding atoms. This leads to a considerable increase of the number of "atomic" contribution values. For this reason group contributions are to be preferred to atomic contributions.

TABLE 4.4 Group contribution of CH₂ to molar volume of liquids

Investigators	CH ₂ contribution to molar volume (cm ³ /mol = 10 ⁻⁶ m ³ /mol)
Traube (1895)	16.1
Kurtz and Lipkin (1941)	16.3
Van Nes and Van Westen (1951)	16.5
Simha and Hadden (1956)	16.5
Li et al. (1956)	16.5
Huggins (1958)	16.5
Tatevskii et al. (1961)	16.1
Davis and Gottlieb (1963)	16.6
Harrison (1965, 1966)	16.4
Exner (1967)	16.6
Rheineck and Lin (1968)	16.5
Fedors (1974)	16.1

In the following sections, exclusively group contributions will be used. Literature data originally expressed in atomic contributions will be converted into group contribution values.

The best confirmations of the additivity of molar volume were obtained from the studies of homologous series. Studies of several series of compounds with increasing numbers of CH₂ groups have led to rather accurate values for the contribution of this group to the molar volume. Values found by several investigators are summarised in Table 4.4. The mean value is 16.45 cm³/mol with a standard deviation of 0.2 cm³/mol.

For other groups, the contributions mentioned by different authors show larger variations. This appears from Table 4.5 where published values of the contributions for a number of groups are compared. All the results are expressed in the form of bivalent groups. This has been done because a number of authors did not make a clear distinction between the contributions of monovalent end groups and the above-mentioned residual volume.

The contributions of several hydrocarbon groups are rather accurately known and can be predicted with an accuracy of about 1 cm³/mol. For other groups, variations range from 2 to 4 cm³/mol. It must be concluded that on the basis of these literature data the molar volume of an organic liquid can be predicted with an accuracy of, at best, some percent. Fedors (1974) proposed an extensive system of group contributions to the molecular volume of liquids. These values, though not very accurate, can be used for a first orientation. They are given in Chap. 7 in Table 7.4, in combination with group contributions for the cohesive energy.

4.3.2. Molar volumes of rubbery amorphous polymers

The rubbery amorphous state of polymers has the greatest correspondence with the liquid state of organic compounds. So it may be expected that the molar volume per structural unit of polymers in this state can be predicted by using the averaged values of the group contributions mentioned in Table 4.5 (Van Krevelen and Hoftyzer, 1969).

$$V_r(298) = \sum_i V_i(298) \quad (4.4)$$

Owing to the very high molecular weight, the residual volume Ω (Eq. (4.3)) may be neglected.

TABLE 4.5 Group contributions to the molar volume of organic liquids at room temperature (cm^3/mol)

Groups	Investigators							
	Traube (1895)	Kurtz and Lipkin (1941)	Li et al. (1956)	Huggins (1954)	Davis and Gottlieb (1963)	Exner (1967)	Rheineck and Lin (1968)	Fedors (1974)
$-\text{CH}_2-$	16.1	16.3	16.5	16.5	16.6	16.6	16.5	16.1
$-\text{CH}(\text{CH}_3)-$	32.2	32.6		32.3	33.2		33.5	32.5
$-\text{C}(\text{CH}_3)_2-$	48.3	48.8		47.6	49.8	49.7		47.8
$-\text{CH}=\text{CH}-$	24.3	26.4		26.5	25.0			27.0
$-\text{CH}=\text{C}(\text{CH}_3)-$	40.4	42.6		40.3	40.6			41.5
$-\text{CH}(\text{CH}=\text{CH}_2)-$	40.4	42.6	43.9		40.6	43.7	43.5	40.0
$-\text{C}_6\text{H}_{10}-$	77.2	78.9			78.5			78.4
$-\text{CH}(\text{C}_6\text{H}_{11})-$	93.3	95.2	97.4		94.1	95.1	94.5	95.5
$-\text{CH}(\text{C}_5\text{H}_9)-$	77.2	82.0	82.6			80.3		79.4
$-\text{C}_6\text{H}_4-$	58.6	60.3			61.8			52.4
$-\text{CH}(\text{C}_6\text{H}_5)$	74.7	76.6	78.8		77.4	75.8	74.5	70.4
$-\text{CHF}-$	18.5			17.8		16.3		17.0
$-\text{CHCl}-$	26.2			26.6		24.1	23.5	23.0
$-\text{CHBr}-$	26.2			30.1		27.4		29.0
$-\text{CHI}-$	26.2			37.3		34.1		30.5
$-\text{CH}(\text{CN})-$	24.4			27.2		23.8		23.0
$-\text{O}-$	5.5				6.8	6.7		3.8
$-\text{CO}-$	15.4					10.2	8.5	10.8
$-\text{COO}-$	20.9			23.9	15.5	19.5	16.5	18.0
$-\text{CH}(\text{OH})-$	18.4		15.8	14.5		11.4	8.2	9.0
$-\text{CH}(\text{CHO})-$	31.5			29.6	27.6	26.3	25.5	21.3
$-\text{CH}(\text{COOH})-$	31.9		30.7	31.7	30.1	28.4	26.5	27.5
$-\text{CH}(\text{NH}_2)-$				21.8		18.8	18.5	18.2
$-\text{CH}(\text{NO}_2)-$				30.1		25.7		23.0–31.0
$-\text{CONH}-$	20.0					17.5		15.3
$-\text{S}-$	15.5				12.2	10.8		12.0
$-\text{CH}(\text{SH})-$	31.6		31.7	30.0		27.0		27.0

At room temperature, those amorphous polymers are in the rubbery state of which the glass transition temperature is lower than 25 °C. The available literature data on the densities for this class of polymers are mentioned in Table 4.6. For each polymer, the molar volume V_r has been calculated from the density. These values of V_r have been compared with Eq. (4.3), using group contributions mentioned in Table 4.4. Although there was an

TABLE 4.6 Molar volumes of rubbery amorphous polymers at 25 °C

Polymer	ρ_r (g/cm ³)	V_r (cm ³ /mol)	V_w (cm ³ /mol)	V_r/V_w (-)
Polyethylene	0.855	32.8	20.5	1.60
Polypropylene	0.85	49.5	30.7	1.61
Polybutene	0.86	65.2	40.9	1.59
Polypentene	0.85	82.5	51.1	1.61
Polyhexene	0.86	97.9	61.4	1.59
Polyisobutylene	0.84	66.8	40.9	1.63
Poly(vinylidene chloride)	1.66	58.4	38.0	1.53
Poly(tetrafluoroethylene)	2.00	50.0	32.0	1.56
Poly(isopropyl vinyl ether)	0.924	93.2	54.9	1.69
Poly(butyl vinyl ether)	0.927	108.0	65.1	1.65
Poly(sec-butyl vinyl ether)	0.924	108.3	65.1	1.65
Poly(isobutyl vinyl ether)	0.93	107.6	65.1	1.65
Poly(pentyl vinyl ether)	0.918	124.4	75.3	1.65
Poly(hexyl vinyl ether)	0.925	138.6	85.5	1.62
Poly(octyl vinyl ether)	0.914	171.0	106.0	1.61
Poly(2-ethylhexyl vinyl ether)	0.904	172.9	106.0	1.65
Poly(decyl vinyl ether)	0.883	208.7	126.3	1.62
Poly(dodecyl vinyl ether)	0.892	238.1	146.9	1.62
Poly(vinyl butyl sulphide)	0.98	118.6	78.9	1.50
Poly(methyl acrylate)	1.22	70.6	45.9	1.54
Poly(ethyl acrylate)	1.12	89.4	56.1	1.56
Poly(butyl methacrylate)	1.053	135.0	86.8	1.56
Poly(hexyl methacrylate)	1.007	169.1	107.3	1.58
Poly(2-ethyl butyl methacrylate)	1.040	163.8	107.2	1.53
Poly(1-methylpentyl methacrylate)	1.013	168.1	107.2	1.57
Poly(octyl methacrylate)	0.971	204.2	127.7	1.60
Poly(dodecyl methacrylate)	0.929	273.8	168.6	1.62
Polybutadiene	0.892	60.7	37.5	1.62
Poly(2-methylbutadiene)	0.91	74.8	47.3	1.58
Polypentadiene	0.89	76.5	47.3	1.62
Poly(chlorobutadiene)	1.243	71.2	45.6	1.56
Poly(ethylene oxide)	1.13	38.9	24.2	1.61
Poly(tetramethylene oxide)	0.98	73.5	44.6	1.65
Poly(propylene oxide)	1.00	58.1	34.4	1.69
Poly[3,3-bis(chloromethylene) oxacyclo butane]	1.386	111.8	71.2	1.57
Average			1.60 ± 0.035	

obvious correspondence between the experimental and calculated values, the inaccuracy of this calculation was too large to provide a prediction of polymer densities that is of any practical value.

Thus another approach proved necessary. This new approach was found by plotting the values of $V_r(298)$ versus the molar Van der Waals volume V_w . Fig. 4.1A shows the result: the molar volumes V_r and V_w , show a simple linear relationship. The ratio $V_r(298)/V_w$ has a value of 1.60 ± 0.035 (see for the numerical values Table 4.6).

4.3.3. Molar volume of glassy amorphous polymers

Those amorphous polymers, for which the glass transition temperature is higher than 25°C , are in the glassy state at room temperature. Table 4.7 gives a survey of the available literature data on the densities of these polymers. For each polymer the molar volume per structural unit has been calculated from the density.

Encouraged by the success with the rubbery polymers, we have also plotted the $V_g(298)$ values versus the molar Van der Waals volumes. The result is shown in Fig. 4.1B. Again a good linear relationship was found. The ratio $V_g(298)/V_w$ is almost identical with that for rubbery polymers; its value is 1.60 ± 0.045 (see for the numerical values Table 4.7).

4.3.4. Volume relaxation

With respect to the values of V_g mentioned it should be noted that a glassy polymer is not in thermodynamic equilibrium below its glass transition temperature T_g . Therefore glassy polymers show *volume relaxation*; the volume gradually changes with time. As amorphous glassy polymers are usually prepared by cooling at a certain rate to below T_g , this relaxation will usually be a contraction. It is a non-linear process that will continue for extremely long periods, except at temperatures in the immediate vicinity of T_g .

The values of $V_g(298)$ should therefore be considered to represent practical conditions of polymer preparation, i.e. "normal" cooling rates. It is possible to prepare glassy polymers with varying molecular volumes by varying the thermal history.

We intend to come back on the phenomenon of volume relaxation in Chap. 13, where it will be discussed and also in context of physical ageing and creep.

4.3.5. Molar volumes of crystalline polymers at 298 K

Fully crystalline polymers do not exist, except in the special case of single crystals. Therefore the density of crystalline polymers cannot be measured directly.

It is, however, possible – by means of modern X-ray analysis – to determine the crystal system of the crystalline domains and also the dimensions of the unit cell as well as the number of the constitutional base units in the unit cell. From these data the real crystalline density can be exactly calculated:

$$\rho_c = \frac{\text{Molar mass of the structural unit}}{\frac{\text{Volume of the unit cell}}{\text{Number of structural units in unit cell}}} \times N_A$$

where N_A is Avogadro's number.

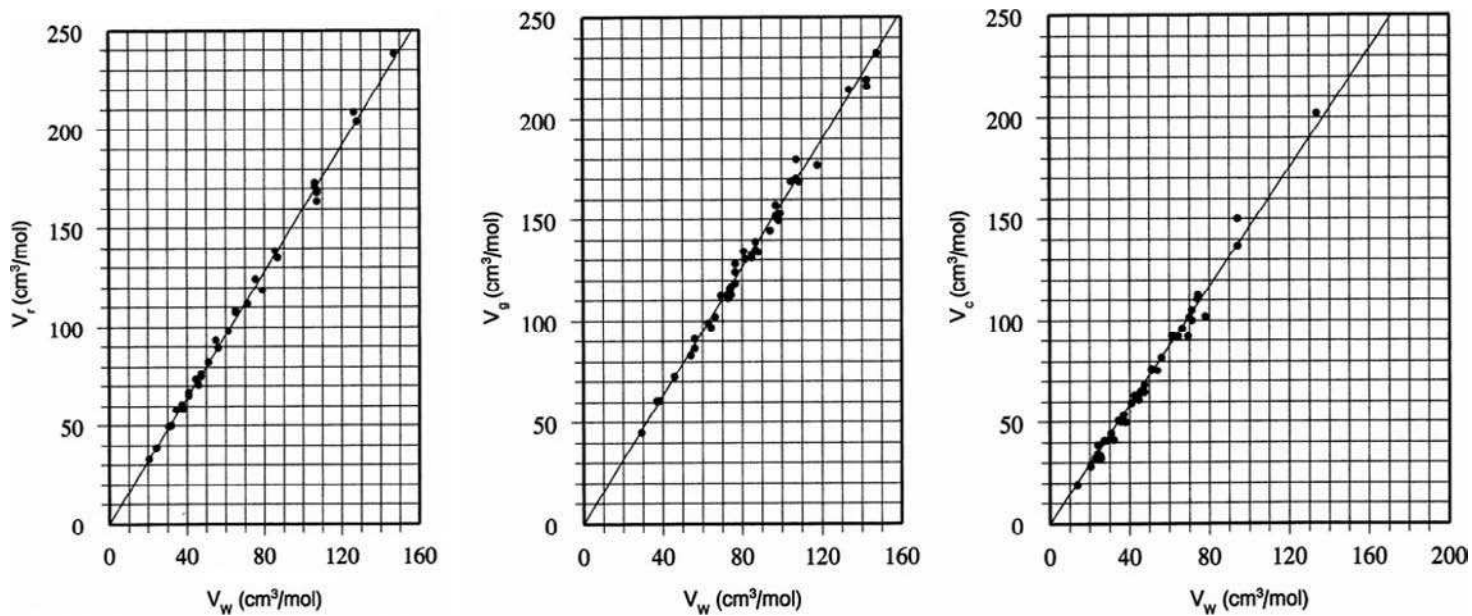


FIG. 4.1 Molar volumes, V_r , V_g and V_c , as functions of the Van der Waals volume.

TABLE 4.7 Molar volumes of glassy amorphous polymers at 25 °C

Polymer	ρ_r (g/cm ³)	V_r (cm ³ /mol)	V_w (cm ³ /mol)	V_r/V_w (-)
Poly(4-methylpentene)	0.84	100.2	61.4	1.63
Polystyrene	1.05	99.0	62.9	1.58
Poly(α -methylstyrene)	1.065	111.0	73.0	1.52
Poly(o-methylstyrene)	1.027	115.1	74.0	1.56
Poly(p-methylstyrene)	1.04	113.7	74.0	1.54
Poly(p-tert.butylstyrene)	0.95	168.7	104.6	1.61
Poly(m-trifluoromethylstyrene)	1.32	130.5	81.6	1.60
Poly(4-fluoro-2-trifluoromethylstyrene)	1.43	132.9	84.9	1.57
Poly(3-phenylpropene)	1.046	113.0	73.0	1.55
Poly(vinyl chloride)	1.385	45.1	29.2	1.54
Poly(chlorotrifluoroethylene)	1.92	60.7	36.9	1.65
Poly(3,3,3-trifluoropropylene)	1.58	60.8	38.3	1.59
Poly(vinylcyclohexane)	0.95	116.0	73.8	1.57
Poly(vinyl acetate)	1.19	72.4	45.9	1.58
Poly(vinyl chloroacetate)	1.45	83.1	54.1	1.54
Poly(tert. butyl acrylate)	1.00	128.2	76.6	1.67
Poly(methyl methacrylate)	1.17	86.5	56.1	1.54
Poly(ethyl methacrylate)	1.119	102.0	66.3	1.54
Poly(propyl methacrylate)	1.08	118.7	76.6	1.55
Poly(isopropyl methacrylate)	1.033	124.1	76.6	1.62
Poly(sec. butyl methacrylate)	1.052	135.2	86.8	1.56
Poly(tert. butyl methacrylate)	1.022	139.1	86.8	1.60
Poly(isopentyl methacrylate)	1.032	151.4	97.0	1.56
Poly(1-methylbutyl methacrylate)	1.030	151.7	97.0	1.56
Poly(neopentyl methacrylate)	0.993	157.3	97.0	1.62
Poly(1,3-dimethyl butyl methacrylate)	1.005	169.5	107.2	1.58
Poly(3,3-dimethyl butyl methacrylate)	1.001	170.1	107.2	1.59
Poly(1,2,2-trimethylpropyl methacrylate)	0.991	171.9	107.2	1.60
Poly(cyclohexyl methacrylate)	1.10	152.9	99.2	1.54
Poly(p-cyclohexylphenyl methacrylate)	1.115	219.1	142.6	1.54
Poly(phenyl methacrylate)	1.21	134.0	88.3	1.52
Poly(benzyl methacrylate)	1.179	149.5	98.5	1.52
Poly(1-phenylethyl methacrylate)	1.129	168.5	108.7	1.55
Poly(diphenylmethyl methacrylate)	1.168	216.0	142.7	1.51
Poly(1,2-diphenylethyl methacrylate)	1.147	232.2	147.7	1.57
Poly(2-chloroethyl methacrylate)	1.32	112.6	74.5	1.51
Poly(2,2,2-trifluoro-1-methylethyl methacrylate)	1.34	134.4	80.8	1.66

(continued)

TABLE 4.7 (*continued*)

Polymer	ρ_r (g/cm ³)	V_r (cm ³ /mol)	V_w (cm ³ /mol)	$V_r/V_w (-)$
Poly(1-o-chlorophenylethyl methacrylate)	1.269	177.1	117.8	1.50
Poly(ethyl chloroacrylate)	1.39	96.8	64.3	1.51
Poly(isopropyl chloroacrylate)	1.27	117.0	74.6	1.57
Poly(butyl chloroacrylate)	1.24	131.1	84.8	1.55
Poly(sec.-butyl chloroacrylate)	1.24	131.1	84.8	1.55
Poly(cyclohexyl chloroacrylate)	1.25	151.0	97.2	1.55
Poly(dimethyl phenylene oxide)	1.07	112.3	69.3	1.62
Poly(diphenyl phenylene oxide)	1.14	214.3	133.7	1.60
Polypivalolactone	1.097	91.2	56.1	1.63
poly(ethylene terephthalate)	1.33	144.5	94.2	1.53
Poly(ethylene phthalate)	1.338	143.6	94.2	1.52
Poly(ethylene isophthalate)	1.335	144.0	94.2	1.53
Poly(tetramethylene isophthalate)	1.268	173.7	114.6	1.52
Poly(cyclohexylenedimethylene terephthalate)	1.19	230.5	147.5	1.56
Nylon 6	1.084	104.4	64.2	1.63
Nylon 8	1.04	135.8	84.6	1.60
Nylon 11	1.01	181.5	115.3	1.57
Nylon 12	0.99	199.3	125.1	1.59
Nylon 6,6	1.07	211.5	128.3	1.65
Nylon 6,10	1.04	271.5	169.2	1.60
Poly(4,4-methylenediphenylene carbonate)	1.24	182.4	115.8	1.58
Poly(4,4-isopropylenediphenylene carbonate)	1.20	211.9	136.2	1.56
Poly(thiodiphenylene carbonate)	1.355	180.2	116.3	1.55
Average				1.60 ± 0.05

There remains one complication: often the polymeric crystallites may occur in several polymorphic forms (e.g. hexagonal, tetragonal, ortho-rhombic, triclinic, etc.) with somewhat different densities. In those cases we have chosen an “average” crystalline density.

Table 4.8 gives a survey of the available data on the density of fully crystalline polymers. From these densities the molar volumes $V_c(298)$ have been calculated.

Also for the crystalline state it was found that the molar volume is directly proportional to V_w (see Fig. 4.1C). The average ratio $V_c(298)/V_w$ is 1.435 ± 0.045 , as is seen in Table 4.8.

TABLE 4.8 Molar volumes of fully crystalline polymers at 25 °C (calculated from X-ray data of crystalline domains)

Polymer	ρ_r (g/cm ³)	V_r (cm ³ /mol)	V_w (cm ³ /mol)	V_r/V_w (-)
Polyethylene (linear)	1.00	28.1	20.5	1.37
Polypropylene (isotactic)	0.95	44.4	30.7	1.45
Polybutene	0.94	59.5	40.9	1.45
Poly(3-methylbutene)	0.93	75.3	51.1	1.47
Polypentene	0.92	76.3	51.1	1.49
Poly(4-methyl-pentene)	0.915	92.0	61.4	1.50
Polyhexene	0.91	92.5	61.4	1.50
Polyoctadecene	0.96	263	184.1	1.43
Polyisobutylene	0.94	59.2	40.9	1.43
Polystyrene	1.13	92.0	64.3	1.43
Poly(α -methyl styrene)	1.16	102.0	78.0	1.40
Poly(2-methyl styrene)	1.07	110.5	74.0	1.49
Poly(vinyl fluoride)	1.44	32.0	22.8	1.41
Poly(vinyl chloride)	1.52	41.0	29.2	1.40
Poly(vinylidene fluoride)	2.00	32.0	25.6	1.25
Poly(vinylidene chloride)	1.95	49.7	38.0	1.31
Poly(trifluoro-ethylene)	2.01	40.8	27.3	1.49
Poly(tetrafluoro-ethylene)	2.35	41.2	32.0	1.29
Poly(trifluoro-chloro-ethylene)	2.19	53.2	36.9	1.49
Poly(vinyl cyclohexane)	0.98	112.5	74.3	1.52
Poly(vinyl alcohol)	1.35	33.6	25.1	1.34
Poly(vinyl-methyl ether)	1.18	50.0	35.7	1.40
Poly(vinyl-methyl ketone)	1.13	62.2	43.4	1.43
Poly(vinyl acetate)	1.34	64.5	45.9	1.42
Poly(methyl methacrylate)	1.23	81.8	56.1	1.46
Poly(ethyl methacrylate)	1.19	96.0	66.3	1.45
Polyacrylonitrile (isotactic)	1.28	41.5	30.7	1.35
Poly(N-isopropyl acrylamide)	1.12	101.5	69.9	1.45
Polybutadiene	1.01	53.5	37.1	1.44
Polyisoprene(<i>cis</i>)	1.00	68.1	47.5	1.44
Polyisoprene (<i>trans</i>)	1.05	64.7	47.5	1.37
Polychloroprene (<i>trans</i>)	1.36	65.0	45.6	1.43
Poly(methylene oxide)	1.54	19.3	13.9	1.39
Poly(ethylene oxide)	1.28	34.5	24.2	1.40
Poly(tetramethylene oxide)	1.18	61.0	44.6	1.37
Poly(acetaldehyde)	1.14	38.7	24.2	1.60
Poly(propylene oxide)	1.15	50.5	34.4	1.47
Poly(trichloro propylene oxide)	1.46	63.1	42.6	1.48
Poly[2,2-bis(chloromethyl)trimethylene Oxide] (=Penton®)	1.47	105.0	71.2	1.47

(continued)

TABLE 4.8 (*continued*)

Polymer	ρ_r (g/cm ³)	V_r (cm ³ /mol)	V_w (cm ³ /mol)	V_r/V_w (-)
Poly(2,6-dimethyl-1,4-phenylene oxide)	1.31	92.0	69.3	1.33
Poly(2,6-diphenyl-1,4-phenylene oxide)	1.21	202.0	133.7	1.51
Poly(1,4-phenylene sulfide)	1.44	75.3	54.1	1.39
Poly(ethylene succinate)	1.36	100.1	71.3	1.49
Poly(ethylene isophthalate)	1.40	137.0	94.2	1.45
Poly(ethylene terephthalate)	1.48	130.0	94.2	1.38
Nylon 6	1.23	92.0	64.2	1.43
Nylon 8	1.18	120	84.6	1.42
Nylon 12	1.15	17.1	115.3	1.49
Nylon 6,6	1.24	183	128.3	1.43
Nylon 6,10	1.19	238	169.2	1.44
Poly [bis(4-amino cyclohexyl)methane-1,10 decanecarboxamide] (<i>trans</i>) (=Qiana)	1.14	388	260.0	1.49
Poly(para-phenylene terephthalamide) (=Kevlar®, Twaron®)	1.48	160	112.6	1.42
Poly[methane bis(4-phenyl)carbonate]	1.30	173	115.8	1.49
Poly[2,2-propane bis(4-phenyl)carbonate]	1.31	195	136.2	1.46
Poly[thio-bis(4-phenyl) carbonate]	1.50	170	116.3	1.46
Poly(paraxylylene)	1.2	87.5	63.8	1.39
Poly[N,N,(p,p'-oxydiphenylene) pyromellitide] (=Kapton®)	1.42	247	184.1	1.36
Poly(dimethyl-siloxane)	1.07	69.1	47.6	1.45
Poly(pivalo lactone)	1.23	81.5	56.1	1.45
Poly(methylene p-phenylene)	1.17	77.0	53.6	1.45
Average				1.435 ± 0.045

4.3.6. Molar volume of semi-crystalline polymers

For a small number of polymers, the densities of both the purely amorphous and the purely crystalline states are known. These data have been collected in Table 4.9. The ratio ρ_c/ρ_a shows a considerable variation; the mean value of this ratio is 1.13 ± 0.08 .

For the highly crystalline polymers the ratio is in the neighbourhood of 1.2, whereas for the low-crystalline polymers it is lower than 1.1.

If semi-crystalline polymers would just be a simple mixture of crystalline and amorphous domains, the following relationship would be valid (with x_c = degree of crystallinity):

$$V_{sc} = x_c V_c + (1 - x_c) V_a \quad (4.5)$$

TABLE 4.9 Data of crystalline polymers

Polymer	ρ_c (g/cm ³)	ρ_a (g/cm ³)	ρ_c/ρ_a
Polyethylene	1.00	0.85	1.18
Polypropylene	0.95	0.85	1.12
Polybutene	0.95	0.86	1.10
Polyisobutylene	0.94	0.84	1.12
Polypentene	0.92	0.85	1.08
Polystyrene	1.13	1.05	1.08
Poly(vinyl chloride)	1.52	1.39	1.10
Poly(vinylidene fluoride)	2.00	1.74	1.15
Poly(vinylidene chloride)	1.95	1.66	1.17
Poly(trifluorochloroethylene)	2.19	1.92	1.14
Poly(tetrafluoroethylene)	2.35	2.00	1.17
Poly(vinyl alcohol)	1.35	1.26	1.07
Poly(methyl methacrylate)	1.23	1.17	1.05
Polybutadiene	1.01	0.89	1.14
Polyisoprene (<i>cis</i>)	1.05	0.91	1.10
Polyisoprene (<i>trans</i>)	1.05	0.90	1.16
Polyacetylene	1.15	1.00	1.15
Poly(methylene oxide)	1.54	1.25	1.25
Poly(propylene oxide)	1.15	1.00	1.15
Poly(tetramethylene oxide)	1.18	0.98	1.20
Poly(pivalo lactone)	1.23	1.08	1.13
Poly(ethylene terephthalate)	1.50	1.33	1.13
Nylon 6	1.23	1.08	1.14
Nylon 6,6	1.24	1.07	1.16
Nylon 6,10	1.19	1.04	1.14
Poly(ethylene oxide)	1.33	1.12	1.19
Poly(bisphenol A carbonate)	1.31	1.20	1.09
Average			1.13±0.08

Substitution of the observed equations for \mathbf{V}_c and $\mathbf{V}_a(298)$ ($=\mathbf{V}_r(298) = \mathbf{V}_g(298)$) gives

$$\begin{aligned} \mathbf{V}_{sc} &= x_c 1.435 \mathbf{V}_W + (1 - x_c) 1.60 \mathbf{V}_W \\ \text{or} \quad \mathbf{V}_{sc} &= 1.60 \mathbf{V}_W [1 - (0.165/1.60)x_c] \\ \text{so} \quad \mathbf{V}_{sc} &= \mathbf{V}_a (1 - 0.103x_c) \end{aligned} \quad (4.6)$$

with the final result

$$\rho_{sc}/\rho_a = \mathbf{V}_a/\mathbf{V}_{sc} = 1/(1 - 0.103x_c) \quad (4.7)$$

This would imply $\rho_c/\rho_a = 1.115$. The variable value 1.13 ± 0.08 confirms the fact that crystallites disturb the structure of the amorphous state, as was mentioned in Chap. 2.

4.3.7. Summary of the correlations between the various molar volumes

The following mean values for the molar volume ratios have been found:

$$\frac{V_r(298)}{V_W} = 1.60 \quad \left. \begin{array}{l} \\ \end{array} \right\} = \frac{V_a(298)}{V_W} \quad (4.8a)$$

$$\frac{V_g(298)}{V_W} \approx 1.6 \quad \left. \begin{array}{l} \\ \end{array} \right\} = \frac{V_a(298)}{V_W} \quad (4.8b)$$

$$\frac{V_c(298)}{V_W} = 1.435 \quad (4.8c)$$

$$\frac{V_{sc}(298)}{V_W} \approx 1.60 - 0.165x_c \quad (4.8d)$$

Since the value of the molar Van der Waals volume of a polymer is derived from universal values of atomic radii and atomic distances, it may be concluded that the method of calculation of the different standard molar volumes (1298 K) as given by Eq. (4.8) provides a sound basis for the estimation of polymer densities under standard conditions.

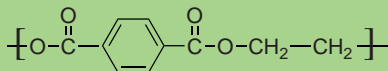
Table 4.10 gives our recommended values for the group contributions (increments) to the various molar volumes at 298 K.

Example 4.1

Estimate the densities of amorphous and crystalline poly(ethylene terephthalate).

Solution

The structural unit is



The molecular weight of this structural unit is 192.2. At room temperature, amorphous poly(ethylene terephthalate) is in the glassy state. The following group contributions may be taken from Table 4.10:

Groups	$V_g(298)$	V_c
1 ($-C_6H_4-$)	65.5	59
2 ($-COO-$)	46.0	43
2 ($-CH_2-$)	32.7	29.4
	144.2	131.4

So $\rho_c(298) = 192.2/144.2 = 1.33 \text{ g/cm}^3$.

This is a good agreement with the experimental value

$\rho_g(298) = 1.33 \text{ g/cm}^3$.

For ρ_g we calculate:

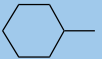
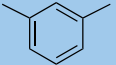
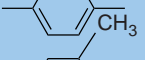
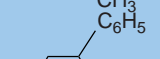
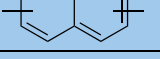
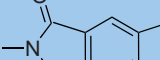
$\rho_c = 192.2/131.4 = 1.465$, in agreement with the experimental value 1.477.

The ratio ρ_c/ρ_a becomes

$$\frac{\rho_c(298)(\text{calc.})}{\rho_g(298)(\text{calc.})} = \frac{1.465}{1.33} = 1.10$$

in good agreement with Eq. (4.7)

TABLE 4.10 Recommended values for molar volume increments at 298 K

Groups (Bivalent)	$V_{a,i}(298)$ (cm ³ /mol)	$V_{c,i}(298)$ (cm ³ /mol)	Groups	$V_{a,i}(298)$ (cm ³ /mol)	$V_{c,i}(298)$ (cm ³ /mol)
-CH ₂ -	16.37	14.68	-SO ₂ -	(32.5)	(29)
-CH(CH ₃)-	32.72	29.35	-CO- al	13.5	12.25
-CH(i-C ₃ H ₇)-	65.44	58.69	ar	18.5	16.8
-CH(t-C ₄ H ₉)-	81.79	73.36	-COO- general	23	21.5
-CH(C ₆ H ₁₁)-	101.76	91.27	acrylics	20.5	18.4
-CH(C ₆ H ₅)-	84.16	75.48	-OCOO-	31	27
-CH(p-C ₆ H ₄ CH ₃)-	102.1	91.55	-CONH-	(21)	(18.7)
-CH(OH)-	22.3	20	-OCONH-	(29)	(26)
-CH(OCH ₃)-	40.8	36.6	-NHCONH-	(29)	(26)
-CH(OCOCH ₃)-	52.4	47	-Si(CH ₃) ₂ -	67.5	60.6
-CH(COOCH ₃)-	56.85	51		86	(77)
-CH(CN)-	30.7	27.5		69	62
-CHF-	20.0	18		65.5	59
-CHCl-	30	27.3		104	94
-C(CH ₃) ₂ -	49.0	44.0			
-C(CH ₃)(C ₆ H ₅)-	100.5	90			
-C(CH ₃)(COOCH ₃)-	74.7	67			
-CF ₂ -	23.7	21			
-CFCl-	33.6	30			
-CCl ₂ -	40.1	36			
-CH=CH-	27.0	24.3			
-CH=C(CH ₃)- { <i>cis</i>	43	40			
{ <i>trans</i>	43	37			
-CH=CCl-	41	37			
-C≡C-	25	23			
-O- al	(8.5)	(7.9)			
ar	(8.0)	(7.1)			
-NH-	(6.4)	(5.7)			
-S-	17.3	15.5			
-S-S-	36	32.5			

4.4. THERMAL EXPANSION

4.4.1. Definitions

A number of different but related notations are used to describe the thermal expansion of matter:

1. The specific thermal expansivity:

$$e \equiv \left(\frac{\partial V}{\partial T} \right)_p \quad (\text{dimension: cm}^3/\text{g/K or m}^3/\text{kg/K})$$

2. The temperature coefficient of density:

$$q \equiv \left(\frac{\partial \rho}{\partial T} \right)_p \quad (\text{dimension: cm}^3/\text{g/K or m}^3/\text{kg/K})$$

3. The coefficient of thermal expansion:

$$\alpha \equiv \frac{1}{V} \left(\frac{\partial V}{\partial T} \right)_p \quad (\text{dimension: K}^{-1})$$

4. The linear coefficient of thermal expansion:

$$\beta \equiv \frac{1}{L} \left(\frac{\partial L}{\partial T} \right)_p \quad (\text{dimension: K}^{-1})$$

5. The molar thermal expansivity:

$$E \equiv \left(\frac{\partial V}{\partial T} \right)_p \quad (\text{dimension: cm}^3/\text{mol/K or m}^3/\text{mol/K})$$

The quantities are interrelated in the following way:

$$\left. \begin{aligned} e &= -V^2 q & e &= \alpha V = \frac{\alpha}{\rho} & \alpha &= 3\beta \\ q &= -e\rho^2 & q &= -\alpha\rho = -\frac{\alpha}{V} & E &= M e = \alpha V = \alpha \frac{M}{\rho} \end{aligned} \right\} \quad (4.9)$$

4.4.2. Phenomenology

Experimental data available suggest that the thermal expansivity of a glass is of the same order as that of the crystal and that no great error is made by putting:

$$\alpha_g \approx \alpha_c \quad \text{or} \quad e_g \approx e_c \quad \text{or} \quad E_g \approx E_c \quad (4.10)$$

The expansivity of a solid polymer is not exactly independent of temperature, but generally shows a gradual increase with temperature (perceptible if the temperature range covered is large). However, it is convenient to ignore this gradual increase compared with the jump in expansivity on passing through the glass transition, and to represent the volume-temperature curve by two straight lines intersecting at the transition point.

It is common practice to report the expansivities immediately below (e_g) and above (e_l) the transition.

TABLE 4.11 Some empirical rules

Rule	Proposed by	Equations
$\alpha_l - \alpha_g \approx 5 \times 10^{-4} \text{ K}^{-1}$	Tobolsky/Bueche (1960/1962)	(4.11)
$\alpha_l T_g \approx 0.16$	Boyer and Spencer (1944)	(4.12)
$\alpha_c T_m \approx 0.11$	Bondi (1968d)	(4.13)
$(\alpha_l - \alpha_g) T_g \approx 0.115$	Simha and Boyer (1962)	(4.14)

Empirically it has been found that often q ($= -\alpha\rho = -e\rho^2$) is practically independent of temperature over a wide range (see Bondi, 1968c).

The expansivity of the rubbery or liquid polymer is always larger than that of the glassy or crystalline polymer.

A number of interesting rules are summarised in Table 4.11. It has to be mentioned, however, that these rules are approximate rules and that they are not to be used to find new equations by substitution of the one in the other!

4.4.3. Theory

The expansion of a material on heating is a phenomenon that depends on internal – mostly intermolecular – forces. Bond lengths between atoms are virtually independent of temperature. This also holds for bond lengths between segments of a polymer chain. Polymer systems, therefore, have lower expansivities than related low-molecular liquids.

Below the glass temperature the expansivity is reduced still further. When passing the glass transition point, the structural changes contributing to the expansion in liquids disappear.

4.4.4. The molar thermal expansion model of polymers (MTE-model)

One of the most useful – though simplified – models to visualise thermal expansion phenomena is based on a concept of Simha and Boyer, and is reproduced in Fig. 4.2. When a liquid is cooled below a potential crystalline melting temperature, two things may happen: it either crystallises or becomes an undercooled liquid; the latter occurs when crystallisation is impeded, e.g. by high viscosity and low molecular symmetry. From Fig. 4.2. it follows that $V_l(0) = V_c(0)$ and $dV_g/dT \approx dV_c/dT$. Undercooling of the liquid may occur until a temperature is reached at which the free volume of the molecules becomes so small that molecular movements of the whole molecule or of large chain segments are no longer possible: then the glassy state is reached. The temperature at which this occurs is the glass transition temperature (T_g).

4.4.5. Inferences from the thermal expansion model

4.4.5.1. Numerical values of the molar thermal expansivities

On the basis of Fig. 4.2 some simple relationships may be derived. From Fig. 4.2 it is obvious that

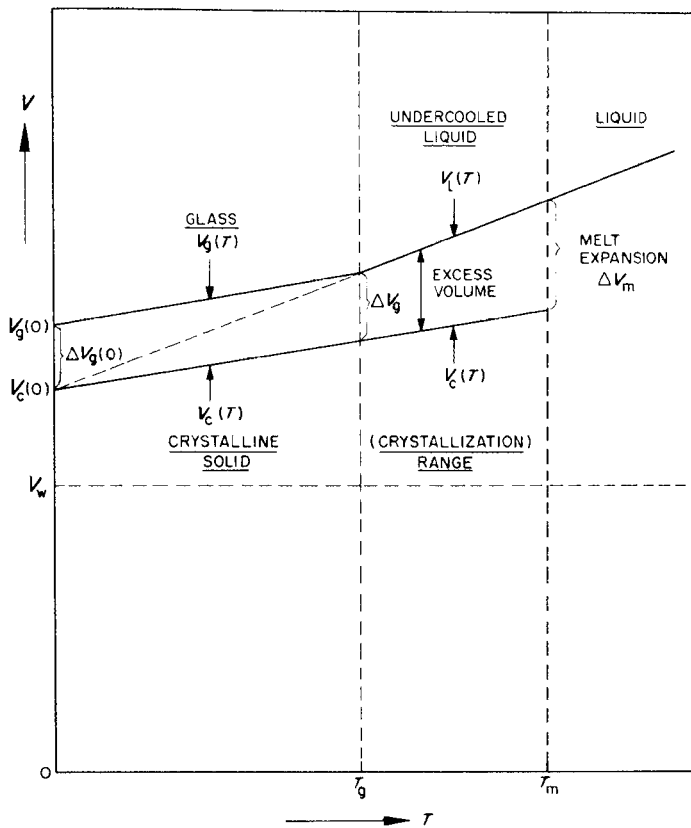


FIG. 4.2 Thermal expansion model of polymers (based on a concept of Simha and Boyer, 1962).

$$E_l = \frac{V_l(T) - V_l(0)}{T} = \frac{V_l(298) - V_c(0)}{298} \approx \frac{V_r(298) - V_c(0)}{298} = E_r \quad (4.15)$$

Likewise

$$E_g = \frac{V_g(T) - V_g(0)}{T} \approx \frac{V_c(T) - V_c(0)}{T} = \frac{V_c(298) - V_c(0)}{298} = E_c \quad (4.16)$$

Values of $E_l (= E_r)$ and $E_g (= E_c)$ are assembled in Table 4.12. Upon plotting these values against V_w , we obtain an interesting result, as shown in Fig. 4.3. Although there is a considerable amount of scatter, the relationship between E_l , E_g and V_w is evident and may approximately be represented by two straight lines, corresponding to the following mean values for the coefficients:

$$E_l (= E_r) = 1.00 \times 10^{-3} V_w \quad (4.17)$$

$$E_g (= E_c) = 0.45 \times 10^{-3} V_w \quad (4.18)$$

Eqs. (4.17) and (4.18) enable us to calculate the numerical values of the molar expansion coefficients. In Table 4.12 the values calculated in this way are compared with the experimental values. The agreement is fair (average deviation for E_l 8% and for

TABLE 4.12 Thermal expansivity of polymers

Polymer	M (g/mol)	V_w (cm ³ /mol)	e_g exp. (10 ⁻⁴ cm ³ /g/K)	e_l exp. (10 ⁻⁴ cm ³ /g/K)	E_g exp. (10 ⁻⁴ cm ³ /mol/K)
Polyethylene	28.0	20.46	2.4/3.6	7.5/9.6	67/101
Polypropylene	42.1	30.68	2.2	5.5/9.4	93
Poly(1-butene)	56.1	40.91	3.8	8.8	214
Poly(1-pentene)	70.1	51.14	—	9.2	—
Polyisobutylene	56.1	40.90	1.6/2.0	5.6/6.9	90/112
Poly(4-methyl-1-pentene)	84.2	61.36	3.85	7.6	324
Polystyrene	104.1	62.85	1.7/2.7	4.3/6.8	177/281
Poly(vinyl chloride)	62.5	29.23	1.4/2.1	4.2/5.2	88/131
Poly(vinylidene fluoride)	64.0	25.56	1.2	2.1/4.6	77
Poly(chlorotrifluoroethylene)	116.5	36.90	1.0/1.5	2.0/3.5	117/175
Poly(vinyl alcohol)	44.0	25.05	3.0	—	132
Poly(vinyl acetate)	86.1	45.88	1.8/2.3	5.0/6.0	155/198
Poly(methyl acrylate)	86.1	45.88	1.8/2.7	4.6/5.6	155/232
Poly(ethyl acrylate)	100.1	56.11	2.8	6.1	280
Poly(isopropyl acrylate)	114.2	66.33	2.2/2.6	6.1/6.3	251/297
Poly(butyl acrylate)	128.2	76.57	2.6	6.0	333
Poly(sec-butyl acrylate)	128.2	76.56	2.75	6.1	353
Poly(2,2-dimethylpropyl acrylate)	142.2	86.78	2.0	6.5	284
Poly(1-ethylpropyl acrylate)	142.2	86.79	3.3	5.9	469
Poly(methyl methacrylate)	100.1	56.10	2.3	5.2/5.5	230
Poly(ethyl methacrylate)	114.1	66.33	2.8	5.4/5.7	319
Poly(propyl methacrylate)	128.2	76.56	3.15	5.8	404
Poly(isopropyl methacrylate)	128.2	76.55	2.0/2.4	6.2	256/308
Poly(butyl methacrylate)	142.2	86.79	—	5.9/6.3	—
Poly(isobutyl methacrylate)	142.2	86.78	2.2/2.5	5.8/6.1	313/356
Poly(sec-butyl methacrylate)	142.2	86.78	3.4	6.3	483
Poly(tert-butyl methacrylate)	142.2	86.77	2.7	6.9	384
Poly(hexyl methacrylate)	170.3	107.25	—	6.3/6.6	—
Poly(2-ethylbutyl methacrylate)	170.3	107.24	—	5.8	—
Poly(octyl methacrylate)	198.4	127.71	—	5.8	—
Poly(dodecyl methacrylate)	254.4	168.63	3.8	6.8	967
Poly(2-methoxyethyl methacrylate)	144.2	80.26	—	5.45	—
Poly(2-propoxyethyl methacrylate)	172.2	100.72	—	6.1	—
Poly(cyclohexyl methacrylate)	168.2	99.23	2.7	—	454
Polybutadiene	54.1	37.40	2.0	6.4/7.7	108
Polyisoprene	68.1	47.61	—	6.0/8.3	—
Polychloroprene	88.5	45.56	—	4.2/5.0	—
Polyformaldehyde	30.0	13.93	1.8	—	54
Poly(ethylene oxide)	44.1	24.16	—	6.2/6.6	—
Poly(tetramethylene oxide)	72.1	44.62	—	6.9	—
Polyacetaldehyde	44.1	24.15	2.1	6.3	93
Poly(propylene oxide)	58.1	34.38	—	7.0/7.3	—
Polyepichlorohydrin	92.5	42.56	—	5.6	—

E_g calc. (10^{-4} cm 3 / mol/K)	E_l exp. (10^{-4} cm 3 / mol/K)	E_l calc. (10^{-4} cm 3 / mol/K)	$e_l - e_g$ (10^{-4} cm 3 /g/K)	T_g (K)	ρ (g/cm 3)	$(\alpha_l - \alpha_g)T_g$ ($\times 10^4$)
92	210/269	205	3.9/7.2	195	0.87	660/1220
138	232/396	307	3.3/7.2	263	0.85	740/1610
184	494	409	5.0	249	0.85	1060
230	645	511	—	—	—	—
184	314/388	409	3.6/5.3	198	0.87	620/910
276	640	614	3.75	302	0.84	950
283	448/708	629	2.6/5.1	373	1.06	1030/2020
132	262/325	292	2.1/3.8	358	1.38	1040/1880
115	134/294	256	0.9/3.4	235	1.74	370/1390
166	233/408	369	0.5/2.5	325	2.03	330/1650
113	—	251	—	—	—	—
206	413/517	459	2.7/4.2	303	1.19	970/1510
206	396/482	459	1.9/3.8	282	1.22	650/1310
252	611	561	3.3	252	1.12	930
298	697/719	663	3.5/4.1	270	1.08	1020/1190
345	769	766	3.4	224	1.08	820
345	782	766	3.35	256	1.05	900
391	924	868	4.5	295	1.04	1380
391	839	868	2.6	267	1.04	720
252	520/550	561	2.9/3.2	387	1.17	1310/1450
298	616/650	663	2.6/2.9	339	1.12	990/1100
345	744	766	2.65	310	1.08	890
345	795	766	3.8/4.2	354	1.04	1400/1540
391	839/896	868	—	—	—	—
391	825/867	868	3.3/3.9	320	1.04	1100/1300
391	896	868	2.9	333	1.04	1000
390	981	868	4.2	380	1.03	1640
483	1073/1124	1073	—	—	—	—
483	988	1072	—	—	—	—
575	1151	1277	—	—	—	—
759	1730	1686	3.0	218	0.93	610
361	786	803	—	—	—	—
453	1050	1007	—	—	—	—
447	—	992	—	—	—	—
168	346/417	374	4.4/5.7	171/259	0.89	670/1310
214	409/565	476	—	—	—	—
205	372/443	456	—	—	—	—
63	—	139	—	—	—	—
109	273/291	242	—	—	—	—
201	497	446	—	—	—	—
109	278	242	4.2	243	1.07	1090
155	407/424	344	—	—	—	—
192	518	426	—	—	—	—

(continued)

TABLE 4.12 (continued)

Polymer	M (g/mol)	V_w (cm ³ /mol)	e_g exp. (10 ⁻⁴ cm ³ /g/K)	e_l exp. (10 ⁻⁴ cm ³ /g/K)	E_g exp. (10 ⁻⁴ cm ³ /mol/K)
Poly(ethylene terephthalate)	192.2	94.18	2.2/2.4	6.0/7.4	423/461
Poly(decamethylene terephthalate)	304.4	176.02	—	5.3	—
Poly(ethylene phthalate)	192.2	94.18	1.7	5.9	327
Poly(ethylene isophthalate)	192.2	94.18	2.0	3.8/5.3	384
Poly[ethylene (2,6-naphthalate)]	242.2	119.86	—	4.9	—
Poly[ethylene (2,7-naphthalate)]	242.2	119.86	—	5.0	—
Nylon 6	113.2	70.71	—	5.6	—
Nylon 7	127.2	80.94	3.5	—	445
Nylon 8	141.2	91.17	3.1	—	438
Nylon 9	155.2	101.40	3.6	—	559
Nylon 10	169.3	111.63	3.5	—	593
Nylon 11	183.3	121.86	3.6	—	660
Nylon 12	197.3	132.09	3.8	—	750
Nylon 10,9	324.5	213.03	—	6.6	—
Nylon 10,10	338.5	223.26	—	6.7	—
Poly(bisphenol carbonate)	254.3	136.21	2.4/2.9	4.8/5.9	610/737

E_g 12%) in view of the fact that the accuracy of the experimental data will also be in the order of $\pm 5\%$.

4.4.5.2. The excess volume of the glassy state

The difference in molar volume of the two solid states of the polymer: the glassy and the crystalline states, is called "excess volume":

$$\Delta V_g = V_g(T) - V_c(T) \quad (4.19)$$

Since the thermal expansivity of the two solid states is equal ($E_g \approx E_c$) it may be presumed that ΔV_g is constant in the whole temperature region below the glass transition, which means:

$$\Delta V_g(0) = \Delta V_g(T \leq T_g) = \Delta V_g(T_g) \quad (4.20)$$

The numerical value of ΔV_g can easily be calculated; since at T_g the molar volumes of the glassy and the liquid state (melt) are equal, so $V_c(T_g) = V_g(T_g)$,

or

$$V_c(0) + E_l T_g = V_g(0) + E_g T_g$$

$$\text{Hence } \Delta V_g = (E_l - E_g)T_g = (1.0 - 0.45) \times 10^{-3} V_w T_g$$

so that

$$\Delta V_g = 0.55 \times 10^{-3} V_w T_g \quad (4.21)$$

E_g calc. (10^{-4} cm 3 / mol/K)	E_l exp. (10^{-4} cm 3 / mol/K)	E_l calc. (10^{-4} cm 3 / mol/K)	$e_l - e_g$ (10^{-4} cm 3 /g/K)	T_g (K)	ρ (g/cm 3)	$(\alpha_l - \alpha_g)T_g$ ($\times 10^4$)
424	1153/1422	942	3.6/5.2	342	1.33	1640/2360
792	1613	1760	—	—	—	—
424	1134	942	4.2	290	1.34	1630
424	730/1019	942	1.8/3.3	324	1.34	780/1430
539	1187	1199	—	—	—	—
539	1211	1199	—	—	—	—
318	634	707	—	—	—	—
364	—	809	—	—	—	—
410	—	912	—	—	—	—
456	—	1014	—	—	—	—
502	—	1116	—	—	—	—
548	—	1219	—	—	—	—
594	—	1321	—	—	—	—
959	2142	2130	—	—	—	—
1005	2268	2233	—	—	—	—
613	1220/1500	1362	1.9/3.5	423	1.20	960/1780

4.4.5.3. Derivation of the basic volume ratios from the MTE model

The numerical values of the molar expansion coefficients provide an independent method to derive the basic volume ratios. We have seen already that $V_c(0) \approx 1.30V_W$ (Eq. (4.2)). Substitution of the Eqs. (4.2), (4.17) and (4.18) in (4.15) and (4.16) gives

$$\frac{V_r(298) - 1.30V_W}{298} = E_r = 1.0 \times 10^{-3}V_W \quad (4.22)$$

$$\frac{V_c(298) - 1.30V_W}{298} = E_c = 0.45 \times 10^{-3}V_W \quad (4.23)$$

which leads to

$$V_r(298) = 1.60V_W \quad (4.24)$$

$$V_c(298) = 1.435V_W \quad (4.25)$$

These equations are identical with (4.8a) and (4.8c). The equivalent expression for $V_g(298)$ is derived as follows.

$$E_g = \frac{V_g(298) - V_g(0)}{298} = \frac{V_g(298) - (V_c(0) + \Delta V_g)}{298} = 0.45 \times 10^{-3}V_W \quad (4.26)$$

Substitution of ΔV_g (Eq. (4.18)) gives, after some arrangement,

$$V_g(298) = [1.43 + 0.55 \times 10^{-3}T_g]V_W \quad (4.27)$$

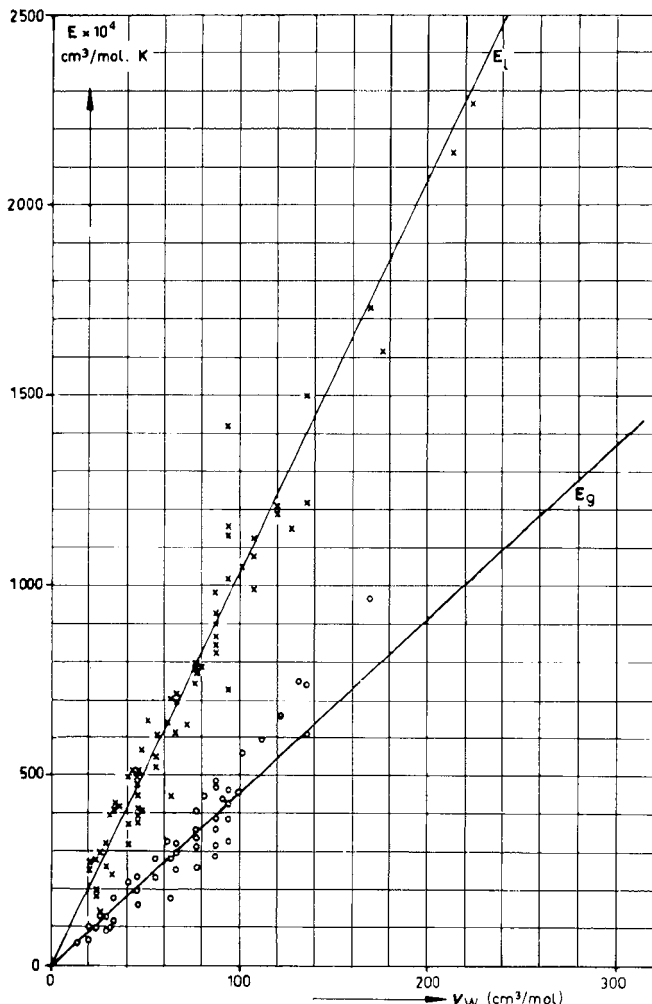


FIG. 4.3 E_l and E_g as functions of V_W .

or

$$V_g(298) = [1.43 + C(T_g)]V_W \quad (4.28)$$

where

$$\begin{aligned} C(T_g) &= 0.165 \text{ at } T_g = 300 \text{ K} & V_g(298) &= 1.595V_W \\ &= 0.220 \text{ at } T_g = 400 \text{ K} & V_g(298) &= 1.650V_W \\ &= 0.275 \text{ at } T_g = 500 \text{ K} & V_g(298) &= 1.705V_W \end{aligned}$$

Earlier we derived from density data

$$V_g(298) = 1.6V_W \quad (4.8b)$$

Compared with Eq. (4.27) this is on the low side; for, e.g. PMMA ($T_g = 387 \text{ K}$) and PS ($T_g = 373 \text{ K}$) Eq. (4.27) yields $V_g(298)/V_W = 1.643$ and 1.635 , respectively. The reason may be twofold. First of all, the T_g 's of the polymers in Table 4.12 are in majority between 300 and 400 K . Secondly, it may be that a number of these glassy amorphous polymers

(which are thermodynamically unstable) have already undergone some volume relaxation at the time of the density measurement.

Summing up we may say that the ratios V_r/V_W , V_g/V_W and V_c/V_W have been derived in two independent ways from quite different experimental data, densities and thermal expansion coefficients respectively.

At the same time we may consider the mutual agreement as a verification of the quantitative applicability of the molar thermal expansion model, given in Fig. 4.2.

4.4.5.4. General expressions for the molar volumes as a function of temperature

We first summarise the basic volumetric correlations:

$$\begin{aligned} V_c(0) &= V_l(0) = 1.30V_W \\ V_r(298) &= 1.60V_W & E_r = E_l = 1.0 \times 10^{-3}V_W \\ V_g(298) &\approx 1.6V_W \\ V_c(298) &= 1.435V_W & E_c = E_g = 0.45 \times 10^{-3}V_W \end{aligned} \quad (4.29)$$

From these values the following general expressions for the molar volumes as a function of temperature have been derived:

$$\begin{aligned} V_r(T) &= V_l(T) = V_r(298) + E_l(T - 298) \\ &\approx V_r(298)[1 + 0.625 \times 10^{-3}(T - 298)] = V_r(298)[0.81 + 0.625 \times 10^{-3}T] \\ &\approx V_W[1.60 + 10^{-3}(T - 298)] = V_W[1.30 + 10^{-3}T] \\ V_g(T) &= V_g(298) + E_g(T - 298) = V_g(298) + E_c(T - 298) \\ &= V_W[1.30 + 0.55 \times 10^{-3}T_g + 0.45 \times 10^{-3}T] \\ V_c(T) &= V_c(298) + E_c(T - 298) \\ &\approx V_c(298)[1 + 0.31 \times 10^{-3}(T - 298)] = V_c(298)[0.907 + 0.31 \times 10^{-3}T] \\ &\approx V_W[1.435 + 0.45 \times 10^{-3}(T - 298)] = V_W[1.30 + 0.45 \times 10^{-3}T] \end{aligned} \quad (4.30)$$

A nice illustration of the value and usefulness of the Eqs. (4.29) and (4.30), in estimating and predicting molar volumes, is shown in Fig. 4.4. This figure was kindly forwarded by Professor R.S.Porter (Amherst).

4.4.5.5. Melting expansion

A quantity that is important both practically and theoretically is the increase in molar volume accompanying the melting process:

$$\Delta V_m = V_l(T_m) - V_c(T_m) \quad (4.31)$$

If it is assumed that Fig. 4.2 is valid up to the melting point, ΔV_m can be calculated if ρ_a , ρ_c , E_l and E_c are known. If one of these data is lacking, it can be estimated with the methods given in this chapter. (Calculation 1, using Eq. (4.30)).

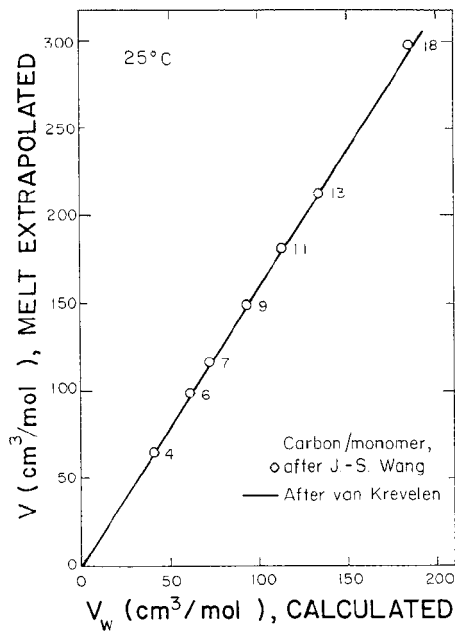


FIG. 4.4 Extrapolated V_l values versus V_w for polyolefins.

The numerical value of ΔV_m can be derived directly from Fig. 4.2 (calculation 2):

$$\Delta V_g / \Delta V_m = T_g / T_m$$

Hence

$$\begin{aligned} E_g (= E_c) &= 0.45 \times 10^{-3} V_W \\ \Delta V_m &= \Delta V_g \frac{T_m}{T_g} = 0.55 \times 10^{-3} V_W T_g \frac{T_m}{T_g} \end{aligned}$$

or

$$\Delta V_m = 0.55 \times 10^{-3} V_W T_m \quad (4.32)$$

Another approximation is via the Eqs. (4.8a)–(4.8c)

$$V_l(298) = V_r(298) = 1.6 V_W; \quad V_c(298) = 1.435 V_W$$

and

$$\frac{V_l(298) - V_c(298)}{298} = \frac{\Delta V_m}{T_m} \quad (\text{from Fig. 4.2.})$$

Substitution gives

$$\frac{0.165}{298} V_W = 0.55 \times 10^{-3} V_W = \frac{\Delta V_m}{T_m}$$

TABLE 4.13 Calculated and experimental values of ΔV_m

Polymer	ΔV_m (cm^3/mol)				References
	Calc. (1) Eq. (4.30)	Calc. (2) Eq. (4.32)	Found		
Polyethylene	6	4.7	3.1/5.9		Starkweather and Boyd (1960)/Robertson (1969)
Polypropylene	8	7.7	9.6		Allen (1964)
Polybutene	9	8.6	8.4		Allen (1964)
Poly(4-methyl pentene)	16	17.4	9.8		Kirshenbaum (1965)
Polyisobutylene	8	6.3	6.7		Allen (1964)
Polystyrene	12	18.3	11.4		Allen (1964)
Poly(tetrafluoroethylene)	11	10.4	7.3/14.5		Starkweather and Boyd (1960)/Allen (1964)
Polyformaldehyde	6	3.7	3.5/5.1		Starkweather and Boyd (1960)/Fortune and Malcolm (1960)
Poly(ethylene oxide)	6	4.5	5.3		Allen (1964)
Poly(ethylene terephthalate)	25	28.8	11.5/16.9		Allen (1964)
Nylon 6,6	44	42	24.8		Allen (1964)

In Table 4.13 values of ΔV_m , calculated according to both methods, are compared with published experimental values. The only conclusion that can be drawn is that the calculated values of ΔV_m are of the correct order of magnitude. The deviations between calculated and experimental values do not exceed the deviations between values mentioned by different investigators.

4.4.5.6. Derivation of the empirical rules from the model

The simple model of Fig. 4.2 may also be used to derive relationships equivalent with Eqs. (4.11)–(4.14) mentioned above.

a. The Tobolski–Bueche rule. Eq. (4.11)

If $E_l = 10.0 \times 10^{-4}V_W$; $E_g = 4.5 \times 10^{-4}V_W$; $V_r(298) = 1.60V_W$ and $V_g(298) \approx 1.6V_W$:

$$\alpha_l(298) = \frac{E_l}{V_l(298)} = \frac{1.0 \times 10^{-3}V_W}{1.60V_W} = 6.25 \times 10^{-4}\text{K}^{-1}$$

$$\alpha_g(298) = \frac{E_g}{V_g(298)} \approx \frac{0.45 \times 10^{-3}V_W}{1.60V_W} = 2.81 \times 10^{-4}\text{K}^{-1}$$

and

$$\alpha_l(298) - \alpha_g(298) \approx 3.5 \times 10^{-4}\text{K}^{-1} \quad (4.11a)$$

Eq. (4.11a) corresponds to the Tobolsky–Bueche equation, Eq. (4.11), except for the much smaller coefficient (i.e. 3.5 versus 5).

b. The Simha–Boyer rule. Eq. (4.14)

The Simha–Boyer rule may be derived if it is assumed that the *fractional excess volume* φ_e at T_g is a universal constant for all polymers. In this case we have

$$\mathbf{V}_l(T_g) = \mathbf{V}_c(0) + \mathbf{E}_l T_g$$

$$\mathbf{V}_g(T_g) = \mathbf{V}_g(0) + \mathbf{E}_g T_g$$

Since at T_g , $\mathbf{V}_l = \mathbf{V}_g$, there results

$$(\mathbf{E}_l - \mathbf{E}_g)T_g = \mathbf{V}_c(0) - \mathbf{V}_g(0) = \Delta\mathbf{V}_g(0) = \Delta\mathbf{V}_g$$

$$\frac{(\mathbf{E}_l - \mathbf{E}_g)T_g}{\mathbf{V}_g(T_g)} = \frac{\mathbf{E}_l T_g}{\mathbf{V}_l(T_g)} - \frac{\mathbf{E}_g T_g}{\mathbf{V}_g(T_g)} = \frac{\Delta\mathbf{V}_g}{\mathbf{V}_g(T_g)} = \varphi_e = \text{const.}$$

so that

$$\frac{(\mathbf{E}_l - \mathbf{E}_g)T_g}{\mathbf{V}_g(T_g)} = (\alpha_l - \alpha_g)T_g = \varphi_e = \text{const.} \quad (4.33)$$

In Table 4.12 Eq. (4.33) is confronted with the available experimental data. The mean value of $\varphi_c = 0.115$ (with a mean deviation of 37%). This is in good correspondence with the value $\varphi_e = 0.115$ proposed by Simha and Boyer.

c. The Boyer–Spencer rule. Eq. (4.12)

In Sect. 4.4.5.6(a) we derived numerical values for $\alpha_l(298)$ and $\alpha_g(298)$; so $\alpha_g/\alpha_l = 0.45$. Substitution of this value in (4.33) leads to

$$(\alpha_l - \alpha_g)T_g = 0.11$$

So $\alpha_l T_g \approx 0.2$, which is very approximately the Boyer–Spencer rule.

d. The Bondi rule. Eq. (4.13)

The Bondi rule is related to the Boyer–Spencer rule (Eq. (4.12)). Since $\alpha_g/\alpha_l = \alpha_c/\alpha_l = 0.45$, substitution of this expression in Eq. (4.12) gives

$$\alpha_l T_g = \frac{\alpha_c}{0.45} T_g = 0.16$$

For semi-crystalline polymers T_g is normally about $2/3 T_m$ so that

$$\frac{\alpha_c}{0.45} 0.667 T_m = 0.16$$

or

$$\alpha_c T_m = \frac{0.45 \times 0.16}{0.667} = 0.11$$

Example 4.2

Estimate the expansion coefficient of the poly(ethylene terephthalate) melt and its density at the extrusion temperature of 277 °C (=550 K).

Solution

Application of Eqs. (4.17) and (4.18) gives for the molar thermal expansivity:

$$E_g = E_c = 4.5 \times 10^{-4} V_W = 4.5 \times 94.18 \times 10^{-4} = 4.2 \times 10^{-2}$$

$$E_l = 10.0 \times 10^{-4} V_W = 10.0 \times 94.18 \times 10^{-4} = 9.4 \times 10^{-2}$$

So with $T_g = 343$ K, the molar volume of the melt at 550 K will be

$$\begin{aligned} V_l(550) &= V_g(298) + E_g(T_g - 298) + E_l(550 - T_g) \\ &= 143.2 + 4.2 \times 10^{-2} \times 45 + 9.4 \times 10^{-2} \times 207 = 164.5 \end{aligned}$$

This results in

$$\rho_l(550) = \frac{192.2}{164.5} = 1.17 \text{ g/cm}^3$$

which is in excellent agreement with the experimental value of 1.16 (determination in the late Prof. van Krevelen's laboratory).

The thermal expansion coefficients follow from the definitions for the specific thermal expansivity:

$$e_l = \frac{E_l}{M} = \frac{9.4 \times 10^{-2}}{192.2} = 4.9 \times 10^{-4} \text{ cm}^3/\text{g/K}$$

$$e_g = \frac{E_g}{M} = \frac{4.2 \times 10^{-2}}{192.2} = 2.2 \times 10^{-4} \text{ cm}^3/\text{g/K}.$$

The average literature values are 6×10^{-4} and 2.3×10^{-4} , respectively, which is in very satisfactory agreement with the calculated values.

4.5. ISOTHERMAL COMPRESSION: EQUATIONS OF STATE

Besides the volume increase by thermal expansion also the volume reduction by compression is an important data for the processing of polymers.

4.5.1. The Tait equation

One of the most useful expressions to represent the $V(P,T)$ -behaviour of liquids, including polymeric liquids, is the Tait-relation (Tait 1888, 1898 and Dorsey 1940):

$$\frac{V(0, T) - V(p, T)}{V(0, T)} = C \ln \left(1 + \frac{p}{B(T)} \right) \quad (4.34)$$

where C is a dimensionless constant and $B(T)$ is a temperature dependent constant with the same dimension as pressure. For practical calculations $V(0, T)$ may be approximated by $V(T, p = 1 \text{ bar})$.

This purely empirical relation was derived by Tait as long ago as 1888; it is still one of the best approximations of the actual *PVT*-behaviour. Reference is usually made to the voyage made by HMS Challenger and the report of experiments undertaken by Tait into the compression of water.

Simha et al. (1973) have shown that C is indeed almost constant (best average value: $C = 0.0894$) and that the temperature dependent factor $B(T)$ can be expressed by

$$B(T) = b_1 \exp(-b_2 T') \quad (4.35)$$

where b_1 and b_2 are empirical constants and T' is the temperature in °C. Substituting (4.35) into (4.34) gives:

$$\frac{V(p=1) - V(p)}{V(p=1)} = 0.0894 \ln \left(1 + \frac{p}{b_1} \exp(b_2 T') \right) \quad (4.36)$$

If we substitute $T' = T - 273$ (T in K) in Eq. (4.35) we then obtain

$$B(T) = b_3 \exp(-b_2 T) \quad (4.37)$$

with $b_3 = b_1 \exp(273b_2)$, so that

$$\frac{V(p=1) - V(p)}{V(p=1)} = 0.0894 \ln \left(1 + \frac{p}{b_3} \exp(b_2 T) \right) \quad (4.38)$$

Table 4.14 exhibits the experimental data of Quach and Simha (1971), Simha et al. (1973), Beret and Prausnitz (1975) and Zoller et al. (1977–1989). The constant b_2 has an average value of 4.5×10^{-3} (°C) $^{-1}$, whereas b_1 and b_3 are obviously dependent on the nature of the polymer. Further analysis showed that b_1 is proportional to the bulk modulus K (the latter will be treated in Chap. 13); roughly

$$b_1 = 6 \times 10^{-2} K \quad (4.39)$$

TABLE 4.14 Constants of the Tait-equation for polymer melts

Polymer	$b_1 (10^3 \text{ bar}) \text{ } ^\circ\text{C}$ as basis	$b_3 (10^3 \text{ bar}) \text{ K}$ as basis	$b_2 (10^{-3} (\text{ } ^\circ\text{C})^{-1})$ or 10^{-3} K^{-1}
Polyethylene (ld)	1.99	8.01	5.10
Polyisobutylene	1.91	5.93	4.15
Polystyrene	2.44	7.56	4.14
Poly(vinyl chloride)	3.52	16.46	5.65
Poly(methyl methacrylate)	3.85	24.11	6.72
Poly(vinyl acetate)	2.23	5.69	3.43
Poly(dimethyl siloxane)	1.04	5.14	5.85
Poly(oxy methylene)	3.12	10.17	4.33
Polycarbonate	3.16	9.63	4.08
Poly(ether ketone)(PEK)	3.88	11.95	4.12
Polysulfone	3.73	10.41	3.76
Polyarylate (Ardel®)	3.03	7.62	3.38
Phenoxy-resin (045C)	3.67	12.13	4.38
Average ± SD			4.54 ± 0.95

Simha et al. (1973) showed that the Tait relation is also valid for polymers in the glassy state. In this case the value of b_1 is about the same as for polymer melts, but b_2 is smaller ($b_2 \approx 3 \times 10^{-3}$). Even nowadays frequently use is made of the Tait equation.

4.5.2. Theoretical approaches

It is not surprising that attempts have been made to derive equations of state along purely theoretical lines. This was done by Flory, Orwoll and Vrij (1964) using a lattice model, Simha and Somcynsky (1969) (hole model) and Sanchez and Lacombe (1976) (Ising fluid lattice model). These theories have a statistical-mechanical nature; they all express the state parameters in a reduced dimensionless form. The reducing parameters contain the molecular characteristics of the system, but these have to be partly adapted in order to be in agreement with the experimental data. The final equations of state are accurate, but their usefulness is limited because of their mathematical complexity.

4.5.3. Semi-empirical equations

Several semi-empirical equations have been proposed, out of which we shall discuss two: the Spencer–Gilmore and the Hartmann–Haque equations.

4.5.4. The Spencer–Gilmore equation (1949)

This equation is based on the Van der Waals equation. It has the following form:

$$(p + \pi)(v - \omega) = RT/M \quad (4.40)$$

where π = internal pressure; ω = specific volume at $p = 0$ and $T = 0$; M = molar mass of the interacting unit, usually taken identical to the structural unit of the polymer.

Since the internal pressure is closely related to the cohesion energy density, we shall postpone further discussion to Chap. 7 (Cohesive Properties).

4.5.5. The Hartmann–Haque equation

A very interesting semi-empirical equation of state was derived by Hartmann and Haque (1985), who combined the zero-pressure isobar of Simha and Somcynsky (1969) with the theoretically derived dependence of the thermal pressure (Pastime and Warfield, 1981). This led to an equation of state of a very simple form:

$$\tilde{p}\tilde{v}^5 = \tilde{T}^{3/2} - \ln \tilde{v} \quad (4.41)$$

where \tilde{p} = reduced pressure = p/B_o ; \tilde{v} = reduced specific volume = v/v_o ; \tilde{T} = reduced temperature = T/T_o .

This equation was verified by application of the p – v – T -data of the melts of 23 polymers of very different structure, adapting the reducing parameters B_o , v_o and T_o to the closest fit with the experiments. The obtained values are shown in the left part of Table 4.15. The average deviation between calculated and experimental $v(P, T)$ data is the same as obtained with the Tait relation. The advantage of Hartmann's equation is that it contains only three constants, whereas the Tait equation involves 4.

Hartmann and Haque applied their equation also on solid polymers, and with success. The reducing parameters appeared to be of the same order as for polymeric melts, but different, as would be expected. Their values are given in the right side part of Table 4.15.

TABLE 4.15 Reducing parameters in equation of state of various polymers (from Hartmann and Haque, 1985)

Polymer	Melts			Solids		
	B_0 (GPa)	v_0 (cm^3/g)	T_0 (K)	B_0 (GPa)	v_0 (cm^3/g)	T_0 (K)
Polyethylene	2.80	1.036	1203	5.59	0.959	1829
Polypropylene	2.05	1.087	1394	—	—	—
Poly(l-butene)	2.10	1.077	1426	—	—	—
Poly(4-methyl pentene-1)	1.67	1.118	1423	2.61	1.121	1658
Poly(vinyl fluoride)	—	—	—	4.86	0.754	1972
Poly(vinylidene fluoride)	—	—	—	5.78	0.589	1490
Poly(trifluoro chloro ethene)	—	—	—	4.97	0.447	2373
Poly(tetrafluoro ethene)	3.64	0.359	875	—	—	—
Poly(vinyl alcohol)	—	—	—	—	—	—
Poly(ethylene terephthalate)	4.14	0.677	1464	—	—	—
Poly(vinyl acetate)	3.82	0.738	1156	4.49	0.796	1955
Poly(methyl methacrylate)	3.84	0.757	1453	4.17	0.813	2535
Poly(butyl methacrylate)	3.10	0.854	1284	3.62	0.885	1781
Poly(cyclohexyl methacrylate)	3.14	0.816	1449	4.43	0.876	2567
Polystyrene	2.97	0.873	1581	4.25	0.919	2422
Poly(o-methyl styrene)	3.11	0.887	1590	4.19	0.936	2301
Poly(dimethyl phenylene ether)	3.10	0.784	1307	3.74	0.913	2947
Polyarylate (Ardel)	3.71	0.738	1590	4.58	0.798	2702
Phenoxy resin	4.27	0.776	1459	5.87	0.817	2425
Polycarbonate	3.63	0.744	1473	4.55	0.804	2476
Polysulfone	3.97	0.720	1585	5.33	0.782	2727
Poly(dimethyl siloxane)	1.85	0.878	999	—	—	—

Hartmann already pointed out that the reducing parameter B_o is equal to the compression modulus or bulk modulus K , extrapolated to zero temperature and pressure and that T_o is related to the glass transition temperature.

Analysing the data of Hartmann and Haque we found the results shown in Table 4.16. The equations given in Table 4.16 are graphically represented in Figs. 4.5–4.7, together with the experimental values. If no values are available from experiments, the equations are recommended as a first approximation.

Hartmann and Haque also gave some useful equations for estimations:

$$\frac{RT_0}{B_0 v_0} = C \quad (4.42)$$

where $C = 5.4 \pm 0.65$ for amorphous solid polymers; $C = 4.2 \pm 1.25$ for semi-crystalline solid polymers, both in the dimension g/mol.

TABLE 4.16 Relationships of the reducing parameters B_o , v_o and T_o

Parameter	For melts	For solid polymers
B_o (GPa)=	2/3 K(298) (dynamic)	K(298) (dynamic)
v_o (cm ³ /g)=	1.425 V _w /M	1.50 V _w /M for glasses 1.40 V _w /M for semi-cryst.
T_o (K)=	$2.0T_g + 700$	$5.0T_g + 500^a$

^a Hartmann mentions as an average: $T_o = 4.92 T_g + 528$.

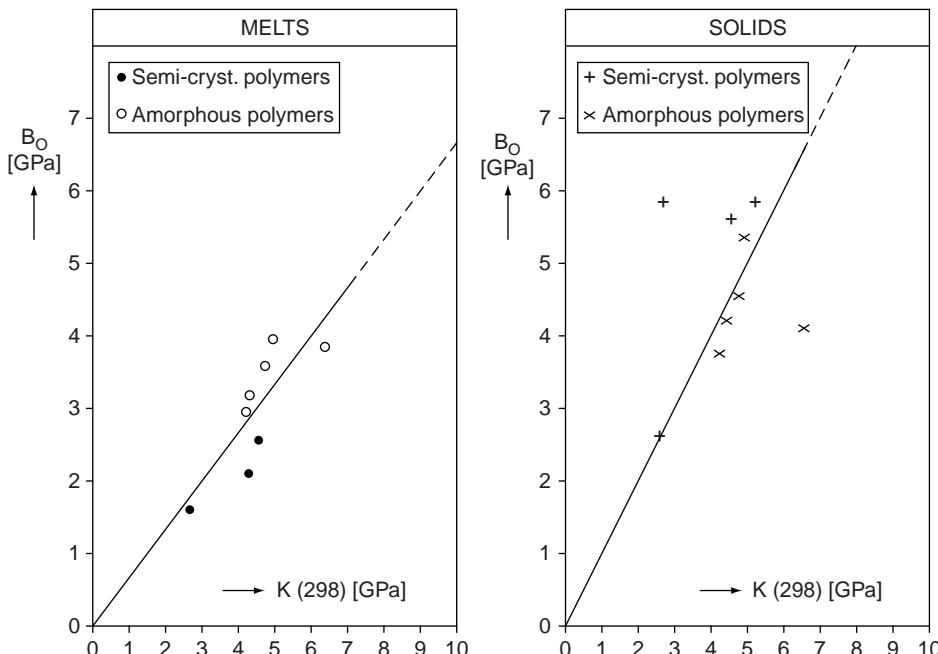


FIG. 4.5 Reducing parameter B_o versus bulk modulus K (298).

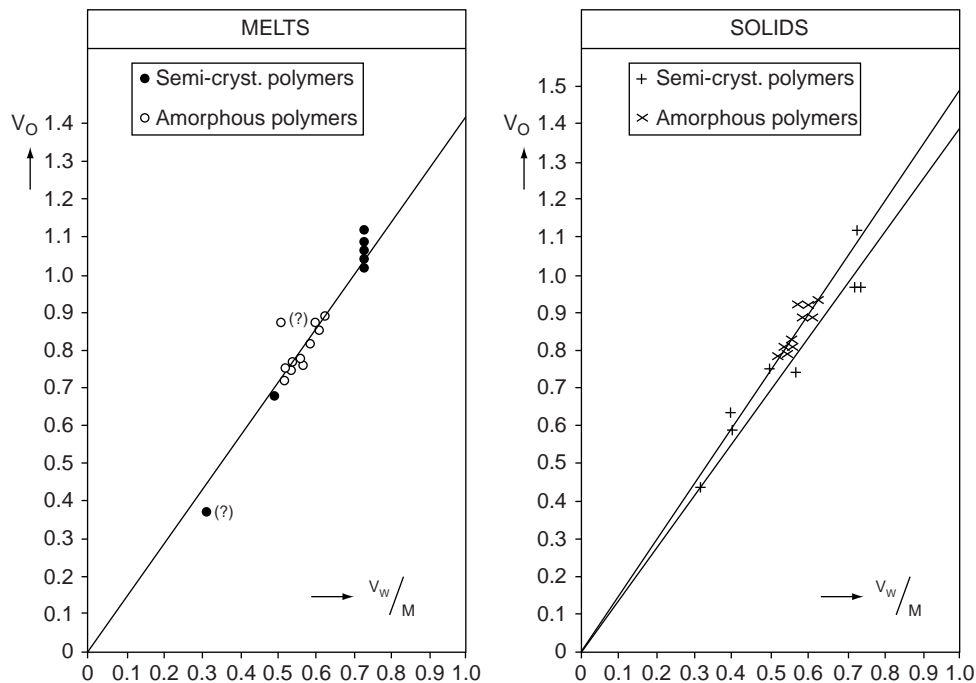


FIG. 4.6 Reducing parameter v_o versus V_w/M .

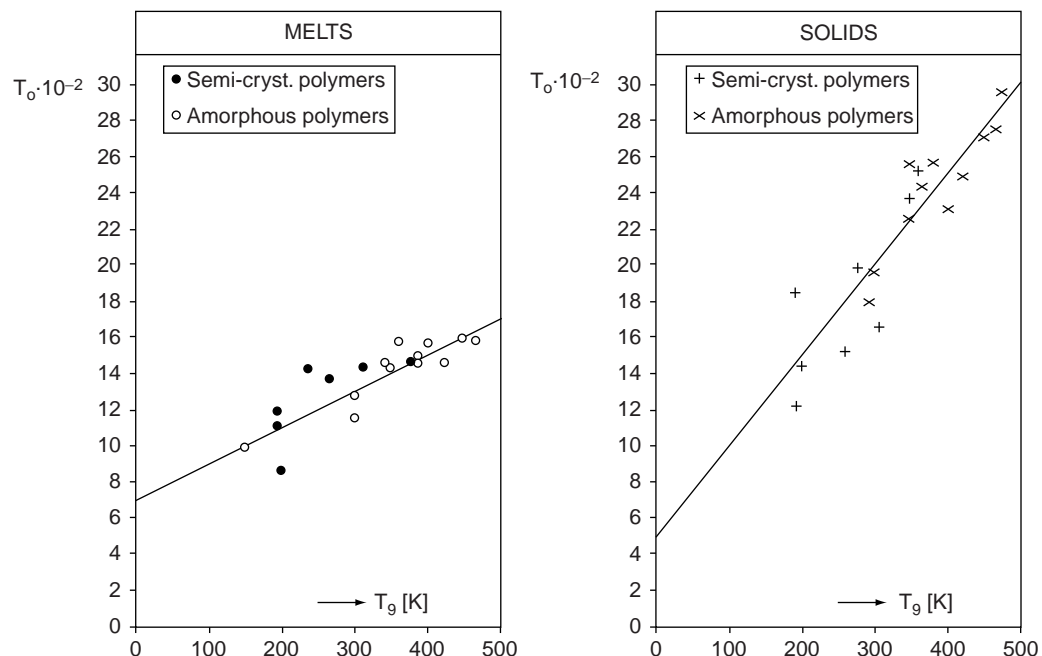


FIG. 4.7 Reducing parameter T_o versus T_g .

From the Hartmann–Haque equation the following expressions for α and K can be derived:

$$\alpha = \frac{1}{v} \left(\frac{\partial v}{\partial T} \right)_p = \frac{\frac{3}{2} \left(\frac{T}{T_o^3} \right)^{1/2}}{1 + \frac{5p}{B_o} \left(\frac{v}{v_o} \right)^5} \quad (4.43)$$

$$\kappa = -\frac{1}{v} \left(\frac{\partial v}{\partial p} \right)_T = \frac{1}{\frac{B_o}{(v/v_o)^5} + 5p} \quad (4.44)$$

BIBLIOGRAPHY

General references

- Bondi A, "Physical Properties of Molecular Crystals, Liquids and Glasses", Wiley, New York, 1968.
 Brandrup J, Immergut EH and Grulke EA (Eds), "Polymer Handbook", Part VII, p 291, Wiley, New York, 4th Ed, 1999.
 Bueche F, "Physical Properties of Polymers", Interscience, New York, 1962.
 Lewis OG, "Physical Constants of Linear Homopolymers", Springer, Berlin, 1968.
 Pauling L, "The Nature of the Chemical Bond", Cornell University Press, Ithaca, New York, 1st Ed 1940, 3rd Ed 1960.
 Tobolsky AV, "Properties and Structure of Polymers", Wiley, New York, 1960.

Special references

- Allen G, J Appl Chem, 14 (1964) 1.
 Askadskii AA, in Pethrick RA and Zaikov GE (Eds), "Chemical Yearbook IV", Harwood Academic Publishers, London, 1987, pp 93–147.
 Beret S and Prausnitz JM, Macromolecules, 8 (1975) 536.
 Biltz W, "Raumchemie der festen Stoffe", Voss, Leipzig, 1934.
 Bondi A, J Phys Chem 68 (1964) 441.
 Bondi A, See General references (1968a) Chaps. 3 and 4; (1968b): Chap. 14; (1968c): p 236 (1968d): p 50.
 Boyer RF and Spencer RS, J Appl Phys 15 (1944) 398.
 Bueche F, see General references (1962) Chap. 4.
 Davis HG and Gottlieb S, Fuel 42 (1963) 37.
 Dorsey NE, "Properties of Ordinary Water Substance". Reinhold, New York, 1940, p 207.
 Exner O, Collection Czech Chem Comm 32 (1967) 1.
 Fedors RF, Polym Eng Sci 14 (1974) 147, 472.
 Flory P, Orwoll RA and Vrij A, J Am Chem Soc 86 (1964) 3507.
 Fortune LR and Malcolm GN, J Phys Chem 64 (1960) 934.
 Harrison EK, Fuel 44 (1965) 339; 45 (1966) 397.
 Hartmann B and Haque MA, J Appl Polym Sci 30 (1985) 1553 and J Appl Phys 58 (1985) 2831.
 Huggins ML, J Am Chem Soc 76 (1954) 843; "Physical Chemistry of High Polymers", Wiley, New York, 1958.
 Kirshenbaum L, J Polym Sci A3 (1965) 1869.
 Krause S, Gormley JJ, Roman N, Shetter JA and Watanabe WH, J Polym Sci A3 (1965) 3573.
 Kurtz SS and Lipkin MR, Ind Eng Chem 33 (1941) 779.
 Le Bas G, "Molecular Volumes of Liquid Chemical Compounds". Longmans, New York, (1915).
 Li K, Arnett RL, Epstein MB, Ries RB, Bitler LP, Lynch JM and Rossini FD, J Phys Chem 60 (1956) 1400.
 Malone WM and Albert R, J Appl Polym Sci 17 (1973) 2457.
 Mathews AP, J Phys Chem 20 (1916) 554.
 Pastine DJ and Warfield RW, Polymer 22 (1981) 1754.
 Quach A and Simha R, J Appl Phys 42 (1971) 4592.
 Rheineck AE and Lin KF, J Paint Technol 40 (1968) 611.
 Robertson RE, Macromolecules 2 (1969) 250.
 Sanchez IC and Lacombe RH, J Phys Chem 80 (1976) 2352.

- Sewell JH, *J Appl Polym Sci* 17 (1973) 1741.
Simha R and Boyer RF, *J Chem Phys* 37 (1962) 1003.
Simha R and Hadden ST, *J Chem Phys* 25 (1956) 702.
Simha R and Somcynsky T, *Macromolecules* 2 (1969) 342.
Simha R, Wilson PS and Olabisi O, *Kolloid-Z* 251 (1973) 402.
Slonimskii GL, Askadskii AA and Kitaygorodskii AI, *Visokomol Soed* 12 (1970) 494.
Spencer RS and Gilmore GD, *J Appl Phys* 20 (1949) 502; 21 (1950) 523.
Starkweather HW and Boyd BH, *J Phys Chem* 64 (1960) 410.
Sugden S, *J Chem Soc* (1927) 1780 and 1786.
Tait PG, *Phys Chem* 2 (1888) 1.
Tait PG, "Physics and Chemistry of the Voyage of the HMS Challenger", Vol. 2, Part 4 (HMSO, London, 1888).
Tait PG, *Scientific Papers*, The University Press, Cambridge, 1898, Vol. 1, p 261.
Tatevskii VM, Benderskii VA and Yarovoi SS, "Rules and Methods for Calculating the Physico-chemical Properties of Paraffinic Hydrocarbons", Pergamon Press, London, 1961.
Timmermans J, *Bull Soc Chim Belg* 26 (1913) 205.
Tobolsky AV (1960), see General references, p 85.
Traube J, *Ber dtsch Chem Ges* 28 (1895) 2722.
Van Krevelen DW and Hoftyzer PJ, *J Appl Polym Sci* 13 (1969) 871.
Van Nes K and Van Westen HA, "Aspects of the Constitution of Mineral Oils". Elsevier, Amsterdam, 1951.
Wang JS, Porter RS and Knox JR, *Polym J* 10 (1978) 619.
Wilson PS and Simha R, *Macromolecules* 6 (1973) 902.

CHAPTER 5

Calorimetric Properties

The following properties belong to the calorimetric category: (1) *specific and molar heat capacities*, (2) *latent heats of crystallization or fusion*. It will be shown that both groups of properties can be calculated as additive molar quantities. Furthermore, starting from these properties the molar *entropy* and *enthalpy* of polymers can be estimated.

5.1. HEAT CAPACITY

5.1.1. Definitions

The specific heat capacity is the heat that must be added per kg of a substance to raise the temperature by one Kelvin or one degree Celsius. The molar heat capacity is the specific heat multiplied by the molar mass (the molar mass of a structural unit in the case of polymers). Specific and molar heat capacity may be defined at constant volume or at constant pressure. The heat added causes a change in the internal energy (U) and in the enthalpy (heat content, H) of the substance. The following notations can be formulated:

1. *Specific heat capacity at constant volume*:

$$c_v = \left(\frac{\partial U}{\partial T} \right)_v \quad (\text{dimension: J kg}^{-1} \text{ K}^{-1}) \quad (5.1)$$

2. *Specific heat capacity at constant pressure*:

$$c_p = \left(\frac{\partial (U + pV)}{\partial T} \right)_p = \left(\frac{\partial H}{\partial T} \right)_p \quad (\text{dimension: J kg}^{-1} \text{ K}^{-1}) \quad (5.2)$$

3. *Molar heat capacity at constant volume*:

$$C_v = M c_v = \left(\frac{\partial U}{\partial T} \right)_v \quad (\text{dimension: J mol}^{-1} \text{ K}^{-1}) \quad (5.3)$$

where \mathbf{U} is the internal energy per mol.

4. *Molar heat capacity at constant pressure*:

$$C_p = M c_p = \left(\frac{\partial H}{\partial T} \right)_p \quad (\text{dimension: J mol}^{-1} \text{ K}^{-1}) \quad (5.4)$$

where \mathbf{H} is the enthalpy (heat content) per mol.

5. Molar heat capacity of solid and liquid polymers at 25°C:

Reliable values for the molar heat capacity in the solid and the liquid state are available for a limited number of polymers only. This emphasizes the importance of correlations between $C_p^s(298)$ and $C_p^l(298)$ and the structure of polymers.

For compounds of low molar mass, correlations are available. Satoh (1948) proposed a method for the prediction of between C_p^s at 200, 300 and 400 K by the addition of group contributions. Shaw (1969) used the same method for $C_p^l(298)$ whereas Johnson and Huang (1955) used it for $C_p^l(293)$. *The question was whether these increments are applicable to polymers.*

A survey of the group contributions to $C_p^s(298)$ by Satoh and to $C_p^l(298)$ by Shaw is given in Table 5.1. Satoh does not mention values for some important groups: $-COO-$, $-CONH-$, $-SO_2-$ and $-F$, while Shaw omits values for $-Cl$, $-F$ and $-CONH-$. The most probable values for these groups, according to the available experimental data, are mentioned in parentheses in Table 5.1. The value for the contribution of $-CONH-$ to C_p^s is still dubious.

In Table 5.2 the available experimental values for $C_p^s(298)$ and $C_p^l(298)$ for polymers are compared with values predicted by the methods of Satoh and Shaw. In general, the correspondence between experimental and calculated values is quite satisfactory. The standard deviation between experimental and calculated values is 2% for $C_p^l(298)$ and 3.5% for $C_p^s(298)$. Values for C_p^l , calculated with Johnson's method show greater deviations from the experimental values than those according to Shaw. For the temperature region of 50–240 K, Wunderlich and Jones (1969) published group contributions for the calculation of C_p^l . If the uncertainty in the extrapolation of these data to 300 K is taken into account, these group contributions correspond with those of Satoh.

Example 5.1

Calculate the heat capacity of polypropylene with a degree of crystallinity of 30% at 25°C.

Solution

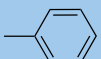
$C_p^s(298)$ and $C_p^l(298)$ may be calculated by the addition of group contributions according to Satoh and to Shaw, respectively (Table 5.1):

	$C_p^s(298)$	$C_p^l(298)$
($-CH_2-$)	25.35	30.4
($>CH-$)	15.6	20.95
($-CH_3$)	30.9	36.9
	71.9	88.3

It is assumed that the semi-crystalline polymer consists of an amorphous fraction with heat capacity C_p^l and a crystalline fraction with heat capacity of C_p^s . For a polymer with 30% crystallinity the estimated molar heat capacity is $C_p(298) = 0.3 \times 71.9 + 0.7 \times 88.3 = 83.4 \text{ J mol}^{-1} \text{ K}^{-1}$. The specific heat capacity is $C_p/M = 1985 \text{ J kg}^{-1} \text{ K}^{-1}$

We may conclude that C_p^s and C_p^l are additive molar functions; their group contributions, also valid for polymers, are given in Table 5.1.

TABLE 5.1 Group contributions to the molar heat at 25 °C ($\text{J mol}^{-1} \text{K}^{-1}$)

Group	C_p^s (Satoh)	C_p^l (Shaw)	C_p^s/R per atom	C_p^l/R per atom
-CH ₃	30.9	36.9	0.92	1.10
-CH ₂ -	25.35	30.4	1.01	1.21
>CH-	15.6	20.95	0.93	1.25
>C<	6.2	7.4	0.74	0.88
=CH ₂	22.6	21.8	0.90	0.87
=CH-	18.65	21.4	1.11	1.28
=C<	10.5	15.9	1.25	1.90
-CH ₂ - (5 ring)	19.9	26.4	0.79	1.05
-CH ₂ - (6 ring)	18.0	26.4	0.71	1.03
>CH _{ar}	15.4	22.2	0.92	1.33
>C _{ar} -	8.55	12.2	1.02	1.45
	85.6	123.2	0.94	1.35
	78.8	113.1	0.95	1.36
	65.0	93.0	0.98	1.40
-F	(21.4)	(21.0)	2.55	2.50
-Cl	27.1	(39.8)	3.23	4.75
-Br	26.3	-	3.14	-
-I	22.4	-	2.67	-
-CN	(25)	-	1.50	-
-OH	17.0	44.8	1.01	2.68
-O-	16.8	35.6	2.01	<4.25
-CO-	23.05	52.8	1.38	3.15
-COOH	(50)	98.9	1.50	2.95
-COO-	(46)	65.0	1.83	2.58
-NH ₂	20.95	-	0.83	-
-NH-	14.25	(31.8)	0.85	1.90
>N-	17.1	(44.0)	2.04	5.25
-NO ₂	41.9	-	1.67	-
-CONH-	(38–54)	(90.1)	1.12–1.63	2.68
-S-	24.05	44.8	2.37	5.35
-SH	46.8	52.4	2.78	3.12
-SO ₂ -	(50)	-	2.00	-

5.1.2. Specific heat as a function of temperature

The complete course of the specific heat capacity as a function of temperature has been published for a limited number of polymers only. As an example, Fig. 5.1 shows some experimental data for polypropylene, according to Dainton et al. (1962) and Passaglia and Kevorkian (1963). Later measurements by Gee and Melia (1970) allowed extrapolation to purely amorphous and purely crystalline material, leading to the schematic course of molar heat capacity as a function of temperature shown in Fig. 5.2.

TABLE 5.2 Experimental and calculated heat capacities of polymers

Polymer	Solid			Liquid			$C_p^l(298)/C_p^s(298)$	$T_m(K)$	$C_p^s(T_m)$	$C_p^l(T_m)$	$C_p^l(T_m)/C_p^s(T_m)$
	$C_p^s(298)$ Exp. (J kg ⁻¹ K ⁻¹)	$C_p^s(298)$ Exp. (J mol ⁻¹ K ⁻¹)	$C_p^s(298)$ Satoh (J mol ⁻¹ K ⁻¹)	$C_p^l(298)$ Exp. (J kg ⁻¹ K ⁻¹)	$C_p^l(298)$ Exp. (J mol ⁻¹ K ⁻¹)	$C_p^l(298)$ Shaw (J mol ⁻¹ K ⁻¹)					
Polyethylene	1550/1760	44/49	51	2260	63	61	1.28/1.46	410	65	71	1.09
Polypropylene	1630/1760	69	72	2140	91	88	1.31	450	100	107	1.07
Polybutene	1550/1760	>87	97	2140	120	119	—	400	127	134	1.06
Poly (4-methylpentene)	1680	141	144	—	—	176	(1.26)	500/520	—	—	—
Polyisobutylene	1680	94	93	1970	111	112	1.18	320	100	114	1.14
Polystyrene	1220	128	127	1720	178	175	1.40	513	211	223	1.06
Poly(vinyl chloride)	960/1090	60/68	68	1220	76	(91)	—	—	—	—	—
Poly(vinylidene chloride)	—	—	86	—	—	(117)	(1.37)	463	—	—	—
Poly(tetrafluoroethylene)	~960	96	(98)	960	96	(99)	~1.00	463	96	96	1.00
Poly (chlorotrifluoroethylene)	920	105	(104)	—	—	(117)	(1.12)	490	165	159?	—
Poly(vinyl alcohol)	1300	57	58	—	—	96	(1.69)	505/535	—	—	—
Poly(vinyl acetate)	~1470	~127	(118)	~1930	~166	153	~1.31	—	—	—	—
Poly(methyl acrylate)	1340	115	(118)	1800	155	153	1.35	—	—	—	—
Poly(ethyl acrylate)	1450	145	(143)	1820	182	184	1.26	—	—	—	—
Poly(butyl acrylate)	1640	210	(194)	1790	230	245	1.10	320	224	236	1.05
Poly(methyl methacrylate)	1380	138	(139)	~1800	~182	177	~1.32	433	194	212	1.09
Poly(ethyl methacrylate)	1450	166	(165)	—	—	207	—	—	—	—	—
Poly(butyl methacrylate)	1680	239	(215)	1860	264	268	1.10	—	—	—	—

Polyacrylonitrile	1260	67	(66)	—	—	—	590	—	—	—	
Polybutadiene	1630	88	88	1890	102	104	1.16	370	107	111	1.04
Polyisoprene	1590	108	111	1930	131	135	1.22	309/340	122	132	1.08
Polychloroprene	—	—	107	—	—	(138)	(1.29)	343	—	—	—
Poly(methylene oxide)	1420	43	42	~2100	63	66	~1.47	460	64	75	1.17
Poly(ethylene oxide)	~1260	<70	68	2050	91	96	>1.30	340	79	95	1.20
Poly(tetramethylene oxide)	~1590	~118	118	2100	150	157	~1.27	310	122	152	1.25
Poly(propylene oxide)	~1420	~83	89	1930	111	124	~1.35	350	96	118	1.23
Poly(2,6-dimethylphenylene oxide)	1260	148	144	~1760	~212	202	~1.43	530	251	271	1.08
Poly(propylene sulphone)	1170	123	(122)	—	—	—	570	—	—	—	
Poly(butylene sulphone)	1220	147	(148)	—	—	—	—	—	—	—	
Poly(hexene sulphone)	1380	205	(198)	—	—	—	—	—	—	—	
Poly(ethylene sebacate)	—	—	(346)	~1930	~442	434	(1.28)	345	—	—	—
Poly(ethylene terephthalate)	1130	218	(222)	~1550	298	304	1.36	540	376	385	1.02
Nylon 6	1470	164	(164)	2140/2470	242	(242)	1.48	496	261	299	1.15
Nylon 6, 6	1470	331	(329)	—	—	(484)	1.47	—	—	—	—
Nylon 6, 10	~1590	~448	(430)	2180	616	(606)	~1.37	496	714	762	1.07
Poly(bisphenol – A carbonate)	1170	303	(289)	1590	410	(408)	1.35	500	487	508	1.05
Diamond	—	6	6	—	—	—	—	—	—	—	—
Graphite	—	9	6	—	—	—	—	—	—	—	—
Sulphur	—	24	24	—	—	—	—	—	—	—	—
Silicon	—	21	—	—	—	—	—	—	—	—	—

Conversion factors: $1 \text{ J kg}^{-1}\text{K}^{-1} = 0.239 \times 10^{-3} \text{ cal g}^{-1}\text{K}^{-1}$; $1 \text{ J mol}^{-1}\text{K}^{-1} = 0.239 \text{ cal mol}^{-1}\text{K}^{-1}$.

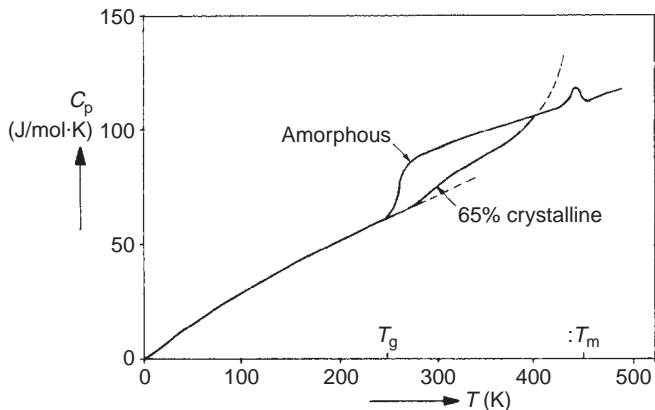


FIG. 5.1 Molar heat capacity of polypropylene.

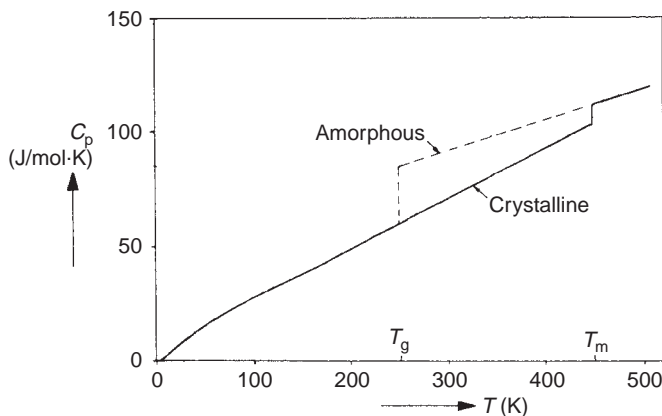


FIG. 5.2 Schematic curve of the molar heat capacity of isotactic polypropylene.

According to this figure a crystalline polymer follows the curve for the solid state to the melting point. At T_m , the value of C_p increases to that of the liquid polymer. *The molar heat capacity of an amorphous polymer follows the same curve for the solid up to the glass transition temperature, where the value increases to that of the liquid (rubbery) material.*

In general a polymer sample is neither completely crystalline nor completely amorphous. Therefore, in the temperature region between T_g and T_m the molar heat capacity follows some course between the curves for solid and liquid (as shown in Fig. 5.1 for 65% crystalline polypropylene). This means that published single data for the specific heat capacity of polymers should be regarded with some suspicion. Reliable values can only be derived from the course of the specific heat capacity as a function of temperature for a number of samples. Outstanding work in this field was done by Wunderlich and his co-workers. Especially his reviews of 1970 and 1989 have to be mentioned here.

Examination of the available literature data showed that, for all the polymers investigated, the curves for the molar heat capacity of solid and liquid might be approximated by straight lines, except for the solid below 150 K. So if the slopes of these lines are known, the heat capacity at an arbitrary temperature may be calculated approximately from its value at 298 K. For a number of polymers the slopes of the heat capacity curves, related to the heat capacity at 298 K, are mentioned in Table 5.3.

TABLE 5.3 Temperature function of the molar heat capacity (K^{-1})

Polymer	$\frac{1}{C_p^s(298)} \frac{dC_p^s}{dT}$	$\frac{1}{C_p^l(298)} \frac{dC_p^l}{dT}$
Polyethylene	3.0×10^{-3}	1.0×10^{-3}
Polybutene	3.1×10^{-3}	1.4×10^{-3}
Poly(4-methylpentene)	3.0×10^{-3}	—
Polyisobutylene	3.3×10^{-3}	2.2×10^{-3}
Polystyrene	3.4×10^{-3}	1.2×10^{-3}
Poly(vinyl chloride)	2.8×10^{-3}	—
Poly(vinyl acetate)	2.9×10^{-3}	—
Poly(methyl acrylate)	2.6×10^{-3}	1.1×10^{-3}
Poly(ethyl acrylate)	2.7×10^{-3}	1.5×10^{-3}
Poly(butyl acrylate)	3.0×10^{-3}	1.5×10^{-3}
Poly(methyl methacrylate)	3.0×10^{-3}	1.5×10^{-3}
Poly(ethyl methacrylate)	3.0×10^{-3}	—
Poly(butyl methacrylate)	3.2×10^{-3}	1.9×10^{-3}
Polybutadiene	3.1×10^{-3}	—
Polyisoprene	3.0×10^{-3}	1.8×10^{-3}
Poly(ethylene oxide)	2.6×10^{-3}	0.5×10^{-3}
Poly(tetramethylene oxide)	2.9×10^{-3}	1.0×10^{-3}
Poly(propylene oxide)	2.9×10^{-3}	1.4×10^{-3}
Poly(phenylene oxide)	2.7×10^{-3}	0.9×10^{-3}
Poly(ethylene sebacate)	—	1.2×10^{-3}
Poly(hexamethylene adipamide)	3.0×10^{-3}	0.5×10^{-3}
Poly(bisphenol-A carbonate)	3.2×10^{-3}	1.4×10^{-3}
Average	3.0×10^{-3}	1.3×10^{-3}
Standard deviation	7%	34%

The slopes of the heat capacity lines for solid polymers show an average value

$$\frac{1}{C_p^s(298)} \frac{dC_p^s}{dT} = 3 \times 10^{-3} K^{-1} \quad (5.5)$$

with a standard deviation of 7%.

For liquid polymers, an analogous expression may be used, but much larger deviations occur. In this case

$$\frac{1}{C_p^l(298)} \frac{dC_p^l}{dT} = 1.3 \times 10^{-3} K^{-1} \quad (5.6)$$

with a standard deviation of 34%.

Nevertheless, if experimental data are lacking, the temperature function of the heat capacity may be approximated with these average values, so that, with T in K:

$$C_p^s(T) = C_p^s(298)[1 + 3 \times 10^{-3}(T - 298)] = C_p^s(298)[0.106 + 3 \times 10^{-3}T] \quad (5.7)$$

$$C_p^l(T) = C_p^l(298)[1 + 1.3 \times 10^{-3}(T - 298)] = C_p^l(298)[0.61 + 1.3 \times 10^{-3}T] \quad (5.8)$$

With the aid of Eqs. (5.7) and (5.8) the specific heat capacity in the solid and the liquid state at temperatures of practical interest may be predicted approximately from their values at room temperature.

As derived from Table 5.2, the ratio $r = C_p^l(298)/C_p^s(298)$ shows a standard deviation of 7% from the average value $r = 1.32$. This ratio will decrease, however, with increasing temperature, as the slope of C_p^s is steeper than that of C_p^l . The linear approximations of the curves for C_p^s and C_p^l as a function of temperature (Eqs. (5.7) and (5.8)) may be used for estimating C_p^s and C_p^l at the melting point. The ratio C_p^l/C_p^s at the melting point shows a standard deviation of 7% from the average value $r = 1.10$. This can also be seen from Table 5.2.

Wunderlich et al. (1988) have confirmed the linear temperature dependence of the liquid heat capacities and derived group contributions for the whole temperature range of 250–750 K. His values are reproduced in Table 5.4.

5.1.3. Theoretical background

Our discussion of the specific heat capacity of polymers on the preceding pages has been quite empirical. There are, in fact, few fundamental rules that can be used for the prediction of specific heat capacity. At very low temperatures, the equations of Debye and Einstein may be used.

On the basis of the equipartition of the energy content of a molecule over the degrees of freedom, the maximum value of the molar heat would correspond to $3R$ per atom. In reality, part of the degrees of freedom are always frozen in, which results in a lower value of the molar heat capacity. The increase of the specific heat capacity with temperature depends on an increase of the vibrational degrees of freedom.

Empirically it has been found that for polymers at room temperature the molar heat capacity is of the order of R per atom. This may be seen from Table 5.1, where the value of C_p/R per atom has been calculated for the group contributions to the molar heat. For hydrocarbon groups C_p^s/R per atom is somewhat lower than unity: the average value of C_p^s/R is about unity. Groups containing other elements show higher values for C_p/R .

It is interesting to note that for some groups C_p/R per atom is greater than the maximum value of 3, which corresponds to all vibrational degrees of freedom of the group. This means that the presence of these groups influences the degrees of freedom of adjacent groups. This is one of the reasons why linear additivity rules do not hold exactly for these groups.

TABLE 5.4 Relationships between liquid C_p and temperature T for different structure groups in linear macromolecules

Group	C_p ($\text{J mol}^{-1}\text{K}^{-1}$)
Methylene, $-\text{CH}_2-$	$0.0433T + 17.92$
Phenylene, $-\text{C}_6\text{H}_4-$	$0.1460T + 73.13$
Carboxyl, $-\text{COO}-$	$0.002441T + 64.32$
Carbonate, $-\text{OCOO}-$	$0.06446T + 84.54$
Dimethylmethylene, $-\text{C}(\text{CH}_3)_2-$	$0.2013T + 18.79$
Carbonyl, $>\text{CO}$	$0.07119T + 32.73$
Naphthylene, $-\text{C}_{10}\text{H}_6-$	$0.2527T + 114.49$
Dimethylphenylene, $-\text{C}_6\text{H}_2(\text{CH}_3)_2-$	$0.2378T + 111.41$
Oxygen, $-\text{O}-$	$-0.00711T + 28.13$
Sulphur, $-\text{S}-$	$-0.02028T + 46.59$

On the basis of the hole theory of liquids, Wunderlich (1960) concluded that the difference $C_p^l - C_p^s$ at the glass transition temperature should be *constant per structural bead* in the polymer. A structural bead in this sense is defined as the smallest section of the molecule that can move as unit in internal rotation.

Equations (5.7) and (5.8) allow the calculation of approximate values for $C_p^l(T_g)$ and $C_p^s(T_g)$ for a number of polymers. The difference in C_p per bead calculated in this way shows a variation from 8.0 to 13.0 J mol⁻¹ K⁻¹, which corresponds reasonably well to the value of 11.3 J mol⁻¹ K⁻¹ mentioned by Wunderlich for small beads. Table 5.5 gives data from Wunderlich et al. (1988) on polymers with "large beads" which give a double or triple increase.

Bicerano (2002) calculated the heat capacity at 298 K for solid as well as soft polymers on the basis of the so-called connectivity indices χ and of rotational degrees of freedom in the backbone ($N_{bb\text{-}rot}$) as well as in the side groups ($N_{sg\text{-}rot}$). He found a close relationship between many calculated and experimental values of both $C_p^s(298)$ and $C_p^l(298)$.

5.1.4. C_p/C_v relationships

So far only c_p and C_p , the specific and the molar heat capacities at constant pressure, have been discussed. Obviously, these quantities are always dealt with in normal measurements. For the calculation of the specific heat capacity at constant volume, c_v some relationships are available. An exact thermodynamic derivation leads to the equation:

$$C_p - C_v = \alpha^2 V T / \kappa \quad (5.9)$$

where V is the molar volume (mol m⁻³), α is the expansion coefficient (K⁻¹), and K is the compressibility (m² N⁻¹).

If insufficient data for the evaluation of Eq. (5.9) are available, a universal expression proposed by Nernst and Lindemann (1911) may be used:

$$C_p - C_v = 0.00511 C_p^2 (T/T_m) \text{ J mol}^{-1} \text{ K}^{-1} \quad (5.10)$$

Approximative relationships for polymers were derived by Warfield et al. (1969, 1974); their results are shown in Figs. 5.3 and 5.4. In Fig. 5.3 C_p/C_v of amorphous polymers is

TABLE 5.5 Heat capacity (ΔC_p increase at the glass transition (T_g))

Polymer	T_g (K)	ΔC_p (J mol ⁻¹ K ⁻¹)	Number of beads ^a	$\Delta C_p/\text{bead}^b$ (J mol ⁻¹ K ⁻¹)
PC	424	56.4	2 + 2	9.4
PET	342	77.8	4 + 1	13.0
PEEK	419	78.1	1 + 3	11.2
PO	358	25.7	0 + 1	12.8
PPS	363	33.0	1 + 1	11.0
PPO	483	32.2	0 + 1 ^c	10.7
PEN	391	81.3	4 + 1 ^c	11.6
PBT	248	107	6 + 1	13.4
Average				11.6 ± 1.3

PC = polycarbonate; PET = poly(ethylene terephthalate); PEEK = poly (aryl-ether-ether-ketone); PO = poly(oxy-1,4-phenylene); PPS = poly (thio-1,4-phenylene); PPO = poly(oxy-2,6-dimethyl-1,4-phenylene); PEN = poly(ethylene-2,6-naphthalenedicarboxylate); PBT = poly (butylene terephthalate). From: Cheng SZD, Pan R, Bu HS, Cao M and Wunderlich B (1988).

^a The first number refers to "small" beads such as CH₂, O, COO, etc. Their ΔC_p is about 11.3 J mol⁻¹ K⁻¹. The second refers to "large" beads such as C₆H₄, C₆H₄O, etc. Their ΔC_p is double that of a "small" bead.

^b Calculated per mole of small beads.

^c The second number refers to "large" beads of C₈H₈ and C₁₀H₄, etc. Their ΔC_p is triple that of a small bead.

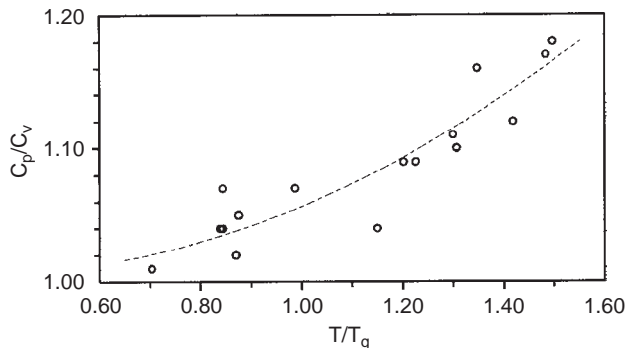


FIG. 5.3 Corresponding state relationship between C_p/C_v and T/T_g for amorphous polymers (after Warfield et al., 1969).

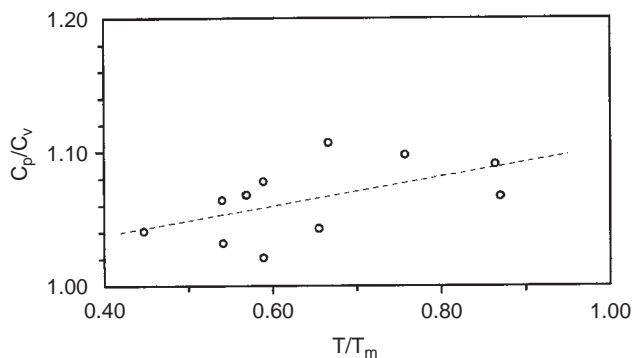


FIG. 5.4 Corresponding state relationship between C_p/C_v and T/T_m for semi-crystalline and crystalline polymers (after Warfield et al., 1969).

plotted vs. T/T_g (in fact vs. $298/T_g$). The authors fitted these results (dashed line) with an equation of the type

$$C_p/C_v = a + b(T/T_g) + c(T/T_g)^2 \quad (5.11)$$

in such a way that for $T/T_g = 0$ the value of C_p/C_v is equal to 1. In Fig. 5.4 C_p/C_v of semi-crystalline and crystalline polymers is plotted vs. T/T_m (in fact vs. $298/T_m$). The authors fitted these results (dashed line) with a linear equation in such a way that for $T/T_m = 0$ the value of C_p/C_v is equal to 1.

5.2. LATENT HEAT OF CRYSTALLIZATION AND FUSION (MELTING)

The latent heat of fusion (crystallization) or the enthalpy difference

$$H_1(T_m) - H_c(T_m) = \Delta H_m(T_m) \quad (5.12)$$

is an important quantity for the calculation of other thermodynamic functions. Furthermore, knowledge of ΔH_m is necessary for the design of a number of polymer processing apparatuses.

Reliable experimental values for ΔH_m are available, however, for a limited number of polymers only. This is probably due to difficulties arising in the experimental determination of ΔH_m . In a direct determination, the degree of crystallinity of the sample has to be taken into account, while indirect determination (e.g. from solution properties) is dependent on the validity of the thermodynamic formulae used. In this connection, a large scatter in published values for ΔH_m may be observed. Another problem might be that many crystals are so small that the surface energy also plays some role; in that case the melting temperature will be lower and the measured ΔH_m will be too small. (This also follows from the gradual decrease of the Young modulus between T_g and T_m , as is shown in Chap. 13). As a general rule, the highest value of ΔH_m mentioned for a given polymer is the best or the most probable one. Table 5.6 gives a survey of the available literature data for ΔH_m . It is very improbable that a method can be derived for the calculation of *accurate* values of ΔH_m by a simple addition of group contributions. Even for compounds of low molecular weight for which a large number of experimental values of ΔH_m are available, such a method could not be derived (Bondi, 1968).

This is in agreement with the experience acquired in another field of thermodynamics. Redlich et al. (1959) tried to calculate the interaction energy between non-electrolyte molecules in a solution as the sum of contributions of the constitutional groups. Instead of attributing a certain contribution to each group present, they had to add contributions corresponding with each pair of interacting groups. This might be called a second-order additivity rule and is the only way to account for the heat of solution.

Application of this method to the heat content of homologous series of organic compounds in the liquid state would result in a non-linear course of the heat content as a function of the number of methylene groups. This is exactly what is found experimentally for the heat of fusion as a function of the number of methylene groups. A second order additivity rule, however, is too complicated for practical application if a large number of structural groups is involved. It would require the compilation of innumerable group pair contributions.

As was stated by Bondi (1968) the entropy of fusion, ΔS_m shows a more regular relation with structure than the enthalpy of fusion. At the melting point T_m the entropy of fusion may be calculated as:

$$\Delta S_m = \frac{\Delta H_m}{T_m} \quad (5.13)$$

The available experimental values of ΔH_m for a number of polymers, mentioned in Table 5.6, permit the calculation of ΔS_m for these polymers; group contributions can be derived according to the equation:

$$\Delta S_m = \sum_i n_i \Delta S_{m,i} \quad (5.14)$$

where n_i is the number of groups of type i , ΔS_i is the entropy contribution per group i .

The (partly still tentative) values of $\Delta S_{m,i}$ are given in Table 5.7. This table also shows tentative values for ΔH_m .

In the derivation of the $\Delta H_{m,i}$ and $\Delta S_{m,i}$ -values, homologous series with increasing numbers of methylene groups played an important role.

Using the derived $\Delta H_{m,i}$ and $\Delta S_{m,i}$ -increments, the values of ΔH_m and ΔS_m of the polymers in Table 5.6 were calculated; the last two columns of Table 5.6 give these values: ΔH_m (estim.) and ΔS_m (estim.). The agreement between experimental and estimated

TABLE 5.6 Enthalpy and entropy of melting of various polymers

Polymer	ΔH_m (exp.) (kJ mol ⁻¹)	T_m (K)	ΔS_m (exp.) (J mol ⁻¹ K ⁻¹)	ΔH_m (estim.) (kJ mol ⁻¹)	ΔS_m (estim.) (J mol ⁻¹ K ⁻¹)
Polyethylene	8.22 ^a	515	19.8	8.0	19.8
Polypropylene	8.70 ^a	461	18.9	8.7	18.9
Poly(1-butene)	7.00 ^a	411	17.0	7.0	17.3
Poly(1-pentene)	6.30 ^a	403	15.6	6.3	15.8
Polyisobutylene	12.0 ^a	317	37.8	12.6	28.9
Poly (4-methyl-1-pentene)	10.0 ^a	523	19.1	10.0	19.1
Polycyclopentene	12.0 ^c	307	39.1	12.0	41.7
Polycyclooctene	23.8 ^c	350	68	24.0	71.4
Polycyclodocene	32.9 ^c	353	93.5	32.0	91.2
Polycyclododecene	41.2 ^c	357	115	40.0	113
Poly(1,4-butadiene) <i>cis</i>	9.20 ^a	285	32.3	9.0	32.3
Poly(1,4-butadiene) <i>trans</i>	7.5 ^a	415	18.1	8	17.8
Poly(1,4-isoprene) <i>cis</i>	8.7 ^a	301	28.9	8.5	28.9
Polystyrene	10.0 ^a	516	19.3	10.0	19.4
Poly(<i>p</i> -xylylene)	{ 10.0 ^a 16.5 ^b	{ 700 713	{ 14.3 23.1	13	24
Poly(vinyl fluoride)	7.54 ^a	503	15.0	7.5	14.9
Poly(vinylidene fluoride)	6.70 ^a	483	13.9	8.0	16.9
Poly(vinyl chloride)	11.0 ^a	546	20.1	11.0	21.0
Poly(trifluoroethylene)	5.44 ^a	495	11.0	7.5	12
Poly(tetrafluoroethylene)	{ 8.20 ^a 9.3 ^b	{ 605 619	{ 13.5 15.0	8.0	14
Poly(trifluoro-chloro ethylene)	5.02 ^b	493	10.2	6.0	16.0
Poly(chloroprene)	8.37 ^c	383	21.9	8.5	21.8
Poly(vinyl alcohol)	6.87 ^a	521	13.2	7.0	13.2
Polyacrylonitrile	5.2 ^c	614	8.5	6.0	9.9
Poly(methyl methacrylate)	9.60 ^a	453	21.2	9.5	21.2
Poly(oxy-methylene) (POM)	{ 9.79 ^a 11.7 ^b	{ 457 456	{ 21.4 25.7	(5.1)	(15)
Poly(oxy-ethylene)	8.67 ^a	346	25.1	9	24
Poly(oxy-trimethylene)	9.44 ^c	309	30.6	13	33
Poly(oxy-tetramethylene)	14.4 ^a	333	43.2	17	42
Poly(oxy-octamethylene)	29.3 ^a	347	84.4	33	78
Poly(bischloromethyl-oxy-tri-methylene) (Penton®)	32 ^a	463	69.1	32	69
Poly(oxy-propylene)	8.4 ^a	348	24.1	9.7	24.0
Poly(oxy-1,4-phenylene)	7.82 ^a	535	14.6	6	11
Poly(oxy-2,6-dimethyl-1,4-phenylene) (PPO)	5.95 ^a	580	10.3	(3)	11
Poly(oxy-2,6-diphenyl-1,4-phenylene) (PPPO)	12.2 ^c	757	16.1	11	16
Poly (oxy-1,4-phenylene-oxy-1,4-phenylene-carbonyl-1,4-phenylene) (PEEK)	{ 37.4 ^a 46.5 ^b	668	{ 56.0 69.0	42	63
Poly(thio-trimethylene)	10.4 ^c	363	28.6	10.5	29

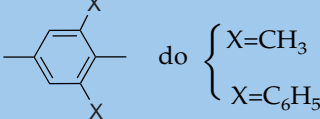
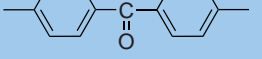
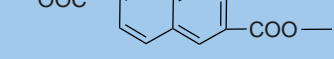
(continued)

TABLE 5.6 (*continued*)

Polymer	ΔH_m (exp.) (kJ mol ⁻¹)	T_m (K)	ΔS_m (exp.) (J mol ⁻¹ K ⁻¹)	ΔH_m (estim.) (kJ mol ⁻¹)	ΔS_m (estim.) (J mol ⁻¹ K ⁻¹)
Poly(propiolactone) (PE 3)	8.52 ^a	366	22.5	6.5	22
Poly(butyrolactone) (PE 4)	11.4 ^a	337	33.8	10.5	31
Poly(valerolactone) (PE 5)	16.0 ^a	331	48.3	14.5	40
Poly(caprolactone) (PE 6)	16.9 ^a	342	49.4	18.5	49
Poly(undecanolactone) (PE 11)	38.2 ^a	365	104.7	38.5	94
Poly(tridecanolactone) (PE 13)	46.1 ^a	368	125.3	45.5	112
Poly(pivalolactone)	14.9 ^c	513	29.0	10.1	33
Poly(ethylene adipate) (PE 2–6)	21.0 ^c	335	62.7	19.0	54
Poly(ethylene suberate) (PE 2–8)	26.5 ^c	348	76.1	19	72
Poly(ethylene sebacate) (PE 2–10)	35.0 ^c	356	89.6	27	88
Poly(decamethyl adipate) (PE 10–6)	45.6 ^c	350	130.3	51	120
Poly(decamethyl azelate) (PE 10–9)	50.7 ^c	343	147.8	63	142
Poly(decamethyl sebacate) (PE 10–10)	56.5 ^c	353	160.1	67	152
Poly(ethylene terephthalate)	26.9 ^a	550	48.9	25	48
Poly(butylene terephthalate)	32.0 ^a	518	61.8	33	64
Poly(hexamethylene terephthalate)	35.3 ^c	434	81.3	41	80
Poly(decamethylene terephthalate)	46.1 ^c	411	112.2	57	112
Poly(ethylene-2,6- naphthalene dicarboxylate (PEN))	25.0 ^a	610	41.0	25	43
Poly(bisphenol carbonate) (PC)	{33.5 ^a 36.9 ^b	608	{55.1 68.7	35	53.5
Poly(caprolactam) (PA-6)	26.0 ^a	533	48.8	22	47
Poly(undecanolactam) (PA-11)	41 ^c	473	86.7	42	92
Poly(pivalolactam)	13 ^c	546	23.8	14.6	31.2
Poly(hexamethylene adipamide) (PA 6–6)	{67.9 ^a 43 ^b	553	{122.8 79.6	44	84
Poly(hexamethyl sebacamide) (PA 6–10)	59 ^c	506	116.6	60	116
Poly(decamethyl azelamide) (PA 10–9)	68.2 ^a	489	139.4	72	140
Poly(decamethyl sebacamide) (PA 10–10)	72 ^c	489	147.2	76	144
Poly(dimethyl siloxane)	2.58 ^a	230	11.2	2.9	11
Poly(diethyl siloxane)	1.71 ^a	276	6.2	1.5	7.8

^a Data, selected by Wunderlich (1989).^b Data of Starkweather et al. (1982–1989).^c Data from Polymer Handbook.

TABLE 5.7 Tentative values of group contributions to the heat and entropy of melting

Group		$\Delta H_{m,l}$ (kJ mol ⁻¹)	$\Delta S_{m,l}$ (J mol ⁻¹ K ⁻¹)
$-\text{CH}_2-$	{ in carbon chains { main chain { side chain	4.0 -0.7	9.9 -1.6
	{ in hetero-chains { 1 hetero-group/unit { 2 hetero-groups/unit		
		4.0 4.0	9.0 8.0
$-\text{CH}(\text{CH}_3)-$		4.7	9.0
$-\text{CH}(\text{isopropyl})-$		6.7	10.8
$-\text{CH}(\text{C}_6\text{H}_5)-$		6	9.5
$-\text{C}(\text{CH}_3)_2-$	{ not enclosed { enclosed between rings	8.6 25	19 58
$-\text{CH}(\text{OH})-$		1.3	3.7
$-\text{CH}(\text{CN})-$		(2)	0
$-\text{CHF}-$		3.5	5
$-\text{CHCl}-$		7	10.2
$-\text{CF}_2-$		4	7
$-\text{CFCl}-$		2	(9)
$-\text{CCl}_2-$		4	11
$-\text{C}(\text{CH}_2\text{Cl})_2-$		2.5	43
$-\text{C}(\text{CH}_3)(\text{COOCH}_3)-$		5.5	11.3
$-\text{CH}=\text{CH}-$	<i>cis</i>	1	12.5
	<i>trans</i>	0	0
$-\text{CH}=\text{C}(\text{CH}_3)-$	<i>cis</i>	0.5	0.1
	<i>trans</i>	(4.5)	(16)
$-\text{CH}=\text{C}(\text{Cl})-$		0.5	2
 non-conjugated		5	5
	do { X=CH ₃ { X=C ₆ H ₅	5 10	5 10
$>\text{CH}-\text{CH}<$		(0)	1.2
$-\text{Si}(\text{CH}_3)_2-$		1.8	5
$-\text{O}-$		1	6
$-\text{S}-$		-1.5	2
$-\text{CO}-$		(0)	(0)
$-\text{COO}-$		-2.5	4
$-\text{CONH}-$		2	2
$-\text{OCOO}-$		(0)	(0)
		17	32
		3.5	46
		17	25

(“predicted”) values is fair, especially in view of the considerable deviations between the experimental values of different investigators; deviations of the order of 10% are quite normal, and even the values given by renowned experts, such as Wunderlich and Zoller, show differences of this order of magnitude (see the examples given in Table 5.6).

The “predicted” values in Table 5.6 have average deviations from the experimental values of 11% for ΔH_m and of 7% of ΔS_m . In accordance with Bondi’s statement the “additivity” of ΔS_m is better than that of ΔH_m .

It must be remarked that the $\Delta S_{m,i}$ -increments of the methylene groups in linear polymers with functional hetero-groups in the main chain, are smaller than the corresponding value for polyethylene, being $9.9 \text{ J mol}^{-1} \text{ K}^{-1}$; they are also variable with the number of hetero-groups per structural unit. The value of $9.9 \text{ J mol}^{-1} \text{ K}^{-1}$ again differs from the still higher values for methylene groups, about 11.1, observed in homologous series of low-molecular compounds (Bondi, 1968). For some series of compounds of low molar mass, however, a contribution for the methylene group of about 9.8 was found.

It may be wise to make the estimations of ΔH_m and ΔS_m by using both sets of increments, with application of Eq. (5.13) for comparison of the results.

5.3. ENTHALPY AND ENTROPY

In determining the course of enthalpy and entropy of a substance with temperature it is usual to start from very accurate specific heat measurements. Enthalpy and entropy may then be calculated by integration:

$$H(T) = H(0) + \int_0^T C_p dT + \sum \Delta H_i \quad (5.15)$$

$$S(T) = S(0) + \int_0^T \frac{C_p}{T} dT + \sum \Delta S_i \quad (5.16)$$

where $H(0)$ and $S(0)$ are the enthalpy and entropy at 0 K and ΔH_i and ΔS_i are the enthalpy and entropy changes at first order phase transitions.

If this method is applied to thermodynamic data of polymers, the same difficulty arises as mentioned in Sect. 5.1 for the determination of the specific heat: most polymer samples are partly crystalline, only. The thermodynamic quantities have values somewhere between those for purely crystalline and purely amorphous polymer. A large number of measurements are needed to derive the data for these two idealized states. Only for a limited number of polymers have data of this kind been published.

As an example, in Figs. 5.5 and 5.6 enthalpy and entropy as a function of temperature are plotted for polypropylene, according to the data of Gee and Melia (1970), Dainton et al. (1962) and Passaglia and Kevorkian (1963).

The corresponding data for some other polymers may be found in a series of articles by Dainton et al. (1962).

As appears from Fig. 5.5, the enthalpy curves for crystalline and amorphous polypropylene run parallel up to the glass transition temperature. The distance between these curves is called $\Delta H(0)$ = the enthalpy of the amorphous polymer at 0 K. From the glass transition temperature on the curve for the amorphous polymer gradually approaches the curve for the melt, while the curve for the crystalline polymer shows a discontinuity at the melting point. The distance between the curves for crystal and liquid at the melting point is the latent heat of fusion, ΔH_m .

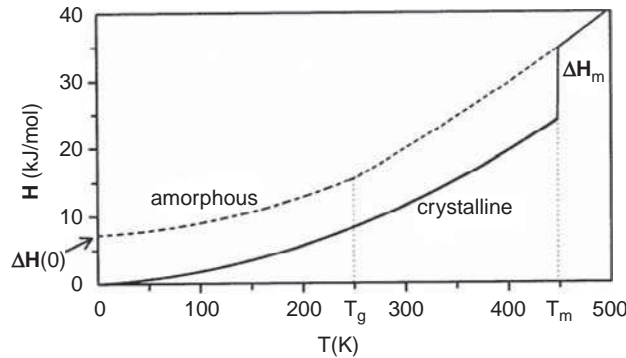


FIG. 5.5 Enthalpy of polypropylene in the glassy, rubbery and crystalline state.

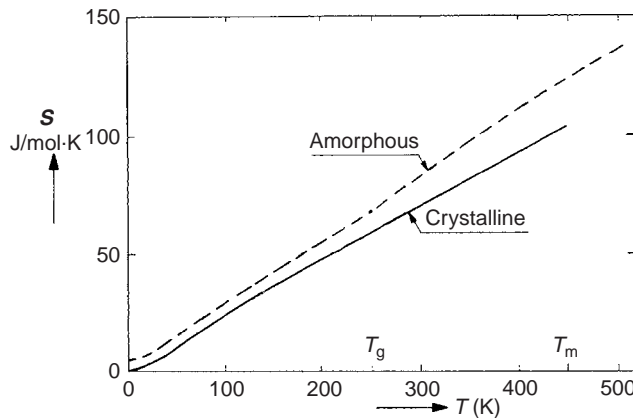


FIG. 5.6 Entropy of polypropylene in the glassy, rubbery and crystalline state.

The curves for the entropy of crystalline and amorphous polymer in Fig. 5.6 show an analogous course.

Application of Eq. (5.15) to crystalline and liquid polymers leads to:

$$H_c(T) = H_c(0) + \int_0^T C_p^s dT, \quad (T < T_m) \quad (5.17)$$

$$H_l(T) = H_c(0) + \int_0^{T_m} C_p^s dT + \int_{T_m}^T C_p^l dT + \Delta H_m, \quad (T > T_m) \quad (5.18)$$

and for amorphous and liquid polymers:

$$H_a(T) = H_c(0) + \Delta H(0) + \int_0^{T_g} C_p^a dT, \quad (T < T_g) \quad (5.19)$$

$$H_l(T) = H_c(0) + \Delta H(0) + \int_0^{T_g} C_p^a dT + \int_{T_g}^T C_p^l dT, \quad (T > T_g) \quad (5.20)$$

According to Fig. 5.5, $\mathbf{H}_l(T_g) = \mathbf{H}_c(T_g) + \Delta\mathbf{H}(0)$. Combination of these equations, substitution of Eqs. (5.7) and (5.8) and assuming $\mathbf{C}_p^a = \mathbf{C}_p^s$ for $T < T_g$ gives:

$$\begin{aligned}\Delta\mathbf{H}_m - \Delta\mathbf{H}(0) &= [0.61\mathbf{C}_p^1(298) - 0.106\mathbf{C}_p^s(298)](T_m - T_g) \\ &\quad + [0.00065\mathbf{C}_p^1(298) - 0.0015\mathbf{C}_p^s(298)](T_m^2 - T_g^2)\end{aligned}\quad (5.21)$$

Although Eqs. (5.7) and (5.8) are certainly not valid at very low temperatures, the deviations cancel out for the greater part, because the curves for \mathbf{H}_a and \mathbf{H}_s run parallel at low temperatures.

Application of Eq. (5.21) to a number of polymers gave the correct order of magnitude for $\Delta\mathbf{H}_m - \Delta\mathbf{H}(0)$. The equation cannot be used for an accurate prediction of $\Delta\mathbf{H}_m$, however, because of lack of data for $\Delta\mathbf{H}(0)$ and the approximate character of Eqs. (5.7) and (5.8). But Eq. (5.11) suggests that $\Delta\mathbf{H}_m$ will increase with increasing values of $\mathbf{C}_p^1(298)$ and of $(T_m - T_g)$. This is proved in Fig. 5.7, where the ratio $\Delta\mathbf{H}_m/\mathbf{C}_p^1(298)$ is plotted against $(T_m - T_g)$ for a number of polymers, for which values of $\Delta\mathbf{H}_m$ have been published. As a first approximation (least squares fit for the curve through the origin: correlation coefficient = 0.98 and a standard deviation of about 25%):

$$\frac{\Delta\mathbf{H}_m}{\mathbf{C}_p^1(298)} = 0.55(T_m - T_g) \quad (5.22)$$

An equation analogous to (5.21) can be derived for the entropy:

$$\begin{aligned}\Delta\mathbf{S}_m - \Delta\mathbf{S}(0) &= [0.61\mathbf{C}_p^1(298) - 0.106\mathbf{C}_p^s(298)]\ln(T_m/T_g) \\ &\quad + [0.0013\mathbf{C}_p^1(298) - 0.003\mathbf{C}_p^s(298)](T_m - T_g)\end{aligned}\quad (5.23)$$

This equation can be checked more accurately than Eq. (5.21) because the order of magnitude of $\Delta\mathbf{S}(0)$ can be estimated. The data given by Bestul and Chang (1964) correspond to a contribution to $\Delta\mathbf{S}(0)$ of about $2.9 \text{ J mol}^{-1} \text{ K}^{-1}$ per chain atom. With these values for $\Delta\mathbf{S}(0)$, $\Delta\mathbf{S}_m$ may be calculated according to Eq. (5.23). Fig. 5.8 shows calculated values of $\Delta\mathbf{S}_m$ for a number of polymers plotted against experimental values of $\Delta\mathbf{S}_m$. The dashed line represents $\Delta\mathbf{S}_m(\text{calc}) = \Delta\mathbf{S}_m(\text{exp})$, whereas the average of $\Delta\mathbf{S}_m(\text{calc})/\Delta\mathbf{S}_m(\text{exp}) = 0.96$

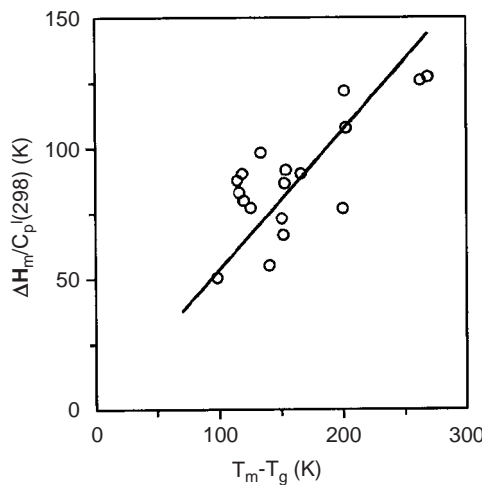


FIG. 5.7 Approximate correlation for $\Delta\mathbf{H}_m$.

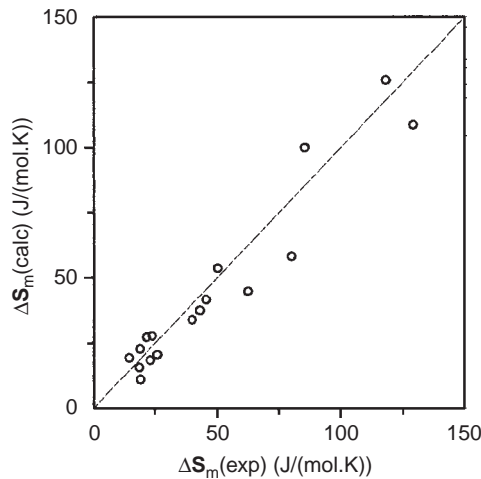


FIG. 5.8 Calculated and experimental values of ΔS_m .

with a standard deviation of 0.21 (= 22%). Considering the inaccuracy of the data used, the result is satisfactory.

Finally, reference is made to a series of articles by Griskey et al. (1966, 1967) mentioning values for enthalpy and entropy as a function of temperature and pressure for a number of commercial plastics.

Example 5.2

Estimate the following properties of poly(ethylene terephthalate) ($M = 192.2$):

- The specific heat of the solid polymer at 25°C (=298 K)
- The specific heat of the liquid polymer at spinning temperature ($277^\circ\text{C} = 550$ K)
- The heat of fusion at the melting point.
- The enthalpy difference between the solid and the rubbery form at the glass transition temperature.

Solution

With the data of Tables 5.1 and 5.7 we find:

Group	$C_p^s(298)$	$C_p^l(298)$	Group	$\Delta H_m \text{ (J mol}^{-1}\text{)}$
$-\text{C}_6\text{H}_4-$	78.7	113.1	$-\text{OOC}-\text{C}_6\text{H}_4-\text{COO}-$	17,000
$2-\text{CH}_2-$	50.7	60.8	$2-\text{CH}_2-$ (carbon main chain)	8,000
$2-\text{COO}-$	92.0	130.0		
	221.4	303.9		25,000

Ad (a) The specific heat of the solid polymer at 25°C will be:

$$c_p^s(298) = \frac{221.4}{192.2} \times 10^3 = 1152 \text{ J kg}^{-1} \text{ K}^{-1}$$

in excellent agreement with the experimental value 1130.

Ad (b) According to Eq. (5.8) the molar heat capacity of the liquid is:

$$C_p^l(550) = C_p^l(298)[0.61 + 0.0013T] = 303.9(0.61 + 0.715) = 402.7$$

The specific heat will be:

$$c_p^l(550) = \frac{402.7}{192.2} \times 10^3 = 2095 \text{ J kg}^{-1} \text{ K}^{-1} \quad (\text{experimental value 2010})$$

Ad (c) The heat of fusion at the melting point is $25,000 \text{ J mol}^{-1}$, in reasonable agreement with the experimental value 26,900

Ad (d) According to Eq. (5.21) we have

$$\begin{aligned}\Delta H(T_g) &= \Delta H(0) = \Delta H_m - [0.61C_p^l(298) - 0.106C_p^s(298)](T_m - T_g) \\ &\quad - [0.65 \cdot 10^{-3}C_p^l(298) - 1.5 \cdot 10^{-3}C_p^s(298)](T_m^2 - T_g^2)\end{aligned}$$

or

$$\begin{aligned}\Delta H(T_g) &= 25,000 - (0.61 \times 303.9 - 0.106 \times 221.4)(543 - 343) \\ &\quad - (0.65 \times 10^{-3} \times 303.9 - 1.5 \times 10^{-3} \times 221.4)(543^2 - 343^2) \\ &= 25,000 - 32,382 + 23,845 = 1.65 \times 10^3 \text{ J mol}^{-1}.\end{aligned}$$

BIBLIOGRAPHY

General references

- Bicerano J, "Prediction of Polymer Properties", Marcel Dekker, New York, 3rd Ed, 2002, Chap. 4.
- Bondi A, "Physical Properties of Molecular Crystals, Liquids and Glasses", Wiley, New York, 1968.
- Godovsky YK, "Thermophysical Properties of Polymers", Springer-Verlag, Berlin, 1992.
- Pan R, Cao MY and Wunderlich B, "Heat Capacities of High Polymers"; in Brandrup J, Immergut EH and Grulke EA, (Eds) "Polymer Handbook", Part VII, p 291, Wiley, New York, 4th Ed, 1999.
- Pyda M and Wunderlich B, "Heat Capacities of High Polymers"; in Brandrup J, Immergut EH and Grulke EA, (Eds) "Polymer Handbook", Part VI p. 483, Wiley, New York, 4th Ed, 1999.
- Reid RC and Sherwood Th K, "The Properties of Gases and Liquids", McGraw-Hill, New York, 1st Ed, 1958, 2nd Ed, 1966, 3rd Ed, 1977 (with Prausnitz JM).
- Tury EA, "Thermal Characterisation of Polymeric Materials", Academic Press, New York, 1981.
- Varna-Nair M and Wunderlich B, "Heat Capacity and other Thermodynamic Properties of Linear Macromolecules", X-Update of the ATHAS (i.e. Advanced Thermal Analysis) Data Bank, a computerized version of the data bank of heat capacities.
- Wen J, "Heat Capacities of Polymers" in Mark JE (Ed), "Physical Properties of Polymers Handbook", Springer-Verlag, 2nd Ed, 2007, Chap. 9.
- Wendtlandt WW, "Thermal Analysis", 3rd Ed, Wiley, New York, 1985.
- Wunderlich B, "Macromolecular Physics", 3 vols, Academic Press, New York, 1973–1980.
- Wunderlich B, Cheng SZD and Loufakis K "Thermodynamic Properties of Polymers", in Mark HF, Bikales NM, Overberger CG, Menges G and Kroschwitz JI (Eds) "Encyclopedia of Polymer Science and Engineering", Vol. 16, pp. 767–807, Wiley, New York, 1989.

Special references

- Baur H and Wunderlich B, Adv Polym Sci 7 (1970), 151.
- Bestul AB and Chang SS, J Chem Phys 40 (1964) 3731.
- Dainton FS, Evans DM, Hoare FE and Melia TP, Polymer 3 (1962) 286.

- Gee DR and Melia TP, *Makromol Chem* 132 (1970) 195.
Griskey RG et al., several articles in *Modern Plastics* 43 (1966); 44 (1967).
Johnson AJ and Huang CJ, *Can J Technol* 33 (1955) 421.
Nernst W and Lindemann FA, *Z Elektrochemie*, 17 (1911) 817.
Passaglia E and Kevorkian R, *J Appl Phys* 34 (1963) 90.
Redlich O, Derr EL and Pierotti GJ, *J Am Chem Soc* 81 (1959) 2283.
Satoh S, *J Sci Res Inst (Tokyo)* 43 (1948) 79.
Shaw R, *J Chem Eng Data* 14 (1969) 461.
Starkweather HW, Zeller P and Jones GA, *J Polym Sci, Polym Phys Ed* 20 (1982) 751; 21 (1983) 295; 22 (1984) 1431, 1615; 26 (1988) 257; 27 (1989) 993.
Warfield RW, Pastine DJ and Petree MC, US Naval Ordnance Lab, RPT NOLTR 69-98, 1969.
Warfield RW, Pastine DJ and Petree MC, *Appl Phys Lett*, 25 (1974) 638.
Wunderlich B *J Phys Chem* 64 (1960) 1052.
Wunderlich B and Jones LD, *J Macromol Sci Phys B* 3 (1969) 67.
Wunderlich B et al., *J Macromol Sci, Phys B* 3 (1969) 67; *J Polym Sci B (Pol Phys Ed)* 16 (1978) 289; 18 (1980) 449; 22 (1984) 379; 23 (1985) 1671; 24 (1986) 575, 595, 1755, 2459; *J Chem Phys, Ref Data* 10 (1981) 1001; 12 (1988) 65, 91; *Polymer* 26 (1985) 561, 1875; 27 (1986) 563, 575; 28 (1987) 10; *Macromolecules* 19 (1986) 1868; 20 (1987) 1630, 2801; 21 (1988) 7, 89; 22 (1989); *Makromol Chem* 189 (1988) 1579.

CHAPTER 6

Transition Temperatures

In this chapter it will be demonstrated that the two main transition temperatures, viz. the glass–rubber transition temperature and the crystalline melting temperature can be correlated with the chemical structure by means of a method based on group contributions.

6.1. INTRODUCTION

As was stated in Chap. 2, it is impossible to understand the properties of polymers if the transitions that occur in such materials and specifically the temperatures at which these occur are not known. The main transitions are the glass–rubber transition and the crystalline melting point. These two will be discussed in this chapter.

However, several other transitions of secondary importance may often be observed. As to the denomination of these transitions there is a complete lack of uniformity. Usually the symbols T_α , T_β , etc., are used, but different authors use different symbols for the same transition.

There may be at least three transitions in the glassy state below T_g viz. in the temperature ranges from $0.5T_g$ to $0.8T_g$, from $0.35T_g$ to $0.5T_g$ and at very low temperatures (4–40 K). Between T_g and T_m transitions may be observed in the rubbery amorphous state and in the crystalline state. Even in the liquid state of the polymer transitions may be observed, e.g. the temperature of melting of “liquid crystals”.

Transition temperatures are extremely “structure-sensitive”, partly due to steric effects, partly due to intra- and inter-molecular interactions.

In order to make the discussion as clear as possible, we shall distinguish the structural groups in two main types:

- a. The *non-functional structural groups*, which are the real “building blocks” of the polymeric chain. To these groups are counted (as extremes) the methylene group ($-\text{CH}_2-$) and the phenylene groups ($-\text{C}_6\text{H}_4-$); in both groups hydrogen atoms may be substituted by other elements or groups;
- b. The *functional structural groups*, originating from the condensation reactions of the functional groups in the “monomers” (such as $-\text{OH}$, $-\text{NH}_2$, $-\text{COOH}$, $-\text{COCl}$, etc.). These groups give the characteristic names to the polymer families, such as polyoxides, -sulphides, -carbonates, -esters, -amides, -urethanes, etc. It are also these groups on which the polymer can be selectively “depolymerised” by smooth chemical treatment, such as hydrolysis, aminolysis, etc. (This is in contrast to the thermal decomposition, in which also the non-functional groups are attacked).

6.2. THE GLASS TRANSITION TEMPERATURE

Several authors have proposed correlations between the chemical structure and the glass transition temperature of polymers. Their methods are usually based on the assumption that the structural groups in the repeating units provide weighed additive contributions to the T_g . In the case of ideal additivity the contribution of a given group is independent of the nature of adjacent groups. Although this ideal case is seldom encountered in practice, additivity can often be approximated by a proper choice of structural groups. We will revert to this point later.

The general form of the correlations for T_g is

$$T_g \sum s_i = \sum s_i T_{gi} \quad (6.1)$$

so that

$$T_g = \frac{\sum s_i T_{gi}}{\sum s_i} \quad (6.2)$$

where T_{gi} is the specific contribution to T_g of a given structural group, and s_i is a weight factor attributed to that structural group.

Different assumptions for s_i were proposed in the literature. Barton and Lee (1968) suggested s_i to be equal to the weight- or mole fraction of the relevant group in relation to the structural unit. Weyland et al. (1970) put s_i equal to Z_i , the number of backbone atoms of the contributing group. Becker (1978) and Kreibich and Batzer (1979) identified s_i with the number of freely and independently oscillating elements in the backbone of the structural unit. In general s_i is held as a kind of "entropy of transition".

With regard to the sum $\sum s_i T_{gi}$ most authors see it as proportional to the cohesion energy, so, e.g. Hayes (1961), Wolstenholme (1968) and Kreibich and Batzer (1979, 1982).

It should be annotated that the *form* of the aforementioned equation is the same as the well-known thermodynamic expression for phase transitions of the first order:

$$\Delta G_{tr} = 0 \quad \text{so that} \quad \Delta H_{tr} = T_{tr} \Delta S_{tr}$$

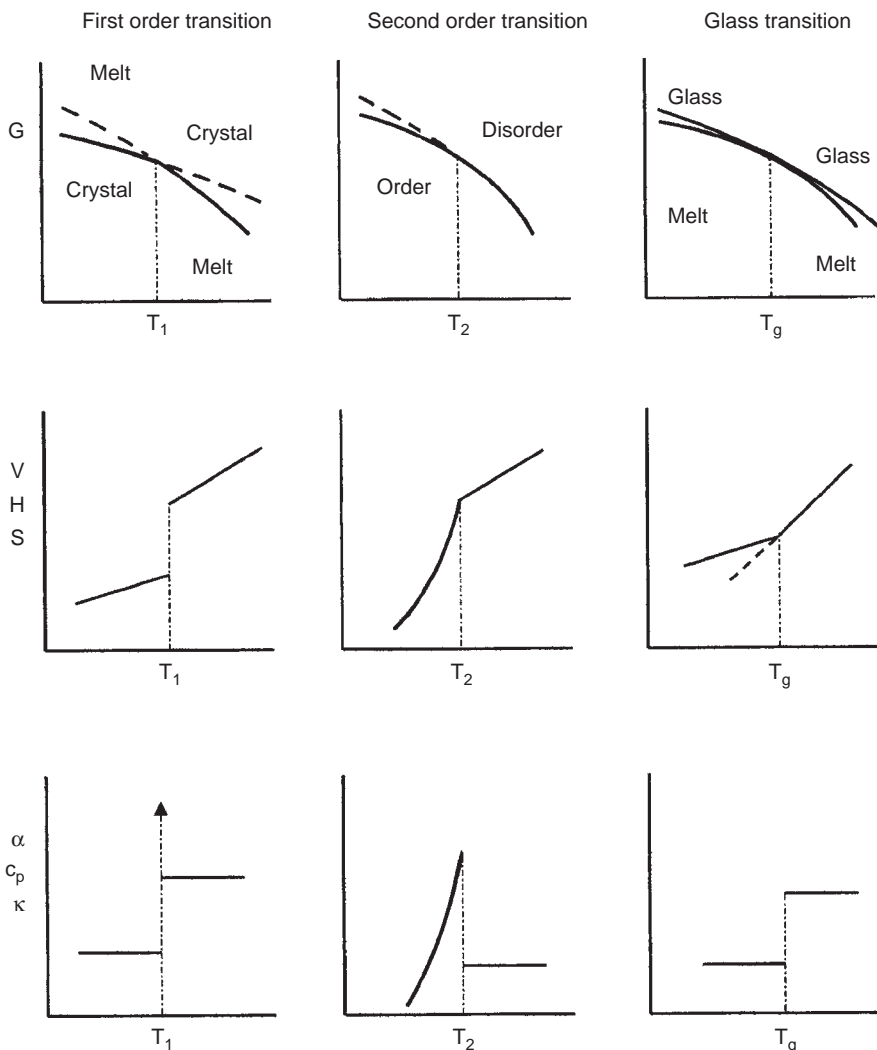
A serious objection against such a thermodynamic analogy, however, for identifying $\sum s_i T_{gi}$ with the molar cohesion energy is twofold:

First, the glass–rubber transition is not a real thermodynamic phase transition, neither a first- nor a second-order transition, as was proved by Staverman (1966) and Rehage et al. (1967, 1980, 1984), (see Scheme 6.1); the glassy state is not thermodynamically stable and thus not defined by the normal state variables; also its history and its age play a part. At the very best the T_g -transition may be seen as a quasi-second-order transition but certainly not as a first-order one.

A second, even more serious, objection against the use of the cohesion energy is that the glass transition is the change from one condensed state (glass) to another condensed state (liquid) whereas the cohesion energy belongs to the change of the condensed state to the completely free state of the molecules (e.g. in ideal diluted solutions or even gas).

A quite different method for calculating T_g was proposed by Marcinčin and Romanov (1975). They developed the formula (also based on cohesive energy):

$$T_g = \frac{V}{V_s} \times 10^{kE_{coh}/(\rho V_s)} \quad (6.3)$$



SCHEME 6.1 Scheme of the change of Thermodynamic Data for transformations of first and second order and for the glass transition. (After Rehage, 1967, 1984).

$$\begin{aligned} S &= - \left(\frac{\partial G}{\partial T} \right)_P; \quad V = \left(\frac{\partial G}{\partial P} \right)_T; \\ C_P &\equiv \left(\frac{\partial H}{\partial T} \right)_P = T \left(\frac{\partial S}{\partial T} \right)_P = -T \frac{\partial^2 G}{\partial T^2}; \quad \kappa \equiv -\frac{1}{V} \left(\frac{\partial V}{\partial P} \right)_T = -\frac{1}{V} \frac{\partial^2 G}{\partial P^2}; \quad \alpha \equiv \frac{1}{V} \left(\frac{\partial V}{\partial T} \right)_P = \frac{1}{V} \frac{\partial^2 G}{\partial T \partial P}. \end{aligned}$$

where V = molar volume of polymer unit; k = constant; E_{coh} = cohesive energy; ρ = density; V_s = parameter with additive properties.

The authors applied Eq. (6.3) to a limited number of polymers; rather large deviations were found, however.

6.2.1. An additive molar function for the calculation of T_g

We come to reach the conclusion that it is wiser not to load the additive function of the glass transition with quasi-theoretical assumptions and to use a pragmatic, empirical approach.

It became evident in work of Van Krevelen and Hoflyzer (1975) that the product $T_g \cdot \mathbf{M}$ behaves in general as an additive function, which was called the *Molar Glass Transition Function*.

$$\mathbf{Y}_g = \sum_i \mathbf{Y}_{gi} = T_g \cdot \mathbf{M} \quad (6.4)$$

so that

$$T_g = \frac{\mathbf{Y}_g}{\mathbf{M}} = \frac{\sum \mathbf{Y}_{gi}}{\mathbf{M}} \quad (6.5)$$

Eq. (6.4) has been applied to the available literature data on T_g 's of polymers, in all nearly 600; from this study the correlation rules for \mathbf{Y}_g have been derived. It appeared that the \mathbf{Y}_{gi} -values of the relevant groups are not independent of some other groups present in the structural unit.

The group contributions and structural corrections found are summarised in Table 6.1. We shall discuss these data step by step.

6.2.2. Derivation of the group contributions to \mathbf{Y}_g

6.2.2.1. The unbranched polymethylene chain

Considerable confusion exists in the literature concerning the real glass transition temperature of polymethylene, i.e. of ideal linear polyethylene. Values between 140 and 340 K have been reported (see Boyer, 1973, 1975). In agreement with Boyer we are convinced, for a variety of reasons (see Boyer, 1973), that the correct T_g of amorphous polymethylene is 195 ± 10 K. This gives for the basic contribution of $-\text{CH}_2-$ to \mathbf{Y}_g :

$$\mathbf{Y}_g(-\text{CH}_2-) = (195 \pm 10) \times 14.03 = 2736 \pm 140 \text{ K mol}^{-1} = 2.74 \pm 0.14 \text{ K kg mol}^{-1}$$

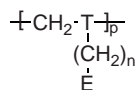
We shall apply a round value of $2.7 \text{ K kg mol}^{-1}$

6.2.2.2. Aliphatic carbon main chains with “small” side groups (substituted polymethylene chains)

The main representative polymer family of this class are the simplest vinyl polymers. The group contributions of the groups OCH_2O and $-\text{CH}_2\text{O}$ are given in Table 6.1.

6.2.2.3. Aliphatic carbon main chains with “long” paraffinic side chains (“comb-polymers”)

The main representatives are the vinyl polymers, viz. of the type



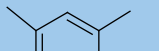
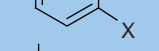
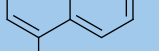
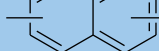
where T stands for a trivalent structural group, e.g. $>\text{CH}-$ or $>\text{C}(\text{CH}_3)-$; the polymer with $N = 0$ will be called the “basic” polymer. A side chain is thus considered as a *univalent end group* E (e.g. methyl, isobutyl, tert-butyl, neo-pentyl, etc.) plus an inserted sequence of CH_2 -groups between T in the main chain and E.

TABLE 6.1 Group contributions (increments) to \bar{Y}_g (K kg mol^{-1})

A. Non-conjugating groups										
	Group	\bar{Y}_{gi}	M_i		Group	\bar{Y}_{gi}	M_i			
$-\text{CH}_2-$	In main chains (gen.)	2.7		Eq. (6.6/8)	Ali-cyclic		<i>cis</i>	(19)	82.1	
	In hydrogen bonded chains	4.3	14.0				<i>trans</i>	27	82.1	
	In side chains									
$-\text{CHR}-$	$-\text{CH}(\text{CH}_3)-$	8.0	28.0		C-Halide	$-\text{CHF}-$		12.4	32.0	
	$-\text{CH}(\text{isopropyl})-$	19.9	56.1			$-\text{CHCl}-$		19.4	48.5	
	$-\text{CH}(\text{tert.butyl})-$	25.6	70.1			$-\text{CFCl}-$		22.8	66.5	
	$-\text{CH}(\text{cyclopentyl})-$	30.7	82.1			$-\text{CF}(\text{CF}_3)-$		24	82.9	
	$-\text{CH}(\text{cyclohexyl})-$	41.3	96.2			$-\text{CF}_2-$		10.5	50.0	
	$-\text{CH}(\text{C}_6\text{H}_5)-$	36.1	90.1			$-\text{CCl}_2-$		22.0	82.9	
	$-\text{CH}(\text{p-C}_6\text{H}_4\text{CH}_3)-$	41.2	104.1		Hetero	$-\text{O}-$		4	16.0	
$-\text{CHX}-$	$-\text{CH}(\text{OH})-$	13	30.0			$-\text{NH}-$		(7)	15.0	
	$-\text{CH}(\text{OCH}_3)-$	11.9	44.1			$-\text{S}-$		8	32.1	
	$-\text{CH}(\text{OCOCH}_3)-$	23.3	72.1			$-\text{SS}-$		16	64.2	
	$-\text{CH}(\text{COOCH}_3)-$	21.3	72.1			$-\text{Si}(\text{CH}_3)_2-$		free	7	58.2
	$-\text{CH}(\text{CN})-$	17.3	39.0					st. hind.	16	58.2
$-\text{CX}_2-$	$-\text{C}(\text{CH}_3)_2-$ free	8.5	42.1		C-hetero	$\text{---O} \begin{array}{c} \text{O} \\ \parallel \\ \text{C} \end{array} \text{---O ---}$		20	60.0	
	$-\text{C}(\text{CH}_3)_2-$ st. hindered	15, ss26	42.1			$\text{---O} \begin{array}{c} \text{O} \\ \parallel \\ \text{C} \end{array} \text{---NH ---}$		20	59.0	
	$-\text{C}(\text{CN})_2-$	22	64.0			$\text{---HN} \begin{array}{c} \text{O} \\ \parallel \\ \text{C} \end{array} \text{---NH ---}$		20	58.0	
	$-\text{C}(\text{C}_6\text{H}_5)_2-$	65	164.2							
$-\text{CXY}-$	$-\text{C}(\text{CH}_3)(\text{COOCH}_3)-$	35.1	86.1							
	$-\text{C}(\text{CH}_3)(\text{C}_6\text{H}_5)-$	51	104.1							

(continued)

TABLE 6.1 (continued)

B. Groups with potential mutual conjugation						
Double-bonded systems			Aromatic ring systems			
Group		γ_{gi}	M_i	Group	γ_{gi}	M_i
$-\text{CH}=\text{CH}-$	<i>cis</i>	3.8	26.0		n	29.5
	<i>trans</i>	7.4	26.0		c	35
$-\text{CH}=\text{CH}(\text{CH}_3)-$	<i>cis</i>	8.1	40.1		cc	41
	<i>trans</i>	9.1			n	25
$-\text{C}(\text{CH}_2)=\text{C}(\text{CH}_2)-$		16.1	54.1		c	29
$-\text{CH}=\text{CF}-$		9.9	44.0		cc	34
$-\text{CH}=\text{CCl}-$		15.2	60.5		X = CH_3	35
$-\text{CF}=\text{CF}-$		20.3	62.0		X = C_6H_5	90.1
$-\text{C}=\text{C}-$		11	24.0		X = Cl	152.2
$\begin{array}{c} \text{O} \\ \parallel \\ -\text{C}- \end{array}$	n	11.5				110.5
	c	15.5	28.0		X = CH_3	54
	cc	19			X = C_6H_5	104.1
$-\text{C}(=\text{O})-\text{O}-\text{C}(=\text{O})-$	n	22	72.0		X = Cl	228.3
					X = CH_3	145.1
$-\text{C}(=\text{O})-\text{O}-$	n	12.5			X = C_6H_5	30
	c	13.5	114.0		X = Cl	90.1
	cc/1)	15			X = CH_3	152.2
$-\text{C}(=\text{O})-\text{NH}-$	n	15			X = C_6H_5	50
	c	21.5	43.0		X = Cl	126.2
	cc/1)	30				
$-\text{S}(=\text{O})-$	n	32.5				
	c	36	64.1			
	cc	40				

n = non-conjugated (isolated in aliphatic chain); *c* = one-sided conjugation with aromatic ring; *cc* = two-sided conjugation /1) between two aromatic rings (rigid).

C. Tentative values for heterocyclic groups

Non-conjugating groups			Conjugating groups				
Group	γ_{gi}	M_i	Group	c = one sided	cc = two sided	γ_{gi}	M_i
	29	84.0		c	(30)	68.0	
	50	110.1		cc	(35)	84.1	
	60	124.1		c	95	145.1	
	75	152.1		cc	(78)	116.1	
	70	132.1		cc	110	156.1	

(continued)

TABLE 6.1 (continued)

C. Tentative values for heterocyclic groups						
Non-conjugating groups			Conjugating groups			
Group	Y_{gi}	M_i	c = one sided	Group	Y_{gi}	M_i
	(100)	182.1			cc	(130) 190.3
	175	214.1				

D. Tentative values of the Exaltation (increase) of group-contribution values (increments) by conjugation of the group with an aromatic ring (system) (values in $K \text{ kg mol}^{-1}$)		
Exaltation by conjugation		
Group	one sided on aromatic ring	two sided between aromatic rings
-COO-	1	2.5
-SO ₂ -	3.5	7.5
-CO-	5	10
-CONH-	6.5	15
-C ₆ H ₄ - para-position	5.5 (2.5) ^a	11.5 (5.5) ^a
-C ₆ H ₄ - meta-position	4 (1.5) ^a	9 (3.5) ^a

^a The values between brackets should be used if these groups are conjugated with the -COO- group, due to the weakness of conjugation of the latter group.

The \mathbf{Y}_g -values of the different "basic polymers" ($=\mathbf{Y}_{go}$) are determined by the chemical structure of the groups T and E; they can be calculated by means of the increments given in Table 6.1.

In the calculation of the \mathbf{Y}_g -values of comb-polymers with different lengths of side chains (i.e. varying values of N_{CH_2}) we meet a difficulty that is "structure determined". If we plot the empirical \mathbf{Y} -values ($=T_g \cdot M$) as a function of N_{CH_2} (Fig. 6.1), we immediately see that the increment of the CH_2 group in the side chain is not constant but varies with the length of the side chain. This is understandable because the side chain starts perpendicularly to the main chain and has to be "fitted" in the eventual ordering: at short lengths the side chain has a disordering effect, whereas at high values of N_{CH_2} the side chains mutually contribute to inter-molecular ordering (a kind of "side chain crystallization").

With increasing length of the methylene chain T_g at first decreases, passes through a minimum and then increases again. This behaviour may be approximately described by starting from the lucky fact that for each series of comb-polymers a minimum value of $T_g = 200$ K is reached at $N = 9$ (see Fig. 6.1). T_g for each member of the series may be predicted with the aid of the equations:

$$N = 9, \quad Y_g \approx 0.2M_9 = Y_{g9} \quad (6.6)$$

$$N < 9, \quad Y_g \approx Y_{go} + \frac{N}{9}(Y_{g9} - Y_{go}) \quad (6.7)$$

$$N > 9, \quad Y_g = Y_{g9} + 7.5(N - 9) \quad (6.8)$$

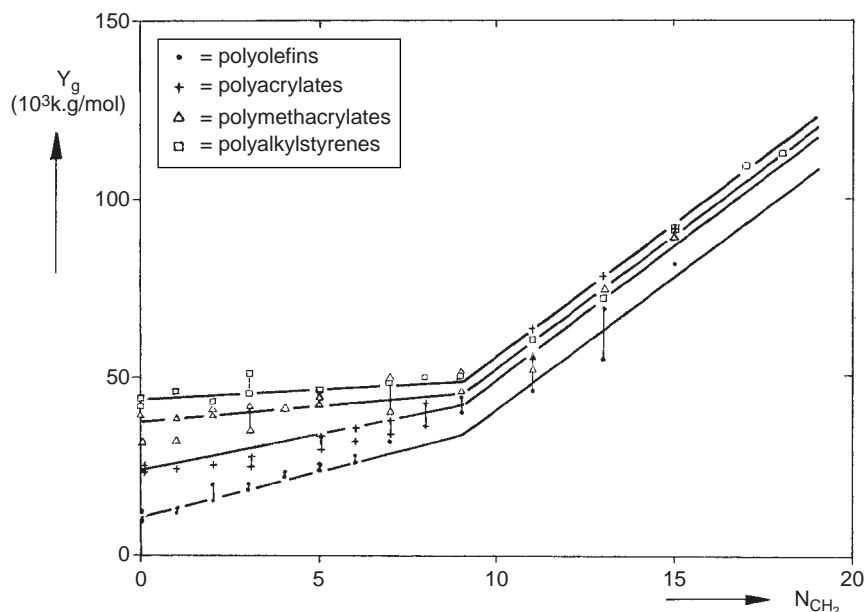


FIG. 6.1 \mathbf{Y}_g values of vinyl polymers with side chains.

Table 6.2 summarises values of Y_{go} and Y_{g9} for some series of comb-polymers. In Fig. 6.2 glass transition temperatures of poly(alkyl methacrylates), calculated with the aid of Eqs. (6.6)–(6.8), and experimental values are shown. In the calculated curve a sharp minimum is present for $N = 9$, due to the change of slope of Y_g in Fig. 6.1 at $N = 9$. The increase of the glass temperature above $N = 9$ might be attributed to the possibility of ordering, but also to the possibility of crystallization of side groups above $N = 9$: in poly(alkyl methacrylates) with higher values of N , synthesized in our laboratory at Delft University of Technology, phase separation was observed clearly (they looked like honey where some crystallization of sugar has occurred).

TABLE 6.2 Basic data for vinyl polymers with long paraffinic side chains (end-group E = methyl)

Series	Basic polymer	Trivalent group T	Y_{go}	Y_{g9}	M_0	M_9
Polyolefins	Polypropylene	$>\text{CH}-$	10.7	33.6	42.0	168.3
Polyalkylstyrenes	Poly(p-methylstyrene)	$>\text{CH}(\text{C}_6\text{H}_4)-$	44.7	48.8	118.2	244.4
Polyvinyl ethers	Poly(vinyl methyl ether)	$>\text{CH}(\text{O}-)-$	14.6	36.8	58.1	184.3
Polyvinyl esters	Poly(vinyl acetate)	$>\text{CH}(\text{OCO}-)-$	26.0	42.4	86.1	212.3
Polyacrylates	Poly(methyl acrylate)	$>\text{CH}(\text{COO}-)-$	26.0	42.4	86.1	212.3
Polymethacrylates	Poly(methyl methacrylate)	$\begin{matrix} -\text{C}(\text{CH}_3) \\ (\text{COO})- \end{matrix}$	37.8	45.2	100.1	226.3

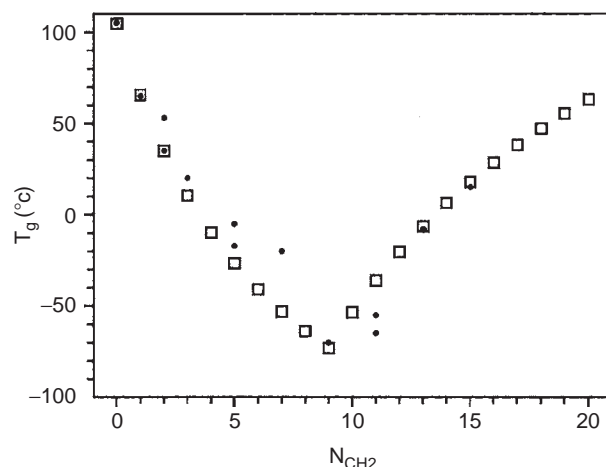


FIG. 6.2 Glass transition temperature of poly(methyl methacrylate) with paraffinic side groups.
□ Estimated values: Eqs. (6.6)–(6.8); ● Experimental values.

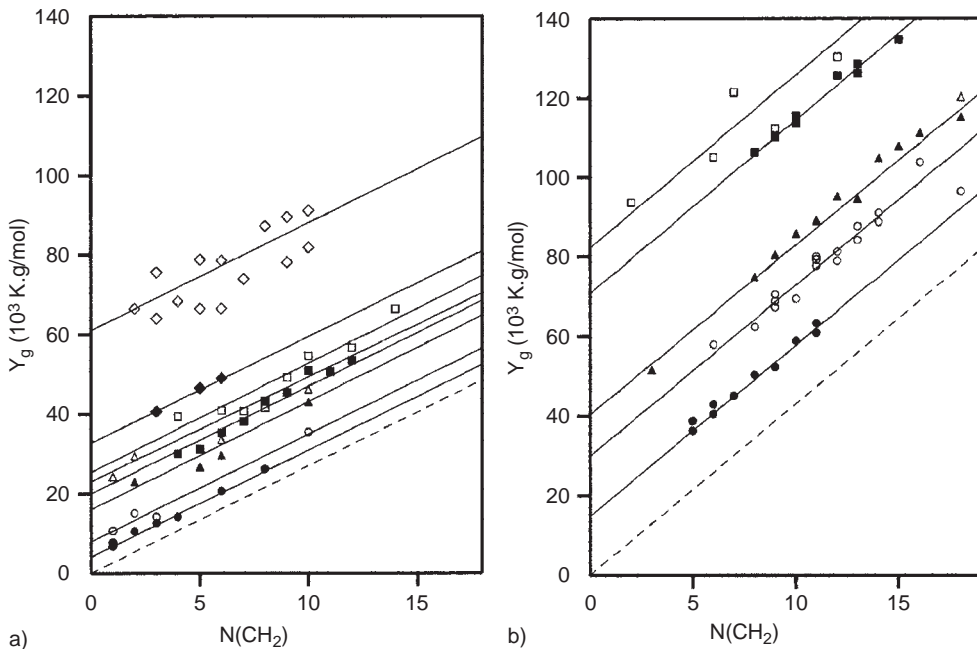


FIG. 6.3 (A) Y_g as a function of the number of $-\text{CH}_2\text{O}$ groups in the main chain (*polymer families without hydrogen bonding groups*). (B) Y_g as a function of the number of $-\text{CH}_2\text{O}$ groups in the main chain (*polymer families containing hydrogen bonding groups*). The empirical values are indicated by the different symbols. The drawn lines are calculated by means of group contributions. The dashed line is the base line, indicating the slope. Note that for all polymer families the relationship between Y_g and $N(\text{CH}_2)$ is a linear function (straight line); for polymers *without* hydrogen bonds the slope is 2.7 (standard value), whereas *with* inter-molecular hydrogen bonds the slope increases to 4.3 (due to hydrogen bonded network formation). The meaning of the symbols is the following: (A) ●, Aliphatic poly(oxides); ○, Aliphatic poly(sulphides); ▲, Aliphatic poly(disulfides); △, Aliphatic poly(carbonates); ■, Aliphatic poly(anhydrides); □, Aliphatic poly(di-esters); ◆, Aliphatic poly(sulphones); ◇, Poly(terephthalates). (B) ●, Aliphatic poly(lactams); ○, Aliphatic poly(di-amides); ▲, Aliphatic poly(di-urethanes); △, Aliphatic poly(di-urea); ■, Aliphatic poly(terephthalamides); □, Poly(xylylene diamides) and Poly(phenylene diethylene diamides).

6.2.2.4. Linear unbranched condensation polymers containing CH_2 groups and single aromatic rings¹

Fig. 6.3 shows the empirical Y_g values of the different series of condensation polymers characterised by their functional groups as a function of the number of the CH_2 groups in the structural unit ($N(\text{CH}_2)$). It is evident that for all series, except the polyamides, polyurethanes and polyurea's, the slope of the lines is constant, viz. 2.7, the increment of the CH_2 group (Fig. 6.3a). Only for the polymers mentioned – all containing hydrogen bonding groups – the slope is 4.3. Networks of inter-molecular hydrogen bonds obviously cause an apparent increase of the CH_2 increment from 2.7 to 4.3 (Fig. 6.3b).

¹ In the second edition of this book an extra parameter I_c was introduced in order to describe the interactions between some functional groups and especially that of intermolecular hydrogen bonding.

In the fourth and this fifth edition we have preferred to use two increments for the CH_2 group, one for the case that no polar interaction between the chains plays a part, the other for the case that strong hydrogen bonding groups are present.

All calculations of Y_g become much easier in this way; the result remains practically unchanged.

From the *intercepts on the Y_g axis* in Fig. 6.3 the increments of the functional groups and also those of the aromatic groups have been derived.

Besides the already discussed *inter-molecular interaction by hydrogen bonding*, there is another effect that stiffens the main chain and thus increases the Y_g value, viz. the *intra-molecular interactions*.

Two types of intra-molecular interactions enlarge the Y_g values of the increments and hence those of the structural unit: π -electron conjugation and steric hindrance by bulky groups. Some examples will be given:

First example: the Y_g -increment of the group $-\text{C}(\text{CH}_3)_2\text{O}-$ is 8.5 (according to Table 6.1.). This value is valid for purely flexible chains. If the same group is found between two aromatic rings, its free rotations are suppressed, the chain is locally stiffened and the increment is enlarged to 15.0 (Table 6.1A);

Second example: the group contribution of a solitary, non-conjugated p-phenylene group is 29.5. If the aromatic ring is conjugated (with another double bonded group) on one side, its increment increases to 35; if it is conjugated on both sides, the stiffening increases and with it the increment of the phenylene group, viz. to 41.0 (Table 6.1B).

6.2.2.5. Aromatic condensation polymers with special structures

The most important representatives of this group are the fully aromatic rigid chains, such as: polyphenylenes, the fully aromatic polyesters ("arylates") and the fully aromatic polyamides ("aramides").

In these cases the increments of both the aromatic groups and the functional groups are enlarged.

The most spectacular member of this group is the poly(p-phenylene-terephthalamide), better known under its commercial names [®]Kevlar and [®]Twaron. Here we have the combined effects of intra-molecular π -electron conjugation between aromatic rings and CONH-groups and the inter-molecular hydrogen-bonding of the CONH-groups. The increment of the latter is, hence, elevated from 15.0 to 30.0 (Table 6.1B).

Frequently occurring combinations of p-phenylene groups with other, mostly functional groups, are given – with their Y_g increments – in Table 6.3.

6.2.2.6. Heterocyclic condensation polymers

The number of reliable T_g data on heterocyclic polymers is restricted. Tentative values of Y_g increments are given in Table 6.1C.

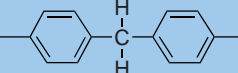
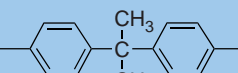
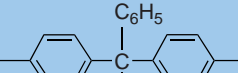
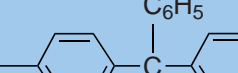
6.2.3. Comparison between calculated and experimental values

Table 6.4 gives a comparison of experimental and calculated values for a selection of polymers. The agreement is satisfactory.

The method of estimation described made it possible to calculate the T_g values of the 600 polymers whose T_g values were measured. About 80% of the T_g values calculated differed less than 20 K from the experimental values. A certain percentage of the literature values is probably unreliable. So as a whole the result may be considered very satisfactory.

Some examples will now illustrate the use of the sketched method of calculating Y_g and estimating T_g

TABLE 6.3 γ_{gi} values of frequently used combinations of groups

Combi-groups	γ_{gi}	M_i	Combi-groups	γ_{gi}	M_i
of hydrocarbon groups only			in flexible chains		
	65	166.2	$-\text{CH}_2-\text{C}_6\text{H}_4-\text{CH}_2-$	35	104.1
	87	194.3	$-\text{O}-\text{C}_6\text{H}_4-\text{O}-$	37.4	108.1
	121	256.3	$-\text{OOC}-\text{C}_6\text{H}_4-\text{COO}-$	62	164.1
	168	316.4	$-\text{OOC}-\text{C}_6\text{H}_4-\text{COO}-$	56.5	164.1
	102	234.3	$-\text{NHCO}-\text{C}_6\text{H}_4-\text{CONH}-$	83	162.1
	137	312.3	$-\text{NHCO}-\text{C}_6\text{H}_4-\text{CONH}-$	70	162.1
			in rigid arylates		
			$-\text{O}-\text{C}_6\text{H}_4-\text{C}(=\text{O})-$	(58)	120.1

(continued)

TABLE 6.3 (continued)

Combi-groups	γ_{gi}	M_i	Combi-groups	γ_{gi}	M_i
	70	152.2		(52)	120.1
with functional groups			in rigid aramides		
	84	180.2		(70)	119.1
	67	168.2		148	238.3
	104	260.2		112	238.3
	72	184.2			
	111	216.3			

TABLE 6.4 Experimental and calculated values of T_g for a number of polymers (K)

	T_g exp.	T_g calc.
Poly(1-butene)	228/249	238
Poly(1-pentene)	221/287	227
Poly(1-octene)	208/228	210
Poly(1-octadecene)	328	312
Poly(p-methylstyrene)	366/379	379
Poly(p-ethylstyrene)	300/351	342
Poly(p-hexylstyrene)	246	250
Poly(p-decylstyrene)	208	200
Poly(p-nonadecylstyrene)	305	314
Poly(vinyl methyl ether)	242/260	252
Poly(vinyl ethyl ether)	231/254	237
Poly(vinyl hexyl ether)	196/223	210
Poly(vinyl decyl ether)	215	200
Poly(methyl acrylate)	279/282	279
Poly(ethyl acrylate)	249/252	260
Poly(hexyl acrylate)	213/216	219
Poly(nonyl acrylate)	184/215	204
Poly(hexamethyl acrylate)	308	295
Poly(methyl methacrylate)	366/399	378
Poly(ethyl methacrylate)	281/338	339
Poly(hexyl methacrylate)	256/268	247
Poly(decyl methacrylate)	203/218	200
Poly(hexamethyl methacrylate)	288	290
Poly(vinyl fluoride)	253/314	338
Poly(vinylidene fluoride)	238/286	206
Poly(1,2-difluoroethylene)	323/371	388
Poly(vinyl chloride)	247/354	354
Poly(vinylidene chloride)	255/288	254
Poly(trifluorochloroethylene)	318/373	330
Poly(vinyl alcohol)	343/372	357
Poly(methylene oxide)	188/243	223
Poly(ethylene oxide)	206/246	213
Poly(trimethylene oxide)	195/228	207
Poly(tetramethylene oxide)	185/194	205
Poly(ethylene adipate)	203/233	228
Poly(ethylene dodecate)	202	216
Poly(decamethylene adipate)	217	213
Poly(ethylene terephthalate)	342/350	361
Poly(decamethylene terephthalate)	268/298	299
Poly(diethyleneglycol malonate)	244	232
Poly(diethyleneglycol octadecanedioate)	205	211
Poly(methaphenylene isophthalate)	411/428	392
Poly(4,4'-methylene diphenylene carbonate)	393/420	368
Poly(4,4'-isopropylidene diphenylene carbonate)	414/423	412
Poly(4,4'-tetramethylene dibenzoinic anhydride)	319	322
Poly(4,4'-methylenedioxy dibenzoinic anhydride)	357	336
Poly(hexamethylene adipamide)	318/330	323
Poly(decamethylene sebacamide)	319/333	318
Poly(heptamethylene terephthalamide)	383/396	435
Poly(paraphenylene diethylene sebacamide)	378	373
Poly(tetramethylene hexamethylene diurethane)	215/332	328

(continued)

TABLE 6.4 (*continued*)

	T_g exp.	T_g calc.
Poly(phenylene dimethylene hexamethylene diurethane)	329	338
Poly(hexamethylene dodecamethylene diurea)	322	319
Poly[methylene bis(oxydiparaphenylene)sulphone]	453	441
Poly[oxy bis(oxydiparaphenylene) ketone]	423	417

Example 6.1

Estimate the limiting value of T_g for polylactams (aliphatic polyamides) at increasing number of CH_2 groups in the chain.

Solution

The structural formula of polylactams is:



From Table 6.1 we take the following values:

$$\begin{aligned} Y_g &= nY_g(\text{CH}_2) + Y_g(\text{CONH}) = 4.3n + 15 \\ M &= nM(\text{CH}_2) + M(\text{CONH}) = 14.0n + 43 \end{aligned}$$

So

$$\lim_{n \rightarrow \infty} \frac{Y_g 1000}{M} = \lim_{n \rightarrow \infty} \frac{4300n + 15,000}{14.0n + 43} = \frac{4300}{14} = 307 \text{ K}$$

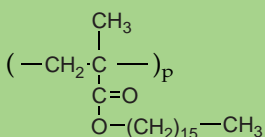
This is in good agreement with the experimental values (307 K).

Example 6.2

Estimate the glass transition temperature of poly(hexadecyl methacrylate).

Solution

The formula of the structural unit is:



For this polymer we find in Table 6.2: $Y_{g9} = 45.2$. By means of Eq. (6.8) we find:

$$\begin{aligned} Y_g &= Y_{g9} + 7.5(N - 9) = 45.2 + 7.5(15 - 9) = 90.2 \\ M &= M_0 (= 100.1) + 15 \times 14.02 = 310.4 \end{aligned}$$

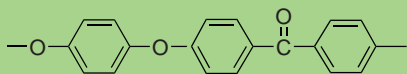
So $T_g = 10^3 \times 90.2 / 310.4 = 291 \text{ K}$.

The value in the literature is $T_g = 288 \text{ K}$, in very good agreement.

Example 6.3

Estimate the glass transition temperature of poly(ether–ether–ketone) or PEEK.

Its repeating unit is:

**Solution**

For this repeating unit the molar mass is $\mathbf{M} = 288.3$.

The \mathbf{Y}_g increments are found in Tables 6.1 and 6.3.

$$\mathbf{Y}_g(-\text{O}-\text{C}_6\text{H}_4-\text{O}-) = 37.4$$

$$\mathbf{Y}_g(-\text{C}_6\text{H}_4-\text{CO}-\text{C}_6\text{H}_4-) = 84$$

So

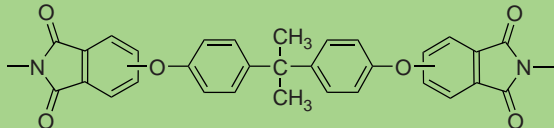
$$\mathbf{Y}_g \text{ of PEEK} = 37.4 + 84 = 121.4$$

and $T_g = 10^3 \times 121.4 / 288.3 = 421 \text{ K}$; the literature values are 414–433. The agreement is good.

Example 6.4

Estimate the T_g of the poly(imide) polymer ULETEM 1000 (produced by General Electric Co)

Formula of the structural unit ($\mathbf{M} = 587$):

**Solution**

From the Tables 6.1 and 6.3 we derive the following increments:

$$2\mathbf{Y}_g(-\text{N}=\text{C}=\text{O}) = 2 \times 95 = 190$$

$$2\mathbf{Y}_g(-\text{O}-) = 2 \times 4 = 8$$

$$\mathbf{Y}_g(-\text{C}_6\text{H}_4-\text{C}(\text{CH}_3)_2-\text{C}_6\text{H}_4-) = \frac{87}{285}$$

So $T_g = 285 \times 1000 / 578 = 493 \text{ K}$; the literature value is 490 K.

Other factors influencing the value of T_g

6.2.3.1. Pressure dependence of T_g

Zoller (1982, 1989) found that the glass transition temperature is a linear function of the pressure:

$$T_g(p) = T_g(0) + s_g p \quad (6.9)$$

The number of numerical values of the constant s_g is very small. Zoller found for semi-rigid aromatic polymers (polycarbonate, polysulphone, polyarylates and polyetherketone) as an average $s_g \approx 0.55 \text{ K MPa}^{-1}$. This means, roughly speaking, that the glass transition temperature increases with approximately 1°C by increasing the pressure with 20 bar (i.e. 50°C kb^{-1}). It is probable, in analogy to the pressure dependence of the melting point, that the value of s_g for flexible aliphatic polymers is lower ($s_g \approx 0.2 \text{ K MPa}^{-1}$). Aharoni (1998) reported some values for s_g (see Table 6.5), with an average of 0.28 and 0.20 K MPa^{-1} for amorphous polymers and semi-crystalline polymers, respectively.

6.2.3.2. The influence of molar mass

The influence of molecular mass on T_g can be approximately described by an equation of the type of Eq. (2.1):

$$T_g = T_g(\infty) - \frac{K_g}{M_n} \quad (6.10)$$

where $T_g(\infty)$ is the value of T_g for very high molecular mass (Fox and Flory (1950)).

According to Cowie (1968), however, T_g shows no further increase if the molecular mass is above a certain critical value. This value corresponds roughly with the critical molecular mass found in melt viscosity experiments, which will be discussed in Chap. 15.

Bicerano (2002) gathered data from literature to find a relationship between K_g and $T_g(\infty)$ and came to the conclusion that $T_g(\infty)$ is larger than the commonly accepted values of T_g at ordinary molecular weights. He suggested, from considerations of chain stiffness and statistics of chain conformations, that the term K_g in Eq. (6.10) should be proportional

TABLE 6.5 Changes in T_g of some amorphous and semi-crystalline polymers as function of applied pressure (after Aharoni, 1998).

Polymer	T_g ($^\circ\text{C}$) (at 1 atm.)	P (MPa)	T_g ($^\circ\text{C}$) (at P MPa)	dT_g/dP (K MPa^{-1})
Polystyrene	108	100	131	0.23
Polystyrene	100	200	182	0.41
Poly(methyl methacrylates)	103	100	121	0.18
Poly(vinyl chloride)	75	100	89	0.14
Poly(vinyl acetate)	32	80	49	0.21
Amorphous poly(ethylene terephthalate)	70	100	93	0.23
Semi-cryst. poly(ethylene terephthalate)	70	100	93	0.23
Poly(butylene terephthalate)	69	200	89	0.10
Polyamide-6	52	200	99	0.24
Polyamide-6,6	60	200	109	0.25
Polyamide-6,9	60	200	102	0.21

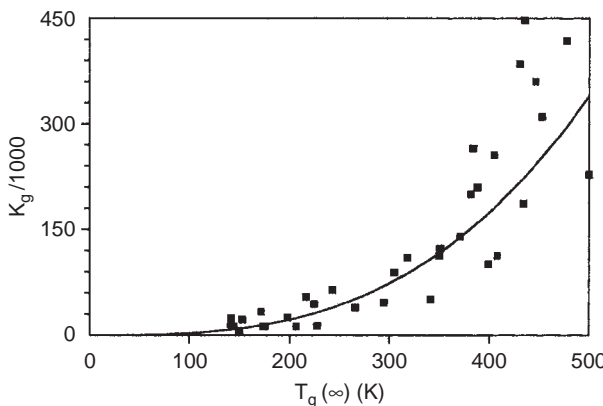


FIG. 6.4 Experimental values of K_g as a function of $T_g(\infty)$. The drawn line represents the equation $K_g = 0.0002715T_g(\infty)^3$ (after Bicerano, 2002).

to a power of $T_g(\infty)$, most likely between $T_g(\infty)^2$ and $T_g(\infty)^4$ and from a statistical analysis of a data set containing 35 polymers, he concluded that K_g should be proportional to $T_g(\infty)^3$. His results are shown in Fig. 6.4, where the drawn line presents the best fit for $T_g(\infty)^3$ dependence²:

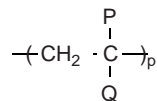
$$K_g = 0.002715T_g(\infty)^3 \quad (6.11)$$

so that Bicerano's analysis leads to

$$T_g = T_g(\infty) - 0.002715 \frac{T_g(\infty)^3}{M_n} \quad (6.12)$$

6.2.3.3. The influence of tacticity

Karasz and Mac Knight (1968) collected the available data for glass transition temperatures of vinyl polymers of the general formula



They observed that steric configuration affects T_g only if $P \neq Q$ and neither P nor Q is hydrogen. Table 6.6 gives glass temperatures for syndiotactic, isotactic and atactic polymers. It shows that for Polystyrene and Poly(alkyl acrylates) $T_{gi} \approx T_{gs}$ ($T_{gs} - T_{gi}$ varies from 8 to 18 K in Table 6.6), whereas for Poly(alkyl methacrylates) and Poly(α -chloro acrylates) $T_{gi} < T_{gs}$ ($T_{gs} - T_{gi}$ varies from 69 to 117 K in Table 6.6). The explanation seems to lie in the added steric repulsion to rotation due to the presence of the asymmetric double-sided groups on alternate chain backbone atoms. There is no possibility for extended planar zigzag configurations and different helical forms of highly isotactic and syndiotactic chains are present and apparently their stiffness differs significantly (Plazek and Ngai, 1996). From Table 6.6 it also follows that T_g of atactic polymers lies approximately halfway the T_g 's of the corresponding syndiotactic and isotactic polymers.

² Upon plotting Bicerano's results in a $\log K_g$ vs. $\log T_g(\infty)$ plot linear regression yields: $K_g = 0.01T_g(\infty)^{2.8 \pm 0.2}$

TABLE 6.6 T_g of stereoregular and atactic polymers (K)

Polymer	T_g (syndio)	T_g (iso)	T_g (atact)
Poly(methyl methacrylate)	433	316	378
Poly(ethyl methacrylate)	393	281	324
Poly(<i>i</i> -propyl methacrylate)	412	300	327
Poly(<i>n</i> -butyl methacrylate)	361	249	293
Poly(isobutyl methacrylate)	393	281	321
Poly(cyclohexyl methacrylate)	436	324	377
Poly(2-hydroxyethyl methacrylate)	377	308	359
Poly(methyl acrylate)	–	283	281
Poly(ethyl acrylate)	–	248	249
Poly(<i>i</i> -propyl acrylate)	270	262	267
Poly(<i>sec</i> -butyl acrylate)	–	250	251
Poly(cyclohexyl acrylate)	–	285	292
Poly(methyl α -chloroacrylate)	450	358	416
Poly(ethyl α -chloroacrylate)	393	310	366
Poly(<i>i</i> -propyl α -chloroacrylate)	409	341	363
Polystyrene	378	360	373
Poly(α -methyl styrene)	453	390	441
Polypropylene	269	255	267
Poly(<i>N</i> -vinyl carbazole)	549	399	423

Data from Karasz and McKnight (1968) for the acrylates and methacrylates and Bicerano (2002) for the other polymers

A theoretical derivation based on the Gibbs–Di Marzio (1958) theory of the glass transition leads to the conclusion that for the series of poly(alkyl methacrylates)

$$T_g(\text{syndiotactic}) - T_g(\text{isotactic}) = \text{constant} \approx 112\text{K}$$

6.2.4.4. The influence of cross-linking

Cross-linking increases the glass transition temperature of a polymer; the change in T_g depends upon the degree of cross-linking.

Nielsen (1969) gave an interesting review of the effect of cross-linking on the physical properties of polymers. At low degrees of cross-linking the shift in T_g is very small, but at high degrees it may be very large indeed. As more and more cross-linking agent is incorporated into the network structure, the chemical composition of the polymer gradually changes and the cross-linking agent can be considered as a type of co-polymerizing unit.

Thus the shift in T_g is made up of two, nearly independent, effects:

1. The “real” effect of cross-linking; this always increases T_g and is largely independent of the chemical composition of the polymer and the cross-linking agent.
2. The copolymer-effect; this may either increase or decrease T_g , depending upon the nature of the cross-linking agent. Quantitatively this effect is difficult to predict. The degree of cross-linking is defined as:

$$x_{\text{crl}} = \frac{\text{number of cross-links}}{\text{number of backbone atoms}}$$

In a representative part of the polymer network 4-functional cross-links are counted double compared with 3-functional cross-links. If the structure of the network is known, e.g. from the structure and functionality of the building blocks (components) in the

polymer synthesis, the value of x_{crl} and thus of M_{crl} , i.e. the average molecular weight between cross-links, can easily be determined

One may expect that at low degrees of cross-linking the shift (upwards) of T_g will be proportional to x_{crl} and thus to the reciprocal values of M_{crl} . Accordingly an empirical equation was mentioned by Nielsen

$$T_{g,\text{crl}} - T_{g,o} = \frac{K_{\text{crl}}}{M_{\text{crl}}} \quad (6.13)$$

with $K_{\text{crl}} = 3.9 \times 10^4 \text{ K mol g}^{-1}$

Nielsen also quotes a (unpublished) theoretical formula of DiBenedetto:

$$T_{g,\text{crl}} - T_{g,o} = 1.2 T_{g,o} \frac{x_{\text{crl}}}{1 - x_{\text{crl}}} \quad (6.14)$$

From both equations $T_{g,\text{crl}}$ becomes very large if x_{crl} tends to unity or when M_{crl} goes to small values.

From data on copolymers of styrene and divinylbenzene (Bicerano et al. 1996) we constructed a plot of T_g vs. $1/M_{\text{crl}}$ in order to determine the constant K_{crl} . Results are shown in Fig. 6.5 and it follows a value of $5.2 \times 10^4 \text{ K mol g}^{-1}$ for K_{crl} . Of course, the value of term K_{crl} depends on the system of consideration.

Also data of Fox and Loshaek (1955) on polystyrene, cross-linked by divinylbenzene and of Loshaek (1955) on poly(methyl-methacrylate) cross-linked by glycol-dimethacrylate, are in fair agreement with Eq. (6.13). The same is true for the data of Kreibich and Batzer (1979) on epoxy-resins, cross-linked by diamines and diacid-anhydrides; in the latter case ΔT_g tends to a constant value at high degrees of cross-linking ($\Delta T_g = 80$). Berger and Huntjens (1979) demonstrated that Eq. (6.13) describes the cross-linking of polyurethanes with diisocyanates in a very satisfactory way. According to Nielsen the same is true for older literature data on cross-linked elastomers (Ueberreiter and Kanig (1950) and Heinze, Schmieder, Schnell and Wolf (1961).

It may be concluded that for low and moderate degrees of cross-linking Eqs. (6.13) and (6.14) lead to fairly reliable results.

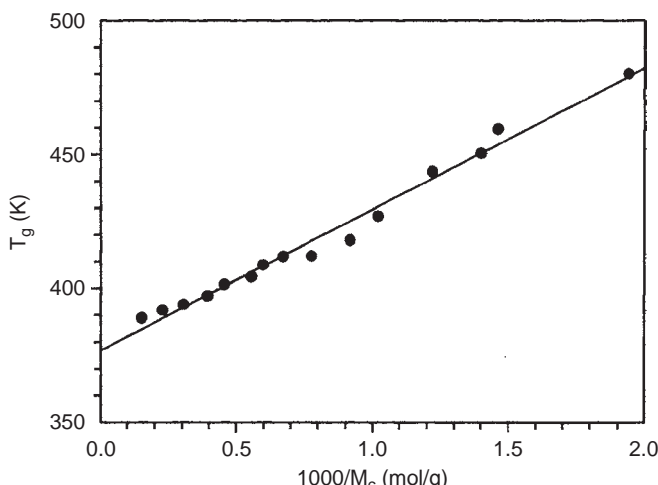


FIG. 6.5 Glass transition temperature, T_g , of styrene-divinylbenzene copolymers as a function of the reciprocal value of the molecular weight between cross-links, $1/M_{\text{crl}}$ (constructed from results presented by Bicerano, 2002).

6.2.3.5. The influence of plasticizer

It is well-known that by the addition of plasticizers the glass temperature of polymers decreases severely: the glass temperature of PVC, e.g. decreases from 90 to 0 °C by the addition of 30% dioctyl phthalate and plasticized PVC finds many applications. We will come back to this important subject in Chap. 16.

6.2.4. Thermodynamics of the glass–rubber transition

In contradiction to the melting point, the glass–rubber transition temperature is not a thermodynamic transition point. It shows some resemblance, however, to a second order transition. For a second-order transition, the following relationships derived by Ehrenfest (1933) hold:

$$\left(\frac{dT_{tr}}{dp} \right)_I = \frac{\Delta\kappa}{\Delta\alpha} \quad (6.15)$$

$$\left(\frac{dT_{tr}}{dp} \right)_{II} = \frac{T_{tr}\Delta\alpha}{\Delta c_p} \quad (6.16)$$

or

$$\frac{T_{tr}(\Delta\alpha)^2}{\Delta\kappa\Delta c_p} = 1 \quad (6.17)$$

where T_{tr} =second order transition temperature; p =pressure; $\Delta\alpha = \alpha_1 - \alpha_2$ =difference in thermal expansion coefficient at T_{tr} ; $\Delta c_p = c_p^1(T_{tr}) - c_p^2(T_{tr})$ =difference in molar heat capacity at T_{tr} ; $\Delta\kappa = \kappa_1 - \kappa_2$ =difference in compressibility at T_{tr} .

Staverman (1966) and Breuer and Rehage (1967) extensively discussed the thermodynamics of the glass–rubber transition. They concluded that it is not a real second-order transition, mainly because the glassy state is not completely defined by the normal state variables p , V and T .

It would be interesting to test the validity of Eqs. (6.15)–(6.17) against experimental data. Unfortunately, the available data show large deviations, so that the calculations merely lead to the correct order of magnitude. Accurate data are those for polystyrene as determined by Breuer and Rehage. They lead to the following results:

$$\Delta\alpha = 3.3 \times 10^{-4} \text{ K}^{-1}$$

$$\Delta\kappa = 1.65 \times 10^{-10} \text{ m}^2 \text{ N}^{-1}$$

$$\Delta c_p(T_g) = 2.63 \times 10^5 \text{ J m}^{-3} \text{ K}^{-1}$$

$$dT_g/dp = 2.5 \times 10^{-7} \text{ K m}^2 \text{ N}^{-1}$$

$$T_g = 375 \text{ K}$$

so that

$$\frac{\Delta\kappa}{\Delta\alpha} = \frac{1.65 \times 10^{-10}}{3.3 \times 10^{-4}} = 5 \times 10^{-7} \text{ Km}^2 \text{ N}^{-1} = 0.5 \text{ K MPa}^{-1}$$

$$\frac{T_g\Delta\alpha}{\Delta c_p} = \frac{375 \times 3.3 \times 10^{-4}}{2.63 \times 10^5} = 4.7 \times 10^{-7} \text{ Km}^2 \text{ N}^{-1} = 0.47 \text{ K MPa}^{-1}$$

$$\frac{T_g(\Delta\alpha)^2}{\Delta\kappa\Delta c_p} = \frac{375 \times (3.3 \times 10^{-4})^2}{1.65 \times 10^{-10} \times 2.63 \times 10^5} = 0.94$$

If we assume that the glass rubber transition is a second order transition, then according to Eqs. (6.15)–(6.17):

$$\frac{\Delta\kappa}{\Delta\alpha} = \frac{T\Delta\alpha}{\Delta c_p} = \frac{dT_g}{dp}$$

Experimental results above show, however, that

$$\frac{\Delta\kappa}{\Delta\alpha} \approx \frac{T\Delta\alpha}{\Delta c_p} \approx 2 \times \frac{dT_g}{dp} (0.5 \approx 0.47 \approx 2 \times 0.25)$$

so that we can conclude that *the glass rubber transition is not a second order transition*.

These values are slightly different from those published earlier by Gee (1966).

The data on polyisobutylene, poly(vinyl acetate), poly(vinyl chloride) and poly(methyl methacrylate) mentioned by Bianchi (1965) and Kovacs (1963) show effects of the same order of magnitude.

6.2.5. The nature of the glass transition

The glassy state is a widespread phenomenon. Besides polymers, also organic liquids, biomaterials, inorganic melts and even certain metallic elements and alloys can exist in the glassy state. Research of the real nature of the glassy state is important for the understanding of the modes of state in which matter can exist.

The first theoretician of the vitrification process was Simon (1930), who pointed out that it can be interpreted as a “freezing-in” process. Simon measured specific heats and entropies of glycerol in the liquid, crystalline and glassy state; below T_g the entropy of the supercooled liquid could, as a matter of fact, only be estimated. Linear extrapolation would lead to a negative entropy at zero temperature (paradox of Kauzmann, 1948) which would be in contradiction with Nernst’s theorem. So one has to assume a sharp change in the slope of the entropy, which suggested a second order transition as defined by Ehrenfest.

This has been the starting point of the theory of Gibbs and Di-Marzio (1958); these authors considered the glass transition “in fact, as the experimental manifestation of the second-order transformation T_g in the Ehrenfest sense”. They concluded to a second order glass transition temperature 50K below the “normal” T_g . This, of course is difficult to determine in a normal way, because the equilibrium time (retardation time) 50K below T_g is something like 10^{12} years (see Table 6.7), as estimated by Rehage (1970) from refractive index relaxation.³ However, from careful experiments on highly concentrated Polystyrene solutions, as reported by Rehage (1973), a glass transition temperature even down to 70 K below the “normal” T_g was not established. In later work Gibbs (with Adam, 1965) took both the equilibrium behaviour of the second order transition and rate effects into account. Most authors at present assume that the glass transition is a kinetically controlled process. The best known experimental evidence in support of the kinetic theory is obtained when the glass transition is studied in cooling runs: T_g always decreases with a decrease in cooling rate; samples which are previously cooled show a hysteresis

³ A straight line with correlation coefficient 0.99994 is obtained by plotting $\log \tau_{\text{ret}}$ vs. $1/T$ (K^{-1}).

TABLE 6.7 Retardation time τ_{ret} as a function of temperature for polystyrene with a glass transition temperature of 89°C. After Rehage (1970).

T (°C)	100	95	91	90	89	88	86.5	85	82	79	77	50	20
τ_{ret}	10^{-2} s	1 s	40 s	2 min	5 min	18 min	1 h	5 h	50 h	60 d	1 a	10^{12} a	10^{34} a

phenomenon. Also results of dynamic mechanical and dielectric measurements show, without exception, transition peaks moving to lower temperatures at decreasing frequency.

Important work on the kinetically interpreted vitrification process was done by Volkenshtein and Ptitsyn (1957), Wunderlich and coworkers (1964–1974) and Moynihan (1974–1978). They considered the vitrification process as a “chemical reaction” involving the passage of “kinetic units” (e.g. “holes”) from one energy level to another.

A comparative study of the kinetic and thermodynamic approaches to the glass transition phenomenon was made by Vijayakumar and Kothandaraman (1987).

A very interesting approach to the thermodynamics of the glassy state was made by Rehage (1980), who pointed out that the non-validity of the Ehrenfest equations results in a path difference of the thermodynamic properties in the glassy state. A new concept, viz. that of “*ordering parameters*” was introduced by Rehage (1973), which allows a thermodynamic treatment of the glass transition and the glassy state. Addition of one ordering parameter (ζ), in addition to the conventional variables T and P , is sufficient to describe the behaviour of conventional polymers such as polystyrene in the glassy state nearly quantitatively (see also Haward, 1975, Chap. 1). In polymer liquid crystals the glass transition is more complicated and requires at least two ordering parameters.

Rehage’s approach combines the thermodynamic theory of second order transitions with the concept of a “freezing-in” of a kinetically determined order.

6.3. THE CRYSTALLINE MELTING POINT

It is remarkable that practically no T_m -structure relationships have been proposed in the literature, although there are more experimental data available for T_m than for T_g .

Many years ago a certain correspondence was already observed between T_g and T_m for the same polymer, which suggests that a treatment analogous to that proposed for T_g could also be used for the prediction of T_m . This leads to a formula equivalent to Eq. (6.1):

$$T_m \sum_i s_i = \sum_i s_i T_{mi} \quad (6.18)$$

There is a fundamental difference between T_g and T_m however, in that the melting point is a *real* first-order transition point, at which the free energies of both phases in equilibrium are equal. Thus:

$$T_m \Delta S_m = \Delta H_m \quad (6.19)$$

where ΔS_m is entropy of fusion, ΔH_m is enthalpy of fusion.

Eq. (6.19) suggests that a method for predicting T_m could be based on calculation of both ΔH_m and ΔS_m by group contribution methods. As was stated in Chap. 5, however, the lack of sufficient data for ΔH_m makes this method impracticable.

6.3.1. An additive molar function for the calculation of T_m

In analogy to the Molar Glass Transition Function, defined by Eq. (6.4), we shall define the equivalent *Molar Melt Transition Function* by:

$$\mathbf{Y}_m = \sum_i \mathbf{Y}_{mi} = T_m \cdot \mathbf{M} \quad (6.20)$$

so that

$$T_m = \frac{\mathbf{Y}_m}{\mathbf{M}} = \frac{\sum_i \mathbf{Y}_{mi}}{\mathbf{M}} \quad (6.21)$$

The function \mathbf{Y}_m (like \mathbf{Y}_g) has the dimension (K kg mol^{-1}). The group increments for this function could be derived from the available literature data on crystalline melting points of polymers, totalling nearly 800. The quantity \mathbf{Y}_m (like \mathbf{Y}_g) does not show simple linear additivity due to intra- and inter-molecular interactions between structural groups. The available group contributions and their structural corrections are summarised in Table 6.8. We shall again discuss these data step by step.

6.3.2. Derivation of the group contributions to \mathbf{Y}_m

6.3.2.1. The unbranched polymethylene chain

It is known from the literature that the melting point of pure polymethylene is 409 K. This gives for the contribution of $-\text{CH}_2-$ to \mathbf{Y}_m

$$\mathbf{Y}_m(-\text{CH}_2-) = 409 \times 14.03 = 5738 \text{ Kg mol}^{-1} = 5.738 \text{ Kkg mol}^{-1}.$$

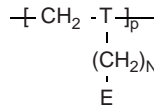
We shall apply a round value of $5.7 \text{ K kg mol}^{-1}$.

6.3.2.2. Aliphatic carbon chains with “small” side groups (substituted polymethylene chains)

The main representatives of this class are the simplest vinyl polymers. The group contributions of the groups $-\text{CHX}-$, $-\text{CX}_2-$ and $-\text{C}(X)(Y)-$ are given in Table 6.8.

6.3.2.3. Aliphatic carbon (main-) chains with “long” side chains (“comb” polymers)

The main type is already mentioned:



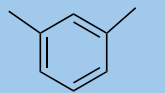
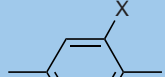
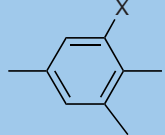
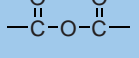
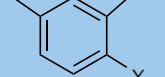
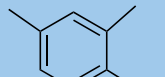
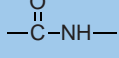
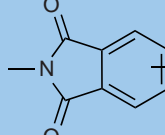
where T is a *trivalent* main chain group and E a *monovalent* end group.

Polymers with $N = 0$ are again called the “*basic*” polymers of this class. Their \mathbf{Y}_m -value has the symbol \mathbf{Y}_{mo} . For T_m we observe a phenomenon, similar to that mentioned for T_g : with increasing N the T_m -values first decrease, pass through a minimum and increase again. In contradistinction to the T_g behaviour the minimum is now located at $N = 5$; for each series the minimum value of T_m is near 235 K. For $N > 5$, the CH_2 increment has again its normal value of $5.7 \text{ K kg mol}^{-1}$ (see Fig. 6.6).

TABLE 6.8 Group contributions (increments) to γ_m (K kg mol^{-1})

A. Non-conjugating groups						
	Group	γ_{mi}	M_i	Group	γ_{mi}	M_i
-CH ₂ -	Limiting value	5.7		ali-cyclic C- halide	31	82.1
	Main chain	Table 6.10	14.0		45	
	Side chain	Eq. (6.22/24)			17.4	32.0
-CHR-	-CH(CH ₃)-	13.0	28.0		27.5	48.5
	-CH(<i>i</i> -propyl)-	35.3	56.1		32	66.5
	-CH(<i>tert</i> -butyl)-	(45)	70.1		-CF(CF ₃)	
	-CH(cyclopentyl)-	-	82.1		-CF ₂ -	25.5
	-CH(cyclohexyl)-	-	96.2		-CCl ₂ -	50.0
	-CH(C ₆ H ₅)-	48	90.1		-O-	39
	-CH(p-C ₆ H ₄ CH ₃)-	(54)	104.1		-NH-	82.9
-CHX-	-CH(OH)-	18	30.0	hetero	-S-	16.0
	-CH(OCH ₃)-	18.7	44.1		-SS-	(18)
	-CH(OCOCH ₃)-	38	72.1		-Si(CH ₃) ₂ - free	22.5
	-CH(COOCH ₃)-	38	72.1		-Si(CH ₃) ₂ - st. hindered	64.2
	-CH(CN)-	26.9	39.0		O —O—C—O—	31
	-C(CH ₃) ₂ - free	12.1	42.1		30	58.2
	-C(CH ₃) ₂ - st. hindered	s 22, ss 39			30	60.0
-CX ₂ -	-(C ₆ H ₅) ₂ -	0	166.2	C- hetero	—O—C—NH—	43.5
-CXY-	-C(CN) ₂ -				—NH—C—NH—	59.0
	-C(CH ₃)(COOCH ₃)-	41.5	86.1		(225)	60
	-H(CH ₃)(C ₆ H ₅)-	54	104.1		58.0	214.1

B. Groups with potential mutual conjugation

Double-bonded systems			Aromatic ring systems		
Group	γ_{mi}	M_i	Group	γ_{mi}	M_i
$-\text{CH}=\text{CH}-$ <i>cis</i>	8.0	26.0		n	38
<i>tr</i>	11			c	47
$-\text{CH}=\text{C}(\text{CH}_3)-$ <i>cis</i>	10	40.1		cc	56
<i>tr</i>	13			n	31
$-\text{C}(\text{CH}_3)=\text{C}(\text{CH}_3)-$	—	54.1		c	(36)
$-\text{CH}=\text{CF}-$	(15)	44.0		cc	(42)
$-\text{CH}=\text{CCl}-$	22	60.5		X = CH_3	(45)
$-\text{CF}=\text{CF}-$	(30)	62.0		X = C_6H_5	
$-\text{C}=\text{C}-$	(16.5)	24.0		X = Cl	90.1
	<i>al</i>	28	28.0		X = CH_3
	<i>ar</i>	29			(67)
			72.0	X = C_6H_5	104.1
	n	35		X = Cl	173
	c	(40)			228.3
	cc	(45)		X = CH_3	
				X = C_6H_5	90.1
			44.0	X = Cl	
	n	25			X = CH_3
	c	29			
	cc ^a	35		X = C_6H_5	
				X = Cl	
	n	45	43.0		(85)
	c	(51)			126.2
	cc ^a	60			
	n	56	64.1		n
	c	(61)			100
	cc	(66)		c	120
					145.1

n = non conjugated (isolated in aliphatic chain); c = one sided conjugation with aromatic ring; cc = two sided conjugation.

^abetween two aromatic rings (rigid).

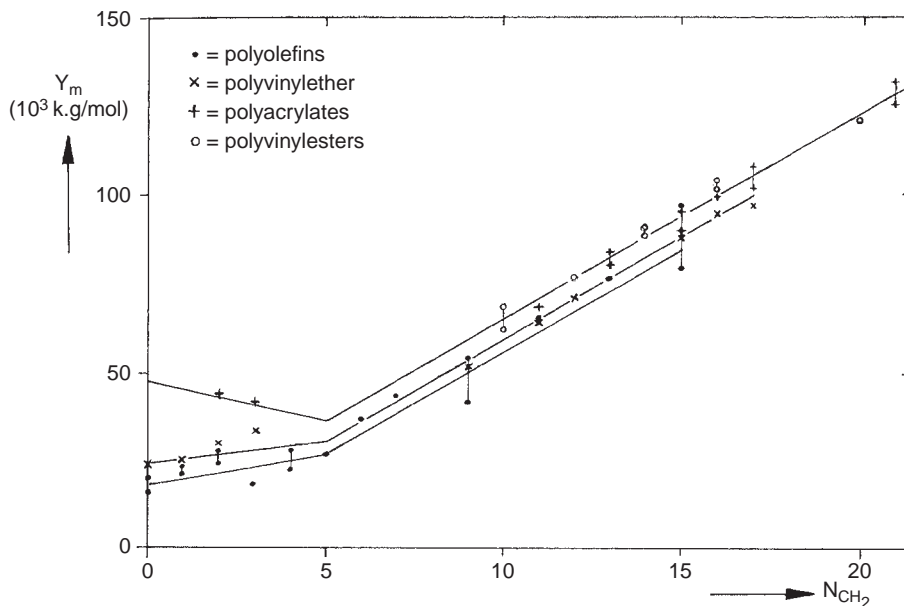


FIG. 6.6 Y_m values of vinyl polymers with side chains.

So the following formulae may be applied:

$$N = 5, Y_m \approx 0.235 M_5 = Y_{m5} \quad (6.22)$$

$$N < 5, Y_m \approx Y_{mo} + \frac{N}{5} (Y_{m5} - Y_{mo}) \quad (6.23)$$

$$N > 5, Y_m \approx Y_{m5} + 5.7(N - 5) \quad (6.24)$$

In Table 6.9 values of Y_m and Y_{mo} are given for the most important vinyl polymers.

The qualitative explanation of this phenomenon is the same as in the case of T_g : small side chains make the fitting into a lattice arrangement more difficult, whereas longer side chains may enhance a secondary inter-molecular order.

6.3.2.4. Linear unbranched condensation polymers containing $-\text{CH}_2-$ (or substituted $-\text{CH}_2-$) groups and solitary aromatic rings⁴

Fig. 6.7 shows a survey of the experimental Y_m values of several series of condensation polymers, each of them characterised by their functional groups. The Y_m 's are plotted versus the total number of CH_2 -groups in the structural unit. The experimental values are indicated by different symbols, each of them belonging to the polymer series concerned.

If we compare Fig. 6.7 with the corresponding Fig. 6.3 for Y_g , the difference of the shape of the graphs is striking. In Fig. 6.3 the relationship is a straight linear function; in Fig. 6.7 one sees curves tending to straight lines at higher N_{CH_2} values.

⁴ In the second edition of this book the curvatures in Fig. 6.7 were described by means of it specially introduced interaction I_x . The use of this extra parameter proved to give some disadvantages: it caused extra calculatory work and it obscured the comparison of the increments of the functional groups. In the fourth and present edition we have abandoned the use of I_x . Instead of it the use of a tabular or graphical device must be preferred (Table 6.9 or Fig. 6.5). The numerical results of the Y_m estimation are practically the same as by means of I_x .

TABLE 6.9 Basic data for vinyl polymers with longer chains (end-group E = methyl)

Series	Basic polymer	T	Υ_{m0}	Υ_{m5}	M_0	M_5
Polyolefins	Polypropylene	$\begin{array}{c} -C- \\ \end{array}$	18.7	26.3	42.0	112.2
Polyvinyl ethers	Poly(vinyl methyl ether)	$\begin{array}{c} -C- \\ \\ O \end{array}$	24.4	30.1	58.1	1282
Polyvinyl esters	Poly(vinyl acetate)	$\begin{array}{c} -C- \\ \\ O \\ C=O \end{array}$	44	36.7	86.1	156.2
Polyacrylates	Poly(methyl acrylate)	$\begin{array}{c} -C- \\ \\ C=O \\ \\ O \end{array}$	48	36.7	86.1	156.2
Polymethacrylates	Poly(methyl methacrylate)	$\begin{array}{c} CH_3 \\ \\ -C- \\ \\ C=O \\ \\ O \end{array}$	47.3	40.0	100.1	170.2

The Υ_m vs. N_{CH_2} curves belong to two types, similar but different. The first type, Fig. 6.7a, is identical in curvature for all polymer families containing only one functional group per repeating unit; poly-oxides, -sulphides, -carbonates, -lactams, -lactones and -sulphones belong to this type.

The second type encompasses the polymer families that possess two functional groups in the repeating unit (Fig. 6.7b); polydiesters, polydiamides, polydiurethanes and polydiurea are in this class. In this type of polymers there are two sets of CH_2 -groups: one between, e.g. the ester groups of the dicarboxylic acid and the other one originated from the diol. This apparently causes the less accurate results in Fig. 6.7b, where the total number of CH_2 -groups is plotted. The most probable explanation is, that the $\Upsilon_m(CH_2)$ increment depends quantitatively on the distance of the relevant CH_2 group from the functional groups enclosing the CH_2 sequence(s). If the positional distance of the CH_2 group to the nearest functional group is defined in atom bond lengths (a.b.l) in the chain, and α corresponds to 1 a.b.l., β to 2 a.b.l., γ to 3, δ to 4, etc., it is easy to derive the values of $\Upsilon_m(CH_2)$ from the curves through the experimental points. The following values are found:

Position	Value of $\Upsilon_m(CH_2)$
α	1.0
β	3.0
γ	4.6
δ	5.7
$>\delta$	5.7 (standard increment)

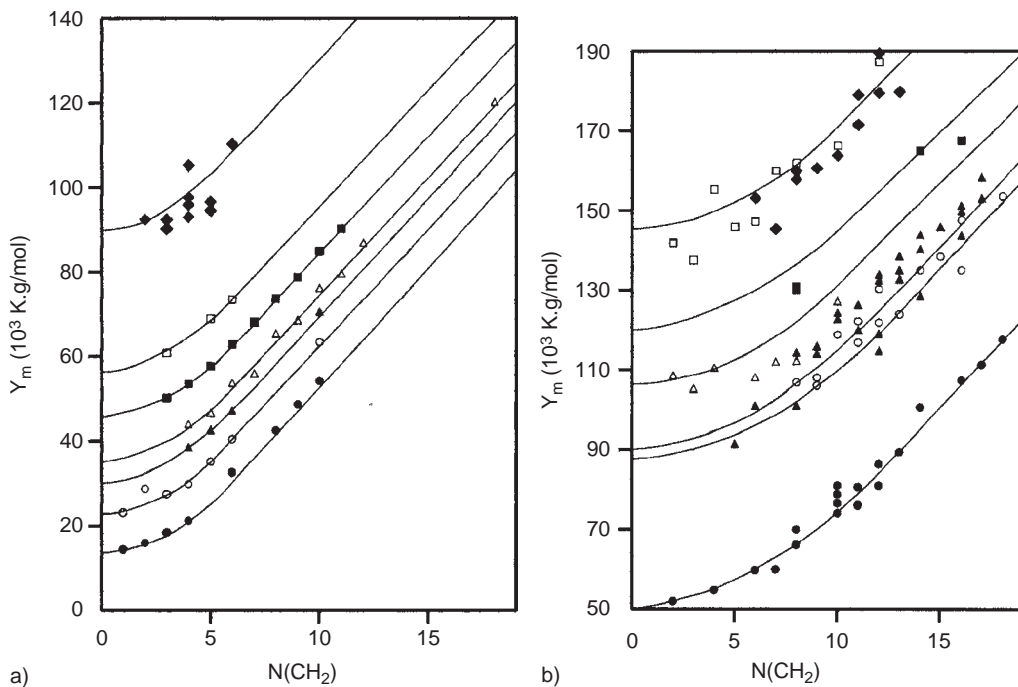


FIG. 6.7 Y_m as a function of the number of $-\text{CH}_2-$ groups in the main chain. The meaning of the symbols is the following: (A) ●, Aliphatic poly(oxides); ○, Aliphatic poly(sulphides); ▲, Aliphatic poly(carbonates); △, Aliphatic poly(anhydrides); ■, Aliphatic poly(lactams); □, Aliphatic poly(sulphones); ◆, Partly aromatic poly(lactams). (B) ●, Aliphatic poly(di-esters); ○, Aliphatic poly(di-urethanes); ▲, Aliphatic poly(di-amides); △, Poly(terephthalates); ■, Aliphatic poly(di-ureas); □, Poly(terephthalamides); ◆, Poly(xylylene diamides) and poly(phenylene diethylene diamides).

Hence, for the polymer polyamide-n, i.e. $\text{H}_2\text{N}-(\text{CH}_2)_{10}-[\text{CONH}-(\text{CH}_2)_{12}]_n-\text{COOH}$, with in the repeating unit 2 CH_2 -groups in the α -position, two in the β -position, two in the γ -position and two in the δ -position and four in higher positions, $\Sigma Y_m(\text{CH}_2) = 2 \times 1 + 2 \times 3 + 2 \times 4.6 + 6 \times 5.7 = 51.4$.

In Table 6.10 the influence of functional groups on the $Y_m(\text{CH}_2)$ increments are given: $m = 0$ means no functional groups in aliphatic carbon chains and $m = 1$ means with one functional group, like in polycaprolactams, polyoxides, etc. (see Fig. 6.7a).

On the other hand for, e.g. polyamide-p,q, with two functional groups in the repeating unit and $p+q$ CH_2 -groups, i.e. $\text{HOOC}-(\text{CH}_2)_q-[\text{CONH}-(\text{CH}_2)_p-\text{NHCO}-(\text{CH}_2)_q]_n-\text{CONH}-(\text{CH}_2)_p-\text{NH}_2$, there are $p + q - 1$ possibilities: p varying from 1 to $p + q - 1$ and q varying from $p + q - 1$ to 1.

In Table 6.11 all values for $\Sigma Y_m(\text{CH}_2)_p + \Sigma Y_m(\text{CH}_2)_q$ are given for all polymers containing two functional groups in the repeating unit, like polydiesters, polydiamides, etc. (see Fig. 6.7b), with p and q varying from 1 to 20. It appears that for $p + q = \text{constant}$ not always constant values for $\Sigma Y_m(\text{CH}_2)_{p+q}$ are found and accordingly different melting points will be found for polymers with the same total number of CH_2 -groups.

Tables 6.9 and 6.10 are very useful for a quick calculation of Y_m ($= \Sigma Y_m(\text{CH}_2) + \Sigma Y_m(\text{funct.gr.})$). The structural interaction mentioned is undoubtedly connected with

TABLE 6.10 Influence of functional groups on the $\Sigma Y_m(\text{CH}_2)$ increment

Total number of CH_2 groups in repeating unit	$\Sigma Y_m(\text{CH}_2)$ in case of m functional groups per repeating unit	
	$m = 0$	$m = 1$
1	5.7	1.0
2	11.4	α
3	17.1	5.0
4	22.8	β
5	28.5	12.6
6	34.2	γ
7	39.9	22.9
8	45.6	δ
9	51.3	> δ
10	57.0	40.0
11	62.7	45.7
12	68.4	51.4
13	74.1	57.1
14	79.8	62.8
15	85.5	68.5
16	91.2	74.2
17	96.9	79.9
18	102.6	85.6
19	108.3	91.3
20	114.0	97.0

molecular lattice fitting. Another phenomenon connected herewith is the well-known "Odd–Even Effect". Odd numbers of CH_2 groups in the repeating unit involve a lower, even numbers a higher T_m (and Y_m) value than the average curve predicts. The magnitude of this structural effect is given in Table 6.12.

Example 6.5

Estimate the melting points for all polyamides-p,q with $p + q = 14$, also taking into consideration the even-odd-effect.

Solution

$\Sigma Y_{m,\text{tot}} = \Sigma Y_m(\text{CH}_2)_p + \Sigma Y_m(\text{CH}_2)_q + 2Y_m(\text{CONH}) \pm 2 \times 2.5$, where, according to Table 6.8 $Y_m(\text{CONH}) = 45$ and $\pm 2 \times 2.5$ means the even-odd-effect. In Table 6.13 results for the various values of $\Sigma Y_m(\text{CH}_2)$ are given. The values of T_m are calculated with the aid of Eq. (6.21) for a molecular weight of 282. It becomes clear that the melting points are strongly depending on the combination p,q. T_m is higher for the small CH_2 -sequences.

TABLE 6.11 Atomic bonds lengths (abl's) of $-\text{CH}_2-$ groups in polymers with repeating units with two functional groups

N_{CH_2}	1	2	3	4	5	6	7	8	9	10	11	12	13	14	15	16	17	18	19	20
1	2.0	3.0	6.0	9.0	13.6	18.2	23.9	29.6	35.3	41.0	46.7	52.4	58.1	63.8	69.5	75.2	80.9	86.6	92.3	98.0
2	3.0	4.0	7.0	10.0	14.6	19.2	24.9	30.6	36.3	42.0	47.7	53.4	59.1	64.8	70.5	76.2	81.9	87.6	93.3	99.0
3	6.0	7.0	10.0	13.0	17.6	22.2	27.9	33.6	39.3	45.0	50.7	56.4	62.1	67.8	73.5	79.2	84.9	90.6	96.3	102.0
4	9.0	10.0	13.0	16.0	20.6	25.2	30.9	36.6	42.3	48.0	53.7	59.4	65.1	70.8	76.5	82.2	87.9	93.6	99.3	105.0
5	13.6	14.6	17.6	20.6	25.2	29.8	35.5	41.2	46.9	52.6	58.3	64.0	69.7	75.4	81.1	86.6	92.5	98.2	103.9	109.6
6	18.2	19.2	22.2	25.2	29.8	34.4	40.1	45.8	51.5	57.2	62.9	68.6	74.3	80.0	85.7	91.4	97.1	102.8	108.5	114.2
7	23.9	24.9	27.9	30.9	35.5	40.1	45.8	51.5	57.2	62.9	68.6	74.3	80.0	85.7	91.4	97.1	102.8	108.5	114.2	119.9
8	29.6	30.6	33.6	36.6	41.2	45.8	51.5	57.2	62.9	68.8	74.3	80.0	85.7	91.4	97.1	102.8	108.5	114.2	119.9	125.6
9	35.3	36.3	39.3	42.3	46.9	51.5	57.2	62.9	68.6	74.3	80.0	85.7	91.4	97.1	102.8	108.5	114.2	119.9	125.6	131.3
10	41.0	42.0	45.0	48.0	52.6	57.2	62.9	68.6	74.3	80.0	85.7	91.4	97.1	102.8	108.5	114.2	119.9	125.6	131.3	137.0
11	46.7	47.7	50.7	53.7	58.3	62.9	68.6	74.3	80.0	85.7	91.4	97.1	102.8	108.5	114.2	119.9	125.6	131.3	137.0	142.7
12	52.4	53.2	56.2	59.2	64.0	68.6	74.3	80.0	85.7	91.4	97.1	102.8	108.5	114.2	119.9	125.6	131.3	137.0	142.7	148.4
13	58.1	59.1	62.1	65.1	69.7	74.3	80.0	85.7	91.4	97.1	102.8	108.5	114.2	119.9	125.6	131.3	137.0	142.7	148.4	154.1
14	63.8	64.8	67.8	70.8	75.4	80.0	85.7	91.4	97.1	102.8	108.5	114.2	119.9	125.6	131.3	137.0	142.7	148.4	154.1	159.8
15	69.5	70.5	73.5	76.5	81.1	85.7	91.4	97.1	102.8	108.5	114.2	119.9	125.6	131.3	137.0	142.7	148.4	154.1	159.8	165.5
16	75.2	76.2	79.2	82.2	86.8	91.4	97.1	102.8	108.5	114.2	119.9	125.6	131.3	137.0	142.7	148.4	154.1	159.8	165.5	171.2
17	80.9	81.9	84.9	87.9	92.5	97.1	102.8	108.5	114.2	119.9	125.6	131.3	137.0	142.7	148.4	154.1	159.8	165.5	171.2	176.9
18	86.6	87.6	90.6	93.6	98.2	102.8	108.5	114.2	119.9	125.6	131.3	137.0	142.7	148.4	154.1	159.8	165.5	171.2	176.9	182.6
19	92.3	93.3	96.3	99.3	103.9	108.5	114.2	119.9	125.6	131.3	137.0	142.7	148.4	154.1	159.8	165.5	171.2	176.9	182.6	188.3
20	98.0	99.0	102.0	105.0	109.6	114.2	119.9	125.6	131.3	137.0	142.7	148.4	154.1	159.8	165.5	171.2	176.9	182.6	188.3	194.0

TABLE 6.12 Even/odd effect of the CH₂ sequence on the value of Y_m

Functional group	Numerical even(+) / odd (-) Effect per functional group
-O-	±0.3
-S-	±1.0
-S-S-	
-CO-O-	
-O-CO-O-	±1.5
-CO-O-CO-	
-CO-NH-	
-O-CO-NH-	±2.5
-NH-CO-NH-	

We may conclude that the structure–property relationship of T_m is more complicated than that of T_g . On the other hand it is less complicated, since there is no influence of hydrogen bonding by groups, like -CONH- on the value of the CH₂ increment. Besides information on structural interaction effects as regards the CH₂ increment, Fig. 6.7 gives other very important information. From the intercepts on the Y_m axis in Fig. 6.7 it is possible to determine the Y_m increments of all functional groups and also those of aromatic ring systems if present. So from the intercept of the curve of polylactams one obtains the Y_m(CONH) value. From the intercept of the polydiamides curve one gets twice the Y_m(CONH) value. From the curves of partly aromatic polydiamides twice the Y_m(CONH) value plus that of the aromatic ring system in the repeating unit can be obtained.

Besides intra-molecular interactions based on the skeleton structure of the chain there are interactions between groups based on π -electron conjugation (“resonance” of groups with double bonds). As an illustration we may use the 1,4-phenylene group. If this group occurs in a non-conjugated position its Y_m increment is 38; if it is conjugated on one side the increment increases to 47; if it is conjugated on both sides (which is mostly the case in conjugation) it is further increased to 56. The conjugation causes stiffening of the adjacent part of the chain.

TABLE 6.13 Results of calculations of Example 6.5

p,q	$\Sigma Y_m(CH_2)_p$	$\Sigma Y_m(CH_2)_q$	$\Sigma Y_m(CH_2)_{12}$	Y _{m,tot}	T _m (K)
1,13	1.0	57.1	58.1	148.1 – 5	509
2,12	2.0	51.4	53.4	143.4 + 5	526
3,11	5.0	45.7	50.7	140.7 – 5	481
4,10	8.0	40.0	48.0	138.0 + 5	507
5,9	12.6	34.3	46.9	136.9 – 5	468
6,8	17.2	28.6	45.8	135.8 + 5	499
7,7	22.9	22.9	45.8	135.8 – 5	464
8,6	28.6	17.2	45.8	135.8 + 5	499
9,5	34.3	12.6	46.9	136.9 – 5	468
10,4	40.0	8.0	48.0	138.0 + 5	507
11,3	45.7	5.0	50.7	140.7 – 5	481
12,2	51.4	2.0	53.4	143.4 + 5	526
13,1	57.1	1.0	58.1	148.1 – 5	509

An analogous effect (stiffening) is caused by steric hindrance. The $-\text{C}(\text{CH}_3)_2-$ group in a flexible chain, e.g. has a group contribution of 12.1 (Table 6.8); if it occurs between two aromatic rings, the increment increases to 24.

6.3.2.5. Aromatic condensation polymers with special structures

In rigid aromatic systems we also meet special effects. The most spectacular examples are the Arylates and Aramides. In arylates (fully aromatic polyesters) the stiffening is so pronounced that the $-\text{COO}-$ increment is raised from 25 to 35; in aramides (fully aromatic polamides) the $-\text{CONH}-$ increment is increased from 45 to 60. Frequently occurring combinations of p-phenylene groups with other, mostly functional groups are shown – with their \mathbf{Y}_m contributions – in Table 6.14.

6.3.2.6. Heterocyclic condensation polymers

The number of reliable data on T_m in this class of polymer families is still smaller than those for T_g . So only a very restricted number of increments could be derived. They are included in Table 6.8.

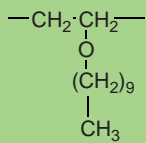
6.3.3. Comparison between calculated and experimental values

Table 6.15 gives a comparison of experimental and calculated values for a random selection of polymers. The agreement is good. Of the nearly 800 polymers whose melting points are reported about 75% gave calculated values which differed less than 20 K from the experimental ones. Part of the experimental values of the other 25% is not fully reliable. The result may be considered satisfactory for the method presented.

We shall now illustrate the method again by some typical examples.

Example 6.6

Estimate the crystalline melting point of poly(vinyl 1-decyl ether). The formula of the structural unit is:



Solution

Eqs. (6.22)–(6.24) give for $N > 5$:

$$\mathbf{Y}_m = \mathbf{Y}_{m5} + 5.7(N - 5)$$

Table 6.9 gives for poly(ethers): $\mathbf{Y}_{m5} = 30.1$ and $\mathbf{M}_o = 58.1$. So

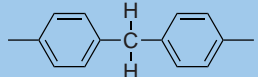
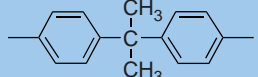
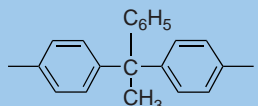
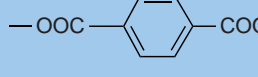
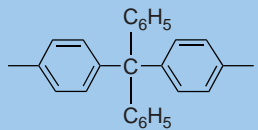
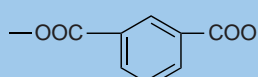
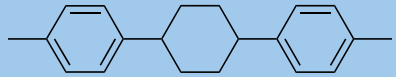
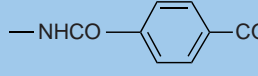
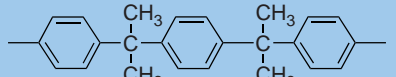
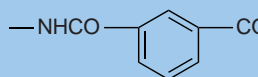
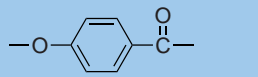
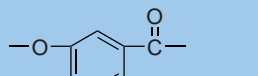
$$\mathbf{Y}_{m5} = 30.1 + 5.7 \times 4 = 52.9$$

$$\mathbf{M} = 58.1 + 9 \times 14.02 = 184$$

$$T_m = \frac{52.9 \times 1000}{184} = 288 \text{ K}$$

The literature value is $T_m = 280 \text{ K}$, in fair agreement.

TABLE 6.14 Υ_{mi} -values of frequently used combinations

Combi-groups	Υ_{mi}	M_i	Combi-groups	Υ_{mi}	M_i
of hydrocarbon groups only			in flexible chains		
	80 ± 10	166.2		47	104.1
	125	194.3		58	108.1
	143	256.3		105	164.1
	190	316.4		85	164.1
	124	234.3		139	162.1
	159	312.3		100	162.1
			in rigid arylates		
				(81)	120.1
				(72)	120.1

(continued)

TABLE 6.14 (continued)

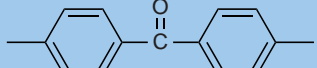
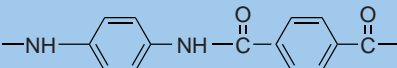
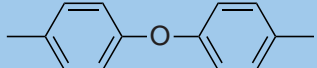
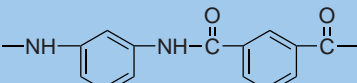
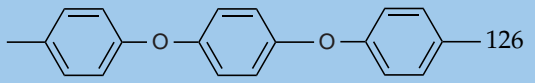
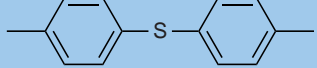
Combi-groups	γ_{mi}	M_i	Combi-groups	γ_{mi}	M_i
	n 99 c 103 cc 110	152.2	in rigid aramides		
with functional groups				98	119.1
	109	180.2		208	238.3
	91	168.2		(125)	238.3
	126	260.2			
	99	184.2			
	133	216.3			

TABLE 6.15 Experimental and calculated values of T_m for a number of polymers (K)

Polymer	T_m exp.	T_m calc.
Polyethylene	410 (268/414)	407
Polyethylidene	463	464
Polypropylene	385/481	445
Polyisobutylene	275/317	318
Polystyrene	498/523	516
Polybutene	379/415	361
Polyoctene	235	235
Polyoctadecene	314/383	330
Poly(vinyl methyl ether)	417/423	420
Poly(vinyl ethyl ether)	359	354
Poly(vinyl heptadecyl ether)	333	329
Poly(propyl acrylate)	388/435	360
Poly(butyl acrylate)	320	309
Poly(docosyl acrylate)	329/345	336
Poly(vinyl dodecanoate)	274/302	288
Poly(methyl methacrylate)	433/473	433
Poly(docosyl methacrylate)	328/334	341
Poly(vinyl fluoride)	503	502
Poly(vinylidene fluoride)	410/511	488
Poly(tetrafluoroethylene)	292/672	510
Poly(vinyl chloride)	485/583	531
Poly(vinylidene chloride)	463/483	461
Poly(trifluoro-chloroethylene)	483/533	494
Poly(ethylene oxide)	335/349	352
Poly(trimethylene oxide)	308	319
Poly(tetramethylene oxide)	308/333	299
Poly(ethylene sulphide)	418/483	407
Poly(decamethylene sulphide)	351/365	363
Poly(decamethylene disulphide)	318/332	343
Poly(ethylene adipate)	320/338	348
Poly(decamethylene adipate)	343/355	345
Poly (decamethylene sebacate)	344/358	349
Poly(ethylene terephthalate)	538/557	563
Poly(decamethylene terephthalate)	396/411	480
Poly(paraphenylene dimethylene adipate)	343/354	395
Poly(tetramethylene anhydride)	350/371	335
Poly(hexamethylene anhydride)	368	369
Poly(tetramethylene carbonate)	332	327
Poly (decamethylene carbonate)	328/378	350
Poly(hexamethylene adipamide)	523/545	518
Poly(decamethylene sebacamide)	467/489	469
Poly(6-aminocaproic acid)	487/506	510
Poly(11-aminoundecanoic acid)	455/493	464
Poly(nonamethylene azelamide)	438/462	436
Poly(ethylene terephthalamide)	728	752
Poly(hexamethylene terephthalamide)	623/644	634
Poly (octadecamethylene terephthalamide)	528	542
Poly(paraphenylene dimethylene adipamide)	606/613	598

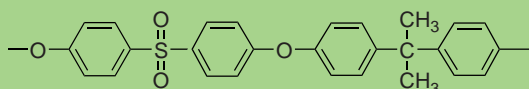
(continued)

TABLE 6.15 (*continued*)

Polymer	T_m exp.	T_m calc.
Poly (hexamethylene-4,4'-oxydibutyramide)	460	513
Poly(tetramethylene hexamethylene diurethane)	446/462	435
Poly(decamethylene hexadecamethylene diurethane)	401	417
Poly(paraphenylene dimethylene tetramethylene diurethane)	500	486
Poly(hexamethylene octamethylene diurea)	498/526	531
Poly(paraphenylene dimethylene hexamethylene diurea)	579	579

Example 6.7

Estimate the crystalline melting point of UDEL® polysulphone, structural formula:

Also estimate the T_g/T_m ratio.**Solution**

From the Tables 6.7, 6.13, 6.1 and 6.3 we take the following data:

	Y_{mi}	Y_{gi}	M_i
	133	111	216.3
	125	87	194.3
2 -O-	27	8	32.0
	285	206	442.6

$$\text{So } T_m = \frac{285 \times 10^3}{442.6} = 645 \text{ K}, \quad T = \frac{206 \times 10^3}{442.6} = 466 \text{ K}, \quad T_g/T_m = 0.71$$

Literature data: $T_g = 465 - 499 \text{ K}$ **6.3.4. Other factors influencing the value of T_m** **6.3.4.1. Pressure dependence of T_m**

Zoller et al. (1988, 1989) found the following relationship for the pressure dependence of the melting point:

$$T_m(p) = T_m(0) + s_m p. \quad (6.25)$$

For flexible aliphatic polymers, e.g. poly(oxy methylene), s_m has a value of 0.175 K MPa^{-1} ; for semi-rigid aromatic polymers (such as PEEK) the value of s_m is much larger, viz. 0.5 K MPa^{-1} .

6.3.4.2. The influence of molecular mass on the crystalline melting point

Flory (1953, 1978) derived the following useful equation for the depression of the melting point by lower molecular constituents of the polymer:

$$\frac{1}{T_m} - \frac{1}{T_{m(\infty)}} = \frac{R}{\Delta H_m} \frac{2}{x_n} \quad (6.26)$$

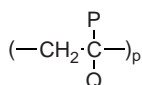
where x_n = degree of polymerisation; ΔH_m = heat of fusion per structural unit; $T_{m(\infty)}$ = melting point of the real "high" polymer.

This formula may also be written as follows

$$\frac{1}{T_m} = \frac{1}{T_{m(\infty)}} + \frac{B}{M_n} \quad (6.27)$$

6.3.4.3. The influence of tacticity

For the structures



some, probably general, rules could be derived.

For P = H we normally find:

$$T_m \text{ (isotactic)} > T_m \text{ (syndiotactic)}$$

For P \neq H and \neq Q the opposite effect is found:

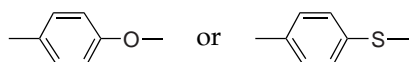
$$T_m \text{ (isotactic)} < T_m \text{ (syndiotactic)}$$

Hence for Polystyrene $T_{mi} > T_{ms}$, whereas for Poly(methyl methacrylate) $T_{mi} < T_{ms}$.

The difference between T_{mi} and T_{ms} is in both cases of the order of 60 K.

6.3.4.4. The influence of molecular asymmetry

Symmetry in the structural unit elevates, asymmetry depresses the melting point. If, e.g. the group combinations



are present in such a way that the structural unit becomes asymmetrical, T_m may decrease by 10 points.

6.4. RELATIONSHIP BETWEEN GLASS TRANSITION TEMPERATURE AND MELTING POINT OF POLYMERS

It has been observed that the ratio of glass transition temperature to melting point (both of course expressed in K) has about the same value for many polymers: $T_g/T_m \approx 2/3$. This feature was first reported by Boyer (1952) and, independently, by Beaman (1953) and Bunn (1953). In later work Boyer (1954, 1963) discussed the subject more fully (Fig. 6.8) and gave the following rules:

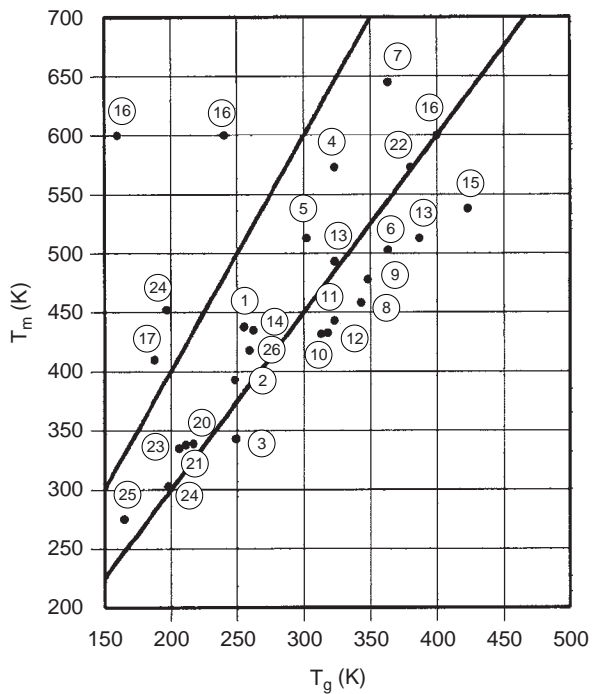


FIG. 6.8 Relation between T_m and T_g for various polymers (Boyer 1963).

Polymer	T_m , °K	T_g , °K	T_m/T_g
1. Polypropylene	438	255	1.71
2. Polybutene-1	393	248	1.58
3. Polypentene-1	343	249	1.37
4. Poly-3-methyl-1-butene	573	323	1.77
5. Poly-4-methyl-1-pentene	513	302	1.70
6. Polystyrene	503	363	1.39
7. Polyvinyl cyclohexane	645	363	1.77
8. Polyallyl benzene	458	343	1.33
9. Polyallyl cyclohexane	478	348	1.37
10. Poly-4-phenyl-1-butene	432	313	1.38
11. Poly-4-cyclohexyl-1-butene	443	323	1.37
12. Isotactic PMMA	433	318	1.36
13. Polymethyl isopropenyl ketone	513	387	1.50
14. Isotactic polyisopropyl acrylate	435	262	1.66
15. Polybisphenol A carbonate	538	423	1.27
16. Teflon (polytetrafluoroethylene)	600	160	3.75
17. Linear polyethylene	600	400	1.67
18. Chlorotrifluoroethylene	410	188	2.18
19. Polyformaldehyde	410	243	1.68
20. Polyethylene oxide	493	323	1.53
21. Polypropylene oxide	452	197	2.3
22. Cellulose triacetate	200	200	2.3
23. <i>Trans</i> -polyisoprene	339	217	1.56
24. <i>Cis</i> -polyisoprene	246	246	1.38
25. <i>Cis</i> -polybutadiene	338	211	1.6
26. <i>Trans</i> -1,4-polybutadiene	573	380	1.51
27. Polydimethylsiloxane	335	206	1.62
	418	259	1.62
	193	150	1.29

$$\frac{T_g}{T_m} \approx \begin{cases} \frac{1}{2} & \text{for symmetrical polymers} \\ \frac{2}{3} & \text{for unsymmetrical polymers} \end{cases} \quad (6.28)$$

Unsymmetrical polymers were defined as those containing a main-chain atom that does not have two identical substituents. Other polymers are regarded as symmetrical. Since then many workers have used this relationship as a rule of thumb.

In an extensive study Lee and Knight (1970) investigated the relationship for 132 polymers and found the ratio to vary widely. In Fig. 6.9 their results are graphically represented. The integral distribution curves show the number N of polymers, for which T_g/T_m is smaller than or equal to a given value, as a function of the value of T_g/T_m . About 80% of both symmetrical and unsymmetrical polymers have values in the range 0.5–0.8 with a maximum number around 0.66, while 20% of the polymers have ratios outside this range. According to these authors there is no real basis for distinguishing between symmetrical and unsymmetrical polymers. They also argue that it is unlikely, from a thermodynamical point of view, that a simple relationship between T_g and T_m can be formulated; the molecular mechanisms of the two phenomena differ fundamentally.

The truth probably lies between these two opinions: the two phenomena show both points of correspondence and points of difference. Thus a constant T_g/T_m ratio may be

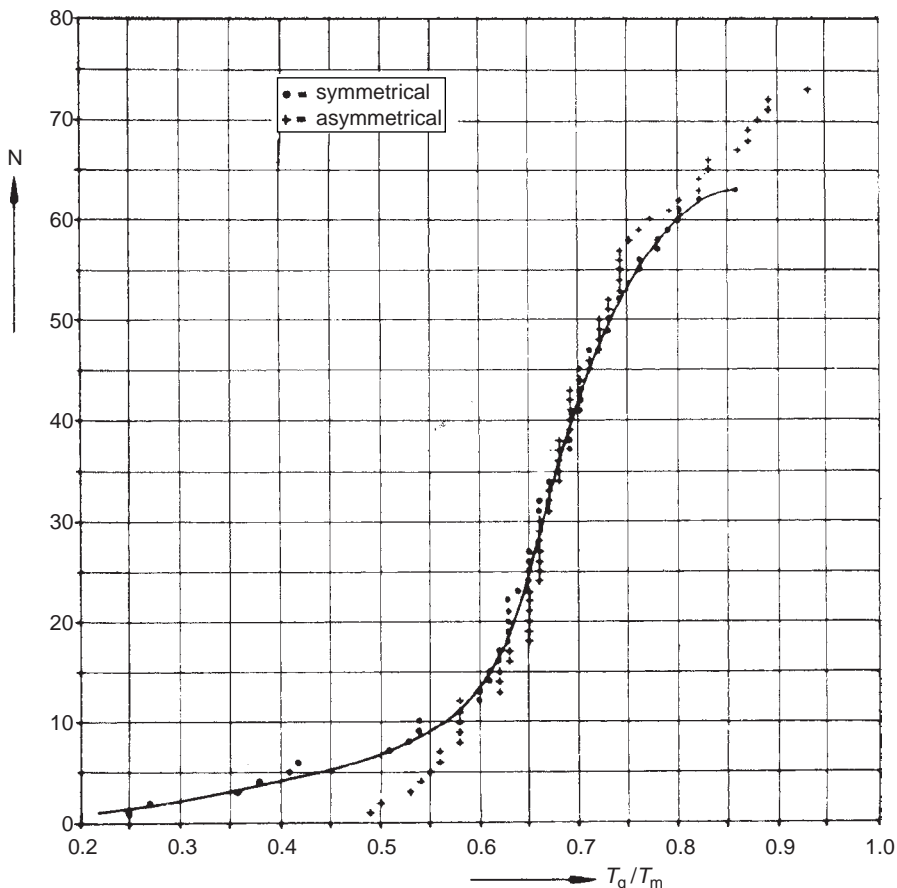


FIG. 6.9 Integral distribution curves of T_g/T_m .

considered as a general rule with a number of exceptions, to be attributed to structural details of the polymers. This is in agreement with the fact that the methods for predicting T_m and T_g described in this chapter, show many points of correspondence, but differ in details (see Appendix II in this chapter).

In conformity with these considerations, the following general rules for the T_g/T_m ratio may be formulated:

1. Polymers with T_g/T_m ratios below 0.5 are highly symmetrical and have short repeating units consisting of one or two main-chain atoms each, carrying substituents consisting of only a single atom (polymethylene, polyethylene, polytetrafluoroethylene, polymethylene oxide). They are markedly crystalline.
2. Polymers with T_g/T_m ratios above 0.67 are unsymmetrical. They can also be highly crystalline if they have long sequences of methylene groups or are highly stereo regular; all have a much more complex structure than the polymers with ratios below 0.5.
3. The majority of the polymers have T_g/T_m ratios between 0.56 and 0.76 with a maximum number around 2/3; both symmetrical and unsymmetrical polymers belong to this group.

These rules may be considered as a modification of Boyer's rules and are useful in practical estimations.

6.4.1. T_g/T_m for co-polymers

In some cases quite different values for the T_g/T_m ratio may be observed in copolymers. In this connection, random copolymers and block copolymers should be distinguished. Owing to the irregularity of the structure, crystallization is more difficult in random copolymers than in each of the pure homopolymers. Therefore the melting point is depressed, while the glass transition temperature may have a normal value between those for the homopolymers. This results in a high value for the T_g/T_m ratio.

In block copolymers, on the other hand, long sequences of equal structural units may crystallize in the same way as in the homopolymer. In some cases, a block copolymer may be obtained that combines a high crystalline melting point (corresponding with the value of one component as a homopolymer) with a low glass transition temperature (corresponding with the other pure homopolymer). This results in a low T_g/T_m ratio. A schematic plot is given in Fig. 6.10.

6.5. RELATIONSHIP BETWEEN T_g , T_m AND OTHER TRANSITION TEMPERATURES

In some papers Boyer (1973–1985) discussed the other transition temperatures which are often encountered in polymers, and the relationships between these transitions and the two main transitions: T_g and T_m .

We shall give here Boyer's main conclusions.

6.5.1. The local mode relaxation, T ($< T_g$) in Boyer's notation

This relaxation involves a very short section of a polymer chain. It is often called the β -relaxation. As a general rule

$$T_\beta \approx 0.75T_g \quad (\text{at } 100 \text{ Hz}) \quad (6.29)$$

It is found in both glassy amorphous and semi-crystalline polymers.

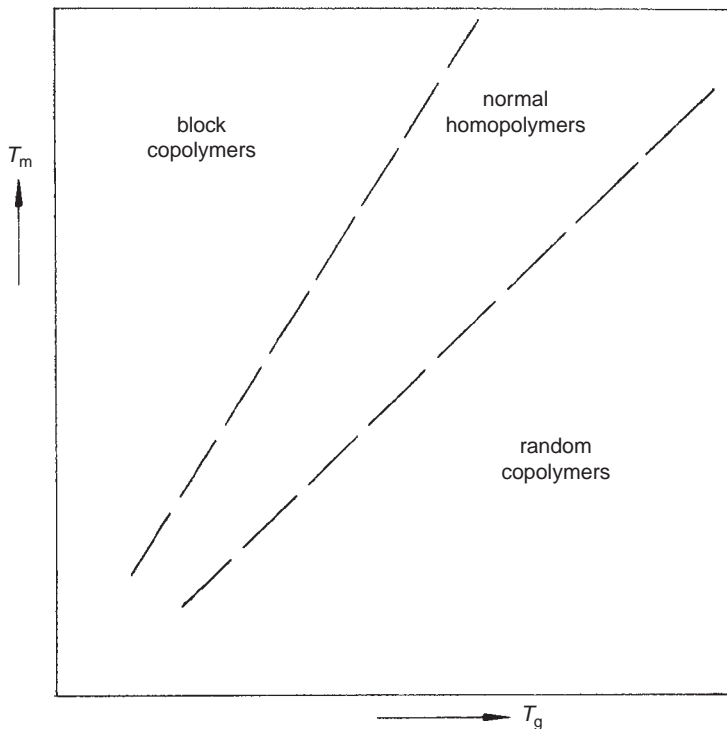


FIG. 6.10 A schematic plot of T_m versus T_g for some types of polymers (from Alfrey and Gurnee, 1967).

6.5.2. A liquid–liquid relaxation above T_g , viz. T_{11}

This relaxation has been discovered in some non-vulcanized amorphous polymers and copolymers. It tends to fall at approximately $1.2T_g$. Because it appears to be connected with the change from the viscoelastic to the normal viscous state it will also depend on the molecular weight and accordingly increases with M_w .

6.5.3. A second glass transition in semi-crystalline polymers

In some semi-crystalline polymers, two glass transitions can be distinguished: a lower glass transition, $T_g(L)$ and an upper glass transition, $T_g(U)$. It may be assumed that $T_g(L)$ arises from purely amorphous material, while $T_g(U)$ arises from amorphous material which is under restraint due to the vicinity of crystallites. Frequently $T_g(U)$ increases with the degree of crystallization. Some general rules are:

$$T_g(U) \approx (1.2 \pm 0.1)T_g(L) \quad (6.30)$$

$$T_g(L) \approx (0.575 \pm 0.075)T_m \quad (6.31)$$

$$T_g(U) \approx (0.7 \pm 0.1)T_m \quad (6.32)$$

6.5.4. A premelting transition ($T_{\alpha c}$)

Some *semi-crystalline* polymers show a mechanical loss peak just below T_m . This $T_{\alpha c}$ is the temperature at which hindered rotation of polymer chains inside the folded crystals can occur. As a general rule

$$T_{zc} \approx 0.9T_m \quad (6.33)$$

Table 6.16 gives a survey of these transitions and their ratios for a number of polymers.

6.5.4.1. The β -relaxation

The first secondary transition below T_g , the so called β -relaxation, is practically important. This became evident after Struik's (1978) finding that polymers are brittle below T_β and establish creep and ductile fracture between T_β and T_g . The β -relaxation is characteristic for each individual polymer, since it is connected with the start of free movements of special short sections of the polymer chain. In view of more recent data of T_β Boyer's relation, Eq. (6.29), is very approximate and fails completely for amorphous polymers with high T_g 's (e.g. aromatic polycarbonates and polysulphones). Some rules of thumb may be given for a closer approximation.

For semi-crystalline polymers the following relation is proposed here:

$$T_\beta \approx 0.8T_g - 40 \approx 0.5T_m - 25 \quad (6.34)$$

This equation is illustrated by Fig. 6.11.

For non-crystallisable glassy polymers another tentative rule is proposed:

$$T_\beta + T_g \approx 635 \text{ K} \quad (6.35)$$

In Table 6.17 a comparison is given between experimental and estimated T_β -values of this type of polymers. It seems that the value for $T_\beta/T_g \approx 0.8$ for the aliphatic polymers and $T_\beta/T_g \approx 0.35$ for the aromatic polymers.

6.5.4.2. Liquid-crystalline transitions

Other transitions that may occur in the case of liquid crystal polymers will be treated in Sect. 6.6.

6.6. TRANSITIONS IN THERMOTROPIC LIQUID CRYSTAL POLYMERS

For polymers which, on heating, yield *Mesophases* (liquid crystal melts), the so-called mesogenic polymers or liquid crystal polymers (LCPs), the situation of phase transitions is much more complex. In this case the simple Volume-Temperature diagram, given in Fig. 4.2 is not valid anymore and has to be substituted by a more complicated one, which is shown in Fig. 6.12.

The liquid crystal melt, which comes into being at the glass-rubber transition or at the crystal-melt transition, may have several phase states (Mesophases): one or more *smectic* melt phases, a *nematic* phase and sometimes a *chiral* or *cholesteric* phase; the final phase will be the isotropic liquid phase, if no previous decomposition takes place. All mesophase transitions are thermodynamically real first order effects, in contradistinction to the glass-rubber transition. A schematic representation of some characteristic liquid crystal phase structures is shown in Fig. 6.13, where also so-called columnar phases formed from disc-like molecules is given.

The designation of the different phase transitions in the literature is confusing. We prefer – as proposed by Wunderlich and Grebowicz (1984) – to reserve the symbol T_m for the “normal” polymers, which do not give mesophases on heating, but a direct transition into the isotropic

TABLE 6.16 Transition temperatures and their ratios for a number of polymers, according to Boyer (1975)

Polymer	Degree of crystallinity	$T < T_g$	$T_g(L)$	$T_g(U)$	$T_{\alpha c}$	T_m	$\frac{T < T_g}{T_g}$	$\frac{T_g(U)}{T_g(L)}$	$\frac{T_g(L)}{T_m}$	$\frac{T_g(U)}{T_m}$	$\frac{T_{\alpha c}}{T_m}$
Polyethylene	(0)	145	{ 195 200 203 206 }	{ (243) 220 235 253 }	378	410	0.75	{ (1.25) 1.10 1.16 1.23 }	0.475	0.60	0.92
	0.3										
	0.5										
	0.7										
Polyoxymethylene		(178)	(235)	(295)	{ 408 433 }	471	(0.75)	(1.25)	(0.50)	(0.63)	{ 0.88 0.92 }
Poly(ethylene oxide)		(140)	(173)	(215)		342	(0.80)	(1.25)	(0.51)	0.72	0.94
Polypropylene (<i>iso</i>)		212	258	300	391	445	0.82	1.18	0.58	0.675	0.89
Polybutene	0.75		236	278	{ 343 323 }	{ 370 407 }		1.29	0.64	0.75	{ 0.925 0.79 }
Polypentene			221	{ 263 291 }				{ 1.19 1.26 }			
Poly(4-methylpentene)	0.05		{ 291 302 }	403		{ 443 463 }	{ 522 551 }		1.36	0.555	0.775
Polybutadiene (<i>trans</i>)			253	308							
Polyisoprene (guta-percha) (<i>trans</i>)			210	265				1.26			
Polyisoprene (<i>cis</i>)	0.2–0.25		202	233				1.15			
Poly(vinyl fluoride)					423	490					0.86
Poly(vinyl chloride)		236	340								
Poly(trifluorochloroethylene)		253	(253)		433	493	(0.71)		0.72		0.88
Poly(vinylidene fluoride)	0.77	176	221	286	{ 363 373 }	443	0.78	1.29	0.51	0.65	{ 0.82 0.85 }
Poly(vinylidene chloride)			288	353				1.23			
Poly(tetrafluoroethylene)		160	220	(300)	400?	470?	0.73				
Poly(vinyl alcohol)			353	393	{ 403 473 }	{ 505 538 }		1.11			{ 0.80 0.75 }
Nylon 6		(140)	{ 323 353 }	{ (405) 398 }					0.65	(0.81)	
Polysulphide (<i>iso</i>)			363	433				1.13			
Polyacrylonitrile			378	413				1.18			
Poly(ethyleneterephthalate)	0.7		339	388				(1.09)			1.14

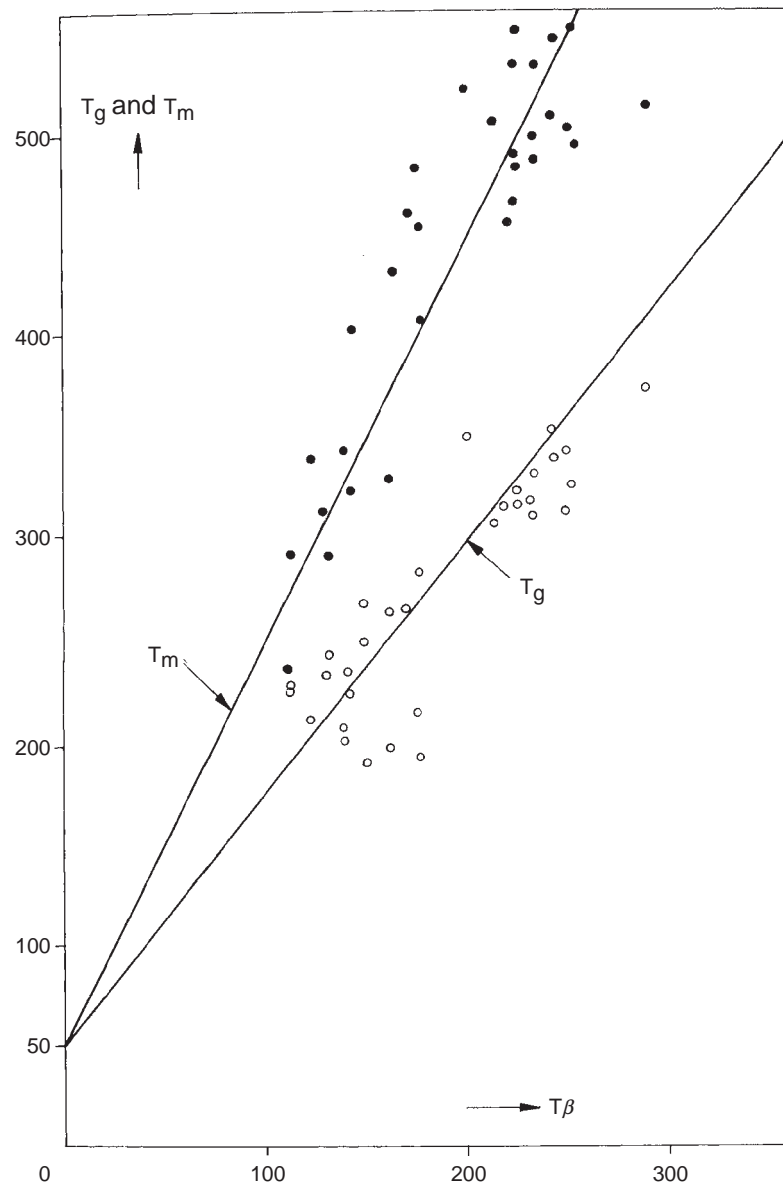


FIG. 6.11 Relationship between T_β and T_g (open points) and between T_β and T_m (filled points) for semi-crystalline polymers.

TABLE 6.17 Some T_β and T_g data of glassy polymers in comparison with estimation

Polymer	T_β (exp.)	T_β (est.)	T_g	T_β/T_g
Polystyrene (atactic)	290	290	373	0.77
Poly(vinyl chloride) (atactic)	250	281	354	0.71
Poly(methyl methacrylate) (atactic)	300	260	378	0.80
Poly(cyclohexyl methacrylate)	311	315	377	0.82
Poly(bisphenol carbonate)	155/243	217	418	0.37/0.58
Polysulphone	173	170	465/499	0.36
Poly(2,6-dimethyl phenylene oxide)	<173	152	483/500	<0.35

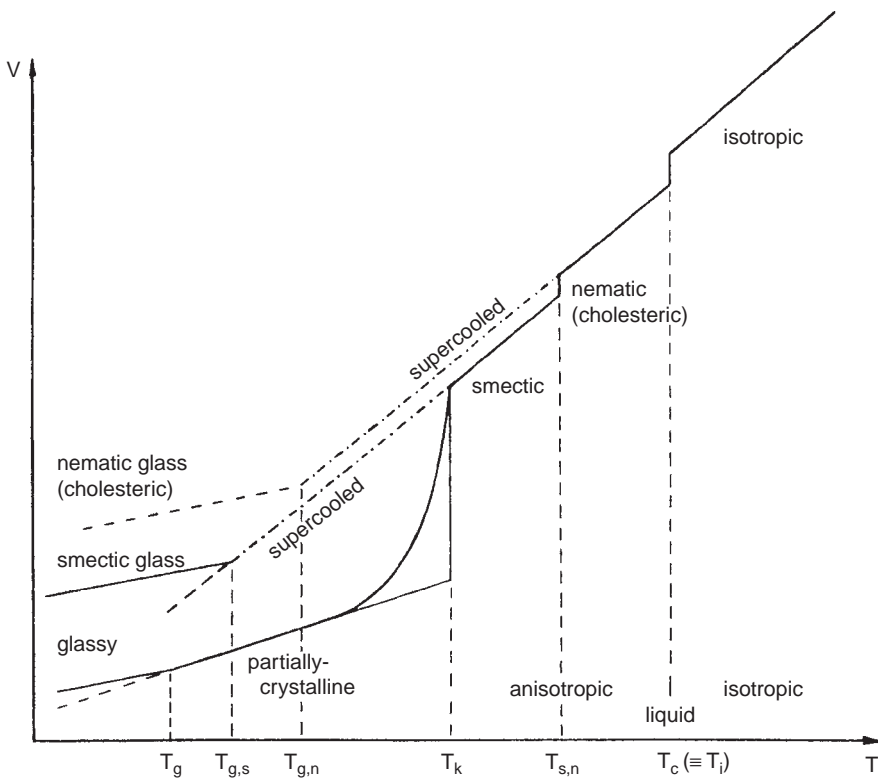


FIG. 6.12 Schematic volume-temperature diagram of a liquid crystal polymer (after Finkelmann and Rehage (1984); Courtesy Springer-verlag).

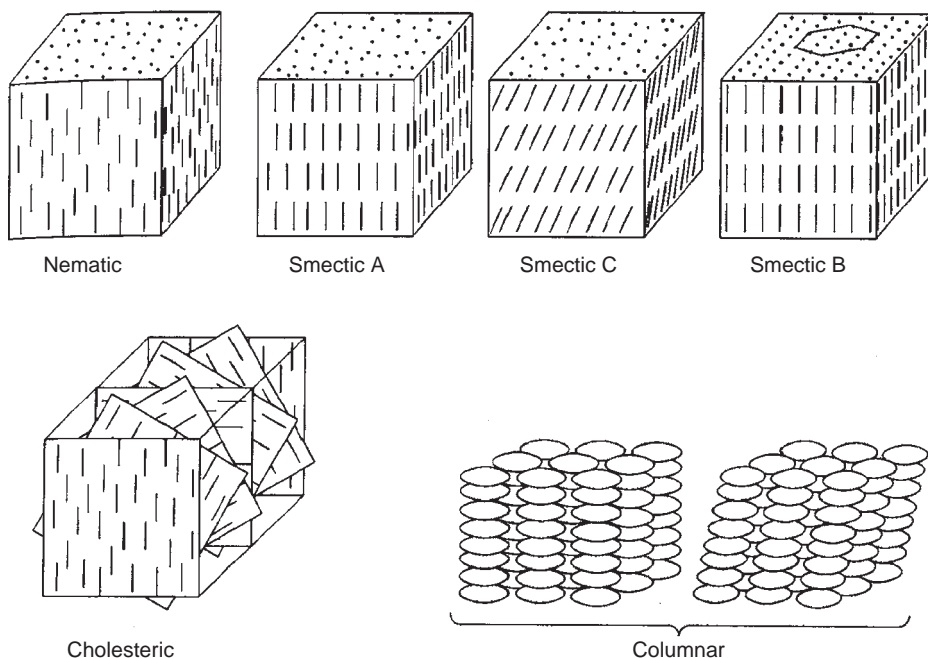
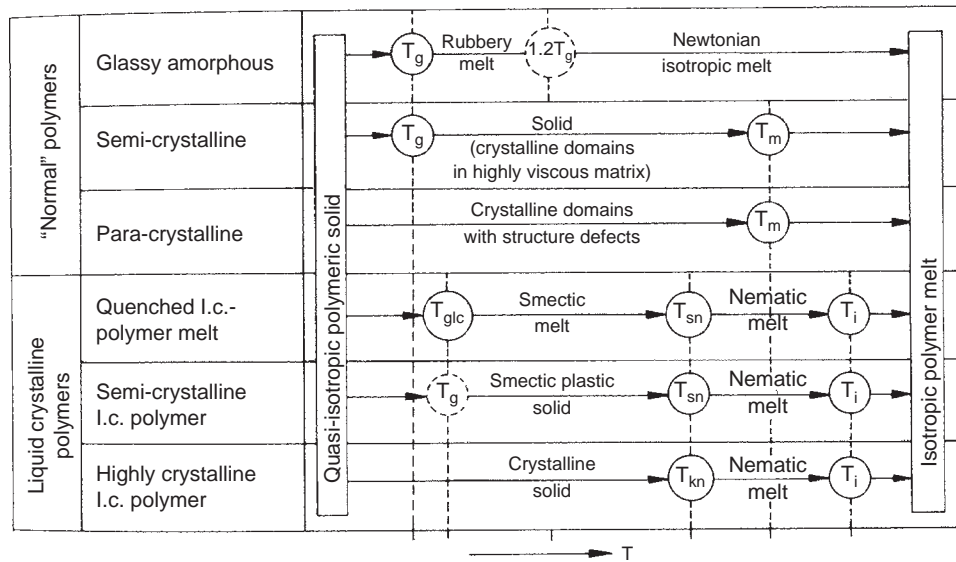


FIG. 6.13 Schematic representation of some characteristic liquid crystal phase structures. Nematic, smectic and cholesteric phases formed from rod-like molecules; columnar phases formed from disc-like molecules (from Jansen, 1996).

melt. The symbol T_k will be used for the “disordering temperature” of the crystalline state into the first liquid crystal state; the symbol T_i will be used for the final transition into the isotropic melt (the latter is often called “clearing temperature”, designated by T_c or T_{cl}). The symbols T_{ks} and T_{kn} may be used as a refinement (if necessary) to designate the transition of the crystalline phase into the smectic or directly to the nematic phase. Furthermore T_{sn} may be used for the transition of the smectic into the nematic phase. If necessary, T_{si} and T_{ni} may be used for the final transition into the isotropic liquid. As a matter of fact all mesophases can be quenched into a glassy state; the glass transitions involved may be designated as $T_{g,s}$ and $T_{g,n}$ in contrast to $T_{g,i}$ the normal T_g . These different T_g ’s are usually fairly close together, so that a restriction to one symbol T_g appears to be allowed. Since in 1.c. polymers usually only one smectic phase can be distinguished, the final designation may be more confined, as visualised in Scheme 6.2. Investigation of about 300 LCPs described in the literature led us to the values given in Table 6.18 for the ratios of the characteristic transition temperatures.

The method of estimation of the numerical values of these characteristic temperatures will now be described.



SCHEME 6.2 Designations of the most important transition temperature (thermotropy).

TABLE 6.18 Ratios of characteristic transition temperatures of thermotropic LCPs

Location of mesogenic group	Functional type of Polymer	T_g/T_k	T_g/T_i	T_{sn}/T_k	T_k/T_i
Main chain	Aromatic polyesters	0.69	0.64	—	0.92
	Azo-benzene type	0.75	0.69	—	0.925
	Siloxanes	—	0.68	—	0.92
	<i>Weighted average</i>	0.72	0.67	—	0.92
	Poly-acrylates and	0.91	0.79	0.98	0.87
Side chain	Poly-siloxanes				
	Poly-methacrylates	0.91	0.86	0.98	0.95
	<i>Weighted average</i>	0.91	0.82	0.98	0.90

NB, Due to the strong influence of the “thermal history” of LCPs the notion of precise temperature transition must be treated with reservation.

All Liquid Crystal Polymers are characterised by the fact that they contain stiff *mesogenic groups*, often inserted in flexible chain systems (so called “*spacers*”) and connected to them by linking functional groups; the mesogenic unit is inserted either in the *main chain* or in the *side chains* or (in exceptional cases) in both. We shall discuss MCLCPs and SCLCPs. A schematic representation of common structures of LCPs is displayed in Fig. 6.14 (Jansen, 1996). An example of a SCLCP with disc-like mesogens is displayed in Fig. 6.15 (Franse et al., 2002, 2004).

6.6.1. Polymers with mesogenic groups in the main chain (MCLCPs)

This type of polymers has the general structure sketched in Fig. 6.16. The usual situation is that the mesogenic group consists of cyclic units (usually *para*-phenylene groups, interconnected by functional groups containing double bonds, so that conjugated cyclic units are formed). These stiff mesogenic groups are often linked to flexible spacers (usually $-\text{CH}_2-$, $-\text{CH}_2\text{CHO}-$ or siloxane sequences) by means of other functional groups.

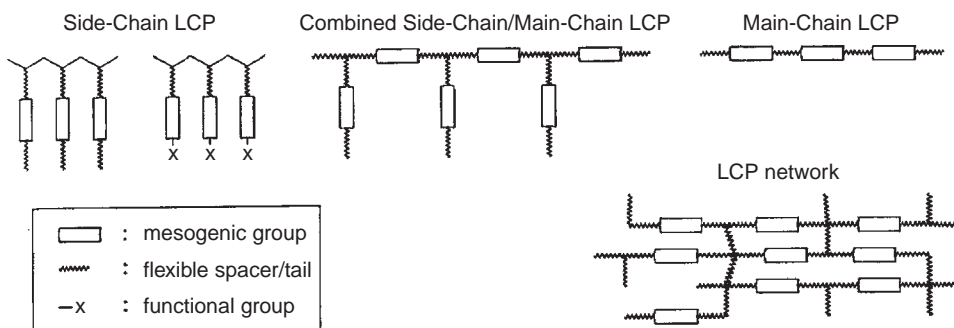


FIG. 6.14 Schematic representation of some common structures of liquid crystalline polymers (From Jansen, 1996).

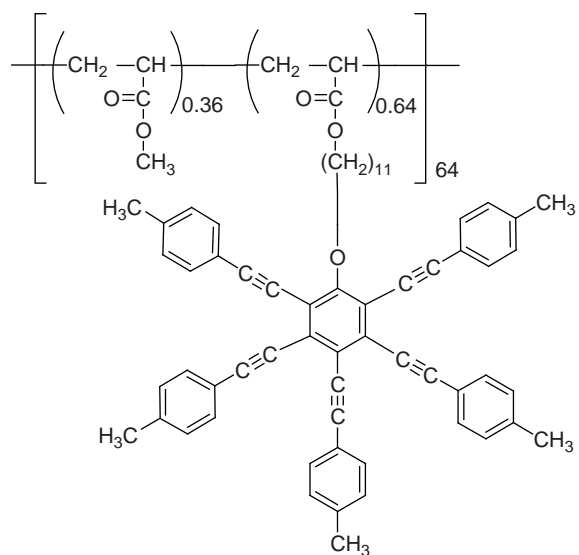


FIG. 6.15 Chemical structure of a discotic side-chain polyacrylate copolymer (from Franse et al., 2002, 2004).

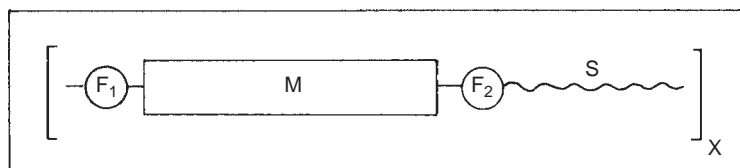


FIG. 6.16 Schematic structure of liquid crystalline polymer with mesogenic group in the main chain. M = stiff mesogenic group, consisting of cyclic units (usually 1,4-phenylene groups), linked by conjugating connector groups (such as $-N=N-$, $-CH=N-$, $-COO-$, $-CONH-$, $-CH=C(R)-$, $-C(R)=N-N=C(R)-$, etc.); S = flexible spacer (usually a sequence of $-CH_2-$, $-CH_2-CH_2-O-$, $-Si(CH_3)_2-O-$, etc.); F = functional group, linking the mesogenic group to the spacer ("linking" z group).

In essence these are normal polymers with normal, be it rather complex structural units, on which the technique of additive group contributions can be applied, if the Y_g - and Y_m -values of the mesogenic groups are known or can be estimated. However, there is a difficulty due to the fact that the melting process is now spread into a stepwise transition region with T_k and T_i as starting and end-points respectively. Empirically we have found that the "fictive" T_m -value, calculated from the group increments is in the middle of T_k and T_i , and that the following relationships exist:

$$T_k = 0.95T_m(\text{calc.}); \quad T_i = 1.05T_m(\text{calc.}) \quad (6.36)$$

Eq. (6.36) is, as a matter of fact, no guarantee that an anisotropic phase will really be observable. In the present state of the art, it is impossible to predict the nature and even the possible existence of a mesophase from the structural formula of a polymer.

6.6.2. Polymers with mesogen groups in the side chain (SCLCPs)

The situation looks more complicated for polymers with mesogenic groups in the side chain, but in fact it is rather simple too. All these polymers can be represented by a general structural formula: structure I in Fig. 6.17. This structure can immediately be derived from the general structure of comb-polymers (structure II in Fig. 6.17): the SCLCP is a comb-polymer with an

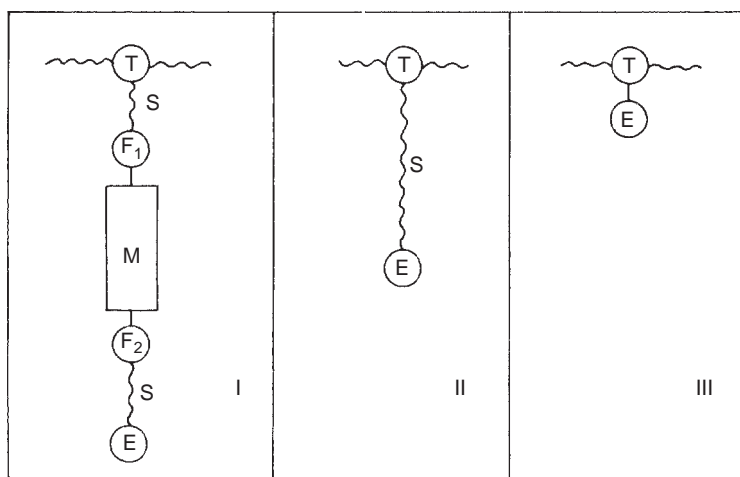


FIG. 6.17 Schematic structure of liquid crystalline polymer with mesogenic group in the side chain (I), in comparison with a normal comb-polymer (II) and their "Basic Polymer" (III). T = trivalent main chain Group ($>CH-$, $>C(CH_3)-$, $>CH(COO-)-$, etc.); E = univalent end group of side chain ($-CH_3$, $-CN$, $-C_6H_5$, etc.); M = mesogenic group; S = spacer ($-(CH_2)_n-$, etc.); F = linking functional group.

inserted mesogenic group (with linking groups) within the sequence of CH₂-groups. The comb-polymer itself may be considered as a “basic” polymer (III) with inserted CH₂-groups between the main chain and an end group (usually -CH₃, -CN or -C₆H₅).

So the logical result of this reasoning is:

$$\mathbf{Y}_g(\text{I}) = \mathbf{Y}_g(\text{II}) + \mathbf{Y}_g(\text{M} + \text{F}) \quad (6.37)$$

$$\mathbf{Y}_m(\text{I}) = \mathbf{Y}_m(\text{II}) + \mathbf{Y}_m(\text{M} + \text{F}) \quad (6.38)$$

The calculation of $\mathbf{Y}_g(\text{II})$ and $\mathbf{Y}_m(\text{II})$ was described earlier in this chapter.

Values for $\mathbf{Y}_g(\text{M} + \text{F})$ and $\mathbf{Y}_m(\text{M} + \text{F})$, derived from the experimental data in the literature, are given in Table 6.19. In principle they may be derived from the increments in the Tables 6.1 and 6.6, but a closer connection with the experimental background (Table 6.22, see later) is preferable.

TABLE 6.19 \mathbf{Y}_g - and \mathbf{Y}_m -increments of some important mesogenic and linking functional groups

Mesogenic groups ^a	\mathbf{Y}_g^b	\mathbf{Y}_m^c
	(70)	100
	(85)	125
	(145)	205
	—	285
	—	295
	70	100
	75	(110)
	70	100
	—	150
	110	160
Linking groups (to spacer)	-O- -Es-	4 12.5
		13.5 25

^a Es = ester group (-COO-).

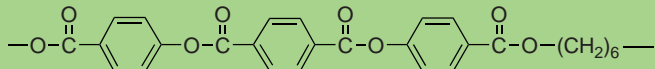
^b Mostly side chain mesogenic groups.

^c Mostly main chain mesogenic groups.

As examples some calculations of T_g , T_k , and T_i will be given for main-chain-, side-chain- and combined main- and side-chain-l.c. polymers.

Example 6.8

Estimate the characteristic temperatures of the MCLCP with the following structural unit



Solution

The structural unit of this polymer has a molar mass of 488 and consists of the following groups with their indicated group contributions:

	\mathbf{Y}_g	\mathbf{Y}_m
1 mesogenic group (use Table 6.19)	(145)	205
2 functional linking groups (-COO-)	25	50
6 -CH ₂ -groups in the main chain, with one functional group per repeating unit (use Table 6.10, for the calculation of \mathbf{Y}_m)	16	17
	(186)	272

Hence:

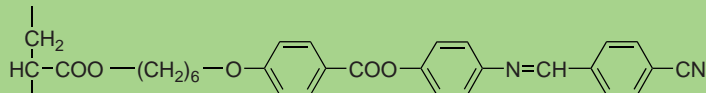
$$T_g = \frac{186}{488} 1000 = 381 \text{ K}, \quad T_m = \frac{272}{488} 1000 = 557 \text{ K} \quad \text{and} \quad T_g/T_m = 0.68$$

so that $T_k = 0.95 \times 557 = 529 \text{ K}$ and $T_i = 1.05 \times 557 = 585 \text{ K}$.

The thermal behaviour of this polymer was investigated by Lenz (1985), who found the following experimental values: $T_k = 500 \text{ K}$ and $T_i = 563 \text{ K}$ (in reasonable agreement).

Example 6.9

Estimate the characteristic temperatures of the liquid-crystalline side-chain polymer with the following structural unit:



Solution

This polymer may be considered as a comb-polymer, based on poly(acrylonitrile), with a mesogenic group and two functional linking groups inserted in the side chain; the molar mass of the whole structural unit is 496.

The calculation has to be done in two steps:

- (a) That of the \mathbf{Y}_g - and \mathbf{Y}_m -values of the comb-polymer. The basic polymer is poly(acrylonitrile) with the data

$$\mathbf{M}_o = 53.1; \mathbf{M}_5 = 123.1; \mathbf{M}_9 = 179.2$$

$$\mathbf{Y}_{go} = 20; \mathbf{Y}_{g9} = 0.2 \quad \mathbf{M}_9 = 35.8$$

$$\text{So} \quad \mathbf{Y}_{g6} = \mathbf{Y}_{g0} + 6/9(\mathbf{Y}_{g9} - \mathbf{Y}_{g0}) = 30.5 \quad (\text{acc to Eq.6.7})$$

In the same way:

$$\mathbf{Y}_{mo} = 32.6; \mathbf{Y}_{m5} = 0.235; \mathbf{M}_5 = 0.235 \times 123.1 = 28.9$$

and

$$Y_{m6} = Y_{m5} + 5.7(6 - 5) = 28.9 + 5.7 = 34.6, \text{ acc to Eq.(6.24).}$$

- (b) That of the Y_g - and Y_m -values of the LCP.

The polymer consists of the comb-polymer, discussed sub (a) with a mesogenic group with two functional linking groups, inserted into the side-chain. Hence:

	Y_g	Y_m
1 comb-polymer unit	30.5	34.6
1 mesogenic unit (see Table 6.19)	110	(160)
2 functional linking groups ($-\text{COO}-$, $-\text{O}-$)	16.5	38.5
	157	233

$$\text{So } T_g = \frac{157}{496} \times 1000 = 317 \text{ K and } T_m = \frac{233}{496} \times 1000 = 470 \text{ K}$$

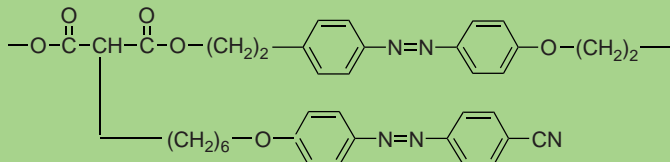
Ringsdorf and Zentel (1982) investigated this polymer and found the following experimental values:

$$T_g = 308 \text{ K; } T_i = 484 \text{ K, from which } T_m = 461 \text{ K}$$

There is a good agreement between estimated and experimental values.

Example 6.10

Estimate the characteristic temperatures of an LCP with mesogenic groups in main- and side-chain, of the following structure:



Solution

The molar mass of the structural unit is 667; it consists of the following structural groups, with the indicated group contributions:

	Y_g	Y_m
1 basic group $-\text{CH}(\text{CN})-$	11.5	17.5
2 functional groups $-\text{COO}-$	25	50
$2 \times 2 -\text{CH}_2-$ groups (Y_m calculated according to Table 6.11)	10.8	4
2 mesogenic units (see Table 6.19)	140	200
2 functional linking groups $-\text{O}-$	8	27
6 inserted $-\text{CH}_2-$ groups in side chain ^a (use Eqs. (6.6)–(6.8) and (6.22)–(6.24))	10.5	9.1
	205.8	307.6

^a The calculation is as follows:

$$Y[\text{inserted } (\text{CH}_2)_6] = (Y(-\text{CH}_2-\underset{\substack{| \\ (\text{CH}_2)_6 \\ | \\ \text{CN}}}{\text{CH}}-)) \text{ minus } Y(-\text{CH}_2-\underset{\substack{| \\ \text{CN}}}{\text{CH}}-))$$

$$\text{So } T_m = \frac{308}{667} \times 1000 = 462 \text{ K}, T_g = \frac{206}{667} \times 1000 = 309 \text{ K and } T_g/T_m = 0.67$$

$$T_i = 1.05 \times 462 = 485 \text{ K}$$

This polymer was investigated by Reck and Ringsdorf (1985), who found: $T_g(\text{exp.}) = 326 \text{ K}$ and $T_i(\text{exp.}) = 475 \text{ K}$. The agreement is very satisfactory.

APPENDIX I

Rules of thumb for substituting an H-atom by a group X

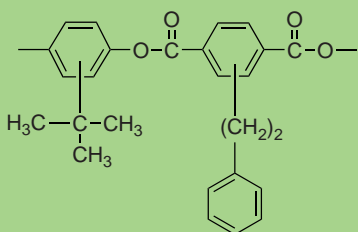
If an H-atom in a structural group is substituted (replaced) by a group X, the numerical values of Y_g and Y_m do increase. Rules for the effects of these substitutions have been derived and are shown in Table 6.20. They are handy when the lists of group increments (Table 6.1 for Y_g and Table 6.8 for Y_m) do not contain the desired values of the substituted group, since its occurrence is rare or occasional. The accuracy of the obtained group contribution is – as a matter of course – somewhat less than listed values.

TABLE 6.20 Increase of the Y_g - and Y_m -values if $-H$ is substituted by $-X$

X	ΔY_g	ΔY_m
$-CH_3$	6	9
$-i.\text{propyl}$	17.5	21
$-tert.\text{ Butyl}$	24	40
$-neopentyl$	31	44
$-cyclohexyl$	37	55
$-phenyl$	33	42
$-p\text{-toluyl}$	39	50
$-C=N$	10	12
$-F$	9	11
$-Cl$	17.5	22
$-Br$	35	11.5

Example 6.11

Estimate the glass transition temperature of the polymer with the following structural unit:



Solution

The structural unit of the polymer has a molar mass of 400. It consists of the following structural groups with their corresponding group contributions:

	γ_g	γ_m
1 mesogenic group	(85)	125
1 linking group (-COO-)	12.5	25
1 H substituted by tert-butyl	24	40
1 H substituted by phenyl	33	42
with -(CH ₂) ₂ -inserted in the side chain	(0)	(-6)
	154.5	(226)

so that the calculated values become:

$$T_g = 1000 \times 154.5/400 = 386, T_m = 1000 \times 226/400 = 565 \text{ and } T_g/T_m = 0.68.$$

The polymer was investigated by Brügging, Kampschulte, Schmidt and Heitz (1988); they found a T_g -value of 373/383 K and a T_m -value of >513 K and remarked that no clearing point was detectable up to 513 K; the polymer started to decompose in air before the T_i could be reached. The agreement of T_g (exp.) and T_g (est.) is good.

APPENDIX II

Similarities and differences between γ_g and γ_m

After our separate discussions on the two main transitions in polymers it looks worthwhile to overview the similarities and differences of γ_g and γ_m .

Similarities

The main transition temperatures have in common that they are both characteristic markings of a collapse of the mechanical stiffness of the polymer. There are many more similarities.

A. Effects of intra-molecular interaction, which usually are the cause of chain stiffening.

These are:

1. *Steric hindrance* of group rotations or oscillations. If, e.g. the groups -C(CH₃)₂- and -Si(CH₃)₂- are located between two aromatic rings, the group increments are increased by about 10 points.
2. *π -Electron conjugation*, which is very marked for the phenylene groups, connected to "double bond" groups, one or two sided. Table 6.21 gives a survey.

TABLE 6.21 π -Electron conjugation effect on the group contribution of phenylene (γ_g and γ_m)

Type of phenylene group	γ_g increment				γ_m increment			
	Standard (no conjugation)	Elevated by conjugation		Standard (no conjugation)	Evaluated by conjugation			
		one sided	two sided		one sided	two sided		
1,4-Phenylene	29.5	35	41	38	47	56		
	Δ	5.5	11.5	Δ	9	18		
1,3-Phenylene	26	31	36	28.5	35	(42)		
	Δ	5	10	Δ	6.5	13.5		

Δ = difference with Standard-increment (no conjugation).

TABLE 6.22 Influence of the nature of the chain (the “environment”) on the increments of the --COO-- and --CONH-- groups

Nature of the chain	Glass transition		Melt transition	
	$Y_g(\text{--COO--})$	$Y_g(\text{--CONH--})$	$Y_m(\text{--COO--})$	$Y_m(\text{--CONH--})$
Full-Aliphatic chain (flexible)	12.5	15	25	45
Mixed aliphatic/ aromatic chain (flexible with rigid elements)	(13.5)	(21.5)	(30)	(51)
Full-aromatic chain (rigid rod)	15	30	35	60

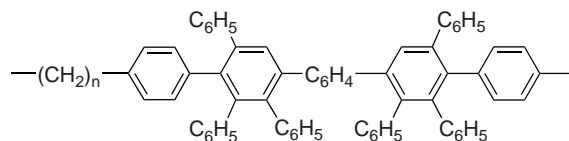
3. The “chemical nature” of the polymer chain: strictly aliphatic (and fully flexible), mixed aromatic/ aliphatic or full-aromatic; this effect is especially clear for the --COO-- and --CONH-- groups. Table 6.22 gives some data.

B. Structural isomer effects.

Similarity of influence on both Y_g and Y_m is observed for:

1. *cis*- versus *trans*-isomers. Always $Y(\text{trans}) > Y(\text{cis})$.
2. *Para/meta*-(or *tere/iso*-, or 1.4/1.3-) in phenylene groups. The magnitude of this effect depends on the extent of the π -electron conjugation of phenylene with its connected groups. Table 6.23 gives a survey of the available data.

The most striking example are two polymer series with very large conjugated aromatic systems, prepared by Stille et al. (1968). The structural unit of these polymers is the following:



where the central $\text{--C}_6\text{H}_4\text{--}$ group is *para*- or *meta*-.

The Y_g 's of the *para*-series are about 40 points higher than those of the *meta*-series. Evidently the structure of the central phenylene group in such an “extended” conjugated system determines the Y values of the whole system.

It is recommended in such a case to estimate (by means of Tables 6.7 and 6.13) first of all the value of the system with 1.4. phenylene in the centre, and to apply thereafter the following rules of thumb:

$$Y_g(1.3.\text{ext.}) = 0.9Y_g(1.4.\text{ext.}) \quad (6.A1)$$

$$Y_m(1.3.\text{ext.}) = 0.75Y_m(1.4.\text{ext.}) \quad (6.A2)$$

C. Side chain effects.

Both T_g and T_m of *comb-polymers* pass through a minimum with increasing length of the side chain, resulting in a kink in Y_g and Y_m (see Figs. 6.1 and 6.3).

TABLE 6.23 Υ_g and Υ_m values of 1.4- and 1.3-phenylene groups and of extended conjugated phenylene group systems, as a function of their size^a

Conjugated group systems	Υ_g Phenylene types 1.4 and 1.3				Υ_m Phenylene types 1.4 and 1.3			
	$\Upsilon_g(1.4.)$	$\Upsilon_g(1.3)$	$\Delta\Upsilon_g$	$\frac{\Upsilon_g(1.3)}{\Upsilon_g(1.4)}$	$\Upsilon_m(1.4.)$	$\Upsilon_m(1.3)$	$\Delta\Upsilon_m$	$\frac{\Upsilon_m(1.3)}{\Upsilon_m(1.4)}$
$-C_6H_4-$	29.5	26	3.5	0.88	38	28	10	0.74
$-OOC-C_6H_4-COO-$	62	56.5	5.5	0.91	105	85	20	0.81
$-NHOC-C_6H_4-CONH-$	83	70	13	0.85	139	100	39	0.72
	131	120	11	0.91	220	160	60	0.73
	485	445	40	0.92	—	—	—	—

^a Type 1.4 = Tere- or Para-substituted; Type 1.3 = Iso- or Meta-substituted.

D. Effects of the average molecular mass (or length).

Below a critical mass (or chain length) the transition temperatures are depressed, often according to simple rules, such as

$$T_g = T_g(\infty) - A/M_n, \quad 1/T_m = 1/T_m(\infty) + B/x_n \quad (6.A3)$$

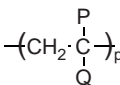
where M_n = average mol. mass; x_n = average degree of polymerisation; index(∞) = very long chain length; A and B are constants.

Differences

There are also a number of marked differences between T_g and T_m partly connected with the completely different nature of the two transitions.

These differences can best be formulated in tabular form. Table 6.24 gives the complete survey.

TABLE 6.24 Difference in behaviour between glass/rubber- and crystal/melt transition

	Quasi-second order	First order
A. Nature of transition	Influence of "history" and "age" of the glassy state	Thermodynamically strictly defined
B. Main chain effects		
1. Shape of plot Y vs N_{CH_2} (length of CH_2 sequence per structural unit)	Strictly linear (see Fig. 6.3)	Curved (see Fig. 6.7)
2. Even/odd effect	Absent	Present; see Table 6.12
3. Influence of hydrogen bond network on the CH_2 increment	Strong; ($T_g(CH_2)$ increases from 2.7 to 4.3)	Absent
4. Influence of number of functional groups per structural unit on value of CH_2 -increment	Absent	Strong; see Table 6.10
5. Influence of asymmetry within structural unit	Small	Strong; depressing influence (about -10)
C. Side group/chain effect		
1. Effect of length	T_g passes through minimum when CH_2 sequence = 9 (see Fig. 6.1)	T_m passes through minimum when CH_2 sequence = 5 (see Fig. 6.6)
2. Limiting value of CH_2 increment at high length	Abnormal; above vs $N_{CH_2} = 9$ Increment ≈ 7.5 (Fig. 6.1)	Normal; above vs $N_{CH_2} = 5$ Increment reaches normal value of 5.7 (Fig. 6.6)
3. Effect of stereoregularity of side groups, for	If P = H: T_g (atact.) $\approx T_g$ (iso) $\approx T_g$ (syndio) If P \neq Q \neq H: T_g (atact.) $\approx T_g$ (syndio) $> T_g$ (iso) $\Delta T_g \approx 100$	If P = H: T_m (iso) $> T_m$ (syndio) If P \neq Q \neq H: T_m (syndio) $> T_m$ (iso) $\Delta T_m \approx 60$
		

BIBLIOGRAPHY

General references

- Alfrey T and Gurnee EF, "Organic Polymers", Chapter 3, Prentice-Hall, Englewood Cliffs, NJ, 1967.
- Bicerano J, "Prediction of Polymer Properties", Chapter 6, Marcel Dekker, New York, 3rd Ed, 2002.
- Blumstein A (Ed), "Liquid Crystalline Order in Polymers", Academic Press, New York, 1978.
- Blumstein A (Ed), "Polymer Liquid Crystals", Plenum Press, New York, 1985.
- Boyer RF (Ed), "Transitions and Relaxations in Polymers", Interscience, New York, 1967.
- Boyer RF, "Encyclopedia of Polymer Science and Technology", Suppl No 2, pp 745–839, Wiley, New York, 1977.
- Brandrup J, Immergut EH and Grulke EA, (Eds), "Polymer Handbook", Part VII, p 291, Wiley, New York, 4th Ed, 1999.
- Brydson JA, "The Glass Transition, Melting Point and Structure", Chapter 3 in Jenkins AD, (Ed), "Polymer Science", North Holland (Elsevier), Amsterdam, 1972.
- Bueche F, "Physical Properties of Polymers" (Chapters 4, 5 and 11), Interscience, New York, 1962.
- Chapoy LL (Ed), "Recent Advances in Liquid Crystalline Polymers", Elsevier Appl Science Publisher, London, 1985.
- Ciferri A, Krigbaum WR and Meyer RB, (Eds) "Polymer Liquid Crystals", Academic Press, New York, 1982.
- Gordon M and Platé NA (Eds), "Liquid Crystal Polymers", Advances in Polymer Science 59, 60 and 61, Springer, Berlin and New York, 1984, (with important contributions of Flory PJ; Uematsu I and Y; Papkow SP; Ober CK; Jin JJ and Lenz RW; Wunderlich B and Grebowicz J; Dobb M and McIntyre JE; Finkelmann H and Rehage G; and Shibaev VP and Platé NA).
- Haward RN, "The Nature of the Glassy State in Polymers", in Ledwith A and North AN (Eds), "Molecular behaviour and development of polymeric materials, pp 404–459, Chapman and Hill, London, 1975.
- Hutchinson JM "Relaxation Processes and Physical Ageing", in Haward RN and Young RS (Eds) "The Physics of Glassy Polymers", Chapter 3, Chapman and Hall, London, 2nd Ed, 1997.
- Mandelkern L and Alamo RG, "Thermodynamic Quantities Governing Melting", in Mark, JE (Ed), "Physical Properties of Polymers Handbook", Chapter 11, AIP Press, Woodbury, NY, 1996.
- McCrumb NG, Read BE and Williams G, "Anelastic and Dielectric Effects in Polymeric Solids", Wiley, New York, 1967.
- Meares P, "Polymers; Structure and Bulk Properties", Van Nostrand, Princeton, 1965.
- Platé NA and Shibaev VP, "Comb-Shaped Polymers and Liquid Crystals", Plenum Press, New York, 1987.
- Plazek DJ and Ngai KL, "The Glass Temperature", in Mark JE (Ed), "Physical Properties of Polymers Handbook", Chapter 12, AIP Press, Woodbury, NY, 1996.
- Shen MC and Eisenberg A, "Glass Transitions in Polymers", Rubber Chem Technol 43 (1970) 95.

Special references

- Adam G and Gibbs JH, J Chem Phys 43 (1965) 139.
- Aharoni SM, Polym Adv Technol 9 (1998) 169.
- Barton JM and Lee WA, Polymer 9 (1968) 602.
- Beaman RG, J Polym Sci 9 (1953) 472.
- Becker R, Faserforschung u Textiltechnik 26 (1978) 361.
- Becker R and Raubach H, Faserforschung u Textiltechnik 26 (1975) 51.
- Berger J and Huntjens FJ, Angew Makromol Chem 76/77 (1979) 109.
- Bianchi U, J Phys Chem 69 (1965) 1497.
- Bicerano J, Sammler RL, Carriere CJ and Seitz JT, J Polym Sci, Polym Phys Ed 34 (1996) 2247.
- Boyer RF, 2nd Int Conf Phys Chem, Paris, June 6, 1952; J Appl Phys 25 (1954) 825; Rubber Chem Technol 36 (1963) 1303; Am Chem Soc Prepr 30 (1970) nr 2; Macromolecules 6 (1973) 288; J Polym Sci, Symp No 50 (1975) 189; J Macromol Sci, Phys B18 (1980) 461; Eur Polym J 17 (1981) 661; Polymer Yearbook (Pethrick RA, Ed) Vol 2, Harwood Publ, 1985, 233 Br Polym J, Dec 1982, 163; J Polym Sci B, Phys 26 (1988) 893.
- Breuer H and Rehage G, Kolloid Z 216/217 (1967) 158.
- Brügging W, Kampschulte U, Schmidt HW and Heitz W, Makromol Chem 189 (1988) 2755.
- Bunn CW, Chapter 12 in "Fibres from synthetic Polymers" (Hill R, Ed) Elsevier Sci Publisher, Amsterdam, 1953.
- Cowie JMC and Toporowski PM, Eur Polym J 4 (1968) 621.
- Ehrenfest P, Proc Kon Akad Wetensch, Amsterdam, 36 (1933) 153.
- Flory FJ, "Principles of Polymer Chemistry," Cornell Univ Press first pr, 1953, 10th pr, 1978, pp 568–571.
- Fox TG and Flory FJ, J Appl Phys 21 (1950) 581.
- Fox TG and Loshaek S, J Polym Sci 15 (1955) 371.
- Franse MWCP, Doctoral Thesis, Delft, The Netherlands, 2002.
- Franse MWCP, Te Nijenhuis K, Groenewold J and Picken SJ, Macromolecules 37 (2004) 7839.
- Gee G, Polymer 7 (1966) 177.
- Gibbs JH and Di Marzio EA, J Chem Phys 28 (1958) 373; Ibid 28 (1958), 807; J Polym Sci 40 (1959) 121.
- Hayes RA, J Appl Polym Sci 5 (1961) 318.
- Heinze HD, Schmieder K, Schnell G and Wolf KA, Kautchuk u Gummi, 14 (1961) 208;
- Rubber Chem Technol 35 (1961) 776.

- Jansen JC, Doctoral Thesis, Delft, The Netherlands, 1996.
- Karasz FE and Mac Knight WJ, *Macromolecules* 1 (1968) 537.
- Kauzmann W, *Chem Rev* 43 (1948) 219.
- Kelley FN and Bueche F, *J Polym Sci* 50 (1961) 549.
- Kovacs AJ, *Adv Polym Sci*, 3 (1963) 394.
- Kreibich UT and Batzer H, *Angew Makromol Chem* 83 (1979) 57 and 105 (1982) 113.
- Lee WA, *J Polym Sci A-2*, 8 (1970) 555.
- Lee WA and Knight GJ, *Br Polym J* 2 (1970) 73.
- Lenz RW, *Faraday Disc Roy Soc No* 79 (1985) 21.
- Loshaek S, *J Polym Sci* 15 (1955) 391.
- Marcinčin CT and Romanov A, *Polymer* 16 (1975) 173, 177.
- Meurisse P, Noël C, Monnerie L, Fayolle B, *Br Polym J* 13 (1981) 55.
- Moynihan CT et al, *J Phys Chem* 78 (1974) 2673 and *J Am Ceram Soc* 59 (1976) 12, 16.
- Ngai KL, "The Glass Transition and the Glassy State" in Mark JE Ngai KL, Graessley WW, Samulski ET, Koenig JL and Mandelkern L, "Physical Properties of Polymers", Cambridge University Press, 3rd Ed, 2004.
- Nielsen LE, *J Macromol Sci*, Part C3 (1969) 69.
- Reck B and Ringsdorf H, *Makromol Chem, Rapid Comm* 6 (1985) 291.
- Rehage G, *Ber Bunsenges* 74 (1970) 796.
- Rehage G, *J Macromol Sci B* 18 (1980) 423.
- Rehage G and Borchard W, in Haward R (Ed), "The Physics of Glassy Polymers", Chapter 1, Applied Science Publishers, London, 1973.
- Ringsdorf H and Zentel R, *Makromol Chem* 183 (1982) 1245.
- Ringsdorf H and Schneller A, *Br Polym J* 13 (1981) 43.
- Simon FE, *Ergebn Exakte Naturwiss* 9 (1930) 244.
- Staverman AJ, *Rheol Acta* 5 (1966) 283.
- Stille JK, Rakutis RO, Mukamal H and Harris FW, *Macromolecules* 1 (1968) 431.
- Struik LCE, "Physical Aging in Amorphous Polymers and Other Materials", p 26, Elsevier, Amsterdam/London/New York, 1978.
- Ueberreiter K and Kanig G, *J Chem Phys* 18 (1950) 399.
- Van Krevelen DW and Hoftyzer PJ, (1975), unpublished.
- Vijayakumar CT and Kothandaraman H, *Thermochim Acta* 118 (1987) 159.
- Volkenshtein MV and Ptitsyn OB, *Sov Phys-Tekhn Phys* 1 (1957) 2138.
- Weyland HG, Hoftyzer PJ and Van Krevelen DW, *Polymer* 11 (1970) 79.
- Wolstenholme AJ, *J Polym Eng Sci* 8 (1968) 142.
- Wunderlich B et al, *J Polym Sci C* 6 (1963) 173; *J Appl Phys* 35 (1964) 95; *Adv Polym Sci* 7 (1970) 151; *J Polym Sci A2* 9 (1971) 1887 and *A2* 12 (1974) 2473.
- Wunderlich B and Grebowicz J, *Adv Polym Sci* 60/61 (1984) 1–59.
- Zoller P, Starkweather H, and Jones G, *J Polym Sci Phys Ed* 16 (1978) 1261; 20 (1982) 1453; 26 (1988) 257; 27 (1989) 993.

CHAPTER 7

Cohesive Properties and Solubility

A quantitative measure of the cohesive properties of a substance is the *cohesive energy*. The cohesive energy per unit of volume is called *cohesive energy density*. The latter is closely related to the *internal pressure*, a quantity appearing in the equation of state.

The square root of cohesive energy density is called *solubility parameter*. It is widely used for correlating polymer solvent interactions. As a refinement, three solubility parameter components can be distinguished, representing dispersion, polar, and hydrogen bond interactions.

Although rigorous additivity rules are not applicable in this case, a fair estimation of the cohesive energy and the solubility parameter of polymers can be made by group contribution methods.

7.1. INTRODUCTION

The cohesive properties of a polymer find direct expression in its solubility in organic liquids. The cohesive properties of a substance are expressed quantitatively in the cohesive energy. This quantity is closely related to the internal pressure, a parameter appearing in the equation of state of the substance.

As early as 1916 Hildebrand pointed out that the order of solubility of a given solute in a series of solvents is determined by the internal pressures of the solvents. Later Scatchard (1931) introduced the concept of "*cohesive energy density*" into Hildebrand's theories, identifying this quantity with the cohesive energy per unit volume. Finally Hildebrand (1936) gave a comprehensive treatment of this concept and proposed the square root of the cohesive energy density as a parameter identifying the behaviour of specific solvents. In 1949 he proposed the term solubility parameter and the symbol δ .

The solubility of a given polymer in various solvents is largely determined by its chemical structure. As a general rule, structural similarity favours solubility. In terms of the above-mentioned quantities this means that the solubility of a given polymer in a given solvent is favoured if the solubility parameters of polymer and solvent are equal. The solubility parameter of the polymer is always defined as the square root of the cohesive energy density in the amorphous state at room temperature. The greater part of this chapter will be devoted to the cohesive energy and the solubility parameter, and to the correlation of these quantities with chemical structure.

Besides the chemical structure, also the physical state of a polymer is important for its solubility properties. Crystalline polymers are relatively insoluble and often dissolve only at temperatures slightly below their crystalline melting points.

As a general rule, the solubility decreases as the molar mass of the solute increases. This property can be used to fractionate polymers according to molar mass.

7.2. COHESIVE ENERGY

7.2.1. Definitions

The cohesive energy E_{coh} of a substance in a condensed state is defined as the increase in internal energy U per mole of substance if all the intermolecular forces are eliminated: The cohesive energy $\equiv E_{coh} = \Delta U$ (dimension: J/mol).

Directly related to the cohesive energy are the quantities

$$\text{Cohesive energy density: } e_{coh} \equiv \frac{E_{coh}}{V} \text{ (at 298 K) in: J/cm}^3 \text{ or MJ/m}^3 \text{ or MPa}$$

$$\text{Solubility parameter } \delta = \left(\frac{E_{coh}}{V} \right)^{1/2} \equiv e_{coh}^{1/2} \text{ (at 298 K) in } (\text{J/cm}^3)^{1/2} \text{ or } (\text{MJ/m}^3)^{1/2} \text{ or MPa}^{1/2}$$

7.2.1.1. Determination of e_{coh}

For liquids of low molar weight, the cohesive energy is closely related to the molar heat of evaporation ΔH_{vap} (at a given temperature):

$$E_{coh} = \Delta U_{vap} = \Delta H_{vap} - p\Delta V \approx \Delta H_{vap} - RT \quad (7.1)$$

Therefore, for low-molar-mass substances E_{coh} can easily be calculated from the heat of evaporation or from the course of the vapour pressure as a function of temperature. As polymers cannot be evaporated, indirect methods have to be used for the determination of their cohesive energy, e.g. comparative swelling or dissolving experiments in liquids of known cohesive energy density. The method is illustrated in Fig. 7.1.

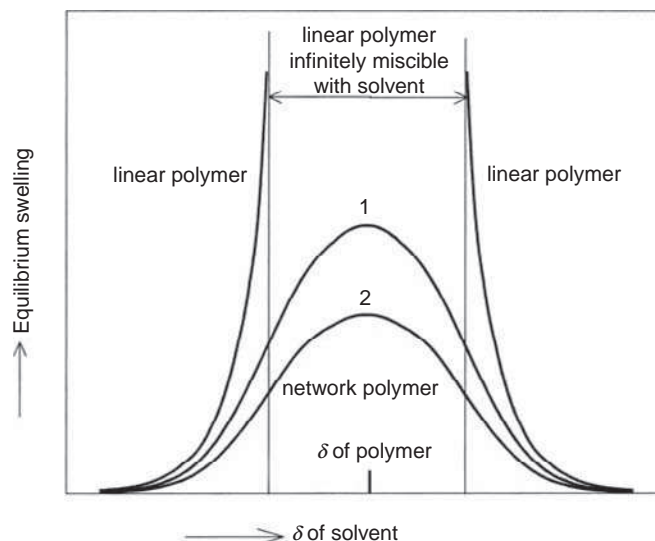


FIG. 7.1 Equilibrium swelling as a function of the solubility parameter of the solvent for linear and cross-linked polymer. The cross-link density of 2 is larger than that of 1.

7.2.2. Prediction of the cohesive energy by means of additive functions

For a prediction of the cohesive energy of substances some group additivity methods have been developed. For substances of low molar weight, E_{coh} , was considered as an additive property many years ago by Dunkel (1928), who derived group contributions for the cohesive energy of liquids at room temperature. Rheineck and Lin (1968), however, found that for homologous series of low-molar-weight liquids, the contribution to the cohesive energy of a methylene group was not constant, but depended on the value of other structural groups in the molecule.

Hayes (1961), Di Benedetto (1963), Hoftyzer and Van Krevelen (1970) and Fedors (1974) have applied Dunkel's original method to polymers.

Bunn (1955) dealt with the cohesive energy at the boiling point, while Bondi (1964, 1968) investigated the cohesive energy properties at 0 K (H^o).

Table 7.1 gives a survey of the contributions of the most important structural groups to E_{coh} (Values between brackets are not given as such in the literature but have been calculated by addition and subtraction).¹

The values given by the different authors show a rough correspondence. Since the cohesive energy will decrease with increasing temperature, the following rule is obeyed in general, as could be expected:

$$H^o > E_{coh}(298) > E_{coh}(T_b)$$

When applied to low-molecular substances, the values of Bunn proved to give by far the best prediction of the cohesive energy. But they can only be applied to substances at the boiling point, so that these values have no direct significance for the cohesive energy of polymers. A good correlation is obtained by the method of Rheineck and Lin, but the disadvantage of their system is that many corrections due to vicinal groups have to be applied. The systems of Di Benedetto and Hayes have the restriction that only values for a limited number of groups are given by these authors.

Although the work of Rheineck and Lin showed that the additivity principle does not apply exactly to the cohesive energy at room temperature, a reasonably good prediction of the cohesive energy of polymers can nevertheless be obtained by this method. The values to be used for the group contributions need not be identical, however, with those for low-molar-weight compounds. Hoftyzer and Van Krevelen (1970) showed that from the available E_{coh} -data on polymers a new set of group contribution values could be obtained that gives the best possible correlation with all available data. Updated values are mentioned in Table 7.1.

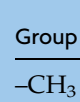
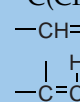
Earlier, Small (1953) had demonstrated that the combination $(E_{coh}/V(298))^{1/2} = F$, the *molar attraction constant*, is a useful additive quantity for low-molecular as well as for high-molecular substances. His set of values is very frequently applied. Accordingly, the corresponding solubility parameter is $\delta_{Small} = F/V$. Later Hoy (1970) proposed group contributions to F , slightly different from those of Small.

Van Krevelen (1965) derived a set of atomic contributions to calculate F . Via F it is possible to derive in an indirect way the value of E_{coh} for polymers. The group contributions to F , proposed by Small, Hoy and Van Krevelen, are mentioned in Table 7.2.

The system of group contributions published by Fedors (1974) gives a less accurate prediction of E_{coh} . As Fedors calculated contributions to E_{coh} for a great number of structural groups, however, these data together with Fedors' group contributions to the

¹ The values in the literature are normally based on the calorie as unit of energy; here (as a matter of system) the Joule is used as unit of energy.

TABLE 7.1 Group contributions to E_{coh} (J/mol)

Group	H_o^o Bondi	E_{coh} (298)					$E_{coh}(T_b)$ Bunn	E_{coh} (298) Hoftzyer and Van Krevelen
		Rheineck and Lin	Dunkel	Di Benedetto	Hayes	Fedors		
-CH ₃	10,560	4150	7460		—	4710	7120	9640
-CH ₂ -	6350	5150	4150	3600	4150	4940	2850	4190
	(-270)	4060	-1590	—	—	3430	(-1840)	420
>C<	(-8000)	—	(-7340)	—	—	1470	(-6280)	-5580
-CH(CH ₃)-	(10,290)	(8210)	(5870)	—	7120	(8140)	5700	(10,060)
-C(CH ₃) ₂ -	(13,120)	—	7580	10,390	11,900	(10,890)	7960	(13,700)
-CH=CH-	—	—	8300	7210	7500	(8620)	7120	10,200
	—	—	(2560)	—	—	(8620)	(2940)	4860
-C(CH ₃)=CH-	—	—	10,020	10,900	11,480	(13,330)	10,060	(14,500)
cyclopentyl	33,770	—	—	—	—	(24,240)	—	—
cyclohexyl	38,210	29,500	—	—	—	(29,180)	—	—
phenyl	41,060	31,220	30,920	—	—	31,940	22,630	31,000
p-phenylene	35,950	—	—	—	23,880	31,940	16,340	25,140
-F	—	—	8630	—	—	4190	(4730)	4470
-Cl	—	11,690	14,250	—	—	11,550	11,730	12,990
-Br	—	—	—	—	—	15,490	12,990	15,500

-I	-	-	-	-	-	19,050	17,600	-
-CN	-	-	-	-	-	25,530	-	25,000
-CHCN-	-	-	-	-	24,130	28,960	-	25,420
-OH	-	32,810	30,380	-	-	29,800	24,300	-
-O-	-	-	6830	-	6830	3350	4190	6290
-CO-	-	-	17,890	-	-	17,370	11,150	-
-COOH	-	32,810	37,580	-	-	27,630	23,460	-
-COO-	-	(19,530)	(16,010)	-	14,160	18,000	12,150	3410
$\begin{array}{c} \text{O} \\ \parallel \\ -\text{O}-\text{C}-\text{O}- \end{array}$	-	-	-	-	-	17,580	-	-
$\begin{array}{c} \text{O} \quad \text{O} \\ \parallel \quad \parallel \\ -\text{C}-\text{O}-\text{C}- \end{array}$	-	-	-	-	-	30,560	16,340	-
$\begin{array}{c} \text{O} \quad \text{H} \\ \parallel \quad \\ -\text{C}-\text{N}- \end{array}$	-	-	67,880	-	44,750	33,490	35,620	60,760
$\begin{array}{c} \text{O} \quad \text{H} \\ \parallel \quad \\ -\text{O}-\text{C}-\text{N}- \end{array}$	-	-	-	-	26,310	26,370	36,620	-
-S-	-	-	-	-	-	14,150	9220	8800

TABLE 7.2 Group contributions to F

Group	Small	Van Krevelen	Hoy ^a
$-\text{CH}_3$	438	420	303.4
$-\text{CH}_2-$	272	280	269.0
$\begin{array}{c} \text{H} \\ \\ -\text{C}- \\ \\ \end{array}$	57	140	176.0
$\begin{array}{c} \\ -\text{C}- \\ \\ \end{array}$	-190	0	65.5
$-\text{CH}(\text{CH}_3)-$	495	560	(479.4)
$-\text{C}(\text{CH}_3)_2-$	686	840	(672.3)
$-\text{CH}=\text{CH}-$	454	444	497.4
$\begin{array}{c} \quad \text{H} \\ -\text{C}=\text{C}- \\ \quad \end{array}$	266	304	421.5
$-\text{C}(\text{CH}_3)=\text{CH}-$	(704)	724	(724.9)
cyclopentyl	-	1384	1295.1
cyclohexyl	-	1664	1473.3
phenyl	1504	1517	1398.4
p-phenylene	1346	1377	1442.2
$-\text{F}$	(250)	164	84.5
$-\text{Cl}$	552	471	419.6
$-\text{Br}$	696	614	527.7
$-\text{I}$	870	-	-
$-\text{CN}$	839	982	725.5
$-\text{CHCN}-$	(896)	1122	(901.5)
$-\text{OH}$	-	754	462.0
$-\text{O}-$	143	256	235.3
$-\text{CO}-$	563	685	538.1
$-\text{COOH}$	-	652	(1000.1)
$-\text{COO}-$	634	512	668.2
$\begin{array}{c} \text{O} \\ \parallel \\ -\text{O}-\text{C}-\text{O}- \end{array}$	-	767	(903.5)
$\begin{array}{c} \text{O} \quad \text{O} \\ \parallel \quad \parallel \\ -\text{C}-\text{O}-\text{C}- \end{array}$	-	767	1160.7
$\begin{array}{c} \text{O} \quad \text{H} \\ \parallel \quad \\ -\text{C}-\text{N}- \\ \\ \end{array}$	-	1228	(906.4)
$\begin{array}{c} \text{O} \quad \text{H} \\ \parallel \quad \\ -\text{O}-\text{C}-\text{N}- \\ \\ \end{array}$	-	1483	(1036.5)
$-\text{S}-$	460	460	428.4

^a In the list of Hoy a "base value" has to be added in the summation of increments, viz. 277.0, if the system is used for small molecules, e.g. monomers or solvent molecules (correction for terminal end groups).

molar volume V are reproduced in Table 7.3. Values of E_{coh} for a series of 41 polymers, calculated by different methods are presented in Table 7.4, in comparison with the experimental data. The experimental data of E_{coh} for some polymers show large variations and the predicted values according to each of the methods mentioned in Table 7.4 fall within the experimental limits of accuracy. There is some evidence, however, that the

TABLE 7.3 Group contributions to E_{coh} and V according to Fedors

Group	E_{coh} (J/mol)	V (cm ³ /mol)
-CH ₃	4710	33.5
-CH ₂ -	4940	16.1
>CH-	3430	-1.0
>C<	1470	-19.2
=CH ₂	4310	28.5
=CH-	4310	13.5
>C=	4310	-5.5
-HC≡	3850	27.4
-C≡	7070	6.5
Phenyl	31,940	71.4
Phenylene (o, m, p)	31,940	52.4
Phenyl (trisubstituted)	31,940	33.4
Phenyl (tetrasubstituted)	31,940	14.4
Phenyl (pentasubstituted)	31,940	-4.6
Phenyl (hexasubstituted)	31,940	-23.6
Ring closure 5 or more atoms	1050	16.0
Ring closure 3 or 4 atoms	3140	18.0
Conjugation in ring for each double bond	1670	-2.2
Halogen attached to carbon atom with double bond	-20% of E_{coh} of halogen	4.0
-F	4190	18.0
-F (disubstituted)	3560	20.0
-F (trisubstituted)	2300	22.0
-CF ₂ - (for perfluoro compounds)	4270	23.0
-CF ₃ (for perfluoro compounds)	4270	57.5
-Cl	11,550	24.0
-Cl (disubstituted)	9630	26.0
-Cl (trisubstituted)	7530	27.3
-Br	15,490	30.0
-Br (disubstituted)	12,350	31.0
-Br (trisubstituted)	10,670	32.4
-I	19,050	31.5
-I (disubstituted)	16,740	33.5
-I (trisubstituted)	16,330	37.0
-CN	25,530	24.0
-OH	29,800	10.0
-OH (disubstituted or on adjacent C atoms)	21,850	13.0
-O-	3350	3.8
-CHO (aldehyde)	21,350	22.3
-CO-	17,370	10.8
-COOH	27,630	28.5
-CO ₂ -	18,000	18.0

(continued)

TABLE 7.3 (*continued*)

Group	E_{coh} (J/mol)	V (cm ³ /mol)
-CO ₃ - (carbonate)	17,580	22.0
-C ₂ O ₃ - (anhydride)	30,560	30.0
-HCOO- (formate)	18,000	32.5
-CO ₂ CO ₂ - (oxalate)	26,790	37.3
-HCO ₃	12,560	18.0
-COF	13,400	29.0
-COCl	17,580	38.1
-COBr	24,150	41.6
-COI	29,300	48.7
-NH ₂	12,560	19.2
-NH-	8370	4.5
-N<	4190	-9.0
-N=	11,720	5.0
-NHNH ₂	21,980	-
>NNH ₂	16,740	16
>NHNH<	16,740	16
-N ₂ (diazo)	8370	23
-N=N-	4190	-
>C=N-N=C<	20,090	0
-N=C=N-	11,470	-
-N=C	18,840	23.1
-NF ₂	7660	33.1
-NF-	5070	24.5
-CONH ₂	41,860	17.5
-CONH-	33,490	9.5
-CON<	29,510	-7.7
HCON<	27,630	11.3
HCONH-	43,950	27.0
-NHCOO-	26,370	18.5
-NHCONH-	50,230	-
-NHCON<	41,860	-
>NCON<	20,930	-14.5
NH ₂ COO-	37,000	-
-NCO	28,460	35.0
-ONH ₂	19,050	20.0
>C=NOH	25,120	11.3
-CH=NOH	25,120	24.0
-NO ₂ (aliphatic)	29,300	24.0
-NO ₂ (aromatic)	15,360	32.0
-NO ₃	20,930	33.5
-NO ₂ (nitrite)	11,720	33.5

(continued)

TABLE 7.3 (*continued*)

Group	E_{coh} (J/mol)	V (cm ³ /mol)
-NH NO ₂	39,770	28.7
-NNO-	27,210	10
-SH	14,440	28.0
-S-	14,150	12
-S ₂ -	23,860	23.0
-S ₃ -	13,400	47.2
>SO	39,140	—
-SO ₃	18,840	27.6
-SO ₄	28,460	31.6
-SO ₂ Cl	37,070	43.5
-SCN	20,090	37.0
-NCS	25,120	40.0
P	9420	-1.0
-PO ₃	14,230	22.7
-PO ₄	20,930	28.0
-PO ₃ (OH)	31,810	32.2
Si	3390	0
SiO ₄	21,770	20.0
B	13,810	-2.0
BO ₃	0	20.4
Al	13,810	-2.0
Ga	13,810	-2.0
In	13,810	-2.0
Tl	13,810	-2.0
Ge	8080	-1.5
Sn	11,300	1.5
Pb	17,160	2.5
As	12,980	7.0
Sb	16,330	8.9
Bi	21,350	9.5
Se	17,160	16.0
Te	20,090	17.4
Zn	14,480	2.5
Cd	17,790	6.5
Hg	22,810	7.5

lower limits of the experimental values are often more reliable. If this effect is taken into account, the methods of Hayes, Small, Hoy, and Hoftyzer and Van Krevelen are superior to the other methods and each of them predicts the cohesive energy with a mean accuracy of about 10%.

TABLE 7.4 Cohesive energy of polymers

Polymer							E_{coh} (calculated) (J/mol)					Hoftyzer and Van Krevelen	
	δ (J ^{1/2} /cm ^{3/2})	V (cm ³ / mol)	E_{coh} (from δ) (J/mol)		Dunkel	Di Benedetto	Hayes	Fedors	Small	Van Krevelen	Hoy		
	From	To	From	To									
Polyethylene	15.8	17.1	32.9	8200	9600	8300	7200	8300	9880	9000	9500	8800	8380
Polypropylene	16.8	18.8	49.1	13,900	17,400	10,020	—	11,270	13,080	12,000	14,400	11,400	14,250
Polyisobutylene	16.0	16.6	66.8	17,100	18,400	11,730	13,990	16,050	15,830	13,700	18,800	13,300	17,890
Polystyrene	17.4	19.0	98.0	29,700	35,400	33,480	41,060	34,270	40,310	34,300	38,300	34,700	35,610
Poly(vinyl chloride)	19.2	22.1	45.2	16,700	22,100	16,810	16,930	21,660	19,920	17,200	17,600	16,500	17,600
Poly(vinyl bromide)	19.4	—	48.6	18,300	—	—	—	—	23,860	21,600	22,000	19,500	20,110
Poly(vinylidene chloride)	20.3	25.0	58.0	23,900	36,300	25,310	—	15,460	25,670	24,300	25,700	23,800	24,590
Poly(tetrafluoroethylene)	12.7	—	49.5	8000	—	19,840	—	9640	17,180	7800	8700	4400	6720
Poly (chlorotrifluoroethylene)	14.7	16.2	61.8	13,400	16,200	25,460	—	—	23,250	13,800	15,000	10,500	15,240
Poly(vinyl alcohol)	25.8	29.1	35.0	23,300	29,600	32,940	—	—	38,170	—	39,400	23,500	—
Poly(vinyl acetate)	19.1	22.6	72.2	26,300	36,900	26,030	28,990	25,430	31,080	27,200	25,300	27,800	27,660
Poly(vinyl propionate)	18.0	—	90.2	29,200	—	30,180	32,590	29,580	36,020	31,000	29,500	31,500	31,850
Poly(methyl acrylate)	19.9	21.3	70.1	27,800	31,800	26,030	28,990	25,430	31,080	28,000	26,100	28,600	27,660
Poly(ethyl acrylate)	18.8	19.2	86.6	30,600	31,900	30,180	32,590	29,580	36,020	32,300	30,800	32,800	31,850
Poly(propyl acrylate)	18.5	—	103.1	35,300	—	34,330	36,190	33,730	40,960	36,700	35,500	37,000	36,040
Poly(butyl acrylate)	18.0	18.6	119.5	38,700	41,300	38,480	39,790	37,880	45,900	41,100	40,200	41,400	40,230
Poly(isobutyl acrylate)	17.8	22.5	119.3	37,800	60,400	36,050	—	36,700	44,160	39,400	40,300	39,300	41,910
Poly(2,2,3,3,4,4,4- heptafluorobutyl acrylate)	13.7	—	148.0	27,800	—	61,110	—	—	56,860	39,400	37,600	31,800	36,760

Poly(methyl methacrylate)	18.6	26.2	86.5	29,900	59,400	27,740	–	30,210	33,830	29,300	30,800	29,900	31,300
Poly(ethyl methacrylate)	18.2	18.7	102.4	33,900	35,800	31,890	–	34,360	38,770	33,900	35,700	34,500	35,490
Poly(butyl methacrylate)	17.8	18.4	137.2	43,500	46,500	40,190	–	42,660	48,650	42,300	44,500	42,600	43,870
Poly(isobutyl methacrylate)	16.8	21.5	135.7	38,300	62,700	37,760	–	41,480	46,910	41,000	45,000	41,000	45,550
Poly(tert.-butyl methacrylate)	17.0	–	138.9	40,100	–	35,320	–	42,110	44,720	37,400	44,000	37,500	45,000
Poly(benzyl methacrylate)	20.1	20.5	151.2	61,100	63,500	55,350	–	–	66,000	56,500	59,600	58,200	56,850
Poly(ethoxyethyl methacrylate)	18.4	20.3	145.6	49,300	60,000	47,020	–	49,490	52,000	44,700	51,100	48,300	50,160
Polyacrylonitrile	25.6	31.5	44.8	29,400	44,500	–	–	28,280	33,900	30,500	43,900	30,600	29,610
Polymethacrylonitrile	21.9	–	63.9	30,600	–	–	–	–	36,650	28,900	44,300	29,100	33,250
Poly(α -cyanomethyl acrylate)	28.7	29.7	82.1	67,600	72,400	–	–	–	54,650	48,400	58,600	50,300	46,660
Polybutadiene	16.6	17.6	60.7	16,700	18,800	16,600	14,410	15,800	18,500	16,400	16,600	17,700	18,580
Polyisoprene	16.2	20.5	75.7	19,900	31,800	18,320	18,100	19,780	23,210	20,600	21,800	21,100	22,880
Polychloroprene	16.8	18.9	71.3	20,100	25,500	25,110	20,950	20,910	30,050	26,600	25,000	26,700	26,230
Polyformaldehyde	20.9	22.5	25.0	10,900	12,700	10,980	–	10,980	8290	6900	11,500	10,200	10,480
Poly(tetramethylene oxide)	17.0	17.5	74.3	21,500	22,800	23,430	–	23,430	23,110	20,400	25,500	23,100	23,050
Poly(propylene oxide)	15.4	20.3	57.6	13,700	23,700	16,850	–	18,110	16,430	14,400	20,900	16,800	20,540
Polyepichlorohydrin	19.2	–	69.7	25,700	–	27,790	–	–	28,210	24,100	29,200	26,900	28,080
Poly(ethylene sulphide)	18.4	19.2	47.9	16,200	17,700	–	–	–	24,030	21,000	21,700	19,500	17,180
Poly(styrene sulphide)	19.0	–	115.8	41,800	–	–	–	–	54,460	45,400	49,600	44,600	44,410
Poly(ethylene terephthalate)	19.9	21.9	143.2	56,700	68,700	–	–	60,500	77,820	69,600	61,200	76,800	60,340
Poly(8-aminocaprylic acid)	26.0	–	135.9	91,900	–	96,930	–	73,800	68,070	–	74,800	57,100	90,090
Poly(hexamethylene adipamide)	27.8	–	208.3	161,000	–	177,260	–	131,000	116,380	–	132,600	97,300	163,420

Conversion factors: $1 \text{ J}^{1/2}/\text{cm}^{3/2} = 0.49 \text{ cal}^{1/2}/\text{cm}^{3/2}$; $1 \text{ cm}^3/\text{mol} = 10^{-6}\text{m}^3/\text{mol}$; $1 \text{ J/mol} = 0.24 \text{ cal/mol}$

Example 7.1

Estimate the cohesive energy and the solubility parameter of benzene (at 20°C)

$$\mathbf{M} = 78.1 \text{ g/mol}, \rho = 0.879 \text{ g/cm}^3, \Delta H_{\text{vap}} = 3.41 \times 10^4 \text{ J/mol}$$

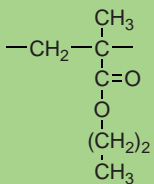
Solution

Substitution in Eq. (7.1) yields: $E_{\text{coh}} = 3.41 \times 10^4 - 8.314 \times 293.15 = 3.16 \times 10^4 \text{ J/mol}$. The correction term for the molar volume of liquid benzene is negligible with respect to the molar gas volume: $22.4 \times 10^{-3} \text{ m}^3/\text{mol}$ vs. $8.9 \times 10^{-5} \text{ m}^3/\text{mol}$.

The solubility parameter is $\delta^2 = E_{\text{coh}}/V = 3.16 \times 10^4 / (78.1/0.879) = 356 \text{ J/cm}^3 = 356 \text{ MJ/m}^3$, so that $\delta = 18.9 (\text{MJ/m}^3)^{1/2}$, in agreement with $\delta = 18.5$ – 18.8 in Table IV of Part VII.

Example 7.2

Estimate the cohesive energy of poly(butyl methacrylate); its structural unit is:



$$\mathbf{M} = 142.2 \text{ g/mol}, \rho_a = 1.045 \text{ g/cm}^3, V_a = 136 \text{ cm}^3/\text{mol}$$

- (a) with the aid of the group contributions proposed in this chapter (H. and V.Kr.)
- (b) according to Small's method

Solution

Addition of group contributions to be found in Tables 7.1 and 7.2 gives the following result:

Groups	ΣE_i	ΣF_i
4 $-\text{CH}_2-$	16,760	1088
2 $-\text{CH}_3$	19,280	876
1 $>\text{C}<$	-5580	-190
1 $-\text{COO}-$	13,410	634
	$E_{\text{coh}} = 43,870$	$F = 2408$

- (a) The direct method gives $E_{\text{coh}} = 43,870 \text{ J/mol}$ unit
- (b) Small's method leads to: $E_{\text{coh}} = F^2/V = 42700 \text{ J/mol}$ unit

Experimental values of the solubility parameter δ range from 17.8 to 18.4. This corresponds to values of $E_{\text{coh}} = \delta^2 V$ from 43,100 to 46,000 J/mol.

The cohesive energy is an important quantity for characterizing the physical state of a given polymer. It is related to other polymer properties for which cohesive forces are important, as will be discussed in other chapters. The cohesive energy has found its most important applications, however, in the interactions between polymers and solvents. For this purpose the solubility parameter δ is generally used. Therefore the greater part of this chapter will be devoted to properties and applications of the solubility parameter.

7.3. SOLUBILITY

7.3.1. The solubility, parameter

At first sight it is rather unpractical to use a quantity δ with dimension $J^{1/2}/cm^{3/2}$ instead of the cohesive energy. The definition of δ is based, however, on thermodynamic considerations, as will be discussed below. In the course of time the values of δ , expressed in $cal^{1/2}/cm^{3/2}$ have become familiar quantities to many investigators. In this connection the change to SI units has some disadvantages. Conversion of $(cal/cm^3)^{1/2}$ into $(J/cm^3)^{1/2}$ or $(MJ/m^3)^{1/2}$ or $MPa^{1/2}$ is simple, however, as it only requires multiplication by a factor of 2 (2.045 to be exact).

The thermodynamic criteria of solubility are based on the free energy of mixing ΔG_M . Two substances are mutually soluble if, at least, ΔG_M is negative. By definition,

$$\Delta G_M = \Delta H_M - T\Delta S_M \quad (7.2)$$

where ΔH_M is enthalpy mixing; ΔS_M is entropy of mixing.

As ΔS_M is generally positive, there is a certain limiting positive value of ΔH_M below which dissolution is possible.

As early as 1916 Hildebrand tried to correlate solubility with the cohesive properties of the solvents. In 1949 he proposed the term solubility parameter and the symbol δ , as defined in the beginning of this chapter. According to Hildebrand, the enthalpy of mixing can be calculated by

$$\Delta h_M = \frac{\Delta H_M}{V_S} = \varphi_1 \varphi_2 (\delta_1 - \delta_2)^2 \quad (7.3)$$

where Δh_M = enthalpy of mixing per unit volume; φ_1 and φ_2 = volume fractions of components 1 and 2; δ_1 and δ_2 = solubility parameters of components 1 and 2.

On the other hand, the Flory-Huggins lattice theory (Flory, 1953) predicts for polymer solutions:

$$\Delta G_M = \Delta H_M - T\Delta S_M = nRT \left[\frac{\varphi}{x} \ln \varphi + (1 - \varphi) \ln (1 - \varphi) + \chi \varphi (1 - \varphi) \right] \quad (7.4)$$

with

$$\Delta H_M = nRT \chi \varphi_1 \varphi_2 = nRT \chi \varphi (1 - \varphi) \quad (7.5)$$

and

$$T\Delta S_M = nRT \left[\frac{\varphi}{x} \ln \varphi + (1 - \varphi) \ln (1 - \varphi) \right] \quad (7.6)$$

where n = number of lattice moles (i.e. $n_{\text{solvent}} + n_{\text{monomeric units}}$); $\varphi = \varphi_2$ = volume fraction of polymer; $1 - \varphi = \varphi_1$ = volume fraction of solvent; x = degree of polymerisation; χ = the so-called Flory Huggins interaction parameter.

Dissolution of high molar weight polymers in a solvent is only possible for $\chi \leq 0.5$ and molecular mixing of low molar weight liquids for $\chi \leq 2$. In Fig. 7.2 $\Delta G_M/(nRT)$ for is shown

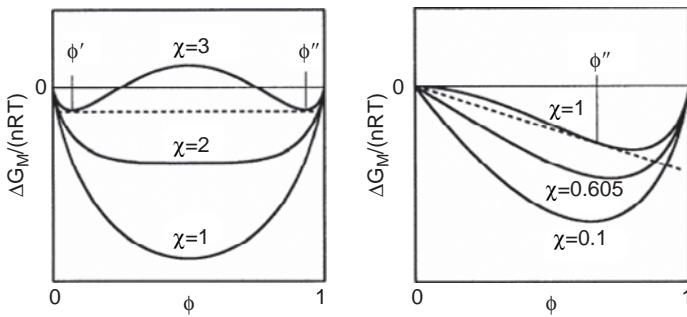


FIG. 7.2 Reduced Gibbs' energy for a solution of a low molecular weight solute ($x = 1$) for various values of χ (left) and for a solution of a polymer with a degree of polymerisation $x = 100$ for various values of χ (right). For $x = 1$ and 100 $\chi_{\text{crit}} = 2$ and 0.605, respectively.

for low-molar weight solvents (left) and for a solution of a polymer with a degree of polymerisation of 100 (right). According to thermodynamics phase separation occurs if it is possible to construct a straight line with two tangent points at the ΔG_M curve. In Fig. 7.2-left this is the case for $\chi = 3$ at φ' and φ'' and accordingly phase separation takes place in the region $\varphi' < \varphi < \varphi''$. For polymer solutions the value of φ' is extremely small, (e.g. $<<10^{-20}$), so that phase separation occurs in such a way that only an extremely low concentrated polymer solution (i.e. practically pure solvent) coexists with a polymer that is swollen with solvent (φ''), as shown in Fig. 7.2-right. The critical value of χ , below which no phase separation occurs, is given by:

$$\chi_{\text{crit}} = \frac{1}{2} + \frac{1}{\sqrt{x}} + \frac{1}{2x} \quad (7.7)$$

and the critical value of φ , where φ' and φ'' coincide

$$\varphi_{\text{crit}} = \frac{1}{1 + \sqrt{x}} \quad (7.8)$$

Critical values χ and ϕ are shown in Table 7.5 for various degrees of polymerisation, x . It follows that for high molar weight polymer χ_{crit} and φ_{crit} tend to 0.5 and 0, respectively. In general χ -parameters are determined from swelling experiments of cross-linked, i.e. non-soluble, polymers.

The concentration and temperature dependence of χ is

$$\chi = \left[d_0 + \frac{d_1}{T} + d_2 \ln(T) + d_3 T \right] \left[1 + b_1(1 - \varphi) + b_2(1 - \varphi)^2 \right] \quad (7.9)$$

where d_0 , d_1 , d_2 , d_3 , b_1 and b_2 are fitting parameters (Bicerano, 2002 and Qian et al., 1991).

Comprehensive tables of Flory–Huggins interaction parameters and their concentration and temperature dependences have been published, e.g. by Schuld and Wolf (1999) and by Orwoll and Arnold (1996).

TABLE 7.5 Critical values of φ and χ

x	1	10	100	1000	10,000	∞
φ_{crit}	0.5	0.240	0.091	0.031	0.010	0
χ	2	1.125	0.605	0.532	0.510	0.5

7.3.1.1. Correlation between the polymer–solvent interaction parameter and the solubility parameters

The polymer–solvent interaction parameter, χ , is considered to be the sum of two components:

$$\chi = \chi_H + \chi_S \quad (7.10)$$

where χ_H is the enthalpic component of polymer–solvent interactions, given by Eq. (7.5), and χ_S is the entropic component or free-volume dissimilarity (see, e.g. Bristow and Watson and Patterson, 1958 and Patterson and Delmas, 1970). The relationship between χ_H and the solubility parameters follows from Eqs. (7.3) and (7.5)

$$\chi_H = \frac{V_s}{RT} (\delta_1 - \delta_2)^2 \quad (7.11)$$

The entropic contribution, χ_S , is usually taken to be a constant of the order 0.35 ± 0.1 and for non-polar systems $\chi_S = 0.34$ is generally used (Scott and Magat, 1949 and Blanks and Prausnitz, 1977), so that

$$\chi \approx 0.34 + \frac{V_s}{RT} (\delta_P - \delta_S)^2 \quad (7.12)$$

It follows from Eq. (7.12) that only positive values of χ are permitted, whereas it was mentioned above that the criterion for complete solvent–polymer miscibility is $\chi_H < 0.5$. The conclusion is that the difference in solubility parameters of solvent and polymer must be small. If we assume that $V_s \approx 80 \text{ cm}^3/\text{mol} = 0.8 \times 10^{-4} \text{ m}^3/\text{mol}$, then at room temperature, the maximum value of $|\delta_P - \delta_S|$ would be $4 \text{ (MJ/m}^3\text{)}^{1/2} = 2 \text{ (cal/cm}^3\text{)}^{1/2}$. This number, of course, depends strongly on the liquid molar volume.

We can conclude that two substances with equal solubility parameters should be mutually soluble due to the negative entropy factor. This is in accordance with the general rule that chemical and structural similarity favours solubility. As the difference between δ_1 and δ_2 increases, the tendency towards dissolution decreases.

The solubility parameter of a given material can be calculated either from the cohesive energy, or from the molar attraction constant F , as $\delta = F/V$

In the derivation of Eq. (7.3) it was assumed that no specific forces are active between the structural units of the substances involved. Therefore it does not hold for crystalline polymers. Also if one of the substances involved contains strongly polar groups or hydrogen bridges, ΔH_M may become higher than predicted by Eq. (7.3), so that ΔG_M becomes positive even for $\delta_1 = \delta_2$ and dissolution does not occur. Conversely, if both substances contain polar groups or hydrogen bridges, solubility may be promoted.

For these reasons a more refined treatment of the solubility parameter concept is often necessary, especially for interactions between polymers and solvents. Nevertheless, the solubility parameters of polymers and solvents are important quantities in all phenomena involving interactions between polymers and solvents.

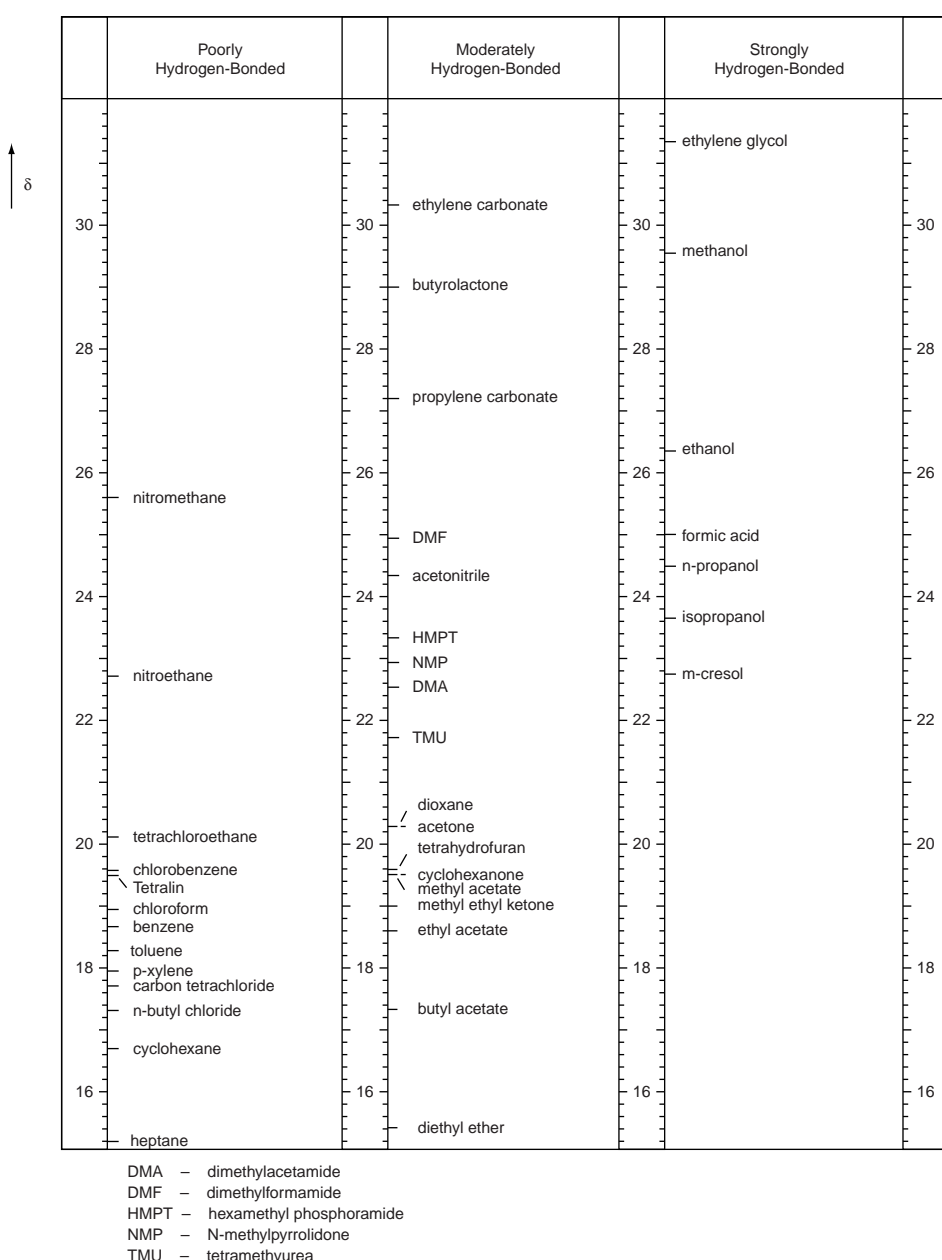
Table 7.6 gives δ -values for some polymers (experimental and calculated) and Table VI, Part VII, gives solubility parameter values for a number of solvents.

Evidently, the most important application of the solubility parameters to be discussed in this chapter is the prediction of the solubility of polymers in various solvents. A first requirement of mutual solubility is that the solubility parameter of the polymer δ_P and that of the solvent δ_S do not differ too much. This requirement, however, is not sufficient. There are combinations of polymer and solvent for which solvent for which $\delta_P \approx \delta_S$, but yet do

TABLE 7.6 Experimental and calculated values of δ for some polymers

Polymer	δ exp. (MJ/m^3) $^{1/2}$		δ calc. (H. + v. K.) (MJ/m^3) $^{1/2}$
	from	to	
Polyethylene	15.8	17.1	16.0
Polypropylene	16.8	18.8	17.0
Polyisobutylene	16.0	16.6	16.4
Polystyrene	17.4	19.0	19.1
Poly(vinyl chloride)	19.2	22.1	19.7
Poly(vinyl bromide)	19.4	—	20.3
Poly(vinylidene chloride)	20.3	25.0	20.6
Poly(tetrafluoroethylene)	12.7	—	11.7
Poly(chlorotrifluoroethylene)	14.7	16.2	15.7
Poly(vinyl alcohol)	25.8	29.1	—
Poly(vinyl acetate)	19.1	22.6	19.6
Poly(vinyl propionate)	18.0	—	18.8
Poly(methyl acrylate)	19.9	21.3	19.9
Poly(ethyl acrylate)	18.8	19.2	19.2
Poly(propyl acrylate)	18.5	—	18.7
Poly(butyl acrylate)	18.0	18.6	18.3
Poly(isobutyl acrylate)	17.8	22.5	18.7
Poly(2,2,3,3,4,4,4-heptafluorobutyl acrylate)	13.7	—	15.8
Poly(methyl methacrylate)	18.6	26.2	19.0
Poly(ethyl methacrylate)	18.2	18.7	18.6
Poly(butyl methacrylate)	17.8	18.4	17.9
Poly(isobutyl methacrylate)	16.8	21.5	18.3
Poly(tert.-butyl methacrylate)	17.0	—	18.0
Poly(benzyl methacrylate)	20.1	20.5	19.3
Poly(ethoxyethyl methacrylate)	18.4	20.3	18.6
Polyacrylonitrile	25.6	31.5	25.7
Polymethacrylonitrile	21.9	—	22.8
Poly(α -cyanomethyl acrylate)	28.7	29.7	23.8
Polybutadiene	16.6	17.6	17.5
Polyisoprene	16.2	20.5	17.4
Polychloroprene	16.8	18.9	19.2
Poly(oxy methylene)	20.9	22.5	20.5
Poly(tetramethylene oxide)	17.0	17.5	17.6
Poly(propylene oxide)	15.4	20.3	18.9
Polyepichlorohydrin	19.2	—	20.1
Poly(ethylene sulphide)	18.4	19.2	18.9
Poly(styrene sulphide)	19.0	—	19.6
Poly(ethylene terephthalate)	19.9	21.9	20.5
Poly(8-aminocaprylic acid)	26.0	—	25.7
Poly(hexamethylene adipamide)	27.8	—	28.0

not show mutual solubility. Mutual solubility only occurs if the degree of hydrogen bonding is about equal. This led Burrell (1955) towards a division of solvents into three classes, viz. poorly, moderately and strongly hydrogen bonded. In combination with the total solubility parameter δ a considerably improved classification of solvents is obtained. The system of Burrell is represented in Table 7.7.

TABLE 7.7 Hydrogen-bonding tendency of solvents

7.3.1.2. Refinements of the solubility parameter concept

In the derivation of Eq. (7.3) by Hildebrand only dispersion forces between structural units have been taken into account. For many liquids and amorphous polymers, however, the cohesive energy is also dependent on the interaction between polar groups and on hydrogen bonding. In these cases the solubility parameter as defined corresponds with the total cohesive energy.

Formally, the cohesive energy may be divided into three parts, corresponding with the three types of interaction forces

$$E_{coh} = E_d + E_p + E_h \quad (7.13)$$

where E_d = contribution of dispersion forces; E_p = contribution of polar forces; E_h = contribution of hydrogen bonding.

The corresponding equation for the solubility parameter is

$$\delta^2 = \delta_d^2 + \delta_p^2 + \delta_h^2 \quad (7.14)$$

The equivalent of Eq. (7.3) becomes

$$\Delta h_M = \varphi_1 \varphi_2 \left[(\delta_{d1} - \delta_{d2})^2 + (\delta_{p1} - \delta_{p2})^2 + (\delta_{h1} - \delta_{h2})^2 \right] \quad (7.15)$$

Unfortunately, values of δ_d , δ_p and δ_h cannot be determined directly. There are, in principle, two ways for a more intricate use of the solubility parameter concept:

- The use of other measurable physical quantities besides the solubility parameter for expressing the solvent properties of a liquid
- Indirect determination of the solubility parameter components δ_d , δ_p and δ_h

The first method was used by Beerbower et al. (1967), who expressed the amount of hydrogen bonding energy by the *hydrogen bonding number* Δv . This quantity was defined by Gordy and Stanford (1939–1941) as the shift of the infrared absorption band in the 4 μm range occurring when a given liquid is added to a solution of deuterated methanol in benzene. Beerbower et al. plotted the data for various solvents in a diagram with the solubility parameter δ along the horizontal axis and the hydrogen bonding number Δv along the vertical axis. All the solvents in which a given polymer is soluble fall within a certain region. As an example, Fig. 7.3 shows such a diagram for polystyrene.

Crowley et al. (1966, 1967) used an extension of this method by including the dipole moment of the solvent in the characterization. However, as this involves a comparison of a number of solvents in a three-dimensional system, the method is impractical.

The second method was developed by Hansen (1967, 1969). Hansen presumed the applicability of Eqs. (7.14) and (7.15) and developed a method for the determination of δ_d , δ_p and δ_h for a number of solvents. The value of δ_d of a given solvent was assumed to be equal to that of a non-polar substance (e.g. hydrocarbon) of about the same chemical structure. This permitted the calculation of $\delta_p^2 + \delta_h^2 = \delta^2 - \delta_d^2 = \delta_a^2$. Now Hansen determined experimentally the solubility of a number of polymers in a series of solvents. All the solvents were characterized by a point in a three-dimensional structure, in which δ_d , δ_p and δ_h could be plotted on three mutually perpendicular axes. The values of δ_p and δ_h for the various solvents were shifted until all the solvents in which a given polymer was soluble were close together in space.

Values of δ_d , δ_p and δ_h for a number of solvents determined in this way can be found in Table VI (Part VII). For comparison also values of the dipole moment μ and the hydrogen bonding number δv are mentioned. Hansen also determined δ_d , δ_p and δ_h of the polymers involved, being the coordinates of the centre of the solvents region in his three-dimensional structure. Table 7.8 shows his parameters for some polymers.² The method of Hansen has the disadvantage that three-dimensional structures are necessary for a

² A number of these values, however, seem to be rather doubtful (see, e.g., the δ_h values of polyisobutylene and polystyrene and the δ_p value of polybutadiene). Koenhen and Smolders (1975) made a critical evaluation of this and similar methods.

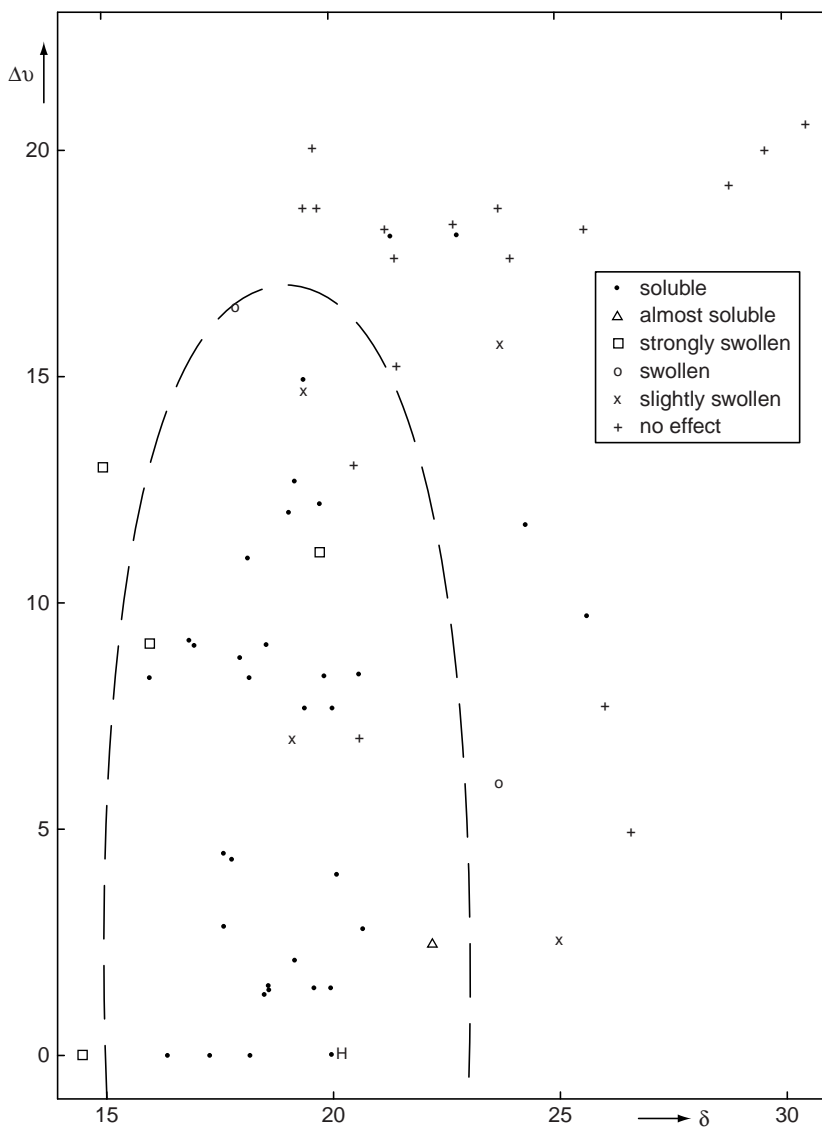


FIG. 7.3 Solubility of polystyrene in various solvents in the $\Delta v-\delta$ diagram.

TABLE 7.8 Hansen's specified solubility parameters and interaction diameter for some polymers ($\text{MJ}/\text{m}^3)^{1/2}$ (Hansen, 1971)

Polymer	δ	δ_d	δ_p	δ_H	$2R$
Polyisobutylene	17.6	16.0	2.0	7.2	12.7
Polystyrene	20.1	17.6	6.1	4.1	12.7
Poly(vinyl chloride)	22.5	19.2	9.2	7.2	3.5
Poly(vinyl acetate)	23.1	19.0	10.2	8.2	13.7
Poly(methyl methacrylate)	23.1	18.8	10.2	8.6	8.6
Poly(ethyl methacrylate)	22.1	18.8	10.8	4.3	10.6
Polybutadiene	18.8	18.0	5.1	2.5	—
Polyisoprene	18.0	17.4	3.1	3.1	9.6

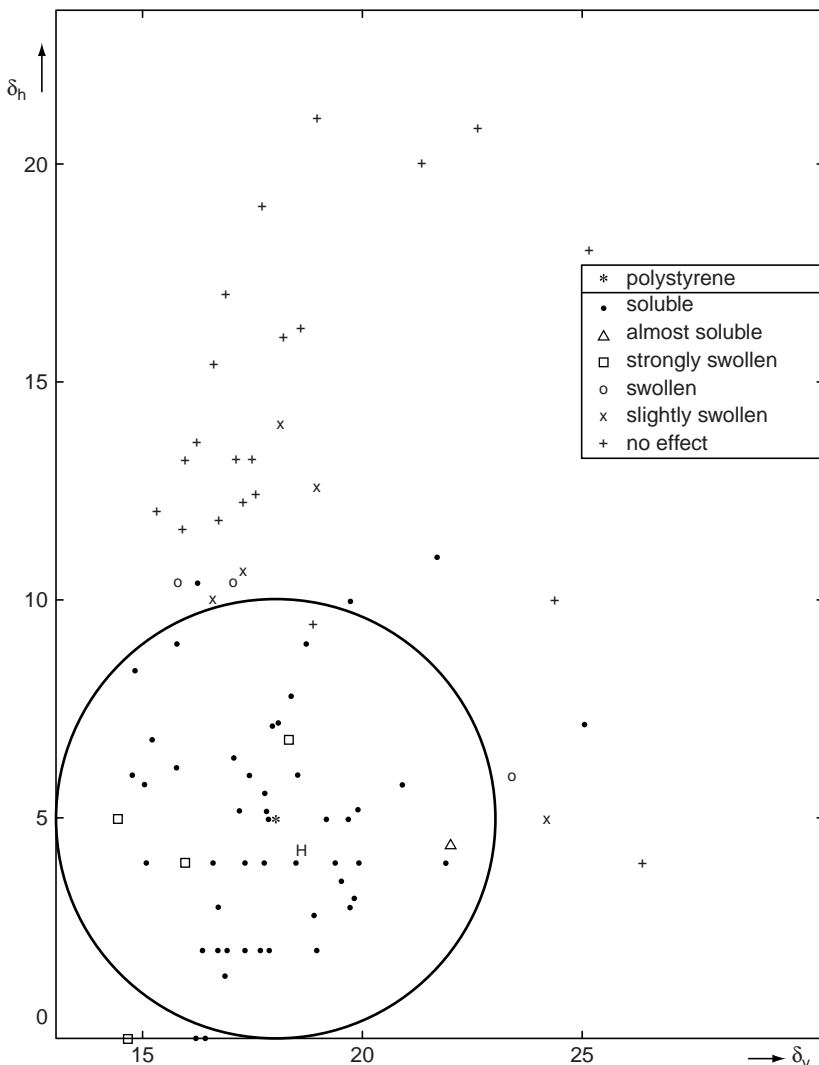


FIG. 7.4 Solubility of polystyrene in various solvents in the δ_v - δ_h diagram.

graphical representation of the interaction between polymers and solvents. For practical applications a two-dimensional method is to be preferred.

Thermodynamic considerations led Bagley et al. (1971) to the conclusion that the effects of δ_d and δ_p show close similarity, while the effect of δ_h is of quite different nature.³

Accordingly, they introduced the parameter $\delta_v = (\delta_d^2 + \delta_p^2)^{1/2}$. This leads to a diagram in which δ_v and δ_h are plotted on the axes. Such a diagram is shown in Fig. 7.4 for the interaction between polystyrene and a number of solvents. The majority of the points for good solvents indeed fall in it single region of Fig. 7.4. This region can approximately be delimitated by a circle the centre of which is indicated by the symbol *. This location differs from that proposed by Hansen, according to the data of Table 7.8, and indicated by the symbol H. Obviously, Fig. 7.4 is superior to Fig. 7.3 in demarcating a solubility region.

³ The hydrogen-bonding parameter is the shift of the infrared absorption band in the 4 μm range occurring when it given liquid is added to it solution of deuterated methanol in benzene.

A method of representation very similar to that of Fig. 7.4 was proposed by Chen (1971). He introduced a quantity

$$\chi_H = \frac{V_s}{RT} \left[(\delta_{dS} - \delta_{dP})^2 + (\delta_{pS} - \delta_{pP})^2 \right] \quad (7.16)$$

where the subscripts S and P denote solvent and polymer, respectively. The solubility data are then plotted in a δ_h - χ_H -diagram. A disadvantage of this method is that the characteristics of the polymer should be estimated beforehand.

Other two-dimensional methods for the representation of solubility data are the δ_p - δ_h -diagram proposed by Henry (1974), the δ - δ_h -diagram proposed by Hoernschemeyer (1974) or the δ - δ_a -diagram.

At the moment the δ_v - δ_h -diagram seems to be the most efficient way to represent polymer-solvent interactions.

The different combinations are all derived from the basic scheme

$$\delta^2 = \overbrace{\delta_d^2 + \delta_p^2}^{\delta_v^2} + \delta_h^2 \quad (7.17)$$

7.3.2. Solubility of polymers in solvents

The solubility region can approximately be delimitated by a circle with a radius of about 5 δ -units. The centre of this circle is indicated by the symbol *; it has the coordinate values: $\delta_v = 18$; $\delta_h = 5$, both in $(\text{MJ}/\text{m}^3)^{1/2}$. It can be seen that the solubility increases approximately as the distance from the centre decreases.

As a general rule, polystyrene is soluble in solvents for which

$$\sqrt{(\delta_v - 18)^2 + (\delta_h - 5)^2} < 5(\text{MJ}/\text{m}^3)^{1/2} \quad (7.18)$$

The literature mentions analogous data for a number of other polymers, which will not be discussed here. When plotted in a δ_h - δ_v -diagram, they generally show the same type of picture. *The reader should be warned, however:*

- (a) For the strong dependence of the radius of the solubility circles on the kind of polymer (see, e.g. Table 7.8)
- (b) For the limited accuracy of this method: the diagrams give only an indication of solubility relationships and always show a number of deviating points

Moreover, temperature dependence plays of course also an important role, as follows from the temperature dependence of the various solubility parameters that are given as (Hansen and Beerbower, 1971):

$$\begin{aligned} \frac{d\delta_d}{dT} &= -1.25\alpha\delta_d \\ \frac{d\delta_p}{dT} &= -\frac{1}{2}\alpha\delta_p \\ \frac{d\delta_h}{dT} &= -\delta_h \left(1.22 \times 10^{-3} + \frac{1}{2}\alpha \right) \end{aligned} \quad (7.19)$$

where α (K^{-1}) is the coefficient of thermal expansion.

TABLE 7.9 Temperature dependence of solubility parameters of some polymers (Chee, 2005)

Polymer	$\delta_g \text{ (MJ/m}^3\text{)}^{1/2}$	$m_g \text{ ((MJ/m}^3\text{)}^{1/2}/\text{K)}$	$m_l \text{ ((MJ/m}^3\text{)}^{1/2}/\text{K)}$
Poly(methyl methacrylate)	18.50	-0.0162	-0.0209
Polystyrene	17.38	-0.0166	-0.0217
Natural rubber	18.85	-0.0131	-0.0241
Low density polyethylene	17.91	-0.0037	-0.0153

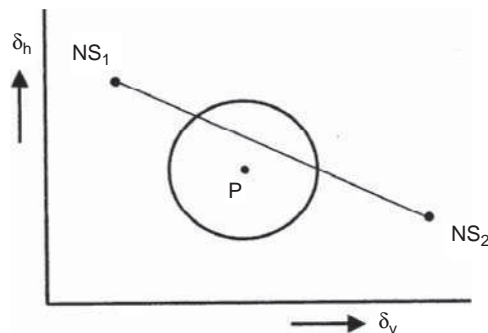
Recently, Chee (2005) suggested temperature dependence for the three parameters of the form:

$$\delta = \delta_g + m_i(T - T_g) \quad (7.20)$$

where m_i is an empirical constant, different above (m_l) and below (m_g) the glass transition temperature T_g . Some of his results are presented in Table 7.9.

7.3.2.1. Solubility in solvent mixtures

The solubility parameter of a solvent mixture can be determined by averaging the Hildebrand value of a solvent of the individual components by volume (see, e.g. Burke, 1984). For example, a mixture of one part acetone and two parts toluene will have a solubility parameter of 18.7 ($= \frac{1}{3} \times 19.7 + \frac{2}{3} \times 18.3$), about the same as that of chloroform. As a result it also shows the possibility to dissolve a polymer in a mixture of two non-solvents: both non-solvents are situated outside the solubility circle of the polymer, whereas the mixture may be situated inside this circle (see Fig. 7.5). It has to be emphasized, however, that the solubility may be limited: only dilute solutions might be possible, sufficient, e.g. for the determination of intrinsic viscosities. This follows from ternary phase diagrams for a polymer and two non-solvents, as presented in Fig. 7.6. From left to right the solubility decreases, e.g. by temperature decrease. It shows that solubility might be very limited, just enough to measure viscosities and osmotic pressures of dilute solutions in order to determine viscosity and number average molecular weights. This low solubility does not follow from the solubility parameters.

**FIG. 7.5** Schematic view of solubility of a polymer in two non-solvents.

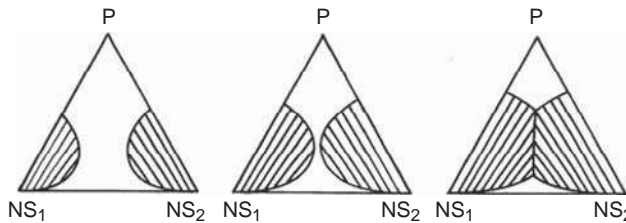


FIG. 7.6 Ternary phase diagrams of polymer and two non-solvents: from left to right decreasing solubility.

7.3.3. Solubility limits and Flory-temperature

The solubility limits of a given polymer are closely related to the Flory-temperatures of the polymer in various solvents.

The *Flory-temperature* or theta-temperature (Θ_F) is defined as the temperature where the *partial molar free energy* due to polymer–solvent interactions is zero, i.e. when $\chi = 0$, so that the polymer–solvent systems show ideal solution behaviour. If $T = \Theta_F$, the molecules can interpenetrate one another freely with no net interactions. For systems with an upper critical solution temperature (UCST) the polymer molecules attract one another at temperatures $T < \Theta_F$. If the temperature is much below Θ_F precipitation occurs. On the other hand for systems with a lower critical solution temperature (LCST) the polymer molecules attract one another at temperatures $T > \Theta_F$. If the temperature is much above Θ_F precipitation occurs. Aqueous polymer solutions show this behaviour. Systems with both UCST and LCST are also known (see, e.g. Napper, 1983).

Thermodynamic considerations have led to the following equation for the temperature at which the solution becomes metastable:

$$T_{\text{cr}} \approx \frac{\Theta_F}{1 + CM^{-1/2}} \quad (7.21)$$

where C is a constant for the polymer-solvent system.

In the metastable state, i.e. between the binodal and the spinodal, phase separation only occurs in the presence of nuclei. Spontaneous phase separation only occurs at temperatures below the spinodal, where the solution becomes unstable. The binodal and spinodal are obtained by constructing curves of ΔG_M vs. φ (Fig. 7.2) for various values of χ (i.e. for various values of temperature) and subsequently plotting the temperature vs. the tangent points and the inflection points to obtain the binodal and spinodal, respectively (see Fig. 7.7).

It is clear that the Flory-temperature is the critical miscibility temperature in the limit of infinite molar weight. Fox (1962) succeeded in correlating Θ_F -temperatures of polymer–solvent systems with the solubility parameter δ_s of the solvent. Plots of δ_s as a function of Θ_F are shown in Fig. 7.8.

Comprehensive Tables of Theta-solvents and Theta-temperatures have been published, e.g. by Elias (1999) and by Sundararajan (1996).

At a given temperature, a solvent for the polymer should have a δ -value approximately between the limits, indicated by the two straight lines in the figure. An even better correlation of Flory-temperatures with solubility parameters can be given in a δ_h – δ_v -diagram. This is shown in Fig. 7.9 for polystyrene. The circle drawn in Fig. 7.9 corresponds again with Eq. (7.18).

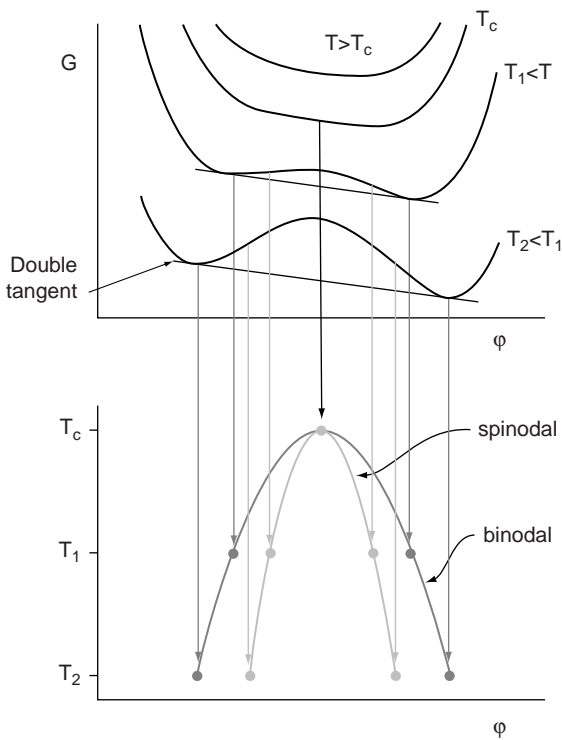


FIG. 7.7 Typical curves of free enthalpy G vs. volume fraction φ as a function of temperature, from above the critical temperature T_c to temperatures below T_c . The diagram below is obtained with the aid of the double tangent curves and the inflection points to construct the binodal curves (phase diagram) and spinodal curves (stability diagram), respectively. It has to be emphasised that this is the result for low molecular weight liquids, for polymer solutions the critical point would be very close to $\varphi = 0$.

7.3.4. Prediction of solubility-parameter components

The solubility parameter components δ_d , δ_p and δ_h , and their combinations $\delta_a = (\delta_p^2 + \delta_h^2)^{1/2}$ and $\delta_v = (\delta_d^2 + \delta_p^2)^{1/2}$, are known for a limited number of solvents only. Therefore a method for predicting these quantities is valuable.

It is to be expected that the polar component δ_p is correlated with the dipole moment μ and that the hydrogen bonding component δ_h is correlated with the hydrogen bonding number Δv . This is not of much use, however, as also μ and Δv are only known for a limited number of solvents. A useful prediction method must be based on the molecular structure of the solvent. The available experimental data prove, however, that it is impossible to derive a simple system for an accurate prediction of solubility parameter components from the chemical structure. Especially the interaction of different structural groups in producing overall polar and hydrogen-bonding properties is so complicated that it does not obey simple rules. If nevertheless such a prediction method is presented here, it does not pretend to give more than rather rough estimates. Yet this may sometimes be preferable to a complete lack of data.

Two approaches have been published, viz. that of Hoytzer and Van Krevelen (1976) and that of Hoy (1985); in both methods the same basic assumption is made, that of Hansen:

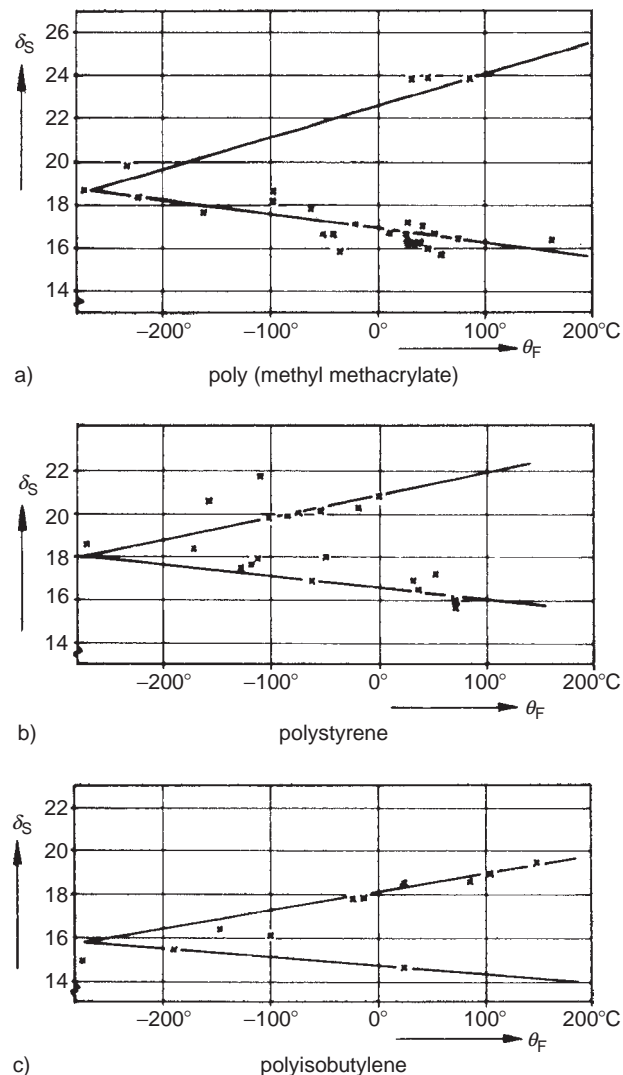


FIG. 7.8 Solubility parameters and Θ -temperatures (Van Krevelen and Hoflyzer, 1967).

$$E_{coh} = E_d + E_p + E_h \text{ (see Eq. (7.15))}, \text{ so:}$$

$$\delta^2 = \delta_d^2 + \delta_p^2 + \delta_h^2 \text{ see Eq. (7.16))}$$

7.3.4.1. Method of Hoflyzer and Van Krevelen (1976)

The solubility parameter components may be predicted from group contributions, using the following equations:

$$\delta_d = \frac{\sum F_{di}}{V} \quad (7.22)$$

$$\delta_p = \frac{\sqrt{\sum F_{pi}^2}}{V} \quad (7.23)$$

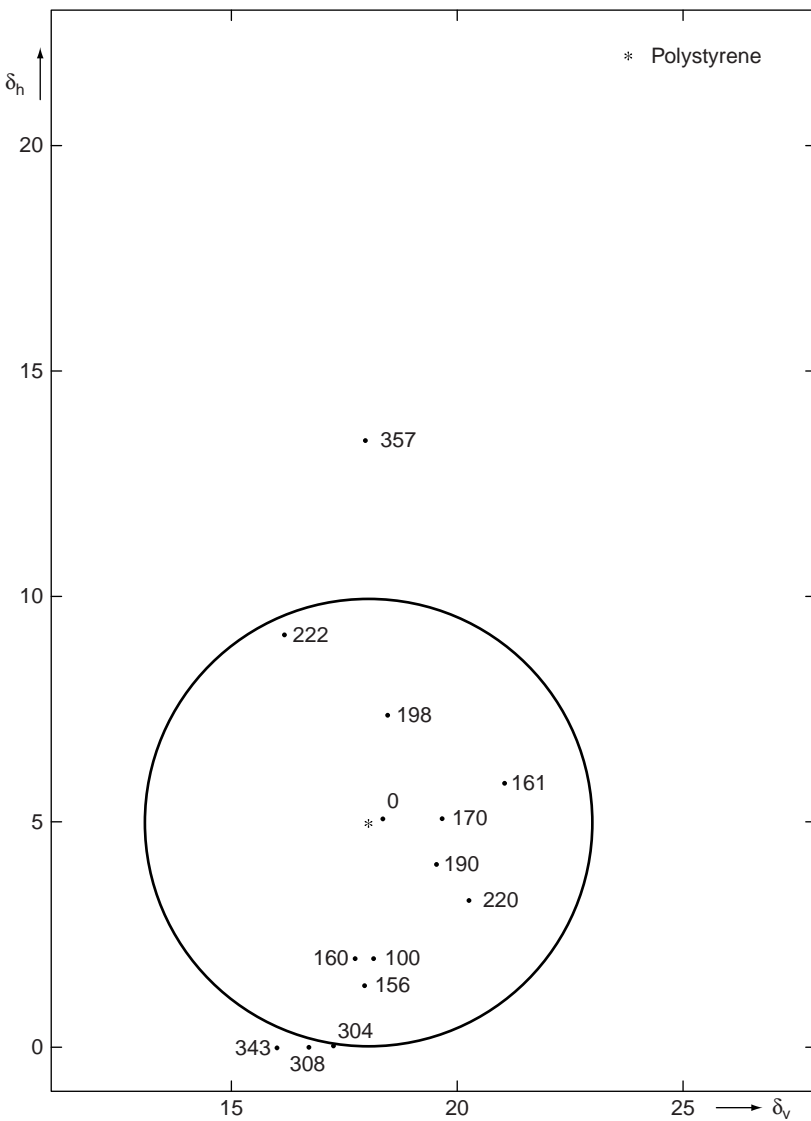


FIG. 7.9 Flory-temperatures (in K) of polystyrene in various solvents.

$$\delta_h = \sqrt{\frac{\sum E_{hi}}{V}} \quad (7.24)$$

This means that for the prediction of δ_d the same type of formula is used as Small proposed for the prediction of the total solubility parameter δ . The group contributions F_{di} to the dispersion component F_d of the molar attraction constant can simply be added.

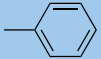
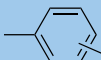
The same method holds for δ_p as long as only one polar group is present. To correct for the interaction of polar groups, the form of Eq. (7.23) has been chosen.

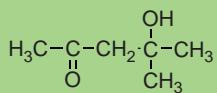
The polar component is still further reduced, if two identical polar groups are present in a symmetrical position. To take this effect into account, the value of δ_p calculated with Eq. (7.23) must be multiplied by a symmetry factor of:

0.5 for one plane of symmetry
0.25 for two planes of symmetry
0 for more planes of symmetry

The F-method is not applicable to the calculation of δ_h . It has already been stated by Hansen that the hydrogen bonding energy E_{hi} per structural group is approximately constant. This leads to the form of Eq. (7.24). For molecules with several planes of symmetry, $\delta_h = 0$. The group contributions F_{di} , F_{pi} and E_{hi} for a number of structural groups are given in Table 7.10.

TABLE 7.10 Solubility parameter component group contributions (method Hoftyzer–Van Krevelen)

Structural group	F_{di} (MJ/m ³) ^{1/2} · mol ⁻¹	F_{pi} (MJ/m ³) ^{1/2} · mol ⁻¹	E_{hi} J/mol
-CH ₃	420	0	0
-CH ₂ -	270	0	0
>CH-	80	0	0
>C<	-70	0	0
=CH ₂	400	0	0
=CH-	200	0	0
=C<	70	0	0
	1620	0	0
	1430	110	0
	1270	110	0
-F	(220)	-	-
-Cl	450	550	400
-Br	(550)	-	-
-CN	430	1100	2500
-OH	210	500	20,000
-O-	100	400	3000
-COH	470	800	4500
-CO-	290	770	2000
-COOH	530	420	10,000
-COO-	390	490	7000
HCOO-	530	-	-
-NH ₂	280	-	8400
-NH-	160	210	3100
>N-	20	800	5000
-NO ₂	500	1070	1500
-S-	440	-	-
=PO ₄	740	1890	13,000
Ring	190	-	-
One plane of symmetry	-	0.50×	-
Two planes of symmetry	-	0.25×	-
More planes of symmetry	-	0×	0×

Example 7.3 Estimate the solubility parameter components of diacetone alcohol**Solution**

The molar volume $V = 123.8 \text{ cm}^3/\text{mol}$. Addition of the group contributions gives

	F_{di}	F_{pi}^2	E_{hi}
3 -CH ₃	1260	0	0
-CH ₂ -	270	0	0
>C<	-70	0	0
-CO-	290	592,900	2000
-OH	210	250,000	20,000
	1960	842,900	22,000

According to Eqs. (7.22)–(7.24)

$$\delta_d = \frac{\sum F_{di}}{V} = \frac{1960}{123.8} = 15.8 \text{ (MJ/m}^3\text{)}^{1/2}$$

$$\delta_p = \frac{\sqrt{\sum F_{pi}^2}}{V} = \frac{\sqrt{842,900}}{123.8} = 7.4 \text{ (MJ/m}^3\text{)}^{1/2}$$

$$\delta_h = \sqrt{\frac{\sum E_{hi}}{V}} = \sqrt{\frac{22,000}{123.8}} = 13.3 \text{ (MJ/m}^3\text{)}^{1/2}$$

The literature values are: $\delta_d = 15.7$, $\delta_p = 8.2$ and $\delta_h = 10.9 \text{ (MJ/m}^3\text{)}^{1/2}$.

From the calculated components an overall value of the solubility parameter is found:

$$\delta = \sqrt{\delta_d^2 + \delta_p^2 + \delta_h^2} = 21.9 \text{ (MJ/m}^3\text{)}^{1/2}$$

The experimental values for δ vary from 18.8 to 20.8 $(\text{MJ}/\text{m}^3)^{1/2}$.

7.3.4.2. Method of Hoy (1985, 1989)

Hoy's method is in many respects different from that of Hoftyzer and Van Krevelen.

Table 7.11 gives a survey of the system of equations to be used. It contains four additive molar functions, a number of auxiliary equations and the final expressions for $\delta_{t(\text{total})}$ and for the components of δ .

F_t is the molar attraction function, F_p its polar component (both as discussed earlier); V is the molar volume of the solvent molecule or the structural unit of the polymer. Δ_T is the Lydersen correction for non-ideality, used in the auxiliary equations. The values for low-molecular liquids were derived by Lydersen (1955); the corresponding values for polymers, which are slightly different, have been derived by Hoy ($\Delta_T^{(P)}$).

Of the other quantities in the auxiliary equations, the significance is the following: α is the *molecular aggregation number*, describing the association of the molecules; n is the

TABLE 7.11 The equations to be used in Hoy's system (1985) for estimation of the solubility parameter and its components. See text for significance of symbols

Formulae	Low-molecular liquids (solvents)	Amorphous polymers
Additive molar functions	$F_t = \sum N_i F_{t,i}$ $F_p = \sum N_i F_{p,i}$ $V = \sum N_i V_i$ $\Delta_T = \sum N_i \Delta_{T,i}$	$F_t = \sum N_i F_{t,i}$ $F_p = \sum N_i F_{p,i}$ $V = \sum N_i V_i$ $\Delta_T^{(P)} = \sum N_i \Delta_{T,i}^{(P)}$
Auxiliary equations	$\log \alpha = 3.39 \log(T_b/T_{cr}) - 0.1585 - \log V$ T_b = boiling point; T_{cr} = critical temp. $T_b/T_{cr} = 0.567 + \Delta_T - (\Delta_T)^2$ (Lydersen equation)	$\alpha(P) = 777 \Delta_T^{(P)}/V$ $n = 0.5/\Delta_T^{(P)}$
Expressions for δ and δ -components (Note that F_t must always be combined with a Base value; B for liquids and B/\bar{n} for polymers)	$\delta_t = (F_t + B)/V$ $B = 277$ $\delta_p = \delta_t \left(\frac{1}{\alpha F_t + B} \right)^{1/2}$ $\delta_h = \delta_t [(\alpha - 1)/\alpha]^{1/2}$ $\delta_d = (\delta_t^2 - \delta_p^2 - \delta_h^2)^{1/2}$	$\delta_t = (F_t + B/\bar{n})/V$ $\delta_p = \delta_t \left(\frac{1}{\alpha^{(P)} F_t + B/\bar{n}} \right)^{1/2}$ $\delta_h = \delta_t [(\alpha^{(P)} - 1)/\alpha^{(P)}]^{1/2}$ $\delta_d = (\delta_t^2 - \delta_p^2 - \delta_h^2)^{1/2}$

number of repeating units per effective chain segment of the polymer. Table 7.12 gives values of increments in Hoy's system for the molar attraction function.

It must be emphasised that Hoy is the only author who uses a "base value" in the calculation of F_t , whereas he neglects a base value in V . It was mentioned earlier that Traube (1895) already proved that for the additive calculation of the molar volume of liquids a base value has to be used (see Chap. 4).

Hoy's method will now be illustrated by two numerical examples.

Example 7.4

Estimate the solubility parameter and its components of diacetone alcohol, $\text{CH}_3\text{COCH}_2\text{C(OH)(CH}_3)_2$

Solution

The values of the group contributions are the following:

Groups	F_t	F_p	Δ_T	V
3 -CH ₃	910.5	0	0.069	64.65
1 -CH ₂ -	269.0	0	0.020	15.55
1 >C<	65.5	0	0	3.56
1 >CO	538	525	0.040	17.3
1 -OH tert.	(500)	(500)	0.082	12.45
Sum	2283	1025	0.211	113.51

Furthermore we get:

$$\mathbf{B} = \text{base value} = 277$$

$$T_b/T_{cr} = 0.576 + 0.211 - 0.045 = 0.742$$

$$\log a = 3.39 \times 0.742 - 0.1585 - 2.055 = 0.3019, \text{ so } a = 2.001$$

Finally we obtain for δ and its components:

$$\delta = \frac{2283 + 277}{113.5} = 22.6 \text{ (MJ/m}^3\text{)}^{1/2}$$

$$\delta_p = 22.6 \left(\frac{1.0}{2.0} \frac{1025}{2560} \right)^{1/2} = 10.1 \text{ (MJ/m}^3\text{)}^{1/2}$$

$$\delta_h = 22.6 \left(\frac{1.0}{2.0} \right)^{1/2} = 16.0 \text{ (MJ/m}^3\text{)}^{1/2}$$

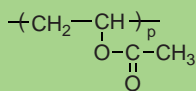
$$\delta_d = (22.6^2 - 10.1^2 - 15.9^2)^{1/2} = 12.4 \text{ (MJ/m}^3\text{)}^{1/2}$$

The comparison with other values is as follows

	Exp.	Small	Hansen	Hoftyzer–Van Krevelen	Hoy
δ	18.8–20.8	23.0	20.7	21.9	22.6
δ_d	–	–	15.7	15.8	12.4
δ_p	–	–	8.2	7.4	10.1
δ_h	–	–	10.9	13.3	16.0

Example 7.5

Estimate the value of δ and its components of poly(vinyl acetate) with the structure



Solution

From the Tables 7.11 and 7.12 we obtain:

Groups	F _t	F _p	$\Delta_T^{(P)}$	V
$-\text{CH}_3$	303.5	0	0.022	21.55
$-\text{CH}_2-$	269.0	0	0.020	15.55
$-\text{CH}<$	176.0	0	0.013	9.56
$-\text{COO}-$	640.0	528	0.050	23.7
Sum	1388.5	528	0.105	70.46

$$\mathbf{B} = \text{base value} = 277$$

$$\alpha = \frac{777 \times 0.105}{70.4} = 1.16; n = \frac{0.5}{0.105} = 4.76$$

So

$$\delta_t = \frac{1388.5}{70.4} + \frac{277/4.76}{70.4} = 20.6$$

$$\delta_p = 20.55 \left(\frac{1}{1.16} \times \frac{528}{1447} \right)^{1/2} = 11.5$$

$$\delta_h = 20.55 \left(\frac{0.16}{1.16} \right)^{1/2} = 7.6$$

$$\delta_d = (20.55^2 - 11.5^2 - 7.6^2)^{1/2} = 15.2$$

The comparison with other values is as follows:

	Exp.	Small	Hansen	Hoftyzer–Van K.	Hoy
δ_t	19.1–22.6	19.2	23.1	19.4	20.6
δ_d	–	–	19.0	16.0	15.2
δ_p	–	–	10.2	6.8	11.5
δ_h	–	–	8.2	8.5	7.6

The results of the two algorithmic methods for estimation of the solubility parameter and its components (Hoftyzer–Van Krevelen and Hoy) are of the same order in accuracy (10%). So the safest way for estimation is to apply both methods, taking the average results.

To conclude we give the full equation that determines the solubility of a polymer in an organic liquid:

$$\Delta\delta = \left[(\delta_{d,P} - \delta_{d,S})^2 + (\delta_{p,P} - \delta_{p,S})^2 + (\delta_{h,P} - \delta_{h,S})^2 \right]^{1/2} \quad (7.25)$$

For it good solubility $\Delta\delta \leq$ must be small, e.g. $\leq 5 \text{ (MJ/m}^3\text{)}^{1/2}$, dependent on the polymer of consideration.

7.3.5. Influence of crystallinity

It was pointed out from the beginning that the concept of the solubility parameter was applicable only to amorphous polymers. In order to adapt the method to highly crystalline polymers some way must be found to deal with the heat of fusion (ΔH_m) in the free enthalpy equation:

$$\Delta G_M = [\Delta H_M + \Delta H_m] - T[\Delta S_M + \Delta S_m]$$

Highly crystalline polymers such as polyethylene and poly(tetrafluoroethylene) are insoluble in all solvents at room temperature. These polymers, however, obey the solubility parameters rules at $T \geq 0.9T_m$. For instance, polyethylene becomes soluble above 80 °C.

TABLE 7.12 Values of increments in Hoy's System (1985), for the molar attraction function

Groups	$F_{t,i}$ ((MJ/m ³) ^{1/2} /mol)	$F_{p,i}$	V_i (cm ³ /mol)	$\Delta_{T,i}^*$	$\Delta_{T,i}^{(P)}$	Groups	$F_{t,i}$ ((MJ/m ³) ^{1/2} /mol)	$F_{p,i}$	V_i (cm ³ /mol)	$\Delta_{T,i}^*$	$\Delta_{T,i}^{(P)}$
-CH ₃	303.5	0	21.55	0.023	0.022	-OH → (H. bonded)	485	485	10.65	0.082	0.034
-CH ₂ -	269.0	0	15.55	0.020	0.020	-OH prim.	675	675	12.45	0.082	0.049
>CH-	176.0	0	9.56	0.012	0.013	-OH second.	591	591	12.45	0.082	0.049
>C<	65.5	0	3.56	0	0.040	-OH tert.	(500)	(500)	12.45	0.082	0.049
=CH ₂	259	67	19.17	0.018	0.019	phenolic	350	350	12.45	0.031	0.006
=CH-	249	59.5	13.18	0.018	0.0185	-O- ether	235	216	6.45	0.021	0.018
=C<	173	63	7.18	0	0.013	-O- acetal	236	102	6.45	0.018	0.018
CH _{ar}	241	62.5	13.42	0.011	0.018	-O- epoxide	361	156	6.45	0.027	0.027
C _{ar}	201	65	7.42	0.011	0.015	-NH ₂	464	464	17.0	0.031	0.035
-HC=O	600	532	23.3	0.048	0.045	-NH-	368	368	11.0	0.031	0.0275
>C=O	538	525	17.3	0.040	0.040	>N-	125	125	12.6	0.014	0.009
-COOH	565	415	26.1	0.039	0.039	-S-	428	428	18.0	0.015	0.032
-COO-	640	528	23.7	0.047	0.050	-F	845	73.5	11.2	0.018	0.006
-CO-O-CO-	1160	1160	41.0	0.086	0.086	-Cl prim.	419.5	307	19.5	0.017	0.031
-C≡N	725	725	23.1	0.060	0.054	-Cl second.	426	315	19.5	0.017	0.032
-N=C=O	736	8.2	25.9	0.054	0.054	arom.	330	81.5	19.5	0.017	0.025
HCON<	1020	725	35.8	0.062	0.055	<(Cl) ₂ twinned	705	572	39.0	0.034	0.052
-CONH ₂	1200	900	34.3	0.071	0.084	-Br aliph.	528	123	25.3	0.010	0.039
-CONH-	1131	895	28.3	0.054	0.073	arom.	422	100	25.3	0.010	0.031
-OCONH-	1265	890	34.8	0.078	0.094						

Configurations	$F_{t,i}$	$F_{p,i}$	V_i	$\Delta_{T,i}^*$	$\Delta_{T,i}^{(P)}$	Configurations	$F_{t,i}$	$F_{p,i}$	V_i	$\Delta_{T,i}^*$	$\Delta_{T,i}^{(P)}$
Base value (B)	277	—	—	—	—	Conjugation isomerism	47.5	—19.8	—	0	0.0035
Ring size (non-aromatic)						cis	—14.6	—14.6	—	0	—0.001
						trans	—27.6	—27.6	—	0	—0.002
4-membered	159	203	—	0	0.012	Aromatic substitution					
5-membered	43	85	—	0	0.003	ortho	20.2	—13.3	—	0	0.0015
6-membered	—48	61	—	0	—0.0035	meta	13.5	—24.3	—	0	0.0010
7-membered	92	0	—	0	0.007	para	83	—34.0	—	0	0.006

For bi-, tri- and tetra-valent groups in saturated rings the Δ_T -values must be multiplied by a factor 2/3.

Furthermore, crystalline polymers do obey the rules even at room temperature in so far as swelling behaviour is concerned. This again is a demonstration that crystalline regions serve as physical cross-links. Some crystalline polymers with strong hydrogen bonding groups can be made to dissolve at room temperature. But in these cases a very specific interaction between polymer and solvent must occur. For example, cellulose is soluble in 70% sulphuric acid and in aqueous ammonium thiocyanate; nylon 6.6 is soluble in phenol and in a 15% calcium chloride solution in methanol.

7.3.6. Other applications of solubility parameter diagrams

Solubility parameter diagrams, e.g. δ_h vs. δ_v -diagrams, may be useful for the correlation of some phenomena attended with polymer-solvent interaction (see, e.g. Xue and Frisch, 1996 and Grulke, 1999). These phenomena will only be mentioned here.

- a. Characteristic parameters of dilute polymer solutions (see Chap. 9), e.g.:
 - (1) The Mark-Houwink exponent $a(\delta)$
 - (2) The composition of solvent mixtures forming Θ -solutions with a given polymer ($\delta, \delta_d, \delta_p, \delta_H$)
 - (3) Partial density of polymers in solution (δ)
- b. Deterioration of polymers by solvents (see Chap. 21), e.g.:
 - (1) Swelling of polymers by solvents (δ)
 - (2) Solvent crazing and cracking ($\delta, \delta_d, \delta_p, \delta_H$)
 - (3) Decrease of mechanical properties, e.g. tensile strength (δ)
- c. Solvents
 - (1) Surface tension (δ_d, δ_p)
 - (2) Index of refraction (δ_d)
 - (3) Van der Waals gas constant (δ)
 - (4) Vaporization enthalpy (δ)
 - (5) Dipole moment (δ_p)
- d. Polymers
 - (1) Internal pressure (δ)
 - (2) Swelling data (δ)
 - (3) Refractive index (δ_d)
 - (4) Dipole moment (δ_p)
- e. Shrinkage of polymer fibres, immersed in solvents (δ)
- f. Crystallization of polymers induced by solvents (δ).

All these applications may lead to better and more consistent values of the parameter components.

7.3.7. Solubility of (semi-) rigid polymers

Since the 1970s the interest in semi-rigid aromatic polymers (aramids and arylates a.o.) is increasing. Dissolving of these polymers may be very difficult and requires rather unusual solvent. A survey of suitable solvents is given in Table 7.13.

TABLE 7.13 Solvents for (Semi-) rigid-rod aromatic polymers (after Lenz (1985))

Solvents	For (S-) R-R Aramids	For (S-)R-R Arylates
Very strong	Sulphuric acid (100%)	Trifluoromethane sulphonic acid
Strong	Hydrofluoric acid Chlorosulphonic acid N,N -Dimethyl formamide + Li, Ca salts N,N -Dimethyl acetamide + Li, Ca salts Hexamethyl phosphoramide + Li, Ca salts N -Methyl pyrrolidone + Li, Ca salts N,N,N',N' -tetramethylurea 1,3-dimethyl-imidazolidinone N,N,N',N' -tetramethyl malonamide	p-Chlorophenol p-Chlorophenol/tetrachloroethane p-Chlorophenol/o-dichlorobenzene p-Chlorophenol/tetrachl. eth/phenol Phenol/tetrachloroethane 60/40 Trifluoroacetic acid/methylene chloride 60/40 or 30/70 Pentafluoro-phenol p-Fluoro-phenol 1,3 Dichloro 1,1,3,3 tetrafluoro acetone hydrate (=DCTFAH) DCTFAH/ perchloroethylene 50/50 DCTFAH/TFA/methylene chloride/ perchloroethylene 25/15/35/25
Weak	N -methyl caprolactam N -acetyl pyrrolidone N,N -dimethyl propionamide N -methyl piperidone	Trifluoroacetic acid (=TFA) Tetrachloroethane N,N -Dimethyl formamide

7.4. INTERNAL PRESSURE

The internal pressure π is closely related to the cohesive energy density e_{coh} . Therefore we pay some attention to this subject. Spencer and Gilmore (1949, 1950) showed that the $p-v-T$ behaviour of polymer melts can be represented reasonably well by the following modified Van der Waals equation of state⁴:

$$(v - \omega)(p + \pi) = \frac{RT}{M_u} \quad (7.26)$$

where p is the applied pressure, v is the specific volume of the polymer and M_u the molar weight of an "interacting unit"; π and ω are constants, which must be determined experimentally, just as the interaction unit M_u . π in this equation is the *internal pressure*, which is independent of specific volume and, therefore, of temperature and pressure. It is obvious that the internal pressure will be related to the cohesive energy density (both have the dimension $J/m^3 = N/m^2$). Ω is the specific volume at $p = 0$ and $T = 0$ (see also Chap. 4).

Spencer and Gilmore evaluated the constants π and M_u from a series of $p-v$ -measurements at fixed temperatures. In synthetic linear polymers M_u could be identified with the molar weight of the structural unit. In this case ($M_u\omega = V(0)$) the equation of state becomes:

⁴ A comparison between some empirical equations of state for polymers with regard to their standard deviations was made by Kamal and Levan (1973).

$$[\mathbf{V} - \mathbf{V}(0)](p + \pi) = RT \quad (7.27)$$

At atmospheric conditions the internal pressure π is much greater than the external pressure p , so that for the liquid polymer:

$$\pi = \frac{RT}{\mathbf{V}(T) - \mathbf{V}(0)} \approx \frac{R}{E_l} \quad (7.28)$$

where $E_l \equiv (dV_l/dT)_p$ = the molar thermal expansion coefficient of a liquid.

The same result is obtained by differentiation of the equation of state:

$$\left(\frac{\partial V}{\partial T}\right)_p = \frac{R}{M_u \pi} \quad (7.29)$$

or

$$\pi = \frac{R}{M_u \left(\frac{\partial V}{\partial T}\right)_p} = \frac{R}{M_u e_1} = \frac{R}{E_l} \quad (7.30)$$

In Table 7.14 the results calculated by means of Eq. (7.28) are compared with the experimental data. The figures obtained are of the right order of magnitude.

Smith (1970) derived an equation of state for liquid polymers based on the hole theory of liquids. For higher temperatures, this equation can be reduced to a form equivalent to that of Eq. (7.26).

It should be remarked that for cellulose derivatives (cellulose acetate, cellulose butyrate and ethyl cellulose) the values of M_u were found to be much smaller than the molar weight of the structural units.

By means of Eq. (7.27) a good impression of the $p-v-T$ behaviour of a polymer melt can be obtained if no data are available at all. Since $\mathbf{V}(0) \approx 1.3\mathbf{V}_W$ and $E_l \approx 1.00 \times 10^{-4}\mathbf{V}_W$, \mathbf{V}_W only has to be calculated from group contributions in this case.

TABLE 7.14 Equation of state constants^a

Polymer	π (bar)		ω (cm^3/g)	
	exp.	calc. $\pi = R/E_l$	exp.	calc. $\omega = \mathbf{V}(0)/M$ $= 1.3\mathbf{V}_W/M$
Polyethylene	3290	3470	0.88	0.95
Polypropylene	2470	2700	0.83	0.95
Poly(1-butene)	1850	2030	0.91	0.95
Poly(4-methylpentene)	1050	1360	0.83	0.95
Polystyrene	1870	1460	0.82	0.79
Poly(methyl methacrylate)	2180	1730	0.73	0.73
Poly(caproamide) (nylon 6)	1110	1180	0.62	0.815
Poly(hexamethylene sebacamide) (nylon 6,8)	540	515	0.77	0.75
Polycarbonate	460	610	0.56	0.695

^a Experimental data from Spencer and Gilmore (1950) and Sagalaev et al. (1974). Conversion factors: 1 bar = $10^5 \text{ N/m}^2 = 0.987 \text{ atm}$; $1 \text{ cm}^3/\text{g} = 10^{-3} \text{ m}^3/\text{kg}$.

Example 7.6

Estimate the specific volume of molten polypropylene

- (a) 200 °C, 1 atm.
- (b) at 250 °C, 1 atm.
- (c) at 200 °C, 600 atm.

Solution

We can calculate v with the aid of a modification of Eq. (7.26)

$$v = \omega + \frac{RT}{M_u(p + \pi)}$$

The following data may be used:

$$R = 83.14 \text{ cm}^3 \text{ bar/mol/K}$$

$$M_u = 42.1 \text{ g/mol} = M$$

$$V_w = 30.68 \text{ cm}^3/\text{mol} \text{ (Table 4.12)}$$

$$\omega = \frac{1.3V_w}{M} = \frac{1.3 \times 30.68}{42.1} = 0.947 \text{ cm}^3/\text{g}$$

$$E_1 = 0.0307 \text{ cm}^3/\text{mol/K}$$

$$\pi = \frac{R}{E_1} = \frac{83.14}{0.0307} = 2700 \text{ bar}$$

Calculation leads to the following results:

T (°C)	p (bar)	v _{calc} (cm ³ /g)	v _{exp} (cm ³ /g)
200	1	1.30	1.34
250	1	1.33	1.39
200	600	1.23	1.28

The experimental data were determined by Foster et al. (1966).

From the equation of state, equations for the *thermal expansion coefficient* (α) and for the *compressibility* (κ) can be obtained. Rearrangement of Eq. (7.27) gives

$$V = V(0) + \frac{RT}{p + \pi} \quad (7.31)$$

from which the following partial derivatives are obtained:

$$\left(\frac{\partial V}{\partial T}\right)_p = \frac{R}{p + \pi} \text{ and } \left(\frac{\partial V}{\partial p}\right)_T = -\frac{RT}{(p + \pi)^2} = -\frac{T}{p + \pi} \left(\frac{\partial V}{\partial T}\right)_p \quad (7.32)$$

Substitution gives:

$$\alpha = \frac{1}{V} \left(\frac{\partial V}{\partial T}\right)_p = \frac{1}{T + \frac{V(0)}{R}(p + \pi)} \quad (7.33)$$

TABLE 7.15 Comparison of π and e_{coh} at 20 °C

Polymer	π (bar)	e_{coh} (bar)	π/e_{coh}
Polyethylene	3200	2500/2900	1.19
Polyisobutylene	3300	2500/2700	1.27
Polystyrene	4600	3000/3600	1.39
Poly(chlorotrifluoroethylene)	3700	2200/2600	1.54
Poly(vinyl acetate)	4300	3600/5100	0.99
Poly(ethyl acrylate)	4400	3500/3700	1.22
Poly(methyl methacrylate)	3800	3400/6900	0.74
Poly(propylene oxide)	3700	2300/4200	1.14
Poly(dimethyl siloxane)	2400	2200/2400	1.04
Average			1.17 ± 0.23

Conversion factor: 1 bar = 10^5 N/m² = 0.987 atm.

$$\kappa = -\frac{1}{V} \left(\frac{\partial V}{\partial p} \right)_T = \frac{1}{(p + \pi) + \frac{V(0)}{RT}(p + \pi)^2} \quad (7.34)$$

The compressibility κ is the reciprocal of the compression modulus or bulk modulus of the material. This important property will be discussed in Chap. 13 (Mechanical properties of solid polymers). The application of Eq. (7.27) is restricted to polymer melts. For amorphous polymers below the melting point, the internal pressure π may be defined as well:

$$\pi = \left(\frac{\partial U}{\partial V} \right)_T = T \left(\frac{\partial p}{\partial T} \right)_V - p \quad (7.35)$$

where U is the internal energy per mole, but here π is dependent on T and p .

Values of the internal pressure for some polymers at room temperature have been mentioned by Allen et al. (1960). They appeared to be of the same order of magnitude as the cohesive energy density e_{coh} . A theoretical deviation by Voeks (1964) resulted in:

$$\pi \approx 1.3e_{coh} \quad (7.36)$$

Values of π and e_{coh} for a number of polymers are compared in Table 7.15, which shows Eq. (7.36) to be valid as a first approximation.

BIBLIOGRAPHY

General references

- Barton AFM, "Handbook of Solubility Parameters and other Cohesion Parameters", CRC Press, Boca Raton, FL, 2nd Ed, 1991
- Burke J, "Solubility Parameters: Theory and Application", The Book and Paper Group Annual, Vol 3, American Institute for Conservation, 1984.
- DuY, Xue Y and Frisch HL, "Solubility Parameters", in Mark JE (Ed), "Physical Properties of Polymers Handbook", AIP Press, Woodbury, NY, 1996, Chapter 16.
- Elias HG, "Macromolecules" 2nd Ed, Plenum Press, New York, 1984.
- Elias HG, "Theta Solvents", in Brandrup J, Immergut EH and Grulke EA (Eds), "Polymer Handbook", Part VII, p. 291, Wiley, New York, 4th Ed, 1999.
- Flory PJ, "Principles of Polymer Chemistry", Cornell Univ Press, Ithaca, NY, 1953.

- Fuchs O, "Löslichkeitstabellen von Makromolekülen", Vol 2 of Lösungsmittel und Weichmachungsmittel, 8th Ed, Wissenschaftliche Verlagsgesellschaft, Stuttgart, FRG, 1980.
- Fuchs O, "Physikalische Grundlagen und Eigenschaften der Lösungen von nieder- und hoch-molekularen Verbindungen", Vol 1 of Lösungsmittel und Weichmachungsmittel, 8th Ed, Wissenschaftliche Verlagsgesellschaft, Stuttgart, FRG, 1980.
- Fuchs O, and Suhr HH in Brandrup J, and Immergut EH, Eds, "Polymer Handbook", 2nd Ed, Wiley, Inc, New York, 1975, pp. IV-241-IV-265.
- Grulke EA, "Solubility Parameter Values", in Brandrup J, Immergut EH and Grulke EA (Eds) "Polymer Handbook", Part VII, p. 675, Wiley, New York, 4th Ed, 1999.
- Hansen CM, "Hansen Solubility Parameters: a user's handbook", CRC Press, Boca Raton, 2000.
- Hansen CM, Ind Eng Chem Prod Res Dev, 8 (1969) 2.
- Hansen CM and Beerbower A, "Solubility Parameters", in: Kirk-Othmer (Eds), "Encyclopaedia of Chemical Technology", Suppl Vol (Standen A Ed), 2nd Ed, Interscience, New York, 1971.
- Hildebrand JH and Scott RL "The Solubility of Non-electrolytes", 3rd Ed, Reinhold Publishing Corp, New York, 1950.
- Molyneux P, "Water-Soluble Synthetic Polymers", CRC Press, Boca Raton, FL, 1983.
- Morawetz H "Macromolecules in Solution", 2nd Ed, Wiley, New York, 1975.
- Orwoll RA and Arnold PA, "Polymer-Solvent Interaction Parameter χ ", in Mark JE (Ed), "Physical Properties of Polymers Handbook", AIP Press, Woodbury, NY, 1996, Chapter 14.
- Rowlinson JS and Swinton FL, "Liquids and Liquid Mixtures", 3rd Ed, Butterworth, London, 1982.
- Sundararajan PR, "Theta Solvents", in Mark JE (Ed), "Physical Properties of Polymers Handbook", AIP Press, Woodbury, NY, 1996, Chapter 15.
- Schuld N and Wolf BA, "Polymer-Solvent Interaction Parameters", in Brandrup J, Immergut EH and Grulke EA (Eds) "Polymer Handbook", Part VII, p. 247, Wiley, New York, 4th Ed, 1999.
- Tanford C, "Physical Chemistry of Macromolecules", Wiley, New York, 1961.
- Tompa H, "Polymer Solutions", Academic Press, New York, 1956.
- Weiss PH, (Ed) "Adhesion and Cohesion", Elsevier, Amsterdam, 1962.

Special references

- Allen G, Gee G, Mangaraj D, Sims D and Wilson GJ, Polymer 1 (1960) 467.
- Bagley EB, Nelson TP and Scigliano JM, J Paint Technol 43 (1971) 35.
- Beerbower A, Kaye LA and Pattison DA, Chem Eng 18 (1967) 118.
- Blanks RF and Prausnitz JM, Ind Eng Chem Fundamentals 3 (1964) 1.
- Bondi A, J Chem Eng Data 8 (1963) 371; J Polym Sci A2 (1964) 3159; "Physical Properties of Molecular Crystals, Liquids and Glasses", Wiley, New York, 1968.
- Bristow GM and Watson WF, Trans Farad Soc 43(1958) 1731.
- Bunn CW, J Polym Sci 16 (1955) 323.
- Burrell H, Official Digest 27, Nr 369 (1955), Nr 394 (1957) 1069 and 1159.
- Burrell H, in Brandrup J and Immergut EH (Eds), "Polymer Handbook", Part IV, p. 337, Interscience, New York, 2nd Ed, 1975.
- Chee KK, Malaysian J Chem 7 (2005) 57.
- Chen S-A, J Appl Polym Sci 15 (1971) 1247.
- Crowley JD, Teague GS and Lowe JW, J Paint Technol 38 (1966) 269; 39 (1967) 19.
- Di Benedetto AT, J Polym Sci A1 (1963) 3459.
- Dunkel M, Z physik Chem A138 (1928) 42.
- Fedors RF, Polym Eng Sci 14 (1974) 147.
- Foster GN, Waldman N and Griskey RG, Polym Eng Sci 6 (1966) 131.
- Fox TG, Polymer 3 (1962) 111.
- Gordy W and Stanford SC, J Chem Phys 7 (1939) 93; 8 (1940) 170; 9 (1941) 204.
- Hansen CM, Doctoral Thesis, Copenhagen, 1967.
- Hansen CM, J Paint Technol 39 (1967) 104 and 511.
- Hansen CM, Ind Eng Chem Prod Res Dev 8 (1969) 2.
- Hansen CM, Skand Tidskr Faerg Lack 17 (1971) 69.
- Hayes RA, J Appl Polym Sci 5 (1961) 318.
- Henry LF, Polym Eng Sci 14 (1974) 167.
- Hildebrand JH, J Am Chem Soc 38 (1916) 1452.
- Hoernschemeyer D, J Appl Polym Sci 18 (1974) 61.
- Hoftyzer PJ and Van Krevelen DW, Paper (Nr 111a-15) presented at the International Symposium on Macromolecules, IUPAC, Leiden (1970)
- Hoftyzer PJ and Van Krevelen DW, in "Properties of Polymers", 2nd Ed, pp. 152-155, 1976, Chapter 7.

- Hoy KL, J Paint Techn 42 (1970) 76; "Tables of Solubility Parameters", Solvent and Coatings Materials Research and Development Department, Union Carbide Corporation (1985); J Coated Fabrics, 19 (1989) 53.
- Kamal HR and Levan NT, Polym Eng Sci 13 (1973) 131.
- Koenhen DM and Smolders CA, J Appl Polym Sci 19 (1975) 1163.
- Lenz RW, Ch 1 in Chapoy LL (Ed), "Recent Advances in Liquid Crystalline Polymers", Elsevier Applied Science Publishers, London, 1985.
- Lydersen AL, "Estimation of Critical Properties of Organic Compounds", Univ Wisconsin Coll Eng Exp Stn Rep 3, Madison Wisconsin, April 1955. See also Chapter 2 in Reid RC, Prausnitz JM and Sherwood THK (Eds), "The Properties of Gases and Liquids" 3rd Ed 1977.
- NapperDH, "Polymeric Stabilization of Colloidal Dispersions", Academic Press, London, 1983.
- Patterson D, Macromolecules 2 (1969) 672.
- Patterson D and Delmas G, Discuss Faraday Soc, 49 (1970) 98.
- Qian C, Mumby SJ and Eichinger BE, Macromolecules 24 (1991) 1655.
- Rheineck AE and Lin KF, J Paint Technol 40 (1968) 611.
- Sagalaev GV, Ismailow TM, Ragimow AM, Makhmudov AA and Svyatodukhov BP, Int Polym Sci Technol 1 (1974) 76 (Russian).
- Scatchard G, Chem Revs 8 (1931) 321.
- Scott RL and Magat M, J Polym Sci, 4 (1949), 555.
- Small PA, J Appl Chem 3 (1953) 71.
- Smith RP, J Polym Sci A2, 8 (1970) 1337.
- Spencer RS and Gilmore GD, J Appl Phys 20 (1949) 21 (1950) 523.
- Van Krevelen DW, Fuel 44 (1965) 236.
- Van Krevelen DW and Hoftyzer PJ, J Appl Polym Sci 11 (1967) 2189.
- Voeks JF, J Polym Sci A2 (1964) 5319.

This page intentionally left blank

CHAPTER 8

Interfacial Energy Properties

The specific surface energy of a polymer can be estimated by means of an additive quantity, the Parachor. Alternatively, it may be calculated from the molar cohesive density (which is also additive). Rules are given for the estimation of the interfacial tension and the contact angle of a liquid on a solid.

8.1. INTRODUCTION

Surface energy is a direct manifestation of intermolecular forces. The molecules at the surface of a liquid or a solid are influenced by unbalanced molecular forces and therefore possess additional energy, in contrast with the molecules inside the liquid or solid.

In liquids the surface energy manifests itself as an internal force that tends to reduce the surface area to a minimum. It is measured in units of force per unit length, or in units of energy per unit area.

The surface of a solid, like that of a liquid, possesses additional free energy, but owing to the lack of mobility at the surface of solids this free energy is not directly observable, it must be measured by indirect methods.

The additional free energy at the interface between two condensed phases is known as *interfacial energy*.

Surface and interfacial energy are important because of their controlling influence on such practical applications as spinning, polymer adhesion, and stability of dispersions and wetting of solids by liquids.

Definitions

The *specific free surface energy* of a material is the excess energy per unit area due to the existence of the free surface; it is also the thermodynamic work to be done per unit area of surface extension. In liquids the specific free surface energy is also called *surface tension*, since it is equivalent to a line tension acting in all directions parallel to the surface.

The *specific interfacial energy* or *interfacial tension* is the excess energy per unit area due to the formation of an interface (solid/liquid; solid/vapour). The surface or interfacial tension is expressed in J/m^2 ($=N/m$) or more often in mJ/m^2 ($=mN/m$). The latter expression is identical with erg/cm^2 ($=dn/cm$) in the c.g.s. unit system. The notation is the following:

- γ_{LV} surface tension of liquid
- γ_S surface tension of solid

- γ_{SL} interfacial tension between liquid and solid
- γ_{SV} surface tension of the solid in equilibrium with the saturated vapour pressure of the liquid
- $\pi_{eq}(= \gamma_S - \gamma_{SV})$ equilibrium film pressure (NB not spreading pressure)

8.2. SURFACE ENERGY OF LIQUIDS AND MELTS

8.2.1. Methods for determining the surface tension of liquids

There are a number of independent methods for determining the surface tension of liquids. First of all there are direct methods measuring the force required to pull, for instance, a metal disk or a metal ring out of a liquid. One of the most popular quasi-static methods is that of capillary rise. Also the drop weight and the bubble-pressure methods are two related methods for measuring the surface tension that depend essentially on the excess pressure under curved surfaces. Finally there are dynamic methods, measuring the wavelength of ripples produced on a surface by a source of known frequency or measuring the period of oscillation of vibrating drops.

8.2.2. Estimation of surface tension of liquids from related properties

Since the surface tension is a manifestation of intermolecular forces, it may be expected to be related to other properties derived from intermolecular forces, such as internal pressure, compressibility and cohesion energy density. This is found to be so indeed. In the first place there exists a relationship between compressibility and surface tension. According to McGowan (1967) the correlation is:

$$\kappa\gamma^{3/2} = 1.33 \times 10^{-8} \text{ (cgs units)} \quad (8.1)$$

Another interesting empirical relationship, viz. between surface tension and solubility parameter, was found by Hildebrand and Scott (1950):

$$\delta = 4.1 \left(\gamma / V^{1/3} \right)^{0.43} \text{ (cgs units)} \quad (8.2)$$

This relationship was examined by Lee (1970) with 129 non-polar and polar liquids. Lee proved that 65% of liquids obey the equation, the major discrepancy being caused by the molar volume term in the case of hydrogen-bonded liquids.

Eq. (8.2) indicates a relationship between surface tension, cohesive energy and molar volume. A quantitative and dimensionally correct relationship between these quantities has been derived by Grunberg and Nissan (1949). For compounds of low molecular weight they defined a quantity W_{coh} , called work of cohesion:

$$W_{coh} = 2\gamma N_A^{1/3} V^{2/3} \quad (8.3)$$

where N_A is the Avogadro number. The ratio E_{coh}/W_{coh} is a characteristic constant of the liquid considered. Its value is about 3.5 for non-polar liquids and between 4 and 8 for hydrogen-bonded liquids.

8.2.3. Calculation of surface tension from an additive function; the Parachor

The molar parachor is a useful means of estimating surface tensions. It is the following additive quantity:

$$P_S = \gamma^{1/4} \frac{M}{\rho} = \gamma^{1/4} V \quad (8.4)$$

The parachor was introduced by Sugden (1924), who gave a list of atomic constants. Later the atomic and group contributions were slightly modified and improved by Mumford and Phillips (1929) and by Quayle (1953).

The conventional numerical values of the parachor and of its group contributions are expressed in $(\text{erg}/\text{cm}^2)^{1/4} \times (\text{cm}^3/\text{mol})$ which is equivalent to $(\text{mJ}/\text{m}^2)^{1/4} \times (\text{cm}^3/\text{mol})$. For obvious reasons we shall keep these numerical values unchanged, although an expression in $(\text{J}/\text{m}^2)^{1/4} \times (\text{m}^3/\text{mol})$ would be more consistent.

The group contributions to the parachor as presented by different investigators are given in Table 8.1. If the group contributions of P_S and V are known, γ results from the expression:

$$\gamma = \left(\frac{P_S}{V} \right)^4 \quad (8.5)$$

Since the parachor (P_S) is practically independent of temperature, Eq. (8.5) can also be used to calculate the temperature-dependence of the surface tension (γ).

TABLE 8.1 Atomic and structural contributions to the parachor

Unit	Values assigned by		
	Sugden	Mumford and Phillips	Quayle
-CH ₂ -	39.0	40.0	40.0
>C<	4.8	9.2	9.0
-H	17.1	15.4	15.5
-O-	20.0	20.0	19.8
-O ₂ (in esters)	60.0	60.0	54.8
>N-	12.5	17.5	17.5
-S-	48.2	50.0	49.1
-F	25.7	25.5	26.1
-Cl	54.3	55.0	55.2
-Br	68.0	69.0	68.0
-I	91.0	90.0	90.3
Double bond	23.2	19.0	16.3–19.1
Triple bond	46.4	38.0	40.6
Three-membered ring	16.7	12.5	12.5
Four-membered ring	11.6	6.0	6.0
Five-membered ring	8.5	3.0	3.0
Six-membered ring	6.1	0.8	0.8
Seven-membered ring		-4.0	4.0

P in $10^6 (\text{mN}/\text{m})^{1/4}(\text{m}^3/\text{mol})$.

8.2.4. Interfacial tension between a solid and a liquid

In Fig. 8.1, S represents a solid surface in contact with faces of liquids; the situations are supposed to continue to the left. The liquid L_1 wets the solid and tends to spread right over the surface. The *contact angle* θ is zero. In the second case (liquid L_2) the tendency to spread over the surface is less marked and the contact angle lies between 0 and $\pi/2$. The third instance (liquid L_3) is one where the liquid does not wet the surface and where the contact angle is greater than $\pi/2$, the liquid tending to shrink away from the solid.

Equilibrium contact angles of liquids on solids (see Fig. 8.2) are usually discussed in terms of *Young's equation*:

$$\gamma_{SV} = \gamma_{SL} + \gamma_{LV} \cos \theta$$

or

$$\gamma_{LV} \cos \theta = \gamma_{SV} - \gamma_{SL}$$

so that

$$\gamma_{LV} \cos \theta = (\gamma_S - \gamma_{SL}) - (\gamma_S - \gamma_{SV}) = (\gamma_S - \gamma_{SL}) - \pi_{eq} \approx \gamma_S - \gamma_{SL} \quad (8.6)$$

The assumption $\pi_{eq} \approx 0$ is allowed for normal polymeric surfaces. $\gamma_{LV} \cos \theta$ is called the *adhesion tension*. Complete wetting occurs when $\cos \theta = 1$ or $\theta = 0^\circ$. In that case the so-called spreading coefficient S , defined as:

$$S = \gamma_{LV} + \gamma_{SL} - \gamma_{SV}$$

is negative.

It is evident that wetting is favoured by relatively low interfacial free energy, high solid surface energy and low liquid surface free energy (surface tension). Unfortunately, only γ_{LV} and θ are eligible for direct experimental determination. In order to understand adhesion phenomena, however, it is essential to know γ_S and γ_{SL} . Fox and Zisman (1952) made an important approach to this problem. They found that for homologous series of liquids on a given solid a plot of $\cos \theta$ versus γ_{LV} is generally a straight line. Zisman (1962, 1963) introduced the concept of *critical surface tension of wetting* (γ_{cr}) which is defined as the value of γ_{LV} , at the intercept of the $\cos \theta - \gamma_{LV}$ – plot with the horizontal line $\cos \theta = 1$. A liquid of γ_{LV} less than γ_{cr} will spread on the surface. Numerically, γ_{cr} is nearly equal to γ_S . Fig. 8.3a gives an illustration of the method.

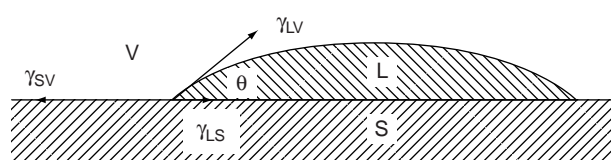


FIG. 8.1 Equilibrium in surface tensions.

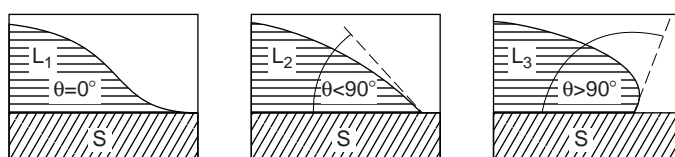


FIG. 8.2 Contact angle of different liquids on a solid.

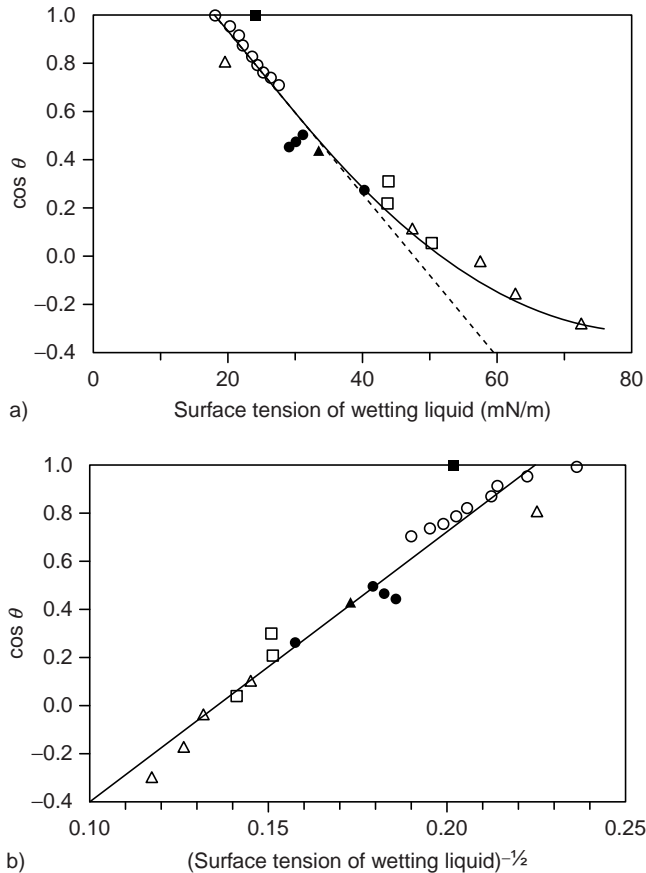


FIG. 8.3 (A) Zisman plot for polytetrafluoroethylene using various testing liquids: (○) n-alkanes; (▲) miscellaneous hydrocarbons; (●) esters; (□) non-fluoro halocarbons; (■) fluorocarbons; (△) miscellaneous liquids. From Wu (1982), based on data of Fox and Zisman (1952). Courtesy Marcel Dekker Inc. (B) Zisman plot for the materials mentioned in (A), but now $\cos \theta$ plotted vs. $\gamma^{-1/2}$.

Another approach is that of Girifalco and Good (1957–1960) who derived the following important relationship between γ_{SV} , γ_{LV} and γ_{SL} :

$$\gamma_{SL} = \gamma_{SV} + \gamma_{LV} - 2\Phi(\gamma_{SV}\gamma_{LV})^{1/2} \quad (8.7)$$

where

$$\Phi \approx \frac{4(V_S V_L)^{1/3}}{(V_S^{1/3} + V_L^{1/3})^2} \quad (8.8)$$

Combining Eqs. (8.6) and (8.7) results in:

$$\gamma_S = \frac{[\gamma_{LV}(1 + \cos \theta) + \pi_{eq}]^2}{4\Phi^2 \gamma_{LV}} \approx \gamma_{LV} \frac{(1 + \cos \theta)^2}{4\Phi^2} \quad (8.9)$$

$$\cos \theta = 2\Phi \left(\frac{\gamma_S}{\gamma_{LV}} \right)^{1/2} - 1 - \frac{\pi_{eq}}{\gamma_{LV}} \approx 2\Phi \left(\frac{\gamma_S}{\gamma_{LV}} \right)^{1/2} - 1 \quad (8.10)$$

By means of Eq. (8.9) the surface tension of the solid can be calculated from measurements of the contact angle. If γ_S is known, Eq. (8.7) provides the possibility of calculating the interfacial tension γ_{SL} . The contact angle can be predicted for solid–liquid systems by means of Eq. (8.10).

8.3. SURFACE ENERGY OF SOLID POLYMERS

8.3.1. Methods to determine surface tension of solids

Three ways are available for the estimation of γ_S , the surface tension of the solid. The first is the method measuring the contact angle between the solid and different liquids and applying Eq. (8.9). The second is the determination of γ_{cr} according to Zisman (1964), with the assumption that $\gamma_S \approx \gamma_{cr}$. The third way is the extrapolation of surface tension data of polymer melts to room temperature (Roe, 1965; Wu, 1969–1971).

8.3.2. Estimation of surface tensions of solid polymers from the parachor

Due to the fact that the extrapolation of surface tensions of melts to room temperature leads to reliable values for the solid polymer, the surface tension of solid polymers may be calculated from the parachor per structural unit by applying Eq. (8.5). The molar volume of the *amorphous* state has to be used, since semi-crystalline polymers usually have amorphous surfaces when prepared by cooling from the melt. We have found that the original group contributions given by Sugden show the best correspondence with experimental values for polymers.

8.3.3. Numerical values and comparison of the different methods

Table 8.2 compares the experimental values of the surface tension of polymers (obtained by different methods) and the calculated values, the latter being obtained by means of the parachor. The discrepancies between the different experimental values are reasonably small. The calculated values are, with a few exceptions, in reasonable agreement with the experimental values.

If no experimental data are available, calculation by means of the group contributions to the parachor gives a reliable approximation. A still higher accuracy can be reached if the methods of “standard properties” or “standard substances”, discussed in Chap. 3, are applied.

From what has been said about the surface tensions of liquids it may be expected that a relation also exists between the surface tension and the cohesive energy density of solid polymers. This proves to be so; with γ expressed in mJ/m^2 and e_{coh} in mJ/m^3 , the following empirical expression may be used:

$$\gamma \approx 0.75e_{coh}^{2/3} \quad (8.11)$$

Table 8.2 also shows γ -values calculated by means of this formula. Only the polymers with strong hydrogen bonding show rather large deviations.

TABLE 8.2 Experimental^a and calculated values of surface tension of polymers expressed in $\text{mJ/m}^2 = \text{mN/m}$

Polymer	γ_s observed			γ_s calculated		γ_{cr}^b
	Extrapolation of γ_{melt}	From contact angle	From γ_{cr}	From $\gamma = (\mathbf{P}_s/\mathbf{V})^4$ Eq. (8.5)	From $\gamma = 0.75e_{coh}^{2/3}$ Eq. (8.11)	
Polyethylene	35.7	33.2	31	31.5	30	31
Polypropylene	29.6		32	32.5	33	29
Polyisobutylene	33.6		27	30.5	31	27
Polystyrene	40.7	42	33–36	43	38	32.8
Poly(2-chlorostyrene)			42	46	40	—
Poly(vinyl fluoride)		36.7	28	32.5	30	28
Poly(vinyl chloride)		41.5	39	42	40	39
Poly(vinylidene fluoride)		32.7	25	28	26	25
Poly(vinylidene chloride)		39.9	40	47	42	40
Poly(trifluoroethylene)	30.9	23.9	22	29	24	22
Poly(trifluorochloroethylene)	30.8		31	27	30	31
Poly(tetrafluoroethylene)	22.6	19.0	18.5	26	20	18.3
Poly(hexafluoropropylene)			16–17	26	20	16.2
Poly(vinyl alcohol)			37	59		37
Poly(methyl vinyl ether)			29	32		—
Poly(vinyl acetate)	36.5		37	40	39	37
Poly(methyl acrylate)	41.0		41	45	40	—
Poly(ethyl acrylate)	37.0		35	42	38	—
Poly(methyl methacrylate)	41.1	40.2	39	42	38	39
Poly(ethyl methacrylate)	35.9		33	42	37	—
Polyacrylonitrile			50	61	57	44
Polybutadiene (<i>cis</i>)			32	32.5	34	25
Polyisoprene (<i>cis</i>)			31	35	34	31
Polychloroprene	43.6		38	43	39	38
Poly(methylene oxide)	45		38	38.5	43	43
Poly(ethylene oxide)	43		43	42	39	43
Poly(tetramethylene oxide)	31.9			31.5	35	—
Poly(propylene oxide)	32		32	32.5	38	32
Poly(ethylene terephthalate)	44.6	43	40–43	49	42	43
Nylon 6		40–47	42	47	64	42
Nylon 11		31.0	33–42	42.5	51	—
Nylon 6,6	46.5	39.3	42–46	47.5	63	42.5
Nylon 10,10		28.5	32	43	53	—
Poly(bisphenol carbonate)			45	42.5		—
Poly(dimethyl siloxane)	19.8		24	21.5		24

^a See: Dann (1970); Fowkes (1964, 1965, 1969); Lee (1967, 1970); Panzer (1973); Roe (1965); Schoenhorn et al. (1966); Wu (1971); Zisman (1962, 1963, 1964).

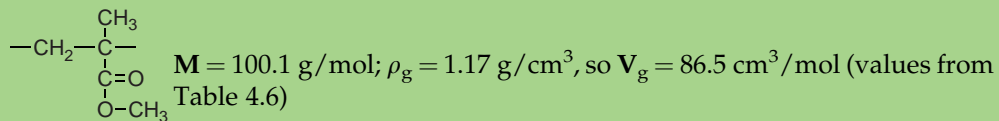
^b After Owen (1996).

Example 8.1

Estimate the surface tension of solid poly(methyl methacrylate) and its contact angle with methylene iodide ($\gamma = 50.8 \text{ mN/m}$).

Solution

The polymeric unit is:



From Table 8.1 (Sugden's values) we obtain the following group contributions to the parachor and the molar volume:

	P_s
1 $-\text{CH}_2-$	39.0
1 $>\text{C}<$	4.8
2 $-\text{CH}_3$	112.2
1 $-\text{COO}-$	64.8
	$[= 2 \times (\text{CH}_2 + \text{H}) = 2 \times (39.0 + 17.1)]$
	220.8
	$[= \text{C} + \text{O}_2 = 4.8 + 60]$
	(expressed as $(\text{mN/m})^{1/4} (\text{cm}^3/\text{mol})$)

$$\text{So } \gamma = \left(\frac{P_s}{V} \right)^4 = \left(\frac{220.8}{86.5} \right)^4 = 42.5 \text{ mN/m} = \gamma_s$$

According to Eqs. (8.10) and (8.8)

$$\cos\theta \approx 2\Phi \left(\frac{\gamma_s}{\gamma_{LV}} \right)^{1/2} - 1 \quad \text{and} \quad \Phi = \frac{4(V_s V_l)^{1/3}}{(V_s^{1/3} + V_l^{1/3})^2}$$

As calculated above, $V_s = 86.5$. For methylene iodide, $M = 267.9$ and $\rho = 3.33$, so that $V_l = 80.5$. With these values for V_s and V_l , $\Phi = 1.00$. For the contact angle with methylene iodide we find:

$$\cos\theta \approx 2 \left(\frac{\gamma_s}{\gamma_{LV}} \right)^{1/2} - 1 \approx 2 \left(\frac{42.5}{50.8} \right)^{1/2} - 1 = 0.83$$

so that $\theta \approx 34^\circ$. The adhesion tension of methylene iodide on poly(methyl methacrylate) will be:

$$\gamma_{LV} \cos \theta = 50.8 \times 0.83 \approx 42 \text{ mN/m}$$

An experimental value of $\theta = 41^\circ$ has been published by Jarvis et al. (1964). Application of Eq. (8.9) gives $\gamma_s = 39 \text{ mN/m}$, which is in good correspondence with experimental values of γ_{cr} .

8.3.4. Temperature dependence of γ

Since the parachor P_s is independent of the temperature it will be clear that

$$\gamma(T) = \gamma(298) \left[\frac{\rho(T)}{\rho(298)} \right]^4 \quad (8.12)$$

Another way to calculate γ at other temperatures is the application of a relationship found by Guggenheim (1945):

$$\gamma = \gamma(0)(1 - T/T_{cr})^{11/9} \quad (8.13)$$

so that, e.g. for PMMA the surface tension at 25 °C is equal to $65.1 \times (1 - 298/935)^{11/9} = 40.73 \text{ mJ/m}^2$ and at 100 °C equal to 34.95 mN/m.

Table 8.3 shows the values of $\gamma(0)$ and T_{cr} (the imaginary critical temperature of the polymer), as given by Wu (1982) for a number of polymers. Differentiation of Eq. (8.13) leads to

$$\frac{d\gamma}{dT} = -\frac{11}{9} \frac{\gamma(0)}{T_{cr}} (1 - T/T_{cr})^{2/9} \quad (8.14)$$

From thermodynamics it follows that $-d\gamma/dT$ is equal to the surface entropy, S^σ , per unit of area. For low values of T/T_{cr} , $d\gamma/dT$ will be approximately constant and typically of the order 0.05–0.08 mN/(m K).

8.3.5. Molecular mass dependence of γ

Two equations for the dependence of γ on M are equally well applicable (Wu (1982)):

$$\gamma = \gamma_\infty - k_e/M_n^{2/3} \quad (8.15)$$

$$\gamma^{1/4} = \gamma_\infty^{1/4} - k_s/M_n \quad (8.16)$$

The values of k_e and k_s according to Wu (1982) are also given in Table 8.3.

According to Sauer and Dee (1994) theoretical predictions show that Eq. (8.15) is appropriate for the lower molecular weights, but that for high molecular weights a M_n^{-1} dependence is more realistic. Nevertheless the difference in surface tension for low and

TABLE 8.3 Temperature and molar mass dependences of the surface tension of some polymers

Polymer	$\gamma(0)$ (mN/m)	T_c (K)	γ_∞ (mN/m)	k_s	k_e
Polyethylene (linear)	53.7	1030	36	31	386
Polyethylene (branched)	56.4	921	—	—	—
Polypropylene	47.2	914	—	—	—
Polyisobutylene	53.7	918	35	46	383
Polystyrene	63.3	967	30	75	373
Polytetrafluoroethylene	44.0	825	25	12	683
Polychloroprene	71.0	892	—	—	—
Poly-vinyl acetate	57.4	948	—	—	—
Poly-methyl methacrylate	65.1	935	—	—	—
Polydimethylsiloxane	35.3	776	21	22	166
Polyethylene oxide	—	—	43	28	343

Data from Wu (1982).

TABLE 8.4 Molecular weight dependence of the surface tension of polystyrene

M_n (g/mol)	γ (mN/m)	
	Eq. (8.15)	Eq. (8.16)
3×10^3	28.20	28.74
5×10^4	29.73	29.92
10^6	29.96	30.00

high molecular weights does in general not exceed 2 mM/m. This also follows from the results for Polystyrene in Table 8.4.

8.3.6. Influence of surface crystallinity on γ_s

When a polymer melt cools and solidifies, an amorphous surface is usually formed, although the bulk phase may be semi-crystalline. Only if the melt solidifies against a nucleating surface, a polymer surface with a certain degree of crystallinity may be obtained.

Semi-crystalline polymer surfaces may be “*trans*-crystalline” (palisades transversely to the surface), spherulitic or lamellar, depending on the rate of cooling and on the nucleating activity of the mould surface. “Low-energy” mould surfaces always give a nearly amorphous polymer surface; “high-energy” mould surfaces yield a certain degree of surface crystallinity. Polypropylene (isotactic) is a typical example. Moulded against aluminium (oxide) it develops a spherulitic surface layer (10–100 µm thickness); moulded against a teflon film it may develop a *trans*-crystalline surface; against a PETP film as mould surface and fast cooling one obtains a spherulitic surface, but with slow cooling the surface will be *trans*-crystalline. Injection moulding in a steel mould may give a lamellar surface.

The highest degree of surface crystallinity is reached if the polymer is moulded on gold foil; then the surface crystallinity is about the same as the bulk crystallinity. The smallest degree of crystallinity is reached if the surface of the melt cools down in nitrogen.

The experimental values of these extremes in surface tensions are given in Table 8.5 (data from Wu, 1982).

The following relationship gives reliable values:

$$\log(\gamma_{SC}/\gamma_a) = \frac{1}{3} f_{c,s} x_{c,max} \quad (8.17)$$

where γ_{SC} = surface tension of semi-crystalline polymer; γ_a = surface tension of amorphous polymer; $x_{c,max}$ = maximum bulk crystallinity of the polymer; $f_{c,s}$ = degree of surface crystallinity (0–1).

TABLE 8.5 Surface tensions of amorphous and semi-crystalline polymers in mN/m

Polymer	Moulded against	
	Nitrogen	Gold foil
	Surface crystallinity ~0%	Surface crystallinity ~100%
Linear polyethylene	$\gamma_s = 36.2$	$\gamma_s = 70$
Isotact. polypropylene	30.1	39.5
Poly(chlorotrifluoro ethylene)	31.1	60
Polyamide 66	46.5	74

8.4. GENERAL EXPRESSION FOR THE INTERFACIAL TENSION

Eq. (8.7) may be generalized to read:

$$\gamma_{12} = \gamma_1 + \gamma_2 - 2\Phi(\gamma_1\gamma_2)^{1/2} \quad (8.18)$$

or

$$\gamma_{12} \approx \left(\gamma_1^{1/2} - \gamma_2^{1/2} \right)^2 \quad (8.19)$$

since $\Phi \approx 1$. This equation, however, is only valid for substances without hydrogen bonds, as was demonstrated by Fowkes (1964).

Fowkes, in a theoretical consideration of attractive forces at interfaces, has suggested that the total free energy at a surface is the sum of contributions from the different intermolecular forces at the surface. Thus the surface free energy may be written:

$$\gamma = \gamma^d + \gamma^p \quad (8.20)$$

where the superscripts d and p refer to the dispersion forces and polar (or a-scalar) forces (the combined polar interactions: dipole, induction and hydrogen bonding). This results into:

$$\gamma_{12} = \gamma_1 + \gamma_2 - F \quad (8.21)$$

For the term F several suggestions were proposed:

$$F_1 = 2(\gamma_1^d\gamma_2^d)^{1/2} \quad (8.21a)$$

$$F_2 = 2(\gamma_1^d\gamma_2^d)^{1/2} + 2(\gamma_1^p\gamma_2^p)^{1/2} \quad (8.21b)$$

$$F_3 = 4\gamma_1^d\gamma_2^d / (\gamma_1^d + \gamma_2^d) + 4\gamma_1^p\gamma_2^p / (\gamma_1^p + \gamma_2^p) \quad (8.21c)$$

F_1 was introduced by Good and Girifalco (1960), F_2 by Owens and Wendt (1969) and F_3 by Wu (1971).

Substances 1 and 2 may either be liquids, solids, or a combination of a solid and a liquid.

The introduction of the frequently used F_2 leads to:

$$\gamma_{12} = \left[(\gamma_1^d)^{1/2} - (\gamma_2^d)^{1/2} \right]^2 + \left[(\gamma_1^p)^{1/2} - (\gamma_2^p)^{1/2} \right]^2 \quad (8.22)$$

If 1 and 2 are immiscible liquids of which γ_1 and γ_2 are known, and of which one is apolar ($\gamma^p = 0$), the γ -components of both liquids may be derived in the following way. The interfacial tension γ_{12} is measured by one of the available methods and the Eqs. (8.21b) and (8.20) are solved. In this way several liquids have been investigated; the values of γ_1 , γ_1^d and γ_1^p are given in Table 8.6. Analogous values for polymers are presented in Table 8.7. Owens and Wendt also gave a more general expression for Eq. (8.10) viz.:

$$1 + \cos \theta \approx \frac{2 \left[(\gamma_{SV}^d \gamma_{LV}^d)^{1/2} + (\gamma_{SV}^p \gamma_{LV}^p)^{1/2} \right]}{\gamma_{LV}} \quad (8.23)$$

This equation permits the derivation of γ_S^d and γ_S^p via measurements of the contact angles θ of two liquids if γ_{LV} , γ_{LV}^d and γ_{LV}^p of both liquids are known.

TABLE 8.6 Force components of surface tension of several liquids (after Fowkes (1964) and Owens and Wendt (1969)) (γ in mN/m)

Liquid	γ_L	γ_L^d	γ_L^P
n-Hexane	18.4	18.4	0
Dimethyl siloxane	19.0	16.9	2.1
Cyclohexane	25.5	25.5	0
Decalin	29.9	29.9	0
Bromobenzene	36.3	36.0	\approx 0
Tricresyl phosphate	40.9	39.2 \pm 4	\approx 1
Aniline	42.9	24.2	18.7
α -Bromonaphthalene	44.6	47 \pm 7	\approx 0
Trichlorobiphenyl	45.3	44 \pm 6	\approx 1.3
Glycol	48.0	33.8	14.2
Methylene iodide	50.8	49.5 \pm 1	\approx 1.3
Formamide	58.2	39.5 \pm 7	\approx 19
Glycerol	63.4	37.0 \pm 4	\approx 26
Water	72.8	21.8 \pm 0.7	51

TABLE 8.7 Components of surface energy for various solid polymers (γ in mN/m)

Polymer	γ_c	γ_s	γ^d	γ^P	Polarity (γ^P/γ_s)	$-d\gamma_s/dT$
Polyethylene-linear	31	35.7	35.7	0	0	0.057
Polyethylene-branched	33	35.3	35.3	0	0	0.067
Polypropylene-isotactic	29	30.1	30.1	0	0	0.058
Polyisobutylene	27	33.6	33.6	0	0	0.064
Polystyrene	32.8	40.7	(34.5)	(6.1)	(0.15)	0.072
Poly(α -methyl styrene)	—	39.0	(35)	(4)	(0.1)	0.058
Poly(vinyl fluoride)	28	36.7	(31.2)	(5.5)	0.15	—
Poly(vinylidene fluoride)	—	30.3	(23.3)	(7)	0.23	—
Poly(trifluoro ethylene)	22	23.9	19.8	4.1	0.17	—
Poly(tetrafluoro ethylene)	18.3	20	18.4	1.6	0.08	0.058
Poly(vinyl chloride)	39	41.5	(39.5)	(2)	(0.05)	—
Poly(vinylidene chloride)	40	45.0	(40.5)	(4.5)	(0.1)	—
Poly(chloro trifluoro ethylene)	31	30.9	22.3	8.6	0.28	0.067
Poly(vinyl acetate)	37	36.5	24.5	1.2	0.33	0.066
Poly(methyl acrylate)	—	41.0	29.7	10.3	0.25	0.077
Poly(ethyl acrylate)	—	37.0	30.7	6.3	0.17	0.077
Poly(methyl methacrylate)	39	41.1	29.6	11.5	0.28	0.076
Poly(ethyl methacrylate)	—	35.9	26.9	9.0	0.25	0.070
Poly(butyl methacrylate)	—	31.2	26.2	5	0.16	0.059
Poly(isobutyl methacrylate)	—	30.9	26.6	4.3	0.14	0.060
Poly(tert. butyl methacrylate)	—	30.4	26.7	3.7	0.12	0.059
Poly(hexyl methacrylate)	—	30.0	(27.0)	(3)	(0.1)	0.062
Poly(ethylene oxide)	43	42.9	30.9	12	0.28	0.076
Poly(tetramethylene oxide)	—	31.9	27.4	4.5	0.14	0.061
Poly(ethyleneterephthalate)	43	44.6	(35.6)	(9)	(0.2)	0.065
Polyamide 66	42.5	46.5	(32.5)	(14)	(0.3)	0.065
Poly(dimethyl siloxane)	24	19.8	19	0.8	0.04	0.048

Data from Owens and Wendt (1969) and from Wu (1982); γ_c from Owen (1996).

For apolar liquids, i.e. $\gamma_{LV}^P = 0$ and thus $\gamma_{LV} = \gamma_{LV}^d$, Eq. (8.23) reduces to

$$1 + \cos \theta = 2 \left(\frac{\gamma_s^d}{\gamma_{LV}} \right)^{1/2} \quad (8.24)$$

In that case plots of $\cos \theta$ vs. $\gamma_{LV}^{-1/2}$ should be linear which makes extrapolation to $\cos \theta = 1$ in order to determine γ_s^d easier. This is shown in Fig. 8.3b. It has to be emphasized that in this plot also polar liquids are included. Nevertheless the plot seems to be rather linear: presumably the polar part of the surface tension is only small.

Example 8.2

Estimate γ^d and γ^P of water if the following data are given:

- a. $\gamma_{H_2O} = 72.8 \text{ mJ/m}^2$ (at 20 °C)
- b. The interfacial tension cyclohexane/water is 50.2 (at 20 °C)
- c. $\gamma_{CH} = 25.5$

Solution

For cyclohexane $\gamma_{CH}^P = 0 = 0$, so that $\gamma_{CH}^d = \gamma_{CH} = 25.5 = 25.5$. From Eq. (8.21) we get:

$$\gamma_{12} = \gamma_{H_2O-CH} = 50.2 = 25.5 + 72.8 - 2(25.5 \times \gamma_{H_2O}^d)^{1/2}$$

from which it follows $\gamma_{H_2O}^d = 22.7$, so that $\gamma_{H_2O}^P = 72.8 - 22.7 = 50.1$ which is in fair agreement with the most reliable values $\gamma_{H_2O}^d = 21.8$ and $\gamma_{H_2O}^P = 51.0 \text{ mJ/m}^2$.

Example 8.3

Estimate γ_s and its components γ_s^d and γ_s^P for poly(vinyl chloride) if the following data (γ in mJ/m^2) are known:

- a. for water: $\gamma_{H_2O} = 72.8$; $\gamma_{H_2O}^d = 21.8$; $\gamma_{H_2O}^P = 51.0$
- b. for methylene iodide: $\gamma_{mi} = 50.8$; $\gamma_{mi}^d = 49.5$; $\gamma_{mi}^P = 1.3$
- c. for the contact angles on PVC: $\theta_{H_2O} = 87^\circ$; $\theta_{mi} = 36^\circ$.

Solution

Substitution of the data in Eq. (8.23) gives:

for water:

$$1 + 0.052 = 2 \frac{(\gamma_{SV}^d)^{1/2} 21.8^{1/2} + (\gamma_{SV}^P)^{1/2} 51.0^{1/2}}{72.8}$$

for methylene iodide:

$$1 + 0.809 = 2 \frac{(\gamma_{SV}^d)^{1/2} 49.5^{1/2} + (\gamma_{SV}^P)^{1/2} 1.3^{1/2}}{50.8}$$

Solution of these simultaneous equations gives: $\gamma_{SV}^d = 40.1$; $\gamma_{SV}^P = 1.5$; $\gamma_{SV} = 41.6$

It has to be emphasized that more refined approaches have been established, in particular by Van Oss and coworkers (1994). They introduced the so-called Lifschitz–Van der Waals (LW) interactions. These interactions include the dispersion or London forces (γ^L), the induction or Debye forces (γ^D) and the dipolar or Keesom forces (γ^K), so that:

$$\gamma^{LW} = \gamma^L + \gamma^D + \gamma^K \quad (8.25a)$$

Besides, they introduced a component γ^{AB} due to Lewis acid-base polar interactions (AB), which is equal to:

$$\gamma^{AB} = 2(\gamma^+ \gamma^-)^{1/2} \quad (8.25b)$$

where γ^+ and γ^- are the electron-acceptor parameter and the electron-donor parameter, respectively. The total surface energy is now equal to:

$$\gamma = \gamma^{LW} + \gamma^{AB} \quad (8.25c)$$

Table 8.8 gives results for some polymers by Van Oss (2006)

8.5. POLYMER ADHESION

A measure of the attraction of two solids S_1 and S_2 across an interface is the reversible work of adhesion W_{adh} . This quantity is given by the relationship of *Dupré*

$$W_{adh} = \gamma_{S_1} + \gamma_{S_2} - \gamma_{S_1 S_2} \approx 2 \left[(\gamma_{S_1}^d \gamma_{S_2}^d)^{1/2} + (\gamma_{S_1}^p \gamma_{S_2}^p)^{1/2} \right] \quad (8.26)$$

W_{adh} is the work required to separate S_1 and S_2 thereby creating unit areas of S_1 and S_2 surface at the expense of a unit area of $S_1 - S_2$ interface.

TABLE 8.8 Surface tension components and parameters of various polymers at 20 °C in mJ/m² (after Van Os, 2006)

Polymer	γ	γ^{LW}	γ^{AB}	γ^+	γ^-
Polyethylene	33.0	33.0	0	0	0
Polypropylene	25.7	25.7	0	0	0
Polyisobutylene	25.0	25.0	0	0	0
Polystyrene	42	42	0	0	0
Poly(vinyl chloride)	43.8	43.0	0.75	0.04	3.5
Poly(vinyl alcohol)	42	42	0	0	17–57
Poly(vinyl pyrrolidone)	43.4	43.4	0	0	29.7
Poly(methyl methacrylate)	40.0	40.0	0	0	14.6
Poly(ethylene oxide)	45.9	45.9	0	0	58.5
Poly(oxy tetramethylene)	44.0	41.4	2.6	0.06	27.6
Polyamide 6,6	37.7	36.4	1.3	0.02	21.6
Cellulose	54.5	44.0	10.5	1.6	17.2
Cellulose acetate	52.6	44.9	7.7	0.8	18.5
Cellulose nitrate	45.1	44.7	0.4	0.003	13.9

In practice it is important to know whether an adhesive joint is stable towards liquids. In this case the work of adhesion or spreading coefficient is

$$W_{\text{adh}} = \gamma_{S_1L} + \gamma_{S_2L} - \gamma_{S_1S_2} \quad (8.27)$$

If an interface $S_1 - S_2$ is immersed in a liquid L and the work of adhesion W_{adh} according to Eq. (8.27) is negative, separation of S_1 and S_2 is favoured and will occur spontaneously, since the free energy of the system is reduced by the separation. The condition for spontaneous separation is:

$$\gamma_{S_1S_2} > \gamma_{S_1L} + \gamma_{S_2L} \quad (8.28)$$

All interfacial tensions may be calculated by means of Eq. (8.21).

It must be emphasized that polymer adhesion is a complex phenomenon. The efficiency of an adhesive is only partly determined by interfacial properties. Cassidy et al. (1972) already found that effects on the glass transition temperature of the adhesive may be more important than interfacial properties. An additive that lowers T_g from a point above the test temperature to below it, causes a decrease in the strength of the system with cohesive failure within the adhesive.

Example 8.4 (after Owens (1970))

Estimate if separation occurs between coating and substrate in the case where flame-treated polypropylene film, coated with vinylidene chloride/methyl acrylate copolymer is immersed in a solution of sodium n-dodecyl sulphate (concentration 0.5%). The data of polymer, coating and liquid are the following (determined in separate experiments):

	γ^d mJ/m ²	γ^p mJ/m ²	γ
Flame-treated polypropylene	33.5	4.1	37.6
Copolymer	38.9	14.7	53.6
Sodium n-dodecyl sulphate solution	29.0	8.2	37.2

Solution

We first calculate the interfacial tensions (γ_{12}), i.e. $\gamma_{S_1S_2}$, γ_{S_1L} and γ_{S_2L} by application of Eq. (8.21), with $F=F_2$. In this way we obtain:

$$\gamma_{S_1S_2} = 37.6 + 53.6 - 2(33.5 \times 38.9)1/2 - 2(4.1 \times 14.7)1/2 = 3.5$$

$$\gamma_{S_1L} = 37.6 + 37.2 - 2(33.5 \times 29.0)1/2 - 2(4.1 \times 8.2)1/2 = 0.9$$

$$\gamma_{S_2L} = 53.6 + 37.2 - 2(38.9 \times 29.0)1/2 - 2(14.7 \times 8.2)1/2 = 1.7$$

Applying the rule (8.27) we get:

$$W_{\text{adh}} = 1.7 + 0.9 - 3.4 = -0.8.$$

Since W_{adh} is negative, accordingly separation will occur.

BIBLIOGRAPHY

General references

- Adamson AW, "Physical Chemistry of Surfaces", Wiley-Interscience, New York, 6th Ed, 1997.
- Bicerano J, "Prediction of Polymer Properties", Marcel Dekker, New York, 3rd Ed, 2002, Ch.7
- Clark DT and Feast WJ (Eds), "Polymer Surfaces", Wiley, New York, 1978.
- Danielli JF, Pankhurst KGA and Riddiford AC (Eds), "Recent Progress in Surface Science", Academic Press, New York, 1964.
- Danielli JF, Rosenberg MD and Cadehead DA (Eds), "Recent Progress in Surface and Membrane Science", Academic Press, New York, Vol 6, 1973.
- Defay R, Prigogine L, Bellemans A and Everett H, "Surface Tension and Adsorption", Wiley, New York, 1966.
- Feast WJ and Munro HS (Eds), "Polymer Surfaces and Interfaces", Wiley, Chichester, 1987.
- Feast WJ, Munro HS and Richards RW (Eds), "Polymer Surfaces and Interfaces II", Wiley, Chichester, 1993.
- Fowkes FM, In "Contact Angle, Wettability and Adhesion", Adv Chem Ser 43, Am Chem Soc 1964, p. 108.
- Fowkes FM, In "Chemistry and Physics of Interfaces", ACS, 1965.
- Fowkes FM (Ed), "Hydrophobic Surfaces", Academic Press, New York, 1969.
- Gould RF (Ed), "Interaction of Liquids at solid Substrates", Adv Chem Ser 87, Am Chem Soc, 1968.
- Hildebrand JH and Scott RL, "The Solubility of Non-electrolytes", Van Nostrand, Princeton, NJ, 1950.
- Kaelble DH, "Physical Chemistry of Adhesion", Interscience, New York, 1971.
- Lee LH (Ed), "Recent Advances in Adhesion", Gordon and Breach Science Publisher, New York, 1973.
- Lee LH (Ed), "Adhesion Science and Technology", Plenum Publishing Corp, New York, 1975.
- Lee LH (Ed), "Characterisation of Metal and Polymer Surfaces", Academic Press, New York, 1975.
- Owen MJ, "Surface and Interfacial Properties" In Mark JE (Ed), "Physical Properties of Polymers Handbook", AIP Press, Woodbury, NY, 1996, Ch 48.
- Matijević E (Ed), "Surface and Colloid Science", 2 Vols, Interscience, New York, 1969.
- Padday JF (Ed) "Wetting, Spreading and Adhesion", Academic Press, New York, 1978.
- Solc K (Ed), "Polymer Compatibility and Incompatibility; Principles and Practice", Vol 2, MMI Symp Series, New York, 1982.
- Sugden S, "The Parachor and Valency", Routledge, London, 1930.
- Van Oss CJ, "Interfacial Forces in Aqueous Media", Taylor and Francis, Boca Raton, FL, 2nd Ed, 2006.
- Wu S, "Polymer Interface and Adhesion", Marcel Dekker, New York, 1982.
- Wu S, J Macromol Sci Rev Macromol Chem 10 (1974) 1.
- Wu SJ, "Surface and Interfacial Tensions of Polymers, Oligomers, Plasticizers and Organic Pigments" In Brandrup J, Immergut EH and Grulke EA (Eds) "Polymer Handbook", Part VI, p 521, Wiley, New York, 4th Ed, 1999.
- Zisman WA, In "Contact Angle, Wettability and Adhesion", Adv Chem Ser 43, Am Chem Soc 1964, pp 1–51; in Weiss P (Ed) "Adhesion and Cohesion", Elsevier, Amsterdam, 1962, pp 176–208.

Special references

- Cassidy PE, Johnson JM and Locke CE, J Adhes 4 (1972) 183.
- Dann JR, J Colloid Interface Sci 32 (1970) 302.
- Fowkes FM, Ind Eng Chem 56 (1964) 40.
- Fox HW and Zisman WA, J Colloid Sci 5 (1950) 514; 7 (1952) 109 and 428.
- Girifalco LA and Good RJ et al, J Phys Chem 61 (1957) 904; 62 (1958) 1418 and 1464 (1960) 561.
- Grunberg L and Nissan AH, Trans Faraday Soc 45 (1949) 125.
- Guggenheim EA, J Chem Phys 13 (1945) 253.
- Jarvis NL, Fox RB and Zisman WA, Adv Chem 43 (1964) 317.
- Lee LH, J Polym Sci A2, 5 (1967) 1103.
- Lee LH, J Paint Techn 42 (1970) 365.
- McGowan JC, Polymer 8 (1967) 57.
- Mumford SA and Phillips JWC, J Chem Soc 130 (1929) 2112.
- Owens DK, J Appl Polym Sci 14 (1970) 1725.
- Owens DK and Wendt RC, J Appl Polym Sci 13 (1969) 1741.
- Panzer J, J Colloid Interface Sci 44 (1973) 142.
- Quayle OR, Chem Revs 53 (1953) 439.
- Roe R-J, J Phys Chem 69 (1965) 2809; 71 (1967) 4190; 72 (1968) 2013.
- Sauer BB and Dee GT, J Colloid Interface Sci 162 (1994) 25
- Schoenborn H, Ryan FW and Sharpe LH, J Polym Sci A2, 4 (1966) 538.
- Sugden S, J Chem Soc 125 (1924) 1177.
- Wu S, J Colloid Interface Sci 31 (1969) 153; J Phys Chem 74 (1970) 632; J Polym Sci C 34 (1971) 19.
- Zisman WA, Ind Eng Chem 55 (1963) 19.

CHAPTER 9

Limiting Viscosity Number (Intrinsic Viscosity) and Related Properties of Very Dilute Solutions

The properties of very dilute polymer solutions are determined by the conformational states of the separate polymer molecules.

The conformational state may be expressed in molecular dimensions (e.g. the mean square end-to-end distance of a polymer molecule) or in the limiting viscosity number (intrinsic viscosity).

If the interaction forces between polymer and solvent molecules can be neglected (the so-called Θ -solution) the polymer molecule is in an unperturbed conformational state. In this situation, the molecular dimensions and the limiting viscosity number can be predicted rather accurately. For a normal dilute polymer solution, however, only approximate values of these quantities can be estimated.

9.1. INTRODUCTION

This chapter deals mainly with the properties of very dilute polymer solutions. It is under these conditions only that isolated linear polymer molecules can be studied.

An isolated linear macromolecule generally tends to assume a random coil configuration. Only for very stiff polymers a rod like configuration is assumed. Several types of measurements can be used to determine the dimensions of the random coil configuration. Conversely, if the appropriate relationships have been established, the same measurements can be used to determine the average molar mass of a given polymer.

The principal types of measurements on very dilute polymer solutions are:

1. Viscosity measurements

The results can be expressed in the limiting viscosity number (intrinsic viscosity) $[\eta]$. This quantity will be discussed further on in this chapter.

2. Light scattering measurements

This phenomenon will be treated in Chap. 10.

3. Small angle X-ray scattering (SAXS) and Small angle neutron scattering (SANS).

4. Osmotic pressure measurements.

The second virial coefficient A_2 in the osmotic pressure equations can also be used to determine random coil dimensions (see Chap. 10).

9.2. MOLECULAR DIMENSIONS OF THE CONFORMATIONAL STATE

9.2.1. Random coil statistics: Definitions of end-to-end distance

Initiated principally by Flory (1953), an extensive literature on the statistical description of macromolecular coil conformations has developed. An extensive survey has been written by Kurata and Stockmayer (1963). Detailed conformational calculations can be found in a monograph by Flory (1969). Here only some headlines can be mentioned.

In the *absence of any type of interaction*, except for the covalent binding forces which fix the length of the chain links, thus assuming completely free internal rotations, a long chain molecule obeys Gaussian or *random-flight statistics*. In such a configuration the mean square value of the end-to-end distance of the chain is given by:

$$\langle r^2 \rangle_{\text{oo}} = nl^2 \quad (9.1)$$

where n is the number of bonds and l the bond length. The double zero subscript denotes neglecting of short-range as well as long-range interactions.

Short-range interactions, i.e. those interactions between atoms or groups separated by only a small number of valence bonds, result in an effective constancy of bond angles and in torques hindering internal rotations.

A theoretical type of conformation, often referred to, is the *free-rotation model with fixed bond angles*. Then the mean square end-to-end distance is

$$\langle r^2 \rangle_{\text{or}} = b \langle r^2 \rangle_{\text{oo}} = bn l^2 \approx nl^2 \frac{1 - \cos \theta}{1 + \cos \theta} \quad (9.2)$$

where b = bond angle factor; θ = bond angle.

For a polymethylene chain, the bond angle is about 110° , so that $\cos \theta \approx -1/3$ and

$$\langle r^2 \rangle_{\text{or}} \approx 2nl^2$$

For fixed bond angles and rotations restricted by short-range interactions the polymer molecule assumes a so-called "unperturbed state" and the effective end-to-end distance becomes

$$\langle r^2 \rangle_o = \sigma^2 \langle r^2 \rangle_{\text{or}} = b\sigma^2 \langle r^2 \rangle_{\text{oo}} = s \langle r^2 \rangle_{\text{oo}} = snl^2 \quad (9.3)$$

where σ = stiffness factor:

$$\sigma^2 = \langle r^2 \rangle_o / \langle r^2 \rangle_{\text{or}} \quad (9.4)$$

$$s = \text{skeletal factor: } s = \langle r^2 \rangle_o / \langle r^2 \rangle_{\text{oo}} = b\sigma^2 \quad (9.5)$$

Both σ and s are used to characterise the flexibility of a chain molecule. In Table 9.1 σ and s are presented for some vinyl polymers.

Long-range interactions, i.e. those interactions between non-bonded groups which are separated in the basic chain structure by many valence bonds. These interactions cause the molecule to pervade a larger volume:

$$\langle r^2 \rangle = \alpha^2 \langle r^2 \rangle_o = \alpha^2 s \langle r^2 \rangle_{\text{oo}} = \alpha^2 snl^2 \quad (9.6)$$

where α is the so-called expansion coefficient.

Only in the so-called theta solvents or Θ -solvents, or more precisely under theta conditions, the volume expansion can be offset. A Θ -solvent is a specially selected poor solvent at

TABLE 9.1 Stiffness factor, σ , skeletal factor, s , and Kuhn length, A , for some vinyl polymers

Polymer	$(\langle r^2 \rangle_o/n)^{1/2}$ (nm)	σ	s	A (nm)	A/l
Polyethylene	0.385	1.77	6.27	0.96	6.2
Poly(vinyl chloride)	0.402	1.84	6.77	1.05	6.8
Poly(methyl methacrylate)	0.457	2.10	8.82	1.36	8.8
Poly(vinyl acetate)	0.462	2.12	8.99	1.39	9.0
Polystyrene	0.507	2.33	10.86	1.67	10.8
Theory	0.218	1	2	0.31	2

a particular temperature, called *theta temperature*. In these Θ -conditions the macromolecule pervades the volume of the unperturbed state, the so-called pseudo ideal state (like the Boyle point in gases). Therefore the concept of a linear macromolecule under Θ -conditions is of paramount importance in treating the properties of the macromolecule per se. Owing to thermal – or Brownian – motion the configuration of a macromolecule is constantly changing.

9.2.2. Conformational models

The methods of conformational statistics, discussed so far, had as starting point *the real polymer chain*. The aim was to relate the dimensions of the coiled polymer molecule statistically to the mutual displaceability of the chain atoms. Nearly exact relationships are obtained for a large number of freely jointed or freely rotating elements. Under conditions of restricted movability, however, the statistical equations can generally not be solved and empirical factors like s , σ and α are introduced.

To avoid the difficulty of unsolvable statistical equations, some *models of a polymer chain* have been developed. The most widely used is the *random-walk necklace model*, or *freely jointed chain model*, proposed by Kuhn (1934). It defines as a statistical element not a single chain atom but a short section of the polymer chain containing several chain atoms. The length of Sect 9.2A, the Kuhn-length, is chosen so that both its ends may be regarded as completely free joints in the chain. Now Eq. (9.1) applies again for a sufficiently large number N of elements, but at the cost of introducing a new empirical factor A . the contour length of this model must be equal to the contour length of the macromolecule, hence

$$\langle r_o^2 \rangle^{1/2} = NA^2 \quad \text{and} \quad NA = L = nl \quad \text{or} \quad \langle r_o^2 \rangle^{1/2} = AL \quad (9.7)$$

so that the length of the statistical chain element is

$$A = \frac{\langle r_o^2 \rangle^{1/2}}{L} = \frac{\langle r_o^2 \rangle^{1/2}}{nl} \quad (9.8)$$

where L is the contour length of the polymer molecule. In Table 9.1 also data for the Kuhn length of some vinyl polymers are presented. It shows that several monomeric units are needed for a Kuhn length. Some authors prefer to assume the contour length to be equal to $nl \times \cos(\theta/2) = 0.816nl$. In that case the Kuhn length is a factor 1.225 larger (see, e.g. Fetters et al., 1999, 2007).

Quite the opposite method has been used by Porod and Kratky (1949) in developing the *wormlike chain model*. A wormlike chain is a continuously bend thread like molecule. The tangent at the starting point of the thread is fixed. Upon walking along the thread the direction of the tangent will change and the cosine of the tangent angle will decrease. The *persistence length* a_p is defined as the length that has to be walked along the thread to obtain an average direction cosine equal to $1/e = 0.368$, or in other words as the length over which correlations in the direction of the tangent are lost. Kratky and Porod showed that the mean square end-to-end distance is given by

$$\langle r_o^2 \rangle = 2a_p \{L - a_p [1 - \exp(-L/a_p)]\} \quad (9.9)$$

For long chains ($L \gg a_p$) this reduces to

$$\langle r_o^2 \rangle = 2a_p L \quad (9.10)$$

This result may be compared with Eq. (9.7), from which it follows that the persistence length is equal to half the length of a statistical chain element or Kuhn length: $a_p = 1/2A$. This representation of the wormlike chain is of particular importance for the description of stiff polymers.

These polymer chain models find their application not so much in the calculation of chain dimensions as in the application of calculated chain conformations for the prediction of other properties of polymer solutions, of which the solution viscosity is the most important.

9.2.3. Quantitative relationships

We shall now consider the quantitative relationships of the isolated macromolecule and of the macromolecule in very dilute solutions.

9.2.3.1. The extended linear macromolecule

If a polymer is fully extended, its end-to-end distance is:

$$r_{\max} = nl \sin(\theta/2) \quad (9.11)$$

For a polyethylene chain, $\theta \approx 110^\circ$ and

$$r_{\max} \approx 0.816nl = 0.816l \left(\frac{M}{M} \right) Z \quad (9.12)$$

where Z = number of backbone atoms per structural unit (see Chap. 6)

For polymer chains containing other structural elements, e.g. polyamides or polyesters, a somewhat different value is calculated for the coefficient in Eq. (9.12).

9.2.3.2. The “unperturbed” random-coil macromolecule

Eq. (9.3) may be written as:

$$\langle r^2 \rangle_o^{1/2} = s^{1/2} n^{1/2} l = s^{1/2} l \left(\frac{M}{M} \right)^{1/2} Z^{1/2} \quad (9.13)$$

$\langle r^2 \rangle_o^{1/2}$ is the root-mean-square unperturbed end-to-end distance. The skeletal factor s has a value between 4 and 16 for most polymers. For polymethylene $s \approx 6.3$. The maximum extension ratio Λ_{\max} of an isolated unperturbed polymethylene molecule is therefore:

$$\Lambda_{\max} = \frac{r_{\max}}{\langle r^2 \rangle_o^{1/2}} \approx \frac{0.816}{6.5^{1/2}} \left(\frac{M}{M} \right)^{1/2} Z^{1/2} \approx 0.32 \left(\frac{M}{M} \right)^{1/2} Z^{1/2} \quad (9.14)$$

This means that a polymer coil with $Z = 2$ and a degree of polymerisation M/M of 10^4 can be extended about 50-fold. This deformability of the isolated molecule is closely related to the reversible deformability of elastomeric polymers in the bulk state.

9.2.3.3. The “normal” macromolecule in solution

The real polymer coil has a larger end-to-end distance than the unperturbed one, due to the molecular interactions with its surroundings:

$$\langle r^2 \rangle^{1/2} = \alpha \langle r^2 \rangle_o^{1/2} = \alpha s^{1/2} l \left(\frac{M}{M} \right)^{1/2} Z^{1/2} \quad (9.15)$$

The expansion factor α is a ratio varying from 1 to ~ 2 ; α is dependent on the chain length (and thus on the molar mass). An empirical approximation is the following:

$$\langle r^2 \rangle^{1/2} = K_r M^b \quad (9.16)$$

9.2.4. Other characteristic quantities of the macromolecular coil

The above-mentioned quantity $\langle r^2 \rangle^{1/2}$ is closely related to the so-called *radius of gyration* R_G , which is the root-mean-square average of the distances of the molecular segments from the centre of gravity of the coil, $\langle S^2 \rangle^{1/2}$. The interrelation of these quantities is (Flory, 1953):

$$R_G \equiv \langle S^2 \rangle^{1/2} = \left(\frac{\langle r^2 \rangle}{6} \right)^{1/2} \quad (9.17)$$

For the Θ -conditions we have:

$$R_{Go} \equiv \langle S^2 \rangle_o^{1/2} = \left(\frac{\langle r^2 \rangle_o}{6} \right)^{1/2} \quad (9.18)$$

Numerical values of these quantities can be obtained from measurements of light scattering (see Chap. 10) and of the limiting viscosity number of polymer solutions, especially in Θ -conditions. From Eq. (9.15) it follows that:

$$R_G = \alpha R_{Go} \quad (9.19)$$

9.3. THE LIMITING VISCOSITY NUMBER (INTRINSIC VISCOSITY)

9.3.1. Definitions

The viscosity of a dilute polymer solution depends on the nature of polymer and solvent, the concentration of the polymer, its average molar mass and molar mass distribution, the temperature and the rate of deformation. In the following exposition it is assumed that the rate of deformation is so low, that its influence can be neglected.

The most important characteristic quantity in very dilute solutions is the *limiting viscosity number*, which is defined as:

$$[\eta] \equiv \lim_{c \rightarrow 0} \frac{\eta - \eta_s}{\eta_s c} = \lim_{c \rightarrow 0} \frac{\eta_{\text{spec}}}{c} \quad (9.20)$$

where η is the viscosity of the solution, η_s that of the pure solvent, c the polymer concentration and η_{spec} the so-called *specific viscosity* (see nomenclature in Table 9.2). $[\eta]$ has the dimensions of a reciprocal concentration or a reciprocal density, for which cm^3/g ($= 10^{-3} \text{ m}^3/\text{kg}$) is used here. Many literature data of $[\eta]$ are expressed in dl/g , which is no longer allowed in the system of S.I. units: $1 \text{ dl/g} = 100 \text{ cm}^3/\text{g} = 0.1 \text{ m}^3/\text{kg}$.

9.3.2. Interrelationships of the limiting viscosity number

The limiting viscosity number is connected with the dimension of the isolated polymer molecule. In the first place there is the well-known empirical expression first proposed by Mark (1938) and Houwink (1940).

$$[\eta] = KM^a \quad (9.21)$$

Furthermore there is a theoretical approach which leads to

$$[\eta] = \Phi \frac{\langle r^2 \rangle_h^{3/2}}{M} \quad (9.22)$$

where $\langle r^2 \rangle_h$ = hydrodynamic equivalent mean-square end-to-end distance of the polymer molecule; Φ = proportionality constant.

TABLE 9.2 Nomenclature of solution viscosity

Common name	Name recommended by the International Union of Pure and Applied Chemistry	Symbol and defining equation
Relative viscosity	Viscosity ratio	$\eta_{\text{rel}} = \frac{\eta}{\eta_s}$
Specific viscosity		$\eta_{\text{spec}} = \eta_{\text{rel}} - 1 = \frac{\eta - \eta_s}{\eta_s}$
Reduced viscosity	Viscosity number	$\eta_{\text{rel}} = \frac{\eta_{\text{spec}}}{c}$
Inherent viscosity	Logarithmic viscosity number	$\eta_{\text{inh}} = \frac{\ln \eta_{\text{rel}}}{c}$
Intrinsic viscosity	Limiting viscosity number (Staudinger index)	$[\eta] = \left(\frac{\eta_{\text{spec}}}{c} \right)_{c \rightarrow 0} = \left(\frac{\ln \eta_{\text{rel}}}{c} \right)_{c \rightarrow 0}$

Eq. (9.22) can be derived from the Einstein equation for suspensions of solid spheres:

$$\eta = \eta_s(1 + 2.5\varphi) \quad (9.23)$$

or

$$\eta_{\text{spec}} = (\eta - \eta_s)/\eta_s = 2.5\varphi = 2.5n_p v_h/V \quad (9.24)$$

where φ is the volume concentration of the suspended particles, v_h the (hydrodynamic) volume per particle, n_p the number of particles and V the volume of the suspension. Assuming that a polymer coil behaves as a particle, and applying the material balance:

$$Vc = n_p M/N_A, \quad n_p/V = cN_A/M \quad (9.25)$$

one gets by substitution of (9.25) into (9.24):

$$\eta_{\text{spec}} = 2.5N_A c \frac{v_h}{M}$$

or

$$\lim_{c \rightarrow 0} \left(\frac{\eta_{\text{spec}}}{c} \right) = [\eta] = 2.5N_A \frac{v_h}{M} \quad (9.26)$$

Taking $k\langle r^2 \rangle_h^{3/2}$ as a measure for the hydrodynamic volume of the coil (with k as a proportionality constant), we get:

$$[\eta] = 2.5N_A \frac{v_h}{M} = 2.5N_A k \frac{\langle r^2 \rangle_h^{3/2}}{M} = \Phi \frac{\langle r^2 \rangle_h^{3/2}}{M}$$

The product of intrinsic viscosity and molecular weight is equal to

$$[\eta]M = \Phi \langle r^2 \rangle_h^{3/2} \quad (9.27)$$

which is proportional to the hydrodynamic volume of the polymer coil and independent of the kind of polymer (linear, branched, stars, ladders, etc.). This is also the basis for Gel Permeation Chromatography.

The hydrodynamic equivalent molecular dimensions can be related to the unperturbed dimensions by the introduction of a hydrodynamic expansion factor α_h . Then Eq. (9.15) reads

$$\langle r^2 \rangle_h^{1/2} = \alpha_h \langle r^2 \rangle_o^{1/2} = \alpha_h s^{1/2} l \left(\frac{M}{M} \right)^{1/2} Z^{1/2} \quad (9.28)$$

α_h appears to increase with increasing molar mass. Substitution of (9.28) into (9.22) gives

$$[\eta] = \alpha_h^3 \Phi_o \frac{\langle r^2 \rangle_o^{3/2}}{M} = \alpha_h^3 [\eta]_\Theta \quad (9.29)$$

A relation between Eqs. (9.21) and (9.29) can be derived, if it is assumed that

$$\alpha_h = C_1 M^{\epsilon/2} \quad (9.30)$$

where $C_1 = \text{constant}$. Then

$$\langle r^2 \rangle_h^{1/2} = C_2 M^{(1+\epsilon)/2} \quad (9.31)$$

where $C_2 = \text{constant}$. Substitution into Eq. (9.22) gives

$$[\eta] = KM^{(1+3\varepsilon)/2} = KM^a \quad (9.32)$$

This is the Mark–Houwink equation, where the formal dimension of K is equal to $\text{cm}^3/\text{g} \times (\text{g}/\text{mol})^a$. In general, however, K is tacitly expressed and tabulated in the same dimension as $[\eta]$ and the resulting polymer molecular weight M is then expressed in g/mol . For polydisperse polymers, M is replaced by M_v the so-called viscosity-average molar mass, so that

$$[\eta] = KM_v^a \quad (9.33)$$

Under theta conditions (unperturbed random coil), $\varepsilon = 0$, so $a = 1/2$:

$$[\eta]_\Theta = K_\Theta M_v^{1/2} \quad (9.34)$$

Combination of Eqs. (9.29) and (9.34) gives

$$[\eta] = \alpha_h^3 [\eta]_\Theta = \alpha_h^3 K_\Theta M_v^{1/2} \quad (9.35)$$

For rod-like molecules, $\varepsilon = 1$, so $a = 2$:

$$[\eta]_{\text{rod}} = K_{\text{rod}} M_v^2 \quad (9.36)$$

Besides the simple experimental relationship, Eq. (9.30), between α_h and M , quite a number of other equations have been proposed. They always contain a parameter that expresses the interaction between polymer and solvent. For a detailed discussion the reader is referred to the literature. A simple equation between α_h and M has been proposed by Stockmayer and Fixman (1963), which can be written as

$$\alpha_h^3 = 1 + BM^{1/2}/K_\Theta \quad (9.37)$$

in which B is an interaction parameter. Combination of Eqs. (9.37) and (9.35) gives the well-known *Stockmayer–Fixman equation*

$$[\eta] = K_\Theta M^{1/2} + BM \quad (9.38)$$

In its converted form

$$\frac{[\eta]}{M^{1/2}} = K_\Theta + BM^{1/2} \quad (9.39)$$

this equation is often used for the determination of K_Θ from viscosity measurements on an arbitrary polymer–solvent system.

It is interesting to note, that an analogous equation has been proposed by Krigbaum (1955). His equation reads

$$[\eta] = K_\Theta M^{1/2} + 0.5A_2 M \quad (9.40)$$

in which A_2 is the second virial coefficient for the polymer–solvent system considered. Values of A_2 may be determined by various experimental techniques, e.g. light scattering or osmometry.

Although there exists a large scatter in the experimental values of both B and A_2 , a global correspondence cannot be denied. In general, the value of the quotient B/A_2 varies

between 0.25 and 0.5. This relationship is too inaccurate, however, to be used for a prediction of the limiting viscosity number from A_2 values.

9.3.3. Prediction of the limiting viscosity number under Θ -conditions

Under Θ -conditions Eq. (9.29) reads

$$[\eta]_{\Theta} = K_{\Theta} M^{1/2} = \Phi_o \frac{\langle r^2 \rangle_o^{3/2}}{M} \quad (9.41)$$

where Φ_o is a universal constant, approximately equal to $2.5 \times 10^{23} \text{ mol}^{-1}$.

Eq. (9.41) may be used to calculate the limiting viscosity number of a theta solution, if the unperturbed dimensions of the macromolecule have been determined by some other method.

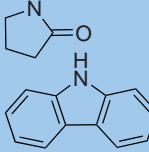
Another method for the estimation of $[\eta]_{\Theta}$ was found by Van Krevelen and Hoflyzer (1967) (see also Van Krevelen (1992) and is based on additive groups. An additive function was discovered, coined *molar intrinsic viscosity function* and defined as:

$$J = K_{\Theta}^{1/2} M - 4.2Z \quad (9.42)^1$$

where $J = \sum_i n_i J_i$; Z = number of backbone atoms per structural unit.

Table 9.3 mentions the group contribution to J . Although formally K_{Θ} has to be expressed in $\text{cm}^3 \text{ mol}^{1/2}/\text{g}^{3/2}$ it is in general expressed in the dimensions of the intrinsic viscosity, so in cm^3/g , so that J is expressed in $\text{g}^{1/4} \text{ cm}^{3/2}/\text{mol}^{3/4}$. Values of K_{Θ}

TABLE 9.3 Group contributions to the molar intrinsic viscosity function

Structural group	J_i	Structural group	J_i	Structural group	J_i
$-\text{CH}_3$	3.55	$-\text{Cl}$	12.25	$-\text{CONH}_2$	(23)
$-\text{CH}_2-$	2.35	$-\text{Br}$	(11)	$-\text{CONH}-$	12.6
$>\text{CH}-$	1.15	$-\text{CN}$	(15)	$-\text{CON}<$	(8)
$>\text{C}<$	0	$-\text{OH}$	(8)	$-\text{OCONH}-$	(25)
$-\text{CH}=\text{CH}-$	0.5	$-\text{O}-$	0.1	$-\text{SO}_2-$	(12)
$-\text{CH}=\text{C}<$	-0.65	$-\text{COOH}$	8.0	$-\text{SO}_2\text{OH}$	(18)
	10.0	$-\text{COO}-$	9.0	$>\text{Si}<$	(5)
		$-\text{COO-}(acrylic)$	6.4		
	8.0	$-\text{OCOO-}$	(27.5)		(18)
	18.25				(18)
	16.3				(41)

¹ Eq. (9.42) is the improved version of the original expression given in 1967. It was introduced in the second edition of this book. The advantage of the new version is that the numerical value of a group contribution in either backbone or side chain is equal.

TABLE 9.4 Experimental and calculated values of K_Θ ($\text{cm}^3 \text{ mol}^{1/2}/\text{g}^{3/2}$)

Polymer	M (g/mol)	z	$\sum j_i$	K_Θ	K_Θ literature	
				Calc.	from	to
Polyethylene	28	2	4.7	0.219	0.20	0.26
Polypropylene	42	2	7.05	0.135	0.12	0.18
Polybutene	56	2	9.4	0.101	0.11	0.13
Polyisobutylene	56	2	9.45	0.102	0.085	0.115
Polystyrene	104	2	21.75	0.084	0.07	0.09
Poly(α -methylstyrene)	118	2	24.15	0.076	0.064	0.084
Poly(vinyl chloride)	62.5	2	15.75	0.149	0.095	0.335
Poly(vinyl alcohol)	44	2	11.5	0.205	0.16	0.30
Poly(vinyl acetate)	86	2	16.05	0.081	0.077	0.103
Poly(methyl acrylate)	86	2	13.45	0.065	0.054	0.081
Poly(methyl methacrylate)	100	2	15.85	0.059	0.043	0.090
Polyacrylonitrile	53	2	18.5	0.258	0.20	0.25
Polymethacrylonitrile	67	2	20.9	0.191	0.22	—
Polybutadiene	54	4	5.2	0.166	0.13	0.185
Polyisoprene	68	4	7.6	0.129	0.11	0.15
Polychloroprene	88.5	4	16.3	0.140	0.095	0.135
Poly(methylene oxide)	30	2	2.45	0.131	0.132	0.38
Poly(ethylene oxide)	44	3	4.8	0.156	0.100	0.23
Poly(tetramethylene oxide)	72	5	9.5	0.179	0.18	0.33
Poly(propylene oxide)	58	3	7.15	0.116	0.105	0.125
Poly(hexamethylene succinate)	200	12	36.8	0.190	0.145	0.185
Poly(hexamethylene sebacate)	284	18	50.9	0.198	0.155	0.275
Poly(ethylene terephthalate)	192	10	39.0	0.178	0.15	0.20
Nylon 6	113	7	24.35	0.226	0.19	0.23
Polycarbonate	254	12	67.2	0.214	0.16	0.28

calculated from these group contributions generally fall within the limits of accuracy of the available literature data. A comparison between experimental and calculated K_Θ values is made in Table 9.4.

By *chain backbone* is understood the polymer chain proper without side groups and branches. For instance, all vinyl polymers have two atoms per structural unit in the chain backbone. If an aromatic ring is part of the backbone, Z is counted as follows: *o*-phenylene, Z = 2; *m*-phenylene, Z = 3; *p*-phenylene, Z = 4. For alicyclic rings the same rule is applied.

9.3.4. Prediction of the limiting viscosity number under non- Θ -conditions

An abundance of data on the limiting viscosity number of polymer solutions can be found in the literature. This is because this quantity is generally used for the determination of the molar mass of polymers. Often the molar mass is not calculated at all and the limiting viscosity number (lvn) is used to characterise the polymer.

Unfortunately these experimental data show large variations, if limiting viscosity numbers determined by different investigators on the same polymer are compared. This

is due to the use of different experimental methods and different ways of interpretation of the data. This means that an exact prediction of the limiting viscosity number of a given polymer solution is out of the question. If, conversely, a limiting viscosity number determination is to be used to calculate the molar mass of a sample, the method has to be standardised on samples of known molar mass.

So a prediction method for the limiting viscosity number can at best give the order of magnitude of this quantity. Such a method will be described on the following pages. The method is based on the empirical relationship between $[\eta]$ and M: the Mark–Houwink Eq. (9.32). In principle, the Stockmayer–Fixman Eq. (9.38) could be used as well, but the majority of the literature data has been expressed in the constant K and the exponent a of the Mark–Houwink equation.

Prediction of $[\eta]$ therefore means: prediction of a and K.

9.3.4.1. Prediction of the exponent a from solvent properties

Obviously the value a is dependent on the nature of the polymer–solvent interaction: in theta solvents $a = 0.5$, while in “good” solvents $a \approx 0.8$. Therefore some relationship between a and the solubility parameter of the solvent, δ_s , may be expected.

The most sophisticated correlation method would make use of the solubility parameter components, discussed in Chap. 7. This would mean, however, a correlation of a with six parameters:

- δ_{dP} dispersion force component for the polymer
- δ_{pP} polar component for the polymer
- δ_{hP} hydrogen bonding component for the polymer
- δ_{dS} dispersion force component for the solvent
- δ_{pS} polar component for the solvent
- δ_{hS} hydrogen bonding component for the solvent

The available experimental data prove to be insufficient for such a correlation.

The next possibility is the use of four parameters: $\delta_{vP} = \sqrt{\delta_{dP}^2 + \delta_{pP}^2}$, $\delta_{hP}, \delta_{vS} = \sqrt{\delta_{dS}^2 + \delta_{pS}^2}$ and δ_{hS} . This four-parameter method was used in Chap. 7 to correlate solubilities of polymers in solvents. As an example, some values of a are indicated in Fig. 9.1 in a δ_{vS} vs. δ_{hS} diagram for poly(methyl methacrylate). The approximate limit of the solubility region is indicated by a circle. The highest values of a are indeed found near the centre.

This method is not suited, however, for an accurate prediction of a from solubility parameter values. This may be caused by the inaccuracy of the parameter values available. For most other polymers even less data can be found in the literature. Therefore these data do not justify the use of solubility parameter components for a prediction of a .

The next logical step is to look for a correlation between a and the total solubility parameters δ_P vs. δ_S . In Fig. 9.2 literature values of a are plotted against $\delta_S - \delta_P$. The values of δ_S have been taken from Table VI (Part VII), while δ_P values have been calculated from E_{coh} in Table 7.2, calculated in its turn from group contributions.

Although Fig. 9.2 shows a considerable amount of scatter, there is a broad correlation, which may be approximated by

$$\begin{aligned} a &\approx 0.8 - 0.1 |\delta_S - \delta_P| & \text{if } |\delta_S - \delta_P| \leq 3 \\ a &= 0.5, & \text{if } |\delta_S - \delta_P| > 3 \end{aligned} \quad (9.43)$$

Large deviations from Eq. (9.43) may be found for highly crystalline polymers, such as polyethylene, and if the solvent has a much higher hydrogen bonding activity than the polymer.

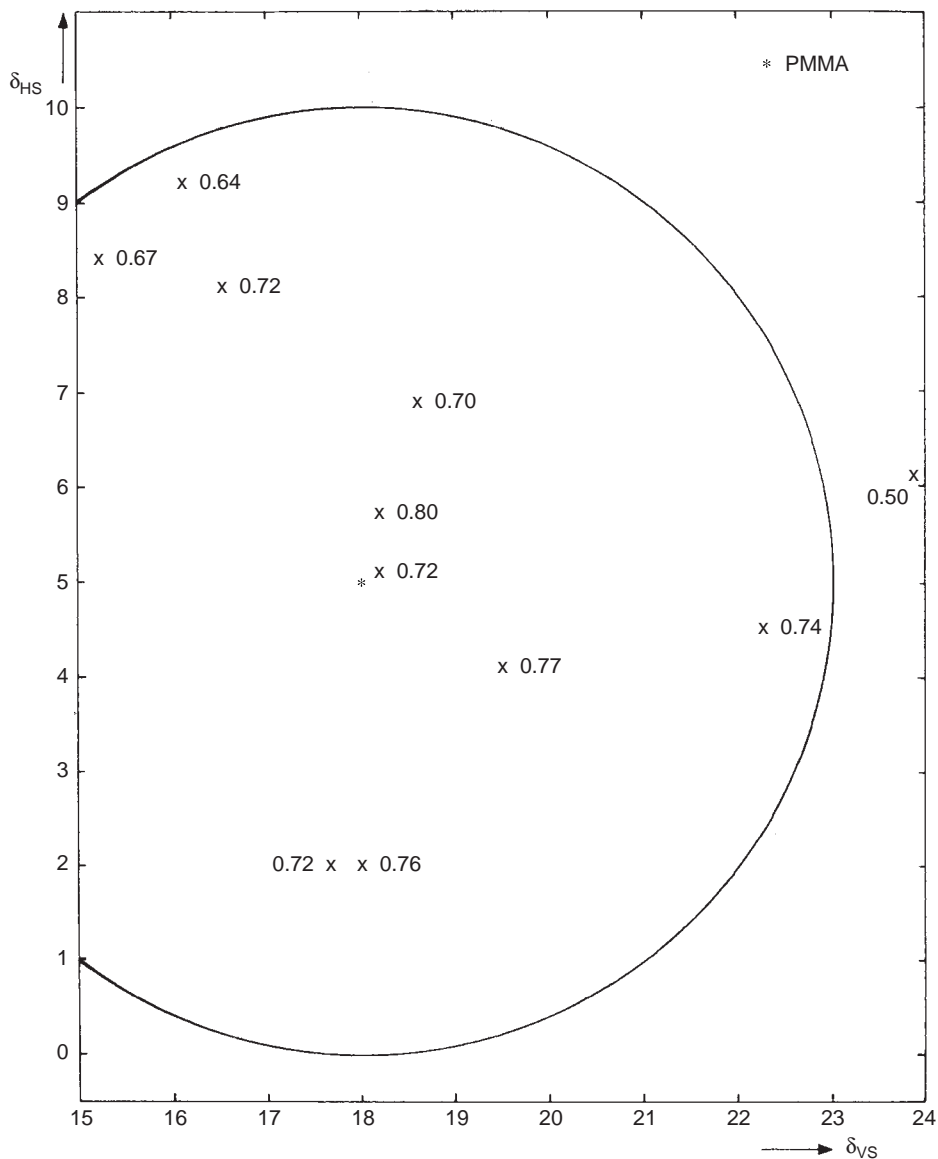


FIG. 9.1 α as a function of δ_{VS} and δ_{HS} for poly(methyl methacrylate).

In Table 9.5, calculated values of the Mark-Houwink exponent α are compared with literature values. There is a reasonable agreement, except if the solvent has hydrogen bonding properties considerably different from that of the polymer.

9.3.4.2. Prediction of K

Van Krevelen and Hoflyzer (1966, 1967) demonstrated the existence of a relationship between K and α . This could be approximated by

$$\log \frac{K_\Theta}{K} = C(\alpha - 0.5) \quad (9.44)$$

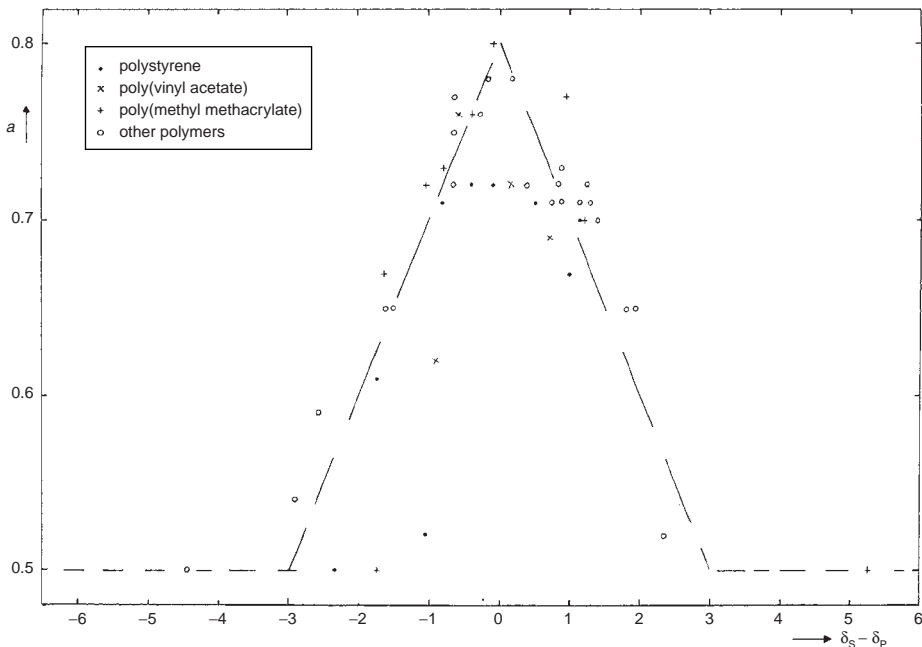


FIG. 9.2 Correlation between the exponent a and the solubility parameters.

where C is a constant, with a numerical value of 3.7 ± 0.7 . This is illustrated in Fig. 9.3 where the available literature data on limiting viscosity numbers of polystyrene solutions are plotted as $(\log K_\Theta/K)$ against a . Although Eq. (9.44) is a fair first approximation, a more accurate equation is desirable, since the average difference between experimental and estimated K -values is about 30%. For this purpose the Mark–Houwink equation will be transformed into a dimensionless form. As the reference value of M the critical molar mass M_{cr} is chosen. This is the molar mass above which molecular entanglements are assumed to play a part in the flow of a molten polymer. This quantity is discussed in Chap. 15, where an empirical relationship between M_{cr} and K_Θ is mentioned:

$$K_\Theta M_{\text{cr}}^{1/2} \approx 13 \text{ (cm}^3/\text{g)} \quad (9.45)$$

If the limiting viscosity number at the critical molecular weight is called $[\eta]_{\text{cr}}$, the Mark–Houwink equation may be written as

$$\frac{[\eta]}{[\eta]_{\text{cr}}} = \left(\frac{M}{M_{\text{cr}}} \right)^a \quad (9.46)$$

Eq. (9.46) has not yet the desired general form, as $[\eta]_{\text{cr}}$ is still dependent on the nature of the polymer–solvent system. As a reference value of the limiting viscosity number the quantity

$$[\eta]_R = [\eta]_{\text{cr},\Theta} = K_\Theta M_{\text{cr}}^{1/2} \quad (9.47)$$

is introduced. $[\eta]_R$ is the limiting viscosity number of a Θ -solution of a polymer with $M = M_{\text{cr}}$. If Eq. (9.45) holds, $[\eta]_R = 13 \text{ cm}^3/\text{g}$.

TABLE 9.5 Comparison of calculated and literature data on the limiting viscosity number (K and $[\eta]$ in m^3/kg)

Polymer	$\log M_{\text{cr}}$	$\log K_{\text{cr}}$	δ_p	Solvent	δ_s	$\log K$ literature	α literature	α calc.	$\log [\eta]$	For $M = 2.5 \times 10^5$ (g/mol)
									Literature	Calc.
Polypropylene	3.96	−0.87	17.0	Cyclohexane	16.7	−4.68 to −4.80	0.76–0.80	0.77	−0.58 to −0.48	−0.51
				Toluene	18.25	−4.66	0.725	0.675	−0.74	−0.82
				Benzene	18.65	−4.57 to −4.47	0.67–0.71	0.635	−0.85 to −0.74	−0.92
Polyisobutylene	4.20	−0.99	16.35	Cyclohexane	16.7	−4.58 to −4.40	0.69–0.72	0.765	−0.85 to −0.51	−0.73
				Carbon tetrachloride	17.7	−4.54	0.68	0.665	−0.87	−1.02
				Toluene	18.25	−4.70 to −4.06	0.56–0.67	0.61	−1.08 to −1.04	−1.13
Polystyrene	4.37	−1.07	19.05	Benzene	18.65	−4.21 to −3.97	0.50–0.56	0.57	−1.27 to −1.19	−1.20
				Cyclohexane	16.7	−4.07 to −3.97	0.48–0.50	0.565	−1.38 to −1.37	−1.31
				Butyl chloride	17.3	−4.82	0.66	0.625	−1.26	−1.13
				Ethylbenzene	17.95	−4.75	0.68	0.69	−1.08	−1.09
				Decalin	18.0	−4.17	0.52	0.695	−1.36	−1.08
				Toluene	18.25	−5.38 to −4.36	0.65–0.79	0.72	−1.12 to −0.85	−0.89
				Benzene	18.65	−5.20 to −4.38	0.60–0.78	0.76	−1.14 to −0.75	−0.88
				Chloroform	18.95	−5.31 to −4.95	0.73–0.795	0.79	−1.04 to −1.01	−0.74 ^a
				Butanone	19.0	−5.52 to −4.41	0.58–0.60	0.795	−1.28	−0.71 ^a
				Chlorobenzene	19.55	−5.13	0.75	0.75	−1.09	−0.92
				Dioxane	20.2	−4.82	0.695	0.685	−1.07	−1.10
Poly(vinyl acetate)	4.40	−1.09	19.55	Methyl isobutyl ketone	17.35	−4.35	0.60	0.58	−1.11	−1.34
				Toluene	18.25	−3.97	0.53	0.67	−1.11	−1.21
				3-heptanone	18.5	−4.09 to −4.03	0.50	0.695	−1.39 to −1.33	−1.14
				Benzene	18.65	−4.66 to −4.25	0.62–0.65	0.71	−1.15 to −0.90	−1.12
				Chloroform	18.95	−4.80 to −4.69	0.72–0.74	0.74	−0.80	−1.04
				Butanone	19.0	−4.97 to −4.38	0.62–0.71	0.745	−1.14 to −1.03	−1.03
				Ethyl formate	19.4	−4.50	0.65	0.785	−0.99	−0.84 ^a
				Chlorobenzene	19.55	−4.03	0.56	0.80	−1.01	−0.78

				Dioxane	20.2	-4.94	0.74	0.735	-0.94	-1.06
				Acetone	20.25	-5.07 to -4.61	0.68–0.74	0.73	-1.10 to -0.95	-1.07
				Acetonitrile	24.3	-4.79 to -4.38	0.62–0.71	0.50	-1.03 to -0.96	-1.44
				Methanol	29.45	-4.50 to -4.42	0.59–0.60	0.50	-1.20 to -1.23	-1.44
Poly(methyl-methacrylate)	4.70	-1.26	19.05	Butyl chloride	17.3	-4.30	0.50	0.625	-1.60	-1.45
				Methyl isobutyrate	17.4	-5.00	0.67	0.635	-1.38	-1.44
				Methyl methacrylate	18.0	-5.17	0.72	0.695	-1.28	-1.36
				Toluene	18.25	-5.15 to -5.09	0.71–0.73	0.72	-1.20 to -0.79	-1.28
				Heptanone	18.5	-4.23 to -4.20	0.48–0.50	0.745	-1.64 to -1.50	-1.22
				Ethyl acetate	18.6	-4.68	0.64	0.755	-1.22	-1.19
				Benzene	18.65	-5.42 to -4.08	0.52–0.79	0.76	-1.27 to -1.04	-1.17
				Chloroform	18.95	-5.47 to -5.02	0.78–0.83	0.79	-1.00 to -0.81	-1.03
				Butanone	19.0	-5.17 to -5.03	0.68–0.72	0.795	-1.36 to -1.26	-1.01
				Dichloroethane	20.0	-5.28 to -4.77	0.68–0.77	0.705	-1.22	-1.19
				Tetrachloroethane	20.05	-4.89	0.73	0.70	-0.95	-1.33
				Acetone	20.25	-5.61 to -5.02	0.69–0.80	0.68	-1.34 to -1.29	-1.37
				Nitroethane	22.7	-5.24	0.74	0.50	-1.24	-1.57
Polyacrylonitrile	3.40	-0.59	25.7	Acetonitrile	24.3	-4.41	0.50	0.50	-1.71–1.47	-1.57
				Dimethyl acetamide	22.45	-4.51	0.76	0.50	-0.40	-0.89
				Dimethyl formamide	24.9	-4.81 to -4.24	0.73–0.81	0.72	-0.63 to -0.30	-0.32
				Dimethyl sulfoxide	26.6	-4.49	0.75	0.71	-0.44	-0.36
				Butyrolactone	28.95	-4.47 to -4.24	0.67–0.73	0.50	-0.69 to -0.52	-0.89
Polybutadiene	3.78	-0.78	17.5	Cyclohexane	16.7	-4.95	0.75	0.72	-0.90	-0.59
				Isobutyl acetate	17.1	-3.73	0.50	0.76	-1.03	-0.43 ^a
				Toluene	18.25	-4.52 to -4.47	0.69–0.725	0.725	-0.75 to -0.60	-0.57
				Benzene	18.65	-5.07 to -4.47	0.715–0.78	0.685	-0.86 to -0.61	-0.69

(continued)

TABLE 9.5 (continued)

Polymer	$\log M_{\text{cr}}$	$\log K_{\text{cr}}$	δ_p	Solvent	δ_s	$\log K$ literature	α literature	α calc.	$\log [\eta]$	For $M = 2.5 \times 10^5$ (g/mol)
									Literature	Calc.
Polyisoprene	4.00	−0.89	17.4	Hexane	14.85	−4.17	0.58	0.545	−1.04	−1.14
				Isooctane	15.8	−4.65	0.685	0.64	−0.96	−0.96
				Toluene	18.25	−4.70 to −4.30	0.67–0.73	0.715	−0.77 to −0.70	−0.76
				Benzene	18.65	−4.73	0.74	0.675	−0.73	−0.87
Poly(ethylene oxide)	3.83	−0.80	19.3	Cyclohexane	16.7	−4.46	0.69	0.54	−0.73	−1.05
				Carbon tetrachloride	17.7	−4.16	0.61	0.64	−0.87	−0.84
				Benzene	18.65	−4.32 to −3.89	0.50–0.68	0.735	−1.19 to −0.65	−0.57
				Chloroform	18.95	−3.69	0.50	0.765	−0.99	−0.44
				Dioxane	20.2	−4.46 to −3.86	0.50–0.71	0.71	−1.16 to −0.63	−0.66
				Acetone	20.25	−3.81	0.50	0.705	−1.11	−0.67 ^a
				Dimethyl formamide	24.9	−4.62	0.73	0.50	−0.68	−1.11 ^a
				Methanol	29.45	−4.48	0.72	0.50	−0.59	−1.11 ^a
				Toluene	18.25	−4.95	0.75	0.735	−0.84	−0.78
				Benzene	18.65	−4.89	0.77	0.775	−0.79	−0.50

^a High δ_{hs} (as compared with δ_{hp}).

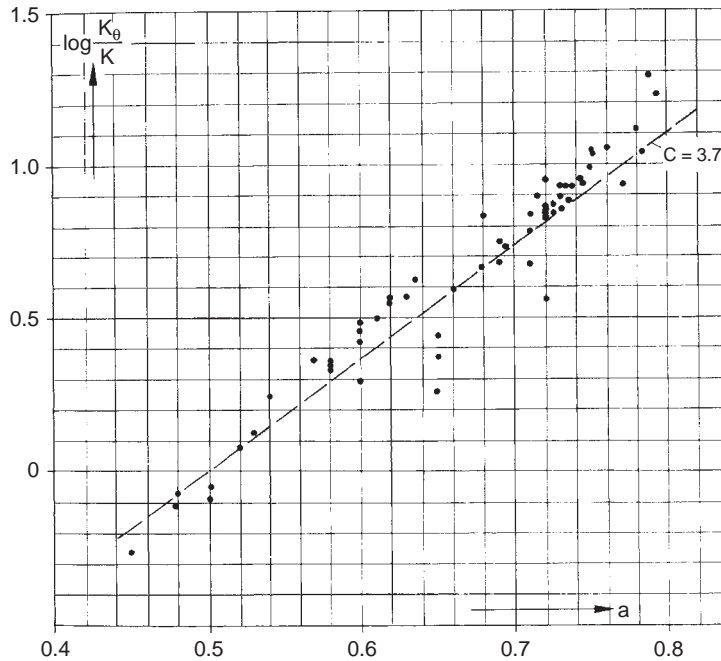


FIG. 9.3 K_{θ}/K as a function of a for polystyrene.

According to Eq. (9.29),

$$[\eta]_{\text{cr}} = \alpha_{h,\text{cr}}^3 [\eta]_R \quad (9.48)$$

so that

$$\frac{[\eta]}{[\eta]_R} = \alpha_{h,\text{cr}}^3 \left(\frac{M}{M_{\text{cr}}} \right)^a \quad (9.49)$$

where $\alpha_{h,\text{cr}}$ = hydrodynamic expansion factor at $M = M_{\text{cr}}$. This is the reduced Mark-Houwink equation, which still contains two parameters: α and α_h . Its relation to the original Mark-Houwink equation is given by:

$$K = \frac{[\eta]_R \alpha_{h,\text{cr}}^3}{M_{\text{cr}}^a} \quad (9.50)$$

Combination of Eqs. (9.47) and (9.50) leads to

$$\log \frac{K_{\theta}}{K} = (a - 0.5) \log M_{\text{cr}} - \log \alpha_{h,\text{cr}}^3 \quad (9.51)$$

Eq. (9.51) may be considered as a corrected form of Eq. (9.44), the correction factor being $\alpha_{h,\text{cr}}$. For a number of selected, reliable literature data on different polymer-solvent combinations, $\alpha_{h,\text{cr}}$ was calculated with the aid of Eq. (9.50). It appears that the quantity $\alpha_{h,\text{cr}}$

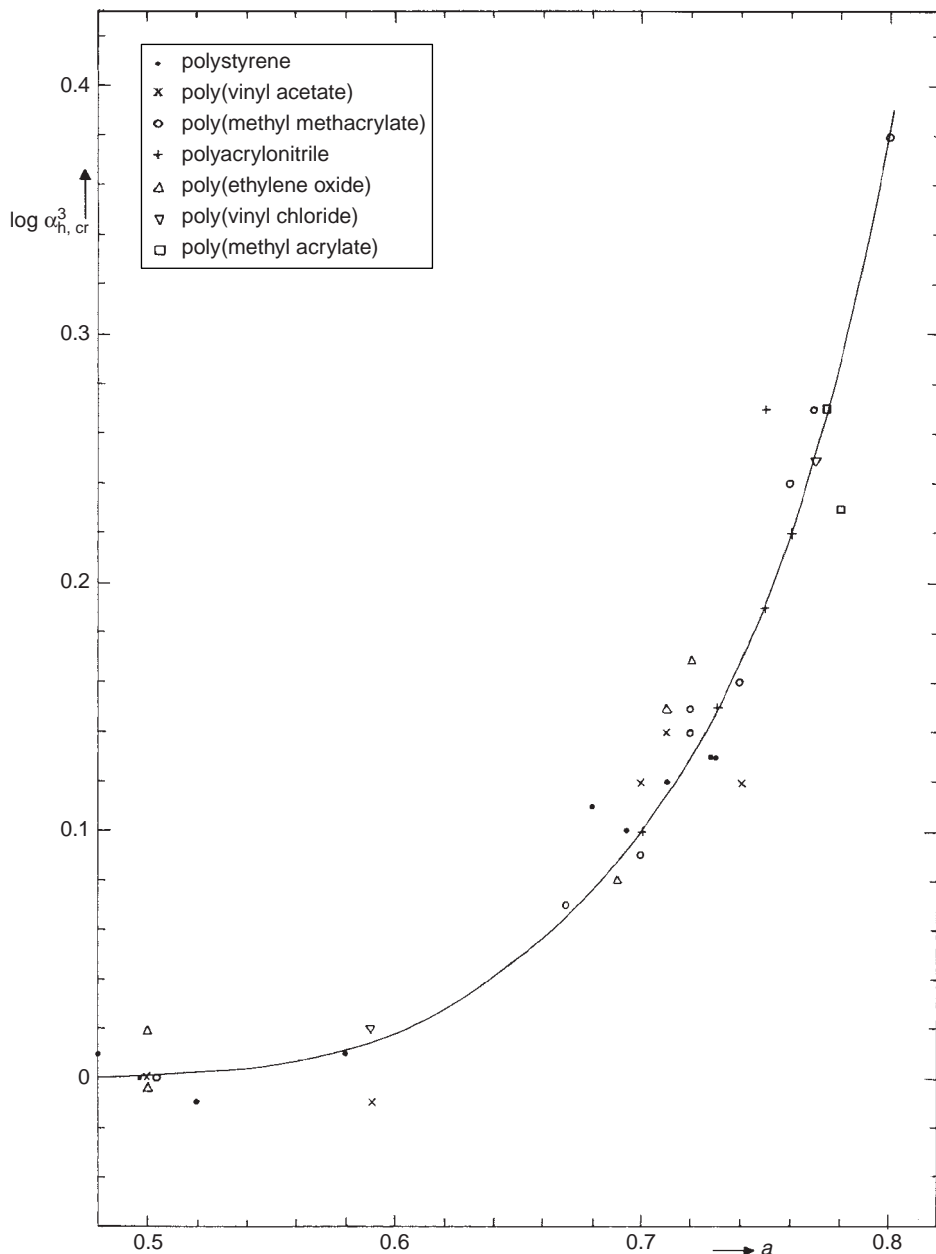


FIG. 9.4 Correlation between $\alpha_{h,cr}^3$ and a .

is correlated with a . This is shown in Fig. 9.4. By definition $\alpha_{h,cr} = 1$ for $a = 0.5$, while it increases to about 2.5 for $a = 0.8$. A good approximation of the curve in Fig. 9.4 is:

$$\log \alpha_{h,cr}^3 \approx 13(a - 0.5)^3 \quad (9.52)$$

The relationship between $\alpha_{h,cr}^3$ and a (Fig. 9.4) makes it possible to represent Eq. (9.49) graphically with only one parameter: the exponent a . Such a diagram is shown in Fig. 9.5.

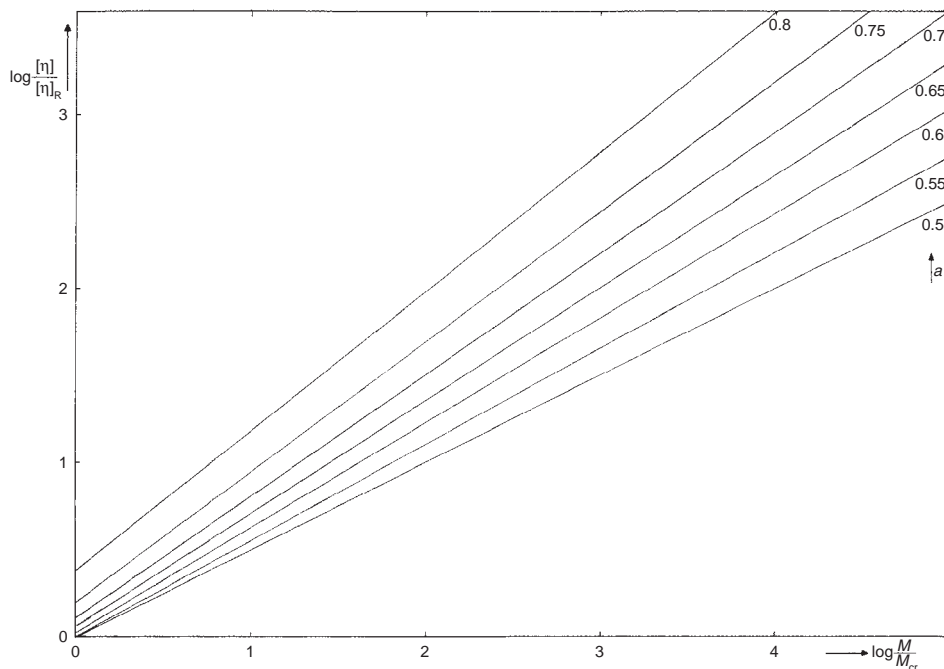


FIG. 9.5 Dimensionless representation of the Mark–Houwink equation.

A similar diagram can be derived from the Stockmayer–Fixman equation, which reads in reduced form:

$$\frac{[\eta]}{[\eta]_R} = \left(\frac{M}{M_{cr}} \right)^{1/2} + B' \frac{M}{M_{cr}} \quad (9.53)$$

where $B' = BM_{cr}/[\eta]_R$. This equation is represented in Fig. 9.6, which shows a certain resemblance to Fig. 9.5. As can be seen in Fig. 9.7, however, a correlation between a and B' is dependent on the ratio M/M_{cr} .

Eq. (9.50) in combination with Fig. 9.4 offers an interesting possibility to determine M_{cr} of a polymer; the data needed are K and a . For this purpose, Eq. (9.50) is rewritten as

$$a \log M_{cr} - \log [\eta]_R = -\log K + \log \alpha_{h,cr}^3 \quad (9.54)$$

If $\log \alpha_{h,cr}^3 - \log K$ is plotted as a function of a , the points may be connected by a straight line, the slope of which corresponds to $\log M_{cr}$. This is shown in Fig. 9.8 for polystyrene.

Table 9.5 besides values of a also compares calculated values of the limiting viscosity number of a given molar mass ($M = 2.5 \times 10^5$) with literature values. In most cases, the correct order of magnitude is predicted.

The comparison between calculated and experimental a -values is shown graphically in Fig. 9.9, while the comparison for $\log [\eta]$ (at $M = 2.5 \times 10^5$) is given in Fig. 9.10.

Example 9.1

Estimate the limiting viscosity, number of poly(methyl methacrylate) with a molar mass $M = 2.5 \times 10^5$ in toluene.

Solution**a. Estimation of α**

According to Chap. 7, $\delta_P = (E_{coh})/V^{1/2}$

The calculated value of E_{coh} in Table 7.4 is $E_{coh} = 31,300 \text{ J/mol}$. With $V = 86.5 \text{ cm}^3/\text{mol}$

$$\delta_P = \left(\frac{31,300}{86.5} \right)^{1/2} = 19.05 \text{ (MJ/m}^3\text{)}^{1/2}$$

In Table IV (part VII) we find for toluene

$$\delta_S = 18.25 \text{ (MJ/m}^3\text{)}^{1/2}$$

$\delta_P - \delta_S = 0.80$, so according to Eq. (9.43)a $\alpha = 0.80 - 0.80/10 = 0.72$.

b. Calculation of M_{cr}

Table 9.3 mentions the following values of the molar intrinsic viscosity function J_i structural group J_i

Structural group	J_i
-CH ₂ -	2.35
>C<	0
2 -CH ₃	7.1
-COO-	6.4
	15.85

$$K_\Theta^{1/2} M = 15.85 + 4.2Z = 15.85 + 8.4 = 24.25$$

$$K_\Theta = \left(\frac{24.25}{100.1} \right)^2 = 0.059 \text{ cm}^3 \text{ mol}^{1/2} / \text{g}^{3/2} \text{ (in practice } 0.059 \text{ cm}^3/\text{g} = 5.9 \times 10^{-5} \text{ m}^3/\text{kg})$$

According to Eq. (9.45)

$$M_{cr} = (13/K_\Theta)^2 = 4.9 \times 10^4$$

c. Estimation of $[\eta]$

For this purpose we use Fig. 9.5.

$$M/M_{cr} = 2.5 \times 10^5 / 4.9 \times 10^4 = 5.1$$

At this value we find by interpolation between the lines for $\alpha = 0.7$ and $\alpha = 0.75$

$$[\eta]/[\eta]_R = 4.4$$

With $[\eta]_R = 13$ we find $[\eta] = 57 \text{ cm}^3/\text{g}$

d. Estimation of K

According to Eq. (9.51) we get:

$$\log K = \log K_\Theta - (a - 0.5)\log M_{\text{cr}} + \log \alpha_{\text{h,cr}}^3$$

For $a = 0.72$ we obtain from Fig. 9.4:

$$\log \alpha_{\text{h,cr}}^3 = 0.13 \quad (\text{so that } \alpha_{\text{h,cr}}^3 = 1.10)$$

With $K_\Theta = 5.9 \times 10^{-5} \text{ m}^3/\text{kg}$ and $M_{\text{cr}} = 4.9 \times 10^4 \text{ g/mol}$ we get after substitution

$$\log K = -5.13, \text{ so } K = 7.4 \times 10^{-6} \text{ m}^3/\text{kg}$$

With the approximative Eq. (9.44) we obtain

$$\log K = -0.504, \text{ so } K = 9.1 \times 10^{-6} \text{ m}^3/\text{kg}$$

e. Comparison with literature value

In the "Polymer Handbook" we find two sets of Mark–Houwink parameters for poly(methyl methacrylate) in toluene at 25 °C

(1) $[\eta] = 7.1 \times 10^{-6} M^{0.73}$ with $M = 2.5 \times 10^5$, $[\eta] = 0.0619 \text{ m}^3/\text{kg}$

(2) $[\eta] = 8.12 \times 10^{-6} M^{0.71}$ with $M = 2.5 \times 10^5$, $[\eta] = 0.0552 \text{ m}^3/\text{kg}$

So the agreement between experimental and calculated values for K , a and $[\eta]$ is very satisfactory.

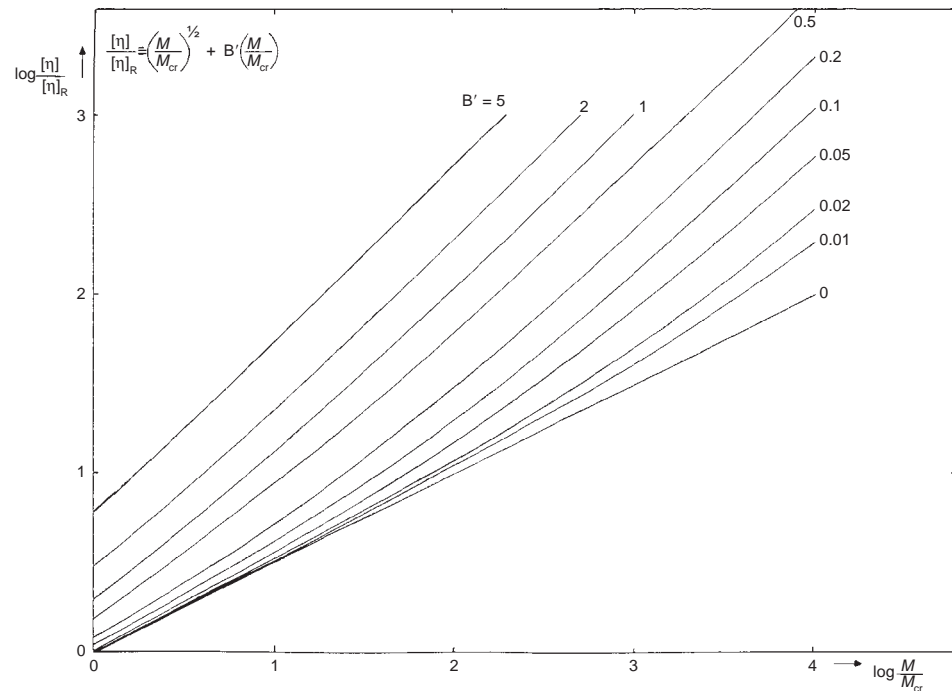


FIG. 9.6 Reduced Stockmayer–Fixman equation.

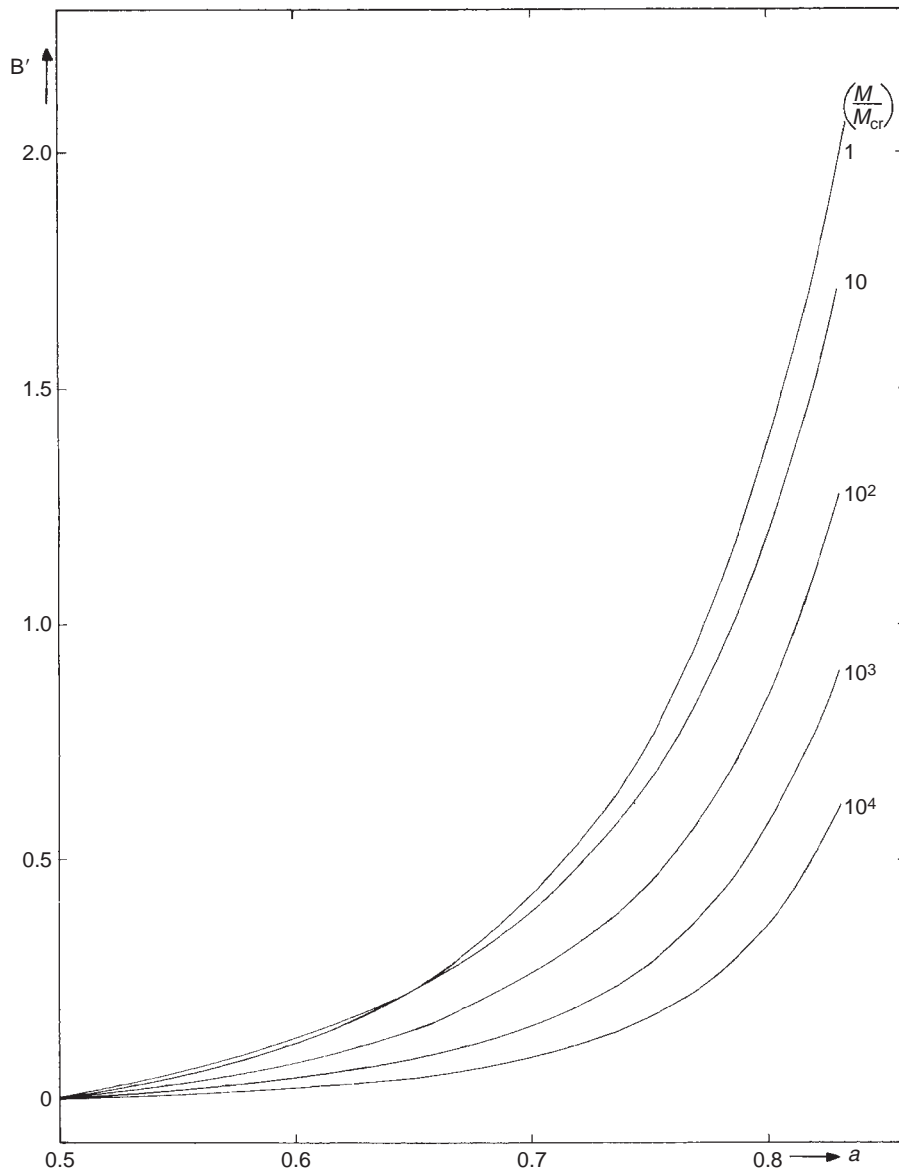


FIG. 9.7 Correlation between a and B' .

9.3.5. The “structure” of polymer solutions and the concepts of De Gennes on the conformation of polymer chains in solution and in melts

The renormalisation theory (concerning magnetic critical and tricritical phenomena) of Wilson and Kogut (1971, 1975) created at that time a new insight in phase transitions. The essence of this theory is that it allows for the effects of fluctuations on different scales. In the neighbourhood of critical transitions (in temperature and concentration) these fluctuations are causing important corrections of the classical theory.

It has been the great merit of De Gennes (1972–1979) that he initiated the application of these ideas on the statistics of polymer molecules. We shall give here a

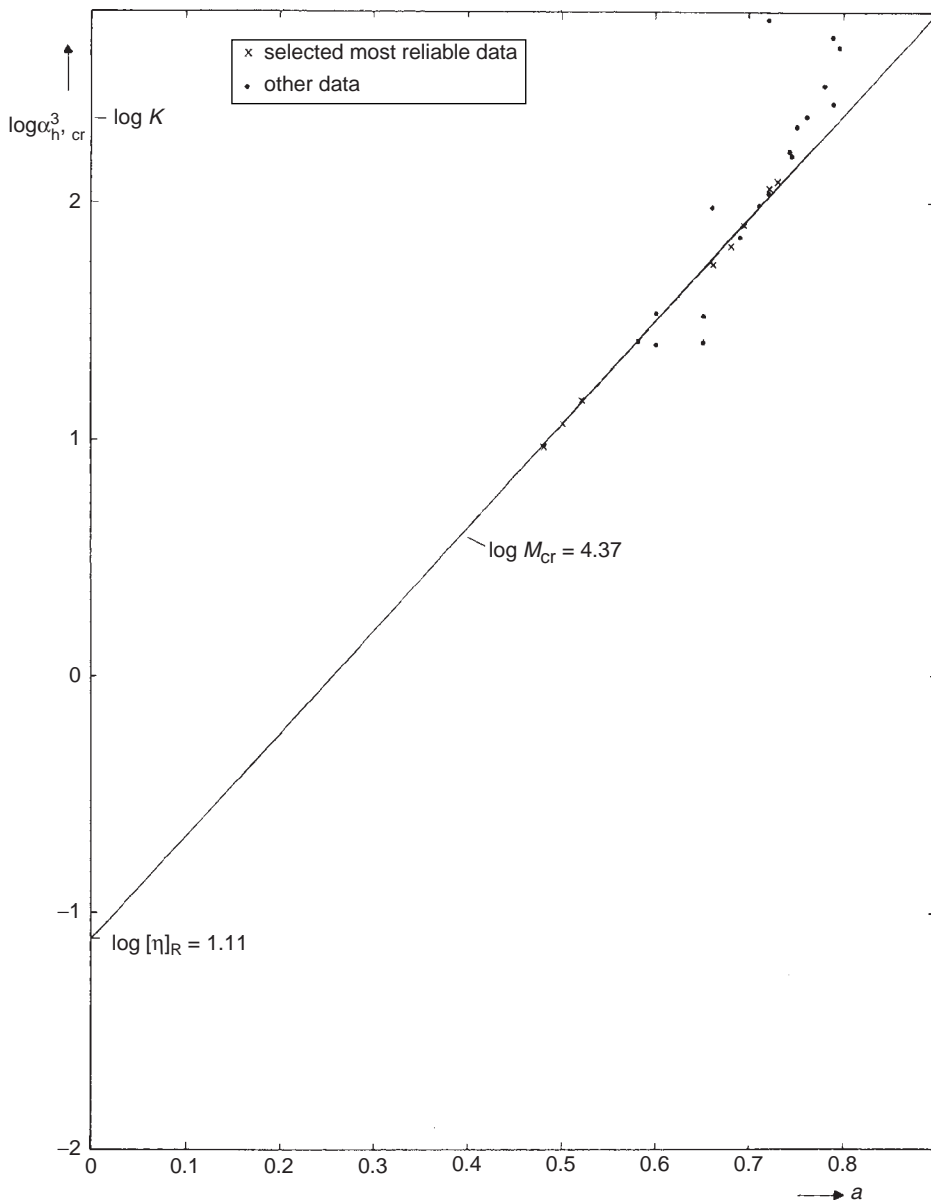


FIG. 9.8 Determination of M_{cr} for polystyrene.

very short summary of De Gennes “scaling” concepts, as much as possible in his own formulation.

De Gennes applied his method to study the chain behaviour similar to that used by Wilson (1971) to study magnetic phenomena. He pointed out that at a certain concentration the behaviour of a polymer chain is analogous to the magnetic critical and tricritical phenomena. De Gennes classifies the concentration c into three categories: the dilute solution c' , the semi-dilute solution c^* and the concentrated solution c'' . The concentration c^* is equivalent to the critical point where the crossover phenomenon occurs from randomness

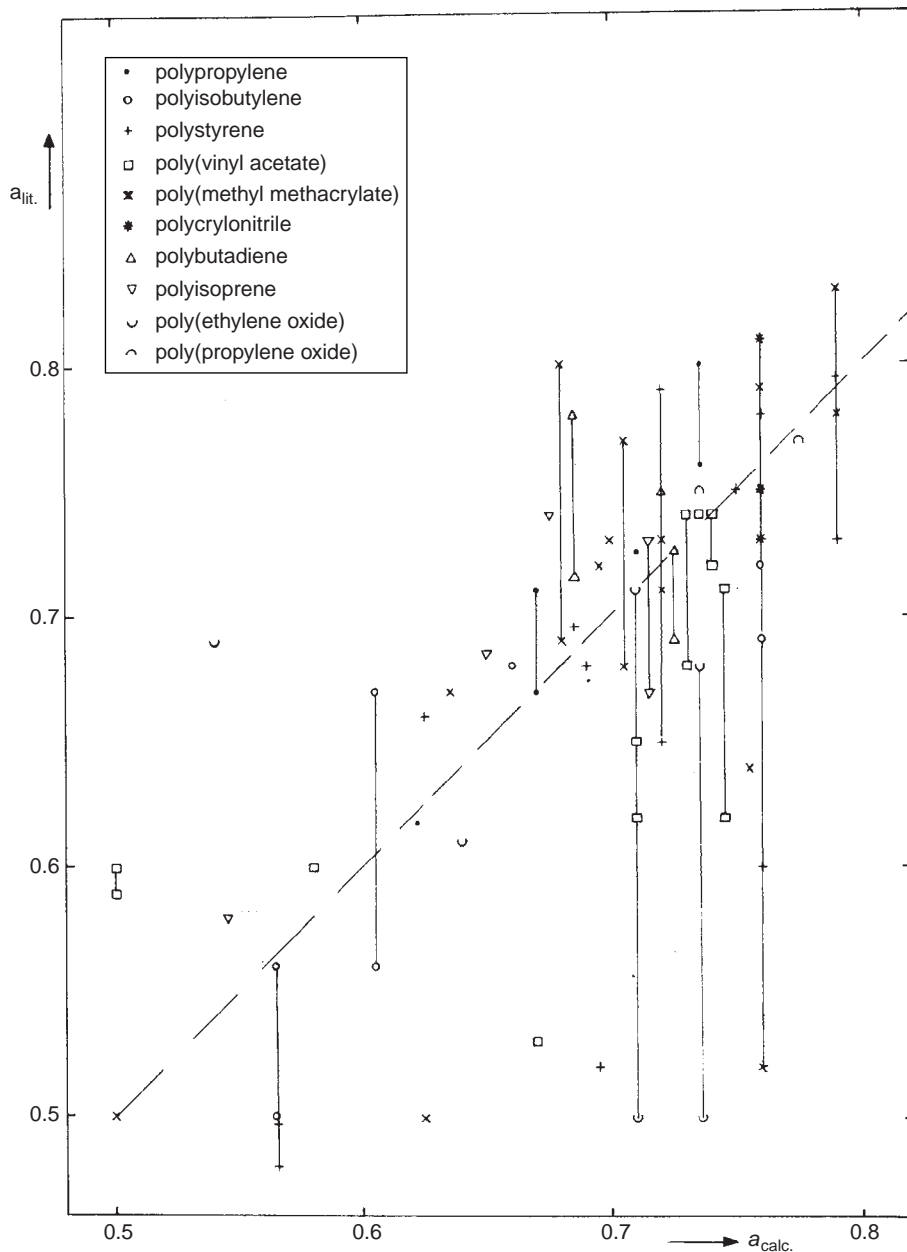


FIG. 9.9 Experimental and calculated values of a .

to order and for a typical polymer of 10^5 units of the order of $0.01 \text{ g/cm}^3 = 10 \text{ kg/m}^3$. The chain conformations in the different zones are schematically represented in Fig. 9.11. De Gennes starts with the ideal, flexible, *single chain* of a polymer. It is characterised by (1) Gaussian statistics, (2) a size proportional to $N^{1/2}$, (3) a large domain of linear relation between force and elongation, and (4) a scattering law of the q^{-2} type. How are these properties altered when we switch from the ideal to the real chain?

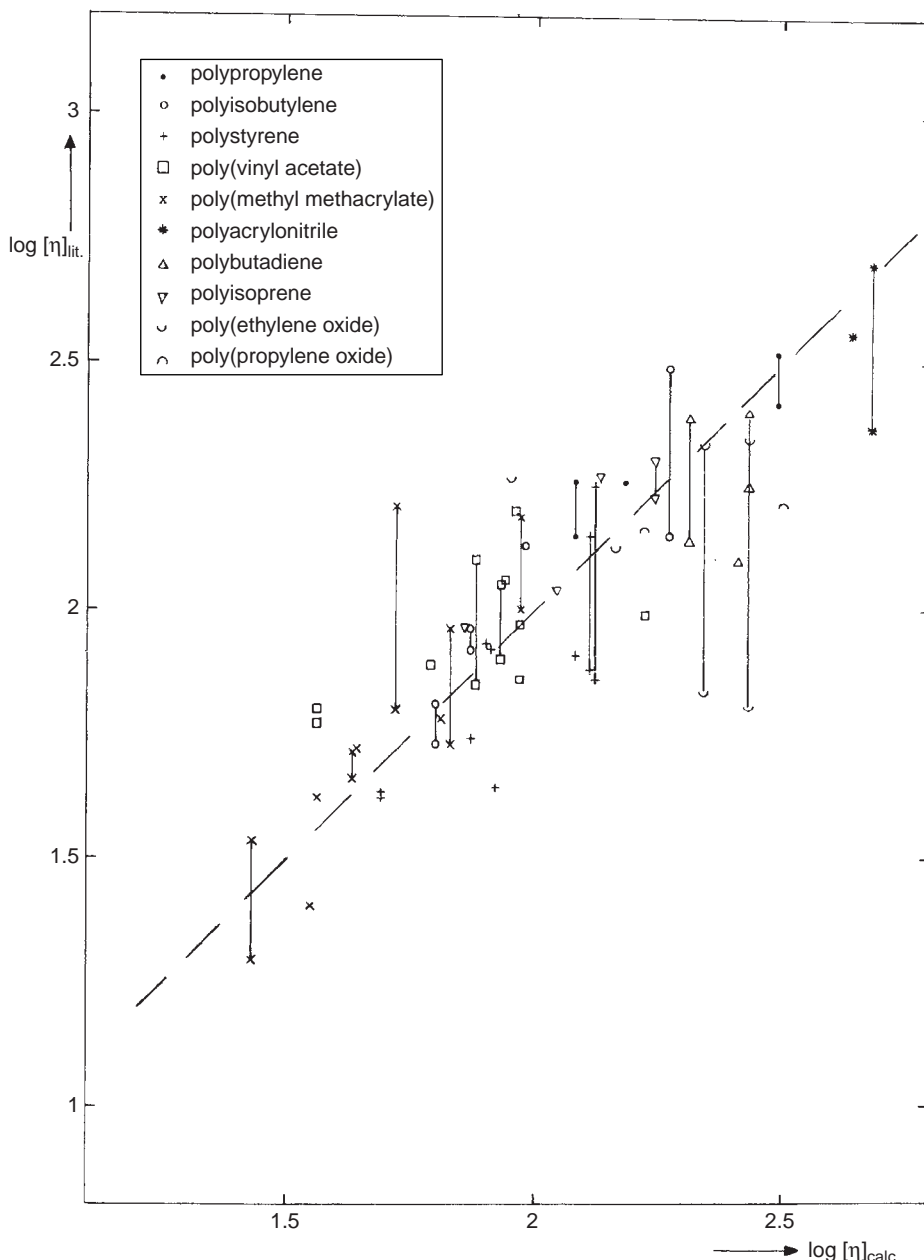


FIG. 9.10 Experimental and calculated values of $[\eta]$ (in cm^3/g for $M = 2.5 \times 10^5 \text{ g/mol}$).

Real chains in good solvents have the same universal features as *self-avoiding walks* on a lattice. These features are described by two “critical” exponents γ and v . The first is related to chain entropy, the second to chain size: a real chain has a size that is much larger than that of an ideal chain (N^v instead of $N^{1/2}$, where $v \approx 3/5$ in good solvents); in good solvents the conformation of the chain is “swollen”.

What is the dynamic behaviour of such a single chain? For uniform translations the polymer coil will behave like a Stokes sphere of the same size. The principal

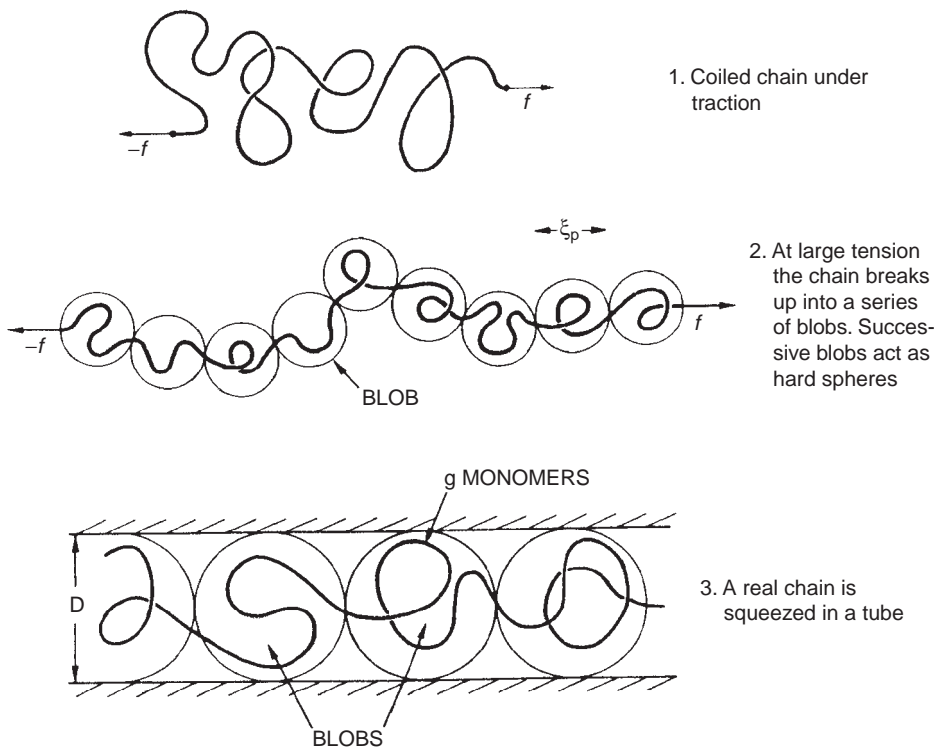


FIG. 9.11 Chain conformation in the dilute, transition and semi-dilute/concentrated regions. From De Gennes (1979). Courtesy of Cornell University Press.

relaxation mode of the coil can be described by an elastic spring constant and a friction constant of the Stokes type; the *inner modes* of the coil can be understood qualitatively as the relaxation of sub-coils. When a coiled chain is *under traction* it will, under large tensions break up into a series of subunits (*blobs*) of size or correlation length ξ . Viewed at larger scales ($r > \xi$) the conformation of the chain may be considered as a string of blobs (see Fig. 9.12).

Also if a chain would be squeezed in a thin tube it would behave as a sequence of blobs of a diameter equal to that of the tube. A polymer chain in a melt is in this situation:

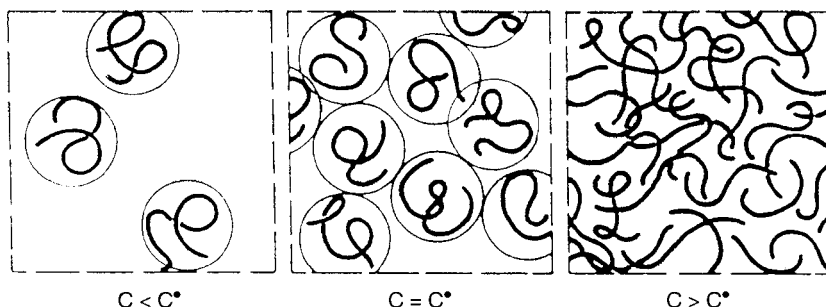


FIG. 9.12 Coiled chains and Blobs (from De Gennes (1979), courtesy Cornell University Press).

the surrounding polymer chains together form the wall of a tube; inside of this tube, formed by its neighbours, the movements of the chain, a string of blobs, is described by the "reptation" model with wiggling, snakelike motions back and forth.

Swollen polymer gels can also be visualised as a collection of adjacent blobs (a kind of network), each blob being associated with one chain and having properties very similar to those of a single chain.

The spatial scales can be distinguished into three types:

- The region between the size of the structural unit and the minimum blob size; "ideal" behaviour
- The region between the minimum and maximum blob size; non-ideal behaviour: excluded volume type
- The region between the maximum blob size and the size of the coil; ideal behaviour; a string of blobs behaves as a flexible chain

We come now to the *polymer solutions*.

A typical phase diagram (temperature versus concentration) is given in Fig. 9.13, reproduced from Daoud and Jannink (1976), elaborated by De Gennes (1979). In poor solvents flexible polymers show a *quasi-ideal* behaviour at Θ -conditions (due to cancellation effects between repulsions and attractions). In Fig. 9.13 the theta-conditions are represented by the line $T_r = 0$ (T_r = reduced temperature = $(T - \Theta)/\Theta$). The real Θ -region is indicated by I'. At slightly lower solvent quality (or temperature) phase separation occurs into a nearly pure solvent phase (containing a few very contracted chains, and a polymer rich phase). The dashed curve in the negative region of T_r (region IV) is a coexistence or phase-separation region. Region I is the dilute region, limited by a T_r -value proportional to R_G^{-1} and the c^* curve. c^* is the *critical concentration* at which the chains begin to overlap, also proportional to R_G^{-1} , and thus proportional to $N^{-0.8}$; for

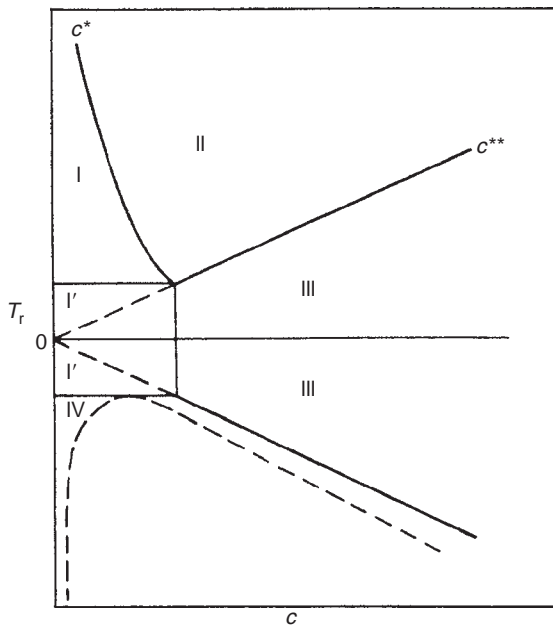


FIG. 9.13 Typical phase diagram of a polymer solution (from Daoud and Jannink, 1976).

a large N value c^* is quite small ($\approx 10^{-3}$ g/cm³). Region III is the semi-dilute and concentrated θ region. The regions II and III are separated by the c^{**} line, which is proportional to T_r .

9.3.6. The Rudin equations

Some very useful equations on dilute polymer solutions were derived by Rudin and co-workers (1976–1982).

Rudin's aim was to predict the size of dissolved polymer molecules and the colligative properties of polymer solutions (hydrodynamic volume, second virial coefficient, interaction parameter, osmotic pressure, etc.) from viscometric data (average molar mass, intrinsic viscosity, etc.).

Rudin combined Flory's theory of the dimension of polymer coils with Zimm's expression (Zimm, 1946) for the second virial coefficient in a dilute suspension of uniform spheres. He further assumed that the swelling factor (ε) of the polymer coil (identical to α^3 in Flory's formalism) reduces to 1 at a certain critical concentration c_x , whereas it tends to a value ε_0 ($= [\eta]/[\eta]_\Theta$) at infinite dilution. The functional relation between ε and c^* , would therefore be

$$\frac{1}{\varepsilon} = \frac{1}{\varepsilon_0} + \frac{c}{c^*} \frac{\varepsilon_0 - 1}{\varepsilon_0} \quad (9.55)$$

For the critical concentration Rudin derived

$$c^* = \frac{3\varphi'}{4\pi N_A [\eta]_\Theta} = \frac{1.24}{[\eta]_\Theta} \text{ kg/m}^3 \quad (9.56)$$

where $\varphi' = 3.1 \times 10^{24}$ mol⁻¹ (according to Flory); $N_A = 6.023 \times 10^{23}$ mol⁻¹ (Avogadro's number)

Rudin gives the following basic equations (for $c < c_x$):

a. Swelling factor

$$\varepsilon = \frac{[\eta]}{[\eta]_\Theta} \frac{3\varphi'}{3\varphi' + 4\pi N_A c([\eta] - [\eta]_\Theta)} \approx \frac{[\eta]}{[\eta]_\Theta} \frac{1}{1 + 0.81c([\eta] - [\eta]_\Theta)} \quad (9.57)$$

b. Hydrodynamic swollen volume

$$v_h = \frac{1.35 \times 10^{-24} [\eta] M}{1 + 0.81c([\eta] - [\eta]_\Theta)} \quad (9.58)$$

c. Osmotic second virial coefficient

$$A_2 = \frac{16\pi N_A [\eta]}{M[3\varphi' + 4\pi N_A c([\eta] - [\eta]_\Theta)]} \left(1 - \frac{[\eta]_\Theta}{[\eta]}\right) \approx \frac{3.24([\eta] - [\eta]_\Theta)}{M[1 + 0.81c([\eta] - [\eta]_\Theta)]} \quad (9.59)$$

where A_2 is expressed in mol cm³/g², M in g/mol, c in g/cm³ and $[\eta]$ in cm³/g or A_2 in mol m³/kg², M in kg/mol, c in kg/m³ and $[\eta]$ in m³/kg.

By means of the last mentioned equation the following expressions lead to the other required data:

d. Osmotic pressure π

$$\pi = RTc \left(\frac{1}{M_n} + A_2 c + A_3 c^2 + \dots \right) \approx \frac{RTc}{M_n} \left(1 + \frac{1}{2} A_2 M_n c \right)^2 \quad (9.60)$$

e. The Flory–Huggins interaction parameter (χ)

$$\chi = \frac{1}{2} - \frac{A_2 \mathbf{M}^2}{\mathbf{V}_s} \quad (9.61)$$

where π is expressed in N/m² if R is expressed in J/(mol K), c in kg/m³ and M_n in kg/mol, and \mathbf{M} = molecular weight of monomeric unit (g/mol or kg/mol); \mathbf{V}_s = molar volume of the solvent (cm³/mol or m³/mol).

Although these equations have been developed quite a long time ago, their advantage is that they are easy to handle.

Example 9.2

Calculate the for solutions in chlorobenzene of polystyrenes with molar weights of 2×10^5 , 5×10^5 and 10^6 g/mol the intrinsic viscosity, the critical concentration, the swelling factor, the hydrodynamic swollen volume, the second virial coefficient and the Flory–Huggins interaction parameter.

Solution

From Table 9.5 it follows for the constants a and K :

Θ -solvent $K = 10^{-4.07} = 8.5 \times 10^{-5}$ m³/kg and $\frac{1}{2}$

Chlorobenzene $K = 10^{-5.13} = 7.41 \times 10^{-6}$ m³/kg, $a = 0.75$ and $\mathbf{V}_s = 101.7 \times 10^{-3}$ m³/mol

The various values can be calculated by substitution in Eqs. (9.56)–(9.60).

Results, where $B = 1 + 0.81c([\eta] - [\eta]_\Theta)$ are the following:

M (kg/mol)	$[\eta]_\Theta$ (m ³ /kg)	$[\eta]$ (m ³ /kg)	c^* (kg/m ³)	B	ε	v_h (10 ²⁴ m ³)	A_2 (mol·m ³ /kg ²)	χ
200	0.0381	0.0701	32.5	$1 + 0.026c$	1.84/B	18.9/B	$5.18 \times 10^{-4}/B$	0.4448
500	0.0601	0.1393	20.6	$1 + 0.064c$	2.32/B	94.0/B	$5.13 \times 10^{-4}/B$	0.4454
1000	0.0851	0.2343	14.7	$1 + 0.121c$	2.32/B	316/B	$4.83 \times 10^{-4}/B$	0.4486

9.3.7. Polymers with special characteristics

9.3.7.1. Branched polymers

The dilute solution properties of branched polymers differ from those of linear polymers of the same composition. Generally, the Mark–Houwink exponent a is lowered by branching (Zimm and Stockmayer, 1949; Zimm and Kilb, 1959). The relationship

between the intrinsic viscosities of linear and branched polymer of the same molecular weight is

$$[\eta]_b / [\eta]_l = g^{3/2} \quad (9.62)$$

where the branching index g , defined as

$$g = \langle S_b^2 \rangle / \langle S_l^2 \rangle \quad (9.63)$$

is strongly dependent on the functionality of the branching points and their distribution.

For determining the molar mass of branched polymers gel permeation chromatography can be used. An important quantity in this connection is the hydrodynamic volume of the polymer coil, which, as shown before in Eq. (9.27), is proportional to the product $[\eta]M$. According to Benoit and co-workers (1966) the hydrodynamic volume is the key size parameter in the establishment of a universal calibration curve for gel permeation chromatography columns (see Chap. 2): if $\log ([\eta]M)$ is plotted versus the elution volume for a variety of polymers, the data fit a single curve.

For linear and branched molecules having the same hydrodynamic volume or elution volume, it follows that the products of their intrinsic viscosities and molar masses can be equated:

$$M_l[\eta]_l = M_b[\eta]_b \text{ (at constant elution volume!)} \quad (9.64)$$

The procedure to determine the molecular weight of a branched polymer is as follows. If for a certain GPC column the universal calibration curve is measured with the aid of a series of monodisperse linear polymers of known molecular weight, the next step is to determine the elution volume and the intrinsic viscosity of the unknown branched fraction. Then the product $[\eta]M$ corresponding to the mean elution volume of a branched fraction is read from the universal calibration curve; this value divided by the determined intrinsic viscosity gives the molar mass of the fraction. At the same molar mass one can also calculate the intrinsic viscosity of the linear polymer by using the Mark–Houwink equation.

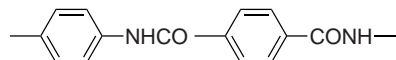
9.3.7.2. Rod-like polymer molecules

The dilute solution properties of polymers discussed so far had to do with randomly coiled macromolecules. In some cases, however, dissolved polymer molecules tend to assume a completely stretched rod-like shape.

This phenomenon can be detected experimentally by a very high value of the Mark–Houwink exponent a , the value of which varies between 0.5 and 0.8 for coiled molecules. Theoretical investigations (Flory, 1953) predict a value $a \approx 1.8$ for rigid stretched molecules. This value is indeed found experimentally in some cases. Another indication of rod-like behaviour of macromolecules is a high ratio of radius of gyration to molar mass.

Rod-like behaviour has been observed with several types of polymers. It is always an indication of a stiff chain skeleton. Some examples are:

- (1) Polyamides containing a large amount of ring-shaped structural elements. A well known representative of this group is poly(p-phenylene terephthalamide)



- (2) Some polypeptide helices and other natural polyelectrolytes
- (3) Some synthetic polyelectrolytes with a high degree of ionisation in dilute aqueous solutions

9.3.7.3. Polyelectrolytes

A polyelectrolyte is defined as a polymer in which the monomeric units of its constituent macromolecules possess ionisable groups. In non-aqueous solvents a polyelectrolyte shows the same behaviour as a normal polymer. In aqueous solutions, however, the charged groups of the polyelectrolytes may be surrounded by small, oppositely charged counter-ions. The conformational properties of polyelectrolytes in aqueous solutions are highly dependent on the nature and concentration of the ions present.

These ions may be divided into two groups:

(1) Ions from neutralising substances

In aqueous solutions of poly(acrylic acid), for instance, the carboxyl groups of the polymer can be neutralised by the hydroxide ions of sodium hydroxide. The fraction of the carboxyl groups neutralised is called the degree of ionisation α_i . For $\alpha_i = 1$, the polymer is called sodium polyacrylate.

(2) Ions from salts

Their concentration is usually expressed in the ionic strength I

In general, the viscosity η of an aqueous polyelectrolyte solution is a complicated function of

c – polyelectrolyte concentration

α_i – degree of ionisation

I – ionic strength of salts present

M – molar mass

T – temperature

$\dot{\gamma}$ – rate of shear

In this chapter, we are mainly concerned with the phenomena in very dilute solutions at zero shear rate, as expressed by the limiting viscosity number $[\eta]$, defined in Eq. (9.20). For several polyelectrolyte solutions, however, it is not even possible to calculate $[\eta]$, as η_{spec}/c does not approach to a constant value for c approaching zero, unless the polyelectrolyte is dissolved in an aqueous salt solution. This is due to the strong electrostatic interaction between the chain segments. Accordingly, the conformational behaviour is highly affected. An aqueous polyelectrolyte solution contains macro-ions and small counter-ions. Because the charges on the macro-ion are fixed only the interaction between the polymer molecules disappears at infinite dilution. The interaction between the charges of a polymer chain itself and its counter-ions does of course not disappear. As a result the macromolecules are expanded and accordingly, in contrast to uncharged polymers, upon plotting η_{spec}/c vs. concentration no straight lines are obtained. A very careful study carried out by Eisenberg and Pouyet (1954) at very low rates of shear led to results shown in Fig. 9.14, where the viscometric behaviour of a poly-salt is shown for various aqueous salt solutions. In the salt-free solution the plot of η_{spec}/c vs. concentration passes through a maximum, since the expansion of the poly-ion eventually reaches an upper limit. As salt is added to the system the charges on the polymer chains will be screened and the polymer molecules will contract. As a result η_{spec}/c will decrease with increasing salt concentration. Fuoss and Strauss (1948, 1951) found that these curves could be described by an empirical equation of the form

$$\frac{\eta_{\text{spec}}}{c} = \frac{A}{1 + B\sqrt{c}} \quad (9.65)$$

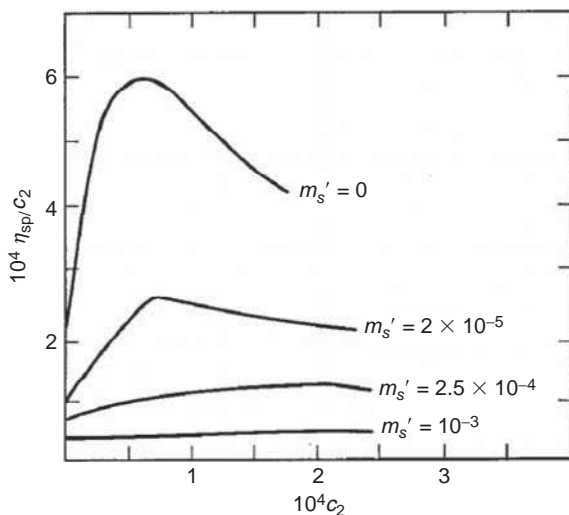


FIG. 9.14 Reduced viscosity ($10^4 \text{ cm}^3/\text{g}$) plots of poly(*N*-butyl-4-vinylpyridinium) bromide vs. concentration ($10^4 \text{ g}/\text{cm}^3$) with various concentrations of added sodium chloride (mol/l). After Eisenberg and Pouyet, 1954.

so that upon plotting c/η_{spec} vs. \sqrt{c} a straight line will be obtained, from which $1/[\eta]$ can be found. In a similar experiment Oth and Doty (1952) showed that for poly(methacrylic acid) in the absence of salt, $[\eta]$ varies as $M^{0.82}$ when the degree of ionisation is 0.001, but as $M^{1.87}$ when the degree of ionisation is 0.7. In the first case the polyelectrolyte behaves as a normal coiled polymer, and in the latter case as a rod-shaped particle. Experimentally it is generally found that linearly rising plots of η_{spec}/c vs. c are obtained if during dilution of the polyelectrolyte solution the ion strength of the mobile small counter-ions remains constant. This so-called iso-ionic dilution makes it possible to determine the intrinsic viscosity without the need of high salt concentrations in order to be able to extrapolate to $c = 0$. An example of the use of constant ionic strength is shown by data of Pals and Hermans (1952) in Figs. 9.15 and 9.16 on solutions of sodium carboxymethylcellulose. Fig. 9.15 shows that normal curves are obtained upon plotting η_{spec}/c vs. c , which can be easily extrapolated to $c = 0$ to obtain the intrinsic viscosity. Fig. 9.16 shows the intrinsic viscosities found in Fig. 9.15 as a function of the ionic strength: at high ionic strengths the screening effect is maximal and there is a sharp change to high intrinsic viscosities occurs at low ionic strengths.

In cases where $[\eta]$ can be calculated, the Mark–Houwink equation, Eq. (9.21), generally holds. The parameters K and a are complicated functions of α_i and I . An extensive literature is devoted to theoretical considerations about this relationship. Some general reviews have been written by Rice and Nagasawa (1961), Oosawa (1970), Mandel (1987), Dautzenberg (1994), Kulicke and Clasen (2004) and Dobrynin and Rubinstein (2005).

Here no attempt at a general survey will be made, but only a specific example of polyelectrolyte behaviour will be given, viz. the viscosity data on solutions of poly(acrylic acid). For this polymer, values of a and K can be found in the literature for different values of α_i and I .

In order to establish a relationship between a and K , the method of Eq. (9.54) has been applied by plotting $\log \sigma_{h,\text{cr}}^3 - \log K$ as a function of a . It appears that the linear relationship of Eq. (9.54) holds for constant values of the degree of ionisation α_i . The

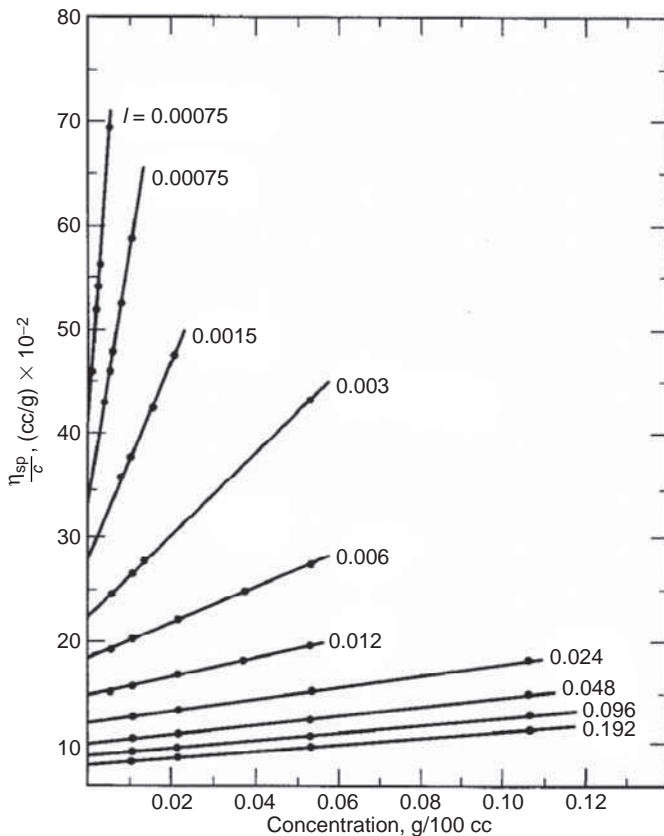


FIG. 9.15 Viscosity data for carboxymethyl cellulose, obtained by dilution at constant ionic strength. After Pals and Hermans, 1952.

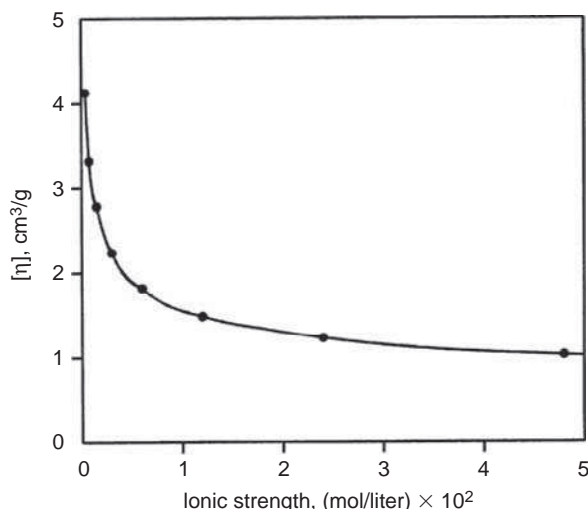


FIG. 9.16 Intrinsic viscosity of carboxymethylcellulose as a function of ionic strength. The data are the intercepts from Fig. 9.15. After Pals and Hermans, 1952.

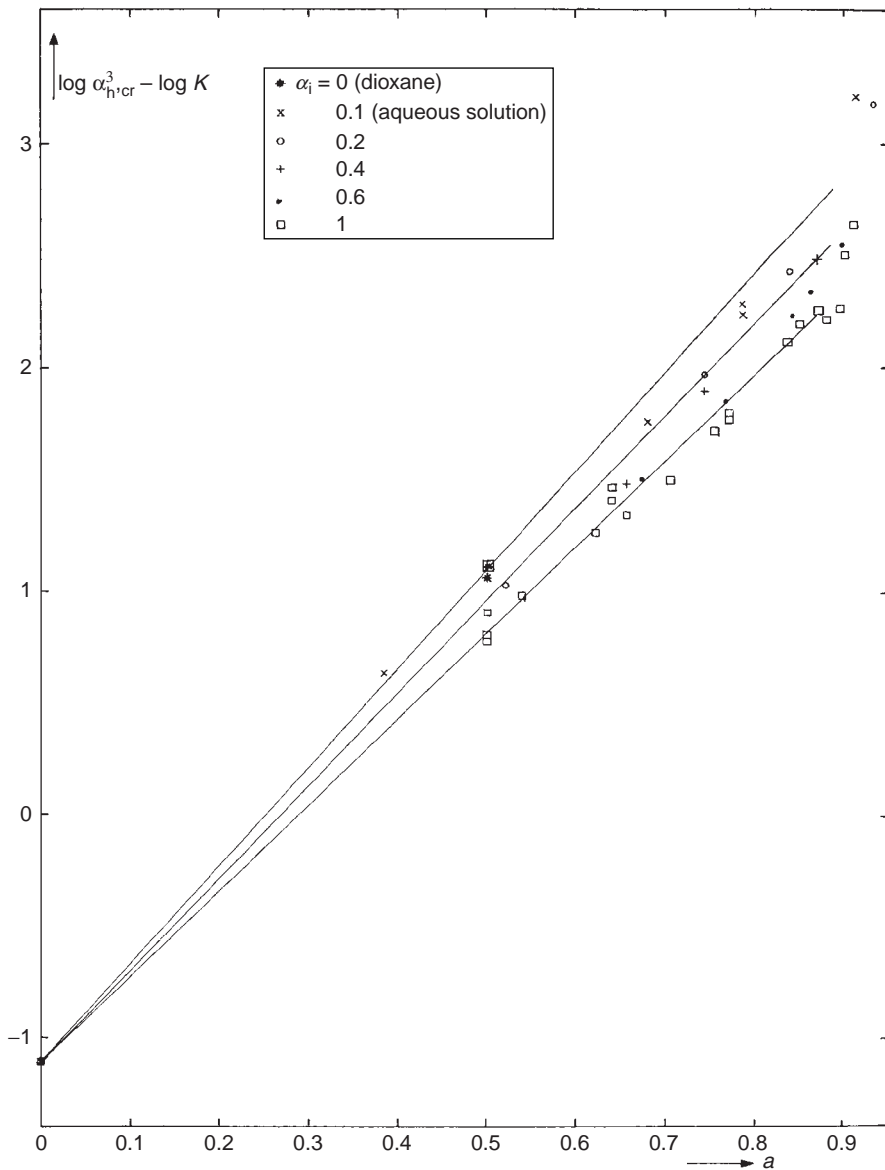


FIG. 9.17 Poly(acrylic acid) solutions. Relationship between K and a .

different values of a and K belonging to the same straight line depend on different values of the ionic strength I . This can be seen in Fig. 9.17.

There is an interesting analogy with the behaviour of normal, neutral, polymers:

- Polyelectrolytes with different degrees of ionisation behave as different polymers.
- At a given value of α_i aqueous solutions with different ionic strength behave as different solvents.
- At a low degree of ionisation the polyelectrolyte shows the same behaviour in an aqueous solution as in an organic solvent.

Fig. 9.18 shows the influence of the ionic strength I on the Mark-Houwink exponent a . Although there is a large amount of scatter, the data clearly indicate a decrease of a with

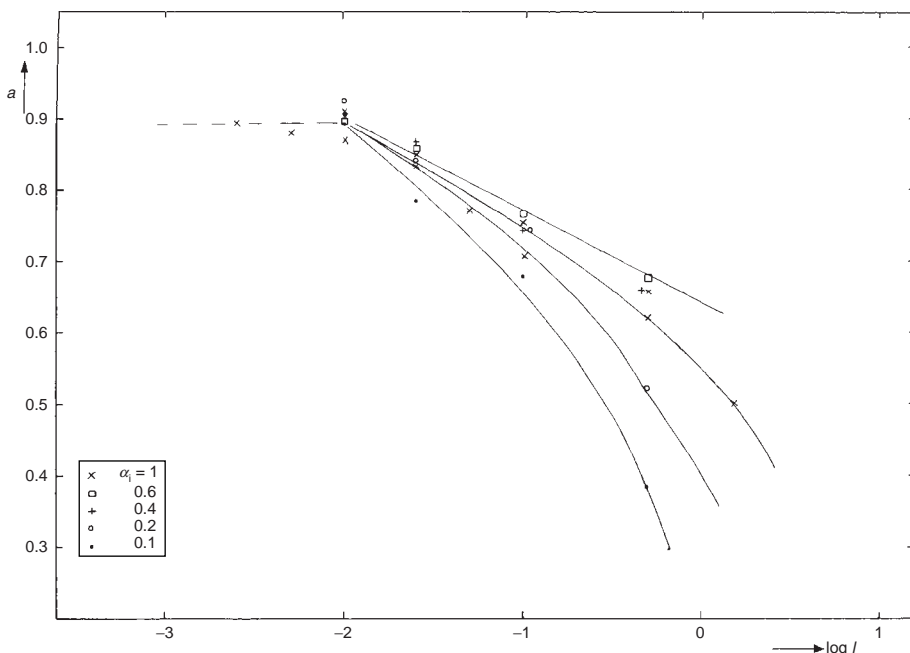


FIG. 9.18 Poly(acrylic acid) solutions. Relationship between α and I .

increasing I . At very low salt concentrations the polyelectrolyte shows a highly expanded state, while at high salt concentrations an unperturbed state is approached. The polymer coil dimensions differ, however, from those of the unperturbed state in organic solvents.

The experimental data on some other polyelectrolytes can be correlated in a similar way, but the relationship between α , K , α_i and I is different for each polymer.

During the 1980s the theoretical insight developed markedly. Combination of the inherent flexibility of the polyelectrolyte chains with the stiffening effect of the interaction of the electrostatic charges was tried. It was found, as shown before, that in very diluted polyelectrolyte solutions the behaviour of the chains, in presence of a surplus of salts, will be quite analogous to that of a conventional uncharged polymer, the conformation being that of individual coils. It became clear, however, that the behaviour becomes different at concentrations of about 10^{-3} g/cm³ (c^* , "critical" concentration, dependent of the molar mass: $c^* \propto M^{3.4}$). At higher concentrations ($c > c^*$) the conformation becomes that of a *dynamic network of "blobs"*, continuously changing in shape by means of wormlike "*reptation*"-movements (a term coined by De Gennes).

Theory (Odijk et al., 1977/79, Mandel et al., 1983/86) predicts that in the dilute state ($c < c^*$) most of the parameters of the solution (intrinsic viscosity, diffusivity, relaxation times) will be functions of the molar mass, but not of the polymer concentration. In the so-called semi-diluted solution state the influence of the polymer concentration (and that of the dissolved salts) becomes very important, whereas that of the molar mass is nearly absent. Experiments have confirmed this prediction.

The above discussion dealt primarily with synthetic polyelectrolytes, which behave in solution more or less as flexible polymers. Another important group, the natural polyelectrolytes, will not be discussed here. They include polynucleic acids, proteins, carbohydrate derivates, etc. They generally behave as rigid-chain polymers, due to their helix conformation.

9.4. INTERRELATIONSHIPS OF “LIMITING” DIFFUSIVE TRANSPORT QUANTITIES

Closely connected with the conformational dimensions of the polymer coil, and therefore with the limiting viscosity number, are some other macroscopic quantities, viz. the limiting sedimentation coefficient and the limiting diffusivity.

9.4.1. Sedimentation

According to Svedberg and Pederson (1940) the sedimentation coefficient is defined as the sedimentation velocity in a unit field of force (e.g. in a centrifuge):

$$s = \frac{dr/dt}{\omega^2 r} \text{ (dimension: second)} \quad (9.66)$$

where dr/dt = instantaneous rate of sedimentation r ; ω = angular velocity.

For a given polymer in a given solvent the sedimentation coefficient is dependent on polymer concentration, molecular weight, temperature and pressure.

Extrapolation of the s -value to zero concentration gives the limiting sedimentation coefficient:

$$s_0 = \lim_{c \rightarrow 0} s(c) \quad (9.67)$$

This limiting sedimentation coefficient is like $[\eta]$ an important polymer property.

The temperature dependence may be approximated by the expression

$$\frac{s(T)}{s(298)} = \frac{\eta_s(298)}{\eta_s(T)} \quad (9.68)$$

where η_s is the viscosity of the solvent.

In analogy with the Mark–Houwink equation the dependence of the sedimentation coefficient on molar mass can be expressed as:

$$s_0 = K_s M^c \quad (9.69)$$

9.4.2. Diffusivity

The diffusivity is defined by Fick's law for unidirectional diffusion

$$D = \frac{\partial c / \partial t}{\partial^2 c / \partial x^2} \text{ (dimension: cm}^2/\text{s or m}^2/\text{s)} \quad (9.70)$$

i.e. the ratio of the rate of change of concentration and the change of the concentration gradient as a function of the distance of transport. Also the diffusivity is a function of the polymer concentration, the molecular weight, the temperature and, to a lesser extent, the pressure. Extrapolation of the D -values to zero concentration gives the limiting diffusion coefficient:

$$D_0 = \lim_{c \rightarrow 0} D(c) \quad (9.71)$$

The temperature dependence can be described by:

$$\frac{D(T)}{D(298)} = \frac{\eta_s(298)}{\eta_s(T)} \frac{T}{298} \quad (9.72)$$

TABLE 9.6 Interrelationships between transport quantities

Method	Equation $\Upsilon = KM^a$	Eq.	Relationship between K and x	Eq.
Viscometry	$[\eta] = KM^a$	(9.21)	Approximate $\log K \approx \log K_\Theta - 3.7(a - \frac{1}{2})$	(9.44)
			Accurate $K \approx \log K_\Theta + \log \alpha_{h,cr}^3 - (a - \frac{1}{2}) \log M_{cr}$	(9.51)
Coil statistics	$\langle r^2 \rangle^{1/2} = K_h M^b$	(9.16)	$\log K_h = \frac{1}{3} \log (K/\Phi_o) = \frac{1}{3} \log K - 7.8$	(9.74)
Sedimentation	$s_o = K_s M^c$	(9.69)	$\log K_s \approx -14.8 + 5.25 (\frac{1}{2} - c)$	(9.75)
Diffusion	$D_o = K_D M^{-d}$	(9.73)	$\log K_D \approx -7.1 + 6.5 (d - \frac{1}{2}) - \log \eta_s^*$	(9.76)

Relationship between a, b, c and d
$a = 3b - 1 = 2 - 3c = 3d - 1$
$b = \frac{1}{3}(a + 1) = 1 - c = d$
$c = \frac{1}{3}(2 - a) = 1 - b = 1 - d$
$d = \frac{1}{3}(a + 1) = b = 1 - c$

* η_s viscosity of solvent, expressed in Ns/m^2 or Pas .

The diffusivity-molar mass dependence frequently takes the form:

$$D_o = K_D M^{-d} \quad (9.73)$$

Table 9.6 gives the functional relationships between $[\eta]$, $\langle r^2 \rangle^{1/2}$, s_o and D_o and the expressions for the numerical calculation of the exponents b , c and d from a and of the constants K , K_h , K_s and K_D from K_Θ and a .

Example 9.3

Estimate the limiting diffusion coefficient, the limiting sedimentation coefficient and the radius of gyration of poly(methyl methacrylate) ($M = 2.5 \times 10^5$) in toluene.

Solution

a. Estimation D_o

According to Eqs. (9.73) and (9.76) (see Table 9.6) we have:

$$\log D_o = \log K_D - d \log M = -7.1 + 6.5(d - \frac{1}{2}) - d \log M - \log \eta_s$$

Eq. (9.77) gives the value of d : $d = \frac{1}{3}(a + 1)$

In Example 9.1 we have found:

$$a = 0.72, \text{ so } d = \frac{1}{3} \times 1.72 = 0.573$$

$$\eta_s = 5.5 \times 10^{-4} \text{ Ns/m}^2 \text{ (from Table VI, Part VII)} \\ \text{so we get}$$

$$\log D_o = -11.1 + 6.5 \times 0.075 - 0.573 \log M - \log \eta_s = 10.46$$

so $D_o = 3.5 \times 10^{-11} \text{ cm}^2/\text{s}$ and $D_o = 4.4 \times 10^{-8} M^{-0.575} \text{ m}^2/\text{s}$

The literature gives no data, but for PMMA in chloroform it gives:

$$D_o = 4.5 \times 10^{-8} M^{-0.60} \quad (\text{Polymer Handbook})$$

b. Estimation of s_o

Table 9.6 (Eqs. (9.69) and (9.75)), gives:

$$\log s_o = \log K_s + c \log M = 14.8 + 5.25(\frac{1}{2} - c) + c \log M$$

since, according to Eq. (9.77) $c = 1 - d = \frac{1}{3}(2 - a)$, we get, with $a = 0.72$ and $d = 0.575$, $c = 0.425$, and according to Eq. (9.15) $\log K_s \approx -14.8 + 5.25(\frac{1}{2} - c) = -14.4$ or $K_s = 4 \times 10^{-15}$.

Substitution gives

$$s_o = 4 \times 10^{-15} M^{0.425} \text{ s}$$

and for $M = 2.5 \times 10^5 \text{ g/mol}$

$$s_o = 7.9 \times 10^{-13} \text{ s}$$

Also in this case the literature does not provide data, but for PMMA in ethyl acetate it gives:

$$s_o = 1.5 \times 10^{-15} M^{0.48} \quad (\text{Polymer Handbook})$$

c. Estimation of $\langle r^2 \rangle_o^{1/2}$

With Eq. (9.29) and (9.34) we find:

$$\log \frac{\langle r^2 \rangle_o^{1/2}}{M^{1/2}} = \frac{1}{3} (\log K_\Theta - \log \Phi_o)$$

In Example 9.1 we have found $\log K_\Theta = -1.23$

Since $\log \Phi_o = 23.4$ we get

$$\log \frac{\langle r^2 \rangle_o^{1/2}}{M^{1/2}} = -8.21$$

$$\frac{\langle r^2 \rangle_o^{1/2}}{M^{1/2}} = 0.62 \times 10^{-8} \text{ cm} = 0.62 \times 10^{-10} \text{ m.}$$

The literature (Polymer Handbook) gives $(640 \pm 60) \times 10^{-3} \text{ \AA} = (0.64 \pm 0.06) \times 10^{-10} \text{ m}$. So in Θ solution we get

$$\langle r^2 \rangle_o^{1/2} = 0.62 \times 10^{-10} \times (25 \times 10^4)^{1/2} \approx 3 \times 10^{-8} \text{ m} = 30 \text{ nm}$$

d. Estimation of $\langle r^2 \rangle^{1/2}$ and R_G .

According to Eqs. (9.15) and (9.17) we find

$$\langle r^2 \rangle^{1/2} = R_G \sqrt{6} = \alpha \langle r^2 \rangle_o^{1/2}$$

$$\text{Since } \alpha^3 = \frac{KM^a}{K_\Theta M^{1/2}} = \frac{K}{K_\Theta} M^{(a-1/2)}$$

we find $\log \alpha = \frac{1}{3}[\log K - \log K_\Theta + (a - \frac{1}{2})\log M]$
 From Example 9.1 we get $\log K = -2.13$ and $\log K_\Theta = -1.23$.
 So $\log \alpha = 0.097$ and $\alpha \approx 1.25$
 and

$$\langle r^2 \rangle^{1/2} = 1.25 \times 3 \times 10^{-8} = 3.75 \times 10^{-8} \text{ m} = 37.5 \text{ nm}$$

$$R_G = 1.53 \times 10^{-8} \text{ m} = 15.3 \text{ nm}$$

This is in fair agreement with Eqs. (9.16) and (9.74) from Table 9.6 from which we get:

$$\log(\langle r^2 \rangle^{1/2}) = \log K_h + b \log M = \frac{1}{3} \log K - 7.8 + b \log M$$

Since $b = d$, we have $b = 0.575$. Substitution of $\log K (= -2.13)$ and of $\log M (= 5.4)$ gives

$$\langle r^2 \rangle^{1/2} = 3.9 \cdot 10^{-6} \text{ cm} = 3.9 \cdot 10^{-8} \text{ m} = 39 \text{ nm}$$

BIBLIOGRAPHY

General references

- Bicerano J, "Prediction of Polymer Properties", Marcel Dekker, New York, 3rd Ed, 2002, Chap. 12.
- Brandrup J and Immergut EH (Eds), "Polymer Handbook", Wiley/Interscience, New York, 2nd Ed, 1975.
- Bueche F, "Physical Properties of Polymers", Wiley, New York, 1962.
- Daoud M, Stanley HE and Stauffer D, "Scaling, Exponents and Fractal Dimensions", In Mark JE (Ed), "Physical Properties of Polymers Handbook", 2nd Ed, Springer-Verlag, Berlin, 2007, Chap. 6.
- Dautzenberg H, Jaeger W and Kotz J, "Polyelectrolytes: Formation, Characterization and Application", Hanser, Munich, 1994.
- De Gennes PG, "Scaling Concepts in Polymer Physics", Cornell University Press, Ithaca, NY, 1979.
- Des Cloizeaux J and Jannink G, "Polymers in Solution: Their Modelling and Structure", Clarendon Press, Oxford, 1990.
- Dobrinin AV and Rubinstein M, Progr Polym Sci 30(2005) 1049.
- Doi M and Edwards SF, "The Theory of Polymer Dynamics", Clarendon Press, Oxford, 1986.
- Eisenberg H, "Biological Macromolecules and Polyelectrolytes in Solution", Clarendon Press, Oxford, 1976.
- Eisenberg A and King M, "Ion-Containing Polymers", Academic Press, New York, 1977.
- Eisenberg A (Ed), "Ions in Polymers", ACS Advances in Chemistry Series No 187, 1980.
- Elias HG, "Makromoleküle", Hüthig & Wepf, Basel, 1971.
- Fetters LJ, Lohse DJ and Colby RH, "Chain Dimensions and Entanglement Spacings", In Mark JE (Ed), "Physical Properties of Polymers Handbook", AIP Press, Woodbury, NY, 2nd Ed, 2007, Chap. 25.
- Flory PJ, "Principles of Polymer Chemistry", Cornell University Press, Ithaca, NY, 1953.
- Flory PJ, "Statistical Mechanics of Chain Molecules", Interscience, New York, 1969.
- Fujita H, "Polymer Solutions", Elsevier Science, New York, 1990.
- Hollyday L (Ed), "Ionic Polymers", Halsted Press/Wiley, New York, 1975.
- Kloczkowski A and Kolinski A, "Theoretical Models of Polymer Chains", In Mark JE (Ed), "Physical Properties of Polymers Handbook", 2nd Ed, Springer-Verlag, Berlin, 2007, Chap. 5.
- Kulicke W-M and Clasen C, "Viscosimetry of Polymers and Polyelectrolytes", Springer Verlag, Berlin, 2004.
- Longworth R, "Developments in Ionic Polymers", Appl Sci PublLondon, 1983.
- Mandel M, "Polyelectrolytes", In: Mark HF, Bikales NM, Overberger CG and Menges G (Eds), "Encyclopedia of Polymer Science and Engineering", Vol 11 (2nd Ed), pp 739–829, Wiley, New York, 1988.
- Morawetz H, "Macromolecules in Solution", 2nd Ed, Wiley/Interscience, 1975.
- Oosawa F, "Polyelectrolytes", Marcel Dekker, New York, 1970.
- Radeva T (Ed), "Physical Chemistry of Polyelectrolytes", Marcel Dekker, New York, 2001.
- Rembaum A and Sé1igny E, (Eds), "Polyelectrolytes and their Applications", Reidel, Dordrecht, NL, 1975.
- Rice SA and Nagasawa M, "Polyelectrolyte Solutions", Academic Press, New York, 1961.

- Sé1igny E, Mandel M and Strauss UP (Eds), "Polyelectrolytes", Reidel, Dordrecht, NL, 1974.
- Sun SF, "Physical Chemistry of Macromolecules, Basic Principles and Issues", Wiley, New York, 1994.
- Tanford C, "Physical Chemistry of Macromolecules", Wiley, New York, 1961.
- Tonelli AE, "Conformation and Configuration" In Mark HF, Bikales NM, Overberger CG, and Menges G (Eds), "Encyclopaedia of Polymer Science and Engineering", Vol 4 (2nd Ed), Wiley, New York, 1986.
- Yamakawa H, "Modern Theory of Polymer Solutions", Harper & Row, New York, 1971.
- Wilson AD and Prosser HJ (Eds), "Developments in Ionic Polymers", Elsevier Applied Science Publisher, London, 1987.
- Zeng W, Du Y, Xue Y and Frisch HL, "Mark-Houwink-Staudinger-Sakurada Constants", In Mark JE (Ed), "Physical Properties of Polymers Handbook", 2nd Ed, Springer-Verlag, Berlin, 2007, Chap. 17.

Special references

- Benoit H, Grubisic Z, Rempp P, Decker D and Zilliox JG, J Chim Phys 63 (1966) 1507.
- Daoud M and Jannink G, J Phys 37 (1976) 973.
- De Gennes PG, et al., J Chem Phys 55 (1971) 572; 60 (1974) 5030; 66 (1977) 5825; J Phys 36 (1975) 1199; 36L (1975) 55; 37 (1976) 1461; 38 (1977) 85; 38L (1977) 355; 39L (1978) 299; Phys Lett 38A (1972) 339; J Polym Sci Pol Lett 15 (1977) 623 J Polym Sci Phys 16 (1978) 1883.
- Eisenberg H and Pouyet J, J Polym Sci 13 (1954) 85.
- Fetters LJ, Lohse DJ and Graessley WW, J Polym Sci Polym Phys 37 (1999) 965.
- Fuoss RM, Discuss Faraday Soc No11 (1951) 125.
- Fuoss RM and Strauss UP, J Polym Sci 3 (1948) 246, 602.
- Houwink R, J Prakt Chem 157 (1940) 15.
- Kratky O and Porod G, Rec Trav Chim 68 (1949) 1106.
- Krigbaum WR, J Polym Sci 18 (1955) 315.
- Kuhn W, Kolloid-Z 68 (1934) 2.
- Kurata M and Stockmayer WH, Adv Polym Sci 3 (1963) 196.
- Mandel M et al., Macromolecules 16 (1983) 220, 227, 231; Macromolecules 19 (1986) 1760.
- Mark H, in Sänger R (Ed), "Der feste Körper", Hirzel, Leipzig, 1938.
- Odijk T et al., J Polym Sci Polym Phys Ed 15 (1977) 477; 16 (1978) 627; Polymer 19 (1978) 989; Macromolecules 12 (1979) 688.
- Oth A and Doty P, J Phys Chem 56 (1952) 43.
- Pals DTF and Hermans JJ, Rec Trav Chim, 71 (1952) 433.
- Porod G, Monatsh Chem 80 (1949) 251.
- Rudin A and Johnstone HK, Polym Lett 9 (1971) 55.
- Rudin A and Wagner RA, J Appl Polym Sci 20 (1976) 1483.
- Rudin A and Kok Ch M, J Appl Polym Sci 26 (1981) 3575; 3583 J Appl Polym Sci 27 (1982) 353.
- Stockmayer WH and Fixman M, J Polym Sci Cl (1963) 137.
- Svedberg T and Pederson KO, "The Ultracentrifuge", Clarendon Press, London, 1940.
- Van Krevelen DW, "Group Contribution Techniques for Correlating Polymer Properties with Chemical Structure", In Bicerano J (Ed), "Computational Modelling of Polymers", Marcel Dekker, New York, 1992, Chap. 1.
- Van Krevelen DW and Hoftyzer PJ, J Appl Polym Sci 10 (1966) 1331; 11 (1967) 1409; 11(1967) 2189.
- Williams MC, AIChE 21 (1975) 1.
- Wilson KG, Phys Rev B4 (1971) 3174, 3184; D3 (1971) 1818.
- Wilson KG and Kogut J, Phys Rep 12C (1975) 75.
- Zimm BH, J Chem Phys 14 (1946) 164.
- Zimm BH and Kilb RW, J Polym Sci 37 (1959) 19.
- Zimm BH and Stockmayer WH, J Chem Phys 17 (1949) 1301.

PROPERTIES OF POLYMERS IN FIELDS OF FORCE

"In the first quarter of the nineteenth century the experimental proof for the interdependence of the composition and properties of chemical compounds resulted in the theory that they are mutually related, so that like composition governs like properties, and conversely"

Wilhelm Ostwald, 1853–1932

This page intentionally left blank

CHAPTER 10

Optical Properties

The *index of refraction* and the *specific refractive index increment* (an important quantity in light scattering) can be estimated via additive molar properties. *Light absorption*, on the other hand, does not show additivity, but is a typically constitutive property. Other optical properties, such as *light reflection*, are dependent on both refraction and absorption.

10.1. OPTICAL PROPERTIES IN GENERAL

In general the interaction of electromagnetic radiation (light) with matter is controlled by three properties:

- (a) The *specific conductivity* (σ_{el})
- (b) The *electric inductive capacity* or *electric permittivity* (ϵ), usually called *dielectric constant*
- (c) The *magnetic inductive capacity* (μ), usually called *magnetic permeability*

These properties are directly related to the refractive index and the extinction index of the medium.

It is sometimes useful to distinguish between conducting or dissipative media ($\sigma_{\text{el}} > 0$) and non-conducting media ($\sigma_{\text{el}} = 0$). For non-conducting media the velocity of an electromagnetic wave is proportional to $(\mu\epsilon)^{1/2}$, just as the velocity of a sound wave is proportional to the square root of the compressibility.

Among the optical properties *refraction*, *absorption*, *reflection* and *scattering* of light are the most important. While the first three properties are determined by the average optical properties of the medium, scattering is determined by local fluctuations in optical properties within the medium.

Light is changed in phase in traversing a medium; some light may be lost from the transmitted beam by extinction. Both the phase change and the extinction may be described by a complex refractive index:

$$n^* = n' - i n'' = n - ik \quad \text{with } i \equiv \sqrt(-1) \quad (10.1)$$

where n and k are the refraction index and extinction index, respectively (both of which are wave-length dependent material properties).

A simple harmonic plane wave travelling in the z-direction with angular frequency ω can be described by a complex disturbance with the amplitude

$$U^* = U_o \exp(iqz) \quad (10.2)$$

where U_o = the time variable, proportional to $\exp(i\omega t)$; q = the wave number ($2\pi/\lambda = 2\pi n^*/\lambda_o = q_o n^*$); q_o = the wave number in free space ($=2\pi/\lambda_o$); λ_o = the wave-length in free space.

After substitution of $q = q_o(n - ik)$, the emergent amplitude becomes

$$U^* = U_o \exp(iq_o nz) \exp(-q_o kz) \quad (10.3)$$

This equation formulates a harmonic wave, with amplitude proportional to $\exp(-iq_o nz)$. The amplitude is exponentially decreasing as it progresses and proportional to $\exp(-q_o kz)$. In Eq. (10.3) n describes only the phase lag caused by the material and k describes the attenuation of the wave, i.e. its extinction due to absorption. The intensity of such a wave is obtained from $|U|^2$, and is

$$I = I_o \exp(-2q_o kz) = I_o \exp(-Ez) \quad (10.4)$$

where $I_o = U_o^2$

This relationship is called Lambert's relationship

The intensity loss $I_o - I$ due to absorption of a light beam propagating over a length of path l is

$$I_o - I = I_o(1 - \exp[-el]) = I_o(1 - \exp[-4\pi kl/\lambda_o]) \quad (10.5)$$

Loss of intensity may also be due to scattering of particles or fluctuating densities:

$$I_o - I = I_o(1 - \exp[-\tau l]) \quad (10.6)$$

Hence, the attenuation or extinction coefficient E is composed of the contributions of absorption and scattering:

$$E = \varepsilon + \tau \quad (10.7)$$

where E = attenuation coefficient or extintcivity; ε = absorption coefficient or absorbance; τ = scattering coefficient or turbidity.

E , ε an τ are all expressed in m^{-1} .

For small values of ε and τ these equations reduce to

$$I_o - I = I_o(\varepsilon + \tau)l = I_o El \quad (10.8)$$

Next to the mentioned optical properties (refraction, absorption and scattering) also reflection is important: it is the part of the light remitted on the surface.

Although, in principle all media transmit part and reflect part of the incident light, for practical purposes a number of descriptive terms are used to discriminate between quantitatively widely different cases. The transmittance of a material, defined as the ratio of the intensity of light passing through to that of light incident on the specimen, is determined by reflection, absorption and scattering. If both absorption and scattering can be neglected, the material is called transparent. An opaque material is one in which

practical transmittance is almost zero because of a high scattering power. Materials with negligible absorption but with a transmittance appreciably higher than zero but lower than 90% may be called *translucent*.

A special case of light absorption is the characteristic absorption. All material bodies possess a number of critical frequencies at which radiation is in resonance with some internal vibration of the body. At these critical frequencies such bodies are strong absorbers of radiation, even if they are transparent to radiation on either side of the critical frequency.

So far only isotropic, quasi-homogeneous materials have been considered. Two other items have to be mentioned before we finish this introduction, viz. *heterogeneity* and *anisotropy*. Heterogeneity is present when the refractive index varies front point to point within the material. No sharp distinction can exist between homogeneous and heterogeneous materials; it is a matter of degree, of scale of heterogeneity. In practice a material is called heterogeneous if the scale becomes comparable with the optical wave length; in that case n'' shows a very marked increase. Polymer solutions and semi-crystalline polymeric solids with small spherilitic crystallites show scattering at small angles. *Anisotropy* is present when the refractive index (n or k) depends on the state of polarisation of the light. Light can be divided into two paths that are polarised at a 90° angle with respect to each other. If the refraction index n differs for the two paths (n_\perp and n_\parallel) the result is *birefringence* or *double refraction*. If the extinction index k differs for the two paths (k_\perp and k_\parallel) the result may be differential selective absorption, called *dichroism* or *pleochroism*, so that the light that leaves the medium may have different colours.

The anisotropy itself may be linear or circular, or a combination of both. In linear anisotropy the refractive index depends on the direction of polarised light. It is found in solid polymers under tension and in viscous polymeric liquids during flow (shear and elongation). The refractive index can also depend on the chirality of polarised light; in this case one speaks of circular or elliptic anisotropy. Thus the so-called "optical activity" is circular birefringence: its extinction analogue is circular dichroism.

Tables 10.1–10.3 give comprehensive surveys of this introduction.

In this chapter the following optical properties will be discussed:

1. Light refraction
2. Light reflection
3. Birefringence
4. Light scattering
5. Differential light absorption

TABLE 10.1 Optical phenomena

	On the surface	In the medium
Observed phenomena	Transmission with refraction Remission by (a) Reflection (b) Scattering (c) Surface absorption	Transmission with extinction Remission by (a) Absorption (b) Scattering

TABLE 10.2 Heterogeneity and anisotropy

Degree (scale) of heterogeneity (h)	Degree of anisotropy (a)			Theoretical approach
	$a = 0$	$0 < a < 1$	$a \approx 1$	
$h = 0,$ $\sigma/\lambda \ll 1^a$	Transparent liquid and glassy solid polymers	(a) Flow oriented polymer melts (b) Solid glassy polymers under tension	Transparent solid semi-crystalline polymers	Continuum physics
$0 < h < 1$	(a) Turbid polymer solutions (b) Turbid solid polymers	Translucent semi-crystalline polymers	Translucent polycrystalline polymers (spherulitic)	Particle physics
$h \approx 1,$ $\sigma/\lambda > 1$	Opaque isotropic polymers	Opaque anisotropic liquid and solid polymers (coatings)	Do.	

^a σ = size of heterogeneity.

TABLE 10.3 Interaction between anisotropic condensed phase and polarised light

Nature of polarised light	Effect based on	
	Real part of $n^* = \text{refractive index } (n' = n)$	Imaginary part of $n^* = \text{extinction index } (n'' = k)$
Linear	Birefringence	Dichroism or PleoChroism
Circular		Circular
Elliptic	Optical Activity	Dichroism or PleoChroism Elliptic Dichroism or PleoChroism

10.2. LIGHT REFRACTION

The first basic law of optical refraction was formulated by Snellius (1618) and (independently) by Des-cartes (1637). It reads

$$n = \frac{\sin \theta_i}{\sin \theta_r} \quad (\text{Snellius' law}) \quad (10.9)$$

where n = index of refraction, characteristic for the material; θ_i = angle of incident light; θ_r = angle of refracted light.

It took more than two centuries before a correlation between the refractive index and the chemical structure was found. In 1858 Gladstone and Dale found that, for organic liquids, the ratio $(n - 1)/\rho$, if measured for a standard wave-length, is a characteristic

"constant" (nearly independent of the temperature) of the substance considered. It was coined "*specific refraction*". They also found that its product with the molar mass $\mathbf{M}(n - 1)/\rho$, coined the molar refraction \mathbf{R} , has additive properties:

$$\frac{\mathbf{M}}{\rho}(n - 1) = \mathbf{R}_{GD} = \sum_i \mathbf{R}_{GD,i} \quad (10.10)$$

A nice qualitative derivation of the Gladstone–Dale equation was given by Schoorl (1920). The Huygens–Fresnel wave optics leads to the conclusion that the refractive index is equal to the ratio of the light velocities in the two media of transmission and also to the ratio of the respective wave-lengths; so Snellius' law can be extended to

$$n = \frac{\sin \theta_i}{\sin \theta_r} = \frac{v_1}{v_2} = \frac{\lambda_1}{\lambda_2}$$

If medium 1 is the vacuum (light velocity v_o) and medium 2 is the transparent material (light velocity v), then

$$\frac{\Delta v}{v} = \frac{v_o - v}{v} = \frac{v_o}{v} - 1 = n - 1$$

which is the *relative "brake power"* of the material and $(n - 1)/\rho$ its *specific relative brake power* versus the light wave.

An expression for the molar refraction, formulated by Lorentz and Lorenz (1880), that has been widely proved with regard to its additivity is

$$\frac{n^2 - 1}{n^2 + 2} \frac{\mathbf{M}}{\rho} = \frac{n^2 - 1}{n^2 + 2} \mathbf{V} = \mathbf{R}_{LL} = \sum_i \mathbf{R}_{LL,i} \quad (10.11)$$

This expression has been widely proved experimentally, especially with regard to its additivity.

Finally, in the 1950s Vogel formulated a very simple expression, only valid at constant temperature:

$$\mathbf{M}n = \mathbf{R}_V = \sum_i \mathbf{R}_{V,i} \quad (10.12)$$

Hence, several definitions of the molar refraction have been proposed in the literature, correlating the refractive index with the chemical structure of electrically insulating materials. Resuming:

(a) The molar refraction, according to Gladstone and Dale (1858):

$$\mathbf{R}_{GD} = (n - 1) \frac{\mathbf{M}}{\rho} = (n - 1) \mathbf{V} \quad (10.10a)$$

(b) The molar refraction, according to Lorentz and Lorenz (1880):

$$\mathbf{R}_{LL} = \frac{n^2 - 1}{n^2 + 2} \frac{\mathbf{M}}{\rho} = \frac{n^2 - 1}{n^2 + 2} \mathbf{V} \quad (10.11a)$$

(c) The molar refraction, according to Vogel (1948–1954):

$$\mathbf{R}_V = n \mathbf{M} \quad (10.12a)$$

(d) The molar refraction, according to Looyenga (1965, 1973):

$$\mathbf{R}_L = (n^{2/3} - 1) \frac{\mathbf{M}}{\rho} = (n^{2/3} - 1) \mathbf{V} \quad (10.13)^1$$

NB \mathbf{R}_{LL} , \mathbf{R}_{GD} and \mathbf{R}_L are expressed in cm^3/mol (or in m^3/mol) and \mathbf{R}_V in g/mol (or in kg/mol)

While (b) and (c) are purely empirical combinations, (a) has its theoretical basis in the electromagnetic wave theory of light; (d) is a simpler approximation of (a).

Several investigators have calculated the atomic, group or bond contributions to the molecular refraction. Among them are Eisenlohr (1911, 1912), Schoorl (1920), Wibaut et al. (1939), Young and Finn (1940), Vogel (1948) and Huggins (1956).

Goedhart (1969) made an extensive regression analysis based on about a thousand liquid organic compounds containing 43 different functional groups. With his group contributions the quantity $(n - 1)$ can be predicted with an average standard deviation of about 1%, which means that n itself can be predicted with an average of about 0.4% (e.g. 1.500 ± 0.006). Goedhart's values are given in Table 10.4.

Because of the relatively strong influence of the benzene ring on other groups, Goedhart made a distinction between groups directly attached to a benzene ring and those separated from the aromatic ring by one or more C atoms. The group contribution of a benzene ring with more substituents is obtained by subtracting an equivalent number of H_{ar} contributions from the contribution of phenyl or phenylene.

A special constitutional increment is the "steric hindrance", which has been introduced to overcome the problem caused by multiple substitutions on adjacent C atoms. If, on a chain, groups like CH_3 , Cl or OH are adjacent or vicinal (i.e. adjacent, on two neighbouring C atoms), this steric hindrance increment has to be used.

From the Eqs. (10.10), (10.11) and (10.12) the following expressions for the refractive index can be easily derived:

$$n = \left(\frac{1 + 2 \frac{\mathbf{R}_{LL}}{\mathbf{V}}}{1 - \frac{\mathbf{R}_{LL}}{\mathbf{V}}} \right)^{1/2}; \quad n = 1 + \frac{\mathbf{R}_{GD}}{\mathbf{V}}; \quad n = \frac{\mathbf{R}_V}{\mathbf{M}}. \quad (10.14)$$

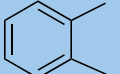
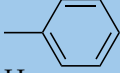
Table 10.5 shows a comparison between calculated and observed values for a series of solid amorphous polymers. Remarkable is the fact that the very simple formula of Vogel (1948–1954), $\mathbf{R}_V = n\mathbf{M}$, gives about the same standard deviation as the more complex and theoretically better explicable formulas of Lorentz–Lorenz and Gladstone–Dale.

A polymer always has a higher average refractive index in the crystalline than in the amorphous state. However, since also the density of the crystalline polymer is higher, the molar refraction according to Lorenz–Lorenz and Gladstone–Dale remains practically constant. The molar refraction according to Vogel is not applicable to crystalline polymers, since it does not contain the polymer density.

It is clear that the ratios $\mathbf{R}_{LL}/\mathbf{V}$, $\mathbf{R}_{GD}/\mathbf{V}$ and \mathbf{R}_V/\mathbf{M} are characteristics of the refractive power of the polymer. This is also true of the structural groups. It is obvious that aromatic groups have a high refractive power, while methyl groups and fluorine atoms have a very, low refractive power.

¹ This is a simplification of the Lorentz–Lorenz equation. Looyenga showed that the expression $(n^2 - 1)/(n^2 + 2)$ can, with high accuracy be approximated by the more simple expressions $(n^{2/3} - 1)$: for the polymer refraction indices mentioned in Table 10.5, the differences vary from 2.9% ($n = 1.35$) to 8.8% ($n = 1.654$).

TABLE 10.4 Group contributions in $10^{-6} \text{ m}^3/\text{mol}$ to the molar refraction ($\lambda = 589 \text{ nm}$)

	Groups	R_{LL}	R_{GD}	R_V
$-\text{CH}_3$	General	5.644	8.82	17.66
	Attached to benzene ring	5.47	8.13	15.4
$-\text{CH}_2-$	General	4.649	7.831	20.64
	Attached to benzene ring	4.50	7.26	18.7
$>\text{CH}-$	General	3.616	6.80	23.49
	Attached to benzene ring	3.52	6.34	21.4
$>\text{C}<$	General	2.580	5.72	26.37
	Attached to benzene ring	2.29	4.96	25.1
	Cyclohexyl	26.686	44.95	122.66
	Phenyl	25.51	44.63	123.51
	<i>o</i> -Phenylenne	24.72	44.2	129.0
	<i>m</i> -Phenylenne	25.00	44.7	128.6
	<i>p</i> -Phenylenne	25.03	44.8	128.6
	Average value	0.59	0.04	-5.2
H_{ar} $-\text{O}-$	Methyl ethers	1.587	2.96	23.85
	Higher ethers	1.641	2.81	23.18
	Attached to benzene ring	1.77	2.84	22.6
	Acetals	1.63	2.75	22.99
	Primary alcohol	2.551	4.13	24.08
$-\text{OH}$	Secondary alcohol	2.458	3.95	23.95
	Tertiary alcohol	2.453	3.85	24.05
	Phenol	2.27	3.53	22.7
	Methyl ketone	4.787	8.42	43.01
$>\text{C} = \text{O}$	Higher ketones	4.533	7.91	43.03
	Attached to benzene ring	5.09	8.82	41.9
	General	5.83	9.63	40.69
$-\text{COOH}$	General	7.212	11.99	64.26
$-\text{COO}-$	Methyl esters	6.237	10.76	65.32
	Ethyl esters	6.375	10.94	64.49
	Higher esters	6.206	10.47	64.20
	Attached to benzene ring	6.71	11.31	64.8
	Acetates	6.306	10.87	64.90

(continued)

TABLE 10.4 (*continued*)

	Groups	R_{LL}	R_{GD}	R_V
-OCOO-	Methyl carbonates	7.75	13.39	87.8
	Higher carbonates	7.74	13.12	86.8
-NH ₂	General	4.355	7.25	22.64
	Attached to benzene ring	4.89	8.40	23.7
>NH	General	3.585	6.29	24.30
	Attached to benzene ring	4.53	8.68	26.9
>N-	General	2.803	5.70	26.66
	Attached to benzene ring	4.05	8.67	30.7
-CONH-	General	7.23	15.15	69.75
	Attached to benzene ring	8.5	18.1	73
-C≡N		5.528	9.08	36.67
-NO ₂		6.662	11.01	66.0
-SH	Primary	8.845	15.22	50.61
	Secondary	8.79	15.14	50.33
	Tertiary	9.27	15.66	49.15
-S-	Methyl sulphide	7.92	14.30	53.54
	Higher sulphides	8.07	14.44	53.53
-SS-		16.17	29.27	107.63
-F	Mono	0.898	0.881	22.20
	Per	0.898	0.702	20.92
-Cl	Primary	6.045	10.07	51.23
	Secondary	6.023	9.91	50.31
	Tertiary	5.929	9.84	50.75
-Br	Attached to benzene ring	5.60	8.82	48.4
	Primary	8.897	15.15	118.5
	Secondary	8.956	15.26	118.4
-I	Tertiary	9.034	15.29	119.1
		13.90	25.0	-
<i>Constitutional increments</i>				
Δ "steric hindrance"	(neighbouring)	-0.118	-0.18	0.41
		0.068	0.05	-0.20
Δ isopropyl group		1.65	1.90	-6.36
		1.76	1.94	-5.56
Δ ethylenic bond (C=C)	General	1.94	2.09	-6.37
	cis	-0.18	-1.15	-5.06
Δ ring structure	trans	-0.13	-0.92	-4.44
	Cyclopentane	-0.12	-0.98	-4.36
	Cyclohexane	-0.086	-0.78	-4.53
	Tetrahydrofuryl	-0.41	-1.94	-5.63
	Furyl			
	Piperidyl			

TABLE 10.5 Observed and calculated values of refractive indices

Polymer	<i>n</i> exp.	<i>n</i> calculated from Eq. (10.14)		
		From \mathbf{R}_{LL}	From \mathbf{R}_{GD}	From \mathbf{R}_V
Polyethylene	1.49	1.479	1.478	1.469
Polystyrene	1.591	1.603	1.600	1.590
Poly(methylstyrene)	1.587	1.577	1.585	1.574
Poly(isopropylstyrene)	1.554	1.562	1.560	1.555
Poly(o-methoxystyrene)	1.593	1.560	1.562	1.575
Poly(p-methoxystyrene)	1.597	1.565	1.566	1.572
Poly(o-chlorostyrene)	1.610	1.612	1.607	1.583
Poly(vinylidene fluoride)	1.42	1.41	1.42	1.43
Poly(tetrafluoroethylene)	1.35	1.28	1.28	1.36
Poly(vinyl chloride)	1.539	1.544	1.543	1.511
Poly(methyl vinyl ether)	1.467	1.450	1.457	1.474
Poly(ethyl vinyl ether)	1.454	1.457	1.460	1.465
Poly(n-butyl vinyl ether)	1.456	1.463	1.465	1.466
Poly(isobutyl vinyl ether)	1.451	1.464	1.466	1.464
Poly(n-pentyl vinyl ether)	1.459	1.465	1.467	1.467
Poly(hexyl vinyl ether)	1.460	1.466	1.468	1.468
Poly(decyl vinyl ether)	1.463	1.469	1.472	1.469
Poly(vinyl acetate)	1.467	1.471	1.475	1.472
Poly(vinyl benzoate)	1.578	1.583	1.583	1.569
Poly(methyl acrylate)	1.479	1.489	1.488	1.477
Poly(ethyl acrylate)	1.469	1.487	1.488	1.468
Poly(butyl acrylate)	1.466	1.481	1.480	1.466
Poly(methyl methacrylate)	1.490	1.484	1.485	1.475
Poly(ethyl methacrylate)	1.485	1.488	1.488	1.467
Poly(isopropyl methacrylate)	1.552	1.479	1.478	1.464
Poly(n-butyl methacrylate)	1.483	1.475	1.475	1.466
Poly(tert.-butyl methacrylate)	1.464	1.467	1.472	1.464
Poly(isobutyl methacrylate)	1.477	1.480	1.480	1.466
Poly(hexyl methacrylate)	1.481	1.476	1.475	1.467
Poly(lauryl methacrylate)	1.474	1.476	1.475	1.469
Poly(cyclohexyl methacrylate)	1.507	1.515	1.513	1.495
Poly(benzyl methacrylate)	1.568	1.563	1.560	1.539
Poly(methyl chloroacrylate)	1.517	1.519	1.521	1.500
Poly(ethyl chloroacrylate)	1.502	1.516	1.518	1.490
Poly(sec.-butyl chloroacrylate)	1.500	1.503	1.502	1.495
Poly(cyclohexyl chloroacrylate)	1.532	1.529	1.528	1.508
Polyacrylonitrile	1.514	1.528	1.529	1.523
Poly(1,3-butadiene)	1.516	1.511	1.513	1.514
Polyisoprene	1.520	1.514	1.514	1.504
Poly(2-tert.-butyl-1,3-butadiene)	1.506	1.517	1.513	1.489
Poly(2-decyl-1,3-butadiene)	1.490	1.487	1.489	1.483
Polychloroprene	1.558	1.560	1.560	1.531
Poly(methylene oxide)	(1.510)	1.416	1.426	1.453
Poly(propylene oxide)	1.457	1.451	1.455	1.463

(continued)

TABLE 10.5 (continued)

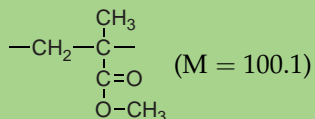
Polymer	<i>n</i> exp.	<i>n</i> calculated from Eq. (10.14)		
		From \mathbf{R}_{LL}	From \mathbf{R}_{GD}	From \mathbf{R}_V
Poly(hexamethylene adipamide)	1.530	1.497	1.521	1.528
Poly(ethylene terephthalate)	1.640	1.580	1.581	1.558
Poly[1,1-ethane bis(4-phenyl)carbonate]	1.594	1.600	1.602	1.594
Poly[2,2-propane bis(4-phenyl)carbonate]	1.585	1.579	1.583	1.590
Poly[1,1-butane bis(4-phenyl)carbonate]	1.579	1.585	1.587	1.582
Poly[2,2-butane bis(4-phenyl)carbonate]	1.583	1.573	1.577	1.584
Poly[1, 1-(2-methylpropane)bis(4-phenyl)-carbonate]	1.570	1.580	1.583	1.582
Poly[diphenylmethane bis(4-phenyl) carbonate]	1.654	1.637	1.630	1.628
Poly[1,1-cyclopentane bis(4-phenyl) carbonate]	1.599	1.589	1.596	1.599
Poly[1,1-cyclohexane bis(4-phenyl) carbonate]	1.590	1.583	1.590	1.595

Example 10.1

Estimate the refractive index of poly(methyl methacrylate).

Solution

The structure unit is



Using the group contributions of Table 10.4 we obtain

$$\begin{aligned}
 \mathbf{R}_{LL} &= 1(-\text{CH}_2-) + 2(-\text{CH}_3) + 1(-\text{COO}-) + 1(>\text{C}<) \\
 &= 4.469 + 2 \times 5.644 + 6.237 + 2.580 = 24.754 \text{ cm}^3/\text{mol} \\
 \mathbf{V} &= 86.5 \text{ cm}^3/\text{mol}
 \end{aligned}$$

So n_D will be

$$\left(\frac{1 + \frac{2 \times 24.754}{86.5}}{1 - \frac{24.754}{86.5}} \right)^{1/2} = 1.484$$

which is in fair agreement with the experimental value ($n_D = 1.490$).

In the same way we obtain:

$$\mathbf{R}_{GD} = 7.831 + 2 \times 8.82 + 10.76 + 5.72 = 41.95 \quad \text{with } n = 1 + 41.95/86.5 = 1.485$$

$$\mathbf{R}_V = 20.64 + 2 \times 17.66 + 65.32 + 26.37 = 147.65 \quad \text{with } n = 147.65/100.1 = 1.475$$

10.3. REFLECTION AND TRANSMISSION

The reflectance of a boundary plane between two non-absorbing media is a function of the refractive indices of the media examined. When light moves from a medium of refractive index n_1 into a second medium with refractive index n_2 , both reflection and transmission of the light may occur (Fig. 10.1). The relationship between θ_i and θ_t is given by Snellius' law (angles are defined as the angle between the beam and the normal on the interface)

$$n_1 \sin \theta_i = n_2 \sin \theta_t \quad (10.15)$$

where θ_i = angle of incidence; θ_t = angle of transmission or refraction.

When no absorption or scattering takes place then the sum of the energies of the reflected and transmitted light waves is equal to the energy of the original wave. There are separate coefficients in the direction perpendicular and parallel to the boundary surface, leading to *reflectances* R_s and R_p , respectively, and to *reflectance coefficients* r_s and r_p , respectively. If the light beam is polarised perpendicular (s-polarised) to the plane of incidence, then, according to Fresnel's relationship (see Pohl, 1943), the reflectance is

$$R_s = \left(\frac{\sin(\theta_i - \theta_t)}{\sin(\theta_i + \theta_t)} \right)^2 = \left(\frac{n_1 \cos \theta_i - n_2 \cos \theta_t}{n_1 \cos \theta_i + n_2 \cos \theta_t} \right)^2 \quad (10.16)$$

If, on the other hand, in two non-absorbing media the light beam is polarised parallel to the plane of incidence (p-polarised) the reflectance is

$$R_p = \left(\frac{\tan(\theta_i - \theta_t)}{\tan(\theta_i + \theta_t)} \right)^2 = \left(\frac{n_2 \cos \theta_i - n_1 \cos \theta_t}{n_2 \cos \theta_i + n_1 \cos \theta_t} \right)^2 \quad (10.17)$$

If in non-absorbing media the incident light is non-polarised, the reflectance is equal to $R = \frac{1}{2}(R_s + R_p)$. Both reflectance coefficients r_s and r_p are equal to the square roots of their corresponding reflectances R_s and R_p .

The corresponding transmittances are:

$$T_s = 1 - R_s \quad \text{and} \quad T_p = 1 - R_p \quad (10.18)$$

For near-normal incidence, i.e. $\theta_i \approx \theta_t \approx 0$, it follows quite easily for non-absorbing media

$$R = R_s = R_p = \frac{(n_2 - n_1)^2}{(n_2 + n_1)^2} \quad (10.19)$$

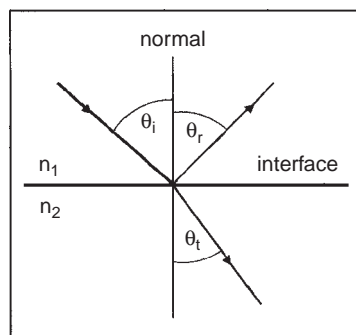


FIG. 10.1 Incident, reflected and refracted beams at an interface.

and for the transmittance

$$T = T_s = T_p = \frac{4n_1 n_2}{(n_2 + n_1)^2} \quad (10.20)$$

If the light is also absorbed in both media (i.e. $n_1' = n_1$, $n_1'' = k_1$ and $n_2' = n_2$, $n_2'' = k_2$) Eq. (10.19) changes into

$$R = R_s = R_p = \frac{|n_2^* - n_1^*|^2}{|n_2^* + n_1^*|^2} = \frac{(n_2 - n_1)^2 + (k_2 - k_1)^2}{(n_2 + n_1)^2 + (k_2 + k_1)^2} \quad (10.21)$$

where k_1 and k_2 denote the extinction indexes of media 1 and 2, respectively.

From Eq. (10.17) an important conclusion may be derived, namely that there must exist an angle θ_i at which $\theta_i + \theta_r = \frac{1}{2}\pi$ rad, so that $R_p = 0$. Hence, the *reflected beam is completely s-polarised*. This angle is coined the *polarising angle* or *Brewster angle* θ_B (see Fig. 10.2), for which holds

$$\tan \theta_B = \frac{n_2}{n_1} \quad (10.22)$$

Apparently the reflected and transmitted beams are perpendicular. In Fig. 10.2, with $n_1 = 1$ and $n_2 = 2$, the Brewster angle is equal to 63.43° .

When moving from a more dense medium into a less dense one (i.e. $n_1 > n_2$), above an incidence angle, known as the critical angle, all light is reflected and $R_s = R_p = 1$ (see Fig. 10.3). At the critical angle, where $\theta_t = 90^\circ$ or $\pi/2$ rad, the transmitted beam just strikes along the interface. For higher incident angles there is no transmission anymore. Measurement of the critical angle is a method to determine the refractive index of non-absorbing media (e.g. the Abbe refractometer). The critical angle follows from

$$\cos \theta_{i,\text{crit}} = n_2/n_1 \quad (10.23)$$

In Fig. 10.3, with $n_1 = 2$ and $n_2 = 1$, the critical angle is equal to 30° .

With strongly absorbing media (10.21), (10.22) and (10.23), are no longer applicable because the refracted light wave will then be inhomogeneous, which renders the relationship between the reflectance and the angles of incidence and refraction very complicated.

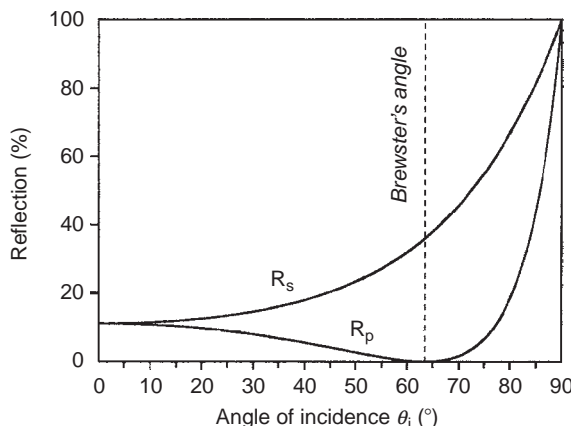


FIG. 10.2 Reflections, R_s and R_p , as a function of the angle of incidence for $n_1 = 1.0$ and $n_2 = 2.0$; indication of the Brewster angle.

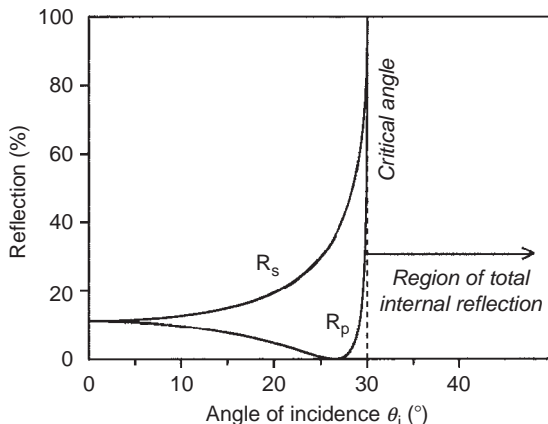


FIG. 10.3 Reflections, R_s and R_p , as a function of the angle of incidence for $n_1 = 2.0$ and $n_2 = 1.0$; indication of the critical angle.

Moreover, in the case of strong absorption, the reflected and absorbed intensities become a strong function of the angle of incidence.

10.4. BIREFRINGENCE (AND OPTICAL ROTATION)

A substance is anisotropic, if it has different properties in different directions. If the refraction index n differs for perpendicular and parallel-polarised light (n_{\perp} and n_{\parallel}) the result is birefringence or double refraction (when transparent). Accordingly, *birefringence* is evidenced by the ability of a material to rotate the plane of polarised light. It is defined as the difference in refractive indices in the directions parallel and perpendicular to the direction of orientation:

$$\Delta n = n_{\parallel} - n_{\perp} \quad (10.24)$$

Birefringence may be a natural property or artificially induced by means of force fields.

Natural birefringence is mainly found in crystalline substances; artificial birefringence is normally based on mechanical orientation, either in the solid or in the liquid state: *stretch* and *flow orientation*, respectively. Melts and solutions may show birefringence, caused by:

- (a) Mechanical orientation: *flow birefringence*
- (b) Electrical fields: the *Kerr effect*
- (c) Magnetic fields: the *Cotton–Mouton effect*

Reliable data on these phenomena are scarce, so that our discussion will be mainly qualitative.

Related to birefringence is the *optical activity* or *optical rotation* (of the plane of polarisation of the light). This also may be a natural or an artificially aroused effect.

Natural optical activity is based on the structure of the molecules (optically active centres). Artificial optical rotation is found in magnetic fields: the *Faraday–Verdet effect* or *Magneto-Optic Effect*, discovered by Michael Faraday in 1845. The theoretical basis for this effect was developed by James Clerk Maxwell in the 1860s and 1870s. From investigations on small molecules we know that the study of magneto-optical rotation offers interesting correlations with the chemical structure and that additive properties of the Verdet constant have been found.

10.4.1. Stress and flow birefringence

Orientation in polymers is normally affected by stretching. One therefore observes the phenomenon of birefringence in polymer melts under forced flow (shear and elongational stresses) or under tension, and in solid polymers after stretch orientation; the oriented polymer is cooled to below its glass transition temperature before the molecules have had a chance to relax to their random coiled configuration. Birefringence is (as a matter of course) not restricted to visible light. Some of the infrared absorption bands of oriented polymers show *infrared dichroism*; they absorb different amounts of polarised infrared radiation in different directions (parallel or perpendicular to the direction of orientation). Dyed oriented polymers often show dichroism to visible light due to orientation of the dye molecules (together with the polymer molecules).

For *rubber-elastic materials* (i.e. cross-linked polymers above their T_g) theory predicts that the degree of orientation is directly proportional to the retractive stress, and the birefringence directly proportional to the orientation. Thus, for uniaxial tension, the birefringence and the retractive stress are related by the simple equation:

$$n_{\parallel} - n_{\perp} = C_{\sigma}\sigma \quad (10.25)$$

C_{σ} is called the *stress optical coefficient*. The value of C_{σ} depends on the chemical structure of the polymer and is somewhat temperature-dependent. The theory of rubber elasticity leads to the following expression:

$$C_{\sigma} = \frac{2\pi(\alpha_{\parallel} - \alpha_{\perp})}{45 kT} \frac{(\bar{n}^2 + 2)^2}{\bar{n}} \quad (10.26)$$

where $\alpha_{\parallel} - \alpha_{\perp}$ is the difference in polarisability of a polymer segment parallel and perpendicular to the direction of the chain. \bar{n} is the average refractive index (\bar{n} equals n of the non-oriented polymer). C_{σ} is normally expressed in $10^{-12} \text{ m}^2/\text{N}$ that are called *Brewsters*. According to theory, C_{σ} is independent of the degree of cross-linking. During stress relaxation the birefringence decreases with the stress, so that their ratio remains constant. The same is true during creep.

Rigid amorphous polymers also become birefringent when a stress is applied to them. A much greater stress is required, however, to produce a given value of birefringence in a rigid polymer than in a rubber: the stress optical coefficient is much lower. It usually changes rapidly with temperature in the neighbourhood of the glass-rubber transition. For some polymers it even changes sign at T_g !

Crystalline polymers, and especially oriented crystalline polymers show birefringence that is made up of two contributions:

- (a) *Intrinsic birefringence* (contribution of the crystallites themselves)
- (b) *Form birefringence*, resulting from the shape of the crystallites or the presence of voids

In crystalline polymers the relations between stress, orientation and birefringence are much more complicated than in amorphous materials.

Polymer solutions show birefringence if orientation is brought about by outside forces; this may occur under the influence of flow (flow birefringence). Janeschitz-Kriegl and Wales (1967) derived dimensionless groups for the correlation of flow birefringence data.

We shall now discuss in more detail the different phase types of polymers as far as data of birefringence, stress-optical coefficient and anisotropies in polarisability are available.

10.4.2. Glassy-amorphous polymers

Table 10.6 shows the data of the stress-optical coefficients as calculated by means of Eq. (10.25). The values are low for aliphatic polymers (about $5 \times 10^{-12} \text{ Pa}^{-1}$); aromatic rings directly linked as side groups on the backbone chain increase the value of C_{σ}

TABLE 10.6 Stress-optical coefficients of glassy polymers in Brewster's ($= 10^{-12} \text{ Pa}^{-1}$)

Poly(methyl methacrylate)		Poly(styrene)		Poly(bis-phenol-A carbonate)	
	-3.3/4.5				111
Poly(chloroethyl methacrylate)		Poly(vinyl toluene)		Aromatic Polyester	
	-5.6				93
Poly(cyclohexyl methacrylate)		Poly(p-tert-butyl styrene)		Aromatic polyamides	
	-59				90

(continued)

TABLE 10.6 (continued)

Poly(phenyl methacrylate)		Poly(p-chlorostyrene)		Aromatic polyimide	
	40		24		111
Poly(benzyl methacrylate)		Poly(α -methyl styrene)		Aromatic polysulphone	
	25/45		2?		150

Data from Lamble and Dahmouch (1958), Rudd and Andrews (1958/1960), Askadskii (1976).

somewhat, but a large increase (to about 100 brewsters) is found when aromatic rings are part of the main chain.

The main investigators in this field are Askadskii and coworkers (1976, 1987). They found that the stress-optical coefficients are correlated with the polymer structure according to the following expression

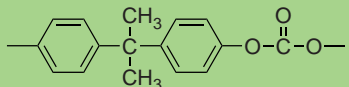
$$C_\sigma = \frac{\sum_i C_i}{V_W} + \Pi \quad (10.27)$$

where V_W = van der Waals volume of structural unit; Π = universal parameter = 0.354×10^{-3} (MPa) $^{-1}$; $\sum_i C_i$ = molar optical sensitivity function, an additive molar quantity, for which increments are given in Table 10.7.

An example of calculation, taken from Askadskii (1987), will illustrate the use of this equation.

Example 10.2

Estimate, the optical-stress coefficient for poly(bisphenol-A carbonate), $[C_{16}H_{14}O_3]_n$, with $V_W = 144 \text{ cm}^3/\text{mol}$ unit.



Solution

Using the increments of Table 10.7, we find

$$\begin{aligned} \sum_i C_i &= 16C_C + 14C_H + 2C_{Ob} + 1C_{Os} + 2C_P + 1\frac{1}{2}C_d \\ &= -16 \times 2.0492 - 14 \times 0.5227 + 2 \times 3.198 - 0.7568 + 2 \times 1.7 - 1\frac{1}{2} \times 2.512 \\ &= -34.834 \times 10^{-3} \text{ (MPa)}^{-1} \text{ cm}^3/\text{mol} \end{aligned}$$

So

$$C_\sigma = \frac{-34.834 \times 10^{-3}}{144} + 0.354 \times 10^{-3} = 112 \times 10^{-6} \text{ (MPa)}^{-1}$$

The experimental value is 111×10^{-6} (MPa) $^{-1}$

10.4.3. Polymer melts and elastomers (above $1.5T_g$)

Table 10.8 gives the available values of the stress-optical coefficients for several polymer types, again calculated by means of Eq. (10.25). These values are higher by some orders of magnitude than those of the glassy polymers. The simplest polymer structure, polymethylene, has a C_σ of about 2000×10^{-12} Pa $^{-1}$. Side groups and side chains do decrease the C_σ -value.

Janeschitz-Kriegel discovered an interesting effect of side groups in polycarbonates. If one methyl group in the 2,2-propylidene group is substituted by a phenyl group, the value of C_σ decreases by 50%; if it is substituted by a benzyl group, however, the value increases by 10% only. This may be explained as follows: the benzyl side group is flexible with regard to the main chain and can orient itself more parallel to the polymer

TABLE 10.7 Increments C_i for different atoms and types of intermolecular interaction

Atom or type of intermolecular interaction	Symbol	$C_i \times 10^3 \text{ cm}^3/(\text{mol} \cdot \text{MPa})$
Carbon	C_C	-2.0492
Hydrogen	C_H	-0.5227
Oxygen in main chain	$C_{O,b}$	3.198
Oxygen in side chain	$C_{O,s}$	-0.7568
Nitrogen in main chain	$C_{N,b}$	7.175
Nitrogen in side chain	$C_{N,s}$	1.303
Chlorine	C_{Cl}	-3.476
Sulfur	C_S	-0.79
Dipole-dipole interaction ^a	C_d	-2.512
Hydrogen bond	C_h	-6.21
Coefficient of symmetry ^b	C_p	1.7

^a Coefficient C_d is used for each polar group of any chemical nature; two similar polar groups at the same atom are considered as one group.

^b Coefficient C_p is used in the case of p-substitution in aromatic cycle positioned in the main chain (in accordance to the amount of the cycles).

backbone (which leads to an increase of α_{\parallel} and thus to an increase of C_{σ} , whereas in the case of the phenyl group, the latter can only orient itself perpendicularly to the backbone, thus increasing α_{\perp} and decreasing C_{σ} .

10.4.4. Flow birefringence of polymer solutions

For dilute polymer solutions the following definitions are well known

$$[n] = \lim_{\substack{c \rightarrow 0 \\ q \rightarrow 0}} \frac{\Delta n - \Delta n_o}{cq\eta_o} \quad \text{and} \quad [\eta] = \lim_{\substack{c \rightarrow 0 \\ q \rightarrow 0}} \frac{\eta - \eta_o}{c\eta_o} \quad (10.28)$$

where $[n]$ = intrinsic flow birefringence ($\text{m}^4 \text{s}^2/\text{kg}^2$); Δn = birefringence of the solution (-); Δn_o = birefringence of the solvent (-); $[\eta]$ = intrinsic viscosity (m^3/kg); η = viscosity of the solution (Ns/m^2); η_o = viscosity of the solvent (Ns/m^2); q = shear rate (s^{-1}); c = concentration of the solution (kg/m^3).

From data on flow birefringence of polymer solutions, values of the segmental anisotropy, $\Delta\alpha = \alpha_1 - \alpha_2$, can be calculated by means of Kuhn's equation on flexible rubber chains:

$$\frac{[n]}{[\eta]} = 2C = \frac{4\pi}{45kT} \frac{(n^2 + 2)^2}{n} (\alpha_1 - \alpha_2) \quad (10.29)$$

where $\Delta\alpha = \alpha_1 - \alpha_2$ = segmental anisotropy of the molecule (m^3).

Preferably a so-called "matching solvent" is used (i.e. $d\eta/dc = 0$). Since $[n]/[\eta] = 2C_{\sigma}$ also the stress-optical coefficient may easily be calculated.

From $\Delta\alpha$ also the value of $\alpha_{\parallel} - \alpha_{\perp}$ may be calculated, which is the difference in polarisability of the structural unit in parallel and perpendicular direction of the chain, by means of the equation:

$$\alpha_{\parallel} - \alpha_{\perp} = (\alpha_1 - \alpha_2) \frac{L\lambda}{\langle r^2 \rangle} \quad (10.30)$$

where L = full length of extended chain; λ = length of structural unit in chain direction; $\langle r^2 \rangle$ = mean square end-to-end distance of coil.

TABLE 10.8 Stress-optical coefficients of polymer melts and elastomers (above their melting temperatures)

Polymers		Temperature (°C)	Stress optical coefficient (brewster)
Polyalkenes	Poly(ethylene), linear (melt)	150/190	1800/2400
	Poly(propylene), isotactic (melt)	210	900
	Poly(ethylene), cross-linked	130/180	1500/2200
Polyvinyls	Poly(vinyl chloride)	210	-500
	Poly(styrene)	120/150	-4100/5200
Polydienes	Polyisobutadienes (melt)	22	3300
	Polyisoprenes (melt)	22	1900
	Poly(<i>cis</i> -isoprene), natural rubber (crossl.)	20/100	1800/2050
	Poly(<i>trans</i> -isoprene), gutta percha (crossl.)	85/250	3000
Polysiloxanes	Poly(dimethyl siloxane)	20/190	135/260
Polycarbonates	Poly(bisphenol-A carbonate) R = CH ₃	170/230	3500/3700
		Do., phenyl substituted R =	250
		Do., benzyl substituted R =	220
			1800/2100
			4000

Data from Saunders (1956), Wales (1976), Vinogradov et al. (1978) and Janeschitz-Kriegl et al. (1988).

Fig. 10.4 gives a survey of the structural influences on $\Delta\alpha$. The data were compiled by Tsvetkov and Andreeva (1975). Carbon main chains have a $\Delta\alpha$ -value of about $75 \times 10^{-25} \text{ cm}^3$. Side chains lower the $\Delta\alpha$ value, especially aromatic side chains with the aromatic ring system directly linked to the main chain. Carboxy-groups in main and side chains also lower the $\Delta\alpha$ value.

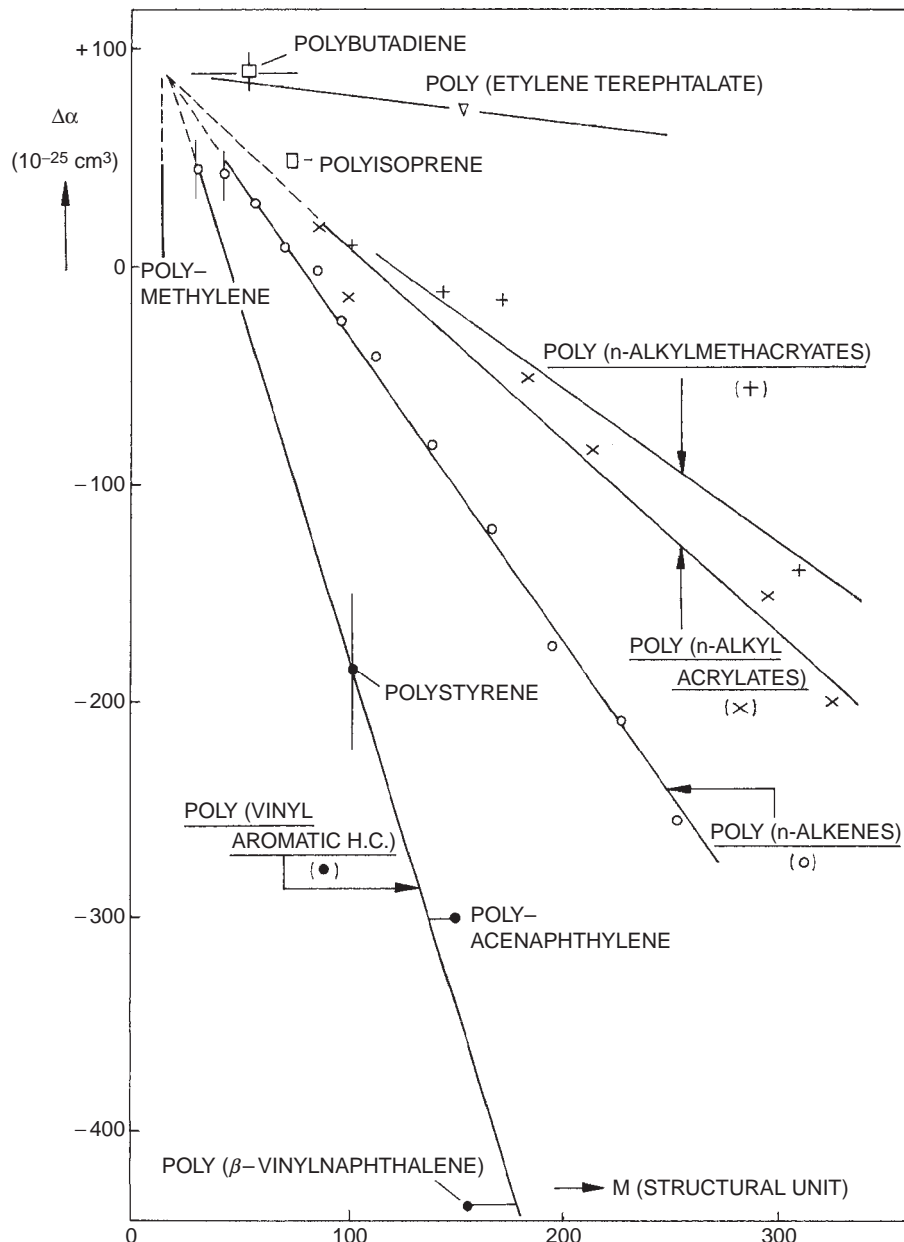


FIG. 10.4 Segmental anisotropy of polymers in solution. Data of Tsvetkov and Andreeva (1975).

10.4.5. Semi-crystalline polymers in fibre form

Data of the birefringence of drawn fibres of semi-crystalline polymers are collected in Table 10.9.

The specific birefringence of a fibre is measured in transverse direction and defined as the difference in refractive index between the two components of a light wave, vibrating parallel and perpendicular to the fibre axis ($\Delta n = n_{\parallel} - n_{\perp}$). The birefringence is made up of contributions from the amorphous and crystalline regions. The increase in birefringence, occurring in semi-crystalline polymers by orientation ("drawing"), is due to the increase in mean orientation of the polarisable molecular segments. In crystalline regions the segments contribute more to the overall birefringence than in less ordered regions. Also the average orientation of the crystalline regions (crystallites) may be notably different from the mean overall orientation. De Vries (1955/1959, 1979/1980) showed that from the measured birefringence of a fibre the applied draw ratio (Λ) can be calculated by means of the empirical formula:

$$\frac{d\Delta n}{d \ln \Lambda} = m + p\Delta n \quad (10.31)$$

or in integrated form:

$$\Delta n = \frac{m}{p} (\Lambda^p - 1) \quad (10.32)$$

Table 10.9 also contains values of p and m . A significant conclusion from these data is that p has a negative value for purely aliphatic chains, whereas p has a positive value for chains containing rings; m is the initial slope of the Δn versus $\ln \Lambda$ curve. De Vries (1959) gave the following tentative scheme of relations between p -values and chemical structure:

	One repeating structural unit	Two alternating structural sub-units
Purely aliphatic chains	$p = -\frac{1}{2}$	$p = -1$
Chain units incorporating a ring structure	$p = +1$	$p = +\frac{1}{2}$

TABLE 10.9 Some numerical data on birefringence of fibres

Polymers		n_{\parallel}	n_{\perp}	Δn	p	m
Ringless chains	Polyethylene	1.556	1.512	0.044	-0.5	0.038
	Nylon 6	1.580	1.530	0.050	-0.5	0.050
	Nylon 66	1.582	1.519	0.063	-1.0	0.072
Chain units incorporating cellulosic rings	Cellulose acetate	1.539	1.519	0.020		
	Rayon	1.539	1.519	0.020	1.0	0.02
	Cellulose	1.578	1.532	0.046	-	-
	Cotton	1.596	1.538	0.068	-	-
Chain units incorporating Aromatic rings	Polyester (PETP)	1.725	1.537	0.118	0.5	0.083
	Aramid (PpPTPA)	2.267	1.605	0.662		

Data from Morton and Hearle (1962), De Vries (1959) and Simmens and Hearle (1980).

10.4.6. Polymer liquid crystals

Liquid crystals are found to be birefringent due to their anisotropic nature.

The last polymer mentioned in Table 10.9 is poly(*p*-phenylene terephthalamide). This polymer is spun from its solution in pure sulphuric acid (100%), a dope that exhibits mesomorphic (=liquid crystalline) behaviour; it is optically anisotropic and is nematic in character. A number of other polymers, containing rigid elements in the chain have melts of polymer liquid crystals, with a high birefringence and a non-linear optical behaviour in electric fields.

Optically non-linear materials show a change in their refractive index when exposed to electrical and electromagnetic fields, which opens the possibility to influence the propagation of light by means of external fields. Practical applications of these effects are in the sphere of optical data transmission and data manipulation.

Liquid crystalline phases are known to couple collectively – and therefore strongly – to external electromagnetic fields, which may be used to induce local variations. If such polymeric liquid crystal phases are rapidly frozen-in, this leads to strongly anisotropic glasses.

10.5. LIGHT SCATTERING

Scattering of light is caused by optical inhomogeneities. Molecules act as secondary sources of light as has been shown by Rayleigh (1871). Since the intensity is the energy crossing unit area per second, we may obtain the total scattering by integrating over a sphere with radius r . For any value of θ we may construct an element of surface having an area $2\pi r^2 \sin \theta d\theta$, over which i_θ/I_o will be constant. Thus, the turbidity (τ) or total scattered intensity is (Debye, 1944–1947; Tanford, 1967)

$$\tau = \int_0^\pi 2\pi r^2 i_\theta \sin \theta d\theta \quad (10.33)$$

In the absence of absorption, τ is related to the primary intensities of a beam before and after it has passed through a thickness l of the medium, by the equation

$$I_o - I = I_o(1 - \exp[-\tau l]) \quad (10.6)$$

In solutions, part of the light scattering arises from fluctuations in refractive index caused by fluctuations in composition. The well-known equation for light scattering from solutions is based on these considerations

$$R_\theta = K \frac{RTc}{d\Pi/dc} \quad (10.34)$$

where c = polymer concentration (kg/m^3)

$$R_\theta \equiv \frac{r^2 i_\theta}{I_o(1 + \cos^2 \theta)} = \text{Rayleigh's ratio } (\text{m}^{-1})$$

r = distance of scattering molecule (m)

$$K = \frac{2\pi^2}{\lambda_o N_A} \left[n \frac{dn}{dc} \right]^2 (\text{m}^2 \text{mol}/\text{kg}) \quad (10.35)$$

N_A = Avogadro's number (mol^{-1}); λ_o = wave-length of the light in vacuum (m); Π = osmotic pressure (N/m^2).

Since

$$\frac{1}{RT} \frac{d\Pi}{dc} = \frac{1}{M} + 2A_2c$$

where A_2 is the second virial coefficient, substitution gives

$$\frac{Kc}{R_\theta} = \frac{1}{M} + 2A_2c \quad (10.36)$$

This equation forms the basis of the determination of polymer molecular masses by light scattering, which is one of the few absolute methods.

Eq. (10.36), however, is correct only for optically isotropic particles, which are small compared to the wave-length. If the particle size exceeds $\lambda/20$ (as in polymer solutions), scattered light waves, coming from different parts of the same particle, will interfere with one another, which will cause a reduction of the intensity of the scattered light to a fraction $P(\theta)$ given by

$$P(\theta) = 1 - \frac{1}{3} q R_G^2 + \dots \quad (10.37)$$

where R_G is the radius of gyration of the particle (polymer molecule) and $q = 4\pi(n/\lambda_o) \sin(\theta/2)$. The formula for the excess light scattered by a polymer solution as compared with pure solvent therefore becomes

$$\frac{Kc}{R_\theta} = \frac{1}{M_w P(\theta)} + 2A_2c + \dots \quad (10.38)$$

As $P(\theta) \rightarrow 1$ for $\theta \rightarrow 0$, Zimm (1960) suggested a plot of Kc/R_θ against $\sin^2(\theta/2) + kc$ (where k is a constant, dependent of the dimension of the concentration, to choose in such a way that clear figures will be created). Thus one obtains a grid which allows extrapolation to $c = 0$ and $\theta = 0$ (see Fig. 10.5). The intercept on the ordinate then gives $1/M_w$, and the two slopes provide values to calculate A_2 (take care of the constant k at the x-axis!) and R_G^2 . By this method polymer molecular masses of the order of $10^4 - 10^7$ g/mol can be measured. In order to find the quantity K , the refractive index of the solution n , and the so-called *specific refractive index increment* (dn/dc), require experimental determination. Because the solutions to be measured are very dilute, the value of n may be replaced by n_s the refractive index of the solvent.

Also for these dilute solutions, the refractive index increment is a constant for a given polymer, solvent and temperature, and is normally measured with an interferometer or with a differential refractometer.

As was shown by Goedhart (1969), it is also possible to calculate (dn/dc) values from group contributions. The best results were obtained with the following simple equation

$$\frac{dn}{dc} = \frac{n_p - n_s}{\rho_p} = \frac{\mathbf{V}}{\mathbf{M}} \left(\frac{\mathbf{R}_V}{\mathbf{M}} - n_s \right) \quad (10.39)$$

where the subscripts s and p identify solvent and polymer, respectively. Since n and ρ of polymers can be calculated by means of additive molar quantities, the specific refractive index increment can be calculated, so that measurement of R_θ only is sufficient for the determination of M_w , R_G^2 and A_2 .

Table 10.10 shows that experimental and calculated values of (dn/dc) are in fair agreement.

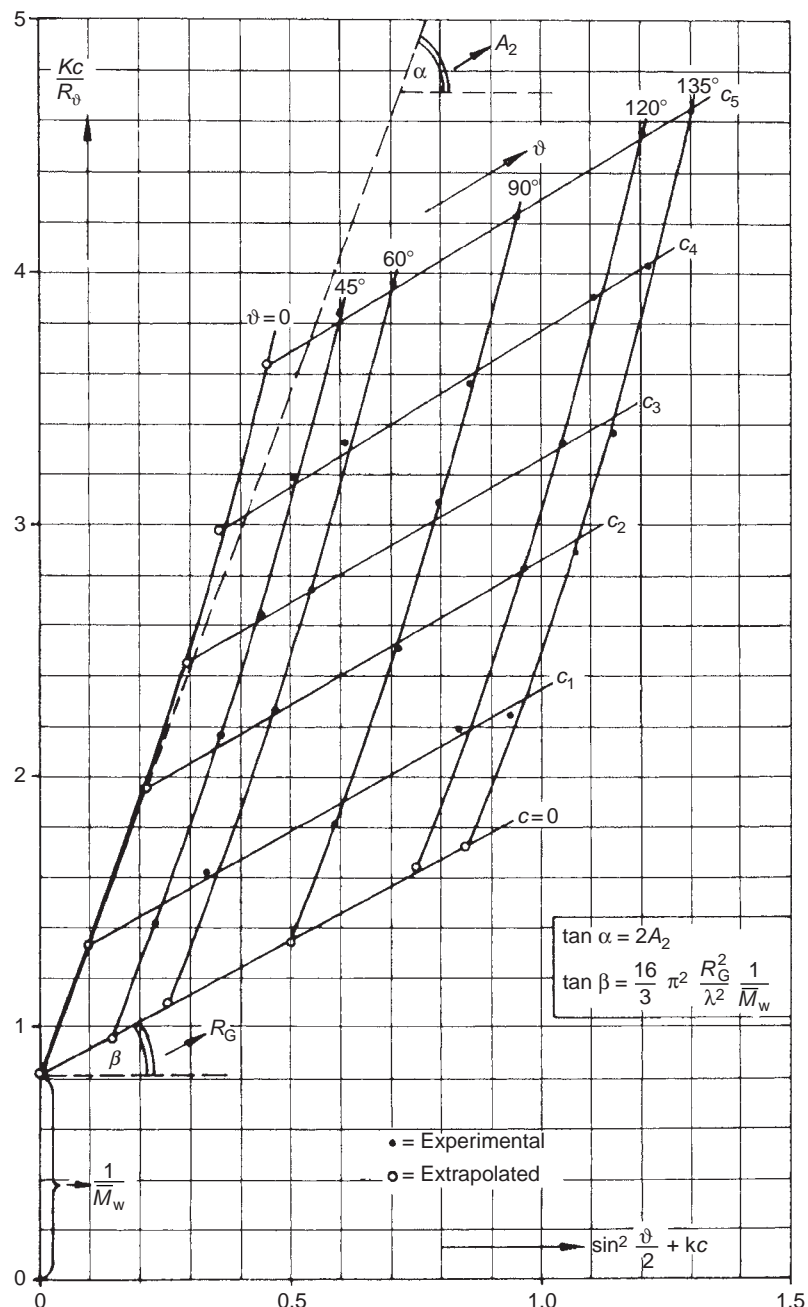


FIG. 10.5 Example of a Zimm plot of light scattering data.

TABLE 10.10 Comparison of calculated and experimental dn/dc values of polymer solutions

Polymer	Solvent	Experimental			Calc. dn/dc with	
		dn/dc	T (°C)	λ (nm)	n_{GD}	n_V
Polystyrene	Benzene	0.106	25	546	0.093	0.084
	Benzene	0.110	25	546	0.093	0.084
	Bromobenzene	0.042	25	546	0.038	0.028
	Bromonaphthalene	-0.051	25	546	-0.056	-0.025
	Carbon tetrachloride	0.146	25	546	0.129	0.120
	Chlorobenzene	0.099	-	436	0.071	0.061
	Chloroform	0.195	20	436	0.145	0.136
	Cyclohexane	0.167	20	546	0.161	0.151
	p-Chlorotoluene	0.093	25	436	0.075	0.066
	Decalin	0.128	20	546	0.122	0.113
	Dichloroethane	0.161	20	546	0.147	0.137
	Dioxane	0.168	25	546	0.167	0.158
	Tetrahydrofuran	0.189	25	546	0.184	0.175
	Toluene	0.104	20	546	0.097	0.088
Poly(vinyl chloride)	Acetone	0.138	20	546	0.133	0.110
	Cyclohexanone	0.078	25	-	0.066	0.043
	Dioxane	0.086	-	546	0.087	0.064
	Tetrahydrofuran	0.102	-	-	0.100	0.077
Poly(vinyl acetate)	Acetone	0.095	20	546	0.097	0.094
	Acetone	0.104	30	436	0.097	0.094
	Acetonitrile	0.104	-	-	0.108	0.105
	Benzene	-0.026	25	560	-0.022	-0.025
	Chlorobenzene	-0.040	25	560	-0.042	-0.045
	Dioxane	0.030	25	560	0.044	0.040
	Ethyl formate	0.095	-	-	0.096	0.093
	Methanol	0.131	25	546	0.121	0.117
	2-Butanone	0.080	25	546	0.079	0.075
	Tetrahydrofuran	0.055	25	546	0.060	0.056
Poly(methyl methacrylate)	Toluene	-0.020	25	560	-0.018	-0.022
	Acetonitrile	0.137	25	546	0.120	0.112
	Bromobenzene	-0.058	25	546	-0.065	-0.073
	1-Bromonaphthalene	-0.147	25	546	-0.151	-0.159
	Butyl acetate	0.097	-	546	0.078	0.069
	Butyl chloride	0.090	20	546	0.072	0.063
	Chlorobenzene	-0.026	25	546	-0.035	-0.043
	Isoamyl acetate	0.091	20	546	0.072	0.063
	Nitroethane	0.094	25	546	0.082	0.074
	1, 1 2-Trichloroethane	0.025	-	560	0.012	0.003
	Acetone	0.129	25	546	0.109	0.100
	Acetone	0.134	25	546	0.109	0.100
	Benzene	-0.010	25	546	-0.014	-0.022
	2-Butanone	0.109	-	546	0.090	0.081
	2-Butanone	0.114	25	546	0.090	0.081
	Carbon Tetrachloride	0.023	25	546	0.019	0.010

(continued)

TABLE 10.10 (continued)

Polymer	Solvent	Experimental			Calc. dn/dc with	
		dn/dc	T (°C)	λ (nm)	n_{GD}	n_V
Poly(propylene oxide)	Chloroform	0.055	–	546	0.034	0.025
	Chloroform	0.063	–	546	0.034	0.025
	Dioxane	0.071	–	546	0.055	0.046
	Ethyl acetate	0.118	–	546	0.098	0.089
	Tetrahydrofuran	0.087	–	546	0.070	0.061
	Benzene	–0.045	25	546	–0.046	–0.042
	Chlorobenzene	–0.064	25	546	–0.069	–0.065
	Hexane	0.078	25	546	0.079	0.083
	2-Methylheptane	0.066	35	546	0.061	0.065
	Methanol	0.118	25	546	0.123	0.127
Poly (hexamethylene adipamide)	m-Cresol	–0.016	25	546	–0.017	–0.011
	Dichloroacetic acid	0.098	25	546	0.051	0.057
	95% Sulphuric acid	0.082	25	546	0.076	0.083

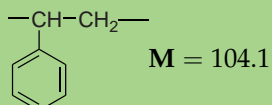
It should be mentioned that light scattering is not restricted to solutions. In fact, the technique can be used to obtain information about the super molecular structure of solid polymers.

Example 10.3

Estimate the specific refractive index increment (dn/dc) of polystyrene in 1,4-dioxane ($n_D = 1.422$).

Solution

The structural unit of polystyrene is



Using the group contributions in Tables 4.2 and 10.4 and using Eq. (4.29) we find

	R_{Vi}	V_i
1 ($-\text{CH}_2-$)	20.64	16.37
1 ($>\text{CH}-$)	21.40	10.85
1 (C_6H_5)	123.51	73.36
	165.55	100.58

using Eq. (10.39) we get:

$$\frac{dn}{dc} = \frac{V}{M} \left(\frac{R_V}{M} - n_s \right) = \frac{100.58}{104.1} \left(\frac{165.55}{104.1} - 1.422 \right) = 0.163$$

which is in fair agreement with the experimental value of 0.168. However, it causes an error of 6% in M_w .

10.6. ABSORPTION

A light beam propagating through a medium over a path l suffers a loss of intensity I characterised by *Lambert's relationship*

$$I = I_0 \exp\left(-\frac{4\pi k l}{\lambda}\right) \quad (10.40)$$

The *absorption index* k is a characteristic function of the wave-length and obviously increases as the wave-length of an absorption peak is approached. Most polymers show no specific absorption in the visible region of the spectrum and are therefore colourless in principle.

10.6.1. Infrared absorption

Since all polymers possess specific absorption bands in the infrared part of the spectrum, the infrared spectrum is one of the most valuable tools in the analysis of polymers. The approximate wave-lengths of some infrared absorption bands arising from structural group and atomic vibrations found in polymers are shown in Fig. 10.6. As some infrared bands are influenced by the conformation of the polymer chain, the IR absorption technique offers a means to determine the crystallinity. Use of polarised IR provides the opportunity to determine the orientation of the amorphous and crystalline parts of a semicrystalline polymer separately. Fourier Transform Infrared Spectroscopy has increased the usefulness tremendously. It is beyond the scope of this book to go into detail of infrared spectroscopy, but it is a technique that in general is used as the first qualitative technique of an unknown sample, because it is a fast method and gives information about chemical composition and structure. The technique might be completed with far-infrared spectra and Raman-spectra. Together they give much information about, e.g.:

- (a) Chemical composition (copolymers, additives tacticity and molecular weight)
- (b) Structure elucidation (conformation, crystallinity, orientation and dispersion)
- (c) Kinetics (degradation and polymerisation, crystallisation and diffusion)
- (d) Temperature effects (melting temperature and glass transition temperature)
- (e) Thickness of plan-parallel films

10.7. OPTICAL APPEARANCE PROPERTIES

The optical appearance properties of a polymer, e.g. its clarity, gloss, dullness or turbidity, have no (direct) correlation with its chemical structure; they are largely determined by physical factors. Commercially these properties are important. Two groups of appearance properties may be distinguished: those connected with the volume (bulk) and those connected with the surface of the material.

The main volume properties of polymers are *colour* and *transparency*. Both may either be inherent to the polymer or caused by additions, e.g. dyes and other additives. Most polymers do not show differential absorption in visible light and are therefore colourless. The volume properties cover a wide range: from *glass clarity* to full *opaqueness*. This is also the case for the surface properties; they may vary from *high gloss* to full *dullness (matt)*.

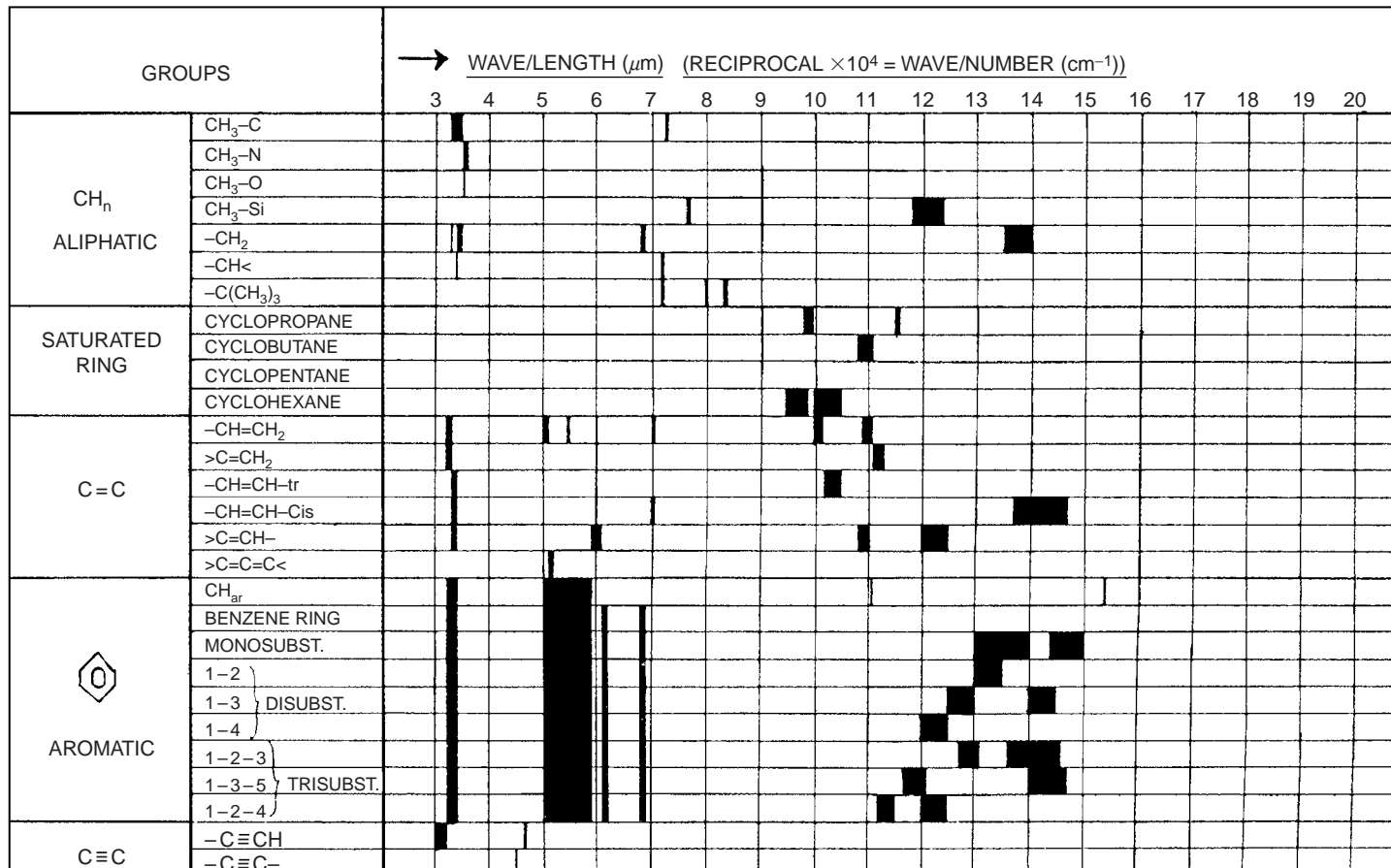


FIG. 10.6 Characteristic absorption bands of structural groups.

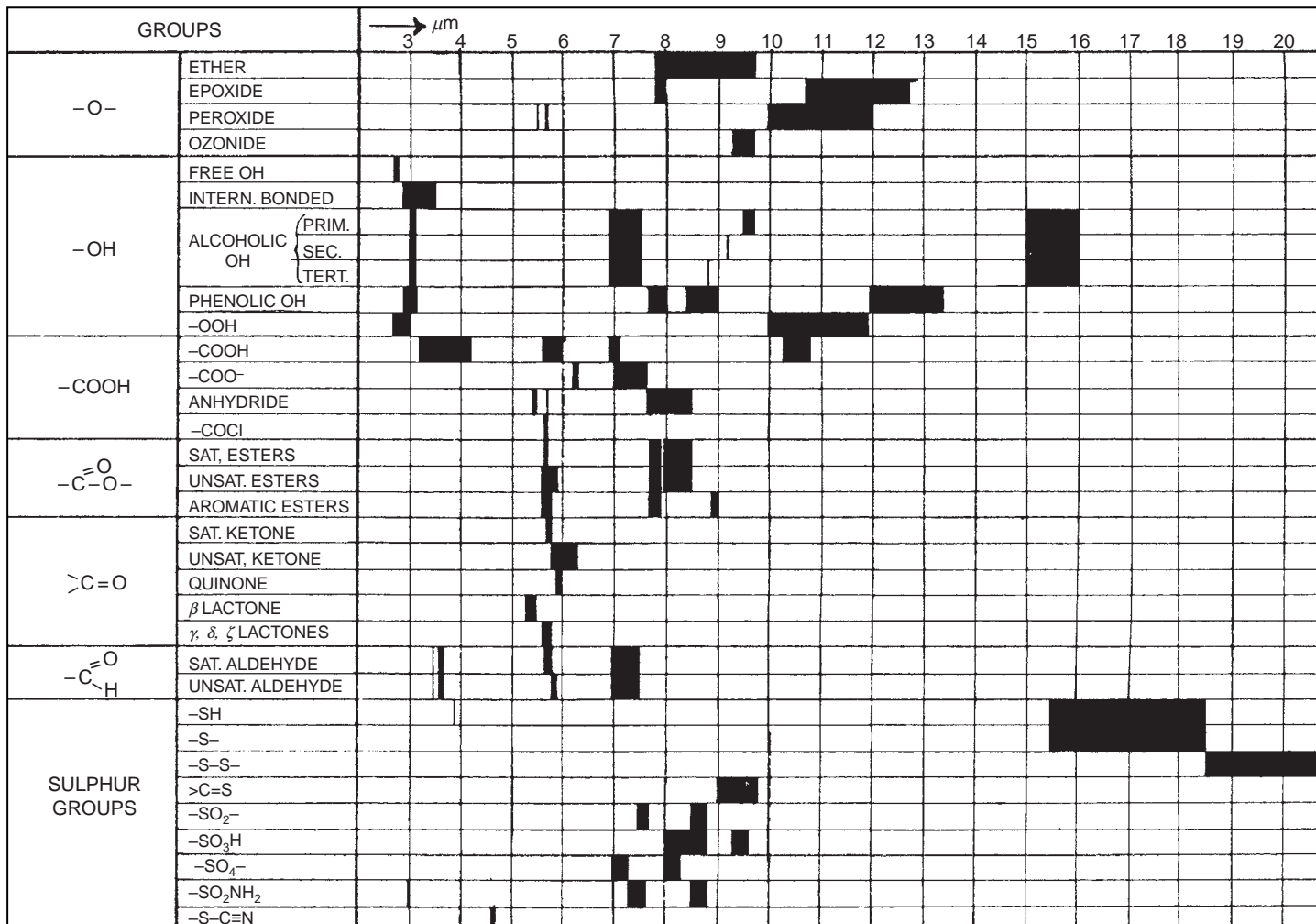


FIG. 10.6 (continued)

TABLE 10.11 Survey of optical appearance properties

Property	Assessment	
	Subjective	Objective
<i>A. Volume properties</i>		
Transparency	Transparency Clarity	Direct transmittance
Translucence	Attenuated Clarity in contrast in detail	Do.
	Haziness	Haze
	Milkiness	Turbidity
Opaqueness	Opaqueness	
<i>B. Surface properties</i>		
High specular reflectance	Glossy	Gloss
Attenuated	Sheen	
Spec. reflect.	Dull	Do.
Specular refl. absent	Matt	—

Table 10.11 gives a tentative survey of the nomenclature. The objective measurement of these properties is not easy. It is based on quantitative measurement of light fluxes. It should always be remembered in this context that the primary instrument is the human eye.

10.7.1. Volume appearance properties

Here the objective measure is the degree of light transmittance: the ratio of the intensity of the non-deviated light passing-through, to that of the incident light; the loss in light flux is the scattered light. The transmittance is nearly 100% for glass-clear materials and 0% for opaque materials.

If the transmittance is > 90%, the material is called *transparent*, for lower values it is called *translucent*. Translucent bodies show loss of contrast and loss of detail. *Haze* or *milkiness* is defined as that fraction of the transmitted light that deviates from the transmitted beam by more than 2½%. It may be caused by flow defects during processing (e.g. *melt elasticity*) or by crystallisation (*size* and *volume fraction* of crystallites and spherulites). Jabarin (1982) determined the haze in polyester (PETP) sheets, crystallised at various temperatures; irrespective of the crystallinity, a maximum of haze was found for spherulite volume fractions of about 0.6 and spherulite radii of about 1.7 µm. These results could be interpreted by means of the *theory of spherulite scattering* developed by Stein et al. (1960–1976).

10.7.2. Surface appearance properties

The objective measure in this case is the intensity and kind of reflectance. Only for highly polished metal mirrors the reflectance may be nearly total; if the specular reflectance is almost nil, the surface is totally *matt*. In between, the material is *glossy* or *sheeny*. *Gloss* is the reflectance of a surface responsible for its lustrous appearance, commonly at maximum near the specular direction, i.e. the direction of pure mirror reflection.

The fraction of the light that neither enters the material, nor follows the direction of mirror reflection, is dispersed by diffraction. The *lustre* of a material is therefore the integral effect of reflection and diffraction.

The major part of the scattered light originates at surface irregularities and other imperfections, such as scratches. Also in this case the dominant rimpling mechanism may be caused by flow defects (and their after-effects) and by crystallisation. Bennett and Porteus (1961) investigated the effect of surface roughness on the reflectance. This effect may be quantified by the equation

$$r_{sr}/r_o = \exp\{-(4n\sigma/\lambda)\cos \theta_i]^2\} \quad (10.41)$$

where r_{sr} = specular reflectance of the rough surface; r_o = specular reflectance of a perfectly smooth surface; n = refractive index; σ = mean surface roughness in nm; λ = wave length of the light in nm; θ_i = angle of incident light.

A thorough theoretical analysis has been carried out by Beckmann and Spizzichino (1963) and by Davies (1954).

BIBLIOGRAPHY

General reading

- Askadskii AA, "Physical Properties of Polymers: Prediction and Control", Gordon and Breach, New York, 1996.
 Bicerano J, "Prediction of Polymer Properties", Marcel Dekker, New York, 3rd Ed, 2002, Chap. 8.
 Galiatsatos V, "Refractive Index, Stress-Optical Coefficient and Optical Configuration Parameters of Polymers", in Mark JE (Ed), "Physical Properties of Polymers Handbook", Springer-Verlag, 2nd Ed 2007, Chap. 50.
 Galiatsatos V, Neaffer RO, Sen S and Sherman BJ, "Refractive Index, Stress-Optical Coefficient and Optical Configuration Parameters of Polymers", in Mark JE (Ed), "Physical Properties of Polymers Handbook", AIP Press, Woodbury, NY, 1996, Chap. 39.

Optics in general

- Born M and Wolf E, "Principles of Optics", 9th Ed, Pergamon Press, Oxford, 1999.
 Born M, Wolf E and Bhatia AB, "Principles of Optics", 7th Ed, Cambridge University Press, Cambridge, 1999.
 Longhurst RS, "Geometrical and Physical Optics", 3rd Ed, Longmans, London, 1973.
 Meeten GH (Ed), "Optical Properties of Polymers", Elsevier Applied Science Publishers, London, 1986.
 Wahlstrom EE, "Optical Crystallography", Wiley, New York, 1969.

Birefringence

- Janeschitz-Kriegel H, "Flow-birefringence of elasto-viscous polymer systems", Adv Polym Sci, 6 (1969) 170.
 Janeschitz-Kriegel H, "Polymer Melt Rheology and Flow Birefringence", Springer Verlag, New York, 1983.

Polarised light

- Azzam RMA and Bashara WM (Eds), "Ellipsometry and Polarised Light", North Holland, Amsterdam, 1977.
 Pye D, "Polarised Light in Science and Nature", IOP, Bristol, 2001.
 Shurcliff WA and Ballard SS, "Polarised Light", Van Nostrand, Princeton, 1964.

Light scattering

- Beckmann P and Spizzichino A, "The Scattering of Electromagnetic Waves from Rough Surfaces", Pergamon, Oxford, 1963.
 Huglin NB (Ed), "Light Scattering from Polymer Solutions", Academic Press, New York, 1972.
 Kerker M, "The Scattering of Light and Other Electromagnetic Radiation", Academic Press, New York, 1969.
 Lenz RW and Stein RS (Eds), "Structure and Properties of Polymer Films", Plenum Press, New York, 1973.
 Van de Hulst HC, "Multiple Light Scattering" (2 Vols), Academic Press, New York, 1978.

Infra-red spectroscopy

- Bellamy LJ, "Advances in Infrared Group Frequencies", Methuen, London, 1968.
 Campbell D and White JR, "Polymer Characterization, Physical Techniques", Chapman and Hall, London, 1989, Chap. 5.

- Conley RT, "Infrared Spectroscopy", Allyn and Bacon, Boston, 1966.
 Dodd RE, "Chemical Spectroscopy", Elsevier, Amsterdam, 1962.
 Flett MSTC, "Characteristic Frequencies of Chemical Groups in the Infrared", Elsevier, Amsterdam, 1963.
 Freeman SK (Ed), "Interpretive Spectroscopy", Reinhold, New York, Chapman, London, 1965.
 Hummel DO, "Infrared Spectra of Polymers: in the Medium and Long Wavelength Regions", Interscience, New York, 1966.
 Szymanski HA, "Infrared Band Handbook", Plenum Press, New York, 1964.
 Zbinden R, "Infrared Spectroscopy of High Polymers", Academic Press, New York, 1964.

Special references

- Andrews RD, J Appl Phys 25 (1954) 1223.
 Askadskii AA, Pure Appl Chem 46 (1976) 19.
 Askadskii AA, "Polymer Yearbook IV" (1987) 128, 145 (Pethrick RA and Zaikov GE Eds, Harwood, London).
 Bennett HE and Porteus JO, J Opt Soc Am 51 (1961) 123 and 53 (1963) 1389.
 Davies H, Proc Inst Electr Eng 11 (1954) 209.
 Debye P, J Appl Phys 15 (1944) 338; J Phys Coll Chem 51 (1947) 18.
 De Vries H, PhD Thesis Delft University of Technology (1953); J Polym Sci 34 (1959) 761, Angew Chem 74 (1962) 574; Coll Polym Sci 257 (1979) 226, 258 (1980) 1.
 Eisenlohr F, Z physik Chem 75 (1911) 585; 79 (1912) 129.
 Gladstone JH and Dale TP, Trans Roy Soc (Lond) A 148 (1858) 887.
 Goedhart DJ, "Communication Gel Permeation Chromatography International Seminar", Monaco, Oct 12–15, 1969.
 Heller W, Phys Rev 68 (1945) 5; J Phys Chem 69 (1965) 1123; J Polym Sci A2–4 (1966) 209.
 Huggins ML, Bull Chem Soc Jpn 29 (1956) 336.
 Jabarin SA, Pol Eng Sci 22 (1982) 815.
 Janeschitz-Kriegl H, Makromol Chem 33 (1959) 55; 40 (1960) 140.
 Janeschitz-Kriegl H and Wales JLS, Nature (1967) 1116.
 Janeschitz-Kriegl H et al., in Lemstra PJ and Kleintjens LA (Eds), "Integration of Fundamental Polymer Science and Technology – 2", pp 405–409, Elsevier Appl Sci 1988.
 Lamble JH and Damiouch ES, Br J Appl Phys 9 (1958) 388.
 Looyenga H, Molecular Physics 9 (1965) 501; J Polym Sci, Polymer Physics Ed 11 (1973) 1331.
 Lorentz HA, Wied Ann Phys 9 (1880) 641.
 Lorenz LV, Wied Ann Phys 11 (1880) 70.
 Morton WE and Hearle JWS, "Physical Properties of Textile Fibres", Textile Inst & Butterworth, London, 1962.
 Pohl RW, "Einführung in die Optik", Berlin, 1943, p 147.
 Rayleigh JW Strutt, Lord, Phil Mag (4) 41 (1871) 107, 224, 447.
 Rudd JF and Andrews RD, J Appl Phys 29 (1958) 1421 and 31 (1960) 818.
 Saunders DW, Trans Faraday Soc 52 (1956) 1414.
 Schoorl N, "Organische Analyse", I Bd 14, Centen, Amsterdam, 1920.
 Simmens S and Hearle JWS, J Polym Sci Phys Ed 18 (1980) 871.
 Stein RS et al., J Appl Phys 31 (1960) 1873; 33 (1962) 1914; 36 (1965) 3072; J Polym Sci, Phys Ed 9 (1971) 1747, 11, (1973) 149, 1047 and 1357; 12 (1974) 735, 763; Polymer J 8 (1976) 369.
 Tanford C, "Physical Chemistry of Macromolecules", Wiley, New York, 5th Pr, 1967.
 Tsvetkov VN and Andreeva LN, "Polymer Handbook" (Eds Brandrup J and Immergut EH, Eds) 2nd Ed, 1975, IV, 377, Wiley, New York.
 Vinogradov GV et al, J Appl Polym Sci 22 (1978) 665.
 Vogel A, J Chem Soc (1948) 1833.
 Vogel A, Chem Ind (1951) 376; (1952) 514.
 Vogel A, Cresswell W and Leicester I, Chem Ind (1950) 358; (1953) 19.
 Vogel A, Cresswell W and Leicester I, J Phys Chem 58 (1954) 174.
 Wales JLS, "The Application of Flow Birefringence to Rheological Studies of Polymer Melts", PhD Thesis Delft University of Technology, Delft University Press, 1976.
 Wibaut JP, Hoog H, Langendijk SL, Overhoff J and Smittenberg J, Rec Trav Chim 58 (1939) 329.
 Young J and Finn A, J Res Natl Bur Standards 24 (1940) 759.
 Zimm BH, "The Normal-Coordinate Method for Polymer Chains in Dilute Solution", Chap. 1 in Eirich FR (Ed), "Rheology", Vol 3, Academic Press, New York, 1960.

CHAPTER 11

Electrical Properties

Two groups of electrical properties of polymers are of interest. The first group of properties is usually assessed from the behaviour of the polymer at low electric field strengths. To this group belong the *dielectric constant*, the *dissipation factor*, the *static electrification*, and the *electrical conductivity*.

The second group consists of properties that are important at very high electric field strengths, such as *electric discharge*, *dielectric breakdown* and *arc resistance*. They may be regarded as the ultimate electrical properties. Properties of the first group are directly related to the chemical structure of the polymer; those of the second are greatly complicated by additional influences in the methods of determination.

Only the dielectric constant can be estimated by means of additive quantities.

11.1. INTRODUCTION

The application of an electric field to a material can produce two effects. It may cause the charges within the material to flow; on removal of the field the flow ceases but does not reverse. In this case the material is called an *electric conductor*.

Alternatively the field may produce field changes in the relative positions of the electric charges, which change is of the nature of an electric displacement and is completely reversed when the electric field is removed. In this case the material is called a *dielectric*.

The common polymers are all dielectrics.

11.2. DIELECTRIC POLARISATION

11.2.1. Dielectric constant (permittivity, electric inductive capacity)

The relative dielectric constant of insulating materials (ϵ) is the ratio of the capacities of a parallel plate condenser measured with and without the dielectric material placed between the plates. The difference is due to the polarisation of the dielectric. It is a dimensionless quantity.

In the 1860s Maxwell published his famous unified theory of electricity, magnetism and light (radiation); he also formulated the so-called *Maxwell relationship* for non-polar materials

$$\varepsilon = n^2 \quad (11.1)$$

where ε is the dielectric constant at the frequency for which the refractive index is n .

For comparison these two quantities should be measured at the same frequency. However, ε is generally measured at relatively low frequencies (10^2 – 10^9 cycles per second), whereas n is measured in the range of visible light (5–7 times 10^{14} cycles per second, usually at the sodium D line). Simple comparison, however, of ε and n_D^2 already gives interesting information. A large disparity of ε and n_D^2 may be an indication of semi-conduction; more frequently the disparity is caused by the occurrence of permanent dipoles in the dielectric.

11.2.2. Relationship between dielectric constant and polarisation

If an electric field is applied to a volume element consisting of molecules without any net dipole, it will cause a change in the distribution of charges in the molecules, resulting in the presence of induced dipoles proportional to the electric field. On molecular level we have (Bower, 2002)

$$P = N_o \alpha E_L \quad (11.2)$$

where P = polarisation (C/m^2); N_o = number of molecules per unit volume (m^{-3}); α = molecular polarisability ($J^{-1} C^2 m^2$); E_L = local electric field ($V/m = J/C/m$).

The relationship between the polarisation and the applied electric field is

$$P = \varepsilon_0 E (\varepsilon - 1) \quad \text{or} \quad \varepsilon = \frac{\varepsilon_0 E + P}{\varepsilon_0 E} = 1 + \frac{P}{\varepsilon_0 E} \quad (11.3)$$

where ε_0 is the permittivity of vacuum ($= 8.854188 \times 10^{-12} J^{-1} C^2/m$). The local field E_L is

$$E_L = E + P/(3\varepsilon_0) = \frac{1}{3}(\varepsilon + 2)E \quad (11.4)$$

Upon substitution Eqs. (11.3) and (11.4) in Eq. (11.2) we finally find

$$\frac{1}{3}N_o \alpha (\varepsilon + 2)E = \varepsilon_0 E (\varepsilon - 1) \quad (11.5)$$

or

$$\frac{\varepsilon - 1}{\varepsilon + 2} = \frac{N_o \alpha}{3\varepsilon_0} \quad (11.6)$$

This relationship between the dielectric constant and the molecular polarisation is known as the *Clausius–Mosotti relation*.

11.2.3. Molar polarisation

The molar polarisation (in m^3/mol) of a dielectric can be defined as follows:

$$\mathbf{P}_{LL} = \frac{\varepsilon - 1}{\varepsilon + 2} \mathbf{V} \quad (\text{compare } \mathbf{R}_{LL} \text{ in Chap. 10}) \quad (11.7)$$

or

$$\mathbf{P}_V = \varepsilon^{1/2} \mathbf{M} \quad (\text{compare } \mathbf{R}_V \text{ in Chap. 10}) \quad (11.8)$$

The group contributions to the molar polarisation (for isotropic polymers) are given in Table 11.1. Application of Eqs. (11.7) and (11.8) permits the calculation of the dielectric

TABLE 11.1 Group contributions to molar dielectric polarisation (\mathbf{P}) in isotropic polymers (cm^3/mol)

Group	For $\mathbf{P}_{\text{LL}} = \frac{\varepsilon - 1}{\varepsilon + 2} \mathbf{V}$ (cm^3/mol)	For $\mathbf{P}_V = \varepsilon^{1/2} \mathbf{M}$ (g/mol)
-CH ₃	5.64	17.66
-CH ₂ -	4.65	20.64
>CH-	3.62	23.5
>C<	2.58	26.4
	25.5	123.5
	25.0	128.6
-O-	5.2	(30)
>C = O	(10)	(65)
-COO-	15	95
-CONH-	30	125
-O-COO-	22	125
-F	(1.8)	(20)
-Cl	(9.5)	(60)
-C ≡ N	11	(50)
-CF ₂ -	6.25	70
-CCl ₂ -	17.7	145
-CHCl-	13.7	90
-S-	8	(60)
-OH (alcohol)	(6)	(30)
-OH (phenol)	~20	~100

constant ε if the structural unit is known. Table 11.2 shows the calculated values of ε in comparison with the observed values and with n^2 . The agreement with the experimental values is satisfactory.

11.2.4. The dielectric constant and the refractive index

For non-polar materials the relationship between the molar polarisation \mathbf{P}_{LL} , the dielectric constant ε and the molecular polarisability α is known as the *molar Clausius–Mosotti relation* and reads

$$\mathbf{P}_{\text{LL}} \equiv \frac{\varepsilon - 1}{\varepsilon + 2} \frac{\mathbf{M}}{\rho} = \frac{N_A \alpha}{3\varepsilon_0} \quad (11.9)$$

The relationship between the molar refraction \mathbf{R}_{LL} , the refractive index n and the polarisability α is known as the *molar Lorentz–Lorenz relation* (1880), which reads

$$\mathbf{R}_{\text{LL}} \equiv \frac{n^2 - 1}{n^2 + 2} \frac{\mathbf{M}}{\rho} = \frac{N_A \alpha}{3\varepsilon_0} \quad (11.10)$$

TABLE 11.2 Dielectrical constants of polymers

Polymer	ε Exp. ^a	n_D^2	ε Calc. from Eq. (11.7)	ε Calc. from Eq. (11.8)
Polyethylene (extrap. to amorphous)	2.3	(2.19)	2.20	2.20
Polypropylene (amorph. part)	2.2	(2.19)	2.15	2.15
Polystyrene	2.55	2.53	2.55	2.60
Poly(o-chlorostyrene)	2.6	2.60	2.82	2.82
Poly(tetrafluoroethylene) (amorphous)	2.1	~1.85	2.00	1.96
Poly(vinyl chloride)	2.8/3.05	2.37	3.05	3.15
Poly(vinyl acetate)	3.25	2.15	3.02	3.30
Poly(methyl methacrylate)	2.6/3.7	2.22	2.94	3.15
Poly(ethyl methacrylate)	2.7/3.4	2.20	2.80	3.00
Poly(methyl α -chloroacrylate)	3.4	2.30	3.45	3.32
Poly(ethyl α -chloroacrylate)	3.1	2.26	3.20	3.16
Polyacrylonitrile	3.1	2.29	3.26	3.15
Poly(methylene oxide)	3.1	2.29	2.95	2.85
Poly(2,6-dimethylphenylene oxide)	2.6	—	2.65	2.75
Penton® (poly [2,2-bis(chloromethyl)-trimethylene-3-oxide])	3.0	—	2.95	2.80
Poly(ethylene terephthalate) (amorphous)	2.9/3.2	2.70	3.40	3.50
Poly(bisphenol carbonate)	2.6/3.0	2.50	3.00	3.05
Poly(hexamethylene adipamide)	4.0	2.35	4.14	4.10

^a Sources of data: Morton and Hearle (1962); Brandrup and Immergut (1999); Hütte (1967).

with

$$\alpha = 4\pi\varepsilon_0\alpha' \quad (11.11)$$

where α = molecular polarisability ($J^{-1} C^2 m^2$); α' = molecular polarisability volume (m^3), a fundamental molecular quantity, earlier introduced by Mosotti (1847) and Clausius (1879).

11.2.5. The dielectric constant and the dipole moment

Molecular polarisability is the result of two mechanisms: (a) *distortional polarisation* and (b) *orientation polarisation*. Distortional polarisation is the result of the change of electric charge distribution in a molecule due to an applied electric field, thereby inducing an electric dipole. This distortional polarisation is coined α_d . Permanent dipoles are also present in the absence of an electric field. At the application of an electric field they will orient more or less in the direction of the electric field, resulting in orientation polarisation. However, the permanent dipoles will not completely align with the electric field due to thermal agitation. It appears that the contribution of molecular polarisability from rotation is approximately equal to $\mu^2/(3kT)$. Accordingly, the total molecular polarisability is

$$\alpha = \alpha_d + \alpha_s = \alpha_d + \mu^2/(3k_B T) \quad (11.12)$$

where μ = the permanent dipole moment of the molecule, expressed in C m, or more usual in *debye units*, D. (1 D = 3.33564×10^{-30} C m).

The molar Clausius–Mosotti relation then reads

$$\mathbf{P}_{LL} \equiv \frac{\epsilon - 1}{\epsilon + 2} \frac{\mathbf{M}}{\rho} = \frac{N_A \alpha_d}{3\epsilon_0} + \frac{N_A \mu^2}{9\epsilon_0 k_B T} \quad (11.13)$$

It has been emphasised that no account has taken of any possible interaction between permanent dipoles, so that the equation will be valid only for polar gases and for dilute solutions of polar molecules in non-polar solvents. Moreover, the equation is not valid at high frequencies, because in that case the dipoles are not able to reorient sufficiently quickly in the oscillatory electric field, so that at optical frequencies $\alpha = \alpha_d$.

In the simplest cases, i.e. when the dielectric is a pure compound and the dipole moment (μ) is small ($\mu < 0.6$ debye units), it is possible to use *Debye's equation* to determine the dipole moment, which reads (at 298 K)

$$\begin{aligned} \mathbf{P}_{LL} - \mathbf{R}_{LL} &= \left[\frac{\epsilon - 1}{\epsilon + 2} - \frac{n^2 - 1}{n^2 + 2} \right] \frac{\mathbf{M}}{\rho} = \frac{N_A \mu^2}{9\epsilon_0 k_B T} \\ &= 1.838 \times 10^{54} \mu^2 (\mu \text{ in C m}) = 2.045 \times 10^{-5} \mu^2 (\mu \text{ in D}) \end{aligned} \quad (11.14)$$

where \mathbf{P}_{LL} and \mathbf{R}_{LL} are quoted in m^3/mol , \mathbf{M} in kg/mol and ρ in kg/m^3 . The equation shows that if permanent dipoles are present, $\epsilon > n^2$. Water, for example, possesses the very high dielectric constant of 81, while its value for n^2 is only 1.77. For all polymers with polar groups $\epsilon > n^2$.

Application of Eq. (11.14) to these polymers (as a first orientation) yields values for the mean dipole moment of the structural units varying from 0 debye units for hydrocarbon polymers to about 1 debye unit for polyamides. The measured values are low compared with the dipole moments of the polar groups in liquids.

Table 11.3 gives the effective average dipole moments in polymers in comparison with those measured in liquids.

Equation (11.14) may also be expressed as:

$$\frac{3(\epsilon - n^2)}{(\epsilon + 2)(n^2 + 2)} \frac{\mathbf{M}}{\rho} = \frac{N_A \mu^2}{9\epsilon_0 k_B T} \quad (11.15)$$

TABLE 11.3 Dipole moments of structural groups in polymers (in Debye units)

Group	Effective μ in polymers	μ in low-molecular liquids
-Cl	0.45	2.0
-CCl ₂ -	0.40	-
-CF ₂ -	0.25	-
-C≡N	0.50	3.5
-O-	0.45	1.1
-COO-	0.70	1.7
-CONH-	1.00	-

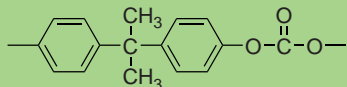
Conversion factor to S.I.: 1 debye unit = $3.34 \times 10^{-30} \text{ C m}$.

Example 11.1

Estimate the dielectric constant and the average dipole moment of poly(bisphenol carbonate).

Solution

The structural unit of polycarbonate is



The molecular weight is 254 g/mol and the molar volume $V(298) = 215 \text{ cm}^3/\text{mol}$. By means of the group contributions in

Table 11.1 we get:

Groups	$P_{LL,i}$	$P_{V,i}$
2	50.0	257.2
1 ($>\text{C}<$)	2.6	26.4
2 ($-\text{CH}_3$)	11.3	35.3
1 ($-\text{O}-\text{COO}-$)	22	125
	85.9	443.9

By substitution in Eqs. (11.7) and (11.8) we calculate $\varepsilon = 3.00$ and $\varepsilon = 3.05$ respectively, in good agreement with the experimental value ($\varepsilon = 2.6-3.0$).

The average dipole moment is estimated by means of the Lorentz–Lorenz molar refraction (Table 10.4)

Groups	R_{iLL}
2	50.06
1 ($>\text{C}<$)	2.29
2 ($-\text{CH}_3$)	11.29
1 ($-\text{O}-\text{COO}-$)	7.74
	71.38

Substitution in Eq. (11.14) gives:

$$20.45\mu^2 = \Sigma P_{iLL} - \Sigma R_{iLL} = 85.9 - 71.4 = 14.5$$

or

$$\mu = \left(\frac{14.5}{20.45} \right)^{1/2} = 0.84 \text{ debye}$$

Important is that Fröhlich (1968) showed that a more exact equation for condensed matter, such as polymers, is

$$\frac{(\varepsilon - n^2)(2\varepsilon + n^2) \mathbf{M}}{\varepsilon(n^2 + 2)^2} \frac{1}{\rho} = \frac{N_A g \mu^2}{9\varepsilon_0 k_B T} \quad (11.16)$$

Unfortunately determination of the so-called correlation factor g , which is the result of the fact that the dipoles do not react independently, is difficult to predict.

11.2.6. Dielectric relaxation or Debye relaxation

It was shown above that the relation between the polarisation, the electric field and the dielectric constant is given by

$$P = \epsilon_0 E(\epsilon - 1) \quad \text{or} \quad \epsilon = 1 + P/(\epsilon_0 E) \quad (11.3)$$

The polarisation itself is, just as the molecular polarisability is, the result of *deformation polarisation* P_d and the *orientation polarisation* P_s . Accordingly, the total polarisation is equal to $P = P_d + P_s$. Because of the resistance to motion of the atom groups in the dielectric, there is a delay between changes in the electric field and changes in the polarisation. The deformation polarisation takes place instantaneously (more precisely in a time of the order of 10^{-14} s) on the application of an electric field. There are two limiting values of ϵ : ϵ_∞ at short times or high frequencies and ϵ_s at long times or low frequencies. This means that we have for the deformation polarisation

$$P_d = \epsilon_0 (\epsilon_\infty - 1) E \quad (11.17)$$

and for the orientation deformation after application of the constant electric field E

$$\frac{dP_s}{dt} = \frac{\epsilon_0 (\epsilon_s - \epsilon_\infty) E - P_s}{\tau} \quad (11.18)$$

$$P_s = \epsilon_0 (\epsilon_s - \epsilon_\infty) (1 - e^{-t/\tau}) E \quad (11.19)$$

Hence, it follows for the time dependent polarisation after application of an electric field E

$$P(t) = \epsilon_0 [\epsilon_\infty - 1 + (\epsilon_s - \epsilon_\infty) (1 - e^{-t/\tau})] E \quad (11.20)$$

so that the time dependent dielectric constant reads

$$\epsilon(t) = \epsilon_\infty + (\epsilon_s - \epsilon_\infty) (1 - e^{-t/\tau}) \quad (11.21a)$$

The static value ϵ_s is called the *relaxed dielectric constant* and the short-time (or high-frequency) value ϵ_∞ the *non-relaxed dielectric constant*; $\epsilon_s - \epsilon_\infty$ is called the *dielectric strength*. They are equal to

$$\epsilon_s = \lim_{t \rightarrow \infty} \epsilon(t); \quad \epsilon_\infty = \lim_{t \rightarrow 0} \epsilon(t); \quad \Delta\epsilon = \epsilon_s - \epsilon_\infty = \frac{N\mu^2}{3\epsilon_0 kT} \quad (11.21b)$$

This equation for the dielectric constant is the analogue of the compliance of a mechanical model, the so-called Jeffreys model, consisting of a Voigt–Kelvin element characterised by G_1 and η_1 and $\tau = \eta_1/G_1$, in series with a spring characterised by G_2 . The creep of this model under the action of a constant stress σ_o is (Bland, 1960)

$$\gamma(t) = \sigma_o J(t) = \sigma_o \{J_2 + J_1[1 - \exp(-t/\tau)]\} \quad (11.22)$$

and the creep compliance

$$J(t) = J_2 + J_1[1 - \exp(-t/\tau)] \quad (11.23)$$

Comparison with Eq. (11.21a) reveals that J_1 corresponds with $\epsilon_0(\epsilon_s - \epsilon_\infty)$ and J_2 with $\epsilon_0\epsilon_\infty$.

If the electric field is an oscillating field

$$E^* = E_0 \exp(i\omega t)$$

the polarisation lags behind by a phase angle δ

$$P^* = P_0 \exp[i(\omega t - \delta)]$$

The equation for the polarisation now becomes

$$P^* = \epsilon_0(\epsilon^* - 1)E^* = \epsilon_0[\epsilon_\infty - 1 + (\epsilon_s - \epsilon_\infty)/(1 + i\omega\tau)]E^* \quad (11.24)$$

so that

$$\epsilon^*(i\omega) = \epsilon_\infty + \frac{\epsilon_s - \epsilon_\infty}{1 + i\omega\tau} = \epsilon_\infty + \frac{\epsilon_s - \epsilon_\infty}{1 + \omega^2\tau^2} - i(\epsilon_s - \epsilon_\infty) \frac{\omega\tau}{1 + \omega^2\tau^2} \quad (11.25)$$

Equation (11.25) is called the *Debye dispersion relation* or the *Debye equation*. The complex dielectric constant is defined to be

$$\epsilon^*(i\omega) \equiv \epsilon'(\omega) - i\epsilon''(\omega) \quad (11.26)$$

where ϵ' is the real part (the *dielectric constant* or *electric inductive capacity*) and ϵ'' the imaginary part (the *dielectric absorption* or *loss factor*) of the complex dielectric constant ϵ^* . Comparison with Eq. (11.25) gives for both dynamic dielectric quantities ϵ' and ϵ''

$$\epsilon'(\omega) = \epsilon_\infty + \frac{\epsilon_s - \epsilon_\infty}{1 + \omega^2\tau^2}; \quad \epsilon''(\omega) = \frac{(\epsilon_s - \epsilon_\infty)\omega\tau}{1 + \omega^2\tau^2} \quad \text{and} \quad \tan \delta = \frac{\epsilon''}{\epsilon'} \quad (11.27)$$

The so-called *loss tangent*, $\tan \delta$, is a very useful dimensionless parameter and is a measure of the ratio of the electric energy loss to energy stored in a periodic field. The product $\epsilon \times \tan \delta$ is directly proportional to the dielectric loss of energy, e.g. in a high-voltage cable.

Comparison with the creep model mentioned above gives (Bland, 1960)

$$J^*(i\omega) \equiv J' - iJ'' = J_1 + \frac{J_2}{1 + i\omega\tau} = J_1 + \frac{J_2}{1 + \omega^2\tau^2} - i \frac{J_2\omega\tau}{1 + \omega^2\tau^2} \quad (11.28)$$

and

$$J' = J_1 + \frac{J_2}{1 + \omega^2\tau^2}; \quad J'' = \frac{J_2\omega\tau}{1 + \omega^2\tau^2} \quad \text{and} \quad \tan \delta = \frac{J''}{J'} \quad (11.29)$$

This kind of behaviour will be one of the subjects to be discussed in Chap. 13.

In Fig. 11.1 the time dependent dielectric constant (left) and both dynamic dielectric constants (right) are plotted vs. reduced time, t/τ , and reduced angular frequency, $\omega\tau$, respectively, for amorphous polyethylene terephthalate at 81°C. It illustrates a continuous increase of $\epsilon(t)$ from 3.8 to 6. It also shows that the $\epsilon'(\omega)$ decreases with frequency in a similar way as $\epsilon(t)$ increases with time. The maximum in ϵ'' , situated at $\omega\tau = 1$, is equal to $(\epsilon_s - \epsilon_\infty)/2 = 1.1$. A Cole–Cole plot where ϵ'' is plotted vs. ϵ' is shown in Fig. 11.2. For a Debye model with only one relaxation time this should be a semi-circle. In reality the decrease of ϵ' from ϵ_s to ϵ_∞ is not so fast and the maximum in ϵ'' not so sharp as the Debye

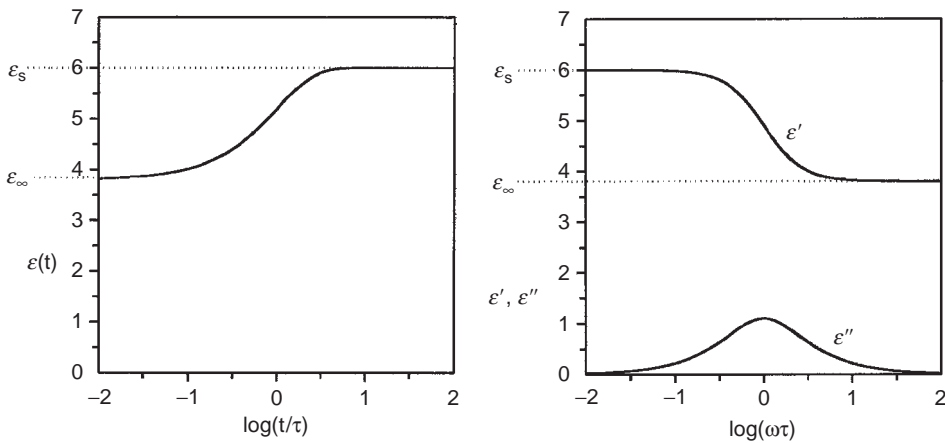


FIG. 11.1 (left) Static dielectric constant $\epsilon(t)$ and (right) dynamic dielectric constants $\epsilon'(\omega)$ and $\epsilon''(\omega)$ of amorphous poly(ethylene terephthalate) at 81°C plotted vs. log reduced time and log reduced angular frequency, respectively, for a simple Debye model with $\epsilon_s = 6$ and $\epsilon_\infty = 3.8$. Analogous to Boyd and Liu, 1997.

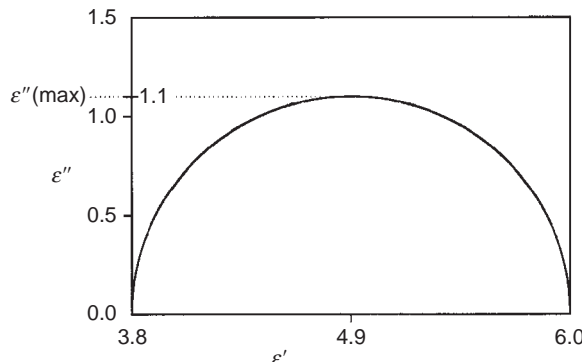


FIG. 11.2 A Cole–Cole plot for the results presented in Fig. 11.1.

model predicts, because in general (much) more relaxation times are present. This is shown in Figs. 11.3, where results are presented for poly(vinyl acetate) and in Fig. 11.4 where Cole–Cole plots are presented for poly(vinyl acetates) of various molecular weights.

The quantity $\tan \delta$ is sometimes called: *dissipation factor*; ϵ^* and δ are usually measured over a wide frequency range and in Fig. 11.3 from 10^{-3} to 10^7 Hz.

The known data of ϵ and $\tan \delta$ for polymers were compiled by Cotts and Reyes (1986). In Fig. 11.5 these data are represented graphically, viz. $\log \tan \delta$ plotted versus $\log \epsilon^*$ ($\tan \delta$ and ϵ^* measured at the same frequency). There is an obvious trend, although the spread is considerable; the approximate correlation (drawn line in Fig. 11.5) is given by:

$$\tan \delta \approx 10^{-5} \epsilon^5 \quad (11.30)$$

At one time it was hoped that the more tedious mechanical studies could be entirely replaced by electrical measurements. There are close similarities between the general shapes and temperature-dependences of the mechanical and dielectric loss curves, but

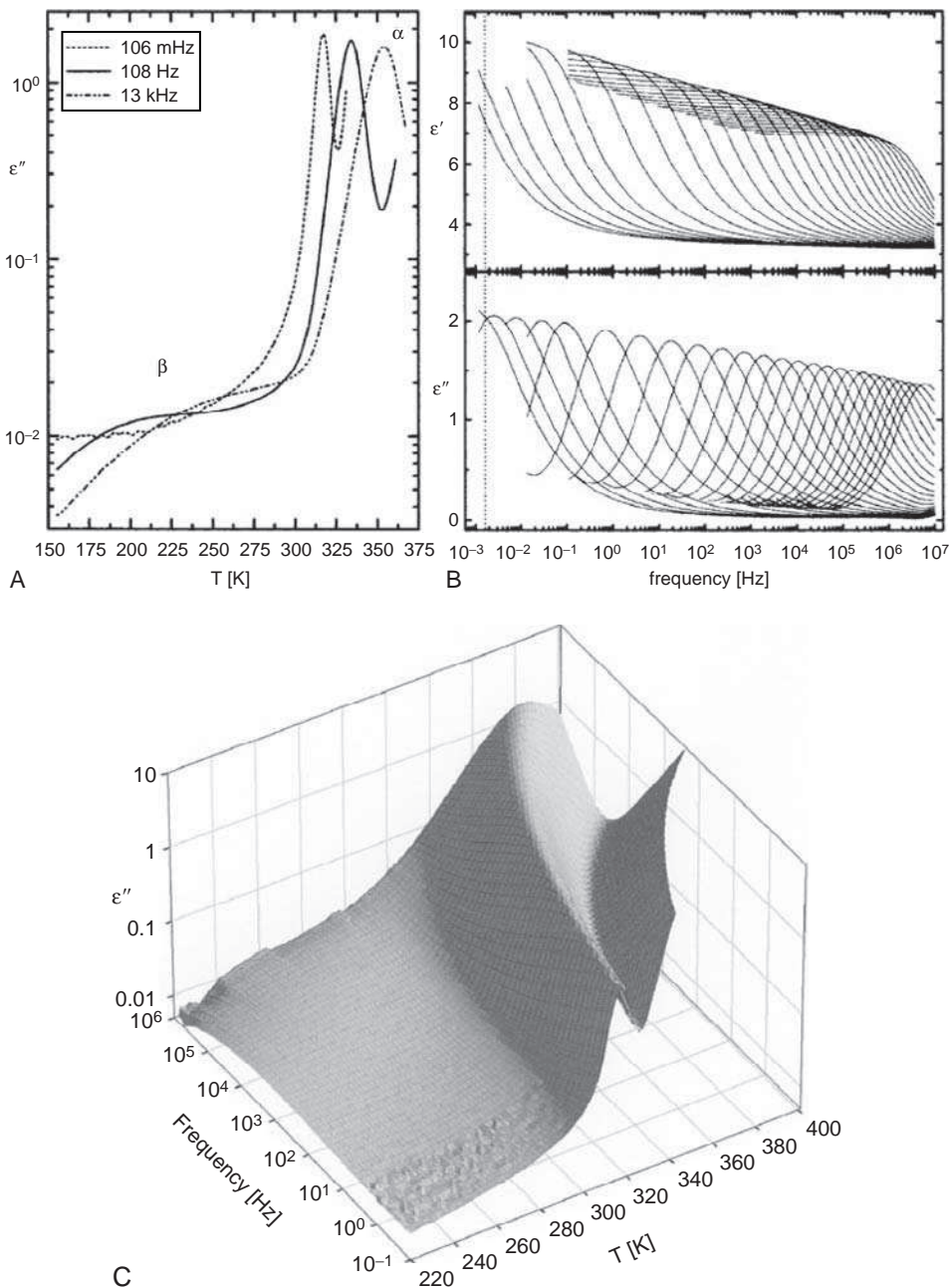


FIG. 11.3 Complex dielectric functions of poly(vinyl acetate). (A) Dielectric loss $\epsilon''(T)$ as a function of temperature for three frequencies. (B) Temperature dependence of the dielectric constant $\epsilon'(v)$ (top panel) and the dielectric loss $\epsilon''(v)$ (bottom panel) of the complex dielectric function; curves from right to left in the temperature range from 377 to 313 K with steps of 4 K and 312.5, 311.5, 310.5, 310 K. (C) 3D plot of the dielectric loss $\epsilon''(v,T)$. The author is much indebted to Prof. M. Wübbenhörst (KU Leuven) for his illustrative measurements on PVAC, especially for the benefit of this book.

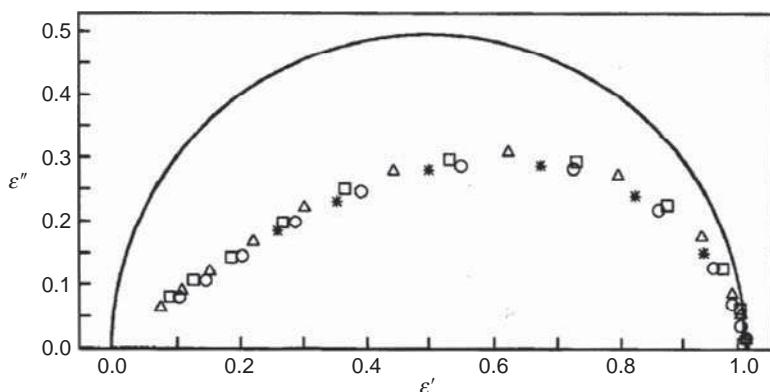


FIG. 11.4 A Cole–Cole plot for samples of Poly(vinyl acetate) of various molar masses (in g/mol): (*) 11,000; (○) 140,000; (□) 500,000 and (△) 1,500,000. The dielectric constant has been normalised so that $\epsilon_s - \epsilon_\infty = 1$. From Havriliak and Havriliak (1997). Courtesy Carl Hanser Verlag.

the quantitative connection between these phenomena is not as simple as was originally believed. Nevertheless, electrical measurements constitute a useful addition to mechanical studies, the more so because they cover a much broader frequency range and are easier to perform.

11.2.7. Thermally stimulated discharge (TSD)

A spectacular relaxation phenomenon of polymeric materials is exhibited in a field-temperature treatment phenomenon. As was shown above, the polarisation of a polymeric material after application of an electric field increases after an instantaneous polarisation to the relaxed polarisation. If the electric field is subsequently released the polarisation decreases again with time. However, if the polarisation took place at a temperature above the glass transition temperature after which the temperature was decreased to a temperature well below T_g , then depolarisation is not possible, due to the immobilisation of the polymer molecules. In this way a so-called electret may be formed, the electric counterpart of a magnet.

An electret is a dielectric material that has a quasi-permanent electric charge or dipole polarisation (carrying opposite charges on two sides), and that generates internal and external electric fields. It is the electrostatic equivalent of a permanent magnet. Heaviside coined the term electret as early as 1885 (*electricmagnet*). Materials with electret properties were already studied since the early eighteenth century and the so-called electrophorus was invented by Wilcke in 1764 and improved by Volta in 1775. Electrets create a strong electric field of about 3000 kV/m, which can be utilised for various purposes. Accordingly, electrets have found commercial and technical interest, such as uses in microphones, in copy machines, electric collection of dust particles and in ion chambers for measuring ionisation radiation or radon (see, e.g. Horiguchi et al., 2005).

If a polarised polymeric material that was cooled down to temperatures well below T_g , is gradually heated again, charge release will occur due to specific molecular

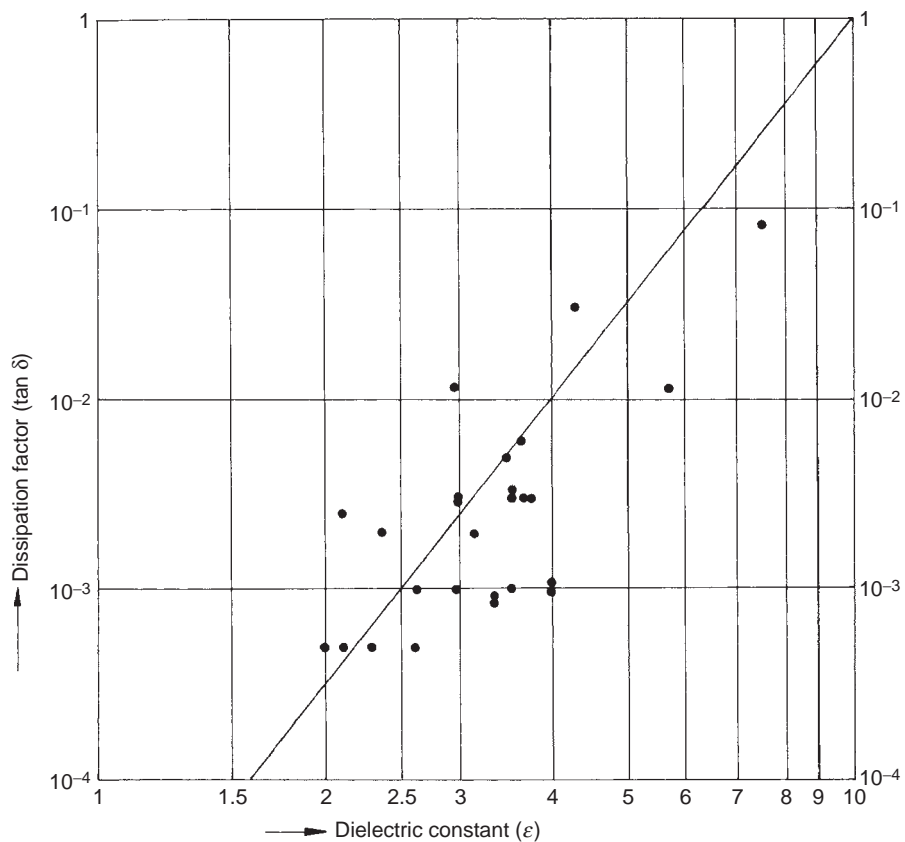


FIG. 11.5 Relationship between ϵ and $\tan \delta$.

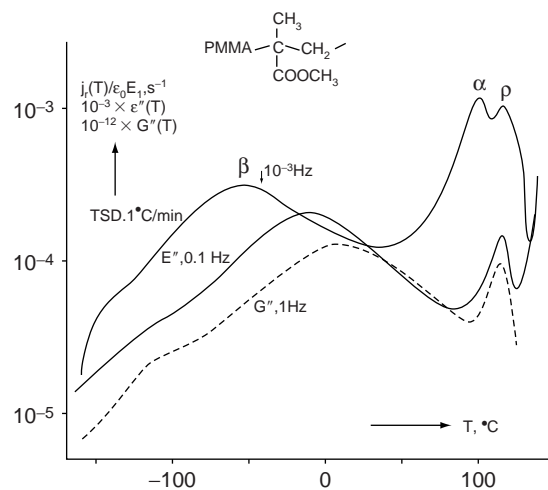


FIG. 11.5A Comparison between current TSD and ϵ'' and G'' data for PMMA. After Van Turnhout (1972).

motions. This is measured as an electric current. In this way relaxation phenomena in the glassy region may be determined. An example is shown in Fig. 11.5a for PMMA. The electret was formed at 140 °C and 7500 kV/m during 1.5 h and subsequently frozen in at -180 °C. PMMA has a polar ester group -COOCH₃ with a dipole moment of 5.3 × 10⁻³⁰ C m = 1.6 debye. It can rotate *with* and *without* the main-chain segments -C-CH₂-.

The thermogram gives the reduced current density vs. temperature. For increasing temperature three maxima were found, designated by β , α and ρ . The β -peak, at -51 °C, is ascribed to the reorientation of the polar side-groups by local motions around the C-C bond. The α -peak at 102 °C is due to the joined reorientation of the polar side-groups with adjacent main-chain segments. This peak corresponds to the glass transition. The α -peak manifests itself also in dynamic mechanical and dielectric measurements, as shown by the G'' and ϵ'' data, respectively, at 0.1 Hz. The ρ -peak is not perceptible. Apparently TSD gives more information than the dynamic techniques (Van Turnhout, 1972).

11.2.8. Relations between dielectric constant and optical quantities

The complex dielectric constant is closely connected with the optical properties, viz. the refractive index (n) and the extinction index (k). The relationships are:

$$\epsilon^* = (n^*)^2 \quad (11.31a)$$

$$\epsilon^* = \epsilon' - i\epsilon''; \quad n^* = n' - in'' = n - ik \quad (11.31b)$$

$$\epsilon' = n^2 - k^2 \quad (11.32a)$$

$$\epsilon'' = 2nk \quad (11.32b)$$

$$\frac{\epsilon''}{\epsilon'} = \tan \delta = \frac{2kn}{n^2 - k^2} \quad (11.33)$$

11.2.9. Correlation between dielectric constant and solubility parameter

As electrical forces due to polarisability and polar moment determine the cohesive energy, a certain correlation between dielectric constant and solubility parameter may be expected. Darby et al. (1967) suggested such a correlation for organic compounds. It appeared that a surprisingly simple correlation holds for polymers, viz.:

$$\delta \approx 7.0\epsilon \quad (11.34)$$

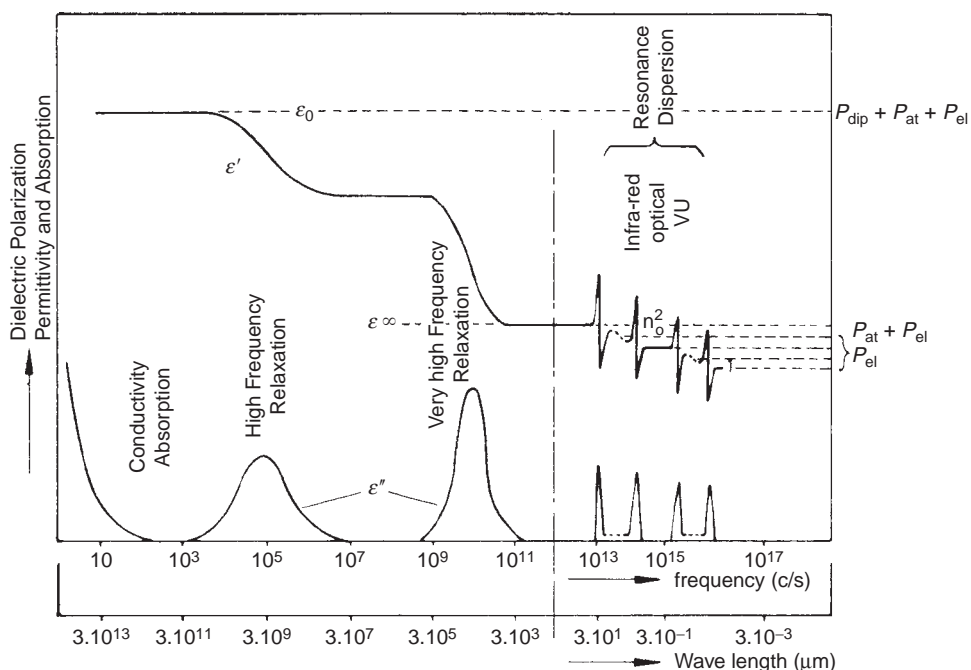
Calculated and experimental values of ϵ are compared in Table 11.4.

11.2.10. Relation between dielectric polarisability and optical dispersion

The main features (simplified) of dielectric polarisability as a function of frequency are shown in Fig. 11.6. At low frequencies the total polarisation manifests itself completely. However, the orientation of the polar groups is relatively slow and as the frequency increases the orientation lags behind. When the frequency reaches a value of about 10¹² c/s, the dipoles are unable to follow the oscillations of the field (P_{dip} , i.e. our P_s disappears). Only random orientations are left and these do not contribute to the resultant

TABLE 11.4 Dielectric constant and solubility parameter

Polymer	δ Calc. ^a	ε Calc.	ε Exp.
Polyleethylene	16.0	2.3	2.3
Polypropylene	17.0	2.4	2.2
Polystyrene	19.1	2.7	2.55
Poly(o-chlorostyrene)	18.2 ^b	2.6	2.6
Poly(vinyl chloride)	19.7	2.8	2.8/3.05
Poly(vinylidene chloride)	20.6	2.9	2.85
Poly(tetrafluoroethylene)	11.7	1.7	2.1
Poly(chlorotrifluoroethylene)	15.7	2.2	2.3/2.8
Poly(vinyl acetate)	19.6	2.8	3.25
Poly(methyl methacrylate)	19.0	2.7	2.6/3.7
Poly(ethyl methacrylate)	18.6	2.7	2.7/3.4
Polyacrylonitrile	25.7	3.7	3.1
Poly(methylene oxide)	20.1	2.9	3.1
Poly(ethylene terephthalate)	20.5	2.9	2.9/3.2
Polycarbonate	20.3 ^b	2.9	2.6/3.0
Nylon 6,6	28.0	4.0	4.0

^a Calculated from the correlation as presented in Chap. 7.^b Experimental value.**FIG. 11.6** Dispersion curves of the dielectric constant (ε') and dielectric absorption (ε'') in the regions of electrical, infrared and optical frequencies.

polarisation. Of the total polarisation only the atomic (P_{at} , i.e our P_d) and the electronic polarisation (P_{el}) remain.

At a somewhat higher frequency the stretching and bending of the bonds become too sluggish, so that no atomic polarisation occurs, either.

The frequency at which this resonance effect occurs (in P_{at}) is of the order of 10^{13} c/s, so dispersion occurs in the infrared region and an infrared absorption band can be observed. Only P_{el} remains above a frequency of 10^{14} c/s.

Finally, at a frequency higher than 10^{15} c/s, which is in the UV range, the distortion of the electronic clouds around the nuclei lags behind, with the consequence that absorption in the optical spectrum occurs.

From Fig. 11.6 it can be seen that the polarisation (and so the refractive index) increases as it approaches a resonance frequency and temporarily falls to a "too" low value just beyond it. This remarkable and sudden change in behaviour was once considered anomalous and was called anomalous dispersion. The electro-magnetic wave theory showed that the "anomalous" dispersion is just as "normal" dispersion and can be explained as a direct consequence of the equation of motion of nuclei and electrons.

11.3. STATIC ELECTRIFICATION AND CONDUCTIVITY

11.3.1. Static electrification

When brought into intimate contact with a neutral surface, e.g. by rubbing, polymers become positively or negatively charged on separation. If two polymers are rubbed against each other and separated, one becomes positively charged (i.e. acts as an *electron donor*) whilst the other becomes negative (i.e. acts as an *electron acceptor*). The sequence of polymers according to their charging behaviour is called the *triboelectric series*.

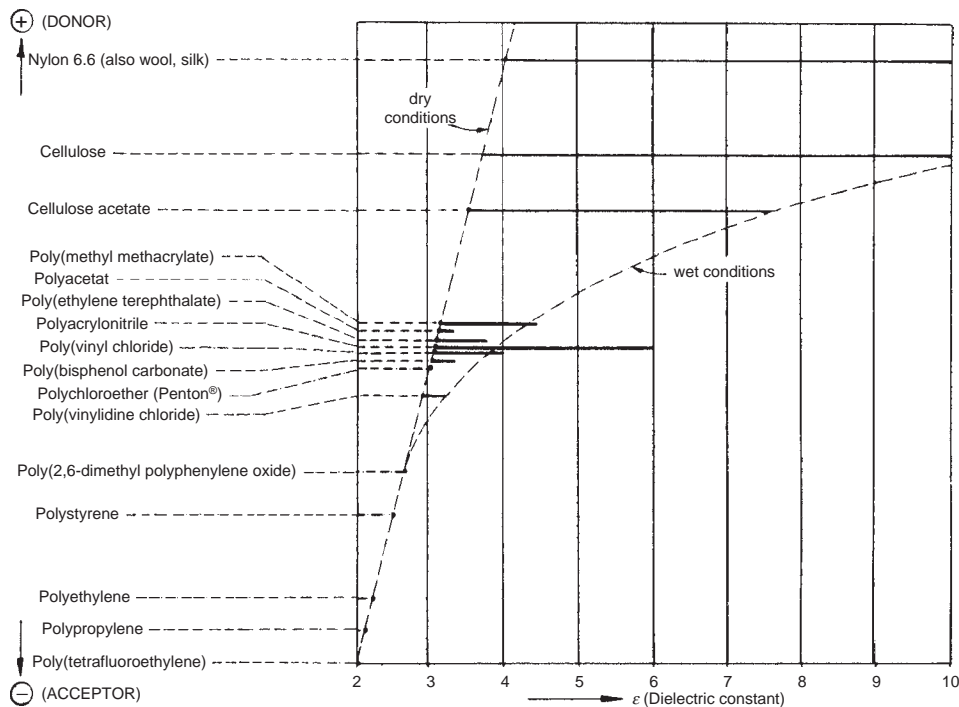
Coehn (1898) derived the general rule that if two substances become charged by mutual contact, the substance with the highest dielectric constant will get the positive charge (i.e. will act as an electron donor). Fig. 11.7 shows that this holds in broad outline: the sequence in the triboelectric series is the same as that of the dielectric constant. Since ϵ for hydrophilic polymers is very moisture-dependent, due to the great influence of the high dielectric constant of water, it is clear that these polymers will be antistatic under humid conditions (wool), but static under very dry conditions. The highest charges observed (500 e.s.u./cm³) are still caused by the transfer of relatively few charges; one electron for every 100 nm², which area covers many hundreds of atoms, would be sufficient.

Strella (1970, 1971) based his triboelectric series on contact potential differences. Table 11.5 shows a reproduction of it.

More important than the electrification itself is the *rate of charge decay*. It was found (Shashoua, 1963) that for a given structural group the fastest charge decay occurs when the group is present as a side chain substituent rather than in the main chain of the polymer. The charge-selective power of a polymer appeared to be related to its ability to bind ions on its surface. This makes it clear how small quantities of impurity can alter the charge-selective power of a given substance (degree of dissociation of ionic impurities).

11.3.2. Conductivity

Electric conductivity, σ (in S/cm or in Ω^{-1} cm⁻¹), of materials in general extends over a wide range, from 10^{-20} to 10^6 S/cm (see Fig. 11.8). This range is subdivided into *conductors* ($\sigma = 10^4$ – 10^6), *semi-conductors* ($\sigma = 10^{-4}$ – 10^2) and *insulators* ($\sigma = 10^{-20}$ – 10^{-6}). The tremendous

**FIG. 11.7** Triboelectric series of polymers.**TABLE 11.5** Work function, Φ , of polymers^a (Strella (1970, 1971))

Polymer	Φ Polymer ^b (eV)
Poly(tetrafluoroethylene) (=Teflon® rod)	5.75
Poly(trifluorochloroethylene)	5.3
Chlorinated polypropylene	5.14
Poly(vinylchloride)	5.13
Chlorinated polyether (= Penton®)	5.11
Poly(4-chlorostyrene)	5.11
Poly(4-chloro, 3-methoxy-styrene)	5.02
Polysulfone	4.95
Epoxy resin (Hydrin®)	4.95
Polystyrene	4.90
Polyethylene	4.90
Polycarbonate (=Lexan®)	4.80
Ethylene/vinylacetate copolymer	4.79
Poly(methylmethacrylate)	4.68
Poly(vinylacetate)	4.38
Poly(vinylbutyral)	4.30
2-vinylpyridine/styrene copolymer	4.27
Nylon 6.6	4.30
Poly(ethyleneoxide)	3.95
	4.50 ^c
	4.50 ^c

^a The assumption is that for $\Phi_1 > \Phi_2$, Φ_1 material will charge negative against Φ_2 material.^b Measured against gold; Φ gold taken as 4.7.^c Changes probably caused by loss of water.

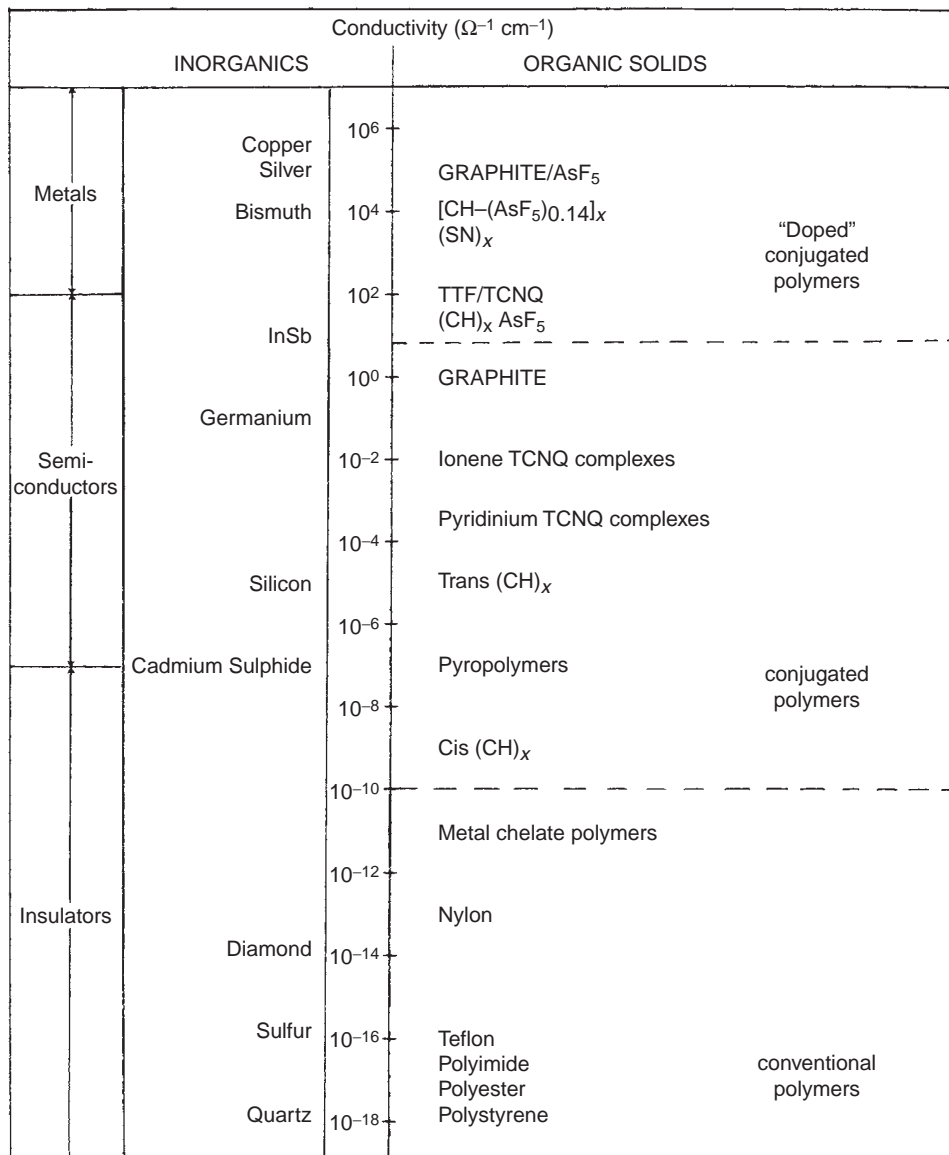


FIG. 11.8 Electrical conductivity of materials.

difference between the three categories is explained by the so-called *band theory*, schematically sketched in Fig. 11.9, where the dashed lines indicate the energy as a function of the distance of electrons to the atomic nuclei. The crosshatched bands are occupied bands and the hatched bands are allowed but not occupied. For *conducting materials* the highest energy level with electrons is not completely filled. Moreover this band overlaps adjoining atoms (Fig. 11.9c). In the other two materials the highest filled bands belong to the matching atoms and the energy bands that overlaps adjoining atoms are in the ground state unoccupied. If the distance between the filled bands and the unoccupied bands is small, as is the case for *semi-conductors* (Fig. 11.9b), then it is quite easy for the electrons to take up some energy (e.g. thermal energy) and to jump to the

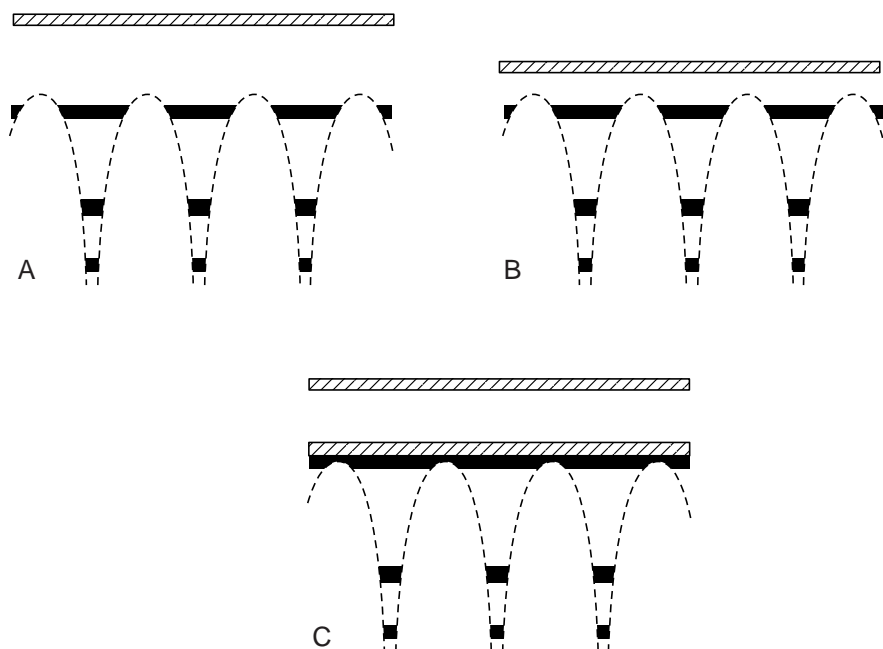


FIG. 11.9 Schematic representation of the band theory of electronic conduction: (A) insulators; (B) semi-conductors and (C) conducting materials. The hatched bands are allowed bands, the cross hatched bands are occupied.

conducting band. If, on the other hand, the distance is too large, as is the case for *insulators* (Fig. 11.9a), then it is almost impossible for electrons to jump to the conducting band.

Metals are the classical conductors. Most organic solids, and notably polymers, are insulators by nature. In the usual polymers the electrical resistance is very high; their conductivity probably results partially from the presence of ionic impurities, whose mobility is limited by the very high viscosity of the medium.

At sufficiently low temperatures (i.e. below a typical transition temperature T_c) most metals lose their electrical resistance completely and become superconductors. Also a number of inorganic semi-conductors, viz. complex oxides of two- and three-valent metals, become superconductors below their T_c , which may be as high as 100 K or more.

The conductivity and also the activation energy of the conduction appear to be practically insensitive to crystallinity. Both surface and volume resistivity are important in the application of polymers as insulating materials.

The conductivity is greatly increased by moisture. An obvious relationship exists between the volume resistivity of pure (and dry) polymers and the dielectric constant, as is shown in Fig. 11.10. Apparently, the volume resistivity (R in $\Omega \text{ cm}$) can be estimated by means of the expression:

$$\log(R/\Omega \text{ cm}) = 15 - 2\epsilon \text{ (at } 298 \text{ K)} \quad (11.35)$$

As said, most organic solids are insulators. There are two exceptions, however.

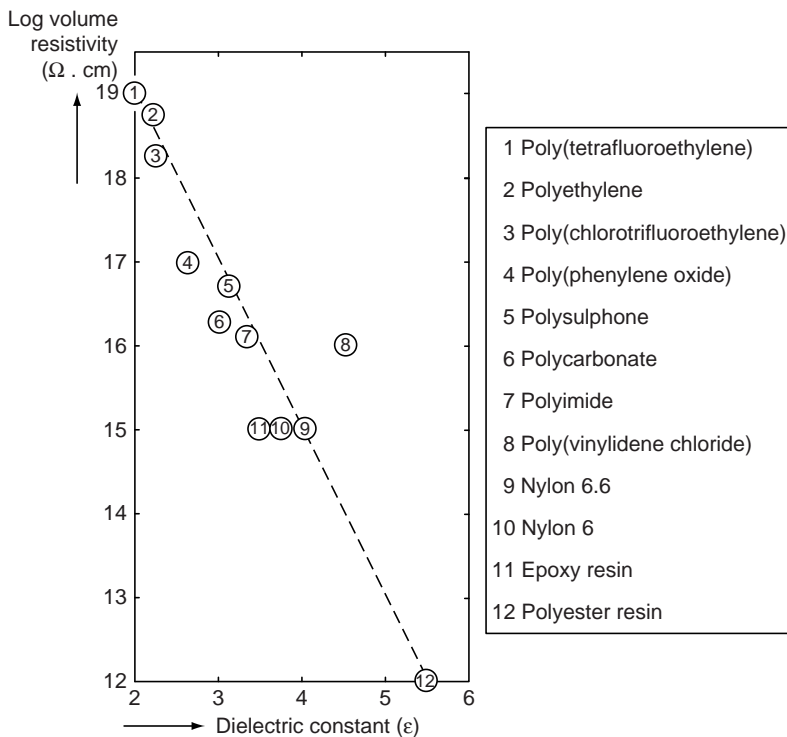


FIG. 11.10 Correlation between electric resistivity and dielectric constant of polymers.

11.3.2.1. Conductive organic crystals with charge transfer

Organic charge-transfer salts can be formed from electron acceptors (e.g. tetracyanoquino-dimethane, TCNQ) and electron donors (e.g. tetrathia-fulvalene, TTF). The combination TCNQ-TTF in the form of single-crystals shows metallic conductivity, as was found by Cowan and co-workers (1972). All organic donors and acceptors suitable for conductive behaviour are planar molecules with extended networks (Fig. 11.11). In the charge-transfer salts mentioned the two molecular species exist in so-called aggregated stacking: the direction of conductivity is along the stacks; it is a case of “one-dimensional metallic conduction” (comparable to stacks of graphitic layers).

11.3.2.2. “Doped” organic polymers with long-distance conjugation

The first organic polymers to show significant conductivity were polyacetylenes. MacDiarmid and Heeger (1977) found that electrical conductivity could be induced by exposing polyacetylene to oxidising agents. This gave rise to a continuing interest in conducting polymers. When polyacetylene is oxidised by electron acceptors (such as iodine or arsenic pentafluoride) or reduced by electron donors (such as lithium), the conductivity increases by orders of magnitude, from 10^{-8} S/cm to values as high as 10^3 S/cm. By mechanically aligning the polymer chains of polyacetylene conductivities as high as 10^5 S/cm have been achieved, comparable to that of copper (10^6 S/cm). The origin of the conductivity of pristine (i.e. non-doped) polyacetylene is the π -conjugated system overlap which is formed by the overlap of carbon p_z orbitals and alternating carbon–carbon bond lengths, thus forming an extended p_z orbital system, through which the electrons can move from one end of the polymer to the other. Besides, other polymers show electrical conductivity, in particular polyaniline (PANI) and polypyrrole (PPY)

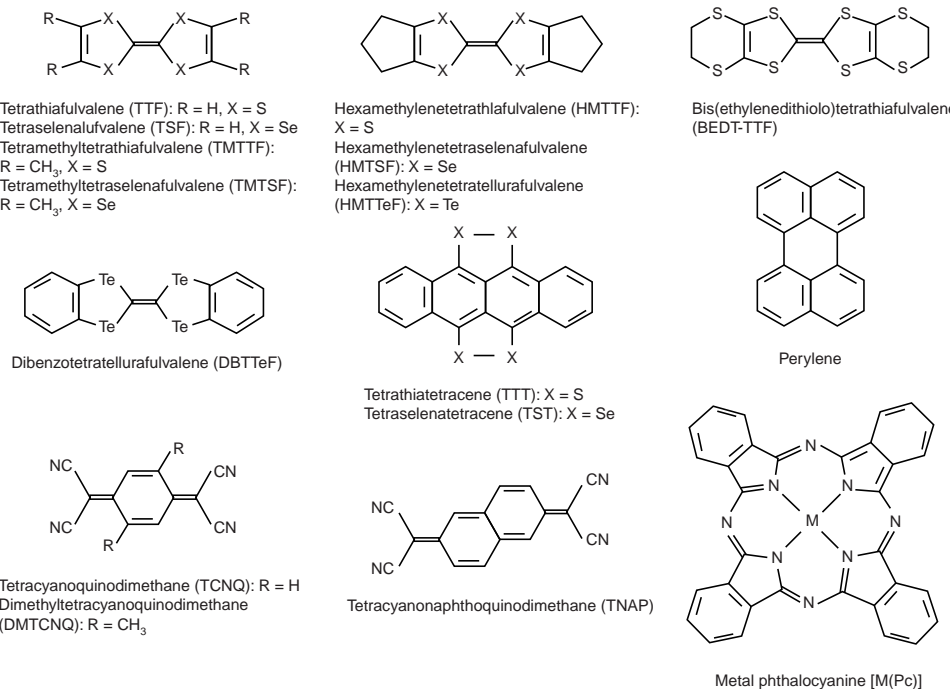
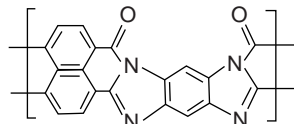


FIG. 11.11 Organic donors and acceptors: planar molecules with extended π -networks (Courtesy Professor Cowan).

(see Fig. 11.12), where C_6 rings or nitrogen p_z orbitals interact in the conjugated system. All of these polymers possess conjugated double bond systems; they can be synthesised by electrochemical or chemical polymerisation of the monomer units. However, those pristine polymers are not really conductive, but at best semi-conductive and it is not until an electron is removed from the valence band (oxidation, p-doping) or added to the conduction band (reduction, n-doping) does a conducting polymer become highly conductive. Doping generates charge carriers that move in an electric field. n-Doping is far less common, because an electron-rich n-doped polymer will react immediately with oxygen to re-oxidise to the neutral state. Hence, chemical n-doping and application as well, have to be done in an environment of inert gas (e.g. argon).

Some discoveries in the late 1980s did possibly challenge theories on conducting polymers and open up the possibility that many other materials may be transformed to conduct electricity. (a) Thakur (1988) showed that the conductivity of natural rubber can be increased by a factor of 10^{10} by doping it with iodine. Rubber does not possess a conjugated system of double bonds. Rather the iodine pulls electrons from the isolated double bonds leaving holes that can leap from chain to chain. Thakur sees the hopping mechanism of electrons and holes as paramount in the conductivity of polymers. (b) Jenekhe and Tibbetts (1988) showed that implantation of high-energy ions (energy above 50 keV = 10^{24} J) is a promising technique for turning polymers in film form into conductors. The polymer investigated was a high-temperature ladder polymer (BBL) with a pristine structure:



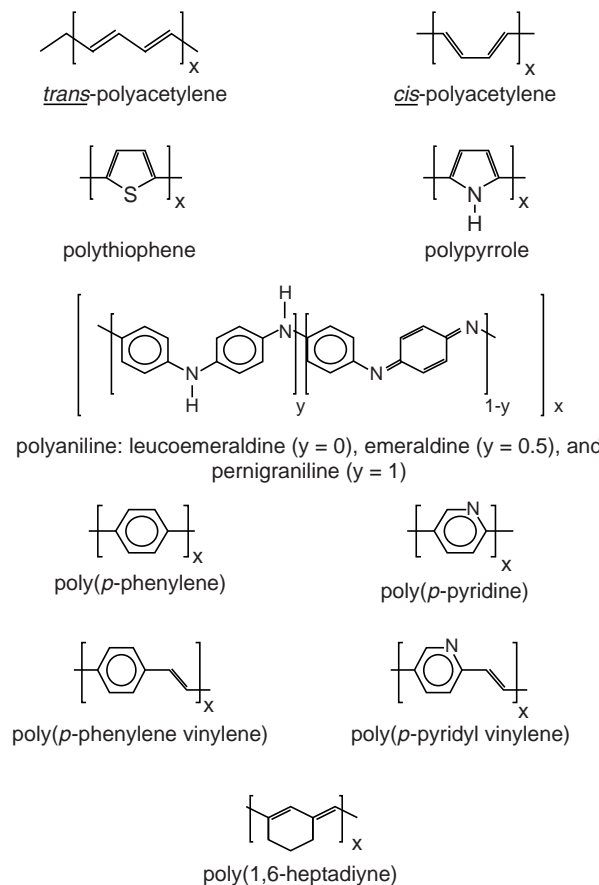


FIG. 11.12 Chemical repeat units of pristine forms of several families of conducting polymers.
Reproduced from Fig. 34.2 in Mark, (1996). Courtesy Springer Verlag.

Without damaging the excellent mechanical properties the conductivity of the polymer could be increased to 10^2 S/cm.

The amount of added doping material needed for polymers is very much higher (a few percent) than is usual in the case of inorganic semi-conductors, based on germanium or silicon (a few parts per million or less) and the mechanisms by which the high conductivity is achieved in polymers are quite different from those in doped semiconductors. In Fig. 11.13 an overview is given of conducting polymers at room temperature.

A complete understanding of the conduction processes has not yet been obtained. It is clear that at least two types of processes are required: charge transport along the chains and charge transport between the chains. Transport along the chains may be possible because of the formation of various kinds of *pseudo-particles*, such as solitons and polarons, which are localised but mobile excitations (Bower, 2002).

Conjugated polymers during doping are partially oxidised (p-doped) or reduced (n-doped) with suitable reagents: halogens and Lewis acids for oxidation and alkali metals for reduction. High conductivity and processibility, both essential for industrial applications, were previously thought to be incompatible. But the addition of long, flexible chains (alkyl substituents or ether- and amide-containing chains) to the monomer units before polymerisation renders them soluble in common organic solvents and hence processible in their doped, conducting, or non-doped, insulating, state.

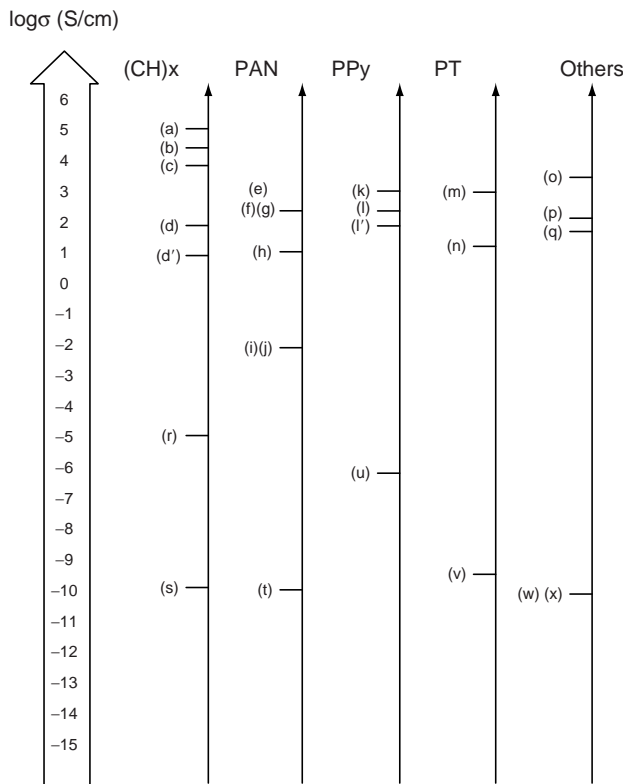


FIG. 11.13 Overview of conductivity of conducting polymers at room temperature. (a) and (b) stretched $[\text{CH}(\text{I}_3)]_n$, (c), (d) and (d') $[\text{CH}(\text{I}_3)]_n$, (e) stretched PANI-HCl, (f) and (g) PANI-CSA from *m*-cresol, (h) PANI derivative POT-CSA fibre from *m*-cresol, (i) POT-HCl, (j) sulfonated PANI, (k) and (l) stretched PPy(PF_6), (l') PPy-TSO, (m) iodine doped poly(dodecylthiophene), (n) FeCl_4^- doped PT, (o) PPV(H_2SO_4), (p) PPP(AsF_6), (q) $^{84}\text{Kr}^+$ implanted poly(phenylenebenzobisoxazole), (r) undoped *trans*-(CH) $_n$, (s) undoped *cis*-(CH) $_n$, (t) undoped PANI(EB), (u) undoped PPy, (v) undoped PT, (w) undoped PPV, (x) undoped PPP. The conductivity reported for the undoped polymers should be considered an upper limit due to the possibilities of impurities. CSA = camphor sulphonate acid, POT = poly(*ortho*-toluidine), i.e. PANI with CH_3 groups on all *ortho* places (mono-substituted). Reproduced from Fig. 34.4 in Mark (1996), where also all references are found. Courtesy Springer Verlag.

Also vinylogues of these polymers (heterocyclic or *p*-phenylene groups linked by a vinyl group) have been prepared and are better processible than the original polymers; they also have smaller band gaps. Also substitution of strongly electro donating alkoxy groups on the rings reduces the band gap and thus increases the conductivity. Sometimes these effects are additive when present in the same polymer.

11.3.3. The concept of doping

As was mentioned above, conjugated organic polymers in their pristine state, are electrical insulators or, at best, semi-conductors. Their conductivity can be increased by orders of magnitude by a doping process. In the “doped” state, the backbone of a conducting polymer consists of a delocalised π -system. Early in the twenty-first century Schon et al. (2001) discovered super-conduction in solution cast doped regioregular poly(3-hexylthiophene) at temperatures below 2.35 K. The appearance of superconductivity seems to be

closely related to the self-assembly properties of the polymer, as the introduction of additional disorder is found to suppress superconductivity.

As before mentioned a possible interpretation in the case of doped polyacetylene is based on the formation of *solitons*. A soliton is a very stable solitary negative or positive solution to the Schrödinger wave equation, a pseudo-particle. In the case of polyacetylene the soliton is in essence a carbo-cation (HC^+), that causes a phase-kink in the double-bond sequence: propagation of this kink under the influence of an electric field would then cause the electrical conductivity (illustrated in Fig. 11.14; see for the soliton concept also Roth (1987 and 2004); a clear explanation has also been given by Bower (2002)). However, most other conducting polymers do not have the proper topology to allow soliton formation. Bredas and Chance et al. (1982) have therefore proposed that *polarons* (radical ions) and *bipolarons* (radical ion pairs) are formed upon doping (Fig. 11.15). In organic materials a polaron is formed when a charge within a molecular chain influences the local nuclear geometry, causing an attenuation of nearby bond alternation amplitudes. This excited state possesses an energy level between the lower and upper bonds. The relatively high conductivity of these polymers probably results from the diffusive motion of the spinless bipolarons. A schematic diagram of some excitations in *trans*-polyacetylene is shown in Fig. 11.16.

There are several methods to “dope” a polymer (MacDiarmid, 2001): redox doping, photo-doping, charge-injection doping and non-redox doping. By controlling the doping level, conductivity anywhere between that of the pristine and that of the fully doped form of the polymer can be easily obtained (MacDiarmid, 2001). Examples are shown in Figs. 11.17 and 11.18 for doping of *trans*-polyacetylene with AsF_6^- and of polyaniline with HCl , respectively. In both cases the conductivity increases by many orders of magnitude up to limiting values of 100 and 1 S/cm, respectively.

11.3.3.1. Redox doping

11.3.3.1.1. Chemical and electrochemical p-doping p-Doping, a partial oxidation of the π -backbone of an organic polymer, was first discovered by treating *trans*-polyacetylene with an oxidising agent such as iodine. Approximately 85% of the positive charge is delocalised over 15 CH units to give a positive soliton. This means that only 7 mol% of iodine is needed per mol of CH. In Scheme 11.1 for simplicity only five units of the soliton are drawn.

p-Doping of $(\text{CH})_n$ can also be accomplished electrochemical anodic oxidation by immersion of a film in a LiClO_4 solution in propylene carbonate.

11.3.3.1.2. Chemical and electrochemical n-doping n-Doping, a partial reduction of the π -backbone of an organic polymer, was also discovered using $(\text{CH})_n$ by treating it with a reducing agent by e.g. sodium naphthalene. It can also be accomplished electrochemically by cathodic reduction of a film in a solution of LiClO in tetrahydrofuran.

In these doping processes, not only of polyacetylene but also of other conjugated polymers, the introduced counter dopant ions stabilise the charge on the polymer backbone. There are doping processes, however, where no counter ions are involved. Examples are *photo doping* and *charge injection doping*.

11.3.3.2. Doping involving no doping ions

11.3.3.2.1. Photo-doping When $(\text{CH})_n$ is exposed to radiation of energy higher than the energy for an electron to jump to the conducting band, the polymer undergoes *photo-doping*. Positive and negative solitons are localised over approximately 15 CH units. In Scheme 11.2 they are for simplicity depicted as residing on one CH unit only. When

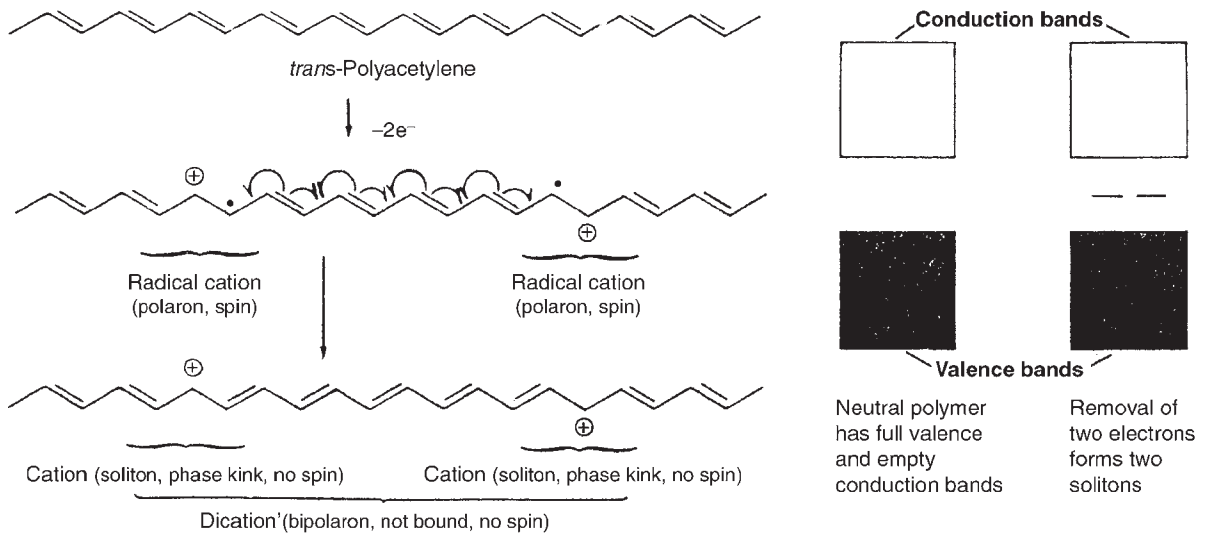


FIG. 11.14 Formation of solitons in oxidised polyacetylene (courtesy Professor Cowan).

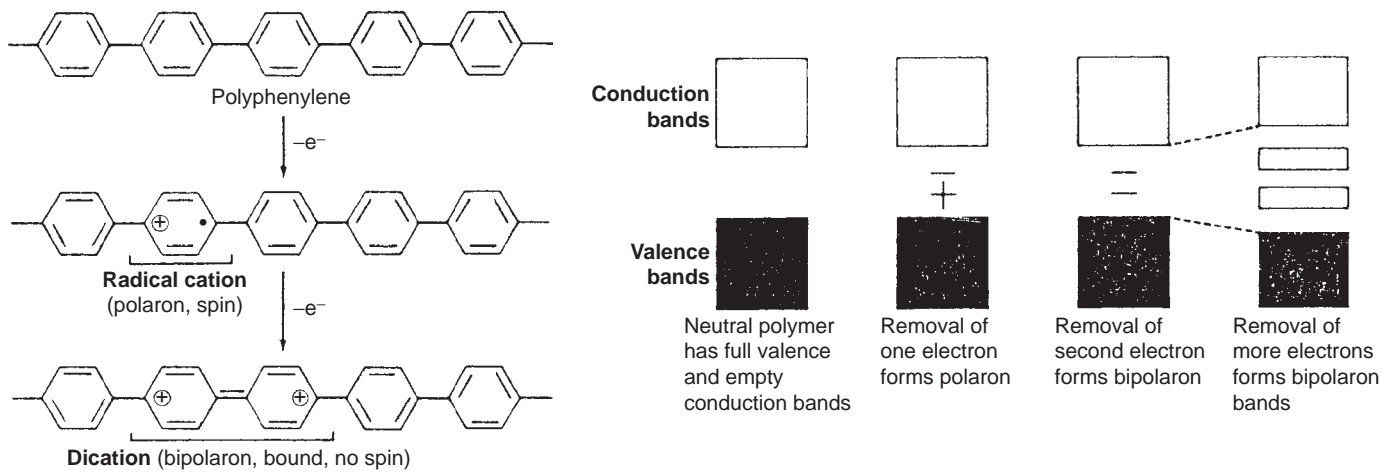


FIG. 11.15 Formation of bipolarons in oxidised polyphenylene (courtesy Professor Cowan).

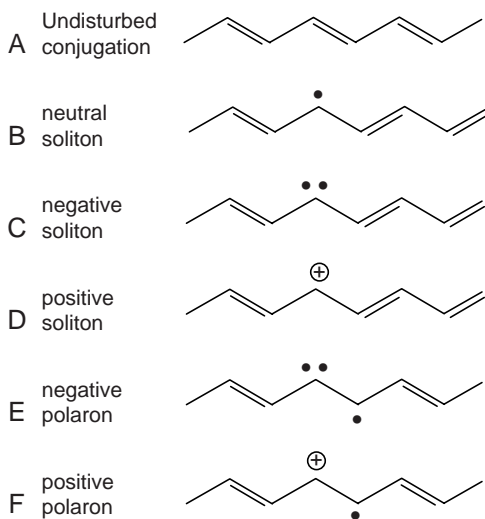


FIG. 11.16 Schematic diagram of some excitations in *trans*-polyacetylene: (•) indicates electrons not involved in bonding and \oplus indicates a missing electron. From Roth (1995). Courtesy John Wiley and Sons, Inc.

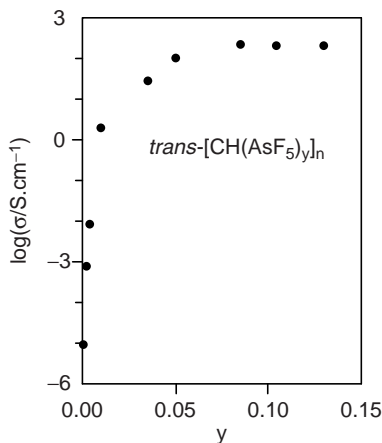


FIG. 11.17 Electrical conductivity of *trans*-(CH)_n as a function of AsF₅ dopant concentration. From Heeger, 2001. Courtesy John Wiley and Sons, Inc.

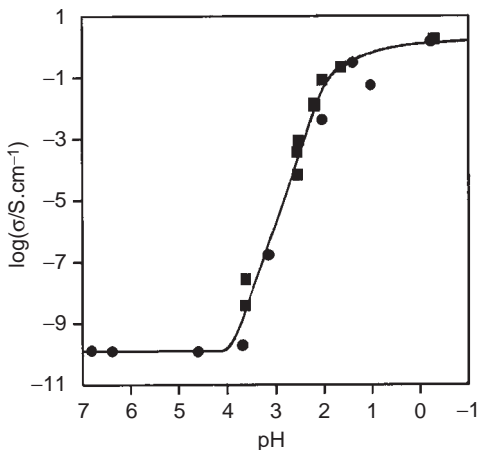
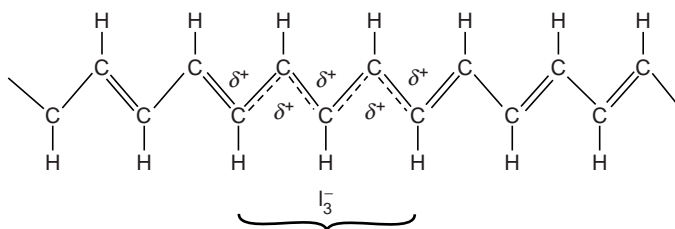
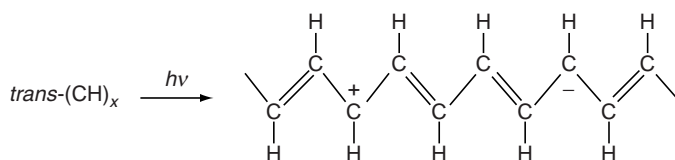


FIG. 11.18 Conductivity of emeraldine base as a function of pH of the HCl dopant solution as it undergoes protonic acid doping; (○) and (■) represent two independent series of experiments. From MacDiarmid, 2001. Courtesy John Wiley and Sons, Inc.



SCHEME 11.1 From MacDiarmid (2001). Courtesy John Wiley and Sons, Inc.



SCHEME 11.2 From MacDiarmid (2001). Courtesy John Wiley and Sons, Inc.

irradiation is stopped they disappear rapidly due to recombination of electrons and holes. Photoconductivity is observed if during irradiation a potential is applied.

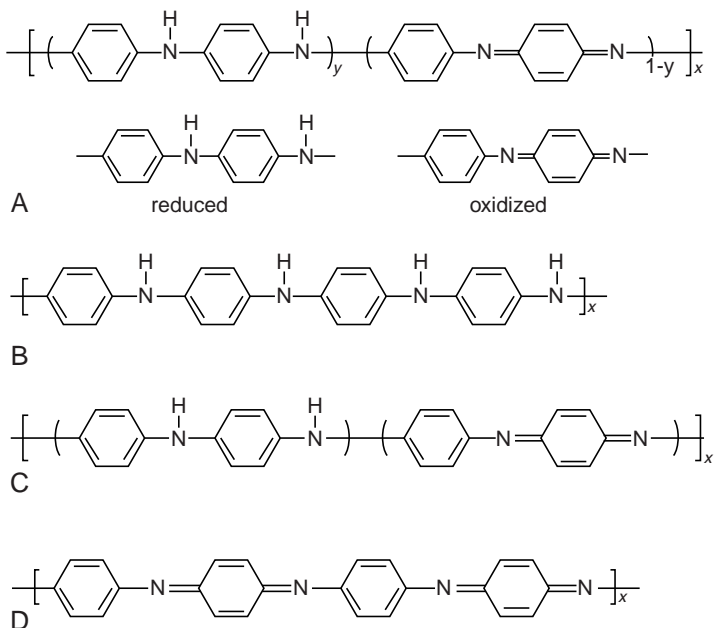
11.3.3.2.2. Charge-injection doping This kind of doping is accomplished in a sandwich structure of metal and a conductive polymer separated by a thin layer of a high dielectric strength insulator. An appropriate potential is applied across the structure, which can give rise to a surface charge layer, without any associated dopant ion. This approach also resulted in the above mentioned superconductivity of poly(3-hexylthiophene).

11.3.3.3. Non-redox doping

In this type of doping the number of electrons does not change: the energy levels are rearranged, however. The most common example for redox doping is polyaniline that has different appearances or oxidation states, as shown in Scheme 11.3. The average oxidation state of polyaniline (y) can be varied continuously $1 \geq y \geq 0$: *leuco-emeraldine* ($y = 1$, fully reduced, insulator), *emeraldine* ($y = 0.5$, half-oxidised, semi-conductor) and *pernigraniline* ($y = 0$, fully oxidised, insulator).

Protonation by acid-base chemistry leads to an internal redox reaction (Fig. 11.19), without change of the number of electrons (Heeger, 2001; MacDiarmic, 2001). The semiconductor (emeraldine base, $\sigma = 10^{-10}$ S/cm) is converted into metal (emeraldine salt, $\sigma \geq 100$ S/cm). Complete protonation of the imine nitrogen atoms in emeraldine base by aqueous HCl results in the formation of a delocalised polysemiquinone radical cation. This is accompanied by an increase in conductivity of more than 12 orders of magnitude.

During reversible chemical or electrochemical doping charge neutrality is maintained by the introduction of counter ions. Metallic polymers are therefore salts. Doped conjugated polymers are good conductors for two reasons: (a) doping introduces carriers into the electronic structure and (b) attraction of an electron in one repeat unit of the nuclei in the neighbouring units leads to carrier delocalisation along the polymer chain and to charge-carrier mobility, which is extended into three dimensions through inter-chain electron transfer (Heeger, 2001).



SCHEME 11.3 From MacDiarmid (2001). Courtesy John Wiley and Sons, Inc.

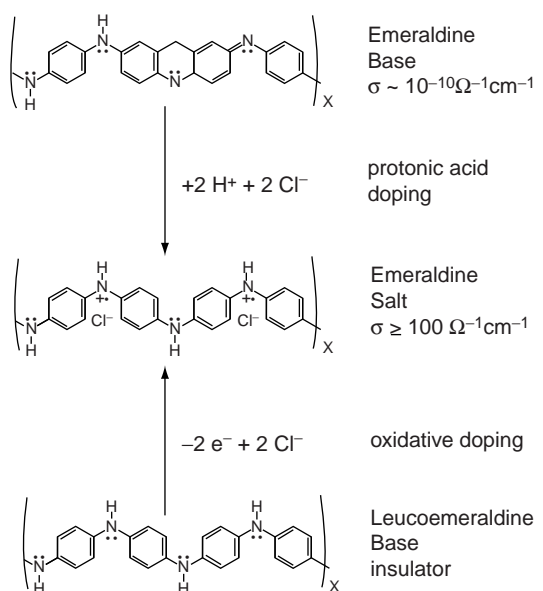


FIG. 11.19 Oxidative doping (*p*-doping) of leuco-emeraldine base and protonic acid doping of emeraldine base, leading to the same final product, emeraldine salt. Reproduced from Fig. 34.3 in Mark (1996). Courtesy Springer Verlag.

11.3.4. Temperature dependence of conduction of doped polymers

In Fig. 11.20 the temperature dependence of the electrical conductivity of iodine doped *cis*-polyacetylene at various doping levels is shown. In the highly doped samples the conductivity changes relatively little with temperature. With decreasing doping concentration the temperature dependence of the conductivity increases tremendously. It is suggested that at higher doping levels the wave functions of the solitons overlap, by which the samples behave more or less like "dirty metals".

Theory for the temperature dependence of the conductivity of doped polyacetylene leads to:

$$\sigma = CT^{-1/2} \exp[-(T_o/T)^{1/4}] \quad (11.36)$$

This equation has found to fit well with the conductivity of some *trans*-polyacetylene samples in the range of 10–300 K (Fig. 11.21).

11.3.5. Non-linear optics (NLO)

A related area in which conducting organic solids play an important part, is the field of nonlinear optics.

Nonlinear optical properties arise when materials are subjected to electromagnetic radiation of very high intensity (usually from lasers). Low-intensity electromagnetic fields give a linear response for the induced dipole moment vector in a molecule:

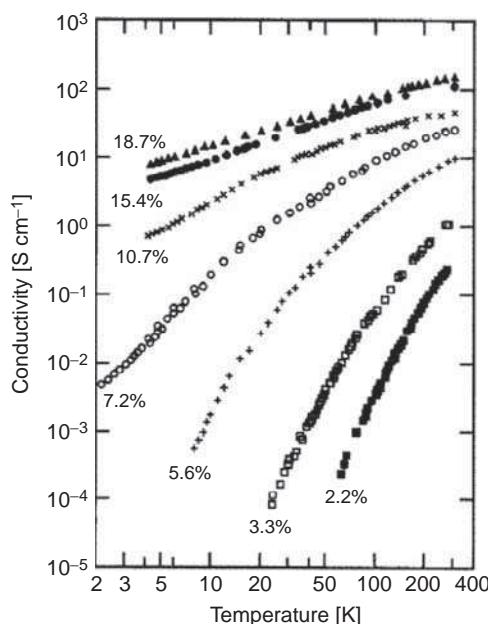


FIG. 11.20 Temperature dependence of the electrical conductivity of *cis*-polyacetylene at various doping levels. From Roth (1987). Courtesy Trans Tech Publications.

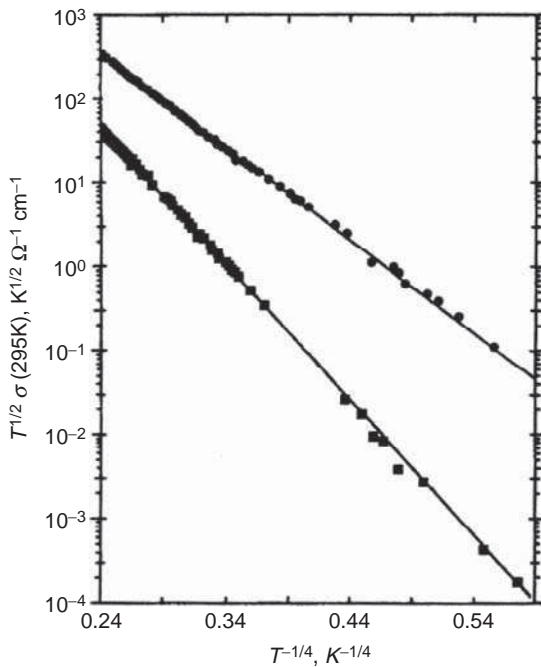


FIG. 11.21 Temperature dependence of iodine doped *trans*-polyacetylene according to Eq. (11.36): (•) 1.7 mol % I₂; (■) 4.2 mol% I₂. From Epstein et al. (1983). Courtesy American Physical Society.

$$\mu = \epsilon_0 \alpha' E \quad (11.37)$$

where ϵ_0 = permittivity of free space (i.e. $(8.8541878176\dots \times 10^{-12}$ F/m = C/V/m = C²/N/m); α' = polarisability of the molecule (m³); E = electric field (V/m).

In vacuum the electric flux density and the electric field are related by

$$\mathbf{D} = \epsilon_0 \mathbf{E} \quad (11.38)$$

where \mathbf{D} = electric flux density vector (C/m²) or electric displacement; \mathbf{E} = electric field vector (V/m¹).

In an *isotropic dielectric medium* polarisation occurs and the flux density is

$$\mathbf{D} = \epsilon_0 \epsilon \mathbf{E} = \epsilon_0 \mathbf{E} + \mathbf{P} \quad (11.39)$$

where \mathbf{P} = polarisation flux density (C/m²) (=dipole moment per unit of volume); ϵ = relative permittivity of the dielectric (or dielectric constant).

The polarisation flux density can be written as

$$\mathbf{P} = \mathbf{D} - \epsilon_0 \mathbf{E} = \epsilon_0 (\epsilon - 1) \mathbf{E} = \epsilon_0 \chi_e \mathbf{E} \quad (11.40)$$

where χ_e = electric susceptibility of the dielectricum, equal to

$$\chi_e = \epsilon - 1 = n^2 - 1 \quad (11.41)$$

where the right hand side expression ($=n^2-1$) is in general valid for most dielectrics.

The equations above are described in the SI system. In the earlier cgs system the definitions and equations are different:

$$\mathbf{D} = \mathbf{E} + 4\pi\mathbf{P} = \mathbf{E}(1 + 4\pi\chi_e) = \epsilon\mathbf{E}$$

or

$$\mathbf{P} = \frac{\mathbf{D} - \mathbf{E}}{4\pi}$$

and

$$\chi_e = \frac{\epsilon - 1}{4\pi}$$

The dimensions of both \mathbf{D} and \mathbf{P} are V/cm in the cgs system.

In an *anisotropic dielectricum* the polarisation \mathbf{P} is not necessarily aligned with the electric field \mathbf{E} , because the induced dipoles have certain preferred directions, related to the physical structure of the material. This can be written as:

$$\mathbf{P} = \epsilon_0 \boldsymbol{\chi}_e \mathbf{E} \quad (11.42)$$

where now the electric susceptibility is not a number, but a second-order tensor: the *second-order electric susceptibility tensor*:

$$\begin{pmatrix} P_1 \\ P_2 \\ P_3 \end{pmatrix} = \begin{pmatrix} \chi_{e,11} & \chi_{e,12} & \chi_{e,13} \\ \chi_{e,21} & \chi_{e,22} & \chi_{e,23} \\ \chi_{e,31} & \chi_{e,32} & \chi_{e,33} \end{pmatrix} \begin{pmatrix} E_1 \\ E_2 \\ E_3 \end{pmatrix} \quad (11.43)$$

From thermodynamic arguments it can be shown that $\chi_{e,ij} = \chi_{e,ji}$, i.e. the tensor $\boldsymbol{\chi}$ is a symmetric tensor. It follows that \mathbf{D} and \mathbf{E} are also related by a tensor

$$\mathbf{D} = \epsilon_0 \mathbf{E} + \mathbf{P} = \epsilon_0 \mathbf{E} + \epsilon_0 \boldsymbol{\chi}_e \mathbf{E} = \epsilon_0(1 + \boldsymbol{\chi}_e) \mathbf{E} = \boldsymbol{\epsilon} \mathbf{E} \quad (11.44)$$

where $\boldsymbol{1}$ = unit tensor; $\boldsymbol{\epsilon}$ = relative permittivity tensor or dielectric tensor.

Non-linear optical properties arise when materials are subjected to electromagnetic radiation of very high intensity (usually from lasers). A second-order non-linear electro-optical (EO) effect, which changes the refractive index for light passing an NLO-material in a strong external electric field, was not observed until 1906, when a light beam of sufficient coherence length was realised. It was first described by Pockels (1906) and nowadays called the Pockels-effect. The second-order opto-optical effect of colour change, known as second harmonic generation (SHG) or frequency doubling, was first described by Franken et al. (1961) when strong laser beams became to their disposal. They detected UV light ($\lambda = 347.1$ nm) at twice the frequency of a ruby laser beam ($\lambda = 694.2$ nm) when this beam traversed a quartz crystal. Another example is the conversion of the commercial infrared laser ($\lambda = 1064$ nm) to green light ($\lambda = 532$ nm). This transformation is useful because it quadruples the amount of information the laser can write on an optical disc. Third-order effects are third harmonic generation (THG), or frequency tripling, where the wavelength of a laser beam decreases by a factor of three, was first observed by Terhune et al. (1962), and the Kerr-effect, discovered in 1875 by the physicist John Kerr, where a material becomes birefringent under the action of an AC or DC electric field. It is distinct from the Pockels effect in that the induced refractive index change is directly proportional to the square of the electric field instead of the magnitude of the field. Third-order effects are extremely small: Terhune et al. detected a conversion of one photon at $\lambda = 231.3$ nm out of about 10^{15} photons at the fundamental wavelength at $\lambda = 693.9$ nm.

Several inorganic single crystalline materials like LiNbO_3 , GaAs , KH_2PO_4 and K_3PO_4 and organic crystals of urea, POM and MAP have strong NLO activity. The advantages of using NLO-polymers with respect of inorganic NLO-materials are many. First, the dielectric constant of polymers is much lower, which increases the speed of the devices they are used in. Secondly, they have a relatively constant refractive index for wavelengths from infrared to microwave region, which ensures proper modulator operation over that range. Thirdly, polymers offer the advantage of ease of integration with semiconductor electronics. Fourthly, they can be prepared as thin films or fibres, they have lower masses, offer low optical loss and are significantly cheaper than their inorganic counterparts.

Organic compounds with an extended conjugated π -electrons system and substituted with electron-donating and electron-withdrawing structural groups display a large first-order hyper polarisability and a large second-order susceptibility (if incorporated in solids). An extensively studied compound of this type is MNA, the 2-methyl-4-nitro-aniline. Compounds like this one generate radiation that has twice the frequency of the original radiation: *frequency doubling*. Possible applications are *frequency-mixing*, *electro-optical modulation* and *optical switching* (see below). Compounds with large third-order susceptibility provide a method for third harmonic generation. Single crystals of polydiacetylenes belong to this group. Functionalised polymers, in particular side chain liquid crystalline polymers offer the possibility to synthesise numerous different polymers, each with his own NLO-properties (see e.g. Fig. 11.22).

In a strong electric field second-order and even third-order effects may be present:

$$\boldsymbol{\mu} = \boldsymbol{\mu}_0 + \boldsymbol{\mu}^{(1)} + \boldsymbol{\mu}^{(2)} + \boldsymbol{\mu}^{(3)} + \dots = \varepsilon_0(\alpha \mathbf{E} + \beta \mathbf{EE} + \gamma \mathbf{EEE} + \dots) \quad (11.45)$$

$$\mathbf{P} = \mathbf{P}_0 + \mathbf{P}^{(1)} + \mathbf{P}^{(2)} + \mathbf{P}^{(3)} + \dots = \varepsilon_0(\chi_e^{(1)} \mathbf{E} + \chi_e^{(2)} \mathbf{EE} + \chi_e^{(3)} \mathbf{EEE} + \dots) \quad (11.46)$$

where:

- (a) The diad \mathbf{EE} and the triad \mathbf{EEE} (second and third-order tensors, respectively) may build up from the same electric field vector \mathbf{E} : they may however, also be build up from different electric fields: $\mathbf{E}^{(1)}\mathbf{E}^{(2)}$ and $\mathbf{E}^{(1)}\mathbf{E}^{(2)}\mathbf{E}^{(3)}$.

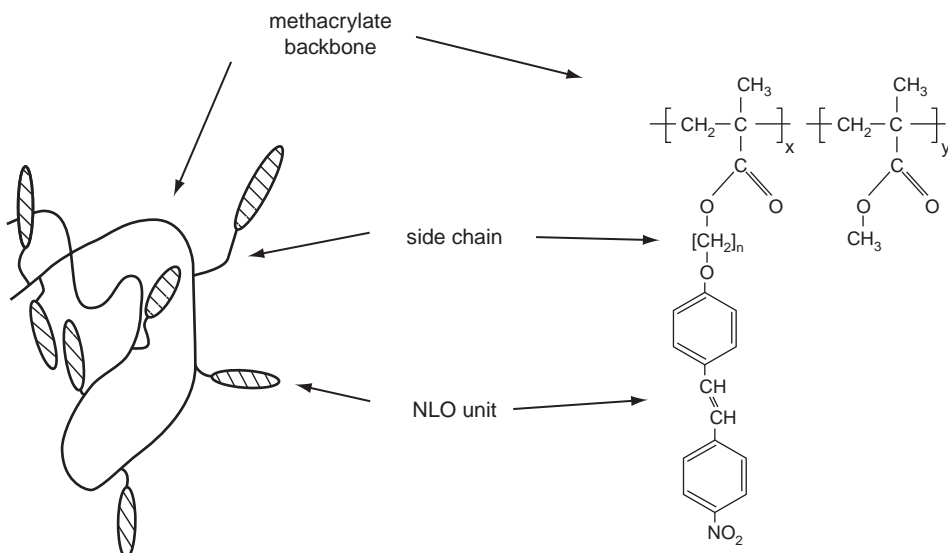


FIG. 11.22 Example of a functionalised side chain liquid crystalline copolymer. After Klaase (2002); See also Jacobson and Landi et al. (1994).

- (b) α , β and γ are the so-called first, second and third-order hyper-polarisability tensors, respectively; with dimensions m^3 , m^4/V and m^5/V , respectively.
- (c) $\chi_e^{(1)}$, $\chi_e^{(2)}$ and $\chi_e^{(3)}$ are second, third and fourth-order tensors, respectively. $\chi_e^{(1)}$ is the susceptibility responsible for linear optics; $\chi_e^{(2)}$ is the second-order non-linear susceptibility (the quadratic field contribution); $\chi_e^{(3)}$ is the third-order nonlinear susceptibility (cubic in field strength E), with dimensions $-m/V$ and m^2/V , respectively.

If the electric field is a sinusoidal field like in electro-magnetic waves, the different fields $E^{(1)}$, $E^{(2)}$ and $E^{(3)}$ may have different amplitudes $E_o^{(1)}$, $E_o^{(2)}$ and $E_o^{(3)}$ and also different angular frequencies ω_1 , ω_2 and ω_3 . The material properties $\chi_e^{(2)}$ and $\chi_e^{(3)}$ are also dependent on the frequencies of the electromagnetic field: $\chi_e^{(2)} = \chi_e^{(2)}(-\omega, \omega_1, \omega_2)$ and $\chi_e^{(3)} = \chi_e^{(3)}(-\omega, \omega_1, \omega_2, \omega_3)$. The first frequency between brackets, ω , refers to the output frequency produced by the device. The frequencies ω_1 , ω_2 and ω_3 represent the input frequencies of the electric field. The notation including $(-\omega)$ refers to the conservation of momentum and energy required in the absence of absorption for the outgoing angular frequency, equal to

$$\omega = \omega_1 + \omega_2 + \omega_3$$

This leads to a wide range of useful NLO phenomena. Some of the relevant processes are listed in Table 11.6.

Some of the results of Table 11.6 become clear from next equations:

$$\begin{aligned} 2 \cos\alpha \cos\beta &= \cos(\alpha + \beta) + \cos(\alpha - \beta) \\ 4 \cos\alpha \cos\beta \cos\gamma &= \cos(\alpha + \beta + \gamma) + \cos(\alpha + \beta - \gamma) \\ &\quad + \cos(\alpha - \beta + \gamma) + \cos(\alpha - \beta - \gamma) \\ 2 \cos^2\alpha &= \cos(2\alpha) + 1 \\ 4 \cos^3\alpha &= \cos(3\alpha) + 3\cos\alpha \end{aligned}$$

For most materials the higher-order non-linear optical effects are small and extremely difficult to detect. So the NLO effects investigated most are the second-order effects.

11.3.6. Current–voltage non-linearity

Some organic compounds, such as the complex copper/TCNQ (see Fig. 11.11), possess the property of current–voltage non-linearity and deviate heavily from Ohm’s law. At some threshold voltage their electrical resistance drops precipitously by orders of magnitude (10^4);

TABLE 11.6 Examples of second and third-order NLO effects

$\chi_e^{(2)}(-\omega_3, \omega_1, \omega_2)$	Three wave mixing, sum and difference frequency generation
$\chi_e^{(2)}(-2\omega, \omega, \omega)$	Second harmonic generation (SHG)
$\chi_e^{(2)}(0, \omega, \omega)$	Optical rectification
$\chi_e^{(2)}(-\omega, \omega, 0)$	Linear electro-optical or Pockels effect
$\chi_e^{(3)}(-\omega_4, \omega_1, \omega_2, \omega_3)$	Four wave mixing
$\chi_e^{(3)}(-\omega, 0, 0, \omega)$	Quadratic electro-optical effect (DC-Kerr)
$\chi_e^{(3)}(-2\omega, 0, \omega, \omega)$	Electric field induced second harmonic (EFISH)
$\chi_e^{(3)}(-\omega, \omega_a, -\omega_a, \omega)$	AC electro-optical effect (AC-Kerr)
$\chi_e^{(3)}(-3\omega, \omega, \omega, \omega)$	Third harmonic generation (THG)

this phenomenon is extremely rapid and takes only nanoseconds. It is a form of electrical switching.

The possible applications of conducting organic solids in the fields of electronics and laser optics are manifold.

11.4. ULTIMATE ELECTRICAL PROPERTIES

11.4.1. Dielectric strength

When the voltage applied to an insulator is increased, a point will be reached where physical breakdown of the dielectric causes a catastrophic decrease in resistance. This voltage is called the dielectric strength. Curves of time-to-failure versus voltage can be plotted and usually show two distinct regions of failure. The short-time failure is due to the inability of the conducting electrons to dissipate rapidly enough the energy they receive from the field. The long-time failure is a breakdown mostly due to the so-called corona attack.

The dielectric strength is highly dependent on the form of the material; this effect is sometimes greater than the change in molecular structure.

The average value of the dielectric strength of pure polymers in kV/cm is 200. Chlorinated polymers show values up to 500, polymers containing aromatic rings are on the low side (about 160).

There is a great similarity between electrical strength and mechanical strength. This is because electrical breakdown involves physical destruction. Within identical temperature regions both modulus and dielectric strength show a substantial reduction in magnitude.

11.4.2. Arc resistance

When exposed to an electrical discharge, the surface of some polymers may become carbonised and conduct current; the arc resistance, a measure of this behaviour, is an important property in the application as insulating material in engine ignition systems.

The arc resistance has the dimension of seconds; its value varies for different polymers from about 400 for poly(chlorotrifluoroethylene) to about 50 for poly(vinylidene fluoride).

No direct correlation with chemical structure can be demonstrated.

BIBLIOGRAPHY

General references

- (A) *Dielectric polarisation*
Atkins PW and De Paula J, "Physical Chemistry", Oxford University Press", Oxford, 8th Ed., 2006.
- Bicerano J, "Prediction of Polymer Properties", Marcel Dekker, New York, 3rd Ed, 2002, Chap. 9.
- Birks JB and Schulman JH (Eds), "Progress in Dielectrics", Wiley, New York, 1959.
- Böttcher CJF, "Theory of Electric Polarisation", Vol. 1, "Dielectrics in Static Fields", 2nd Ed, revised by Van Bel OC, Elsevier, Amsterdam, 2nd Ed, 1973.
- Böttcher CJF and Bordewijk P, "Theory of Electric Polarisation", Vol. 2, "Dielectrics in Time-dependent Fields", Elsevier, Amsterdam, 2nd Ed, 1973.
- Boyd RH and Liu F, "Dielectric Spectroscopy of Semicrystalline Polymers", in Runt JP and Fitzgerald JJ (Eds), "Dielectric Spectroscopy of Polymeric Materials: Fundamentals and Applications", American Chemical Society, Washington DC, Chap. 4.
- Bower DI, "An Introduction to Polymer Physics", Cambridge University Press, 2002, Chap. 9.
- Brandrup J, Immergut EH and Grulke EA (Eds) "Polymer Handbook", Part VII, Wiley, New York, 4th Ed, p 291, 1999.

- Fröhlich H, "Theory of Dielectrics", Oxford Univ Press, 2nd Ed, 1968.
- Karasz FE (Ed), "Dielectric Properties of Polymers", Plenum Press, New York, 1972.
- McCrum NG, Read BL and Williams G, "Anelastic and Dielectric Effects in Polymeric Solids", Wiley, New York, 1967.
- Morton WE and Hearle JWS, "Physical Properties of Textile Fibres", Textile Institute, Butterworth, London 1962, Chap. 21.
- Sessler GM (Ed.) "Electrets", 3rd Ed, Laplacian Press, Morgan Hill, 1999.
- Van Turnhout J, "Thermally Stimulated Discharge of Polymer Electrets", PhD Thesis, Leiden, 1972; as book published by Elsevier, Amsterdam (1975).
- Würstlin F and Thurn H, "Struktur und Elektrische Eigenschaften", in Stuart HA (Ed) "Die Physik der Hochpolymeren", Vol. IV, Springer, Berlin, 1956, Chap. 8.

(B) Static electrification and conduction

- Bower DI, "An Introduction to Polymer Physics", Cambridge University Press, 2002, Chap. 9.
- Bredas JL, Chance RR, et al., "Structural Basis for Semi-conducting and Metallic Polymer/Dopant Systems", Chemical Reviews 82 (1982) 209.
- Cotts DB and Reyes Z, "Electrically Conductive Organic Polymers for Advanced Applications", Noyes Data Corp, Park Ridge, NJ, 1986.
- Cowan DO and Wlygul FM, "The Organic Solid State", C & EN Special Report, Chem & Eng News, July 21, pp 28–45, 1986.
- Epstein AJ, "Conducting Polymers: Electrical Conductivity", in Mark JE (Ed), "Physical Properties of Polymers Handbook", Springer-Verlag, 2nd Ed, 2007, Chap. 46.
- Gayler J, Wiggins RE and Arthur JB, "Static Electricity; Generation, Measurement and its Effects on Textiles", N Carolina State University, School of Textiles, Rayleigh, 1965.
- Gutman F and Lyons LE, "Organic Semi Conductors", Wiley, New York, 1967.
- Kohlman RS, Joo J and Epstein AJ, "Conducting Polymers: Electrical Conductivity", in Mark JE (Ed), "Physical Properties of Polymers Handbook", AIP Press, Woodbury, NY, 1996, Chap. 34.
- Koton JE (Ed), "Organic Semiconducting Polymers", Marcel Dekker, New York, 1968.
- Loeb LB, "Static Electrification", Springer, Berlin/New York, 1958.
- Mair HJ and Roth S (Eds), "Elektrisch leitende Kunststoffe", Carl Hanser, München, 1986.
- Mort J and Pfister G (Eds), "Electronic Properties of Polymers", Wiley, New York, 1982.
- Nalwa HS, "Handbook of Organic Conductive Molecules and Polymers"; Vol. 1, "Charge-Transfer Salts, Fullerenes and Photoconductors"; Vol. 2, "Conductive Polymers: Synthesis and Electrical Properties"; Vol. 3, "Conductive Polymers: Spectroscopy, Photo-Physics and Applications"; Vol. 4, "Conductive Polymers: Transport and Physical Properties", Wiley, Chichester, 1997.
- Pratt C, "Applications of Conducting Polymers", <http://homepage.ntlworld.com/colin.pratt/appcp.htm>.
- Ramakrishnan S, Resonance, 2 (1997) 48.
- Roth S and Carroll D, "One-Dimensional Metals: Conjugated Polymers, Organic Crystals, Carbon Nanotubes", Wiley-VCH, Weinheim, New York, 2nd Ed, 2004.
- Seanor DA (Ed), "Electrical Properties of Polymers", Academic Press, New York, 1982.
- Seymour RB, "Conductive Polymers", Plenum Press, New York, 1981.
- Skotheim TA (Ed), "Handbook of Conducting Polymers", 2 vols, Marcel Dekker, New York, 1986.
- Skotheim TA, Elsenbaumer RL and Reynolds JR (Eds), "Handbook of Conducting Polymers", Dekker, New York, 2nd Ed, 1998.

(C) Non-linear optics

- Barford W, "Electronic and Optical Properties of Polymers", Oxford University Press, Oxford, 2005.
- Bower DI, "An Introduction to Polymer Physics", Cambridge University Press, 2002, Chap. 9.
- Butcher PN and Cotter D, "The Elements of Nonlinear Optics", Cambridge University Press, 1991.
- Heeger AJ, Angew Chem Int Ed 40 (2001) 2591.
- Heeger AJ, Orenstein J and Ulrich DR (Eds), "Nonlinear Optical Properties of Polymers", Materials Res Soc Symposium Proceedings, Vol. 109, Pittsburgh, 1988.
- Klaase PTA, "Structure Dependent Electro-optical Properties of Chromophore Functionalised Polymers", Doctoral Thesis, Delft, 2002.
- MacDiarmid AG, Nobel Lecture "Synthetic Metals, A Novel Role for Organic Polymers", Angew Chem Int Ed 40 (2001) 2581; Rev Mod Phys 73 (2001) 701.
- Mark JE (Ed), "Physical Properties of Polymers Handbook, Part VIII, Electro-optical and Magnetic Properties", Springer-Verlag, 2nd Ed, 2007.
- Paschotta R, "Encyclopedia of Laser Physics and Technology", WWW Virtual Library, 2005.
- Pockels F, "Lehrbuch der Kristallphysik", Tuebner, Leipzig, 1906.
- Prasad SV and Ulrich DR, "Nonlinear Optical Polymers", Plenum Press, New York, 1988.

- Shen YR, "The Principles of Nonlinear Optics", Wiley, New York, 1984.
- Van der Vorst CPJM and Picken SB, "Electric Field Poling of Nonlinear Optical Side Chain Polymers", in Shibaev VP (Ed.) "Polymers as Electro-optical and Photo-optical Active Media", Springer Verlag, Berlin, 1996, Chap. 5; "Electric Field Poling of Acceptor-Donor Molecules", J Opt Soc Am B 7 (1990) 320.
- Wijekoon WMKP and Prasad PN, "Nonlinear Optical Properties of Polymers", in Mark JE (Ed), "Physical Properties of Polymers Handbook", AIP Press, Woodbury, NY, 1996, Chap. 38.
- Wijekoon WMKP, Lee K-S and Prasad PN, "Nonlinear Optical Properties of Polymers", in Mark JE (Ed), "Physical Properties of Polymers Handbook", Springer-Verlag, 2nd Ed, 2007, Chap. 49.
- Yariv A, "Optical Electronics", Saunders, Orlando, Florida, 1991.

Special references

- Baeriswyl D, Campbell DK and Mazumdar S, in Keiss HG (Eds), "Conjugated Conducting Polymers", Springer Verlag, Berlin, p 7, 1992.
- Bland DR, "The Theory of Linear Viscoelasticity", Pergamon Press, Oxford, 1960.
- Bredas JL, Chance RR, et al., Phys Rev B 29 (1984) 6761.
- Bredas JL, Street GB, et al., Phys Rev B 30 (1984) 1023.
- Clarke TC, Street GB, et al., Mol Cryst Liq Cryst 83 (1982) 253.
- Coehn A, Ann Phys 64 (1898) 217.
- Cole RH and Cole KS, J Chem Phys 9 (1941) 341.
- Debye P, Phys Z 13 (1912) 97.
- Darby JR, Touchette NW and Sears K, Polym Eng Sci 7 (1967) 295.
- Epstein AJ, Rommelmann H, Bigelow R, Gibson HW, Hoffmann DM and Tanner DB, Phys Rev Lett 50 (1983) 1866.
- Franken PA, Hill AE, Peters CW and Weinreich G, Phys Rev Lett 7 (1961) 118.
- Goss Levi B, Physics Today, 53 (2000) 19.
- Hall N, J Chem Soc Chem Commun (2003) 1.
- Heeger AJ, MacDiarmid AG, et al., Phys Rev Lett 39 (1977) 1098.
- Horiguchi et al., "Manufacturing Method and Device for Electrets Processed Product", U.S. Patent 6,969,484 November 29, 2005.
- Jacobson S and Landi P, J Appl Polym Sci 53 (1994) 649.
- Jenekhe SA and Tibbetts SJ, J Polym Sci B, 26 (1988) 201.
- Mosotti OF, Mem Matem e Fisica Moderna 24 (1850) 11.
- Müller FH and Schmelzer CHR, Ergebn exakt Naturwiss 25 (1951) 359.
- Roth S, Mater Sci Forum 21 (1987) 1.
- Schmieder K and Wolf K, Kolloid-Z 127 (1952) 65.
- Schon JH, Dodabalapur A, Bao Z, Kloc C, Schenker O and Batlogg B, Nature 410 (2001) 189 Seanor DA, Adv Polym Sci 4 (1965) 317.
- Shashoua J, J Polym Sci A1, 1 (1963) 169.
- Shirakawa H, Luois EJ, MacDiarmid AG, Chiang CK and Heeger AJ, J Chem Soc Chem Comm (1977) 579.
- Strella S (1970, 1971), quoted by Seanor DA, in Frisch KC and Patsis A (Eds) "Electric Properties of Polymers", Technonomic Publishers Co Westport, CO, pp 37–51, 1972 Chap. 3.
- Terhune RW, Maker PD and Savage CM, Phys Rev Lett, 8 (1962) 404.
- Thakur M, Macromolecules 21 (1988) 661.
- Würstlin F, Kolloid-Z 120 (1951) 102.

CHAPTER 12

Magnetic Properties

The principal magnetic properties of polymers are the *diamagnetic susceptibility* and the *magnetic resonance*. The former is a property of the material as a whole; the latter is connected with magnetic moments of electrons and nuclei within the material.

Only the diamagnetic susceptibility and the second moment of the nuclear magnetic resonance show additive molar properties.

12.1. MAGNETIC SUSCEPTIBILITY (MAGNETIC INDUCTIVE CAPACITY)

Matter is diamagnetic, paramagnetic or ferromagnetic. This means that their presences in a magnetic field influence the magnetic field strength in different ways. In vacuum the magnetic flux density and the magnetic field are related by

$$\mathbf{B} = \mu_0 \mathbf{H} \quad (12.1)$$

where \mathbf{B} = magnetic flux density vector or magnetic induction vector or magnetic field strength vector (in $T = \text{Wb m}^{-2} = \text{kg A}^{-1} \text{s}^{-2} = \text{N A}^{-1} \text{m}^{-1} = \text{V s m}^{-2}$); \mathbf{H} = magnetic field vector or magnetic field intensity (A m^{-1}); μ_0 = magnetic permeability of vacuum ($4\pi \times 10^{-7} \text{ H m}^{-1} = \text{N A}^{-2}$) ($H = \text{Henry}$).

It has to be mentioned that a field strength of 1 T (SI unit) is equal to 10^4 G (cgs unit).

The magnetisation of a material is equal to the density of magnetic dipole moments

$$\mathbf{M} = \boldsymbol{\mu}_{\text{total}} / V \quad (12.2)$$

where \mathbf{M} = magnetisation vector (dimension equal to that of \mathbf{H}); $\boldsymbol{\mu}$ = magnetic dipole moment vector (A m^2).

The total magnetic field in the material is

$$\mathbf{B} = \mathbf{B}_0 + \mu_0 \mathbf{M} = \mu_0 (\mathbf{H} + \mathbf{M}) = \mu_0 \mathbf{H} (1 + \chi_v) = \mu_0 \mu_r \mathbf{H} \equiv \mu \mathbf{H} \quad (12.3)$$

where χ_v = volume magnetic susceptibility (or shortly the magnetic susceptibility) of the material; $\mu_r = 1 + \chi_v$ = relative magnetic susceptibility of the material; $\mu = \mu_0 \mu_r$ = magnetic permeability of the medium.

It follows that the magnetic susceptibility χ_v is equal to the ratio between the magnetisation and the magnetic field intensity:

$$\mathbf{M} = \chi_v \mathbf{H} \quad (12.4)$$

The magnetic susceptibility is negative and small (-10^{-4} to -10^{-6}) and temperature independent for diamagnetic materials ($\chi_v = -8.8 \times 10^{-6}$ for copper), and positive, small (10^{-5} to 10^{-3}) and strongly temperature dependent for paramagnetic materials ($\chi_v = 23 \times 10^{-6}$ for aluminium). On the other hand ferromagnetic materials show large values for χ_v , which, moreover, is strongly dependent on temperature and on magnetic field strength (for annealed iron χ_v varies from 150 to a maximum value of 5000 with increasing field strength; it subsequently decreases strongly at still higher field strengths). Criteria of this classification are given Table 12.1.

In organic polymers ferromagnetism occurs when impurities are present. These may completely mask the true susceptibility of the substance to be investigated. In the following we shall only consider substances free from ferromagnetism, since polymers normally are non-ferromagnetic.

Already in the 1980s some, probably real, ferromagnetic polymers were synthesised. Ovchinnikov (1987) polymerised a stable biradical monomer, consisting of a cyclic nitroxyl group attached to either end of a diacetylene fragment. Only a small fraction (0.1%) of the polymer was ferromagnetic and remained so on heating up to about 150 °C. Also Torrance et al. (1987) succeeded to produce a ferromagnetic polymeric material by reacting 1,3,5-triamino benzene with iodine. Again the yield was very low and not very reproducible. The significance of these studies is, that it shows that the electron spins of polymer-bound radicals can align along the length of the polymer chain.

However, cases like these are exceptional. Normally pure polymers are diamagnetic. Diamagnetism is a universal property of matter. Paramagnetism occurs in only two classes of organic substances: those containing metals of the transition groups of the periodic system and those containing unpaired electrons in the free radical or the triplet state. Since

$$\chi_{v,\text{total}} = \chi_{v,\text{dia}} + \chi_{v,\text{para}} \quad (12.5)$$

and $\chi_{v,\text{para}}$ is inversely proportional to the temperature, the value of χ_v extrapolated to infinite temperature, or to $1/T = 0$, gives the value of the diamagnetic part of the susceptibility only.

There are two other measures of susceptibility, the mass magnetic susceptibility χ or χ_g (in $\text{m}^3 \text{ kg}^{-1}$), and the molar magnetic susceptibility χ_m (in $\text{m}^3 \text{ mol}^{-1}$). The interrelations between the three magnetic susceptibilities are:

$$\begin{aligned} \chi_g &= \chi_v / \rho = \chi_m / M \\ \chi_m &= M \chi_g = M \chi_v / \rho \\ \chi_v &= \rho \chi_g = \rho \chi_m / M \end{aligned} \quad (12.6)$$

TABLE 12.1 Classification (χ_v) of various forms of magnetism

Class	Susceptibility range	Dependence on temperature	Dependence on field
Diamagnetic	-10^{-4} to -10^{-6}	Nearly independent	Nearly independent
Paramagnetic	10^{-5} to 10^{-3}	Inversely proportional to absolute temperature	Nearly independent
Ferromagnetic	10 to 10^5	Highly dependent	Dependent, reaches (after a maximum) a saturation value

12.1.1. Additivity of the molar magnetic susceptibility

The diamagnetic properties of homologous series of organic compounds were first investigated by Henricksen (1888), who called attention to the additive character of the magnetic susceptibility per gram molecule.

For a long period, from 1910 to 1952, Pascal worked on the elaboration of a consistent method for calculating the quantity

$$X_m = M\gamma_g \quad (12.7)$$

He used the formula

$$X_m = \sum_i X_{m,i} + \sum_i \lambda_i \quad (12.8)$$

where $X_{m,i}$ is the so-called atomic susceptibility, while λ_i represents the structure increments (i.e. structural correction factors). Following the work initiated by Pascal, various investigators have screened a large number of homologous series. A survey is given in Table 12.2.

Also Dorfman (1964) and Haberditzl (1968) have done important work in this field. They calculated a large number of contributions to the susceptibility per atomic bond, arriving also at a consistent method.

Since this book invariably uses contributions per structural group, Pascal's values (from 1935 and 1952) and those of Dorfman and Haberditzl have been converted into group contributions. They are summarised in Table 12.3. The mutual deviations are not large.

TABLE 12.2 Molar magnetic susceptibility X_m of the CH_2 -group (in $10^{-12} \text{ m}^3 \text{ mol}^{-1}$)

Year	Author	$-X_m(\text{CH}_2)$	Extremes	Error (%)	Type of compounds	Number of compounds
1910	Pascal	149.0	145–157	1.5	11 series	35
1927	Vaidyanathan	140.7			Liquid and gaseous org. compounds	
1929	Bitter	182.2	166–212	7.3	Hydrocarbons (gaseous)	5
1934	Cabrera and Fahlenbrach	144.3	139–152	2.3	Alcohols, esters, acids	6
1934	Bhatnagar et al.	142.8	141–145	0.9	Nitrogenous compounds	20
1935	Gray and Cruikshank	149.0				
1935	Woodbridge	146.7	141–152	2.1	Esters	4
1936	Bhatnagar and Mitra	146.8	133–157	2.1	11 different series	82
1937	Farquharson	146.3	143–149	1.6	Acids	5
1943	Angus and Hill	146.8	138–151	1.4	Different homologous series (hydrocarbons, alcohols, esters, acids)	27
1949	Broersma	142.9				48
1951	Pascal et al.	142.8				36
Average \pm SD		148 \pm 11				

TABLE 12.3 Group contributions to molar diamagnetic susceptibility $-X_m$ (in $10^{-12} \text{ m}^3 \text{ mol}^{-1}$)

Group	Pascal (ca. 1935)	Pascal (1952)	Dorfman (1964)	Haberdlitzl (1968)	Recommended value (SI units)
$-\text{CH}_3$	176.4	180.3	175.9	182.8	180
$-\text{CH}_2-$	142.8	142.8	143.3	142.7	143
$>\text{CH}-$	109.1	118.1	115.6	111.8	110
$>\text{C}<$	75.4	93.0	100.5	81.7	90
$=\text{CH}_2$	108.1	108.7	128.2	120.0	110
$=\text{CH}-$	74.5	83.6	84.2	82.3	83
$=\text{C}<$	40.8	58.4	69.1	60.9	57
$=\text{CH}_{\text{ar}}-$	116.0	114.4	116.0	115.6	116
$\text{>C}_{\text{ar}}-$	70.4	89.2	90.9	75.4	90
$\text{>C}_{\text{ar}}^{\text{endo}}$	121.9	—	—	119.4	119
$-\text{C}_6\text{H}_5$	—	666.0	—	653.5	670
$-\text{C}_6\text{H}_4-$	—	640.9	—	628.3	630
$\equiv\text{CH}$	104.3	—	114.4	—	110
$=\text{C}-$	70.5	—	99.3	—	90
$-\text{F}$	82.9	82.9	—	83.6	83
$-\text{Cl}$	251.3	232.5	226.2	232.4	230
$-\text{Br}$	402.1	349.3	—	339.3	350
$-\text{I}$	552.9	530.3	—	540.4	540
$-\text{CF}_3$	—	—	—	314.2	315
$-\text{CH}_2\text{Cl}$	394.6	—	—	377.0	380
$-\text{CCl}_2-$	—	—	540.4	490.1	500
$-\text{CCl}_3-$	—	—	754.0	754.0	750
$-\text{OH}$	91.7	91.7	84.2	100.5	94
$-\text{O}-$	57.8	66.6	502.7	66.6	60
$-\text{CH=O}$	81.1	105.6	109.3	104.9	106
$>\text{C=O}$	54.0	80.4	94.2	69.1	82
$-\text{COOH}$	198.5	215.5	233.7	261.4	240
$-\text{COO}-$	164.6	190.4	144.5	178.4	180
$-\text{NH}_2$	140.7	162.4	137.0	157.0	150
$>\text{NH}$	106.8	138.2	109.3	105.6	110
$>\text{N}-$	69.1	113.1	81.7	69.1	75
>N	155.8	—	—	—	150
$-\text{CONH}_2$	211.1	—	—	226.2	210
$-\text{CONH}-$	181.0	—	—	175.9	180
$-\text{CON}<$	144.5	—	—	138.2	140
$-\text{C}\equiv\text{N}$	138.2	138.2	150.8	125.6	140
$-\text{NO}_2$	—	—	103.0	—	100
$-\text{SH}$	222.4	237.5	—	—	230
$-\text{S}-$	188.5	212.4	—	—	200
$>\text{S=O}$	—	—	130.7	—	130
$>\text{Si}<$	—	—	—	—	140

12.1.2. Comparison with experimental χ_g -values of polymers

The number of reliable data on the magnetic susceptibility of polymers is relatively small. Table 12.4 shows that on the whole there is a good agreement with the additively calculated values.

Example 12.1

Estimate the values of χ_g , χ_m and χ_y for Polystyrene ($M = 104.1 \text{ g mol}^{-1}$, $\rho = 1.05 \text{ g cm}^{-3}$)

Solution

From Table 12.3 it follows for $10^{12}X_{m,i}$

Group	$X_{m,i}$
$-\text{CH}_2-$	-143
$>\text{CH}-$	-110
C_6H_5-	-670
	<hr/>
	-923

from which we calculate with the aid of Eq. (12.6):

$$\chi_g = -923 \times 10^{-12} / 0.1041 = -8.88 \times 10^{-9} \text{ m}^3 \text{ kg}^{-1}$$

$$\chi_m = -923 \times 10^{-12} \text{ m}^3 \text{ mol}^{-1}$$

$$\chi_y = -8.88 \times 10^{-9} \times 1050 = -9.32 \times 10^{-6}$$

These results are in agreement with Table 12.4.

12.2. MAGNETIC RESONANCE

Magnetic resonance occurs when a material, placed in a static magnetic field, absorbs energy from an superimposed oscillating magnetic field, perpendicular to the static field, due to the presence of small magnetic elementary particles in the material. The nature of the absorption is connected with transitions between energy eigenstates of the magnetic dipoles.

There are two kinds of transitions that may be responsible for magnetic resonance:

- Transitions between energy states of the magnetic moment of the nuclei in the steady magnetic field; this effect is called *nuclear magnetic resonance* (NMR).
- Transitions between energy states of the magnetic moment of the electrons in the steady magnetic field; this effect is known as *electron spin resonance* (ESR).

ESR occurs at a much higher frequency than the NMR in the same magnetic field, because the magnetic moment of an electron is about 1800 times that of a proton. ESR is observed in the *microwave region* (9–38 GHz), nuclear spin resonance at *radio frequencies* (10–950 MHz).

In ordinary absorption spectroscopy one observes the interaction between an oscillating electric field and matter, resulting in transition between naturally present energy levels of a system of electrically charged dipoles. So it would be appropriate to call this “*electric resonance spectroscopy*”.

TABLE 12.4 Comparison of experimental and calculated values of magnetic susceptibilities of polymers

Polymer	Investigator	$-\gamma_g$ exp. ($10^{-9} \text{ m}^3 \text{ kg}^{-1}$)	$-X_m$ calc. ($10^{-12} \text{ m}^3 \text{ mol}^{-1}$)	M ($10^{-3} \text{ kg mol}^{-1}$)	$-\gamma_g$ calc. ($10^{-9} \text{ m}^3 \text{ kg}^{-1}$)	$-\chi_v$ (10^{-6})
Polyethylene	Maklakov (1963)	10.30	285	28.1	10.20	9.5
	Baltá-Calleja et al. (1965)					
Polypropylene	Rákoš et al. (1966)	10.05	439	42.1	10.40	9.4
Polystyrene	Hoarau (1950); Maklakov (1963)	8.86	922	104.1	8.86	9.3
Poly(tetrafluoroethylene)	Wilson (1962)	4.78	508	100.2	5.03	10.1
Poly(methyl methacrylate)	Bedwell (1947)	7.41	771	100.1	7.67	9.1
Poly(2,3-dimethyl-1,3-butadiene)	Hoarau (1950)	9.04	763	82.1	9.30	8.5
Polycyclopentadiene	Hoarau (1950)	9.04	535	66.1	8.17	—
Polyoxymethylene	Sauteray (1952)	6.53	205	30.0	6.85	8.6
Poly(ethylene oxide)	Baltá-Calleja et al. (1965)	7.92	348	44.1	7.92	8.9
Poly(2,6-dimethyl-1,4-phenylene oxide)	Baltá-Calleja and Barrales-Rienda (1972)	5.91(?)	1005	120.1	8.36	8.9
Poly(ethylene terephthalate)	Selwood et al. (1950)	6.35	1265	192.2	6.60	9.2
Nylon 6,6	Rákoš et al. (1968)	9.55(?)	1778	226.3	7.92	8.8
Poly(dimethyl siloxane)	Bondi (1951)	7.79	565	74.1	7.67	7.5
Poly(methylphenyl siloxane)	Bondi (1951)	7.54	2099	136.1	7.73	—

Magnetic resonance spectroscopy deals with the observation of the interaction between an oscillating magnetic field and matter, which results in transition between energy levels of the magnetic dipoles, the degeneracy of which is usually removed by an externally applied steady magnetic field.

The important practical difference between electric and magnetic resonance spectroscopy is that the former technique usually permits observation of transitions in the absence of externally applied fields. In magnetic resonance spectroscopy this is hardly ever possible.

NMR spectra of nuclei such as ^{57}Fe (spin $\frac{1}{2}$) in magnetic materials can be measured without external magnetic field. Also in the case of nuclear quadrupole resonance (NQR) no static magnetic field is necessary. For this reason NQR is sometimes called "zero field NMR". It is used to detect atoms whose nuclei have a nuclear quadrupole moment, such as ^{14}N and ^{35}Cl .

12.2.1. Nuclear magnetic resonance spectroscopy

NMR spectroscopy is probably the most powerful research tool used in structural chemical investigations today. It was first described independently by Felix Bloch (paraffin, 30 MHz) and Edward Mills Purcell (water, 8 MHz) in 1945/1946. They shared the Nobel Prize in Physics in 1952 for their discovery. Atomic nuclei experience this phenomenon if they possess a *spin*: the nuclei of some elements possess a net *magnetic moment* (μ), viz. in the case that the spin (I) of the nucleus is non-zero. This condition is met if the mass number and the atom number of the nucleus are *not both even* (as is the case for ^{12}C and ^{16}O).

NMR was for many years restricted to a few nuclei of high natural abundance and high magnetic moment (^1H , ^{19}F and ^{31}P). Less receptive nuclei, such as ^{13}C and ^{29}Si , required too long observation times to be applicable. With modern pulsed *Fourier-Transform (FT)* spectrometers, which have largely replaced the old continuous wave (CW) technique, individual spectra can be collected much more rapidly, so that ^{13}C NMR has become a routine.

The advances in NMR spectroscopy, since the beginning of the 1970s, have led to such a formidable array of new techniques (with their corresponding acronyms!) that even the professional spectroscopist sometimes feels himself bewildered.

The first revolution in NMR was the increased convenience of *signal averaging*; earlier only in solution good spectra could be obtained.

The major breakthroughs, however, have come from the use of *high magnetic fields* and further from the use of different *multiple pulse sequences* to manipulate the nuclear spins in order to generate more and more information: *time domain NMR spectroscopy*, that is used to probe molecular dynamics in solutions. The latter made it also possible to "edit" sub-spectra and to develop different *two-dimensional* (2D) techniques, where correlation between different NMR parameters can be made in the experiment (e.g. δ_{H} versus $\delta_{^{13}\text{C}}$, see later). *Solid state NMR spectroscopy* is used to determine the molecular structure of solids.

This is the reason that – after all – the NMR became such a highly professional field, that in a book like this one, only a rather superficial survey can be given.

Formerly (also in the second edition of this book) the field of NMR was subdivided into the so called *High-Resolution NMR* (restricted to solutions) and the "*broad band*" or "*wide line*" NMR (characteristic for solids). Due to the great advances in NMR techniques the barrier between these two – once quite separate – disciplines has almost disappeared.

The NMR phenomenon

The two most important nuclei for NMR in polymer chemistry, viz. the hydrogen isotope ^1H (protonium) and the carbon isotope ^{13}C . Proton-NMR gives information on the *skin* of the molecule (since the skin consists mainly of hydrogen atoms in different combinations) whereas ^{13}C -NMR provides information on the carbon *skeleton* of the molecule. Other isotopes nowadays frequently used in NMR are ^{19}F , ^{29}Si and ^{31}P . Important data on several nuclei are given in Table 12.5. We shall restrict ourselves from now on to ^1H and ^{13}C NMR.

A rotating nucleus, i.e. a rotating electric charge, behaves as a bar magnet, but a bar magnet so small that, when placed in an external magnetic field B_o , the spinning nuclei will not obediently align their magnetic moments in the field direction. Instead, their spin axes undergo a precession (due to the uncertainty principle of Heisenberg) around the direction of the magnetic field (like gyroscopes in a gravitational field), as shown in Fig. 12.1. The frequency of this so-called *Larmor precession*, the *Larmor frequency* v_L , is proportional to the field strength B_o :

$$v_L = \frac{\gamma}{2\pi} B_o \quad \text{or} \quad \omega_L = \gamma B_o$$

where γ is the so called *magnetogyric ratio* of the nucleus, which is a constant for every nucleus and defined as the ratio of its magnetic dipole moment to its angular momentum (as follows below), and expressed in Hz T $^{-1}$ or (T s) $^{-1}$ (this value is also included in Table 12.5). Increase of the field strength will not result in a better alignment, but in faster precession of the spinning nuclei.

TABLE 12.5 Some data of nuclei in NMR

Isotope		^1H	^2H	^{13}C	^{15}N	^{19}F	^{29}Si	^{31}P
Atomic number	Z	1	1	6	7	9	14	15
Mass number (atomic mass)	A	1	2	13	15	19	29	31
Natural abundance (%)	–	99.9844	0.0156	1.108	0.365	100	4.70	100
Nuclear spin quantum number	I	$^1/2$	1	$^1/2$	$^1/2$	$^1/2$	$^1/2$	$^1/2$
Magnetic moment ^a	μ	2.7927	0.8574	0.7022	-0.2830	2.6273	-0.5548	1.1305
Magneto-gyric ratio (MHz T $^{-1}$)	γ	267.52	41.07	67.26	-27.11	251.67	-53.16	108.29
Dimensionless constant	g_N	5.5854	0.8574	1.4042	-0.566	5.2576	-1.110	2.261
Relative sensitivity ($^1\text{H} = 1$)	–	1	0.00964	0.0159	0.00104	0.834	0.0785	0.0664
Resonance frequency (MHz) in a 1 T field	v_o	42.577	6.536	10.705	4.315	40.055	8.460	17.235

Most data from Tonelli and White (2007).

^a In units of the nuclear magneton: $\mu_N = eh/(4\pi m_p) = 5.05082 \times 10^{-27} \text{ J T}^{-1}$.

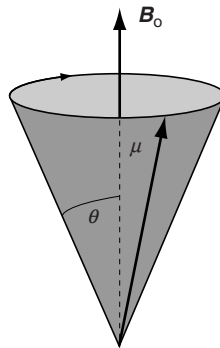


FIG. 12.1 Precession of a nuclear angular momentum in a magnetic field.

Nuclear spin is associated with an angular momentum which is characterised by the *orbital angular momentum vector I* . The magnitude of I is related to the nuclear spin quantum number I , which for ^1H and ^{13}C is equal to $1/2$, by

$$|I| = \frac{h}{2\pi} \sqrt{I(I+1)} \quad (12.9)$$

where h is Planck's constant.

The spin angular moment of a nucleus can take orientations from $+I$ to $-I$ in integral steps; hence, there are $2I + 1$ orientations. These values are known as the magnetic quantum numbers m_I . Accordingly, for a nucleus with $I = 1/2$, like ^1H and ^{13}C , there are only two orientations, leading to the magnetic quantum numbers $m_I = 1/2$ and $m_I = -1/2$. The component of the *spin angular momentum vectors* in the direction of the applied magnetic field, its z-component, is (Fig. 12.2)

$$I_z = m_I h / (2\pi) \quad (12.10)$$

which for $I = 1/2$ leads to

$$I_z = h / (4\pi) \quad \text{and} \quad I_z = -h / (4\pi) \quad (12.11)$$

in the direction and opposite direction of the magnetic field, respectively.

Spin of the nucleus gives rise to a magnetic field with strength proportional to its angular momentum. The magnetic moment due to the nucleus' spin interacts with this

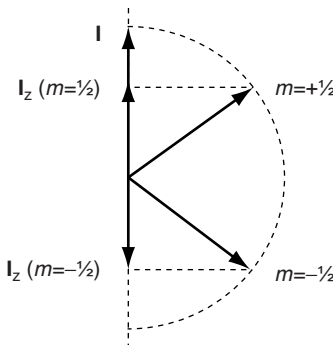


FIG. 12.2 Magnetic quantum numbers and spin angular momentum vectors for $I = 1/2$.

magnetic field. The orientation of the spin magnetic moment is determined by the orientation of the spin angular momentum

$$\boldsymbol{\mu}_m = \gamma \mathbf{I} \quad (12.12)$$

Placing an isolated magnetic moment μ in a magnetic field B_o results in a change of energy

$$E = -\boldsymbol{\mu} \cdot \mathbf{B}_o = -\mu B_o \cos\theta = -\mu_z B_o \quad (12.13)$$

where θ is the (precession) angle between the magnetic moment $\boldsymbol{\mu}$ and the magnetic field B_o . For $I = \frac{1}{2}$ the precession angle is $54^\circ 44'$.

The component of the magnetic moment in the direction of a magnetic field is

$$\mu_z = \gamma m_I h / (2\pi) \quad \text{or also} \quad \boldsymbol{\mu}_z = g_N \beta_N I \quad (12.14)$$

where g_N = a dimensionless constant (depending on the nucleus, see Table 12.5; $\beta_N = eh/(4\pi m_H) = 5.50082 \times 10^{-27} \text{ J T}^{-1}$ is the *nuclear magneton*; m_H = the mass of a proton = $1.67265 \times 10^{-27} \text{ kg}$).

For the energy we now can write

$$E = -\mu_z B_o = -\gamma m_I h B_o / (2\pi) = -g_N \beta_N m_I B_o \quad (12.15)$$

As long as there is no external magnetic field for nuclei for which the nuclear spin quantum number $I = \frac{1}{2}$, the number of nuclei with $m_I = -\frac{1}{2}$ equals the number of nuclei with $m_I = +\frac{1}{2}$: there is a dynamic equilibrium

$$A(\uparrow) + A(\downarrow) \rightleftharpoons A(\downarrow) + A(\uparrow) \quad \text{or} \quad m\left(+\frac{1}{2}\right) + m\left(-\frac{1}{2}\right) \rightleftharpoons m\left(-\frac{1}{2}\right) + m\left(+\frac{1}{2}\right)$$

where the number of $A(\uparrow)$ is equal to the number of $A(\downarrow)$.

For nuclei for which $I = \frac{1}{2}$ the nuclei with spin $m_I = +\frac{1}{2}$ are oriented parallel to the external magnetic field and they have a lower energy than the nuclei with spins $m_I = -\frac{1}{2}$, that are oriented antiparallel to the magnetic field; these states are labelled α -state and β -state, respectively. The energy difference between the two nuclei is

$$\Delta E = E_\beta - E_\alpha = \gamma h B_o / (2\pi) = g_N \beta_N B_o \quad (12.16)$$

In the presence of the external field the dynamic equilibrium mentioned above will be shifted in the direction of lower energy nuclear spins $A(\uparrow)$. This causes a surplus of low energy nuclear spins. Their population (N) will be given by a Boltzmann equation: ($N_o = N_\alpha + N_\beta$)

$$N_\beta / N_\alpha = \exp(-\Delta E / k_B T) \approx 1 - \frac{\Delta E}{k_B T} \quad (12.17)$$

or

$$\Delta N = N_\alpha - N_\beta \approx N_o \frac{\Delta E}{2k_B T} \quad (12.18)$$

or

$$\frac{N_\alpha - N_\beta}{N_\alpha + N_\beta} \approx \frac{\Delta E}{2k_B T} = \frac{\gamma h B_o}{4\pi k_B T} = \frac{g_N \beta_N B_o}{2k_B T} \quad (12.19)$$

So the population difference is dependent both on the field and on the nuclear species under observation. In practice ΔE is very small: for the proton in a magnetic field of 2.34 T $\Delta E \approx 6.6 \times 10^{-26} \text{ J}$ or 0.04 J mol^{-1} , so that at room temperature the relative surplus of protons in the α -state is only 1.6×10^{-5} . The corresponding Larmor frequency is 100 MHz.

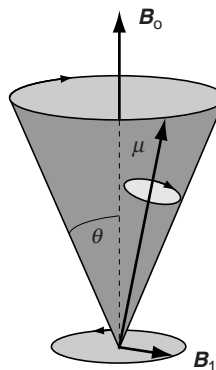


FIG. 12.3 Precession of a nuclear angular moment at resonance frequency for any $+m$; for $-m$ the precession is opposite.

Upon applying a second magnetic field B_1 at right angles to B_0 and causing this field to rotate exactly at the precession frequency v_L the lower energy α -spins will absorb energy until the situation is reached that the number of spins in the β -state equals that in the α -state, or $N_\alpha = N_\beta$. This is attended with large oscillations in the angle between μ and B_0 (see Fig. 12.3, where for the sake of simplicity the rotating field B_1 is drawn much larger than it is in practice with respect of B_0). This rotation frequency of B_1 is called the resonance frequency v_r , which is equal to v_L :

$$hv_r = \Delta E = g_N \beta_N B_0 = \gamma h B_0 / (2\pi) = hv_L \quad (12.20)$$

It follows that the resonance frequency is linear dependent on the magnetic field strength, just as the Larmor frequency is. In Fig. 12.4 the splitting of the energy levels for $I = \frac{1}{2}$ nuclei is shown, and in Fig. 12.5 in the case of protons the splitting is shown as a function of the magnitude of the magnetic field B_0 , with the resonance frequency v_r of the magnetic field as a parameter.

12.2.1.1. Detection of NMR phenomena

There are two basic methods to determine the resonance condition and to record a NMR spectrum, viz. a) the continuous wave technique (CWNMR) and b) the pulsed NMR or pulsed Fourier Transform technique (FTNMR).

12.2.1.1.1. CWNMR Throughout the first NMR decades (until the 1970s) the CW technique was practised to determine the resonance state: a) *frequency sweep*: the homogeneous magnetic field B_0 is static and the radio frequency of an extra oscillating magnetic field

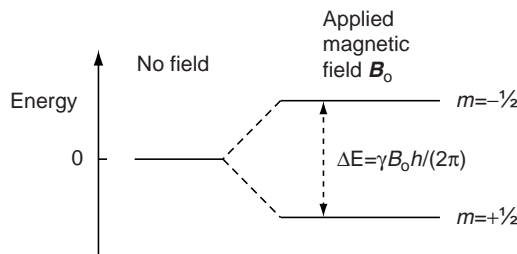


FIG. 12.4 Magnetic energy levels for spin $\pm \frac{1}{2}$.

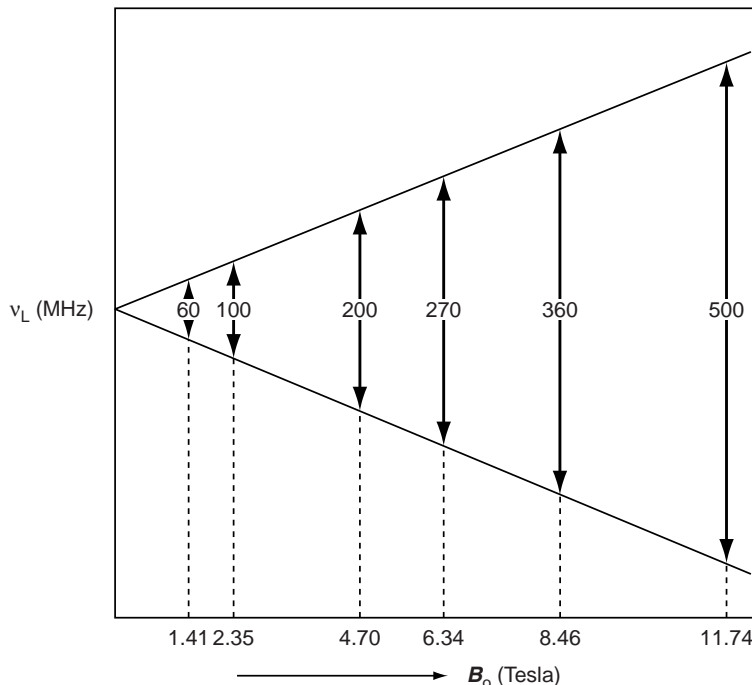


FIG. 12.5 The splitting of magnetic energy levels of protons, expressed as frequency v_o in varied magnetic field B_o .

B_1 is varied; the corresponding resonance frequency v_r is determined and b) most common: *field sweep*: the radio frequency of the oscillating magnetic field B_1 is held constant and the magnetic field strength B_o is varied to determine the resonance state.

Differences in the magnetogyric ratio γ lead to different observation frequencies for different nuclei. In a field of 4.7 T, the signal for a proton occurs at 200 MHz. At the same field a ^{13}C signal would be observed at 50.3 MHz, since γ for ^{13}C is about one quarter the γ for a proton (see Table 12.5). It is common among chemists to describe spectrometers by the proton frequency (in MHz) rather than by the magnetic field strength.

12.2.1.1.2. FT-NMR A major breakthrough occurred in 1966 when Ernst (the Nobel prize winner for Chemistry in 1991) and Anderson (Ernst et al. 1987, 1992), found that the accuracy of the measurements could be increased up to a hundredfold if the slow frequency sweep was replaced by short, intense radio frequency pulses that contain many frequencies in a broad band around v_r and thus excites the resonance of all spins in a sample at the same time. The pulses cause a signal to be emitted by the nuclei. This signal is measured as a function of time after the pulse, but could not be interpreted directly. Ernst discovered that it was possible to extract the resonance frequencies from such a signal and to convert the signal into a NMR spectrum by Fourier Transformation (FT), performed rapidly in a computer. Possibilities to averaging of many very fast recorded spectra (e.g. 1600 scans) leads to an excellent signal-to-noise ratio and therefore to a ten to hundred fold increase in sensitivity. An example of a ^{13}C spectrum of a dilute solution of ethyl benzene obtained with the aid of FT-NMR is given in Fig. 12.6.

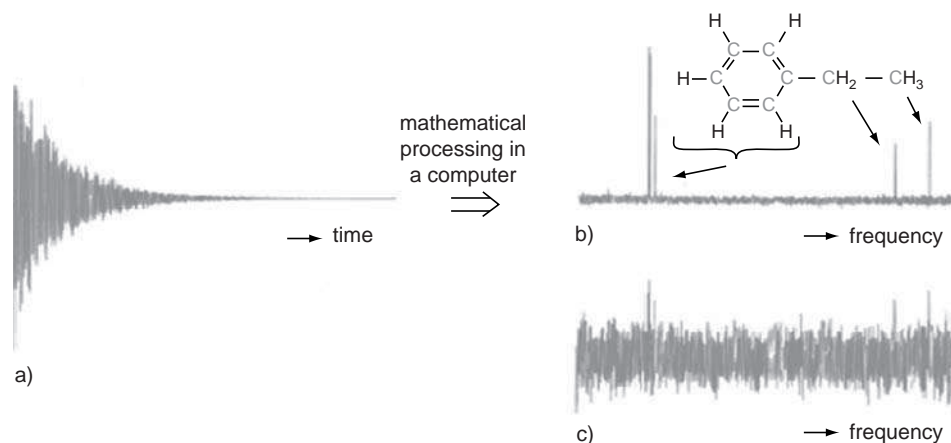


FIG. 12.6 ^{13}C FT-NMR spectrum of ethyl benzene: diagram (A) shows a NMR signal from ^{13}C nuclei obtained with the pulse technique by accumulating the response of the nuclear spins to 200 pulses. The total experiment time was 20 min. After Fourier Transformation one obtains the ^{13}C NMR spectrum in diagram (B). If the experiment was performed with the old technique, in the same time one would only manage to perform a single sweep and the spectrum would look like diagram (C). From http://nobelprize.org/nobel/nobel_prizes/chemistry/laureates/1991/illpress/fourier.html.

In the early NMR-days field strengths were normally in the range 1.4–2.3 T, corresponding with operating frequencies of 60 and 100 MHz and use was made of permanent magnets and electromagnets with maximum field strengths of 2.1 and 2.3 T, respectively. (The earth magnetism at the equator is approximately 3×10^{-5} T). Higher field strengths require the use of superconducting solenoids, operating at a temperature of 4 K and the present time (2007) magnetic fields up to 22.3 T, corresponding to 950 MHz, are possible. Commercial instruments at present operate at 300–950 MHz.

Accordingly, the present powerful instruments are of the pulsed Fourier Transform type. Here at a constant value of the external magnetic field B_0 , strong pulses of an oscillating magnetic field B_1 (a radio frequency field or RF field, perpendicular to B_0) are given to the sample repeatedly, from parts of seconds to a few seconds. Between the pulses the magnetic response from the sample is measured. In this way the measuring time is shortened at least hundredfold.

Fourier Transform NMR is very important for ^{13}C NMR where the signals are very weak owing to the low natural abundance of ^{13}C isotopes. Here *computer accumulation of the responses*, obtained after each RF pulse, gives spectra of sufficient quality in a relatively short time. The resolution of the NMR measurements is such that even very small changes in the position of the resonance line caused by the environment of the nuclei (electron density) can be determined with great accuracy. So a wealth of information on chemical and physical structure can be obtained from NMR.

In the absence of other interactions, for a given applied frequency and nuclear spin type, NMR resonance would only be observed at a single value of field strength, as determined by Eqs. (12.16) and (12.17) and this would result in a single absorption peak and NMR spectroscopy would be very limited as an analytical technique. However, the magnetic field experienced by the nuclei is slightly modified by the presence of surrounding electrons (*Chemical Shift*) and by the presence of interacting neighbouring

nuclei (*Spin–spin Coupling*, causing the *multiplet structure*). In liquids, where the molecules can rotate freely and the spectral lines are extremely narrow, these multisplit structures are observed (*high-resolution NMR*). In solids, where all the nuclei are more or less fixed in position, dipole–dipole interaction causes a broadening of the resonance absorption (*wide-line NMR*). In this case line narrowing can be obtained by suitable NMR techniques and pulse sequence programs.

12.2.1.2. High-resolution NMR (HR NMR) in liquids

The major chemical applications of NMR are derived from three secondary phenomena: “*chemical shift*”, “*spin–spin coupling*” and “*time-dependent effects*”.

12.2.1.2.1. Chemical shift As mentioned before, the field experienced by nuclear spins of the same species, e.g. of protons, is modified due to magnetic shielding by the cloud of electrons around each nucleus. This is accompanied by a small local magnetic field proportional to B_o , but opposite to B_o . As a result a slightly higher value of B_o is needed to achieve resonance, because

$$B_{\text{loc}} = B_o(1 - \sigma) \quad (12.21)$$

where σ is the electronic shielding constant, which is highly sensitive to molecular structure but independent of B_o . The resonance frequency now becomes

$$\nu_r = \gamma B_{\text{loc}} / (2\pi) = \gamma B_o(1 - \sigma) / (2\pi) \quad (12.22)$$

and the separation between the nuclear spin energy levels

$$\Delta E = \gamma h B_{\text{loc}} / (2\pi) = \gamma h B_o(1 - \sigma) / (2\pi) \quad (12.23)$$

Due to chemical shift for ethanol, e.g. (CH₃–CH₂–OH), the proton NMR spectrum exhibits three peaks with relative peak intensities 3:2:1.

The most important differences arise from changes in *electro negativity* of substituents. Other differences, especially in proton magnetic resonance, arise from long-range effects due to movements of electrons in multiple bonds under the influence of the applied magnetic field, setting up magnetic fields of their own. Multiple bonds, for instance, exhibit pronounced magnetic anisotropy; aromatic structures, having delocalised electrons in closed-loop systems, actually show evidence of the presence of “ring currents” under the influence of the magnetic field.

At constant ν_r the magnetic sweep ΔB is only a tiny fraction (10^{-5} for ¹H MR and 10^{-4} for ¹³C NMR) of the total field strength and therefore the position of the various resonance signals, determined by their chemical shift, cannot be recorded in absolute units. Instead, a reference compound is included in the sample and the chemical shift is defined as:

$$\delta = \frac{B_R - B}{B_R} \times 10^6 \quad (12.24)$$

where B is the magnetic field strength corresponding to the resonance frequency of the nucleus in the compound under investigation, and B_R is the magnetic field strength corresponding to the resonance frequency of the same nucleus in the reference substance. A corresponding equation in terms of resonance frequencies is

$$\delta = \frac{\nu_R - \nu}{\nu_R} \times 10^6 \quad (12.25)$$

where ν_R is the operating frequency of the NMR spectrometer.

For proton and ¹³C magnetic resonance studies of non-aqueous solutions the most recommended reference compound is tetramethyl silane, (CH₃)₄Si, which is magnetically

and electrically isotropic, chemically reasonably inert, and non-associating with any common compound. When the high-field-absorbing tetramethyl silane is used as a reference, most δ values, defined as in Eqs. (12.24) and (12.25) are positive. Fig. 12.7 summarises the chemical shifts for protons in the principal functional groups. It should be remarked that chemical shifts are, to a certain extent, solvent-dependent. Fig. 12.8 gives the chemical

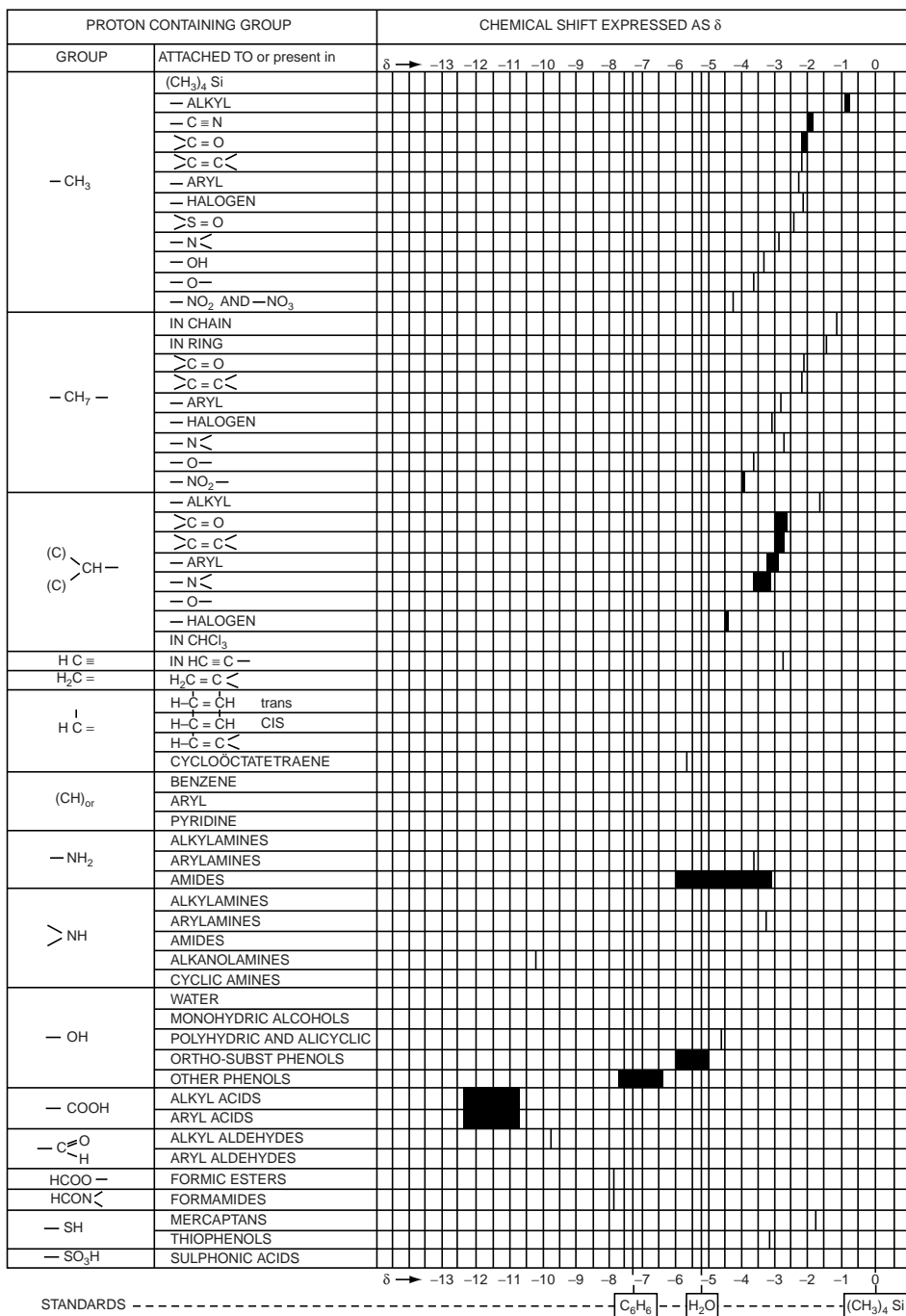


FIG. 12.7 Proton chemical shifts of principal structural groups.

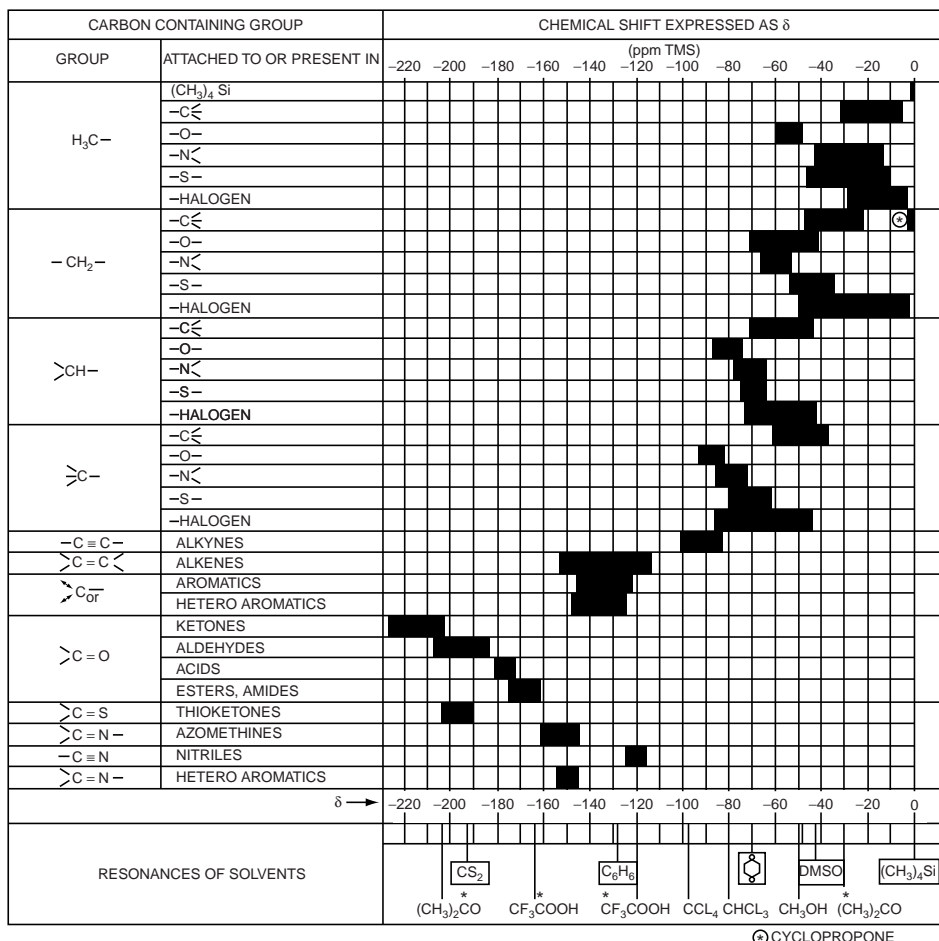


FIG. 12.8 ^{13}C -chemical shifts of principal structural groups.

shifts for ^{13}C in the principal functional groups (see Slothers (1972), Levy and Nelson (1972) and Breitmaier et al. (1971)).

Carbon resonances of organic compounds are found over a range of 230 ppm, compared with 12 ppm for proton nuclei. By controlled elimination of the spin–spin splitting it is also possible to obtain narrower resonance lines in CMR than in PMR. These advantages of CMR make this technique superior to PMR, for instance in determining the tacticity of vinyl polymers, the configuration of polybutadienes, the sequence length of copolymers and the nature and number of side groups in low-density polyethylenes.

Keller (1982) developed an additive increment system for the calculation of the ^{13}C chemical shift in polymers as a function of the substitution of the (neighbouring) C atoms.

12.2.1.2.2. Spin–spin interactions The signals often show a fine structure with a characteristic splitting pattern due to spin–spin interactions with neighbouring nuclei. These interactions occur mostly between nuclei that are one to four bonds away from each other in the molecule. The splitting corresponds to the slightly different energy levels of nuclei whose spins are parallel and anti-parallel to those of their neighbours; in some cases it may lead to a considerable complication of the spectra. As an example, again ethanol is considered.

The proton nuclei have spins $m_1 = \pm \frac{1}{2}$, indicated as + and −, or as \uparrow and \downarrow . The occurrence of the different proton spins of CH_2 are $(\uparrow\uparrow)$, $(\uparrow\downarrow$ and equivalent $\downarrow\uparrow)$ and $(\downarrow\downarrow)$. The three protons of the CH_3 group feel the different magnetic fields of these proton spins and the PNMR spectrum exhibits a CH_3 peak which is composed of three peaks with relative intensities 1:2:1. On the other hand the occurrence of the different proton spins of CH_3 are $(\uparrow\uparrow\uparrow)$, $(\uparrow\uparrow\downarrow, \uparrow\downarrow\uparrow,$ and $\downarrow\uparrow\uparrow)$, $(\uparrow\downarrow\downarrow, \downarrow\uparrow\downarrow$ and $\downarrow\downarrow\uparrow)$ and $(\downarrow\downarrow\downarrow)$. The two protons of the CH_2 group feel the different magnetic fields of these proton spins and the PNMR spectrum exhibits a CH_2 peak which is composed of four peaks with relative intensities 1:3:3:1.

These spin–spin interactions called *Coupling Constants* can be experimentally determined even in very complex spectra. Coupling constants, e.g. between two protons or a ^{13}C nucleus and a proton, are molecular parameters, independent of the applied external magnetic field. Expressed in Hertz, they can have positive or negative values depending on the numbers of bonds between the two nuclei.

In proton spectra of polymers knowledge of the exact values of the coupling constants and the chemical shifts makes it possible to simulate the experimental spectra by computer calculations. In this way it is possible to interpret quantitatively the complex spectra of many homopolymers and copolymers in terms of configuration (or “tacticity”) and monomer sequences (copolymers). The obtained sequence lengths can be directly related to the polymerisation mechanism.

As the coupling constants, especially between two protons on adjacent carbon atoms, are very sensitive to rotational changes, one can also derive from them the preferred conformation of the polymer chain (see Diehl et al., 1971).

12.2.1.2.3. Time-dependent effects The NMR signals are sometimes influenced by time-dependent phenomena such as conformational or prototropic changes, which take place at a rate faster than the line width and comparable to (or faster than) the inverse of the differences between the frequencies of the transitions of the different sites. This means that kinetic phenomena may be studied by the NMR technique, especially if the temperature of the sample can be adapted. As an example we mention the two chair forms of cyclohexane, which are energetically stable; there is a fast inversion from the one into the other via the boat form. At room temperature the PNMR spectrum exhibits one sharp peak, corresponding to the mean of the two chemical shifts. At -120°C the dynamic equilibrium is frozen and the spectrum exhibits two sharp peaks, whereas at -60°C the inversion is slow and the spectrum exhibits one broad peak.

We can conclude that “simple” PNMR enables us to determine:

- Kind of protons (chemical shift)
- Number of protons (intensity of the peaks)
- Neighbouring groups (spin–spin coupling: splitting of peaks in sub-peaks)
- Kinetics of fast reactions (width of the peak)

It is possible to record HR NMR spectra of polymer solutions with the aid of the wide range of solvents available for NMR, sometimes at elevated temperatures. The viscosity of the solution does not always affect the line width. Thus HR NMR can successfully be applied to elucidate the chemical structure, configuration (tacticity!) and conformation of polymers and copolymers.

Since the signal intensity is proportional to the number of absorbing nuclei, HR NMR can also be used as a quantitative tool, e.g. in polymer end group determinations.

The availability of pulsed FT spectrometers at high frequencies (300–750 MHz for protons and 75–188 MHz for ^{13}C) with signal averaging has greatly enhanced the possibility of polymer analysis in HR NMR.

12.2.1.3. Relaxation phenomena in NMR

When a small and oscillating second field B_1 , perpendicular to the field B_o , is applied, the magnetic moment of the spinning nucleus will now experience the combined effects of B_o and B_1 , if the angular frequency of B_1 , coincides with the Larmor frequency of the spinning nucleus. Accordingly, the nucleus absorbs energy from B_1 and the orientation between the magnetic moment μ_m of the spinning nucleus and the field B_o changes. Upon varying the rotation rate, or frequency, of B_1 around the Larmor frequency to be found, a resonance condition is achieved and a transfer of energy from B_1 to the spinning nucleus occurs, resulting in an oscillation of the precession angle θ .

The presence of relaxation processes affects the shape of the absorption lines. This is because the lifetimes of the spin levels are shortened if relaxation occurs and so their energy is made imprecise: this is the so-called lifetime broadening effect. There are two processes responsible for this effect: *spin-lattice relaxation* and *spin-spin relaxation*.

12.2.1.3.1. Spin-lattice relaxation In equilibrium the nuclei spins are precessing around B_o . Upon application of the proper extra field B_1 the precession changes and energy is absorbed, because the spins in the α state are transferred into the β state, so that there will be a surplus on β spin with respect of the Boltzmann equilibrium state. If the extra field B_1 has returned to zero, the surplus of β -spins will return to the α state, thereby returning to the Boltzmann equilibrium state corresponding to Eq. (12.17). The surplus of energy is lost to the thermal motions of the polymer, due to interaction of the spins with the surroundings, or lattice, thereby causing a tiny rise of the temperature. This exponential return to the Boltzmann equilibrium state is characterised by T_1 , the *spin-lattice relaxation time* or *longitudinal relaxation time*, which is the time to reduce the difference between the excited and equilibrium populations by a factor of e:

$$\Delta N = \Delta N_{eq}[1 - \exp(-t/T_1)] \quad (12.26)$$

and corresponding the longitudinal magnetisation vector (i.e. in the z-direction)

$$\mu_z = \mu_{zo}[1 - \exp(-t/T_1)] \quad (12.27)$$

where ΔN_{eq} is given by Eq. (12.18).

T_1 can give information of rotations and translations of molecules or molecule groups in liquids and of thermal vibrations in a crystal lattice. Accordingly, T_1 is a function of thermal motions, concentration of nuclear spins, viscosity of the medium etc. The coupling between fluctuating magnetic fields (due to molecular motions) and the spinning system is strongest (i.e. T_1 is minimal) when the spectrum of molecular motions contains a dominating component with a frequency approximately equal to the NMR frequency. Every minimum in T_1 corresponds to a single process of molecular motions.

In liquids T_1 usually ranges from 10^{-2} to 10^2 s, but in rigid solid samples it may be as long as hours (see Table 12.6).

TABLE 12.6 Spin-lattice relaxation times (T_1) and spin-spin relaxation times (T_2) in seconds for various materials of various phases

	Solids	Melts and conc. solutions	Dilute solutions and liquids
T_1	hours	10^{-2} to 10	10^{-2} to 10^2
T_2	10^{-5} to 10^{-4}	10^{-5} to 10^{-2}	10^{-3} to 10^2

12.2.1.3.2. Spin–spin relaxation Interaction between neighbouring nuclei with identical precession frequencies but differing quantum states ($m = \pm \frac{1}{2}$) can cause an exchange of quantum states as shown in Eq. (12.15). This of course does not cause a net change in populations of the energy states, but the average lifetime of a nucleus in the excited state will decrease. This process is characterised by T_2 , the *spin–spin relaxation time* or *transverse relaxation time*, which is the time that describes the return of the transverse magnetisation to the equilibrium state and is thus a measure for the coupling of nuclear magnetic dipoles:

$$\mu_{xy} = \mu_{xy,0} \exp(-t/T_2) \quad (12.28)$$

The net magnetisation in the XY plane goes to zero and then the longitudinal magnetisation μ_z grows until we have μ_{z0} along the Z-axis. Two factors contribute to the decay of transverse magnetisation (Hornak, 1997):

- (1) Molecular interactions (said to lead to a pure T_2 molecular effect)
- (2) Variations in B_o (said to lead to inhomogeneous T_2 effect)

The combination of these two factors is what actually results in the decay of the transverse magnetisation. The combined time constant T_2^* and the relationship between T_2 from the molecular processes and that from inhomogeneities in the magnetic field is

$$1/T_2^* = 1/T_{2,\text{molecular}} + 1/T_{2,\text{inhomogeneities}} \quad (12.29)$$

The dipole–dipole coupling and the inhomogeneities are responsible for line broadening in a NMR spectrum when the molecular motions are slow. From line width and form of the spectrum data may be obtained of nuclear positions. Hence, T_2 determines the width of the resonance line, but has no correspondence with the saturation or the overall degree of occupation of the nuclear energy levels, like T_1 has. T_2 is always less than or equal to T_1 (see Table 12.6).

12.2.1.4. Wide-line NMR (WL NMR)

Solids give rise to the “wide-line” or (broad-line) spectra, because the local fields arising from nuclear magnetic dipole interactions contribute significantly to the total field experienced by a nucleus in the solid state. A measure of this direct spin–spin interaction is the spin–spin relaxation time T_2 (see Sect. 12.2.1.3), which is much shorter in solids than in liquids, and thus gives rise to broader lines (of the order of 10^{-6} to 10^{-4} T, depending on the kind of nucleus). Now the contour of the absorption line provides information as to the relative position of the neighbouring nuclei.

For a symmetrical spectrum the centre of the resonance line B_c is given by

$$B_c = \int_0^\infty B f(B) dB \quad (12.30)$$

$f(B)$ is the line shape function, i.e. the shape of the curve if the magnetic field varies and the frequency is kept constant.

The broadening of the resonance band may be characterised by the line width at half height ($\Delta B_{1/2}$) or by the second moment of the curve which is defined as

$$S_2 = \frac{\int_0^\infty (B - B_o)^2 f(B) dB}{\int_0^\infty f(B) dB} \quad (12.31)$$

where B_o is the value of the magnetic field where resonance occurs.

Correlated with the line width at half height is the spin–spin relaxation time T_2 . In case the line shape is Lorentzian, we get

$$T_2 \approx \frac{1}{\pi K \Delta B_{1/2}} \quad (12.32)$$

where $K = h/(\pi g_N \beta_N)$.

In addition to this spin–spin interaction there exists an interaction between the spins and the surroundings, the so-called spin–lattice interaction. The characteristic constant is called the spin–lattice relaxation time T_1 . T_2 is, below a certain temperature, nearly independent of temperature, whereas T_1 is highly temperature-dependent (see Sect. 12.2.1.3). This provides means of studying the two rate processes separately.

Richards et al. (1955, 1958) measured line widths at low temperatures (90 K) and found that the second moment (S_2) depended very much on the inter-hydrogen distance. Since the hydrogen atoms in an aromatic ring are more widely spaced than those in aliphatic groups, the variation in the line widths can be associated with variation of the ratio aromatic/aliphatic components. Richards et al. derived additive group contributions to the second moment from the resonance spectra of a number of model substances; they are shown in Table 12.7. Because of the differences in mobility it is also possible to determine, e.g. the plasticizer content in Polyvinyl chloride.

The line-width behaviour as a function of temperature may provide useful information on transition temperatures in the solid state.

Since the different types of transitions have different energies of activation, the line width sometimes decreases discontinuously with varying temperature. At characteristic transition temperatures the spin–lattice relaxation time T_1 reaches a minimum. Comparative study of this NMR method of measuring transition temperatures with the dynamic mechanical and dielectric methods is sometimes very valuable to the understanding of structural or conformational effects.

WL NMR applications to polymers have been reviewed by Slichter (1958, 1970), one of the pioneers in this field.

Another important application of wide-line NMR is the determination of crystallinity. Some polymers give spectra, which can be graphically separated into a broader and a narrower component. In this way Wilson and Pake determined the crystallinity of polyethylene and poly(tetrafluoroethylene) as early as 1953.

NMR spectroscopy can be also used in investigations of polymer aggregates in solution, gels etc, i.e. in systems which are between liquids and solids. As an example, studies of the formation and structure of a stereo-complex of poly(methyl methacrylate) (PMMA) by Spevacek and Schneider (1974, 1975) can be mentioned. The formation of ordered associated structures of the stereo-complex upon mixing solutions of isotactic and syndiotactic PMMA manifests itself by the broadening of all polymer lines and results in disappearance of HR-NMR signals; wide-lines then can be detected.

TABLE 12.7 Group contributions to the second moment in NMR (90 K)

Group	Contribution per hydrogen atom to the second moment (10^{-4} T)
Aromatic CH	9.7
(Aliphatic CH)	(10)
Aliphatic CH_2	27.5
Aliphatic CH_3	10.0
peri- CH_3	22.4

12.2.1.5. Methods of line narrowing in the NMR spectroscopy of solid polymers

As mentioned above, one of the major successes of modern NMR spectroscopy is the development of pulse techniques to obtain narrow resonance lines of solid specimens.

Even for such complicated materials as coals and comparable carbonaceous products, spectra are obtained which can be, qualitatively and sometimes quantitatively, interpreted in terms of a structural group composition.

Before going into some detail on the applied techniques, we shall first summarise the causes of line broadening in the spectra of solids. Line broadening in ^{13}C NMR spectra of solids will be discussed below.

In principle the following four factors are responsible:

1. *The strong, direct, dipolar coupling.* In most substances protons contribute to local magnetic fields and have, due to their abundance and their relatively large magnetic moment, a marked effect on all magnetic resonance phenomena. In liquids this type of broadening is absent, since the local fields are averaged by the quick molecular motions; in solids this averaging effects is lacking. In general at a point a distance r from a proton at an angle φ to the direction of B_o with spin m_I there is a magnetic field given by

$$B^{\text{nucl}} = \frac{h}{2\pi} \gamma_H m_I (1 - 3 \cos^2 \varphi) r^{-3} = \pm \frac{1}{2} g_N \beta_N (1 - 3 \cos^2 \varphi) r^{-3}$$

Accordingly, the local field at a ^{13}C nucleus, caused by a proton is given by the formula:

$$B^{\text{nucl}} = \pm \frac{h \cdot \gamma_H}{4\pi} \frac{3 \cos^2 \varphi_{\text{C-H}} - 1}{r_{\text{C-H}}^3} \quad (12.33)$$

where φ = angle between the inter-nuclear vector (the magnetic dipole) and the direction of the applied magnetic field B_o . $r_{\text{C-H}}$ = distance between the ^1H and ^{13}C nuclei; the \pm sign indicates that B_{loc} is aligned with or against the direction of B_o .

In the liquid and gaseous states the continuous motion of the molecules cancels out the spin-spin coupling, because $\langle 1 - 3 \cos^2 \varphi \rangle = \int_0^\pi (1 - 3 \cos^2 \varphi) \sin \varphi d\varphi / \int_0^\pi \sin \varphi d\varphi = 0$.

In polymer solutions there are some restrictions of chain conformations, so that $\langle 1 - 3 \cos^2 \varphi \rangle \neq 0$ and accordingly the resonance lines are broadened to some extent, which makes interpretation more difficult. However, the temperature dependence of the conformation restrictions may be an advantage. In the solid state the presence of spin-spin interactions results much more line broadening, unless the term $1 - 3 \cos^2 \varphi = 0$, which is the case at $\varphi_m = 54^\circ 44'$, the so-called *magic angle*. By mechanically rotating the sample (usually at 1–70 kHz) at the magic angle with respect to the direction of the magnetic field (so-called *magic-angle spinning*), the isotropic chemical shift is obtained, identical with that in solution and as a result the normally broad lines become narrower, increasing the resolution for better identification and analysis of the spectrum. This technique was proposed independently by Andrew et al. (1958) and Lowe (1959). CSA line width depends on the static magnetic field B_o . Consequently, the rotation frequency of the sample must at least be of the order of the CSA line width. Since the latter is of the order of a few kHz for aliphatic carbon, the MAS experiment is usually conducted at about 3–12 kHz.

2. *The weaker indirect coupling of the spins via intervening covalent bonds.* This is a *scalar coupling*, similar to the coupling in HR NMR, known as *J-coupling*; its strength is denoted by *coupling constants J* usually expressed in Hz. This kind of coupling is nearly independent of the magnetic field B_o .

Nuclear coupling between ^{13}C nuclei and directly bonded protons (a relatively strong interaction) causes the multiplicity of lines – sometimes a helpful effect in making resonance assignments.

3. The chemical shift anisotropy. The chemical shift, the most important tool for structural diagnostics, is caused by the shielding (or de-shielding) of nuclei by electrons. More shielding means an increase of the internal, opposing, magnetic field, the cause of the shift. If there is no spherical distribution of electrons around the nucleus, so if the shift is anisotropic as is in general the case in solids, line broadening is obtained owing to an angular distribution of the bonds with respect to the magnetic field. Also this effect has an angular dependence of the form $(3 \cos^2\theta - 1)$ with respect to the magnetic field B_0 .

4. The influence of time dependent (relaxation) effects. In order to remove the influence of these four factors, a number of *special techniques* can be used.

The strong dipolar coupling (1) can be greatly reduced by application of *high power decoupling* (HPD) techniques; in case of ^1H NMR multiple pulse sequences are necessary.

The scalar J -coupling (2), much smaller than the dipolar coupling, is simultaneously removed by application of the high power decoupling field.

The influence of the chemical shift anisotropy (CSA) (3) can be removed by the so-called *Magic-Angle Spinning* (MAS), as mentioned before.

If the CSA is large (10–20 kHz, as for carbons in aromatic and in other conjugated bond systems), spinning at 3 kHz will not be sufficient and spinning side bands (SSB) will be obtained around the isotropic resonance line. By application of special pulse techniques these side bands (time dependent effects, (4)) can be removed or at least minimised in most of the cases.

To enhance the sensitivity of ^{13}C solid state NMR, polarisation (magnetisation) transfer from the abundant proton spins to the rare carbon spins is applied. This technique is called *cross polarisation* (CP). This is achieved by first exciting the proton resonance and then simultaneously turning on the ^{13}C and ^1H radio frequency fields. The so called *Hartmann–Hahn condition* should then be satisfied:

$$\gamma_C B_{1,C} = \gamma_H B_{1,H}$$

Since according to Table 12.5 $\gamma_H = 4\gamma_C$, this means $B_{1,C} = 4B_{1,H}$ where B_1 is the radio-frequency field.

Under these conditions the carbons obtained a significant (maximum fourfold) enhancement in signal intensity.

Cross Polarisation not only provides a better signal-to-noise ratio, but the experiment can also be done faster, because the repetition rate of the pulses is now determined by the proton relaxation times, which are a factor 10–100 smaller than those of the carbons.

The greatest improvements are obtained by *combination*: dipolar decoupling (DD) in combination with magic angle spinning (MAS) and cross polarisation (CP).

A survey of the many highly specialised techniques, to be used for the most difficult NMR analyses (e.g. those of high-carbon materials such as coals and asphalts) was given by Snape (1989). It is reproduced here as Table 12.8.

Fig. 12.9 gives a good impression how powerful the modern techniques are in dissolving the broad bands into – what could be nearly called – a line spectrum.

12.2.1.5.1. Polymer chain dynamics in the solid state Several relaxation time parameters can be distinguished in solid state NMR. For the study of polymer dynamics T_2 , $T_{1\rho}$ and T_{CP} are mostly used.

T_2 , the *spin–spin relaxation time*, is governed both by static as by Larmor frequency motions.

TABLE 12.8 Summary of the principal solid state ^{13}C NMR techniques

Name	Use	Notes
High power decoupling	Removal of ^1H - ^{13}C dipolar interactions of several kHz	Dipolar interactions are much larger than scalar coupling. Therefore more power needed than for decoupling in solution-state ^{13}C NMR
Magic-angle spinning (MAS)	Removal of chemical shift anisotropy (CSA) – greater than 100 ppm broadening for aromatic peaks	Sample spun at speeds of >2 kHz at an angle of $54^\circ 44'$ to magnetic field
Cross-polarisation (CP)	To avoid long relaxation delays required for normal FID methods	Magnetisation transferred from ^1H to ^{13}C under Hartmann-Hahn conditions. Sensitivity improvement $\times 4$, variable CP time often used determine maximum intensities of aromatic and aliphatic bands
Dynamic nuclear polarisation (DNP)	To increase sensitivity	Magnetisation transferred from unpaired electrons to ^{13}C spins via ^1H spins if required. Sensitivity improvement of about 100-fold
Spectral editing techniques TOSS and PASS pulse sequences	Removal of spinning sidebands in high field spectra	Pulse sequences modulate phase of sidebands, but loss of intensity is unavoidable
Variable CP time	Resolution of protonated carbons	Observed at short contact times
Dipolar dephasing	Separation of tertiary and quaternary aromatic C peaks; and aliphatic C peaks due to mobile (CH_3 and alkyl CH_2) groups from more rigid CH_2 and CH groups	Dipolar decoupling removed for about 50 μs after CP
Sideband analysis	Resolution of bridgehead, non-bridgehead and tertiary aromatic carbons	Relative intensities of sidebands used in high field spectra

Acronyms not explained in the accompanying text: FID = Free inductive decay; TOSS = Total suppression of side bands; PASS = Phase altered spinning side band.

T_{CP} , the *cross polarisation relaxation time*, is a measure of the strength of the dipolar contact between the ^1H and the ^{13}C nuclei. This strength depends both on the inter-nuclear distance and on the mobility of the chain or chain segments. The cross polarisation is less effective when the motion is fast, whereas rigid systems will cross-polarise rapidly. So a study of T_{CP} will yield insight into the proximity of the nuclei and the mobility of the molecular chain or chain segments.

$T_{1\text{p}}$ (^{13}C), the *rotating frame spin-lattice relaxation time* can partially be correlated with dynamic mechanical data. It has been shown to characterise qualitatively the

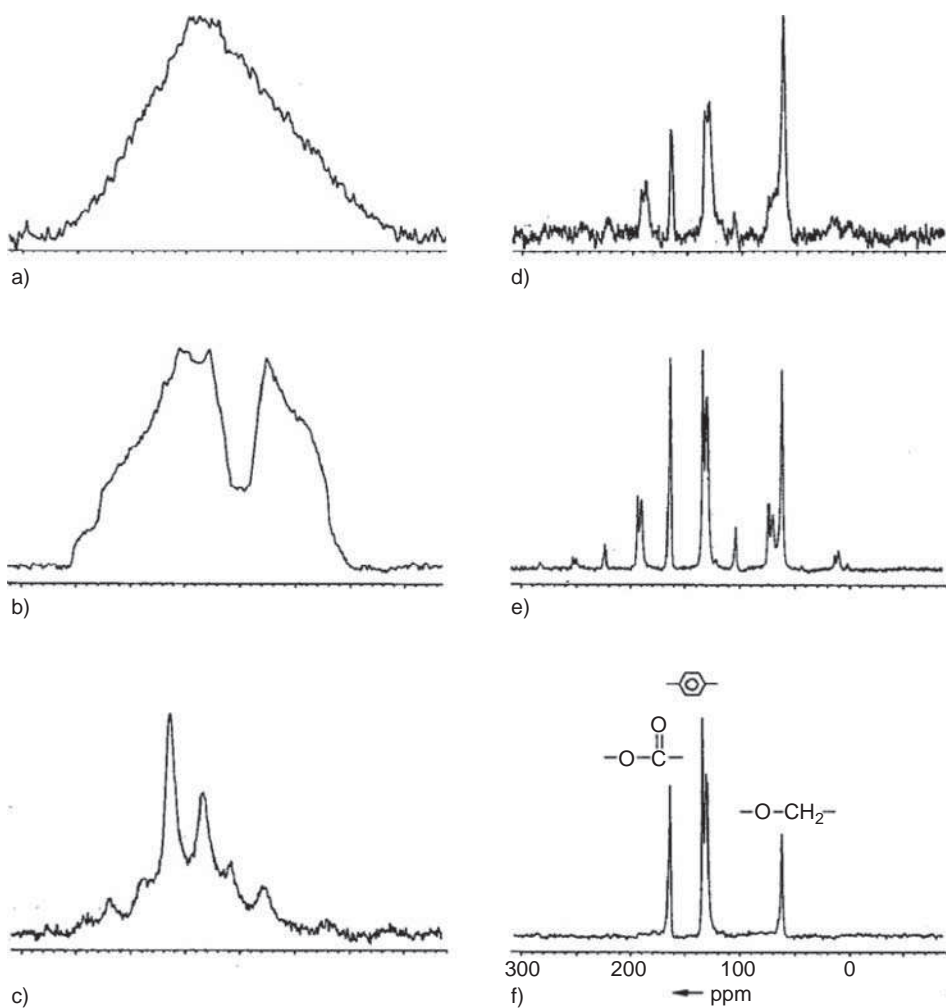


FIG. 12.9 ^{13}C -NMR solid state spectra of a poly(ethylene terephthalate) fiber (50.3 MHz); Effect of band and line narrowing by different special techniques. Courtesy H. Angad Gaur, AKZO Corp. Res., 1989.
 (A). Static spectrum; cross polarised, no decoupling. (B). Static spectrum; cross polarised, decoupled.
 (C). MAS spectrum (magic angle spinning, at $v_r = 3$ kHz), no decoupling. (D). MAS spectrum, with decoupling.
 (E). MAS spectrum, cross polarised and decoupled. (F). MAS spectrum, cross polarised and decoupled, with spinning side bands elimination by special pulse technique (TOSS-sequence).

kilo- to mid-kilo hertz main chain motions. Furthermore, high resolution ^{13}C NMR permits, by means of the different resonances, the separation between main chain and side chain motions in a relatively easy way.

In semi-crystalline polymers T_2 and T_{1G} measurements can be used to separate the crystalline from the amorphous phase, so creating a possibility to study each of the phases separately.

Though less easy accessible, the same kind of relaxation parameters in ^1H solid state NMR can also be used to study polymers.

All together relaxation time measurements are a powerful tool to study the dynamic behaviour of polymers in the solid state.

12.2.2. Electron magnetic resonance

This type of resonance, often called ESR or electron paramagnetic resonance (EPR), is formally observed in paramagnetic substances (thus having a permanent magnetic moment) and particularly in systems with odd numbers of electrons as for example in organic radicals or ions of transition metal complexes. The energy of an unpaired electron depends on whether its spin magnetic moment is oriented parallel (α state: $m_s = +\frac{1}{2}$) or antiparallel (β state: $m_s = -\frac{1}{2}$) to the local magnetic field B . The energies of the two states are

$$E = g_e \beta_B m_s B, \quad m_s = \pm \frac{1}{2} \quad (12.34)$$

where g_e = gyromagnetic ratio of the electron or the spectroscopic splitting factor (whose value is about two for organic radicals); approximately equal to 2; $\beta_B = eh/(4\pi m_e) = 9.27498 \times 10^{-24} \text{ J T}^{-1}$ is the Bohr magneton, i.e. the magnetic moment of an electron; m_e = mass of the electron = $9.10953 \times 10^{-31} \text{ kg}$.

Therefore the energy difference between those two positions is:

$$\Delta E = g_e \beta_B B \quad (12.35)$$

To move between the two energy levels, the electron can absorb electromagnetic radiation of the correct energy:

$$\Delta E = h\nu = g_e \beta_B B \quad (12.36)$$

Accordingly, thanks to their magnetic dipole moment the unpaired electrons may interact with an electromagnetic field; resonance is obtained when the frequency satisfies the condition:

$$\nu = \frac{g_e \beta_B}{h} B \approx 2.8 \times 10^{10} B \quad (12.37)$$

where B is expressed in T.

Again, the result of the interaction is net absorption of electromagnetic energy.

It is customary to keep the frequency constant while the field B is varied. At the commonly used frequency of 9.5 GHz (known as X-band microwave radiation and thus giving rise to X-band spectra) resonance occurs at a magnetic field of 0.34 T. Disturbances again cause a band of finite width, characterised by the line width at half height ($\Delta B_{1/2}$); again dipole-dipole interactions of the spins is a reason of the width of the resonance lines.

Characteristic of the order-disorder transition caused by this interaction is the so-called spin-spin relaxation time (T_2), which is correlated with the line width at half height; for a line of Lorentzian shape:

$$T_2 = \frac{h}{\pi g_e \beta_B \Delta B_{1/2}} = \frac{1}{\pi K' \Delta B_{1/2}} \quad (12.38)$$

where $K' = h/(\pi g_e \beta_B)$

In addition to the spin-spin interaction, also in this case there exists interaction between the spins and their surroundings: the so-called spin-lattice interaction. The characteristic constant of the order-disorder transition of this interaction process is the spin-lattice relaxation time (T_1). T_1 is highly dependent on temperature, whereas T_2 is nearly temperature-independent.

In solution, the line width is small enough to observe hyperfine splitting, caused by interaction of the unpaired spin with magnetic nuclei in the radical (e.g. H, F, N).

Thus, electron magnetic resonance is an important tool in the detection and structure analysis of radicals in polymeric systems (during formation, oxidation, irradiation, pyrolysis and mechanical rupture). From these patterns the chemical structure of the radicals may be derived. For the study of short-lived radicals flow systems have been developed. Free radicals in glassy polymers, however, may have an extremely long life.

BIBLIOGRAPHY

General references

- Atkins PW and De Paula J, "Physical Chemistry", Oxford University Press", Oxford, 8th Ed, 2006.
 Campbell D and White JR "Polymer Characterization, Physical Techniques", Chapman and Hall, London, 1989.

(A) Magnetic susceptibility

- Dorfman JG, "Diamagnetismus und Chemische Bindung", Verlag H Deutsch, Frankfurt, Zurich, 1964.
 Haberdlitzl W, "Magnetochemie", Akademie, Berlin, 1968.
 Selwood PW, "Magnetochemistry", Interscience Publishers, New York, 1943.

Nuclear magnetic resonance spectroscopy

- Becker ED, "High Resolution NMR", Academic Press, New York, 2nd Ed, 1980.
 Bovey FA, "Nuclear Magnetic Resonance Spectroscopy", Academic Press, New York, 1969.
 Bovey FA, "High Resolution NMR of Macromolecules", Academic Press, New York, 1972.
 Bovey FA and Jelinski LW, "Chain Structure and Conformation of Macromolecules" Academic Press, New York, 1982.
 Bovey FA and Jelinski LW, "Nuclear Magnetic Resonance", in "Encyclopaedia of Polymer Science and Engineering", Wiley, New York, Vol. 10, 1987, pp 254–327
 Bovey FA and Mirau PA, "NMR of Polymers", Academic Press, San Diego, 2nd Ed, 1996.
 Bower DI, "An Introduction to Polymer Physics", Cambridge University Press, 2002, Chap. 2.
 Breitmaier E and Voelter W, "¹³C NMR Spectroscopy – Methods and Applications in Organic Chemistry", Verlag Chemie, Weinheim, 1978.
 Cowan B, "Nuclear Magnetic Resonance and Relaxation", Cambridge University Press, Cambridge, 1997.
 Das S, Resonance, January 2004, 34.
 Dybowski CR and Lichten RL (Eds), "Practical NMR Spectroscopy", Marcel Dekker, New York, 1986.
 Emsley JW, Feeney J and Sutcliffe LH, "High Resolution Nuclear Magnetic Resonance Spectroscopy", Vol. I and II, Pergamon Press, Oxford, 1969.
 Ernst RR, "Kernresonanz-Fourier-Transformations-Spektroskopie" (Nobel-Vortrag), Angewandte Chemie 104 (1992) 817–836.
 Ernst RR, Bodenhausen G and Wokaun A, "Principles of Nuclear Magnetic Resonance in one and Two Dimensions", Clarendon Press, Oxford, 1987.
 Farrar TC and Becker ED, "Pulse and Fourier Transform NMR", Academic Press, New York, 1971.
 Hornak JP, "The Basics of NMR" <http://www.cis.rit.edu/htbooks/nmr>, 1997
 Jackman LM and Sternhell S, "Applications of Nuclear Magnetic Resonance in Organic Chemistry", Pergamon, Oxford, 2nd Ed, 1969.
 Jelinski LW, Ann Rev Mater Sci 15 (1985) 359.
 Komoroski RA (Ed), "High Resolution NMR of Synthetic Polymers in Bulk", VCH Publishers, Deerfield Beach, FL, 1986.
 Levy GC (Ed), "Topics in Carbon-13 NMR Spectroscopy", Wiley, New York, 1979.
 Levy GC and Nelson GL, "C-13 Nuclear Magnetic Resonance for Organic Chemists", Wiley Interscience, New York, 1972.
 Levy GC, Lichten RL and Nelson GL, "Carbon-13 Nuclear Magnetic Resonance Spectroscopy", Wiley, New York, 2nd Ed, 1980.
 Martin ML, Delpuech JJ and Martin GJ, "Practical NMR Spectroscopy", Heyden, Philadelphia, 1980.
 McBrierty VJ and Packer KJ, "Nuclear Magnetic Resonance in Solid Polymers", Cambridge Solid State Science Series, Cambridge University Press, Cambridge, 1993.
 Pham OT, Petiaud R, Llauro MF and Waton H, "Proton and Carbon NMR Spectra of Polymers", Vols. 1–3, Wiley, New York, 1984.
 Pretsch F, Seibl J, Simon W and Clerc T, "Tables of Spectral Data for Structure Determination of Organic Compounds", Springer, Berlin, New York, 1983.
 Randall JC (Ed), "NMR and Macromolecules", ACS Symp Ser 247, American Chemical Society, Washington DC, 1984.

- Sanders JKM and Hunter BK, "Modern NMR Spectroscopy – A Guide for Chemists", Oxford University Press, Oxford, 1988.
- Slichter CP, "Principles of Magnetic Resonance", Springer, Heidelberg, 1978.
- Slothers JB, "C-13 NMR Spectroscopy", Academic Press, New York, 1972.
- Tonelli AE and White JL, "NMR Spectroscopy of Polymers", in Mark JE (Ed), "Physical Properties of Polymers Handbook", Springer, 2nd Ed, 2007, Chap. 20.
- Wherli FW and Wirthlin T, "Interpretation of Carbon-13 NMR Spectra", Heyden, London, 1978.

(B) Electron spin resonance

- Boyer RF and Keinath SE (Eds), "Molecular Motion in Polymers by ESR", Harwood Academic Press, New York, 1980.
- Ingram DJE, "Free Radicals as Studied by Electron Spin Resonance", Butterworth, London, 1958.
- Hudson A, Electron Spin Resonance, 11A (1988) 55–76.
- Kinell P (Ed), "ESR Applications to Polymer Research", Wiley, New York, 1973.
- McMillan JA, "Electron Paramagnetism", Reinhold, New York, 1968.
- Poole CP, "Electron Spin Resonance", Wiley, New York, 2nd Ed, 1983.
- Poole Jr CP and Farach HA, "Theory of Magnetic Resonance", 2nd Ed, Wiley New York, 1987
- Poole Jr CP and Farach HA, "Handbook of Electron Spin Resonance", American Institute of Physic Press, New York, 1994.
- Ranby B and Rabek JF, "ESR Spectroscopy in Polymer Research", Springer, Heidelberg, 1977.
- Scheffler K and Stegmann HB, "Elektronenspinnresonanz", Springer, Berlin, 1970.
- Wertz JE, and Bolton JR, "Electron Spin Resonance", McGraw-Hill, New York, 1972.

Special references

(A) Magnetic susceptibility

- Angus WR and Hill WK, Trans Faraday Soc 39 (1943) 185.
- Baltá-Calleja FJ, Hosemann R and Wilke W, Trans Faraday Soc 61 (1965) 1912; Kolloid-Z 206 (1965); 118 Makromol Chem 92 (1966) 25.
- Baltá-Calleja FJ, J Polym Sci C 16 (1969) 4311.
- Baltá-Calleja FJ and Barrales-Rienda JM, J Macromol Sci Phys B 6 (1972) 387.
- Bedwell MF, J Chem Soc (1947) 1350.
- Bhatnagar SS and Mitra NG, J Indian Chem Soc 13 (1936) 329.
- Bhatnagar SS, Mitra NG and Das Tuli G, Phil Mag 18 (1934) 449.
- Bitter F, Phys Rev 33 (1929) 389.
- Bondi AJ, J Phys Coll Chem 55 (1951) 1355.
- Broersma S, J Chem Phys 17 (1949) 873.
- Cabrera B and Fahlenbrach H, Z Physik 89 (1934) 682.
- Cabrera B and Colyon H, Comput Rend 213 (1941) 108.
- Farquharson J, Trans Faraday Soc 32 (1936) 219; 33 (1937) 824.
- Gray FW and Cruikshank JH, Trans Faraday Soc 31 (1935) 1491.
- Hoarau J, Bull Soc Chim France (1950) 1153.
- Maklakov AJ, Zh Fiz Khim 37 (1963) 2609.
- Ovchinnikov A, Nature 326 (1987) 370.
- Pascal P, Ann Chim Phys 16 (1909) 531; 19 (1910) 5; 25 (1912) 289; 28 (1913) 218; Comput Rend 147 (1908) 56, 242, 742; 148 (1909) 413; 150 (1910) 1167; 152 (1911) 862, 1010; 156 (1913) 323; 158 (1914) 37; 173 (1921) 144; 176 (1923) 1887; 177 (1923) 765; 180 (1925) 1596: Bull Soc Chim France 11 (1912) 636; Rev Gen Sci 34 (1923) 388.
- Pascal P, Pacault A and Hoarau J, Comput Rend 233 (1951) 1078.
- Pascal P, Gallais F and Labarre JF, Comput Rend 252 (1961) 18, 2644.
- Rákoš M, Šimo R and Varga Z, Czech J Phys B 16 (1966) 112, 167; B 18 (1968) 1456.
- Sauterey R, Ann Chim 7 (1952) 5.
- Selwood PW, Parodi JA and Pace A, J Am Chem Soc 72 (1950) 1269.
- Torrance JB et al, Synthetic Metals 19 (1987) 709.
- Vaidyanathan VI, Phys Rev 30 (1927) 512.
- Wilson CW, J Polym Sci 61 (1962) 403.
- Woodbridge DB, Phys Rev 48 (1935) 672.

(B) Magnetic resonance

- Andrew ER, Bradbury A and Eades RG, Nature 182 (1958) 1659.
- Anet FAL and Levy GC, Science 180 (1973) 141.
- Bell CLM, Richards RE and Yorke RW, Brennstoff-Chem 39 (1958) 30.

- Bovey FA, "Polymer Conformation and Configuration", Academic Press, New York, 1969.
- Bovey FA and Jelinski LW, in Mark HF, Bikales NM, Overberger CG, Menges G and Kroschwitz JI (Eds), "Encyclopedia of Polymer Science and Engineering", Vol. 10, Wiley, New York, 2nd Ed (1987) pp 254–327.
- Breitmaier E, Jung G and Voelter W, Angew Chem 83 (1971) 659.
- Diehl P, Fluck E and Kosfeld R, "NMR Basic Principles and Progress", Vol 4: "Natural and Synthetic High Polymer", Springer, Berlin, 1971.
- Keller F, Plaste u Kautschuk 29 (1982) 634.
- Lowe IJ, Phys Rev Lett 2 (1959) 285.
- McCall DW and Falcone DR, Trans Faraday Soc 66 (1970) 262.
- McCall DW, Douglass DC and Falcone DR, J Phys Chem 71 (1967) 998.
- Mochel VD, J Macromol Sci-Rev Macromol Chem C 8 (1972) 2, 289.
- Richards RE, Newman PC, Pratt L and Richards RE, Nature 175 (1955) 645.
- Slichter WP, Fortschr Hochpolym Forsch 1 (1958) 35; J Chem Ed 47 (1970) 193.
- Snape CE Fuel 68 (1989) 548.
- Spěváček J and Schneider B, Makromol Chem 175 (1974) 2939; 176 (1975) 729.
- Wilson CW and Pake GE, J PolymSci 10 (1953) 503.

CHAPTER 13

Mechanical Properties of Solid Polymers

The mechanical properties of polymers are controlled by the *elastic parameters*: the three moduli and the Poisson ratio; these four parameters are theoretically interrelated. If two of them are known, the other two can be calculated. The moduli are also related to the different sound velocities. Since the latter are again correlated with additive molar functions (the molar elastic wave velocity functions, to be treated in Chap. 14), the elastic part of the mechanical properties can be estimated or predicted by means of the additive group contribution technique.

There is also an empirical relationship between the shear modulus and the transition temperatures.

Since polymers are no purely elastic materials but are viscoelastic, they exhibit time and temperature dependence; these also may be estimated if the transition temperatures are known.

In oriented polymers (e.g. stretched filaments) the tensile modulus is a function of the stretch ratio; tentative expressions are provided.

13.1. INTRODUCTION

The mechanical properties of polymers are of interest, in particular in all applications where polymers are used as structural materials. Mechanical behaviour involves the deformation of a material under the influence of applied forces.

The simplest mechanical properties are those of homogeneous isotropic and purely elastic materials; their mechanical response can be defined by only two constants, e.g. the Young modulus E and the Poisson ratio v . For anisotropic, oriented-amorphous, crystalline and oriented-crystalline materials more constants are required to describe the mechanical behaviour.

13.2. ELASTIC PARAMETERS

The most important and most characteristic mechanical properties are called moduli. A *modulus* is the ratio between the stress and the applied deformation. The reciprocal of a modulus is called *compliance*, which is defined as the ratio between the deformation and the applied stress.

The nature of modulus and compliance depend on the nature of the deformation. The three most important elementary modes of deformation and the moduli (and compliances) derived from them are given in Fig. 13.1 and Table 13.1: compression, tensile and shear moduli, K , E and G , respectively and the corresponding compliances, κ , S and J , respectively.

Other very important, but more complicated, deformations are *bending* and *torsion*. From the bending or flexural deformation the tensile modulus can be derived. The torsion is determined by the shear modulus or rigidity.

The *true stress* is the load divided by the *instantaneous* cross-sectional area of the sample, whereas engineers often use the nominal stress, which is the load divided by the *initial* (undeformed) cross-sectional area of the sample:

$$\sigma = F/A \quad \text{and} \quad \sigma_{\text{eng}} = F/A_0 \quad (13.1)$$

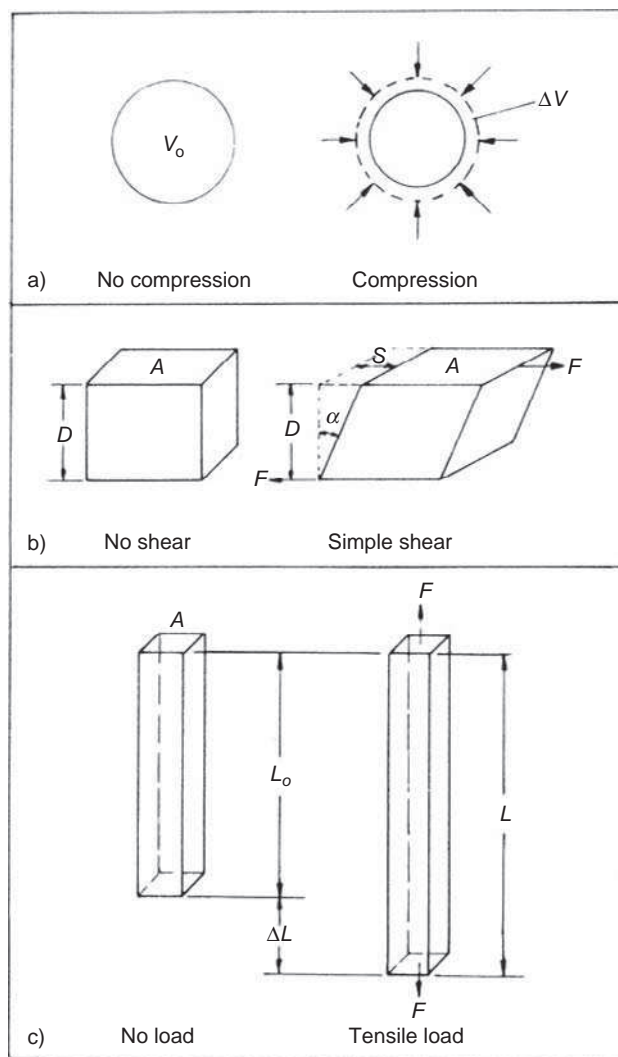


FIG. 13.1 Deformations. (A) Under hydrostatic pressure; (B) under shear; (C) under tension.

TABLE 13.1 Survey of the elastic parameters and their definitions

Elementary mode of deformation	Elastic parameter	Symbol	Definition	Equations
Isotropic (hydrostatic) compression	Bulk modulus	K^a	$\frac{\text{Hydrostatic pressure}}{\text{Volume change per unit volume}} = \frac{p}{\Delta V/V_o} = \frac{pV_o}{\Delta V}$	(13.4)
	Bulk compliance or compressibility	κ $(\kappa = 1/K)$	Reciprocal of the foregoing	
Simple shear	Shear modulus or rigidity	G	$\frac{\text{Shear force per unit area}}{\text{Shear strain}} = \frac{F/A}{\tan \alpha} = \frac{\tau}{\tan \alpha} = \frac{\tau}{\gamma}$	(13.5)
	Shear compliance	$(J = 1/G)$	Reciprocal of the foregoing	
Uniaxial extension	Tensile modulus or Young's modulus	E	$\lim_{L \rightarrow L_o} \frac{\text{Force per unit cross-sectional area}}{\text{Strain}} = \lim_{L \rightarrow L_o} \frac{F/A}{\ln(L/L_o)} = \lim_{\epsilon \rightarrow 0} \frac{\sigma}{\epsilon} = \lim_{\Delta L \rightarrow 0} \frac{F/A}{\Delta L/L_o}$	(13.6)
	Tensile compliance	S^b $(S = 1/E)$	Reciprocal of the foregoing $\left(= \frac{\text{strain}}{\text{stress}}\right)$	
Any	Poisson ratio	ν	$\frac{\text{Change in width per unit width}}{\text{Change in length per unit length}} = \frac{\text{lateral contraction}}{\text{axial strain}}$	(13.7)

^a Often the symbol B is used.

^b In older literature the symbol D is often used.

Directly measured is the *nominal strain or engineering strain* ε_o :

$$\varepsilon_o = \frac{L - L_o}{L_o} = \frac{\Delta L}{L_o} \quad (13.2)$$

The *true strain* is the integral of the nominal strain:

$$\varepsilon_{\text{tr}} = \int_{L_o}^L \frac{dL}{L} = \ln(L/L_o) \quad (13.3)$$

13.2.1. Definitions

The definitions of the elastic parameters are given in Table 13.1 (Eqs. (13.4)–(13.7); see also commentary to the definitions of E and S). The three elastic moduli have the dimension: force per unit area, so in the S.I.-system N/m² or Pa. For practical reasons the numerical values below the glass transition temperature are usually given in GPa. The Poisson ratio is dimensionless; theoretically it varies from -1 to $\frac{1}{2}$, and in practice from 0 to $\frac{1}{2}$ (incompressible rigid solids and liquids).

The (theoretical) inter-relations between the elastic parameters are shown in Table 13.2 and Fig. 13.2 (Eqs. 13.8)–(13.11).

In the past also some other elastic constants were used: the so-called *Lamé constants* λ and μ , constants in a well-known rheological constitutive equation. They have the following significance:

$$\mu = G \quad \text{and} \quad \lambda = K - \frac{2}{3}G \quad (13.12)$$

13.2.2. Measurement techniques

A survey of the different experimental techniques of measurement is given as Table 13.3.

There are quasi-static and dynamic experimental techniques. The first are mostly isothermal, the second usually adiabatic. Because of the thermodynamic work done in volume expansion in isothermal experiments, the values of the bulk moduli are somewhat different from those obtained in adiabatic determinations:

$$\frac{K_{\text{adiabatic}}}{K_{\text{isothermal}}} = \frac{C_p}{C_v} \quad (13.13)$$

TABLE 13.2 Theoretical inter-relations of elastic parameters

$K =$	$\frac{\frac{1}{3}E}{1 - 2\nu}$	$\frac{\frac{2}{3}G(1 + \nu)}{1 - 2\nu}$	$\frac{\frac{1}{3}E}{3 - E/G}$	(13.8)
$G =$	$\frac{\frac{1}{2}E}{1 + \nu}$	$\frac{3}{2}K \cdot \frac{1 - 2\nu}{1 + \nu}$	$\frac{E}{3 - \frac{1}{3}E/K}$	(13.9)
$E =$	$2G(1 + \nu)$	$3K(1 - 2\nu)$	$\frac{3G}{1 + \frac{1}{3}G/K}$	(13.10)
$\nu =$	$\frac{1}{2} - \frac{1}{6}E/K$	$\frac{1}{2}E/G - 1$	$\frac{1 - \frac{2}{3}G/K}{2(1 + \frac{1}{3}G/K)}$	(13.11)

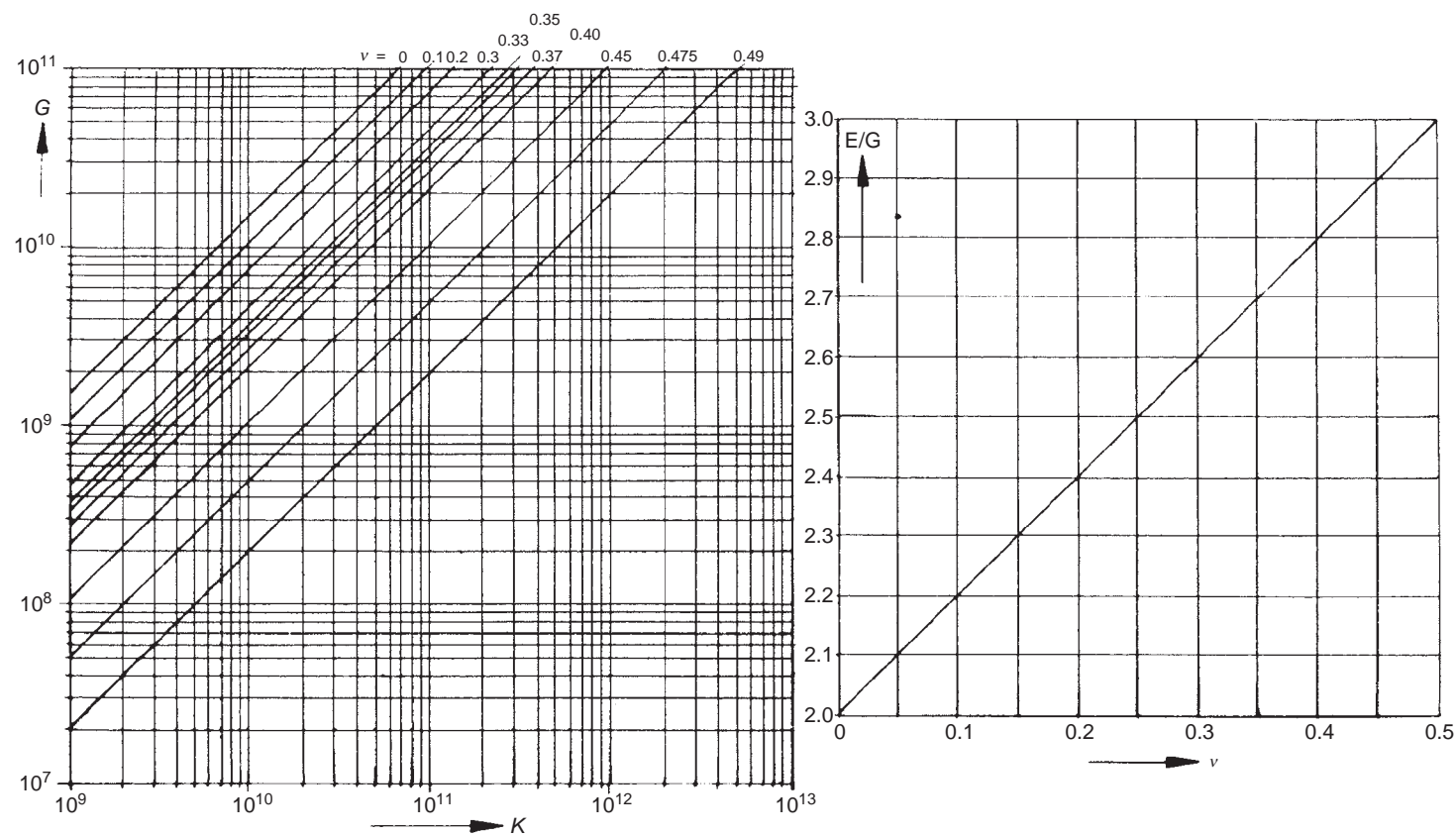


FIG. 13.2 Relationship between the elastic moduli.

TABLE 13.3 Measurement techniques of the elastic moduli of solid polymers

Modulus	(Quasi-)static techniques	Dynamic techniques
K	Measurement of volume change as a function of pressure; a. Dilatometer method (Bekkedahl, 1949) (sample immersed in mercury) b. Piston-cylinder method (Warfield, 1980) (cylindrical sample in bore of rigid container under varying pressure)	Combined measurement of speed of longitudinal and shear waves (Hartmann, 1980) $K = \rho(u_L^2 - \frac{4}{3}u_{sh}^2)$
G	Torsion pendulum method (Nielsen, 1962) (measurement of frequency of oscillations and rate of damping, at different temperatures)	Measurement of speed of shear wave (Schuyer et al., 1954, Hartmann, 1980) $G = \rho u_{sh}^2$
E	Stress-strain measurements (measurement of initial slope in stress-strain diagram)	Filament damping technique (Tokita, 1956; Van der Meer, 1970) magnetostrictive technique (Ballou and Silverman, 1944)

For shear and tensile moduli the adiabatic and isothermal values are equal since the shear and extension deformations occur at constant volume and almost constant volume, respectively.

There may be, however, another reason why for polymers the results of dynamic and static experiments can differ. Polymers are not really elastic, but viscoelastic materials. The high frequencies of most adiabatic techniques do not allow equilibrium to be reached in viscoelastic materials; at high frequencies they will behave more elastic and less viscous.

For the reasons mentioned, values of moduli obtained by different techniques do not always agree in the literature.

13.2.3. Numerical values of elastic parameters

Table 13.4 gives characteristic values of the moduli and Poisson ratios for different metals, ceramic materials and polymers.

The moduli of polymers cover a wider range than those of other materials (from 10^5 N/m² for rubber to 10^{10} N/m² = 10 GPa for rigid polymers), which is one of the reasons why polymers are so versatile in application. Absolute stiffness and strength of polymers are much lower than those of metals, but on the basis of equal weight polymers compare favourably due to their much lower density. The specific moduli, defined as the moduli divided by the density, of isotropic polymers are of the order of one tenth of those of the stronger metals. The hyper-strong and hyper-stiff polymeric fibres such as fully extended polyethylene, stretched poly-(p-phenylene terephthalic amide) and carbon,

TABLE 13.4 Mechanical properties of various materials

Class of materials	Material	Density $\rho(10^3 \text{ kg/m}^3)$	Poisson ratio ν	Moduli (10^9 N/m^2)			Specific moduli (10^6 Nm/kg)		
				E	G	K	E/ρ	G/ρ	K/ρ
Organic and inorganic liquids	Benzene	0.88	0.5	0	0	1.25	0	0	1.4
	Carbon disulphide	1.26	0.5	0	0	1.5	0	0	1.2
	Water	1.0	0.5	0	0	2.0	0	0	2.0
Polymers	Natural rubber	0.91	(0.49 ⁵)	10.5×10^{-4}	3.5×10^{-4}	2.0	11.5×10^{-4}	4×10^{-4}	2.2
	Polyethylene (LD)	0.92	0.49	0.2	0.07	3.3	0.22	0.076	3.6
	Nylon	1.14	0.44	1.9	0.7	5.0	1.66	0.61	4.4
	Poly(methyl methacrylate)	1.17	0.40	3.2	1.1	5.1	2.7	0.95	4.4
	Polystyrene	1.05	0.38	3.4	1.2	5.0	3.2	1.14	4.8
Metals	Epoxy resin	1.18	0.4	2.5	0.9	6.4	2.15	0.77	5.5
	Mercury	13.55	0.5	0	0	25	0	0	1.85
	Lead	11.0	0.44	16	6	41	1.45	0.55	3.7
	Gold	19.3	0.42	80	28	165	4.15	1.45	8.5
	Copper	8.9	0.34	110	44	135	12.4	4.95	15.2
Inorganic solids	Steel (mild)	7.8	0.28	220	80	160	28	10.2	20.5
	Tungsten	19.3	0.28	390	150	300	20	7.8	15.5
	Granite	2.7	0.30	30	12	25	11.1	4.45	9.2
	Glass	2.5	0.23	60	25	37	24.0	10.0	14.8
	Vitreous silica	2.2	0.14	70	30	32	31.8	13.6	14.5
Refractory materials	Alumina (Whiskers)	3.96	(0)	(2000)	(1000)	(667)	(500)	(250)	(170)
	Carborundum	3.15	(0)	1000	500	333	320	160	106
	Diamond	3.51	(0)	1180	590	395	338	168	112

Conversion factors: $1 \text{ kg/m}^3 = 10^{-3} \text{ g/cm}^3$; $1 \text{ N/m}^2 = 10 \text{ dn/cm}^2$.

possess, in the direction of the fibre axis, specific moduli and strengths that may even exceed those of metals (see, e.g. Black, 1980).

For a number of linear polymers, values of E for single crystals have been determined. This has been performed by direct measurements or by calculation from molecular dimensions and force constants for bond stretching and valence angle deformation (Treloar, 1960; Frensdorff, 1964; Sakurada and co-workers, 1962, 1970; Frank, 1970).

The values of E for polymer crystals are of the order of magnitude of $10^{11} \text{ N/m}^2 = 100 \text{ GPa}$, which is much higher than the values mentioned in Table 13.2 for commercial polymers. These values of the elastic moduli of single crystals must be considered as the limiting values of the tensile moduli of stretched polymeric fibres.

The most rigid, fully cross-linked, fully isotropic and fully crystalline "polymer" is diamond, the purest three-dimensional polymer of aliphatic carbon. It has a Poisson ratio of nearly zero and elasticity moduli of the order of $10^{12} \text{ N/m}^2 (=10^3 \text{ GPa})$.

The *Poisson ratio* is a very important parameter. Its value varies from 0 for diamond to $\frac{1}{2}$ for purely elastic incompressible solid materials.

Shamov (1966) has pointed out the importance of the time dependence of the Poisson ratio of polymers. Measurements on polymers at very low frequency will yield values near $\frac{1}{2}$, whereas data obtained at very high frequencies will yield values asymptotically approaching $\frac{1}{3}$. The value of ν is thus a function of the *rate of measurement*. This fact is illustrated by data of Warfield and Barnet (1972) and Schuyer (1959):

Values of ν		
Polyethylene sample ρ (kg/m^3)	Warfield, ν statically determined	Schuyer's ν measurements at 2 MHz
920	0.49	0.45
950	0.45	0.42

The reason of these differences is the viscoelastic nature of polymers (see Sect. 13.4).

13.2.4. Theoretical relationship of the elastic parameters with the velocities of sound waves

Theoretically the elastic parameters are directly related to the speeds of the different sound waves.

Whereas in liquids only one type of sound wave occurs, viz. the bulk or compression wave, the situation in solids is more complicated.

In isotropic solids one can distinguish longitudinal waves and shear waves. When the lateral dimensions are much less than the wavelength (threads) an extensional wave is propagated.

The equations for the speeds of the different kinds of wave are:

$$u_B = \left[\left(K + \frac{4}{3}G \right) / \rho \right]^{1/2} \quad (13.14)$$

$$u_{sh} = (G/\rho)^{1/2} \quad (13.15)$$

$$u_{ext} = (E/\rho)^{1/2} \quad (13.16)$$

where u_B = bulk velocity; for liquids it is called u_L ; u_{sh} = velocity of propagation of shear or transverse waves; u_{ext} = velocity of propagation of extensional waves.

In liquids $G = 0$ and $E = 0$, so that bulk velocity becomes

$$u_L = (K/\rho)^{1/2} \quad (13.17)$$

As will be demonstrated in Chap. 14, the different sound speeds are related with additive molar functions of the form:

$$\mathbf{U} = \mathbf{V}u^{1/3} \quad \text{or} \quad u = (\mathbf{U}/\mathbf{V})^3 \quad (13.18)$$

\mathbf{U} is called *Molar Elastic Wave Function*; it is independent of temperature or polymeric phase state and can be calculated from additive group contributions. In this way the elastic parameters can be estimated or predicted.

There are two additive \mathbf{U} -functions, \mathbf{U}_R and \mathbf{U}_H

$$\mathbf{U}_R = \mathbf{V}u_B^{1/3}; \quad \text{it is also called Rao-function} \quad (13.19)$$

$$\mathbf{U}_H = \mathbf{V}u_{Sh}^{1/3}; \quad \text{we shall call it Hartmann-function} \quad (13.20)$$

If the additive group contributions of these molar functions are known, the moduli can be calculated:

$$K = \rho(\mathbf{U}_R/\mathbf{V})^6 \quad (13.21)$$

$$G = \rho(\mathbf{U}_H/\mathbf{V})^6 \quad (13.22)$$

so

$$G/K = (\mathbf{U}_H/\mathbf{U}_R)^6 \quad (13.23)$$

By means of these equations and Eqs. (13.8)–(13.11) mentioned in Table 13.2 all elastic parameters can be estimated.

13.2.5. Empirical relationships of elastic parameters with other physical quantities

a. With thermodynamic quantities

In the literature three useful empirical rules are to be found:

a1. The Grüneisen rule

Grüneisen (1926) derived a semi-empirical relation between thermal expansion, specific heat, specific volume and compressibility for *solid crystalline substances*.

$$\frac{\alpha v}{c_V \kappa} = \text{const.} \approx \text{unity} \quad (13.24)$$

a2. The Grüneisen–Tobolsky rule

According to Grüneisen (see also Tobolsky, 1962) the following relation applies to simple *molecular crystals*:

$$K \approx 8.04 \frac{E_{\text{subl}}}{V} \quad (13.25)$$

where E_{subl} is the lattice energy (sublimation energy) of the molecular crystal.

a3. The McGowan rule

McGowan (1967) has demonstrated that for liquids the compressibility is closely related to the surface tension:

$$\kappa\gamma^{3/2} = \text{const.} \quad (13.26)$$

These empirical rules are also applicable to polymers in the respective phase state.

b. With transition temperatures

Another way to obtain a fairly good estimation of the rigidity of a polymer at room temperature is the application of an empirical relationship found by Van Krevelen and Hoflyzer (1970)

$$G_{sc}(298) = G_g(298) + x_c^2[G_c(298) - G_g(298)] \quad (13.27)$$

where x_c is degree of crystallinity and G_{sc} , G_c and G_g are the rigidities of semi-crystalline, fully crystalline and fully glassy polymers (all of them isotropic).

$$G_c(298) \approx \frac{T_m - 298}{100} \times 10^9 \text{ N/m}^2 \quad (13.28)$$

$$G_g(298) \approx \frac{3}{1 + 600/T_g} \times 10^9 \text{ N/m}^2 \quad (13.29)$$

If $T_g < 298$ K, $G_g(298)$ has to be neglected in Eq. (13.27).

The results of the application of these equations to a number of polymers are given in Table 13.5 in comparison with the experimental data. The agreement is very satisfactory.

TABLE 13.5 Shear moduli of polymers

State of polymer	Polymer	$G_{\text{exp.}}$ (10^9 N/m^2)	$G_{\text{calc.}}$ (10^9 N/m^2)
Amorphous	Polystyrene	1.1–1.2	1.15
	Poly(vinyl chloride)	1.1	1.10
	Poly(vinyl acetate)	1.0	1.0
	Poly(vinyl carbazole)	1.24	1.33
	Poly(methyl methacrylate)	1.0–1.5	1.15
	Poly(bisphenol carbonate)	0.8–1.1	1.25
	Polyurethane 6,4	0.9	1.0
Semi-crystalline	Polyethylene ($x_c \approx 0.8$)	0.1–1.0	0.8
	Polypropylene ($x_c \approx 0.5$)	0.7	0.75
	Poly(vinyl fluoride) ($x_c \approx 0.25$)	0.1	0.1
	Poly(vinylidene chloride) ($x_c \approx 0.75$)	1.2	1.05
	Polyoxymethylene ($x_c \approx 1$)	1.2–2.0	1.6
	Poly(ethylene oxide) ($x_c \approx 1$)	0.2	0.35
	Poly(propylene oxide) ($x_c \approx 0.3$)	0.05	(0.05)
	Poly(ethylene terephthalate) ($x_c \approx 0.3$)	~1	1.1
	Poly(tetramethylene terephthalate) ($x_c \approx 0.2$)	~1	1.0
	Nylon 6 ($x_c \approx 0.35$)	~1	1.2

Example 13.1

Estimate the bulk modulus of a medium density polyethylene, density 0.95 g/cm³ (degree of crystallinity 70%) by means of the three methods available.

Solution

- a. Estimation by means of the Rao function:

According to Eq. (13.21) we have:

$$K/\rho = (\mathbf{U}_R/\mathbf{V})^6$$

For \mathbf{V} we get:

$$\mathbf{V} = \mathbf{M}/\rho = 28/0.95 = 29.5 \text{ cm}^3/\text{mol}$$

For \mathbf{U}_R we get: (see Table 14.4)

$$\mathbf{U}_R = 2 \times 880 = 1760 \text{ (cm}^3/\text{mol})(\text{cm/s})^{1/3}$$

So

$$(\mathbf{U}_R/\mathbf{V})^6 = \left(\frac{1760}{29.5}\right)^6 = 59.6^6 = 4.5 \times 10^{10} \text{ cm}^2/\text{s}^2 = 4.5 \times 10^6 \text{ m}^2/\text{s}^2$$

and

$$K = 0.95 \times 4.5 \times 10^{10} = 4.3 \times 10^{10} \text{ g}(\text{cm/s}^2)^{-1} \quad \text{or} \quad \text{dn/cm}^2 = 4.3 \times 10^9 \text{ N/m}^2$$

- b. Estimation by means of the Grüneisen relation:

According to Eqs. (13.24) and (13.31) (see later) we have:

$$K = \left(\frac{\mathbf{C}_v}{\mathbf{C}_p}\right) \left(\frac{\mathbf{C}_p}{\mathbf{E}}\right)$$

For \mathbf{C}_p we get:

$$\mathbf{C}_p = x_c \mathbf{C}_p^s + (1 - x_c) \mathbf{C}_p^r = 0.7 \times 51 + 0.3 \times 63 = 54.5 \text{ J/(mol K)}$$

and for \mathbf{E}

$$\begin{aligned} \mathbf{E} &= x_c \mathbf{E}_c + (1 - x_c) \mathbf{E}_r = 0.7 \times 92 \times 10^{-4} + 0.3 \times 205 \times 10^{-4} \\ &= 126 \times 10^{-4} \text{ cm}^3/(\text{mol K}) = 1.26 \times 10^{-8} \text{ m}^3/(\text{mol K}) \end{aligned}$$

From Fig. 5.4 we read $(\mathbf{C}_p/\mathbf{C}_v) \approx 1.07$, so that

$$K = \left(\frac{1}{1.07}\right) \left(\frac{54.5}{126}\right) \times 10^{10} = 4.0 \times 10^9 \text{ N/m}^2$$

- c. Estimation by means of the Grüneisen–Tobolsky relation:

From Eq. (13.25) we get:

$$K = 8.04 \frac{E_{\text{subl}}}{\mathbf{V}}$$

Since $E_{\text{subl}} \approx \mathbf{E}_{\text{coh}} + x_c \Delta \mathbf{H}_m$, we first derive \mathbf{E}_{coh} and $\Delta \mathbf{H}_m$.

From the group contributions mentioned in Chap. 5 for ΔH_m and in Chap. 7 for E_{coh} we derive

$$E_{coh} = 8380 \text{ J/mol} \quad \text{and} \quad \Delta H_m = 8000 \text{ J/mol}$$

so

$$E_{subl} = 8380 + 0.70 \times 8000 = 14,000 \text{ J/mol}$$

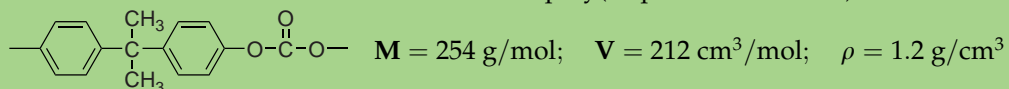
and

$$K = 8.04 \times \frac{E_{subl}}{V} = 8.04 \frac{14,000}{29.5 \times 10^{-6}} = 3.8 \times 10^9 \text{ N/m}^2$$

The experimental value is $4.5 \times 10^9 \text{ N/m}^2$, in good agreement with the average value of the three estimation methods ($= 4.1 \times 10^9 \text{ N/m}^2$).

Example 13.2

Estimate the moduli and the Poisson ratio of poly(bisphenol carbonate)



Solution

1. Bulk modulus

From Table 14.4 the increments to the Rao function are obtained:

	U_{Ri}
	11,000
$-O-COO-$	$\frac{1575}{12,575} = U_R$

So $(U_R/V)^6 = (12,575/212)^6 = 4.4 \times 10^{10} \text{ (cm/s)}^2 = K/\rho$ and $K = 4.36 \times 10^{10} \times 1.20 \text{ g}/(\text{cm s}^2)$ or $dn/\text{cm}^2 = 5.23 \times 10^9 \text{ N/m}^2$, which is in good agreement with the experimental value of $5.0 \times 10^9 \text{ N/m}^2$.

2. Shear modulus

From Table 14.4 we get the tentative increments for the Hartmann function:

	U_{Hi}
	8700
$-O-COO-$	$\frac{1200}{9900} = U_H$

$$\text{So } (\mathbf{U}_H/\mathbf{V})^6 = (9900/212)^6 = 1.03 \times 10^{10} \text{ (cm/s)}^2 = G/\rho \text{ and } G = 1.03 \times 10^{10} \times 1.20 \text{ dn/cm}^2 \\ = 1.24 \times 10^9 \text{ N/m}^2$$

3. Poisson ratio

According to Eq. (13.10, Table 13.2) the Poisson ratio is a function of G/K , viz.

$$\nu = \frac{1 - \frac{1}{3}G/K}{2(1 + \frac{1}{3}G/K)} = \frac{1 - 0.16}{2(1 + 0.075)} = 0.39 \text{ (exp. value: 0.39)}$$

4. Young's modulus

According to Eq. (13.10) in Table 13.2 the Young modulus is:

$$E = 3G/(1 + \frac{1}{3}G/K) = 3.52 \times 10^9 \text{ N/m}^2,$$

in excellent agreement with the exp. value $3.09 \times 10^9 \text{ N/m}^2$.

13.2.6. Estimation and prediction of the bulk modulus from additive molar functions

We now summarise the relationships between K and some additive molar functions of a very different nature:

$$\text{Eq. (13.22) gives: } K = \rho(\mathbf{U}_R/\mathbf{V})^6 = (\mathbf{M}/\mathbf{V})(\mathbf{U}_R/\mathbf{V})^6 \quad (13.30)$$

$$\text{Eq. (13.24) gives: } K \approx \frac{c_v}{\alpha V} = \frac{\mathbf{C}_v}{\mathbf{E}_c} = \frac{\mathbf{C}_v \mathbf{C}_p}{\mathbf{C}_p \mathbf{E}_c} \quad (13.31)$$

$$\text{Eq. (13.25) gives: } K \approx 8.04 \frac{E_{\text{subl}}}{V} \approx 8.04 \frac{E_{\text{coh}} + x_c \Delta H_m}{V} \quad (13.32)$$

By means of these equations three independent methods for estimation or prediction of the Bulk Modulus are available.

13.2.6.1. Results

The results of the three independent methods of calculation of K are given in Table 13.6 and compared with experimental values. For the partly crystalline polymers the method of calculation is illustrated in Example 13.1.

All methods lead to the right order of magnitude and agree within 20%, which is surprisingly good. If no experimental data are available at all, it is best to use the average of the three values obtainable from the additive functions.

13.2.7. Change of stiffness (G and E) at phase transitions

If a modulus is plotted as a function of temperature, a very characteristic curve is obtained which is different in shape for the different types of polymer: amorphous (glassy) polymers, semi crystalline polymers and elastomers (cross-linked amorphous polymers).

A typical example is polystyrene. This normally is amorphous (atactic); it can be cross-linked in this state. But it can also be crystalline (isotactic). The so-called 10 s curves (see later) are shown in Fig. 13.3.

TABLE 13.6 Bulk modulus of some polymers, experimental versus calculated values

Polymers	ρ (g/cm ³)	K (10 ⁹ N/m ²)			
		Exp. ^a	$(U_R/V)^6$	C_V/E Eq. (13.31)	E_{subl}/V Eq. (13.32)
			$\times \rho$ Eq. (13.30)		
Polyethylene (am) (extrapol.)	0.85	(1.9)	1.95	2.5	2.0
Polyethylene (ld)	0.92	3.4	3.55	3.15	3.0
Polyethylene (md)	0.95	4.5	4.3	4.0	3.8
Polyethylene (HD)	0.97	5.0	5.05	4.35	4.0
Polyethylene (cr) (extrapol.)	1.00	(6.0)	6.3	5.1	4.6
Polypropylene	0.91	3.5	3.85	3.5	3.4
Polybutene-1	0.91	3.8	3.8	3.95	3.4
Polystyrene	1.05	5.0	5.15	4.35	2.7
Poly(vinyl chloride)	1.42	5.5	5.25	5.1	3.2
Poly(vinylidene fluoride)	1.77	5.4	4.2	6.2	2.4
Poly(chlorotrifluoroethylene)	2.15	5.2	4.55	6.6	2.8
Poly(tetrafluoroethylene)	2.35	2.5	3.6	6.6	2.2
Poly(vinyl butyral)	1.11	4.2	3.1	5.2	2.6
Poly(methyl methacrylate)	1.19	5.1	5.25	5.35	2.8
Poly(isobutyl methacrylate)	1.04	2.9	3.2	5.25	2.6
Polyisoprene (natural rubber)	0.91	2.0	1.9	2.4	2.1
Poly(chlorobutadiene)	1.24	2.3	2.3	2.7	2.6
Poly(methylene oxide)	1.43	6.9	7.4	5.8	6.3
Poly(ethylene oxide)	1.21	5.7	6.9	3.4	4.1
Poly(2,6-dimethyl-p-phenylene oxide)	1.07	4.1	4.0	4.35	3.2
Poly(ethylene terephthalate)	1.40	>4	7.4	5.0	4.0
Nylon 6	1.14	5.1	6.05	4.9	7.2
Nylon 66	1.14	8.1	6.05	4.9	7.9
Polyimide	1.44	6.0	6.05	4.15	?
Poly(bisphenol carbonate)	1.20	5.0	5.3	4.6	3.1
Polysulphone	1.24	5.3	6.2	4.2	?
Phenolformaldehyde resin	1.22	7.4	5.4	4.3	—
Epoxy resin	1.18	6.4	6.8	6.2	—

^a i.a. Warfield and co-workers (1968, 1970, 1972).

The curve of the tensile modulus versus temperature for the amorphous polymer shows five regions of elastic behaviour (Fig. 13.4):

The *glassy* region ($T \leq T_g$; $E \approx 10^9$ N/m²)

The *transition ("leathery")* region ($T \approx T_g$; E varies from 10^9 to 3×10^5 N/m²)

The *rubbery "plateau"* (E remains fairly constant $\approx 3 \times 10^5$ N/m²; and $G \approx 10^5$ N/m²)

The region of *rubbery flow* (E varies from 3×10^5 to 3×10^3 N/m²)

The state of *liquid flow* ($E < 10^3$ N/m²)

The shear and Young moduli of semi-crystalline polymers not only depend on amount of crystallinity but also on the sizes of the micro-crystallites: for very small crystallites the

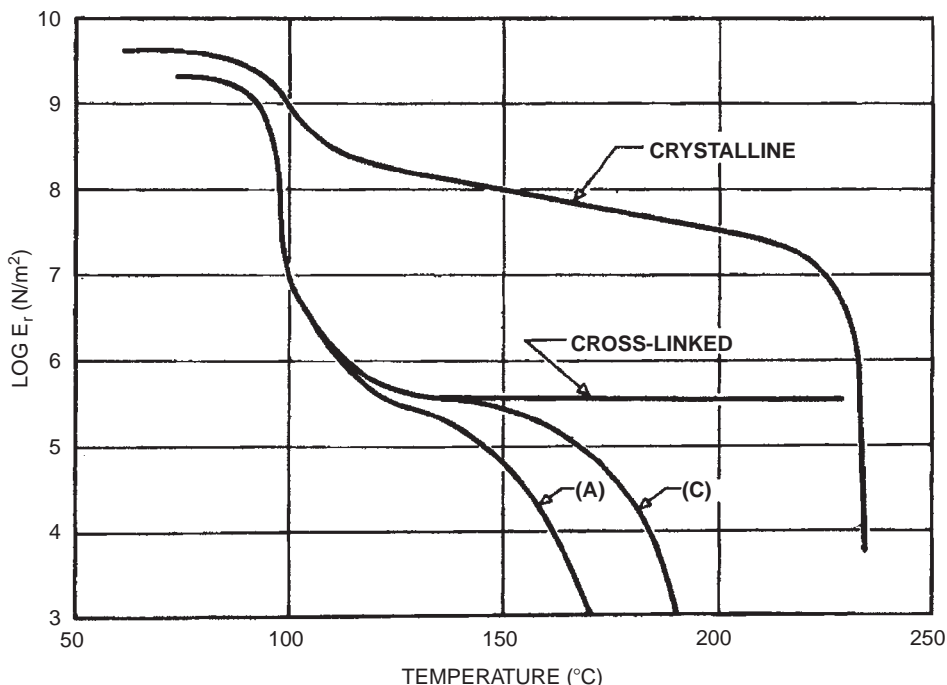
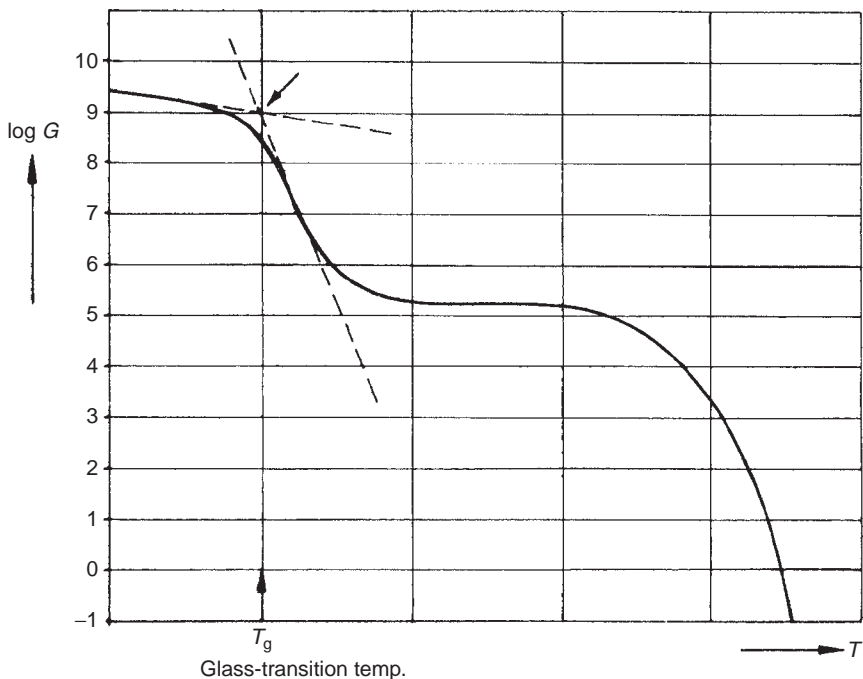


FIG. 13.3 E versus temperature for crystalline isotactic polystyrene, for two linear atactic polystyrene samples A and C ($M_{w,C} > M_{w,A}$) and for lightly cross-linked atactic polystyrene. From Tobolsky (1962). Courtesy John Wiley & Sons, Inc.

surface energy plays an important role, resulting in a lower melting point. In general the modulus decreases continuously from the glass transition temperature up to the melting temperature. This shows that micro-crystallites of various sizes are present in the polymer. It means that Eq. (13.27) has to be used with careful judgement. An example of such behaviour is shown in Fig. 13.5 (Illers and Brever, 1963), where the storage shear modulus of poly(ethylene terephthalate) of various degrees of crystallinity is shown as a function of temperature. 0% crystallinity is obtained by quenching the polymer from above its melting temperature (280°C) to below its glass transition temperature (70°C). The three degrees of crystallinity were obtained by heating the quenched samples at the temperatures T_c prior to the temperature scan.

Copolymers can also show significant differences in moduli with respect of both homopolymers. Random copolymers have in general intermediate properties, whereas block and graft copolymers have mechanical spectra that in some respects remind of crystalline polymers. This effect is illustrated in Fig. 13.6. The two homopolymers are polybutadiene and polystyrene each with its own mechanical spectrum, depicted as $\log G'$ and Λ , the logarithmic decrement (equal to $\pi \times \tan \delta$), vs. temperature, with T_{gS} of approximately -100 and 100°C , respectively. The random copolymer behaves like a homopolymer, with intermediate behaviour: the glass transition temperature depends of course on the fraction of both monomers the copolymer consists of. The behaviour of the block and graft copolymers is completely different: it shows two transitions at the two T_{gS} , a high "rubber" plateau that lies in between the glass plateau and normal pseudo-rubber plateau, its height depending on the fraction of both monomers, and a second pseudo-rubber plateau of "normal" value of approximately 10^5 N/m^2 .



Mechanical Behaviour	Glassy	Leathery	Rubbery-elastic	Rubberly flow	Liquid flow
Molecular Behaviour	Only vibrations of atomic groups	Short-range diffusional motion (chain segments)	Rapid short-range diffusional motions Retarded long-range motions	Slippage of long-range entanglements	Long-range configurational changes (whole molecules)

FIG. 13.4 Regions of viscoelastic behaviour of amorphous polymers.

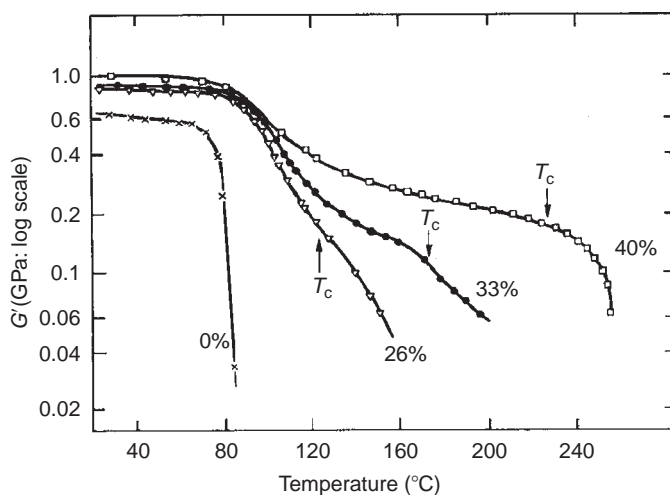


FIG. 13.5 Storage shear modulus for poly(ethylene terephthalate) with different degrees of crystallinity vs. temperature. From McCrum, Buckley and Bucknall, 1988. Courtesy Oxford University Press.

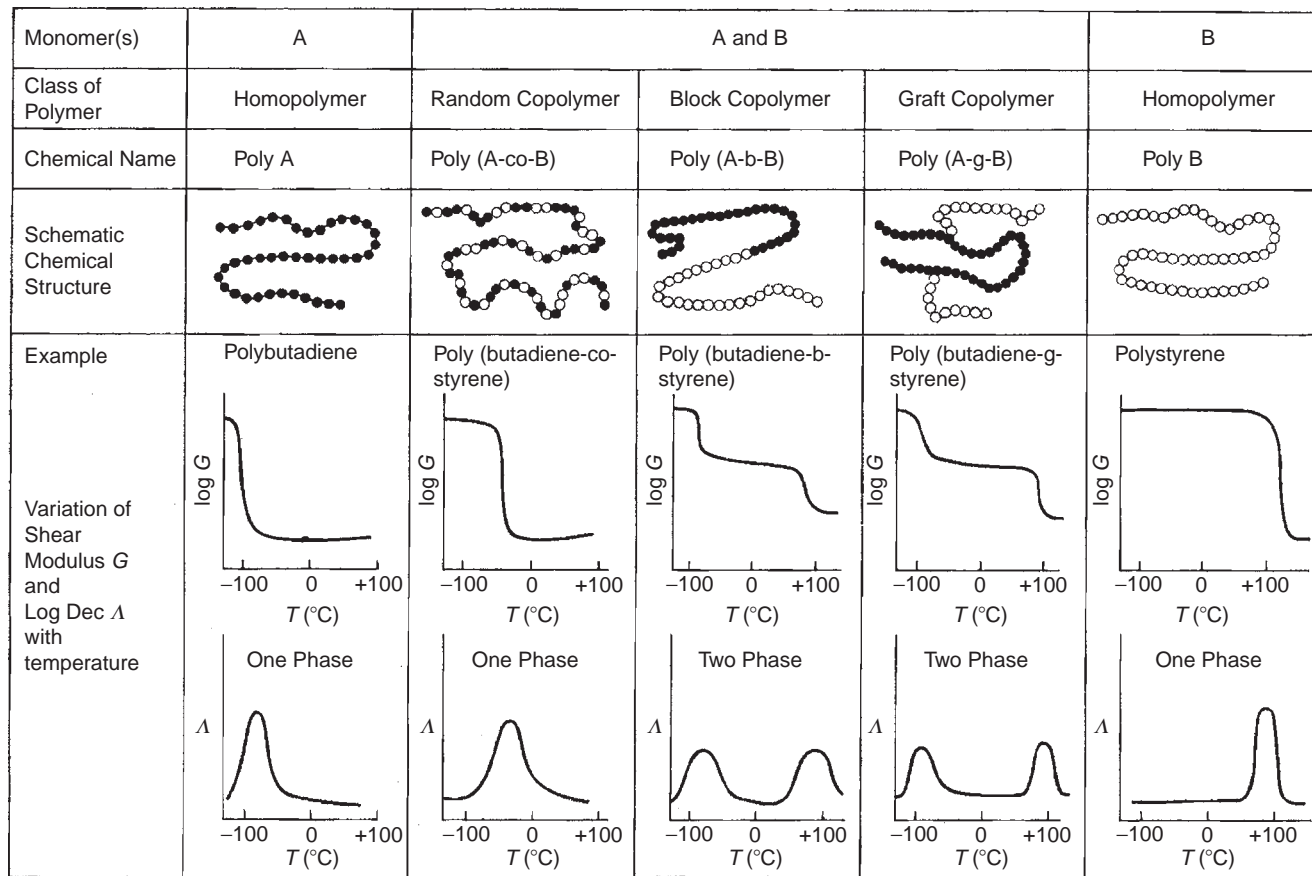


FIG. 13.6 The mechanical spectra ($\log G'$ and Λ , i.e. $\pi \tan \delta$, at ~ 1 Hz vs. temperature) for copolymers of styrene and butadiene (random, block and graft) and their homopolymers. From McCrum, Buckley and Bucknall, 1988. Courtesy Oxford University Press.

Chain entanglements are the cause of rubber-elastic properties in the liquid. Below the "critical" molecular mass (M_c) there are no indications of a rubbery plateau. The length of the latter is strongly dependent on the length of the molecular chains, i.e. on the molar mass of the polymer. From the shear modulus of the pseudo rubber plateau the molecular weight between entanglements may be calculated:

$$\frac{1}{3}E_r = G_r = \frac{\rho RT}{M_e} \left(1 - \frac{2M_e}{M_n}\right) \quad (13.33)$$

or

$$M_e = \left(\frac{G_r}{\rho RT} + \frac{2}{M_n}\right)^{-1} \quad (13.34)$$

where M_e = molecular weight between entanglements (kg/mol); M_n = number average molecular weight of polymer (kg/mol); G_r = shear modulus of the pseudo rubber plateau (N/m²); ρ = polymer density (kg/m³); R = gas constant = 8.314 J/(mol K); T = temperature (K).

The term $1 - 2M_e/M_n$ corrects for the dangling ends, which is important if the molecular weight is relatively small.

The rubbery plateau can be "stabilised" by cross-linking, the regions of rubbery flow and liquid flow are completely suppressed if enough chemical cross-links are introduced to serve as permanent network junctions in place of the temporary chain entanglements. Crystallisation is a kind of physical cross-linking with (numerically) many junctions. It is understandable that the amorphous state is more or less "stabilised" by crystallisation, so that the transition becomes less pronounced.

We see from Fig. 13.3 that at the glass transition temperature the rigidity of the amorphous polymers declines rapidly. In the semi-crystalline polymers there is a decline, too, but certain rigidity is retained up to the melting point. For highly crystalline polymers there is hardly any influence of the glass transition; their rigidity breaks down at the crystalline melting point. In the glassy polymers the rigidity is obviously highly dependent on the glass transition temperature; for the highly crystalline polymers it is mainly the location of the melting point that determines the rigidity. In the semi-crystalline polymers both transitions are important.

The empirical Eq. (13.27)/(13.28)/(13.29) of Van Krevelen and Hoflyzer (1970) can be extended to describe the polymer rigidity as a function of temperature.

$$\begin{aligned} \frac{G_g(T)}{G_g(T_R)} &\approx \frac{E_g(T)}{E_g(T_R)} = \frac{T_g/T_R + 2}{T_g/T_R + 2T/T_R} \quad (\text{for } T < T_g) \\ \frac{G_c(T)}{G_c(T_R)} &\approx \frac{E_c(T)}{E_c(T_R)} = \exp \left[-2.65 \frac{T_m/T_R - T_m/T}{T_m/T_R - 1} \right] \quad (\text{for } T > T_R - 100) \\ G_{sc} &= G_g + x_c^2(G_c - G_g) \end{aligned} \quad (13.35)$$

where T_R is reference temperature, e.g. room temperature.

To semi-crystalline polymers with a glass transition temperature well below the reference temperature, Eq. (13.28) may directly be applied.

$$\text{In this special case } \frac{G_{sc}(T)}{G_{sc}(T_R)} = \frac{G_c(T)}{G_c(T_R)}$$

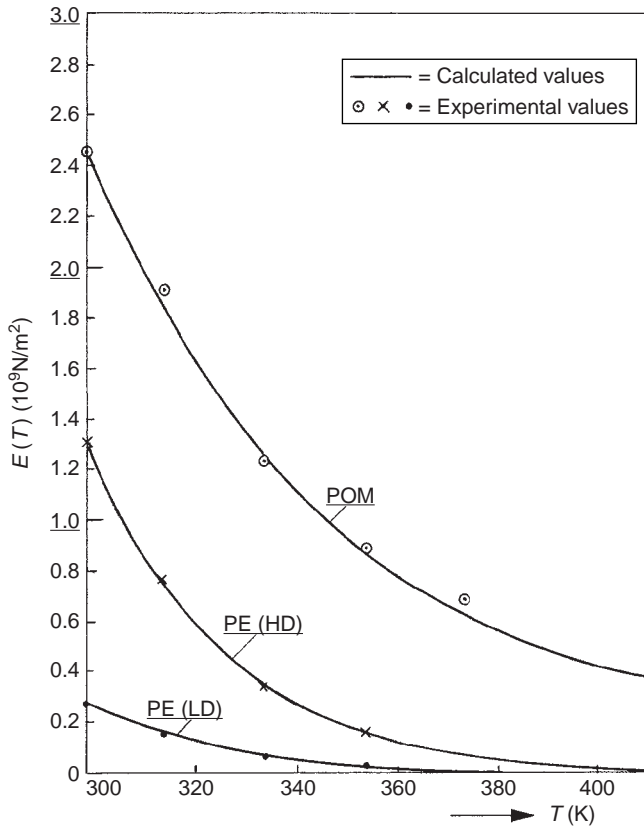


FIG. 13.7 Tensile modulus (10^2 s, 0.2% strain).

The following form is the easiest for numerical calculations:

$$\log \frac{G(T_R)}{G(T)} \approx \log \frac{E(T_R)}{E(T)} = 1.15 \times \frac{T_m/T_R - T_m/T}{T_m/T_R - 1} \quad (13.36)$$

Fig. 13.7 shows how well Eq. (13.36) describes the experimental data reported by Ogorkiewicz (1970).

13.3. RUBBER ELASTICITY

Cross-linked elastomers are a special case. Due to the cross-links this polymer class shows hardly any flow behaviour.

The kinetic theory of rubber elasticity was developed by Kuhn (1936–1942), Guth, James and Mark (1946), Flory (1944–1946), Gee (1946) and Treloar (1958). It leads, for Young's modulus at low strains, to the following equation:

$$E = \frac{3\rho RT}{M_c} \left(1 - \frac{2M_c}{M_n}\right) = \frac{3z_c RT}{V} \left(1 - \frac{2M_c}{M_n}\right) = 3C_o \left(1 - \frac{2M_c}{M_n}\right) \quad (13.37)$$

where E = Young's modulus (N/m^2); R = gas constant = $8.314 \text{ J}/(\text{mol K})$; M_c = number average molecular weight of the polymer segments between cross-links (kg/mol);

ρ = density (kg/m^3); z_c = average number of cross-links per structural unit (i.e. per primary polymer molecule) = M/M_c ; V = molar volume of structural (i.e. monomer) unit (m^3/mol); $C_o = z_c RT/V = \rho RT/M_c$ (N/m^2)

The term $1 - 2M_c/M_n$ corrects for the dangling ends, which is important if the cross-link density is small.

Eq. (13.37) shows that the modulus of a rubber increases with temperature; this is in contrast with the behaviour of polymers that are not cross-linked. The reason of this behaviour is that rubber elasticity is an *entropy elasticity* in contrast with the *energy elasticity* in "normal" solids; the modulus increases with temperature because of the increased thermal or Brownian motion, which causes the stretched molecular segments to tug at their "anchor points" and try to assume a more probable coiled-up shape.

Eq. (13.37) shows that E increases with z_c . Normally z_c is of the order of 10^{-2} so that $E \approx 10^6 \text{ N/m}^2$ at 25°C .

The theory of rubber elasticity also leads to the following stress-deformation expression (for unidirectional stretching and compression):

$$\sigma = C_o(\Lambda^2 - \Lambda^{-1}) \quad (13.38)$$

where $\Lambda = L/L_o$ = ratio of stretched length to unstretched length.

The significance of C_o becomes clear from Eq. (13.38) by calculating the Young modulus:

$$E = \lim_{\varepsilon \rightarrow 0} \frac{\sigma}{\varepsilon} = \lim_{\varepsilon \rightarrow 0} \frac{C_o \left[(1 + \varepsilon)^2 - (1 + \varepsilon)^{-1} \right]}{\varepsilon} = 3C_o$$

It follows that the constant C_o is equal to $\frac{1}{3}E$ and also equal to the shear modulus G , because for rubbers the Poisson constant $\nu \approx \frac{1}{2}$.

The expression (13.38) is valid for small extensions only. The actual behaviour of cross-linked rubbers in unidirectional extension is well described by the empirical *equation of Mooney–Rivlin* (1940, 1948):

$$\sigma = C_1(\Lambda^2 - \Lambda^{-1}) + C_2(\Lambda - \Lambda^{-2}) = (C_1 + C_2\Lambda^{-1})(\Lambda^2 - \Lambda^{-1}) \quad (13.39)$$

where C_1 and C_2 are empirical constants.

In the same way as above it becomes clear that

$$C_1 + C_2 = \frac{1}{3}E = G$$

The *Mooney stress*, σ_M , is obtained by dividing the stress by $(\Lambda^2 - \Lambda^{-1})$:

$$\sigma_M = \sigma / (\Lambda^2 - \Lambda^{-1}) = C_1 + C_2\Lambda^{-1} \quad (13.40)$$

It follows that the constants C_1 and C_2 can easily be obtained by plotting the Mooney stress σ_M vs. the reciprocal elongation $1/\Lambda$.

The Mooney–Rivlin equation is readily available from the *Constitutive Equation for isotropic elastic materials*:

$$\mathbf{T} = -p_0 \mathbf{I} + C_1 \mathbf{B} - C_2 \mathbf{B}^{-1} \quad (13.41)$$

where \mathbf{T} = stress tensor; \mathbf{I} = unit tensor; \mathbf{B} = Finger deformation tensor; \mathbf{B}^{-1} = reciprocal Finger deformation tensor or Cauchy deformation tensor.

For uniaxial deformation the Finger and Cauchy tensors read

$$\mathbf{B} = \begin{pmatrix} \Lambda^2 & 0 & 0 \\ 0 & \Lambda^{-1} & 0 \\ 0 & 0 & \Lambda^{-1} \end{pmatrix} \quad \text{and} \quad \mathbf{B}^{-1} = \begin{pmatrix} \Lambda^{-2} & 0 & 0 \\ 0 & \Lambda & 0 \\ 0 & 0 & \Lambda \end{pmatrix} \quad (13.42)$$

The tensile stress is equal to the first normal stress difference:

$$\sigma = N_1 \equiv T_{11} - T_{22} \quad (13.43)$$

It follows

$$T_{11} = -p_o + C_1\Lambda^2 - C_2\Lambda^{-1} \quad \text{and} \quad T_{22} = -p_o + C_1\Lambda^{-1} - C_2\Lambda$$

so that Eq. (13.39) now readily follows from Eq. (13.43).

In the equations above σ is the true tensile stress, i.e. F/A . In practice in general use is made of σ_{eng} , the engineering stress, which is equal to F/A_o , where F is the tensile load and A and A_o are the cross-sectional surface areas of the sample in the deformed and non-deformed state, respectively. Because the Poisson constant $\approx 1/2$ for rubbers $A = A_o/\Lambda$, so that the equations for the tensile stress become:

$$\sigma_{\text{eng}} = C_o(\Lambda - \Lambda^{-2}) \quad (13.44)$$

$$\sigma_{\text{eng}} = C_1(\Lambda - \Lambda^{-2}) + C_2(1 - \Lambda^{-3}) = (C_1 + C_2\Lambda^{-1})(\Lambda - \Lambda^{-2}) \quad (13.45)$$

and the Mooney engineering stress

$$\sigma_{M,\text{eng}} = \sigma_{\text{eng}}/(\Lambda - \Lambda^{-2}) = C_1 + C_2\Lambda^{-1} \quad (13.46)$$

Fig. 13.8 gives an illustration of the engineering stress σ_{eng} during uniaxial deformation for a NR-IR rubber (Eisele, 1990), whereas Fig. 13.9 shows the Mooney engineering stress as a function of the reciprocal elongation. The constants C_1 and C_2 are calculated to be $C_1 = 2.80 \times 10^5 \text{ N/m}^2$ and $C_2 = 2.67 \times 10^5 \text{ N/m}^2$, respectively. It follows that the Young modulus is equal to $E = 1.64 \times 10^6 \text{ N/m}^2$. The dashed line in Fig. 13.8 is obtained by substituting C_1 and C_2 in Eq. (13.46). The Mooney–Rivlin equation is obeyed up to $\Lambda = 4$. Above that value the measured stress increases faster, due to non-linear (non-Gaussian)

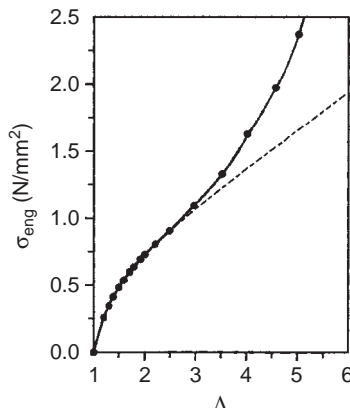


FIG. 13.8 Stress–elongation curve for a natural rubber (after Eisele, 1990); the dashed line is obtained by substituting C_1 and C_2 , as found in Fig. 13.9, in Eq. (13.46).

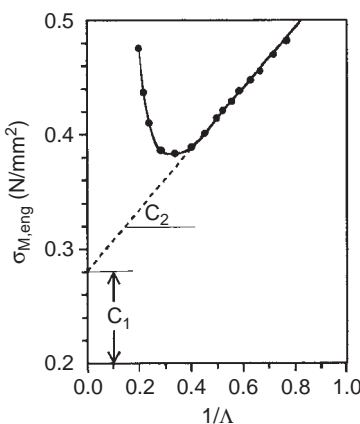


FIG. 13.9 Mooney engineering stress vs. reciprocal elongation of the rubber from Fig. 13.8.

behaviour of the rubber and possibly also by crystallisation. In compression and in shear the ideal elastic behaviour is more closely followed.

Eq. (13.45) may also be expressed as:

$$\sigma_{\text{eng}} = (C_1 + C_2) \left[1 - \frac{C_2}{C_1 + C_2} \left(1 - \frac{1}{\Lambda} \right) \right] (\Lambda - \Lambda^{-2}) \quad (13.47)$$

Table 13.7 shows the values of C_1 and C_2 for different families of elastomers. Obviously the Mooney–Rivlin equation may also be written as

$$\sigma_{\text{eng}} \approx C_o \left[1 - 0.4 \left(1 - \frac{1}{\Lambda} \right) \right] (\Lambda - \Lambda^{-2}) \quad (13.48)$$

where $C_o = C_1 + C_2$. Apparently C_2 is approximately equal to $0.4G_e$.

The theory of rubber elasticity was extended by Blokland (1968). On the basis of photoelasticity, light scattering and electron microscopy studies he found a structure in his (polyurethane) networks that can be interpreted as rod like correlated regions of chain segments or “bundles” (involving about 5% of the chain segments). He derived an equation of the following type: On the basis of this model he derived an equation of the following type:

$$\sigma_{\text{eng}} = C_o [1 - C_3(\Lambda)] (\Lambda - \Lambda^{-2}) \quad (13.49)$$

where now C_3 is deformation dependent.

TABLE 13.7 Constants of the Mooney–Rivlin equation (numerical values derived from Blokland (1968))

Elastomer	C_1	C_2	$C_1 + C_2$	$\frac{C_1}{C_1 + C_2}$
Natural	2.0 (0.9–3.8)	1.5 (0.9–2)	3.5	0.4 (0.25–0.6)
Butyl rubber	2.6 (2.1–3.2)	1.5 (1.4–1.6)	4.1	0.4 (0.3–0.5)
Styrene-butadiene rubber	1.8 (0.8–2.8)	1.1 (1.0–1.2)	2.9	0.4 (0.3–0.5)
Ethene-propene rubber	2.6 (2.1–3.1)	2.5 (2.2–2.9)	5.1	0.5 (0.43–0.55)
Polyacrylate rubbers	1.2 (0.6–1.6)	2.8 (0.9–4.8)	3	0.5 (0.3–0.8)
Silicone rubbers	0.75 (0.3–1.2)	0.75 (0.3–1.1)	1.5	0.4 (0.25–0.5)
Polyurethanes	3 (2.4–3.4)	2 (1.8–2.2)	5	0.4 (0.38–0.43)

C_1 and C_2 expressed in 10^5 N/m^2 .

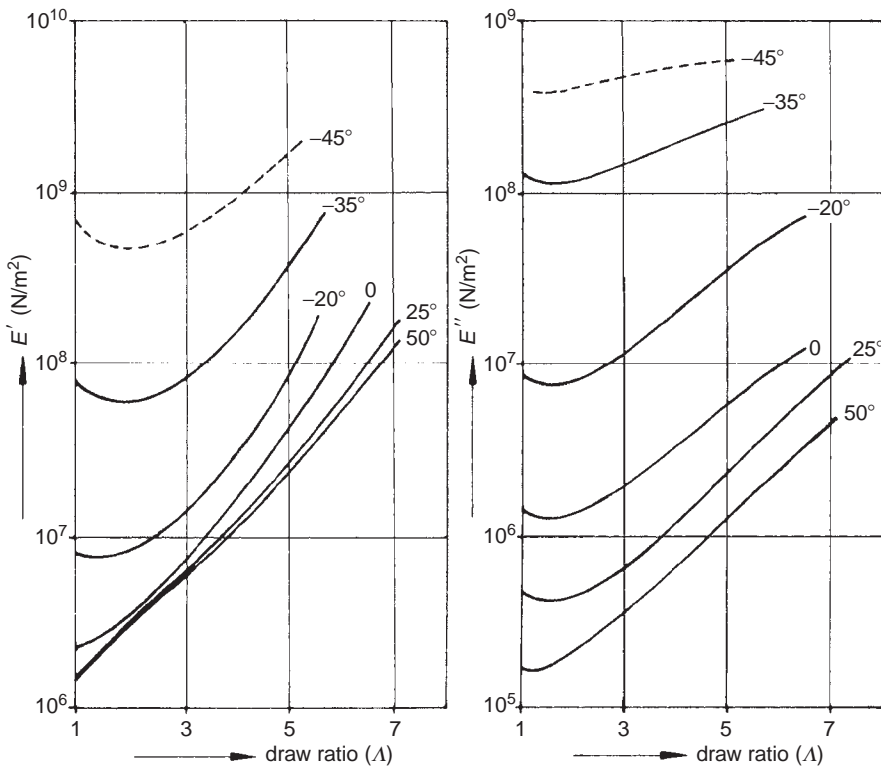


FIG. 13.10 Dynamic Young's moduli, E' and E'' of natural rubber as a function of the elongation at 1 kc/s. From Mason (1961).

Fig. 13.10 gives typical results of dynamic-mechanical measurements on natural rubber during elongation. Natural rubber beyond 200% elongation shows induced crystallisation, by which the mechanical properties are strongly influenced; the dynamic Young modulus, E' increases rapidly with orientation. Also viscoelastic damping, E'' , is observed (for the significance of E'' see Sect. 13.4.1).

13.4. VISCOELASTICITY

Sections A and B of this chapter dealt with purely elastic deformations, i.e. deformations in which the strain was assumed to be a time-independent function of the stress and vice versa. In reality, materials are never purely elastic: under certain circumstances they have non-elastic properties. This is especially true of polymers, which may show non-elastic deformation under circumstances in which metals may be regarded as purely elastic. For a better understanding three phenomena may be distinguished, the combination of which is called viscoelasticity. This is elucidated in Table 13.8. *The only modulus which is time-independent is the bulk modulus*; hence its advantage as a basis for additivity.

It is customary to use the expression *viscoelastic deformations* for all deformations that are not purely elastic. This means that viscoelasticity deals with a number of quite different phenomena. Literally the term viscoelastic means the combination of viscous and elastic properties. Examples are stress relaxation, creep and dynamic mechanical

TABLE 13.8 Fundamental viscoelastic phenomena

Phenomenon	Tensile			Shear		
	Adj.	Meas.	Calc.	Adj.	Meas.	Calc.
Stress relaxation	ε_0	$\sigma(t)$	$E(t)$	γ_0	$\sigma_{sh}(t)$	$G(t)$
Creep	σ_0	$\varepsilon(t)$	$S(t)$	$\sigma_{sh,o}$	$\gamma(t)$	$J(t)$
Dynamic Mechanical	ε_o, ω	σ_o, δ	$E'(\omega), E''(\omega)$	γ_o, ω	$\sigma_{sh,o}, \delta$	$G'(\omega), G''(\omega)$

Adj = adjustable, Meas. = measured; Calc. = calculated. In practice the phase angle φ of the measuring device is measured, and the loss angle δ is calculated.

behaviour (all in tensile and in shear deformation), and also volume retardation. This does not mean that these phenomena can always be easily distinguished. Many practical deformation processes form a complicated combination.

13.4.1. Stress relaxation

In stress relaxation a sample is stepwise deformed to a tensile deformation ε_0 or to a shear deformation γ_0 and the decreasing stress is measured as a function of time: $\sigma(t)$ or $\sigma_{sh}(t)$, respectively. The proportionality factors between stress and deformation are the Young modulus $E(t)$ and the shear modulus $G(t)$

$$E(t) = \frac{\sigma(t)}{\varepsilon_0} \quad \text{and} \quad G(t) = \frac{\sigma_{sh}(t)}{\gamma_0} \quad (13.50)$$

The relationship between $E(t)$ and $G(t)$ is

$$E(t) = 2[1 + v(t)]G(t) \quad (13.51)$$

where $v(t)$ = time dependent Poisson's constant.

For amorphous thermoplastic polymers the general view of the Young modulus is shown as a function of time in Fig. 13.11. In this figure the various regions are present as they were also shown in Figs. 13.3 and 13.7. In those figures, however, the modulus is presented as a function of temperature. Formally a modulus temperature curve is obtained by measuring stress relaxation as a function of time at many different

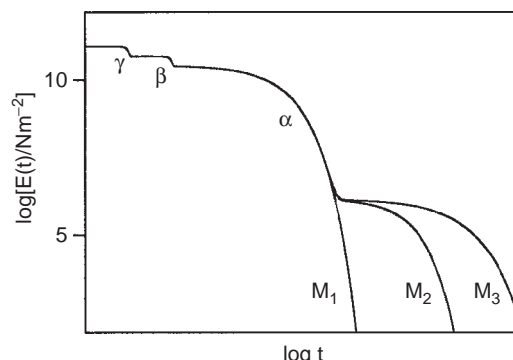


FIG. 13.11 Schematic logarithmic plot of Young modulus, $E(t)$, against time for an amorphous polymer with glass transition (α) and secondary transitions (β and γ): $M_1 \approx 20,000 \text{ g/mol}$; $M_1 < M_2 < M_3$.

temperatures. The modulus vs. temperature curve is then obtained by choosing a single time t_1 and subsequently plotting $E(T, t_1)$ vs. T . In Fig. 13.11 also secondary, sub- T_g transitions are depicted. The glass–rubber transition is a transition with micro-Brownian movements: relatively large chain parts are able to move with respect to each other and to fit themselves to the stress, that subsequently decreases fast. In the glassy region itself, i.e. in the period that the deformation has been applied only a short time ago, only small parts of the backbone chains, or side groups are able to fit themselves very fast to the stress, e.g. by rotations. For every kind of secondary transition, each with its own movement possibility, a certain time is needed, so that various transitions may be present in the glassy region. These secondary transitions may affect the impact strength of polymers. Following the terminology of Deutsch, Hoff and Reddish (1954) the various transitions are designated, starting with the glass transition and going down to lower temperatures, by the α , β , γ , δ and ϵ transitions.

It is clear that the determination of such a modulus temperature curve takes an awful lot of time. Moreover, the transitions in the glassy region are difficult to determine, because the time needed for such a transition will be very small: it may be of the order of or even much faster than the time in practice to apply an instantaneous deformation. For that reason in general use is made of dynamic mechanical measurements as a function of frequency to elucidate the modulus temperature curves, in particular in the glassy region. An additional advantage is that elastic and viscous forces are separated in this kind of measurements.

13.4.2. Dynamic-mechanical measurements

Measurement of the response in deformation of a material to *periodic forces* or of the response in stress to *periodic deformations*, for instance during forced vibration, shows that stress and strain are not in phase; the strain lags behind the stress by an angle δ , the loss angle.

13.4.2.1. The storage and loss moduli

If the deformation is of a sinusoidal type (see Fig. 13.12), one gets:

$$\varepsilon = \varepsilon_0 \sin(\omega t) \quad (\text{tensile strain}) \quad (13.52)$$

$$\sigma = \sigma_0 \sin(\omega t + \delta) \quad (\text{tensile stress}) \quad (13.53)$$

where ε_0 = the amplitude of the sinusoidal tensile deformation (–); σ_0 = the amplitude of the sinusoidal tensile stress (N/m); ω = the angular frequency (rad/s), which is equal to $2\pi\nu$ where ν is the frequency in cycles per second (or Hz); δ = phase angle (rad).

For ideal elastic materials $\delta = 0$, whereas for purely viscous fluids $\delta = \pi/2$ rad.

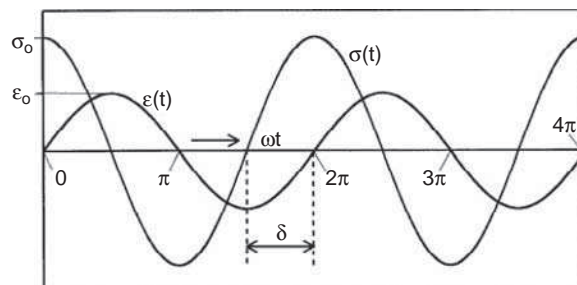


FIG. 13.12 Sinusoidal strain and stress with phase angle δ .

Development of Eq. (13.53) yields

$$\sigma = \sigma_0[\sin(\omega t) \cos \delta + \cos(\omega t) \sin \delta] = \varepsilon_0[E' \sin(\omega t) + E'' \cos(\omega t)] \quad (13.54)$$

with

$$E'(\omega) \equiv \frac{\sigma_0}{\varepsilon_0} \cos \delta \quad \text{and} \quad E''(\omega) \equiv \frac{\sigma_0}{\varepsilon_0} \sin \delta \quad (13.55)$$

where $E'(\omega)$ and $E''(\omega)$ are the tensile storage and tensile loss moduli, respectively (N/m).

The term $\varepsilon_0 E' \sin(\omega t)$ in Eq. (13.54) is the part of the stress that is in phase with the deformation and thus represents the elastic part of the stress, i.e. the part of the stress where energy is stored. For that reason E' is called the (*tensile storage modulus*). The term $\varepsilon_0 E'' \cos(\omega t)$ in Eq. (13.54) is the part of the stress that is $\pi/2$ rad out of phase with the deformation and thus represents the viscous part of the stress, i.e. the part of the stress where energy is dissipated. For that reason E'' is called the (*tensile loss modulus*).

Complex notation, as generally used by physicists, is:

$$\varepsilon^* = \varepsilon_0 \exp(i\omega t) \quad (13.56)$$

$$\sigma^* = \sigma_0 \exp[i(\omega t + \delta)] \quad (13.57)$$

Then

$$E^* \equiv \frac{\sigma^*}{\varepsilon^*} = \frac{\sigma_0}{\varepsilon_0} \exp(i\delta) = \frac{\sigma_0}{\varepsilon_0} (\cos \delta + i \sin \delta) = E' + iE'' \quad (13.58)$$

where $E^* = E^*(\omega)$ = the *complex dynamic tensile modulus*; $E' = E'(\omega) = \sigma_0/\varepsilon_0 \cos \delta$ is the real part of E^* , or *tensile storage modulus*; $E'' = E''(\omega) = \sigma_0/\varepsilon_0 \sin \delta$ is the imaginary part of E^* , or *tensile loss modulus*; $i = \sqrt{-1}$.

In the same way also the dynamic shear modulus may be found

$$\gamma = \gamma_0 \sin(\omega t) \quad (\text{shear strain}) \quad (13.59)$$

$$\sigma_{sh} = \sigma_{sh,o} \sin(\omega t + \delta) \quad (\text{shear stress}) \quad (13.60)$$

This leads to

$$G'(\omega) \equiv \frac{\sigma_{sh,o}}{\gamma_0} \cos \delta \quad \text{and} \quad G''(\omega) \equiv \frac{\sigma_{sh,o}}{\gamma_0} \sin \delta \quad (13.61)$$

where G' and G'' are the shear storage and loss moduli, respectively, or shortly *storage modulus* and *loss modulus*.

In complex notation:

$$G^* \equiv \frac{\sigma_{sh}^*}{\gamma^*} = \frac{\sigma_{sh,o}}{\gamma_0} \exp(i\delta) = \frac{\sigma_{sh,o}}{\gamma_0} (\cos \delta + i \sin \delta) = G' + iG'' \quad (13.62)$$

The curves of storage modulus vs. angular frequency resemble the Young modulus-temperature curves, but they are almost their mirror image. In Fig. 13.13 the storage and loss moduli for an amorphous high molecular weight polymer are presented as functions of the angular frequency. In the plateaus of the storage moduli, with almost no relaxation processes, the loss modulus has minimum values; in the regions where G' decreases in a

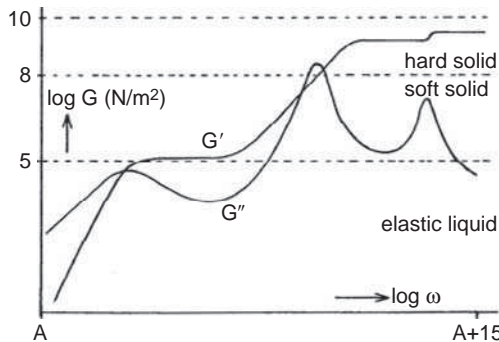


FIG. 13.13 The dynamic shear moduli, G' and G'' , for a high molecular weight polymer, as functions of the angular frequency. Classification is also indicated. Analogous to Ferry (1970) and Te Nijenhuis (1980, 2006).

relaxation process G'' shows a maximum value. At very low frequencies the slopes of both moduli are 2 and 1 for G' and G'' , respectively. This leads to the following relationships

$$\lim_{\omega \rightarrow 0} \frac{G'}{\omega^2} = \Psi_{10} \quad \text{and} \quad \lim_{\omega \rightarrow 0} \frac{G''}{\omega} = \eta_0 \quad (13.63)$$

where Ψ_{10} appears to be the first normal stress coefficient and η_0 the viscosity, both defined in steady shear experiments

$$\Psi_{10} \equiv \lim_{q \rightarrow 0} \frac{T_{11} - T_{22}}{q^2} = \frac{N_1}{q^2} \quad \text{and} \quad \eta_0 \equiv \lim_{q \rightarrow 0} \frac{T_{21}}{q} \quad (13.64)$$

Here T_{ij} are the components of the stress tensor as defined in rheology: $T_{11} - T_{22}$ is the first normal stress difference and T_{21} the shear stress, equal to N_1 and σ_{sh} , respectively. Hence, from dynamic mechanical measurements it is possible to determine the zero shear first normal stress coefficient Ψ_{10} and zero shear viscosity η_0 .

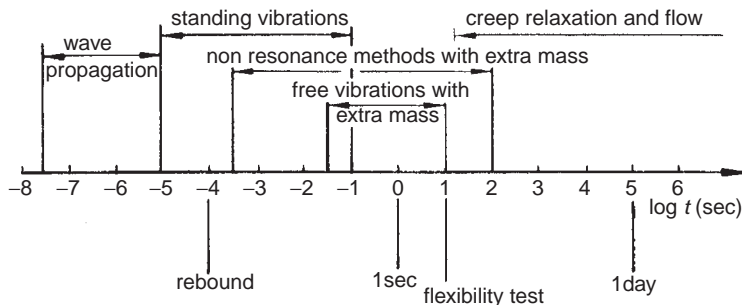
Fig. 13.13 also gives a rough classification of amorphous polymers:

- Hard viscoelastic solids, which cover a G' region of 10^8 – 10^{10} N/m²; test pieces have to be small in torsion and bending tests.
- Soft viscoelastic solids and liquids of high viscosity, which cover a G' region of 10^5 – 10^8 N/m²; in this region the storage and loss moduli have comparable values, so that $\tan \delta$ is neither very small nor very large; test pieces are softer than the instruments they are confined in.
- Elastic liquids of relatively low viscosity; these liquids have to be confined in the measuring devices in order to prevent flow under the action of gravitational forces.

From Fig. 13.13 it also follows that the frequency region covers at least 15 decades. This, of course, is not realisable with only one instrument. In Table 13.9 a classification of experimental techniques for the determination of the dynamic moduli is presented. It appears that even a combination of those techniques is not sufficient to cover the whole frequency range. Other, non-dynamic mechanical measurement techniques are needed, like creep, relaxation and flow measurements. This is illustrated in Fig. 13.14 where a survey of available methods is given.

TABLE 13.9 Classification of experimental techniques to determine G' and G''

Experimental technique	Frequency range (Hz)
Free damped vibrations	0.1–30
Forced vibrations: resonance	$0.01\text{--}10^4$
Forced vibration: non-resonance	$10^{-4}\text{--}10^2$
Wave propagation	$1\text{--}3 \times 10^9$

**FIG. 13.14** The position of different experimental techniques on logarithmic time scale (Staverman and Schwarzl, 1956).

For the complex moduli the basic interrelation formula (Table 13.2) remain valid. The complex moduli are related to the complex viscosities by the following equations:

$$\begin{aligned} \eta_e^* &= E^*/(i\omega), & \eta^* &= G^*/(i\omega) \\ \eta_e'' &= E'/\omega, & \eta'' &= G'/\omega \\ \eta_e' &= E''/\omega, & \eta' &= G''/\omega \end{aligned} \quad (13.65)$$

η_e^* is the so-called complex dynamic *tensile viscosity* and η^* the complex dynamic *shear viscosity*. Their relation is:

$$\frac{\eta_e^*}{\eta^*} = \frac{E^*}{G^*} = 2(1 + v) \quad (13.66)$$

For incompressible liquids $v = \frac{1}{2}$, so that $\eta_e^* = 3\eta^*$

The general expressions for the dynamic mechanical parameters are:

$$\begin{aligned} E^* &= E' + iE'', & |E^*| &= \left[(E')^2 + (E'')^2 \right]^{1/2} \\ S^* &= S' - iS'' = 1/E^*, & |S^*| &= \left[(S')^2 + (S'')^2 \right]^{1/2} \\ G^* &= G' + iG'', & |G^*| &= \left[(G')^2 + (G'')^2 \right]^{1/2} \\ J^* &= J' - iJ'' = 1/G^*, & |J^*| &= \left[(J')^2 + (J'')^2 \right]^{1/2} \\ \eta^* &= \eta' - i\eta'' = G^*/(i\omega), & |\eta^*| &= \left[(\eta')^2 + (\eta'')^2 \right]^{1/2} = |G^*|/\omega \end{aligned} \quad (13.67)$$

13.4.2.2. The loss tangent

The characteristic measure of damping is the ratio of energy dissipated per cycle to the maximum potential energy stored during a cycle. It is related to the called dissipation factor or loss tangent, which is defined to be

$$\tan \delta_E \equiv \frac{E''}{E'} = \frac{S''}{S'} = \frac{\eta'_e}{\eta''_e}; \quad \tan \delta_G \equiv \frac{G''}{G'} = \frac{J''}{J'} = \frac{\eta'}{\eta''}; \quad \tan \delta_E \approx \tan \delta_G \quad (13.68)$$

An extensive study by Koppelman (1958) of viscoelastic functions through one of the secondary mechanisms in Poly(methyl methacrylate) is shown in Fig. 13.15. Dynamic storage moduli and $\tan \delta$'s near 25 °C are plotted vs. angular frequency. It shows first, that a secondary mechanism is present, secondly that E' and G' are not completely parallel, because the Poisson constant is not a real constant, but also dependent on frequency (the numbers in between both moduli are the actual, calculated Poisson constants) and thirdly that $\tan \delta_E$ is practically equal to $\tan \delta_G$.

Sinusoidal motion is attended by elastic energy stored and viscous energy dissipated. The total energy involved during a quarter of cycle is

$$\int_0^{\varepsilon_0} \sigma d\varepsilon = \sigma_0 \varepsilon_0 \int_0^{\frac{1}{2}\pi} \sin(\omega t + \delta) \cos(\omega t) d(\omega t) = \frac{1}{2} E' \varepsilon_0^2 + \frac{1}{4} \pi E'' \varepsilon_0^2 = W_{\max} + \frac{1}{4} Q \quad (13.69)$$

where the heat developed per cycle per unit volume is

$$Q = \pi E'' \varepsilon_0^2 \quad (13.70)$$

and the maximum energy per unit volume stored during a cycle is (i.e. the energy stored per first quarter of a deformation cycle):

$$W_{\max} = \frac{1}{2} E' \varepsilon_0^2 \quad (13.71)$$

It follows for the loss tangent:

$$2\pi \tan \delta = \frac{Q}{W_{\max}} = \psi \quad (13.72)$$

where ψ = the specific damping capacity or internal friction.

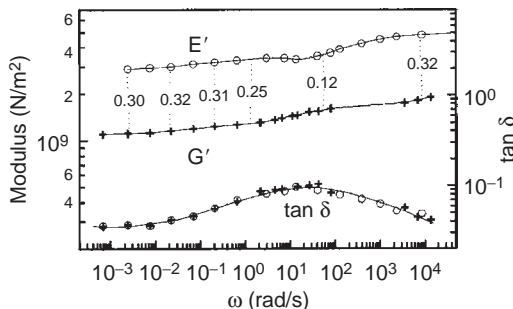


FIG. 13.15 Storage moduli in shear (G') and extension (E') and the loss tangents $\tan \delta_G$ and $\tan \delta_E$, of poly (methyl methacrylate) near 25 °C, plotted logarithmically vs. angular frequency. The numbers between E' and G' denote the values of Poisson's ratio. From Koppelman (1958). Courtesy Springer Verlag.

13.4.2.3. Rebound resilience

In close agreement is the so-called rebound resilience, which is a material property for which different definitions are given in the literature. Most often it is used as an inverse measure of damping. A rigid ball is released at a fixed height h_0 above a rubber test piece. During the resulting collision part of the kinetic energy of the rigid ball is dissipated as heat in the rubber test piece. As a consequence the ball does not return to its original height, but to a lower height h_1 and after the second collision to a still lower height h_2 etc. The dissipated energy is equal to the difference in kinetic energy just before and after the collision:

$$\Delta W = W_0 - W_1 = W_1 - W_2 = \dots = W_n - W_{n+1} \quad (13.73)$$

According to the British Standard, BS903, PartA8, the rebound resilience is defined as "*The proportion of the applied energy usefully returned after an impact*"

$$R = \frac{W_1}{W_0} = \frac{W_2}{W_1} = \dots = \frac{W_{n+1}}{W_n} = \frac{h_1}{h_0} = \frac{h_2}{h_1} = \dots = \frac{h_{n+1}}{h_n} \quad (13.74)$$

For small damping, different definitions result in (Marvin, 1952):

$$R = \exp(-\pi \tan \delta) \quad \text{or} \quad \tan \delta = \frac{1}{\pi} \ln(h_n/h_{n+1}) \quad (13.75)$$

The resilience of a polymer will be high (i.e. $\tan \delta$ is small) in temperature regions where no mechanical damping peaks are found. This applies in particular to rubbery networks ($T \gg T_g$), which therefore possess a high resilience. Various rubbers behave quite differently: at room temperature the rebound resilience is for natural rubber, butadiene-styrene rubber and butyl rubber high, medium and low, respectively. In practice this means that tyres for cars must have medium rebound resilience: high rebound resilience causes bumping on the road, whereas low rebound resilience causes a tyre to become very hot.

13.4.3. Models of viscoelastic behaviour

In order to describe and imitate the viscoelastic behaviour several models have been developed (Fig. 13.16).

1. The *ideal elastic element* is represented by a spring that obeys Hooke's law (with a defined modulus of elasticity) (*Hooke element*). The elastic deformation is instantaneous. In a dynamic experiment the stress is in phase with the deformation: $\sigma_e = E\varepsilon$. An ideal rubbery solid exhibits such a simple behaviour.

2. The *ideal viscous element* can be represented by a dashpot filled with a Newtonian fluid, whose deformation is linear with time while the stress is applied, and is completely irrecoverable (*Newton element*). In a dynamic mechanical experiment the stress is exactly 90° out of phase with the strain: $\sigma_v = \eta d\varepsilon/dt$.

These two basic elements may be combined in series or parallel, giving the Maxwell-element and the Voigt–Kelvin element.

3. The *Maxwell element* (elastic deformation plus flow), represented by a spring and a dashpot in series. It symbolises a material that can respond elastically to stress, but can also undergo viscous flow. The two contributions to the strain are additive in this model, whereas the stresses are equal:

$$\varepsilon = \varepsilon_e + \varepsilon_v \quad \text{and} \quad \sigma = \sigma_e = \sigma_v \quad (13.76)$$

NUMBER OF ELEMENTS IN MODEL	MODEL	
1	Hooke Model 	Newton Model
2	Maxwell Model 	Voigt Model
4	Burgers Model 	

FIG. 13.16 Models for viscoelastic behaviour.

In a stress relaxation experiment the Maxwell-element is subjected to an instantaneous deformation ε_0 which is held constant. It means that:

$$\varepsilon_0 = \varepsilon_e + \varepsilon_v = \text{constant} \quad \text{or} \quad \frac{d\varepsilon_e}{dt} + \frac{d\varepsilon_v}{dt} = 0 \quad (13.77)$$

so that

$$\frac{1}{E} \frac{d\sigma}{dt} + \frac{\sigma}{\eta} = 0 \quad (13.78)$$

which leads to:

$$\sigma(t) = \sigma_0 \exp(-t/\tau) = \varepsilon_0 E \exp(-t/\tau) \quad (13.79)$$

where $\tau = \eta/E$, i.e. the *relaxation time*, which is the time needed for the stress to decrease from σ_0 to $\sigma_0/e \approx 0.37\sigma_0$. In Fig. 13.17 the relative stress $\sigma(t)/\sigma_0$ is plotted vs. $\log t/\tau$: it shows that in approximately two time decades the relative stress decreases from 1 to zero.

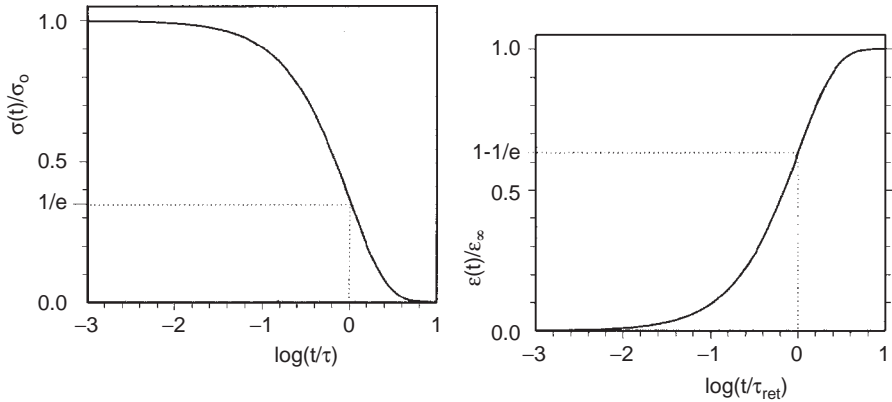


FIG. 13.17 Left: time dependent reduced stress, $\sigma(t)/\sigma_0$, of a Maxwell element after applying a constant strain vs. log reduced time, $\log(t/\tau)$. Right: time dependent reduced strain, $\varepsilon(t)/\varepsilon_\infty$, of a Voigt–Kelvin element after applying a constant stress vs. log reduced time, $\log(t/\tau_{\text{ret}})$.

The time dependent modulus of a Maxwell element is given by

$$E(t) = \frac{\sigma_0}{\varepsilon_0} \exp(-t/\tau) = E \exp(-t/\tau) \quad (13.80)$$

In practice the stress relaxation behaviour has to be described expressed with N Maxwell elements connected in parallel, each with its own spring constant E_i and relaxation time τ_i (the so-called Maxwell–Wiechert model):

$$\sigma(t) = \varepsilon_0 \sum_{i=1}^N E_i \exp(-t/\tau_i) \quad (13.81)$$

4. The *Voigt–Kelvin element* (retarded elastic response), represented by a spring and a dashpot in parallel. The elastic response is not instantaneous but retarded by a viscous resistance. The two contributions to the stress are additive in this model whereas the strains are equal:

$$\sigma = \sigma_e + \sigma_v \quad \text{and} \quad \varepsilon = \varepsilon_e = \varepsilon_v \quad (13.82)$$

In a creep experiment the Voigt–Kelvin element is instantaneously subjected to a stress σ_0 which is held constant. It means that

$$\sigma_0 = \sigma_e + \sigma_v = \text{constant} \quad \text{or} \quad \frac{d\sigma_e}{dt} + \frac{d\sigma_v}{dt} = 0 \quad (13.83)$$

so that

$$\frac{1}{E} \frac{d\varepsilon}{dt} + \frac{1}{\eta} \frac{d^2\varepsilon}{dt^2} = 0 \quad (13.84)$$

which leads to

$$\varepsilon(t) = \frac{\sigma_o}{E} [1 - \exp(-t/\tau_{\text{ret}})] = \sigma_o S [1 - \exp(-t/\tau_{\text{ret}})] = \varepsilon_\infty [1 - \exp(-t/\tau_{\text{ret}})] \quad (13.85)$$

where $\tau_{\text{ret}} = \eta/E = \eta S$, i.e. the *creep retardation time*, which is the time needed for the strain to increase from 0 to $\varepsilon_o(1-1/e) \approx 0.63 \varepsilon_o$; S = the compliance of the spring, equal to $1/E$.

In Fig. 13.17 also the relative strain $\varepsilon(t)/\varepsilon_\infty$ is plotted vs. $\log(t/\tau_{\text{ret}})$. It shows that in approximately two time decades the relative strain increases from zero to 1.

The time dependent compliance of a Voigt–Kelvin element is

$$S(t) = \frac{\varepsilon(t)}{\sigma_o} = \frac{1}{E} [1 - \exp(-t/\tau_{\text{ret}})] = S [1 - \exp(-t/\tau_{\text{ret}})] \quad (13.86)$$

The limiting value of the creep is equal to $\varepsilon_\infty = \sigma_o/E = \sigma_o S$. The Voigt–Kelvin element is only able to describe qualitatively the creep behaviour of rubberlike materials with a limited creep and not the creep of an elastic liquid. In general the creep compliance may be expressed as

$$S(t) = S_e(t) - t/\eta = S_{eo}[1 - \psi(t)] - t/\eta \quad (13.86a)$$

where $\psi(t) = 1$ for $t = 0$ and $\psi(t) = 0$ for $t = \infty$, e.g. $\psi(t) = \exp(-t/\tau_{\text{ret}})$ and where $S_e(t)$ is known as the elastic compliance. It is clear that the compliance of a Voigt–Kelvin element does not contain the viscous term t/η . In order to take into account such a viscous term the Burgers element has been introduced.

5. The Burgers element

The basic models contain a modulus E and a viscosity η that are assumed to be time-independent. Many attempts have been made to describe real time-dependent phenomena by combinations of these basic models.

The simplest model that can be used for describing a single creep experiment is the Burgers element, consisting of a Maxwell model and a Voigt–Kelvin model in series. This element is able to describe qualitatively the creep behaviour of viscoelastic materials

$$\varepsilon(t) = \frac{\sigma_o}{E_{VK}} [1 - \exp(-t/\tau_{\text{ret}})] + \frac{\sigma_o}{E_M} + \frac{\sigma_o t}{\eta_M} \quad (13.87)$$

Hence, the compliance of the Burgers element is given by

$$S(t) = \frac{\varepsilon(t)}{\sigma_o} = S_{VK}[1 - \exp(-t/\tau_{\text{ret}})] + S_M + \frac{t}{\eta_M} \quad (13.88)$$

where $S_{VK} = 1/E_{VK}$, $S_M = 1/E_M$ and $\tau_{\text{ret}} = \eta_{VK}/E_{VK} = \eta_{VK} S_{VK}$.

In Fig. 13.18 the strain of a Burgers element, after applying a constant stress σ_o at time zero, is plotted vs. time. It clearly shows the various contributions and how the various model constants can be determined: there is an instantaneous strain ε_{mom} equal to $\sigma_o S_M$, a viscous contribution equal to $\sigma_o t / \eta_M$ and an exponential time dependent part belonging to the Voigt–Kelvin part. For long times (e.g. $t \gg 10\tau$) the strain becomes a linear function of time, with a slope equal to σ_o / η_M .

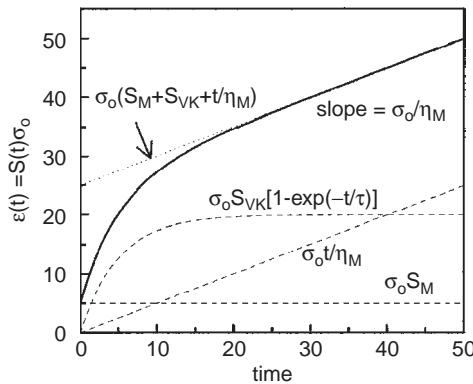


FIG. 13.18 Time dependent strain of a Burgers element after applying a constant stress σ_o . Values of the various parameters are $\sigma_o = 1$, $S_M = 5$, $S_{VK} = 20$, $\eta_M = 2$, $\eta_{VK} = 0.25$, $\tau_{ret} = 5$.

If at time t_1 the stress is released, recoil will take place, according to

$$\varepsilon(t > t_1) = \sigma_o \left\{ S_{VK} [\exp(-(t - t_1)/\tau) - \exp(-t/\tau)] + t_1/\eta_M \right\} \quad (13.89)$$

Apparently, there is an instantaneous recoil equal to $\varepsilon_{inst} = \sigma_o S_M$, which is equal to the instantaneous strain after applying the stress σ_o . For long times t both exponential functions vanish, so that the remaining strain is equal to $\varepsilon_{rem} = t_1/\eta_M$. This is demonstrated in Fig. 13.19.

In practice the creep compliance of polymeric materials can be described by one Maxwell element in series with N Kelvin–Voigt elements in series:

$$S(t) = \frac{\varepsilon(t)}{\sigma_o} = \frac{1}{E_M} + \frac{t}{\eta_M} + \sum_{i=1}^N \frac{1}{E_{VK,i}} \left[1 - \exp(-t/\tau_{ret,i}) \right] = S_M + \frac{t}{\eta_M} + \sum_{i=1}^N S_{VK,i} \left[1 - \exp(-t/\tau_{ret,i}) \right] \quad (13.90)$$

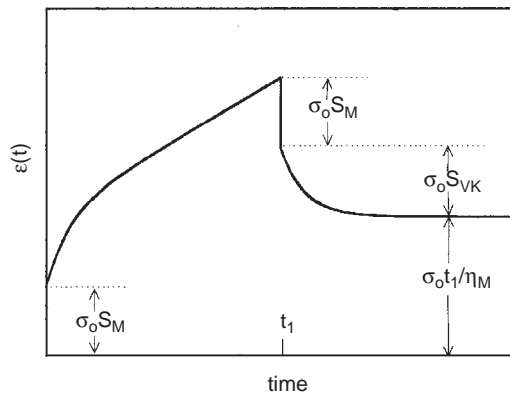


FIG. 13.19 Creep and recoil for a Burgers element.

The number N of retardation times needed depends on the required agreement between theory and experimental behaviour that is required. Instead of a description of viscoelastic behaviour with the aid of a discrete spectrum of relaxation and retardation times, also continuous relaxation or retardation time spectra can be used. In some cases these are easier to handle.

Although the Maxwell–Wiechert model and the extended Burgers element exhibit the chief characteristics of the viscoelastic behaviour of polymers and lead to a spectrum of relaxation and retardation times, they are nevertheless of restricted value: it is valid for very small deformations only. In a qualitative way the models are useful. The flow of a polymer is in general non-Newtonian and its elastic response non-Hookean.

6. The Maxwell element in dynamic mechanical deformation

If a Maxwell element is subjected to a sinusoidal shear deformation that starts at time $t = 0$, Eq. (13.77) becomes

$$\gamma = \gamma_e + \gamma_v = \gamma_0 \sin(\omega t) \quad \text{or} \quad \frac{d\gamma_e}{dt} + \frac{d\gamma_v}{dt} = \gamma_0 \omega \cos(\omega t) \quad (13.91)$$

which leads to

$$\sigma_{sh}(t) = \frac{\omega \tau}{1 + \omega^2 \tau^2} [\omega \tau \sin(\omega t) + \cos(\omega t) - \exp(-t/\tau)] \quad (13.92)$$

For long times (e.g. $t > 5\tau$) the exponential term vanishes, so that the shear stress becomes also sinusoidal:

$$\sigma_{sh}(t) = G\gamma_0 \frac{\omega^2 \tau^2}{1 + \omega^2 \tau^2} \sin(\omega t) + G\gamma_0 \frac{\omega \tau}{1 + \omega^2 \tau^2} \cos(\omega t) \quad (13.93)$$

Comparison with Eq. (13.54), replacing E by G , yields for the dynamic moduli of a Maxwell element

$$G'_M = G \frac{\omega^2 \tau^2}{1 + \omega^2 \tau^2} \quad \text{and} \quad G''_M = G \frac{\omega \tau}{1 + \omega^2 \tau^2} \quad (13.94)$$

In Fig. 13.20 the reduced moduli G'_M/G and G''_M/G are plotted vs. $\omega\tau$ on double logarithmic scales. They show straight lines at low frequencies with slopes of 2 and 1, respectively; the moduli cross at the maximum of the loss modulus; at high frequencies the storage modulus becomes constant with a value equal to $2 \times G''_{M,\max}$ and the loss modulus decreases with a slope -1 .

In a Maxwell–Wiechert model both moduli become

$$G'_M = \sum_i^N G_i \frac{\omega^2 \tau_i^2}{1 + \omega^2 \tau_i^2} \quad \text{and} \quad G''_M = \sum_i^N G_i \frac{\omega \tau_i}{1 + \omega^2 \tau_i^2} \quad (13.95)$$

In Fig. 13.21 the reduced moduli are plotted vs. angular frequency on double logarithmic scales for a MW-model with relaxation times of 1 and 10^4 s and corresponding spring constants of $100G$ and G , respectively. In this case two plateaus in the storage modulus and two maxima in the loss modulus are present, just as in general is found in polymers above the glass temperature.

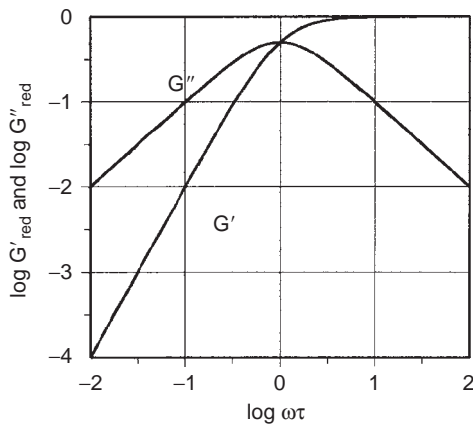


FIG. 13.20 Double logarithmic plot of the reduced dynamic moduli of a Maxwell model vs. the angular frequency.

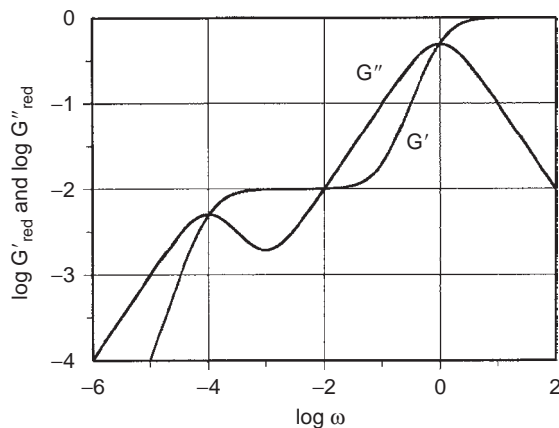


FIG. 13.21 Double logarithmic plot of the reduced dynamic moduli of a Maxwell–Wiechert model with two relaxation times of 10,000 s and 1 s, vs. angular frequency. The corresponding spring constants are G and $100G$, respectively.

13.4.4. Dynamic mechanical parameters and the polymer structure

In many investigations dynamic-mechanical properties have been determined not so much to correlate mechanical properties as to study the influence of polymer structure on thermo-mechanical behaviour. For this purpose, complex moduli are determined as a function of temperature at a constant frequency. *In every transition region (see Chap. 2) there is a certain fall of the moduli, in many cases accompanied by a definite peak of the loss tangent* (Fig. 13.22). These phenomena are called dynamic transitions. The spectrum of these damping peaks is a characteristic fingerprint of a polymer. Fig. 13.23 shows this for a series of polymers.

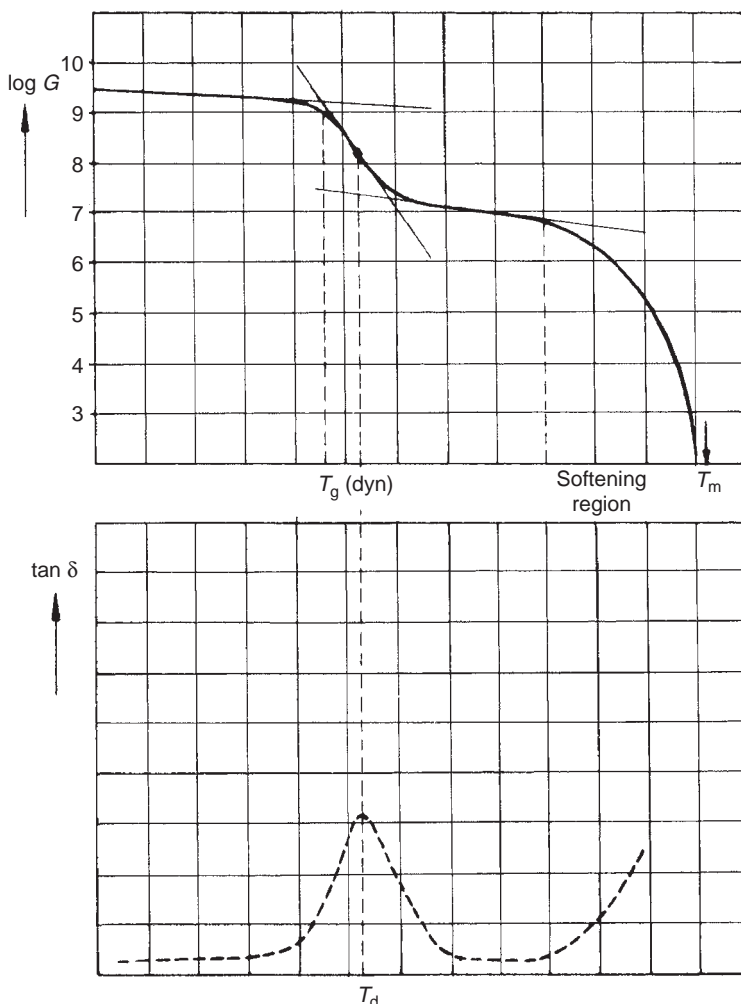


FIG. 13.22 Shear modulus (G) and $\tan \delta$ as functions of temperature for partly crystalline polymers.

Damping peaks between 130 and 170 K (i.e. around -120°C) are frequently connected with sequences of more than three CH_2 groups in the backbone chain; examples are not only polyethylene but also aliphatic polyamides. Also the dispersion region around 200 K is connected with movements (rotations?) of chain segments. The main dispersion region is always related to the conventional glass–rubber transition. (In series of methacrylates it is clear that long side-chains act as plasticizers, but that long side groups also will crystallise.) Between glass transition and (pre-)melting there are sometimes transitions in the solid structure which give rise to damping peaks (e.g. poly(tetrafluoro ethylene), polyethylene, poly(methyl methacrylate)).

The temperature at which the damping peak occurs is not the same as that at which the discontinuous change in a thermodynamic quantity is found. The damping peak will always nearly coincide with the point of inflection of the modulus–temperature curve, whereas the conventional transition temperature is at the intersection of the two tangents

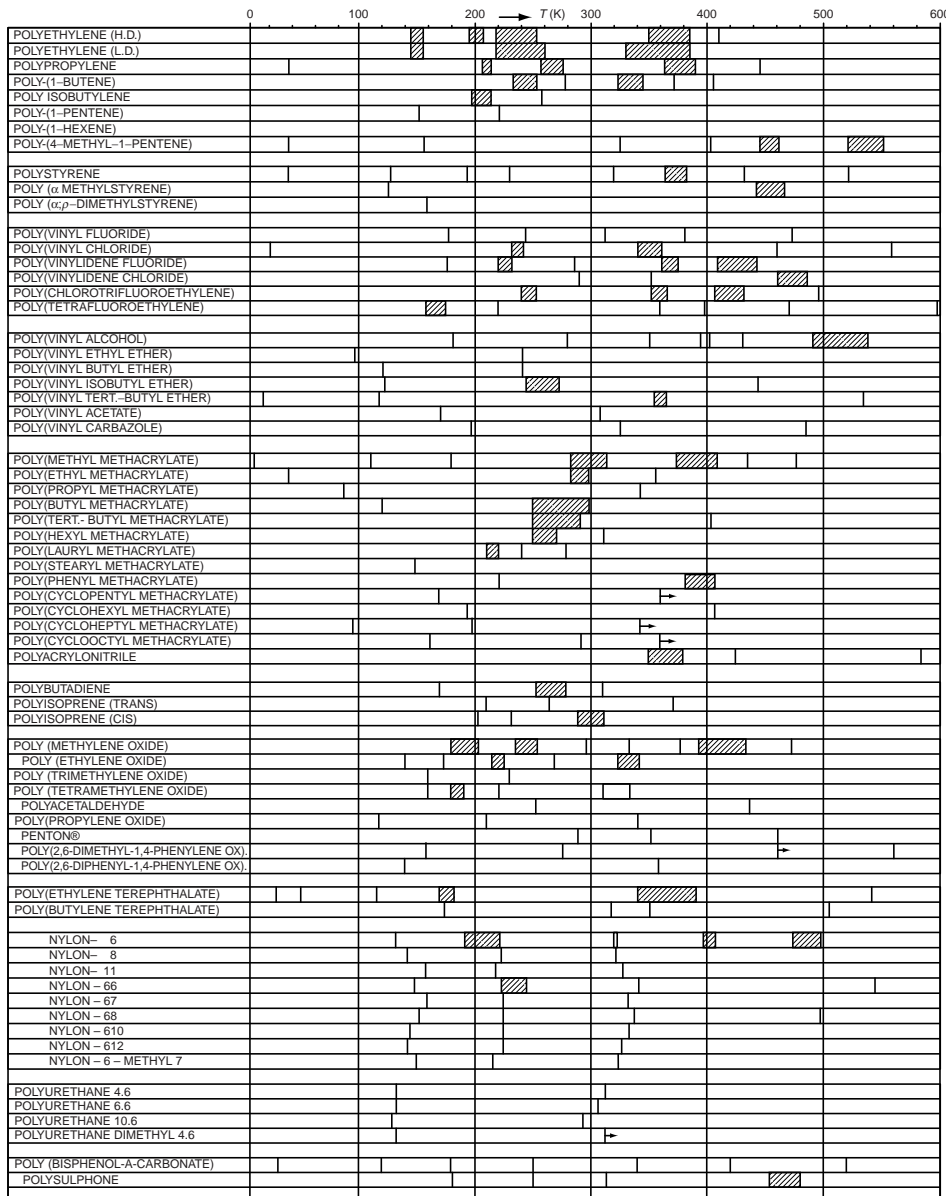


FIG. 13.23 Dynamic transitions of a series of polymers at a frequency of 1 Hz.

of the modulus-temperature curve, at least if the frequency is low. For many polymers this difference $T_d - T_{g,dyn}$ (see Fig. 13.22) can be of the order of 25 °C. This is the reason why instead of the maximum in $\tan \delta$ the maximum in G'' is chosen nowadays: the maximum in $\tan \delta$ is not only dependent on the maximum in G'' , but also on how fast G' decreases in a relaxation process. Sometimes a maximum in $\tan \delta$ is not detectable or not present at all. Even for a Maxwell element $\tan \delta$ decreases with increasing frequency ($\tan \delta = 1/(\omega\tau)$) and therefore does not show a maximum, notwithstanding the presence of a sharp maximum in G'' .

13.4.4.1. Temperature dependence of the transitions

The temperature dependence of the glass rubber transition is different from that of the secondary transitions. The transitions are defined as the frequency of the maximum in G'' (or in $\tan \delta$), which of course is dependent on temperature. For the glass transition we have the WLF-equation (Williams et al., 1955)

$$\omega_{\max}(T) = \omega_g \exp \left[\frac{2.303 c_1^g c_2^g}{c_2^g + T - T_g} \right] \quad (13.96)$$

whereas the secondary transitions are of the Arrhenius type

$$\omega(T) = \omega_0 \exp(-E_A/RT) \quad (13.97)$$

where E_A is the activation energy of the mobilities of those parts of the polymer molecules that are responsible for the transition and c_1^g and c_2^g are the WLF constants at the glass transition temperature (the so-called universal constants c_1^g and c_2^g are equal to 17.4(–) and 51.6(K), respectively, but in practice they are strongly dependent on the kind of polymer). In Fig. 13.24 temperature dependences of the α - and β -transitions are shown. The full curves depict the WLF and Arrhenius equations, respectively.

Very important work on the influence of the chemical structure on the temperature of the damping maximum was done by Heijboer (1956–1972), especially regarding the structure of the ester groups in polymethacrylates.

The temperature dependence of a secondary transition can be used to determine the mechanism of the transition, by comparing it with that of other polymers. In Fig. 13.25 the for poly(cyclohexyl methacrylate), PCHMA, G' and $\tan \delta$ are plotted vs. temperature for a number of frequencies varying from 10^{-4} to 8×10^5 Hz. Upon plotting $\log \nu_{\max}$, where ν_{\max} is the frequency at the maximum in $\tan \delta$, vs. $1/T$ a straight line is obtained as depicted in Fig. 13.26. It is not clear beforehand what mechanism is responsible for this transition. Therefore in Fig. 13.26 also results are shown not only for poly(cyclohexylacrylate), PCHA, i.e. PCHMA without the α -CH₃ group, but also for the liquid cyclohexanol (two measurements at very high frequencies). It appears that the results for the three materials fall on

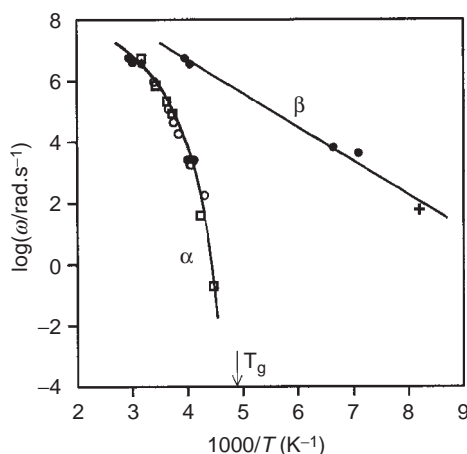


FIG. 13.24 Frequency-temperature correlation map for dynamic mechanical, dielectric and NMR measurements on Polyisobutylene. The α and β relaxation regions are shown. Measurements: (●) NMR; (○) Dielectric; (□) Mechanical. The full lines are the WLF equation (curved) and the Eyring Equation (straight). From Schlichter (1966). Courtesy John Wiley & Sons, Inc.

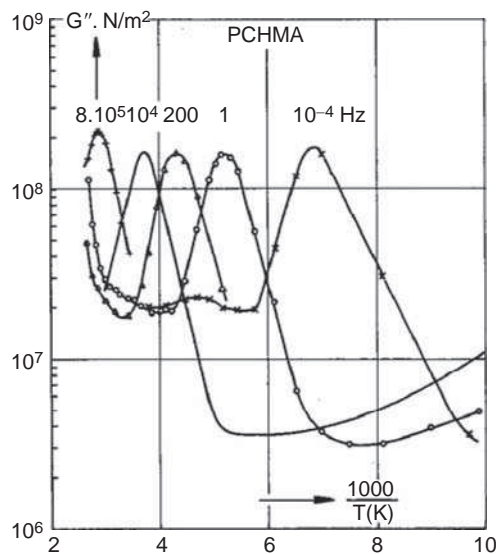


FIG. 13.25 Loss modulus G'' as function of temperature T at six frequencies for poly(cyclohexyl methacrylate) (PCHMA). From Heijboer (1972).

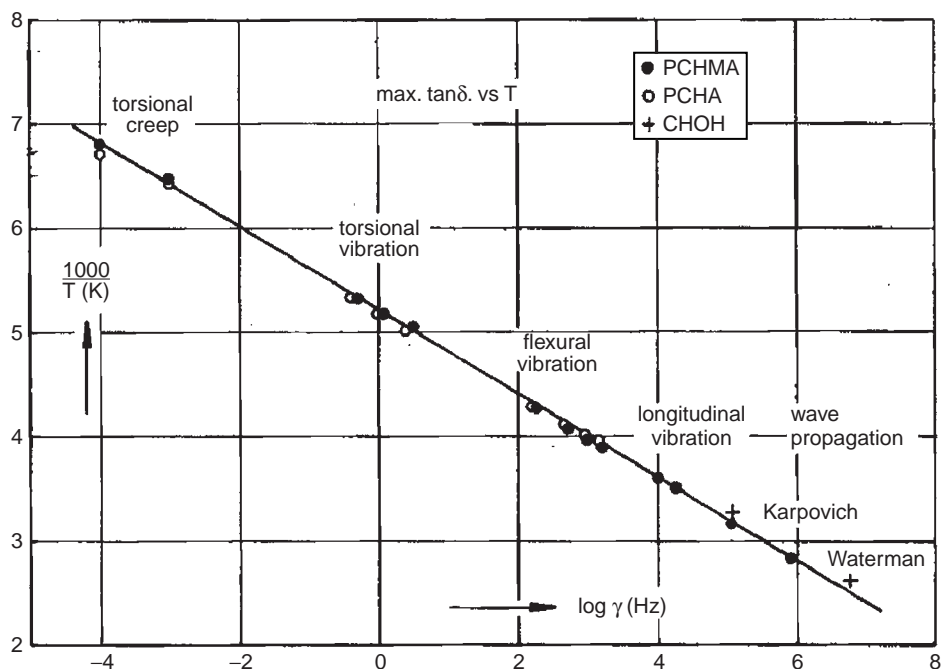


FIG. 13.26 Arrhenius plot for the loss maxima of poly(cyclohexyl methacrylate) (PCHMA), poly(cyclohexyl acrylate) (PCHA) and cyclohexanol (CHOH). The maxima are obtained from $\tan \delta$ vs. T curves. From Heijboer (1972).

the same line. The only correspondence between them is the cyclohexyl ring and the discussed transition is attributed to the mobility of the cyclohexyl ring; the molecular motion is believed to be the flipping of the saturated six-membered ring and involves an activation energy from this analysis of 47.3 kJ/mol, which is in good agreement with the NMR value of 47.7 kJ/mol for the chair-chair-transition of the cyclohexyl ring (Heijboer, 1972).

Another example is shown in Fig. 13.27, where for four poly(n-alkylmethacrylates) with increasing lengths of the side chain ester groups, G' and $\tan \delta$ at 1 Hz are plotted logarithmically vs. temperature. The sharp transitions at the high temperatures are the α -transitions that shift to lower temperatures with increasing length of the side chains. This is in agreement with the decrease of the glass transition temperature. A β -transition is clearly visible at 20 and 10 °C for PMMA and PEMA, respectively, but with increasing side chain length it is overtaken by the α -transition and almost invisible in the PnBuMA polymer. Near -180 °C a third mechanism, the γ -transition appears, but only in the n-propyl and n-butyl polymers.

The temperature dependences of the various transitions in PMMA are quite different, as shown in Fig. 13.28. Because the slopes are decreasing in the direction $\alpha, \beta, \gamma, \delta$ the correspondent heats of activation are also decreasing. Accordingly, the resolution decreases with increasing frequencies, hence with increasing temperature. According to

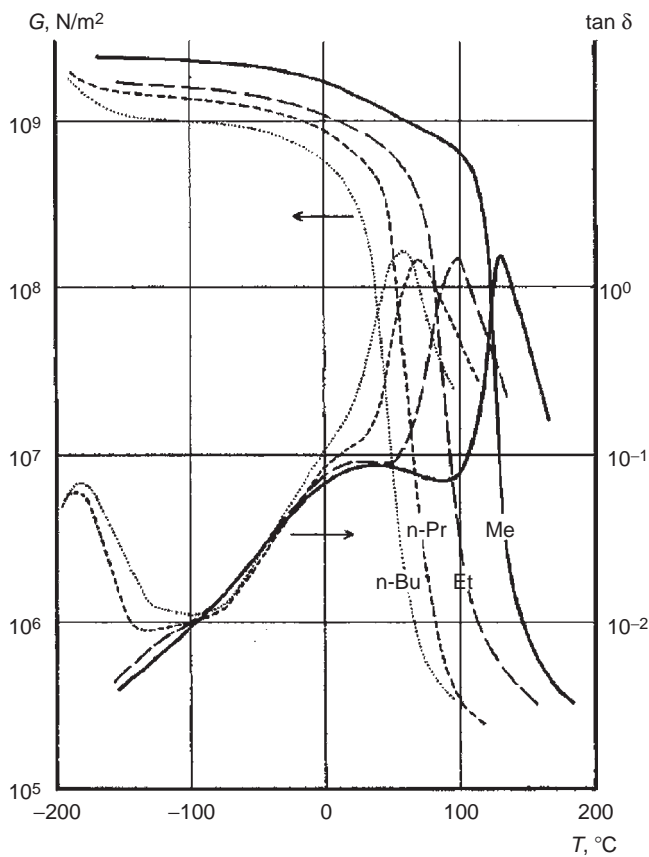


FIG. 13.27 Shear modulus G' and $\tan \delta$ at 1 Hz plotted vs. temperature for four poly(alkyl methacrylates) Me = methyl; Et = ethyl; n-Pr = n-propyl; n-Bu = n-butyl. After Heijboer (1965). From Heijboer (1965). Courtesy Elsevier Science Publishers.

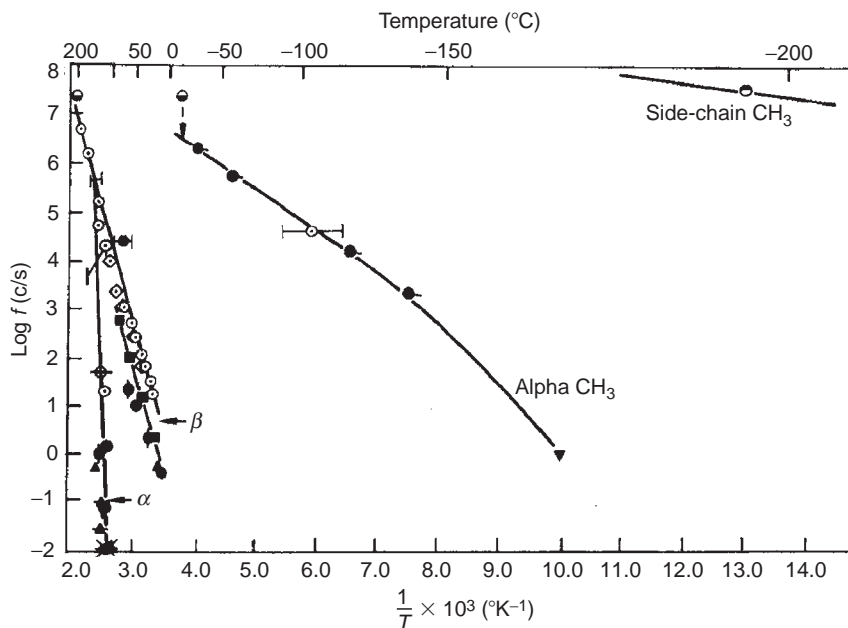


FIG. 13.28 Frequency-temperature correlation map for poly(methyl methacrylate) (PMMA). Dynamic mechanical measurements are indicated by filled points and dielectric measurements by open points; (α) = glass transition; (β) = ester group rotation; (γ) = α -methyl group rotation; (δ) = side chain methyl group motion. From McCrum et al. (1967). Courtesy John Wiley & Sons, Inc.

Heijboer the straight lines come together at $\log \nu = 13.5 \pm 1$ at $1/T = 0$. Another example is shown for polystyrene in Fig. 13.29, where besides the glass transition four secondary transitions are visible and the δ -transition only in dielectric dispersion. These two figures show that mechanical data are often supplemented by dielectric and nuclear magnetic resonance data. The advantage of dielectric measurements is their very large frequency region; they are however, appropriate for polymers with some polarisability. In some cases, the δ -transition in polystyrene, e.g., is only detectable with the aid of dielectric measurements. Mechanical measurements are of course of great value, but they are not appropriate for rotational motions, whereas NMR measurements are pre-eminently

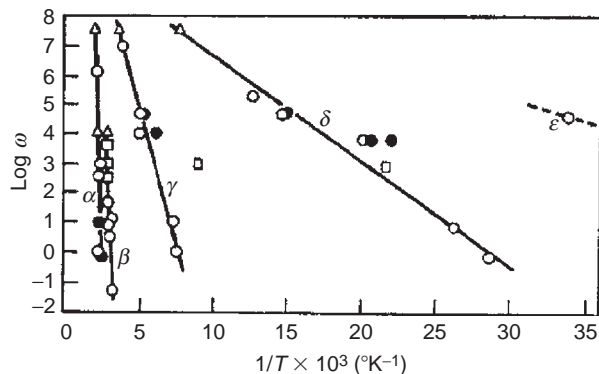


FIG. 13.29 Frequency-temperature correlation map for polystyrene. (\circ , \bullet) mechanical loss peaks; (\square , \blacksquare) dielectric loss peaks; (\triangle , \blacktriangle) NMR narrowing and T_1 (i.e. spin-lattice relaxation time) minima for (open symbols) atactic and (filled symbols) isotactic polystyrenes. From Yano and Wada (1971). Courtesy John Wiley & Sons, Inc.

suitable for rotational motions. For a detailed discussion about the background of the transitions in PMMA and PS the reader is referred to the monographs of Haward (1973) and of Haward and Young (1997).

13.4.4.2. Types of secondary transition

As was mentioned above, the glass transition results from molecular motions involving relatively large segments of the polymer backbone. In contrast, the secondary transitions are due to short-range, much more localised motions. Those motions significantly affect the mechanical and physical properties. Examples are the Young modulus, the dielectric constant, the thermal expansion coefficient and the specific heat capacity. These properties show a stepwise change upon passing a transition. Impact strength and toughness of polymers are primarily dependent on secondary relaxations.

There have been proposed several types of short-range molecular motions to account for the various transitions. Following Heijboer (1977), Fig. 13.30 illustrates schematically possible modes of molecular motion in secondary relaxation in glassy polymers. The classification is outlined below.

- Type A. From Wilbourn's observations (1958) it became clear that many amorphous polymers with successive $-\text{CH}_2-$ groups in the backbone show a mechanical dispersion at $-120\text{ }^\circ\text{C}$ and 1 Hz. Various mechanisms have been proposed to explain this behaviour. It involves a small segment in the backbone, e.g. 6 $-\text{CH}_2-$ groups, and it is attributed to a so-called crank-shaft mechanism: a rotation of the six $-\text{CH}_2-$ groups around the C_1-C_7 axes. 4 and 5 CH_2 groups are also mentioned. An illustration of various models is shown in Fig. 13.31. According to Schatzki the model is also useful for polymers with small side groups, e.g. $-\text{CH}_3$ groups or Cl atoms. A disadvantage is that much free volume is needed and the secondary transitions are in general not very much dependent on pressure. Nevertheless this type of motion has been attributed to the β -relaxation in rigid poly(vinyl chloride), to the γ -relaxation in polycarbonate and to secondary loss peaks in polysulphon, polyesters and polyamides.
- Type B. This type of molecular motion involves the rotation of a whole side group, e.g. the n-alkyl ester group in poly (n-alkyl methacrylates) and poly (n-alkyl acrylates). It does not necessarily mean that a complete rotation is made. Moreover a cooperative motion of the backbone might be required for this partly rotation.
- Type C. A localised motion of a part of the side group involved in Type B, e.g. the alkyl group of the ester group. This motion is responsible for the γ -relaxation in poly (n-alkyl methacrylates) and poly (n-alkyl acrylates). In addition, the δ -relaxation in poly(n-alkylmethacrylates) is due to rotation of the side chain $-\text{CH}_3$ group, directly bound to the backbone.

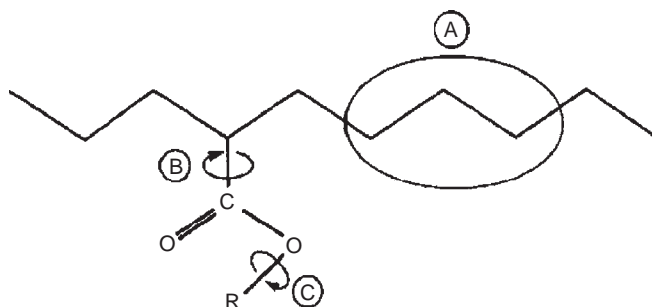


FIG. 13.30 Schematic illustration of the possible modes of molecular motion in secondary relaxation in glassy polymers. Reproduced with permission from Heijboer J (1977), Int J Polym Mat 6 (1&2) 11. Copyright Taylor and Francis Ltd., <http://www.informaworld.com>.

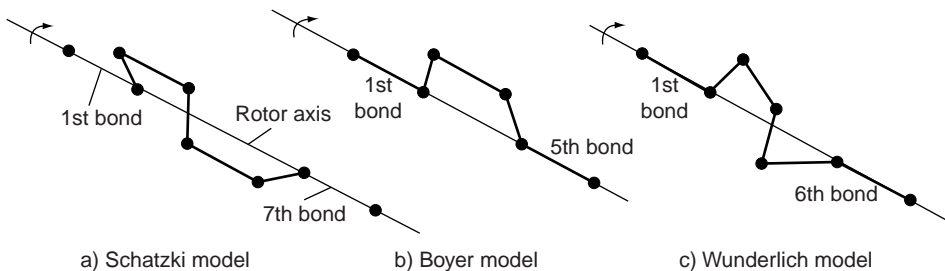


FIG. 13.31 Crankshaft models of rotability of main chain according to (a) the Schatzki model with rotation around the first and seventh bond; (b) the Boyer model with rotation around the first and fifth bond; (c) the Wunderlich helix model with rotation around the first and sixth bond. From Haward (1973). Courtesy Chapman & Hall.

For the molecular origins of the secondary relaxation processes the reader is referred to McCrum, Read and Williams (1967) to start with. However, since that time considerable progress has been made in the determination of the relation between the secondary processes and molecular motions (see, e.g. Chap. 3.3 in Haward and Young, 1997).

13.4.5. Glass transition temperature and volume retardation

Creep and stress relaxation of polymeric solids depend on the state of the polymer. Both effects are much faster and stronger for a material that was quenched from the liquid state (i.e. the state above the glass transition temperature) to room temperature than for a material that was cooled down slowly. This is due to the process of volume retardation.

When an amorphous polymer is gradually cooled from above the glass transition temperature T_g its volume decreases (see Fig. 13.32) according to its thermal expansion coefficient α_l . In the region around the T_g the volume decrease will lag behind, starting at temperature T_{e1} because the rate of reorganisation process becomes too small. The polymer starts to vitrify and a temperature T_{e2} will be reached where the reorganisation completely stops and where the vitrification process is completed. Decrease of volume is only the result of normal volume contraction with expansion coefficient α_g . The relationship between both thermal expansion coefficients is

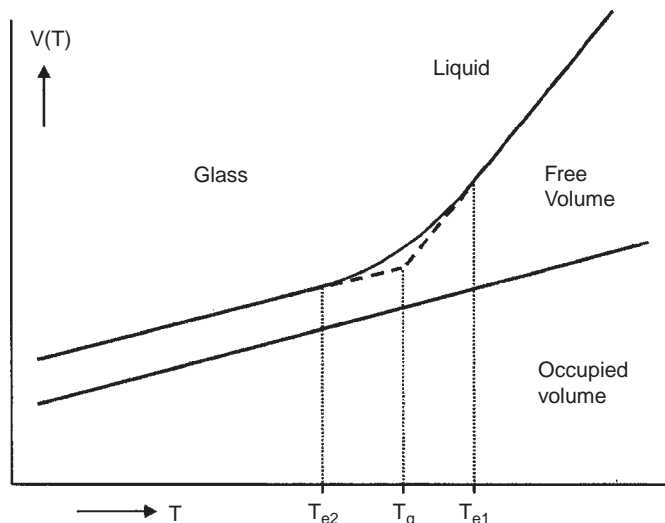


FIG. 13.32 Schematic diagram of volume-temperature relationship for an amorphous polymer around the glass transition temperature.

$$\alpha_l - \alpha_g = \Delta\alpha = \alpha_f \quad (13.98)$$

where α_f depicts the thermal expansion of free volume relative to total volume, and accordingly determines the increase of the amount of free volume with temperature above T_g (see also Eq. (13.120)):

$$f(T > T_g) = f_g + \alpha_f(T - T_g) \quad (13.99)$$

Very careful volume-temperature measurements were reported by Greiner and Schwarzl (1984) on various polymers: in this way they were able not only to determine the glass transition temperature, but also the secondary transition temperatures in e.g. PMMA, PS, PVC and PC and also the corresponding changes in the thermal expansion coefficients.

The value of T_g depends on the rate of the temperature decrease: it decreases with decreasing cooling rate, as is shown in Fig. 13.33 where the cooling rate decreases from q_1 to q_3 . This alone already shows that the glass transition temperature is not a thermodynamic parameter but kinetically determined.

When a sample is quickly cooled down from the liquid state to point A, in the glassy region, a relatively high glass temperature is obtained (see Fig. 13.34). If this point is not far from the "normal" glass transition temperature, in the course of time the volume will decrease and the equilibrium state will be reached at point B, where the glass transition temperature has a lower value. This process is called *volume retardation*. On the other hand, after cooling down to a lower temperature, point D, volume relaxation will also occur, but the rate of the process is so small, that within reasonable time (years, e.g.) the equilibrium state will not be reached: volume retardation will occur so slowly that point D will be reached only. Upon heating from this point on the equilibrium state will be reached at point E.

13.4.5.1. Hysteresis in the V-T-diagram

Cooling down from a temperature above T_{e1} to a temperature below T_{e2} immediately followed by heating up with the same rate as the cooling process is a source for hysteresis. This is shown in Fig. 13.35. In the vitrification region between T_{e1} and T_{e2} some volume

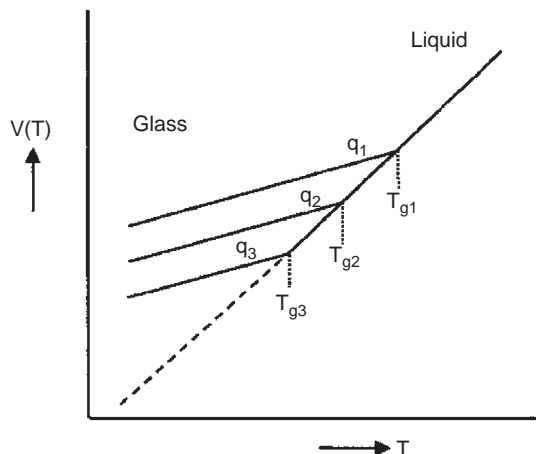


FIG. 13.33 Schematic diagram of volume-temperature relationship for an amorphous polymer around the glass transition temperature for three different cooling rates: $q_1 > q_2 > q_3$.

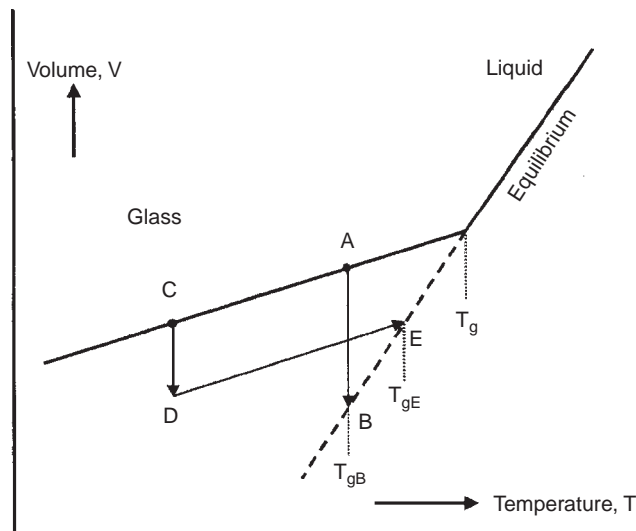


FIG. 13.34 Volume retardation after a jump of temperature; at point A complete retardation is possible, whereas at point C only partial retardation is possible in reasonable time.

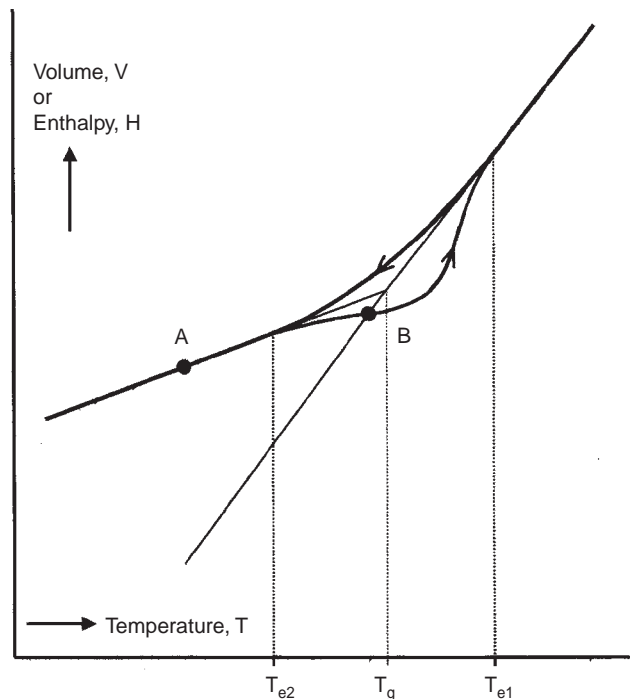


FIG. 13.35 Schematic diagram of volume hysteresis at cooling and subsequent heating with the same rate.

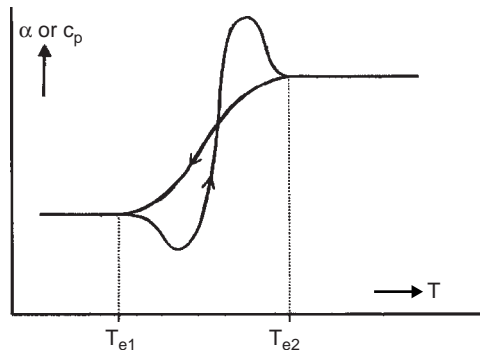


FIG. 13.36 Schematic diagram of volume expansion coefficient α during cooling, followed by heating with the same rate.

retardation will take place. The upper curved line between the two temperatures shows this. Upon heating from point A volume retardation will start again at temperature T_{e2} , so that the volume does not increase as fast as expected. Upon reaching the equilibrium line at point B volume decrease will stop. Point B is the glass transition temperature that would be reached upon cooling the sample from the liquid state with a very low cooling rate. Because the heating rate is too high, the opposite retardation, with increase of volume, will lag behind so that the equilibrium line will be crossed. Close to the temperature T_{e1} the volume retardation is so fast that the equilibrium line will be reached again. Qualitatively the same curve will be obtained upon measuring the enthalpy H as a function of temperature.

The result for the thermal expansion coefficient, α , which is equal to $(dV/dT)/V$, is shown in Fig. 13.36 for the cooling and heating process. In the cooling process α decreases gradually from α_l to α_g . Hysteresis in the volume causes in the subsequent heating process an anomalous effect in the thermal expansion coefficient, depicted by undershoot and overshoot, as also shown in Fig. 13.36. A similar effect occurs in enthalpy H and accordingly in c_p , the specific heat capacity, equal to dH/dT . This effect is frequently observed in DSC (Differential Scanning Calorimetry) experiments.

13.4.5.2. Volume retardation

After a temperature quench from T_0 to T_1 with $\Delta T = T_1 - T_0 > 0$ an almost instantaneous volume decrease from V_0 to V_1 occurs, determined by the thermal expansion coefficient α_g . Subsequently the volume gradually decreases (*volume retardation*) to V_∞ as determined by the $\Delta\alpha = \alpha_l - \alpha_g$ (see Figs. 13.37 and 13.38):

$$V_1 - V_0 = V_0\alpha_g(T_1 - T_0) = V_0\alpha_g\Delta T \quad \text{and} \quad V_\infty - V_0 = V_0\alpha_l(T_1 - T_0) = V_0\alpha_l\Delta T \quad (13.100)$$

Volume retardation occurs according to

$$V(t) = V_\infty + (V_1 - V_\infty)f(t) = V_\infty + (V_1 - V_\infty)\sum_i \exp(-t/\tau_{ri}) \quad (13.101)$$

where $f(t)$ is the retardation function, which might be approximated by a single exponential function $\exp(-t/\tau_r)$, where τ_r is the retardation time. In many cases, however, a sum of exponentials is needed to describe the retardation behaviour as depicted in Eq. (13.101).

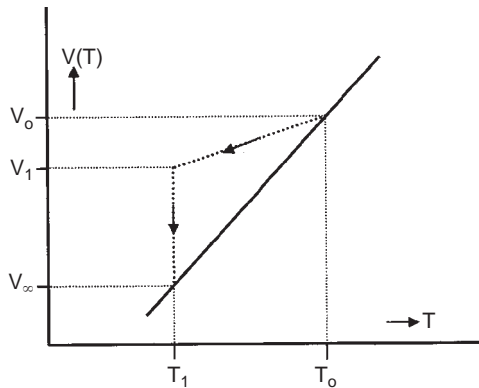


FIG. 13.37 Schematic diagram of volume–temperature path in the temperature jump method. The solid line is the equilibrium line.

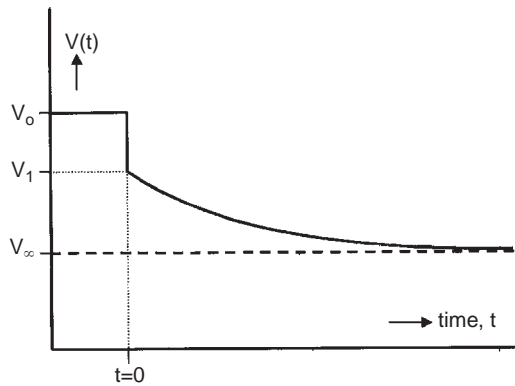


FIG. 13.38 Schematic diagram of volume retardation curve after a jump of temperature.

The retardation curve is normalised by plotting $[V(t) - V_\infty]/[V_1 - V_\infty]$ vs. $\ln t$. Because the volume retardation immediately starts after the temperature quench the volume V_1 is difficult to determine, but it can be calculated by subtracting both Eqs. (13.100):

$$V_1 = V_\infty + V_0(\alpha_g - \alpha_l)(T_1 - T_0) = V_\infty - V_0\Delta\alpha\Delta T \quad (13.102)$$

Another problem is that several minutes are needed to obtain thermal equilibrium, whereas volume retardation immediately starts after the temperature quench. In order to overcome this equilibrium time volume retardation can also be measured following a pressure quench, which takes only a few seconds to reach equilibrium. The corresponding equations are

$$V_1 - V_0 = -V_0\kappa_g(P_1 - P_0) = -V_0\kappa_g\Delta P \quad \text{and} \quad V_\infty - V_0 = -V_0\kappa_l(P_1 - P_0) = -V_0\kappa_l\Delta P \quad (13.103)$$

$$V_1 = V_\infty - V_0(\kappa_g - \kappa_l)(P_1 - P_0) = V_\infty + V_0\Delta\kappa\Delta P \quad (13.104)$$

Classic studies concerning volume retardation were made by Kovacs (1963) and by Goldbach and Rehage (1966, 1967). Illustrations of typical isothermal volume retardation curves are shown in Fig. 13.39 for atactic polystyrene, where the volume retardation is

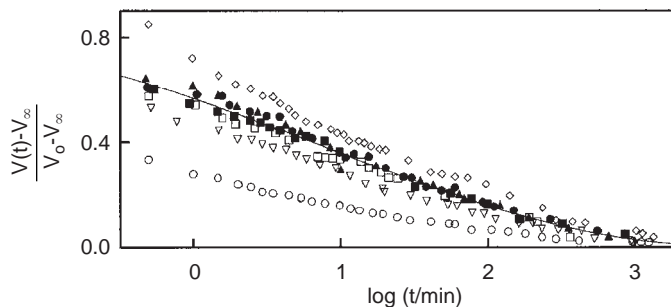


FIG. 13.39 Volume-retardation curves after a jump of temperatures $\Delta T = T_1 - T_0$ from T_0 to $T_1 = 90.70\text{ }^\circ\text{C}$ at 1 atm. $\Delta T = (\diamond) + 1.04\text{ }^\circ\text{C}; (\blacktriangle) + 0.60\text{ }^\circ\text{C}; (\bullet) - 0.60\text{ }^\circ\text{C}; (\blacksquare) - 1.12\text{ }^\circ\text{C}; (\square) - 1.80\text{ }^\circ\text{C}; (\triangledown) - 3.23\text{ }^\circ\text{C}; (\circ) - 10.79\text{ }^\circ\text{C}$. From Goldbach and Rehage (1967). Courtesy Springer Verlag.

shown after quenching from temperatures T_0 , varying from 89.66 to $101.49\text{ }^\circ\text{C}$, to the retardation temperature $T_1 = 90.70\text{ }^\circ\text{C}$ (Goldberg and Rehage). The ordinate is the normalised retardation. It can be concluded that the retardation cannot be described with one retardation time only, because in that case the normalised volume would decrease in two time decades from 1 to 0. It also shows that the retardation process is not linear, which means that increasing the temperature quench by a factor of 2 does not imply that the retardation is increased by a factor of 2: linearity is only obtained for small temperature quenches, viz. $-0.5\text{ }^\circ\text{C} < \Delta T < 2\text{ }^\circ\text{C}$. This means that the dilatation retardation ($\Delta T > 0$) is linear over a larger temperature quench than the contraction retardation ($\Delta T < 0$). Goldberg and Rehage also showed (Fig. 13.40) that the retardation curve is linear for (negative) pressure quenches of more than 25 atm, i.e. $\Delta P < 0$. Finally they mentioned that reasonable retardation curves are obtained for ageing temperatures $-10\text{ }^\circ\text{C} < T_1 - T_g < 10\text{ }^\circ\text{C}$. For lower ageing temperatures the retardation is too slow and for higher ageing temperatures it is too fast.

From the preceding discussion it is clear that ageing does substantially affect the glass-rubber transition. The effect of ageing on secondary transitions has been the subject of many studies (see, e.g. Howard and Young, 1997). From Struik's observations on a large number of amorphous polymers it has become clear that thermal history does not affect the secondary transitions (Struik, 1987).

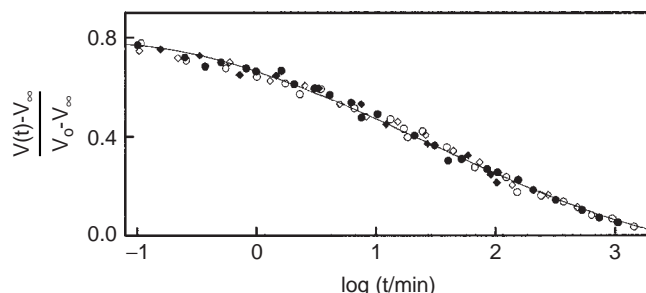


FIG. 13.40 Volume-retardation curves after a jump of pressures $\Delta P = P_1 - P_0$ from P_0 to $P_1 = 1\text{ atm}$ at $91.84\text{ }^\circ\text{C}$. $\Delta P = (\circ) -22.3\text{ atm}; (\bullet) -11.2\text{ atm}; (\diamond) -5.6\text{ atm}; (\blacklozenge) -2.8\text{ atm}$. From Goldbach and Rehage (1967). Courtesy Springer Verlag.

13.4.6. Stress relaxation and creep

Stress relaxation and creep are measured with the aid of two distinct experimental methods, which are frequently used in the mechanical testing of solid polymers, especially over longer periods.

13.4.6.1. Stress relaxation

Stress relaxation is the time-dependent change in stress after an instantaneous and constant deformation and constant temperature. As the shape of the specimen does not change during stress relaxation, this is a pure relaxation phenomenon in the sense defined at the beginning of this section. It is common use to call the time dependent ratio of tensile stress to strain the *relaxation modulus*, E , and to present the results of the experiments in the form of E as a function of time. This quantity should be distinguished, however, from the tensile modulus E as determined in elastic deformations, because stress relaxation does not occur upon deformation of an ideal rubber.

The stress-relaxation behaviour of polymers is extremely temperature-dependent, especially in the region of the glass temperature.

In the transition region a plot of the logarithm of the tensile relaxation function $(\sigma(t)/\varepsilon_0)$ against the logarithm of time is an almost straight line with a negative slope. This behaviour can be approximated by the empirical formula:

$$\frac{\sigma(t)}{\varepsilon_0} \equiv E(t) \approx Kt^{-n} \quad (13.105)$$

where ε_0 is the instantaneous deformation and K and n are constants.

For amorphous polymers the constant n may vary between 0.5 and 1.0; n , a dimensionless number, is a measure of the relative importance of elastic and viscous contributions to stress relaxation; it is closely related to $\tan \delta$:

$$\tan(n\pi/2) \approx \tan \delta \quad (13.106)$$

Another approximation of the tensile relaxation function is that of the Maxwell model:

$$\frac{\sigma(t)}{\varepsilon_0} \equiv E(t) = E \exp(-t/\tau) \quad (13.80)$$

Eq. (13.80) is valid only in a rather limited time interval. If the behaviour over a longer time period must be described, a number of equations of this type can be superposed, each with a different relaxation time. Ultimately, a whole *relaxation time spectrum* may be developed:

$$\frac{\sigma(t)}{\varepsilon_0} \equiv E(t) = \sum_{i=1}^N E_i \exp(-t/\tau_i) \quad (13.81)$$

In practice the stress relaxation also depends on the time elapsed since the sample was cooled down from above to temperatures below T_g . This is due to the volume retardation phenomenon, which, as mentioned before, is a decrease of free volume. This volume retardation hinders to an increasing degree the movements of (parts of) the polymer chains and thus causes the relaxation times to increase with ageing. For a material that experienced a temperature quench only shortly ago, the volume retardation is still relatively fast, so that the relaxation times are relatively large. In the course of time the relaxation times increase, and consequently the stress relaxation will proceed slower. An illustrative example is shown in Fig. 13.41, where the effect of cooling rate on stress relaxation of poly(methyl methacrylate) is shown. Small and large cooling rates gives

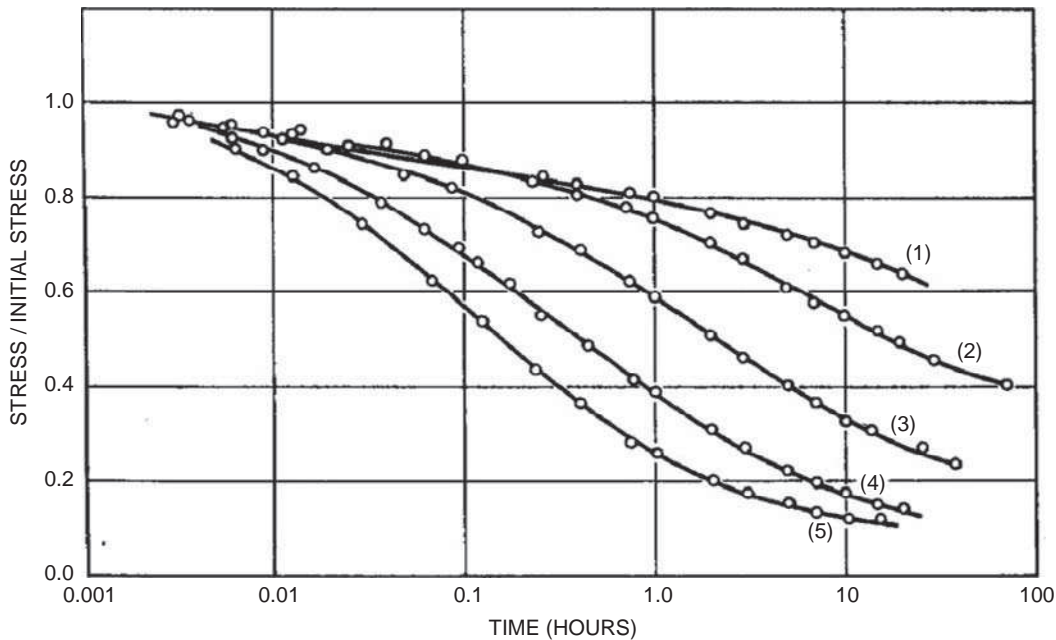


FIG. 13.41 Effect of cooling rate on stress relaxation of poly(methyl methacrylate) at 80 °C. Sample cooled from 130 °C as follows: (1) 5 °C/h; (2) 30 °C/h; (3) convection in 25 °C air; (4) plunged in 25 °C oil; (5) plunged in dry ice-naphtha bath (~ -80 °C) and subsequently measured at 80 °C. From McLoughlin, and Tobolsky (1951). Courtesy John Wiley & Sons, Inc.

rise to a relatively small and large free volumes and accordingly relatively slow and fast stress relaxations.

Equations proposed by Struik (1977, 1978) that are able to describe experimental stress relaxation below T_g are:

for short-time experiments

$$\frac{\sigma(t)}{\varepsilon_0} \equiv E(t) = E_0 \exp [(-t/\tau_0)^m]; \quad m \approx 1/3 \quad (13.107)$$

and for long-term tests

$$\frac{\sigma(t)}{\varepsilon_0} \equiv E(t) = E_0 \exp [-(t_e/\tau_0)^m \ln^m (1 + t/t_e)] \quad (13.108)$$

where ε_0 = instantaneous deformation; $\sigma_0 = E_0 \varepsilon_0$, i.e. stress at start of test; t_e = time of polymer, elapsed after quenching of melt, also called ageing time; τ_0 = characteristic constant for the material, dependent on T and on t_e ; m = constant with a value about $1/3$.

Eq. (13.108) is graphically represented in Fig. 13.42.

The relationship between t_o and t_e is approximated by Struik (1977, 1978) to be constant, but t_e/t_o increases with increasing temperature. In Fig. 13.43 it becomes more clear that the relaxation is slower with increasing ageing time t_e .

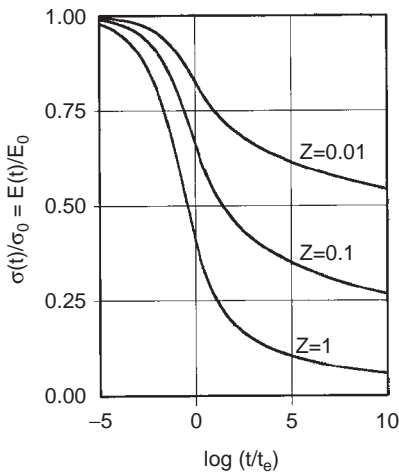


FIG. 13.42 Stress-relaxation according to Eq. (13.90) for various values of $Z = t_e/t_o$. From Struik (1977, 1978). Courtesy of the author and of Elsevier Science Publishers.

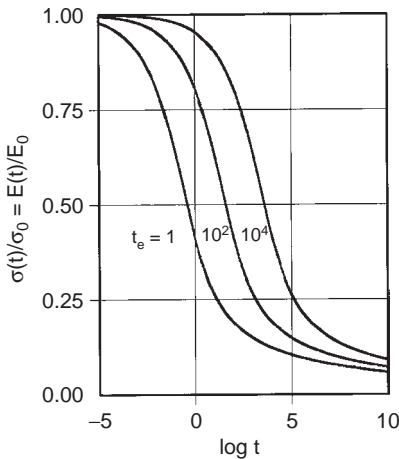


FIG. 13.43 Stress relaxation according to Eq. (13.90) for various values of ageing time t_e .

13.4.6.2. Creep (elasto-plasticity)

Dimensional stability is one of the most important properties of solid materials, but few materials are perfect in this respect. Creep is the time-dependent relative deformation under a constant force (tension, shear or compression). Hence, creep is a function of time and stress. For small stresses the strain is linear, which means that the strain increases linearly with the applied stress. For higher stresses creep becomes non-linear. In Fig. 13.44 typical creep behaviour of a glassy amorphous polymer is shown: for low stresses creep seems to be linear. As long as creep is linear, time-dependence and stress-dependence are separable; this is not possible at higher stresses. The two possibilities are expressed as (Haward, 1973)

$$\varepsilon(\sigma, t) = f_1(\sigma)f_2(t) \quad \text{and} \quad \varepsilon(\sigma, t) = F(\sigma, t) \quad (13.109)$$

The first equation is much easier to manipulate than the second one. A simple check for separability of the variables is that curves of log strain vs. log time with stress as

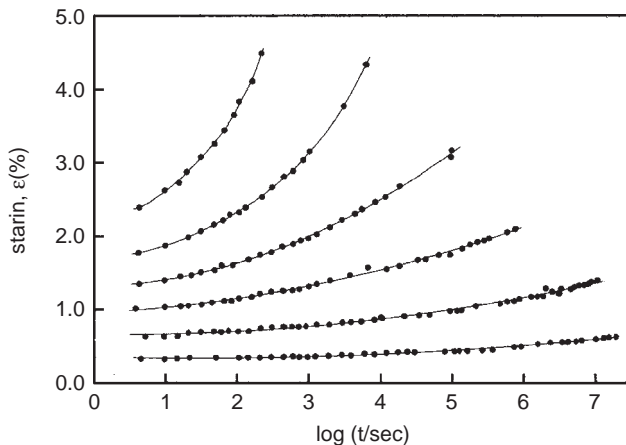


FIG. 13.44 Typical tensile creep behaviour of a glassy amorphous polymer (a modified PMMA at 20 °C), where strain is plotted vs. log time, for various values of tensile stress. From bottom to top 10, 20, 30, 40, 50 and 60 MPa. From Haward (1973). Courtesy Chapman & Hall.

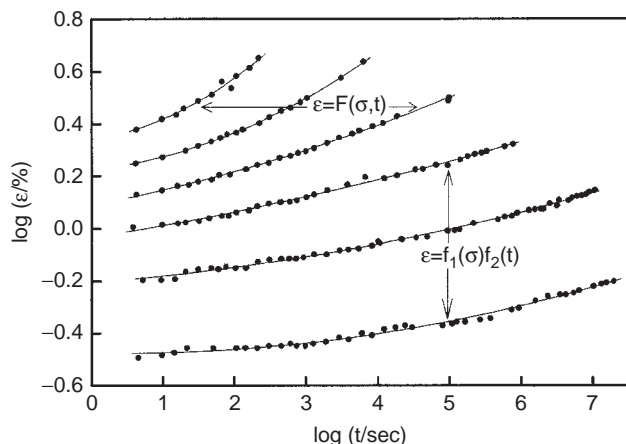


FIG. 13.45 The results from Fig. 13.44, now plotted as log strain vs. log time. From bottom to top 10, 20, 30, 40, 50 and 60 MPa. The stress-dependence and time dependence are separable at stresses below about 35 MPa and inseparable at stresses above about 35 MPa.

parameter, will be parallel. This is shown in Fig. 13.45, where it is clear that at low stresses the first equation is fulfilled and at high stress the second equation.

As the amount of deformation increases, viscous phenomena become increasingly important. At a given moment the specimen may show *yielding*, i.e. rapid viscous deformation.

The results of creep experiments are usually expressed in the quantity *creep compliance*, the time-dependent quotient of strain and stress.

Creep properties are very much dependent upon temperature. Well below the glass transition point very little creep will take place, even after long periods of time. As the temperature is raised, the rate of creep increases. In the glass-transition region the creep properties become extremely temperature-dependent. In many polymers the creep rate goes through a maximum near the glass-transition point.

A well-known simplified equation for the tensile creep function is *Nutting's empirical formula* (1921):

$$\frac{\varepsilon(t)}{\sigma_0} = S(t) = Kt^n \quad (13.110)$$

where σ_0 = the instantaneous applied stress and K and n are constants. For n the same reasoning is valid as for the stress relaxation. If $n\pi/2 \ll 1$:

$$\tan(n\pi/2) \approx \tan \delta \quad (13.111)$$

A second approximation of the tensile creep function is the Voigt-Kelvin model

$$\frac{\varepsilon(t)}{\sigma_0} = S_{\text{ret}}(t) = S[1 - \exp(-t/\tau)] \quad (13.86)$$

Also in this case, several retardation phenomena with different retardation times may be superposed.

The simple relaxation and retardation phenomena described by Eqs. (13.80) and (13.86) show some analogy with a chemical reaction of the first order. The reaction rate constant corresponds with the reciprocal relaxation (or retardation) time. In reality, these phenomena show even more correspondence with a system of simultaneous chemical reactions.

Here again two formulae proposed by Struik (1977, 1978) have to be mentioned:
for short-time tests:

$$\frac{\varepsilon(t)}{\sigma_0} \equiv S(t) = S_0 \exp\left[\left(t/\tau_0\right)^m\right]; \quad m \approx 1/3 \quad (13.112)$$

and for long-time tests:

$$\frac{\varepsilon(t)}{\sigma_0} \equiv S(t) = S_0 \exp\left[\left(t_e/\tau_0\right)^m \ln^m(1 + t/t_e)\right] \quad (13.113)$$

The symbols in Eqs. (13.112) and (13.113) have the same significance as in Eqs. (13.107) and (13.108). Fig. 13.46 gives illustrations of Eqs. (13.112) and (13.113). Of course the reciprocals of the various compliances are equal to the elastic moduli presented in Fig. 13.42 Equations of the same form are valid for the shear compliance $J(t)$.

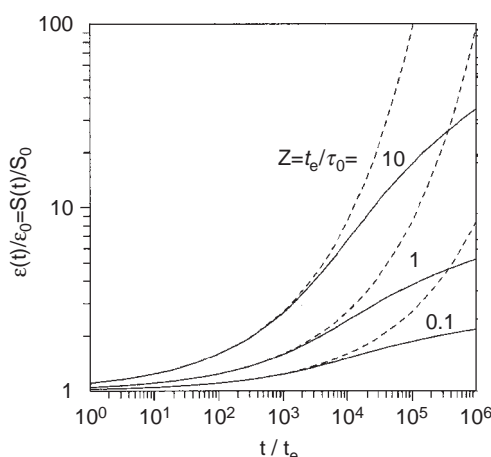


FIG. 13.46 Creep according to Eq. (13.112) (dashed lines) and to Eq. (13.113) (full lines) for various values of Z.

13.4.7. Struik's rules on physical ageing

Outstanding work has been accomplished in the complex field of time-dependent viscoelastic phenomena (volume relaxation, physical ageing, stress relaxation, creep, etc.) by Struik (1977, 1978). He studied nearly all aspects of this field, but paid special and careful attention on tensile and torsional creep. An example of his careful measurements are creep measurements on poly(vinyl chloride). Creep measurements in general suffer from ageing processes during long time creep, just as was mentioned for stress relaxation, because the creep retardation times increase (approximately) proportional to the ageing time t_e . In order to distinguish between creep with constant time constants (retardation times) and ageing, PVC samples were quenched from 90 °C (i.e. above T_g of 80 °C) to 40 °C and further kept at 40 °C for a period of 4 years. During that time at various ageing times t_e creep measurements were carried out on samples during a time shorter than 15% of the actual ageing time. During those measurements the retardation times may be considered to be constant. Results are shown in Fig. 13.47. The creep rate decreases with increasing ageing time due to decrease of free volume, but the curves are parallel and superposition by almost horizontal shifts is possible, in order to obtain one master curve. Master curves obtained at different temperatures could also be superposed by almost horizontal shifts to obtain one super master curve (see Fig. 13.48 (left)) at one chosen temperature and one chosen ageing time. In Fig. 13.48 (right) final results at other temperatures are shown. There, the effect of creep measurements where measuring time exceeds the ageing time, also becomes clear: creep turns out to be less fast, because during the measurements the volume retardation is continuing in the way described before, thereby causing the free volume to decrease. Both the shortly aged and long-aged curves in Fig. 13.48 (right) resemble theoretical curves presented in Fig. 13.46.

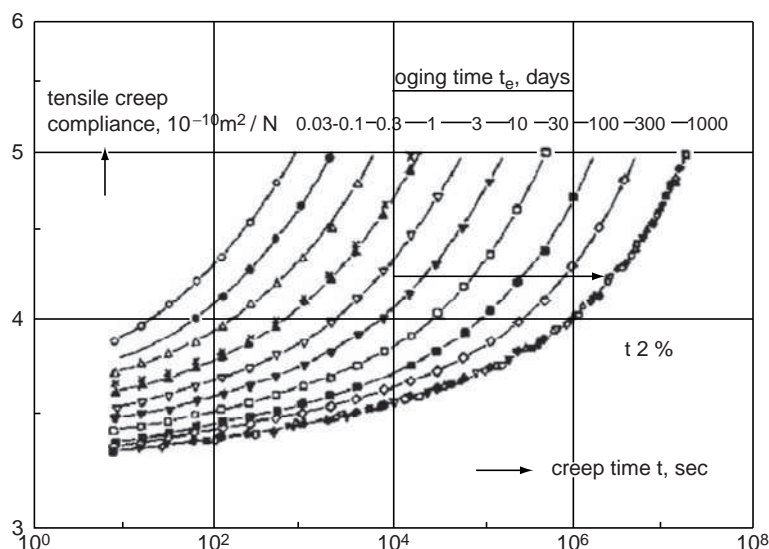


FIG. 13.47 Small strain tensile creep curves of rigid PVC quenched from 90 °C (i.e. about 10 °C above T_g) to 40 °C and further kept at 40 ± 0.1 °C for a period of 4 years. The different curves were measured for various values of time t_e elapsed after the quench. The master curve gives the result of a superposition by shifts that were almost horizontal; the arrow indicates the shifting direction. The crosses refer to another sample quenched in the same way, but only measured for creep at a t_e of 1 day. From Struik (1977, 1978). Courtesy of the author and of Elsevier Science Publishers.

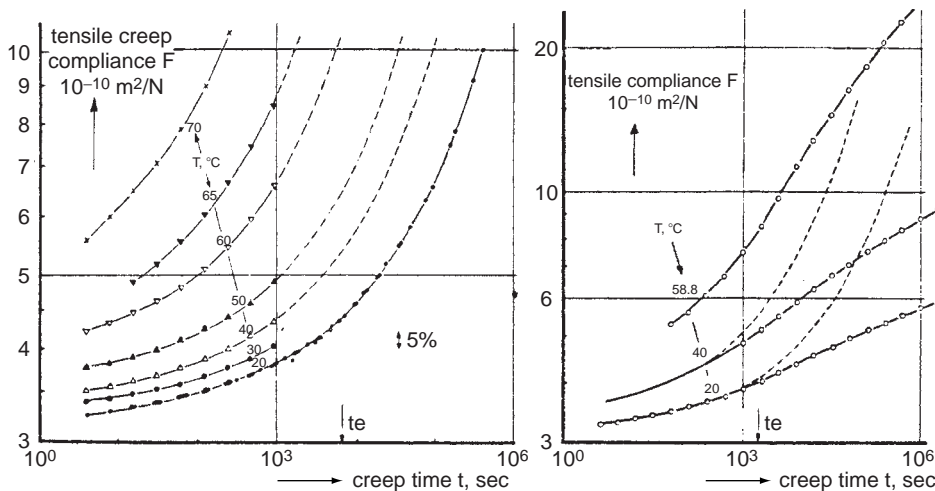


FIG. 13.48 Small-strain tensile creep of rigid PVC. Left: short-time tests ($t \leq 1000 \text{ s}$) at a t_e of 2 h after quenches from 90 °C to various temperatures ($t/t_e \leq 0.13$). The master curve at 20 °C was obtained by time-temperature superposition (compare Section 13.4.8); the dashed curves indicate the master curves at other temperatures. Right: long-term tests ($t = 2 \times 10^6 \text{ s}$, $t_e = 1/2 \text{ h}$, $t/t_e = 1100$). The dashed lines are the master curves at 20 and 40 °C for a t_e of 1/2 h; they were derived from the left-hand diagram. From Struik (1977, 1978). Courtesy of the author and of Elsevier Science Publishers.

We shall try to summarise Struik's work in 10 conclusions, or better "propositions"

1. Physical ageing or "age stiffening" – is a thermo-reversible process, that occurs in all glassy materials and affects their properties primarily by changing the relaxation times, all of them in the same way.
2. The origin of the phenomenon of ageing lies in the fact that glasses are not in thermodynamic equilibrium; their volume and entropy are too large, hence there is a tendency to volume reduction (volume retardation). Decreases of rates of stress relaxation and creep are consequences of this phenomenon.
3. Nearly all aspects of physical ageing can be explained by means of the "free volume" concept, i.e. the hypothesis that the mobility of particles (atoms, molecules) is mainly determined by their packing density.
4. Ageing does not affect secondary thermodynamic transitions; so the range of ageing falls between T_g and the first secondary transition T_β .

Propositions 1–4 are schematically illustrated by Figs. 13.49 and 13.50.

5. Physical ageing is important from a practical point of view. Application of polymeric materials is even based on ageing: without progressive stiffening, due to physical ageing, polymeric materials would not be able to resist mechanical loads during long periods of time.
6. All polymers age in the same way, their relaxation times increasing proportionally to the ageing time. Proposition 6 is illustrated by Fig. 13.51.
7. The small-strain viscoelastic behaviour of all amorphous polymers is similar, so that in a limited region it can be described by a single universal formula

$$J(t) = J_0 \exp[(t/t_0)^m], \quad \text{with } m = 1/3 \quad (13.114)$$

where $J(t)$ = creep compliance; J_0 = constant related to the vertical shift factor; t_0 = constant related to the horizontal shift factor.

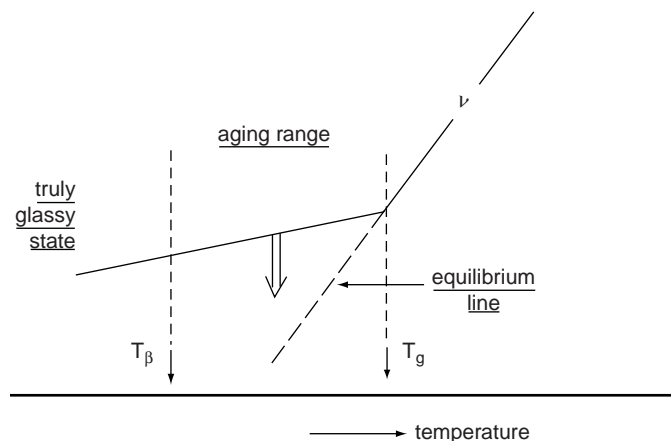


FIG. 13.49 Origin of aging. T_g is the glass transition temperature, T_β the temperature of the highest secondary transition, and ν the specific volume. From Struik (1977, 1978). Courtesy of the author and of Elsevier Science Publishers.

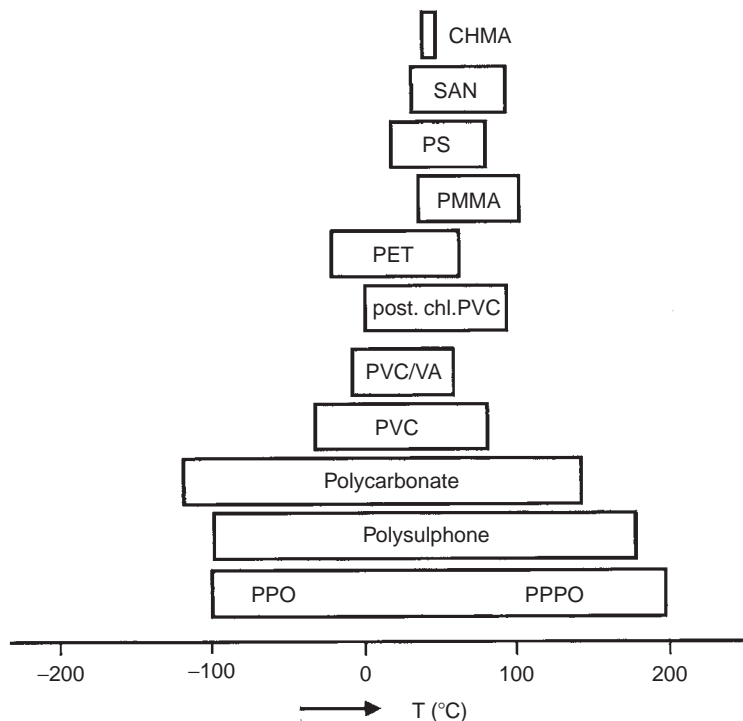


FIG. 13.50 Temperature ranges of strong ageing for various polymers. From Struik (1977, 1978). Courtesy of the author and of Elsevier Science Publishers.

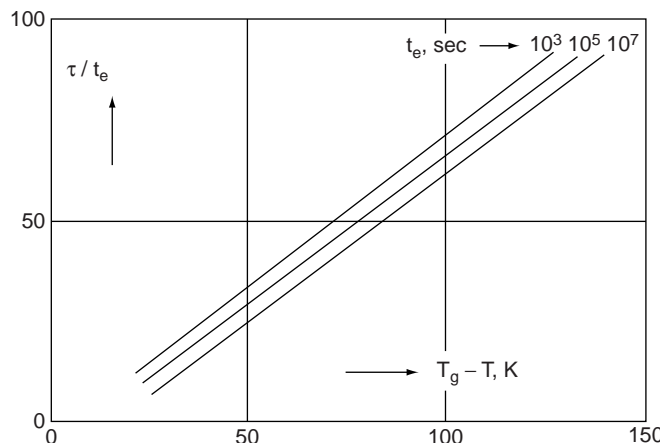


FIG. 13.51 Variation of relaxation time τ in the glassy state with temperature, T , and aging time, t_e . From Struik (1977, 1978). Courtesy of the author and of Elsevier Science Publishers.

- By means of horizontal and vertical shifting the curves of all materials can be superimposed. Proposition 7 is illustrated by Fig. 13.52.
8. Physical ageing persists for very long periods; at temperatures well below ($T_g - 25$) K it may persist for hundreds of years. Fig. 13.53 is the illustration.

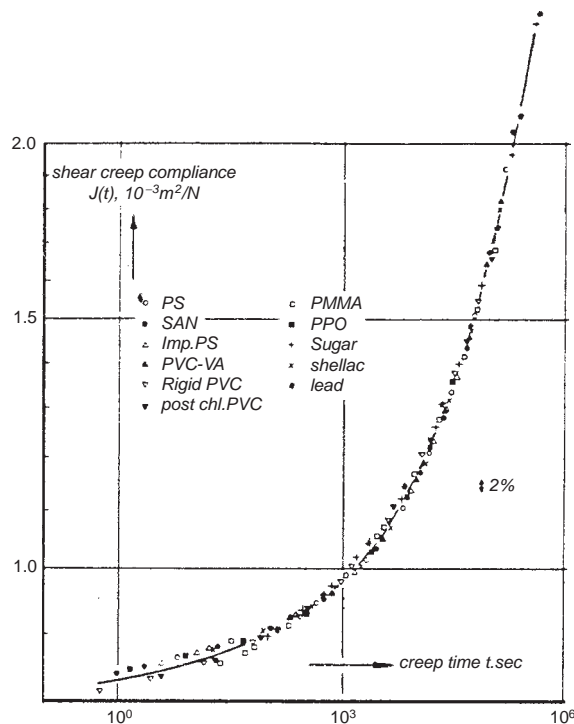


FIG. 13.52 Temperature ranges in which the data were originally measured are indicated. The master curves for the different materials were superimposed by horizontal and vertical shifts. From Struik (1977, 1978). Courtesy of the author and of Elsevier Science Publishers.

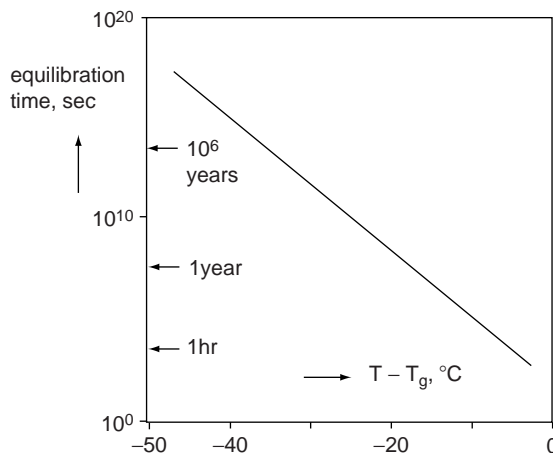


FIG. 13.53 Time t_∞ necessary for attainment of thermodynamic equilibrium. From Struik (1977, 1978). Courtesy of the author and of Elsevier Science Publishers.

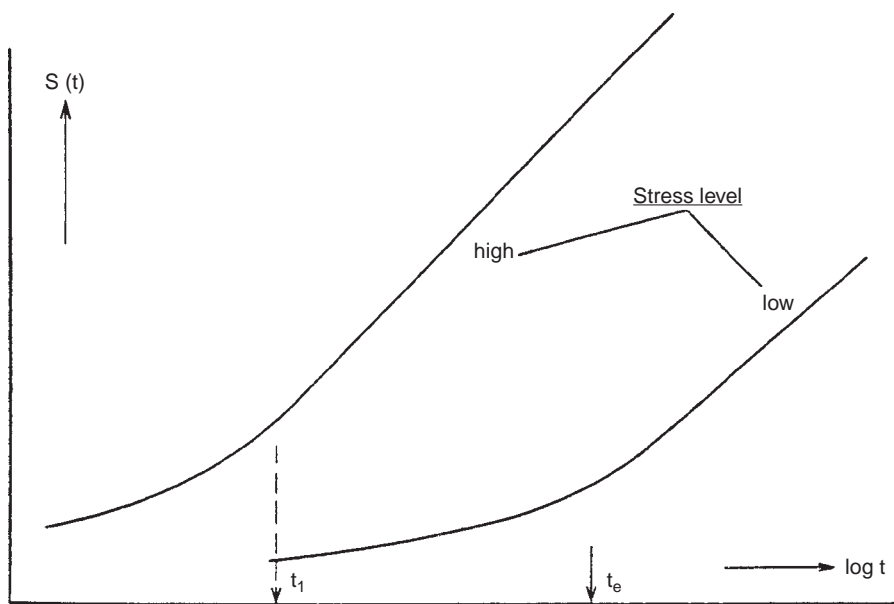


FIG. 13.54 Effect of the stress level on creep compliance $F(t) = \varepsilon(t)/\sigma_0$; ε is the strain, σ_0 the constant stress. For very low stresses (spontaneous ageing), the $F(t)$ versus $\log t$ curve becomes straight for $t > t_e$. For high stresses, the straight line region sets in at $t_1 < t_e$ because of stress-activated ageing.

9. Physical ageing is counter-acted by high stresses and large deformations, due to formation of "new" free volume. Proposition 9 is illustrated by Fig. 13.54.
10. The long-term behaviour of polymers is fundamentally different from the short time behaviour; the first cannot be explained from the latter, if the ageing time is neglected. So the value of "accelerated tests" is dubious. Proposition 10 is illustrated by Fig. 13.48.

Thermo-reversible has the following meaning: if an amorphous polymer is heated to above T_g , it readily reaches thermodynamic equilibrium: by definition the sample has then "forgotten" its history, any previous ageing it may have undergone below T_g having been erased. In other words it is completely rejuvenated. Ageing therefore is a thermo-reversible process to which one and the same sample can be subjected an arbitrary number of times. It has just to be retreated each time to the same temperature above T_g .

Struik also (1987–1989) showed that his concept of physical ageing and its affects on the mechanical behaviour can be extended to semi-crystalline polymers; the only additional assumption needed is that in semi-crystalline polymers the glass transition is broadened and extended towards the high temperature side. Fig. 13.55 illustrates this.

Struik showed furthermore that for amorphous and semi-crystalline polymers the ageing effect after complicated thermal histories is strikingly similar. In both cases high stresses can erase previous ageing and "rejuvenate" the material.

Filled rubbers behave in the same way as semi-crystalline materials.

13.4.8. The time-temperature and time-pressure superposition principles (TTSP and TPSP)

13.4.8.1. The TTSP for amorphous polymers above T_g

Above T_g the stress relaxation and the creep behaviour of amorphous polymers obey the "time-temperature superposition (or equivalence) principle".

Leaderman (1943) was the first to suggest that in viscoelastic materials time and temperature are equivalent to the extent that data at one temperature can be superimposed upon data taken at a different temperature, merely by shifting curves. Williams et al. (1955), Tobolsky (1962) and Ferry (1962, 1970, 1980) have worked out this suggestion and demonstrated the validity of the principle; with their procedures it is possible to convert stress-relaxation data at widely different temperatures to a single curve covering many decades of time at some reference temperature. This superposition is frequently used because the time scale or frequency scale of the viscoelastic behaviour of polymers from the glass transition to the flow region covers 10 to 15 decades, depending on the molecular weight of the polymer. There are no instruments available to cover this range. Time temperature superposition is the remedy.

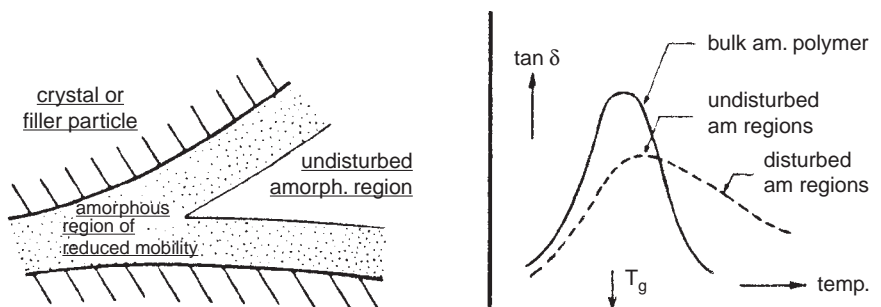


FIG. 13.55 Extended glass transition in semi-crystalline polymers and filled rubbers. From Struik (1977, 1978). Courtesy of the author and of Elsevier Science Publishers.

The principle can be applied as follows: The relaxation modulus:

$$\frac{\sigma(t)}{\varepsilon_0} = E(t) \quad (13.115)$$

is determined as a function of time (or frequency) and temperature.

Fig. 13.56 is chosen as an example showing the curves of polyisobutylene. These curves were corrected (reduced) for density and temperature. An arbitrary temperature T_o (K) (25 °C) was selected as the reference temperature. The reduced modulus values were calculated by

$$E(t)_{\text{red}} = \frac{\rho_o T_o}{\rho T} E(t) \quad (13.116)$$

The correction comes from the kinetic theory of rubber elasticity; it is relatively small and is sometimes neglected. (This reduction is of course not necessary for $\tan \delta$). The reduced curves can now be shifted, one at a time, with respect to the reference curve (at $T_o = 25$ °C), until portions of the curves superimpose to give a master curve such as also shown in Fig. 13.56. The amount each reduced modulus has to be shifted along the logarithmic time axis in making the master curve, the so-called *shift factor*, a_T , is a function of temperature. The determination of $\log a_T$ is quite difficult in the pseudo-rubbery region, where the curves are rather flat. As will be shown later, the same values of the shift factor are obtained by plotting $G'(\omega)$ and $G''(\omega)$ versus $\log \omega$. In the pseudo-rubbery region the curves for storage modulus are also rather flat, but the loss modulus goes through a minimum and accordingly the values of the shift factor are easier to determine.

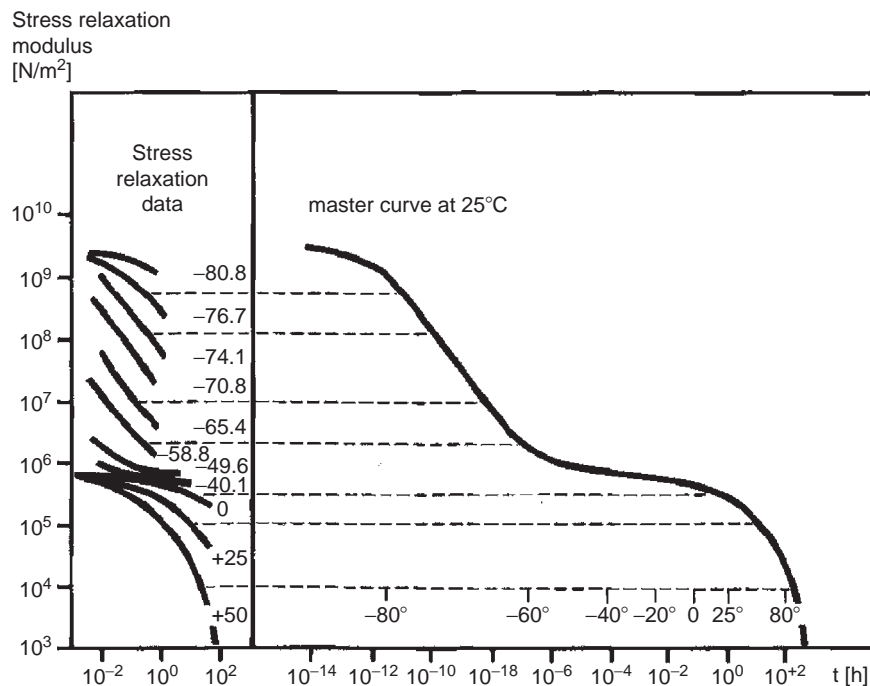


FIG. 13.56 Use of the time-temperature superposition illustrated with polyisobutylene data. The reference temperature of the master curve is 25 °C. From Eisele (1990), as reconstructed from Castiff and Tobolsky (1955, 1956). Courtesy Springer Verlag.

The generalised formula for the shift factor is, according to *Williams, Landel and Ferry* (1955):

$$\log(a_T)_{T_0} = \log[t(T_0)/t(T)] = \log[\omega(T)/\omega(T_0)] = \frac{-c_1^o(T - T_0)}{c_2^o + T - T_0} \quad (13.117)$$

From this equation it appears that the constants c_1^o and c_2^o may be obtained by plotting $(T - T_0)/\log a_T$ against $(T - T_0)$, because

$$\frac{T - T_0}{\log a_T} = -\frac{c_2^o}{c_1^o} - \frac{1}{c_1^o}(T - T_0) \quad (13.118)$$

If T_g is chosen as the reference temperature, then in Eq. (13.117) the subscripts and superscripts "o" has to be replaced by "g". The relationships between the constants c_1 and c_2 at the different reference temperatures are

$$\begin{aligned} c_2^g &= c_2^o + T_g - T_0 \\ c_1^g c_2^g &= c_1^o c_2^o \end{aligned} \quad (13.119)$$

The two pretended universal constants c_1^g and c_2^g are theoretically (under special assumptions) equal to 17.4 and 51.6, respectively. In general, different values are experimentally found for different polymers (see Table 13.10). Relationships between c_1^g and c_2^g and polymer properties are

$$\begin{aligned} c_1^g &= B/(2.303 f_g) \\ c_2^g &= f_g/\alpha_f \\ f_g &= B/(2.303 c_1^g) \approx 0.25B \\ \alpha_f &= B/(2.303 c_1^g c_2^g) \approx 4.8 \times 10^{-4} B \\ f(T > T_g) &= f_g + \alpha_f(T - T_g) \end{aligned} \quad (13.120)$$

where B = a constant, often taken equal to 1; f and f_g = fraction of free volume at T and T_g ; $\alpha_f = \Delta\alpha = \alpha_l - \alpha_g$.

Accordingly the WLF equation may also be expressed as

$$\log(a_T)_{T_g} = \frac{B}{2.303} \left(\frac{1}{f} - \frac{1}{f_g} \right) = -\frac{[B/(2.303 f_g)](T - T_g)}{f_g/\alpha_f + T - T_g} \quad (13.121)$$

If the following values are chosen: $B = 1$, $f_g = 0.025$ and $\alpha_f = 4.84 \times 10^{-4} \text{ }^\circ\text{C}^{-1}$, then the so-called "universal" constants are obtained: $c_1^g = 17.4$ and $c_2^g = 51.6$. That one has to be careful in using these values for c_1^g and c_2^g becomes clear from Table 13.10.

This WLF equation enables us to calculate the time (frequency) change at constant temperature, which – as far as the dynamic-mechanical behaviour is concerned – is equivalent to a certain temperature change at constant time (frequency). For temperatures below T_g deviations from the WLF equation are of course to be expected. This has been stated, for instance, by Rusch and Beck (1969).

TABLE 13.10 Parameters characterising temperature dependence of α_T for various polymer systems. Most data from Ferry (1980).

Polymer	T_o (K)	$c_1^0(-)$	$c_2^0(K)$	T_g (K)	$c_1^g(-)$	$c_2^g(K)$	f_g/B (-)	$\alpha_f/B \times 10^4$ (K^{-1})	$\Delta\alpha \times 10^4$ (K^{-1})
"Universal"					17.44	51.6	0.025	4.8	4.8
<i>General</i>									
Polyisobutylene	298	8.61	200.4	205	16.07	107.4	0.026	2.5	4.9
Poly(vinyl acetate)	349	8.86	101.6	305	15.63	57.6	0.028	5.9	4.4
Poly(vinyl chloroacetate) ^a	346	8.86	101.6	296	17.45	51.6	0.025	6.2	
Polystyrene	373	13.70	50.0	373	13.70	50.0	0.032	6.3	3.7
Poly(α -methyl styrene)	441	16.80	53.5	441	16.80	53.6	0.026	6.4	3.8
Poly(hexene-1)	218	17.40	51.6	218	17.40	51.6	0.020	9.7	
Poly(dimethyl siloxane)	303	1.90	222.0	150	6.11	69.0	0.071	10.3	10.9
Polyacetaldehyde ^a	243	14.50	24.0	243	14.50	24.0	0.030	12.5	
Poly(propylene oxide) ^a	198	16.20	24.0	198	16.20	24.0	0.027	11.3	
Styrene-n-hexyl methacrylate copolymer ^b	373	7.11	192.6	277	14.17	96.6	0.030	3.2	
Styrene-n-hexyl methacrylate copolymer ^c	373	6.56	156.4	287	14.57	70.4	0.030	4.2	
<i>Rubbers</i>									
Hevea rubber	248	8.86	101.6	200	16.80	53.6	0.026	4.8	
Polybutadiene, <i>cis-trans</i> ^d	298	3.64	186.5	172	11.22	60.5	0.039	6.4	
Polybutadiene, high <i>cis</i> ^e	298	3.44	196.6	161	11.35	59.6	0.039	6.4	
Polybutadiene, <i>cis-trans-vinyl</i> ^f	263	5.97	123.2	205	11.28	65.2	0.038	5.9	
Polybutadiene, high vinyl ^g	298	6.23	72.5	261	12.72	35.5	0.034	9.6	
Styrene-butadiene copolymer ^h	298	4.57	113.6	210	20.28	25.6	0.034	9.6	
Butyl rubber ⁱ	298	9.03	201.6	205	16.76	108.6	0.026	2.4	
Ethylene-propylene copolymer ^j	298	5.52	96.7	242	13.11	40.7	0.033	8.1	
Ethylene-propylene copolymer ^k	298	4.35	122.7	216	13.11	40.7	0.033	8.1	
Polyurethane ^l	283	8.86	101.6	238	15.90	56.6	0.028	8.5	
Polyurethane ^m	231	16.70	68.0	221	19.58	58.0	0.022	3.8	

(continued)

Table 13.10 (continued)

Polymer	T_o (K)	$c_1^0(-)$	c_2^0 (K)	T_g (K)	$c_1^g(-)$	c_2^g (K)	f_g/B (-)	$\alpha_f/B \times 10^4$ (K $^{-1}$)	$\Delta\alpha \times 10^4$ (K $^{-1}$)
<i>Methacrylate polymers</i>									
Methyl	381	34.00	80.0	381	34.00	80.0	0.013	1.6	4.1
Ethyl	373	11.18	103.5	335	17.67	65.5	0.025	3.7	3.0
<i>n</i> -Butyl	373	9.70	169.6	300	17.03	96.6	0.026	2.6	3.0
<i>n</i> -Hexyl	373	9.80	234.4	268	17.75	129.4	0.025	1.9	~2.5
<i>n</i> -Octyl	373	7.60	227.3	253	16.10	107.3	0.027	2.5	~2.5
2-Ethyl hexyl	373	11.58	208.9	284	20.18	199.9	0.021	1.8	
<i>Diluted systems</i>									
Poly(<i>n</i> -butyl methacrylates) in DEP 50%	273	9.98	153.1	206	17.74	86.1	0.024	2.8	3.0
Poly(<i>n</i> -butyl methacrylates) in DEP 60%	273	12.80	157.3	227	18.09	111.3	0.024	2.2	1.0
Pol(methyl methacrylates) in DEP 30%	298	7.11	130.1	211	22.50	41.1	0.020	4.7	2.0
Poly(vinyl chloride) in DBP ⁿ 10%	274	5.58	178.7	178	17.20	58.0	0.025	4.4	
Poly(vinyl chloride) in DOP ⁿ 10%	274	6.98	152.0	186	16.60	64.0	0.026	4.1	

^a From dielectric rather than mechanical data.^b Styrene: *n*-hexyl methacrylates = 0.26:0.74 (by mole);^c 0.41:0.59 (by mole).^d *cis:trans:vinyl* = 43:50:7;^e 96:2:2;^f 27:37:36;^g 7:1.5:91.5.^h Styrene: butadiene = 23.5:76.5 (by weight).ⁱ Lightly vulcanised with sulphur.^j Ethylene: propylene = 16:84 (by mole);^k 56:44 (by mole).^l Copolymer of adipic acid and ethylene and propylene glycols, cross-linked by naphthalene 1,4-diisocyanate and 1,4-butanediol.^m Poly(propylene ether) cross-linked by toluene diisocyanate and trimethylol propane.ⁿ Data by Te Nijenhuis (1974, 1979).

The time-temperature equivalence principle can also be applied to other viscoelastic functions in a similar way. Again, this leads to shift factors that are identical with those obtained from stress relaxation:

$\log G_o(t) = \log[G(t)\rho_o T_o / (\rho T)]$	Versus	$\log(t/a_T)$	and analogous	$\log E_o(t)$
$\log G'_o(\omega) = \log[G'(\omega)\rho_o T_o / (\rho T)]$	Versus	$\log(\omega a_T)$	and analogous	$\log E'_o(\omega)$
$\log G''_o(\omega) = \log[G''(\omega)\rho_o T_o / (\rho T)]$	Versus	$\log(\omega a_T)$	and analogous	$\log E''_o(\omega)$
$\log J_o(t) = \log[J(t)\rho T / (\rho_o T_o)]$	Versus	$\log(t a_T)$	and analogous	$\log S_o(t)$
$\log J'_o(\omega) = \log[J'(\omega)\rho T / (\rho_o T_o)]$	Versus	$\log(a_T/\omega)$	and analogous	$\log S'_o(\omega)$
$\log J''_o(\omega) = \log[J''(\omega)\rho T / (\rho_o T_o)]$	Versus	$\log(a_T/\omega)$	and analogous	$\log S''_o(\omega)$
$\log \tan \delta$	Versus	$\log(\omega a_T)$		

13.4.8.2. The TPSP for amorphous polymers above T_g

The rates of relaxation and retardation processes above the glass temperature are strongly dependent on the viscosity and thus on the fraction of free volume present. Because the viscosity not only depends on temperature but also on static pressure (the glass transition temperature increases approximately 1 °C per 20 bar of pressure) it is not surprising that pressure also affects the viscoelastic processes. A qualitatively relation analogous to Eq. (13.121) can be readily derived (Ferry, 1980):

$$\log(a_P)_{P_o} = -\frac{[B/(2.303f_o)](P - P_o)}{f_o/\beta_o - (P - P_o)} \quad (13.122)$$

with

$$f_P = f_o - \beta_f(P - P_o) \quad (13.123)$$

where β_f is the compressibility of the free volume, defined as $\beta_f = -(1/v)(\partial v_f / \partial P)_T \approx -(\partial f / \partial P)_T$. For more details the reader is referred to Ferry's monograph (1980). An example of measurements on a chlorosulfonated polyethylene lightly filled with 4% carbon black at pressures from 1 to 4600 bar and a constant temperature of 25 °C is shown in Fig. 13.57 (Fillers and Tschoegl, 1977): the polymer is rubbery at low pressures (shear modulus of the order of 10^6 N/m²) over the time scale covered, a hard glass at high pressures ($G_R \approx 6 \times 10^8$ N/m²) and at intermediate pressures $G(t)$ goes through a transition zone as a function of time. These data together with others at different temperatures are combined with reduced variables in Fig. 13.58, which shows also in a three-dimensional insert the forms of temperature and pressure dependence of the combined shift factor $a_{T,P}$. The treatment appears to be very successful. The expression for the combined shift factor reads (Ferry, 1980):

$$\log a_{T,P} = \frac{[B/(2.303f_o)][T - T_o - \Theta(P)]}{f_o/\alpha_f(P) + T - T_o - \Theta(P)} \quad (13.124)$$

where $\Theta(P)$ is a rather complicated function of the bulk modulus.

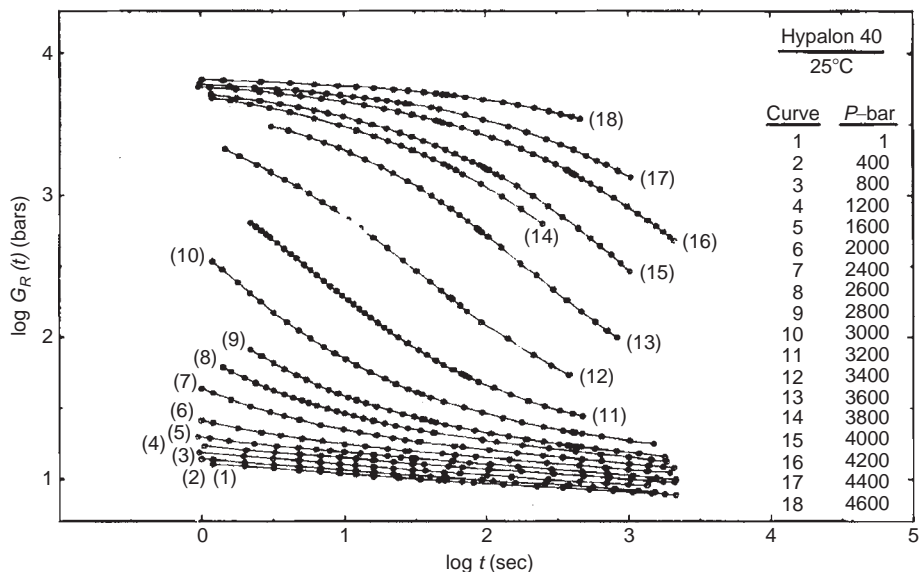


FIG. 13.57 Logarithmic plot of shear relaxation modulus vs. time at 25 °C and various pressures from 1 to 4600 bars as indicated for a chlorosulfonated polyethylene. From Fillers and Tschoegl (1977). Courtesy The American Institute of Physics.

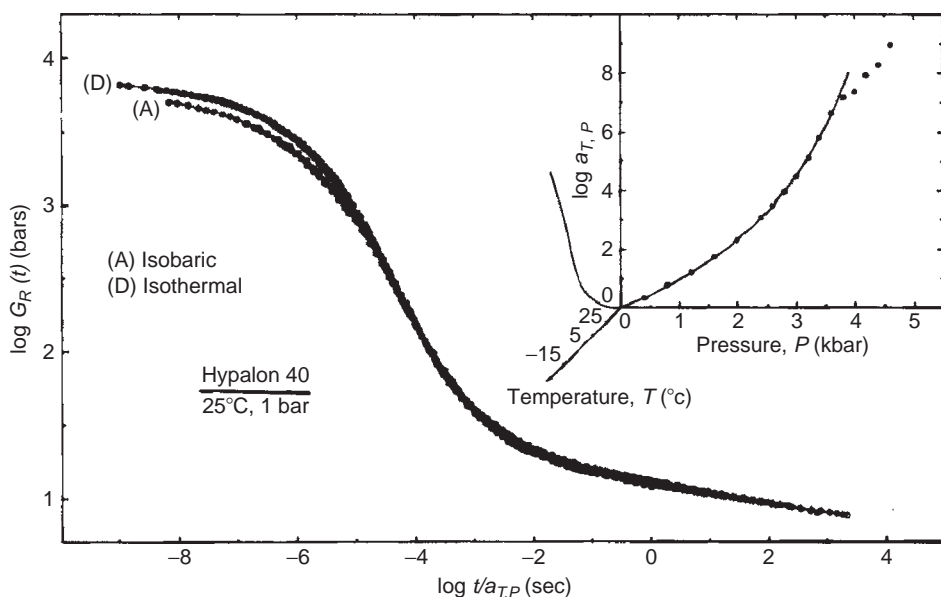


FIG. 13.58 Data of Fig. 13.57 (isothermal) and others at different temperatures down to -15 °C (isobaric) reduced to 25 °C and 1 bar by shift factors $a_{T,P}$ whose magnitudes are indicated in the three-dimensional insert. From Fillers and Tschoegl (1977). Courtesy The American Institute of Physics.

Example 13.3

The stress relaxation modulus of polyisobutylene at 25 °C and a measuring time of 1 h is $3 \times 10^5 \text{ N/m}^2$. Estimate (a) the stress relaxation modulus at a measuring time of 1 h at -80 °C, (b) the temperature at which the modulus for a measuring time of 10^{-6} h is the same as that at -80 °C for a measuring time of 1 h.

Solution

- a. The shift factor at -80 °C can be obtained by applying Eq. (13.117). For polyisobutylene T_g is 200 K. Hence,

$$\log a(298 \text{ K}) = \frac{-17.44 \times (298 - 200)}{51.6 + (298 - 200)} = -11.42$$

$$\log a(193 \text{ K}) = \frac{-17.44 \times (193 - 200)}{51.6 + (193 - 200)} = 2.73$$

$$\log \frac{a(193 \text{ K})}{a(298 \text{ K})} = 2.73 + 11.42 = 14.15$$

$$t(193 \text{ K}) = \frac{t(298 \text{ K})}{a(193 \text{ K}/298 \text{ K})} = 1 \text{ h} \times 10^{-14.15} = 7 \times 10^{-15} \text{ h}$$

This result for $t(193)$ is quite different from Fig. 13.56, where $t(193 \text{ K})$ is approximately equal to $3 \times 10^{-12} \text{ h}$. If we take for the WLF constants not the universal values of 17.44 and 51.6 but those from Table 13.10 for polyisobutylene ($c_1^g = 16.85$ and $c_2^g = 102.4$), we then calculate $t(193 \text{ K}) = 3 \times 10^{-10} \text{ h}$ which is slightly better in agreement with Fig. 13.56. However, as said before, because of the flatness of the pseudo-rubber plateau the determination of $\log a_T$ is rather inaccurate, so that the shift from temperatures below to above this plateau, thus from -80 to 25 °C is rather problematic. This means that the value of $3 \times 10^{-12} \text{ h}$ will also be wrong. The values of 16.85 and 102.4 have been determined with the aid of the storage and loss moduli, by which these problems were bypassed, so that the value of $t(193 \text{ K}) = 3 \times 10^{-10} \text{ h}$ will be more realistic than the other two values for $t(193 \text{ K})$.

For $t(193 \text{ K}) = 7 \times 10^{-15} \text{ h}$ the master curve gives a modulus of about $3 \times 10^9 \text{ N/m}^2$ and for $t(193) = 1.3 \times 10^{-11} \text{ h}$ a modulus of about $4 \times 10^8 \text{ N/m}^2$.

- b. The stress relaxation modulus at -80 °C and a measuring time of 1 h is 10^9 N/m^2 . We have to calculate the temperature change corresponding to a shift factor of 10^{-6} . We again apply Eq. (13.117):

$$\log a(193) = 2.73 \quad \text{and} \quad \log[a(193)/a(T)] = 6 = 2.73 + 3.27$$

$$\log a(T) = -3.27 = \frac{-17.44\Delta T}{51.6 + \Delta T} \quad \text{so that} \quad \Delta T = 12 \text{ °C}$$

or

$$T = T_g + 12 = 200 + 12 = 212 \text{ K} = -61 \text{ °C}$$

With the aid of the more realistic values of the WLF constants we obtain $T = 226 \text{ K} = -43 \text{ °C}$

13.4.8.3. The TTSP for (semi)crystalline polymers between T_g and T_m

For crystalline polymers well below their melting points the WLF equation is not valid. Seitz and Balazs (1968) proved that the interrelation between a_T and T is a simple Arrhenius type of equation

$$\log a_T = \log(t/t_o) = \frac{E_{\text{act}}}{2.303R} \left(\frac{1}{T} - \frac{1}{T_o} \right) \quad (13.125)$$

In this respect it is interesting that Eq. (13.36) can be written in the following form:

$$\log \frac{E(T)}{E(T_o)} = 1.15 \frac{T_m}{(T_m/T_o) - 1} \left(\frac{1}{T} - \frac{1}{T_o} \right)$$

which means that the activation energy of the creep (and stress relaxation) process is proportional to

$$T_m / [(T_m/T_o) - 1]$$

The available data in the literature substantiate this equation as long as $T_g \ll T_o$. Combination of Eq. (13.125) with Eq. (13.36) gives:

$$\log \frac{E_o}{E} \approx \log \frac{G_o}{G} \approx A \log \frac{t}{t_o} + B \left(\frac{1}{T_o} - \frac{1}{T} \right) \quad (13.126)$$

where $B \approx T_m / (T_m/T_o - 1)$

Some characteristic values for engineering plastics have been derived from the literature data on creep measurements (see, e.g., Ogorkiewicz (1970)) and are given in Table 13.11.

The “activation energy” of the shift factor in the formula of Seitz and Balazs (Eq. (13.125)) is:

$$E_{\text{act}}/R = 2.3B/A$$

For HDPE this gives $E_{\text{act}}/R = 2.31 \times 1265/0.11 = 2.66 \times 10^4 \text{ K}$, in good agreement with the experimental value obtained by Seitz and Balazs in stress relaxation measurements, viz. 28,000 ($E_{\text{act}} = 235 \text{ kJ/mol}$).

13.4.8.4. Significance of the shift factor (a_T)

As we have seen, the shift factor is the *relative* change in time (t/t_o) needed to *simulate* a certain property (which is known at a reference temperature (T_o) and a reference time (t_o)) at a changed temperature. The shift factor proves to be the relative *time shortening* to

TABLE 13.11 Values of constants in Eq. (13.126)

Polymer	E_o at 298 K; 100 s (10^9 N/m^2)	A (-)	B (K)	$T_m / [(T_m/T_o) - 1](\text{K})$
Polyethylene HD	1.3	0.11	1265	1170
Polypropylene (isotactic)	1.5	0.08	800	900
Polyoxymethylene	2.5	0.06	675	800
Nylon 66	2.5	0.1	875	700

simulate (at the reference temperature) a *low-temperature* property; it is the relative *time lengthening* to simulate (at the reference temperature) a *high-temperature* property.

The shift factor is also the relative time *shortening* needed to simulate at a *higher* temperature a property measured at the reference temperature; it is the time *lengthening* to simulate at a *lower* temperature a property measured at the reference temperature.

Example 13.4

The creep modulus of polypropylene at room temperature (298 K) is $1.5 \times 10^9 \text{ N/m}^2$ (100s creep modulus). Estimate the creep modulus at 333 K after 10^4 h ($=3.6 \times 10^7 \text{ s}$).

Solution

Eq. (13.126) is used, with constants found in Table 13.11:

$$\log \frac{E_0}{E} \approx 0.08 \log \frac{3.6 \times 10^7}{100} + 800 \left(\frac{1}{298} - \frac{1}{333} \right) = 0.727$$

So $\frac{1.5 \times 10^9}{E} \approx 5.33 \quad \text{or} \quad E(333 \text{ K}, 10^4 \text{ h}) \approx 0.28 \times 10^9 \text{ N/m}^2$

The experimental value is $0.21 \times 10^9 \text{ N/m}^2$

13.4.9. Interrelations between different viscoelastic functions of the same material

For a given material the viscoelastic properties – the relaxation behaviour for solid materials – can be determined by a number of different techniques. The results obtained by each technique are expressed in the form of a characteristic function. In tensile deformation these functions are:

a. Stress relaxation:

The relaxation modulus as a function of time: $E(t)$

b. Creep:

The retardation compliance as a function of time: $S(t)$

c. Periodic deformation:

The components of the dynamic modulus or the dynamic compliance as functions of the frequencies $E'(\omega)$ and $E''(\omega)$ or $S'(\omega)$ and $S''(\omega)$

It will often be desirable to convert the results of one type of experiment into the characteristic quantities of another type. Unfortunately, there are no rigorous rules for these conversions. The problem may be approached in two ways. In the first place, exact interrelations can be derived from the theory of linear viscoelasticity. This method has two disadvantages.

- a. The theory of linear viscoelasticity is applicable to rather small deformations only.
- b. The exact relations are not very suitable for numerical calculations, because the moduli or compliances must be known for zero to infinite times and the dynamic moduli or compliances from zero to infinite frequencies.

In practice, the exact interrelations will thus seldom be applicable. This is the reason why a great number of approximate interrelations have been derived by several

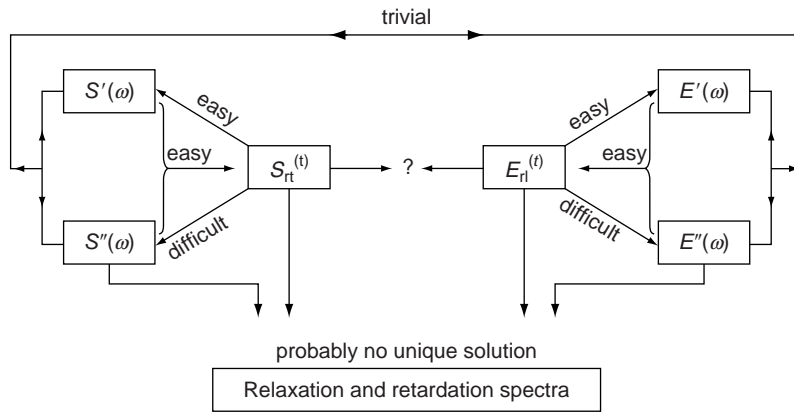


FIG. 13.59 Accuracy of interrelationships between static and dynamic viscoelastic functions.

investigators. For a survey of these relationships the reader is referred to the monographs of Ferry (1980) and Schwarzl (1990).

Schwarzl (1970) studied the errors to be expected in the application of this type of equations, starting from the theory of linear viscoelasticity. His results are given schematically in Fig. 13.59. For non-linear viscoelastic behaviour, the exactitude of the approximate equations cannot be predicted.

As it is impossible to mention all the approximate relationships that have been proposed in the literature; just to show, only a few examples will be given.

13.4.9.1. Stress relaxation from creep

$$E(t) = \frac{\sin(m\pi)}{m\pi S(t)} \quad \text{and} \quad G(t) = \frac{\sin(m\pi)}{m\pi J(t)} \quad (13.127)$$

$$\text{in which } m = \frac{d \log S(t)}{d \log t} \quad \text{or} \quad m = \frac{d \log J(t)}{d \log t}$$

For small values of m we have $S(t) = 1/E(t)$ and $J(t) = 1/G(t)$

13.4.9.2. Stress relaxation from dynamic quantities

Approximate relations are

$$E(0.48t) \approx E'(\omega)|_{t=1/\omega} \quad (13.128)$$

$$E(0.48t) \approx [E'(\omega) - 0.257E''(0.299\omega)]|_{t=1/\omega} \quad (13.129)$$

$$E(1.25t) \approx [E'(\omega) - 0.5303E''(0.5282\omega) - 0.021E''(0.085\omega) + 0.042E''(6.73\omega)]|_{t=1/\omega} \quad (13.130)$$

Eqs. (13.128)–(13.130) illustrate how the exactitude of the formula can be increased by the addition of more modulus values at different values of ω . The applicability, however, decreases with an increasing amount of information required.

13.4.9.3. Dynamic quantities from stress relaxation

Exact relations are:

$$\begin{aligned} E'(\omega) &= \omega \int_0^{\infty} E(t) \sin(\omega t) dt \\ E''(\omega) &= \omega \int_0^{\infty} E(t) \cos(\omega t) dt \end{aligned} \quad (13.131)$$

Approximate relations are

$$\begin{aligned} E'(\omega) &\approx [E(t) + 0.86\{E(t) - E(2t)\}]|_{t=1/\omega} \\ E''(\omega) &= \left[-0.470\{E(2t) - E(4t)\} + 1.674\{E(t) - E(2t)\} + 0.198\{E(\frac{1}{2}t) - E(t)\} + \dots \right]|_{t=1/\omega} \end{aligned} \quad (13.132)$$

13.5. ULTIMATE MECHANICAL PROPERTIES

13.5.1. Deformation properties

The strength properties of solids are most simply illustrated by the stress-strain diagram, which describes the behaviour of homogeneous brittle and ductile specimens of uniform cross section subjected to uniaxial tension (see Fig. 13.60). Within the linear region the strain is proportional to the stress and the deformation is reversible. If the material fails and ruptures at a certain tension and a certain small elongation it is called *brittle*. If permanent or plastic deformation sets in after elastic deformation at some critical stress, the material is called *ductile*.

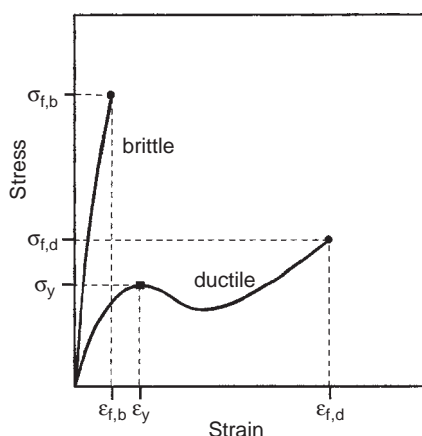


FIG. 13.60 Generalised tensile stress-strain curves for brittle and ductile plastics; $\varepsilon_{f,b}$, ε_y and $\varepsilon_{f,d}$ = strain at brittle fracture, at yield and at ductile fracture, respectively; $\sigma_{f,b}$, and $\sigma_{f,d}$ = ultimate strength at brittle fracture and ductile fracture, respectively; σ_y = yield strength; (●) fracture points; (■) yield point.

We have seen already (Sect. 13.4.7) that every amorphous material (including that in semi-crystalline polymers) becomes brittle when cooled below the first secondary transition temperature (T_β) and becomes ductile when heated above the glass transition point (T_g). Between these two temperatures the behaviour – brittle or ductile – is mainly determined by the combination of temperature and rate of deformation.

During the deformation of ductile polymers there is often an increase in stress with deformation; this is known as *work-hardening*. If at some point the stress is removed, the material recovers along a path nearly parallel to the linear region; the sample then shows a permanent plastic deformation.

There is a basic difference between rupture above the glass transition temperature (where the polymer backbones have an opportunity to change their configurations before the material fails) and well below T_g (where the backbone configurations are essentially immobilised within the period of observation: brittle materials).

Fig. 13.61 shows the stress–strain curves for the different types of polymeric materials.

13.5.2. Ultimate strength

13.5.2.1. Ultimate strength of brittle materials

The theoretical value for the brittle strength of a material is of the order of

$$\sigma_{b,th} \approx \frac{E}{10}$$

where E is the Young modulus.

The observed brittle strength is generally very variable, but is always 10–100 times smaller than the theoretical value. Only some very fine fibres (e.g. silica) have been

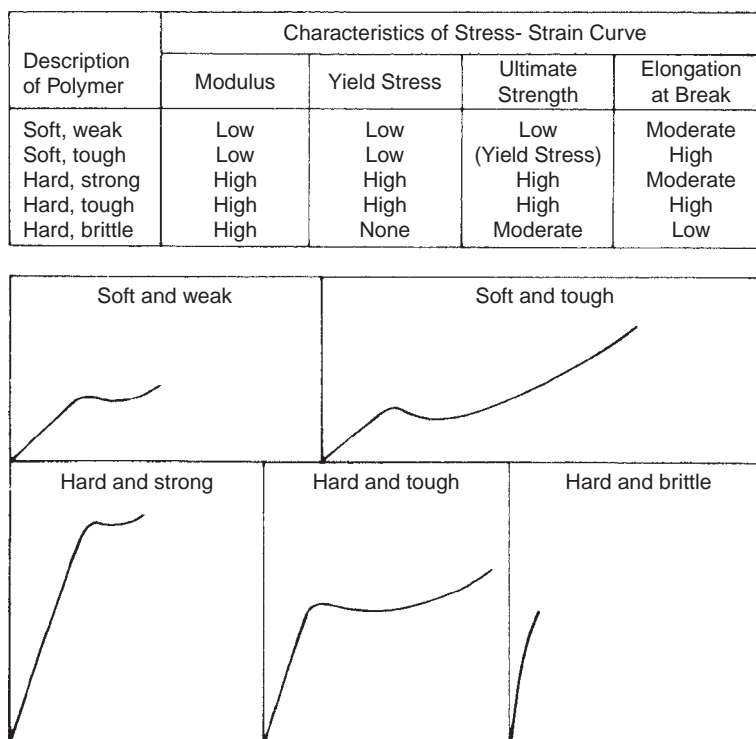


FIG. 13.61 Tensile stress–strain curves for several types of polymeric materials (Winding and Hiatt, 1961).

prepared which have tensile strengths approaching the theoretical value. The source of this "weakness" is the presence of flaws or cracks in the solid, especially at the surface. These cracks act as "stress-multipliers". If there is a crack in a sample with a length L and a tip radius r , the tensile stress at the tip of the crack is multiplied by a factor of the order $\sqrt{L/r}$. The multiplication factor can easily be of the order of 10–100. But even if the crack-tip tends to zero the material still possesses certain strength, so that there must be an extra effect to explain the facts.

Griffith (1921) gave the answer to this problem by showing that for a crack to grow, it is not sufficient for the stresses at the crack-tip to exceed the theoretical strength; in addition sufficient elastic energy must be released to provide the extra surface energy that a growing crack demands. This will be discussed in more detail in Sect. 13.59.

13.5.2.2. Ultimate strength of ductile materials

If a material does not appreciably work-harden after yielding, in tension, its *yield stress* will be very nearly the maximum stress the material can support before it pulls apart, i.e. its ultimate tensile strength.

Tabor (1947) showed that the yield stress of a material is proportional to the indentation hardness (see Chap. 25). Since the latter is a power function of the modulus, the yield stress will be:

$$\sigma_y = \sigma_{\max} \propto E^n \quad (13.133)$$

where $n \approx 0.75$.

If a material shows work-hardening, as in many crystalline polymers (due to *orientation* during the plastic deformation), the ultimate strength (if calculated on the basis of original cross section) will of course be higher than the yield stress.

13.5.2.3. Transition from ductility to brittleness, and vice versa

As we have seen, mobility of the molecules is one of the sources of ductility. However, if the mobility is obstructed by some barrier, an internal crack may form, and initiate crack propagation. In this way a ductile solid may become brittle.

On the other hand a brittle solid may be made ductile by applying hydrostatic pressure. Let us consider a brittle solid, which fails at a tensile stress σ . If a hydrostatic pressure p is applied, the tensile stress necessary for failure is $p + \sigma$. Associated with this tensile stress is a shear stress equal to $\frac{1}{2}(p + \sigma)$. If the critical shear stress is less than this, the material will flow in a ductile manner before the tensile stress is large enough to produce brittle failure.

Phenomena like this are well known. At great depths rocks can flow although they are normally very brittle. Even quartz can flow plastically under sufficiently high hydrostatic pressure.

Well-known yield criteria are the Tresca criterion and the Von Mises criterion. Discussion of this subject falls beyond the scope of this book, but a clear description is presented in, e.g. the monograph of Ward and Hadley (1993). If stresses increase above a certain value yield will occur. For metals this critical value is almost independent of pressure, whereas for polymers it is strongly dependent on pressure. An example is shown in Fig. 13.72 for PMMA in Sect. 13.5.4.

Many polymers, which are brittle in tension or bending, may readily yield in other types of deformation, and show a high ductility. In indentation hardness experiments, plastic indentation can often be made in relatively brittle materials. Hardness values thus obtained are a measure of the plastic properties of the brittle solid!

Another effect, which greatly influences the type of rupture, is orientation. If a polymer is heated just above the glass transition temperature, stretched several hundred percent in one direction and cooled to room temperature while under stress, the polymer chains will be trapped in a non-random distribution of conformations: more orientation parallel to the stretching direction. The material becomes markedly anisotropic and will be considerably stronger in the direction of orientation (and weaker in the transverse direction). The effect may be dramatic: a glassy polymer which, unoriented, would undergo brittle fracture at $\varepsilon_{\max} = 0.03$, may, when oriented, exhibit ductile yielding with failure at $\varepsilon_{\max} = 0.50$. The area under the stress-strain curve (energy per unit volume), a rough measure of toughness, may be 20 times as large for a properly oriented specimen of the same material.

If crystallisation and orientation go together, the strength can be further improved. The strongest polymeric materials (synthetic fibres) are oriented crystalline polymers.

13.5.2.4. Crazing

Crazing is a form of non-catastrophic failure that may occur in glassy polymers, giving rise to irreversible deformation. Crazes scatter light and are readily visible to the unaided eye as whitened planes *perpendicular* to the direction of stress. A craze is a narrow zone of highly deformed and voided material (40–60%). The molecular chains in a craze are aligned *parallel* to the direction of stress; they are drawn into a lacework of oriented threads or sheets, separated from each other by a maze of interconnected voids. This leads to visual impairment and enhanced permeability. Craze formation is now considered to be a mode of plastic deformation peculiar to glassy polymers (or to glassy regions in a polymer) that is competitive with shear ductility. Thus, when subject to a tensile stress, high-molecular-mass glassy polymers can exhibit three main types of response:

- a. They can extend uniformly
- b. They can extend in a necking mode
- c. They can craze – and finally break

It seems reasonable to assume that crazing is a process which can occur quite naturally in any orientation hardening material, which exhibits plastic instability at moderate strains and in which the yield stress is much higher than the stress required for the nucleation of voids (cavitations).

It is interesting to remark that like most mechanical parameters the crazing stress exhibits viscoelastic characteristics, decreasing with increasing temperature and with decreasing strain rate (which is an indication that it is better to speak of a crazing strain). We come back to the discussion of crazes in Sect. 13.5.5.

13.5.2.5. Numerical values

Table 13.12 gives the numerical values of the strength properties of a series of polymers. The data on the tensile strength are graphically reproduced in Fig. 13.62, where σ_{\max} (i.e. the tensile strength at break of brittle (linear) polymers and the tensile strength at yield of ductile (linear) polymers) is plotted as a function of E , the tensile modulus. As an approximation the following empirical expression may be used (drawn line):

$$\sigma_{\max} = 30E^{2/3} \quad \text{or} \quad \sigma_{\max} = 0.03E^{2/3} \quad (13.134)$$

where σ_{\max} and E are expressed in N/m² or in GPa, respectively.

TABLE 13.12 Ultimate mechanical properties of polymers (unmodified) (moduli in 10^9 N/m^2 ; strengths in 10^7 N/m^2)

Polymer ref. no.	Polymer	Tensile strength at yield	Elongation at yield (%)	Tensile strength at break	Elongation at break (%)	Tensile modulus	Flexural strength	Flexural modulus	Compressive strength	Poisson ratio (stat.)
1	Polyethylene (LD)	0.8	20	1.0	800	0.2				0.49
2	Polyethylene (HD)	3.0	9	3.0	600	1	4.5	0.8	2	0.47
3	Polypropylene	3.2	12	3.3	400	1.4	4.9	1.5	4.5	0.43
4	Poly(1-butene)			3.0	350	0.75				0.47
5	Polystyrene			5.0	2.5	3.4	8	3.3	9.5	0.38
6	Poly(vinyl chloride)	4.8	3	5.0	30	2.6	9	3.5	7	0.42
7	Poly(chlorotrifluoroethylene)	3.0	10	3.5	175	1.9	5.5	2	4	0.44
8	Poly(tetrafluoroethylene)	1.3	62.5	2.5	200	0.5		0.35	0.8	0.46
9	Poly(methyl methacrylate)			6.5	10	3.2	11	3	10.5	0.40
10	Poly(methylene oxide)			6.5	40	2.7		2.5	12	0.44
11	Poly(phenylene oxide)			6.5	75	2.3				0.41
12	Poly(phenylene sulphide)			6.5	3	3.4	11			
13	Poly(ethylene terephthalate)		6	5.4	275	3.0		2.9	9	0.43
14	Poly(tetramethylene terephthalate)			5.0		2.5			8	0.44
15	Nylon 66	5.7	25	8.0	200	2.0		2.3	10	0.46
16	Nylon 6	5.0	30	7.5	300	1.9		2.0	9	0.44
17	Poly(bisphenol carbonate)	6.5	30	6.0	125	2.5	9	2.5	7	0.42
18	Polysulphone			6.5	75	2.5	10		8	0.42
19	Polyimide			7.5	7	3.0	10			0.42
20	Cellulose acetate	4	6	3	30	2	5	1.25		
21	Phenol formaldehyde resin			5.5	1	3.4	9	4	13	0.35
22	Uns. polyester resin			6.0	3	5.0	9	5.0	15	0.36
23	Epoxy resin			5.5	5	2.4	11	2.5	13	0.37

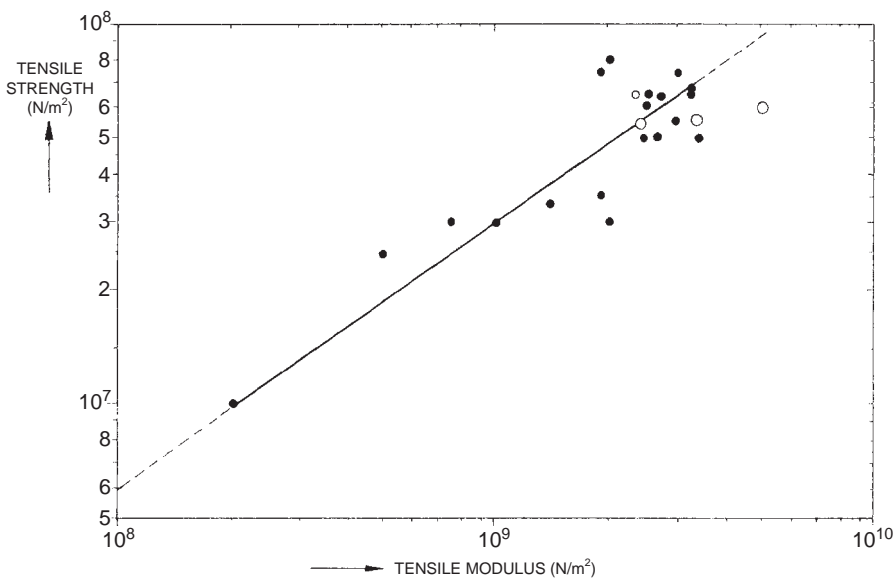
**FIG. 13.62** Tensile strength of polymers, correlated with modulus.

Table 13.12 permits a comparison of the values of the tensile, flexural and compressive strength. The strength ratios of polymers are compared with those of other materials in Table 13.13. Obviously there is a strong influence of the Poisson ratio on the value of the compressive/tensile strength ratio. The following empirical equation provides a good estimate (see Fig. 13.63):

$$\log \frac{\sigma_{\max}(\text{compressive})}{\sigma_{\max}(\text{tensile})} \approx 2.2 - 5v \quad (13.135)$$

where v is the Poisson ratio.

On the other hand, the flexural/tensile strength ratio is nearly constant (average value 1.6) for polymers. (The same is true for the flexural/tensile modulus ratio).

Finally there is a rough relationship between the maximum elongation and the Poisson ratio of polymers. This is not expected, since the Poisson ratio is a measure of

TABLE 13.13 Strength ratio in different materials

Material	Strength ratio (exp)		
	Compressive tensile	Flexural tensile	Poisson ratio (v)
Vitreous silica	30	—	0.14
Silicate glass	12.5	—	0.225
Phenol formaldehyde	2.5	—	0.35
Polystyrene	1.9	1.9	0.37
Poly(methyl methacrylate)	(1.6)	1.6	0.40
Poly(vinyl chloride)	1.4	1.8	0.42
Polyethylene HD	0.67	1.5	0.47

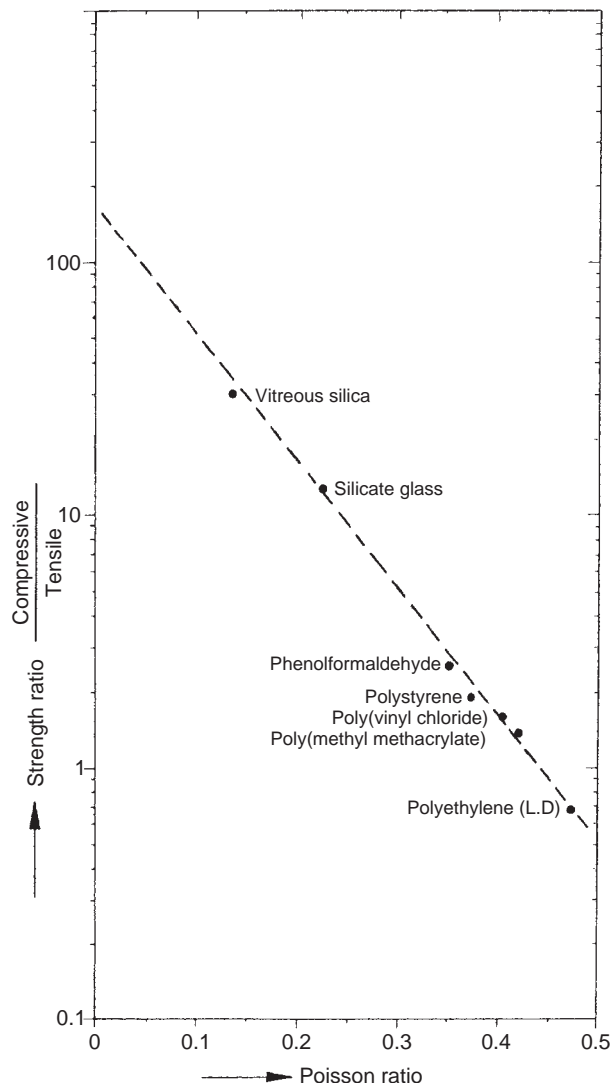


FIG. 13.63 Strength ratios of polymers.

the liquid-like character of a solid. The correlation is illustrated in Fig. 13.64. ν characterises the polymer's ability to be deformed by shear forces. The dashed line in Fig. 13.64 corresponds to the following equation:

$$\log \varepsilon_{br}(\%) = 27.5\nu - 10 \quad (13.136)$$

13.5.2.6. Rate dependence of ultimate strength

When the rate of elongation is increased, the tensile strength and the modulus also increase; the elongation to break generally decreases (except in rubbers). Normally an increase of the speed of testing is similar to a decrease of the temperature of testing. To lightly cross-linked rubbers even the time-temperature equivalence principle can be applied. The rate dependence will not surprise in view of the viscoelastic nature and the influence of the Poisson ratio on the ultimate properties.

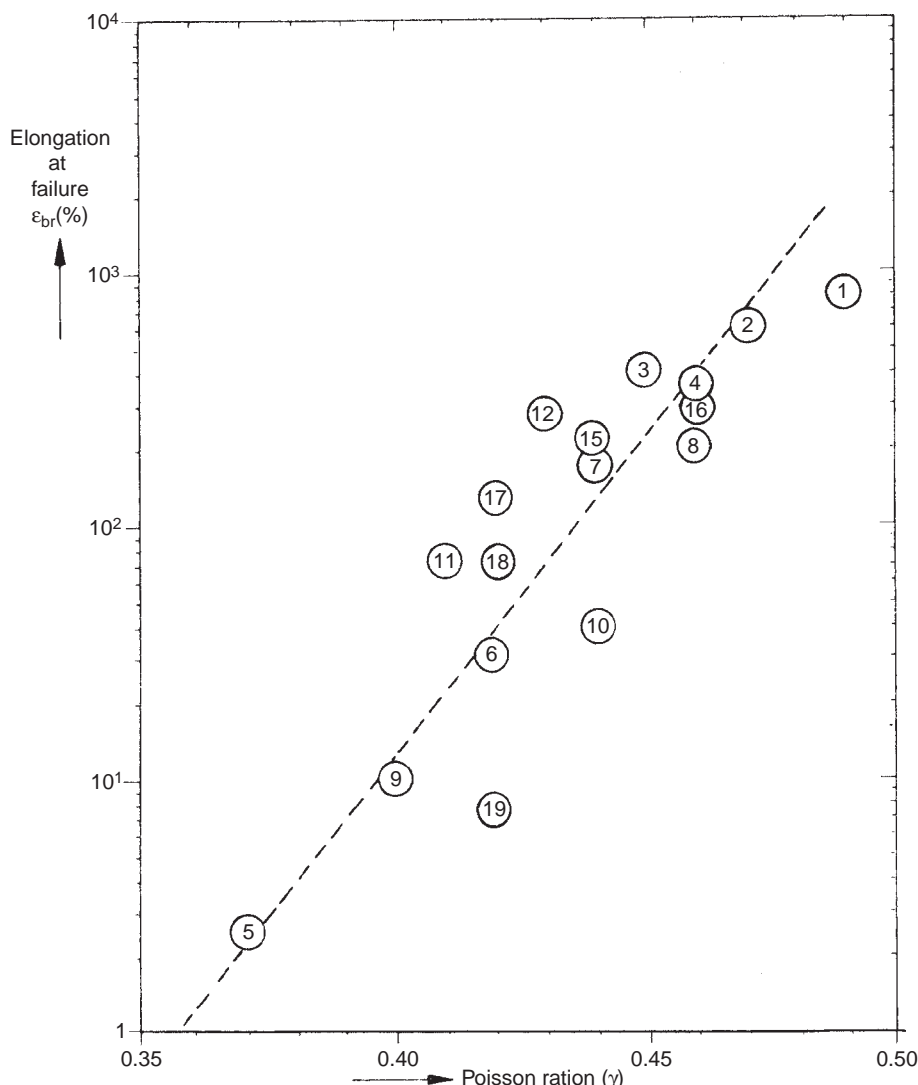


FIG. 13.64 Relationship between maximum elongation and Poisson ratio of polymers (for reference numbers, see Table 13.11).

Shamov (1966) has pointed out the importance of the time dependence of the Poisson ratio of polymers. Measurements on polymers at very low frequency will yield values near $\frac{1}{2}$, whereas data obtained at very high frequencies will yield values asymptotically approaching $\frac{1}{3}$. The value of v is thus a function of the rate of measurement. This fact is illustrated by data of Warfield and Barnet (1972) and Schuyler (1959) (see page 390).

13.5.3. Introduction

Stress-strain behaviour of poly(methyl methacrylate) is shown in Fig. 13.65 at various temperatures. At low temperatures the polymer behaves brittle (at this rate of deformation) and at high temperatures ductile. At 40 °C a transition from brittle to ductile

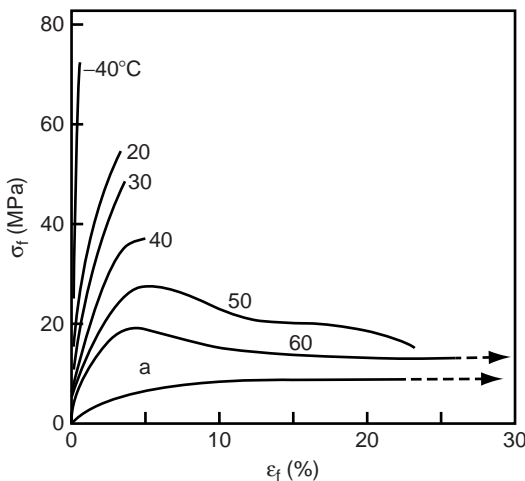


FIG. 13.65 Stress–strain behaviour of PMMA at various temperatures. Curve a shows rubberlike behaviour of a cross-linked thermoplastic above T_g . According to Andrews (1968).

behaviour is present and the corresponding temperature is called the *brittle–ductile transition temperature* or shortly the *brittle temperature*. Above this temperature the stress–strain curves show a maximum after which the stress decreases. This maximum in the curve is called the *yield point*, with corresponding yield stress σ_y and yield strain ε_y . Ductile deformation increases fast with increasing temperature: the fracture deformation ε_f of some percents at brittle fracture can increase to several hundreds of percents at ductile fracture. The brittle temperature is dependent on the rate of deformation, not only for plastic materials but also for metals, as is shown in Fig. 13.66. Hence, a material can behave ductile in a tensile tester whereas it behaves brittle at the same temperature in an impact tester, in particular in the presence of a notch. In this respect the fracture energy per unit volume, i.e. the surface area below the stress–strain curve, plays an important role. It strongly depends on the rate of deformation: at low rates, where the material behaves

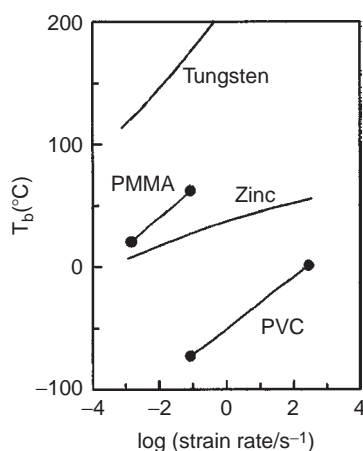


FIG. 13.66 Rate of strain dependence upon brittle–ductile transition temperatures of various solids. According to Vincent (1962).

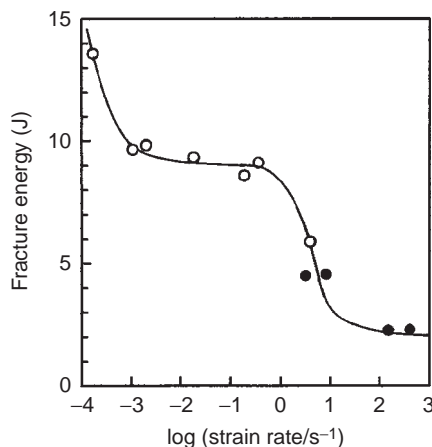


FIG. 13.67 Fracture energy of Penton (a chlorinated polyethylene) as function of strain rate. According to Warburton-Hall and Hazell (1963).

ductile, the fracture energy is high, whereas at high rates where the material behaves brittle, the fracture energy is low (see Fig. 13.67). In practice the difference between brittle fracture and ductile fracture is that broken pieces that were obtained by brittle fracture can in principle be glued together; this is not possible with broken pieces obtained by ductile fracture.

13.5.4. Yield behaviour

13.5.4.1. Yield point

In ductile materials the maximum in the stress-strain curve is the yield point. Two definitions of yield points are in use (see Fig. 13.68):

- (a) Intrinsic yield point, i.e. the maximum in the true stress vs. nominal deformation curve
- (b) Extrinsic yield point, i.e. the maximum in the nominal stress vs. the nominal deformation curve

A tangent line from the point $(\sigma, \varepsilon_n) = (0, -1)$ on the true stress curve hits this curve at that value of ε_n where the engineering stress curve has its maximum value. This is called

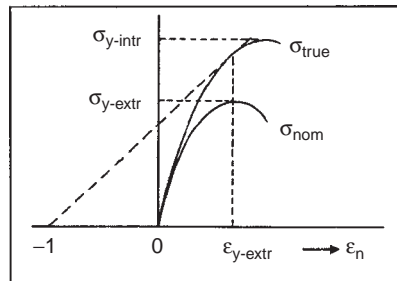


FIG. 13.68 Intrinsic and extrinsic yield points and the Considère construction.

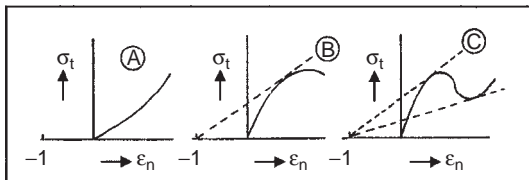


FIG. 13.69 Three possibilities of Considère's construction.

the Considère construction. There are in practice three possibilities for stretch behaviour, as shown in Fig. 13.69:

- No tangent line is possible from the point $(0, -1)$: the polymer stretches uniformly under increasing stress and no necking occurs; examples are vulcanised rubber and cellulose nitrate.
- There is one tangent line from the point $(0, -1)$: the sample stretches uniformly till the tangent point, where necking of the sample starts; the neck becomes thinner and thinner because of the deformation softening; examples are copper and poly(vinyl chloride) at high stretching rates.
- There are two tangent lines from the point $(0, -1)$: there is a stable neck that extends with increasing stretching due to strain hardening; examples are polycarbonate, high density polyethylene and many other polymers.

13.5.4.2. Influences of the yielding process

The yielding process is influenced by several parameters, e.g. rate of deformation, temperature and pressure.

(a) Dependence on rate of deformation

The yield stress is strongly dependent on the rate of deformation, as shown in Fig. 13.70. For many polymers the relationship between the σ_y and $\ln(d\varepsilon/dt)$ is linear

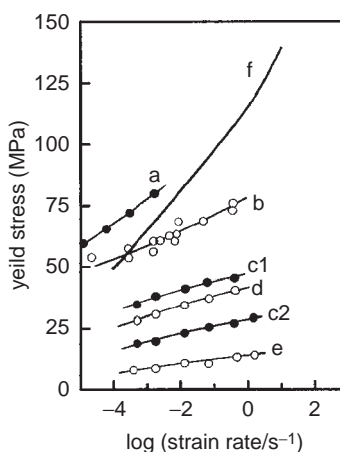


FIG. 13.70 Yield stresses of various polymers as function of the rate of testing. (A) PMMA; (B) rigid PVC; (C1 and C2) "Kralastic B" (two ABS resins); (D) polypropylene; (E) polyethylene. Compare (F) Copper at 600°C . According to Vincent (1962).

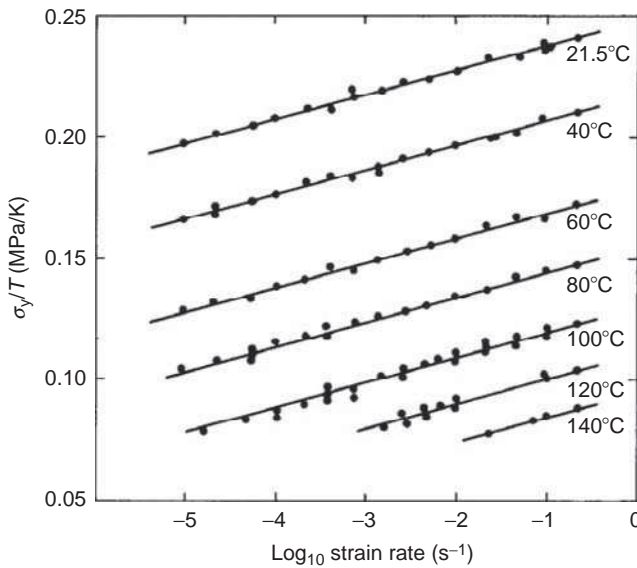


FIG. 13.71 Eyring plot of σ_y/T vs. \log (strain rate) for polycarbonate at different temperatures. From Bauwens-Crowet et al. (1969). Courtesy John Wiley & Sons.

and the slope $d\sigma/d\ln(d\varepsilon/dt)$, is determined by the volume of activation, V_{act} , and according to the Eyring equation, Eq. (13.137) below, equal to $2RT/V_{act}$. It is for PMMA much higher (5.2 MPa per decade of strain rate) than, e.g. for PC and PVC (1.3 and 1.8 MPa per decade of strain rate, respectively). Apparently the activation volume is quite small for PMMA.

(b) *Dependence on temperature*

In Fig. 13.71 the ratio of yield stress and temperature of polycarbonate is plotted vs. \log rate of deformation at various temperatures. The lines appear to be parallel and their mutual distance can be described by a WLF equation. This behaviour shows that the yielding process is a viscoelastic phenomenon.

(c) *Dependence on pressure*

The dependence of yield behaviour of PMMA-tubes in shear in internal pressure was studied by Rabinowitz et al. (1970). Results for pressures from 0.1 to 703 MPa are presented in Fig. 13.72. It appears that

- Both the yield stress and the yield deformation increase with increasing pressure
- The initial Young modulus also increases with increasing pressure: from 0.7 to 1.3 GPa
- The yield depends on the pressure according to $\sigma_{sh,y} = \sigma_{sh,yo} + \mu P = 50.3 + 0.204P$ MPa; such a relationship has been found for many amorphous, glassy polymers: μ , i.e. *the coefficient of internal friction*, usually shows values between 0.1 and 0.25, depending on the polymer, whereas for semi-crystalline polymers this coefficient is smaller
- Above a pressure of 300 MPa the polymer fails in a brittle way
- The dashed line connects all failure points, in ductile as well as in brittle failure; this line is called *the failure envelope* or *fracture envelope*

For a discussion of these results the reader is referred to the monograph by Ward and Hadley (1993).

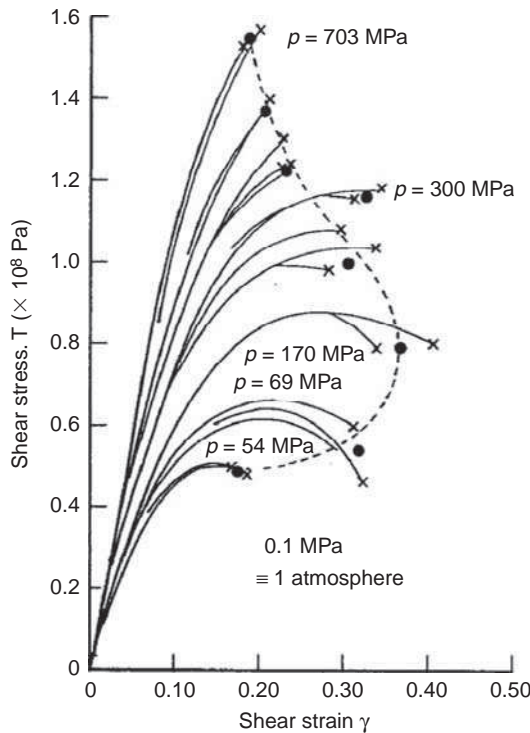


FIG. 13.72 Shear stress–strain curves for PMMA at 22 °C under different pressures at a strain rate of approximately $4 \times 10^{-4} \text{ s}^{-1}$. The filled circles connect all fracture points in a *fracture envelope*. From Rabinowitz et al. (1970). Courtesy Springer Verlag.

13.5.4.3. The Eyring model for yield

The flow model of Eyring provides a basis to correlate the effects of temperature and strain rate on flow stress. The idea is that a segment of a polymer molecule must pass over an energy barrier in moving from the one position to another in the solid. This leads to a relationship between the strain rate and the yield stress (see, e.g. McCrum et al., 1997 or Ward and Hadley, 1993)

$$\dot{\epsilon}_y = 2\dot{\epsilon}_o \exp\left(-\frac{\Delta E_{\text{act}}}{RT}\right) \sinh\left(\frac{\sigma_y V_{\text{act}}}{2RT}\right) \quad (13.137)$$

where E_{act} = the activation energy required to take a mole of segments to the top of the energy barrier; V_{act} = activation volume, e.g. the volume of jumping segments.

For high values of the stress $\sinh(\sigma) \approx \frac{1}{2}\exp(\sigma)$, so that for high yield stresses Eq. (13.137) reduces to

$$\dot{\epsilon}_y = \dot{\epsilon}_o \exp\left(-\frac{\Delta E_{\text{act}}}{RT}\right) \exp\left(\frac{\sigma_y V_{\text{act}}}{2RT}\right) \quad (13.138)$$

or

$$\frac{\sigma_y}{T} = \frac{2}{V_{\text{act}}} \left[\frac{\Delta E_{\text{act}}}{T} + R \ln \frac{\dot{\epsilon}_y}{\dot{\epsilon}_o} \right] \quad (13.139)$$

TABLE 13.14 A comparison of the statistical segment volume for flow for a polymer measured in solution with the flow volumes, V_{act} , derived from the Eyring theory

Polymer	Volume of statistical link in solution (nm ³)	Eyring flow volume V_{act} (nm ³)	Number of stat. links in V_{act}
Poly(vinyl chloride)	0.38	8.6	22.6
Polycarbonate	0.48	6.4	13.3
Poly(methyl methacrylate)	0.91	4.6	5.1
Polystyrene	1.22	9.6	7.9
Cellulose trinitrate	2.62	6.1	2.3
Cellulose triacetate	2.06	17.6	8.5

After Haward and Thackray (1968).

Straight lines should be obtained upon plotting σ_y/T vs. $\log \dot{\varepsilon}_y$. This is in agreement with results for polycarbonate, presented in Fig. 13.71.

The slopes of those parallel curves, with temperature as a parameter, are equal to $2.303R/V_{act}$ and the relationship between the horizontal shift $\log b_T$ and the temperature is

$$\log(b_T)_{T_o} = \frac{\Delta E_{act}}{2.303R} \left(\frac{1}{T_o} - \frac{1}{T} \right) \quad (13.140)$$

Values of activation volumes for some polymers are mentioned in Table 13.14.

Example 13.5

Calculate the activation energy and the activation volume of polycarbonate from the results presented in Fig. 13.71.

Solution

From Fig. 13.71 and Eq. (13.138) we find

$$\frac{d(\sigma_y/T)}{d(\log \dot{\varepsilon}_y)} = \frac{2 \times 2.303 \times R}{V_{act}} = 9.8 \text{ kPa/K per decade}, \text{ so that}$$

$V_{act} = 3.9 \times 10^{-3} \text{ m}^3/\text{mol}$ of jumping segments = $6.5 \text{ nm}^3/\text{jumping segment}$. According to Table 13.14 on the average 13.3 segments are involved in the activation volume. According to McCrum et al. (1997) in a segment of polyethylene of 6.5 nm^3 260 CH₂ groups would be involved.

Results for Eq. (13.140) are presented in the figure: a straight line is obtained:

$$\log(b_T)_{T_1} = 50.9 - 14.8 \times 10^3 / T, \text{ from which it follows: } E_{act} = 284 \text{ kJ/mol (Fig. 13.73).}$$

13.5.5. Brittle fracture, crazing

For brittle materials the stress-strain curves are almost linear up to the fracture point and the fracture strain is small, of the order of a few percentages. Figs. 13.74 and 13.75 show the tensile strain and flexural strength as functions of temperature for PMMA. At 10 °C the fracture strain increases, which points to a transition to ductile behaviour. The brittle

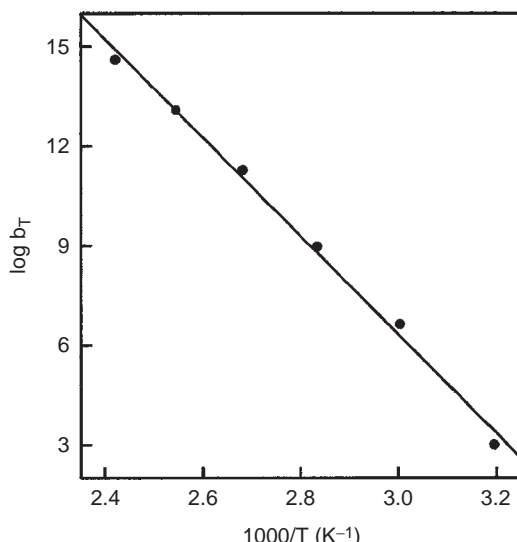


FIG. 13.73 Eyring plots of horizontal shift of the polycarbonate results presented in Fig. 13.71.

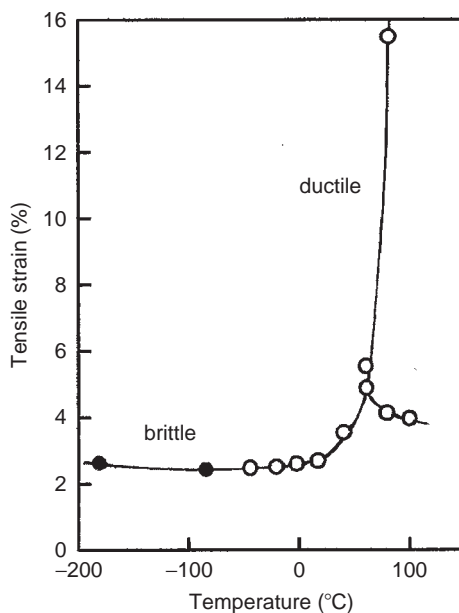


FIG. 13.74 Fracture and yield strains for poly(methyl methacrylate) as functions of temperature. According to Vincent (1961).

strength curve meets the ductile curve at approximately 50 °C, which means that above 50 °C the material will fail in a ductile manner. Hence, the brittle temperature is the temperature where the brittle and ductile curves cross each other.

There are several parameters that affect the brittleness and the brittle–ductile transition temperature, such as molecular weight, presence of cross-links, crystallinity and the presence of notches. A schematic way, following Fig. 13.75 to depict the influence of the various parameters, is shown in Fig. 13.76.

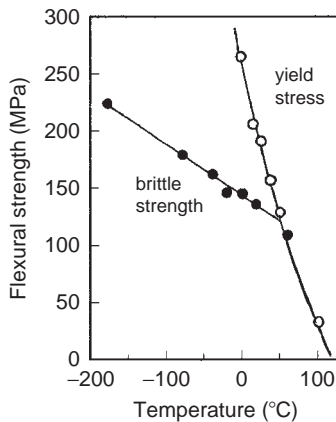


FIG. 13.75 Brittle and yield stresses of poly(methyl methacrylate) as functions of temperature. According to Vincent (1961).

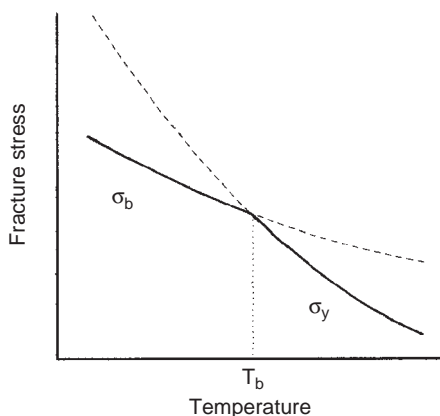


FIG. 13.76 Schematic view of brittle and yield stresses as functions of temperature. Below T_b the brittle stress is smaller than the yield stress, so that the material fails in a brittle way. Above T_b the yield stress is smaller than the brittle stress, so that the material fails in a ductile way.

(a) *Dependence of molecular weight*

The brittle strength of polymers decreases with decreasing number average molecular weight, whereas the yield stress is practically independent of molecular weight. The reason for the decreasing brittle strength is that a low molecular weight polymer has more chain ends, thus more inhomogeneities, where fracture can find its way. The result is that the brittle curve in Fig. 13.76 decreases with decreasing number average molecular weight, so that the brittle temperature increases: the material becomes more brittle.

(b) *Dependence of presence of cross-links*

By cross-linking polymer molecules the number of chain ends does not change and the brittle curve will almost not move. On the other hand, the yield stress will be increased

considerably and accordingly the brittle temperature will increase. The material becomes more brittle. It is worthwhile mentioning that at high cross-link densities also the brittle strength will decrease.

(c) *Crystallinity*

The yield stress curve will be increased by crystallinity, but within certain limits the brittle strength will not be affected. Consequently the brittle temperature will increase with increasing crystallinity: the material becomes more brittle.

(d) *Presence of notches*

Samples for impact measurements are frequently provided with a notch. Such a notch will of course in principle not affect the brittle temperature, but it does affect the distribution of the applied force in the sample. Near the notch the stresses are triaxially distributed and a higher yield stress in the direction of the net force causes the "normal" yield stress in the sample near the notch. Accordingly, the yield stress curve will be increased and consequently the brittle temperature will apparently be shifted to higher values.

As an example, in Table 13.15 the glass and brittle temperatures are mentioned for six polymers. For PMMA, PC and PVC the differences between T_g and T_b are large and for NR, PS and PIB rather small. It is well-known that σ_y increases fast upon temperature decrease close to the glass transition or close to the β -transition. If σ_y increases fast upon a temperature decrease in the neighbourhood of T_g , as is often the case for amorphous polymers like PS and PIB, then the brittle temperature T_b lies closely to T_g . If crystallinity is present so that the glass transition covers a broad temperature region, or if there is a secondary transition far away from T_g , then σ_y will increase slowly upon a temperature decrease and only in the region of T_β , hence far away from T_g , σ_y will increase fast. Accordingly T_b will be considerably lower. This is the case for PMMA, PC and PVC.

13.5.6. Fatigue failure

A material that is subjected to cyclic application of stresses may fail after a large number of load cycles without nearly reaching the maximum failure stress of direct loading. The effect of such cyclic stresses is to initiate microscopic cracks at centres of stress concentration within the material or on the surface, and subsequently to enable these cracks to propagate, leading to eventual failure. For high stress amplitudes less cycles are needed for failure than for low stress amplitudes. For high frequencies less cycles are needed for

TABLE 13.15 Glass and brittle temperatures in °C of some polymers

Polymer	T_g	T_b	$T_g - T_b$
Polymethyl(methacrylate)	105	45	60
Polycarbonate	150	-200	350
Poly(vinyl chloride)	74	-20	94
Natural Rubber	-70	-65	5
Polystyrene	100	90	10
Polyisobutylene	-70	-60	10

failure than for low frequencies. Many polymers will “never” fail if the stress amplitude is low enough. This limit reaches generally 20–35% of their tensile strength. This limiting stress is called the *fatigue limit* or *durability* or *endurance limit*. This is an important property for materials that are subject to frequently changing stresses, like, e.g. propellers in modern windmills (see also Chap. 25).

13.5.7. Creep failure

Fracture by creep is the phenomenon that fracture takes place only some time after applying a constant load. This is also called “*static fatigue*”. The time needed for fracture of the material is shorter for higher loads. An outstanding example of creep fracture is shown in Fig. 13.77. Here results are presented of measurements at different temperatures on high density polyethylene (HDPE) tubes that are subjected to internal biaxial stresses (Van der Vegt, 2005). The various curves consist of two straight lines: the upper ones for ductile fracture and the lower ones for brittle fracture. The positions of the bends in the various curves form a straight line. Accordingly, long-term behaviour at room temperature may be obtained by extrapolation of short-term measurements at high temperatures. In order to explain this apparently anomalous behaviour (ductile fracture at shorter times than brittle fracture) the curves shown in Fig. 13.76 have to be extended to higher temperatures or, as shown in Fig. 13.78 (Van der Vegt, 2005), to longer times. Due to the time-temperature superposition increasing temperature and longer times are qualitatively identical. In Fig. 13.78 three fracture stress regions are shown: two brittle regions and in between a ductile region. At the highest stresses (region A) the applied stress will cause brittle fracture already after a short time, with broken pieces (that can be glued together). At lower stresses (region B) more time is needed for failure and the material fails in a ductile way. At still lower stresses (region C) and longer times again brittle fracture appears, but now by the formation of brittle micro-voids.

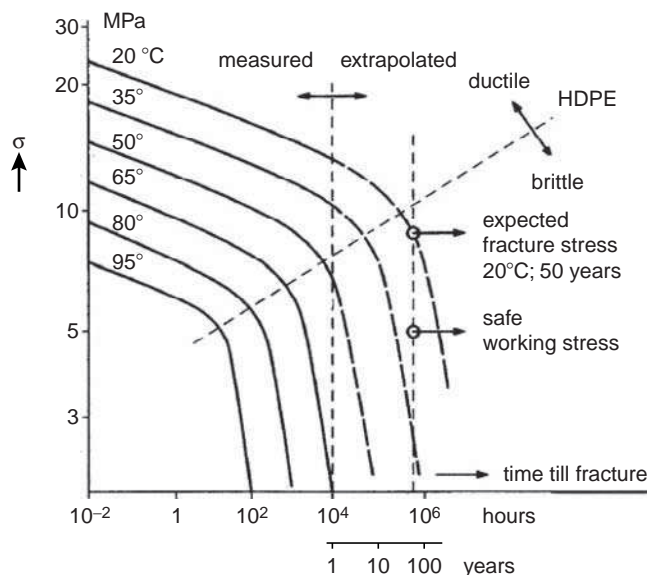


FIG. 13.77 Extrapolation procedure for HDPE tubes. According to Van der Vegt (2005).

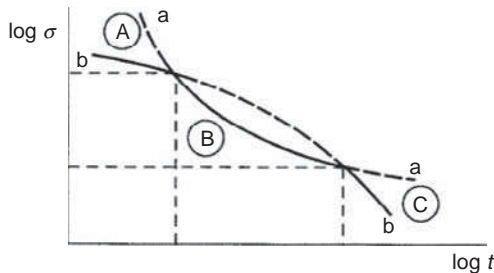


FIG. 13.78 Schematic view of brittle stresses as functions of time, an extension of Fig. 13.76. (a) brittle curve; (b) ductile curve; (A) brittle fracture region; (B) ductile fracture region; (C) brittle fracture region (evolution of micro-voids). According to Van der Vegt (2005).

13.5.8. Crazes and cracks

Crazing is a phenomenon that frequently precedes fracture in many glassy polymers and that occurs in regions of high hydrostatic tensions. It leads to the formation of interpenetrating micro-voids and small fibrils, as schematically presented in Fig. 13.79. The empty space in these crazes is of the order of 45–60%. Crazing occurs mostly in brittle polymers like polystyrene and poly(methyl methacrylate) and is typified by a whitening of the crazed region, due to differences in refractive index, and thus by light scattering from the fibrils. Fig. 13.79 also shows that crazes still support load and that the stress at the tip of the craze is (much) higher than the average stress in the material (see also Sect. 13.5.9). Accordingly, crazes have a tendency to grow in the direction perpendicular to the principal stress (see Fig. 13.80). If the applied load is sufficient, the polymer bridges elongate and

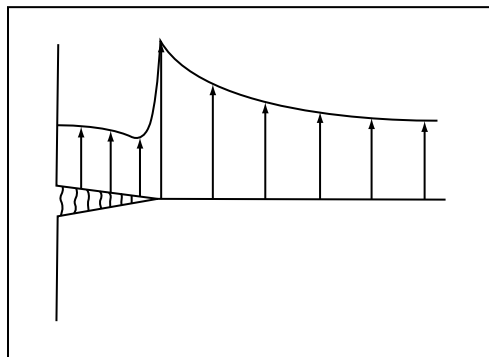


FIG. 13.79 Schematic view of a craze in a polymeric material and stress distribution in the adjacent material. Polymer bridges connect opposite surfaces.

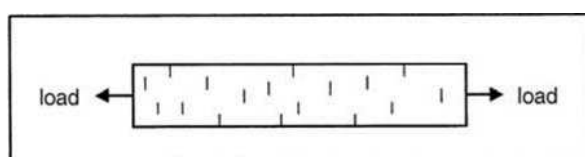


FIG. 13.80 Craze formation in the direction perpendicular to the principal stress.

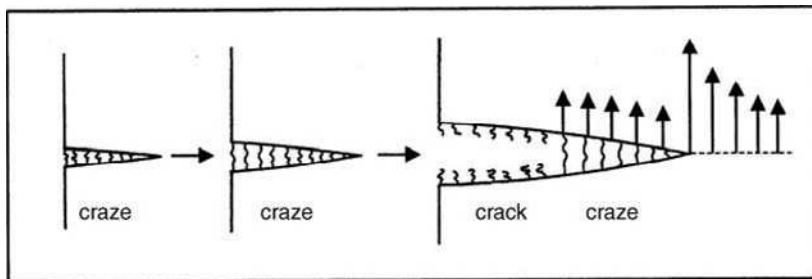


FIG. 13.81 Continuous craze growth and formation of a crack, which cannot support load, as shown in the stress distribution.

may eventually break under the formation of a crack, as schematically shown in Fig. 13.81. In cracks the space is completely empty, so that cracks are different from crazes that they are not able to support a load. Another difference between crazes and cracks is that crazes may disappear upon unloading and rejuvenating the sample above the glass transition temperature. This is not possible with cracks (see also Chap. 25).

13.5.9. Fracture mechanics

According to Williams (1973) the tensile stress σ_t at the tip of a crack (see Fig. 13.82) in the direction of the applied stress is:

$$\sigma_t = \sigma_o(1 + 2\sqrt{a/\rho}) \quad (13.141)$$

where σ_o = the applied tensile stress; $2a$ = the crack length; ρ = radius of curvature.

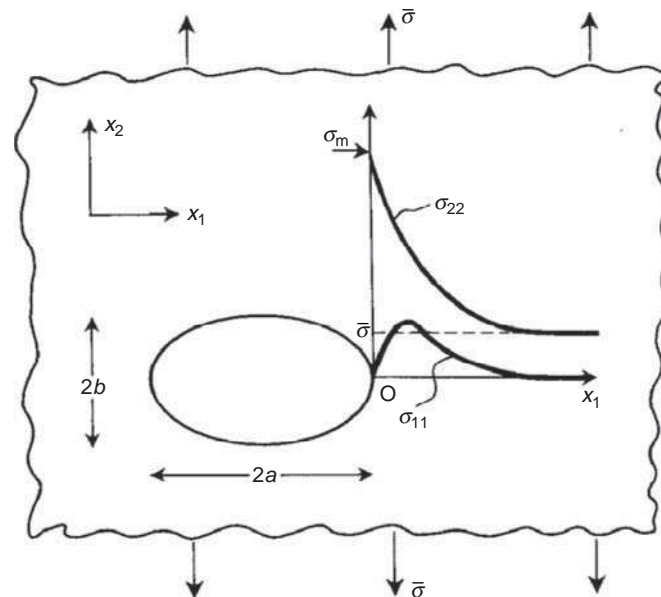


FIG. 13.82 An elliptical, through thickness crack in an elastic sheet subject to a stress $\bar{\sigma}$ in the x_2 -direction along Ox_1 as shown; σ_{22} is amplified from $\bar{\sigma}$ to σ_m at both tips of the crack; σ_{11} is perpendicular to σ_{22} . From McCrum, Buckley and Bucknall, 1997. Courtesy Oxford University Press.

For an elliptical hole (a = long semi axis, b = short semi axis) the radius of curvature at the end of the long axis is b^2/a so that

$$\sigma_t = \sigma_o(1 + 2a/b) \quad (13.142)$$

Besides the maximum tensile stress, also the stress distributions in the tensile direction and the opposite direction are shown in Fig. 13.82. Failure occurs where the stress concentration is highest, i.e. at the tip of the crack. It shows that the stress increases for longer (a increases) and sharper (ρ decreases) cracks. For thin elliptical cracks, e.g. with $a/b = 500$, the maximum stress amplification is 1000. Of course cracks are in general not elliptical, but it shows the enormous amplification of the average stress at the crack tip.

For sharp cracks, where ρ is almost zero, the stress concentration σ_t/σ_o becomes infinite. Hence the equation has to be modified and in general use is made of the classical analysis of Griffith (1920). Elastic energy is released by putting a sharp crack of length $2a$ into a thin plate, but energy is also needed to form two new surfaces. The work done per unit area of crack surface is G_C . If no heat is dissipated, as in the original derivation by Griffith, then $G_C = 2\gamma$, where γ is the surface energy of the newly formed surface. The factor 2 arises because of the formation of two new surfaces. For polymers 2γ is approximately 1 J/m^2 , whereas G_C is measured to be approximately 500 J/m^2 . This is caused by viscoelastic energy: for the formation of polymer cracks not only two new surfaces are formed but the majority of energy is needed to pull apart polymer molecules (microscopically it is shown that a crack has not a very smooth surface, but a surface with many coiled polymer molecules that are pulled apart). The total energy involved to form this crack in a wide plate is

$$U = -\frac{\sigma^2 \pi a^2 B}{E} + 2aB G_C \quad (13.143)$$

where B = thickness of the plate; E = Young's modulus.

The dependence of U on the crack length is shown in Fig. 13.83. This figure resembles the formation of critical nuclei in crystallisation processes (see Chap. 19). U first increases

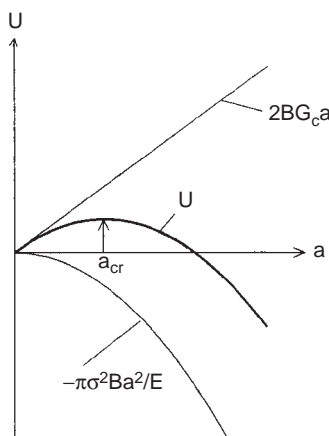


FIG. 13.83 Dependence of the change in energy of a wide sheet, U , on the half-length, a , of a crack, at constant tensile stress, σ . The total energy U is the sum of the surface energy, $2BG_c a$, and the strain energy, $-\pi\sigma^2 Ba^2/E$. For crack half-lengths smaller than $2a_{cr}$ the crack is stable under the applied stress; for half-lengths larger than $2a_{cr}$ the crack will grow under the applied stress σ .

with increasing crack length $2a$, but a maximum ($dU/da = 0$) is obtained for the critical crack length

$$2a_{\text{cr}} = \frac{2EG_C}{\pi\sigma_f^2} \quad (13.144)$$

Cracks larger than $2a_{\text{cr}}$ will grow spontaneously under the applied stress, because the energy will decrease in that case, whereas cracks smaller than $2a_{\text{cr}}$ are stable under the applied stress. Accordingly, the fracture tensile stress, i.e. the stress needed to increase the length of a crack, is

$$\sigma_f = \left(\frac{EG_{\text{IC}}}{\pi a_{\text{cr}}} \right)^{1/2} \quad (\text{plane - stress}) \quad (13.145)$$

Eq. (13.145) is called the *Griffith equation* for thin sheets, i.e. in plane stress, where G_{IC} , known as the fracture energy, has replaced 2γ . A frequently used parameter in plane stress is the *critical stress energy factor* K_C , which in the case of a wide sheet (plane stress) is defined as

$$K_{\text{IC}} = \sigma_f (\pi a_{\text{cr}})^{1/2} \quad (13.146)$$

or

$$K_{\text{IC}} = (EG_{\text{IC}})^{1/2} \quad (\text{plane - stress}) \quad (13.147)$$

The index I in G_{IC} refers to the mode of fracture deformation. Mode I is deformation due to tensile stresses, mode II is deformation in sliding and mode III in tearing.

From Eq. (13.146) it becomes clear that K_{IC} is easy to determine from the fracture tensile stress and the crack length, so that also G_{IC} can be calculated easily. The equations above are valid for thin, wide sheets, i.e. if the width W is very large with respect of the crack length (in mathematical terms as long as $\tan(a/W) \approx a/W$, see, e.g. McCrum et al., General References, 1997). If this condition is not obeyed, K_{IC} becomes dependent on the width of the sheet, so that, in contrast with G_{IC} , the stress intensity factor K_{IC} is not a material property.

The equations above are valid for plane-stress situations, i.e. for thin sheets. For thicker sheets plain-strain conditions occur at the crack tip. In that case for a thick plate of infinite width containing a crack of length $2a$ the fracture stress is

$$\sigma_f = \left[\frac{EG_{\text{IC}}}{\pi(1-\nu^2)a_{\text{cr}}} \right]^{1/2} \quad (\text{plane - strain}) \quad (13.148)$$

where ν is Poisson's ratio

Substitution in Eq. (13.146) gives the relationship for K_{IC} in plain strain

$$K_{\text{IC}} = \left[\frac{EG_{\text{IC}}}{1-\nu^2} \right]^{1/2} \quad (\text{plane - strain}) \quad (13.149)$$

It follows that for plane-stress parameters G_C and K_C have been replaced by the plane-strain parameters G_{IC} and K_{IC} which are in general smaller than their plane-stress analogues.

According to Eqs. (13.145) and (13.148) the fracture stress in plane strain is a factor $1/(1-v^2) \approx 1/0.84 \approx 1.2$ higher than in plane stress. Experimentally, however, the difference is much bigger. The reason for this discrepancy is that Griffith's equations were developed in linear fracture mechanics, which is based on the results of linear elasticity theory where the strains are supposed to be infinitesimal and proportional to the stress.

Example 13.6

A sharp central crack of length 30 mm in a wide, thick plate of a glassy plastic commences to propagate at $\sigma_f = 4.61$ MPa. (a) Find K_{IC} ; (b) Find G_{IC} , given that $E = 1.6$ GPa and that the Poisson constant = 0.4; and (c) will a crack of length 5 mm in a similar sheet fracture under a tensile stress of 10 MPa?

Solution

$$(a) \text{ Substitution in Eq. (13.146): } K_{IC} = 4.61 \times (\pi \times \frac{1}{2} \times 30 \times 10^{-3})^{1/2} = 1.00 \text{ MPa m}^{1/2}.$$

$$(b) \text{ Substitution in Eq. (13.149): } G_{IC} = \frac{K_{IC}^2(1-v^2)}{E} = \frac{10^{12}(1-0.4^2)}{1.6 \times 10^9} = 525 \text{ J/m}^2.$$

$$(c) K_I = \sigma(\pi a)^{1/2} = 10 \times (\pi \times \frac{1}{2} \times 5 \times 10^{-3})^{1/2} = 0.89 \text{ MPa m}^{1/2}.$$

K_I is 89% of K_{IC} and thus the plate will not fracture.

13.5.10. Ultimate stress-strain properties of amorphous elastomers

Lightly cross-linked elastomers follow a simple pattern of ultimate behaviour. Smith (1958) has shown that the ultimate properties of this class of polymers follow a time-temperature equivalence principle just as the viscoelastic response to small non-destructive stresses does.

Curves of stress (divided by absolute temperature) versus log time-to-break at various temperatures can be made to coincide by introducing the temperature-dependent shift factor a_T . Application of the same shift factor causes the curves of the elongation at the break ε_{br} versus the logarithm of time-to-break at various temperatures to coincide. A direct consequence is that all tensile strengths (divided by absolute temperature), when plotted against elongation at break, fall on a common failure envelope, independent of the temperature of testing. Fig. 13.84 shows the behaviour of Viton B elastomer.

Crystallisation accompanying stretching invalidates the simple time-temperature equivalence principle.

Fig. 13.84c, known as the *Smith failure envelope*, is of great importance because of its independence of the time scale. Moreover, investigations of Smith, and Landel and Fedors (1963, 1967) proved that the failure envelope is independent of the path, so that the same envelope is generated in stress relaxation, creep and constant-rate experiments. As such it serves a very useful failure criterion. Landel and Fedors (1967) showed that a further generalisation is obtained if the data are reduced to v_e , i.e. the number of elastically active network chains (EANCs). The latter is related to the modulus by

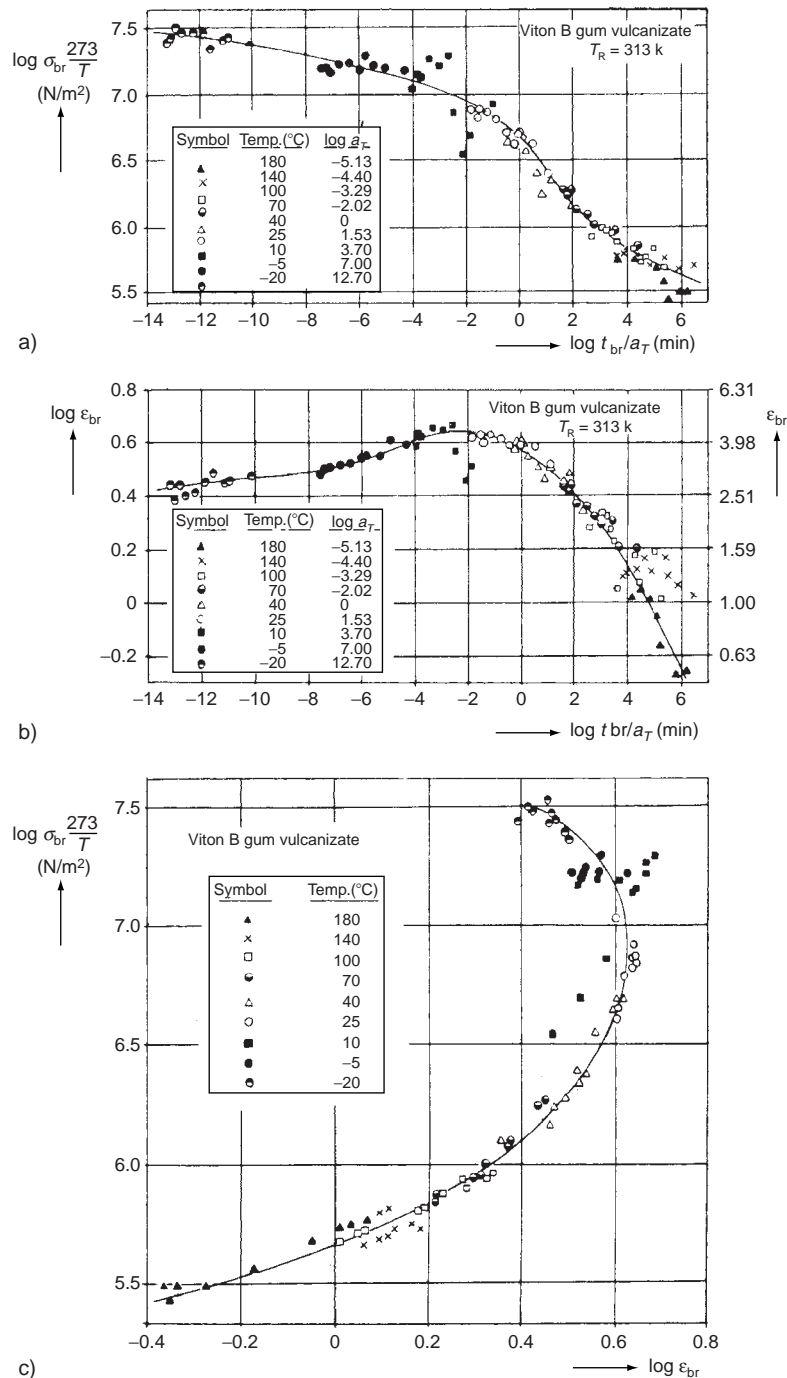


FIG. 13.84 Generalised ultimate parameters of an elastomer (after Smith, 1962, 1964). (A) Logarithmic plot of stress-at-break ($\sigma_{br} 273/T$) versus reduced time-to-break (t_{br}/a_T) for Viton B vulcanizate. Reference temperature for a_T is 313 K (40 °C); (B) logarithmic plot of ultimate strain (ϵ_{br}) versus reduced time to break (t_{br}/a_T) for Viton B vulcanizate; reference temperature for a_T is 313 K (40 °C); (C) failure envelope for Viton B vulcanizate.

$$E = 3RT\nu_e \quad (13.150)$$

By plotting

$\frac{\sigma_{br} 273}{T}$ vs. $\varepsilon_{br} = \Lambda_{br} - 1$, where Λ_{br} is the stretch ratio at break, they obtained a generalised diagram which is somewhat simplified in Fig. 13.85. It is valid for polybutadiene, polyisobutylene, silicon and fluorocarbon elastomers and for epoxy resins. At higher temperatures these polymers follow a common response curve, at lower temperatures they diverge due to their different T_g -temperatures, their different chain flexibilities and their different degrees of cross-linking.

For glassy and semi-crystalline polymers the number of investigations is restricted and no generalisations have been found.

13.5.10.1. Other mechanical properties of polymers

The other mechanical properties of polymers have the typical character of product properties: they are not only dependent on the intrinsic nature of the material but also on the environmental conditions, in other words, they are systemic quantities. They will be treated separately in Chap. 24.

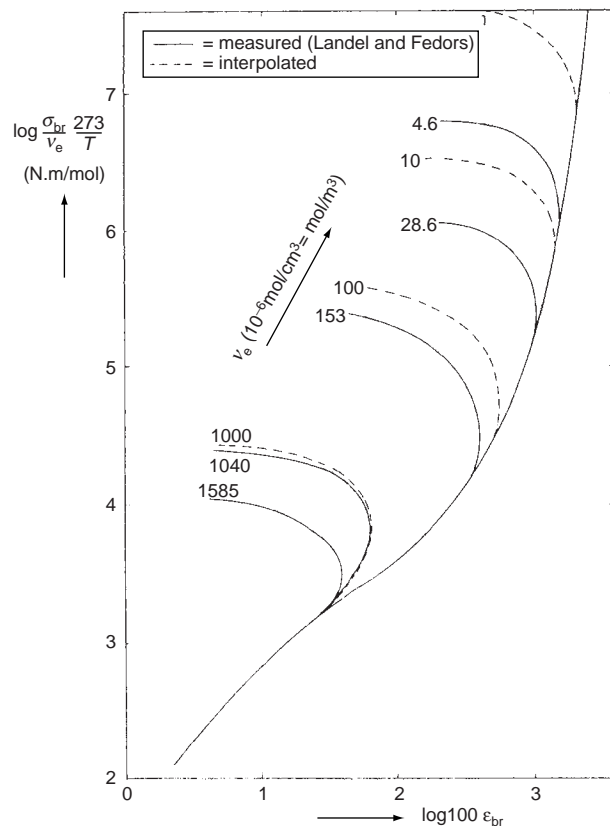


FIG. 13.85 Generalised failure envelope.

13.6. MECHANICAL PROPERTIES OF UNIAXIALLY ORIENTED POLYMERS (FIBRES)

If an isotropic polymer is subjected to an imposed external stress it undergoes a structural rearrangement called *orientation*. In amorphous polymers this is simply a rearrangement of the randomly coiled chain molecules (molecular orientation). In crystalline polymers the phenomenon is more complex. Crystallites may be reoriented or even completely rearranged and oriented recrystallisation may be induced by the stresses applied. The rearrangements in the crystalline material may be read from the X-ray diffraction patterns.

Nearly all polymeric objects have some orientation; during the forming (shaping) of the specimen the molecules are oriented by viscous flow and part of this orientation is frozen in as the object cools down. But this kind of orientation is negligible compared with the stress-imposed orientation applied in drawing or stretching processes.

Orientation is generally accomplished by deforming a polymer at or above its glass transition point. Fixation of the orientation takes place if the stretched polymer is cooled to below its glass transition temperature before the molecules have had a chance to return to this random orientation. By heating above the T_g the oriented polymer will tend to retract: in amorphous polymers the retractive force is even a direct measure of the degree of orientation obtained.

Orientation has a pronounced effect on the physical properties of polymers. Oriented polymers have properties, which vary in different directions, i.e. they are *anisotropic*.

Uniaxial orientation is accomplished by stretching a thread, strip or bar in one direction. Usually this process is carried out at a temperature just above the glass transition point. The polymer chains tend to line up parallel to the direction of stretching, although in reality only a small fraction of the chain segments becomes perfectly oriented.

Uniaxial orientation is of the utmost importance in the production of man-made fibres since it provides the desired mechanical properties like modulus and strength. In addition, it is only by stretching or drawing that the spun filaments become dimensionally stable and lose their tendency to creep – at least at room temperature. The filaments as spun possess a very low orientation unless spinning is performed at extreme velocities. Normally a separate drawing step is required to produce the orientation necessary for optimum physical properties. In practice a drawing machine consists of two sets of rolls, the second running faster depending on the stretch ratio, which is usually about four.

As mentioned already, the effects of orientation on the physical properties are considerable. They result in increased tensile strength and stiffness with increasing orientation. Of course, with increasing orientation the anisotropy of properties increases too. Oriented fibres are strong in the direction of their long axis, but relatively weak perpendicular to it.

If the orientation process in semi-crystalline fibres is carried out well below the melting point (T_m), the thread does not become thinner gradually, but rather suddenly, over a short distance: the *neck*. The so-called *draw ratio* (Λ) is the ratio of the length of the drawn to that of the undrawn filament; it is about 4–5 for many polymers, but may be as high as 40 for linear polyolefins and as low as 2 in the case of regenerated cellulose.

The degree of crystallinity does not change much during drawing if one starts from a specimen with a developed crystallinity (before drawing); if on the other hand, the crystallinity of the undrawn filament is not, or only moderately, developed, crystallinity can be greatly induced by drawing. The so-called “cold drawing” (e.g. nylon 6, 6 and 6) is carried out more or less adiabatically. The drawing energy involved is dissipated as heat, which causes a rise of temperature and a reduction of the viscosity. As the polymer thread reaches its yield-stress, it becomes mechanically unstable and a neck is formed.

During the drawing process the crystallites tend to break up into microlamellae and finally into still smaller units, possibly by unfolding or despiralizing of chains. Spherulites present tend to remain intact during the first stages of drawing and often elongate into ellipsoids. Rupture of the filament may occur at spherulite boundaries; therefore it is a disadvantage if the undrawn thread contains spherulites. After a first stage of reversible deformation of spherulites, a second phase may occur in which the spherulites are disrupted and separate helices of chains (in the case of polyamides) become permanently arranged parallel at the fibre axis. At extreme orientations the helices themselves are straightened.

13.6.1. Measurement of the orientation

13.6.1.1. Orientation can be measured by a number of methods

13.6.1.1.1. Birefringence or double refraction This is often the easiest method (Stein and Tobolsky, 1948; De Varies, 1953 and Andrews, 1954). The specific birefringence (Δn) of a fibre is defined as the difference in refractive index between the two components of a light wave vibrating parallel and perpendicular to the fibre axis ($\Delta n = n_{||} - n_{\perp}$). Birefringence is made up of contributions from the amorphous and crystalline regions.

The increase in birefringence occurring in crystalline polymers by orientation is due to the increase in mean orientation of the polarisable molecular chain segments. In crystalline regions the segments contribute more to the overall birefringence than in less ordered regions. Also the average orientation of the crystalline regions (behaving as structural units) may be notably different from the mean overall orientation.

13.6.1.1.2. X-ray diffraction (in crystalline polymers) Unoriented crystalline polymers show X-ray diffraction patterns, which resemble powder diagrams of low-molecular crystals, characterised by diffraction rings rather than by spots. As a result of orientation the rings contract into arcs and spots. From the azimuthal distribution of the intensity in the arcs the degree of orientation of the crystalline regions can be calculated (Kratky, 1941).

13.6.1.1.3. Infrared dichroism In oriented samples the amount of absorption of polarised infrared radiation may vary greatly when the direction of the plane of polarisation is changed. If stretching vibrations of definite structural groups involve changes in dipole moment that are perpendicular to the chain axis, the corresponding absorption bands are strong for polarised radiation vibrating perpendicular to the chain axis (and weak for that vibrating along the axis).

Sometimes separate absorptions can be found for crystalline and amorphous regions; in such a case the dichroism of this band gives information about orientation in both regions.

The X-ray diffraction measurements result in a numerical parameter $\langle \sin^2 \varphi \rangle$, where φ is the angle between the chain axis, being parallel to the symmetry axis of the crystallite, and the fibre axis. $\langle \sin^2 \varphi \rangle$ is called *orientation distribution parameter*. It has a zero value for ideal orientation and is equal to one in the case of isotropy ("ideal disorientation").

There exists a linear relation between Δn and $\langle \sin^2 \theta \rangle$, as was found by Hermans and Platzenk (1939):

$$\Delta n = (\Delta n)_{\max} \left(1 - \frac{3}{2} \langle \sin^2 \theta \rangle \right) \quad (13.151)$$

This expression is called the *Hermans function*; it is a nice example of unification in physics, in this case between optics and X-ray diffraction. This relation has a broad theoretical validity.

13.6.2. Mechanical properties of yarns (filaments, fibres)

The mechanical properties of fibres and yarns are quite complex and have been the subject of much experimental work. A stressed fibre is a very complicated viscoelastic system in which a number of irreversible processes, connected with plasticity, can take place.

The most important mechanical properties of fibres and filaments are:

The *tensile modulus*, E , in the direction of the fibre axis

The *tensile strength*, σ_{br} in the same direction

The *elongations* (ϵ , in %) at yield and at break

Since for the application of fibres in textile products (knitted and woven products, tire yarn canvas, reinforcement of plastics) a high specific weight is a disadvantage, it is customary also to express modulus and strength in another way, viz. as *specific* quantities; this is done by division of E and σ by the density ρ . E/ρ and σ/ρ have the dimension Nm/kg = J/kg. In order to relate these quantities to the *yarn count number* (expressed in Tex), the specific quantities are also expressed in N/tex.

1 denier = 1 g per 9000 m length of yarn;

1 tex = 1 g per 1000 m length of yarn = 10^{-6} kg/m;

1 tex = 9 denier;

$1 \text{N/tex} = 10^6 \text{J/kg} = 10 \text{MJ/kg} = 10^6 \text{Nm/kg} = 10^6 (\text{N/m}^2)/(\text{kg/m}^3)$.

A simple rule for conversion of numerical values is the following: divide the *numerical* value of the modulus or strength (expressed in GPa) by the numerical value of the specific weight (in g/cm³); then the numerical value of the specific modulus or strength is obtained, expressed in N/tex.

In the past the specific quantities were expressed in gf/denier; the latter had a value of $1/(9 \times 10^{-3} \times 9.81) = 11.3$ times the value in N/tex.

tenacity = tensile strength expressed in gf/denier:

$1 \text{gf/denier} = 9 \text{gf/tex} = 9 \times 10^{-3} \text{kgf/tex} = 88.29 \times 10^{-3} \text{N/tex} = 8.83 \times 10^4 \text{N m/kg}$.

Accordingly, tensile strength in GPa = $1 \text{gf/denier} \times \rho (\text{kg/m}^3) \times 8.83 \times 10^{-5}$

A very important diagram for fibres and yarns is the *stress-strain diagram*, where the specific stress is plotted as a function of the elongation (extensional strain) in %. The curve starts at an elongation of zero and ends in the breaking point at the *ultimate specific stress* (=tensile strength or *tenacity*) and the *ultimate elongation* (=strain at break).

Typical stress-strain curves are shown in Fig. 13.86. In addition Fig. 13.87 gives a survey of specific tenacity versus specific modulus for the modern high-performance filaments. The range of the specific modulus varies from 3 to 300 N/tex (i.e. modulus approximately from 3 to 500 GPa), that of tenacity from 0.2 to 3.5 N/tex (i.e. tenacity approximately from 0.2 to 5 GPa). Diagonal lines show the ratio σ_{br}/E_o ; the average value is about 0.02. In comparison Fig. 13.88 shows the same parameters for the conventional man made fibres. Here the ranges are much smaller and the average value of σ_{br}/E_o is about 0.08.

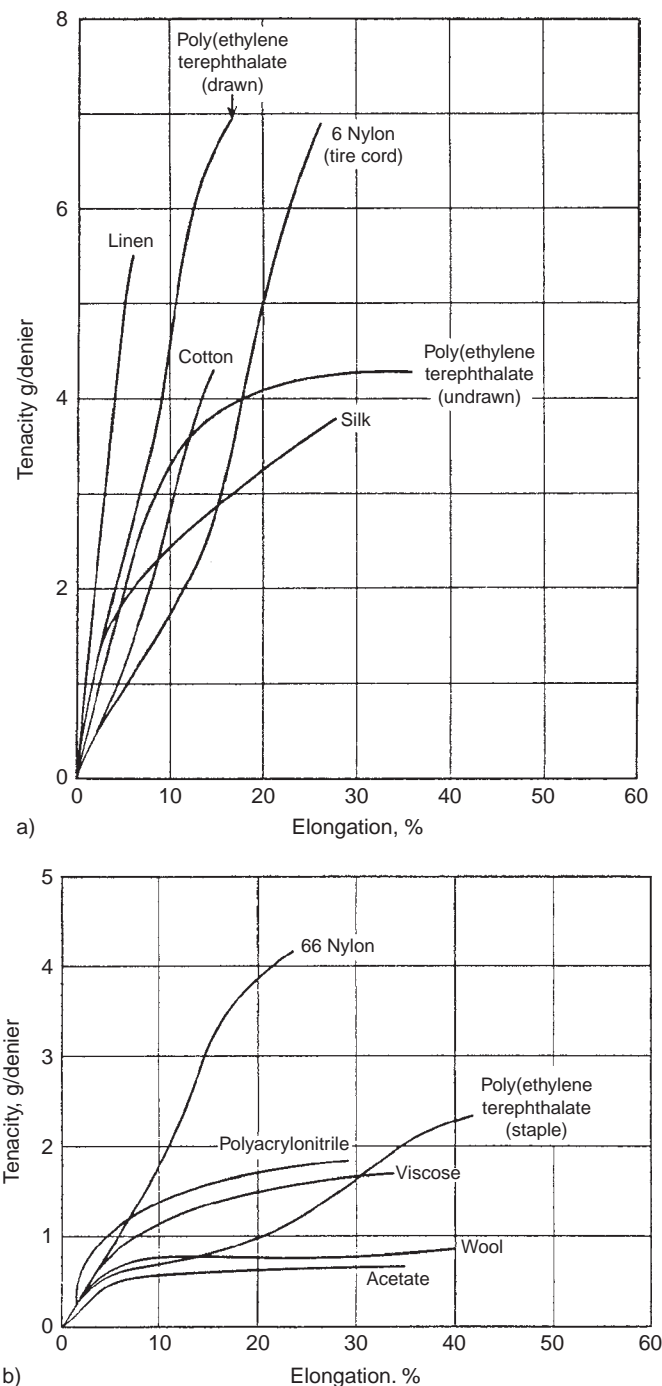


FIG. 13.86 (A) Stress-strain curves of silklike fibres (Heckert, 1953). (B) Stress-strain curves of woollike fibres (Heckert, 1953).

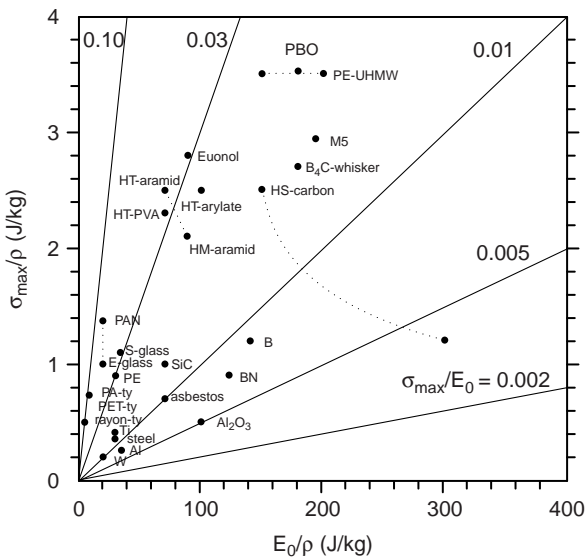


FIG. 13.87 Diagram of the specific tenacity (σ_{br}/ρ) versus specific dynamic tensile modulus (E_o/ρ), for modern high-performance filaments. The diagonal lines have the indicated ratio, which is the theoretical elongation at break (fractional); high-performance yarns have σ_{br}/E_o -values between 0.025 and 0.03 when the yarns are polymeric, whereas filaments of refractory materials have values between 0.025 and 0.005. (ty = tire yarn).

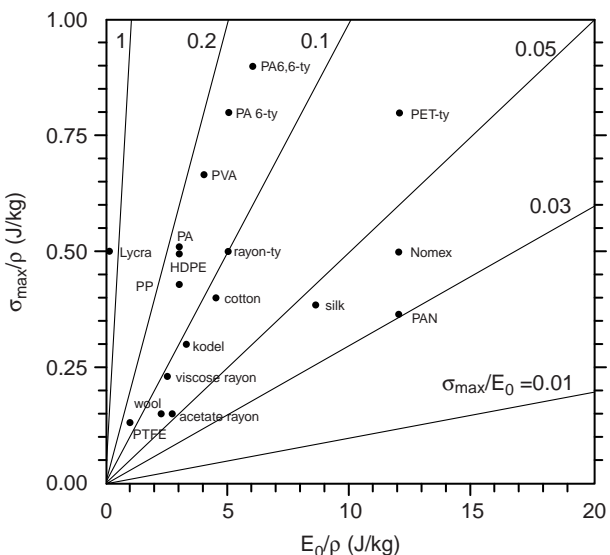


FIG. 13.88 Diagram of the specific tenacity (σ_{br}/ρ) versus the initial specific modulus (E_o/ρ) for conventional man made fibres. E_o is the limiting tangential slope in the stress-strain diagram for strain tending to zero. The diagonal lines show the indicated σ_{br}/E_o -ratio; this varies from = 1 for elastomeric filaments and ~0.2 for tyre yarns (ty) to 0.03 for yarns such as polyacrylonitrile.

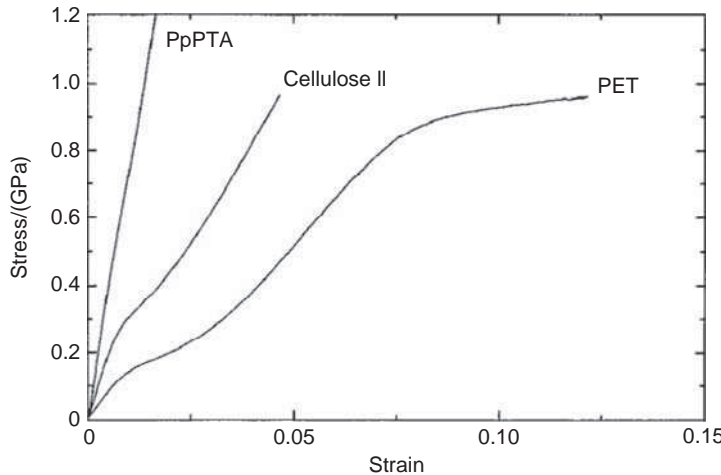


FIG. 13.89 Typical stress–strain curves of PET, cellulose II and PpPTA fibres. From Northolt and Baltussen (2002). Courtesy John Wiley & Sons, Inc.

The very wide range of the numerical values of the mechanical properties is evident. The modulus of organic polymer fibres varies between 1 and 350 GPa. The tenacities or tensile strengths may even vary from about 0.07 GPa (0.05 N/tex) for the weakest (cellulose acetate) to about 7 GPa (4 N/tex) for the strongest fibre (PIP or M5®); the compressive strengths reaches up to 1.7 GPa and the temperature resistance up to 400 °C. The ultimate elongation may vary from about 1% for the stiffest fibre (carbon) to about 600% for the most rubber–elastic.

Notwithstanding this great variety of mechanical properties the deformation curves of fibres of linear polymers in the glassy state show a great similarity. Typical stress–strain curves of poly(ethylene terephthalate) (PET), cellulose II and poly(*p*-phenylene terephthalamide (PpPTA) are shown in Fig. 13.89. All curves consist of a nearly straight section up to the yield strain between 0.5 and 2.5%, a short yield range characterised by a decrease of the slope, followed by a more or less concave section almost up to fracture. Also the sonic modulus versus strain curves of these fibres are very similar (see Fig. 13.90). Apart from a small shoulder below the yield point for the medium- or low-oriented fibres, the sonic modulus is an increasing, almost linear function of the strain.

We shall now discuss to what extent it is possible to estimate/predict the mechanical behaviour of filaments and fibres. Important properties of several high-performance fibres are listed in Table 13.16 (Sikkema et al., 2003).

13.6.3. Empirical relations for partly oriented yarns

Many years ago De Vries discovered two important relations, when he was studying the orientation in drawing viscose-rayon yarns: one for the relationship between draw ratio and modulus, the other for the stress–strain correlation in drawn yarns.

a. The compliance of a fibre as a function of the draw ratio (Λ)

De Vries found the following empirical relationship:

$$\frac{1}{E} = \frac{1}{E_{\text{iso}}} - \frac{\ln \Lambda}{C_\Lambda} \quad \text{or} \quad S = S_{\text{iso}} - \frac{\ln \Lambda}{C_\Lambda} \quad (13.152)$$

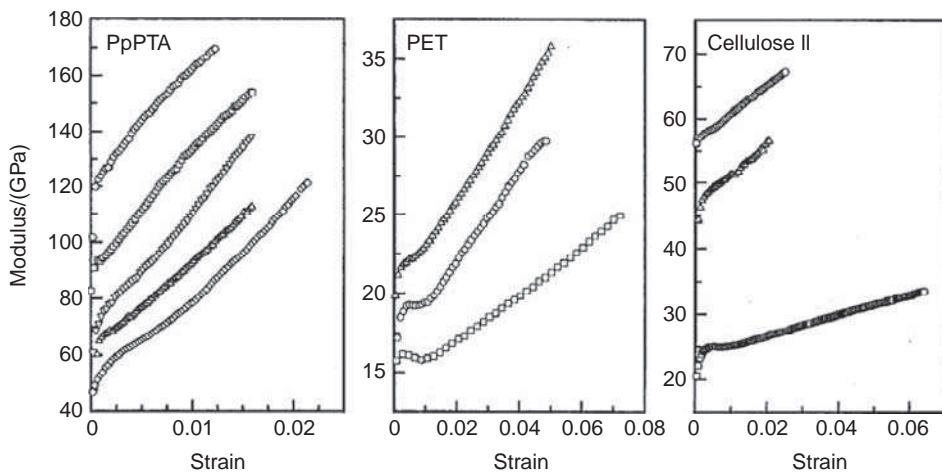


FIG. 13.90 Typical sonic modulus vs. strain curves of PET, cellulose II and PpPTA fibres. The differences in initial moduli per polymer are due to differences in orientation angles. From Northolt and Baltussen (2002). Courtesy John Wiley & Sons, Inc.

TABLE 13.16 Values of E_o and C_ε (in GPa) for some commercial yarns

Yarn	E_o	C_ε	E_o/C_ε
Native cellulose (cotton)	16	2.0	8.0
Rayon tire yarn	40	5.5	7.3
Linear polyethylene HD	11.7	1.65	7.1
Nylon 66	7	0.9	7.8
Nylon 6	4.5	0.65	7.0
PET polyester yarn	18.5	2.3	8.0

E_o measured at 9000 Hz (De Vries, 1953–1959; Weyland, 1961).

C_Λ is a constant having the value of approximately 8 GPa for viscose-rayon yarn. De Vries also investigated some other synthetic fibres; his values for the constant C_Λ were found to be proportional to E_{iso} , so that the product $C_\Lambda S_{iso}$ is a constant:

$$C_\Lambda S_{iso} = 1.65 \quad (13.153)$$

Substituting this value in (13.152) we obtain

$$S = S_{iso}(1 - 1.4 \log \Lambda) \quad (13.154)$$

This relation is shown in Fig. 13.91 and describes the experimental data of PET-polyester fibre very well for compliances $>0.1 \text{ GPa}^{-1}$. The same applies for nylon yarns.

b. The stress-strain behaviour of drawn yarns

In this case De Vries found the correlation:

$$\ln(1 + \varepsilon) = C_\varepsilon \left(\frac{1}{E_o} - \frac{1}{E} \right) = C_\varepsilon (S_{iso} - S) \quad (13.155)$$

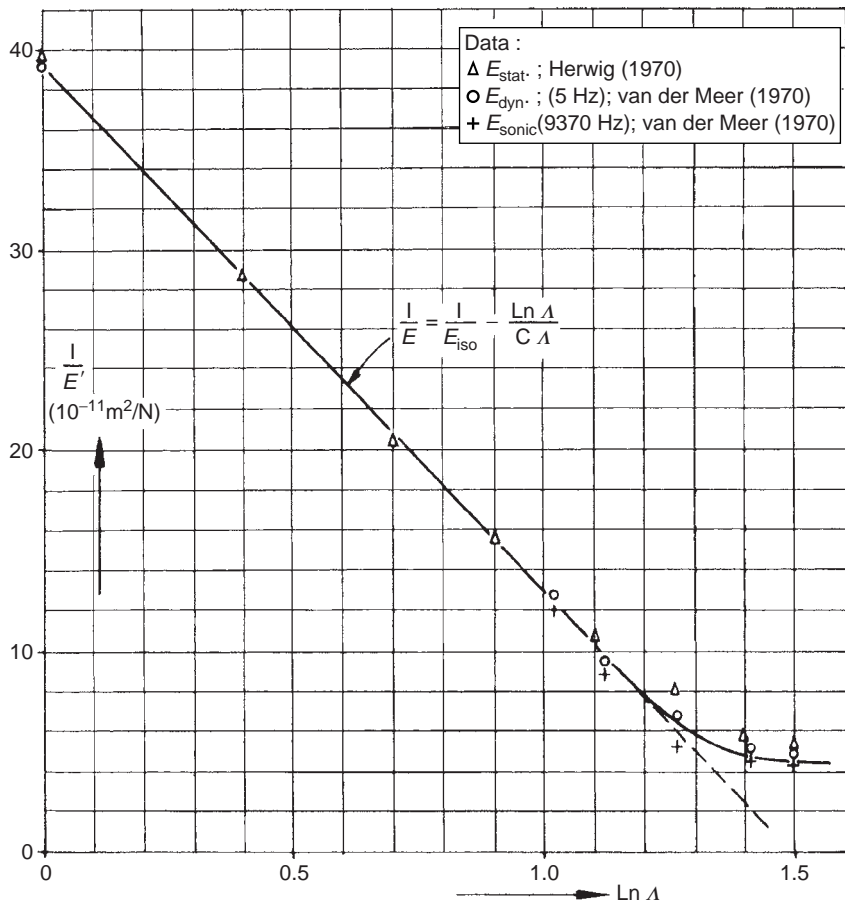


FIG. 13.91 Influence of draw ratio on modulus of elasticity (E') (three drawing series of polyester (PETP) yarns).

The similarity of Eqs. (13.155) and (13.152) can easily be understood, since drawing and elongation are, in principle, very similar; if a yarn with a draw ratio Λ_o and an initial modulus E_o (under the same conditions) were subjected to further elongation ε , the total resulting draw ratio would be:

$$\Lambda_{\text{tot}} = \Lambda_o(1 + \varepsilon) \quad (13.156)$$

Table 13.17 gives the values of some synthetic yarns. The average value of the ratio E_o/C_ε is 7.5, where E_o is the initial modulus of the yarn. For yarns with helical molecular chains (silk, hair, isot. polypropylene, etc.) the value of E_o/C_ε is lower (about 2). Native cellulose (cotton) is added to the series for comparison. After substitution of $E_o/C_\varepsilon = 7.5$ and $E = \sigma/\varepsilon$ we get, after some rearrangement:

$$\sigma = \varepsilon \frac{E_o}{1 - 7.5 \ln(1 + \varepsilon)} \quad (13.157)$$

TABLE 13.17 Mechanical and physical properties of high-performance fibres (after Sikkema et al., 2003)

Property	Aramid fibre	Carbon fibre ^a	PBO ^b fibre	M5 fibre (exp.)
	High E	High strength	High E	High E
Tenacity (specific strength) (GPa)	3.2	3.5	5.5	5.0
Elongation (%)	2.0	1.5	2.5	1.5
Elastic modulus (GPa)	115	230	280	330
Compressive strength (GPa)	0.58	2.10	0.40	1.70
Compressive strain (%) ^c	0.50	0.90	0.15	0.50
Density (kg/m ³)	1450	1800	1560	1700
Water regain ^d (%)	3.5	0.0	0.6	2.0
Limiting oxygen index (LOI) ^e (%O ₂)	29	—	68	59
Onset of thermal degradation, air (°C)	450	800	550	530

^a Mechanical properties of carbon fibre are evaluated in resin-impregnated strands to protect the material against premature brittle failure in the tensile test machine. The organic fibres are tested as such; averages of 10 filament measurements (10 cm gauge) are given for the tensile data.

^b PBO = poly(benzobisoxasole); Toyoba data.

^c Measured in unidirectional composite test bars, three-point bending test, onset of deflection for the organic-fibre-reinforced composites; catastrophic failure for the carbon composites. M5 composites proved to be able to carry much higher loads than the load at onset of deflection and to absorb more energy at high compressive strains in a mode analogous to the flow behaviour in steel being damaged.

^d Fibres are first dried in an oven, then exposed to 65% RH at 23 °C for 24 h.

^e Percentage of oxygen in the atmosphere that will sustain burning of the material (see Chap. 26).

or, for the general case

$$\sigma = \frac{\varepsilon E_o}{1 - (E_o/C_e)\ln(1 + \varepsilon)} \quad (13.158)$$

In contrast to the Young modulus the shear modulus is nearly independent of orientation (the torsional strength, however, decreases!).

c. Empirical relation between compliance and birefringence

Very interesting are the classic results obtained by Northolt in investigating a stretch series of polyester (PET) tire yarns. Poly(ethylene terephthalate) used to be an extremely useful polymer for studying mechanical properties of fibres, since it may be spun as an isotropic filament and can be stretched to a very wide range of yarns of increasing degrees of orientation. Experimental data of the dynamic compliance and the birefringence of this stretch series are given in Fig. 13.92. It is striking that the plotted “curve” consists of two branches, linear relations: one for well-oriented fibres ($\Delta n > 0.07$, $S < 0.15$) and one, with a significantly lower slope for the low-oriented fibres ($\Delta n < 0.05$, $S > 0.2$). An analogous effect was found by Northolt and De Vries (1985) in a stretch series of regenerated cellulose (viscose-rayon), see Fig. 13.93. The two branches in the $\Delta n - S$ diagram could be explained by the two versions of the series aggregate model. The classical version, with elements of cubical shape, provides a satisfactory interpretation of the data of low-oriented fibres; the modified version of the single-phase series model, with the oblong-shaped elements, explains the data of well-oriented fibres. The latter model also includes in its interpretation the aramid, arylate and even the carbon fibres.

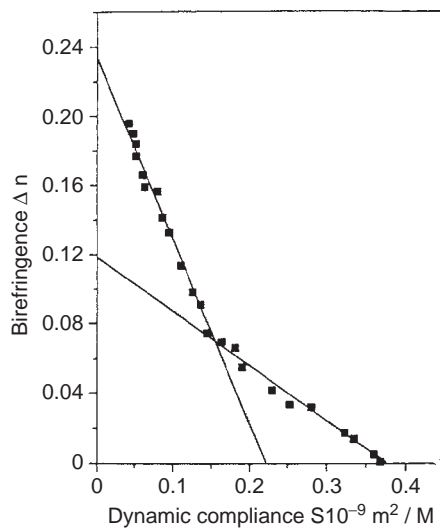


FIG. 13.92 Birefringence Δn as a function of the dynamic compliance $E^{-1} = S$ for various polyester tire yarns.

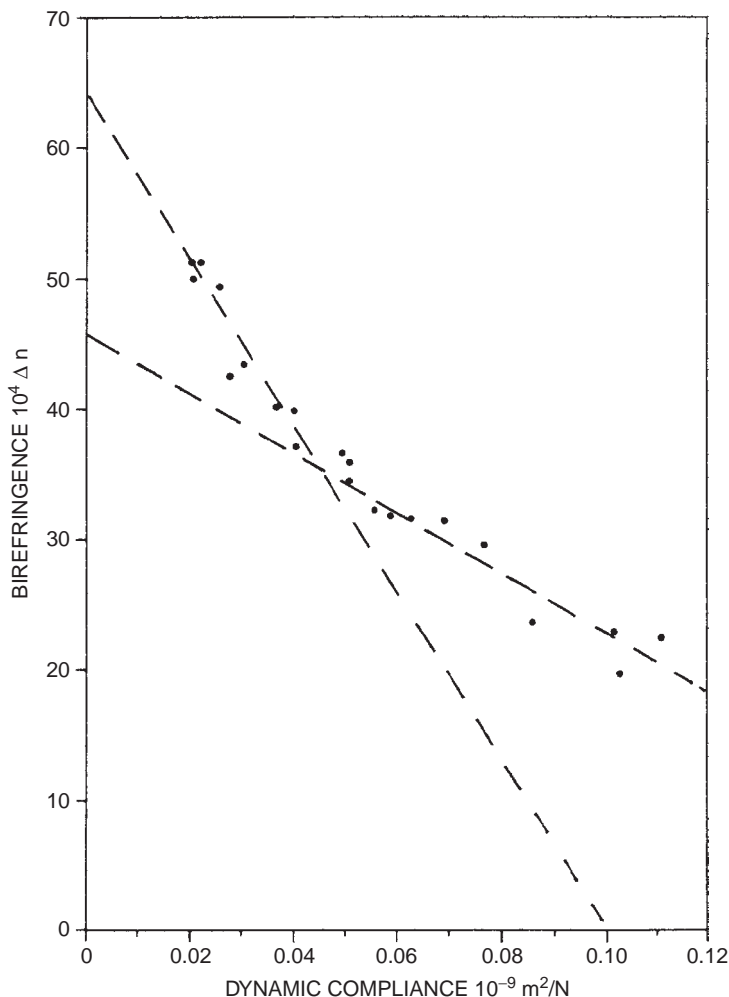


FIG. 13.93 Birefringence Δn as a function of the dynamic compliance $E^{-1} = S$ for various regenerated cellulose fibres.

13.6.4. Generalised stress-strain relationship for polymers

An interesting relation found by Herwig (1970) for a nylon 6 drawing series may be mentioned. Every yarn in such a drawing series, having a certain draw ratio (Λ_o) has its own stress-strain diagram, in which the stress (σ) refers to the cross-section of the yarn and the strain (ε) to the initial length of the (drawn) yarn. If, however, the stress is related to the original spinning cross-section and the strain to the original spinning length, it appears that all the stress-strain curves above the yield value merge into one "master curve", as shown in Fig. 13.94. This master curve is the stress-strain curve of the undrawn yarn.

For this purpose the "reduced" stress and strain are calculated from the following equations:

$$\sigma_{\text{red}} = \sigma_{\text{obs}} / \Lambda_o \quad (13.159)$$

$$1 + \varepsilon_{\text{red}} = (1 + \varepsilon_{\text{obs}}) \Lambda_o \quad (13.160)$$

where Λ_o is the draw ratio at which the yarn has been produced. Comparison of this equation with Eq. (13.156) shows that $1 + \varepsilon_{\text{red}} = \Lambda_{\text{tot}}$ as far as the conditions of drawing and elongation are equivalent.

Fig. 13.94 shows that if the stress-strain diagram of the undrawn yarn is determined, the stress-strain diagrams of all the drawn yarns, obtained at definite draw ratios, can be estimated.

The relationships between the stress-strain curves of undrawn and drawn yarn, borne out by the "master curve", again stress the key role of the draw ratio and elongation with respect to the physical properties of yarns, as already shown by the relations to birefringence (Eq. (10.24)) and dynamic modulus of elasticity (Eqs. (13.98) and (13.101)).

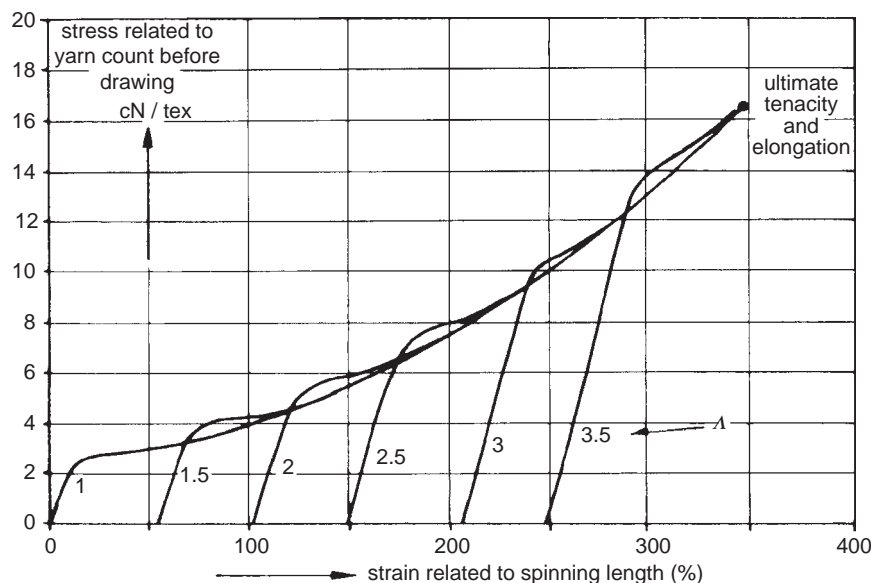


FIG. 13.94 Generalised stress-strain diagram for nylon 6. The tex is a standardised symbol for the linear density of a yarn: 1 tex = 1 g per 1000 m. Divided by the density it is proportional to the cross-section of the yarn (after Herwig, 1970).

13.6.5. Theoretical approach of the mechanical properties of well-oriented polymer fibres

(a) Introduction

The theoretical treatment of the mechanical properties of fibres is, as a matter of fact, more complicated than that of isotropic polymers. Instead of two elastic parameters, e.g. the tensile modulus and the Poisson ratio, we now need five, because of the anisotropy.

A useful fibre model is the series aggregate model. The original model has been developed by Ward (1983). In this model the fibre is considered as being built up of a series of elements, together forming a fibril. Each element is a transversely isotropic body of cubical shape, having five elastic constants e_{ch} , e_{\perp} , g_d , v_{12} and v_{13} , which have the following meaning:

e_{ch} = tensile modulus parallel to the chain axis of the polymer

e_{\perp} = tensile modulus perpendicular to this symmetry axis

g_d = shear modulus parallel to the symmetry axis

v_{12} = Poisson ratio for a stress directed normal to the symmetry axis

v_{13} = Poisson ratio for a stress, parallel to the symmetry axis

By means of these elastic constants and the orientation distribution of the symmetry axes with respect to the fibre axis, the Compliance ($S = 1/E$ = reciprocal modulus) of the fibre could be calculated.

Later Northolt and Van der Hout (1985) developed a *modified model*, in which the fibre is considered to be composed of a series arrangement of *oblong-shaped elements* with their longest dimension parallel to the chain axis. It is also assumed that the oblong-shaped elements change in shape and thus in length under an applied stress. The model takes into account the coupling of the successive elements throughout the orientation process caused by extension of the fibre.

In a subsequent investigation, with Roos and Kampschreur (1989), Northolt extended the modified series model to include viscoelasticity. For that an additional assumption was made, viz. that the relaxation process is confined solely to shear deformation of adjacent chains. The modified series model may be applied to well-oriented fibres having a small plastic deformation (or set). In particular it explains the part of the tensile curve beyond the yield stress in which the orientation process of the fibrils takes place. The main factor governing this process is the modulus for shear, g_d , between adjacent chains. At high deformation frequencies g_d attains its maximum value, g_{do} ; at lower frequencies or longer times the viscoelasticity lowers the value of g_d , and it becomes a function of time or frequency. Northolt's relations, that directly follow from his theoretical model for well-oriented fibres, are in perfect agreement with the experimental data if acceptable values for the elastic parameters are substituted.

For low-oriented fibres the theory leads to a much more complicated expression, which can only be simplified under special conditions. Moreover, in low-oriented fibres not only elastic and viscoelastic, but also plastic deformations play a part. So no analytical relations can be derived for low-oriented fibres and we have to resort to empirical equations.

(b) The Northolt and Baltussen continuous chain model for well-oriented fibres

For fibres below their glass transition temperature the dominant structural parameter for their tensile properties is the chain orientation function. Structural details, except for the orientation distribution are less important. The tensile deformation of fibres is caused by a

combined effect of the elongation of the polymer chains themselves and the shear deformation of a small domain containing the considered chain element. Main parameters are the domain shear modulus g_d , the chain modulus e_{ch} and the orientation distribution $f(\theta)$ of the polymer chains with respect of the fibre axis. Values for e_{ch} can be calculated (from bond strengths and valence angles) or independently determined (from crystallite strain measurements, using X-ray diffraction on fibres, see Sect. 13.6.1). The chain modulus is very large (of the order of 250 GPa) with respect of the domain shear modulus (of the order of 2 GPa), and accordingly the deformation of medium and low oriented fibres is dominated by the local shear deformation. A simple theory shows that the yield strain in tension varies from 0.5% for well-oriented fibres to 2.5% for randomly oriented fibres (1995).

In the 1990s Northolt and Baltussen developed the so-called *continuous chain model*, which is able to describe the tensile deformation properties of well-oriented polymer fibres properly. We will not go into detail in describing this outstanding model, but for an exact description of this model the reader is referred to the many publications of these two authors and their co-authors in the years from 1995 to 2005, and in particular to the doctoral thesis (1996) by Baltussen, the 2002 paper by Northolt and Baltussen and the 2005 paper by Northolt et al. on the strength of polymer fibres.

(b1) Introduction of the NB-model; the initial modulus and compliance

The model is based on the simple model for the structure of para-crystalline polymers represented in Fig. 13.95. The immediate surroundings of a small chain segment are called a domain. The chain, chain segment and the surrounding domain are schematically represented in Fig. 13.96. The chain segment is the symmetry axis of the domain and subtends an angle Θ with the fibre axis in the unloaded state. The orientation angle Θ follows a distribution $\rho(\Theta)$, where $N(\Theta)d\Theta = \rho(\Theta) \sin\Theta d\Theta$ is the fraction of segments with an orientation between Θ and $\Theta + d\Theta$. The fibre is deformed by a tensile stress σ^F parallel to the fibre axis. The angle between the fibre axis and the chain segment of a deformed domain is denoted by θ . The strain of the fibre is given by:

$$\varepsilon^F = (L - L_o)/L_o \quad (13.161)$$

where L_o is the projection length of the chain onto the fibre axis in the unloaded state:

$$L_o = L_{ch} \langle \cos \Theta \rangle \quad (13.162)$$

L_{ch} being the contour length of the chain. The projection length L of the chain at a tensile stress σ is equal to

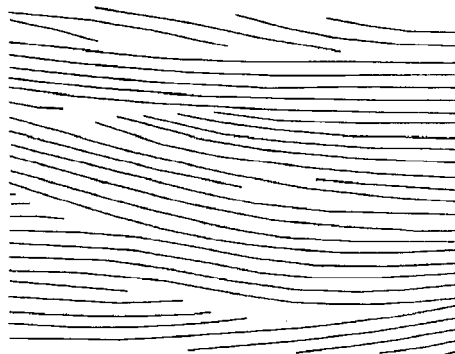


FIG. 13.95 The single-phase structural model for a polymer fibre. From Northolt and Baltussen (2002). Courtesy John Wiley & Sons, Inc.

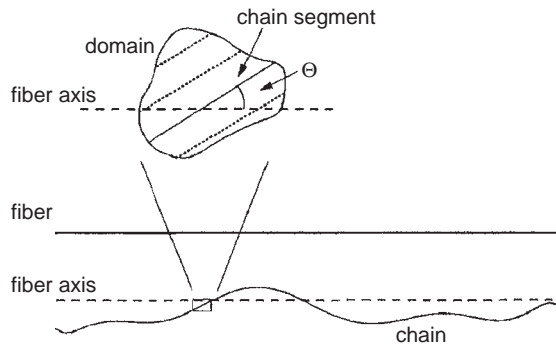


FIG. 13.96 A schematic picture of a chain, a chain segment and the surrounding domain. From Northolt and Baltussen (2002). Courtesy John Wiley & Sons, Inc.

$$L = L_{\text{ch}} \langle [1 + \varepsilon_{\text{ch}}(\Theta, \sigma^F)] \cos \theta(\Theta, \sigma^F) \rangle \quad (13.163)$$

where ε_{ch} is the strain of a chain segment and where in general the average of a function $f(\Theta)$ is defined here as

$$\langle f(\Theta) \rangle \equiv \frac{\int f(\Theta) \rho(\Theta) \sin \Theta \, d\Theta}{\int \rho(\Theta) \sin \Theta \, d\Theta} \quad (13.164)$$

A schematic representation of the domain contributions to the tensile deformation of a fibre is depicted in Fig. 13.97 and shows that the total deformation consists of chain stretching and shear deformation resulting in rotation of the chain axis. For an infinitesimal deformation and well-oriented fibres Northolt and Baltussen found for the initial modulus, E_{in}^F , and for the initial compliance, S_{in}^F , of the fibre

$$S_{\text{in}}^F = \frac{1}{E_{\text{in}}^F} = \frac{1}{e_{\text{ch}}} + \frac{\langle \sin^2 \Theta \rangle_E}{2g_d} \quad (13.165)$$

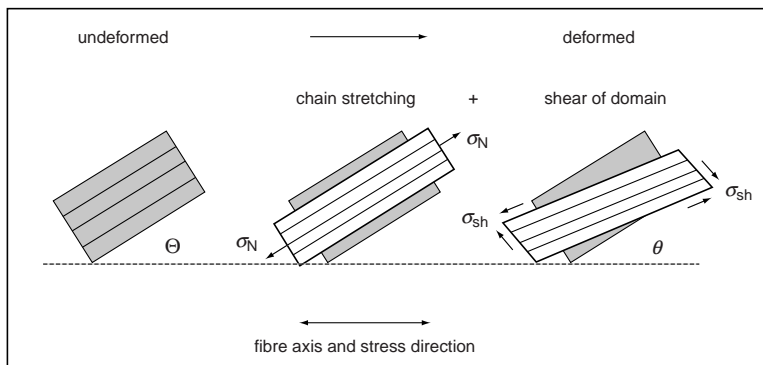


FIG. 13.97 Schematic representation of the domain contributions to the tensile deformation of the fibre: chain stretching and chain rotation due to shear deformation. The chains make an angle Θ in the undeformed state and angle θ in the deformed state. From Northolt et al. (2005). Courtesy Springer Verlag.

where e_{ch} is the chain modulus, g_d the shear modulus of the surrounding domain and $\langle \sin^2 \Theta \rangle_E$ is the strain orientation parameter of the chains, defined by

$$\langle \sin^2 \Theta \rangle_E = \frac{\langle \sin^2 \Theta \cos \Theta \rangle}{\langle \cos \Theta \rangle} \quad (13.166)$$

Because e_{ch} is much larger than g_d (see, e.g. Table 13.18), Eq. (13.165) shows that the fibre modulus is largely determined by the orientation of the fibre and by the value of the shear modulus g_d .

If Eq. (13.165) is substituted in the Hermans function Eq. (13.151) we obtain a general relationship between the birefringence and the compliance of well-oriented fibres:

$$\Delta n = (\Delta n)_{max} \left[\left(1 + 3 \frac{g_d}{e_{ch}} \right) - 3g_d S \right] \quad (13.151a)$$

Although initially the model has been developed for well-oriented para-crystalline fibres, experimental results have shown that it can also be applied to well-oriented semi-crystalline fibres.

(b2) The modulus and compliance under stress

Due to the elastic deformation of the domain of well-oriented polymer fibres the orientation angle Θ of the chain decreases approximately according to

$$\tan(\theta - \Theta) = -\frac{\sigma^F}{2g_d} \sin \theta \cos \theta = -\frac{\sigma^F}{4g_d} \sin 2\theta \quad (13.167)$$

TABLE 13.18 The basic elastic constants g_d and e_{ch} , the highest filament values of the modulus, E and the strength, σ_b , together with the average values of the creep compliance, $j(t)$ (ratio of time dependent creep and local stress), at 20 °C and the interchain bond for a variety of organic polymeric fibres (after Northolt et al., 2005)

Fibre	e_{ch} (GPa)	g_d (GPa)	E (GPa)	σ_b (GPa)	$j(t)$	Interchain bond
UHMW PE	280–300	0.7–0.9	264	7.2	0.3	Van der Waals
PET	125	1.0–1.3	38	2.3	0.13	Van der Waals/dipole
Cellulose II	88	2.0–5.0 ^a	55	1.8	0.4 ^b	Bidirectional hydrogen
Cellulose I (native fibre)	136	1.5	110	–	–	Unidirectional hydrogen/Van der Waals
PpPTA	240	1.5–2.7	140	4.5	0.02–0.04	Unidirectional hydrogen/Van der Waals
PBO	500	1.0–1.5	280	7.3	0.005	Van der Waals/dipole
PIPD ^c	550	6.0	330	6.6	0.0035	Bidirectional hydrogen

^a Depending on water content.

^b Conditioned at 65% R.H.

^c PIPD is a fibre in an early stage of development

where of course $\theta = \theta(\sigma^F)$. For well-oriented fibres the fibre strain ε^F , which, as shown before, is equal to the sum of the strain of the chain segment and the rotational shear strain, reads:

$$\varepsilon^F = \varepsilon_{ch} + \varepsilon_{sh} = \frac{\sigma^F (\cos^2 \theta)}{e_{ch}} + \frac{\langle \cos \theta \rangle - \langle \cos \Theta \rangle}{\langle \cos \Theta \rangle} \quad (13.168)$$

A combination of Eqs. (13.167) and (13.168) yields the typical concave shape of the elastic stress-strain curve of well-oriented fibres. In Fig. 13.98 the calculated stress-strain curve is compared with the experimental curve at decreasing stress of a Twaron® 1000 fibre. It shows almost elastic behaviour. By including the simple theory the tensile curve with yield can be calculated as shown in Fig. 13.99.

The compliance, i.e. the reciprocal of the dynamic modulus of the fibre, can now be approximated at a stress σ by

$$S^F = \frac{1}{E^F} = \frac{1}{e_{ch}} + \frac{\langle \sin^2 \theta \rangle_E}{2g_d \left(1 + \frac{\sigma^F}{2g_d}\right)} \quad (13.169)$$

E^F is the sonic modulus of the fibre. From Eq. (13.167) it follows that measurement of Θ and $\theta(\sigma^F)$ (by X-ray diffraction) during extension of a fibre, yields the value of σ^F/g_d and thus of g_d . Eq. (13.169) predicts a linear relation between the compliance and the orientation parameter $\langle \sin^2 \theta \rangle_E / [1 + \sigma^F / (2g_d)]$. This relation has been verified experimentally by a combined sonic modulus-X-ray diffraction experiment on a PpPTA fibre (Baltussen and Northolt, 2002), as shown in Fig. 13.100. Linear regression yields $e_{ch} = 240$ GPa and $g_d = 1.60$ GPa.

(b3) The failure envelope

For fibres made from the same polymer but with different degrees of chain orientation the end points $(\varepsilon_f^F, \sigma_f^F)$ of the tensile curves are approximately located on a hyperbola. Typical examples of this fracture envelope are shown in Fig. 13.101 for cellulose II fibres.

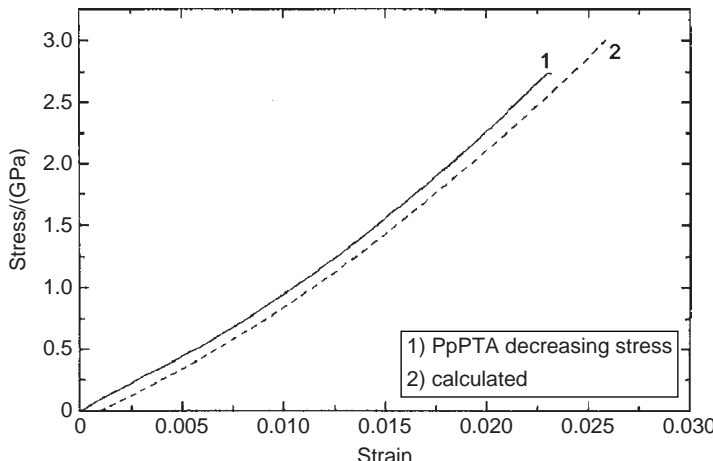


FIG. 13.98 The stress-strain curve of a Twaron® 1000 fibre at decreasing stress compared with the calculated curve. From Northolt and Baltussen (2002). Courtesy John Wiley & Sons, Inc.

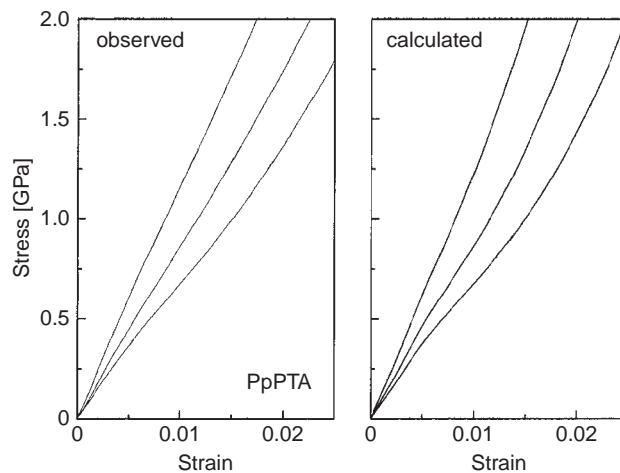


FIG. 13.99 The observed stress–strain curves of three PpPTA fibres compared to the calculated curves. From Northolt et al. (1996). Courtesy John Wiley & Sons, Inc.

A simple explanation for the shape of the fracture envelope starts with the assumption that the tensile curve is linear with modulus E^F . The work of fracture or the strain energy per unit volume up to the fracture point is given by

$$W_f^F = \int_0^{e_f^F} \sigma^F d\epsilon^F = \frac{1}{2} E^F (e_f^F)^2 = \frac{1}{2} \sigma_f^F e_f^F \quad (13.170)$$

If it is assumed that W_f^F is independent of the initial modulus of the fibres made from the same polymer, then the end points are located on a hyperbola $\sigma_f^F = 2W_f^F/e_f^F$. In Fig. 13.101 $W_f^F = 0.058 \text{ GJ/m}^3$ gives the best fit. Cellulose II has a chain modulus $e_{ch} = 88 \text{ GPa}$ (see Table 13.18), which yields for the strain energy of the chain up to fracture of

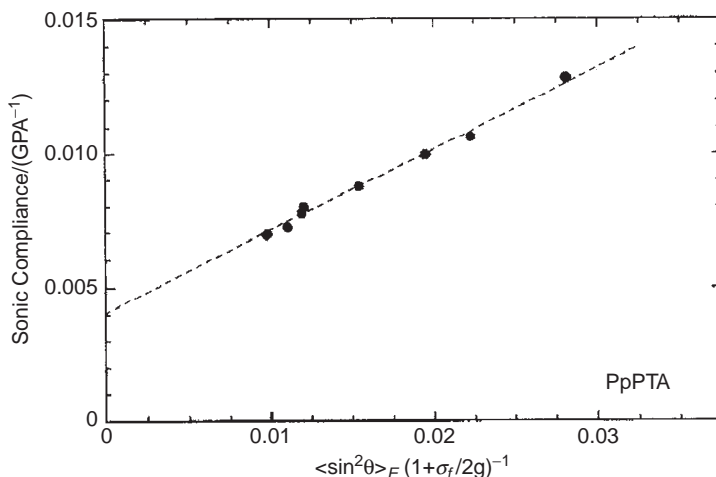


FIG. 13.100 The sonic compliance versus the orientation measured by X-ray diffraction during extension of a low-modulus PpPTA fibre. From Northolt and Baltussen (2002). Courtesy John Wiley & Sons, Inc.

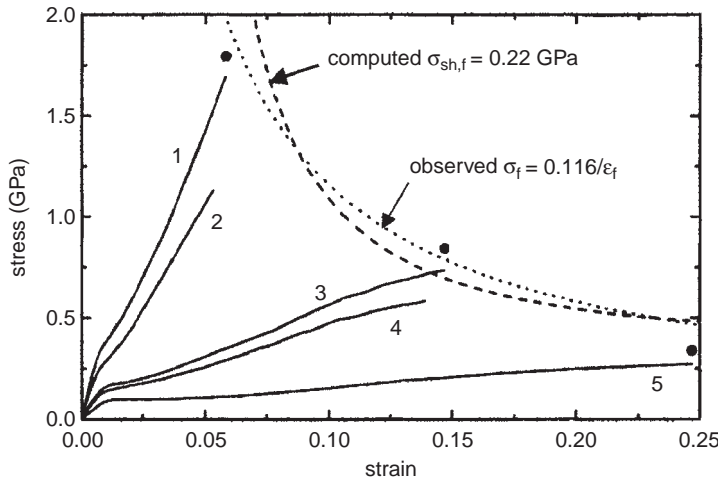


FIG. 13.101 Tensile curves of cellulose II fibres measured at an RH of 65%; (1) Fibre B; (2) Cordenka EHM yarn; (3) Cordenka 700 tyre yarn; (4) Cordenka 660 tyre yarn and (5) Enka viscose textile yarn. The solid circles represent the fracture strength corrected for the reduced cross section. The dotted curve is the hyperbola fitted to the end points of the tensile curves 1, 3, and 5. The dashed curve is the fracture envelope calculated using a critical shear stress $\sigma_{sh,f}^F = 0.22$ Gpa. From Northolt et al. (2005). Courtesy Springer Verlag. For the original filament tensile curves see Boerstoel (1998), Boerstoel et al. (2001), Northolt and Boerstoel et al. (2001).

the fibre with the largest modulus $W_f^{ch} = 1/2(\sigma_f^F)^2/e_{ch} = 0.017 \text{ GJ/m}^3$ (Fibre 1 in Fig. 13.101). This implies that *the major part of the strain energy of the cellulose fibres is stored in the straining of the intermolecular hydrogen bonds as a result of the shear deformation between the chains*. The total energy content of the hydrogen bonds in cellulose II is 0.24 GJ/m^3 , so that for fibre breakage a fraction of only 7% of the intermolecular hydrogen bonds needs to be broken (Northolt et al., 2005). By adopting a constant critical shear stress, irrespective of the degree of orientation in the fibre, it can be shown that the fracture envelope is a hyperbola. Together with the observed fact that the fracture morphology of fibres that do not have a melting temperature has a more or less fibrillar nature, this strongly indicates that the fracture of fibres is due to the rupture of the intermolecular bonds. Further development of the theory of the strength of fibres (Northolt et al., 2005) was achieved by considering the polymer fibre as a molecular composite of chains embedded in a matrix of secondary bonds and resulted in a relation between the initial compliance, S_{in}^F (or the reciprocal initial modulus, $1/E_{in}^F$), and the fracture tensile strength,

$$S_{in}^F = \frac{1}{E_{in}^F} = \frac{1}{e_{ch}} + \frac{\beta^2(2g_d + \sigma_f^F)^2}{2g_d(\sigma_f^F)^2} - \frac{(2g_d + \sigma_f^F)^2}{10.4g_d^2 e_{ch}} \quad (13.171)$$

where β is the critical or maximum shear strain value.

Fig. 13.102 shows this theoretical relation between the tensile strength and the initial modulus of PpPTA fibres for five values of β varying from 0.10 to 0.12 rad (i.e. from 5.7° to 6.9°) and for $g_d = 1.8 \text{ GPa}$ and $e_{ch} = 240 \text{ GPa}$ (see Table 13.18). A rapid increase in strength of PpPTA is observed in the modulus range from 40 to 80 GPa and there the best fit agrees with $\beta = 0.115$. For higher moduli the tensile strength levels off. This is also the case with the theoretical curves, but not until a modulus of 110 GPa (not shown here).

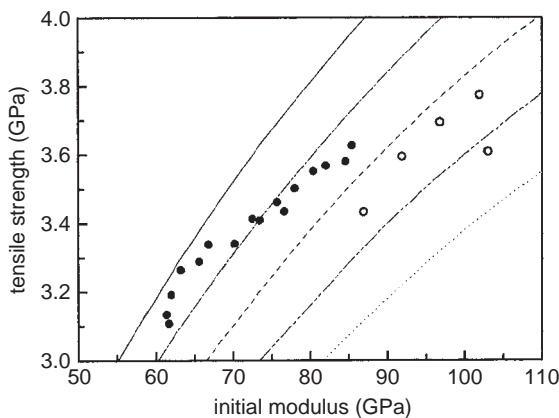


FIG. 13.102 PpPTA yarn data showing the relation between tensile strength and initial modulus together with the curves calculated with Eq. (13.171) for five different values of critical shear strain, β ; from left to right $\beta = 0.12, 0.115, 0.11, 0.105$ and 0.10 rad; used values are $g_d = 1.8$ GPa and $e_{ch} = 240$ GPa (see Table 13.18). Constructed from Figs. 22 and 23 in Northolt et al. (2005). The points above (●) and below (○) the line for $\beta = 0.11$ are from different sets of PpPTA fibres.

The authors state that their approach that leads to Eq. (13.171) does not take into account that during the first loading of the fibre viscoelastic and plastic deformation contribute to the shear deformation. Therefore they have applied a slightly different method for the calculation of the tensile strength as a function of the initial modulus. However, there is still room for a slight discrepancy between the theoretical and experimental results as the derivation of Eq. (13.171) is based on the application of a single orientation angle as a measure of the whole distribution in the fibre.

Example 13.7

Estimate for a Poly(*p*-phenylene terephthalamide) fibre with a single orientation angle $\Theta = 11^\circ$, which is loaded to a stress of 3 GPa, the initial modulus, the actual modulus, the strain stretching and the strain due to chain rotation (from Northolt et al., 2005).

Solution

Typical values for PpPTA are (see Table 13.18) $e_{ch} = 240$ GPa and $g_d = 1.8$ GPa. Substitution in Eq. (13.165) yields

$$1/E_{in} = 1/240 + (\sin 11^\circ)^2 / (2 \times 1.8) = 1.43 \times 10^{-2} \quad \text{or} \quad E_{in} = 70 \text{ GPa}$$

The actual orientation angle θ is calculated with the aid of Eq. (13.167):

$$\tan(11 - \theta) = \frac{3}{2 \times 1.8} \sin \theta \cos \theta = 0.417 \sin 2\theta$$

from which it follows $\theta = 6^\circ$.

The actual value of the modulus is calculated with the aid of Eq. (13.169):

$$\frac{1}{E} = \frac{1}{240} + \frac{(\sin 6^\circ)^2}{2 \times 1.8 + 3} = 5.8 \times 10^{-3} \quad \text{or} \quad E = 172 \text{ GPa.}$$

This is in good agreement with results presented in Fig. 13.90.

According to Eq. (13.168) the strain due to strain stretching is equal to $\varepsilon_{ch} = 3 \times (\cos 6^\circ)^2 / 240 = 0.012$

Also according to Eq. (13.168) the strain due to chain rotation is

$$\varepsilon_{sh} = \frac{\cos 6^\circ}{\cos 11^\circ} - 1 = \frac{0.9945}{0.9816} - 1 = 0.013$$

The conclusion is that a considerable fraction of the fibre strain is caused by contraction of chain orientation distribution, which increases for decreasing fibre modulus.

Example 13.8

If for the polymer fibre in Example 13.7 the fracture stress σ_f^F is equal to 3.35 GPa (see Fig. 13.102), then estimate the orientation at fracture and the strains at fracture due to stretching and to chain rotation.

Solution

According to Eq. (13.171)

$$\frac{1}{70} = \frac{1}{240} + \frac{\beta^2(3.6 + 3.35)^2}{3.6 \times 3.35^2} - \frac{(3.6 + 3.35)^2}{10.4 \times 1.8^2 \times 240} \text{ or } \beta = 0.116, \text{ which, of course is in}$$

agreement with the experimental results presented in Fig. 13.102. The orientation angle at fracture is

$$\theta_f = 11 - 0.116 \times 360 / (2\pi) = 4.4^\circ.$$

The two fracture strains now follow as

$$\varepsilon_{ch} = \sigma_f^F / e_{ch} = 3.35 \times (\cos 4.4^\circ)^2 / 240 = 0.014;$$

$$\varepsilon_{sh} = \cos \theta_f / \cos \Theta - 1 = \cos 4.4^\circ / \cos 11^\circ - 1 = 0.016$$

(b4) Creep of fibres under constant load

Understanding of the mechanism of creep failure of polymeric fibres is required for the prediction of lifetimes in technical applications (Northolt et al., 2005). For describing the viscoelastic properties of a polymer fibre use is made of a rheological model as depicted in Fig. 13.103. It consists of a series arrangement of an “elastic” spring representing the chain modulus e_{ch} and a “shear” spring, g_d with viscoelastic and plastic properties

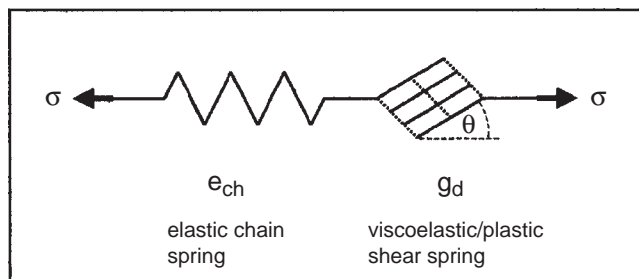


FIG. 13.103 The rheological model of a polymer fibre consisting of a series arrangement of an “elastic” spring representing the chain modulus e_{ch} and a “shear” spring, g_d with viscoelastic and plastic properties representing the intermolecular bonding. From Northolt et al. (2005). Courtesy Springer Verlag.

characterising the shear deformation of the domain. The viscoelastic extension of the fibre is written as

$$\varepsilon^F(t) = \frac{\sigma_o^F \langle \cos^2 \theta(t) \rangle}{e_{ch}} + \frac{\langle \cos \theta(t) \rangle - \langle \cos \Theta \rangle}{\langle \cos \Theta \rangle} \quad (13.172)$$

For well-oriented fibres with a single orientation angle Θ the creep equation reduces to

$$\varepsilon^F(t) = \frac{\sigma_o^F}{e_{ch}} + \frac{\cos \theta(t) - \cos \Theta}{\cos \Theta} \quad (13.173)$$

The term σ_o^F/e_{ch} is the momentary elastic chain extension, while the second term is in this equation includes the momentary elastic shear strain as well as the viscoelastic and plastic shear strain of the creep deformation. According to Baltussen (1996) and to Northolt et al. (2005), Eq. (13.173) can be developed to

$$\varepsilon^F(t) \approx \frac{\sigma_o^F}{E} + \frac{1}{2} j(t) \sigma_{sh,n}^F \quad (13.174)$$

where $j(t)$ is the time dependent creep compliance and $\sigma_{sh,n}$ is the normalised shear stress, that may be expressed as

$$\sigma_{sh,n}^F = 2g_d \left(\frac{1}{E_{in}} - \frac{1}{e_{ch}} \right) \frac{\sigma_o^F}{\left(1 + \frac{\sigma_o^F}{2g_d} \right)^3} \quad (13.175)$$

It has been experimentally verified that the creep compliance may be expressed as

$$j(t) = j_1 \log(t) \quad (13.176)$$

Hence, it follows for the creep rate, defined as $d\varepsilon/d \log t$

$$\frac{d\varepsilon}{d \log t} = j_1 \sigma_{sh,n}^F \quad (13.177)$$

Fig. 13.104 shows that the creep rate calculated as a function of the initial modulus agrees well with the experimental data of a series PpPTA. This creep model has been confirmed for PpPTA fibres up to a stress of 2 GPa (Baltussen and Northolt, 2001).

(b5) Life time of fibres under stress

In this respect also the time needed for creep failure, t_f , is also an important property of fibres. According to Northolt et al. this lifetime reads

$$^{10}\log(t_f) = \frac{\beta(2g_d + \sigma_f^F)^2}{2j_1 g_d^2 \sigma_f^F \tan \Theta} - \frac{2g_d + \sigma_f^F}{2j_1 g_d^2} \quad (13.178)$$

In Fig. 13.105 the observed data for a PpPTA fibre by Wu et al. (1988) are with the calculated life time curve using the parameters $\beta = 0.08$, $\tan \Theta = 0.1483$, $g_d = 1.6$ GPa and $j_1 = 0.032$ GPa⁻¹ (this implies a fibre with a sonic modulus of 91.8 GPa, obtained by substitution in Eq. (13.165), thereby also using $e_{ch} = 240$ GPa). The agreement is very good, but it shows that fibres that were tested at high stresses had shorter lifetimes than calculated from Eq. (13.178). The lifetime is strongly depending on the initial orientation angle or on the initial modulus. This is shown in Fig. 13.106, for the lifetime of PpPTA

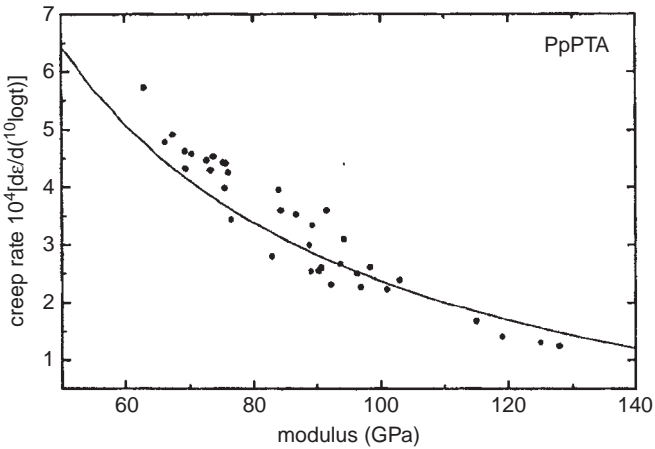


FIG. 13.104 Comparison of the calculated creep rate with the observed data of a series PpPTA yarns with different initial moduli for a creep stress of 0.9 GPa. The fitted parameters are $g_d = 1.9$ GPa and $j_1 = 0.045 \text{ GPa}^{-1}$. From Northolt et al. (2005). Courtesy Springer Verlag.

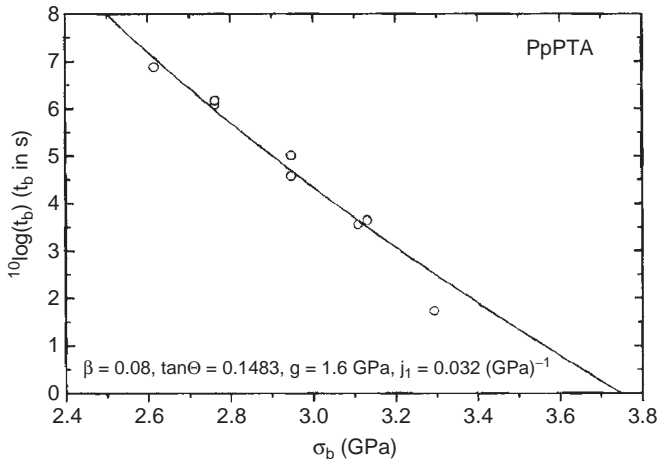


FIG. 13.105 The calculated lifetime curve according to Eq. (13.178) compared with the experimental results on PpPTA filaments by Wu (1988). From Northolt et al. (2005). Courtesy Springer Verlag.

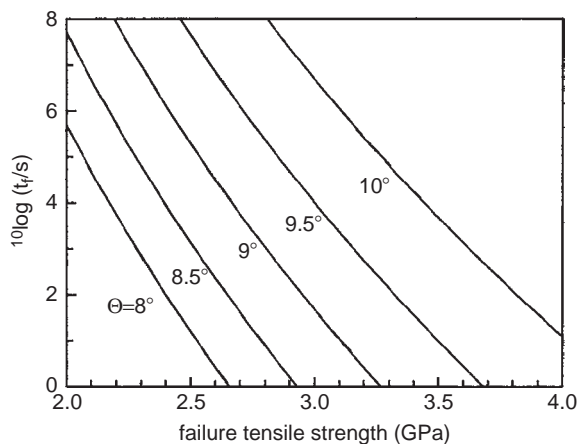


FIG. 13.106 Calculated lifetime curve for PpPTA fibres according to Eq. (13.178), for five values of the initial orientation angle Θ . The other parameters are the same as in Fig. 13.105: $\beta = 0.08 \text{ rad}$; $g_d = 1.6$ GPa; $e_{ch} = 240$ GPa and $j_1 = 0.032 \text{ GPa}^{-1}$.

fibres, calculated with Eq. (13.178) for various initial orientation angles, Θ , varying from 8° to 10° (or E_{in} varying from 98 to 74 GPa and the orientation angle at failure varying from 3.4° to 5.4°).

For a more complete description of the time and the temperature dependence of the fibre strength a theoretical description of the viscoelastic and plastic tensile behaviour of polymer fibres has been developed. Baltussen (1996) has shown that the yielding phenomenon, the viscoelastic and plastic extension of a polymer fibre can be described by the Eyring reduced time model. This model uses an activated site model for the plastic and viscoelastic shear deformation of adjacent chains in the domain, in which the straining of the intermolecular bonding is now modelled as an activated shear transition between two states, separated by an energy barrier. It provides a relation between the lifetime, the creep load and the temperature of the fibre, which for PpPTA fibres has been confirmed for a range of temperatures (Northolt et al., 2005).

BIBLIOGRAPHY

General references

- Aklonis JJ, MacKnight WJ and Shen M, "Introduction to Polymer Viscoelasticity", Wiley, Inc, New York, 1972.
- Alfrey T, "Mechanical Behaviour of High Polymers", Interscience, New York, 1948.
- Andrews EH, "Fracture in Polymers", Oliver and Boyd Ltd, Edinburgh, 1968.
- Bunn CW, "Polymer Texture; Orientation of Molecules and Crystals in Polymer Specimens", in Hill R (Ed), "Fibres from Synthetic Polymers", Elsevier, Amsterdam, 1953, Chap. 10.
- Ciferri A and Ward IM (Eds), "Ultra-high Modulus Polymers", Applied Science Publishers, London, 1979.
- Eirich FR (Ed), "Rheology", Academic Press, New York, 1959, 1960.
- Ferry JD, "Viscoelastic Properties of Polymers", Wiley, New York, 3rd Ed, 1982.
- Flory PJ, "Principles of Polymer Chemistry", Cornell University Press, Ithaca, 1953.
- Fried JR, "Sub-T_g Transitions", in Mark JE (Ed), "Physical Properties of Polymers Handbook", Springer, 2nd Ed, 2007, Chap. 13.
- Gent AN, "Rubber Elasticity: A Review", J Polym Sci, Polymer Symp 48 (1974) 1.
- Haward RN (Ed), "The Physics of Glassy Polymers", Applied Science Publishers, London, 1973.
- Haward RN and Young RL (Eds), "The Physics of Glassy Polymers", Chapman and Hall, 2nd Ed, 1997.
- Hermans PH, "Contributions to the Physics of Cellulose Fibres", Elsevier, Amsterdam, 1946.
- Hill R, "The Mathematical Theory of Plasticity", Clarendon Press, Oxford, 1950.
- Janssen M, Zuidema J and Wanhill RJH, "Fracture Mechanics", Taylor and Francis, London, 2nd Ed, 2004.
- Kausch HH, Hassel JA and Jaffee RJ (Eds), "Deformation and Fracture of High Polymers", Plenum Press, New York, 1973.
- Kinloch AJ and Young RJ, "Fracture Behaviour of Polymers", Elsevier, London, 1983.
- Kolski H, "Stress Waves in Solids", Clarendon Press, Oxford, 1953.
- Lockett FJ, "Non-linear Viscoelastic Solids", Acad Press, Inc, London, 1972.
- Love AE, "A Treatise on the Mathematical Theory of Elasticity", New York, 1944.
- McCrumb NG, Read BE and Williams G, "Anelastic and Dielectric Effects in Polymeric Solids", Wiley, New York, 1967.
- McCrumb NG, Buckley CP and Bucknall CB, "Principles of Polymer Engineering", Oxford University Press, Oxford, 1988, 2nd Ed, 1997.
- Morton WE and Hearle JWS, "Physical Properties of Textile Fibres", The Textile Institute and Butterworths, London, 1962.
- Nielsen LE, "Mechanical Properties of Polymers", Reinhold, New York, 1962.
- Ogorkiewicz RM (Ed), "Thermoplastics, Properties and Design", Wiley-Interscience, London, 1974.
- Ogorkiewicz RM (Ed), "Engineering Properties of Thermoplastics", Wiley-Interscience, London, 1970.
- Plazek DJ and Ngai KL, "The Glass Temperature", in Mark JE (Ed), "Physical Properties of Polymers Handbook", Springer, 2nd Ed, 2007, Chap. 12.
- Rohn LR, "Analytical Polymer Rheology; Structure-Processing-Property Relationships", Carl Hanser, Munich, 1995.
- Rosen SL, "Fundamental Principles of Polymeric Materials", Wiley, New York, 2nd Ed, 1993.
- Schwarzl FR, "Polymermechanik", Springer, Berlin, 1990.
- Shen M and Croucher M, "Contribution of Internal Energy to the Elasticity of Rubberlike Materials", J Macromol Sci: Revs Macromol Chem C 12 (1975) 287.

- Stein RS, "The Optical and Mechanical Properties of High Polymers", in Research Report Nr 14, High Polymer Series, US Army Quartermaster Res & Eng Center, Natick, MA, 1960, Chaps. 8 and 9.
- Stein RS and Onogi S (Eds), US-Japan Seminar in Polymer Physics (J Polymer Sci, C 15) Interscience, New York, 1966.
- Strobl G, "The Physics of Polymers", Springer, Berlin, 2nd Ed, 1997.
- Struik LCE, "Physical Aging in Amorphous Polymers and other Materials", Phd Thesis, Delft, 1977; as book published by Elsevier, Amsterdam, 1978.
- Stuart HA, "Die Physik der Hochpolymeren", Springer, Berlin, 1956.
- Te Nijenhuis K, "Survey of Measurement Techniques for the Determination of the Dynamic Moduli", in Astarita G, Marrucci G and Nicolais L (Eds) "Rheology", Plenum Publishing Company, New York, Vol. 1, 1980.
- Te Nijenhuis K, "Viscoelastic Polymeric Fluids" Chap. 9.1 and "Entrance Correction and Extrudate Swell" Chap. 9.4 in Tropea C, Yarin AL and Foss JF (Eds) "Handbook of Experimental Fluid Mechanics", Springer, Berlin, 2007, Chap. 9.1.
- Tobolsky AV, "Properties and Structure of Polymers", Wiley, New York, 2nd Ed, 1962.
- Treloar LRG, "The Physics of Rubber Elasticity", 2nd Ed, Wiley, Chichester, 1983.
- Ward IM Ed, "Structure (and Properties of Oriented Polymers" Applied Science Publishers, London, 1975.
- Ward IM Ed, "Developments in Oriented Polymers", Applied Science Publishers, London, Vol. 1, 1982.
- Ward IM, "Mechanical Properties of Solid Polymers", Chichester, Wiley, 2nd Ed, 1983.
- Ward IM and Hadley DW, "An Introduction to the Mechanical Properties of Solid Polymers", Wiley, Chichester, 1993.
- Warfield RW, in "Methods of Experimental Physics", Fava RA, Ed, Academic Press, New York, Vol. 16C, pp 91–116, 1980.
- Whorlow R, "Rheological Techniques", Ellis Horwood, Chichester, 2nd Ed, 1992.
- Williams JG "Stress Analysis of Polymers," Ellis Horwood, Chichester, 2nd Ed, 1983.
- Williams JG "Fracture Mechanics of Polymers", Ellis Horwood, Chichester, 1984.
- Winding CC and Hiatt GD "Polymeric Materials", McGraw-Hill, New York, 1961.
- Zachariades AE and Porter RS (Eds), "Mechanics of High Modulus Fibres", Marcel Dekker, Inc, New York, 1983.

Special references

- Andrews RD, J Appl Phys 25 (1954) 1223.
- Baltussen JJM and Northolt MG, Polym Bull 36 (1996) 125.
- Baltussen JJM and Northolt MG, J Rheol 41 (1997) 575.
- Baltussen JJM and Northolt MG, Polymer 42 (2001) 3835.
- Baltussen JJM, "Tensile Deformation of Polymer Fibres", PhD Thesis, Delft, The Netherlands, 1996.
- Bauwens-Crowet C, Bauwens JC and Homès G, J Polym Sci A2, 7 (1969) 735.
- Bekkedahl N, J Res Natl Bur of Standards 42 (1949) 145.
- Black WB, Annu Rev Mater Sci 10 (1980) 311.
- Blokland R, "Elasticity and Structure of Polyurethane Networks", Thesis, Delft University of Technology, 1968.
- Blokland R and Prins W, J Polym Sci (A2) 7 (1969) 1595.
- Boerstoel H, "Liquid Crystalline Solutions of Cellulose in Phosphoric Acid", Doctoral Thesis Groningen, The Netherlands, 1998.
- Boerstoel H, Maatman H, Westerink JB and Koenders BM, Polymer 42 (2001) 7371.
- Catsiff E and Tobolsky AV, J Colloid Sci 10 (1955) 375; J Polym Sci 19 (1956) 111.
- Cleereman KJ, Karam HJ and Williams JL, Modern Plastics 30 (1953) 119.
- Crawford SM and Kolski H, Proc Phys Soc B 64 (1951) 119.
- De Vries H, Thesis Delft, The Netherlands, "On the Elastic and Optical Properties of Cellulose Fibres", 1953.
- De Vries H, Appl Sci Res A3 (1952) 111; J Polym Sci 34 (1959) 761; Angew Chem 74 (1962) 574.
- De Vries H, Coll Polym Sci 257 (1979) 226; 258 (1980) 1.
- Deutsch K, Hoff EAW and Reddish W, J Polym Sci, 13 (1954) 565.
- Eisele U, "Introduction to Polymer Physics", Springer, Berlin, 1990.
- Eiermann K, J Polym Sci C 6 (1964) 157.
- Fedorov RF and Landel RF, Trans Soc Rheol 9: 1 (1965) 195.
- Fillers RW and Tschoegl NW, Trans Soc Rheol 21 (1977) 51.
- Flory PJ, Chem Rev 35 (1944) 51; Ind Eng Chem 38 (1946) 417.
- Frank FC, Proc Roy Soc A (London) 319 (1970) 127.
- Frensdorff HK, J Polym Sci A 2 (1964) 333, 341.
- Gee G, Trans Farad Soc 42 (1946) 585.
- Goldbach G, PhD Thesis, Aachen, 1966
- Goldbach G and Rehage G, Rheol Acta 6 (1967) 30.
- Greiner R and Schwarzl FR, Rheol Acta 23 (1984) 378.
- Griffith AA, Phil Trans Roy Soc (London) A 221 (1921) 163.
- Grüneisen E, "Handbuch der Physik", Vol. 10, Springer, Berlin, p 52, 1926.

- Guth E, James HM and Mark IT, "The Kinetic Theory of Rubber Elasticity", in Mark H and Whitby GS (Eds), "Scientific Progress in the Field of Rubber and Synthetic Elastomers" Interscience Publishers, New York, Vol. II, pp 253–299, 1946.
- Hartmann B, "Ultrasonic Measurements", in "Methods of Experimental Physics", Fava RA (Ed), Academic Press, New York, Vol. 16C, pp 131–160, 1980.
- Howard RN and Thackray G, Proc Roy Soc A 302 (1968) 453.
- Heckert WW, in McFarlane SB, Ed, "Technology of Synthetic Fibres", Fairchild Publications, New York, 1953.
- Heijboer J, Kolloid-Z 148 (1956) 36 and 171 (1960) 7; Plastica 10 (1957) 824; 11 (1958) 34; 12 (1959) 110, 598; Makromol Chem 35A (1960) 86; Proc Intern Conf Physics of Non-Crystalline Solids, Delft (1965) p 231; Br Polym J 1 (1969) 3; Intern J Polym Mater 6 (1977) 11.
- Heijboer J, "Mechanical Properties of Glassy Polymers, Containing Saturated Rings", PhD Thesis, Leiden, 1972.
- Heijboer J, Baas JMA, Van de Graaf B and Hoefnagel MA, Polymer 33 (1992) 1359.
- Heijboer J, Schwarzel FR, in Nitsche R, and Wolf KA (Eds), "Kunststoffe", Springer, Berlin, 1962.
- Hermans PH and Platzek P, Kolloid Z 88 (1939) 68.
- Hermans PH, Kolloid Z 103 (1943) 210.
- Hermans PH and Vermaas D, Trans Faraday Soc 42B (1946) 155.
- Herwig HU, Unpublished, Internal report Akzo Res (1970).
- Hertz H, J Reine Angew Mathem 92 (1881) 156.
- Illers KH and Brever H, Colloid Sci 18 (1963) 1.
- Jackson GB and Ballman RL, Soc Plastics Eng J 16 (1960) 1147.
- James HM and Guth E, J Chem Phys 11 (1943) 455.
- Koppelman J, Rheol Acta 1 (1958) 20.
- Kordes E, Günther F, Büchs L and Göltner W, Kolloid-Z 119 (1950) 23.
- Kovacs AJ, Adv Polym Sci 3 (1963) 394.
- Kratky O, Z Physik Chem B50 (1941) 255.
- Kratky O, Kolloid Z 64 (1933) 213.
- Kuhn W and Grün F, Kolloid Z 101 (1942) 248.
- Landel RF and Fedors RF, J Polym Sci B 1 (1963) 539; Rubber Chem Technol 40 (1967) 1049.
- Leaderman H, "Elastic and Creep Properties of Filamentous Materials and other High Polymers", The Textile Foundation, Washington DC, 1943.
- Marvin RS, Ind Eng Chem 44 (1952) 696.
- McGowan JC, Polymer 8 (1967) 57.
- McLoughlin JR and Tobolsky AV, J Polym Sci 7 (1951) 658.
- Mason P, J Appl Polym Sci 5 (1961) 428.
- Mooney M, J Appl Phys 11 (1940) 582.
- Northolt MG, J Mater Sci 16 (1981) Letters, 2025.
- Northolt MG and Van der Hout R, Polymer 26 (1985) 310.
- Northolt MG and De Vries H, Angew Makromol Chem 133 (1985) 183.
- Northolt MG, Kroon-Batenburg LMJ and Kroon J, Polym Commun, 27 (1986) 290.
- Northolt MG, Roos A and Kampschreur JH, J Polym Sci B, Phys 27 (1989) 1107.
- Northolt MG, Baltussen JJM and Schaffers-Korff B, Polymer 36 (1995) 3485.
- Northolt MG, Boerstoel H, Maatman H, Huisman R, Veurink J and Elzerman H, Polymer 42 (2001) 8249.
- Northolt MG and Baltussen JJM, J Appl Polym Sci 83 (2002) 508.
- Northolt MG, Sikkema DJ, Zegers HC and Klop EA, Fire Mater 26 (2002) 169.
- Northolt MG, Den Decker P, Picken SJ, Baltussen JJM and Schlatmann R, Adv Polym Sci 178 (2005) 1.
- Nutting P, Proc Am Soc Testing Mater 21 (1921) 1162.
- Picken SJ, Boerstoel H and Northolt MG, "Processing Rigid Polymers to High Performance Fibres" in "Encyclopaedia of Materials: Science and Technology", Elsevier, Amsterdam, 2001.
- Rabinowitz S, Ward IM and Parry JCS, J Mat Sci 5 (1970) 29.
- Rao R, Indian J Phys 14 (1940) 109; J Chem Phys 9 (1941) 682.
- Rivlin RS, Phil Trans Roy Soc (London) A240 (1948) 459, 491, 509 and A241 (1948) 379.
- Rusch KC and Beck RH, J Macromol Sci B 3 (1969) 365.
- Sakurada I, Nakushina Y and Ito T, J Polym Sci 57 (1962) 651.
- Sakurada I and Keisuke K, J Polym Sci C 31 (1970) 57.
- Schlchter WP, J Polym Sci C 14 (1966) 40.
- Schmieder K and Wolf K, Kolloid-Z 134 (1953) 149.
- Schuyler J, Dijkstra H and Van Krevelen DW, Fuel 33 (1954) 409.
- Schuyler J, Nature 181 (1958) 1394; J Polym Sci 36 (1959) 475.
- Schwarzl FR, Kolloid-Z 165 (1959) 88.
- Schwarzl FR and Staverman AJ, J Appl Phys 23 (1952) 838.

- Schwarzl FR, in Houwink R and Staverman AJ (Eds), "Chemie und Technologie der Kunststoffe", Akademie Verlagsgesellschaft, Leipzig, 4th Ed, 1963, Chap.6.
- Schwarzl FR, Pure Appl Chem 23 (1970) 219.
- Seitz JT and Balazs CF, Polym Eng Sci (1968) 151.
- Shamov L, Polym Mech (USSR) 1 (1966) 36.
- Sikkema DJ, Northolt MG and Pourdeyhimi B, MRS Bulletin 28 (2003) 579.
- Sikkema DJ, "Manmade Fibers One Hundred Years: Polymers and Polymer Design". J Appl Polym Sci 83 (2001) 484.
- Smith ThL, J Polym Sci 32 (1958) 99; 31 (1963) 3597.
- Smith ThL, J Appl Phys 31 (1960) 1892; 35 (1964) 27.
- Smith ThL, Rubber Chem Technol 35 (1962) 753; 40 (1967) 544.
- Smith THL, ASD-TDR 62-572 Report, Wright Patterson Air Force Base, Ohio (1962).
- Staverman AJ and Schwarzl FR, in Stuart HA, Ed "Die Physik der Hochpolymeren", Springer, Berlin, Vol. 4, 1956, Chaps. 1-3.
- Stein RS and Tobolsky AV, Textile Res J 18 (1948) 201, 302.
- Struik LCE, Rheol Acta 5 (1966) 202; Plastics Rubber Process Appl 2 (1982) 41.
- Struik LCE, Polymer 21 (1980) 962; 28 (1987) 1521, 1533; 30 (1989) 799, 815.
- Struik LCE, Polymer 28 (1987) 57.
- Tabor D, Proc Roy Soc (London) 192 (1947) 247.
- Te Nijenhuis K, PhD Thesis, Delft, The Netherlands
- Te Nijenhuis K and Dijkstra HJ, Rheol Acta, 14 (1975) 71
- Tjader TC and Protzman TF, J Polym Sci 20 (1956) 591.
- Tokita N, J Polym Sci 20 (1956) 515.
- Treloar LRG, Polymer 1 (1960) 95, 279.
- Van der Meer SJ, PhD Thesis, Delft, 1970; Lenzinger Ber 36 (1974) 110.
- Van der Vegt AK and Govaart LE, "Polymeren, van Keten tot Kunstsof", 5th Ed, Delft University Press, Delft, 2005.
- Van Krevelen DW and Hoflyzer PJ, (1970) unpublished.
- Vincent PI, Plastics, Lond 26, Nov 141 (1961).
- Vincent PI, Plastics, Lond 27, Jan 115 (1962).
- Warburton Hall H and Hazell EA, "Techniques of Polymer Science", SCI Monograph No 17, p 226, 1963.
- Ward IM, Proc Phys Soc 80 (1962) 1176.
- Warfield RW, Cuevas JE and Barnet FR, J Appl Polym Sci 12 (1968) 1147; Rheol Acta 8 (1970) 439.
- Warfield RW and Barnet FR, Angew Makromol Chem 27 (1972) 215; 44 (1975) 181.
- Weyland HG, Textile Res J 31 (1961) 629.
- Wilbourn AH, Trans Farad Soc 54 (1958) 717.
- Williams ML, Landel RF and Ferry JD, J Am Chem Soc 77 (1955) 3701.
- Wu HF, Phoenix SL and Schwartz P, J Mater Sci 23 (1988) 1851.
- Yano O and Wada Y, J Polym Sci A2, 9 (1971) 669.

This page intentionally left blank

CHAPTER 14

Acoustic Properties

The speeds of longitudinal and transverse (shear) sonic waves can be estimated, c.q. predicted via two additive molar functions. From these sound velocities the four most important elastic parameters (the three elastic moduli and the Poisson ratio) can be estimated.

Sonic absorption on the other hand is – for linear polymers – a typical constitutive property, dependent of temperature and frequency, for which no additivity techniques are available. For cross-linked polymers the integrated loss modulus–temperature function (the “loss area”) in the glass–rubber transition zone shows additive properties.

14.1. INTRODUCTION

Acoustic properties are important, both from a theoretical and from a practical point of view.

In Chap. 13 we have already discussed the use of sound speed measurements for the derivation of elastic parameters. We shall come back on that, more elaborately, in this chapter. We have also seen that sound speeds can be expressed in terms of additive molar functions; these are of course basic for estimations, as well for mechanical properties as for thermal conductivity (Chap. 17).

Acoustic measurements can also be used as a structural probe, since the acoustic properties, especially sound absorption, are related to many structural factors, such as transition temperatures, morphology, cross-link density, etc. Finally, they can be used as a source of engineering data, especially in the building and construction field: for the absorption of unwanted sound, the construction of acoustically transparent windows, underwater acoustics, etc.

The phenomenon *sound* comes about by periodic pressure waves, which are called acoustic or *sonic* waves. The term acoustic is sometimes reserved for vibrations that are in the audible range of frequencies, nominally from 20 to 20,000 Hz. Higher frequencies are referred to as ultra-sonic and lower frequencies as infra-sonic. In the physics of sound and acoustics they play a similar role as the electromagnetic waves in the field of light and optics. Acoustics were unified with mechanics during the development of theoretical mechanics, in the same way as optics were unified with electromagnetism by the famous theory of Maxwell in the nineteenth century.

The most important contributions to polymer acoustics were: in the period 1940–1955 those of Rao, Ballou, Guth, Mason and Nolle; in the years 1955–1970 those of Maeda, Wada

and Schuyer; in the 1970s till the 1990s those of Perepechko, Pethrick and Hartmann; all of them of course with their respective collaborators.

In an acoustic sense a material is fully characterised by four parameters: the longitudinal and transverse sound speeds, and the longitudinal and transverse sound absorption. We shall successively discuss sound propagation and sound absorption.

14.2. SOUND PROPAGATION AND ABSORPTION

As all waves, sound waves are characterised by speed, frequency and amplitude.

Sound speed gives the magnitude of the sound velocity vector; it is expressed in units of m/s and symbolised by the symbol u (or sometimes by v or c).

Sound frequency is the reciprocal of the period of the sound wave. It is denoted by the symbol ν and expressed in cycles per second with the Hertz (s^{-1}) as unit. Also the angular frequency is used; the latter is symbolised by ω , which is identical with $2\pi\nu$.

In Chap. 13 we have already mentioned that in an (isotropic) solid two independent types of elastic waves are propagated. The propagation of an acoustic wave through a solid polymer can be characterised by two parameters: sound velocity and sound absorption. Sound speed, u (in m/s) is the rate at which sound waves travel through the medium. Sound absorption or attenuation α (in dB/m) is a measure of the loss of energy of the sound wave as it travels through the medium: the energy of the sound wave is converted into thermal motions or heat, but usually with a negligible rise of temperature only. Instead of referring to absorption per unit of distance (dB/m), it is sometimes more convenient to refer to the absorption per wave-length, λ , which is equal to $\alpha\lambda$ (in dB).

In isotropic solids there are two independent modes of acoustic propagation: longitudinal modes and shear modes. In *longitudinal waves*, also called compression, dilatational or irrotational waves, the solid is subjected to alternate local compressions and expansions. The movements of the individual particles of a solid transmitting these waves are normal to the advancing wave front; they vibrate in the direction of propagation of the wave. In *shear waves*, also called transverse, dilatation-free (or iso-voluminous) or distortional waves, the solid is locally subjected to shearing forces and the wave consists in the spreading throughout the solid of an oscillating shearing motion. The motion of the individual particles of the material takes place parallel to the wave front and perpendicular to the direction of propagation of the wave. Hence, in principle four parameters are required to specify the acoustic properties of an unbounded solid, isotropic polymer: longitudinal and shear speed and longitudinal and shear absorption: u_L , u_S , α_L and α_S (Hartmann, 1980, 1984, 1996; Sinha and Buckley, 2007).

In fluid media, such as gases or liquids and melts, which have no rigidity, only longitudinal waves can occur. In media that have rigidity but are incompressible, only transverse waves can occur.

So the Poisson ratio plays an important part in sound propagation.

14.2.1. Sound speed

When there is negligible absorption the two sound speeds are related to the elastic parameters (see Chap. 13):

$$u_L = [(K + \frac{4}{3}G)/\rho]^{1/2} \quad (14.1)$$

$$u_S = (G/\rho)^{1/2} \quad (14.2)$$

These equations are valid only when absorption is zero or low. The absorption correction is found by making the moduli complex: the real part equal to the modulus and the imaginary part proportional to the absorption (a situation completely similar to that in optics).

In threads or filaments, where the lateral dimensions are much smaller than the wave-length, the longitudinal wave is almost purely extensional; its speed is given by the expression

$$u_{\text{ext}} = (E/\rho)^{1/2} = \left[\frac{3G}{(1 + 1/3 G/K)\rho} \right]^{1/2} \quad (14.3)$$

In melts $G \ll K$ so that there is a pure compression wave, hence the bulk velocity of sound is

$$u_B = (K/\rho)^{1/2} \quad (14.4)$$

14.2.2. Sound absorption

Absorption is a material property, usually symbolised by α , which is a measure of the energy removed from the sound wave by conversion to heat as the wave propagates through a given thickness l of material. It is expressed in units of decibel/cm (dB/cm).

The decibel is based on 10 times the common logarithm of the ratio of the acoustic energy to its standard value: $\alpha l = 10 \log(E/E_0) = 10 \log(A/A_0)^2 = 20 \log(A/A_0)$ dB (A = amplitude), where α is the sonic absorption coefficient. Alternatively the natural logarithm can be used. In this case the units of α are Np/cm, where one Neper (Np) is equal to 8.686 dB ($8.686 = 20 \log e$).

Sound absorption is related to various molecular mechanisms in the polymer structure, such as glass transition, melting break down, secondary transitions, curing (formation of cross-links), annealing (relaxation of internal constraints, e.g. tensions), etc. It is a measure of dissipative energy loss (conversion to heat) as the wave travels through the polymer. Transitions are characterised by peaks in the absorption. Just as in dielectric properties is absorption related to dynamic terminology, as damping, loss factor and loss tangent. Sound absorption is related to the loss factor

$$\alpha\lambda = 8.686\pi \tan \delta \quad (14.5)$$

in units of dB, where $8.686 = 20 \log e$. According to Ferry (1980) this approximation is, for small values of $\tan \delta$, almost always good to 1%.

As in light absorption one uses the term *attenuation* for the sum of energy losses due to absorption, reflection and scattering. It is expressed in the same units as absorption, but it is not a material property, as depends, e.g. on the sample thickness.

The conclusion is that the acoustic approach and the modulus approach are thus alternate and equivalent ways of describing the same physical phenomenon (Hartman, 1990).

14.2.3. Measurement techniques

Among the various techniques of measurement one may be indicated as the most versatile: the *immersion technique* (see Hartmann and Jarzynski, 1974; Hartmann, 1980). In this method acoustic waves are generated and received by two piezo-electric transducers, one acting as transmitter, the other as receiver; the transducer material is

either quartz or lead zirconate/titanate (PZT). The polymer specimen is placed between the two transducers, and the whole combination is immersed in a liquid, preferably a low viscosity silicone liquid. The pulse generator and the transducer combination are connected with an oscilloscope. Pulses are sent from the transmitter to the receiver, both with and without the sample in the path of the sound beam. From the changes in the detected signal, displayed on the oscilloscope, before and after removal of the sample, the speed and the absorption of the sound can be calculated.

Both longitudinal and shear waves are generated in the specimen. If the sample is held at an angle, larger than the critical angle, the longitudinal wave is totally reflected and only the shear wave is propagated and measured. If the sample surface is perpendicular to the direction of propagation the longitudinal wave speed is measured.

The absorption can be measured by using two specimens of different thickness but otherwise identical; the change in amplitude as a function of the path difference can be measured and thus the difference in absorption.

Other techniques can only be mentioned here. The most important are the "delay rod technique" and the "multiple echo techniques". In the first method the sample is placed between two quartz rods which are directly bonded (by a silicone liquid) to the transducers. Longitudinal and shear measurements are made separately with different sets of quartz transducers (X-cut crystal for longitudinal, Y-cut crystal for shear waves).

In the second method wave pulses bounce back and forth with continually diminished amplitude. From the oscilloscope signals the sound parameters can be calculated.

The measurement of the sound speed in filaments and yarns requires special techniques, viz. by means of a magnetostrictive oscillator (see Ballou et al. 1944/1949). The dynamic modulus, determined in this way is considerably larger than the Young modulus from stress-strain experiments: $E_{\text{dyn}} \approx 1.5 E_{\text{stat}}$.

14.2.4. Experimental data

Hartmann (1984) made a comprehensive list of the available experimental data. These data are the basis of Table 14.1. It contains the speed, temperature dependence and absorption data for longitudinal and shear wave for various polymers.

These data will also be the basis and check for our correlations. Some illustrative examples of the experimental data are shown in the Figs. 14.1 and 14.2.

(a) Density and crystallinity dependence of sound speed

It is well known that crystallinity affects the density and the moduli of polymers. Hence sound speed will also depend on those properties, but it is beforehand not clear how it depends on these properties. In Fig. 14.3 U_{EXT} is plotted vs. both density and crystallinity. In both cases the sound speed varies linearly with these properties, at least in the region shown, whereas according to Eq. (14.3) U_{EXT} is equal to $(E/\rho)^{1/2}$.

(b) Temperature dependence of sound speed

The acoustic properties of polymers are just as for many properties strongly dependent on temperature around the glass-rubber transition: the sound speed decreases rapidly from a relatively high value at $T < T_g$ to a relatively low value at $T > T_g$. During this transition the absorption shows a maximum value. An example is given in Fig. 14.4, where data for a poly(metacarborane siloxane) are displayed. The measurements were made in the longitudinal mode as a function of temperature at a frequency

of 2 MHz. At the peak the absorption per wavelength has a value of $\alpha\lambda = 1.3$ dB (as can be calculated from Fig. 14.4) so that with the aid of Eq. (14.5) it follows $\tan \delta = 0.05$. The effects of secondary transitions are less frequently studied, because of the relatively small effects.

(c) Frequency dependence of sound speed

Because of the time-temperature (or frequency-temperature) relation for the viscoelastic properties of polymers there is of course also a corresponding frequency dependence of the acoustic properties of polymers. In Table 14.2 frequency derivatives of sound speeds and absorptions are listed.

(d) Pressure dependence of sound speed

Although few experimental data are available sound speed and absorption are pressure dependent. This thought to be due to the pressure dependence of free volume in the polymer. In Table 14.3 pressure derivatives of sound speeds and absorptions are listed for a few polymers.

TABLE 14.1 Sound propagation and elastic parameter data for various polymers

Polymer	General data			Sound speeds	
	M (g/mol)	ρ (g/cm ³)	V (cm ³ /mol)	u_L (m/s)	u_{sh} (m/s)
Polyethylene (LID)	28.1	0.96	29.4	2430	950
Polypropylene	42.1	0.91	46.1	2650	1300
Poly(4-methyl 1-pentene)	84.2	0.835	100.8	2180	1080
Polystyrene	104.1	1.05	99.0	2400	1150
Polyvinylchloride	62.5	1.39	44.9	2376	(1140)
Poly(vinylidene fluoride)	64.0	1.78	36.0	1930	775
Polytetrafluoro-ethylene	100.0	2.18	45.9	1380	(710)
ABS (acrylonitril/butadiene/styrene copolymer)	211	1.02	206	2040	830
Poly(vinyl butyral)	98.1	1.11	88.7	2350	(1125)
Poly(methyl methacrylate)	100.1	1.19	84.5	2690	1340
Poly(oxymethylene)	30.1	1.425	21.1	2440	1000
Poly(ethylene oxide)	44.1	1.21	36.5	2250	(406)
Polyamide 6	113.2	1.15	98.8	2700	1120
Polyamide 66	226.4	1.15	197.6	2710	1120
Poly(ethylene terephthalate)	192.2	1.335	144.0	—	—
Poly(2,6 dimethyl phenylene oxide)	120.1	1.08	111.1	2293	(1000)
Poly(bisphenol carbonate)	254.3	1.19	213.7	2280	970
Polysulfone	442.5	1.24	356.9	2297	1015
Poly(ether sulfone)	232.3	1.37	169	2325	990
Poly(phenyl quinoxaline)	484	1.21	400	2460	1130
Phenol-formaldehyde resin	106	1.22	87	2480	1320
Epoxy resin (DGEBA/MPDA)	788	1.205	664	2820	1230
Epoxy-resin (RDGE/PDA)	518	1.27	407	3090	1440

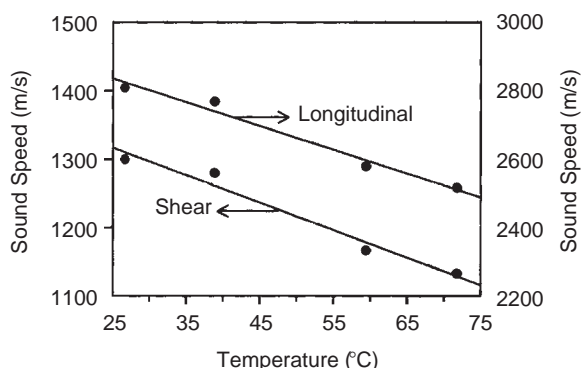
DGEBA=diglycidyl ether of bisphenol A; RDGE=resorcinol diglycidyl ether; MPDA=m-phenylene diamine; PDA=propane diamine.

(continued)

TABLE 14.1 (*continued*)

Code	Elastic parameters				Secondary sonic data			
	K (GPa)	G (GPa)	E (GPa)	v (-)	-du _L /dT (m/s/K)	-du _{sh} /dT (m/s/K)	α _L (dB/cm)	α _{sh} (dB/cm)
PE (HD)	4.54	0.91	2.55	0.41	9.6	6.8	3.0	25.0
PP	4.37	1.54	4.13	0.34	15.0	6.7	—	—
PMP	2.67	0.97	2.61	0.34	4.2	1.8	1.4	6.7
PS	4.21	1.39	3.76	0.35	1.5	4.4	—	—
PVC	(5.5)	(1.81)	(4.90)	0.35	—	—	—	—
PVDF	5.18	1.07	3.00	0.40	—	—	—	—
PTFE	(2.66)	(1.1)	(2.87)	0.31	—	—	—	—
ABS	3.33	0.70	1.96	0.40	4.1	1.5	—	—
PVB	(3.88)	(1.71)	(4.40)	0.31	—	—	—	—
PMMA	6.49	2.33	6.24	0.34	2.5	2.0	1.4	4.3
POM	6.59	1.43	4.01	0.40	—	—	—	—
PEO	(5.80)	0.2	0.45	0.36	—	—	7.1	—
PA-6	6.45	1.43	4.00	0.40	—	—	—	—
PA-66	6.53	1.43	3.99	0.40	—	—	—	—
PETP	>4	1.1	~3.0	(0.40)	—	—	—	—
PPO	(4.22)	(1.09)	3.00	0.38	1.5	—	—	—
PC	4.72	1.10	3.09	0.39	3.6	—	—	—
PSF	5.3	1.0	3.55	0.38	1.4	—	—	—
PESF	5.6	1.35	3.73	0.39	—	—	—	—
PPO	5.21	1.54	4.20	0.37	3.0	1.3	3.5	15.0
PF	7.0	2.13	5.8	0.36	7.5	4.0	4.1	19.0
EP-DM	6.8	2.00	5.05	0.38	6.5	3.7	5.5	27.7
EP-RP	8.65	2.64	7.20	0.36	8.9	4.7	5.1	26.6

(Data from B. Hartmann et al. (1980–1984))

**FIG. 14.1** Sound speeds vs. temperature for phenolic resin. From Hartmann (1975). Courtesy of John Wiley & Sons, Inc.

(e) Frequency dependence of absorption: hysteresis

If absorption is measured not too close to the damping peak ($\tan \delta$) both longitudinal and shear absorption often increase linearly with frequency. This is demonstrated in Fig. 14.5 for polyethylene (Hartmann and Jarynski, 1972). This phenomenon is called hysteresis behaviour in acoustics (it does not refer to absorption as is common among polymer scientists (Hartmann, 1990). At any frequency shear absorption is much higher than longitudinal absorption.

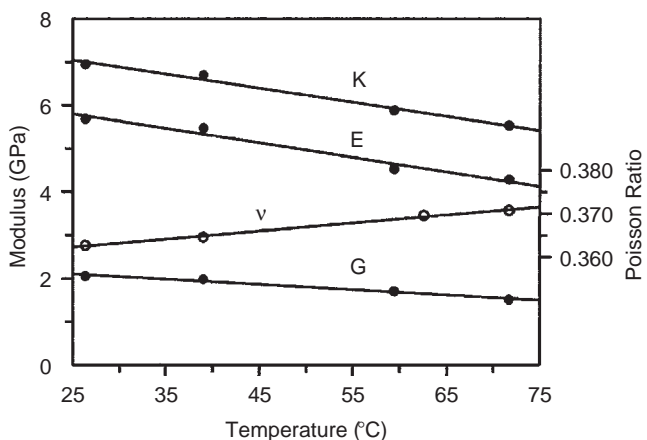


FIG. 14.2 Elastic constants vs. temperatures for phenolic resin. From Hartmann (1975). Courtesy John Wiley & Sons, Inc.

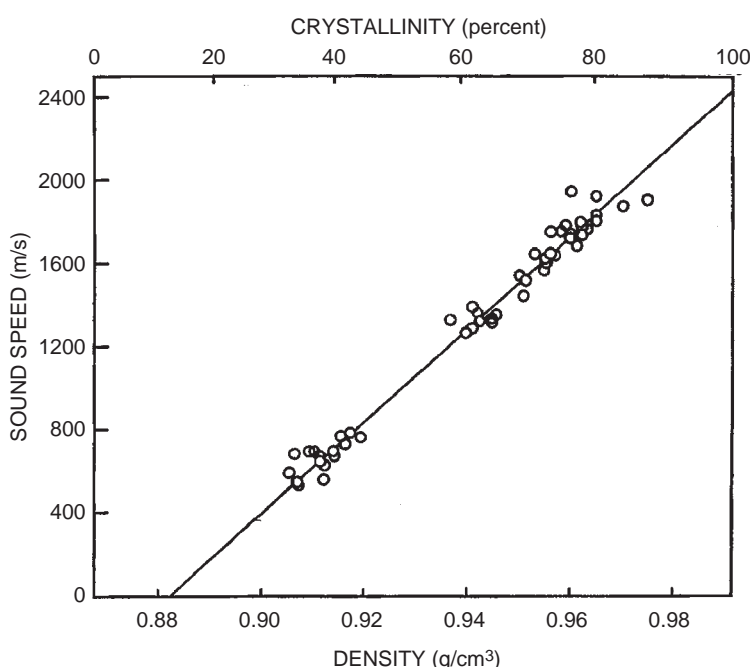


FIG. 14.3 Extensional sound speed vs. density and crystallinity for polyethylene. From Hartman (1996). Courtesy Springer Verlag.

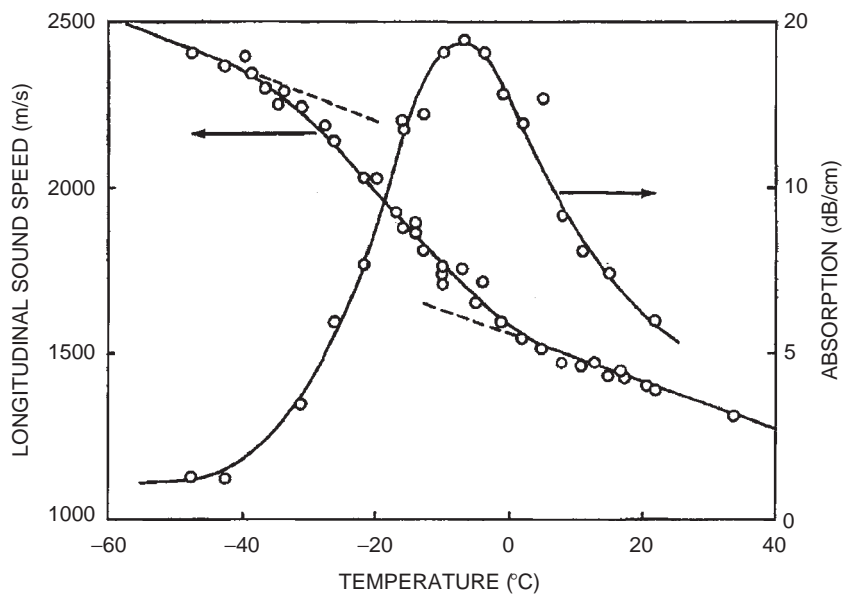


FIG. 14.4 Longitudinal sound speed and absorption for poly(carborane siloxane) at 2 MHz. From Hartman (1996); Courtesy Springer Verlag.

TABLE 14.2 Frequency derivatives of longitudinal and shear sound speeds and sound absorptions

Polymer	ρ (kg/m ³)	$du_L/d \log \omega$ (m/s)	$du_S/d \log \omega$ (m/s)	$d\alpha_L/d \log \omega$ (dB/m)	$d\alpha_S/d \log \omega$ (dB/m)
Polyethylene	957	3.3	25.0	1700	3400
Polystyrene	1046	1.4	—	—	—
Poly(methyl methacrylate)	1180	13.0	6.6	2100	7200
Poly(4-methyl-1-pentene)	835	1.4	6.7	—	—
Poly(vinyl chloride)	1386	11.0	—	—	—
Poly(ethylene oxide)	1208	7.1	—	2900	—
Poly(acrylonitrile-butadiene-styrene)	1023	1.8	15.0	—	—
Polycaprolactam	1084	13.0	—	—	—
Polycarbonate	1194	9.4	—	12,000	—
Polysulfone	1236	4.0	—	7700	—
Poly(ether sulfone)	1373	5.0	—	7200	—

Data from B. Hartmann (1996).

TABLE 14.3 Pressure derivatives of longitudinal and shear sound speeds and longitudinal sound absorption

Polymer	ρ (kg/m ³)	$d(\ln u_L)/dP$ (GPa ⁻¹)	$d(\ln u_S)/dP$ (GPa ⁻¹)	$d(\ln \alpha_L)/dP$ (GPa ⁻¹)
Polyisobutylene	914	2.7	—	2.7
Polystyrene	1046	0.9	0.5	—
Poly(methyl methacrylate)	1180	0.89	0.69	—

Data from B. Hartmann (1996).

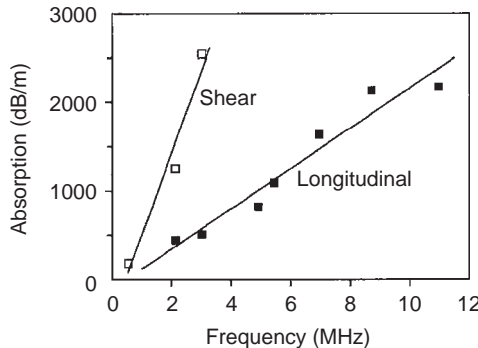


FIG. 14.5 Shear and longitudinal absorption at 25 °C vs. frequency for polyethylene. From Hartman and Jarzynski (1972); Courtesy of American Institute of Physics.

14.3. ADDITIVE MOLAR FUNCTIONS FOR SOUND PROPAGATION

In Chap. 10 we have seen that the relative speed of light waves (i.e. the ratio of the speed in vacuum to that in a material), alias the refractive index (n), can be related to a temperature-independent material constant: the specific refraction $(n - 1)/\rho$. Multiplied with the molar mass this gives the Molar Refraction \mathbf{R} :

$$\mathbf{R} = \mathbf{M}(n - 1)/\rho$$

which has additive properties and correlates the speed of light in a material with the chemical structure. An analogous correlation was found for the speed of sound. In 1940 Rama Rao showed that for organic liquids the ratio $u^{1/3}/\rho$ is also nearly independent of the temperature; multiplied with the molar mass it gives also a molar function with additive properties; it is called now the Rao function or Molar Sound Velocity Function:

$$\mathbf{U}_R = \mathbf{M}u^{1/3}/\rho = \mathbf{V}u^{1/3} \quad (14.6)$$

A set of additive group contributions for \mathbf{U}_R valid for liquids was derived by Sakiades and Coates (1955).

The Rao function has the same form as the Sugden function or Molar Parachor ($\mathbf{P}_s = \mathbf{M}\gamma^{1/4}/\rho$), derived by Sugden in 1924, which correlates the surface tension with the chemical structure. Also the Small function or Molar Attraction Function, which correlates the cohesion energy density, e_{coh} , and the solubility parameter, δ , with the chemical structure, has this form:

$$\mathbf{F} = \mathbf{M}e_{coh}^{1/2}/\rho = \mathbf{M}\delta/\rho = \mathbf{V}\delta$$

In solids the situation is more complicated than in liquids. Here we have two types of waves, viz. the longitudinal and the shear waves. In contrast with liquids the longitudinal wave in solids is not only determined by the bulk or compression modulus but also by the shear modulus, or alternatively by the Poisson ratio.

Schuyer (1958, 1959) proved that instead of the simple relationship $u_L^2 = K/\rho$, valid for liquids, a more complicated expression must be used in the case of solids:

$$u_L^2 = \frac{K}{\rho} \frac{3(1-v)}{1+v} \quad (14.7)$$

For the Rao function we also have to use a corrected, generalised form:

$$\mathbf{U}_R = \mathbf{V} u_L^{1/3} \left[\frac{1+v}{3(1-v)} \right]^{1/6} \quad (14.8)$$

For liquids $v = 1/2$, so that Eqs. (14.7) and (14.8) reduce to Eqs. (14.4) and (14.6), respectively. Rearrangement of Eq. (14.8) gives:

$$u_L = \left(\frac{\mathbf{U}_R}{\mathbf{V}} \right)^3 \left[\frac{3(1-v)}{1+v} \right]^{1/2} \quad (14.9)$$

Schuyer showed that for polyethylenes the Rao function according to Eq. (14.8) does not vary with the density, irrespective of whether variations in density are caused by changes in temperature or in structure. Since v is nearly independent of the density, Eq. (14.9) predicts that the longitudinal sound velocity will be roughly proportional to the third power of the density of polyethylene. This is confirmed by Fig. 14.6.

The group contributions to the Rao function, defined by Eq. (14.8), are given in Table 14.4. The numerical values of the Rao function and of its group contributions are expressed in the usual way in $(\text{cm}^3/\text{mol})(\text{cm}/\text{s})^{1/3} = \text{cm}^{10/3}/\text{s}^{1/3}/\text{mol} = 2.154 \times 10^{-7} \text{ m}^{10/3}/\text{s}^{1/3}/\text{mol}$.

Combination of Eqs. (14.7) and (14.9) gives:

$$\frac{K}{\rho} = \left(\frac{\mathbf{U}_R}{\mathbf{V}} \right)^6, \quad \text{so} \quad \mathbf{U}_R = \mathbf{V}(K/\rho)^{1/6} \quad (14.10)$$

This expression makes it possible to calculate the compression (bulk) modulus from the additive molar functions \mathbf{U} and \mathbf{V} .

Hartmann (1984) found that the analogous additive property for the shear modulus is $\mathbf{V}(G/\rho)^{1/6}$; it is also temperature independent and additive as long as the material is in the solid state well below T_g . We shall coin this molar function as \mathbf{U}_H the Hartmann function:

$$\mathbf{U}_H = \mathbf{V}(G/\rho)^{1/6} \quad (14.11)$$

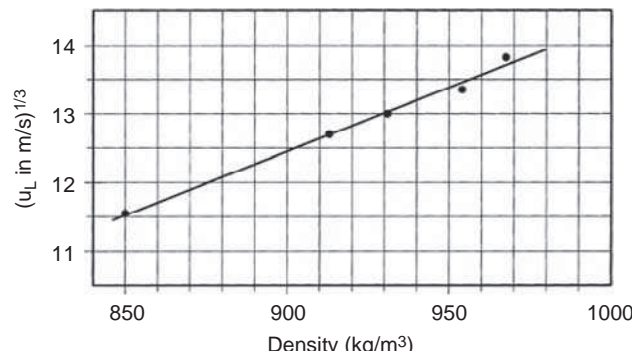
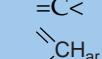
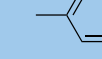
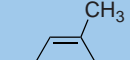
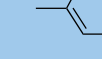
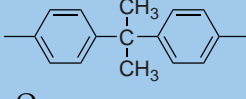
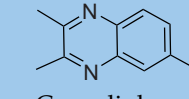


FIG. 14.6 Cubic root of longitudinal sound velocity of polyethylene as a function of density.

TABLE 14.4 Group contributions to the Rao and Hartmann-functions (cm^3/mol) (cm/s) $^{1/3}$; Increments of \mathbf{U}_H are tentative

Bivalent groups	\mathbf{U}_R	\mathbf{U}_H	Other groups	\mathbf{U}_R	\mathbf{U}_H
$-\text{CH}_2-$	880	675	$-\text{CH}_3$	1400	1130
$-\text{CH}(\text{CH}_3)-$	1875	1650	$>\text{CH}-$	460	370
$-\text{CH}(\text{i-C}_3\text{H}_7)-$	4800	4050	$>\text{C}<$	40	35
$-\text{CH}(\text{C}_6\text{H}_5)-$	4900	4050	$=\text{CH}-$	745	600
$-\text{CH}(\text{COCH}_3)-$	2500	2250	$=\text{C}<$	255	200
$-\text{CHCl}-$	1725	1450		830	665
$-\text{C}(\text{CH}_3)_2-$	2850	2350		400	320
$-\text{C}(\text{CH}_3)(\text{COOCH}_3)-$	4220	3650			
$-\text{CF}_2-$	1100	900		4500	3650
	4100	3300		5000	4000
	4050	3100		3700	2900
	6100	4800		3300	2600
	11,000	8700	$-\text{N}<$ $>\text{Si}<$ $-\text{CN}$	65 100 1400	50 80 1150
$-\text{O}-$	400	300	$-\text{OH}$	630	500
$-\text{CO}-$	875	600			
$-\text{COO}-$	1225	900	$-\text{F}$	(530)	(400)
$-\text{OCOO}-$	1575	1200	$-\text{Cl}$	1265	(1000)
			$-\text{Br}$	(1300)	(1000)
$-\text{CONH}-$	1750	1400			
$-\text{NH}-$	875	800			
$-\text{S}-$	(550)	(440)		5350	4300
$-\text{SO}_2-$	1250	1000			
$-\text{Si}(\text{CH}_3)_2-$	2900	—	Cross-link	600	600

so that

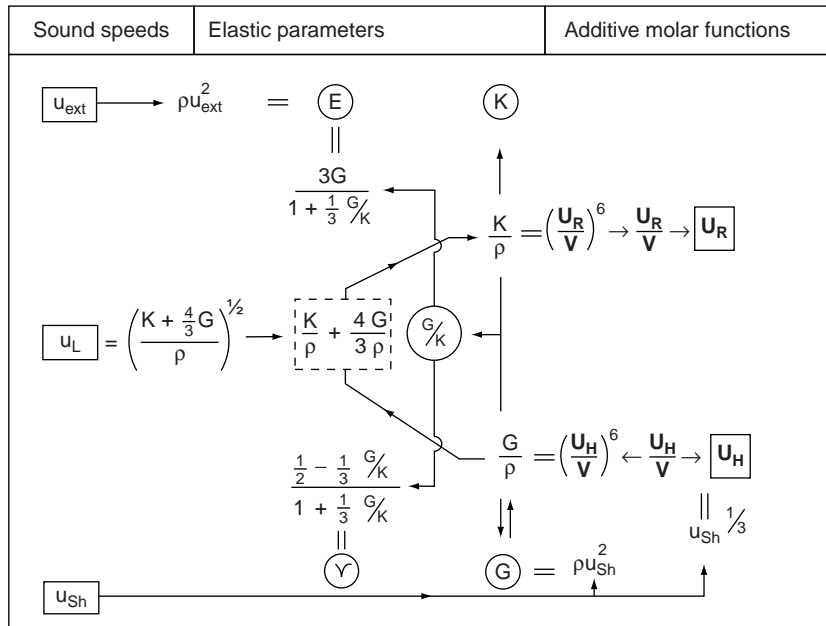
$$\frac{G}{\rho} = \left(\frac{\mathbf{U}_H}{\mathbf{V}} \right)^6 \quad (14.12)$$

Also for this function the group contributions are given in Table 14.4. They are tentative.

Table 14.5 shows the comparison of the values of the \mathbf{U}_R and \mathbf{U}_H functions derived from experimental sound speed data with the values derived from the group contributions. It also shows a comparison between experimental sound speed values with those calculated purely from additive molar functions. The agreement is on the whole very satisfactory.

TABLE 14.5 Comparison between experiment and calculation of sound speeds and molar functions

Polymer	Experimental					Calculated			
	u_L (m/s)	u_{Sh} (m/s)	V (cm ³ /mol)	U_R	U_H	U_R	U_H (m/s)	u_L (m/s)	u_{Sh}
PE(HD)	2430	950	29.4	1760	1335	1760	1350	2410	960
PP	2650	1300	46.1	2750	2340	2755	2325	2586	1280
PMP	2180	1080	100.8	5700	4740	5680	4725	2170	1020
PS	2400	1150	99.0	5795	4720	5780	4725	2270	1080
PVC	2376	(1140)	44.9	2620	(2120)	2605	2125	2425	1140
PVDF	1930	775	360	1995	1520	1980	1575	1925	840
PTFE	1380	(710)	45.9	2200	1900	2200	1800	1306	610
ABS	2040	830	206	11,650	9000	11,750	9470	2190	970
PVB	2350	1125	88.7	5050	4260	5140	4275	2420	1100
PMMA	2690	1340	84.5	5100	4320	5100	4325	2700	1360
POM	2440	1000	21.1	1295	980	1280	975	2420	990
PEO	2250	(406)	36.5	2210	(1250)	2160	1650	(2400)	(925)
PA-6	2700	1120	98.8	6150	4770	6150	4750	2785	1120
PA-66	2710	1120	196.8	12,300	9600	12,300	9500	2785	1120
PPO	2293	(1000)	111.1	6450	5120	6500	5100	2347	955
PC	2280	970	213.7	12,400	9950	12,575	9900	2402	995
PSF	2257	1015	356.9	20,650	16,700	21,250	16,600	2470	1020
PESF	2325	990	169	9900	7800	9850	7600	2330	1080
PPO	2460	1130	400	22,700	19,000	—	—	—	—
PF	2840	1320	87	5400	4420	5570	4375	3015	1270
EP-DM	2820	1230	664	41,250	33,000	41,600	33,300	2925	1270
EP-RP	3090	1440	407	25,900	21,200	26,400	20,935	3290	1450



SCHEME 14.1 Calculation of the elastic parameters EP and the additive molar functions **U** from the sound speed measurement u and vice versa. Valid only for elastic isotropic materials.

Finally the method of calculation, from sound speeds to molar functions (via elastic parameters) and vice versa, is illustrated in Scheme 14.1 (see also Examples 14.1 and 14.2).

Our conclusion is that by means of four additive molar functions (M , V , U_R and U_H) all modes of dynamic sound velocities and the four dynamic elastic parameters (K , G , E and ρ) can be estimated, c.q. predicted from the chemical structure of the polymer, including cross-linked polymers.

14.4. SONIC ABSORPTION

Sonic absorption has been less systematically studied than sonic speed. Yet it is of considerable practical importance. Vibration damping in machinery, automobiles and aircraft constitutes an important task for both the reduction of noise and the prevention of fatigue failure of the materials.

As to the absorption values in the literature (see Table 14.1) some tentative conclusions may be drawn:

- (a) In transition zones and in a “gel” state the absorption α tends to high values
- (b) Below a Poisson ratio of 0.3 the absorption becomes very low to negligible
- (c) Rubbers with a low cross-link density show high to very high sound absorption
- (d) High cross-link density leads to low absorption
- (e) The ratio $\alpha_{\text{sh}}/\alpha_L$ is nearly constant, viz. ≈ 5 (14.13)
- (f) In temperature regions, wherein no transitions are observed, the following tentative rule can be observed:

$$\alpha_L (\text{dB/cm}) \approx 40(v - 0.30) \quad (14.14)$$

This rule is valid for linear, non-cross-linked polymers.

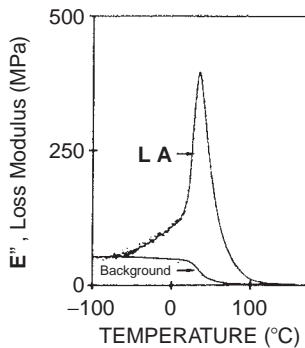


FIG. 14.7 Linear loss modulus versus temperature for a PMA/PEMA 55/45 IPN. The background correction for E'' is also shown. From Chang et al. (1988). Courtesy John Wiley & Sons, Inc.

The highest sonic damping is obtained in transition zones. The glass transition can be used for this purpose if cross-linked polymers are applied, with a rubbery solid state until far above T_g . Very interesting work in this field was done by Sperling and his co-workers (1987, 1988) who studied the damping behaviour of homopolymers, statistical copolymers and interpenetrating networks (IPNs) of polyacrylics, polyvinyls and polystyrenes.

Sperling et al. made an important discovery, viz. that the area under the linear loss modulus–temperature curve (coined by them *loss area*, LA) (see Fig. 14.7) is a quantitative measure of the damping behaviour and moreover, possesses additive properties:

$$LA = \int_{T_g}^{T_r} E'' dT \quad (14.15)$$

where T_g and T_r are the glassy and rubbery temperatures just below and just above the glass transition; E'' is the tensile loss modulus, which is a measure for the conversion of mechanical energy into molecular motion during the transition.

The glass transition results from large scale conformational motion of the polymer chain backbone; all moieties making up the structural unit of the polymer contribute to it. The main chain motions also satisfy the De Gennes reptation model (1971), where the chains move back and forth in snakelike motions.

Chang, Thomas and Sperling also derived the following equation:

$$LA = \int_{T_g}^{T_r} E'' dT = (E'_G - E'_R) \frac{\pi R T_g^2}{2 E_{act}} \quad (14.16)$$

where E'_G and E'_R are the glass and rubber tensile storage moduli, respectively and E_{act} is the activation energy of the glass–rubber transition.

The additivity relationship of LA reads as follows:

$$LA = \frac{\sum_i (LA)_i \mathbf{M}_i}{\sum_i \mathbf{M}_i} = \frac{\sum_i \mathbf{G}_i}{\mathbf{M}} \quad (14.17)$$

or

$$\mathbf{G} = \mathbf{M}(LA) = \sum_i \mathbf{G}_i \quad (14.18)$$

where \mathbf{G} is the molar loss area.

Table 14.6 gives the group contributions \mathbf{G}_i that have been determined so far. As said, these values have been derived from polyacrylates, polymethacrylates, polyvinyls and polystyrenes. Sperling et al. demonstrated that for these polymer families the additivity according to Eq. (14.17) is valid for networks of homopolymers, statistical copolymers, interpenetrating polymer networks and *polymer blends*. The LA-values obtained are invariant for a given composition and independent of subsequent decross-linking or annealing.

For polymer blends the following additive mixing rule has to be used:

$$(LA)_M = w_1(LA)_1 + w_2(LA)_2 + \dots \quad (14.19)$$

where w = weight fraction.

Example 14.3 illustrates the application of the given relations.

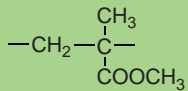
The \mathbf{G}_i -values in Table 14.6 demonstrate that the backbone motions and the moieties attached directly to the backbone, contribute the most to the damping peak and that long side chains act as "diluants".

TABLE 14.6 Group contributions to molar loss area (\mathbf{G}) (from Chang et al., 1988)

Bi- and trivalent groups	In chain backbone	Attached to chain backbone	Not attached to chain backbone
$-\text{CH}_2-$	(32)		-42
$-\text{CH}<$	(60)		7
$-\text{CH}_2-\text{CH}<$	92		
$-\text{O}-$	306		
Univalent groups		Attached to chain backbone	Not attached to chain backbone
$-\text{CH}_3$		165	(-32)
$-\text{CH}(\text{CH}_3)_2$			(-56)
$-\text{CH}_2\text{CH}(\text{CH}_3)_2$			-98
		916	166
			287
$-\text{OH}$		80	
$-\text{OCH}_3$		674	
$-\text{COO}- (\dots) -\text{H}$		936	
$-\text{OCO}- (\dots) -\text{H}$		905	
$-\text{C}\equiv\text{N}$		603	377
$-\text{Cl}$		327	556

Example 14.1

Estimate the elastic parameters of poly(methyl methacrylate). The structural unit is



with $M = 100.1 \text{ g/mol}$, $\rho = 1.19 \text{ g/cm}^3$ and $\mathbf{V} = 84.5 \text{ cm}^3/\text{mol}$.

Solution

Table 14.4 gives the group contributions:

	\mathbf{U}_{Ri}	\mathbf{U}_{Hi}
$-\text{CH}_2-$	880	675
$-\text{C}(\text{CH}_3)(\text{COOCH}_3)-$	4220	3650
	5100	4325

For the specific calculations we follow Scheme 14.1.

$$K = \rho \left(\frac{\mathbf{U}_{\text{R}}}{\mathbf{V}} \right)^6 = 1.19 \left(\frac{5100}{84.5} \right)^6 = 5.75 \times 10^{10} \text{ g}/(\text{cm s}^2) \text{ or } \text{dn}/\text{cm}^2 = 5.75 \text{ GPa}$$

$$G = \rho \left(\frac{\mathbf{U}_{\text{H}}}{\mathbf{V}} \right)^6 = 1.19 \left(\frac{4325}{84.5} \right)^6 = 2.14 \times 10^{10} \text{ g}/(\text{cm s}^2) \text{ or } \text{dn}/\text{cm}^2 = 2.14 \text{ GPa}$$

So $G/K = 2.14/5.75 = 0.372$. For E we then find:

$$E = 3G/[1 + G/(3K)] = 6.54/1.126 = 5.71 \text{ GPa}$$

and for v

$$v = [\sqrt{2} - G/(3K)]/[1 + G/(3K)] = 0.334$$

In comparison with the experimental values this result is satisfactory:

	Exp.	Estimated
K	6.49 (GPa)	5.75
G	2.33 (GPa)	2.14
E	6.24 (GPa)	5.71
v	0.34 –	0.334

Example 14.2

Estimate the sound velocities and the sound absorptions of PMMA.

Solution

Using the estimated values of Example 14.1 for K and G we find:

$$K/\rho = (5.75/1.19) \times 10^{10} (\text{cm/s})^2 = 4.83 \times 10^{10} (\text{cm/s})^2$$

$$G/\rho = (2.14/1.19) \times 10^{10} (\text{cm/s})^2 = 1.80 \times 10^{10} (\text{cm/s})^2$$

$$u_L = (4.83 + 4/3 \times 1.80)^{1/2} \times 10^5 \text{ cm/s} = 2.69 \times 10^3 \text{ m/s}$$

$$u_{\text{Sh}} = (1.80 \times 10^{10})^{1/2} \text{ cm/s} = 1.34 \times 10^3 \text{ m/s}$$

Both values for the sound speed are in excellent agreement with the experimental ones: $u_L = 2690 \text{ m/s}$ and $u_{Sh} = 1340 \text{ m/s}$. For the sound absorption coefficients we use the tentative Eqs. (14.14) and (14.13). Example 14.1 gave as a value for the Poisson ratio 0.332. Substituted in Eq. (14.14) this gives

$$\alpha_L = 40 \times (0.332 - 0.3) = 1.28 \text{ dB/cm}$$

$$\alpha_{Sh} = 5\alpha_L = 6.4 \text{ dB/cm}$$

in fair agreement with the experimental values 1.4 and 4.3 dB/cm.

Example 14.3

Estimate the LA-value for a Polystyrene/Polymethylacrylate 33/67 statistical copolymer (cross-linked).

Solution

Eq. (14.19) gives

$$LA_{copol} = 0.33LA_{PS} + 0.67LA_{PMA}$$

From the data in Table 14.6 we get

$$LA_{PS} = (92 + 916)/104.1 = 9.7 \quad \text{and} \quad LA_{PMA} = (92 + 936 - 42)/86.1 = 11.45$$

So $LA_{copol} = 0.33 \times 9.7 + 0.67 \times 11.45 = 10.9$ in good agreement with the experimental value 11.2.

BIBLIOGRAPHY

General references

- Bhatia AB, "Ultrasonic Absorption", Oxford University Press, London, 1967.
 Bicerano J, *Prediction of Polymer Properties*, Marcel Dekker, New York, 3rd Ed, 2002, Chap. 11.
 Corsaro RD and Sperling LH (Eds), "Sound and Vibration Damping with Polymers", ACS Symposium Series 424, ACS Press, Washington DC, 1990.
 Ferry JD, "Viscoelastic Properties of Polymers", Wiley, New York, 3rd Ed, 1980.
 Hartmann B, "Ultrasonic Measurements", In "Methods of Experimental Physics", Fava RA (Ed), Academic Press, New York, Vol. 16C, 1980, pp 59–90.
 Hartmann B, "Acoustic Properties", In Mark HF, Bikales NM, Overberger CG, Menges G and Kroschwitz JI (Eds), "Encyclopaedia of Polymer Science and Engineering", Wiley, New York, Vol. 1, 2nd Ed, 1984, pp 131–160.
 Hartmann B, "Relation of Polymer Chemical Composition to Acoustic Damping" In Corsaro RD and Sperling LH (Eds), "Sound and Vibration Damping with Polymers", ACS Symposium Series 424, ACS Press, Washington DC, 1990, Chap. 2.
 Hartmann B, "Acoustic Properties" In Mark JE (Ed), "Physical Properties of Polymers Handbook", AIP Press, Woodbury, NY, 1996, Chap. 49.
 Herzfeld KF and Litovitz TA, "Absorption and Dispersion of Ultrasonic Waves", Academic Press, New York, 1959.
 Mason WP, "Physical Acoustics and the Properties of Solids", Van Nostrand, Princeton, NJ, 1958.
 McCrum NG, Read BE and Williams G, "Anelastic and Dielectric Effects in Polymeric Solids", Wiley, London, 1967.
 Sinha M and Buckley DJ, "Acoustic Properties of Polymers", In Mark JE (Ed), "Physical Properties of Polymers Handbook", Springer, 2nd Ed 2007, Chap. 60.
 Truell R, Elbaum C and Chick BB "Ultrasonic Methods in Solid State Physics", Academic Press, New York, 1969.

Special references

- Ballou JW and Silverman J, Acous Soc Am 16 (1944) 113.
Ballou JW and Smith JC, J Appl Phys 20 (1949) 493.
Chang MCO, Thomas DA and Sperling LH, J Polym Sci Polym Phys 26 (1988) 1627.
De Gennes PG, J Chem Phys 55 (1971) 572.
Gilbert AS, Pethrick RA and Phillips DW, J Appl Polym Sci 21 (1977) 319.
Hartmann B, J Appl Polym Sci 19 (1975) 3241; J Appl Phys 51 (1980) 310; Polymer 22 (1981) 736; "Acoustic Properties" (1984), see General reference.
Hartmann B, and Jarzynski J, J Polym Sci A-2 (1971) 763; J Appl Phys 43 (1972) 4304; J Acous Soc Am 56 (1974) 1469.
Hartmann B and Lee GF, J Appl Phys 51 (1980) 5140; J Polym Sci Phys Ed 20 (1982) 1269; Bull Am Phys Sec 35 (1990) 611.
Ivey DG, Mrowca BA and Guth E, J Appl Phys 20 (1949) 486.
Maeda Y, J Polym Sci 18 (1955) 87.
Mason WP et al. Phys Rev 73 (1948) 1091; 74 (1949) 1873; 75 (1949) 939.
Nolle AW and Mowry SC, J Acous Soc Am 20 (1948) 432.
Nolle AW and Sieck PW, J Appl Phys 23 (1952) 888.
North AM, Pethrick RA and Phillips DW, Polymer 18 (1977) 324.
Perepechko II et al., Polym Sci USSR 13 (1971) 142; 16 (1974) 1910/15.
Pethrick RA, "Acoustic Studies in Polymer Solutions", Rev Macromol Sci 10 (1973) 91.
Phillips DW and Pethrick RA, J Macromol Sci Rev 16 (1977) 1.
Phillips DW, North AM and Pethrick RA, J Appl Polym Sci 21 (1977) 1859.
Rao MR, Ind J Phys 14 (1940) 109; J Chem Phys 9 (1941) 682.
Sakiades BC and Coates J, AIChem Eng J 1 (1955) 275.
Schuyer J Nature 181 (1958) 1394; J Polym Sci 36 (1959) 475.
Sperling LH et al., Macromolecules 5 (1972) 340; 9 (1976) 743; 15 (1982) 625; Rubber Chem Techn 59 (1986) 255; Polymer 19 (1978) 188; J Appl Polym Sci 17 (1973) 2443; 19 (1975) 1731; 21 (1977) 2609; 33 (1987) 2637; 34 (1987) 409; Polym Eng Sci 21 (1981) 696; 22 (1982) 190; 23(1983) 693; 26 (1986) 730; J Polym Sci Polym Phys 26 (1988) 1627.
Wada Y et al., J Phys Soc Jpn 11 (1956) 887; 16 (1961) 1226; J Polym Sci Part C 23 (1968) 583; J Polym Sci Phys Ed 11 (1973) 1641.
Warfield RW, Kayser G and Hartmann B, Makromol Chem 104 (1983) 1927.

PART

IV

TRANSPORT PROPERTIES OF POLYMERS

"Πάντα ρει: Everything flows"

Heraclitus the Ephesian, ca 535–475 BC

This page intentionally left blank

CHAPTER 15

Rheological Properties of Polymer Melts

The principal quantities determining the rheological behaviour of polymer melts are the viscosity and normal stress coefficients in shear and extensional viscosity.

The shear viscosity of polymers depends on the average molecular weight, the molecular-weight distribution, the temperature, the shear stress (and shear rate) and the hydrostatic pressure. Semi-empirical relationships for these dependencies permit estimations of shear viscosities of polymer melts under arbitrary experimental conditions.

Extensional viscosity is obviously dependent on average molecular weight, temperature and rate of extension. Apparently, also the tensile strain (degree of extension) is important.

At high shear rates catastrophic deformations are possible which are known as "melt fracture". Empirical expressions for the conditions under which melt fracture occurs are given, but the phenomenon is still not completely understood.

15.1. INTRODUCTION

The flow behaviour of polymer melts is of great practical importance in polymer manufacturing and polymer processing. Therefore, the development of a quantitative description of flow phenomena based on a number of material properties and process parameters is highly desirable.

In the same way as the mechanical behaviour of solid polymers can be described in terms of moduli (ratios of stress and deformation), the flow behaviour of polymer melts can be characterised by viscosities (ratios of stress and rate of deformation).

For common liquids, the viscosity is a material constant which is only dependent on temperature and pressure but not on rate of deformation and time. For polymeric liquids, the situation is much more complicated: viscosities and normal stress coefficients differ with deformation conditions. Because polymer melts are viscoelastic their flow is accompanied by elastic effects, due to which part of the energy exerted on the system is stored in the form of recoverable energy. For this reason the viscosities are time and rate dependent: polymer melts are viscoelastic.

Some typical viscoelastic phenomena are: (a) the *Weissenberg effect*. In a stirred vessel, a common liquid shows it vortex with the liquid level at the centre lower than at the wall. In stirring polymer melts the opposite effect is observed, the so-called rod-climbing effect; this can give rise to the construction of a normal-force pump; (b) the *Barus effect* or *die swell*. If a polymer melt is extruded from a capillary into the air, the jet shows an increase in diameter; (c) open-siphon flow, where a liquid is sucked out of the surface, e.g. with a syringe; subsequently the syringe can be brought far above the liquid surface without disturbing the flow; (d) another open-siphon effect is the transfer of a solution of high molecular weight polymer from one full container to a lower empty container without making use of a siphon pipe. Other effects can be found in literature, e.g. in Barnes, Hutton and Walters (General references, 1989) and in Boger and Walters (1993).

15.2. MODES OF DEFORMATION AND DEFINITION OF VISCOSITY AND NORMAL STRESS COEFFICIENTS

15.2.1. Modes of deformation

As in the elastic-mechanical behaviour of solid polymers, so in the flow behaviour of polymer melts the mode of deformation determines the nature of the characteristic property, in this case the viscosity.

There are two prominent elementary modes of deformation, viz. simple shear and simple extension.

15.2.1.1. Simple shear

Viscosity of a liquid is defined as the ratio between shear stress, σ_{sh} , and shear rate, $d\gamma/dt$, so that a simple measurement of can be determined by measurement the shear stress and shear rate.

15.2.1.1.1. Shear rate Under idealised conditions, the polymer melt subjected to *simple shear* is contained between two (infinitely extending) parallel walls, one of which is translated parallel to the other at a constant distance. The result of the shear stress (σ_{sh} , the force exerted on the moving wall per unit of surface area) is a velocity gradient in the melt in a direction perpendicular to the wall. If the velocity increases linearly from the one plate to the other one, then the flow is *rectilinear*. In that case, the velocity gradient is constant (see Fig. 15.1):

$$v_1 = \frac{v_w}{d} x_2 \quad \text{and} \quad \frac{dv_1}{dx_2} = \frac{v_w}{d} \quad (15.1)$$

The rate of shear is equal to:

$$\dot{\gamma} \equiv \frac{d\gamma}{dt} = \frac{d \tan \alpha}{dt} = \frac{d}{dt} \left(\frac{dx_1}{dx_2} \right) = \frac{d}{dx_2} \left(\frac{dx_1}{dt} \right) = \frac{dv_1}{dx_2} \quad (15.2)$$

where α is the angle shown in Fig. 15.1.

Accordingly, under these ideal conditions the velocity gradient is equal to the rate of shear. If the shear rate is independent of time, the flow is called *stationary* $\dot{\gamma} = \dot{\gamma}_0 = \text{constant} = q$.

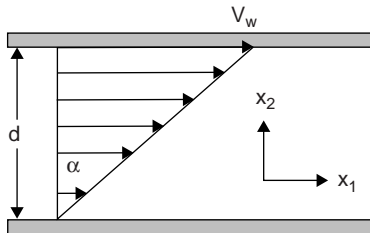


FIG. 15.1 Rectilinear shear flow; x_1 is the direction of flow and x_2 is the direction of the velocity gradient.

Although the geometry of simple shear as defined above is seldom encountered in practice, it may be approximated under real conditions. An example of an approximation of infinitely extended, parallel plates is the Couette geometry, consisting of two coaxial cylinders, where the liquid of consideration is confined in the narrow slit between the two cylinders. The cylinders rotate with respect of each other with different angular velocities, Ω (in rad/s), and in general one of them is fixed. If the diameters of the cylinders are large with respect to the slit width and small with respect to their lengths, then in the slit a shear flow is obtained which to a high approximation is equal to the shear flow between two infinitely extended parallel plates. In Couette geometry (Fig. 15.2) the velocity gradient is equal to:

$$\frac{dv}{dr} = \frac{d(\Omega r)}{dr} = \Omega + r \frac{d\Omega}{dr} \quad (15.3)$$

where r is the distance to the axis.

If the inner and outer cylinder rotate together with the fluid as a rigid system, then $\Omega = \text{constant}$ and thus $d\Omega/dr = 0$. In that case, the velocity gradient is equal to Ω , whereas the shear rate is equal to zero. Hence, in the determination of the shear rate, we have to take into consideration the fact that the velocities of neighbouring shearing planes contain a rigid-body rotation component, Ω . We have to subtract this term from the difference in velocities, in order to calculate the shear rate, so that for:

Couette flow between two concentric cylinders:

$$\dot{\gamma} = \frac{dv}{dr} - \Omega = r \frac{d\Omega}{dr} \approx \frac{r_{av} \Omega_o}{\Delta r} \quad (15.4)$$

where Ω_o = angular velocity of the outer cylinder if the inner cylinder is fixed; $r_{av} = \frac{1}{2}(r_o + r_i)$, i.e. the average distance to the axis; r_o and r_i are the radius of the outer and inner cylinder, respectively.

Similar considerations lead to expressions of shear rates in other geometries shown in Fig. 15.2:

Torsional flow between parallel plates:

$$q = q(r) = r \frac{d\Omega}{dz} \approx r \frac{\Omega_o}{z_o} \quad (15.5)$$

Torsional flow between a cone and a plate:

$$q \approx \frac{\Omega_o}{\Delta\Theta} \quad (15.6)$$

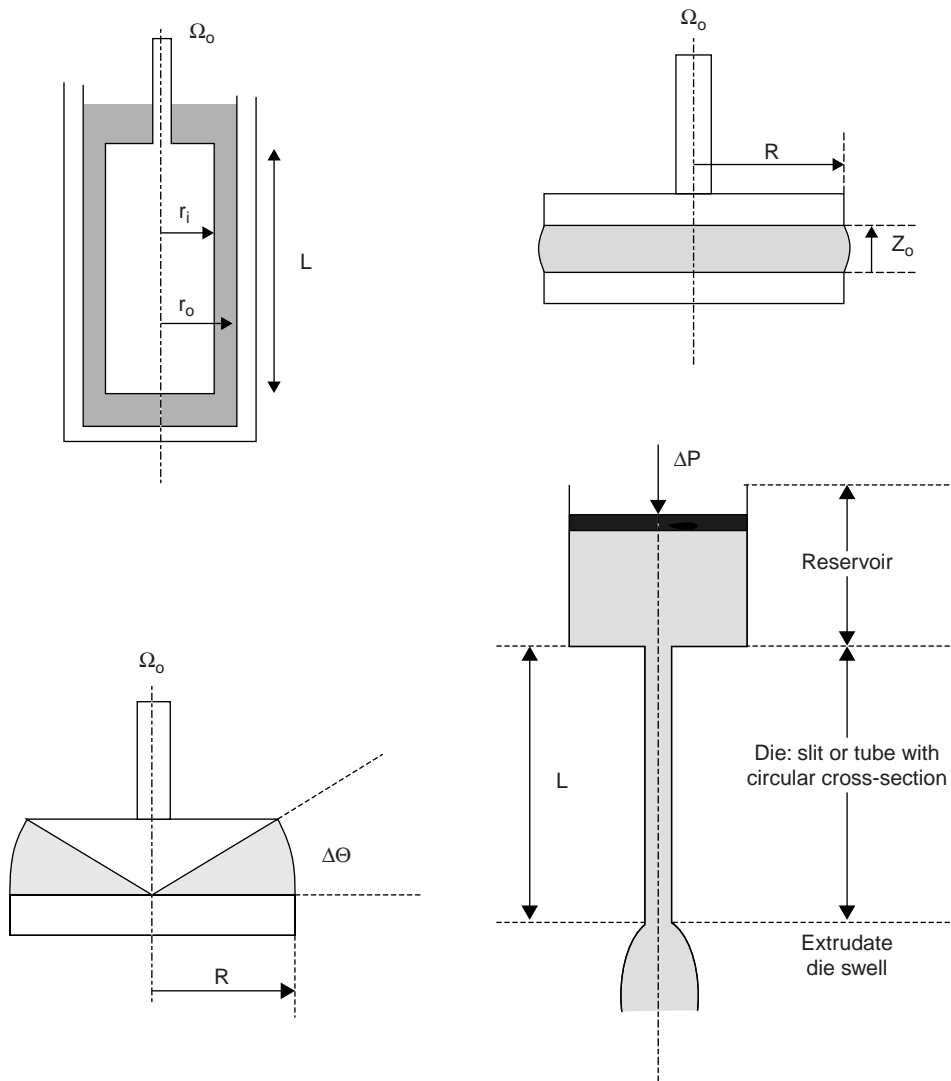


FIG. 15.2 Types of simple shear flow. (A) Couette flow between two coaxial cylinders; (B) torsional flow between parallel plates; (C) torsional flow between a cone and a plate and (D) Poisseuille flow in a cylindrical tube. After Te Nijenhuis (2007).

Telescopic flow in a cylindrical tube:

$$q = q(r) = \frac{dv(r)}{dr} \quad (15.7)$$

where Ω_0 = angular velocity of inner cylinder, upper plate or cone (rad/s); z_o = distance between the parallel plates (m); $\Delta\Theta$ = angle between cone and plate (rad).

In Couette flow and in torsional flow between a cone and a plate the shear rate may be considered constant, provided the slit Δr between the two cylinders and the angle $\Delta\Theta$ between cone and plate, respectively, are small. On the other hand, the shear rates in

torsional flow between parallel plates and Poisseuille flow in a cylindrical tube are highly dependent on the distance r to the axis. In principle, it is difficult to determine the shear rate dependent viscosity in these two geometries. However, there are possibilities to overcome these problems.

15.2.1.1.2. Shear stress The shear stress in the four mentioned geometries can be determined by measuring the moment M (in Nm), or pressure ΔP (in N/m²) during flow. For the Couette flow and the cone and plate flow the relationships for shear stress and shear rate are easy to handle in order to determine the viscosity. For the parallel plates flow and Poisseuile flow, however, more effort is needed to determine the shear stress at the edge of the plate, q_R , in parallel plates flow or the shear rate at the wall, q_w , in Poisseuile flow. In Table 15.1 equations for shear stresses and shear rates are shown.

15.2.1.1.3. Normal stresses For the exact definition of shear stresses and normal stresses, we use the illustration of the stress components given in Fig. 15.3. The stress vector t on a body in a Cartesian coordinate system can be resolved into three stress vectors t_i perpendicular to the three coordinate planes. In this figure t_2 the stress vector on the plane perpendicular to the x_2 -direction. It has components T_{21}, T_{22} and T_{23} in the x_1, x_2 and x_3 -direction, respectively. In general, the stress component T_{ij} is defined as the component of the stress vector t_i (i.e. the stress vector on a plane perpendicular to the x_i -direction) in the x_j -direction. Hence, the first index points to the normal of the plane the stress vector acts on and the second index to the direction of the stress component. For $i = j$ the stress

TABLE 15.1 Equations for shear stress, normal stress functions and shear rate for various geometries

Type of flow	Shear stress/Normal stresses	Shear rate
Couette flow, cc	$\sigma_{sh} = \frac{M}{2\pi L}$ $N_1 = \frac{\Delta T_{22}}{\Delta r} r_{av}$	$q = \frac{r_{av}\Omega_o}{\Delta r}$
Torsional flow, pp	$\sigma_{sh}(q_R) = \frac{M}{2\pi R^3} \left(3 + \frac{d \log M}{d \log \Omega_o} \right)$ $N_1(q_R) - N_2(q_R) = \frac{F_n}{\pi R^2} \left(2 + \frac{d \log F_n}{d \log \Omega_o} \right)$	$q_R = \frac{R\Omega_o}{z_o}$
Torsional flow, cp	$\sigma_{sh} = \frac{3M}{2\pi R^3}$ $N_1 = \frac{2F_n}{\pi R^2}, \quad N_1 + 2N_2 = \frac{d T_{22}(r)}{d \ln(r/R)}$	$q = \frac{\Omega_o}{\Delta \Theta}$
Capillary flow, cf	$\sigma_{sh}(q_w) = -\frac{R\Delta P}{2L}$ $2N_1(q_w) + N_2(q_w) = -T_{22}(R) \left(2 + \frac{d \log T_{22}(R)}{d \log \Delta P} \right)$	$q_w = \frac{4Q}{\pi R^3} \left(\frac{3}{4} + \frac{1}{4} \frac{d \log Q}{d \log \Delta p} \right)$

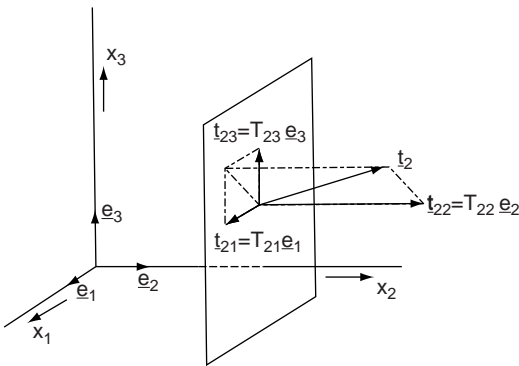


FIG. 15.3 Components of the stress vector t_2 .

components are normal stresses: T_{11}, T_{22} and T_{33} , whereas for $i \neq j$ the stress components are shear stresses: $T_{12}, T_{21}, T_{13}, T_{31}, T_{23}$ and T_{32} . In Fig. 15.4, all components of the stress tensor T are shown.

If the flow points in the x_1 -direction and the velocity gradient in the x_2 -direction then:
 $T_{21} = \sigma_{sh}$ = shear stress

T_{11} = normal stress component in the direction of flow

T_{22} = normal stress component in the direction of the velocity gradient or of the shear

T_{33} = normal stress component in the third direction and perpendicular to the third direction

Normally the coordinate system is chosen in such a way that $T_{13} = T_{31} = T_{23} = T_{32} = 0$

In general, use is made of normal stress differences, N_1 and N_2 , because they do not include undetermined hydrostatic pressures that are always present but not affect the material properties (as long as they are not too high). In Table 15.1, also the possibilities to determine the normal stress differences or combinations are depicted. In the modern rheogoniometers also normal stress differences can be determined but. They follow from measurements of normal forces, F_n , or normal stresses, T_{22} , as is also depicted in Table 15.1. For the measurements of the normal stresses T_{22} pressure gauges have to be mounted in the Couette cylinders, in the capillary of the capillary rheometer (in both cases quite difficult to mount) and in the plate of a cone and plate instrument at several distances from the axis (not that difficult). Sometimes use is made of a slit rheometer instead of a capillary rheometer, because pressure gauges are much easier to mount (Te Nijenhuis, 2007, Chap. 9.1.2).

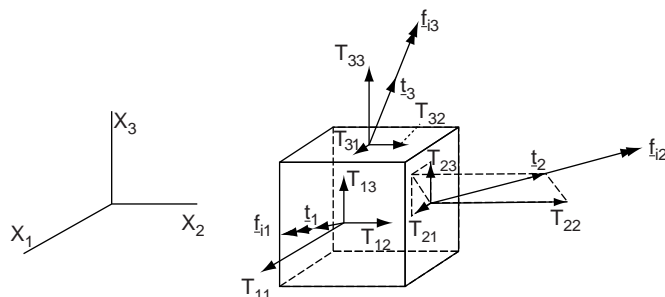


FIG. 15.4 Components of the stress tensor T .

The stresses arising from simple shear flow may be generally expressed by the following set of equations:

$$\text{Shear stress } T_{21} = \sigma_{sh} = \eta(\dot{\gamma})\dot{\gamma} \quad (15.8)$$

$$\text{First normal stress difference : } N_1 = T_{11} - T_{22} = \Psi_1(\dot{\gamma})\dot{\gamma}^2 \quad (15.9)$$

$$\text{Second normal stress difference : } N_2 = T_{22} - T_{33} = \Psi_2(\dot{\gamma})\dot{\gamma}^2 \quad (15.10)$$

where the viscosity, η , the first normal and second normal stress coefficients, Ψ_1 and Ψ_2 , respectively, are shear rate dependent quantities. For low shear rates they have constant, so called zero shear values: η_0 , $\Psi_{1,0}$ and $\Psi_{2,0}$. The first normal stress difference is in general positive for polymeric systems and its existence is the background for the above mentioned Weissenberg effect or rod climbing effect. The second normal stress coefficient is in general negative and its absolute value is for polymeric systems in general not more than 20% of the first normal stress difference. In the case of simple shear flow

$$\eta \equiv \frac{T_{21}}{\dot{\gamma}} = \text{viscosity} \quad (\text{in N s/m}^2) \quad (15.11)$$

$$\Psi_1 \equiv \frac{N_1}{\dot{\gamma}^2} = \frac{T_{11} - T_{22}}{\dot{\gamma}^2} = \text{first normal stress coefficient} \quad (\text{in N s}^2/\text{m}^2) \quad (15.12)$$

$$\Psi_2 \equiv \frac{N_2}{\dot{\gamma}^2} = \frac{T_{22} - T_{33}}{\dot{\gamma}^2} = \text{second normal stress coefficient} \quad (\text{in N s}^2/\text{m}^2) \quad (15.13)$$

$$\frac{T_{11} - T_{22}}{T_{21}} = \gamma_{rec} = \text{recoverable shear or elastic shear deformation} \quad (15.14)$$

$$G \equiv \frac{T_{21}}{\gamma_r} = \text{shear modulus} \quad (\text{in N/m}^2) \quad (15.15)$$

It should be mentioned that according to some theories the elastic shear deformation should be defined as $\gamma_e = (T_{11} - T_{22})/(2T_{21})$.

For linear (e.g. Newtonian) behaviour G and η are material constants:

$$G_0 = \lim_{\dot{\gamma} \rightarrow 0} G(\dot{\gamma}) \quad (15.16)$$

$$\eta_0 = \lim_{\dot{\gamma} \rightarrow 0} \eta(\dot{\gamma}) \quad (15.17)$$

It has to be mentioned that $G(\dot{\gamma})$ is equal to the initial slope in the plot of shear stress vs. shear deformation:

$$G(\dot{\gamma}) = \lim_{t \rightarrow 0} \frac{\sigma_{sh}}{q t} = \lim_{\gamma \rightarrow 0} \frac{\sigma_{sh}}{\gamma} \quad (15.18)$$

15.2.1.1.4. Experimental determination of viscosity and normal stress coefficients Since the range of η may extend from 10^{-2} to 10^{11} N s/m² and the normal stress coefficients, Ψ_1 and Ψ_2 , cover also a wide range of values, a number of different experimental techniques have been developed to cover this wide range. Some methods are listed in Table 15.2.

TABLE 15.2 Survey of possible results of measurement techniques

Instrument	Shear rate	viscosity	Normal stress differences/coefficients
Couette	$q \approx \text{constant}$	$\eta(q)$	$N_1(q)$
Parallel plates	$q = q(r)$	$\eta(q_R)$	$N_1(q_R) - N_2(q_R)$
Cone and plate	$q = \text{constant}$	$\eta(q)$	$N_1(q)$ and $N_1(q) + N_2(q)$
Cap. rheometer	$q = q(r)$	$\eta(q_w)$	$2N_1(q_w) + N_2(q_w)$
Slit rheometer	$q = q(h)$	$\eta(q_w)$	$\Psi_1(q_w) + \Psi_2(q_w)$
			$\Psi_1(q_w)$

Bold parameters mean that these measurements are possible in commercially available instruments; the others are not easy to measure and it is in general not possible to measure them in commercially available instruments.

15.2.1.2. Simple extension

Extensional flow (also called elongational flow) is defined as a flow where the velocity changes in the direction of the flow: dv_1/dx_1 in contradistinction with shear flow where the velocity changes normal to the direction of flow (dv_1/dx_2). In *uniaxial flow* in the x_1 direction the extensional rate of strain is defined as:

$$\dot{\varepsilon} \equiv \frac{1}{l_{x1}} \frac{dl_{x1}}{dt} \quad (15.19)$$

For constant extensional rate of strain, q_e , the length of a line element increases exponentially in the x_1 -direction:

$$l_{x1}(t) = l_{o,x1} \exp(q_e t) \quad (15.20)$$

If the volume is constant, then the flows in the other directions are

$$l_{x2}(t) = l_{o,x2} \exp(-\frac{1}{2} q_e t), \quad l_{x3}(t) = l_{o,x3} \exp(-\frac{1}{2} q_e t) \quad (15.21)$$

For correct measurements, the extensional rate of strain is in general controlled and the extensional stress is measured.

In practice, simple extension is found in melt spinning of polymeric fibres, although the situation is complicated by the non-isothermal character.

The extensional viscosity is defined as

$$\eta_e = \frac{\text{tensile stress}}{\text{extensional rate of strain}} = \frac{\sigma_e}{q_e} = \frac{T_{11} - T_{22}}{q_e} \quad (15.22)$$

Because also the extensional viscosity is dependent on the strain rate, we have:

$$\eta_{eo} = \lim_{\dot{\varepsilon} \rightarrow 0} \eta_e(\dot{\varepsilon}) \quad (15.23)$$

Other forms of extensional flow are *biaxial extensional flow* and *planar extensional flow* or *pure shear flow*.

Biaxial extensional flow is extensional flow in two directions with the same constant extensional strain rate q_e . If the volume is constant then

$$l_x(t) = l_{o,x} \exp(q_e t), \quad l_y(t) = l_{o,y} \exp(q_e t), \quad l_z(t) = l_{o,z} \exp(-2q_e t) \quad (15.24)$$

Planar extensional flow or pure shear flow is extensional flow with the same but opposite rates of strain in two directions; in the third direction, there is no flow:

$$l_x(t) = l_{o,x} \exp(q_e t), \quad l_y(t) = l_{o,y} \exp(-q_e t), \quad l_z(t) = l_{o,z} \quad (15.25)$$

15.2.2. Complicated modes of deformation

Several published studies have been devoted to more complicated flow situations, e.g.:

- a. *Convergent flow*, in which an extensional deformation and a shear deformation are superposed, as encountered in the entry and exit effects of capillary flow.
- b. *Biaxial shear*, in which shear processes in different directions are superposed, as encountered in the barrel of a screw extruder.

15.3. NEWTONIAN SHEAR VISCOSITY OF POLYMER MELTS

This section will be devoted to the Newtonian viscosity η_o , that is to situations where the shear rate is proportional to the shear stress. This is the case under *steady-state conditions at low shear rates*. Although η_o may be directly measured at low shear rates in a cone and plate rheometer, it is in general not measured directly but found by extrapolation of viscosity values, as measured in a capillary rheometer, as a function of shear rate:

$$\eta_o = \lim_{\dot{\gamma} \rightarrow 0} \eta(\dot{\gamma}) \quad (15.26)$$

This may introduce a certain inaccuracy, however, into the values of η_o .

The best method to determine the zero shear viscosity is to calculate η_o from the loss modulus G'' measured in dynamic shear experiments at a series of frequencies such low that by plotting $\log G''$ vs. $\log \omega$ a straight line is obtained with slope equal to 1:

$$\eta_o = \lim_{\substack{\omega \rightarrow 0 \\ \gamma_o \rightarrow 0}} \frac{G''}{\omega} \quad (15.27)$$

where ω is the angular frequency and γ_o is the amplitude of the sinusoidal shear deformation.

The parameters which η_o is dependent on for a given polymer are molar mass, temperature and hydrostatic pressure. Table 15.3 gives some typical values of η_o for different polymers.

TABLE 15.3 Some typical values of η_0

Polymer	$T(^{\circ}\text{C})$	M_w	$\eta_0 (\text{N s/m}^2)$
Polyethylene, high density	190	10^5	2×10^4
Polyethylene, low density	170	10^5	3×10^2
Polypropylene	220	3×10^5	3×10^3
Polyisobutylene	100	10^5	10^4
Polystyrene	220	2.5×10^5	5×10^3
Poly(vinyl chloride)	190	4×10^4	4×10^4
Poly(vinyl acetate)	200	10^5	2×10^2
Poly(methyl methacrylate)	200	10^5	5×10^4
Polybutadiene	100	2×10^5	4×10^4
Polyisoprene	100	2×10^5	10^4
Poly(ethylene oxide)	70	3×10^4	3×10^2
Poly(ethylene terephthalate)	270	3×10^4	3×10^2
Nylon 6	270	3×10^4	10^2
Polycarbonate	300	3×10^4	10^3
Poly(dimethyl siloxane)	120	4×10^5	2×10^3

Conversion factor: $1 \text{ N s/m}^2 = 10 \text{ poise}$ or $1 \text{ m N s/m}^2 = 1 \text{ cP}$.

15.3.1. Effect of molar mass on η_0

As is to be expected, the viscosity of polymer melts increases with increasing molar mass. The difference in behaviour of polymers from low-molar mass substances becomes striking, however, for molecular mass higher than a certain critical value, M_{cr} . In this instance

$$\log \eta_0 = 3.4 \log M_w + A \quad (15.28)$$

where A is an empirical constant, dependent on the nature of the polymer and the temperature. For molecular mass lower than M_{cr} a number of empirical relationships can be found in the literature, for instance

$$\log \eta_0 = n \log M_w + B \quad (15.29)$$

where $n \approx 1$ and B is an empirical constant.

In Fig. 15.5 for many polymers, $\log \eta$ is plotted against $\log M_w$ and the 3.4 law appears to be really universal.

Originally it was supposed that there is a rather sudden transition from Eqs.(15.28) to (15.29) at $\bar{M}_w = M_{\text{cr}}$. Later investigations showed a gradual transition from Eqs. (15.28) to (15.29). Nevertheless, M_{cr} may still be defined as the molecular mass at which the two extrapolated logarithmic linear relationships intersect.

The very strong influence of molecular mass on the viscosity of polymer melts required some mechanism of molecular interaction for a theoretical interpretation. Bueche (1952) could derive Eq. (15.28) with certain assumptions on the influence of chain entanglements on polymer flow. Later, numerous other interpretations have been offered which will not be discussed here.

A consequence of these theories is that chain entanglements are not important to flow behaviour if $\bar{M}_w < M_{\text{cr}}$. The critical molecular mass M_{cr} may vary from 2000 to 60,000, depending on the structure of the polymer. It was shown by Fox et al. (1956) that the critical value of the number of atoms in the backbone of the polymer chain, Z_{cr} gives a smaller variation. Nevertheless, the values of Z_{cr} still show great differences.

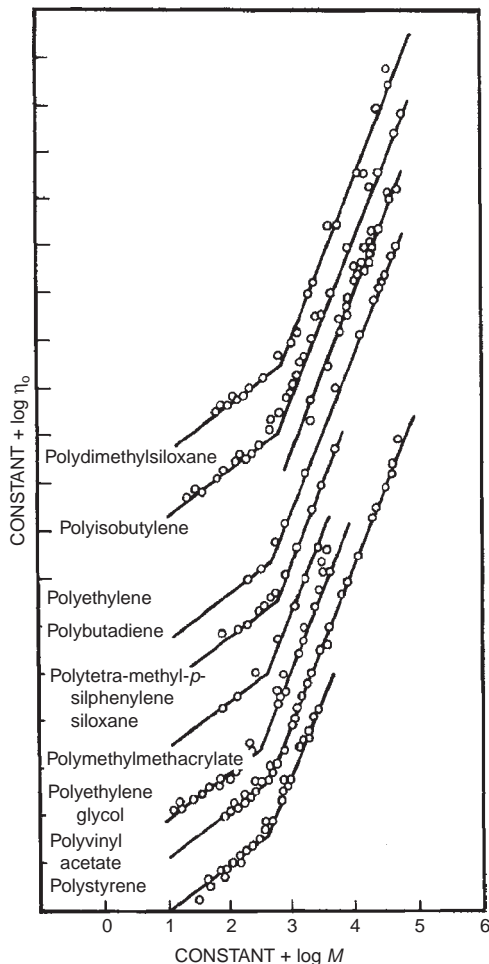


FIG. 15.5 Viscosity vs. weight average molecular weight for several polymers, on double logarithmic scales. The data are shifted to avoid overlap. The lines for the low and high molecular weights have slopes of 1.0 and 3.4, respectively. From Berry and Fox, 1948, Courtesy Springer Verlag.

It is a very interesting fact that M_{cr} also proved to be the best available relative measure for the "brittleness" of the solid polymer (below T_g).

Fox and Allen (1964) correlated M_{cr} with molecular dimensions, i.e. with the group

$$R_{\text{Go}}/(Mv)$$

where R_{Go} is the unperturbed radius of gyration (see Chap. 9) and v is the specific volume.

An even better correlation can be obtained, however, with K_Θ the coefficient in the equation for the intrinsic viscosity of Θ -solutions (Chap. 9). Approximately

$$K_\Theta M_{\text{cr}}^{1/2} \approx 13 \text{ cm}^3/\text{g} = 0.013 \text{ m}^3/\text{kg} \quad (15.30)$$

In Table 15.4 values for M_{cr} , Z_{cr} and the product $K_\Theta M_{\text{cr}}^{1/2}$ are listed for a number of polymers.

TABLE 15.4 Critical molecular mass for a number of polymers

Polymer	M_{cr} (g/mol) (lit.)	Z_{cr}	K_θ ($\text{cm}^3 \text{mol}^{1/2}/\text{g}^{3/2}$)	$K_\theta (\text{m}^3 \text{mol}^{1/2}/\text{kg}^{3/2}) \times 10^3$	$K_\theta M_{cr}^{1/2}$ ($\text{cm}^3 \text{g}$)
Polyethylene	3500	250	0.219	6.92	13
Polypropylene	7000	330	0.135	4.27	11
Polyisobutylene	16,000	570	0.102	3.23	13
Polystyrene	35,000	670	0.084	2.66	16
Poly (α -methylstyrene)	40,000	680	0.076	2.40	15
Poly(vinyl chloride)	6200	200	0.149	4.71	12
Poly(vinyl alcohol)	7500	340	0.205	6.48	18
Poly(vinyl acetate)	25,000	580	0.081	2.56	13
Poly(methyl acrylate)	24,000	560	0.065	2.06	10
Poly(methyl methacrylate)	30,000	600	0.059	1.87	10
Poly(butyl methacrylate)	60,000	840	0.049	1.55	12
Poly(hexyl methacrylate)	61,000	720	0.044	1.39	11
Poly(octyl methacrylate)	110,000	1100	0.042	1.33	14
Polyacrylonitrile	1300	50	0.258	8.16	9
Polybutadiene	6000	440	0.166	5.25	13
Polyisoprene	10,000	590	0.129	4.08	13
Poly(ethylene oxide)	3400	230	0.156	4.93	9
Poly(propylene oxide)	5800	300	0.116	3.67	9
Poly (tetramethylene adipate)	6000	360	0.190	6.01	15
Poly (decamethylene succinate)	4000	250	0.196	6.20	12
Poly (decamethylene adipate)	4500	285	0.198	6.26	13
Poly (decamethylene sebacate)	4000	260	0.202	6.39	13
Poly(ethylene terephthalate)	6000	310	0.178	5.63	14
Poly(ϵ - caprolactam)	5000	310	0.226	7.15	16
Polycarbonate	3000	140	0.214	6.77	12
Poly(dimethyl siloxane)	30,000	810	0.077	2.43	13
Average				12.6 ± 2.2	

If the Newtonian viscosity at the critical molecular mass is denoted by η_{cr} Eqs. (15.28) and (15.29) may be rewritten as:

$$\begin{aligned}\log \eta_o &= \log \eta_{\text{cr}} + 3.4 \log(M_w/M_{\text{cr}}), && \text{if } M_w > M_{\text{cr}} \\ \log \eta_o &= \log \eta_{\text{cr}} + \log(M_w/M_{\text{cr}}), && \text{if } M_w < M_{\text{cr}}\end{aligned}\quad (15.31)$$

15.3.2. Effect of temperature on η_o

The effect of temperature on the viscosity of polymer melts is very complicated. Several mathematical formulations of this effect have been presented in the literature, but none has been found to hold for every arbitrary polymer over the whole range of temperatures. This is mainly because for many semi-crystalline polymers the temperature range of the viscosity data extends far below the crystalline melting point, often even into the vicinity of the glass transition temperature. Obviously, the flow behaviour of a polymer changes essentially over such a temperature range. For temperatures far enough above the melting point of a given polymer, the temperature dependence of viscosity follows a simple exponential relationship

$$\eta = B \exp[E_\eta/(RT)] \quad (15.32)$$

where E_η is an activation energy for viscous flow and B is a constant.

This expression was first formulated by Andrade (1930). Eyring (1941) interpreted this equation with the aid of his hole-theory of liquids. According to this theory, a liquid contains unoccupied sites or holes, which move at random throughout the liquid as they are filled and created anew by molecules jumping from one site to another. Each jump is made by overcoming an energy barrier of height E_η . This energy of activation is (for low-molecular liquids) related to the heat of vaporisation of the liquid, since the removal of a molecule from the environment of its neighbours forms part of both processes.

In polymers, however, E_η levels off at a value independent of molecular mass. This means that in long chains the unit of flow is considerably smaller than the complete molecule. It seems that viscous flow in polymers takes place by successive jumps of segments until the whole chain has shifted.

As was stated by Magill and Greet (1969) Eq. (15.32) does not hold in the vicinity of the melting point and even not for liquids of low molecular mass. So it is quite obvious that Eq. (15.32) cannot be used for semi-crystalline polymers in the temperature range between T_m and T_g . Sometimes values of E_η for this situation are mentioned in the literature, but these relate to formal application of Eq. (15.32) over a small temperature range. Such values of E_η increase with decreasing temperature.

The decrease of E_η with increasing T may be explained by the extra free volume created by thermal expansion. This was suggested by Batchinski in 1913 already. Several attempts have been made to formulate a joint temperature function for polymer melts and rubbery amorphous polymers on this basis. Doolittle (1951) formulated the equation:

$$\eta = A \exp(B/f) \quad \text{or} \quad \ln \eta = \ln A + B/f \quad (15.33)$$

where A and B are constants and f is the free volume fraction.

If it is assumed that f increases linearly with temperature, e.g. $f = f_g + \alpha_f(T - T_g)$ (see Eq. (13.99)) substitution into Eq. (15.33) gives

$$\ln \frac{\eta(T)}{\eta(T_g)} = -\frac{B}{f_g} \left(\frac{T - T_g}{f_g/\alpha_f + T - T_g} \right) \quad (15.34)$$

This equation was proposed by Williams et al. (1955). In its generalised form the equation reads:

$$\log \eta(T) = \log \eta(T_S) - \frac{c_1^S(T - T_S)}{c_2^S + (T - T_S)} \quad (15.35)$$

where T_S is a standard temperature. If T_g is chosen as standard temperature, the “universal” values of c_1^S and c_2^S are 17.44 and 51.6, respectively. They are not universal at all, however, as has already been shown in Table 13.10, Chap. 13. If the standard temperatures are arbitrarily selected in order to obtain the best universal function (see Table 15.5 for these T_S -values of different polymers), the values of the universal constants c_1^S and c_2^S are 8.86 and 101.6, respectively. This would mean that $T_S - T_g = 50$ K. However, the difference $T_S - T_g$ is about 43 K for a wide range of polymers so that the values of the universal constants c_1^S and c_2^S should be 9.51 and 94.6, respectively. As we have seen, the WLF equation also plays an important role in the time-temperature superposition principle in viscoelastic processes (see Chap. 13).

Eq. (15.35) gives a fair description of the effect of temperature on viscosity for a number of polymers. For some other polymers, however, considerable deviations are found. According to Eq. (15.35), $\eta(T)/\eta(T_g)$ should be a universal function of $(T - T_g)$, which is not confirmed by experimental data.

Another attempt to derive an equation for the whole temperature range based on a free-volume theory was made by Litt (1973). His equation reads:

$$\log \frac{\eta(T)}{\eta(T_R)} = \left(\frac{T_R}{T} \right)^{3/2} \frac{\exp(T_R/T)}{1 + (T_R/T)} \quad (15.36)$$

in which T_R is a specific reference temperature. Litt found T_R to be proportional to T_g for a number of polymers ($T_R \approx 2.8T_g$).

Eq. (15.36) would imply that $\eta(T)/\eta(T_g)$ is a universal function of T_g/T . However, this relationship is not confirmed, either, by experimental data.

TABLE 15.5 T_g and T_S values for different polymers

Polymer	T_S (K)	T_g (K)	$T_S - T_g$
Poly(hexene-1)	268	223	45
Polyisobutylene	243	197	46
Polystyrene	413	373	40
Poly(vinyl chloride)	395	358	37
Poly(vinyl acetate)	350	305	45
Poly(methyl acrylate)	324	282	42
Poly(methyl methacrylate)	433	387	46
Poly(cis-isoprene)	249	206	43
Polyurethane	283	238	45
Average			43

Finally a quite empirical equation, proposed by Fox and Loshaek (1955), should be mentioned:

$$\log \eta = A + \frac{B}{T^{1+a}} \quad (15.37)$$

where A, B, and a are constants (usually $a \approx 1$).

A similar formula was proposed by Cornelissen and Waterman (1955) for several oils, bituminous products, silicones and glasses.

15.3.3. The Vankrevelen–Hoftijzer viscosity–temperature relationship

As no completely satisfactory equation is available for the effect of temperature on η_o , a correlation of the available experimental data will be given here in graphical form. Such a correlation should satisfy Eq. (15.32) for high temperatures and should correspond to some WLF-type relationship in the neighbourhood of T_g . This can be realised by plotting by plotting $\log \eta$ against T_g/T .

The same temperature effect is found for all polymers if $T = 1.2T_g$ (in the region where also the WLF correlation approximately holds). So a generalised η -T correlation may be obtained by plotting $\eta_o(T)/\eta_o(1.2T_g) = \eta_{cr}(T)/\eta_{cr}(1.2T_g)$ as a function of T_g/T . This is shown in Fig. 15.6 in which the available experimental data of zero-shear viscosities of polymer melts are plotted. It can be seen that for T_g/T values exceeding 1/1.2 (= 0.83) all points indeed lie on a single curve. For higher temperatures, however, the curves for different polymers follow completely different paths. For high values of T , i.e. low values of T_g/T , the curves asymptotically approach to straight lines.

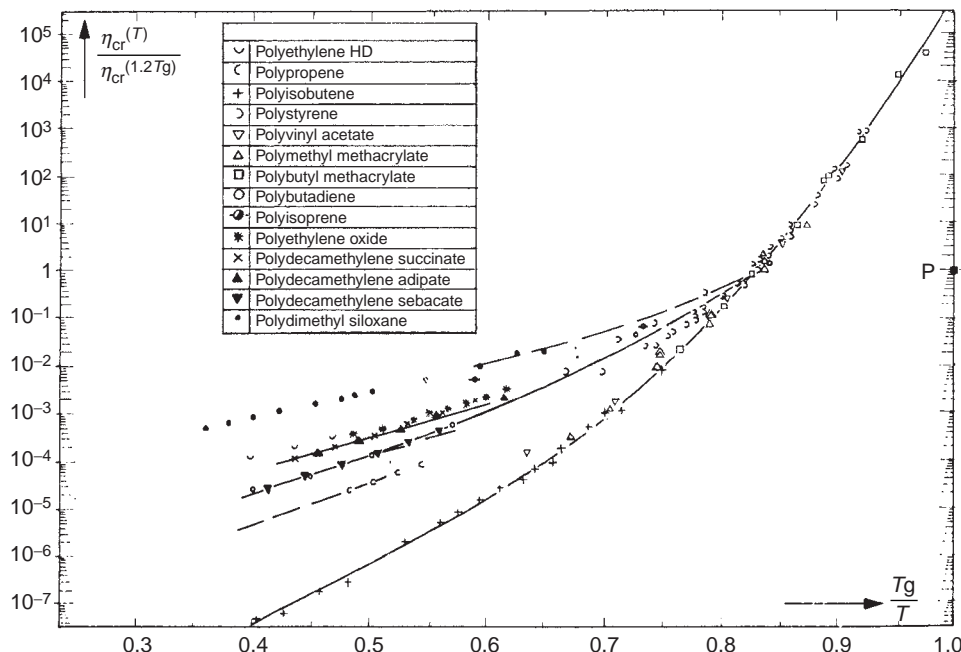


FIG. 15.6 Graphical correlation of η_{cr} data (Van Krevelen and Hoftijzer, 1976).

It is remarkable that all these lines, when extrapolated, pass through one point, indicated by P in Fig. 15.6. The coordinates of this point are

$$\log[\eta_{\text{cr}}(T)/\eta_{\text{cr}}(1.2T_g)] = 0 \quad \text{and} \quad T_g/T = 1$$

The general equation of these asymptotes is:

$$\log \frac{\eta_o(T)}{\eta_o(1.2T_g)} = \log \frac{\eta_{\text{cr}}(T)}{\eta_{\text{cr}}(1.2T_g)} = A \left(\frac{T_g}{T} - 1 \right) \quad (15.38)$$

Comparison with Eq. (15.32) shows that

$$E_\eta(\infty) = 2.303 A R T_g \quad \text{or} \quad A = \frac{0.4343 E_\eta(\infty)}{R T_g} \quad (15.39)$$

So with the aid of Fig. 15.6 $\log \eta_{\text{cr}}$ at a given temperature can be estimated, if E_η and $\log \eta_{\text{cr}}(1.2T_g)$ are known. Table 15.6 gives a survey of the available data. It should be borne in mind that there are rather large differences between the values of E_η and $\log \eta_{\text{cr}}(1.2T_g)$ obtained from the data of different investigators. The data mentioned in Table 15.6 are mean values.

TABLE 15.6 Parameters of the $\eta_{\text{cr}}(T)$ correlation

	A (-)	$E_\eta(\infty)$ (kJ/mol)	$\log \eta_{\text{cr}}(1.2T_g)$ (N s/m ²)	T_g (K)	$E_\eta(\infty)$ (calc.) (kJ/mol)
Polyethylene	8.5	25	5.05	195	27
Polypropylene	9.0	44	2.4	253	43
Polyisobutylene	12.5	48	7.8	198	48
Polystyrene	8.2	59	1.8	373	58
Poly(vinyl chloride)	~12.5	~85	~6	354	85
Poly(vinyl acetate)	11.5	67	4.45	301	63
Poly(methyl methacrylate)	9.0	65	3.1	378	64
Poly(butyl methacrylate)	12.5	72	4.5	300	75
Polybutadiene (<i>cis</i>)	8.0	26	3.8	171	26
Polyisoprene	5.5	23	2.05	220	26
Poly(ethylene oxide)	6.7	27	2.6	206	27
Poly(decamethylene succinate)	7.0	28	3.75	210	30
Poly(decamethylene adipate)	7.0	29	3.45	217	29
Poly(decamethylene sebacate)	7.8	30	3.95	197	29
Poly(ethylene terephthalate)	~7	~45	~2	343	47
Nylon 6	~6	~36	~1	323	36
Polycarbonate	~11	~85	~2	414	85
Poly(dimethyl siloxane)	5.2	15	2.5	150	15

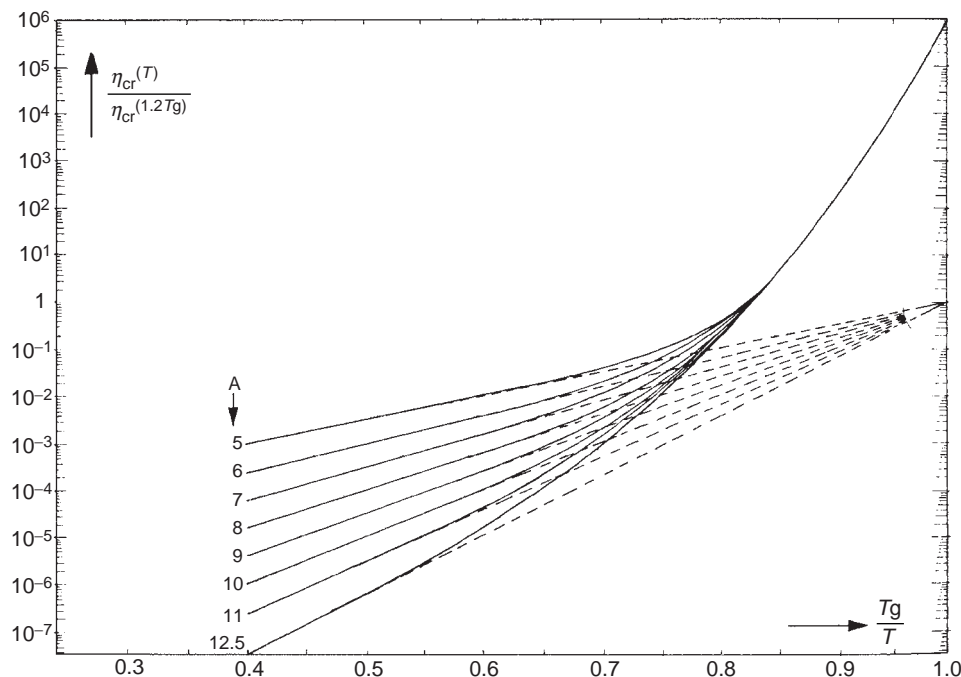


FIG. 15.7 Master curves for $\eta_{cr}(T)$ (Van Krevelen and Hoflyzer, 1976).

For practical use, a number of master curves for $\eta_{cr}(T)/\eta_{cr}(1.2T_g)$ against T_g/T have been drawn in Fig. 15.7, for different values of A , in correspondence with Fig. 15.6.

Of course, it would be very desirable to have a method for using the curves of Fig. 15.7 with polymers for which E_η and $\eta_{cr}(1.2T_g)$ are not yet known. This means that these quantities have to be predicted from the structure of the polymer, a task that is facilitated by the existence of a correlation between E_η and $\eta_{cr}(1.2T_g)$.¹ In order to demonstrate this, Eq. (15.32) may be rewritten as

$$\log \eta_{cr}(T) = \log \eta_{cr}(\infty) + \frac{E_\eta(\infty)}{2.3RT} \quad (15.40)$$

where $\eta_{cr}(\infty)$ is a formally defined viscosity at $T = \infty$. Combination with Eq. (15.38) gives

$$\log \eta_{cr}(\infty) = \log \eta_{cr}(1.2T_g) - A \quad (15.41)$$

In Fig. 15.8 $\log \eta_{cr}(\infty)$ is plotted against E_η . The data approximately satisfy the simple equation

$$\log \eta_{cr}(\infty) = -1.4 - 8.5 \times 10^{-5} E_\eta(\infty) \quad (\eta \text{ in N s/m}^2 \text{ and } E_\eta \text{ in kJ/mol}) \quad (15.42)$$

Combination of (15.41), (15.42) and (15.39) gives:

$$\log \eta_{cr}(1.2T_g) = -1.4 - 8.5 \times 10^{-5} E_\eta(\infty) + 0.052 \frac{E_\eta(\infty)}{T_g} \quad (15.43)$$

¹ Such a correlation is often found in related activated mass transfer processes (diffusion, chemisorption, etc.).

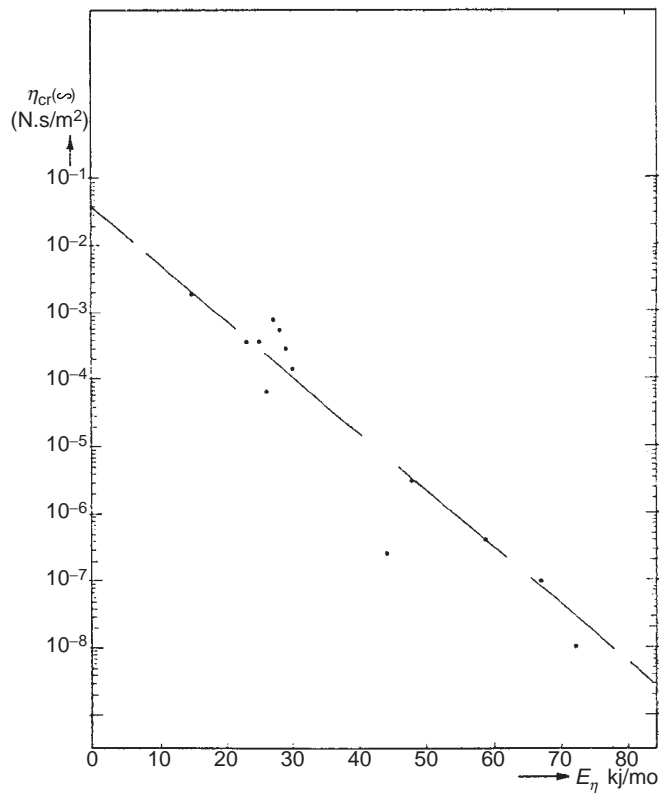


FIG. 15.8 $\eta_{cr}(\infty)$ as a function of E_η .

or

$$\log \eta_{cr}(1.2T_g) = E_\eta(\infty) \left(\frac{0.052 - 8.5 \times 10^{-5} T_g}{T_g} \right) - 1.4 \quad (15.44)$$

As can be seen from Table 15.6, there exists a general correlation between E_η and polymer structure. A low value of E_η , 25 kJ/mol, is found for an unbranched polymethylene chain. About the same value is found for linear polymers, containing methylene groups and oxygen or double bonds. For linear polymers, containing other groups, E_η increases with increasing bulkiness of these groups.

Higher values of E_η are found for polymers containing side chains, and E_η increases with increasing length of the side chain.

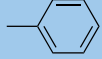
The activation energy of poly(dimethyl siloxane) is evidently much lower than the value to be expected for the corresponding carbon-containing polymer.

15.3.4. An additive function for the prediction of $e_\eta(\infty)$

It was found (Van Krevelen and Hoflyzer, 1976) that the function

$$H_\eta = M [E_\eta(\infty)]^{1/3} \text{ (dimension: gJ}^{1/3} \text{ mol}^{-4/3}\text{)}$$

TABLE 15.7 Group contributions to the molar viscosity-temperature function ($\text{g J}^{1/3}/\text{mol}^{4/3}$)

Group	$H_{\eta i}$	Group	$H_{\eta i}$
Bivalent		Monovalent	
$-\text{CH}_2-$	420	$-\text{CH}_3$	810
$-\text{CH}(\text{CH}_3)-$	1060		3350
$-\text{C}(\text{CH}_3)_2-$	1620		
$-\text{CH}(\text{C}_6\text{H}_5)-$	3600		
$-\text{CHCl}-$	2330	$-\text{Cl}$	2080
$-\text{O}-$	480	Trivalent	
$-\text{COO}-$	1450	$>\text{CH}-$	250
$-\text{OCOO}-$	3150	$=\text{CH}-$	380
$-\text{CONH}-$	1650	Tetravalent	
	3200	$>\text{C}<$	0
$-\text{Si}(\text{CH}_3)_2-$	1350	$>\text{C}=$	0
		$>\text{Si}<$	-270
		Extra effect of side chain, per $-\text{CH}_2-$ or other bivalent group	250

has additive properties. Table 15.7 gives the group contributions to this function, and the last column of Table 15.6 gives the $E_{\eta}(\infty)$ values as calculated by means of these increments. The correlation is very satisfactory. The function H_{η} will be called *molar viscosity-temperature gradient*.

Table 15.7 enables the prediction of E_{η} for other polymers. Inaccuracies in the prediction of E_{η} are reduced by the compensative character of Eq. (15.39).

Example 15.1

Estimate the Newtonian viscosity of poly(ethylene terephthalate) with a molecular mass $M_w = 4.7 \times 10^4$ at a temperature of 280°C ; $T_g = 70^\circ\text{C} = 343\text{ K}$.

Solution

1. According to Table 15.7 the H_{η} function of PETP is calculated as follows

$$\begin{array}{ll} -\text{C}_6\text{H}_4- & 3200 \\ 2-\text{COO}- & 2900 \\ 2-\text{CH}_2- & 840 \\ H_{\eta} & = 6940 \text{ g J}^{1/3}/\text{mol}^{4/3} \end{array}$$

Since $\mathbf{M} = 192 \text{ g/mol}$ we find

$$E_{\eta}(\infty) = \left(\frac{H_{\eta}}{\mathbf{M}} \right)^3 = \left(\frac{6940}{192} \right)^3 = 4.7 \times 10^4 \text{ J/mol}$$

2. Substitution in Eq. (15.44) gives:

$$\log \eta_{\text{cr}}(1.2T_g) = 4.7 \times 10^4 \left(\frac{0.052 - 8.5 \times 10^{-5} \times 343}{343} \right) - 1.4 = 1.7$$

3. According to Eq. (15.39) we get:

$$A = \frac{0.4343 \times 4.7 \times 10^4}{8.3 \times 343} = 7.2$$

4. In Fig. 15.7, the curve for $A = 7.2$ runs close to that for $A = 7$. At $T_g/T = 343/553 = 0.62$, interpolation gives

$$\log \frac{\eta_{\text{cr}}(T)}{\eta_{\text{cr}}(1.2T_g)} = -2.7$$

$$\text{So } \log \eta_{\text{cr}}(553) = 1.7 - 2.7 = -1.0.$$

5. The critical molar mass M_{cr} of PETP is 6000. So

$$\log(M_w/M_{\text{cr}}) = \log(4.7 \times 10^4 / 6 \times 10^3) = 0.89.$$

According to Eq. (15.31)

$$\log \eta_o(553) = \log \eta_{\text{cr}}(553) + 3.4 \log(M_w/M_{\text{cr}}) = -1 + 3.4 \times 0.89 = 2(\text{N s/m}^2)$$

This is in fair agreement with the experimental value as determined by Gregory (1972), viz. $\log \eta_{\text{cr}}(553) = 2.54 \text{ N s/m}^2$.

15.3.5. Effect of hydrostatic pressure on viscosity

Just as for liquids of low molecular mass, the viscosity of polymers increases with the hydrostatic pressure. The *pressure coefficient of viscosity*, β_p is defined as

$$\beta_p = \frac{\partial \ln \eta}{\partial p} = \frac{1}{\eta} \frac{\partial \eta}{\partial p} \quad (15.45)$$

Experimental data of β_p for polymers are scarce; available data are mentioned in Table 15.8. In principle, for a prediction of β_p , the following equation that can be derived from thermodynamics, might be used

$$\frac{\beta_p}{\beta_T} \approx -\frac{\kappa}{\alpha} \quad (15.46)$$

where κ = compressibility; α = thermal expansion coefficient and the *temperature dependence of viscosity* is defined as

$$\beta_T = \frac{\partial \ln \eta}{\partial T} = \frac{1}{\eta} \frac{\partial \eta}{\partial T}$$

However, as a rule the thermodynamic data for the calculation of the quotient κ/α are not readily available. In this case, the average value of the β_p/β_T ratio of Table 15.8 can be used.

TABLE 15.8 The pressure coefficient of viscosity

Polymer	T (°C)	$\beta_P (10^{-8} \text{ m}^2/\text{N})$	$\beta_T (\text{K}^{-1})$	$-\beta_P/\beta_T (10^{-7} \text{ m}^2 \text{ K}/\text{N})$	References
Polyethylene	190	1.4	-0.028	5.0	Westover (1961)
Polyethylene LD	210	1.43	-0.027	5.3	Cogswell and McGowan (1972)
Polyethylene HD	170	0.68	-0.025	2.7	Cogswell and McGowan (1972)
Polypropylene	210	1.50	-0.028	5.4	Cogswell and McGowan (1972)
Polystyrene	165	4.3	-0.078	5.5	Hellwege et al. (1967)
Polystyrene	190	3.5	-0.103	3.4	Cogswell and McGowan (1972)
Poly(methyl methacrylate)	235	2.14	-0.057	3.8	Cogswell and McGowan (1972)
Polycarbonate	270	2.35	-0.058	4.1	Cogswell and McGowan (1972)
Poly(dimethyl siloxane)	40	0.73	-0.018	4.0	Holzmüller and Dinter (1960)
Average				4.3 ± 0.9	

$$\frac{\beta_P}{\beta_T} = 4 \times 10^{-7} \text{ K m}^2/\text{N} \quad (15.47)$$

So

$$\frac{\partial \ln \eta}{\partial p} \approx -4 \times 10^{-7} \frac{\partial \ln \eta}{\partial T} \quad (15.48)$$

or

$$\frac{\Delta \ln \eta}{\Delta p(\text{bar})} \approx -0.04 \frac{\Delta \ln \eta}{\Delta T} \quad (15.49)$$

This means that a pressure increase of 1000 bar has about the same effect as a temperature decrease of 40 °C.

15.4. NON-NEWTONIAN SHEAR VISCOSITY AND FIRST NORMAL STRESS COEFFICIENT OF POLYMER MELTS

15.4.1. Viscosity as a function of shear rate

The most obvious viscoelastic phenomenon in polymer melts is the decrease of viscosity with increasing shear rate. This decrease may amount to several decades. At the same time, elastic behaviour may be observed.

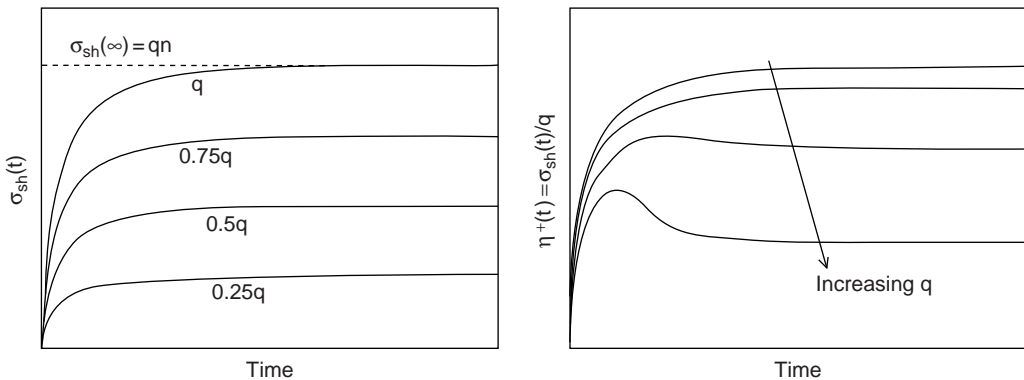


FIG. 15.9 (left) Increase of shear stress after starting steady shear flow at zero time for constant shear rate in the Newtonian region. (right) Time dependent shear viscosity, $\eta^+(t)$ from Newtonian to non-Newtonian behaviour.

Upon starting a steady shear flow with constant shear rate $\dot{\gamma}_0 = q$ the shear stress for a Maxwell element increases gradually in time to a steady state value ηq according to (see Chap. 13)

$$\sigma_{sh}(t) = \eta q [1 - \exp(-t/\tau)] \quad (15.50)$$

This, of course, is not the time dependence of shear stress upon starting a steady shear flow of a polymer melt, but it shows that the stress increases fast and then slows down reaching a steady state value. It also shows that upon starting such a flow with a shear rate two times as high that the shear stress also increases by a factor of 2. As long as this linearity exists in polymers melts, as shown schematically in Fig. 15.9 (left), the viscosity has a constant value. However, in polymer melts the stress does not increase linearly with shear rate if the shear rate is not low anymore, but it slows down and the viscosity decreases accordingly. For high shear rates, there is even a so-called stress overshoot, after which the shear stress decreases with time before reaching a steady state value. This is demonstrated in Fig. 15.9 (right). Accordingly, the viscosity decreases in the same way. In Fig. 15.9 $\eta^+(t)$, which is defined as

$$\eta^+(t) \equiv \sigma_{sh}(t)/q \quad (15.51)$$

is plotted against time for various increasing values of shear rate. It shows the overshoot at high shear rates and the shear thinning behaviour.

A number of empirical equations have been proposed to describe the influence of shear rate on viscosity. The most popular equation represents the so-called power law formulated by Ostwald (1925) and De Waele (1923):

$$\sigma_{sh} = K\dot{\gamma}^n \quad \text{or} \quad \eta = K\dot{\gamma}^{n-1} \quad (15.52)$$

In addition, the viscosity behaviour of many polymers follows the power law. In many cases, the power law index n is only constant over a few decades in the shear rate and in general, decreases with increasing shear rate. Table 15.9 gives this extreme decrease in n -values for some typical polymers.

In the shear range of polymer processing the power law is a good approximation, but not in the low shear rate range. For this reason a better approximation is *Spriggs' truncated power law model law* (Spriggs, 1965):

TABLE 15.9 Values of power-law index, n for six materials

Shear rate (s^{-1})	Poly(methyl methacrylate) 230 °C	Acetal copolymer 200 °C	Nylon 6,6 285 °C	Propylene–ethylene copolymer 230 °C	Low-density polyethylene 170 °C	Unplasticised PVC 150 °C
10 ⁻¹	—	—	—	0.93	0.7	—
1	1.00	1.00	—	0.66	0.44	—
10	0.82	1.00	0.96	0.46	0.32	0.62
10 ²	0.46	0.80	0.91	0.34	0.26	0.55
10 ³	0.22	0.42	0.71	0.19	—	0.47
10 ⁴	0.18	0.18	0.40	0.15	—	—
10 ⁵	—	—	0.28	—	—	—

After P.C. Powell (1974).

$$\eta(\dot{\gamma}) = \eta_o, \quad \text{for } \dot{\gamma} \leq \dot{\gamma}_o \\ \eta(\dot{\gamma}) = \eta_o (\dot{\gamma}/\dot{\gamma}_o)^{n-1}, \quad \text{for } \dot{\gamma} \geq \dot{\gamma}_o \quad (15.53)$$

where $\dot{\gamma}_o$ is equal to the shear rate where shear thinning starts.

A number of other power law equations have been proposed that predict an approach to constant viscosity at low shear rates. Cross (1965, 1968) formulated a three-parameter model:

$$\eta(\dot{\gamma}) = \frac{\eta_o}{1 + (\tau\dot{\gamma})^m} \quad (15.54)$$

In addition, Carreau (1969) proposed the following three-parameter model:

$$\eta(\dot{\gamma}) = \eta_o [1 + (\tau\dot{\gamma})^2]^{(n-1)/2} \quad (15.55)$$

In both models, τ is a time constant that determines the position of the transition from Newtonian to non-Newtonian behaviour.

For a better fit of experimental data Yasuda, Armstrong and Cohen (1981) added a fourth parameter:

$$\eta(\dot{\gamma}) = \eta_o [1 + (\tau\dot{\gamma})^a]^{(n-1)/a} \quad (15.56)$$

The Ellis model is in general given as a shear stress dependent viscosity $\eta(\sigma)$:

$$\eta(\sigma) = \eta_o \frac{1}{1 + (\sigma/\sigma_{1/2})^{n-1}} \quad (15.57)$$

where $\sigma_{1/2}$ is the stress where the viscosity is equal to $1/2\eta_o$ and n the slope of the curve $\log[(\eta/\eta_o) - 1]$ vs. $\log \sigma_{1/2}$.

The advantage of these models is that they predict a Newtonian plateau at low shear rates and thus at low shear stresses. We will see back these models in Chap. 16 where an extra term η_∞ is added to the equations to account for the viscosity of polymer solutions at high shear rates. At high shear rates the limiting slopes at high shear rates in $\log \eta$ vs. $\log \dot{\gamma}$ curves are for the Cross, the Carreau and the Yasuda et al. models $-m$, $(n-1)$ and $(n-1)$, respectively.

Other empirical equations have been used by Ferry (1942):

$$\eta = \frac{\eta_o}{1 + \sigma_{sh}/G_i} \quad (15.58)$$

and by Spencer and Dillon (1949):

$$\eta = \eta_0 \exp(-\sigma_{sh}/b) \quad (15.59)$$

In these equations K , n , G , and b are constants.

All these empirical equations have a limited applicability, and the constants involved have different values for different polymer samples.

In this chapter a general empirical correlation of rheological properties of polymer melts will be given. The form of this correlation is based on theoretical interpretations of the decrease of viscosity with increasing rate of shear. The pioneer in this field has been Bueche (1962), who based his derivations on a simplified model of polymer structure. A more intricate theory, which is often cited, is that of Greassley (1967). For details of these models, the reader is referred to the literature. In the discussion of the extensional viscosity of polymer melts (Sect. 15.5) we will also meet some integral rheological constitutive equations, that also are able to describe the shear thinning behaviour of polymer melts.

One important aspect of polymer structure should be mentioned here, however, viz. the very important role of very long polymer molecules in the viscoelastic behaviour. Accordingly, the viscoelastic phenomena are also highly dependent on the molecular mass distribution.

15.4.2. Rheological quantities and their interrelations

The viscoelastic quantities η , γ_e , G , Ψ_1 and τ were defined at the beginning of this chapter. For a system with *only one relaxation time*, e.g. for a Maxwell element, the following interrelations exist between these rheological quantities:

$$\begin{aligned} \eta &= G\tau = \frac{\Psi_1}{2\tau} = (\gamma_2\Psi_1 G)^{1/2}, \quad G = \frac{\eta}{\tau} = \frac{2\eta^2}{\Psi_1} = \frac{\Psi_1}{2\tau^2} \\ \Psi_1 &= 2\eta\tau = 2G\tau^2 = \frac{2\eta^2}{G}, \quad \tau = \frac{\eta}{G} = \frac{\Psi_1}{2\eta} = \left(\frac{\Psi_1}{2G}\right)^{1/2} \\ \gamma_r &= \dot{\gamma}\tau = \frac{\dot{\gamma}\eta}{G} = \frac{\dot{\gamma}\Psi_1}{2\eta} = \left(\frac{\dot{\gamma}^2\Psi_1}{2G}\right)^{1/2} \end{aligned} \quad (15.60)$$

15.4.3. Lodge's rheological constitutive equation

The reality, however, is not as simple as that. There are several possibilities to describe viscosity, η , and first normal stress difference coefficient, Ψ_1 . The first one originates from Lodge's rheological constitutive equation (Lodge 1964) for polymer melts and the second one from substitution of a sum of N Maxwell elements, the so-called Maxwell–Wiechert model (see Chap. 13), in this equation (see General references: Te Nijenhuis, 2005).

15.4.3.1. Transient properties

When Lodge's constitutive equation is applied to shear flow, that starts at time $t = 0$ with constant shear rate $\dot{\gamma}$, then the following equations are found for the shear stress T_{21} and the first normal stress difference $T_{11} - T_{22}$

$$T_{21}(t) = q \int_0^t G(t-s)ds \rightarrow q \sum_{i=1}^N G_i \tau_i [1 - \exp(-t/\tau_i)] \quad (15.61)$$

and

$$N_1(t) = (T_{11} - T_{22})(t) = 2q^2 \int_0^t sG(t-s)ds \rightarrow 2q^2 \sum_{i=1}^N G_i \tau_i^2 [1 - (1+t/\tau_i)\exp(-t/\tau_i)] \quad (15.62)$$

The arrows in these equations mean that in the derived equations, for $G(t-s)$ a sum of Maxwell elements is substituted:

$$G(t-s) = \sum_{i=1}^N G_i \exp[(t-s)/\tau_i] \quad (15.63)$$

These equations show that both the shear stress and the first normal stress difference gradually increase from zero to a steady state value for $t \rightarrow \infty$. This results in values for the viscosity and the first normal stress coefficient equal to

$$\frac{T_{21}}{q} = \frac{\sigma_{sh}}{q} = \eta = \int_0^\infty G(t)dt \rightarrow \sum_{i=1}^N G_i \tau_i \quad (15.64)$$

$$\frac{T_{11} - T_{22}}{q^2} = \frac{N_1}{q^2} = \Psi_1 = 2 \int_0^\infty tG(t)dt \rightarrow 2 \sum_{i=1}^N G_i \tau_i^2 \quad (15.65)$$

It is clear that the relationship between η and Ψ_1 is not as simple as it is in Eqs. (15.60).

From Eqs. (15.61) and (15.62) it follows that the shear stress and the first normal stress difference gradually increase from 0 to the steady state value. In this respect sometimes the following definitions are suggested for the transient values of viscosity and first normal stress coefficient

$$\eta^+(t) \equiv \frac{T_{21}(t)}{q} = \int_0^t G(t-s)ds \rightarrow \sum_{i=1}^N G_i \tau_i [1 - \exp(-t/\tau_i)] \quad (15.66)$$

$$\Psi_1^+(t) \equiv \frac{N_1(t)}{q^2} = 2 \int_0^t sG(t-s)ds \rightarrow 2 \sum_{i=1}^N G_i \tau_i^2 [1 - (1+t/\tau_i)\exp(-t/\tau_i)] \quad (15.67)$$

An important conclusion is that *it is clear that Lodge's constitutive equation is not able to describe non-Newtonian behaviour in steady shear, because both the viscosity and the first normal stress coefficient appear to be no functions of the shear rate.*

15.4.3.2. Oscillatory flow: Coleman–Markovitz relationship

It is also possible to calculate the dynamic moduli $G'(\omega)$ and $G''(\omega)$ with Lodge's constitutive equation. This results in

$$G'(\omega) = \omega \int_0^\infty G(t) \sin(\omega t) dt \rightarrow \sum_{i=1}^N G_i \frac{\omega^2 \tau_i^2}{1 + \omega^2 \tau_i^2} \quad (15.68)$$

$$G''(\omega) = \omega \int_0^\infty G(t) \cos(\omega t) dt \rightarrow \sum_{i=1}^N G_i \frac{\omega \tau_i}{1 + \omega^2 \tau_i^2} \quad (15.69)$$

Very interesting is the value of both dynamic moduli at low frequencies, and comparing them with Eqs. (15.64) and (15.65):

$$\lim_{\omega \rightarrow 0; (\gamma_o \rightarrow 0)} \frac{G'}{\omega^2} = \int_0^\infty t G(t) dt = \lim_{t \rightarrow \infty; (q \rightarrow 0)} \frac{N_1}{2q^2} \rightarrow \sum_{i=1}^N G_i \tau_i^2 = \eta_0 \Psi_{1,0} \quad (15.70)$$

$$\lim_{\omega \rightarrow 0; (\gamma_o \rightarrow 0)} \frac{G''}{\omega} = \int_0^\infty G(t) dt = \lim_{t \rightarrow \infty; (q \rightarrow 0)} \frac{T_{21}}{q} \rightarrow \sum_{i=1}^N G_i \tau_i = \eta_0 \quad (15.71)$$

The conclusion is that Lodge's rheological constitutive equation results in relationships between steady shear and oscillatory experiments. The limits $\gamma_o \rightarrow 0$ (i.e. small deformation amplitudes in oscillatory flow) and $q \rightarrow 0$ (i.e. small shear rates) do not come from Lodge's equation but they are in agreement with practice. These interrelations between sinusoidal shear deformations and steady shear flow are called the *relationships of Coleman and Markovitz*.

The dynamic moduli can also be defined in the complex plane:

$$\gamma^* = \gamma_o \exp(i\omega t), \quad \sigma^* = \sigma_o \exp[i(\omega t + \delta)] \quad \text{and} \quad G^* \equiv \frac{\sigma^*}{\gamma^*} = \frac{\sigma_o}{\gamma_o} \exp(i\delta) = |G^*| \exp(i\delta) \quad (15.72)$$

where:

$$G^* = G' + iG'' \quad \text{and} \quad i = \sqrt{-1} \quad (15.73)$$

The complex viscosity is defined as:

$$\eta^* \equiv \frac{\sigma^*}{d\gamma^*/dt} = \frac{\sigma^*}{-i\omega\gamma^*} = -\frac{iG^*}{\omega} = \frac{G''}{\omega} - i\frac{G'}{\omega} = \eta' - i\eta'' \quad (15.74)$$

with:

$$\eta' = \frac{G''}{\omega} \quad \text{and} \quad \eta'' = \frac{G'}{\omega} \quad (15.75)$$

The absolute values of the complex modulus and viscosity are:

$$|G^*| = \sqrt{G'^2 + G''^2} \quad \text{and} \quad |\eta^*| = \sqrt{\eta'^2 + \eta''^2} = \frac{|G^*|}{\omega} \quad (15.76)$$

In Fig. 15.10 the complex material properties are demonstrated in the complex plane for $\omega = 1/2$ rad.

15.4.3.3. Recoverable shear strain during steady shear flow

In Chap. 13 the creep recovery of a Burgers element was discussed and from Fig. 13.18 it becomes clear that the recoverable shear creep strain is in the present terms equal to

$$\gamma_{\text{rec,cr}}(t) = \sigma_{\text{sh}} J_e(t) = \sigma_{\text{sh}} J_e^0 [1 - \exp(-t/\tau)] \quad (15.77)$$

According to a thorough calculation by Janeschitz-Kriegl (General references, 1983, Appendix A3) the elastic shear compliance is equal to

$$J_e^0 = \frac{1}{2} \Psi_{1,0} / \eta_o^2 = \lim_{\omega \rightarrow 0} \frac{G'(\omega)}{(G''(\omega))^2} \rightarrow \sum_{i=1}^N G_i \tau_i^2 / \left(\left(\sum_{i=1}^N G_i \tau_i \right)^2 \right) = \langle \tau \rangle / \eta_o \quad (15.78)$$

where the average relaxation time is defined as

$$\langle \tau \rangle = \sum_{i=1}^N G_i \tau_i^2 / \sum_{i=1}^N G_i \tau_i = \frac{\frac{1}{2} \Psi_{1,0}}{\eta_o} \quad (15.79)$$

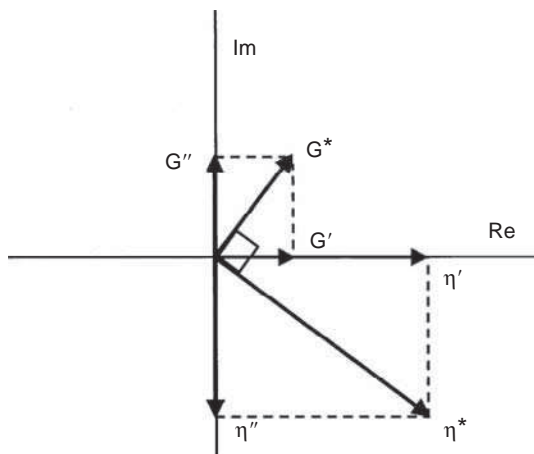


FIG. 15.10 The dynamic moduli and viscosities in the complex plane for $\omega=1/2$.

so that from Eq. (15.77) it follows

$$\gamma_{\text{rec,cr}} \equiv \gamma_{\text{rec,cr}}(\infty) = \sigma_{\text{sh}} J_e^0 \rightarrow q\langle\tau\rangle \quad (15.80)$$

During steady shear flow the strain $\gamma(t)$ is composed of irrecoverable viscous strain, $\gamma_{\text{vis}}(t)$ and elastic or recoverable strain, $\gamma_{\text{rec}}(t)$:

$$\gamma(t) = \gamma_{\text{vis}}(t) + \gamma_{\text{rec}}(t) \quad (15.81)$$

A thorough solution of this equation, making use of the Lodge equation, was again presented by Janeschitz-Kriegl (General references, 1983, Appendix A3), with as the result

$$\gamma_{\text{rec}}(t) = qt \left(1 - \frac{\eta^+(t)}{\eta_o}\right) + \frac{q\Psi_1^+(t)}{2\eta_o} \quad (15.82)$$

In the steady state it becomes

$$\gamma_{\text{rec}} \equiv \gamma_{\text{rec}}(\infty) = \frac{1}{2}\Psi_{1,0}/(q\eta_o) \rightarrow q \sum_{i=1}^N G_i \tau_i^2 / \sum_{i=1}^N G_i \tau_i = q\langle\tau\rangle \quad (15.83)$$

which is equal to $\gamma_{\text{rec,cr}}$ in Eq. (15.80)

When the shear flow is stopped in the steady state, then the time dependent strain is given by

$$\gamma(t \geq t_1) = qt_1 - \frac{\frac{1}{2}q\Psi_1^+(t')}{\eta_o} \quad (15.84)$$

where $t' = t - t_1$.

For $t \gg t_1$ the remaining shear deformation is

$$\gamma(t \geq t_1) = qt_1 - \frac{\frac{1}{2}\Psi_{1,0}}{q\eta_o} \quad (15.85)$$

This recoverable shear strain shows up when the flow of a polymer melt in a capillary rheometer is suddenly stopped. The material that has just left the capillary rheometer will clearly recover to a certain extent, in principle equal to $\frac{1}{2}\Psi_{1,0}/(q\eta_o)$. In Fig. 15.11 the various strains are shown after starting a steady shear flow at time $t = 0$ and stopping it at time t_1 .

15.4.4. Experimental methods

A number of experimental techniques have been developed for measuring the viscosity and the first (and second) normal stress coefficient. In Table 15.2 a survey of these methods has already been given.

In practice it appears that in a figure where $\log \eta$ is plotted vs. $\log q$ and $\log \eta'$ vs. $\log \omega$, both lines coincide not only in the linear region but also, to some extent, in the region where both viscosities decrease. The agreement is even better if $\log \eta^*$ instead of $\log \eta'$ is plotted vs. $\log \omega$. This is demonstrated for polystyrene in Figs. 15.12 and 15.13

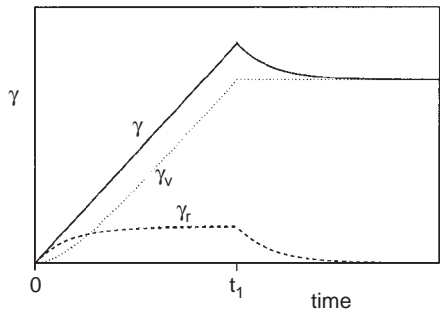


FIG. 15.11 Total, viscous and recoverable (i.e. elastic) deformations, γ , γ_{vis} and γ_{rec} , respectively, during steady shear flow and recovery after cessation of flow at time t_1 .

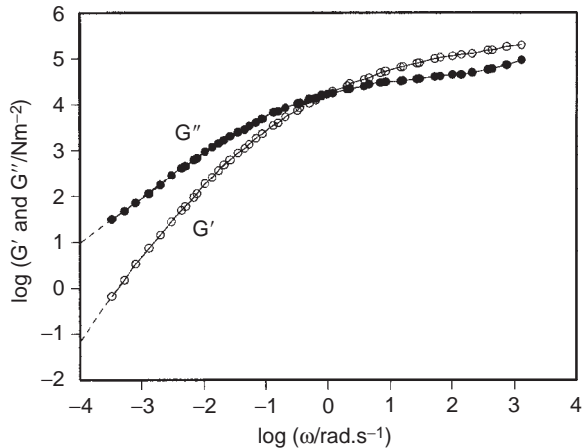


FIG. 15.12 Double logarithmic plot of the dynamic shear moduli G' and G'' vs. angular frequency ω for Polystyrene Hostyren N4000V, measured at temperatures varying from 140 to 206 °C and reduced to the reference temperature of 170 °C. After Gortemaker (1976) and Gortemaker et al. (1976).

(Gortemaker (et al.), 1976). In Fig. 15.12, the dynamic moduli are plotted vs. reduced angular frequency. From these results the complex viscosity η^* and its components η' and η'' were calculated. They were plotted vs angular frequency in Fig. 15.13, where also experimental values of the steady shear viscosity are shown. The agreement between $\eta(q)$ and $\eta^*(\omega)$ is clearly visible. This relationship between steady shear and sinusoidal experiments

$$\eta(\dot{\gamma}) \approx |\eta^*(\omega)|_{\omega=\dot{\gamma}} \quad (15.86)$$

is called the *Cox-Merz relationship* (Cox and Merz, 1958). This rule was confirmed by many other investigators. From Fig. 15.13 it appears that for low shear rates and angular frequencies η^* is primarily determined by η' , whereas at higher shear rates and angular frequencies η^* is primarily determined by η'' . It seems strange that a linear oscillatory property, $\eta^*(\omega)$ can be compared with a non-linear transient property $\eta(q)$.

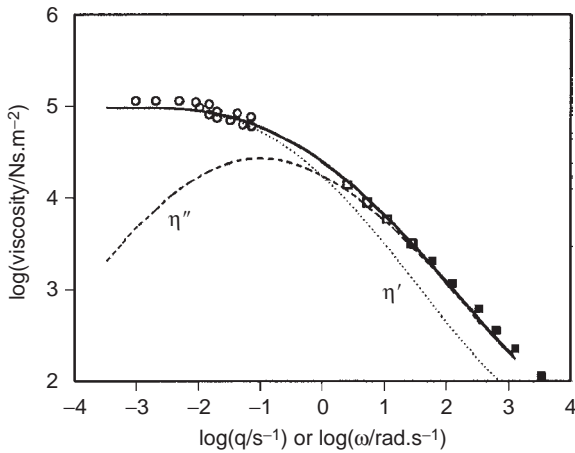


FIG. 15.13 Non-Newtonian shear viscosity $\eta(q)$ at 170 °C vs. shear rate, q , for the polystyrene mentioned in Fig. 15.12, measured in a cone and plate rheometer (\circ) and in a capillary rheometer (\square and ■) and the dynamic and complex viscosities, $\eta'(\omega)$ (dotted line), $\eta''(\omega)$ (dashed line) and $|\eta^*(\omega)|$ (full line), respectively, as functions of angular frequency, as calculated from Fig. 15.12. From Gortemaker (1976) and Gortemaker et al. (1976). Courtesy Springer Verlag.

Another method to calculate viscoelastic quantities uses measurements of flow birefringence (see Chap. 10). In these measurements, two quantities are determined as functions of the shear rate $\dot{\gamma}$: the birefringence Δn and the extinction angle χ . The following relationships exist with the stress tensor components:

$$2T_{21} = C_\sigma \Delta n \sin(2\chi) \quad (15.87)$$

$$N_1 = C_\sigma \Delta n \cos(2\chi) \quad (15.88)$$

where C_σ is the so-called stress-optical coefficient, the value of which depends on the nature of the polymer.

Even if the value of C_σ is not known beforehand, the normal stress component can be estimated by using the quotient of Eqs. (15.87) and (15.88):

$$N_1 = 2T_{21} \cot \chi \quad (15.89)$$

The (approximate) validity of Eq. (15.89) has been confirmed by experiments of Adamse et al. (1968) (see also Janeschitz-Kriegl, General References, 1968 and 1983).

15.4.5. Non-Newtonian viscosity and molecular weight c.q. molecular-weight distribution

In Fig. 15.14 the viscosity is schematically plotted vs. shear rate for the same kind of three polymers of different molecular weights and molecular-weight distributions. A and B are monodisperse polymers, whereas C is a polydisperse polymer. Their molecular weights are $M_{w,C} = M_A = 2M_B$. The zero shear viscosities of A and C are equal, whereas the zero shear viscosity of B is $2^{3.4} = 10$ times smaller. A high molecular weight gives rise to a stronger deviation from Newtonian behaviour than a low molecular weight, just as a broader molecular weight with respect of the high molecular weight. An example of the

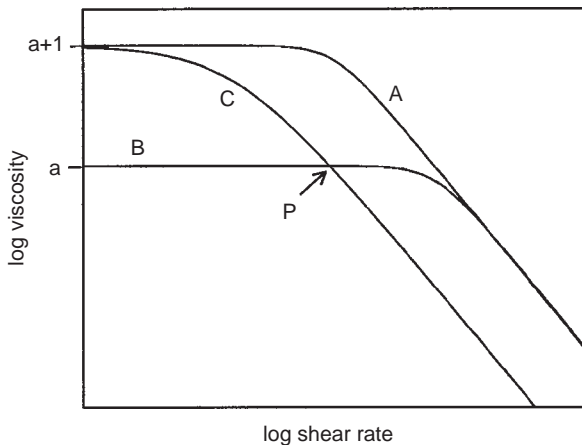


FIG. 15.14 Schematic representation of the shear rate dependence of the viscosities of polymers of the same kind, but of different molecular weights and molecular-weight distributions. (A, B): monodisperse polymers; (C) polydisperse polymer. Molecular weights: $M_{w,C} = M_A = 2M_B$. The symbols values a and $a + 1$ on the viscosity axis are introduced just to show that the zero shear viscosity of polymer A is ten times that of polymer B.

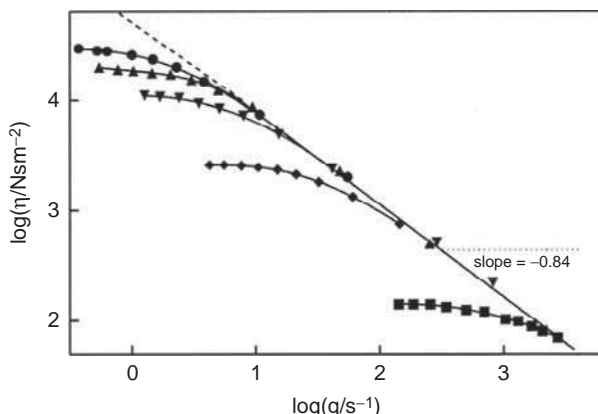


FIG. 15.15 Logarithmic plots of apparent viscosity vs. shear rate for "monodisperse" polystyrenes of different molecular weights (in kg/mol): (●) 242; (◆) 217; (■) 179; (▲) 117; (▼) 48.5. All data are reduced to 183 °C. The dashed line has a slope of -0.84 . From Stratton (1966). Courtesy Elsevier Science Publishers.

molecular weight dependence of the viscosity for a series of polystyrenes of narrow weight distributions is given in Fig. 15.15 (Stratton, 1966). In the high shear rate region, the viscosities of both monodisperse polymers coincide; the slope at high shear rates is equal to -0.84 , so that the power-law index is equal to -0.16 . Fig. 15.14 is a figure to show the difficulties that arise in the interpretation of so-called melt index measurements, used in application laboratories to characterise polymer samples. In a melt index instrument, a polymer melt is extruded at a specified temperature in a specified capillary and at a specified shear stress or volume flow rate. The amount of material in grams extruded in

a specified time is called the melt index. It is a measure for the viscosity of the molten polymer. If this point happens to be point P in Fig. 15.14 the melt index does not characterise the polymer adequately: it might be a low molecular weight monodisperse polymer or a high molecular weight polydisperse polymer. A second measurement at another shear rate would very useful to characterise the polymer much better.

15.4.6. Correlation of non-Newtonian shear data

It proved possible to correlate all the available data on viscoelastic shear quantities. The basis for this correlation has been laid by Bueche (1962) and by Vinogradov and Malkin (1964).

In order to elucidate the correlation method it may be recalled that the viscosity η approaches asymptotically to the constant value η_o with decreasing shear rate q . Similarly, the characteristic time τ approaches a constant value τ_o and the shear modulus G has a limiting value G_o at low shear rates. Bueche already proposed that the relationship between η and q be expressed in a dimensionless form by plotting η/η_o as a function of $q\tau_o$. According to Vinogradov, also the ratio τ/τ_o is a function of $q\tau_o$. If the zero shear rate viscosity and first normal stress are determined, then a time constant τ_o may be calculated with the aid of Eqs. (15.60). This time constant is sometimes used as relaxation time, in order to be able to produce general correlations between viscosity, shear modulus and recoverable shear strain as functions of shear rate.

The product $q\tau_o$ is sometimes called the Weissenberg number, We .

Vinogradov originally correlated with the product $q\eta_o$ instead of $q\tau_o$. The correlations given hold for steady-state shearing conditions. Some literature data are also available about the transient state at the start of a shearing experiment at constant shear rate $\dot{\gamma}$, for instance for the experiments of Meissner (1972) with low-density polyethylene.

During the transient period, the viscosity increases with time. For a correlation of the viscoelastic quantities two dimensionless groups are needed: $q\tau_o$ and τ_o/t . These correlations will not be discussed here.

In addition, for the correlation of dynamic viscoelastic shear quantities two dimensionless groups are needed: $\tau_o\omega$ and $\tau_o\omega\gamma_o$ as was shown by Vinogradov et al. (1970, 1971). γ_o is the amplitude of the imposed dynamic shear.

The relationship between η/η_o and $q\tau_o$ appears to be dependent on the molecular-weight distribution. As a first approximation, this influence may be taken into account by using the distribution factor $Q = \bar{M}_w/\bar{M}_n$ as a parameter. The available experimental data do not show an influence of the molecular-weight distribution on the relationship between τ/τ_o and $q\tau_o$. Consequently, the factor Q should also be used as a parameter in correlating the data on G/G_o as a function of $q\tau_o$.

Figs. 15.16–15.19 show the correlation between η/η_o , τ/τ_o , G/G_o , γ_r with $q\tau_o$, with Q as a parameter. For low shear rates ($\log q\tau_o < -0.5$ or $q\tau_o < 0.3$)

$$\eta/\eta_o = 1, \quad \tau/\tau_o = 1, \quad G/G_o = 1, \quad \gamma_r = q\tau_o = q \frac{\eta_o}{G_o} \quad (15.90)$$

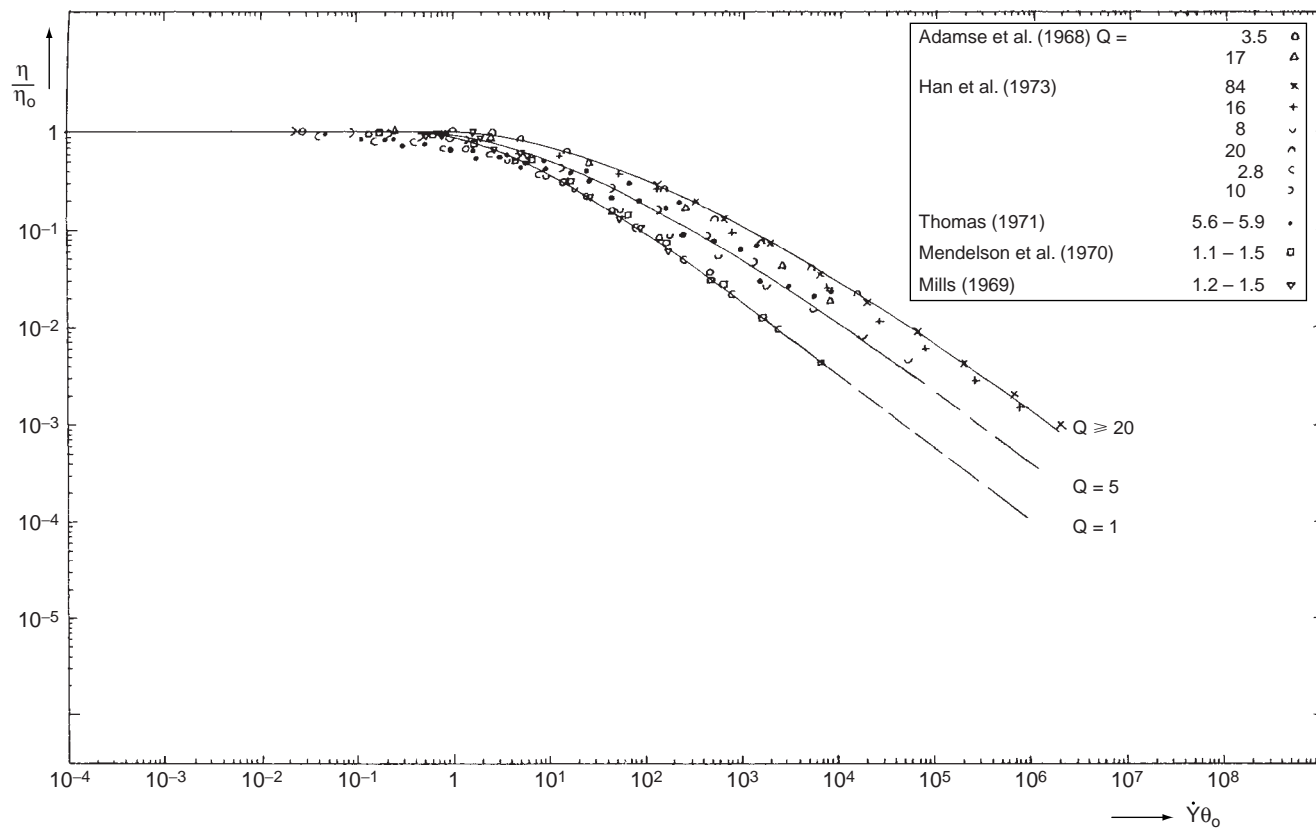


FIG. 15.16 η/η_0 as a function of $\dot{\gamma}\theta_0$.

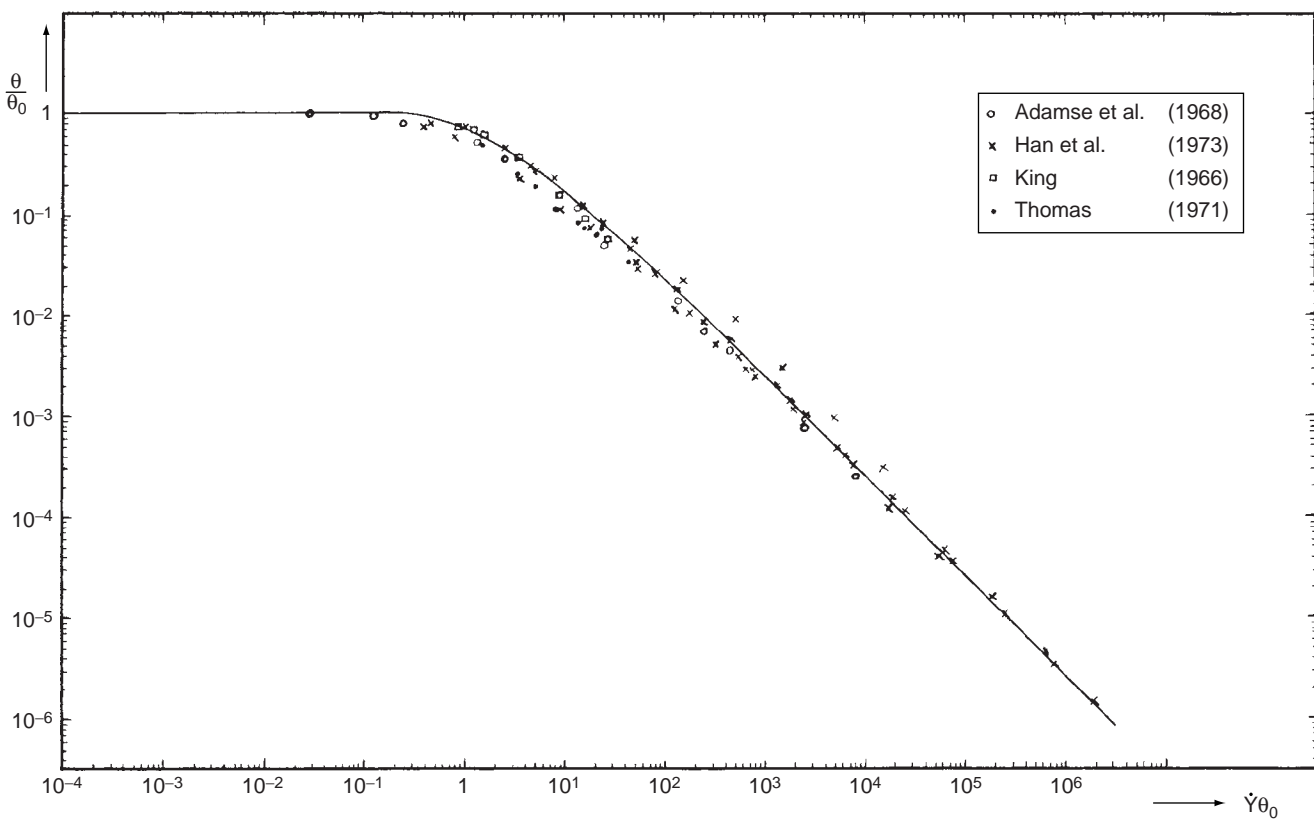


FIG. 15.17 τ/τ_0 as a function of $\dot{\gamma}\tau_0$.

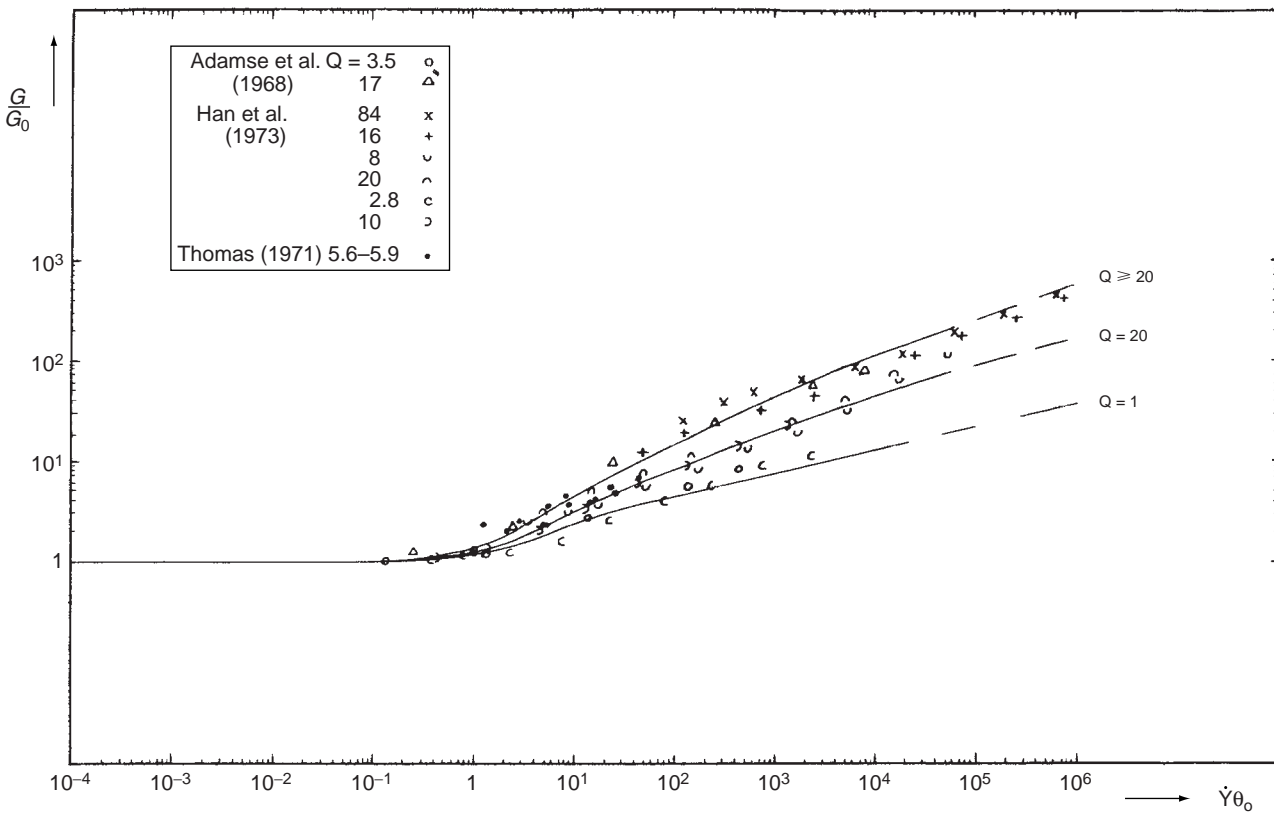


FIG. 15.18 G/G_0 as a function of $\dot{\gamma}\theta_0$.

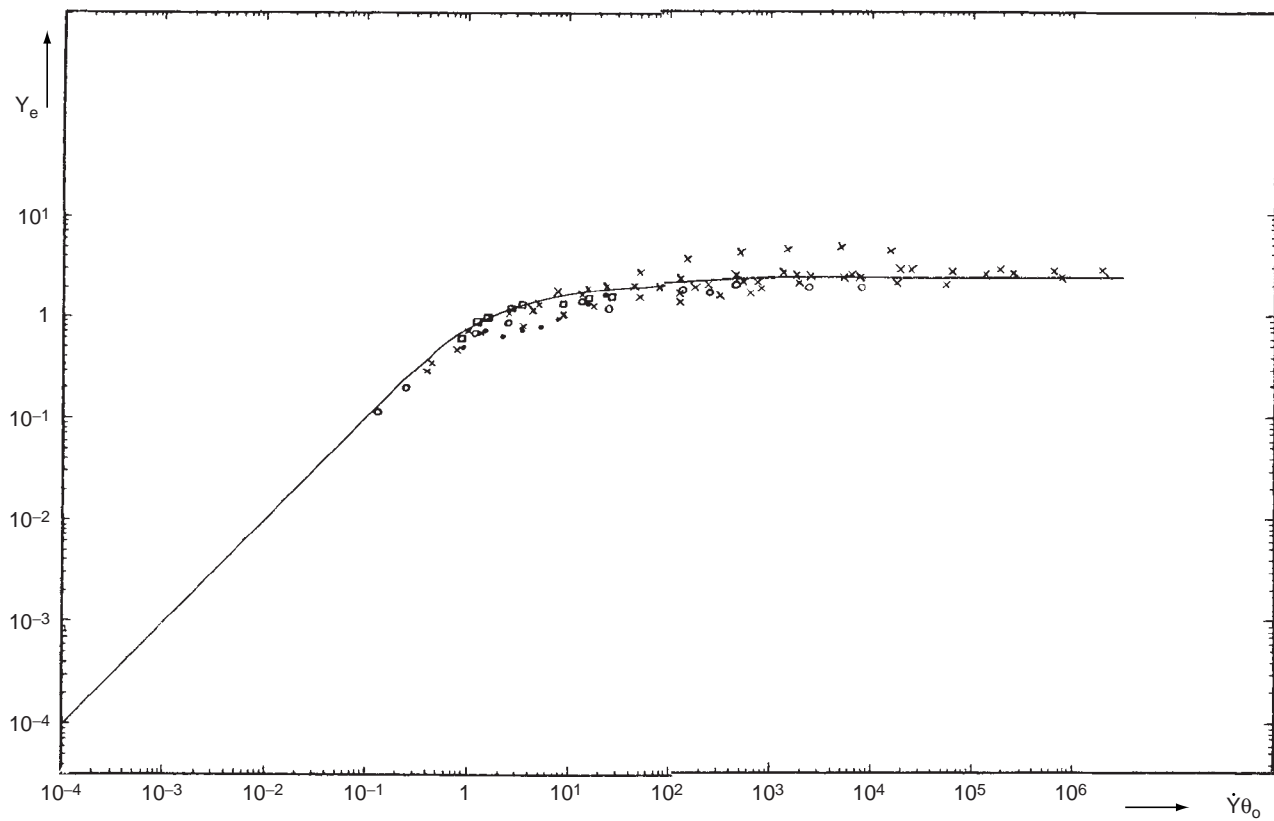


FIG. 15.19 γ_r as a function of $\gamma\tau_0$.

For high shear rates ($\log q\tau_o > 3$), the curves can be described by the following linear relationships

$$\begin{aligned}\log(\eta/\eta_o) &= 0.5 - 0.75 \log(q\tau_o) \quad (\text{for } Q = 1) \\ \log(\tau/\tau_o) &= 0.4 - \log(q\tau_o) \\ \log(G/G_o) &= 0.1 + 0.25 \log(q\tau_o) \quad (\text{for } Q = 1) \\ \log \gamma_r &= 0.4\end{aligned}\tag{15.91}$$

15.4.7. Prediction of viscosity as a function of shear rate

For many technical calculations a method for the prediction of polymer melt viscosity as a function of shear rate would be very valuable. A basis for this prediction forms Fig. 15.16, where η/η_o has been plotted as a function of $\dot{\gamma}\tau_o = q\tau_o$, with Q as a parameter. Obviously, η_o and τ_o should be known if η is to be calculated as a function of q .

A method for the prediction of η_o as a function of molecular mass and temperature has been given earlier in this chapter. There remains the prediction of the characteristic time constant τ_o .

Calculations with molecular structure models, as performed by Bueche, Rouse and others, in general based on bead spring models, predict that for monodisperse polymers the largest relaxation time is equal to

$$\tau_1 = \frac{6 \eta_o M}{\pi^2 \rho R T} = \frac{0.608 \eta_o M}{\rho R T}\tag{15.92}$$

Various authors have obtained this equation with slight differences in the term $6/\pi^2$. The available data on (nearly) monodisperse polymers seem to confirm these rules. For polydisperse polymers, however, the situation is more complicated. For a number of polydisperse polymer samples, experimental values of τ_1 can be found in the literature. These values of τ_1 are always larger than those calculated with Eq. (15.92), using M_w for the molecular mass:

A more direct prediction method uses a formal time constant τ_{1w}

$$\tau_{1w} = \frac{0.608 \eta_o M_w}{\rho R T}\tag{15.93}$$

Experimental values of η/η_o are plotted against the product $q\tau_{1w}$ with Q as a parameter. A graph of this type is shown in Fig. 15.20. This correlation, however, should be considered as a first approximation only. Some literature values show considerable deviations. This will at least partly be caused by large inaccuracies in the values of M_w .

An empirical method to cope with the effect of molecular-weight distribution was proposed by Van der Vegt (1964). He determined viscosities of several grades of polypropylenes with different M_w and MMD as a function of the shear stress σ_{sh} . A plot of η/η_o vs. the product $\tau_{vdv} = \tau_{1w}Q$ proved to give practically coinciding curves. This generalised curve has been reproduced in Fig. 15.21.

The results of Van der Vegt suggest that for polydisperse polymer melts the terminal relaxation time might be predicted by

$$\tau_{1,vdv} \approx \frac{0.608 \eta_o M_w}{\rho R T} Q\tag{15.94}$$

so that again η can be calculated with the aid of Fig. 15.21.

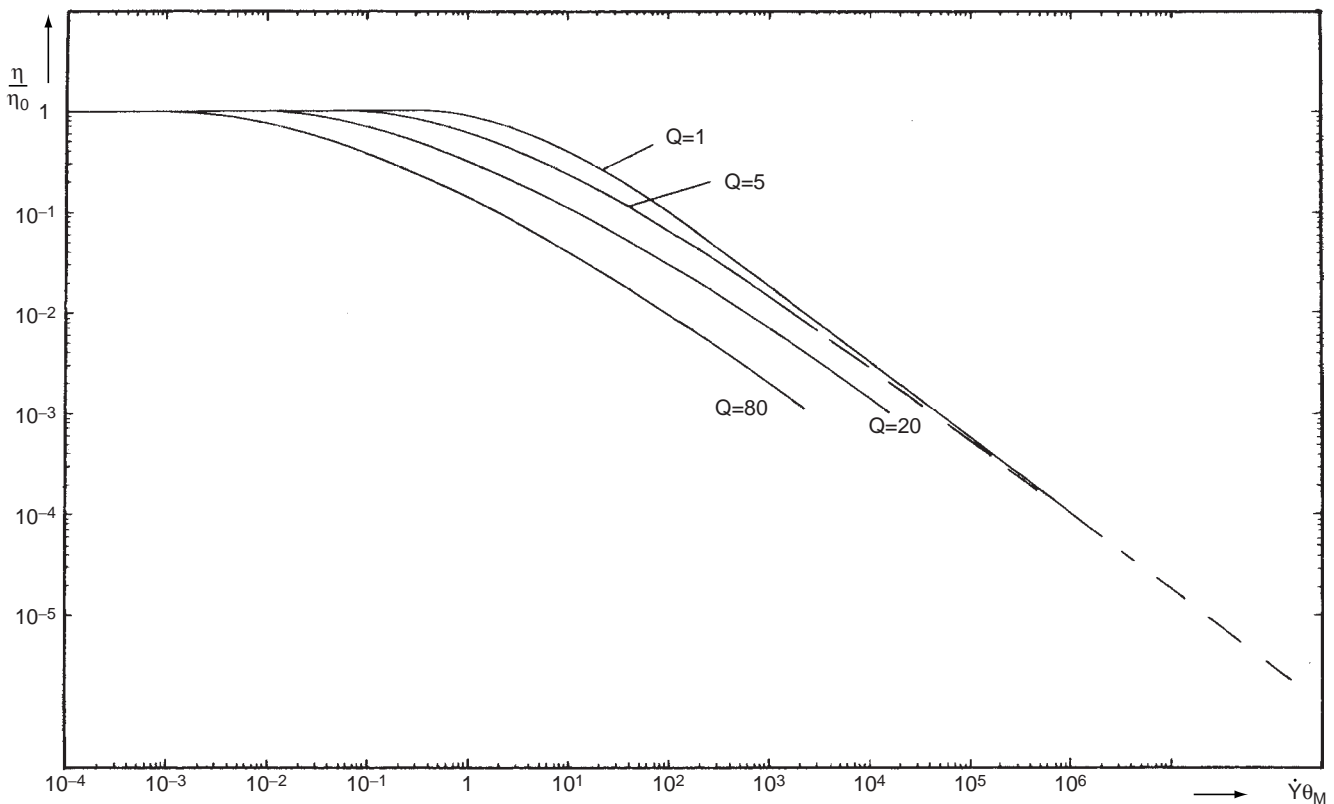


FIG. 15.20 η/η_0 as a function of $\dot{\gamma}\tau_M$.

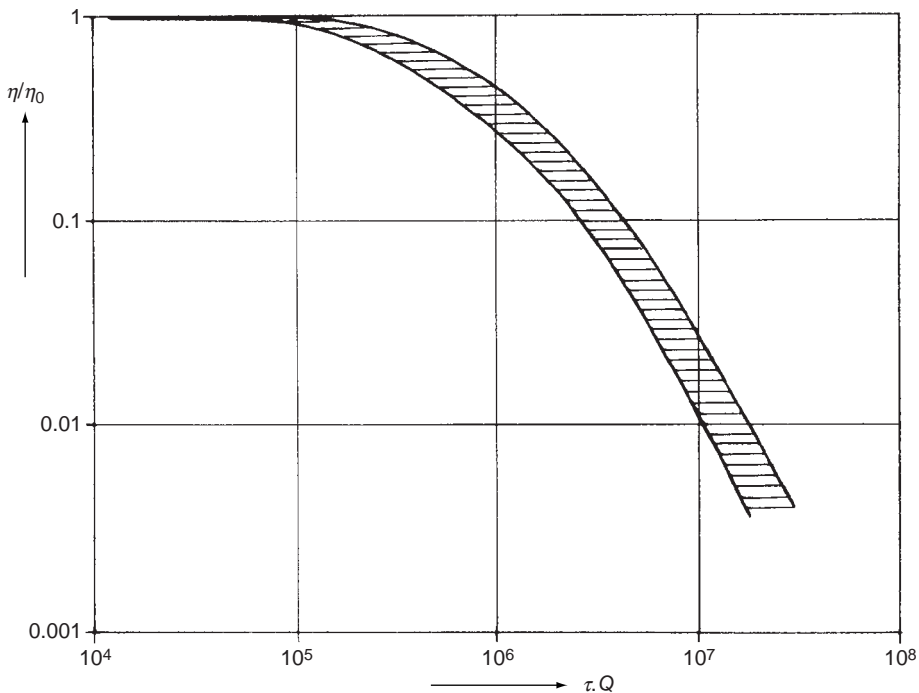


FIG. 15.21 Reduced viscosity of 33 polypropylene grades at 210 °C (Q between 3.5 and 25) (Van der Vegt, 1964).

It is interesting to note that an analogous result is obtained with a theoretical derivation of η as a function of q by Greassley (1967, 1970). This calculation can be used with an arbitrary molecular mass distribution. Calculations carried out with Greassley's equations by Cote and Shida (1973) showed that the parameter $Q = M_w/M_n$ was insufficient for a complete description of the effect of molecular mass distribution.

A serious drawback, however, is that the calculations are based on an unspecified time constant. According to experiments of Saeda (1973) this time constant does not correspond with τ_o or τ_M . This makes the method less suited for prediction purposes.

Stratton (1966) showed that coinciding curves of a series of monodisperse polystyrenes were obtained by plotting $\log(\eta/\eta_o)$ vs. $\log([q\eta_o M_w^{0.75}/(\rho RT)])$.

Example 15.2

Estimate the decrease in the viscosity of a poly(ethylene terephthalate) melt at a shear rate of 5000 s^{-1} . $M_w = 3.72 \times 10^4 = 37.2 \text{ kg/mol}$; $Q = 3.5$; $T = 553 \text{ K}$; $\eta_o = 156 \text{ N s/m}^2$; $\rho = 1160 \text{ kg/m}^3$.

Solution

According to Eq. (15.93):

$$\tau_{1,w} = \frac{0.6\eta_o M_w}{\rho RT} = \frac{0.6 \times 156 \times 37.2}{1160 \times 8.314 \times 553} = 6.6 \times 10^{-4} \text{ s}$$

$$q\tau_{1,w} = 5000 \times 6.6 \times 10^{-4} = 3.3$$

In Fig. 15.20 we read at $q\tau_{1,w} = 3.3$ and $Q = 3.5$: $\eta/\eta_o \approx 0.50$. So the estimate is $\eta \approx 80 \text{ N s/m}^2$ under the conditions given. The experimental value mentioned by Gregory (1972) is $\eta \approx 81.5 \text{ N s/m}^2$

15.4.8. Second Newtonian flow region

Up to now, two regions of shear flow have been discussed: Newtonian flow at low shear rates and non-Newtonian flow at high shear rates. In the first region, the viscosity is independent of the shear rate, while in the second region the viscosity decreases with increasing shear rate.

Under special experimental conditions a third region may be found at still higher shear rates. In this region, the viscosity becomes again independent of the shear rate. Therefore, this region is called second Newtonian flow region. Data on the existence of this region for polymer melts and on the role of molecular mass have been discussed by Porter et al. (1968). In practice, the second Newtonian flow region, if it indeed exists, will not often be encountered, as under normal conditions melt fracture will occur in the second flow region already.

15.5. EXTENSIONAL VISCOSITY OF POLYMER MELTS

15.5.1. Experimental techniques

Measurements of rheological quantities on the tensile deformation of polymer melts used to be extremely difficult and required the development of special techniques.

The usual shear measurements on polymer melts are performed as steady-state experiments in which a stationary state of shear deformation is maintained. A steady-state experiment on tensile deformation, however, means an imitation of a melt spinning process. This type of experiment has several disadvantages:

- (1) The deformation conditions (rate of deformation, tensile stress, temperature) vary from point to point
- (2) The local deformation conditions cannot easily be determined
- (3) Die-swell occurs in the first stages of deformation

In a number of publications in this field an incorrect interpretation of the experimental results may have been presented. Therefore, in a number of investigations on tensile deformation, non-steady-state techniques have been used. In these experiments, a cylindrical beam of the material is gradually extended from its original length L_o at $t = 0$ to a length L at time t . From the definition of the rate of deformation $\dot{\epsilon}$, a constant value

of $\dot{\varepsilon}$ cannot be obtained by moving one end of the beam at a constant linear velocity. A constant rate of deformation could be realised by special experimental devices.

In these experiments, the tensile force is measured as a function of time, so that at a constant rate of deformation $\dot{\varepsilon}$ it is possible to calculate the true tensile stress and the extensional viscosity $\eta_e = \sigma_e / \dot{\varepsilon}$ at an arbitrary time t . The elastic properties of the deformation can be determined by measuring the elastic strain ε_e .

15.5.2. Correlation of extensional viscosity data

For correlating extensional viscosity data, it is obvious to attempt the same method as was used for non-steady state shear viscosity. Thus, the ratio η_e / η_{eo} is presumed to be determined by two dimensionless groups $\dot{\varepsilon}\tau_o$ and t/τ_o . As $\dot{\varepsilon}$ is constant (i.e. q_e), the ratio of these groups is equal to the tensile deformation ε . Therefore, τ/τ_o will likewise be a function of t/τ_o and ε .

By way of example, the experimental results of Meissner (1971) on low-density polyethylene have been represented in Fig. 15.22, by plotting η_e / η_{eo} against t/τ_o with ε as a parameter. For low values of ε all points lie on a single curve, which shows some correspondence to the curves of Fig. 15.16 for η/η_o against $\dot{\gamma}\tau_o$. If $\varepsilon > 1$, however, the extensional viscosity increases considerably with increasing extension.

This effect may be responsible for the popular belief that the extensional viscosity of polymer melts increases with increasing rate of deformation. Obviously, this statement is too simplistic, as one more parameter is needed to describe the relationship between extensional viscosity and rate of deformation. The situation is even more complicated. It is certain that the correlation of Fig. 15.22 has no universal validity, but depends on the nature of the polymer. Therefore, at this moment it is not possible to predict the extensional viscosity behaviour of an arbitrary polymer.

The available data on continuous tensile deformation indicate that in this situation the same conclusions hold as given above for non-steady state deformation:

1. The ratio τ/τ_o is not a simple function of the group $\dot{\varepsilon}\tau_o$, but requires an additional parameter (e.g. ε) for correlation
2. This correlation is dependent on the nature of the polymer

The available data on continuous tensile deformation are insufficient to justify a presentation at this place.

The elastic properties of tensile deformation may be correlated by plotting τ/τ_o , E/E_o or ε_e vs. $\dot{\varepsilon}\tau_o$ or t/τ_o . The same types of correlation are found as for shear viscosity, but also in this case the data are too scarce to provide general relationships.

As mentioned above, it is far more difficult to measure extensional viscosity than shear viscosity, in particular of mobile liquids. The problem is not only to achieve a constant stretch rate, but also to maintain it for a sufficient time. As shown before, in many cases Hencky strains, $\varepsilon = q_e t$, of at least 7 are needed to reach the equilibrium values of the extensional viscosity and even that is questionable, because it seems that a stress overshoot is reached at those high Hencky strains. Moreover, if one realises that that for a Hencky strain of 7 the length of the original sample has increased 1100 times, whereas the diameter of the sample of 1 mm has decreased at the same time to 33 μm , then it will be clear that the forces involved with those high Hencky strains become extremely small during the experiment.

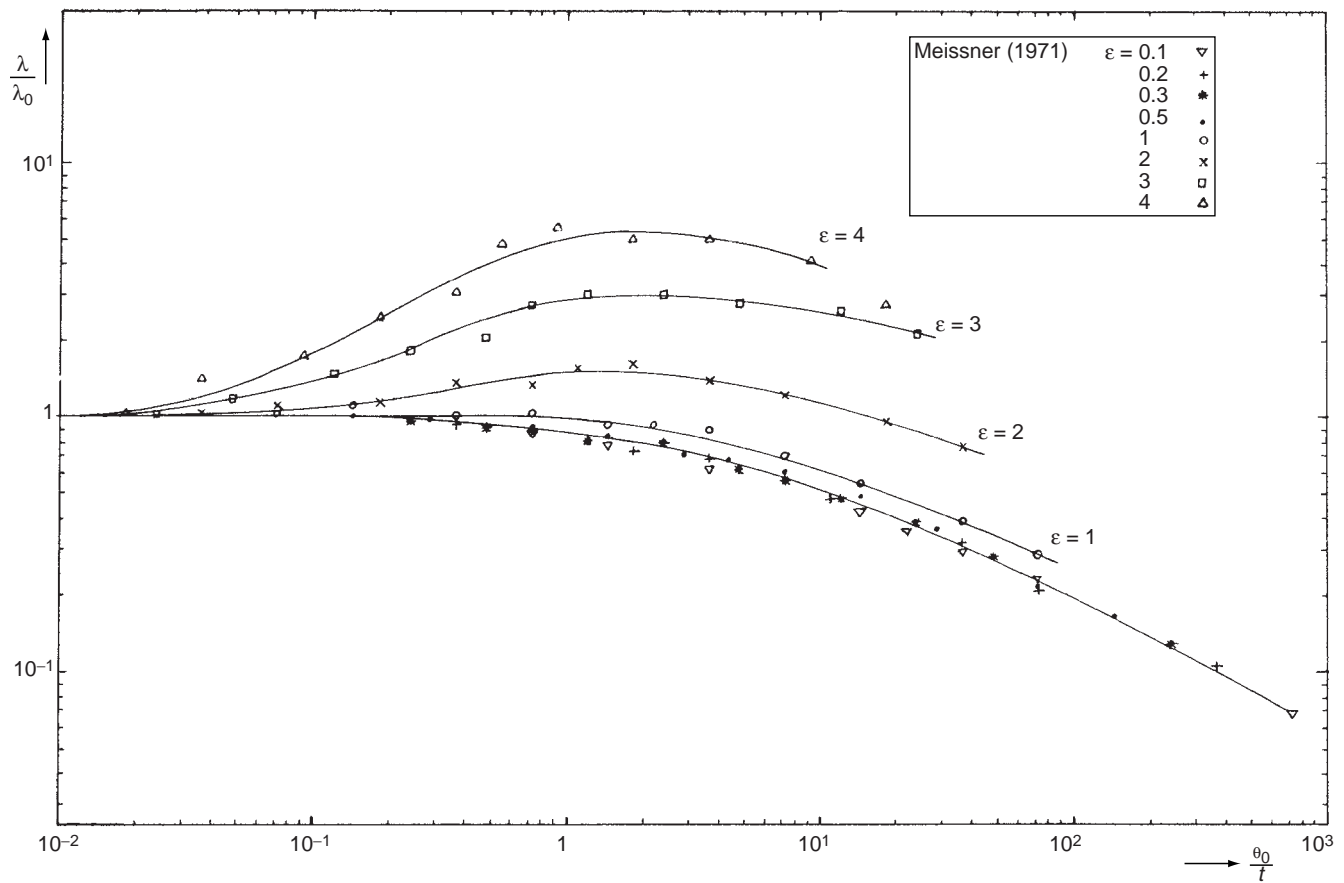


FIG. 15.22 Extensional viscosity of polyethylene.

Example 15.3

Estimate for an extensional viscosity of 10^5 N s/m^2 the force needed to maintain a stretching rate of 1 s^{-1} of a sample with an original diameter of 1 cm at a Hencky strain of 7.

Solution

The tensile stress is equal to $N_1 = \eta_e q_e = 10^5 \times 1 = 10^5 \text{ N}$. The tensile deformation is equal to $\exp(7) = 1097$; the area of the original cross section is equal to $1/4\pi \times 10^{-4} \text{ m}^2$ and the actual area equal to $1/4\pi \times 10^{-4}/1097 = 7.16 \times 10^{-8} \text{ m}^2$ (provided the volume is constant). Accordingly the tensile force is equal to $10^5 \times 7.16 \times 10^{-8} = 7.16 \times 10^{-3} \text{ N} = 7.3 \times 10^{-4} \text{ kgf} = 0.73 \text{ gf}$. It shows the very small forces that have to be measured at high deformations.

For the measurement of the stationary extensional viscosity, it is important that a steady state or equilibrium situation is being created. This theoretical equilibrium will not be reached completely in practice. For highly viscous systems, the conditions for equilibrium will be reached approximately, so that η_e may be calculated. In this case, the so-called controllable measurement techniques can be used. Examples are the extensional rheometer developed by Münstedt (1979), as schematically shown in Fig. 15.23, where a servo control system is used to maintain a specified extensional strain rate or a specified tensile stress. A cylindrical polymer sample is glued between two small metal clamps. Difficulties that arise are the temperature control in order to have isothermal conditions, in particular at high Hencky strains. Other problems are gravitational forces that become important at high Hencky strains and interfacial tensions. These problems had already overcome in 1971 by Meissner by making use of rotating clamps, as shown in Fig. 15.24. The sample floats on a thermostated liquid bath, in such a way that the sample floats on the surface of the liquid to withstand gravitational forces. In a commercialised version, use is made of a

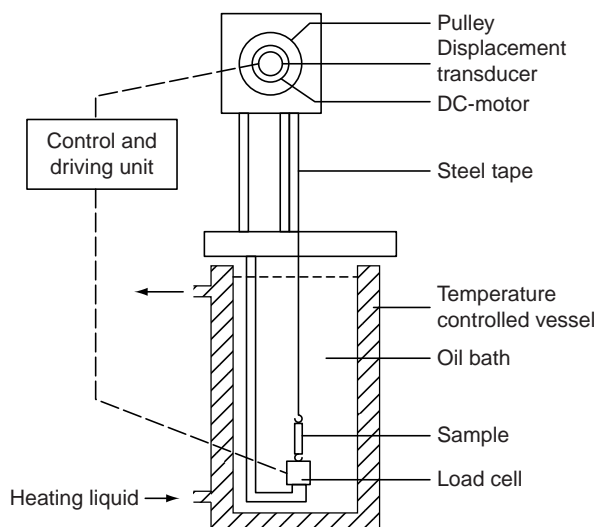


FIG. 15.23 Extensional rheometer, designed by Münstedt (1979). A servo control system is used to maintain a specified extensional rate of strain or a specified tensile stress. Courtesy Society of Rheology. For a modern version, see Münstedt et al., 1998.

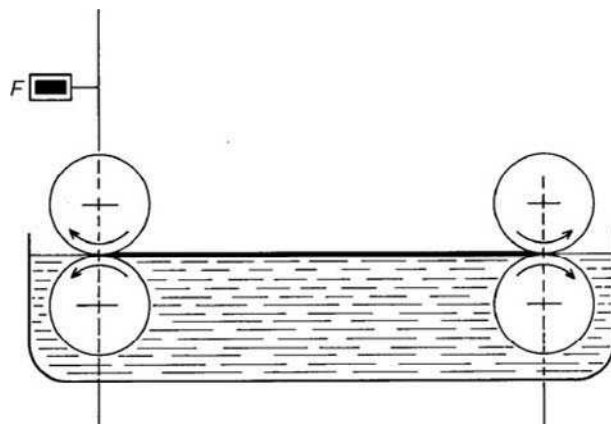


FIG. 15.24 Schematic representation of the four roller extensional rheometer, designed by Meissner (1972) to attain high Hencky strains. Two sets of rotary clamps are individually driven by two motors at constant rotation rates. The force in the sample is measured by a transducer F mounted on a leaf spring. From Barnes, Hutton and Walters (Gen Ref 1993). Courtesy Elsevier Science Publishers.

nitrogen flow where the sample floats on and the clamps are replaced by gear wheels. The length of the sample does not change in this experiment, and upon constant rotational speed of the clamps, the rate of extension is constant. Hencky strains as high as 7 are reached in this device.

For mobile liquids, the use of this kind of controllable instruments is practically impossible. For these liquids, the non-controllable measurement techniques are available only and in general an apparent transient viscosity will be obtained. Nevertheless these measurements are still of great value, because in many cases they approximate industrial process conditions. Mostly used is the spinning line rheometer, where an elastic liquid is pressed through a spinneret and the liquid is pulled from the die by winding the filament around a rotating drum or by sucking the tread into a capillary tube. This is schematically shown in Fig. 15.25. A serious problem is the translation of the obtained data to the extensional viscosity. Many other non-controllable devices are discussed by,

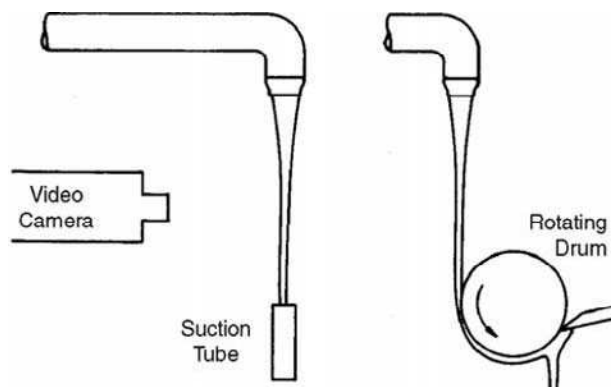


FIG. 15.25 Schematic diagram of the spinning technique. The fluid leaving the nozzle is pulled downwards by a rotating drum or a sucking tube. From James and Walters (General References, 1993). Courtesy Chapman & Hall.

e.g. Barnes et al. (General References, 1998), by James and Walters (1993) and by Macosko (General References, 1994). In Chap. 16, we go into more detail on the subject of mobile liquids.

It has already been shown before that in uniaxial extensional flow or stretching flow the length in the direction of the flow changes according to

$$l = l_0 e^{q_e t} = l_0 e^{\varepsilon(t)} \quad (15.95)$$

where $\varepsilon(t)$ is the so-called Hencky strain. Upon substitution Eq. (15.95) in Lodge's constitutive equation we find for the tensile stress, which is equal to the first normal stress difference:

$$N_1(t) = q_e \int_0^t (2e^{2q_e t} + e^{-q_e t}) G(t) dt \quad (15.96)$$

Upon substituting a sum of Maxwell elements, we find a rather complicated solution:

$$N_1(t) = 2q_e \sum_{i=1}^N \frac{G_i \tau_i}{1 - 2q_e \tau_i} [1 - e^{-(1-2q_e \tau_i)t/\tau_i}] + q_e \sum_{i=1}^N \frac{G_i \tau_i}{1 + q_e \tau_i} [1 - e^{-(1+q_e \tau_i)t/\tau_i}] \quad (15.97)$$

This result is not quite clear to understand and therefore we will look to some limiting cases to get some insight in its merits.

15.5.2.1. Very slow extensional flow: $2q_e \tau_1 \ll 1$ (where τ_1 is the longest relaxation time)

In this case Eq. (15.97) is simplified to

$$N_1(t) = 3q_e \sum_{i=1}^N G_i \tau_i (1 - e^{-t/\tau_i}) \quad (15.98)$$

Eq. (15.98) strongly resembles Eq. (15.61), that we obtained for shear stress build up after starting a steady shear flow with shear rate q at time $t = 0$. Accordingly, the elongational or extensional viscosity, which is defined to be

$$\eta_e = \lim_{t \rightarrow \infty} \frac{N_1(t)}{q_e}$$

has for very slow extensional flows the value

$$\lim_{q_e \rightarrow 0} \eta_e = 3 \int_0^\infty G(t) dt \rightarrow 3 \sum_{i=1}^N G_i \tau_i \quad (15.99)$$

This is, according Eq. (15.64), three times the zero shear viscosity, which in agreement with practice. It is a result already obtained by Trouton in 1906. Accordingly, the *Trouton ratio*, defined as

$$T_R = \frac{\eta_e}{\eta} \quad (15.100)$$

is equal to 3 for Newtonian behaviour.

15.5.2.2. Slow extensional flow: $2q_e\tau_1 < 1$

In this case, the tensile stress in the limit for $t \rightarrow \infty$ becomes

$$\lim_{t \rightarrow \infty} N_1(t) = 2q_e \sum_{i=1}^N \frac{G_i \tau_i}{1 - 2q_e \tau_i} + q_e \sum_{i=1}^N \frac{G_i \tau_i}{1 + q_e \tau_i} \quad (15.101)$$

The result is that the extensional viscosity increases with increasing extensional rate of strain. This is also in agreement with practice.

15.5.2.3. Fast extensional flow: $2q_e\tau_1 > 1$

As soon as the flow becomes so fast that $q_e > 1/(2\tau_1)$, the first term in Eq. (15.97) increases without limit with time. However, as long as t is still small, $N_1(t)/q_e$ is still independent of q_e . The deviation from this linear behaviour occurs earlier, i.e. at shorter times, when the extensional rate of strain becomes higher (approximately at $q_e t = 0.5$).

In Fig. 15.26 an example is given of Eq. (15.97) for a Maxwell element with $G = 1000 \text{ N/m}^2$ and $\tau = 1 \text{ s}$. For small extensional rates of strain, the extensional viscosity is constant and equal to 3000 N s/m^2 . For higher extensional rates of strain, the viscosity increases. At the extensional rate of strain of 0.5 s^{-1} there is a transition to infinite extensional viscosities. The dotted line is the transient shear viscosity $\eta^+(t)$ at low shear rates and equal to $\frac{1}{3}$ of the transient extensional viscosity $\eta_e^+(t)$ at low extensional rates of strain.

In Fig. 15.27, the transient extensional viscosity of a low-density polyethylene, measured at 150°C for various extensional rates of strain, is plotted against time (Münstedt and Laun, 1979). Qualitatively this figure resembles the results of the Lodge model for a Maxwell model in Fig. 15.26. For small extensional rates of strain ($q_e \leq 0.001 \text{ s}^{-1}$) $\eta_e^+(t)$ is almost three times $\eta^+(t)$. For $q_e > 0.01 \text{ s}^{-1}$ $\eta_e^+(t)$ increases fast, but not to infinite values, as is the case in the Lodge model. The drawn line was estimated by substitution of a spectrum of relaxation times of the polymer (calculated from the dynamic shear moduli, G' and G'') in Lodge's constitutive equation. The resulting viscosities are shown in Fig. 15.28: after a constant value at small extensional rates of strain the viscosity increases to a maximum value, followed by a decrease to values below the zero extension viscosity.

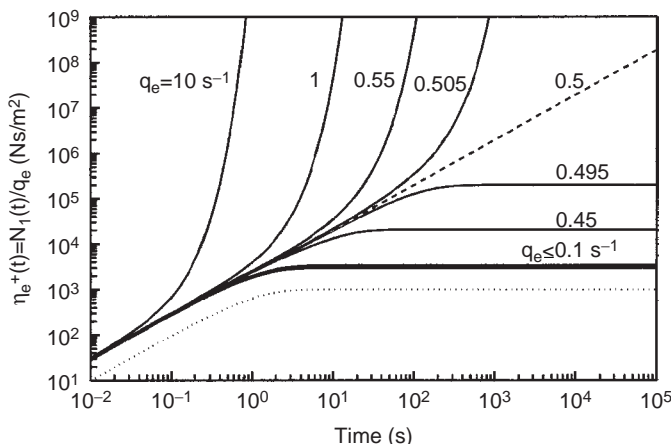


FIG. 15.26 Transient extensional viscosity, $\eta_e^+(t)$, vs. time, calculated with Lodge's constitutive equation for a Maxwell element with $G = 1000 \text{ N/m}^2$ and $\tau = 1 \text{ s}$.

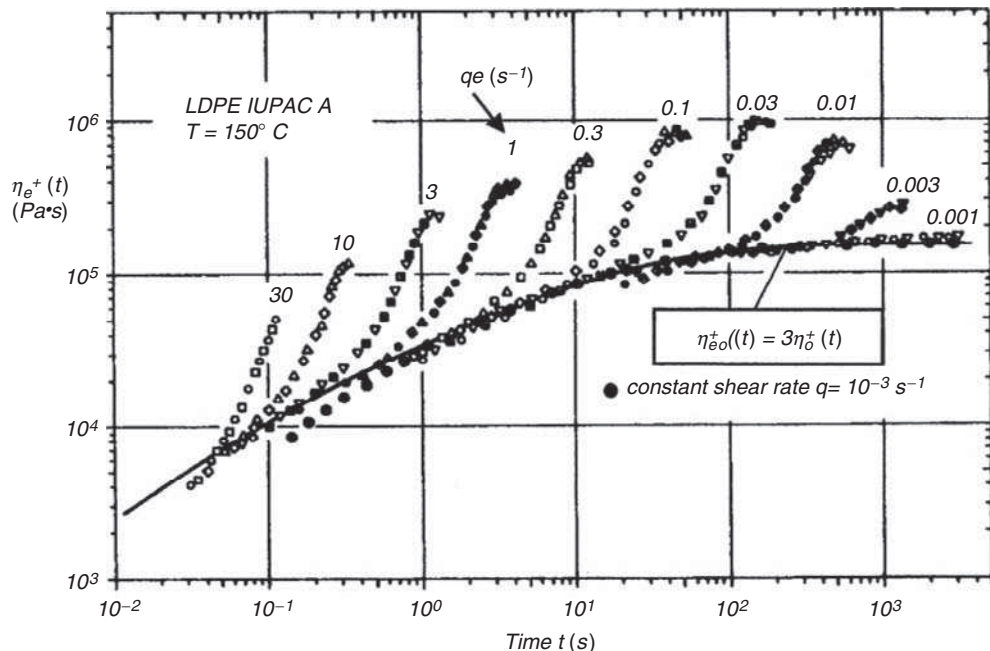


FIG. 15.27 Transient extensional viscosity, $\eta_e^+(t)$ of low-density polyethylene LDPE IUPAC A at 150 °C, vs. time, for various extensional rates of strain. From Münstedt and Laun (1979). Courtesy Springer Verlag.

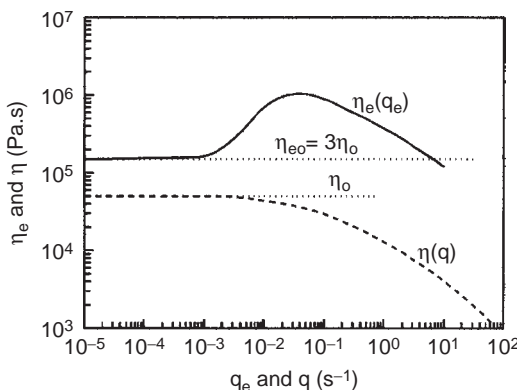


FIG. 15.28 Steady state extension and shear viscosities of LDPE IUPAC A at 150 °C (Fig. 15.27), as functions of extension and shear rate, respectively. After Münstedt and Laun (1979).

In Sect. 15.4 it was shown how the shear thinning behaviour of the viscosity could be described empirically with the aid of many suggestions found in literature. It was not mentioned there that the first normal stress coefficient also shows shear thinning behaviour. In this Sect. 15.5 it became clear that also the extensional viscosity is not a constant, but depending on the strain rate: upon increasing the strain rate q_e the extensional viscosity depart from the Trouton behaviour and increases (called strain hardening) to a maximum value, followed by a decrease to values below the zero extensional viscosity. It has to be emphasised that results in literature may show different behaviour for the extensional behaviour, but in many cases this is due to the limited extensions used,

so without reaching the “steady” state. For the first normal stress coefficient and the extensional viscosity no empirical relations are available like those for the viscosity. However, it is possible to fit the results for the three parameters by substitution of a so-called damping function in the relaxation modulus. In this way, Wagner’s constitutive equation is obtained. This subject is discussed in many monographs on rheology, e.g. Janeschitz-Kriegl (1983), Larson (1988) and Te Nijenhuis (2005). Equations found for viscosity and first normal stress coefficient are

$$\eta(q) \rightarrow \int_0^\infty t \sum_{i=1}^N (G_i/\tau_i) e^{-t/\tau_i} [f e^{-n_1 q t} + (1-f) e^{-n_2 q t}] dt = \sum_{i=1}^N G_i \tau_i \left[\frac{f}{(1+n_1 q \tau_i)^2} + \frac{1-f}{(1+n_2 q \tau_i)^2} \right] \quad (15.102)$$

$$\Psi_1(q) \rightarrow 2 \int_0^\infty t^2 \sum_{i=1}^N (G_i/\tau_i) e^{-t/\tau_i} [f e^{-n_1 q t} + (1-f) e^{-n_2 q t}] dt = 2 \sum_{i=1}^N G_i \tau_i \left[\frac{f}{(1+n_1 q \tau_i)^3} + \frac{1-f}{(1+n_2 q \tau_i)^3} \right] \quad (15.103)$$

In Fig. 15.29 results are shown for a low-density polyethylene where the fitting parameters are: $n_1 = 0.310$, $n_2 = 0.106$ and $f = 0.57$. The full lines were calculated with the damping function as shown in both equations between square brackets.

In the same way, but much more complicated, with a damping function depending on the Hencky strain, it proved to be possible to calculate the transient extensional viscosity as a function of q_e . The result is illustrated in Fig. 15.30 for the same polymer. It shows that extensional viscosity remains finite and increases with increasing strain rate up to a maximum at $q_e = 2 \text{ s}^{-1}$, after which it decreases again. The calculated lines coincide quite well with the experiments, but the calculated viscosities are somewhat too high.

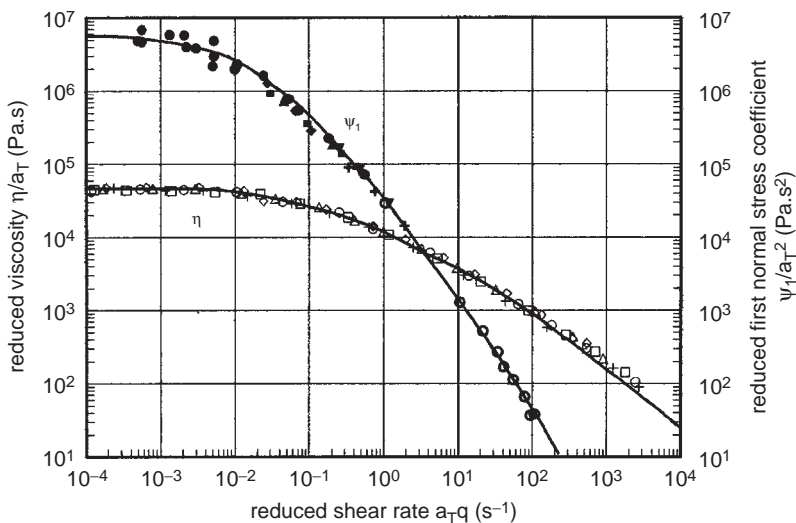


FIG. 15.29 Steady state viscosity (open symbols) and first normal stress coefficient (filled symbols) vs. shear rate for the LDPE Melt I at 150 °C. Measurements were taken at temperatures varying from 115 to 210 °C and WLF reduced to 150 °C. From Laun (1978). Courtesy Springer Verlag. (\times ; ∇ ; \blacktriangledown) 115 °C; (\circ ; \bullet) 130 °C; (\square ; \blacksquare) 150 °C; (\triangle ; \blacktriangle) 170 °C; (\diamond ; \blacklozenge) 190 °C; (\lozenge ; \blacklozenge) 210 °C.

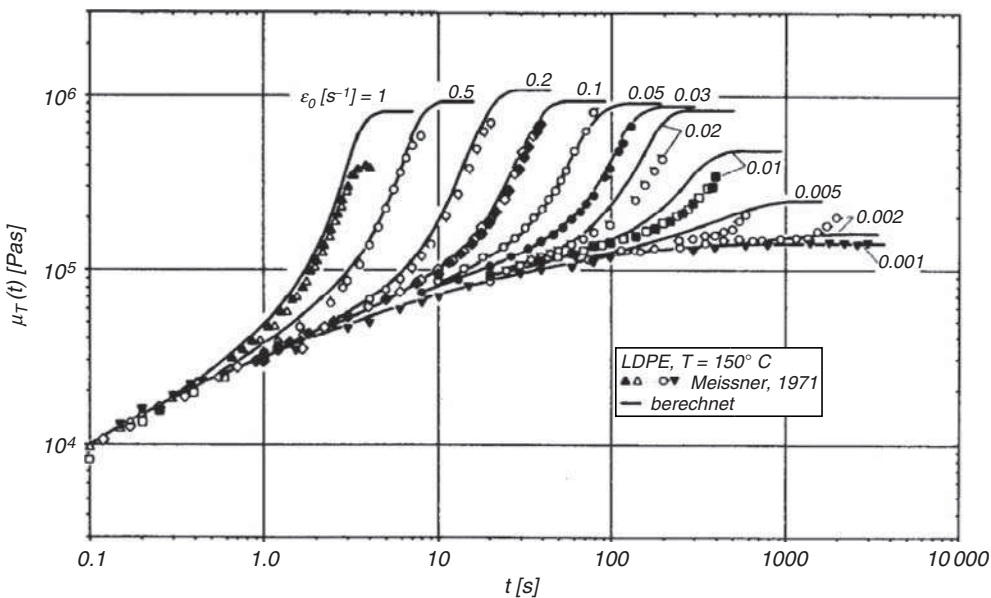


FIG. 15.30 Transient extensional viscosity of LDPE Melt I for extensional rates of strain varying from 0.001 to 1 s^{-1} , at 150°C . From Wagner and Meissner (1980). Courtesy John Wiley & Sons, Inc.

15.6. ELASTIC EFFECTS IN POLYMER MELTS

15.6.1. Converging flow phenomena

Converging flow occurs in a wedge or tapering tube (restrained converging flow) and in the drawing of a molten filament (unrestrained converging flow). Polymer melts often behave very differently from Newtonian fluids under these circumstances.

The extreme case of converging flow arises when a melt is forced from a large reservoir into a narrow tube. Figure 15.31 gives a diagrammatic indication for a highly elastic fluid. Tordella (1957) and Clegg (1958) have already observed the large ring vortex as shown

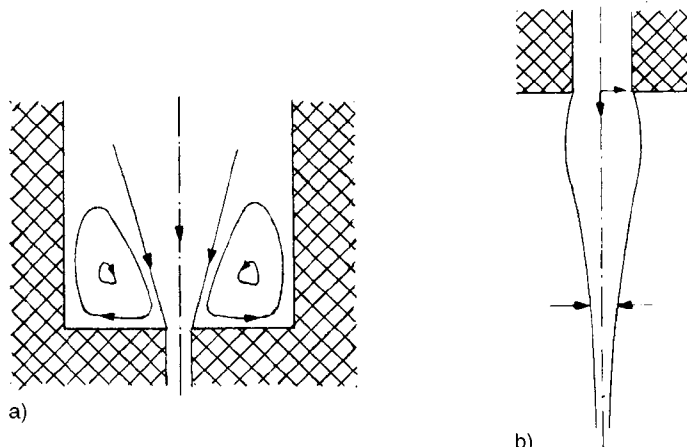


FIG. 15.31 (A) Efflux of an elastic fluid into a narrow tube from a large reservoir. (B) Die swell at efflux of an elastic fluid from a capillary.

with many polymer melts. The phenomenon is a direct consequence of a high extensional viscosity linked with a relatively low shear viscosity; the material flowing into the tube is restricted to a narrow-angle cone and the large recirculating vortex occupies a "dead" volume around it.

In general, when a thermoplastic melt flowing in a channel encounters an abrupt decrease in channel diameter, the material conforms to a natural angle of convergence for streamline flow. Cogswell (1972) derived the following expressions:

$$\text{for conic-cylindrical flow: } \tan \alpha = \left(\frac{2\eta}{\eta_e} \right)^{1/2} \quad (15.104)$$

$$\text{for wedge-flow: } \tan \beta = \frac{3}{2} \left(\frac{2\eta}{\eta_e} \right)^{1/2} \quad (15.105)$$

where α and β are in both cases the half angle of natural convergence.

In appendix II of this chapter the most important rheological equations for converging flow are summarised.

15.6.2. Extrudate swell ratio or die swell

Most polymer melts, when extruded, expand in diameter once they emerge into an essentially unrestrained environment. Especially in short dies (in the extreme case in dies of "zero length") the tensile component of flow induced by convergence of the flow cannot relax before reaching the die exit. This swelling behaviour is the consequence of the elastic properties of a polymer melt. Let us in an experiment in thought press a cross-linked rubber through a capillary. When the rubber leaves the capillary, it will swell again, trying to recover its original dimensions, due to its elasticity. A polymer melt will swell almost like as the rubber. However, upon leaving the die the original dimensions of the reservoir will not be reached again, because of stress relaxation, primarily due to coil-stretch-recoil transition of macromolecules. In Fig. 15.32 a cartoon of this concept is shown.

In principle, extrudate swell or die swell is dependent on the terminal relaxation time and on the time of residence in a capillary. The shorter the time of residence in the capillary or the longer the relaxation time the higher the die swell. This leads to (see, e.g. Te Nijenhuis, General References, 2007, Chap. 9.4)

$$B \equiv D/D_o = B(\dot{\gamma}_w, T, t, L/D_o, M, MWD) \quad (15.106)$$

Accordingly, die swell increases with increasing flow rate and decreases with increasing length of the capillary. Both effects are depicted in Fig. 15.33 for high-density polyethylene (Han et al., 1970). This is also in agreement with Fig. 15.34, where die swell and viscosity of polystyrene are plotted vs. shear rate (Greassley et al., 1970). Die swell decreases with

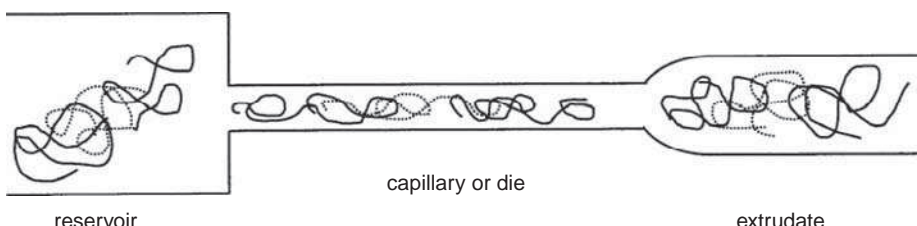


FIG. 15.32 Schematic representation of a macromolecule in the course of time during flow in a capillary rheometer.

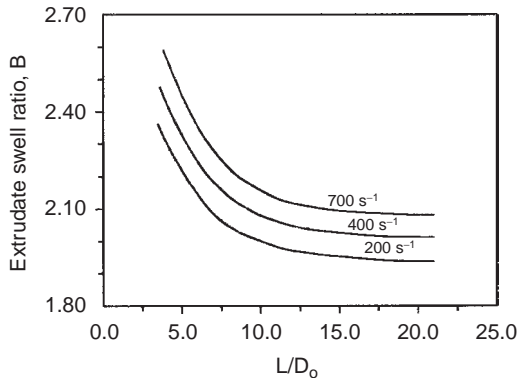


FIG. 15.33 Extrudate swell ratio as a function of L/D_o for high-density polyethylene at 18 °C for shear rates as indicated. From Han et al. (1970). Courtesy Society of Rheology.

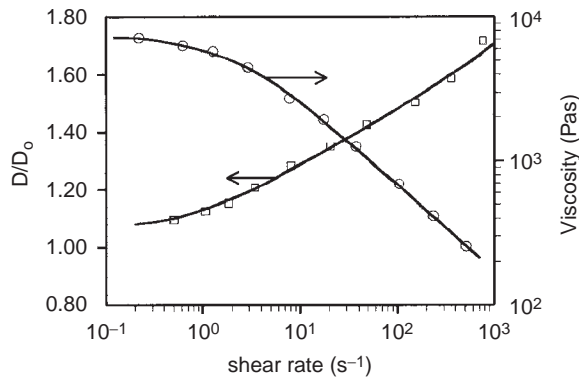


FIG. 15.34 Extrudate swell ratio and viscosity, both as functions of shear rate, for a polystyrene melt of $M_w = 2.2 \times 10^5$ and $M_w/M_n = 3.1$. From Greassley et al. (1970). Courtesy Society of Rheology.

increasing temperature. This is obvious from Fig. 15.35 where die swell of a polystyrene melt measured at 160, 180 and 200 °C is plotted vs. shear rate. A single curve is obtained by plotting the die swell vs. shear stress, as shown in Fig. 15.36. This is due to the time temperature superposition of viscoelasticity and because the shear stress is proportional to the viscosity. Furthermore, the extrudate swell ratio increases with increasing molecular weight and, broader molecular-weight distribution. This is shown in Fig. 15.37 (Greassley et al., 1970), where the open and filled symbols refer to polystyrenes with narrow and broad molecular-weight distributions. The broad polymer exhibits much higher extrudate swell ratios than the narrow polymer, whereas its viscosity is only three times higher ($M_{w,\text{broad}}/M_{w,\text{narrow}} \approx 1.4$). Of course, the viscosity is not the only parameter that is responsible for die swell. It is obvious that recoverable shear strain will be responsible for extrudate swell. Hence, the normal stress coefficients will also have an important effect. For that reason Tanner (1970, 1985) has proposed the following simple expression for extrudate swell ratio:

$$\frac{D}{D_o} = 0.1 + \left[1 + \frac{1}{2} \left(\frac{N_1}{2T_{21}} \right)_w^2 \right]^{1/6} = 0.1 + \left[1 + \left(\frac{\Psi_1 \dot{\gamma}_w}{2\eta} \right)^2 \right]^{1/6} = 0.1 + [1 + \gamma_{\text{rec}}^2]^{1/6} \quad (15.107)$$

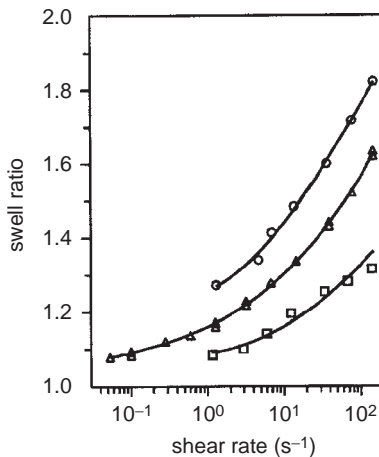


FIG. 15.35 Extrudate swell ratio of the same polystyrene as in Fig. 15.34 plotted vs. shear strain for temperatures of (○) 160 °C, (△) 180 °C and (□) 200 °C. L/D_o ratios varied from 27 to 56. From Greassley et al. (1970). Courtesy Society of Rheology.

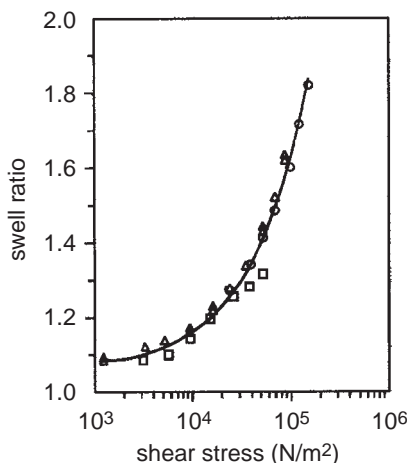


FIG. 15.36 Extrudate swell ratio of the same polystyrene melts as in Fig. 15.35, now plotted vs. shear stress for temperatures of (○) 160 °C, (△) 180 °C and (□) 200 °C. L/D_o ratios varied from 27 to 56. From Greassley et al. (1970). Courtesy Society of Rheology.

According to Eq. (15.80) recoverable shear strain is proportional to the elastic shear compliance, J_e^0 . The elastic shear compliance depends on the molecular-weight distribution in the following way

$$J_e^0 \propto \frac{M_z M_{z+1}}{M_w^2}$$

Accordingly, the recoverable shear strain is for polymers with a broad MWD larger than for a polymer with a narrow MWD with the same M_w and thus the extrudate swell ratio will be higher for the “broad” polymer. This is in agreement with Fig. 15.37. Eq. (15.107) proved to be quite successful in describing data on extrudate swell, as long as it only concerns molecular-weight distribution.

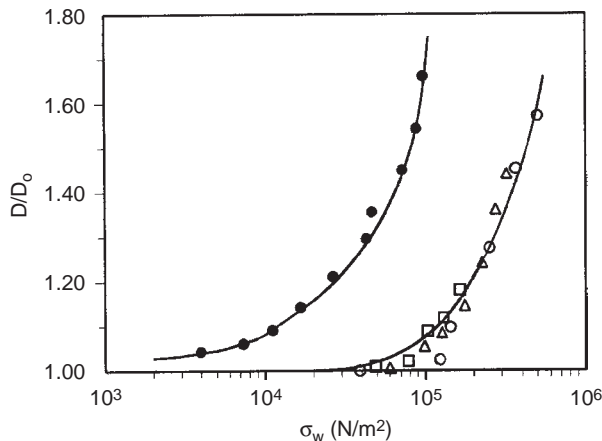


FIG. 15.37 Extrudate swell ratio vs. shear stress at the wall, for melts of polystyrenes of broad and narrow molecular-weight distributions. Filled symbols: the broad polystyrene mentioned in Fig. 15.34–15.36: $M_w = 2.2 \times 10^5$ and $M_w/M_n = 3.1$. Open symbols: narrow polystyrene: $M_w = 1.6 \times 10^5$ and $M_w/M_n < 1.1$. From Greassley et al. (1970). Courtesy Society of Rheology.

Finally, it has to be mentioned that die swell is also dependent on the kind of convergence of the flow. Fig. 15.38 shows the relationships between swelling and recoverable shear strain as derived by Cogswell (1970) for long capillaries and slit dies: B_{ER} represents the swelling ratio in capillaries B_{SH} and B_{ST} that in slit dies in the thickness direction and transverse direction, respectively. Fig. 15.39 shows the analogous relationships for very

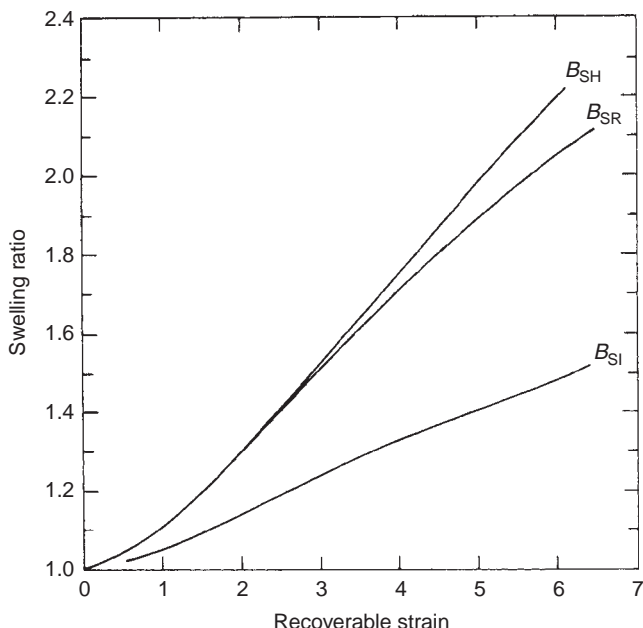


FIG. 15.38 Relationship between swelling ratio and recoverable shear strain for long capillary and slit dies. After Powell (1974).

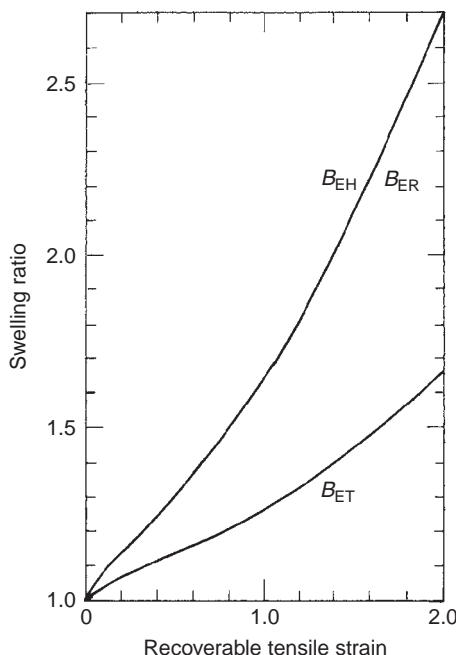


FIG. 15.39 Relationship between swelling ratio and recoverable tensile strain for short capillary and slit dies.
After Powell (1974).

short (zero length) dies: B_{ER} is the swelling ratio in radial direction in a very short circular die, whereas B_{SH} and B_{ST} give the corresponding relationships for slit dies in the thickness direction and transverse direction, respectively.

In appendix II the expressions for the swelling ratio in different cases of convergent flow are given.

15.6.3. Unstable flow and melt fracture

Newtonian shear flow of polymer melts is a stable process. This means that small disturbances in the flow conditions, caused by external effects, are readily suppressed. As the rate of shear increases, however, the elastic response of the melt becomes more pronounced relative to the viscous response. In other words, components of the stress tensor in directions different from the direction of the shear stress become more important. As a result, small disturbances are not so readily compensated and may even be magnified.

In extrusion, for instance, high shear rates may result in rough surfaces of the extrudate, poor surface gloss and poor transparency. For low flow rates, the flow is smooth and only die swell of the extrudate will occur. With increasing flow rates the extrudate surface starts to exhibit ripples or undulations that become progressively stronger as the flow rate increases. At still higher flow rates the distortions can become so severe that they cause the extrudate to break. This ultimate disastrous effect of melt flow instability is called *melt fracture*. For beautiful photographs of melt fracture, the reader is referred to, e.g. Boger and Walters, (1993) and Kissi and Piau (1996).

There is an extensive literature on attempts to give quantitative criteria for the onset of melt fracture. The simplest criterion has been proposed by Benbow and Lamb (1963), viz.

that melt fracture occurs if the shear stress exceeds $1.25 \times 10^5 \text{ N/m}^2$. Bartos (1964) suggested a critical value of viscosity reduction

$$\eta_{Mf} = 0.025\eta_0 \quad (15.108)$$

Barnett (1967) defined a "melt fracture number"

$$Mf = \frac{\eta_0 q}{Q} \quad (15.109)$$

where $Q = M_w/M_n$. Melt fracture is observed if $Mf > 10^6 \text{ N/m}^2$ (η_0 is expressed in N s/m^2 and q in s^{-1}).

It is doubtful, however, if melt fracture can be predicted from shear rate criteria alone, without taking the geometry of the apparatus into account. Especially the form of the channel at the entrance of the die is very important. In using extrusion dies with a conical entrance, flow instabilities are suppressed by decreasing the cone angle. This effect has been found experimentally by Tordella (1956), Clegg (1958) and Ferrari (1964).

From these results, Everage and Ballman (1974) concluded that melt fracture originates at a point where fluid elements are subjected primarily to extensional deformation. They could correlate the results of Ferrari with a critical extension rate of about 1000 s^{-1} .

Some general observations are (Brydson, General References, 1981, Chap. 5.3):

- (a) The critical value of the shear stress is of the order of $0.1 - 1 \text{ MN/m}^2$ for most commercial polymers
- (b) The form of the distortion varies widely: screwed thread, spiral, regular ripple, random, periodic bambooing
- (c) Increase in temperature causes a large increase in the critical shear rate, whereas it has less effect on the critical shear stress (see Fig. 15.40, Howells and Benbow, 1962)
- (d) The product $\sigma_c M_w$ is approximately constant, as becomes clear from in Fig. 15.41 for poly(methyl methacrylate) (Howells and Benbow, 1962), but that has been observed also for other polymers

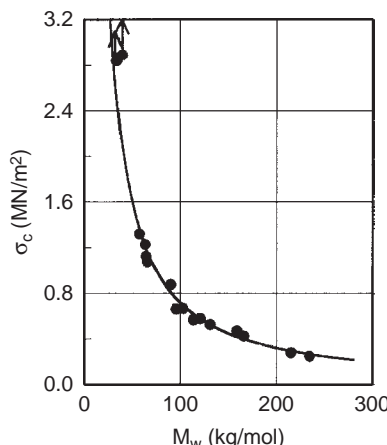


FIG. 15.40 Effect of melt temperature on onset of elastic turbulence in polyethylene. From Brydson (1981, Gen Ref, his Fig. 5.6 as reproduced from Howells and Benbow, 1962). Courtesy The Plastics & Rubber Institute.

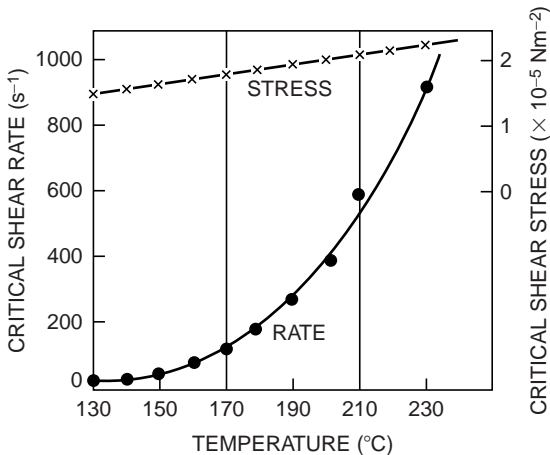


FIG. 15.41 Effect of molecular weight on critical shear stress at onset of elastic turbulence in poly(methyl methacrylate). From Brydson (1981, Gen Ref, his Fig. 5.8 as reproduced from Howells and Benbow, 1962). Courtesy The Plastics & Rubber Institute.

- (e) The product $\sigma_c M_w$ appears to increase with an increase in the solubility parameter (Benbow and Lamb, 1963)
- (f) Widening the molecular-weight distribution seems to increase the critical shear rate, although there are conflicting conclusions

De Gennes (2007) has constructed a model for slippage planes in a sheared melt, based on a balance between reptation bridging and shear debonding (slip stick model). He proposed that slippage occurs on solid walls: either at the container surface or on dust particles floating in the melt. There is critical stress for slippage, approximately equal to $\frac{1}{3}$ of the plateau modulus, which means that melt fracture is expected at moderate stresses.

It is the great merit of Van Saarloos and his group (Bertola et al., 2003; Meulenbroek et al., 2003) to have thrown light on the physical background of the phenomenon of melt fracture. It is well known that, even for low Reynolds numbers, viscoelastic fluids may exhibit instabilities for Weissenberg numbers larger than 1, provided the streamlines are curved (Couette rheometer and cone and plate rheometer, e.g.), due to the normal forces. In the 1970s, however, it had already been proven that for polymer fluids in a straight tube or between parallel plates (capillary rheometer and slit rheometer) the flow is *linear stable*. This is in agreement with the phenomenon that instabilities only occur in flows with curved streamlines. Therefore, many investigators assumed that such flow patterns are also *non-linear stable*. However, the essence of studies in the Van Saarloos group is based on the “simple” idea that this cannot be true. For the reason that introducing a disturbance of sufficient big amplitude the streamlines are locally curved, the flow must be unstable. In other words, *such a flow must be linear stable but non-linear unstable*. The authors were able to predict this non-linear instability. Van Saarloos et al. came to the following conclusions:

- (a) It is possible to calculate the effect of a small disturbance in the flow, e.g. by a little burr in the capillary or by the presence of dust particles
- (b) If the disturbance is sufficiently small, it will be damped down
- (c) Above a specific flow rate some disturbances do not damp down
- (d) Disturbances above a specific critical size even intensify themselves

It means that melt fracture is an inherent phenomenon. It might be postponed by taking special cares, but it always will occur, if the flow is fast enough.

15.7. RHEOLOGICAL PROPERTIES OF THERMOTROPIC LIQUID CRYSTALLINE POLYMERS

Isotropic and Anisotropic (LCP- or Mesophase-) melts have very different flow behaviour, qualitatively and quantitatively. Very striking is the viscosity-temperature curve, as shown in Fig. 15.42a for thermotropic LCPs. As usual, the viscosity decreases with increasing temperature in the nematic phase. However, upon approaching the clearing temperature $T_{n,1}$ the viscosity increases again because the Brownian motion starts to disturb the alignment of the LCP rods in the flow direction. At further increase of temperature above $T_{n,1}$ the viscosity decreases again in the normal way for polymers in the isotropic state. A similar effect is the viscosity-concentration curve, as shown in Fig. 15.42b for lyotropic LCPs. As usual, the viscosity increases with increasing concentration in the isotropic phase. At the phase transition concentration $c_{i,n}$ however, the viscosity starts to decrease because of orientation of the LCP rods. The lower viscosity of the anisotropic solution can be attributed to a partial orientation of the rod like molecules, parallel to each other and in the direction of flow. The viscosity reaches a minimum value and upon further increase of the concentration, the viscosity increases in a usual way.

When compared with conventional melts, the LCP melts show a number of other characteristic deviations:

- A high elastic response to small amplitude oscillations, but absence of gross elastic effects, such as post-extrusion swelling
- A flow curve (viscosity vs. flow rate) which clearly shows several (usually three) regions, incorporating a "yield stress" region, a "pseudo-Newtonian" region and a region of "shear thinning" (Onogi and Asada, 1980);
- A strong dependence of the rheological properties on the thermo-mechanical history of the melt
- A low or even very low thermal expansion coefficient

Cogswell (1985) expressed it in the following words: "To make the connection from the basic material properties to the performance in the final product, industrial technologists had to learn a new science". It is more or less so, that – for liquid crystal polymers – properties like stress history, optical and mechanical anisotropy, and texture seem to be independent variables; this in contradistinction to the situation with conventional polymers.

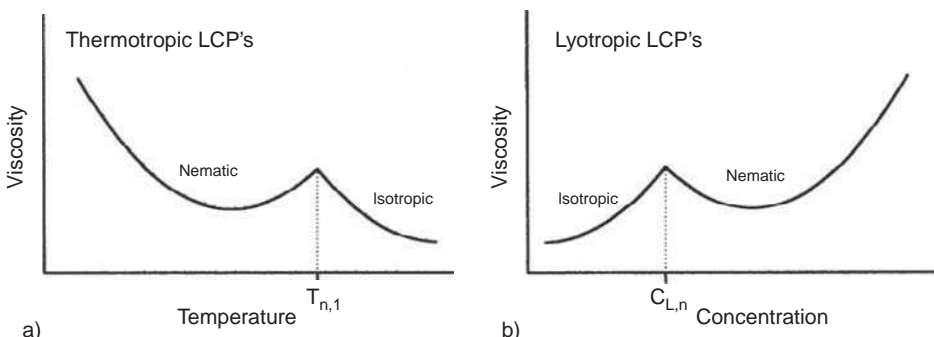


FIG. 15.42 Schematic representation of the viscosity (A) as a function of temperature for thermotropic LCPs and (B) as a function of concentration for lyotropic LCPs.

Liquid crystal polymers have a potentially low viscosity, but that potential becomes only manifest when the system is flowing. Since they have a yield stress, LCP melts cannot be assumed to have a low viscosity at rest.

The main rheological properties, as a function of the main variables, of the thermotropic LCP melts in comparison to conventional polymer melts are summarised in Fig. 15.43.

15.7.1. Thermotropic main chain liquid crystalline polymers, MCLCPs

The dependence of the viscosity on shear rate for thermotropic LCPs may be represented by the curve schematically shown in Fig. 15.44 (Onogi and Asada, 1980; Beekmans, 1997). The behaviour is divided into three regions with respect of the shear rate. In Region I the flow is not strong enough to disturb the existing random polydomain structure and application of a stress results in yield and plastic flow of piled domains. The apparent viscosity decreases rapidly with increasing shear rate. In Region II the flow disturbs the polydomain structure

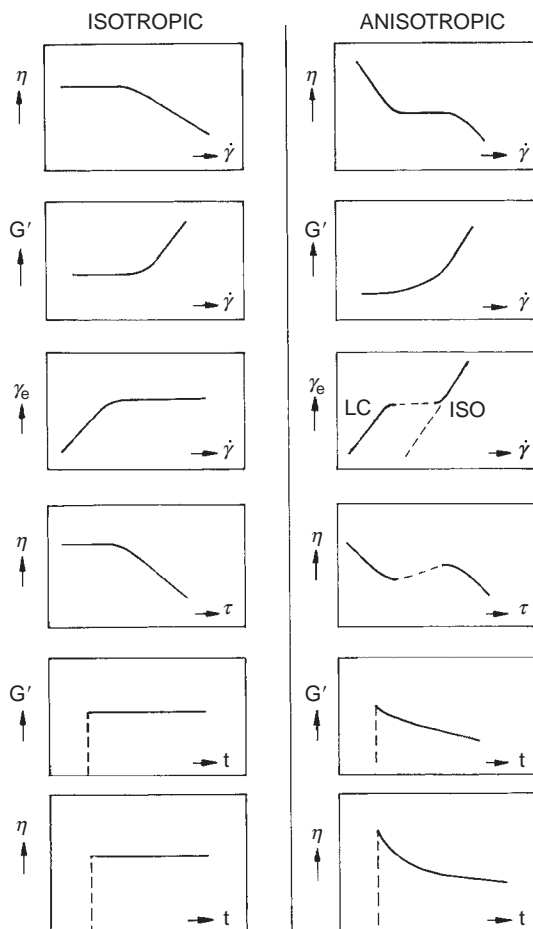


FIG. 15.43 Rheological behaviour of isotropic vs. anisotropic melts. All graphs are double logarithmic.

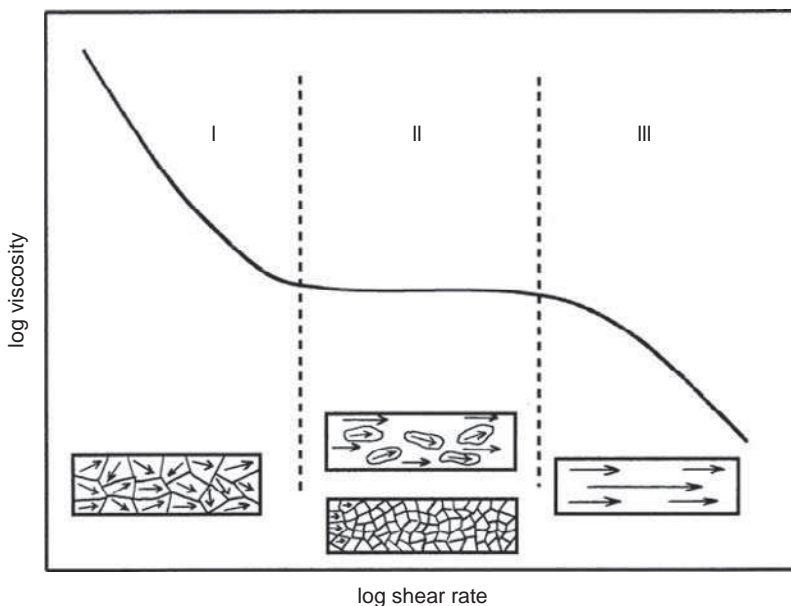


FIG. 15.44 Schematic representation of the bulk structure of an LCP during shear flow in the respective regions of the three-region flow curve, as proposed by Onogi and Asada (1980) and by Beekmans (1997). The lower cartoon in region II is in agreement with newer ideas of the structure obtained in the 1990's by Burghardt & Fuller, 1991, Vermant et al., 1994, Walker et al., 1995.

considerably, resulting in flow of randomly oriented domains dispersed in an oriented nematic melt (upper cartoon in Region II). The viscosity is approximately constant and the plateau zone is called the Newtonian region. At still higher shear rates this texture evolves to a uniformly aligned sample in Region III, which is called the power-law shear thinning region. The flow behaviour of LCPs in Region I is non-Newtonian and thus the zero-shear viscosity can not be determined. Moreover, in this region the flow properties of LCPs depend strongly on their texture and thus on their thermal and deformation history. It will be clear that the viscosity in region II has to be used as a characteristic viscosity of these polymers, but this region can be very narrow for LCPs. The flow properties in Region III seem to be least dependent on the sample history.

It has to be pointed out that the vision on Region II has changed in the 1990s (Burghardt & Fuller, 1991; Vermant et al., 1994; Walker et al., 1995): instead of a gradual texture enlargement into a monodomain, a texture refinement is observed at these shear rates (lower cartoon in Region II). As the domains are broken down to smaller and smaller sizes, the increasing surface area of the domains may cause again an increase of the resistance to flow. When the whole structure is homogenised the now rapidly increasing flow orientation of the individual polymer molecules will lower the viscosity anew. It is then that *Region III* starts: the "shear-thinning" region, the region of high shear rates. The LCP melt then has a much lower viscosity than the isotropic melt, even though its temperature is lower. Cogswell visualised the rheological behaviour of LCPs *in connection with texture* in a scheme that is reproduced in Fig. 15.45. Note that the viscosity is now plotted vs. shear stress instead of shear rate.

An example of such behaviour is shown in Fig. 15.46 for Vectra A900, which is a copolymer consisting of 73 mol% HBA (1,4-hydroxy benzoic acid) and 27 mol% HNA (2,6-hydroxy naphthoic acid) (Langelaan and Gotsis, 1996). In this figure, Regions I and III are undoubtedly present, but Region II is very narrow, if indeed it exists for this polymer,

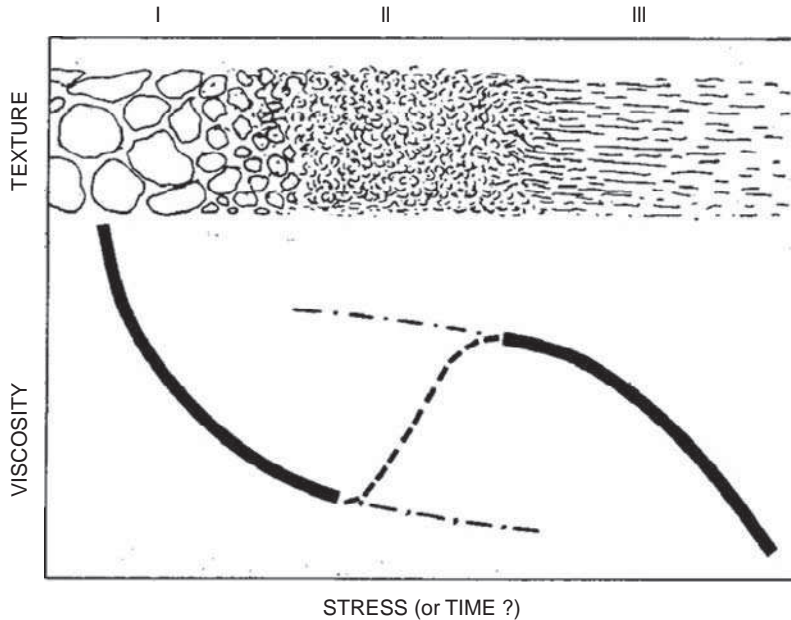


FIG. 15.45 Relationship between morphology and rheology. From Cogswell (1985).

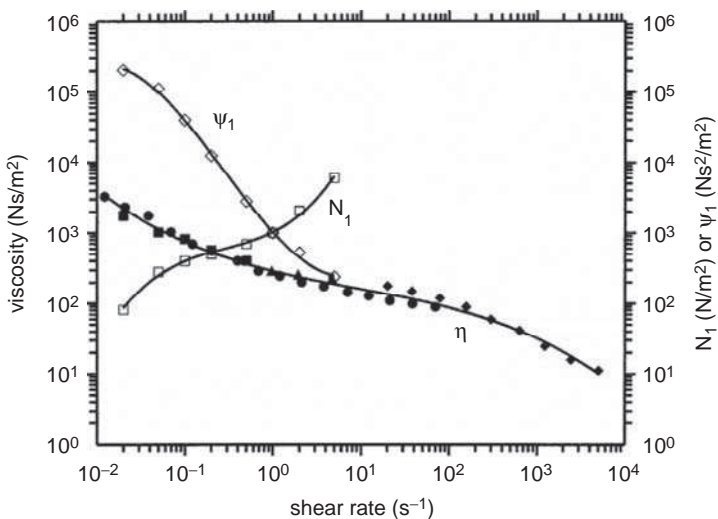


FIG. 15.46 Viscosity, η , and first normal stress difference, N_1 , of Vectra 900 at 310 °C as functions of shear rate, according to Langelaan and Gotsis (1996). The first normal stress coefficient, Ψ_1 , is estimated from N_1 by the present author. (◆) Capillary rheometer; (■) and (□) cone and plate rheometer; (●) complex viscosity η^* ; (▲) non-steady state values of the cone and plate rheometer. Courtesy Society of Rheology.

around a shear rate of 1 s^{-1} . Practically the same curve was reported by Cogswell and Wissbrun (1996), based on the observations of five different groups of investigators. In Fig. 15.46 also N_1 , the first normal stress difference, is presented as a continuously increasing function of shear rate. In liquid crystalline polymers, in particular in lyotropic LCPs (see Chap. 16) N_1 often reaches a maximum, then decreases even to negative values

at higher shear rates; subsequently N_1 increases again to positive values at still higher shear rates. It is not clear yet if this is also the case in this polymer Vectra 900, although it is the polymer that has been studied by many independent investigators (Cogswell and Wissbrun, 1996).

It is amazing that in many cases the viscosity and the first normal stress differences are reported together: it would be wise to compare the viscosity and the first normal stress coefficient, Ψ_1 , because these both are material properties. For that reason in Fig. 15.46, the present author also incorporated Ψ_1 . It also seems to reach a Region II.

Another peculiar property of LCPs is shown in Fig. 15.47, where the transient behaviour of the shear stress after start up of steady shear flow is shown for Vectra A900 at 290 °C at two shear rates. We will come back to this behaviour in Chap. 16 for lyotropic systems where this behaviour is quite common and in contradistinction to the transient behaviour of conventional polymers, as presented in Fig. 15.9. This damped oscillatory behaviour is also found for simple rheological models as the Jeffreys model (Te Nijenhuis 2005) and according to Burghardt and Fuller, it is explicable by the classic Leslie–Ericksen theory for the flow of liquid crystals, which tumble, rather than align, in shear flow. Moreover, it is extra complicated due to the interaction between the tumbling of the molecules and the evolving defect density (polynomial structure) of the LCP, which become finer, at start up, or coarser, after cessation of flow.

According to Gotsis and Odriozola (2000) the uniaxial elongational viscosity of the thermotropic liquid crystalline polymer Vectra A950 is much higher than three times the shear viscosity at equivalent strains. Further, it is strain-hardening and depends on the flow and thermal history of the sample. A modification of mesoscopic theory of Larson and Doi (1991) can predict the stress growth in elongational flows. The elongational rheology of LCPs at low strain rates seems to be influenced strongly by the domain texture, which cannot become a monodomain, even at high stretch ratios and at very high levels of average orientation. The extensional viscosity of polydomain LCPs is higher when the initial texture is finer.

Some of the more than 35 known Liquid Crystal phases are illustrated in Fig. 15.48.

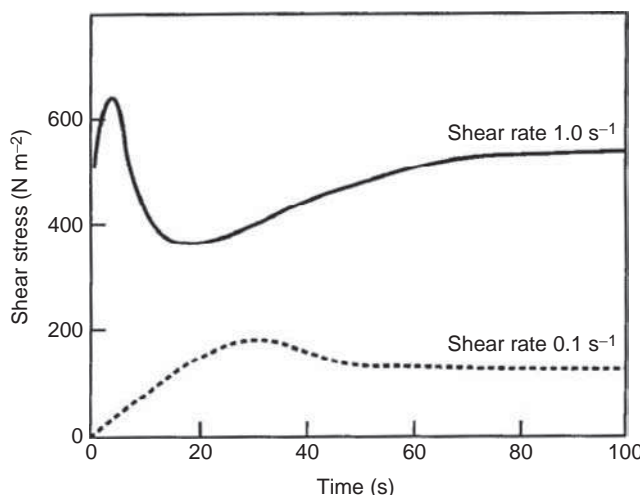


FIG. 15.47 Transient behaviour after start up of steady state flow in Vectra A900 at 290 °C at shear rates of 0.1 and 1 s⁻¹, based on results of Guskey and Winter (1991). From Cogswell and Wissbrun, 1996. Courtesy Chapman & Hall.

Liquid Crystal Phases (known approx. 35 and rising)

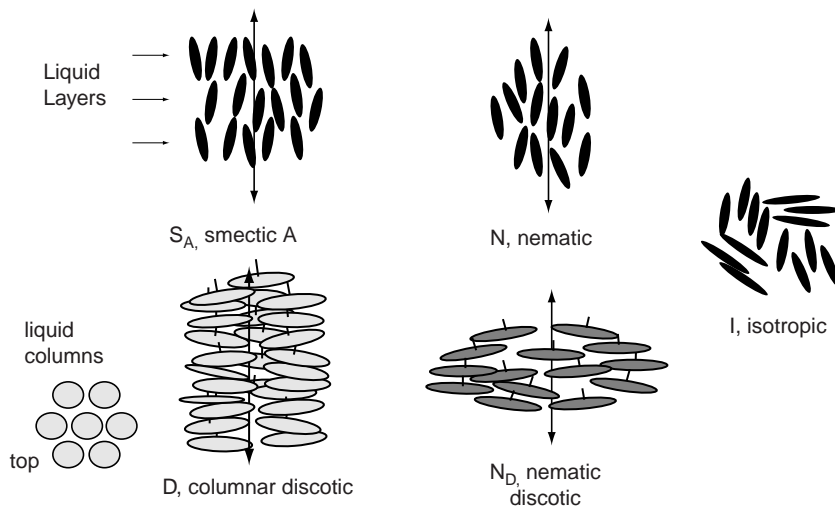


FIG. 15.48 Schematic view of some liquid crystal phases. Kindly provided by Prof. S.J. Picken (2003).

Nematic phases are characterised by a uniaxial symmetry of the molecular orientation distribution function $f(\theta)$, describing the probability density of finding a rod with its orientation between θ and $\theta + d\theta$ around a preferred direction, called the director \mathbf{n} (see Fig. 15.49). An important characteristic of the nematic phase is the order parameter $\langle P_2 \rangle$, also called the *Hermanns orientation function* (see also the discussion of oriented fibres in Sect. 13.6):

$$\langle P_2 \rangle = \frac{1}{2}(3\langle \cos^2 \theta \rangle - 1) = 1 - \frac{3}{2}\langle \sin^2 \theta \rangle \quad (15.110)$$

where θ is the angle of an individual molecule (described by the vector \mathbf{u} (in Fig. 15.49) and the director \mathbf{n} . The order parameter is zero for isotropic systems, $-\frac{1}{2}$ for fully perpendicular alignment and 1 for perfect parallel alignment. Several models describing the phase transitions from isotropic to nematic result in different predictions regarding the order parameter in the nematic phase: it jumps from zero to 0.44 or 0.84 in the various models (see, e.g. Fig. 15.50). The quality of the alignment of the orientation director might be very good, but if the molecular orientation is not high, the overall result is poor.

The big difference between normal isotropic liquids and nematic liquids is the effect of anisotropy on the viscous and elastic properties of the material. Liquid crystals of low molecular weight can be Newtonian anisotropic fluids, whereas liquid crystalline polymers can be rate and strain dependent anisotropic non-Newtonian fluids. *The anisotropy gives rise to 5 viscosities and 3 elastic constants*. In addition, the effective flow properties are determined by the flow dependent and history dependent texture. This all makes the rheology of LCPs extremely complicated.

The five viscosities are the Miesowicz viscosities, called after Miesowicz, who introduced them already in 1946. The background of the first three viscosities is shown in Fig. 15.51 (Jadzyn and Czechowski, 2001): η_1 where the director is perpendicular to the direction of flow; η_2 where the director is perpendicular to the velocity gradient and η_3 where the director is perpendicular to both the flow direction and the

velocity gradient. The fourth viscosity η_{12} is the extensional viscosity and the fifth one γ_1 is a rotational viscosity.

The three elastic constants are the Frank elastic constants, called after Frank, who introduced them already in 1958. They originate from the deformation of the director field as shown in Fig. 15.52. A continuous small deformation of an oriented material can be distinguished into three basis distortions: *splay*, *twist* and *bend* distortions. They are required to describe the resistance offered by the nematic phase to orientational distortions. As an example, values for Miesowicz viscosities and Frank elastic constants are presented in Table 15.10. It should be mentioned that those material constants are not known for many LCs and LCPs. Nevertheless, they have to be substituted in specific rheological constitutive equations in order to describe the rheological peculiarities of LCPs. Accordingly, the viscosity and the dynamic moduli will be functions of the Miesowicz viscosities and/or the Frank elastic constants. Several theories have been presented that are more or less able to explain the rheological peculiarities. Well-known are the Leslie–Ericksen theory and the Larson–Doi theory. It is far beyond the scope of this book to go into detail of these theories. The reader is referred to, e.g. Acierno and Collyer (General References, 1996).

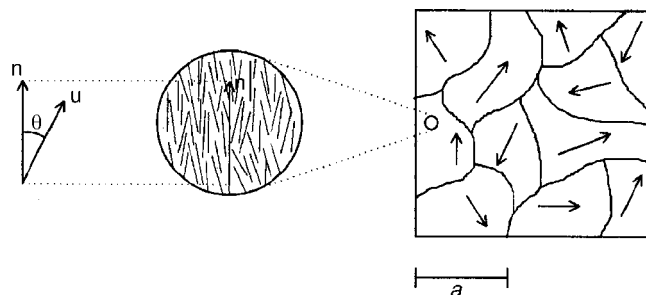


FIG. 15.49 Orientation angle θ between rodlike molecules, described by unit vector \mathbf{u} and director \mathbf{n} within one nematic domain of a macroscopically isotropic polydomain sample; a denotes the size of the domain. From Beekmans, 1997.

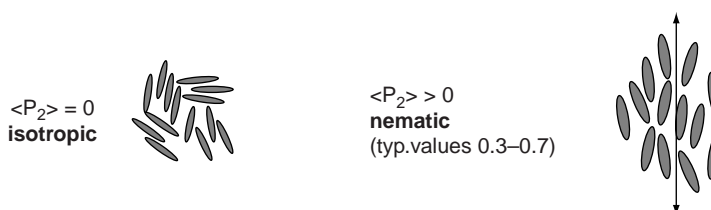


FIG. 15.50 Order parameters of rodlike molecules in the isotropic and the nematic states. Kindly provided by Prof. S.J. Picken (2003).

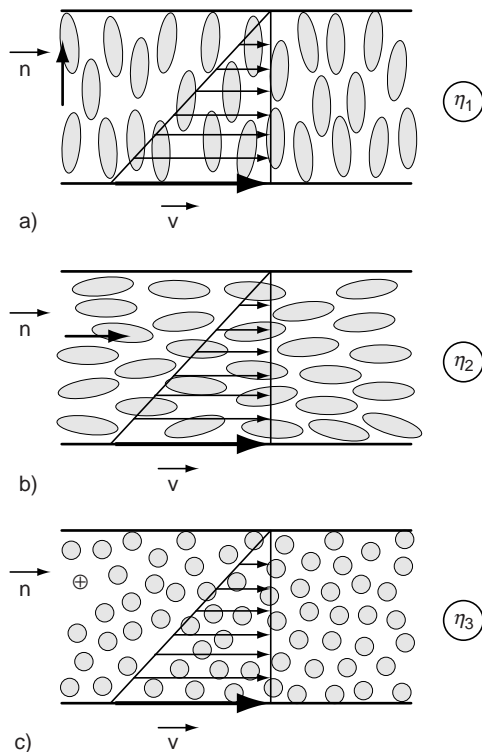


FIG. 15.51 The experimental conditions for measurement of the first three Miesowicz viscosities of nematic liquid crystals: (A) $\mathbf{n} \perp \mathbf{v}$ and $\mathbf{n} \parallel \text{grad } \mathbf{v}$; (B) $\mathbf{n} \parallel \mathbf{v}$ and $\mathbf{n} \perp \text{grad } \mathbf{v}$; (C) $\mathbf{n} \perp \mathbf{v}$ and $\mathbf{n} \perp \text{grad } \mathbf{v}$. From Jadzyn and Czechowski, 2001. Courtesy IPO Publishing.

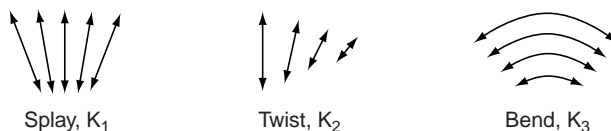


FIG. 15.52 Elastic responses due to the deformation of the director field: Frank elastic constants. Kindly provided by Prof. S.J. Picken (2003).

TABLE 15.10 Some values for the Miesowicz viscosities and Frank elastic constants

Low MW (MBBA 25 °C) ^a	Polymers
$\eta_1 = 121 \times 10^{-3} \text{ N s/m}^2$	Viscosities of the order of magnitude: 500–10,000 N s/m ²
$\eta_2 = 24 \times 10^{-3} \text{ N s/m}^2$	
$\eta_3 = 42 \times 10^{-3} \text{ N s/m}^2$	Aramid solutions (80 °C): $\sigma_{sh} = 1200q^{0.7}$ (power law)
$\eta_{12} = 6.5 \times 10^{-3} \text{ N s/m}^2$	
$\gamma_1 = 95 \times 10^{-3} \text{ N s/m}^2$	PBG in <i>m</i> -cresol (20 °C):
$K_1 = 7.1 \times 10^{-12} \text{ N}$	$K_1 = 4.1 \times 10^{-12} \text{ N}$
$K_2 = 4.0 \times 10^{-12} \text{ N}$	$K_2 = 0.36 \times 10^{-12} \text{ N}$
$K_3 = 9.2 \times 10^{-12} \text{ N}$	$K_2 = 4.7 \times 10^{-12} \text{ N}$

^a MBBA = N-(*p*-methoxybenzilidene)-*p*-butylaniline.

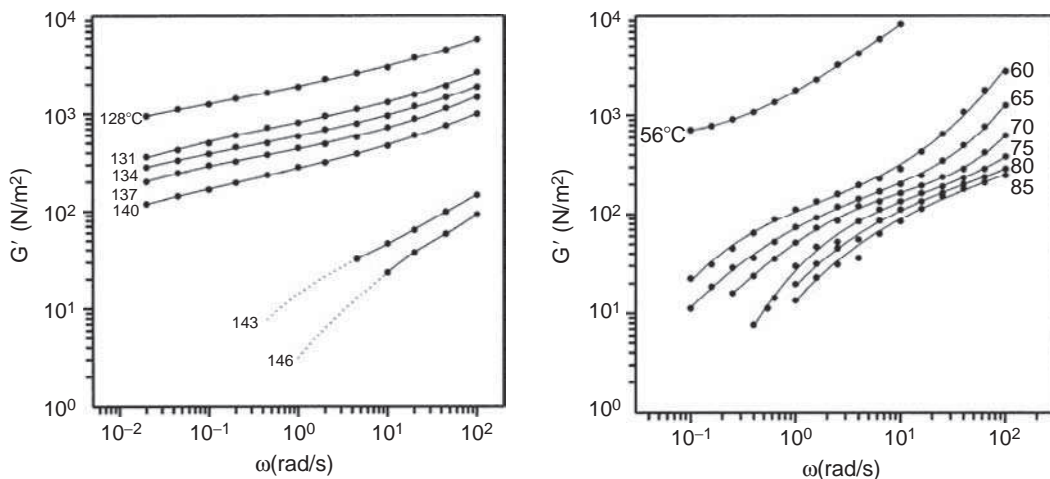
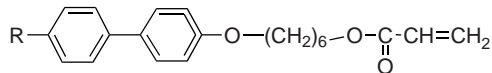


FIG. 15.53 Storage moduli vs. angular frequency as functions of temperature for (A) Polymer 1; and (B) Polymer 2. From Rottink et al. (1993). Courtesy Springer Verlag.

15.7.2. Thermotropic side chain liquid crystalline polymers, SCLCPs

The study of rheological properties of SCLCPs has been much less the subject of investigation than those of MCLCPs. The reason is that the application of SCLCPs is much more sophisticated than of MCLCPs, such as, e.g. data storage and switching of displays. Nevertheless, measurement of viscosity and dynamic mechanical properties is of importance as one of the means of structure determination. A first example is given in Fig. 15.53 (Rottink et al., 1993). The storage moduli of two acrylic polymers with mesogenic side groups (for their monomers: see Scheme 15.1) are plotted vs. angular frequency. Their characteristics are shown in Table 15.11. Polymer 1 is an LCP, with transitions: K 129 °C S_a 140 °C N 148 °C I, whereas polymer 2 shows only crystalline behaviour with a melting point of 57 °C, notwithstanding the LC behaviour of the side group. In Fig. 15.53 (left) two transitions are clearly visible: one between 128 and 131 °C, from crystalline to smectic-A, and one between 140 and 143 °C, from the smectic-A to the nematic state. The third transition, from the nematic to the isotropic state at 148 °C was not detectable with the rheogoniometer used. The second polymer, in Fig. 15.53 (right) only shows the transition from the crystalline to the isotropic state between 56 and 60 °C. The mesogenic structure of the side chains comes into view in the isotropic state: instead of liquid-like behaviour with



SCHEME 15.1 Mesogenic acrylate monomer; 1: R = OCH₃; 2: R = H.

TABLE 15.11 Characteristics of polymers P1 and P2

Polymer	Mn (kg/mol)	Mw (kg/mol)	Phase behaviour	T _g (°C)
1	9.0	22.5	K 129 S _a 140 N 148 I	65
2	7.9	22.4	K 57 I	48

slope 2 at low frequencies, a clear transition is present. Apparently, this is the result of interaction between the side groups in the formation of a fragile network. This kind of interactions is only visible in dynamic mechanical behaviour.

A second example is shown in Fig. 15.54 (Jin, 1995), where the storage moduli of polyurethane with N-substituted HMDI-nitrostilbene mesogenic side groups (see Scheme 15.2) are presented as a function of angular frequency. This SCLCP has a clearing temperature of 57 °C. A very distinct, large drop between 53 and 58 °C is visible. This is attributed to the dissociation of the double layer smectic structures. At higher temperatures around 82–87 and 117–122 °C two other moderate gaps are discernable. The first one is attributed to the breakdown of part of the hydrogen bonds between the polymer chains and the second one might be the result of breakdown where also the nitrostilbene dipoles are involved.

The conclusion is for SCLCPs that the study of viscoelastic properties is a powerful tool in revealing the occurrence of possible transitions, thus of changes in structure, but it is in general not possible to fully characterise the SCLCP structure by this method only. For that purpose also other, independent techniques are needed. By combination of results obtained from rheological investigations and at least one other technique, insight into the SCLCP structure can be deepened tremendously. In many cases, even only ripples are detectable, in, e.g. DSC, IR or X-ray diffraction measurements, whereas rheological investigations show some clear transition. Hence, one discovers where to look at in the other techniques (Te Nijenhuis, 1997).

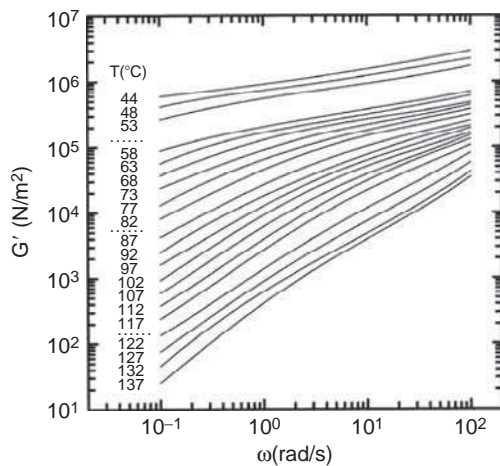
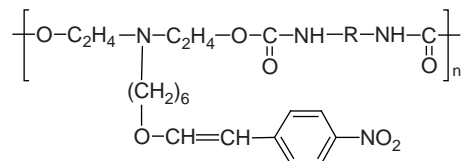


FIG. 15.54 Storage moduli vs. angular frequency as functions of temperature for a Polyurethane-HMDI SCLCP with a clearing temperature of 57 °C. From Jin (1995).



SCHMЕE 15.2 Polymer PU-HMDI.

APPENDIX I

Flow of polymer melts through narrow tubes and capillaries

For the flow of a Newtonian fluid through a capillary the Hagen–Poiseuille law is:

$$Q = \frac{\pi R^4}{8\eta} \frac{\Delta p}{L} \quad (\text{m}^3/\text{s}) \quad (15.A1)$$

where Q is the volume flow rate, R the capillary radius and $\Delta p/L$ the pressure gradient.

The shear stress at the wall and the shear rate at the wall of a Newtonian fluid are:

$$\sigma_w = \frac{R \Delta p}{2 L} \quad \text{and} \quad q_w = \frac{4Q}{\pi R^3} \quad (15.A2)$$

The equation for the shear stress at the wall is equal for Newtonian and non-Newtonian liquids, but the shear rate at the wall is for non-Newtonian liquids different from that in this equation.

If the melt is non-Newtonian, corrections have to be made, the Bagley correction and the Rabinowitz correction.

(a) Bagley correction

The first correction is for entrance and end effects and was suggested by Bagley (1957). Due to these effects, in the calculation of the shear stress at the wall one has to use an effective flow length L_{eff} :

$$\sigma_w = \frac{R \Delta p}{2 L_{\text{eff}}} = \frac{\Delta p}{2 \left(\frac{L}{R} + e \right)} \quad (15.A3)$$

e being a correction factor which can be determined by plotting (at constant shear rate) Δp vs. L/r .

(b) Rabinowitsch correction

The second correction is for the non-Newtonian character as such. It is the so-called correction of Rabinowitsch (1929).

For non-Newtonian liquids, an *apparent* shear rate at the wall is defined to be

$$q_a = \frac{4Q}{\pi R^3} \quad (15.A4)$$

which is certainly not equal to the real shear rate at the wall. With the aid of this definition the shear rate at the wall can be written as

$$q_w = \frac{3}{4} q_a + \frac{1}{4} \sigma_w \frac{dq_a}{d\sigma_w} = q_a \left(\frac{3}{4} + \frac{1}{4} \frac{d \log q_a}{d \log \sigma_w} \right) = \frac{4Q}{\pi R^3} \left(\frac{3}{4} + \frac{1}{4} \frac{d \log Q}{d \log \Delta p} \right) \quad (15.A5)$$

Accordingly, the shear rate at the wall can be found by measuring the volume flow rate Q as a function of the pressure Δp and subsequently plotting $\log Q$ vs. $\log \Delta p$. The slope at every point in the curve gives then, with the aid of Eq. (15.A5), the value of the shear rate at

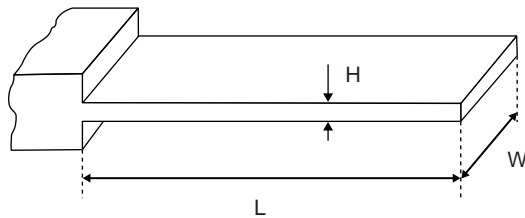


FIG. 15.A1 Schematic view of a slit rheometer.

the wall. For Newtonian liquids this slope is equal to 1, so that the result is equal to that in Eq. (15.A2). For a power law fluid the slope is equal to $1/n$, so that the shear rate at the wall is then equal to

$$\dot{\gamma}_w = \frac{4Q}{\pi R^3} \frac{3n+1}{4n} \quad (15.A6)$$

For slit rheometers of rectangular cross-section, with length L and sides W and H ($L \gg W \gg H$) (see Fig. 15.A1) the shear rate at the wall is given by

$$\dot{\gamma}_w = \dot{\gamma}_a \left(\frac{2}{3} + \frac{1}{3} \frac{d \log \dot{\gamma}_a}{d \log \sigma_w} \right) = WH^2 \left(\frac{2}{3} + \frac{1}{3} \frac{d \log Q}{d \log \Delta p} \right) \quad (15.A7)$$

where the apparent shear rate at the wall is equal to

$$\dot{\gamma}_a = \frac{6Q}{WH^2} \quad (15.A8)$$

APPENDIX II

Analysis of flow in processing operations

In the processing equipment of thermoplastics, many kinds of complicated flow configurations exist. The flow in a tapered die, for example, produces three components of deformation: that due to flow from the reservoir into the die; that due to telescopic shear within the die; that due to extensional flow within the die. These may be assumed separable and the separately calculated pressure drops may be added to give the total pressure drop. But in addition, each deformation mechanism contributes to post extrusion swelling. The components due to simple shear and extension at the die exit determine the swell ratio.

Table 15.12 gives a survey of the more important rheological equations. Figs. 15.36 and 15.37 (already discussed) show the relationship between swelling ratio and recoverable strain. It is far beyond the scope of this book to go into detail of this subject. The interested reader is referred to, e.g. Collyer (1993), Collyer and Clegg (1998) and Denys (2003).

TABLE 15.12 Some important rheological equations

Class of flow	Pressure drop			Swell ratio
	Shear	Extensional	Die entry	
(1) Constant section die Circular: long	$2L\sigma_{sh}/R$	0	$\frac{4\sqrt{2}}{3(n+1)}\dot{\gamma}(\eta\eta_e)^{1/2}$	$B_{SR} = \left[\frac{2}{3}\gamma_w \left\{ \left(1 + \frac{1}{\gamma_w^2} \right)^{3/2} - \frac{1}{\gamma_w^3} \right\} \right]^{1/2}$
Circular: zero length	0	0	$\frac{4\sqrt{2}}{3(n+1)}\dot{\gamma}(\eta\eta_e)^{1/2}$	$B_{ER} = (\exp \varepsilon_w)^{1/2}$
Slit: long	$2L\sigma_{sh}/H$	0	$\frac{4}{3(n+1)}\dot{\gamma}(\eta\eta_e)^{1/2}$	$\begin{cases} B_{ST} = \left[\frac{1}{2} \left\{ (1 + \gamma_w^2)^{1/2} + \frac{1}{\gamma_w} \ln \left\{ \gamma_w + (1 + \gamma_w^2)^{1/2} \right\} \right\} \right]^{1/3} \\ B_{SH} = B_{ST}^2 \end{cases}$
Slit: zero length	0	0	$\frac{4}{3(n+1)}\dot{\gamma}(\eta\eta_e)^{1/2}$	$\begin{cases} B_{ET} = (\exp \varepsilon_w)^{1/4} \\ B_{EH} = B_{ET}^2 \end{cases}$
(2) Tapered section die Coni- cylindrical	$\frac{2\sigma_{sh}}{3n \tan \theta} [1 - (R_1/R_o)^{3n}]$	$\frac{1}{3}\eta_e \dot{\gamma} \tan \theta [1 - (R_1/R_o)^3]$ $\left(\dot{\varepsilon}_{max} = \frac{1}{2} \left(\frac{3n+1}{n+1} \right) \dot{\gamma} \tan \theta \right)$	$\frac{4\sqrt{2}}{3(n+1)}\dot{\gamma}_o(\eta\eta_e)^{1/2}$ $\left(\sigma_{max} = \frac{3}{8} (3n+1) P_o \right)$	$\begin{cases} B_{SR} = \left[\frac{2}{3}\gamma_w \left\{ (1 + 1/\gamma_w^2)^{3/2} - 1/\gamma_w^3 \right\} \right]^{1/2} \\ B_{ER} = (\exp \varepsilon_w)^{1/2} \end{cases}$

(continued)

TABLE 15.12 (continued)

Class of flow	Pressure drop			Swell ratio
	Shear	Extensional	Die entry	
Wedge	$\frac{2\sigma_{sh}}{2n\tan\theta} [1 - (H_1/H_o)^{2n}]$	$\frac{1}{2}\sigma_{av}[1 - (H_1/H_o)^2]$ $\left(\dot{\varepsilon}_{max} = \frac{1}{3}\dot{\gamma}\tan\theta \right)$	$\frac{4}{3(n+1)}\dot{\gamma}(\eta_e)^{1/2}$	$\begin{cases} B_{ET} = (\exp \varepsilon_w)^{1/4} \\ B_{EH} = B_{ET}^2 \end{cases}$
(3) Spreading disc flow (circular disc, centre gate)				
Isothermal	$\frac{2CQ^n R^{1-n}}{(1-n)x^{1+2n}}$	$\frac{\eta_e Q}{4\pi x R^2}$		
Non-isothermal	$\frac{2CQ^n R^{1-n}}{(1-n)(xZ)^{1+2n}}$	$\frac{\eta_e Q}{4\pi x R^2 Z}$		

Data from Powell (1974), Cogswell (1970), Cogswell and McGowan (1972) and Barrie (1970).

B_{SR} – swelling ratio in radial direction; B_{ST} – swelling ratio in transverse direction; B_{SH} – swelling ratio in thickness direction; B_{ER} – tensile swelling ratio in radial direction for $L \rightarrow 0$; B_{ET} – tensile swelling ratio in transverse direction for $L \rightarrow 0$; B_{EH} – tensile swelling ratio in thickness direction for $L \rightarrow 0$; C – power law constant; H – die gap; H_o – entry die gap; H_1 – exit die gap; L – length of section; n – power law exponent; P_o – entry pressure; Q – volume flow rate; R – radius; R_o – entry radius; R_1 – exit radius; W – width of wedge; x – separation of plates; Z – effective thickness correction factor; $\dot{\gamma}$ – shear rate = $4Q/(\pi R^3)$ or $3Q/(2WH^2)$; γ_R – recoverable shear strain = σ_{sh}/G ; ε – tensile strain; ε_R – recoverable tensile strain = σ_e/E ; $\dot{\varepsilon}$ – tensile strain rate; η – shear viscosity; θ – half angle of taper; τ – relaxation time; η_e – extensional viscosity; σ_e – tensile stress; σ_{sh} – shear stress = $C(4Q/\pi R^3)^n$.

BIBLIOGRAPHY

General references

- Acieno D and Collyer AA (Eds), "Rheology and Processing of Liquid Crystal Polymers", Chapman and Hall, London, 1996.
- Astarita G, Marucci G and Nicolais L (Eds), "Rheology", Vols. 1, 2 and 3, Plenum Press, New York, 1980.
- Barnes HA, Hutton JF and Walters K, "An Introduction to Rheology", Elsevier, Amsterdam, 1989.
- Bird RB, Armstrong RC and Hassager O, "Dynamics of Polymeric Liquids", Vol. 1, "Fluid Mechanics", Wiley, New York, 1987.
- Brydson JA, "Flow Properties of Polymer Melts", George Godwin, London, 2nd Ed., 1981.
- Bueche F, "Physical Properties of Polymers", Interscience, New York, 1962.
- Dealy JM and Wissbrun KF, "Melt Rheology and its Role in Plastics Processing", Van Nostrand Reinhold, New York, 1990.
- De Gennes PG, "The Physics of Liquid Crystals", Clarendon Press, Oxford, 1974.
- De Gennes PG, "Scaling Concepts in Polymer Physics", Cornell University Press, Ithaca, NY, 1979.
- Doi M and Edwards SF, "The Theory of Polymer Dynamics", Oxford, Clarendon Press, 1986.
- Eirich FR (Ed), "Rheology", 5 Vols, Academic Press, New York, 1956–1969.
- Ferry JD, "Viscoelastic Properties of Polymers", Wiley, New York, 1961; 2nd Ed, 1970; 3rd Ed, 1980.
- Frederickson AG, "Principles and Applications of Rheology", Prentice-Hall, Englewood Cliffs, NJ, 1964.
- Glasstone S, Laidler KJ and Eyring H, "The Theory of Rate Processes", McGraw-Hill, New York, 1941.
- Greassley WW, "The Entanglement Concept in Polymer Rheology", Adv Polym Sci 16 (1974) 1–179.
- Harris J (Ed), "Karl Weissenberg, 80th Birthday Celebration Essays", East African Literature Bureau, Nairobi, 1973; <http://innfm.swan.ac.uk/bsr/weissenburg/index.htm>.
- Janeschitz-Kriegel H, "Flow Birefringence of Elastico-Viscous Polymer Systems", Adv Polym Sci 6 (1969) 170–318.
- Janeschitz-Kriegel H, "Polymer Melt Rheology and Flow Birefringence", Springer, Berlin, 1983.
- Larson RG, "Constitutive Equations for Polymer Melts and Solutions", Butterworth, London, 1988.
- Larson RG and Doi M, J Rheol 35 (1991) 539.
- Lodge AS, "Elastic Liquids", Academic Press, New York, 1964.
- Macosko CW, "Rheology: Principles, Measurements and Applications", VCH Publishers, New York, 1994.
- Mason P and Wookey N (Eds), "The Rheology of Elastomers", Pergamon Press, New York, 1958; 2nd Ed, 1964.
- Middleman S, "The Flow of High Polymers", Interscience, New York, 1968.
- Nguyen TQ and Kausch H-H, "Flexible Polymer Chain Dynamics in Elongational Flow", Springer, Berlin, 1999.
- Reiner M, "Deformation and Flow", Lewis, London, 1948.
- Rohn LR, "Analytical Polymer Rheology; Structure–Processing–Property Relationships", Carl Hanser, Munich, 1995.
- Strobl G, "The Physics of Polymers", Springer, Berlin, 2nd Ed, 1997.
- Tadmor Z and Gogos CG, "Principles of Polymer Processing", Wiley, New York, 2nd Ed, 2006.
- Te Nijenhuis K, "Rheology of Polymeric Liquids", 4th impression, Delft, 2nd Ed, 2005.
- Te Nijenhuis K, "Viscoelastic Polymeric Fluids" Chap. 9.1 and "Entrance Correction and Extrudate Swell" Chap. 9.4 in Tropea C Yarin AL and Foss JF (Eds), "Handbook of Experimental Fluid Mechanics", Springer, Berlin, 2007, Chap. 9.1.
- Vinogradov GV and Malkin AYA, "Rheology of Polymers: Viscoelasticity and Flow of Polymers", Springer, Berlin, 1980.
- Walters K, "Rheometry", Chapman & Hall, London, 1975.

Special references

- Adamse JWC, Janeschitz-Kriegel H, Den Otter JL and Wales JLS, J Polym Sci A2–6 (1968) 871.
- Andrade, Da Costa EN, Nature 125 (1930) 309, 582.
- Bagley EB, J Appl Phys 28 (1957) 624; Trans Soc Rheol 5 (1961) 355.
- Barnett SM, Polym Eng Sci 7 (1967) 168.
- Barrie IT, Plastics and Polymers 38 (1970) 47.
- Bartos O, J Appl Phys 35 (1964) 2767.
- Batchinski AJ, Z physik Chem 84 (1913) 643.
- Beekmans F, "Rheology and Changes in Structure of Thermotropic Liquid Crystalline Polymers", PhD Thesis, Delft, 1997.
- Benbow JJ and Lamb P, SPE Trans 3 (1963) 1.
- Berry GC and Fox TG, Adv Polym Sci 5 (1968) 261.
- Bertola V, Meulenbroek B, Wagner C, Storm C, Mozorov A, Van Saarloos W and Bonn D, Phys Rev Lett 90 (2003) 114502.
- Boger DV and Walters K, "Rheological Phenomena in Focus", Elsevier, Amsterdam, 1993
- Bueche F, J Chem Phys 20 (1952) 1959; 22 (1954) 603; 25 (1956) 599.
- Bueche F, (1962): see General references.

- Burghardt WR and Fuller GG, *J Rheol* 34 (1990) 959, *Macromolecules* 24 (1991) 2546.
- Carreau PJ, PhD Thesis, Univ of Wisconsin, 1969.
- Clegg PL, in "Rheology of Elastomers" (1958): see General references; *Brit Plastics* 39 (1966) 96.
- Cogswell FN, *Plastics Polym* 38 (1970) 391.
- Cogswell FN, *Polym Eng Sci* 12 (1972) 64.
- Cogswell FN, in Chapoy LL (Ed), "Recent Advances in Liquid Crystalline Polymers", Elsevier Applied Science Publishers, 1985, Chap. 10.
- Cogswell FN and Lamb P, *Plastics Polym* 38 (1970) 331.
- Cogswell FN and McGowan JC, *Brit Polym J* 4 (1972) 183.
- Cogswell FN and Wissbrun KF, "Rheology and Processing of Liquid Crystal Polymer Melts" in Acierno D and Collyer AA (Eds), "Rheology and Processing of Liquid Crystal Polymers", Chapman and Hall, London, 1996, Chap. 4.
- Cogswell FN, Webb PC, Weeks JC, Maskell SG and Rice PDR, *Plastics Polym* 39 (1971) 340.
- Collyer AA, "Techniques in Rheological Measurement", Chapman & Hall, London, 1993.
- Collyer AA, Clegg DW (Eds), "Techniques in Rheological Measurement", Kluwer Academic Publishers, Boston, 2nd Ed, 1998.
- Cornelissen J and Waterman HI, *Chem Eng Sci* 4 (1955) 238.
- Cote JA and Shida MJ, *Appl Polym Sci* 17 (1973) 1639.
- Cox WP and Merz EH, *J Polym Sci* 28 (1958) 619.
- Cross MM, *J Colloid Sci* 20 (1965) 417.
- Cross MM, in Wetton RE and Whorlow RW (Eds), "Polymer Systems: Deformation and Flow", Macmillan, London, 1968.
- De Gennes PG, *Eur Phys J*, E23 (2007) 3.
- Denys KFJ, "Flow of Polymer Solutions through Porous Systems", PhD Thesis, Delft, 2003.
- De Waele A, *J Oil Col Chem Assoc* 4 (1923) 33.
- Doolittle AK, *J Appl Phys* 22 (1951) 1031, 1471; 23 (1952) 236.
- Ellis SB, see Reiner M (Ed), "Deformation, Strain and Flow", Interscience, New York, 1960, p 246.
- Everage AE and Ballman RL, *J Appl Polym Sci* 18 (1974) 933.
- Eyring H (1941): see General references Glasstone et al.
- Ferrari AG, *Wire and Wire Products* 39 (1964) 1036.
- Ferry JD, *J Am Chem Soc* 64 (1942) 1330.
- Fox TG and Allen VR, *J Chem Phys* 41 (1964) 344.
- Fox TG and Loshaek S, *J Polym Sci* 15 (1955) 371.
- Fox TG, Gratch S and Loshaek S, in "Rheology" in Eirich FR (Ed), Academic Press, New York, Vol. 1, 1956, p 431.
- Gortemaker FH, Hansen MG, De Cindio B, Laun HM and Janeschitz-Kriegl H, *Rheol Acta* 15 (1976) 256.
- Gotsis AD and Odriozola MA, *J Rheol* 44 (2000) 1205.
- Greassley WW, *J Chem Phys* 47 (1967) 1942.
- Greassley WW and Segal L, *AIChE J* 16 (1970) 261.
- Greassley WW, Glasscock SD and Crawley RL, *Tran Soc Rheol* 14 (1970) 519.
- Gregory DR, *J Appl Polym Sci* 16 (1972) 1479, 1489.
- Guskey SM and Winter HH, *J Rheol* 35 (1991) 1191.
- Han CD, Charles M and Philippoff W, *Trans Soc Rheol* 14 (1970) 393.
- Han CD, Kim KU, Siskovic N and Huang CR, *J Appl Polym Sci* 17 (1973) 95.
- Hellwege KH, Knappe W, Paul P and Semjonow V, *Rheol Acta* 6 (1967) 165.
- Holzmüller W and Dinter R, *Exp Techn Physik*, 8 (1960) 118.
- Howells ER and Benbow JJ, *Trans Plastic Inst* 30 (1962) 240.
- Hudson NE and Jones TER, *J Non-Newtonian Fluid Mech* 46 (1993) 69.
- Jadzyn J and Czechowski G, *J Phys: Condensed Matter* 13 (2001) L261–L265.
- James DF and Walters K, "A Critical Appraisal of Available Methods for the Measurement of Extensional Properties of Mobile Systems" in Collyer AA (Ed), "Techniques in Rheological Measurement", Chapman & Hall, London, 1993.
- Jin S, "Synthesis and Characterization of Side-Chain Liquid Crystalline Polyesters and Polyurethanes", PhD Thesis, Delft, 1995.
- King RG, *Rheol Acta* 5 (1966) 35.
- Kissi NE and Piau J-M, "Stability Phenomena During Polymer Melt Extrusion" in Piau J-M and Agassant J-F (Eds), "Rheology for Polymer Melt Processing", Rheology Series, Vol. 5, Elsevier, Amsterdam, 1996, pp 389–420.
- Langelaan HC and Gotsis AD, *J Rheol* 40 (1996) 107.
- Laun HM, *Rheol Acta* 17 (1978) 1.
- Litt M, *Polym Preprints* 14 (1973) 109.
- Magill JH and Greet RJ, *Ind Eng Chem Fundamentals* 8 (1969) 701.
- Meissner J, *Kunststoffe* 61 (1971) 576, 688.

- Meissner J, *Rheol Acta* 10 (1971) 230.
- Meissner J, *Trans Soc Rheol* 16 (1972) 405.
- Metzner AB, Houghton WT, Sailor RA and White JL, *Trans Soc Rheol* 5 (1961) 133.
- Metzner AB, Uebler EA and Chan Man Fong CF, *AIChE J* 15 (1969) 750.
- Meulenbroek B, Storm C, Bertola V, Wagner C, Bonn D and Van Saarloos W, *Phys Rev Lett* 90 (2003) 024502.
- Mills NJ *Europ Polym J* 5 (1969) 675.
- Münstedt H, *J Rheol* 23 (1979) 421.
- Münstedt H, Kurzbeck S and Egersdörfer, *Rheol Acta* 37 (1998) 21.
- Münstedt H and Laun HM, *Rheol Acta* 18 (1979) 492.
- Onogi S and Asada T, "Rheo-Optics of Polymer Liquid Crystals", in "Rheology" (see Gen Ref: Astarita, Marrucci and Nicolai, Eds) Vol 1, pp 127-147.
- Ostwald Wo, *Kolloid-Z* 36 (1925) 99.
- Picken SJ, "Rheology of Liquid Crystals and Liquid Crystal Polymers", Lecture notes in Te Nijenhuis K, post academic RPK course on "Rheology", Utrecht & Delft 2003.
- Porter RS, Mac Knight WJ and Johnson JF, *Rubber Chem Technol* 41 (1968) 1.
- Powell PC, "Processing methods and properties of thermoplastic melts", in Ogorkiewicz RM (Ed), "Thermoplastics", Wiley, London, 1974, Ch 11.
- Rabinowitsch B, *Z physik Chem* A145 (1929) 1.
- Rottink JBH, Te Nijenhuis K, Addink R and Mijs WJ, *Polym Bull* 31 (1993) 221.
- Saeda S, *J Polym Sci (Phys)* 11 (1973) 1465.
- Shore JD, Ronis D, Piché L and Grant M, *Phys Rev Lett* 77 (1996) 655.
- Shore JD, Ronis D, Piché L and Grant M, *Phys Rev E* 55 (1997) 2976.
- Special issue *J Non-Newtonian Fluid Mech* 35, 2+3 (1990).
- Spencer RS and Dillon RE, *J Colloid Sci* 4 (1949) 241.
- Spriggs TW, University of Wisconsin-Madison, unpublished, 1965; see also Bird, Armstrong, Hassager, 1987 in General References.
- Stratton RA, *J Colloid Interface Sci* 22 (1966) 517.
- Tanner RI, *J Polym Sci A8* (1970) 2067; "Engineering Rheology", Oxford University Press, Oxford, 1985; 2nd Ed, 2000.
- Te Nijenhuis K, "Thermoreversible Networks", *Adv Polym Sci* 130 (1997) 1-267.
- Thomas DP, *Polym Eng Sci* 11 (1971) 305.
- Thomas DP and Hagan RS, *Polym Eng Sci* 9 (1969) 164.
- Tordella JP, *J Appl Phys* 27 (1956) 454; *Trans Soc Rheol* 1 (1957) 203; *Rheol Acta* 2/3 (1961) 216.
- Van der Vegt AK, *Trans Plastics Inst* 32 (1964) 165.
- Van Krevelen DW and Hoflyzer PJ, *Angew Makromol Chem* 52 (1976) 101.
- Vermant J, Moldenaers P, Picken SJ and Mewis J, *J Non Newt Fluid Mech* 53 (1994) 1.
- Vinogradov GV, *Pure Appl Chem* 26 (1971) 423.
- Vinogradov GV and Malkin AYA, *J Polym Sci A2* (1964) 2357.
- Vinogradov GV and Prozorovskaya NV, *Rheol Acta* 3 (1964) 156.
- Vinogradov GV, Malkin AYA, Yanovsky Yu G, Dzyura EA, Schumsky VF and Kulichikhin VG, *Rheol Acta* 8 (1969) 490.
- Vinogradov GV, Malkin AYA and Kulichikhin VG, *J Polym Sci A2-8* (1970) 333.
- Vinogradov GV, Radushkevich BV and Fikhman VD, *J Polym Sci A2-8* (1970) 1.
- Vinogradov GV, Yanovsky Yu and Isayev AI, *J Polym Sci A2-8* (1970) 1239.
- Wagner MH and Meissner J, *Makromol Chem* 181 (1980) 1533.
- Walker LM, Wagner NJ, Larson RG, Mirau PA and Moldenaers P, *J Rheol* 39 (1995) 925.
- Weissenberg K, *Nature* 159 (1947) 310.
- Westover RF, *SPE Trans* 1 (1961) 14.
- Williams ML, Landel RF and Ferry JD, *J Am Chem Soc* 77 (1955) 3701.
- Yasuda K, Armstrong RC and Cohen RE, *Rheol Acta* 20 (1981) 163.

This page intentionally left blank

CHAPTER 16

Rheological Properties of Polymer Solutions

The rheology of a polymer solution increases with the polymer concentration. A transition exists at the so-called critical concentration (which decreases with increasing molecular mass) separating "dilute" from "concentrated" solutions.

The viscosity of dilute polymer solutions can be estimated with fair accuracy.

For concentrated polymer solutions the viscosity is proportional to the 3.4th power of the molecular mass and about the 5th power of the concentration. The effects of temperature and concentration on viscoelastic properties are closely interrelated. The validity of a time-concentration superposition is shown. A method is given for predicting the viscosity of concentrated polymer solutions.

16.1. INTRODUCTION

The rheology of polymer solutions is a subject of considerable practical interest. It is important in several stages of the manufacturing and processing of polymers, e.g. in the spinning of fibres and the casting of films from solutions, and especially in the paints and coatings industry.

Despite the large amount of literature on this subject, the rheology of polymer solutions is less completely understood than that of polymer melts. This is because two more parameters are involved: the nature and the concentration of the solvent.

Theoretical investigations of the properties of polymer solutions may use two different starting points:

- a. The very dilute solution (nearly pure solvent)
- b. The pure solute (polymer melt)

These two approaches can be clearly distinguished in the literature on the rheology of polymer solutions. It is remarkable that both approaches use quite different methods. Only a few authors have tried to establish a relationship between the two fields of investigation.

In conformity with the literature, dilute polymer solutions and concentrated polymer solutions will be discussed separately in this chapter.

It is difficult to give an exact definition of the terms "dilute" and "concentrated". Usually there is a gradual transition from the behaviour of dilute to that of concentrated solutions, and the concentration range of this transition depends on a number of parameters. As a rule of thumb, however, a polymer solution may be called concentrated if the solute concentration exceeds 5% by weight.

16.2. DILUTE POLYMER SOLUTIONS

In Chap. 9 the following definition of the limiting viscosity number or intrinsic viscosity was given

$$[\eta] = \lim_{c \rightarrow 0} \frac{\eta - \eta_s}{\eta_s c} = \lim_{c \rightarrow 0} \frac{\eta_{sp}}{c} \quad (16.1)$$

where $\eta_{sp} \equiv \frac{\eta - \eta_s}{\eta_s}$; $[\eta]$ = intrinsic viscosity (m^3/kg); η = viscosity of the solution; η_s = viscosity of the solvent; c = solute concentration (kg/m^3).

Eq. (16.1) implies that the relationship between η_{sp} and c can be approximated by a linear proportionality as c approaches zero. At finite concentrations, however, the relationship between η_{sp} and c is certainly not linear. Therefore some extrapolation method is required to calculate $[\eta]$ from viscosity measurements at a number of concentrations.

The most popular extrapolation method was introduced by Huggins (1942):

$$\eta_{sp} = [\eta]c + k_H[\eta]^2c^2 \quad (16.2)$$

where k_H is called the Huggins constant.

Another well-known extrapolation formula was proposed by Kraemer (1938):

$$\ln \frac{\eta}{\eta_s} = [\eta]c - k_K[\eta]^2c^2 \quad (16.3)$$

where k_K is the so-called Kraemer constant.

In fact, several authors used both extrapolation methods for the calculation of $[\eta]$. In several cases this led to identical values of $[\eta]$. Moreover, it was found that

$$k_H + k_K \approx 0.5 \quad (16.4)$$

which was to be expected theoretically, provided η_{sp} is small, i.e. as long as $\ln(1 + \eta_{sp}) \approx \eta_{sp} - \frac{1}{2}\eta_{sp}^2$.

Eqs. (16.2) and (16.3) are truncated versions of the complete virial equation

$$\frac{\eta_{sp}}{c} = [\eta]\{1 + k_1[\eta]c + k_2[\eta]^2c^2 + k_3[\eta]^3c^3 + \dots\} \quad (16.5)$$

where $k_1 = k_H$.

Rudin et al. (1973) compared correlations with one, two and three terms of Eq. (16.5) and found that a two-term equation provided very accurate values of $[\eta]$. With a two-term equation (i.e. the Huggins equation) slightly different values of $[\eta]$ were found, but for most purposes the accuracy of these $[\eta]$ values was sufficient.

The coefficients of Eq. (16.5), however, proved to be very sensitive to the number of terms applied. Especially the coefficient $k_1 (= k_H)$ showed a large amount of scatter if it was calculated with the two-term Eq. (16.2). The scatter of k_1 was considerably reduced

with the three-term or four-term equation. This conclusion is confirmed by the large amount of scatter found in the literature values of k_H . These data generally cannot be correlated with other system parameters.

There seems to exist a correlation between k_H and the exponent a of the Mark–Houwink equation, $[\eta] = K(M_v)^a$, in the same polymer–solvent system, but owing to large variations in both k_H and a values, such a correlation cannot be determined exactly. As a general rule, for ordinary polymer solutions, showing values of $a \approx 0.7$, the Huggins constant is about $k_H \approx 0.4$. For θ -solutions, $0.5 < k_H < 0.64$, according to Sakai (1970). On the other hand, under conditions where the exponent a approaches the value 1.0, as in solutions of nylon 6,6 in formic acid, $k_H \approx 0.1$. Very approximately, the relationship between k_H and a could therefore be described as:

$$k_H + a \approx 1.1 \quad (16.6)$$

Table 16.1 shows values of k_H and a for some polymer–solvent systems.

Eq. (16.2) can be used for predicting the viscosity of a dilute polymer solution if the Huggins constant k_H is known. But literature values of k_H or values predicted with Eq. (16.6) are rather inaccurate. So they do not permit a good prediction of η .

TABLE 16.1 Huggins constants and a -values of polymer–solvent systems

Polymer	Solvent	k_H	a	$k_H + a$
Poly(methyl methacrylate)	Toluene	0.43	0.73	1.16
	Chloroform	0.32	0.82	1.14
	Benzene	0.35	0.76	1.11
	Acetone	0.48	0.70	1.18
	Butanone	0.40	0.72	1.12
Poly(vinyl acetate)	Acetone	0.37	0.70	1.07
	Chlorobenzene	0.41	0.56	0.97
	Chloroform	0.34	0.74	1.08
	Dioxane	0.34	0.74	1.08
	Methanol	0.47	0.59	1.06
	Toluene	0.50	0.53	1.03
	Benzene	0.37	0.65	1.02
Polystyrene	Toluene	0.37	0.72	1.09
	Cyclohexane	0.55	0.50	1.05
	Benzene	0.36	0.73	1.09
	Chloroform	0.33	0.76	1.09
	Butanone	0.38	0.60	0.98
	Ethylbenzene	0.23	0.68	0.91
	Decalin	0.60	0.56	1.16
Polybutadiene	Benzene	0.49	0.76	1.25
	Isobutyl acetate	0.64	0.50	1.14
	Cyclohexane	0.33	0.75	1.08
	Toluene	0.33	0.70	1.03
Average	—	—	—	1.08

Application of Eq. (16.5) would provide a prediction of the viscosity with a greater accuracy if the coefficients k_1 , k_2 , etc. were available. Lack of these data prohibits the application of this equation.

In order to overcome this difficulty, Rudin and Strathdee (1974) developed a semi empirical method for predicting the viscosity of dilute polymer solutions. The method is based on an empirical equation proposed by Ford (1960) for the viscosity of a suspension of solid spheres:

$$\frac{\eta_s}{\eta} = 1 - 2.5\varphi + 11\varphi^5 - 11.5\varphi^7 \quad (16.7)$$

where φ is the volume fraction of the suspended spheres.

Rudin and Strathdee assume that Eq. (16.7) may be used for dilute polymer solutions if is replaced by φ_{sp} , the volume fraction of the solvated polymer. They calculate φ_{sp} by

$$\varphi_{sp} = \frac{N_A c V_{sp} \varepsilon}{M} \approx \frac{c \varepsilon}{\rho} \quad (16.8)$$

where N_A = Avogadro's number (mol^{-1}); c = polymer concentration (kg/m^3); V_{sp} = volume of a solvated polymer molecule (m^3); ε = swelling factor (-); M = molecular weight of polymer (kg/mol); ρ = bulk polymer density (kg/m^3).

They further assume that ε is a linear function of φ_{sp} between two limits:

- (a) $\varphi_{sp} = 0$, i.e. at infinite dilution; here the swelling has its maximum value: $\varepsilon = \varepsilon_o$
- (b) $\varphi_{sp} = 0.524$, i.e. the occupied volume in cubical packing of uniform spheres; it is assumed that there is no swelling in this situation: $\varepsilon = 1$

This function is:

$$\frac{1}{\varepsilon} = \frac{1}{\varepsilon_o} + \frac{c}{0.524\rho} \frac{\varepsilon_o - 1}{\varepsilon_o} \quad (16.9)$$

Substituting (16.9) into (16.8) gives:

$$\varphi_{sp} = \frac{0.524c\varepsilon_o}{0.524\rho + c(\varepsilon_o - 1)} \quad (16.10)$$

Finally ε_o is calculated by combining Eq. (16.8) with the Einstein equation

$$\frac{\eta}{\eta_s} = 1 + 2.5\varphi \quad (16.11)$$

or

$$[\eta] = \lim_{c \rightarrow 0} \frac{\eta - \eta_s}{c\eta_s} = 2.5 \frac{\varphi_{sp}}{c} = 2.5 \frac{\varepsilon_o}{\rho} \quad (16.12)$$

resulting in

$$\varepsilon_o = \frac{[\eta]\rho}{2.5} = \frac{KM^a\rho}{2.5} \quad (16.13)$$

where K and a are the Mark–Houwink constants. Combination of (16.10) and (16.13) gives:

$$\varphi_{sp} = \frac{0.4[\eta]c}{1 + 0.765[\eta]c - 1.91 \frac{c}{\rho}} \quad (16.14)$$

So η can be calculated as a function of c by means of Eqs.(16.7), (16.10) and (16.13) if the following parameters are known:

- the Mark–Houwink constants K and a
- The molecular weight M
- The bulk polymer density ρ
- The solvent viscosity η_s

Rudin and Strathdee tested their method against available literature data with remarkably good results, at of course only for low concentrations, not exceeding 1% by weight.

For dilute polymer solutions, the effect of temperature on the viscosity can be described with Andrade's equation:

$$\eta = B \exp(E_\eta/RT) \quad (16.15)$$

where B = constant; E_η = energy of activation of viscous flow; R = gas constant; T = temperature.

Example 16.1

Estimate the viscosity of a solution of polystyrene in toluene at 20 °C, if $c = 0.02 \text{ g/cm}^3$ and $[\eta] = 124 \text{ cm}^3/\text{g}$:

- a. With Huggins' equation
- b. With the method of Rudin and Strathdee.

Solution

- a. Literature values of k_H for polystyrene in toluene range from 0.31 to 0.39. The lower value gives in Eq. (16.2)

$$\eta_{sp} = [\eta]c + k_H[\eta]^2c^2 = 124 \times 0.02 + 0.31 \times 124^2 \times 0.02^2 = 4.39$$

$$\eta_s = 5.56 \times 10^{-4} \text{ N s/m}^2$$

$$\eta = \eta_s(\eta_{sp} + 1) = 5.56 \times 10^{-4} \times 5.39 = 3.00 \times 10^{-3} \text{ N s/m}^2$$

The higher value of k_H gives $\eta = 3.27 \times 10^{-3} \text{ N s/m}^2$. With the Mark–Houwink exponent $a = 0.72$, Eq. (16.6) predicts $k_H = 1.1 - 0.72 = 0.38$. This corresponds with $\eta = 3.23 \times 10^{-3} \text{ N s/m}^2$.

- b. With Eq. (16.14) and $\rho = 1.05 \text{ g/cm}^3$

$$\varphi_{sp} = \frac{0.4[\eta]c}{1 + 0.765[\eta]c - 1.91c/\rho} = \frac{0.4 \times 124 \times 0.02}{1 + 0.765 \times 124 \times 0.02 - 1.91 \times 0.02/1.05} = 0.347$$

Eq. (16.7) gives

$$\frac{\eta_s}{\eta} = 1 - 2.5\varphi_{sp} + 11\varphi_{sp}^5 - 11.5\varphi_{sp}^7 = 1 - 0.868 + 0.055 - 0.007 = 0.180$$

$$\eta = \frac{\eta_s}{0.180} = \frac{5.56 \times 10^{-4}}{0.180} = 3.09 \times 10^{-3} \text{ N s/m}^2$$

The experimental value mentioned by Streeter and Boyer (1951) is $\eta = 3.16 \times 10^{-3} \text{ N s/m}^2$. From their experimental results these authors calculated $k_H = 0.345$. With this value, the calculated viscosity is $\eta = 3.11 \times 10^{-3} \text{ N s/m}^2$.

As a first approximation

$$E_\eta(\text{solution}) = \varphi_1 E_\eta(\text{solvent}) + \varphi_2 E_\eta(\infty)(\text{polymer}) \quad (16.16)$$

where φ_2 = volume fraction of polymer; φ_1 = volume fraction of solvent; $E_\eta(\infty)$ = the value of E_η of the polymer for $T \gg T_g$. This quantity has been described in Chap. 15.

16.2.1. Other transport properties in dilute polymer solutions

In Chap. 9 the limiting sedimentation coefficient s_o and the limiting diffusion coefficient D_o have been discussed. These are the values of the sedimentation coefficient s and the diffusion coefficient D , extrapolated to zero concentration.

The dependence of s_o and D_o on polymer molecular weight and temperature is also mentioned in Chap. 9.

For dilute polymer solutions, the effect of concentration on s and D may be described by equations which show great analogy with Eq. (16.2) as far as the effect of concentration on viscosity is concerned. These equations are

$$\frac{\eta_{sp}}{[\eta]c} = 1 + k_H[\eta]c \quad (16.17)$$

$$\frac{s_o}{s} = 1 + k_S[\eta]c \quad (16.18)$$

$$\frac{D_o}{D} = 1 + k_D[\eta]c \quad (16.19)$$

where k_H = Huggins' constant (dimensionless); k_S = concentration coefficient of sedimentation (dimensionless); k_D = concentration coefficient of diffusion (dimensionless).

The literature (see Brandrup and Immergut, 1999) contains a number of data of k_s for several polymer-solvent systems. It is found that k_s as defined in Eq. (16.18), is independent of the molecular mass of the polymer. The order of magnitude is $k_s \approx 1$.

Since only few experimental data on k_D are available, no general conclusions can be drawn.

16.3. CONCENTRATED POLYMER SOLUTIONS

The rheology of concentrated polymer solutions shows a striking correspondence with that of polymer melts, which has been discussed in Chap. 15. The influences of the parameters molecular mass, temperature and shear rate on the viscosity are largely analogous, but the situation is made more complicated by the appearance of a new parameter: the concentration of the polymer.

Like polymer melts, concentrated polymer solutions show the phenomenon of a critical molecular mass. This means that in a plot of $\log \eta$ against $\log M$ the slope of the curve changes drastically if M exceeds a critical value M_{cr} . For polymer solutions, M_{cr} increases with decreasing polymer concentration. A similar phenomenon is observed if $\log \eta$ is plotted against $\log c$ for a constant value of M : the slope of the curve changes at $c = c_{cr}$.

The critical phenomena will now be described before the influence of the parameters mentioned is discussed.

16.3.1. Critical values of molecular mass and concentration

As was mentioned in Chap. 15, the strong effect of M on η for $M > M_{\text{cr}}$ is attributed to entanglements between coil polymer molecules. Obviously, the conditions become less favourable for entanglements as the polymer concentration decreases. So M_{cr} increases with decreasing concentration, and vice versa.

Onogi et al. (1966) investigated the mutual influence of c and M on η for a number of polymer-solvent systems. They found that the critical conditions obeyed the general formula

$$c_{\text{cr}}^p M_{\text{cr}} = \text{constant} \quad (16.20)$$

where $p \approx 1.5$.

It is difficult, however, to derive accurate values of c_{cr} and M_{cr} from experimental data, because the change of slope in a $\log \eta - \log M$ curve or a $\log \eta - \log c$ curve is very gradual. An additional difficulty is that the concentration is expressed in different units in different articles. Moreover, the values mentioned for the polymer molecular mass are not completely comparable.

With these restrictions as to accuracy, a number of literature data on $c_{\text{cr}} - M_{\text{cr}}$ combinations will now be correlated. For this purpose the concentrations will be expressed in φ_p , the volume fraction of (unsolvated) polymer. This makes it possible to compare values of M_{cr} for polymer solutions with those for polymer melts ($\varphi_p = 1$). In Fig. 16.1 $\log [M_{\text{cr}}(\text{solution})/M_{\text{cr}}(\text{melt})]$ is plotted against $\log \varphi_p$ for a number of polymer-solvent systems.

In agreement with the rules mentioned by Onogi et al., the majority of the data on polystyrene and poly(vinyl acetate) fall on a straight line, with a slope of -1.5 . This corresponds with $p = 1.5$ in Eq. (16.20). For a number of other polymers, however, lower values of p are found. The available literature data do not permit more definite conclusions about the relationship between M_{cr} and c_{cr} .

Rudin and Strathdee (1974) remarked that the equations presented for the viscosity of dilute polymer solutions were valid approximately up to the critical concentration. This leads to a more general definition of a concentrated polymer solution, viz. a solution for which $c > c_{\text{cr}}$.

16.3.2. Effect of molecular mass and concentration on the viscosity of concentrated polymer solutions

In accordance with the foregoing remarks, the influences of molecular mass and concentration should be discussed simultaneously. This principle is actually applied in the literature, but in two different ways.

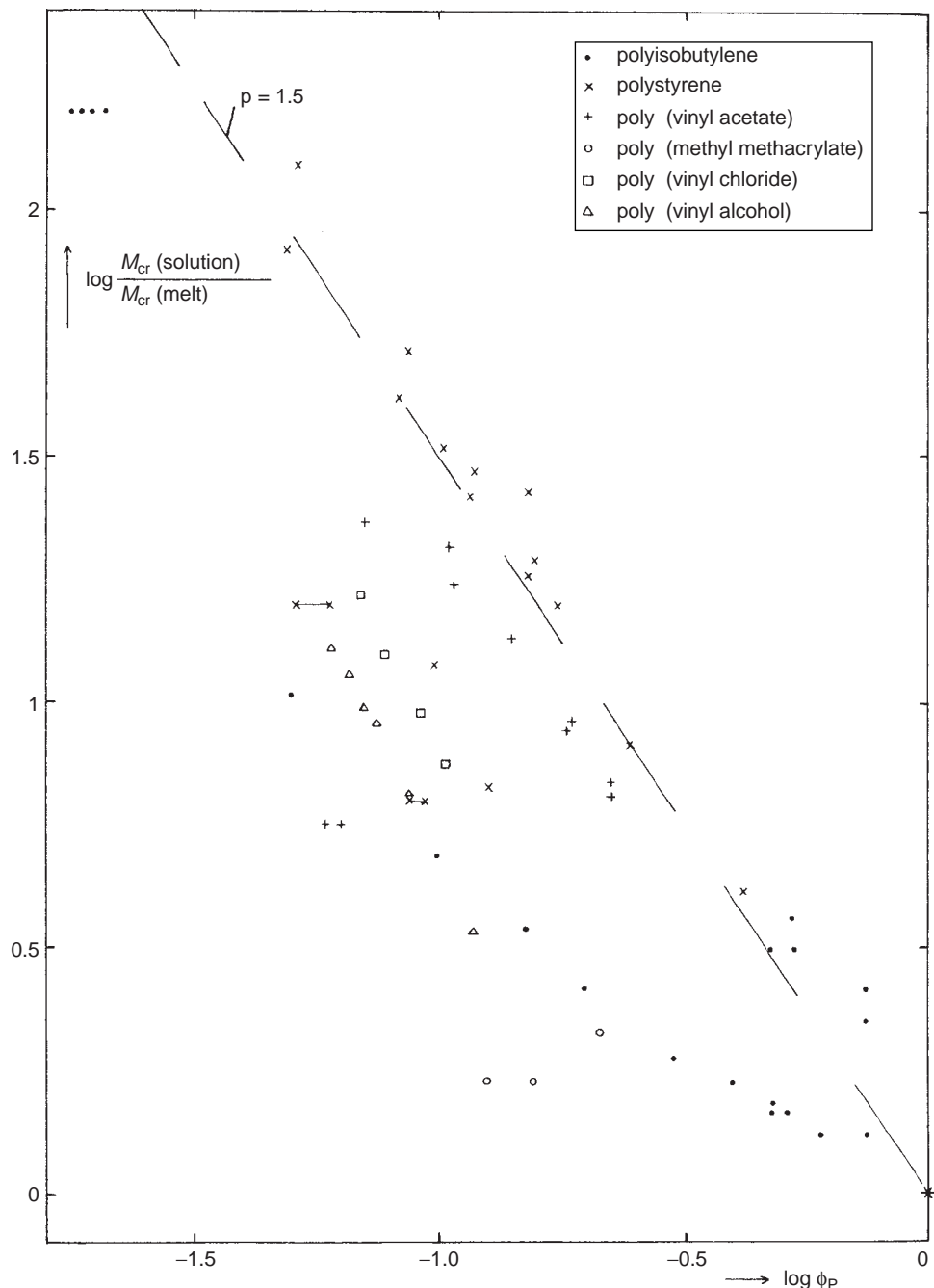
The first method uses the power-law equation:

$$\eta = K c^\alpha M^\beta \quad (16.21)$$

where K = constant, dependent on the nature of the system.

This equation was applied by Onogi et al. (1966), but had already been proposed in principle by Johnson et al. (1952). The exponent of the molar mass, β , is always quite close to the value of 3.4 found for polymer melts. The value of α , however, may vary from 4.0 to 5.6. The mean value is about $\alpha \approx 5.1$, corresponding with $\alpha/\beta = p = 1.5$.

By way of illustration this method of correlation is applied to the experimental data of Pezzin and Gligo (1966) on poly(vinyl chloride) in cyclohexanone. In Fig. 16.2 $\log \eta$ is plotted against $\log c + 0.63 \log M$, and indeed all the data points fall approximately on one

**FIG. 16.1** M_{cr} of polymer solutions.

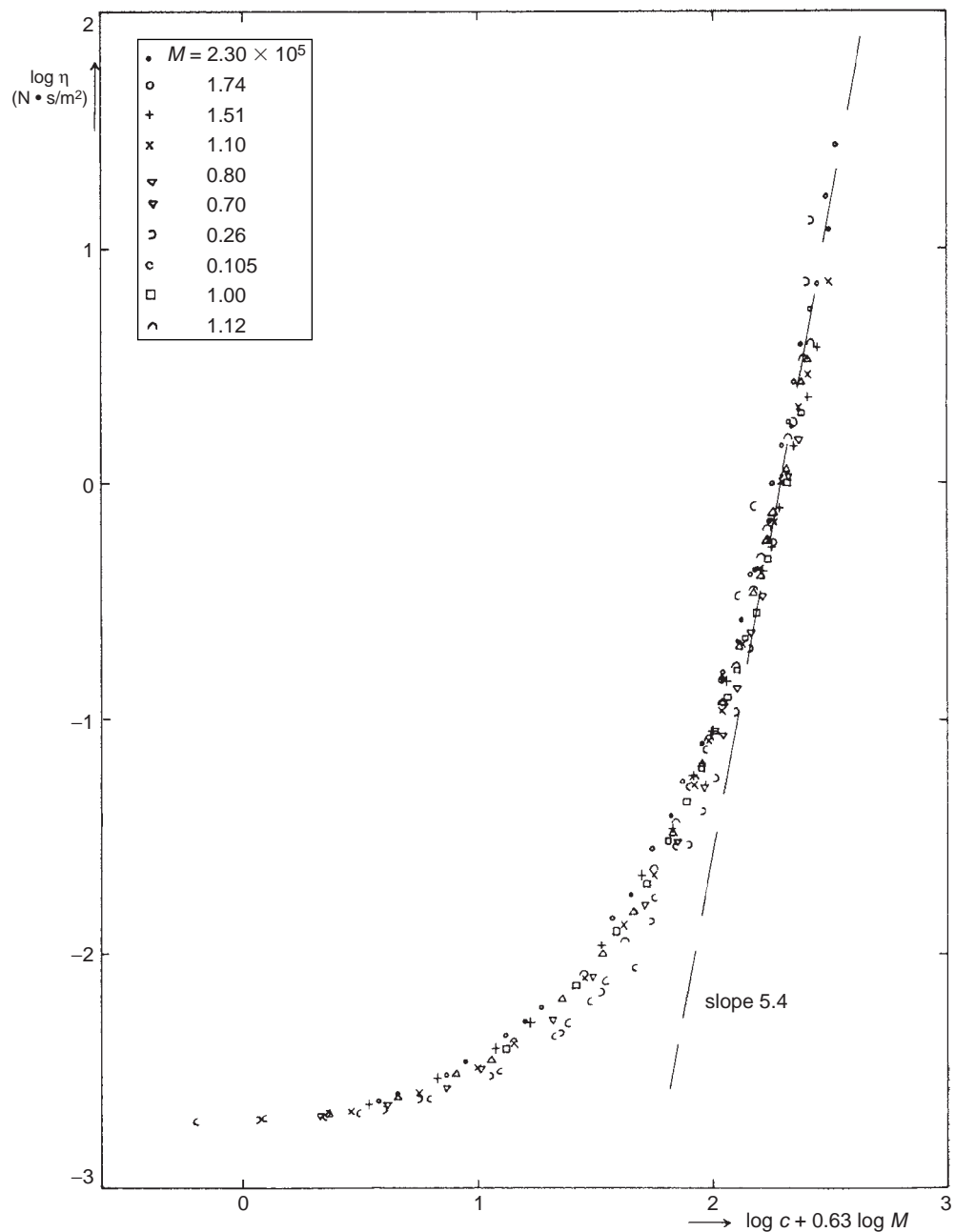


FIG. 16.2 Viscosity of solutions of PVC in cyclohexanone (power-law method).

curve. This curve approaches asymptotically to a straight line with a slope of 5.4 for the higher concentrations. So for concentrated solutions Eq. (16.21) is valid:

$$\eta = Kc^{5.4}M^{3.4}$$

The other method has been described by Simha and Utracki in several articles (1963–1973). The method is called a corresponding states principle. A reduced viscosity $\tilde{\eta}$ is plotted against a reduced concentration \tilde{c} , where

$$\tilde{\eta} = \frac{\eta_{sp}}{c[\eta]} \quad (16.22)$$

and

$$\tilde{c} = c/a_{M,T}$$

where $a_{M,T}$ is a shift factor, depending on molar mass and temperature.

Simha and Utracki show that indeed all the experimental data for a given polymer solvent system fall on the same master curve. The master curve is different, however, for each different polymer–solvent system, while the shift factors $a_{M,T}$ differ also. Therefore this method is less suited for predicting the viscosity of a new polymer–solvent system.

To illustrate the application of this method the same data of Fig. 16.2 are plotted in Fig. 16.3 as $\log \tilde{\eta}$ against $\log \tilde{c}$, where $\log \tilde{c} = \log c + 0.63 \log M$.

A peculiar effect of concentration and molar mass on viscosity show solutions of rod-like macromolecules. These phenomena have originally been described by Flory (1956) and Hermans (1962) for polypeptides. They were also observed by Papkov et al. (1974) with polyparabenzamide and by Sokolova et al. (1973) with poly(paraphenylene terephthalamide) (LCP-solutions; see also Sect. 16.5 of this chapter).

Solutions of these substances at first show the normal increase of viscosity with concentration. Above a certain critical concentration, however, the viscosity decreases rapidly. This phenomenon is explained by orientation of the rod-like macromolecules in the flow direction. An analogous behaviour is observed, if the viscosity is plotted as a function of molecular weight at constant concentration.

Flory (1956) proposed the following equation for the critical concentration, at which transition from an isotropic to an anisotropic state takes place

$$\varphi^* = \frac{8}{x} \left(1 - \frac{2}{x}\right) \quad (16.23)$$

where φ^* = critical concentration (expressed in volume fraction); x = aspect ratio, i.e. length-to-diameter ratio of the rod-like particles, i.e. L/D .

16.3.3. The effect of temperature on the viscosity of concentrated polymer solutions

It is to be expected that the influence of temperature on the viscosity of a polymer solution lies somewhere between that of the pure solvent and that of a polymer melt.

The temperature effect on the viscosity of solvents can be described by Andrade's equation

$$\eta_s = B \exp(E_\eta/RT) \quad (16.15a)$$

where B = constant; E_η = energy of activation, for most solvents between 7 and 14 kJ/mol.

As was discussed in Chap. 15, a plot of $\log \eta$ against $1/T$ for polymer melts shows a curved line with increasing slope. This slope approaches very high values as T approaches T_g .

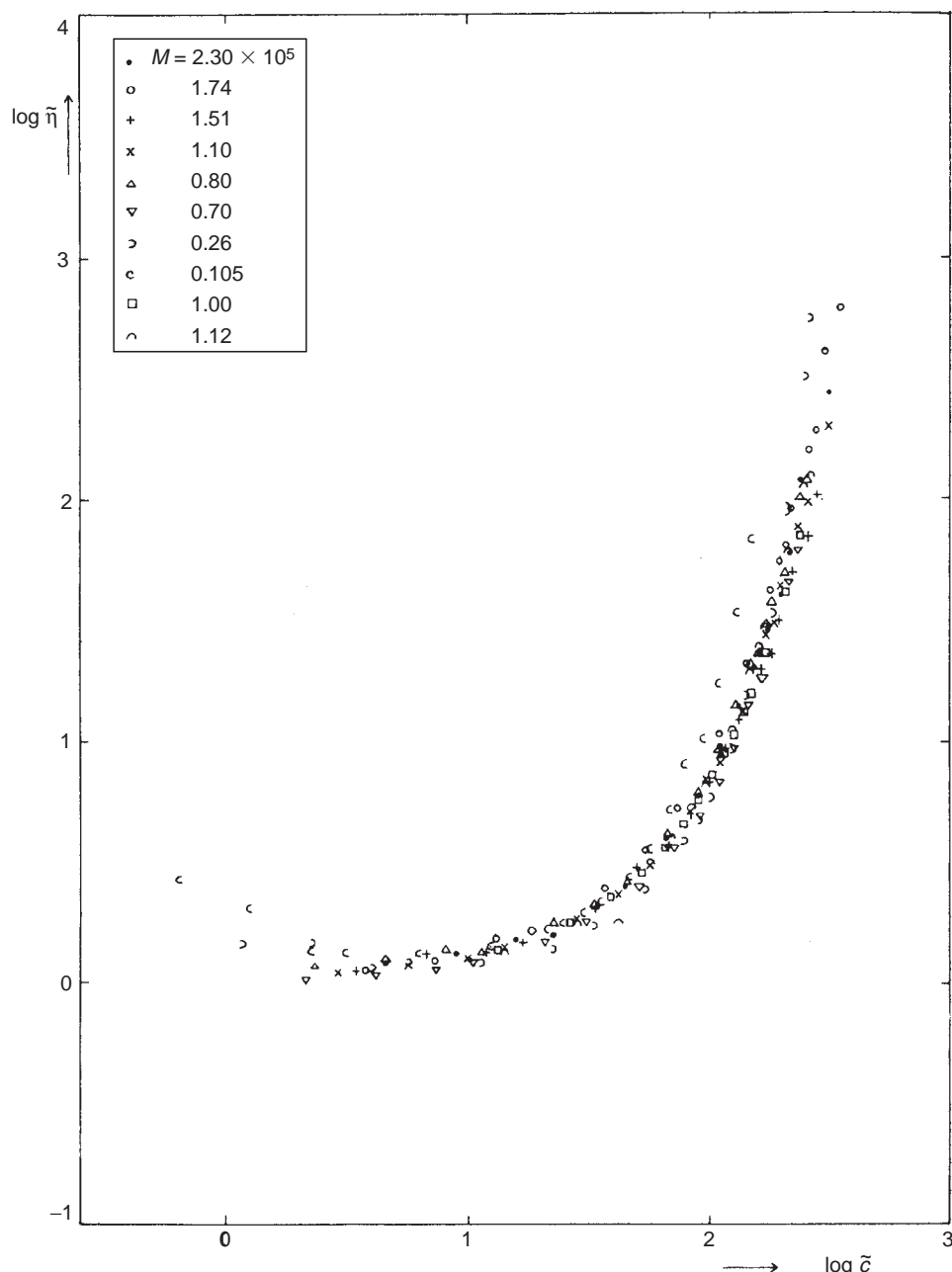


FIG. 16.3 Viscosity of solutions of PVC in cyclohexanone (method of reduced parameters).

For low values of $1/T$, that is for temperatures far above T_g Eq. (16.15) holds, but even in this region the energy of activation of polymer melts is much higher than that of solvents. Values of $E_\eta(\infty)$ for most polymers range from 25 to 85 kJ/mol.

For a number of polymer solutions experimental data on the effect of temperature on viscosity are available. By way of example, Fig. 16.4 shows $\log \eta$ against $1/T$ for polystyrene in xylene, together with the curve for the melt and the straight line for the pure solvent.

For concentrated polymer solutions the relationship between $\log \eta$ and $1/T$ often is a curved line, its slope (so the activation energy) varying with the polymer concentration.

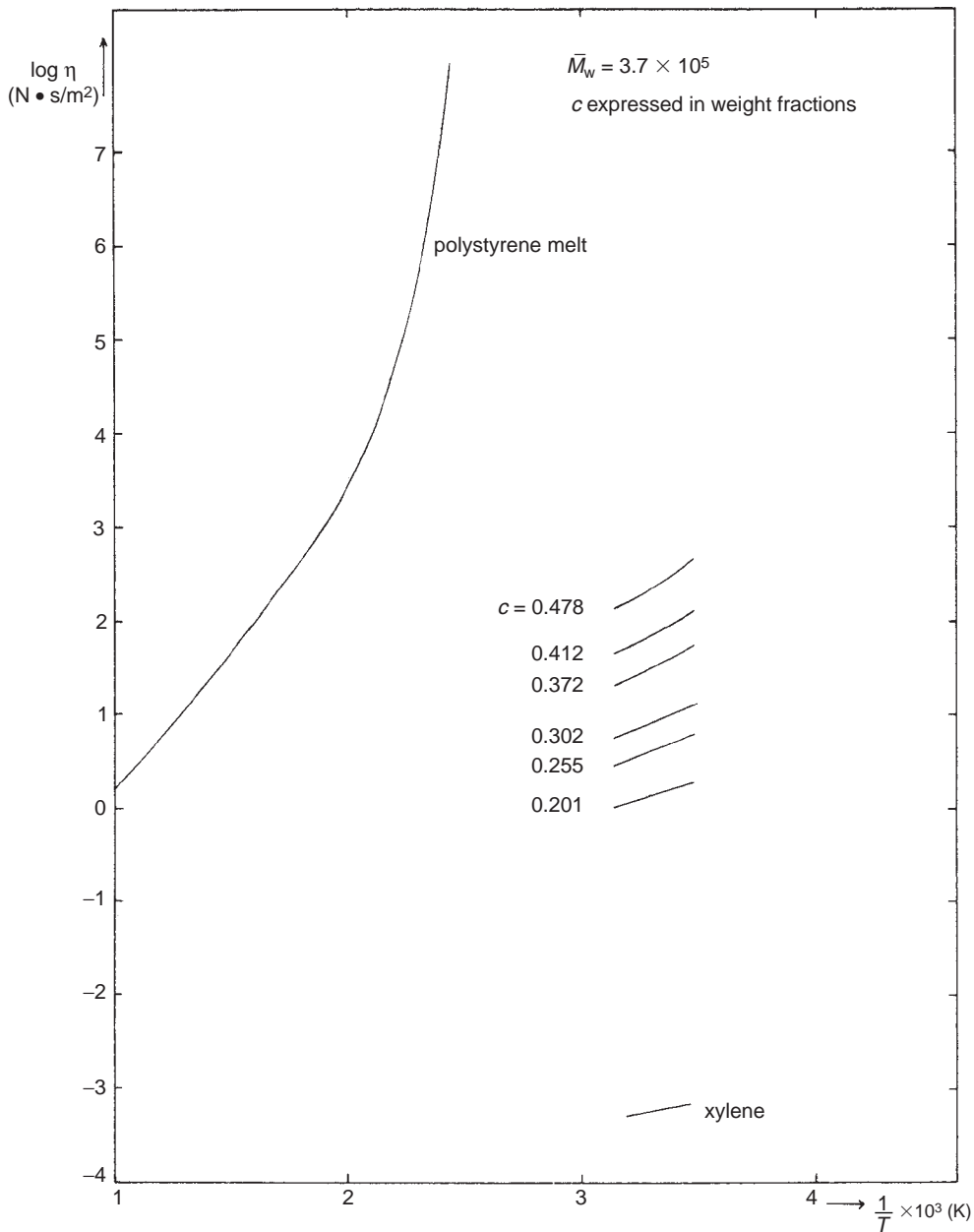


FIG. 16.4 Viscosity of solutions of polystyrene in xylene.

Summarising we may state:

For solvents $E_\eta = E_\eta(T)$

For polymer melts $E_\eta = E_\eta(T, T_g)$

For polymer solutions $E_\eta = E_\eta(T, T_g, c)$

Furthermore we know (a) that in concentrated solutions $\eta \propto c^\alpha$ (with $\alpha \approx 5$) and (b) that T_g is a function of the solvent concentration (the well-known plasticizer effect). An important

conclusion can be drawn: the effects of concentration and temperature on the viscosity of polymer solutions show complicated interactions, so that they should not be treated separately. Especially at high polymer concentrations part of the effect of concentration on viscosity is caused by the variation of T_g and only part of the effect is a proper dilution effect.

16.3.4. The glass transition temperature of polymer solutions

It is well-known that by the addition of plasticizers the glass temperature of polymers decreases severely: the glass temperature of PVC, e.g. decreases from 90 to 0 °C by the addition of 30% dioctyl phthalate and plasticized PVC finds many applications. Unfortunately, there are only a few literature data on this subject. One of the most extensive investigations, that of Jenckel and Heusch, dates back to 1953. Moreover, published T_g values of polymer solutions are rather inaccurate and generally cover a limited concentration range. Fig. 16.5 shows results by Jenckel and Heusch (1953) for Polystyrene in many solvents. In this figure the compositional variation of T_g shows a continuous decreasing function of the weight fraction of solvent, with a continuously decreasing negative slope. This behaviour may be explained by assuming that the fractional free volumes are not quite additive (Braun and Kovacs, 1965; see also Ferry, General references, 1980, Chap. 17) but also depend on a negative interaction parameter k , of the order of 10^{-2} , as follows

$$f = \varphi_1 f_1 + \varphi_2 f_2 + k\varphi_1\varphi_2 \quad (16.24)$$

This leads to a dependence of glass transition temperature on composition

$$T_g = \frac{\varphi_1 \alpha_{f1} T_{g1} + \varphi_2 \alpha_{f2} T_{g2} - k\varphi_1\varphi_2}{\varphi_1 \alpha_{f1} + \varphi_2 \alpha_{f2}} \quad (16.25)$$

Such behaviour, with a continuously decreasing slope, is not always found. There are many examples where two descending curves that come together in a cusp (Braun and Kovacs, 1965). Results by Pezzin et al. (1968, 1971) are shown in Fig. 16.6 for PVC in two plasticizers. For this kind of behaviour results can be fitted with two equations: one above and the other below the temperature T_c of the cusp. For temperatures above T_c use can be made of the Kelley–Bueche equation (1961):

$$T_g = \frac{\varphi_1 \alpha_{f1} T_{g1} + \varphi_2 \alpha_{f2} T_{g2}}{\varphi_1 \alpha_{f1} + \varphi_2 \alpha_{f2}} \quad (16.26)$$

and for temperatures below T_c of the Braun and Kovacs equation (1965)

$$T_g = T_{g1} + \frac{f_{g2}}{\alpha_{f1}} \frac{\varphi_2}{\varphi_1} \quad (16.27)$$

where φ_1 and φ_2 are the volume fractions of solvent and polymer, respectively; α_{f1} and α_{f2} are the thermal expansion coefficients of the fractional free volume of solvent and polymer, respectively; T_{g1} and T_{g2} are the glass temperatures of solvent and polymer, respectively; f_{g2} is the fractional free volume of the polymer at its T_{g2} .

In Fig. 16.6 the dashed lines are calculated with the aid of these two equations: they agree very well with the experimental points.

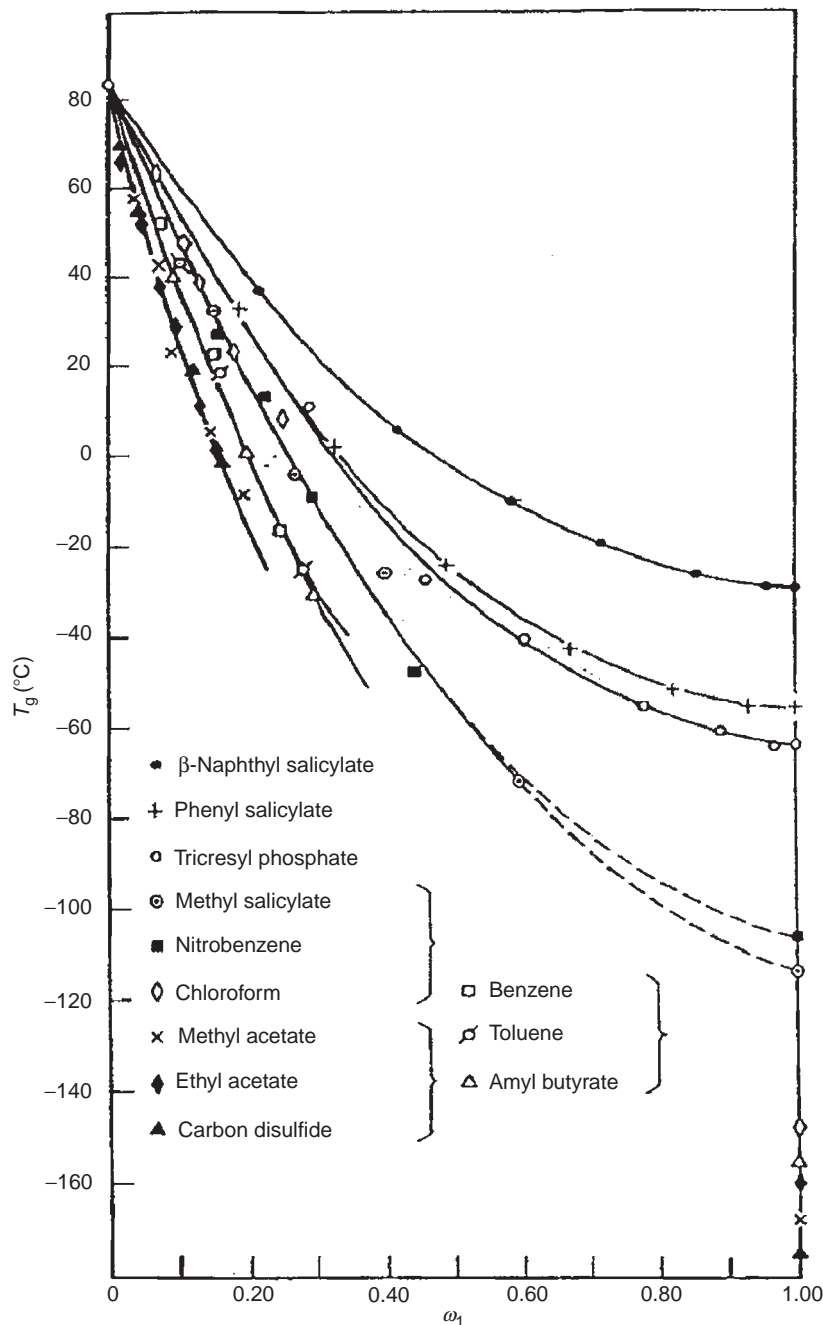


FIG. 16.5 Glass transition temperature of solutions of Polystyrene in 12 different solvents as a function of the weight fraction of solvent, w_1 . After Jenkel and Heusch (1953). Courtesy Hüthig and Wepf Verlag.

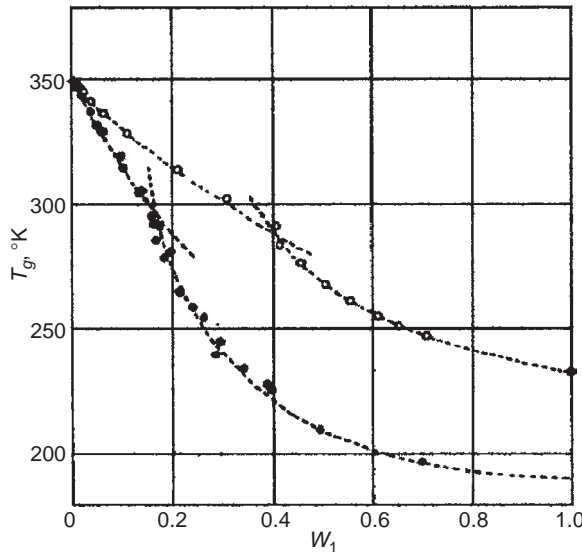


FIG. 16.6 Glass transition temperature of solutions of Poly(vinyl chloride) in two plasticizers as a function of weight fraction of plasticizer, w_1 . ● dibutyl phthalate; ○ dicyclohexyl phthalate. The dashed lines above and below the cusp temperature were calculated with the aid of Eq. (16.26) and Eq. (16.27), respectively. From Pezzin (1971). Courtesy The IUPAC Secretariat.

A reduced treatment of the plasticizer effect starts with the equation developed by Bueche (1962), who gave the following equation for the glass transition temperature of a plasticized polymer

$$T_g = \frac{T_{g2} + (KT_{g1} - T_{g2})\varphi_1}{1 + (K - 1)\varphi_1} \quad (16.28)$$

where

$$K = \frac{\alpha_{f1}}{\alpha_{f2}} \approx \frac{\alpha_{l1} - \alpha_{g1}}{\alpha_{l2} - \alpha_{g2}}$$

The constant K normally has values between 1 and 3.

From Eq. (16.28) one can derive

$$T_{g,\text{red}} = \frac{T_{g2} - T_g}{T_{g2} - T_{g1}} = \frac{1 - \varphi_2}{1 - \varphi_2(1 - 1/K)} \quad (16.29)$$

In order to check this expression, the T_g values of solvents should be known. Actually this is the case for a few solvents only. Table 16.2 gives a survey. It is striking that also for these small molecules the relationship found for polymers:

$$T_g/T_m \approx 2/3 \quad (16.30)$$

appears to be valid. So if T_{gS} is unknown, $2/3T_{mS}$ may be used as a good approximation.

Fig. 16.7 gives a graphical representation of Eq. (16.29) for different values of K in comparison with the available T_g data of polymer-solvent systems in the literature. If no K value for the system is known, one should take as an average $K = 2.5$.

TABLE 16.2 Experimental values of T_g for a number of compounds of low molecular weight

Compound	T_g (K)	T_m (K)	T_g/T_m
Pentane	64	142	0.45
Hexane	70	179	0.39
Heptane	84	182	0.46
Octane	85	216	0.39
2,3-Dimethylpentane	83	~149	~0.56
3-Methylhexane	~85	154	~0.55
Cyclohexane	80	280	0.29
Methylcyclohexane	85	147	0.58
Toluene	106	178	0.60
Ethylbenzene	111	180	0.62
n-Propylbenzene	122	171	0.71
Isopropylbenzene (cumene)	123	176	0.70
n-Butylbenzene	124	192	0.65
sec.-Butylbenzene	127	190	0.67
tert.-Butylbenzene	142	215	0.66
n-Pentylbenzene	128	195	0.66
Methanol	110	175	0.63
Ethanol	100	157	0.64
n-Propanol	109	146	0.75
n-Butanol	118	183	0.64
tert-Butanol	180	299	0.60
n-Pentanol	124	194	0.64
Isopropanol	121	184	0.66
Glycerol	187	293	0.64
Butanone	97	187	0.52
Isobutyl chloride	88	142	0.62
Dimethyl sulphoxide	153	291	0.53
Abietic acid	320	446	0.72
Glucose	298	418	0.71
Sulphur	243	353	0.69
Selenium	303	488	0.63
Boron trioxide	513	723	0.71
Silicon dioxide	1410	1975	0.72

Eq. (16.28) equals Eq. (16.25) if the interaction parameter k is neglected. Accordingly, the glass transition temperatures calculated with Eq. (16.28) are somewhat higher than those calculated with Eq. (16.25). If we start with Eq. (16.25) the reduced glass transition temperature is given by

$$T_{g,\text{red}} = \frac{T_{g2} - T_g}{T_{g2} - T_{g1}} = \frac{1 - \varphi_2}{1 - \varphi_2(1 - 1/K)} - \frac{1}{T_{g2} - T_{g1}} \frac{\varphi_2(1 - \varphi_2)k/\alpha_{f1}}{1 - \varphi_2(1 - 1/K)} \quad (16.31)$$

The minor effect of the correction term is demonstrated in Fig. 16.8 where $T_{g2} - T_{g1} = 200$; $K = 2.5$, $k = 10^{-2}$ and $\alpha_{f1} = 3 \times 10^{-4}$ is chosen. In this case the effect of the correction term is the same as changing K from 2.5 to 1.9 in Eq. (16.31). At $\varphi_2 = 0.5$ we find $T_g = 257$ and $T_g = 269$ with the aid of Eqs. (16.31) and (16.29), respectively.

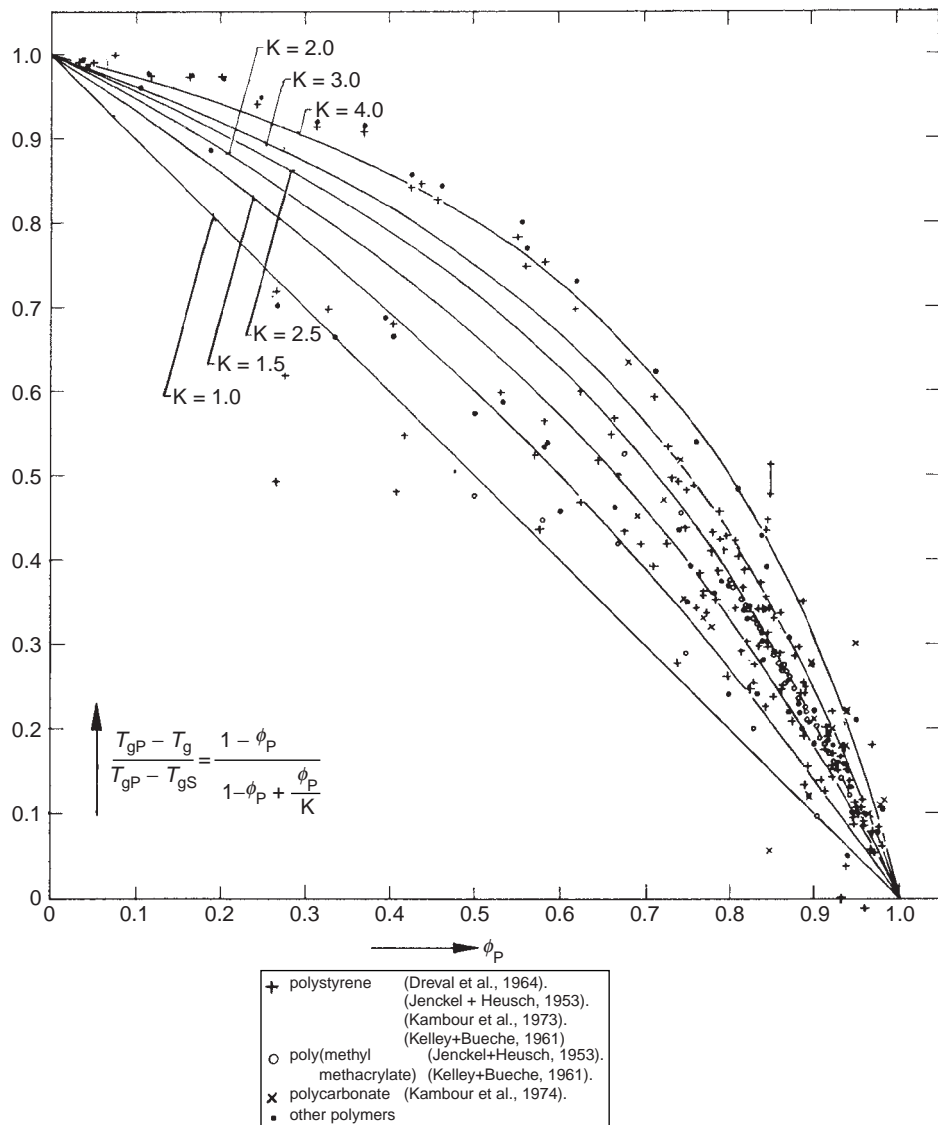


FIG. 16.7 Glass transition temperature of polymer solutions.

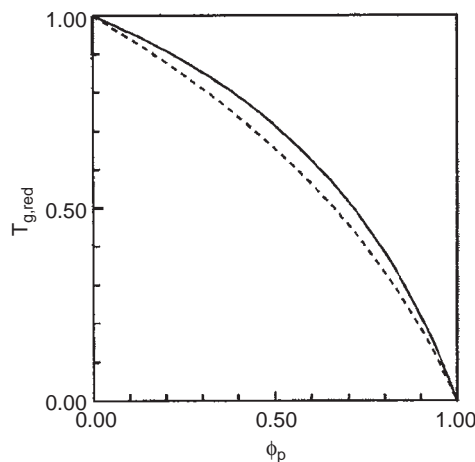


FIG. 16.8 Reduced glass temperature with and without interaction parameter k ; full line Eq. (16.30); dashed line Eq. (16.31).

Example 16.2

Estimate the glass transition temperature for a solution of polystyrene in benzyl alcohol with $\varphi_P = 0.85$.

Solution

According to Fig. 16.7 at $\varphi_P = 0.85$ and $K = 2.5$

$$\frac{T_{g2} - T_g}{T_{g2} - T_{g1}} = 0.29$$

For polystyrene $T_{g2} = 373$ K. The value of T_{g1} for benzyl alcohol cannot be found in the literature. So the estimated value is derived from $T_{m1} = 258$ K:

$$T_{g1} = \frac{2}{3} T_{m1} = 172 \text{ K}$$

With these data, the estimated value is $T_g = 315$ K. The experimental value of Kambour et al. (1973) is $T_g = 324$ K.

Example 16.3

The glass temperature of PVC decreases from 90 °C to 0 °C by the addition of 30% dioctyl phthalate:

- (a) Estimate the value of the constant K of the system PVC + 30% dioctyl phthalate ($T_{gs} = -89$ °C).
- (b) Estimate T_g of PVC with 30% dibutyl phthalate ($T_{gs} = -97$ °C) for the same value of K.
- (c) Estimate the amounts of both plasticizers, DOP and DBP, needed to PVC to reach a T_g of 20 °C.

Solution

(a) $\varphi_P = 100/(100 + 30) = 0.77$. Substitution in Eq. (16.29) yields $\frac{90 - 0}{90 - (-89)} = 0.503 = \frac{1 - 0.77}{1 - 0.77 \times (1 - 1/K)}$ so that $K = 3.4$.

(b) Substitution in Eq. (16.29) yields: $\frac{90 - T_g}{90 - (-97)} = \frac{1 - 0.77}{1 - 0.77 \times (1 - 1/3.4)}$ so that $T_g = -4.2$ °C.

(c) Substitution in Eq. (16.29) yields for DOP: $\frac{90 - 20}{90 + 89} = \frac{1 - \varphi_2}{1 - \varphi_2(1 - 1/3.4)}$ so that $\varphi_2 = 0.84 = 100/(100 + \% \text{DOP})$, from which it follows that 19% DOP has to be added. In the same way it follows that 17.6% DBP has to be added.

16.3.5. The Van Krevelen–Hoftyzer method for estimating the viscosity of concentrated polymer solutions

In the preceding sections it was shown that there can be two causes for the decrease in viscosity upon addition of a solvent to a polymer:

- (a) A decrease of the viscosity of the pure polymer as a result of a decrease of the glass transition temperature
- (b) A real dilution effect, which causes the viscosity of the solution to fall between that of the pure polymer (as mentioned under a) and that of the pure solvent.

For this reason the effects of concentration and temperature on the viscosity of polymer solutions cannot be separated.

In reality the interactions between polymer and solvent molecules, which determine the solution viscosity, are very complicated and dependent on a great number of parameters. The literature mentions the solubility parameters of polymer and solvent, polymer chain stiffness, free volume of the solution, etc. In principle, all these factors should be taken into account in predicting the viscosity of a polymer solution. However, the available experimental data are insufficient for this purpose.

Instead, a simple prediction method has been developed by Hoftyzer and Van Krevelen (1976), which provides approximate values of the viscosity for a number of polymer solvent systems. This method is based on the following three assumptions:

- (1) The glass transition temperature of the solution can be calculated with the method described in the preceding section (Eqs. (16.24) and (16.25)).
- (2) The viscosity of the undiluted polymer (η_p^*) at new T_g (glass transition temperature of the solution) can be calculated from the normal $\log \eta$ vs. T_g/T relationship given in Chap. 15. The glass transition temperature of the solution has to be used in the T_g/T ratio in Fig. 15.7.
- (3) For a description of the dilution effect, a modified form of Eq. (16.21) can be applied: it is assumed that η is proportional to the fifth power of φ_p , the volume fraction of the polymer. As $\eta = \eta_p^*$ at $\varphi_2 = 1$,

$$\log \eta = \log \eta_p^* + 5 \log \varphi_2 \quad (16.32)$$

The applicability of this method will be demonstrated in the following example.

Example 16.4

For concentrated solutions of polyisobutylene in decalin ($\varphi_p > 0.1$), estimate the viscosity as a function of the volume fraction of polymer at a temperature of 20 °C. The viscosity of the bulk polymer at this temperature is $\eta_p = 6.5 \times 10^9 \text{ Ns/m}^2$.

Solution

1. The glass transition temperatures. For the polymer, the literature value is $T_{gp} = 198 \text{ K}$. A glass transition temperature of decalin has not yet been published. Therefore T_{gS} is estimated by

$$T_{g1} = \frac{2}{3} T_{m1} = \frac{2}{3} \times 230 = 150 \text{ K}$$

Now for the solutions T_g can be calculated with the aid of Fig. 16.7 or Eq. (16.29), using $K = 2.5$. These values are mentioned in Table 16.3.

2. For the calculation of η^* use can be made of Fig. 15.7, where $\eta_P(T)/\eta_P(1.2T_g)$ is plotted against the ratio T_g/T . This graph shows a number of curves for different values of a parameter A. As has been mentioned in Chap. 15, for polyisobutylene A = 12.5, $\eta(1.2T_g)$ can be calculated from the viscosity of the bulk polymer. With $T_{gP} = 198$ K and $T = 293$ K, $T_g/T = 0.676$. According to Fig. 15.7 this corresponds to $\log \{\eta_P(T)/\eta_P(1.2T_g)\} = -3.5$. So $\log \eta_P(1.2T_g) = \log \eta_P(293) + 3.5 = \log 6.5 \times 10^9 + 3.5 = 13.3$. For each value of T_g in Table 16.3, $\eta_P(T)/\eta_P(1.2T_g) = \eta^*/\eta_P(1.2T_g)$ can be read in Fig. 15.7 and η_P^* can be calculated.
3. Application of Eq. (16.32) gives the estimated values of $\log \eta$. These are compared in Table 16.3 with the experimental values of Tager et al. (1963).

While in this example the agreement between calculated and experimental viscosity values is excellent, it should be mentioned that for several series of experimental data it is less.

16.3.6. Equations for the viscosity of polymer solutions over the whole concentration range

In this chapter, different methods for predicting the viscosity are described that are valid for dilute or concentrated polymer solutions. The same distinction is made in most of the literature. This has a natural justification, because a discontinuity in behaviour can be observed near the critical concentration.

Nevertheless, Lyons and Tobolsky (1970) proposed an equation for the concentration dependence of the viscosity of polymer solutions, which is claimed to be valid for the whole concentration range from very dilute solutions to pure polymer. The equation reads:

$$\frac{\eta_{sp}}{c[\eta]} = \exp\left(\frac{k_H[\eta]c}{1-bc}\right) \quad (16.33)$$

where η_{sp} = specific viscosity (-); $[\eta]$ = intrinsic viscosity (m^3/kg); c = concentration (kg/m^3); k_H = Huggins constant (-); b = constant (m^3/kg).

TABLE 16.3 Solutions of polyisobutylene in decalin (η in Ns/m^2)

φ_P	T_g (K)	T_g/T	$\log \frac{\eta_P^*}{\eta_P(1.2T_{gP})}$	$\log \eta_P^*$	$5 \log \varphi_P$	$\log \eta$ (calc.)	$\log \eta$ (exp.)
1.00	198	0.676	-3.5	9.8	0	9.8	9.81
0.77	177	0.606	-4.7	8.6	-0.58	8.0	8.30
0.70	177	0.591	-4.9	8.4	-0.77	7.65	7.83
0.61	168	0.575	-5.1	8.2	-1.08	7.1	7.24
0.51	164	0.560	-5.3	8.0	-1.48	6.5	6.51
0.42	161	0.549	-5.4	7.9	-1.89	6.0	5.94
0.31	157	0.537	-5.65	7.65	-2.54	5.1	5.04
0.21	155	0.528	-5.8	7.5	-3.41	4.1	3.87
0.10	152	0.519	-6.0	7.3	-4.94	2.35	2.23

For a given polymer–solvent system, k_H and $[\eta]$ can be determined in the usual manner. The only remaining constant, b , can be calculated from the bulk viscosity of the polymer, where $c = \rho$ (polymer density).

Lyons and Tobolsky successfully applied Eq. (16.33) to the systems poly(propylene oxide)-benzene and poly(propylene oxide)-methylcyclohexane. The application was restricted, however, to a polymer of molecular mass 2000, which is below the critical molecular mass M_{cr} .

The applicability of Eq. (16.33) will be limited by the fact that the bulk viscosity of the polymer is often extremely high and unknown at the temperature at which the solution viscosities are determined. On the basis of theoretical considerations, Rodriguez (1972) concludes that the applicability of Eq. (16.33) is limited to systems for which $M < M_{cr}$.

A certain generalisation is permitted with respect to the relationship between the effects of concentration and molecular mass on the viscosity of polymer solutions. It is restricted to solutions of polymers with $M > M_{cr}$ in good solvents.

At high concentrations Eq. (16.21) holds, according to which η is proportional to c^α and M^β , and $\alpha/\beta \approx 1.5$. At very low concentrations η_{sp} is proportional to the first power of c and, according to the Mark–Houwink equation, to a power of M of about 0.7. This gives the same power ratio of about 1.5. This ratio seems to hold over the whole concentration range.

As the intrinsic viscosity $[\eta]$ is proportional to $M^a \approx M^{\beta/\alpha}$, the product $c[\eta]$ is proportional to c and M in the correct power ratio. Therefore η_{sp} will be a unique function of the product $c[\eta]$. This was discussed by Vinogradov et al. (1973).

16.4. VISCOELASTIC PROPERTIES OF POLYMER SOLUTIONS IN SIMPLE SHEAR FLOW

Viscoelastic properties of polymer solutions may be of practical importance, e.g. in the flow of these solutions through technical equipment. For concentrated polymer solutions the viscoelastic properties show great analogy with those of polymer melts. For dilute solutions ($c < c_{cr}$) the analogy decreases with decreasing concentration.

16.4.1. Viscoelastic properties of dilute solutions

Rouse (1953) and Zimm (1956) presented in the 1950s their classical models for viscoelastic properties in dilute solutions. Both of them made use of a bead-spring model. Zimm took hydrodynamic interaction between polymer and solvent (so-called non-draining assumption) into consideration, whereas Rouse ignored it (so-called free-draining assumption). The advantage of Zimm's assumption is that it also includes partial hydrodynamic interaction, which can be fitted with experiments to an intermediate state between non-draining and free-draining. Both models make use of the following equations for the shear and dynamic moduli

$$G(t) = nkT \sum_{p=1}^N \exp(-t/\tau_p) = \frac{cRT}{M} \sum_{p=1}^N \exp(-t/\tau_p) \quad (16.34)$$

$$G'(\omega) = nkT \sum_{p=1}^N \frac{\omega^2 \tau_p^2}{1 + \omega^2 \tau_p^2} = \frac{cRT}{M} \sum_{p=1}^N \frac{\omega^2 \tau_p^2}{1 + \omega^2 \tau_p^2} \quad (16.35)$$

$$G''(\omega) - \omega \eta_s = nkT \sum_{p=1}^N \frac{\omega \tau_p}{1 + \omega^2 \tau_p^2} = \frac{cRT}{M} \sum_{p=1}^N \frac{\omega \tau_p}{1 + \omega^2 \tau_p^2} \quad (16.36)$$

where η_s is the viscosity of the solvent.

In Rouse's model the relaxation times are approximated by

$$\tau_p = \frac{[\eta]\eta_s M}{S_{1,R} p^2 RT} = \frac{\tau_1}{p^2} \quad (16.37)$$

where $S_{1,R} = \zeta 1/p^2 = \pi^2/6 = 1.645$ and τ_1 is the longest relaxation time.

For sufficiently low ω the curves for $\log G'$ and $\log G''$ plotted vs. $\log \omega$ are straight lines with slopes 2 and 1, respectively. For sufficiently high frequencies

$$G'(\omega) = G''(\omega) - \omega\eta_s = \frac{cRT}{M} \frac{\pi}{2\sqrt{2}} (\omega\tau_1)^{1/2} \quad (16.38)$$

So that $G'(\omega)$ and $G''(\omega) - \omega\eta_s$ coincide at high frequencies and the slopes of the straight lines are $\frac{1}{2}$ in the above mentioned plot and $\tan \delta = \tan(\frac{1}{2}\pi n) = \tan(\pi/4) = 1$, where n is the slope at high frequencies.

In Zimm's model the expression for the relaxation times is more complex: the relaxation times τ_i are proportional to $p^{-3/2}$ in the non-draining case instead of to p^{-2} in the free-draining case and $S_{1,Z} = 2.369$. This leads to slopes of 2 and 1 at sufficiently low frequencies, whereas for sufficiently high frequencies

$$G'(\omega) = 1.05 \frac{cRT}{M} (\omega\tau_1)^{3/2} \quad \text{and} \quad G''(\omega) - \omega\eta_s = 1.82 \frac{cRT}{M} (\omega\tau_1)^{3/2} \quad (16.39)$$

Accordingly, $G'(\omega)$ and $G''(\omega)$ are parallel at high frequencies with slope $\frac{2}{3}$ and their mutual distance is $\tan \delta = \tan(\frac{1}{2}\pi n) = \tan(\pi/3) = 1.732$, which is of course equal to $1.82/1.05$.

In Fig. 16.9 the reduced dynamic moduli $[G'(\omega)]_R$ and $[G''(\omega)]_R$ are plotted vs. $\omega\tau_1$ on double logarithmic scales. The reduced moduli are defined to be

$$[G'(\omega)]_R = \sum_{p=1}^N \frac{\omega^2 \tau_p^2}{1 + \omega^2 \tau_p^2} \quad \text{and} \quad [G''(\omega)]_R = \sum_{p=1}^N \frac{\omega \tau_p}{1 + \omega^2 \tau_p^2} \quad (16.40)$$

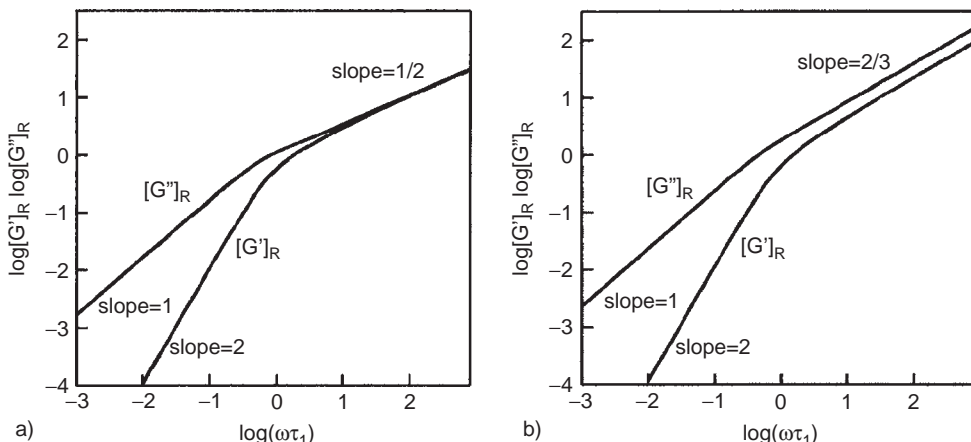


FIG. 16.9 Logarithmic plots of $[G']_R$ and $[G''']_R$ vs. $\omega\tau_1$ for bead-spring models. (A) Rouse: free-draining (negligible hydrodynamic interaction); (B) Zimm: non-draining (dominant hydrodynamic interaction). After Ferry, General References, 1980.

Fig. 16.9 shows the low frequency slopes of 2 and 1, respectively, as expected for viscoelastic liquids and the high frequency slopes $\frac{1}{2}$ and $\frac{2}{3}$ for Rouse's and Zimm's models, respectively. Experimentally it appears that in general Zimm's model is in agreement with very dilute polymer solutions, and Rouse's model at moderately concentrated polymer solutions to polymer melts. An example is presented in Fig. 16.10. The solution of the high molecular weight polystyrene (III) behaves Rouse-like (free-draining), whereas the low molecular weight polystyrene with approximately the same concentration behaves Zimm-like (non-draining). The higher concentrated solution of this polymer illustrates a transition from Zimm-like to Rouse-like behaviour (non-draining nor free-draining, hence with intermediate hydrodynamic interaction).

These conclusions are in agreement with results reported by Janeschitz-Kriegl (1969), who measured the shear compliance J_{eR} of highly concentrated to very dilute solutions of a series of polystyrenes with narrow molecular weight distributions. For the melt down to moderately concentrated solutions J_{eR} appeared to be equal to 0.4, which is the value to be expected for free-draining solutions. In very dilute solutions J_{eR} tended to decrease to the non-draining case, where $J_{eR}=0.205$.

16.4.2. Viscoelastic properties of concentrated solutions

As an example of the concentration dependence of viscoelastic properties in Fig. 16.11 the shear creep compliance of poly(vinyl acetate) is plotted vs. time for solutions of poly(vinyl acetate) in diethyl phthalate with indicated volume fractions of polymer, reduced to 40 °C with the aid of the time temperature superposition principle (Oyanagi and Ferry, 1966). From this figure it becomes clear that the curves are parallel. We may conclude that the various may be shifted over the time axis to one curve, e.g. to the curve for $\varphi_2 = 1$, the pure polymer. In general it appears that viscoelastic properties measured at various concentrations may be reduced to one single curve at one concentration with the aid of a time-concentration superposition principle, which resembles the time-temperature superposition principle (see, e.g. Ferry, General references, 1980, Chap. 17). The Doolittle equation reads for this reduction:

$$\log a_c = \frac{B}{2.303} \left(\frac{1}{f_c} - \frac{1}{f_p} \right) \quad (16.41)$$

where f_c = the fractional free volume at concentration c ; f_p = the fractional free volume of the undiluted polymer; B = constant, frequently taken equal to 1.

In the linear range where T_g decreases linearly with the volume fraction of solvent, φ_s a linear dependence of f on φ_s is expected:

$$f(T, \varphi_s) = f_p(T) + \beta \varphi_s \quad (16.42)$$

where φ_s is the volume fraction of solvent. An expression for β might be

$$\beta = \alpha_{fs}(T - T_{gs}) - \alpha_{fp}(T - T_{gp}) \quad (16.43)$$

where α_{f1} and α_{f2} are the fractional free volume expansion coefficients of solvent and polymer, respectively.

Substitution of Eqs. (16.42) and (16.43) into (16.41) leads to

$$\log a_c = - \frac{\varphi_s}{2.303 f_p (\varphi_s + f_p / \beta)} \quad (16.44)$$

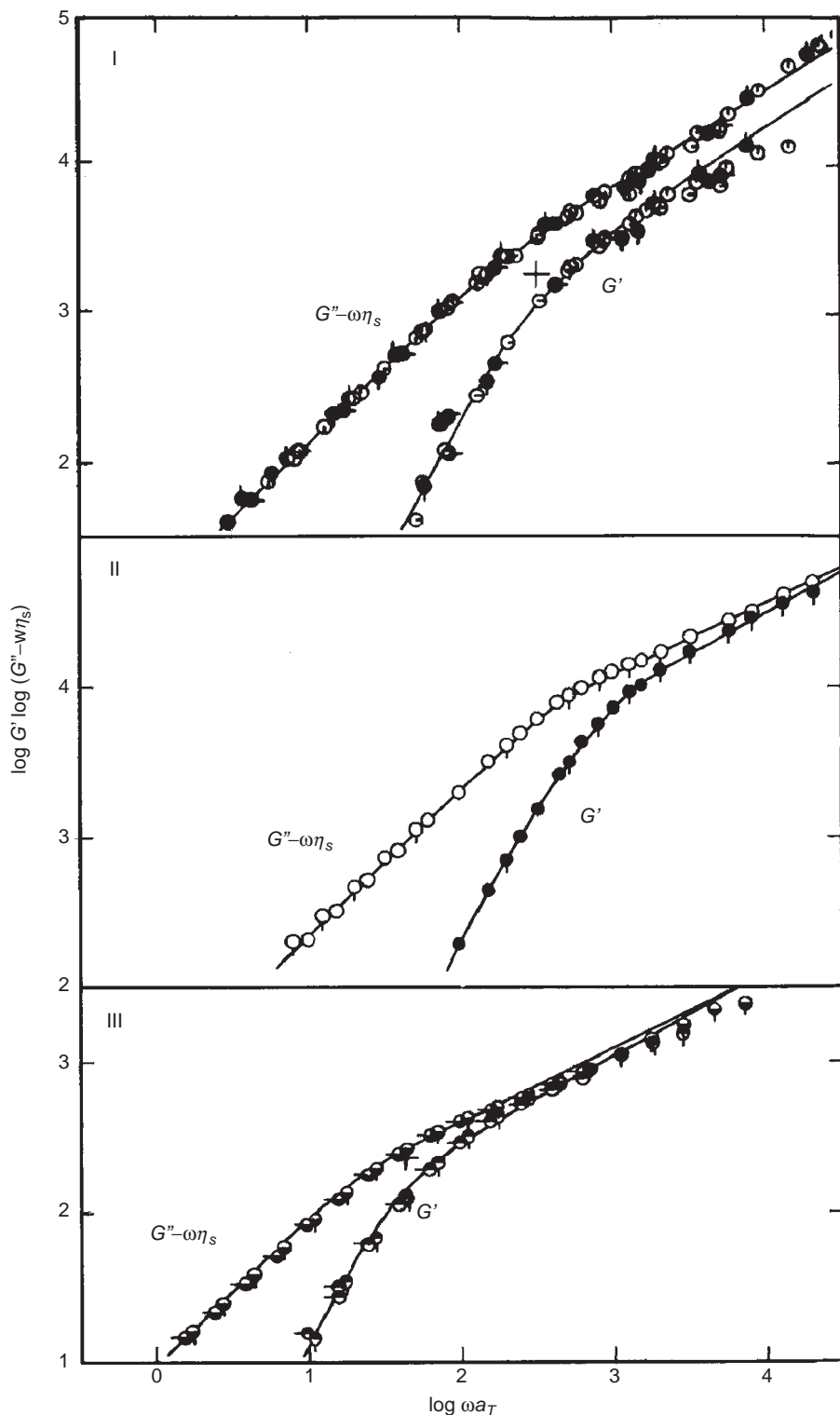


FIG. 16.10 Logarithmic plots of G' and $G'' - \omega\eta_s$ vs. angular frequency reduced to a reference temperature of 25.0 °C for polystyrenes with narrow molecular weight distribution in chlorinated diphenyl. (I) $M = 2.67 \times 10^5$, $c = 0.0286 \text{ g/cm}^3$; (II) $M = 2.67 \times 10^5$, $c = 0.12 \text{ g/cm}^3$; (III) $M = 1.7 \times 10^6$, $c = 0.0253 \text{ g/cm}^3$. From Ferry, General References, 1980. Courtesy John Wiley & Sons, Inc.

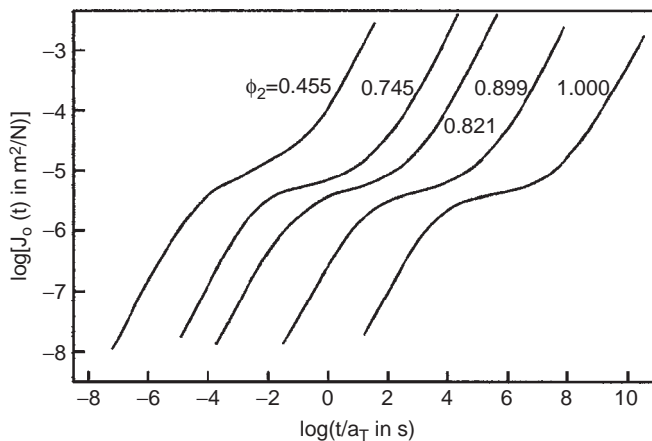


FIG. 16.11 Shear creep compliance of poly(vinyl acetate), $M = 240 \text{ kg/mol}$, and four solutions in diethyl phthalate with indicated values of the polymer volume fraction, φ_2 , reduced to 40°C . From Oyanagi and Ferry (1966). Courtesy John Wiley & Sons, Inc.

The values of f_P and β may be obtained by determining slopes and intercepts of

$$-\frac{1}{\ln a_c} = f_P + \frac{f_P^2}{\beta \varphi_S} \quad (16.45)$$

$$-\frac{\varphi_S}{\ln a_c} = \frac{f_P^2}{\beta} + f_P \varphi_S \quad (16.46)$$

An example of the application of Eqs. (16.44) to (16.46) on the data in Fig. 16.11 is presented in Figs. 16.12–16.14. In the three figures the full lines are calculated for $f_P = 0.039$ and $\beta = 0.0096$.

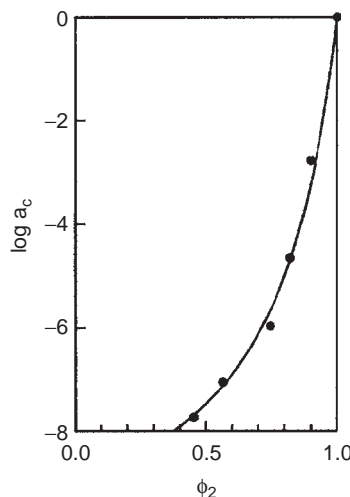


FIG. 16.12 Plot of $\log a_c$ vs. volume fraction of polymer, for data of Fig. 16.11 in the transition region. Curve drawn from Eq. (16.44) with $f_2 = 0.039$ and $\beta = 0.0096$.

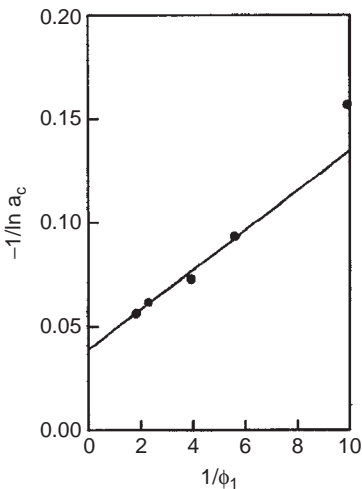


FIG. 16.13 Plot of $-\ln a_c$ vs. $1/\varphi_1$ for data of Fig. 16.12. Curve drawn from Eq. (16.45) with $f_2 = 0.039$ and $\beta = 0.0096$.

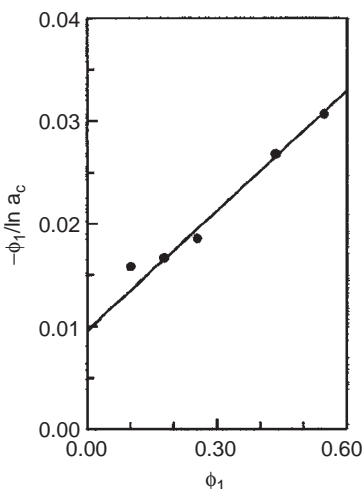


FIG. 16.14 Plot of $-\varphi_1/\ln a_c$ vs. φ_1 for data of Fig. 16.12. Curve drawn from Eq. (16.46) with $f_2 = 0.039$ and $\beta = 0.0096$.

It has to be mentioned that the effect of dilution is in the terminal zone (long times) greater than in the glass–rubber transition zone (short times), which is specified by $\log a_c$. This becomes also clear from Fig. 16.11: the values of $\log a_c$ in Figs. 16.12–16.14 were taken in the transition zone. It is beyond the scope of this book to go into more detail into this subject. For more details of the time-concentration superposition principle the reader is referred to the monograph by Ferry (General references, 1980, Chap. 17).

16.4.3. Non-Newtonian behaviour of concentrated polymer solutions

At low rates of shear (i.e. for $q\tau < 1$) polymer solutions, as polymer melts, show Newtonian behaviour. This is determined by the Newtonian viscosity η_o . For $q\tau > 1$, the viscosity η decreases with increasing shear rate. The value of η can be estimated as a function of q with the aid of Fig. 15.10, which was derived for polymer melts.

Finally a phenomenon should be mentioned which polymer solutions show more often than polymer melts: viz. *a second Newtonian region*. This means that with increasing shear rate the viscosity at first decreases, but finally approaches to another constant value. As the first Newtonian viscosity is denoted by η_o , the symbol η_∞ is generally used for the second Newtonian viscosity. Empirical equations as those presented in Chap. 15 now need an extra term η_∞ to account for this second Newtonian region. This leads to:

(a) The equation of Cross (1965)

$$\frac{\eta(q) - \eta_\infty}{\eta_o - \eta_\infty} = \frac{1}{1 + (\tau q)^m} \quad (16.47)$$

For many systems $\eta_o \gg \eta_\infty$ so that for very small shear rates the viscosity tends to η_o , whereas for very high shear rates

$$\eta(q) \approx \eta_\infty + \eta_o m q^{n-1} \quad (16.48)$$

where $m = \tau^{1-n}$.

(b) The equation of Carreau (1969)

$$\frac{\eta(q) - \eta_\infty}{\eta_o - \eta_\infty} = [1 + (\tau q)^2]^{(n-1)/2} \quad (16.49)$$

(c) The equation of Yasuda et al. (1981)

$$\frac{\eta(q) - \eta_\infty}{\eta_o - \eta_\infty} = \eta_o [1 + (\tau q)^a]^{(n-1)a} \quad (16.50)$$

The ratio η_o/η_∞ increases with the molecular weight of the polymer and with the concentration. Experimental data are scarce and show a large amount of scatter, but the order of magnitude of can be estimated in the following way.

If it is assumed that the influence of entanglements on viscosity starts at $M = M_{cr}$ while $\eta \propto M$ for unentangled molecules

$\eta \propto M^{3/4}$ for entangled molecules

and η_∞ represents unentangled conditions, the distance between the two lines in Fig. 16.15 corresponds with $\log(\eta_o/\eta_\infty)$ for polymer melts and

$$\log(\eta_o/\eta_\infty) = 2.4 \log(M/M_{cr})$$

For polymer solutions, the difference between and η_∞ decreases with decreasing concentration. A number of literature data could approximately be correlated with the following empirical equation

$$\log(\eta_o/\eta_\infty) = 2.4 \log(M_w/M_{cr}) + 2 \log \varphi_P \quad (16.51)$$

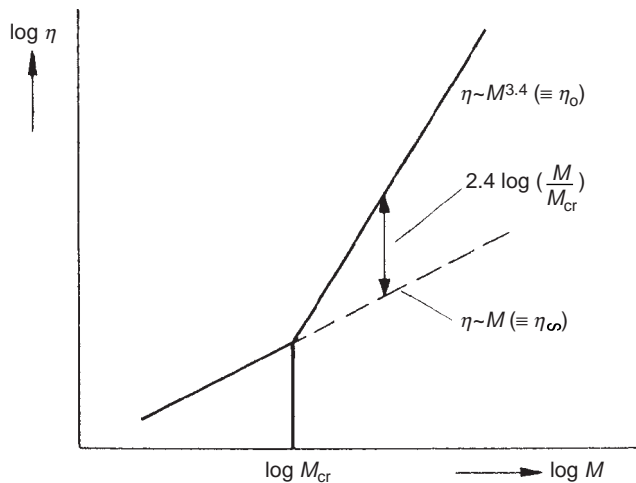


FIG. 16.15 Influence of entanglements on viscosity.

Example 16.5

Estimate the viscosity of a solution of polystyrene ($\rho = 1050 \text{ kg/m}^3$) in diethyl phthalate under the following conditions:

Temperature 20 °C

Polymer concentration: $c = 0.44 \text{ g/cm}^3 = 440 \text{ kg/m}^3$

$M_w = 3.5 \times 10^5 \text{ g/mol} = 350 \text{ kg/mol}$; $Q = M_w/M_n = 2$

$\eta_o = 4 \times 10^3 \text{ N s/m}^2$

Shear rates 0.1, 10 and 1000 s^{-1}

(Experimental data of Ito and Shishido, 1975).

Solution

The time constant $\tau_{1,\text{vdy}}$ may be estimated with the "solution-equivalent" of Eq. (15.94):

$$\tau_{1,\text{vdy}} \approx \frac{6}{\pi^2} \frac{\eta_o M_w Q}{c R T} = \frac{6 \times 4 \times 10^3 \times 350 \times 2}{\pi^2 \times 440 \times 8.314 \times 293} = 1.6 \text{ s}$$

The values of η/η_o can be read in Fig. 15.10

$\dot{\gamma} (\text{s}^{-1})$	$\dot{\gamma}\tau_{1,\text{vdy}}$	η/η_o	$\eta (\text{Ns/m}^2)$	$\eta \exp (\text{Ns/m}^2)$
0.1	0.16	1.00	4.0×10^3	4.0×10^3
10	16	0.30	1.2×10^3	1.0×10^3
10^3	1.6×10^3	0.016	64	≈ 150

There is a reasonable correspondence between the experimental and calculated viscosity values at a shear rate of 10 s^{-1} . The calculated η value at $\dot{\gamma} = 10^3 \text{ s}^{-1}$ is too low, however, because at this shear rate the second Newtonian region is approached. To estimate η_∞ Eq. (16.51) can be applied with

$$\begin{aligned}
 M_{\text{cr}} &= 350 \text{ kg/mol} \\
 \varphi_p &\approx c/\rho(\text{polymer}) = 440/1050 = 0.42 \\
 \log(\eta_o/\eta_\infty) &= 2.4 \log(M_w/M_{\text{cr}}) + 2 \log \varphi_p = 2.4 - 2 \times 0.38 = 1.64 \\
 \eta_o/\eta_\infty &= 44 \\
 \eta_\infty &= 4000/44 = 91 \text{ N s/m}^2
 \end{aligned}$$

An alternative method for the estimation of η/η_o is the use of Fig. 15.19. In this case τ_1 must be calculated with Eq. (15. 92); for the example $\tau_1 = 0.8 \text{ s}$ and at $\dot{\gamma} = 10 \text{ s}^{-1}$ the product $\dot{\gamma}\tau_1 = 8$. According to Fig. 15.19 $\eta/\eta_o = 0.35$ at $Q = 2$.

The character of non-Newtonian viscosity of concentrated polymer solutions resembles closely that of undiluted polymers as discussed in Chap. 15, if the shear rate is not very high. An example is shown in Fig. 16.16 for polystyrene with a narrow molecular weight distribution in *n*-butyl benzene (Graessley, 1967). With decreasing concentration the onset to non-Newtonian behaviour shifts to higher shear rate. At high shear rates the plot becomes linear, but the slope $n-1$ becomes less negative with decreasing concentration. This is not very clear in this figure. In Fig. 16.17 $-\beta = 1-n$ is plotted vs. $c[\eta]$ for solutions of polystyrene and poly(α -methyl styrene) in chlorinated biphenyls (Graessley, 1974). The product $c[\eta]$ is a measure of the degree of overlap of polymer coils. At high concentrations the slope reaches a value -0.8 . This is observed in many undiluted polymers and in Graessley's model (1967) for non-Newtonian viscosities this slope is equal to $-9/11 = -0.82$ and in Bueche's model (1968) equal to $-6/7 = -0.86$. A single curve for polystyrene solutions of various concentrations and molecular weights is obtained, provided the concentration is high enough for a concentration independent slope, i.e. above $c[\eta] = 30$ (Graessley, 1974). This is shown in Fig. 16.18 where η/η_o is plotted vs. q/q_o where q_o is an empirical characteristic shear rate locating the onset of shear rate dependence in viscosity, corresponding to $\eta/\eta_o \approx 0.8$.

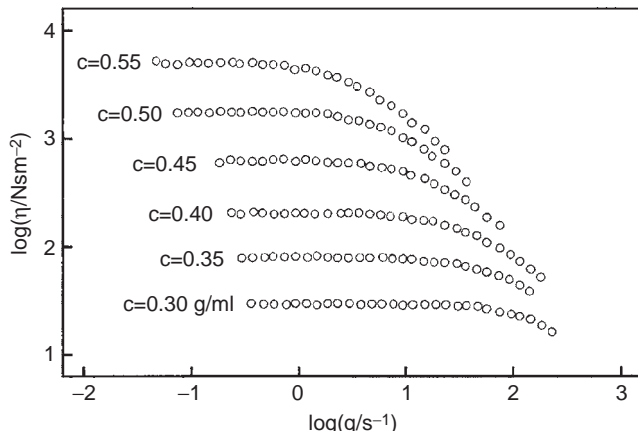


FIG. 16.16 Shear rate dependence of viscosity as a function of concentration. Data were obtained on a single narrow molecular weight distribution of polystyrene ($M_w = 411 \text{ kg/mol}$) in *n*-butyl benzene at 30°C . From Graessley, Hazleton and Lindeman (1967). Courtesy Society of Rheology.

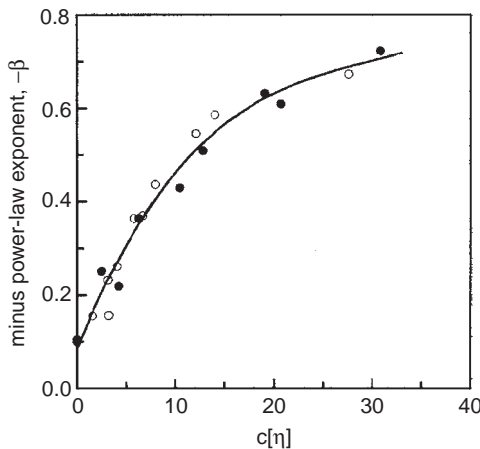


FIG. 16.17 Power law exponent $-\beta = 1 - n$ as a function of the coil overlap parameter $c[\eta]$, for solutions of polystyrene (filled symbols) and poly(α -methyl styrene) in chlorinated biphenyls (open symbols). The values of $[\eta]$ were obtained in toluene. Molecular weights range from 860 to 13,600 kg/mol for polystyrene and from 440 to 7500 kg/mol for poly(α -methyl styrene). From Graessley (1974). Courtesy Springer Verlag.

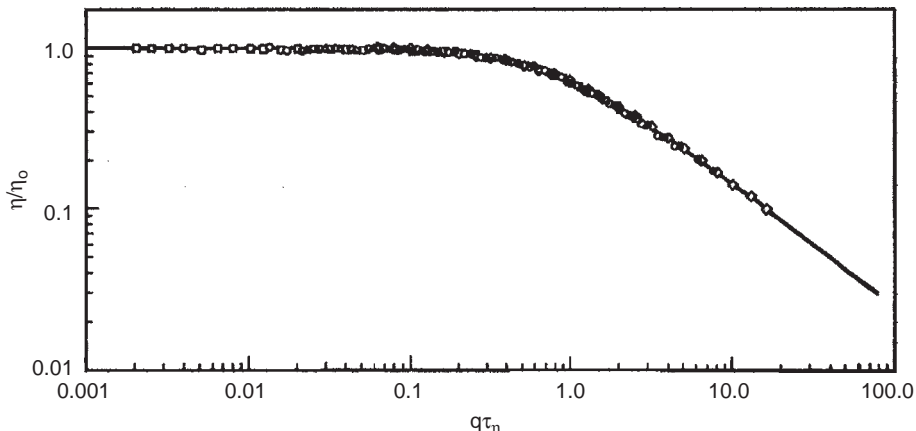


FIG. 16.18 Non-Newtonian viscosity ratio η/η_0 for solutions of narrow molecular weight distribution polystyrenes in *n*-butyl benzene, plotted vs. reduced shear rate q/q_0 , where q_0 , equal to the reciprocal of the characteristic time constant τ_η , is chosen empirically for each solution. The data were obtained for molecular weights ranging from 160 to 2400 kg/mol and for concentrations ranging from 0.255 to 0.55 g/ml at temperatures from 30 to 60 °C. The full line is calculated with the aid of Eqs. (16.52)–(16.55). From Graessley, Hazleton and Lindeman (1967). Courtesy Society of Rheology.

This characteristic shear rate is equal to the reciprocal average entanglement time τ_η at equilibrium. The solid curve is from Graessley's model, which reads

$$\eta = \eta_0 g^{3/2} h \quad (16.52)$$

in which

$$g(\theta) = \frac{2}{\pi} \left[\cot^{-1} \theta + \frac{\theta}{1 + \theta^2} \right] \quad (16.53)$$

$$h(\theta) = \frac{2}{\pi} \left[\cot^{-1} \theta + \frac{\theta(1 - \theta^2)}{(1 + \theta^2)^2} \right] \quad (16.54)$$

and

$$\theta = \frac{\eta}{\eta_0} \frac{q\tau_\eta}{2} \quad (16.55)$$

The functions $g(\theta)$ and $h(\theta)$ represent two separate effects of disentanglement: $g(\theta)$ is the fractional reduction of entanglement density due to steady shear flow and $h(\theta)$ is the fractional reduction in energy dissipation rate per molecule due to dis-entanglement in steady shear flow (for details, see Graessley, 1974, Chap. 8). Eqs. (16.52)–(16.55) define an implicit expression for the master curve η/η_0 vs. $q\tau_\eta$, the reduced viscosity also being present in the arguments of the functions $g(\theta)$ and $h(\theta)$.

16.4.4. First normal stress coefficient and creep

The first normal stress coefficient at low shear rates, $\Psi_{1,0}$, and the elastic shear compliance, J_e^0 , are related by Eq. (15.78) which reads

$$\Psi_{1,0} = 2\eta_0^2 J_e^0 \quad (16.56)$$

At high shear rates this relationship is not simple anymore. Ψ_1 decreases fast with increasing shear rate. This is shown in Fig. 16.19 for a 20% solution of PIB in Primol D oil at 25 °C (Huppler et al., 1967). It appears that Ψ_1 falls by several orders of magnitude with increasing q , but the slope is less steep than -2 predicted by many rheological models. Moreover, at high shear rates it starts to level off, although a second plateau region, like that for viscosities of polymer solutions, has never been found, as far as the present author knows.

The ratio S_q , which is defined to be equal to $1/2\Psi_1/\eta^2$, is equal to the elastic shear compliance J_e^0 for shear rates approaching zero. Both Ψ_1 and η are shear rate dependent, but it is previously not clear whether it increases or decreases with increasing shear rate. In Fig. 16.20 both η/η_0 and S_q/J_e^0 are plotted vs. $q\tau_o$ on double logarithmic scales for solutions and melts of poly (α -methyl styrene) as well (Sakai et al., 1972). First, it appears that the

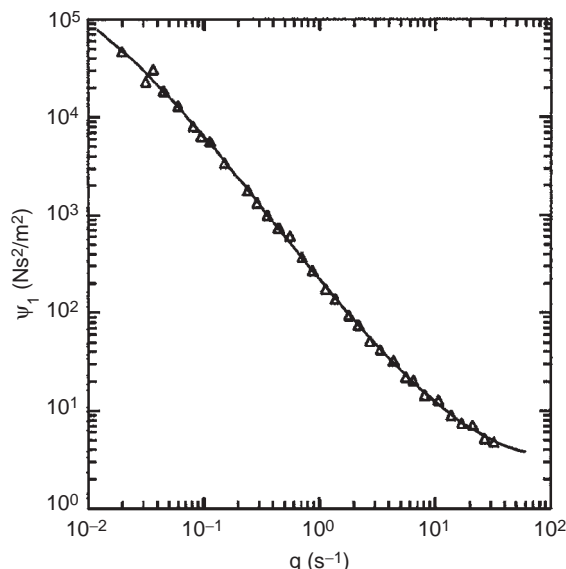


FIG. 16.19 First normal stress coefficient Ψ_1 vs. shear rate q on double logarithmic scales for a 20% solution of PIB in Primol D at 25 °C. Data from Huppler et al. (1967) and reproduced from Bird et al. (1987).

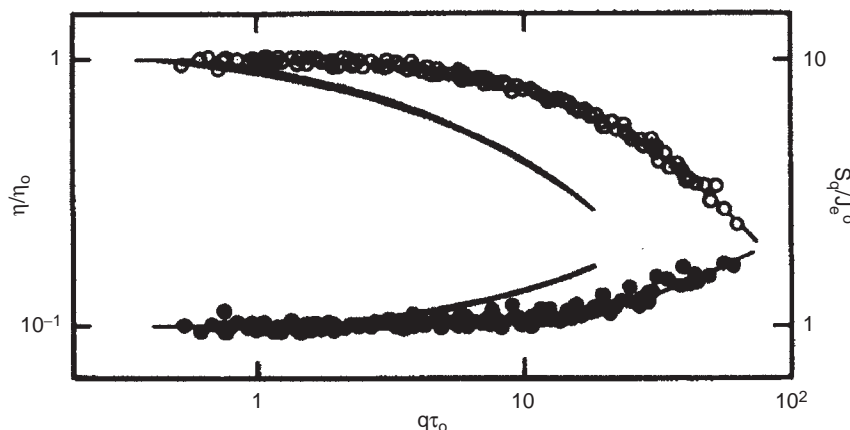


FIG. 16.20 Superimposed plots of η/η_0 (open symbols) and S_q/J_e^0 (closed symbols) as functions of shear rate for high concentrations and molecular weights of poly(α -methyl styrene) solutions. The full lines are empirical results for low concentrations and molecular weights. Replotted from Sakai et al. (1972).

term S_q/J_e^0 increases with increasing shear rate. Apparently the viscosity decreases relatively faster with increasing shear rate than the first normal stress coefficient. Secondly, the polymer solutions are behaving non-Newtonian already at lower values of $q\tau_0$ than the polymer melts. This is different from results in Fig. 16.19. Apparently τ_0 decreases faster with increasing shear rate for dilute polymer solutions than that for concentrated polymer solutions.

16.5. EXTENSIONAL FLOW OF POLYMER SOLUTIONS

Extensional deformation of polymer solutions is applied technically in the so-called dry spinning of polymer fibres. The literature data in this field are not as numerous as in the field of shear viscosity, so that only a qualitative picture can be given here.

For concentrated polymer solutions, the behaviour in extensional deformation shows a great correspondence to that of polymer melts. At low rates of deformation the extensional viscosity has the theoretical value of three times the shear viscosity. At higher rates of deformation, the experimental results show different types of behaviour. In some cases, the extensional viscosity decreases with increasing rate of extension in the same way as the shear viscosity decreases with increasing shear rate. In other cases, however, a slight increase of the extensional viscosity with increasing rate of extension was observed.

By contrast, quite different results have been obtained with dilute polymer solutions. Here the extensional viscosity may be as much as thousand times the shear viscosity. Measurement of extensional viscosity of such mobile liquids is far more difficult than shear viscosity, or even impossible. According to Barnes et al. (General references, 1993): "The most that one can hope for is to generate flow which is dominated by extension and then to address the problem of how best to interpret the data in terms of material functions that are rheologically meaningful". An example of the difficulties that arise with the measurement of extensional viscosity is shown in Fig. 16.21 for a Round Robin test

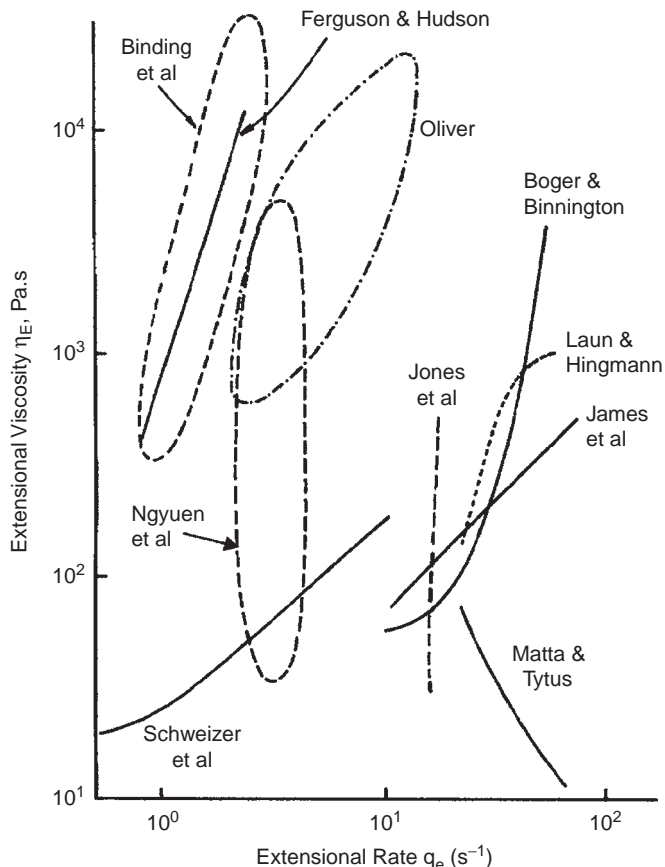


FIG. 16.21 Apparent or transient extensional viscosity of the round robin test fluid M1 as a function of Hencky strain, measured in many different devices (James and Walters, 1993). The various instruments are *spin line*: Binding et al.; Ferguson and Hudson; Ngyuen et al.; *horizontal spin line*: Oliver; *open siphon*: Binding et al.; *stagnation flow*: Laun and Hingmann; Schweizer et al.; *contraction flow*: Binding et al.; Boger and Binnington; *converging flow*: James et al.; *falling pendant drop*: Jones et al.; *falling cylinder*: Matta and Tytus. See special issue J Non-Newtonian Fluid Mech, 35, 2+3 (1990). Courtesy Chapman & Hall.

fluid M1 consisting of 0.244% w/w solution of high molecular weight polyisobutylene ($M = 3.79 \times 10^6$ g/mol) in a mixed solvent of 7% kerosene and 93% polybutene oil. Its viscosity was moderately high, being about 3 Ns/m^2 at 20°C . This test fluid was rheologically examined in shear and in extension with the aid of various instruments all over the world, commercially available and home made as well. A special issue of J Non-Newtonian Fluid Mechanics [35, 2+3 (1990)] is devoted to the rheological characterisation of this Round Robin fluid. Shear measurements coincided remarkably well (Te Nijenhuis and Van Benschop, 1990). In Fig. 16.21 results of extensional measurements are shown as the transient extensional viscosity, $\eta_e^+(t)$, vs. Hencky strain rate, q_e . It shows that different (kinds of) instruments yield different results. It also shows that the extensional viscosity exceeds the shear viscosity by many order of magnitude, with Trouton ratios of at least 10,000. As already became clear in Chap. 15, the transient extensional viscosity plotted vs. measurement time, is highly dependent on time of residence and on extensional rate of

strain: large parts of the graphs were covered with theoretical and experimental results. Hence, it is reasonable now that results obtained in a special instrument cover a limited part of the rheogram only. As pointed out by J. Ferguson (see Hudson and Jones, 1993), a three-dimensional plot should be used to present the transient extensional viscosity as a function of Hencky strain and time of residence. It seems that results that show no correspondence at all in a 2D-plot, like those in Fig. 16.21, cover a surface in a 3D-plot with a quite clear correlation. From Fig. 16.21 it is also obvious that there are many different kinds of devices to measure the extensional viscosity, each covering a certain part of the rheogram. As already mentioned in Chap. 15, they can be divided in controllable and non-controllable instruments, where imposed parameters are whether or not controllable, respectively.

Indeed, a number of extensional rheometers have spawned in the last decades (James and Walters, 1993) and most of them are able to capture the high extensional viscosities, which are known to exist. An example of such an instrument is schematically shown in Fig. 16.22. By this technique a liquid is sucked out of a reservoir into a capillary with the aid of a vacuum pump. After the flow has started, the suction opening is brought above the liquid surface in the reservoir. For liquids with sufficient elasticity the upgoing liquid flow remains intact. This is called for the open-siphon flow or Fano flow after the physician who first (1908) reported this technique. The volume flow rate and the dimensions of the flowing liquid column, as measured with the video camera, yield necessary information. The stress may be obtained by measuring the force at the top of the liquid column needed to maintain the flow. It is the reverse of spin line flows (Te Nijenhuis, 2005), which has already been discussed in Chap. 15. It has the advantage, however, that the material is at rest before it is suddenly stretched, in contrast to the spinning line experiment. A disadvantage is the presence of some shear (see, e.g. Makosko, 1994). Other, more sophisticated methods to study the elongation behaviour of dilute polymer solutions are, e.g. falling drop, stagnation flow, lubricated compression, converging flow and contraction flow techniques. For a description of these methods the reader is referred to the paper by James and Walters (1993).

We will finish this Section with some interesting experimental results on dilute polymer solutions. In Fig. 16.23 extensional viscosity data are shown, obtained from a spin-line rheometer on a solution of polybutadiene in decalin (Hudson and Ferguson, 1976). Here η_e not only shows normal behaviour, starting with an increase, followed by a substantial decrease, but also at very high extensional rates a substantial increase. It is not clear yet whether this ultimate tension thickening also occurs for stiff polymeric systems. Concentration dependent extensional viscosities are presented in Fig. 16.24 for 0.0125–0.75%

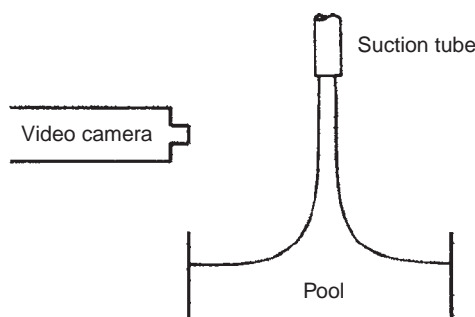


FIG. 16.22 Schematic view of Fano flow.

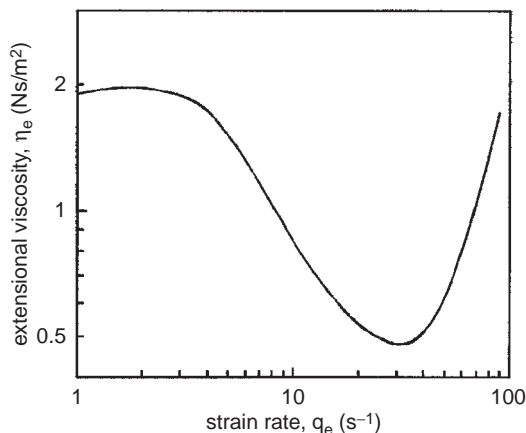


FIG. 16.23 Extensional viscosity curve for a 6.44% solution of polybutadiene in decalin determined with a commercial spin-line rheometer. Analogous to Hudson and Ferguson (1976).

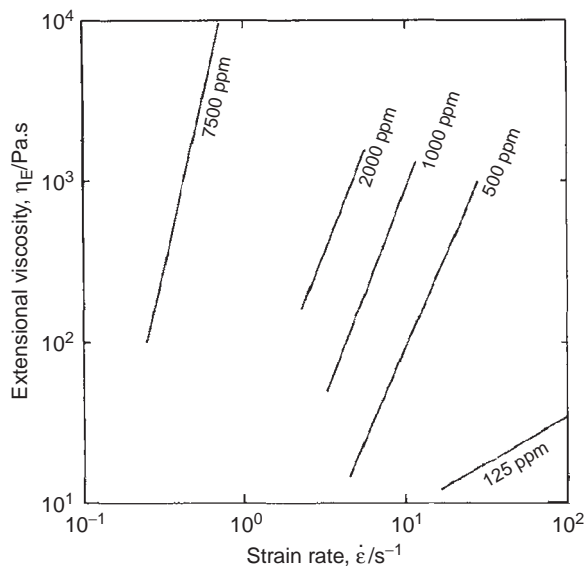


FIG. 16.24 Extensional viscosity data obtained from a spin-line rheometer for very dilute aqueous poly(acryl amide) (1175 grade) solutions, as specified. From Walters and Jones (1988, 1989). Courtesy Elsevier Science Publishers.

aqueous solutions of high molecular weight poly(acryl amide) also obtained from a spin-line rheometer (Walters and Jones, 1988, 1989). It is amazing that such dilute solutions have such extremely high extensional viscosities, up to 10,000 N s/m², whereas the shear viscosities of these solutions are of the order of 0.1–10 N s/m². Trouton ratios, η_e/η , of more than 10,000 are shown in Fig. 16.25 for less dilute solutions of an obviously lower molecular weight poly(acryl amide) and of xanthan gum. Although the Xanthan gum solution is tension-thinning, the associated Trouton ratios increase with strain rate and are still significantly in excess of the low rate value of 3.

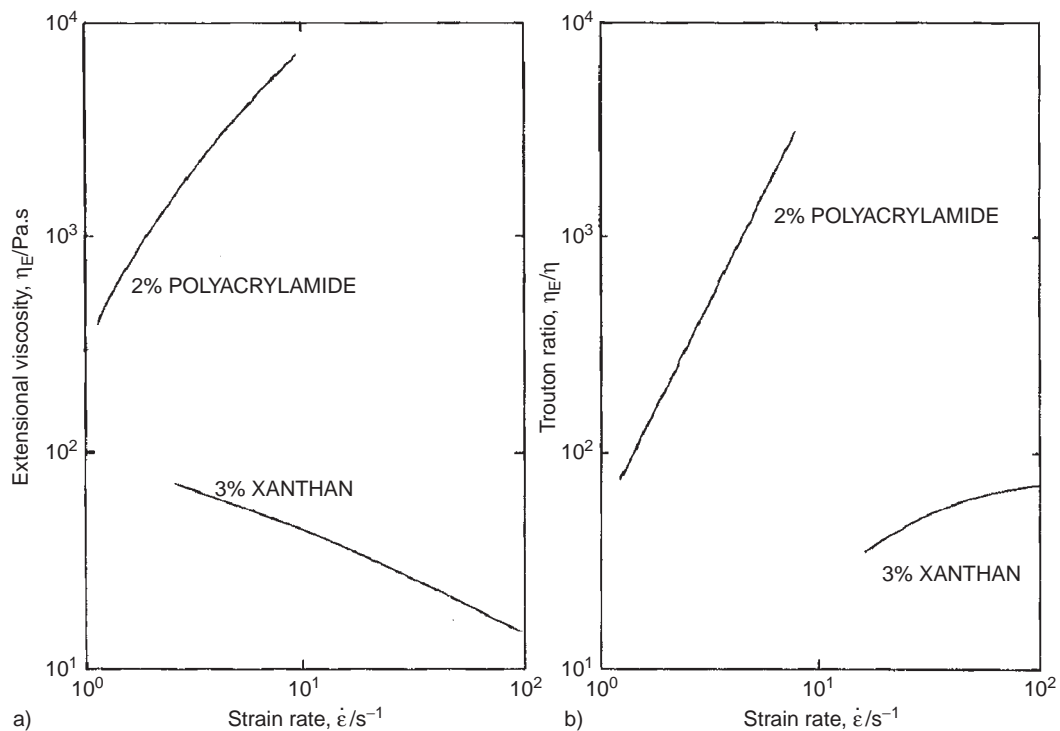


FIG. 16.25 (A) Extensional viscosity data obtained from a spin-line rheometer for dilute aqueous poly(acryl amide) (E10 grade) and Xanthan solutions; (B) Trouton ratios for both polymer solutions. From Barnes, Hutton and Walters (1989). Courtesy Elsevier Science Publishers.

16.6. SOLUTIONS OF LYOTROPIC LIQUID CRYSTALLINE POLYMERS

16.6.1. Lyotropic main chain LCPs

Solutions of the aromatic polyamides (PpBA, PpPTA and PmPTA), the polybenzazoles (PBT and PBO), poly(benzyl glutamate) (PBG) and hydroxypropylcellulose (HPC) are the most studied main chain lyotropic systems and our understanding of the behaviour of lyotropics is based on investigations of this relatively small number of materials (Moldenaers, 1996). They form main chain liquid crystals because of their rigid molecular structure in the appropriate solvents. Two kinds of solvents are used (Collyer, 1996):

1. Powerfully protonating acids such as 100% sulphuric acid, chlorofluoro acid, methanesulphonic acid and anhydrous hydrogen fluoride
2. Aprotic dipolar solvents such as dimethylacetamide containing about 2.5% of a salt as lithium chloride or calcium chloride

Moreover, in order to obtain a nematic mesophase instead of an isotropic solution several conditions have to be fulfilled:

1. A polymer concentration above a critical concentration: $c_{\text{nem}} > c_{\text{crit}}$
2. A polymer molecular weight above a critical molecular weight $M_{\text{nem}} > M_{\text{crit}}$
3. A temperature below a critical level $T_{\text{nem}} < T_{\text{crit}}$

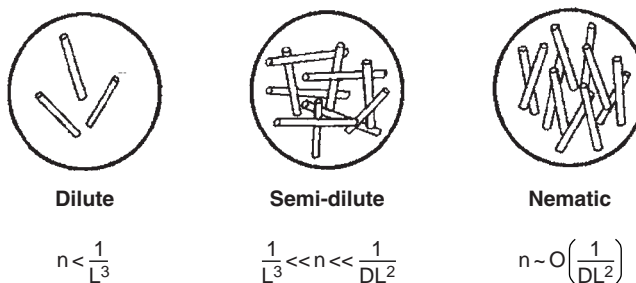


FIG. 16.26 Doi and Edwards classification of regimes for long rigid rods in solution: L = length of rod, D = diameter of rod; n = number of rods.

An example of the concentration dependence of a solution with rigid rods is illustrated in Fig. 16.26.

For a specific polymer, critical concentrations and temperatures depend on the solvent. In Fig. 15.42b the concentration condition has already been illustrated on the basis of solution viscosity. Much work has been reported on PpPTA in sulphuric acid and of PpPBA in dimethylacetamide/lithium chloride. Besides, Boerstoel (1998), Boerstoel et al. (2001) and Northolt et al. (2001) studied liquid crystalline solutions of cellulose in phosphoric acid. In Fig. 16.27 a simple example of the phase behaviour of PpPTA in sulphuric acid (see also Chap. 19) is shown (Dobb, 1985). In this figure it is indicated that a direct transition from mesophase to isotropic liquid may exist. This is not necessarily true, however, as it has been found that in some solutions the nematic mesophase and isotropic phase coexist in equilibrium (Collyer, 1996). Such behaviour was found by Aharoni (1980) for a 50/50 copolymer of *n*-hexyl and *n*-propylisocyanate in toluene and shown in Fig. 16.28. Clearing temperatures for PpPTA (Twaron® or Kevlar®, PIPD (or M5), PABI and cellulose in their respective solvents are illustrated in Fig. 16.29. The rigidity of the polymer chains increases in the order of cellulose, PpPTA, PIPD. The very rigid PIPD has a LC phase already at very low concentrations. Even cellulose, which, in principle, is able to freely rotate around the ether bond, forms a LC phase at relatively low concentrations.

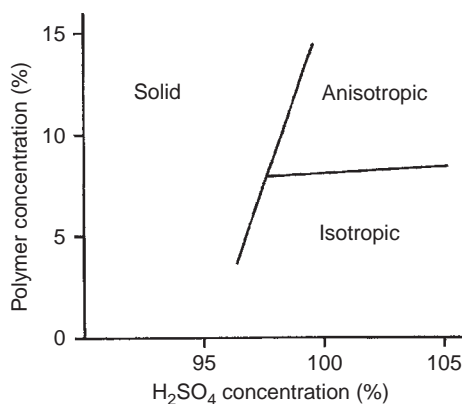


FIG. 16.27 A typical phase diagram for poly (p-phenylene terephthalamide) showing percentage polymer plotted against solvent concentration. >100% sulphuric acid is obtained by adding SO₃ (this is coined oleum). After Dobb (1985).

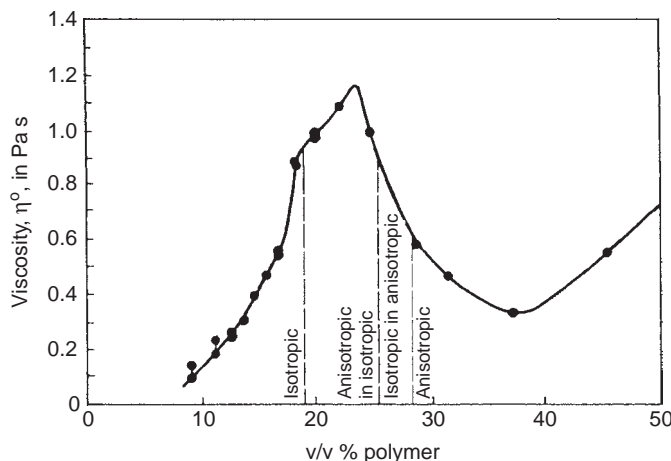


FIG. 16.28 Viscosity vs. concentration of 50/50 copolymer of *n*-hexyl and *n*-propylisocyanate in toluene at 25 °C. From Aharoni (1980); Courtesy of John Wiley & Sons, Inc.

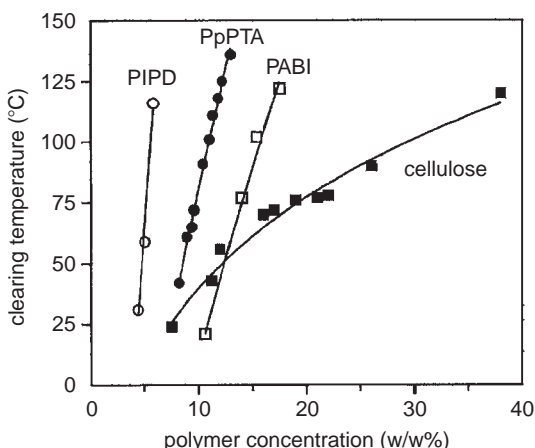


FIG. 16.29 Clearing temperature vs. concentration for PpPTA in sulphuric acid (Picken, 1989), for PIPD and cellulose in phosphoric acid (Lammers, 1998 and Boerstoel et al., 2001) and PABI homopolymer in sulphuric acid (Smirnova and Iovleva, 2003). The full lines are calculated according to Eq. (16.63) (Courtesy of Dr. H. Boerstoel).

An important dimensionless relationship between viscosity and concentration was found by Papkov et al. (1974) and reproduced in Fig. 16.30, where the variation of viscosity with polymer concentration for different molecular weights, expressed as intrinsic viscosities, is shown (left). The reduced viscosity η/η^* vs. the reduced concentration c/c^* is shown on the right. The viscosity of the solution jumps down rapidly above the critical concentration as the nematic mesophase forms. The dimensionless relationship is remarkable. The relationship between the viscosity at the maximum and the intrinsic viscosity (see inset) appears to be $\eta_{\max} = 5.5[\eta]^{1.5}$, where η is expressed in Ns/m² and $[\eta]$ in m³/kg.

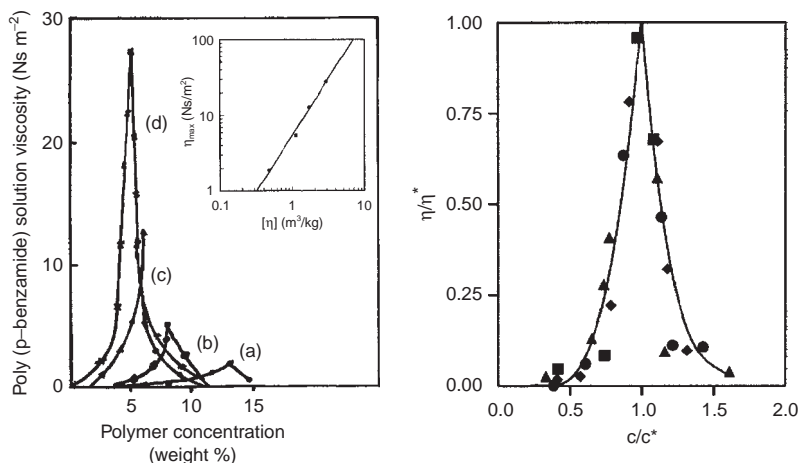


FIG. 16.30 (left) Variation of the viscosity of PpBA in dimethylacetamide/lithium chloride solutions with polymer concentration for various molecular weights expressed as intrinsic viscosities (in m³/kg): (A) 0.47; (B) 1.12; (C) 1.68 and (D) 2.96. The inset is produced by the present author: $\eta_{\text{max}} = 5.5[\eta]^{1.5}$, where η is expressed in N s/m² and $[\eta]$ in m³/kg; (right) Reduced viscosity vs. reduced concentration of the same solutions. After Papkov et al. (1974). Courtesy of John Wiley and Sons, Inc.

Several theories attempt describe the critical conditions for the formation of a lyotropic liquid crystalline structure.

(A) *Onsager's rigid-rod model* (1949) was the first correct model of an athermal Isotropic → Nematic phase transition. It is a relatively simple model that predicts phase transitions. It is based on excluded volume between two rigid rods, which reads

$$V_{\text{excl}} = 2DL^2 \langle \sin \beta \rangle \quad (16.57)$$

where L = length of rigid rod (or particle); D = width of rigid rod (or particle); β = is the angle between two rods.

If the cylinders are at some angle β to one another, then there is a large volume surrounding the rod where the approaching rod's centre-of-mass enters. If, however, the rods are oriented parallel to one another there is little volume that is excluded. This gives rise to an effective potential of the form $2kTDL^2 \langle \sin \beta \rangle$. It leads in a virial expansion to a critical volume fraction φ_{crit} for appearance of an anisotropic liquid crystalline phase

$$\phi'_{\text{crit}} = \frac{3.34}{x} \quad (16.58)$$

where $x = L/D$, i.e. aspect ratio of the rod.

The solution becomes fully anisotropic beyond a volume fraction of

$$\phi''_{\text{crit}} = \frac{4.49}{x} \quad (16.59)$$

The Onsager model is only able to describe the phase behaviour of low concentrated solutions. A second drawback is that it is athermal, and thus is not able to describe temperature dependent phase transitions, and accordingly cannot describe the occurrence of a clearing temperature.

(B) *Flory's lattice theory* (1956) has received most attention. It is an extension of Onsager's model to higher concentrations. It is ideally suited for lyotropic LCPs consisting of solvent and rigid rods. It predicts that at a phase transition an isotropic and a nematic phase coexist with respective volume fractions

$$\phi' \approx \frac{8}{x} \left(1 - \frac{2}{x}\right) \quad \text{and} \quad \phi'' \approx \frac{12.5}{x} \quad (16.60)$$

Eq. (16.60) is considered to be valid for values of the aspect ratio larger than 10. For large values of x the equation reduces to

$$\phi_{\text{crit}} = \frac{8}{x} \quad (16.61)$$

The general description of Eq. (16.60) is in agreement with experiment for a variety of lyotropic LCPs. A consequence of the theory is that for a polydisperse system of rods fractionation will occur: longer rods will become part of the anisotropic phase and the smaller ones of the isotropic phase. The major drawback to his lattice theory is that it is athermal, just like the Onsager model and therefore also fails to predict the occurrence of the clearing temperature.

Later Flory (1978) extended his theory to semi-flexible particles. For that purpose he suggested that the persistence length would determine the effective aspect ratio. If the persistence length is temperature dependent then the phase behaviour will also be temperature dependent and thus, in addition, concentration dependent. He made use of Ciferri's suggestion for the temperature dependence of the persistence length

$$L_p = AT^{-n} \quad (16.62)$$

From Ciferri's equation it follows that for flexible polymers the exponent n is larger than for stiff polymers (see, e.g. Fig. 16.29).

(C) *Maier–Saupe's mean field theory* (1958–1960) is widely used to describe low molecular weight nematics. It includes contributions from an attractive intermolecular potential between the rods that tends to align them. In contrast to the virial expansion and the lattice theory, enthalpy effects are considered, rather than entropic ones. The anisotropic attraction stabilises parallel alignment of neighbouring molecules and a mean field average of the interactions is considered. This statistical theory predicts first order phase transitions, from the isotropic to the nematic phase, consistent with experiment. The excluded volume models (Onsager and Flory approaches) fail to predict anisotropy at small aspect ratios. The M–S theory gives a fairly good description of orientation in the nematic phase and a prediction of a clearing temperature, for low molecular weight nematics only, however. Accordingly, it has not found much application to the theory of LCPs.

It has been the merit of Picken (1989, 1990) having modified the Maier–Saupe mean field theory successfully for application to LCPs. He derived the stability of the nematic mesophase from an anisotropic potential, thereby making use of a coupling constant that determines the strength of the orientation potential. He also incorporated influences of concentration and molecular weight in the Maier–Saupe model. Moreover, he used Ciferri's equation to take into account the temperature dependence of the persistence length. In this way he found a relationship between clearing temperature (i.e. the temperature of transition from the nematic to the isotropic phase) and concentration:

$$T_{\text{cl}} = \text{constant} \times c^{2/(1+2n)} \quad (16.63)$$

In this equation the temperature dependence of the persistence length is incorporated in the parameter n . The equation is used to calculate the best fit of the full lines in Fig. 16.29. We found for the parameters n the values: PIPD $n = 0.6$; PPpPTA $n = 1.2$; PABI $n = 1.2$ and cellulose $n = 5.6$ (correlation coefficients 0.988–0.997). It shows that cellulose is indeed a relatively flexible polymer, whereas the other three polymers show rigid-rod behaviour, in particular PIPD.

16.6.2. Flow behaviour of Lyotropic Main Chain LCPs

Flow behaviour as illustrated in Figs. 15.44 and 15.45 for thermotropic MCLCPs, manifests itself also at lyotropic MCLCPs. The three-region flow curve for the dependency of the viscosity on shear rate, suggested by Onogi and Asada (1980), consists of three regions shown in Fig. 16.31. This well-known curve consists of a shear-thinning region (I) at low shear rates, a “Newtonian” region (II) at intermediate shear rates and a shear thinning region (III) at still higher shear rates. In Chap. 15 it was shown that the particle structures are different in the three regions. This type of flow behaviour has also been reported for many lyotropic systems. The three regions are perceptible. In some cases region I is only present if the polymer concentration is high enough. It has also been reported that region I is preceded by a real Newtonian region with constant viscosity (e.g. Walker et al., 1995). It is not always sure whether these solutions were fully anisotropic.

The first normal stress difference of lyotropic LCPs shows, in contradistinction to ordinary polymers, a very typical behaviour as a function of shear rate. With increasing shear rate N_1 goes through a maximum, subsequently decreases, even to negative values, to reach a minimum value and increases again to positive values. An example is shown in Fig. 16.32 for 16.4% poly(benzyl L-glutamate) in m-cresol from the pioneering work of Kiss and Porter (1978, 1980). If in such a figure also the viscosity is added, then a kink is perceptible in this curve. It is slightly perceptible in Fig. 16.33 for a 12% solution of PBLG in m-cresol (Mewis and Moldenaers, 1987) just where the first normal stress difference is negative. In some cases it is much more pronounced with even a maximum in the viscosity. It is attributed to the transition from tumbling to flow aligning (Marrucci, 1996).

In addition, the second normal stress difference, which for conventional polymers is in general negative with an absolute value of not more than 20% of the first normal stress

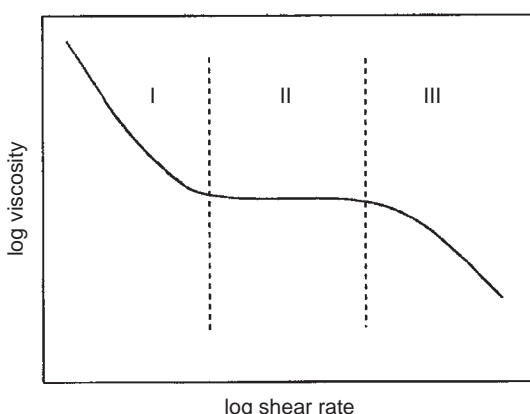


FIG. 16.31 Simplified version of the three-region flow behaviour of LCPs (non-simplified version: see Fig.15.44).

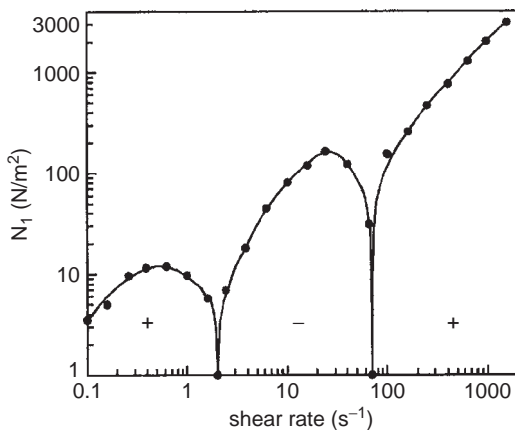


FIG. 16.32 First normal stress difference vs. shear rate of 16.4wt% PBLG in m-cresol. NB the positive and negative regions are indicated by + and -. After Kiss and Porter (1978, 1980). Courtesy John Wiley & Sons, Inc.

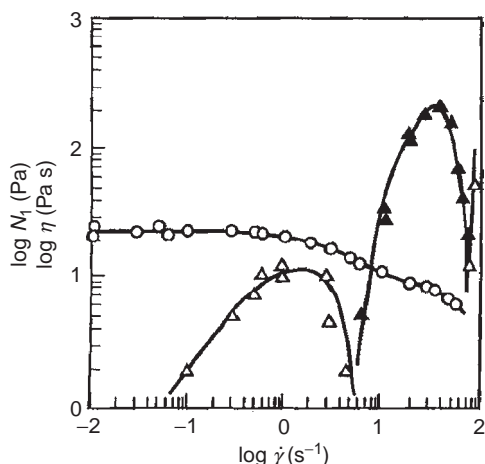


FIG. 16.33 Steady shear flow results for 12% PBLG solution in m-cresol at 293K: (○) viscosity; (△) positive N_1 ; (▲) negative N_1 . Reproduced with permission from Mewis J and Moldenaers P (1987) Mol Cryst Liq Cryst 153, 291. Copyright Taylor and Francis Ltd., <http://www.informaworld.com>.

difference, also shows changes in sign. This is illustrated in Fig. 16.34 (Magda et al., 1991) for a 12.5% PBLG solution in m-cresol. N_2 again is the opposite of N_1 . N_2 changes sign at approximately the same shear rates as N_1 and in absolute values N_2 is less than 20% of N_1 . NB: the characteristics of N_1 are similar to that shown in Fig. 16.33, but in Fig. 16.34 the ordinate is linear, instead of logarithmic.

Transient behaviour of lyotropic MCLCPs is similar to that of thermotropic MCLCPs as discussed in Sect. 15.7 (Fig. 15.47). An example is given in Fig. 16.35 for PpPTA in sulphuric acid (Doppert and Picken, 1987). It shows damped oscillating behaviour, which is in contradistinction to conventional polymers, but which is also found as a result of simple rheological models, like the Jeffreys model (see Chap. 15). This behaviour turns out to be a general feature of lyotropic MCLCPs. The oscillatory behaviour is easier to measure for lyotropic than for thermotropic systems, where it is less pronounced.

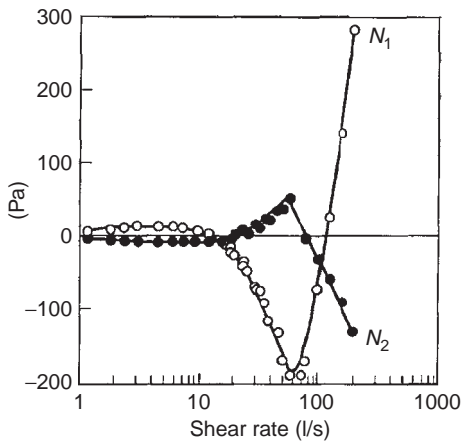


FIG. 16.34 The first and second normal stress differences in the shear flow of a 12.5% nematic solution of PBLG in m-cresol. From Magda et al. (1991). Courtesy The American Chemical Society.

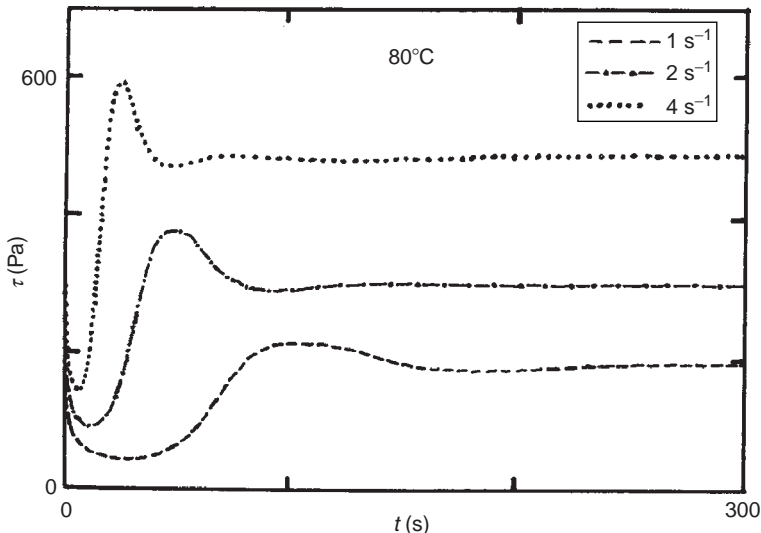


FIG. 16.35 Transient shear stress vs. time upon starting steady shear flow at three different shear rates for a 20% (w/w) solution of PpPTA in concentrated sulphuric acid. Reproduced with permission from Doppert HL and Picken SJ (1987) Mol Cryst Liq Cryst 153, 109. Copyright Taylor and Francis Ltd., <http://www.informaworld.com>.

The steady state is reached after several oscillations and the time of the minima and maxima may be scaled by qt , where q is the constant shear rate. As already said in Chap. 15, this behaviour is according to Burghardt and Fuller explicable by the classic Leslie-Ericksen theory for the flow of liquid crystals, which tumble, rather than align, in shear flow. Again it is far beyond the scope of this book to go into detail of this theory.

Finally, it has to be mentioned that stress growth experiments turn out to be very sensitive to the previous history (Moldenaers, 1996).

As a résumé the rheological responses of MCLCP solutions (in comparison with conventional polymer solutions) to the most important variables are shown (qualitatively) in the comprehensive Fig. 16.36.

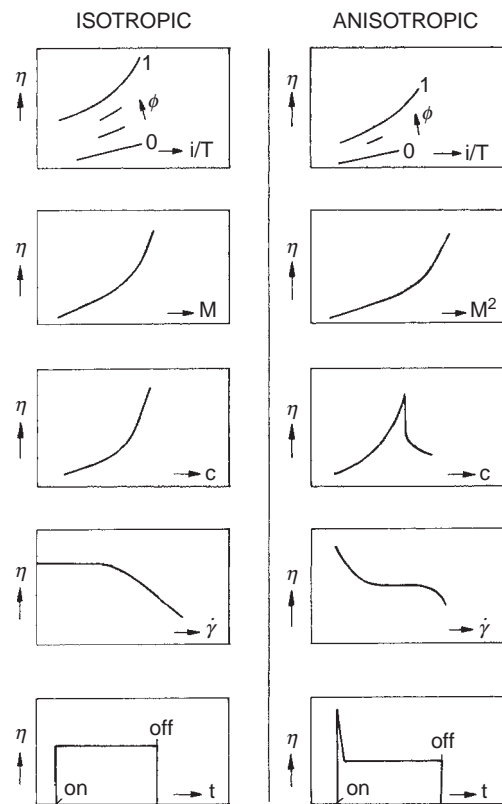


FIG. 16.36 Rheological behaviour of isotropic vs. anisotropic solutions. All graphs are double logarithmic.

16.6.3. Lyotropic side chain LCPs

Lyotropic SCLCP are far less well studied by rheology than lyotropic MCLCPs. An example is the discotic SCLCP, as mentioned in Chap. 6 (Fig. 6.15), by Franse et al. (2002–2004). Fig. 16.37 gives a schematic representation of side chain discotic polymers (Franse, 2002). In solution the polymers have a tendency to form networks due to interaction between the discotic side chains. From viscoelastic measurements (G' and G'' as functions of angular frequency) it appeared that the networks formed in a 13% solution in 1,1,2-trichloroethane are very fragile, with a rubber modulus of not more than 1 N/m^2 .

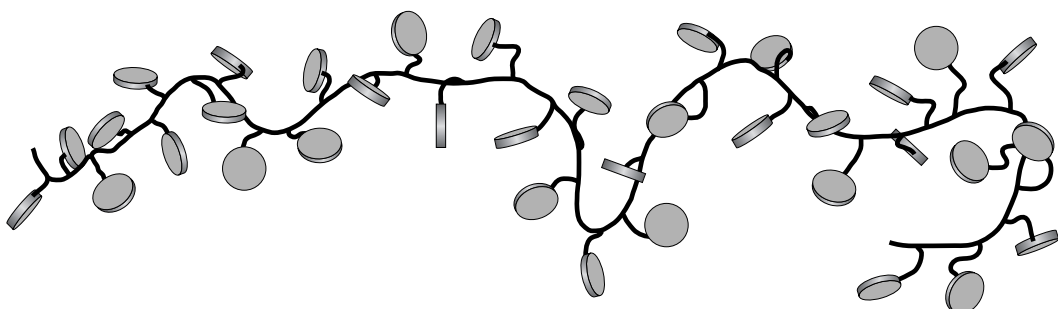


FIG. 16.37 Cartoon of discotic side-chain liquid crystalline polymers. After Franse, 2002.

From model calculations it became clear that the formation enthalpy of cross-links formed in the solution is of the order of 3 kJ/mol only and the conclusion is that pair and pair interactions between two discs only, form the cross-links.

BIBLIOGRAPHY

General references

- Acierno D and Collyer AA (Eds) "Rheology and Processing of Liquid Crystal Polymers", Chapman & Hall, London, 1996.
 Barnes HA, Hutton JF and Walters K, "An Introduction to Rheology", Elsevier, Amsterdam, 1989.
 Brandrup J, Immergut EH and Grulke EA (Eds) "Polymer Handbook", Wiley, New York, 4th Ed, 1999.
 Bueche F, "Physical Properties of Polymers", Wiley, New York, 1962.
 Doi M and Edwards SF, "The Theory of Polymer Dynamics", Clarendon Press, Oxford, 1986.
 Eirich FR, "Rheology", Vol. 1, Academic Press, New York, 1956.
 Flory PJ, "Principles of Polymer Chemistry", Cornell Univ Press, Ithaca, NY, 1953.
 Larson RG, "Constitutive Equations for Polymer Melts and Solutions", Butterworth, London, 1988.
 Morawetz H, "Macromolecules in Solution", Wiley, New York, 1975.
 Tanford C, "Physical Chemistry of Macromolecules", Wiley, New York, 1961.
 Te Nijenhuis K, "Rheology of Polymeric Liquids", 4th impression, Delft, 2nd Ed, 2005.
 Tompa H, "Polymer Solutions", Academic Press, New York, 1956.
 Vollmert B, "Grundriss der Makromolekularen Chemie", Springer, Berlin, 1962.

Special references

- Aharoni SM, *Polym.*, 21 (1980) 1413.
 Bird RB, Armstrong RC and Hassager O, "Dynamics of Polymeric Liquids", Vol. 1: "Fluid Mechanics", Wiley, New York, 1987.
 Boerstoel H, "Liquid Crystalline Solutions of Cellulose in Phosphoric Acid", Doctoral Thesis Groningen, The Netherlands, 1998.
 Boerstoel H, Maatman H, Picken SJ, Remmers R and Westerink JB, *Polymer* 42 (2001) 7363.
 Boerstoel H, Maatman H, Westerink JB and Koenders BM, *Polymer* 42 (2001) 7371.
 Bondi A, "Physical Properties of Molecular Crystals, Liquids and Glasses", Wiley, New York, 1968.
 Braun G and Kovacs AJ, in Prins JA (Ed), "Proc Int Conf on Phys Non-Crystalline Solids, Delft, July, 1964", North Holland Publishing Co, Amsterdam, 1965.
 Bueche F, *J Chem Phys* 48 (1968) 4781.
 Bueche F and Harding SW, *J Polym Sci* 32 (1958) 177.
 Burghardt WR and Fuller GC, *J Rheol* 34 (1990) 959.
 Carreau PJ, PhD Thesis, Univ of Wisconsin, 1969.
 Ciferri A and Marsano E, *Gazz Chim Ital* 117 (1989) 567.
 Collyer AA, "Introduction to Liquid Crystal Polymers" in Acierno D and Collyer AA (Eds) "Rheology and Processing of Liquid Crystal Polymers", Chapman & Hall, London, 1996, Chap. 1.
 Cross MM, *J Colloid Sci* 20 (1965) 417.
 Cross MM, in Wetton RE and Whorlow RW (Eds) "Polymer Systems: Deformation and Flow", Macmillan, London, 1968.
 Dobb MG, in Watt W and Perov BV (Eds), "Strong Fibres", North Holland, Amsterdam, 1985, pp 673–704.
 Doppert HL and Picken SJ, *Mol Cryst Liq Cryst* 153 (1987) 109.
 Dreval VYe, Tager AA and Fomina AS, *Polym Sci USSR* 5 (1964) 495.
 Ferry JD, "Viscoelastic Properties of Polymers", Wiley, New York, 3rd Ed, 1980; Dilute solutions, Chap. 9; Concentrated Solutions, Chap. 17.
 Fitzgerald ER and Miller RF, *J Coll Sci* 8 (1953) 148.
 Flory PJ, *Proc Royal Soc A* 234 (1956) 73.
 Flory PJ, *Macromolecules* 11 (1978) 1141.
 Ford TF, *J Phys Chem* 64 (1960) 1168.
 Franse MWCP, "A Rheological and Structural Study of Polymer Networks", Doctoral Thesis, Delft, The Netherlands, 2002.
 Franse MWCP, Te Nijenhuis K and Picken SJ, *Rheol Acta* 42 (2003) 443.
 Franse MWCP, Te Nijenhuis K, Groenewold J and Picken SJ, *Macromolecules* 37 (2004) 7839.
 Graessley WW, *J Chem Phys* 47 (1967) 1942.
 Graessley WW, "The Entanglement Concept in Polymer Rheology", *Adv Polym Sci* 16 (1974) 1–179.
 Graessley WW, Hazleton RL and Lindeman LR, *Trans Soc Rheol* 11 (1967) 267.
 Hermans J, *J Colloid Sci* 17 (1962) 638.
 Hoftyzer PJ and Van Krevelen DW, *Angew Makromol Chem* 54 (1976) 1.

- Hudson NE and Ferguson J, Trans Soc Rheol 20 (1976) 265.
- Huggins ML, J Am Chem Soc 64 (1942) 2716.
- Huppler JD, Ashare E and Holmes LA, Trans Soc Rheol 11 (1967) 159.
- Ito Y and Shishido S, J Polymer Sci, Polymer Phys 13 (1975) 35.
- James DF and Walters K, "A Critical Appraisal of Available Methods for the Measurement of Extensional Properties of Mobile Systems" in Collyer AA (Ed), "Techniques in Rheological Measurement", Chapman & Hall, London, 1993.
- Janeschitz-Kriegel H, "Flow Birefringence of Elastico-Viscous Polymer Systems", Adv Polym Sci 6 (1969) 170–318.
- Jenckel E and Heusch R, Kolloid-Z 130 (1953) 89.
- Johnson MF, Evans WW and Jordan T, J Coll Sci 7 (1952) 498.
- Kambour RP, Romagosa EE and Gruner CL, Macromolecules 5 (1972) 335.
- Kambour RP, Gruner CL and Romagosa EE, J Polymer Sci, Polymer Phys 11 (1973) 879; Macromolecules 7 (1974) 248.
- Kiss G and Porter RS, J Polym Sci, Polym Symp 65 (1978) 193.
- Kiss G and Porter RS, J Polym Sci, Polym Phys Ed 18 (1980) 361.
- Kelley FN and Bueche F, J Polymer Sci 50 (1961) 549.
- Kraemer EO, Ind Eng Chem 30 (1938) 1200.
- Lammers M, "PIPD Rigid-Rod Polymer Fibres and Films", PhD Thesis, ETH 12685, Zürich (1998).
- Lettinga P, Dogic Z, Wang H and Vermant J, Langmuir 21 (2005) 8048.
- Lyons PF and Tobolsky AV, Polymer Eng Sci 10 (1970) 1.
- Macosko CW, "Rheology: Principles, Measurements and Applications", VCH Publishers, New York, 1994.
- Magda JJ, Baek SG, De Vries L and Larson RG, Macromolecules 24 (1991) 4460.
- Maier W and Saupe A, Z Naturf A13 (1958) 564; A14 (1959) 1909 and A15 (1961) 282.
- Marrucci G, "Theoretical Aspects of the Flow of Liquid Crystal Polymers", in Acierno D and Collyer AA (Eds) "Rheology and Processing of Liquid Crystal Polymers", Chapman & Hall, London, 1996, Chap. 2.
- Mewis J and Moldenaers P, Mol Cryst Liq Cryst 153 (1987) 291.
- Moldenaers P, "Time-dependent Effects in Lyotropic Systems", in Acierno D and Collyer AA (Eds) "Rheology and Processing of Liquid Crystal Polymers", Chapman & Hall, London, 1996, Chap. 8.
- Northolt MG, Boerstoel H, Maatman H, Huisman R, Veurink J and Elzerman H, Polymer 42 (2001) 8249.
- Onogi S and Asada T, "Rheo-Optics of Polymer Liquid Crystals", in "Rheology" (see Gen Ref: Astarita, Marrucci and Nicolai, Eds) Vol. 1, pp 127–147.
- Onogi S, Kimura S, Kato T, Masuda T and Miyanaga N, J Polymer Sci C15 (1966) 381.
- Onsager L, Ann NY Acad Sci 98 (1949) 627.
- Oyanagi Y and Ferry JD, J Colloid Sci 21 (1966) 547.
- Papkov SP, Kulichikhin VG, Kalmykova VD and Malkin AY, J Polymer Sci: Polymer Phys 12 (1974) 1753.
- Pezzin G, Pure Appl Chem 26 (1971) 241.
- Pezzin G and Gligo N, J Appl Polym Sci 10 (1966) 1.
- Pezzin G, Omacini A and Zilio-Grandi F, Chim Ind (Milan) 50 (1968) 309.
- Picken SJ, Macromolecules 22 (1989) 1766 and 23 (1990) 464.
- Picken SJ, "Orientational Order in Aramid Solutions", PhD Thesis, Utrecht, 1990.
- Rodriguez F, Polym Lett 10 (1972) 455.
- Rudin A and Strathdee GB, J Paint Techn 46 (1974) 33.
- Rudin A, Strathdee GB and Brain Edey W, J Appl Polym Sci 17 (1973) 3085.
- Sakai T, Macromolecules 3 (1970) 96.
- Sakai M, Fujimoto T and Nagasawa M, Macromolecules 5 (1972) 641.
- Simha R and Chan FS, J Phys Chem 75 (1971) 256.
- Simha R and Utracki L, J Polym Sci A2–5 (1967) 853.
- Simha R and Utracki L, Rheol Acta 12 (1973) 455.
- Smirnova VN and Iovleva MM, Fibre Chem 35 (2003) 290.
- Sokolova TS, Yefimova SG, Volokhina AV, Kudryavtsev GI and Papkov SP, Polym Sci USSR 15 (1973) 2832.
- Streeter DJ and Boyer RF, Ind Eng Chem 43 (1951) 1790.
- Tager AA, Dreval VYE and Khasina FA, Polym Sci USSR 4 (1963) 1097.
- Te Nijenhuis K and Van Benschop HJ, J Non-Newtonian Fluid Mech 35 (1990) 169.
- Utracki L and Simha R, J Polym Sci A1 (1963) 1089.
- Vinogradov GV, Malkin AyA, Blinova NK, Sergeyevkov SI, Zabugina MP, Titkova LV, Yanovsky YuG and Shalganova VG, Eur Polym J 7 (1973) 1231.
- Walker LM, Wagner NJ, Larson RG, Mirau PA and Moldenaers P, J Rheol 39 (1995) 925.
- Walters K and Jones DM, in Uhlherr PHT (Ed) "Proceedings of the 10th International Congress on Rheology", Vol. 1, Australian Society of Rheology, 1988, pp 103–109; Rheol Acta 28 (1989) 482.
- Yasuda K, Armstrong RC and Cohen RE, Rheol Acta 20 (1981) 163.

CHAPTER 17

Transport of Thermal Energy

In this chapter it is demonstrated that the *heat conductivity* of amorphous polymers (and polymer melts) can be calculated by means of additive quantities (Rao function, molar heat capacity and molar volume). Empirical rules then also permit the calculation of the heat conductivity of crystalline and semi-crystalline polymers.

The rate of heat transport in and through polymers is of great importance. For good thermal insulation the thermal conductivity has to be low. On the other hand, polymer processing requires that the polymer can be heated to the processing temperature and cooled to ambient temperature in a reasonable time.

17.1. THERMAL CONDUCTIVITY

Thermal conductivity is the intensive property of a material that indicates its ability to conduct heat. For one-dimensional heat flow in the x -direction the steady state heat transfer can be described by Fourier's law of heat conduction:

$$Q = -\lambda \frac{dT}{dx} \quad (17.1)$$

where Q = heat flux in the x -direction per unit area perpendicular to the heat flow ($\text{J}(\text{m}^2\text{s})^{-1}$); λ = thermal conductivity ($\text{J}(\text{m s K})^{-1}$); dT/dx = temperature gradient in the x -direction (K m^{-1}).

Hence, thermal conductivity, λ , is the heat flux transported through a material due to a temperature gradient.

For non-stationary heat conduction in a semi-infinite stationary medium the one-dimensional transient heat conduction without heat production, we have next parabolic differential equation

$$\frac{\partial T}{\partial t} = h \frac{\partial^2 T}{\partial x^2} \quad (17.2)$$

where the *heat transfer coefficient* or *thermal diffusivity* h is defined as

$$h = \frac{\lambda}{\rho c_p} (\text{m}^2\text{s}^{-1}) \quad (17.3)$$

where ρ = density (kg m^{-3}); c_p = specific heat capacity at constant pressure ($\text{J}(\text{kg K})^{-1}$).

An adequate theory that might be used to predict accurately the thermal conductivity of polymeric melts or solids does not exist. Most of the theoretical or semi-theoretical

expressions proposed are based on Debye's treatment of heat conductivity (1914), which leads to the equation:

$$\lambda = \Lambda c_v \rho u l \quad (17.4)$$

where c_v = specific heat capacity at constant volume ($\text{J}(\text{kg K})^{-1}$); u = velocity of elastic waves (sound velocity) (m s^{-1}); l = average free path length (m); Λ = a constant in the order of magnitude of unity.

Kardos (1934) and, later, Sakiadis and Coates (1955, 1956) proposed an analogous equation:

$$\lambda \approx c_p \rho u L \quad (17.5)$$

where L = the distance between the molecules in "adjacent isothermal layers" (m).

Most theories have the common feature that they explain the phenomenon of heat conductivity (in melts and amorphous solids) on the basis of the so-called "phonon" model. The process is supposed to occur in such a way that energy is passed quantumwise from layer to layer with sonic velocity and the amount of energy transferred is assumed to be proportional to density and heat capacity. No large-scale transfer of molecules takes place.

In crystalline solids, and therefore also in highly crystalline solid polymers, the thermal conductivity is enlarged by a concerted action of the molecules.

17.1.1. Amorphous polymers and polymer melts

The general shape of the $\lambda - T$ curve of amorphous polymers and of polymer melts is given in Fig. 17.1. The curve passes through a rather flat maximum at T_g , and shows a gradual but slow decline in the liquid state. In the same figure also the $c_p - T$, $\rho - T$ and $u - T$ curves are shown, being the components of the $\lambda - T$ curve according to Eqs. (17.4) and (17.5). Indeed, multiplication of c_p , ρ and u gives the expected behaviour of λ .

Assuming that ΛL in (17.4) or L in (17.5) are nearly constant and independent of temperature, it may be expected that a direct proportionality exists between the thermal diffusivity $h = \lambda / (\rho c_p)$ and the sound velocity u . Using the method of calculation of u , explained in Chap. 14, i.e. putting

$$u_{\text{long}} = \left(\frac{\mathbf{U}_R}{\mathbf{V}} \right)^3 \left[\frac{3(1-v)}{1+v} \right]^{1/2} \quad (17.6)$$

one may expect

$$h = \frac{\lambda}{\rho c_p} = L \left(\frac{\mathbf{U}_R}{\mathbf{V}} \right)^3 \left[\frac{3(1-v)}{1+v} \right]^{1/2} \quad (17.7)$$

The factor $\left(\frac{3(1-v)}{1+v} \right)^{1/2}$ is nearly constant for solid polymers (≈ 1.05). Table 17.1 gives the adequate data at room temperature as published by Eiermann, Hellwege and Knappe (see references) and by Hands et al. (1973). The value of L is of the expected order of magnitude with an average of $L \approx 5 \times 10^{-11} \text{ m}$.

Since $\rho c_p = C_p / V$, the approximate value of λ can be estimated by means of the expression:

$$\lambda(298) = L \frac{C_p}{V} \left(\frac{\mathbf{U}_R}{\mathbf{V}} \right)^3 \text{ J}(\text{m s K})^{-1} \quad (17.8)$$

where $L \approx 5 \times 10^{-11} \text{ m}$.

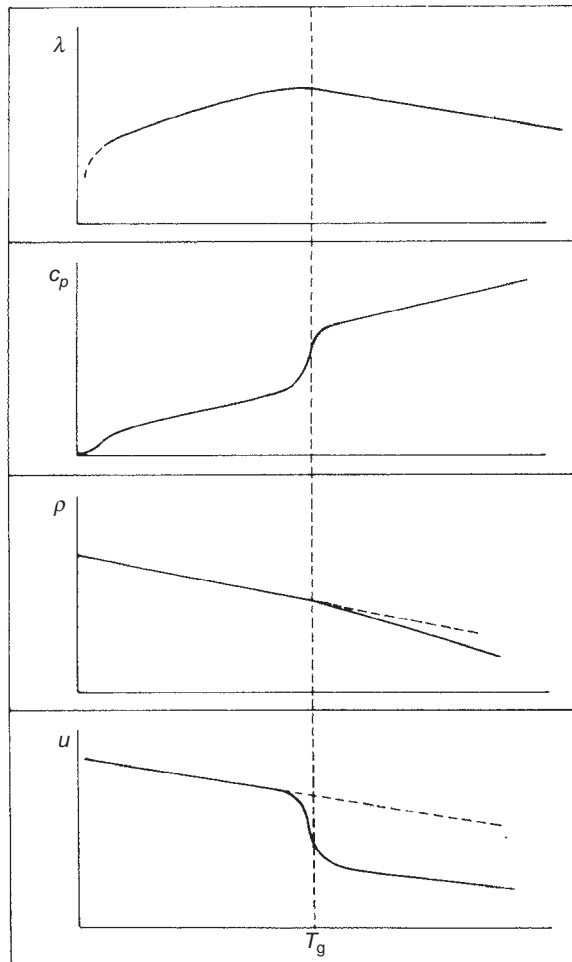


FIG. 17.1 Thermal conductivity λ and its components for amorphous polymers.

The thermal conductivity of polymers is temperature-dependent. Fig. 17.2 shows a generalized curve as a function of T/T_g based on the available experimental data. According to Bicerano (2002) the results may be approximated by (the drawn lines in Fig. 17.2):

$$\begin{aligned} T < T_g, \quad \lambda(T)/\lambda(T_g) &= (T/T_g)^{0.22} \\ T > T_g, \quad \lambda(T)/\lambda(T_g) &= 1.2 - 0.2T/T_g \end{aligned} \tag{17.9}$$

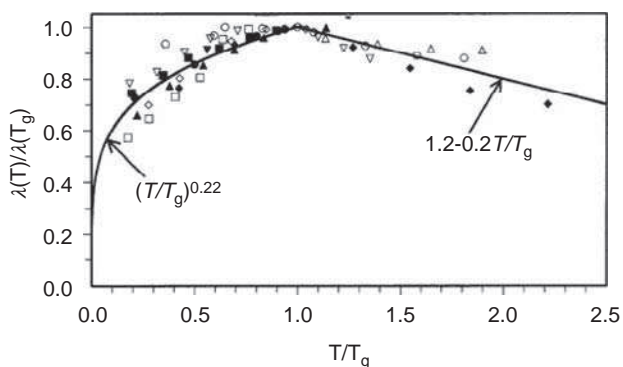
17.1.2. Highly crystalline polymers

Crystalline polymers show a much higher thermal conductivity. As an example Fig. 17.3 gives the measured value of polyethylenes as a function of the degree of crystallinity.

Using an extrapolation method, Eiermann (1962–1965) found the following relationship for polymers such as polyethylene and polyoxymethylene of “100% crystallinity”.

TABLE 17.1 Heat conductivities of amorphous polymers

Polymer	λ (J (m s K) $^{-1}$)	C_p (J (kg K) $^{-1}$)	ρ (kg m $^{-3}$)	$h = \lambda / (\rho C_p)$ (10 $^{-8}$ m 2 s $^{-1}$)	U_{long} (m s $^{-1}$)	L (10 $^{-11}$ m)
Polypropylene (at.)	0.172	2140	850	9.5	1715	5.5
Polyisobutylene	0.130	1970	860	7.7	1770	4.3
Polystyrene	0.142	1210	1050	11.1	2600	4.3
Poly(vinyl chloride)	0.168	960	1390	12.5	2000	6.3
Poly(vinyl acetate)	0.159	1470	1190	9.1	1610	5.7
Poly(vinyl carbazole)	0.155	1260	1190	10.4	2460	4.4
Poly(methyl methacrylate)	0.193	1380	1170	11.8	2370	5.0
Polyisoprene	0.134	1890	910	7.8	1470	5.3
Polychloroprene	0.193	1590	1240	9.8	1360	7.2
Poly(ethylene oxide)	0.205	2010	1130	9.0	2120	4.1
Poly(ethylene terephthalate)	0.218	1130	1340	14.3	2140	6.7
Polyurethane	0.147	1700	1050	8.3	1710	4.8
Poly(bisphenol carbonate)	0.193	1200	1200	13.5	2350	5.8
Poly(dimethyl siloxane)	0.163	1590	980	10.4	1700	6.1
Phenolic resin	0.176	1050	1220	13.7	2320	5.9
Epoxide resin	0.180	1250	1190	12.0	2680	4.5
Polyester resin	0.176	1250	1230	11.3	2430	4.6

Conversion factor: 1 J (m s K) $^{-1}$ = 2.4 × 10 $^{-3}$ cal (cm s °C) $^{-1}$ **FIG. 17.2** Generalized curve for the thermal conductivity of amorphous polymers. (◆) silicon rubber; (Δ) polyisobutylene; (○) natural rubber; (◊) polypropylene; (▲) poly(trifluoro chloro ethylene); (●) poly(ethylene terephthalate); (▽) poly(vinyl chloride); (■) poly(methyl methacrylate); (□) poly(bisphenol carbonate); (▼) poly(vinyl carbazole); lines are drawn according to Eq. (17.9).

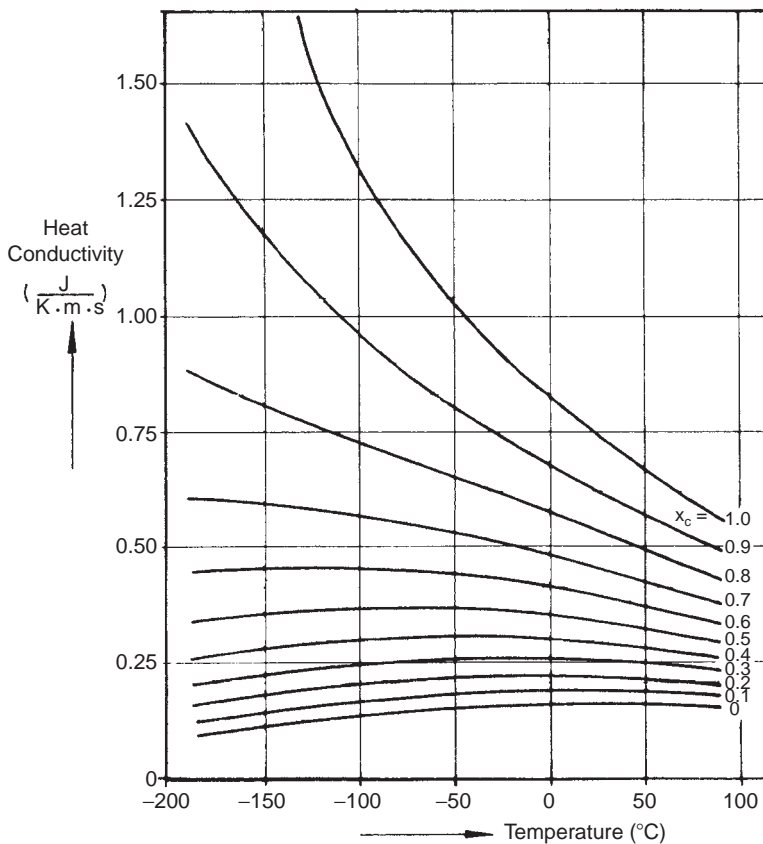


FIG. 17.3 Heat conductivity of polyethylene as a function of crystallinity (after Eiermann, 1965).

$$\lambda \approx \frac{C}{T} \left(\text{J}(\text{m s K})^{-1} \right) \quad (17.10)$$

where C is a constant with a value of about 210.

Therefore the thermal conductivity at room temperature of these *highly regular polymers* is found to be approximately $0.71 \text{ J} (\text{m s K})^{-1}$ as compared with about $0.17 \text{ J} (\text{m s K})^{-1}$ for the same polymers in the amorphous state.

For the highly regular polymers one may, as a rule of thumb, use the equation:

$$\frac{\lambda_c}{\lambda_a} \approx \left(\frac{\rho_c}{\rho_a} \right)^6 \quad (17.11)$$

by which the heat conductivity at room temperature of fully crystallized polymers can be calculated if the ratio ρ_c/ρ_a is known.

For the "normal", less regular, crystalline polymers Eiermann (1965) found the following relationship:

$$\frac{\lambda_c}{\lambda_a} - 1 = 5.8 \left(\frac{\rho_c}{\rho_a} - 1 \right) \quad (17.12)$$

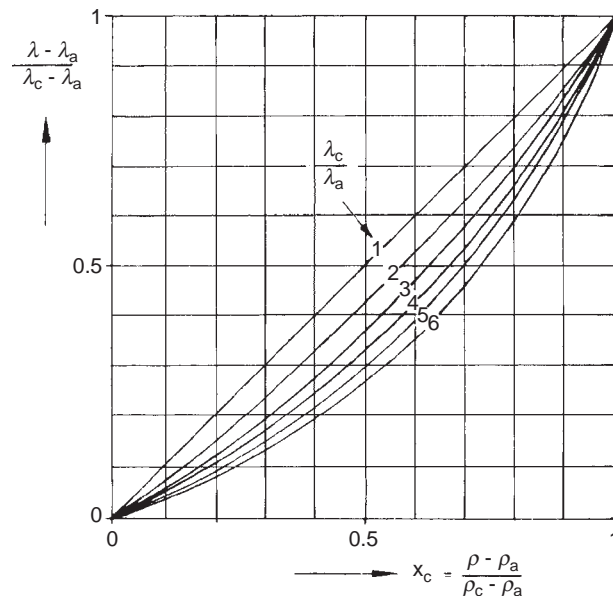


FIG. 17.4 Correlation of heat conductivity with crystallinity and density.

17.1.3. Partly crystalline polymers

Eiermann also derived equations for partly crystalline polymers of which the degree of crystallinity x_c and the ratio λ_c/λ_a are known. These equations are graphically reproduced in Fig. 17.4.

Example 17.1

Estimate the heat conductivity of amorphous poly(methyl methacrylate) (a) at room temperature and (b) at 200 °C.

Solution

(a) We use Eq. (17.7) with $c_p = 13.80 \text{ J} (\text{kg K})^{-1}$ (Chap. 5), $\rho = 1.17 \text{ g cm}^{-3} = 1170 \text{ kg m}^{-3}$ (Chap. 4), $v = 0.40$ (Chap. 13) and $M = 100.1 \text{ g mol}^{-1}$. We first calculate the Rao function (Chap. 14)

	U_{Ri}
1($-\text{CH}_2-$)	880
1($>\text{C}<$)	40
2($-\text{CH}_3$)	2800
1($-\text{COO}-$)	<u>1225</u>
	4945 ($\text{cm}^3 \text{ mol}^{-1}$) (cm s^{-1}) $^{1/3}$

$$\text{So } U_R/V = \frac{4945}{100.1/1.17} = 58(\text{cm/s})^{1/3}$$

$$\text{and } (U_R/V)^3 = 1.97 \times 10^5 \text{ cm/s} = 1.97 \times 10^3 \text{ m/s.}$$

According to Eq. (17.7)

$$\begin{aligned}\lambda &= \rho c_p L (\mathbf{U}_R / \mathbf{V})^3 \left[\frac{3(1-\nu)}{1+\nu} \right]^{1/2} = 1170 \times 1380 \times 5 \times 10^{-11} \times 1.97 \times 10^3 \times 1.13 \\ &= 0.180 \text{ J (m s K)}^{-1}\end{aligned}$$

This is in fair agreement with Eiermann's data (0.193).

- (b) We first calculate λ at T_g by means of Fig. 17.2 or of Eq. (17.9). Since $T_g = 378 \text{ K}$ we find at room temperature

$$T/T_g = 298/378 = 0.79; \lambda(T)/\lambda(T_g) = 1.2 \times 0.79 = 0.95$$

so that

$$\lambda(T_g) = 0.180/0.95 = 0.190.$$

This being known we find at $T = 200 \text{ }^\circ\text{C} = 473 \text{ K}$, so that $T/T_g = 473/378 = 1.25$ and from Fig. 17.2 or Eq. (17.9)

$$\frac{\lambda(473)}{\lambda(T_g)} = 1.2 - 0.2 \times 1.25 = 0.95$$

So λ at $200 \text{ }^\circ\text{C}$ will be $0.95 \times 0.190 = 0.180 \text{ J (m s K)}^{-1}$

Example 17.2

The heat conductivity of amorphous poly(ethylene terephthalate) at room temperature is $0.218 \text{ J (m s K)}^{-1}$. Calculate the heat conductivity of semi-crystalline PETP at a degree of crystallinity of 0.40.

Solution

Since $\rho_c = 1.465$ and $\rho_a = 1.335$, we can calculate λ_c by means of Eq. (17.12)

$$\lambda_c = \lambda_a \left[1 + 5.8 \left(\frac{\rho_c}{\rho_a} - 1 \right) \right] = 0.218 \left[1 + 5.8 \left(\frac{1.465}{1.335} - 1 \right) \right] = 0.218 \times 1.565 = 0.341$$

By means of Fig. 17.4 we may find $\lambda(x_c)$. At $\lambda_c/\lambda_a = 1.565$ and $x_c = 0.4$ we read from the graph:

$$\frac{\lambda - \lambda_a}{\lambda_c - \lambda_a} \approx 0.36 \text{ or } \frac{\lambda - 0.218}{0.341 - 0.218} \approx 0.36$$

So that $\lambda = 0.262 \text{ J (s m K)}^{-1}$, in good agreement with the experimental value (0.272).

17.2. APPENDIX

It is interesting to compare the *thermal* conductivities of polymers with those of other materials. Fig. 17.5 gives a survey.

Fig. 17.5 is an analogue of Fig. 11.5 (on the *electrical* conductivities of various materials, including polymers).

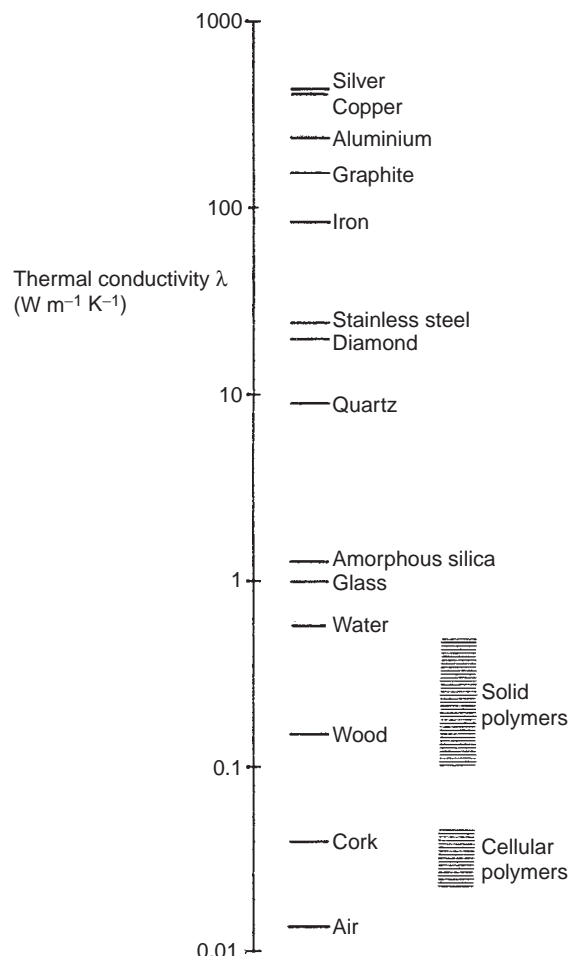


FIG. 17.5 Thermal conductivities of various materials in comparison with polymers.

BIBLIOGRAPHY

General references

- Bicerano J, "Prediction of Polymer Properties", Marcel Dekker, New York, 3rd Ed, 2002, Chap. 14.
 Bridgman PW, Proc Am Acad Arts Sci 59 (1923) 154.
 Carslaw HS and Jaeger JC, "Conduction of Heat in Solids", Clarendon Press, Oxford, 2nd Ed, 1959.
 Debye P, Math Vorlesungen Univ Gottingen 6 (1914) 19.
 Godovsky YK, "Thermophysical Properties of Polymers", Springer, Berlin, 1992.
 Knappe W, "Wärmeleitung in Polymeren", Adv Polym Sci 7 (1971) 477–535.
 Thompson EV, "Thermal Properties", in Mark HF, Bikales NM, Overberger CG, Menges G and Kroschwitz JI (Eds), "Encyclopaedia of Polymer Science and Engineering", Wiley, New York, Vol 16, 2nd Ed, 1985, pp 711–737.
 Tye RP (Ed), "Thermal Conductivity", Academic Press, New York, 2 Vols, 1969.
 Wen J, "Heat Capacities of Polymers" in Mark JE (Ed), "Physical Properties of Polymers Handbook", Springer, 2nd Ed, 2007, Chap. 9.
 Yang Y, "Thermal Conductivity" in Mark JE (Ed), "Physical Properties of Polymers Handbook", Springer, 2nd Eds, 2007, Chap. 10.
 Ziman JM, "Electrons and Phonons", Clarendon Press, Oxford, 1960.

Special references

- Eiermann K, Kunststoffe 51 (1961) 512; 55 (1965) 335.
Eiermann K, Kolloid-Z 180 (1962) 163; 198 (1964) 5 and 96; 199 (1964) 63 and 125; 201 (1965) 3.
Eiermann K and Hellwege KH, J Polym Sci 57 (1962) 99.
Eiermann K, Hellwege KH and Knappe W, Kolloid-Z 171 (1961) 134.
Hands D, Lane K and Sheldon RP, J Polym Sci, Polym Symp No 42 (1973) 717.
Hellwege KH, Henning J and Knappe W, Kolloid-Z (1962) 29; 188 (1963) 121.
Kardos A, Forsch Geb Ingenieurw 5B (1934) 14.
Knappe W, Z Angew Physik 12 (1960) 508; Kunststoffe 51 (1961) 707; 55 (1965) 776.
Sakiadis BC and Coates J, AIChEJ 1 (1955) 275; 2 (1956) 88.

This page intentionally left blank

CHAPTER 18

Properties Determining Mass Transfer In Polymeric Systems

Permeation and dissolution are the main processes determined by diffusive mass transfer. Permeation of polymers by small molecules depends on their solubility and diffusivity. For both quantities reasonable estimations are possible if some basic data of the permeating molecules (e.g. critical temperature and collision diameter) and of the polymer (structure, glass transition temperature, crystallinity) are known. For the estimation of the permeability of thin layers (films) an additive quantity, the permachor, is available.

Dissolution of polymers is controlled by processes of diffusion and convection. The rate of diffusion may be estimated from the intrinsic properties of the polymer and the Reynolds number of the dissolving liquid.

18.1. INTRODUCTION

In this chapter the diffusive mass transfer, as observed in practical applications of polymeric systems will be discussed. Three categories will be considered.

First of all, the permeation of simple gases through thin layers of polymers, as occurs in protective coatings and in packaging films, will be treated. This category is the most widely studied; for simple gases (such as hydrogen, air, oxygen, carbon dioxide) the permeation rules are relatively simple. Generally the knowledge within this category is well-rounded, though not yet complete, as far as the full understanding of the diffusive mechanism is concerned.

The second category is that of the mass transfer of heavier organic vapours and liquids as occurs in polymeric constructions such as plastic containers and bottles. In this case the situation is more complicated; very often there is stronger interaction between penetrant and polymer. The performance of useful and repeatable experiments and the acquiring of quantitative knowledge can be very difficult.

The last category of mass transfer problems is the dissolution of polymers by liquids. The study of this category is still in its infancy.

We shall discuss these three categories in succession.

18.2. PERMEATION OF SIMPLE GASES

The *permeability* or *permeability coefficient* P of a membrane is:

$$P = \frac{QL}{\Delta\varphi} \quad (18.1)$$

where Q = flux of permeant; L = thickness of the membrane; $\Delta\varphi$ = potential difference between both sides of the membrane.

It illustrates that the permeability P is equal to the flux Q of permeant that is transported through a membrane of thickness L under the influence of a difference $\Delta\varphi$ in potential. As shown in Table 18.1 the potential φ may be a pressure (N/m^2), a mass concentration (kg/m^3) or a molar concentration (mol/m^3). This, of course, influences the dimensions of flux and permeability.

Other important properties are the *barrier performance*, which is defined as the resistance to the transport of permeant molecules and thus is the inverse of permeability, and the *selectivity* of a polymer between two types of molecules, which is the ratio of its permeabilities to those molecules, e.g. P_{O_2}/P_{N_2} is the selectivity between oxygen and nitrogen.

For simple gases a general relationship between the three main permeation properties P (permeability), S (solubility) and D (diffusivity) is almost exactly valid:

$$P = SD \quad (18.2)$$

where D = a mutual diffusion coefficient or diffusivity, which is a kinetic factor; S = solubility or solubility coefficient, which is a thermodynamic factor.

For the dimensions concerning the permeability parameters see Table 18.1.

This means that permeation is a sequential process, starting with solution of the gas on the outer surface of the polymer (where equilibrium nearly exists), followed by slow inward diffusion ("reaction with pre-established equilibrium"). For all three physical quantities P , S and D , the temperature dependence can be described by a Van't Hoff-Arrhenius equation:

$$S(T) = S_o \exp\left(-\frac{\Delta H_S}{RT}\right) \quad (18.3)$$

$$D(T) = D_o \exp\left(-\frac{E_D}{RT}\right) \quad (18.4)$$

$$P(T) = P_o \exp\left(-\frac{E_P}{RT}\right) \quad (18.5)$$

where ΔH_S = molar heat of sorption; E_D = activation energy of diffusion; E_P = apparent activation energy of permeation.

TABLE 18.1 Dimensions concerning permeability

Potential $\Delta\varphi$	$N\ m^{-2} = Pa$	$kg\ m^{-3}$	$mol\ m^{-3}$
Flux Q	$m^3(STP)\cdot(m^2 s)^{-1}$	$kg\cdot(m^2 s)^{-1}$	$mol\cdot(m^2 s)^{-1}$
Diffusivity D	$m^2 s^{-1}$	$m^2 s^{-1}$	$m^2 s^{-1}$
Solubility S	$m^3(STP)\cdot(m^3 Pa)^{-1}$	—	—
Permeability P	$m^3(STP)\cdot(m s Pa)^{-1}$	$m^2 s^{-1}$	$m^2 s^{-1}$

As a consequence of Eq. (18.2), we also have

$$P_o = S_o D_o \quad (18.6)$$

$$E_P = \Delta H_S + E_D \quad (18.7)$$

The Eqs. (18.3–18.4) may also be written in the following way:

$$\log S(T) = \log S_o - 0.4343\Delta H_S/(RT) \quad (18.3a)$$

$$\log D(T) = \log D_o - 0.4343E_D/(RT) \quad (18.4a)$$

$$\log P(T) = \log P_o - 0.4343E_P/(RT) \quad (18.5a)$$

and:

$$\log S(298) = \log S_o - 1.457 \times 10^{-3}\Delta H_S/R \quad (18.3b)$$

$$\log D(298) = \log D_o - 1.457 \times 10^{-3}E_D/R \quad (18.4b)$$

$$\log P(298) = \log P_o - 1.457 \times 10^{-3}E_P/R \quad (18.5b)$$

where $\Delta H_s/R$, E_D/R and E_P/R have the dimension of a temperature (K). By means of the Eqs. (18.3–18.4) the six basic parameters S_o , D_o , P_o , ΔH_S , E_D and E_P can be derived from measurements of $S(T)$, $D(T)$ and $P(T)$ at different temperatures.

We shall first of all consider the main characteristic physical data of simple gases; then solubility, diffusivity and permeability will be separately discussed; finally some useful inter-conversion ratios will be given.

18.2.1. Main characteristic physical data of simple gases in connection with solubility and diffusive transport

In simple gases the molecular interactions are small. As a consequence some “model laws” may successfully be applied, e.g. the “laws” of Van der Waals, Trouton and Lennard-Jones. *Van der Waals’ law* is an extension of the law of Boyle-Gay Lussac, with corrections for the weak interaction and the proper volume of the gas molecules. For simple gases it is a fair approximation of the P - V - T -behaviour. It reads:

$$(p + a/V^2)(V - b) = RT \quad (18.8)$$

where a and b are the Van der Waals constants. The critical pressure, temperature and volume can be calculated as an expression in a , b and R :

$$V_{m,cr} = 3b, \quad p_{m,cr} = a/(27b^2), \quad T_{m,cr} = 8a/(27Rb) \quad (18.9)$$

Trouton’s rule is the relationship between the boiling temperature and the molar heat of vaporisation; it reads:

$$\Delta H_V = 10.5RT_b \quad (18.10)$$

Deviations are observed as soon as stronger (polar) interaction plays a part.

TABLE 18.2 Molar enthalpy and entropy of vaporisation and boiling temperature of some simple liquids

Liquid	$\Delta H_{\text{vap,m}}$ (kJ/mol)	$\Delta S_{\text{vap,m}}$ (J/(mol K))	T_b (°C)
Methane	8.2	73.2	-116.5
Carbon tetrachloride	30.0	85.8	76.7
Cyclohexane	30.1	85.1	80.7
Benzene	30.8	87.2	80.1
Hydrogen sulphide	18.7	87.9	-60.4
Methanol	35.3	104.6	64.0
Water	40.7	109.1	100.0

Trouton's rule states that the molar entropy of vaporisation has for many kinds of liquids the same value of about 87 J/(K mol):

$$\Delta S_{\text{vap,m}} \approx 87 \text{ J}/(\text{mol K}) \approx 10.5 R \quad (18.11)$$

$\Delta S_{\text{vap,m}}$ is equal to ratio between the molar enthalpy of vaporisation and the boiling temperature, which leads to Eq. (18.10). The molar enthalpy and entropy of vaporisation and the boiling temperature of some simple liquids are presented in Table 18.2. Some liquids deviate sharply from the rule. This is often because these liquids have structure and so a greater amount of disorder is introduced when they evaporate. Examples are water and methanol due to hydrogen bonds between the molecules. (Atkins and De Paula, 2006)

The *Lennard-Jones equation* for the potential energy at high compression reads:

$$\varphi(r) = 4\epsilon \left[\left(\frac{\sigma}{r} \right)^{12} - \left(\frac{\sigma}{r} \right)^6 \right]$$

where $\varphi(r)$ = molecular interaction energy as a function of the separation distance; r = separation distance; ϵ = potential energy constant; σ = potential length constant.

ϵ and σ are the Lennard-Jones scaling factors. Division of ϵ by the Boltzmann constant k gives the *Lennard-Jones temperature* ϵ/k , expressed in K. The constant σ may be considered as the collision diameter of the molecule. In Table 18.3 a survey of the most important physical data of simple gases is given.

18.2.2. Solubility

S is the *amount* of substance (gas) per unit volume of solvent (polymer) in equilibrium with a unit partial pressure, as expressed in the equation:

$$c = Sp \text{ (Henry's law)}$$

For simple gases S is usually given in cm^3 (STP) per cm^3 polymer per bar; the conversion into S.I. units is easy:

$$1 \text{ cm}^3 \text{ (STP)} / (\text{cm}^3 \text{ bar}) = 10^{-5} \text{ m}^3 \text{ (STP)} / (\text{m}^3 \text{ Pa})$$

TABLE 18.3 Some physical data of simple gases

Gas	T_g (K)	T_{cr} (K)	ε/k (K)	ΔH_b (kJ/mol)	$\Delta H_b/(RT_b)$ (-)	σ (nm)
He	4.3	5.3	10.2	0.36	10.0	0.255
{ H ₂	20	33	60	1.66	10.0	0.283
{ Ne	27	44.5	33	2.70	10.0	0.282
{ N ₂	77	126	71	6.47	10.1	0.380
{ CO	82	133	92	6.75	9.9	0.369
{ Ar	87.5	151	93	7.3	10.0	0.354
{ O ₂	90	155	107	7.5	10.0	0.347
{ CH ₄	112	191	149	9.4	10.0	0.376
{ Kr	121	209	179	10.1	10.0	0.366
{ Xe	164	290	231	13.7	10.0	0.405
{ C ₂ H ₄	175	283	225	14.4	10.1	0.416
{ C ₂ H ₆	185	305	216	15.6	10.1	0.444
{ CO ₂	195	304	195	16.2	(10)	0.394
H ₂ S	212	373	301	(19.3)	(11)	0.362
C ₃ H ₈	231	370	237	19.0	9.8	0.512
NH ₃	240	406	558	23.3	11.6	0.290
{ (CH ₃) ₂ O	250	500	395	22.6	10.9	0.431
{ SO ₂	263	431	335	24.8	11.3	0.411
C ₄ H ₁₀	272	425	331	24.3	10.7	0.469
{ CH ₂ Cl ₂	313	510	356	31.6	12.1	0.490
{ (CH ₃) ₂ CO	329	509	560	31.9	11.7	0.460
CH ₃ OH	338	513	482	39.2	13.9	0.363
C ₆ H ₆	353	562	412	34.0	11.6	0.535
H ₂ O	373	647	809	41.0	13.2	0.264

N.B. For organic vapours the solubility is normally expressed in weight per weight of polymer at equilibrium vapour pressure. In order to convert this into cm³(STP)/(cm³ bar) one has to multiply by the factor:

$$\frac{22,400 \times \rho(\text{polymer})}{M(\text{vapour}) \times p(\text{vapour})}$$

where 22,400 is the STP molar volume of vapour (in cm³/mol) (M expressed in g/mol).

The *solubility* of gases in polymers is not so easy to determine, since the solubilities of simple gases in polymers are low. The most accurate procedure is to establish sorption equilibrium between polymer and gas at known pressure and temperature, followed by desorption and measurement of the quantity of gas desorbed.

For fairly soluble organic vapours the determination of S is easier; a sample of polymer of known weight is kept at a fixed temperature and pressure in contact with the vapour and the weight increase is measured, usually by means of a quartz-spiral balance.

A survey of the numerical data of the solubilities of the most important simple gases in polymers at room temperature is given in Table 18.4. It is evident that for a given gas the solubilities in the different polymers do not show large variations. The nature of the gas, however, is important. Taking the solubility of nitrogen as 1, that of oxygen is roughly 2, that of carbon dioxide 25 and that of hydrogen 0.75 (see later Table 18.9).

TABLE 18.4 Solubility of simple gases in polymers

	S(298) in $\text{cm}^3 \text{ (STP)} / (\text{cm}^3 \text{ bar}) = 10^{-5} \text{ cm}^3$ $(\text{STP}) / (\text{cm}^3 \text{ Pa})^a$				Heat of solution (ΔH_s in kJ/mol)			
	N_2	O_2	CO_2	H_2	N_2	O_2	CO_2	H_2
<i>Elastomers</i>								
Polybutadiene	0.045	0.097	1.00	0.033	4.2	1.3	-8.8	6.2
cis-1,4-polyisoprene (natural rubber)	0.055	0.112	0.90	0.037	2.1	-4.2	-12.5	-
Polychloroprene	0.036	0.075	0.83	0.026	-	-	-9.6	6.2
Styrene-butadiene rubber	0.048	0.094	0.92	0.031	0.3	2.3	-	-
Butadiene-acrylonitrile rubber 80/20	0.038	0.078	1.13	0.030	5.8	2.0	-9.2	4.1
Butadiene-acrylonitrile rubber 73/27	0.032	0.068	1.24	0.027	4.1	2.0	-10.8	4.1
Butadiene-acrylonitrile rubber 68/32	0.031	0.065	1.30	0.023	4.6	0.8	-12.5	5.2
Butadiene-acrylonitrile rubber 61/39	0.028	0.054	1.49	0.022	4.0	4.6	4.6	5.0
Poly(dimethyl butadiene)	0.046	0.114	0.91	0.033	3.8	0.8	-6.6	2.0
Polyisobutylene (butyl rubber)	0.055	0.122	0.68	0.036	1.7	-5.0	-8.8	2.5
Polyurethane rubber	0.025	0.048	(1.50)	0.018	-	-	-	-
Silicone rubber	0.081	0.126	0.43	0.047	-	-	-	-
<i>Semi-crystalline polymers</i>								
Polyethylene H.D.	0.025	0.047	0.35	-	2.1	-1.7	-5.3	-
Polyethylene L.D.	0.025	0.065	0.46	-	7.9	2.5	0.4	-
trans-1,4-Polyisoprene (Gutta-percha)	0.056	0.102	0.97	0.038	-	-	-	-
Poly(tetrafluoroethylene)	-	-	0.19	-	-5.4	-7.2	-14.7	-
Polyoxymethylene	0.025	0.054	0.42	-	-	-	-	-
Poly(2,6-diphenyl-1,4-phenylene oxide)	0.043	0.1	1.34	-	-	-	-	-
Poly(ethylene terephthalate)	0.039	0.069	1.3	-	-11.4	-13.0	-31.4	-
<i>Glassy polymers</i>								
Polystyrene	-	0.055	0.65	-	-	-	-	-
Poly(vinyl chloride)	0.024	0.029	0.48	0.026	7.1	1.3	-7.9	0
Poly(vinyl acetate)	0.02	0.04	-	0.023	-	-4.6	-24.5	10.3
Poly(bisphenol A-carbonate)	0.028	0.095	1.78	0.022	-	-12.9	-21.7	-

^a Van Amerongen (1950, 1964) and Polymer Handbook.

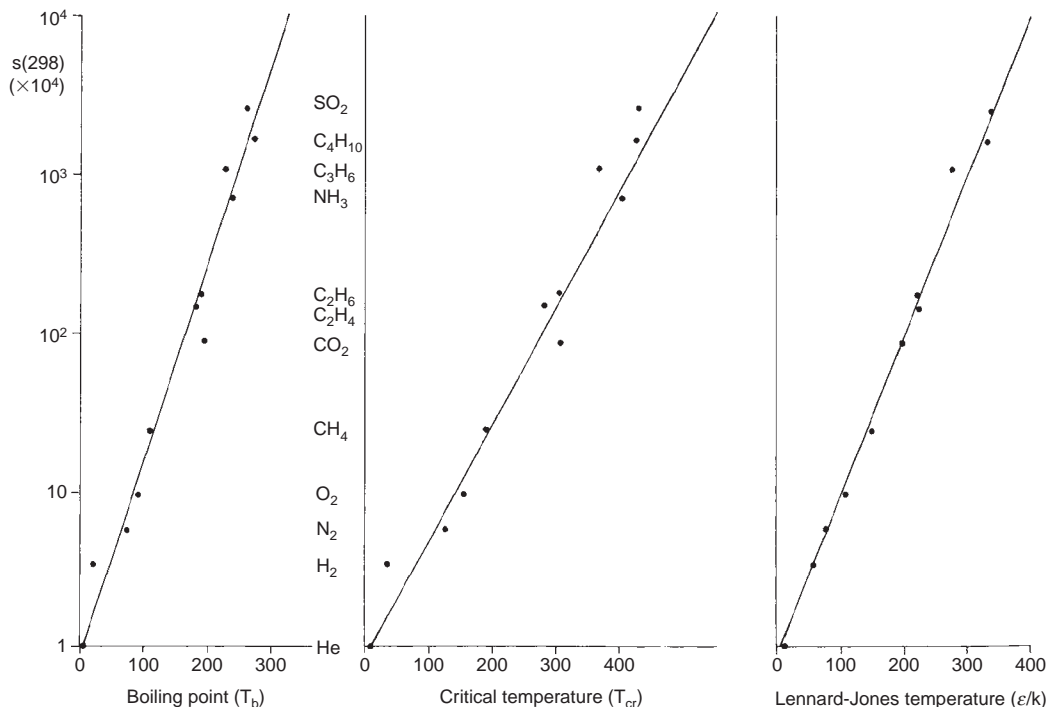


FIG. 18.1 The solubility $S(298)$ of different gases in natural rubber as a function of the boiling point, the critical temperature and the Lennard-Jones temperature. $S(298)$ is expressed in $\frac{m^3(STP)}{m^3Pa} \times 10^{-7}$.

A simple linear relationship has been found by Van Amerongen (1950, 1964) between the solubility of various gases in rubber and their boiling points or their critical temperatures. The solubility of these simple gases in natural rubber is shown in Fig. 18.1. The drawn lines can be described by the following expressions, where S is expressed in $m^3 \cdot (m^3 Pa)^{-1}$:

$$\log S(298) \approx -7.0 + 0.0074 T_{cr} \quad (18.12a)$$

$$\log S(298) \approx -7.0 + 0.0123 T_b \quad (18.12b)$$

$$\log S(298) \approx -7.0 + 0.010 \varepsilon/k \quad (18.12c)$$

The last expression is possibly the most accurate one, as was demonstrated by Michaels and Bixler (1961).

The nature of the polymer slightly affects the solubility and is probably related to the solubility parameter of the polymer. For amorphous elastomers without strong polar groups (and even for amorphous polymers in general!) Eq. (18.12c) may be used as a first approximation (with an accuracy of ± 0.25).

Van Amerongen found a pronounced selective effect of the polarity of the polymer on gas solubility in butadiene-acrylonitrile copolymers. As the acrylonitrile content of the copolymer increases, the solubility of carbon dioxide increases, whereas that of hydrogen, nitrogen and oxygen decreases.

The temperature dependence of the solubility, as follows from Eq. (18.3), obeys the Clausius–Clapeyron equation:

$$\frac{\Delta H_S}{R} = -\frac{d \ln S}{d(1/T)}$$

where ΔH_S is the heat of solution, expressed in J/mol.

For the smallest gas molecules dissolving in elastomers ΔH_S is positive (endothermic effect); for the larger gas molecules the reverse is true (exothermic effect). The process is exothermic if the sorption energy evolved exceeds the energy needed to make a hole of molecular size in the polymer.

Van Amerongen measured the heat effects of various gases in several elastomers. He found that ΔH_S of elastomers also mainly depends on the boiling points (or the Lennard-Jones temperatures) of the gas and is hardly dependent on the nature of the polymer. A representative expression is:

$$10^{-3}\Delta H_S/R = 1.0 - 0.010\varepsilon/k \pm 0.5 \quad (18.13)$$

By means of the Eqs. (18.12c), (18.13) and (18.3b) an expression for S_o can be derived:

$$\log S_o = -5.5 - 0.005\varepsilon/k \pm 0.8 \quad (18.14)$$

Eqs. (18.12) and (18.13) are valid for elastomers (and for polymers in the rubbery state). As was already mentioned earlier: no *systematic* correlation with the polymer structure could be demonstrated (it is small anyhow).

For *glassy amorphous* polymers analogous expressions could be derived from the experimental data in the literature. The numerical values of the constants in the equations are somewhat lower, and also the accuracy is lower (this is probably due to the fact that the physical structure of the glassy state strongly depends on the processing of the polymer).

It seems useful to summarise the derived expressions for the three main parameters of the solubility: $S(298)$, S_o and $\Delta H_S/R$.

For *rubbers (elastomers)* the equations are:

$$\log S(298) = -7.0 + 0.010\varepsilon/k \pm 0.25 \quad (18.12a1)$$

$$10^{-3}\Delta H_S/R = 1.0 - 0.010\varepsilon/k \pm 0.5 \quad (18.13a1)$$

$$\log S_o = -5.5 - 0.005\varepsilon/k \pm 0.8 \quad (18.14a)$$

and for *glassy polymers*:

$$\log S(298) = -7.4 + 0.010\varepsilon/k \pm 0.6 \quad (18.12b1)$$

$$10^{-3}\Delta H_S/R = 0.5 - 0.010\varepsilon/k \pm 1.2 \quad (18.13b1)$$

$$\log S_o = -6.65 - 0.005\varepsilon/k \pm 1.8 \quad (18.14b)$$

For all types of amorphous polymers:

$$\log S(T) = \log S_o - 0.4343\Delta H_S/RT = \log S(298) - 0.4343\frac{\Delta H_S}{R}\left(\frac{1}{T} - \frac{1}{298}\right) \quad (18.3a, b)$$

For fully *crystalline polymers* the solubility of gases is nearly zero; for *semi-crystalline polymers* it depends on the degree of crystallinity. Michaels and Bixler (1961) demonstrated that the following simple rule is valid for a considerable number of gases:

$$S(298) \approx S_a(298)(1 - x_c) \quad (18.15)$$

where x_c is the degree of crystallinity and S_a the solubility in the amorphous state.

Our conclusion is, that the three parameters of the solution (sorption) process of simple gases can be estimated from three hall-marks of the polymer-gas combination: the Lennard-Jones temperature of the gas (ε/k), the glass transition temperature (T_g) and the degree of crystallinity (x_c) of the polymer.

Example 18.1 gives an illustration of a calculation; Table 18.5 shows a comparison of calculated versus experimental values.

Example 18.1

Estimate the solubility and the heat of solution (sorption) of oxygen in poly(ethylene terephthalate) (PETP), both in the quenched amorphous glassy state and in the semi-crystalline state ($x_c = 0.45$).

Solution

PETP has a T_g of 345 K; so at room temperature the amorphous matrix is in the *glassy state*. We apply Eq. (18.12b1); substituting $\varepsilon/k = 107$ for O₂, gives:

$$\log S_a(298) = -7.4 + 1.07 \pm 0.6 = -6.33 \pm 0.6$$

So the value of $S_a(298)$ will be 4.7×10^{-7} with a margin between 1.2×10^{-7} and 18.5×10^{-7} . The experimental value in the literature is 9.9×10^{-7} in fair agreement (Polymer Handbook)

For the *semi-crystalline state* we find:

$$S_{sc}(298) = S_a(298)(1 - x_c) = 4.7 \times 10^{-7} \times 0.55 = 2.6 \times 10^{-7}$$

with a margin between 0.7×10^{-7} and 10×10^{-7} . The experimental value is 7.4×10^{-7} , in fair agreement.

For the value of ΔH_S we use Eq. (18.13b1):

$$10^{-3} \times \Delta H_S/R = 0.5 - 1.07 \pm 1.2 = -0.57 \pm 1.2$$

so that $\Delta H_S \times 10^{-3} = -4.7$ with a margin between -14.8 and 5.2 . The experimental value in the literature is -11.6 kJ/mol. This value determines the temperature dependence of $S(T)$ in the semi-crystalline state. The *heat effect* per mol PETP will be $\Delta H_S(1 - x_c) = -2.6 \pm 5.5$ kJ per mol PETP, and thus is very inaccurate.

18.2.3. Diffusivity

The *Diffusivity* or *Diffusion Coefficient* (D) is the amount of matter (m) passing per second through a unit area, under the influence of a unit gradient of concentration (the "driving force"), as expressed in the equation (Fick's Law):

$$\frac{dm}{dt} = -DA \frac{dc}{dx} \quad (18.16)$$

The dimension of D is m²/s, or more usual in the literature cm²/s.

TABLE 18.5 Calculated versus experimental data of $\log S(298)$ and $\Delta H_S/R$

Data	Polymer	T_g	Gas										
			He $\varepsilon/k = 10$		$H_2 \varepsilon/k = 60$		$N_2 \varepsilon/k = 71$		$O_2 \varepsilon/k = 107$		$CO_2 \varepsilon/k = 195$		
			Calc.	Exp.	Calc.	Exp.	Calc.	Exp.	Calc.	Exp.	Calc.	Exp.	
log S(298)	Silicon rubber	146		-6.37		-6.24		-6.70		-5.51		-	
	Butyl rubber	200	-6.9	-6.81	-6.40	-6.45	-6.29	-6.26	-5.93	-5.92	-5.05	-5.17	
	Natural rubber	213	± 0.25	-6.67	± 0.25	-6.43	± 0.25	-6.53	± 0.25	-5.99	± 0.25	-5.04	
	Neoprene rubber	230		-7.15		-6.59		-6.44		-6.13		-5.07	
	PVAC	306		-6.98		-6.58		-6.70	-6.20			-5.00	
	PETP	345	-7.3	-7.10	-6.80	-6.40	-6.69	-6.33	-6.00	-6.33	-5.45	(-4.53)	
	PVC	360	± 0.6	-7.26	± 0.60	-6.59	± 0.60	-6.63	-6.54	± 0.6	± 0.6	-5.35	
	PC	423		-7.88		(-5.86)		-6.80	-6.30			-5.91	
	$10^{-3} \times \Delta H_S/R$	Silicon rubber	146	-	-	-	0.80	-	-	-	-	-	
		Butyl rubber	200	0.9	0.90	0.40	0.40	0.29	0.21	0.07	-0.60	-1.05	-1.06
$10^{-3} \times \Delta H_S/R$	Natural rubber	213	± 0.5	-	± 0.50	-	± 0.50	0.25	± 0.5	-0.51	± 0.5	-1.50	
	Neoprene rubber	230	-		0.75		-			0.28		-1.15	
	PVAC	306		1.06		1.23		-0.81		-0.55		-	
	PETP	345	0.4	0.13	-0.10	-	-0.21	(-2.88)	-0.57	-1.40	-1.45	-2.9	
	PVC	360	± 1.2	1.10	± 1.20	0	± 1.20	0.84	± 1.2	0.16	± 0.12	-0.95	
	PC	423	-		0.21		-1.35		-1.55			-2.61	

If D only depends on temperature (and thus not on concentration or time), the diffusion process is called Fickian. Simple gases show *Fickian diffusion* and so do many dilute solutions (even in polymers). The diffusivity can be determined directly either from sorption or from permeation experiments. In the first case the reduced sorption, $c(t)/(c_\infty - c_0)$, is plotted versus the square root of the sorption time and D is calculated from the equation:

$$D = \frac{\pi}{16} \delta^2 K^2$$

where δ = film thickness (m) and K = slope of the reduced sorption curve ($s^{-1/2}$).

In the second case D can be calculated from the *permeation time lag* by means of the equation:

$$D = \frac{1\delta^2}{6\Theta}$$

where Θ is the time lag in seconds obtained by extrapolating the linear part of the pressure-versus-time graph to zero pressure.

Indirectly D can be determined by measuring the permeability and solubility, and applying Eq. (18.2).

For simple gases the interactions with polymers are weak, with the result that the diffusion coefficient is independent of the concentration of the penetrant. In this case the penetrant molecules act effectively as "probes of variable size" which can be used to investigate the polymer structure.

In general, diffusion of gases may be regarded as a thermally activated process, expressed by an equation of the Arrhenius type:

$$D = D_0 \exp(-E_D/(RT)) \quad (18.4)$$

where D_0 and E_D are constants for the particular gas and polymer.

All the known data on the diffusivity of gases in various polymers were collected by Stannett (1968).

Table 18.6 gives a survey of the data of the most important simple gases. It is evident that the diffusivities – in contradistinction to the solubilities – of a given gas in different polymers show large variations; also the nature of the gas plays an important part.

The activation energy of diffusion (E_D) is the most dominant parameter in the diffusion process; it is the energy needed to enable the dissolved molecule to jump into another "hole". It is clear that larger holes are necessary for the diffusion of larger gas molecules; hence the activation energy will be larger for the diffusion of bigger molecules and the diffusivity will be smaller. This is indeed found to be true in all cases.

The available data show a somewhat scattered correlation between the energy of activation and the diameter of the gas molecule, varying between the first and the second power of the molecular diameter of the penetrant molecule. In our experience the best correlation is obtained if E_D is assumed to be proportional to second power of the collision diameter (see Fig. 18.2, where the data of Table 18.3 for the collision diameters are used). If nitrogen is taken as the standard gas for comparison, we can use the product

$$\left(\sigma_{N_2}/\sigma_X\right)^2 \frac{E_D}{R} = p \quad (18.17)$$

as a characteristic parameter for the polymer, for which a correlation may be found with other parameters of the polymer. In the parameter p the influence of the diffusing gas (via its collision diameter) on E_D is "neutralised".

TABLE 18.6 Diffusivity of simple gases in polymers values of $D(298)$ in $10^{-10} \text{ m}^2/\text{s}$; D_o in $10^{-4} \text{ m}^2/\text{s}$; E_D/R in 10^3 K

Polymers	Diffusing gas			
	N_2		E_D/R	$D(298)$
	$D(298)$	D_o		
<i>Elastomers</i>				
Polybutadiene	1.25	0.19	3.6	1.5
cis-1,4-polyisoprene (natural rubber)	1.21	2.4	4.35	1.6
Polychloroprene (Neoprene)	0.29	9.3	5.15	0.43
Styrene-butadiene rubber	1.14	0.53	3.9	1.4
Butadiene-acrylonitrile rubber 80/20	0.56	0.78	4.25	0.79
Butadiene-acrylonitrile rubber 73/27	0.28	9.5	5.2	0.43
Butadiene-acrylonitrile rubber 68/32	0.17	50	5.85	0.28
Butadiene-acrylonitrile rubber 61/39	0.07	126	6.35	0.14
Poly(dimethyl butadiene)	0.10	8.8	6.2	0.14
Polyisobutylene (butyl rubber)	0.05	33	6.05	0.08
Polyurethane rubber	0.09	8.7	5.35	0.24
Silicone rubber	13	0.0014	1.35	25
<i>Semi-crystalline polymers</i>				
Polyethylene H.D.	0.12	0.36	4.5	0.17
Polyethylene L.D.	0.31	5.7	4.95	0.46
trans-1,4-polyisoprene (Gutta-percha)	0.58	6.9	4.9	0.70
Poly(tetrafluoroethylene)	0.10	0.015	3.55	0.15
Polyoxymethylene	0.021	1.31	5.35	0.037
Poly(2,6-diphenyl-1,4-phenylene oxide)	0.39	1.23×10^{-5}	1.0	0.72
Poly(ethylene terephthalate)	0.0013	0.063	5.25	0.0036
<i>Glassy polymers</i>				
Polystyrene	0.06	0.094	4.25	0.11
Poly(vinyl chloride)	0.004	288	7.45	0.012
Poly(vinyl acetate)	0.03	27.5	6.15	0.05
Poly(ethyl methacrylate)	0.025	0.68	5.1	0.11
Poly(bisphenol-A-carbonate)	0.015	0.0328	4.35	0.021

In Fig. 18.3 the parameter p is plotted versus T_g , as an index of the molecular stiffness of the polymer. The data show a considerable scattering, but the general course is unmistakable (Van Krevelen, 1972). The drawn curve corresponds to the following equation, as obtained by linear regression (correlation coefficient is only 0.86) of all data:

$$p = 6.4 \times 10^3 - 0.16(298 - T_g)^2 \pm 1.5 \times 10^3 (\text{K}) \quad (18.17a)$$

The factors $(298 - T_g)$ and $(T_g - 298)$ are the "thermal distances" of T_g from room temperature for rubbers and glasses respectively. The influence of these "thermal distances" is probably connected with the *fractional free volume* of the polymer; in rubbery amorphous polymers this f.f.v. increases with decreasing T_g , in glassy amorphous polymers the f.f.v. increases with increasing T_g (increasing formation of micro-voids), hence lowering of the activation energy.

The second important parameter of the diffusion process is the "constant" D_o . Here we are favoured by the existence of a lucky correlation of D_o with E_D . If the values of $\log D_o$

O_2		CO_2			H_2		
D_o	E_D/R	$D(298)$	D_o	E_D/R	$D(298)$	D_o	E_D/R
0.135	3.4	1.05	0.22	3.65	9.6	0.050	2.55
1.79	4.15	1.1	3.36	4.45	10.2	0.24	3.0
3.0	4.7	0.27	20	5.4	4.3	0.28	3.3
0.21	3.55	1.0	0.80	4.05	9.9	0.052	2.55
0.63	4.05	0.43	2.17	4.6	6.4	0.21	3.1
2.2	4.6	0.19	11.9	5.35	4.5	0.48	3.45
9.0	5.15	0.11	61	6.0	3.85	0.49	3.5
12.3	5.45	0.038	220	6.7	2.45	0.85	3.8
17	5.55	0.063	134	6.4	3.9	1.14	3.75
38	5.95	0.06	33	6.0	1.5	1.20	4.05
6.5	5.1	0.09	36	5.9	2.6	0.90	3.8
0.0010	1.1	15	0.0014	1.35	75	0.0030	1.1
0.44	4.4	0.12	0.19	4.25	—	—	—
4.55	4.8	0.37	1.87	4.6	—	—	—
3.5	4.6	0.47	6.5	4.9	5.0	1.9	3.8
0.0058	3.15	0.10	0.0009	3.4	—	—	—
0.22	4.65	0.024	0.20	4.75	—	—	—
3.41×10^{-5}	1.15	0.39	8×10^{-6}	0.9	—	—	—
0.37	5.5	0.0015	0.70	5.95	—	—	—
0.123	4.15	0.06	0.131	4.35	4.4	0.0036	2.0
42.2	6.55	0.0025	493	7.75	0.50	5.9	4.15
6.13	5.55	—	—	—	2.1	0.013	2.6
0.038	3.8	0.030	0.017	3.95	—	—	—
0.0085	3.85	0.005	0.018	4.5	0.64	0.0028	2.5

are plotted versus E_D a remarkably simple relationship is observed, as is shown in Fig. 18.4 for elastomers. For the amorphous glassy polymers the correlation is less accurate but shows a similar tendency, as is clear from Fig. 18.5.

So if for a certain gas–polymer combination the activation energy, E_D , is known, the diffusivity can be calculated. Equations to be used are:
for elastomers:

$$\log(D_o/m^2 s^{-1}) = 0.001 E_D/R - 8.0 \pm 0.4 \quad (18.18a)$$

and for glassy polymers:

$$\log(D_o/m^2 s^{-1}) \approx 0.001 E_D/R - 9.0 \pm 0.8 \quad (18.18b)$$

Eqs. (18.18a) and (18.18b) are interesting examples of the so-called *compensation effect* (partial offset of the effect of higher E_D by higher D_o).

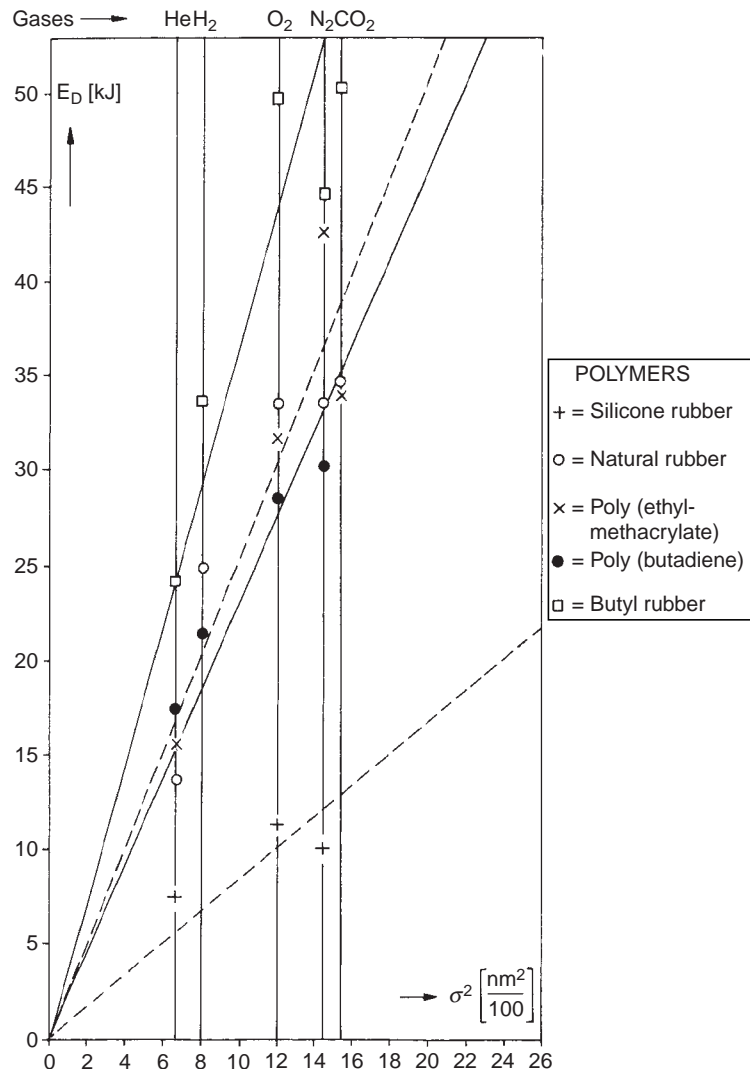


FIG. 18.2 Activation energy of diffusion versus mean square collision diameter.

With useful equations for E_D/R (18.17) and for D_o (18.18a)–(18.8b) at our disposal it is possible to calculate the diffusivity at room temperature $D(298)$ and at arbitrary temperature $D(T)$ by means of the Eqs. (18.4b) and (18.4a):

$$\log[D(T)] = \log D_o - 0.4343 E_D/(RT) \quad (18.4a)$$

$$\log[D(298)] = \log D_o - 1.457 \times 10^{-3} E_D/R \quad (18.4b)$$

As a consequence of the compensation effect mentioned earlier, the scattering of the E_D/R data is less harmful than might be expected. Some examples of estimations of $\log D(298)$ in comparison with experimental values are given in Table 18.7.

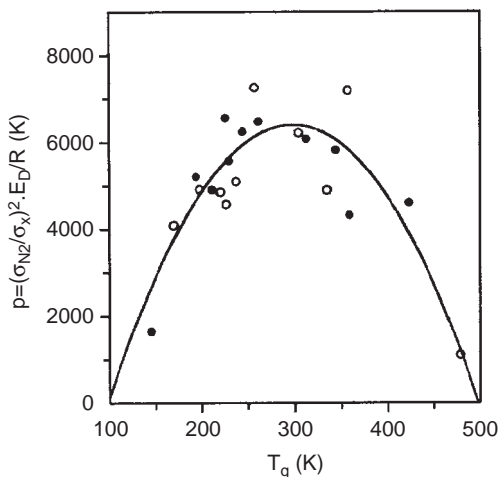


FIG. 18.3 Activation energy of diffusion as a function of T_g for 21 different polymers: from low to high temperatures, (●) odd numbers; (○) even numbers: 1. Silicone rubber; 2. Butadiene rubber; 3. Hydropol (hydrogenated polybutadiene = amorphous polyethylene); 4. Styrene/butadiene rubber; 5. Natural rubber; 6. Butadiene/acrylonitrile rubber (80/20); 7. Butyl rubber; 8. Ethylene/propylene rubber; 9. Chloroprene rubber (neoprene); 10. Poly(oxy methylene); 11. Butadiene/acrylonitrile rubber (60/40); 12. Polypropylene; 13. Methyl rubber; 14. Poly(vinyl acetate); 15. Nylon-11; 16. Poly(ethyl methacrylate); 17. Poly(ethylene terephthalate) 18. Poly(vinyl chloride); 19. Polystyrene; 20. Poly (bisphenol A carbonate); 21. Poly(2,6 dimethyl-p.phenylene oxide).

Crystallisation of polymers tends to decrease the volume of amorphous material available for the diffusion; crystalline regions obstruct the movement of the molecules and increase the average length of the paths they have to travel.

As a first approximation the following equation for (semi-)crystalline polymers

$$D = D_o(1 - x_c) \quad (18.19)$$

may be used, where x_c = degree of crystallinity.

This equation has been experimentally verified by Michaels et al. (1963) for the diffusion of several gases in poly(ethylene terephthalate).

Our final conclusion is, that the three determining parameters of the diffusion process of simple gases can be estimated from three hall-marks of the polymer-gas combination: the (collision) diameter of the gas (σ), the glass transition temperature (T_g) and the degree of crystallinity (x_c) of the polymer.

It is useful to summarise the whole set of equations, available for the estimation of the diffusion parameters:

for all polymers:

$$\frac{E_D}{R} = \left(\frac{\sigma_x}{\sigma_{N_2}} \right)^2 \left[\underbrace{6.4 \times 10^3 - 0.16(298 - T_g)^2}_p \right] \pm 1.5 \times 10^3 = p \left(\frac{\sigma_x}{\sigma_{N_2}} \right)^2 \quad (18.17b)$$

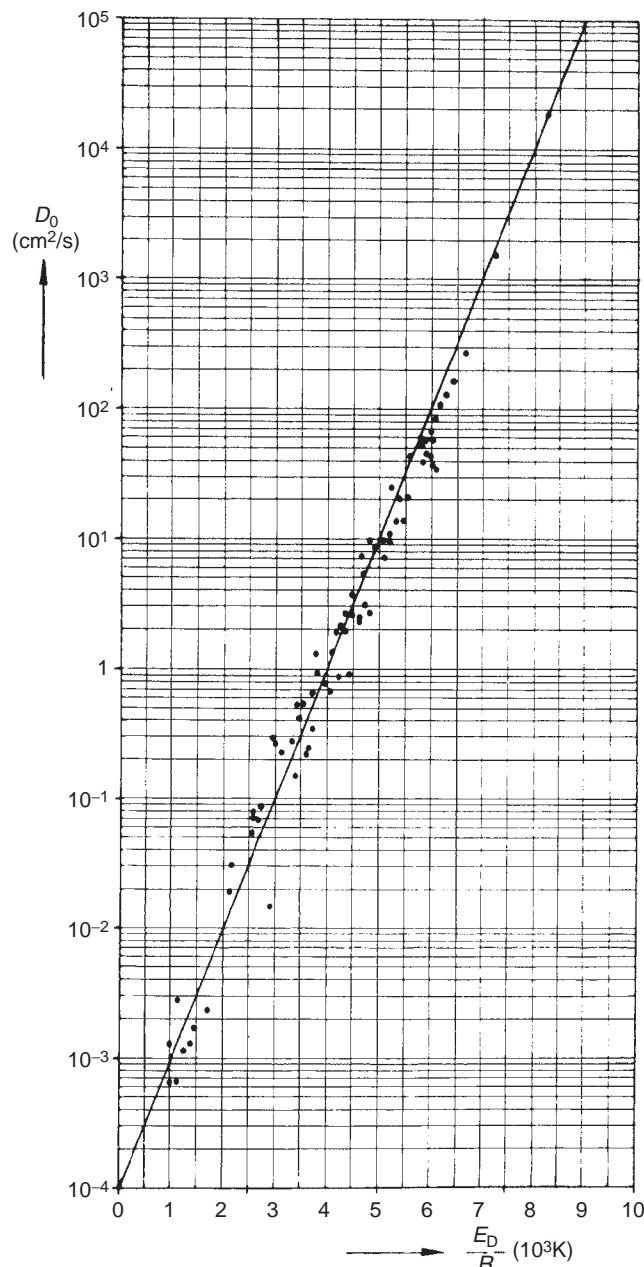


FIG. 18.4 $D_o - E_D$ relationship for elastomers.

for rubbers (elastomers):

$$\log(D_o/\text{m}^2\text{s}^{-1}) = 0.001E_D/R - 8.0 \pm 0.4 \quad (18.18a)$$

for glassy amorphous polymers:

$$\log(D_o/\text{m}^2\text{s}^{-1}) = 0.001E_D/R - 9.0 \pm 0.8 \quad (18.18b)$$

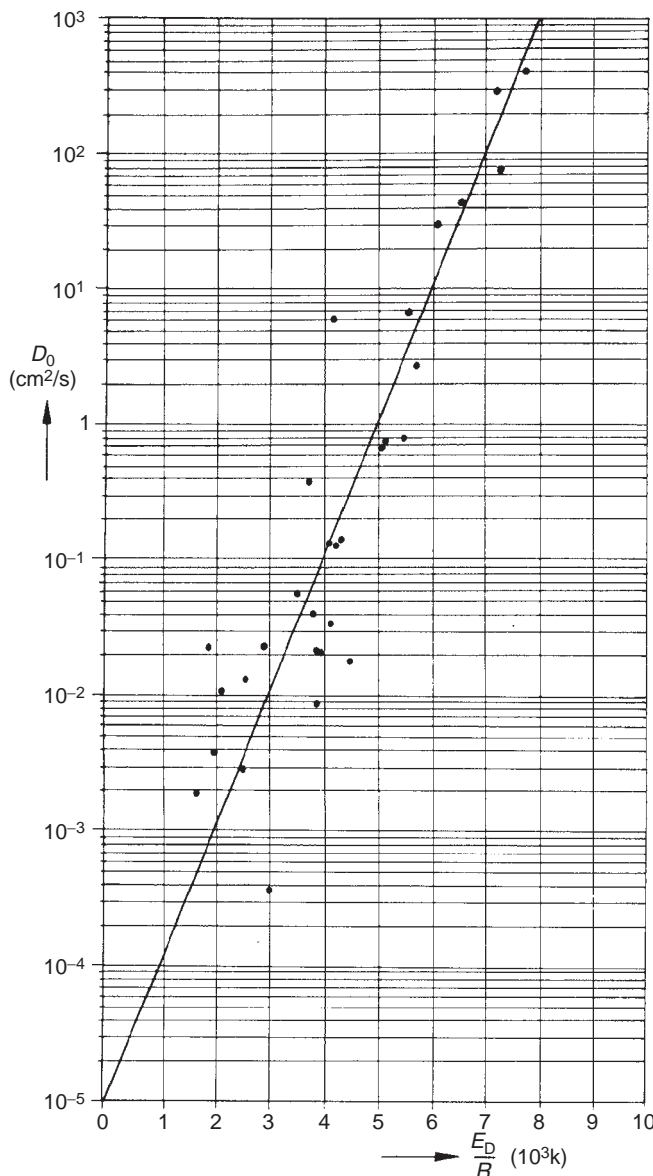


FIG. 18.5 $D_o - E_D$ relationship for glassy polymers.

for semi-crystalline polymers:

$$D_{sc} = D_a(1 - x_c) \quad (18.19)$$

for all polymers:

$$\log D(298) = \log D_o - 1.457 \times 10^{-3} \frac{E_D}{R} = -8.0 - 0.457 \times 10^{-3} \frac{E_D}{R} \quad (18.20)$$

$$\log D(T) = \log D_o - \frac{0.4343 E_D}{RT} = \log D(298) - \frac{0.4343 E_D}{R} \left(\frac{1}{T} - \frac{1}{298} \right) \quad (18.21)$$

TABLE 18.7 Calculated and experimental values of $\log D(298)$; values of $D(298)$ in cm^2/s or $10^{-4} \text{ m}^2/\text{s}$

Polymer	T_g	Gas									
		He		H ₂		O ₂		N ₂		CO ₂	
		$\sigma = 0.255 \text{ nm}$		$\sigma = 0.283$		$\sigma = 0.347$		$\sigma = 0.380$		$\sigma = 0.394$	
		Calc.	Exp.	Calc.	Exp.	Calc.	Exp.	Calc.	Exp.	Calc.	Exp.
Silicone rubber	146	-4.55	-4.20	-4.68	-4.33	-5.03	-4.87	-5.24	-5.07	-5.34	-4.82
Butadiene rubber (poly-butadiene)	171	-4.79	-4.80	-4.97	-5.02	-5.46	-5.83	-5.76	-5.96	-5.90	-5.98
Butyl-rubber (poly-isobutene cpl)	200	-5.01	-5.23	-5.23	-5.58	-5.86	-7.1	-6.23	-7.37	-6.41	-7.24
Natural rubber (poly-cis-isoprene)	213	-5.08	-4.67	-5.33	-	-6.03	-5.66	-6.41	-5.93	-6.60	-5.90
Neoprene rubber (poly-chloroprene)	230	-5.17	-	-5.43	-5.35	-6.16	-6.37	-6.60	-6.54	-6.81	-6.57
Methyl rubber (poly-dimethyl butadiene)	262	-5.28	-	-5.57	-5.41	-6.36	-6.85	-6.85	-7.10	-7.08	-7.2
Poly(vinyl acetate)	306	-6.3	-6.0	-6.6	-5.6	-7.4	-7.3	-7.9	-7.5	-8.2	-
Poly(ethylene terephthalate)	345	-6.3	-5.5	-6.5	-	-7.3	-8.3	-7.8	-8.7	-8.0	-9.1
Poly(vinyl chloride)	360	-6.2	-5.6	-6.5	-7.3	-7.2	-7.9	-7.7	-8.4	-7.9	-8.6
Poly(bisphenol carbonate)	423	-5.8	-	-6.0	-7.2	-6.5	-7.6	-6.8	-7.7	-6.9	-8.3

Example 18.2

Estimate the diffusivity at 298 K and the activation energy of diffusion for oxygen in PETP, both in the glassy and in the semi-crystalline state.

Solution

For the derivation of E_D we use Fig. 18.3 or Eq. (18.17a), where we find at $T_g = 345$ K: $p = 6.05 \times 10^3$. From Table 18.3 we find: $(\sigma_{O_2}/\sigma_{N_2})^2 = (0.91)^2 = 0.83$. So

$$\frac{E_D}{R} = p \left(\frac{\sigma_{O_2}}{\sigma_{N_2}} \right)^2 = (6.05 \pm 1.5 \times 10^3) 0.83 = (5.0 \pm 1.25) \times 10^3$$

which gives: $E_D = (41.6 \pm 10.5) \times 10^3$ J/mol = 41.6 ± 10.5 kJ/mol. Two experimental values are mentioned in the literature, viz. 46.1 and 48.5 kJ/mol, so in reasonable agreement with our estimation.

Eq. (18.18b) will be used for the estimation of $\log D_o$:

$$\log(D_o/m^2 s^{-1}) = -9.0 + 0.001 E_D / R \pm 0.8 = -9.0 + 5.0 \pm 0.8 = -4.0 \pm 0.8$$

By means of Eq. (18.20) we then find $D(298)$:

$\log D(298) = \log D_o - 1.46 \times 10^{-3} E_D / R \pm 0.8 = -4.0 - 7.3 \pm 0.8 = -11.3 \pm 0.8$, so $D_a(298) = 5.0 \times 10^{-12}$ m²/s, with a margin between 0.8×10^{-12} and 32×10^{-12} m²/s. Two experimental values are available in the literature: 0.23×10^{-12} and 0.5×10^{-12} m²/s. Our estimated value is a reasonable good approximation (see also Table 18.7).

Finally we find for the semi-crystalline state:

$D_{sc}(298) = D_a(1 - 0.45) = 2.8 \times 10^{-12}$ m²/s with a margin of 0.4×10^{-12} to 18×10^{-12} m²/s. The literature gives 0.35×10^{-12} m²/s. Also in this case a reasonable estimation.

All literature data refer to the Polymer Handbook.

18.2.4. Permeability

The Permeability or permeation coefficient (P) is the amount of substance passing through a polymer film of unit thickness, per unit area, per second and at a unit pressure difference. Here we shall use the meter as unit of length and the Pa (i.e. Pascal) as unit of pressure, so that the dimension of P becomes: m³(STP). m/(m² s Pa) = m²/(Pa s).

In the literature many units are used which easily leads to confusion and errors in computation: see Table 18.8.

TABLE 18.8 Multiplication factors with respect of SI unit: unit = a × m²/(s Pa)
1 m³ (STP) is the amount of gas in m³ at standard temperature and pressure (273 K, 1 bar)

P expressed in	do., Abbreviated	Multiplication factor a
m ³ (STP) m/(m ² s Pa)	m ² /(s Pa)	1
cm ³ (STP) cm/(cm ² s Pa)	cm ² /(s Pa)	10 ⁻⁴
cm ³ (STP) cm/(cm ² s mm Hg)	cm ² /(s mm Hg)	7.5 × 10 ⁻⁷
cm ³ (STP) cm/(cm ² s cm Hg)	cm ² /(s cm Hg)	7.5 × 10 ⁻⁸
cm ³ (STP) cm/(cm ² s atm)	cm ² /(s atm)	0.9868 × 10 ⁻⁹
cm ³ (STP) cm/(cm ² s bar)	cm ² /(s bar)	10 ⁻⁹

1 bar = 10^5 Pa; 1 atm = 760 mm Hg = 1.0135 bar = 1.0135×10^5 Pa; 1 mm Hg = 133.33 Pa; 1 Pa = 7.5×10^{-3} mm Hg;
1 mil = 1 milli-in. = 10^{-3} in.

For practical purposes the permeability is the most important of the permeation properties. Since methods of estimation of solubility and diffusivity are available, estimation of permeability is possible by means of Eq. (18.4).

As an illustration, Fig. 18.6 shows the permeability of nitrogen (at room temperature) for a great variety of polymers (elastomers, semi-crystalline polymers and glassy polymers). It can be seen that the values of P vary by a factor of nearly one million if silicone rubber on the one hand is compared with poly(vinylidene chloride) on the other!

Values of $P(298)$, P_o and E_P/R can be calculated by application of the Eqs. (18.2), (18.6) and (18.7), using the corresponding values of S and D .

By analogy with Eqs. (18.17a–18.17), the following empirical correlations could be derived from the available experimental permeability data

for rubbers:

$$\log[P_o(\text{m}^2\text{Pa}^{-1}\text{s}^{-1})] = -14.1 + 10^{-3}E_P/R \pm 0.25 \quad (18.22a)$$

$$\log P(298) = -14.1 - 0.457 \times 10^{-3}E_P/R \pm 0.25 \quad (18.23a)$$

for glassy polymers:

$$\log[P_o(\text{m}^2\text{Pa}^{-1}\text{s}^{-1})] = -15.25 + 10^{-3}E_P/R \pm 0.75 \quad (18.22b)$$

$$\log P(298) = -15.25 - 0.457 \times 10^{-3}E_P/R \pm 0.75 \quad (18.23b)$$

for semi-crystalline polymers:

$$P_{sc} = S_{sc}D_{sc} = S_aD_a(1-x_c)^2 = P_a(1-x_c)^2 \quad (18.24)$$

for all polymers:

$$\log P(T) = \log P(298) - \frac{0.4343E_P}{R} \left(\frac{1}{T} - \frac{1}{298} \right) \quad (18.25)$$

$$E_P/R = \Delta H_S/R + E_D/R \quad (18.7)$$

18.2.5. Relationships between the permeation parameters of different gases

Stannett and Szwarc (1955), Rogers et al. (1956) and Frisch (1963) have shown that simple relationships exist between the ratios of the permeability constants for either a series of gases through two polymers or the ratio between two gases through a series of polymers. If we take nitrogen as the standard gas, the permeabilities of the other gases can be calculated by a simple factor, which is given in Table 18.9.

A similar relationship as for the permeabilities is valid for the diffusivities and for the solubilities, although here the range in actual values is less impressive than with the permeability constants. These ratios are also given in Table 18.9.

Finally, even the activation energies of diffusion and permeation can be estimated in this way, as was already quantitatively described by the relationship $E_D \propto \sigma^2$. We may conclude that if two of the three quantities D , S and P are known (or can be estimated) for nitrogen in a given polymer, those for the other gases can be estimated very quickly and rather accurately.

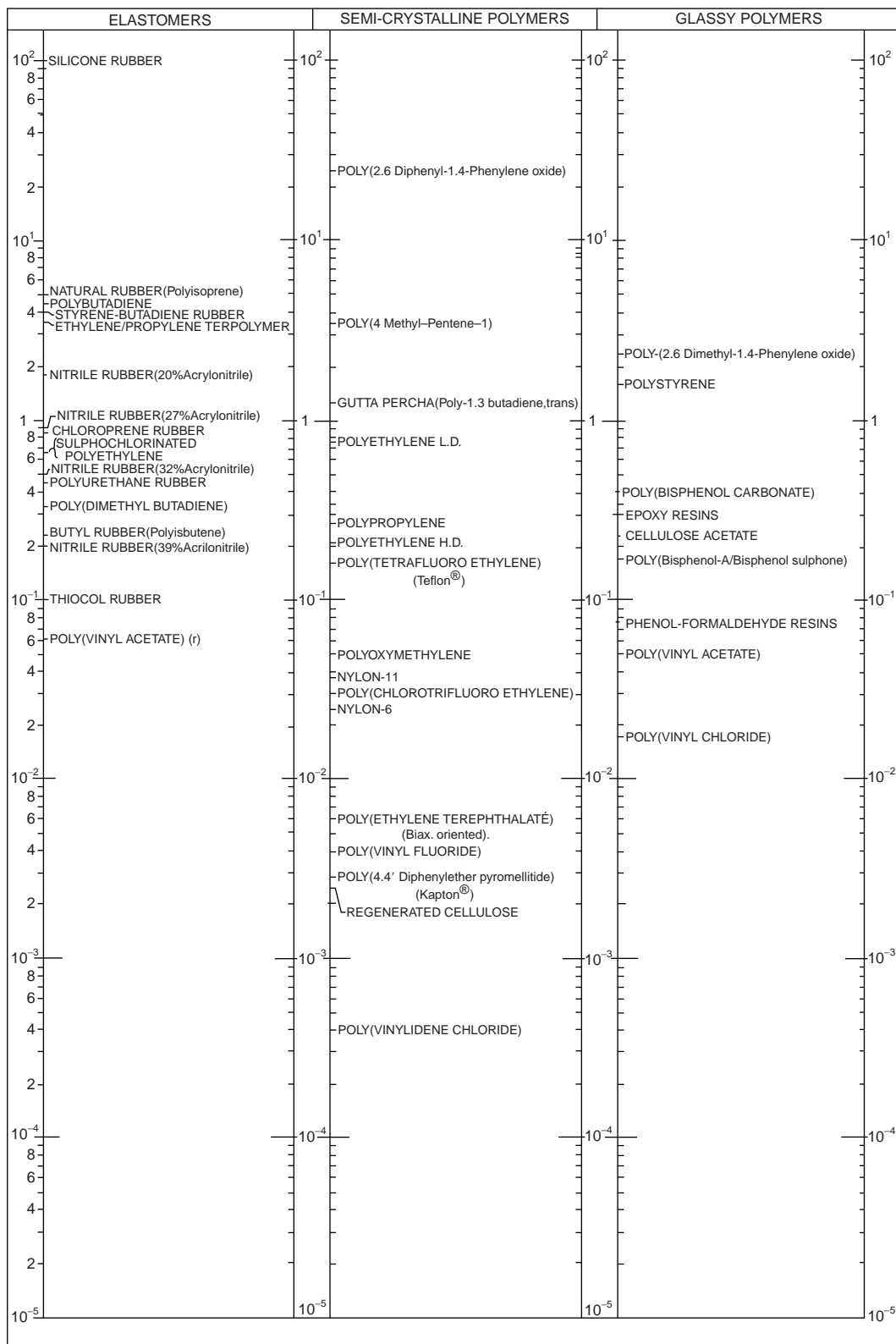


FIG. 18.6 Permeability of polymers for nitrogen (units: $10^{-12} \text{ m}^2/(\text{s bar}) = 10^{-17} \text{ m}^2/(\text{s Pa})$).

TABLE 18.9 Relative values of permeability parameters (rules of thumb)

Gas	P	D	S	E_P	E_D	σ^2	σ^{-2}
$N_2 (=1)$	1	1	1	1	1	1	1
CO	1.2	1.1	1.1	1	1	0.94	1.06
CH_4	3.4	0.7	4.9	(1)	(1)	0.98	1.02
O_2	3.8	1.7	2.2	0.86	0.90	0.83	1.20
He	15	60	0.25	0.62	0.45	0.45	2.22
H_2	22.5	30	0.75	0.70	0.65	0.55	1.80
CO_2	24	1	24	0.75	1.03	1.08	0.931
H_2O	(550)	5	–	0.75	0.75	0.48	2.07

18.2.6. The Permachor, an additive molar function for the estimation of the permeability

In 1986 Salame introduced a new physical parameter π , for which he coined the name (specific) Permachor. It is defined by the equation

$$P(298) = P^*(298)\exp(-s\pi) \quad (18.26)$$

or

$$\pi = -\frac{1}{s} \ln \frac{P(298)}{P^*(298)} = -\frac{2.303}{s} \log \frac{P(298)}{P^*(298)} \quad (18.27)$$

where $P(298)$ = permeability of an arbitrary simple gas in an arbitrary polymer at 298 K; $P^*(298)$ = permeability of the same gas in a chosen standard polymer at 298 K; s = a scaling factor, that will be described below.

As a *standard gas* nitrogen is used by preference, but in principle any other simple gas may be used, since the permeabilities of the different gases have a constant ratio determined by the collision diameter of the gas molecules (Table 18.3).

As a *standard polymer* Salame selected natural rubber, for several reasons. First of all it is a generally available polymer with a well-defined chemical composition: poly(*cis*-isoprene). Furthermore it is, on the scale of permeabilities, rather representative for the “average” elastomer (with a relatively high permeability). This implies, according to Eq. (18.26) that for natural rubber π is by definition zero. Furthermore the value of $\log P^*$ of nitrogen in natural rubber at 298 K is equal to -16 ± 0.3 . Salame chose as a second fixed point on the π -scale a very “impermeable” polymer, viz. poly(vinylidene chloride (Saran®)), which has a $\log P(298)$ value of -21 ± 0.5 ; the assigned π -value for it is chosen to be 100. By its definition π is proportional to the negative logarithm of the relative permeability: $\pi \propto -\log[P(298)/P^*(298)]$.

Since a linear relationship between $\log P(298)$ and π is implied in the definition of π , a graphical representation can be made in which the two fixed points are connected by a straight line. If $\log P(298)$ of a polymer is known, the value of π can be read from this graph. As an illustration Fig. 18.7, gives the position of a number of polymers; numerical values are given in Table 18.10. The scaling factor s is, as a matter of fact, determined by the choice of the second fixed point of the π -scale. For the gases N_2 , O_2 and CO_2 s has a value of 0.115 at 298 K, i.e. slope of line in Fig. 18.7 divided by -2.303 .

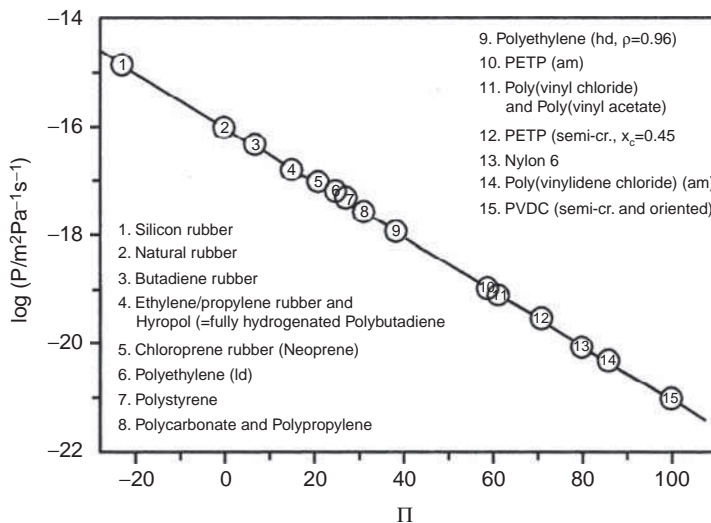


FIG. 18.7 Logarithm of permeability versus specific Permachor.

TABLE 18.10 Values of π for different polymers (Salame, 1986)

Polymer	π
Elastomers	
Silicone rubber	-23
Butyl rubber	-2
<i>Natural rubber (poly-cis-isoprene)</i>	0
Butadiene rubber (poly-butadiene)	6
Poly(methyl pentene)	7
Neoprene rubber (poly-chloroprene)	21
Glassy amorphous polymers	
Hydropol (hydrogenated p. butadiene)	15
Polystyrene	27
Poly(bisphenol) (carbonate)	31
Poly(vinyl fluoride)(quenched)	50
Poly(ethylene terephthalate) am.	59
Poly(vinyl acetate)	61
Poly(vinyl chloride)	61
Poly(vinylidene chloride) am.	86
Poly(acrylonitrile)	110
Semi-crystalline polymers	
Poly(ethylene) ld ($a = 0.57$)	25
Poly(propylene) ($a = 0.40$)	31
Poly(ethylene) hd ($a = 0.26$)	39
Poly(vinyl fluoride) ($a = 0.60$)	59
Poly(ethylene terephthalate) ($a = 0.7$)	65
Do. ($a = 0.55$)	70
Nylon 66 ($a = 0.6$)	73
Nylon 6 ($a = 0.4$)	80
<i>Poly(vinylidene chloride) (or. cr.)</i>	100
Poly(vinyl alcohol) (dry, $a = 0.3$)	157

Salame found that the product $N\pi$, the *Molar Permачor* (Π) is an additive function:

$$N\pi = \Pi = \sum_i (N_i \Pi_i) \quad (18.28)$$

where N = number of characteristic groups per structural unit; Π_i = increment of the group i .

Table 18.11 gives the list of group contributions to the molar permачor.

The numerical value of π being known, the permeability at room temperature can be estimated from the equation (P in $m^2/(s \text{ Pa})$):

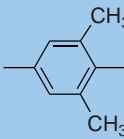
$$\log P(298) = \log P^*(298) - 0.4343s\pi \quad (18.27a)$$

For permeation of nitrogen $\log P^*(298) = -16$ and $s = 0.115$, so that in that case the equation reduces to:

$$\log P(298) = -16 - 0.05\pi \quad (18.29)$$

A disadvantage of the permачor method is that in case of different gases a set of values for $P^*(298)$ and for s should be known. It must be advised therefore to calculate first of all $\log P(298)$ for nitrogen (taking this gas as the standard gas) and then to apply the relative P -values given in Table 18.9 in order to estimate the P -value of the relevant gas. For other temperatures the permeability can be estimated by means of Eq. (18.21). For this E_p must be known ($=\Delta H_s + E_D$).

TABLE 18.11 Group contributions to the molar permачор

Group	Π_i	Group	Π_i
$-\text{CH}_2-$	15	$-\text{CH}(\text{OH})-$	255 wet 100
$-\text{CH}(\text{CH}_3)-$	15	$-\text{CH}(\text{CN})-$	205
$-\text{CH}(\text{C}_6\text{H}_5)-$	39	$-\text{CHF}-$	85
$-\text{CH}(\text{i butyl})-$	-1	$-\text{CF}_2-$	120
$-\text{C}(\text{CH}_3)_2-$	-20	$-\text{CHCl}-$	108
		$-\text{CCl}_2-$	155
		$-\text{CH}(\text{CH}_2\text{Cl})-$	50
$-\text{CH} = \text{CH}-$	-12		
$-\text{CH} = \text{C}(\text{CH}_3)-$	-30	$-\text{Si}(\text{CH}_3)_2-$	-116
$-\text{CH} = \text{C}(\text{Cl})-$	33	$-\text{O}-$	70
	-54	$-\overset{\text{O}}{\underset{\parallel}{\text{C}}}-\text{O}-$	102
	60	$-\text{O}-\overset{\text{O}}{\underset{\parallel}{\text{C}}}-\text{O}-$	24
	-44	$-\overset{\text{O}}{\underset{\parallel}{\text{C}}}-\text{NH}-$	309 wet 210

The π -values calculated by means of the Molar Permachor are valid for amorphous polymers. For semi-crystalline and oriented polymer films a correction must be made. Salame recommends for semi-crystalline polymers the following expression:

$$\pi_\infty \approx \pi_a - 18 \ln a \approx \pi_a - 41.5 \log(1 - x_c) \quad (18.30)$$

where a = volume fraction amorphous and x_c = crystallinity. For oriented crystalline polymer films Salame gives the expression:

$$P_{\text{oriented,sc}} = P_{\text{sc}}/\tau_o \quad (18.31)$$

where τ_o = "tortuosity" of crystallites $\approx 1.13/a^{1/2}$

In his 1986-paper Salame also gave a derivation of his equations of departure from the basic permeation Eqs. (18.2)–(18.7) that can be summarised as follows:

$$P(T) = S(T)D(T) = S_o D_o \exp[-(\Delta H_s + E_D)] \quad (18.2) - (18.7)$$

Salame substituted four empirical expressions in this basic equation, which he derived from literature data, viz. for E_D , D_o , ΔH_s and S_o . In these expressions he used his parameter π as the characteristic datum of the polymer (instead of T_g used as such in our treatment of Diffusivity given earlier).

Salame's four equations read as follows (using the S.I. units m, s, J and Pa):

Equation for	(a) Rubbers	(b) Glasses		
I	E_D/R	$\left(\frac{\sigma_x}{\sigma_{N_2}}\right)^2 (3125 + 78\pi)$	$\left(\frac{\sigma_x}{\sigma_{N_2}}\right)^2 (2875 + 45\pi)$	(18.32)
II	$\log D_o$	$-8.0 + 10^{-3}E_D/R$	$-7.5 + 0.6 \times 10^{-3}E_D/R$	(18.33)
III	$\Delta H_s/R$	$1550 - 13.25\varepsilon/k$	$450 - 13.25\varepsilon/k$	(18.34)
IV	$\log S_o$	$-5.3 - 0.0057\varepsilon/k - 0.013\pi$	$-6.5 - 0.0057\varepsilon/k - 0.013\pi$	(18.35)

Equation I is similar to our Eq. (18.17) (but π is used for characterising the polymer instead of T_g); II is almost equal to (18.18a/b); III is nearly identical to Eqs. (18.13a/b) and IV is an extension of Eqs. (18.14a/b).

Salame then combined all terms containing π into a product $s \times \pi$ (giving so the full expression of the exponent in Eq. (18.26) and all terms not containing π into a quantity $A(T)$, which is identical to P^* .

Salame finally found (1987) that π is a linear function of $\log(e_{\text{coh}}/f_v)$, where e_{coh} = cohesive energy density and f_v = fractional free volume of the polymer.

Example 18.3

Estimate the permeability $P(298)$ for oxygen of two polymer films: one a neoprene rubber film, the other a PVC film.

Use two methods of estimation: one via the solubility and diffusivity ($P = SD$), the other via the permachor-method. For oxygen $\varepsilon/k = 107$ and $(\sigma_o/\sigma_N)^2 = 0.83$; for neoprene $T_g = 230$ K, for PVC $T_g = 360$ K.

Solution*(a) Estimation via S and D*

Neoprene is a rubber, so we use successively Eqs. (18.17a), (18.12c), (18.17), (18.18a) and (18.4b):

$$p = 6400 - 0.16 \times 58^2 = 5862$$

$$\log S(298) = 0.010\varepsilon/k - 7.0 \pm 0.25 = -5.93 \pm 0.25$$

$$E_D/R = p(\sigma_{O_2}/\sigma_{N_2})^2 = 5862 \times 0.83 = (4.9 \pm 0.4) \times 10^3$$

$$\log(D_o/m^2 s^{-1}) = -8.0 + 10^{-3}E_D/R \pm 0.4 = -3.1 \pm 0.4$$

$$\log D(298) = \log D_o - 1.457 \times 10^{-3}E_D/R \pm 0.4 = -10.24 \pm 0.4$$

So we get $\log P(298) = \log S(298) + \log D(298) = -5.93 - 10.24 \pm 0.6 = -16.2 \pm 0.6$ or $P(298) = 6.3 \times 10^{-17} m^2/(s Pa)$ with a margin of 1.6×10^{-17} to 25×10^{-17} ; the experimental value (Polymer Handbook) is 3×10^{-17} , in fair agreement with our estimation.

Polyvinyl chloride is an amorphous polymer in the glassy state, so we use successively Eqs. (18.17a), (18.8c), (18.17), (18.14b) and (18.4b)

$$p = 6400 - 0.16 \times 62^2 = 5785$$

$$\log S(298) = 0.010\varepsilon/k - 7.4 \pm 0.6 = -6.33 \pm 0.6$$

$$E_D/R = p(\sigma_{O_2}/\sigma_{N_2})^2 = 5785 \times 0.83 = (4.8 \pm 0.8) \times 10^3$$

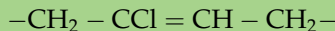
$$\log(D_o/m^2 s^{-1}) = -9.0 + 10^{-3}E_D/R \pm 0.8 = -4.2 \pm 0.8$$

$$\log D(298) = \log D_o - 1.457 \times 10^{-3}E_D/R \pm 0.8 = -11.2 \pm 0.8$$

So $\log P(298) = \log S(298) + \log D(298) = -6.33 - 11.2 = -17.5 \pm 1.4$ or $P(298) = 3.2 \times 10^{-18} m^2/(s Pa)$ with a margin between 0.1×10^{-18} and 79×10^{-18} . The experimental value is 0.34×10^{-18} . The accuracy is less than for neoprene.

(b) Estimation via the permachor (π)

The structural unit of *neoprene* (poly-chloroprene) is



The contributions to the molar parachor are:

$$\begin{array}{rcccl}
 & 2 & -\text{CH}_2- & = 2 \times 15 = 30 \\
 & 1 & -\text{CH} = \text{C(Cl)}- & = 33 \\
 \hline
 & \text{N} = 3 & & & \boldsymbol{\Pi} = 63
 \end{array}$$

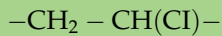
The specific parachor then becomes: $\pi = \boldsymbol{\Pi} / \text{N} = 63/3 = 21$. Now Salame's equation can be applied:

$$\log P(298) = \log P^*(298) - s\pi/2.303.$$

For the standard gas (nitrogen) in the standard polymer (natural rubber) we have: $\log P^*(298) = -16$ and $s = 0.115$. Substitution gives $\log P(298) = -16 - 0.12 \times 21/2.303 = -17.0$ or $P(298) = 9 \times 10^{-18} m^2/(s Pa)$ for nitrogen in neoprene; the experimental value (Polymer Handbook) is 9×10^{-18} , in excellent agreement. The conversion factor for P , from nitrogen to oxygen (Table 18.9), is 3.8. So for oxygen in neoprene $P(298)$ becomes

$3.8 \times 9 \times 10^{-18} = 3.4 \times 10^{-17} \text{ m}^2/(\text{s Pa})$. The experimental value (Polymer Handbook) is 3.0×10^{-17} , again in good agreement.

For PVC the structural formula is:



Hence the contributions to the Molar Permachor are:

$$\begin{array}{rcl} 1 & \text{--CH}_2\text{--} & = 15 \\ 1 & \text{--CH(Cl)}\text{--} & = 108 \\ \hline \text{N} = 2 & & \text{II} = 123 \end{array}$$

So $\pi = \text{II}/\text{N} = 123/2 = 61.5$.

For nitrogen in PVC we then find:

$\log P(298) = -16 - 0.115 \times 61.5/2.303 = -19.07$ or $P(298) = 8.5 \times 10^{-20} \text{ m}^2/(\text{s Pa})$ (experimental value 8.9×10^{-20} , Polymer Handbook).

So for oxygen in PVC the result is $3.8 \times 8.5 \times 10^{-20} = 3.2 \times 10^{-19}$;

This is to be compared with the experimental value 3.4×10^{-19} . For a glassy polymer this is a very good agreement.

18.3. PERMEATIONS OF A MORE COMPLEX NATURE

18.3.1. Introduction

Until now we have considered the simplest case of more or less ideal permeation behaviour: Henry's law for sorption (sorbed penetrant randomly dispersed within the polymer) and Fick's first law for diffusion (diffusion coefficient independent of the concentration of the sorbed penetrant). This ideal behaviour is observed in practice only when "permanent gases" are the penetrants and if the gas pressure is nearly atmospheric. In this case there are no strong polymer–penetrant interactions and no specific interactions between the penetrant molecules.

As soon as interactions become important, also other types of sorption are observed. Fig. 18.8 gives a classification of sorption isotherms, proposed by Rogers (1965, 1985).

Type I is of course the ideal sorption behaviour according to Henry's law. As said before, it is observed in the sorption of permanent gases at moderate pressures.

Type II is the well-known sorption isotherm according to Langmuir. This type of isotherm will result when gases are sorbed at specific sites at higher pressure; the concentration of the sorbed substance will reach a "saturation capacity". This isotherm is also found when non-permanent gases at higher pressures are sorbed in glassy amorphous polymers having pre-existing micro-voids.

Type III is the sorption isotherm of Flory–Huggins. Here the solubility coefficient increases continuously with pressure. It represents a preference for formation of penetrant pairs and clusters; it is observed when the penetrant acts as a swelling agent for the polymer without being a real solvent. An example is water in relatively hydrophobic polymers containing also some polar groups.

Type IV is the typical 2-stage isotherm according to Brunauer, Emmett and Teller (BET-isotherm), which may be considered as a combination of the other types (e.g. II at low with III at high pressure). This type is especially found if water is sorbed in hydrophilic polymers.

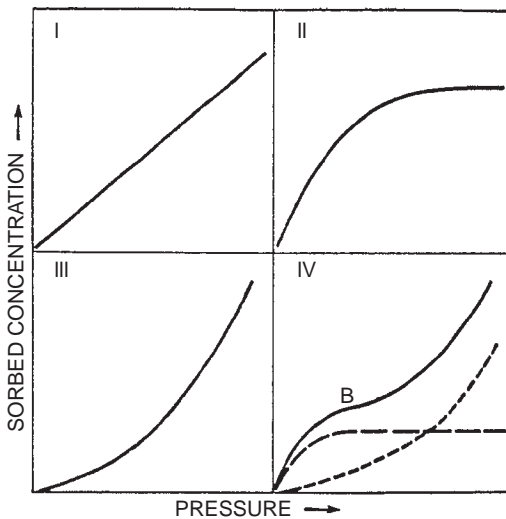


FIG. 18.8 Typical isotherm plots of sorbed concentration versus ambient vapour pressure. (I) Henry's law, S is a constant; (II) Langmuir equation; (III) Flory-Huggins equation; (IV) BET equation, site saturation at point B (from C.F. Rogers, 1985).

Types II–IV are coined as “anomalous sorption isotherms”. As a matter of fact the type of sorption isotherm has a profound effect on the permeation behaviour.

18.3.2. Partially immobilising sorption (“dual-mode” model)

Precise studies of sorption of non-permanent gases in glassy polymers showed that the sorption isotherms do not follow Henry's law (see Fig. 18.9a). A very good approximation of the isotherm is:

$$C = C_H + C_L - SP + \frac{C_H^s bp}{1 + bp} \quad (18.36)$$

Here C = total concentration of sorbed penetrant; C_H^s = saturation capacity of Langmuir isotherm (in “holes”); b = affinity coefficient of Langmuir isotherm; p = pressure; S = solubility.

This equation has become known as the “dual sorption model”, because obviously two separate sorption mechanisms are operative for gases in glassy polymers. One mode (first term on the right in Eq. (18.36)) follows the Henry's law; the other mode (second term) follows a Langmuir form. This additional mode is attributed to sorption into micro-voids that apparently pre-exist in the glassy state of the polymer (and only there!); it disappears above T_g (see Fig. 18.9b).

The dual-sorption model was first suggested by Barrer et al. (1958) and Vieth et al. (1965/72), and developed by Petropoulos (1970) and in particular by Paul and Koros et al. (1969/88).

Early investigations of the dual-sorption model started from the assumption that only Henry's part of the sorbed gas contributed to the gas transport, whereas the Langmuir part would not contribute to it, due to immobilisation. Then the transport flux would be

$$J = -D \frac{dC_D}{dx} \quad (18.37)$$

where $C_D = Sp$ (randomly dispersed).

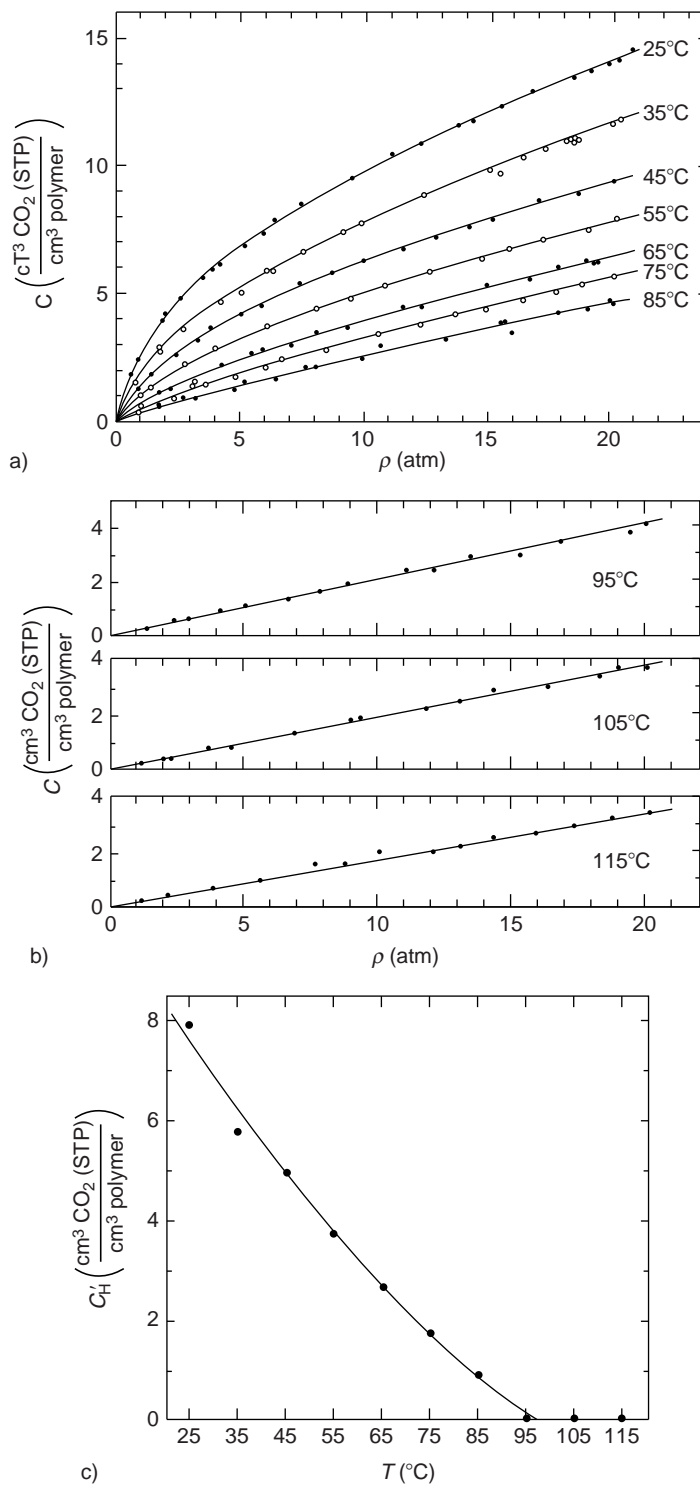


FIG. 18.9 (A) CO_2 sorption in PET below T_g . From Paul (1979); Courtesy of Verlag Chemie. (B) CO_2 sorption in PET above T_g . From Paul (1979); Courtesy of Verlag Chemie. (C) Effect of temperature on Langmuir capacity for CO_2 sorption in PET. From Paul (1979); Courtesy of Verlag Chemie.

(Continued)

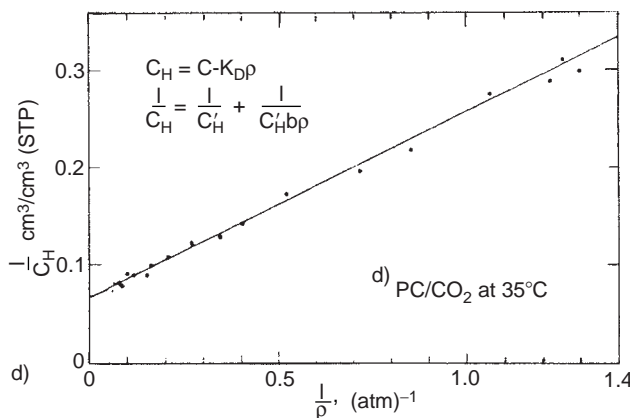


FIG. 18.9—cont'd (D) A graphical test to show how well C_H is described by the Langmuir isotherm for CO_2 sorption in Polycarbonate at 35 °C. From Koros et al. (1976); Courtesy of John Wiley & Sons, Inc.

However, Petropoulos (1970) speculated that the Langmuir part might have a certain mobility and proposed a more general form of Fick's law:

$$J = -D_D \frac{dC_D}{dx} - D_H \frac{dC_H}{dx} \quad (18.38)$$

where C_H = concentration of the gas held in "holes" (micro-voids); D_D and D_H are separate diffusion coefficients of the two species (randomly dispersed and holes).

This form is actually used by Koros and Paul (1978). Eq. (18.38) can be solved for the boundary conditions of transient permeation. The set of equations then obtained is given in Table 18.12. These Eqs. (18.39)–(18.42) enable us to derive SC_H^S and b from experimental sorption isotherms, as presented by Eq. (18.36), and the values of D_D and D_H from transient permeation experiments. The equations contain a number of dimensionless groups:

$D_D\tau/L^2$, a "model numeric" (see Chap. 3);

$a = b/S$ and $K = C_H^S b/S$: "intrinsic numerics" of the polymer/gas combination;

$F = D_H/D_D$, a "resultant numeric", expressing an experimental result.

Fig. 18.10a,b shows an example of a calculated (and experimentally confirmed) behaviour of the diffusional time lag (τ) and the permeability (P) in dimensionless form, as a function of the dimensionless variable bp ; K is held constant at a (realistic) value 10.

If $F = 0$, there is *total immobilisation* of the penetrant population in the microvoids; if $F = 1$ there is *no immobilisation* at all. In practice F has values in the neighbourhood of 0.1 (see Fig. 18.10c).

Table 18.12 also gives a formula for the "effective diffusivity" at varying F , K and αC_D . Fig. 18.10d shows its graphical representation.

The available experimental data on the dual-mode sorption and mobility parameters have been summarised in Table 18.13. Their number is too small to derive correlations with the chemical structure; only some tentative conclusions can be drawn. D_D and S may be estimated along similar rules as D and S in Sect. 1. From Table 18.13 we may conclude that the values of a and F are of the order of 0.4 and 0.15, respectively. The parameter C_H^S remains as the great "unknown". Barbari, Koros and Paul (1988) suggested that C_H^S probably would be proportional to the fractional volume of the holes; as a measure

TABLE 18.12 Main formulae of the dual-mode model of permeation^a

Experiment	To measure	To find	Formula of dual mode model to be used	Equations	Limiting case in simplest (ideal) model
Sorption isotherm $C = f(p)$	C, p	S, b and C_H^S Calculate α and C_D	$C = Sp + \frac{C_H^S bp}{1 + bp} = C_D + C_H = C_D \left[1 + \frac{K}{1 + \alpha C_D} \right]$	(18.39)	$C = Sp$
Transient permeation $P = f(p)$	P	$D_o \approx D$ and $\frac{FK}{C_H \text{ and } D_H}$ Calculate	$P = SD_D \left[1 + \frac{FK}{1 + bp} \right]; \text{ in } \lim_{bp \rightarrow 0} = SD_D[1 + FK] = SD_D + bC_H^S D_H$	(18.40)	$P = SD$
Diffusion time lag $\Theta = f(D)$	D	$\frac{D_D}{FK \text{ and } K}$ Calculate	$\frac{\Theta D_D}{L^2} = \frac{1}{6} \left[1 + f(F, K, b, p) \right]; \text{ in } \lim_{bp \rightarrow 0} = \frac{1}{6} \left[\frac{1 + K}{1 + FK} \right]$	(18.41)	$\frac{\Theta D}{L^2} = \frac{1}{6}$
Effective diffusivity $D_{\text{eff}} = f(p, C, F)$	D_{eff}	$\frac{D_D, F, K}{\text{Calculate } D_o}$	$D_{\text{eff}} = D_D \left[\frac{1 + \frac{FK}{(1 + \alpha C_D)^2}}{1 + \frac{K}{(1 + \alpha C_D)^2}} \right]; \text{ in } \lim_{\alpha C_D \rightarrow 0} = D_o = D_D \left[\frac{1 + FK}{1 + K} \right]$	(18.42)	$D_{\text{ef}} = D = D_o$

^a Index D means: (randomly) dispersed; index H means: in holes (microvoids).

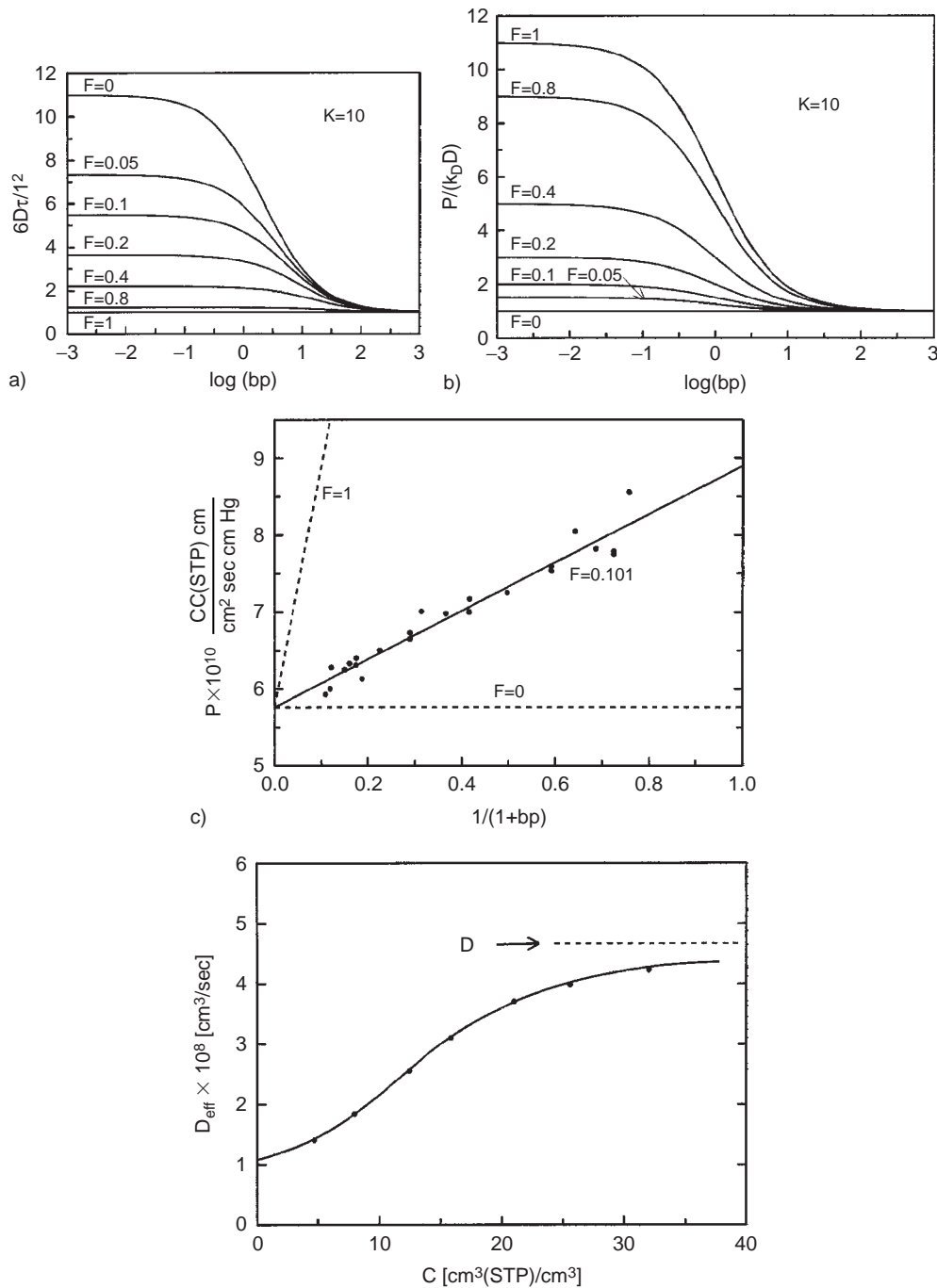


FIG. 18.10 (A) Time lag predicted from assumption that D is constant. From Paul & Koros (1976); Courtesy of John Wiley & Sons, Inc. (B) Permeability predicted from assumption that D is constant. From Paul & Koros (1976); Courtesy of John Wiley & Sons, Inc. (C) Permeability plotted in accordance with the partial immobilisation model with D constant. From Koros et al. (1976); Courtesy of John Wiley & Sons, Inc. (D) Concentration dependence of the effective diffusion coefficient of CO₂ in Polycarbonate at 35 °C. From Koros et al. (1976); Courtesy of John Wiley & Sons, Inc.

for it we may take the fractional unrelaxed volume of the glassy state: $f_H = (\mathbf{V}_g - \mathbf{V}_1)/\mathbf{V}_g$. If for $\mathbf{V}_g(T)$ and $\mathbf{V}_1(T)$ the values derived in Chap. 4 are substituted (Eqs. (4.26)), we obtain:

$$f_H = \frac{\mathbf{V}_g(T) - \mathbf{V}_1(T)}{\mathbf{V}_g(T)} \approx 0.33 \times 10^{-3}(T_g - T) \quad (18.43)$$

Barbari, Koros and Paul derived as full expression for C_H^S

$$C_H^S = \frac{22,400}{V_p} f_H \quad (18.44)$$

where

$$\frac{22,400}{V_p} = \frac{\text{Molar Volume (STP) of penetrant in gaseous state}}{\text{Molar Volume of penetrant in sorbed state (in 'holes')}}$$

For permanent gases V_p will be of the order of the molar volume in the gaseous state, so that C_H^S will be small (of the order of 0.05); accordingly the values of K and FK will also be very small.

For vapours whose critical temperature is higher than room temperature, however, V_p will be almost equal to the molar volume in the liquid state (capillary condensation) and C_H^S becomes:

$$C_H^S = 7.5(T_g - T)/V_p \quad (18.44a)$$

CO_2 is a typical “border case” ($T_{\text{cr}} = 304$ K). For the V_p of CO_2 an average value for V_p of 50 cm^3/mol can be calculated from the experimental data of $C_H^S(\text{CO}_2)$ for different glassy polymers (Table 18.13); this is of the order of the critical molar volume of CO_2 (i.e. 94 cm^3/mol).

An estimation of all the dual mode parameters is therefore possible in cases where no experimental data are available.

The dual-mode model proved rather successful to describe the isotherms and permeabilities at higher pressures.

Barrer (1984) suggested a further refinement of the dual-mode mobility model, including diffusive movements from the Henry's law mode to the Langmuir mode and the reverse; then four kinds of diffusion steps are basically possible. Barrer derived the flux expression based on the gradients of concentration for each kind of diffusion step. This leads to rather complicated equations, of which Sada (1987, 1988) proved that they describe the experimental results still better than the original dual-mode model. This, however, is not surprising, since two extra adaptable parameters are introduced.

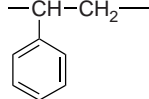
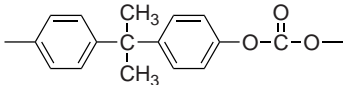
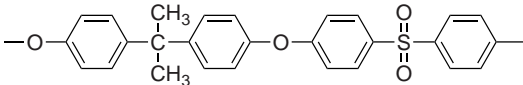
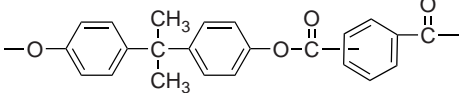
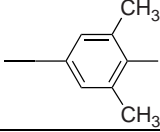
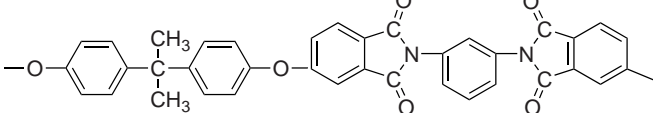
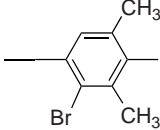
18.3.3. The “gas–polymer-matrix model”

Another model for the sorption and transport of gases in glassy polymers at super atmospheric pressures is the gas–polymer-matrix model, proposed by Raucher and Sefcik (1983). The premise of this model is that the penetrant molecules exist in the glassy polymer as a *single* population and that the observed pressure dependence of the mobility is *completely* due to gas–polymer interactions. In the mathematical representation of this model the following expression for sorption and transport is used:

$$P(T, C_2) = S(T, C_2)D(T, C_2) = S(T)\exp(-\alpha C_2)D(T)\exp(\beta C_2) \quad (18.45)$$

where $S_o(T)$ and $D_o(T)$ are defined the temperature dependent infinite dilution solubility and diffusion coefficients, respectively; the constants α and β describe the effect of

TABLE 18.13 Dual mode sorption and mobility data of glassy amorphous polymers (values at 35 °C) Data from Sada et al. (1987), Chern et al. (1987) and Barbari, Koros and Paul (1988).

Polymer	Structural unit	T_g °C	T_g K	ρ (kg/m ³)
Polystyrene PS		100	373	1050
Polycarbonate PC Lexan®		150	423	1200
Polysulfone PSF		186	451	1240
Polyarylate PAR Ardel 100®		190	463	1210
Poly oxide PDMPO PPO®		210	483	1060
Polyetherimide PEI Ultem® Brominated PPO		215	488	1280
(91% aryl substitution)		262	535	1380

gas–polymer interactions on changes in solubility and mobility, respectively. Accordingly, in this case:

$$S(T, C_2) = S(T)\exp(-\alpha C_2) = S_0 \exp[-\Delta H_S/(RT)]\exp(-\alpha C_2) \quad (18.46)$$

$$D(T, C_2) = D(T)\exp(\beta C_2) = D_0 \exp[-E_D/(RT)]\exp(\beta C_2) \quad (18.47)$$

The terms $S(T)$ and α follow from equilibrium sorption measurements, using the expression

$$C_2(T, p) = pS(T, C_2) = pS(T)\exp(-\alpha C_2) \quad (18.48)$$

which for small values of αC_2 can be simplified to

$$C_2 = S(T)p(1 - \alpha C_2) \text{ or } \frac{1}{C_2} = \frac{1}{S(T)p} + \alpha \quad (18.49)$$

Hence, upon plotting $1/C_2$ vs. $1/p$, the values of $S(T)$ and α can be determined.

Also this model describes the experimental data very properly.

Gases	S (m^3 STP/ m^3)	C_H^s (m^3 STP/ m^3)	b (bar $^{-1}$)	D_D ($\text{m}^2/$ $\text{s} \times 10^{12}$)	D_H ($\text{m}^2/$ $\text{s} \times 10^{12}$)	$\alpha =$ b/S	$K =$ αC_H^s	$F = D_H$ $/D_D$	FK
CO ₂	0.65	9.45	0.11	11.9	3.8	0.17	1.6	0.32	0.51
CH ₄	0.26	4.7	0.055	1.9	0.9	0.21	0.95	0.47	0.45
N ₂	-	-	-	6	-	-	-	-	-
CO ₂	0.69	18.8	0.26	6.22	0.49	0.38	7.1	0.08	0.56
CH ₄	0.29	8.4	0.084	1.09	0.13	0.29	4.7	0.12	0.54
N ₂	0.09	2.1	0.056	1.76	0.51	0.63	1.3	0.29	0.38
CO ₂	0.66	17.9	0.33	4.5	0.54	0.53	9.0	0.12	1.1
CH ₄	0.16	9.9	0.7	0.69	0.12	0.44	6.9	0.17	1.2
N ₂	0.075	10.0	0.015	0.93	0.53	0.20	2.1	0.60	1.25
CO ₂	0.63	22.7	0.215	6.9	0.86	0.34	7.7	0.13	0.96
CH ₄	0.18	6.5	0.10	1.3	0.21	0.53	3.6	0.16	0.57
N ₂	0.08	1.2	0.07	2.75	0.41	0.88	1.1	0.16	0.17
CO ₂	0.92	32.7	0.20	36.8	3.7	0.24	7.1	0.10	0.71
CH ₄	0.32	22.7	0.107	6.2	0.43	0.34	7.4	0.07	0.52
N ₂	0.15	10.0	0.048	-	-	0.32	-	-	-
CO ₂	0.76	25.0	0.37	1.14	0.07	0.49	12.0	0.063	0.76
CH ₄	0.21	7.3	0.14	0.11	0.01	0.67	4.9	0.073	0.36
N ₂	0.063	4.15	0.045	0.57	0.02	0.71	2.9	0.042	0.12
CO ₂	2.57	37.5	0.29	4.82	3.3	0.11	4.3	0.07	0.30
CH ₄	1.32	26.9	0.12	6.1	0.2	0.10	2.5	0.05	0.13
N ₂	0.57	15.1	0.06	-	-	0.10	-	-	-

Barbari, Koros and Paul (1988) compared the two models ("dual-mode" and "matrix") on the basis of their experimental data. They state that both models give a good description of the experiments; yet the dual mode model has their preference, since it has simple physical interpretations of the parameters and can be related rather well to gas and polymer characteristics. The parameters of the matrix model do, however, not follow any consistent trend.

Although the dual-mode model seems to be favoured, the relative validity of the two models is not firmly established. Quoting Rogers (1985) we may conclude: "it must be realised that both models are only approximations which require estimation of a number of parameters".

18.3.4. Moisture absorption and transport

The behaviour of water in polymers presents a special case, due to the nature of the water molecule. This molecule is relatively small and has a strong tendency towards hydrogen bond formation in its own liquid and solid state as well as with other polar groups.

In polar polymers both equilibrium sorption and diffusivity are strongly influenced by these interactions, but also in less polar polymers anomalies, e.g. association of sorbed water molecules, may occur ("clustering").

Equilibrium sorption of water (solubility) is described by the different isotherms of the Brunauer–Emmett–Teller classification.

In most hydrophilic polymers, such as cellulose and proteins, each polar group interacts strongly with one water molecule only. In hydrophobic polymers such as polyolefins, on the other hand, Henry's law is obeyed over the complete range of relative pressures and only minute quantities of water are sorbed.

The more polar groups are present in the polymer matrix, the higher its sorptive affinity for water will be. However, the accessibility of the polar groups, the relative strength of the water–water versus the water–polymer bonds and the degree of crystallinity of the polymer matrix are very important factors, which explain the fact that no simple correlation between number of polar groups and solubility exists. For instance, well-defined crystallites are inaccessible to water, but on the surfaces of the crystallites the polar groups will "react with water".

Barrie (1968) collected all the known data on water sorption. From these data it is possible to estimate the effect of the different structural groups on water sorption at different degrees of humidity. Table 18.14 presents the best possible approach to the sorptive capacity of polymers versus water, i.e. the amount of water per structural group at equilibrium, expressed as molar ratio. From these data the solubility (cm^3 water vapour (STP) per cm^3 of polymer) can be easily calculated. (The multiplication factor is $22.4 \times 10^3 / V$, where V is the molar volume per structural polymer unit.)

The heat of sorption is of the order of 25 kJ/mol for non-polar polymers and 40 kJ/mol for polar polymers.

TABLE 18.14 Molar water content of amorphous polymers per structural group at different relative humidities at 25 °C

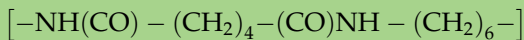
Group	Relative humidity				
	0.3	0.5	0.7	0.9	1.0
$-\text{CH}_3$					
$-\text{CH}_2-$	(1.5×10^{-5})	(2.5×10^{-5})	(3.3×10^{-5})	(4.5×10^{-5})	(5×10^{-5})
$-\text{CH}<$					
	0.001	0.002	0.003	0.004	0.005
$>\text{C} = \text{O}$	0.025	0.055	(0.11)	(0.20)	(0.3)
	0.025	0.05	0.075	0.14	0.2
$-\text{O}-$	0.006	0.01	0.02	0.06	0.1
$-\text{OH}$	0.35	0.5	0.75	1.5	2
$-\text{NH}_2$	0.35	0.5	0.75	(1.5)	(2)
$-\text{NH}_3^+$			2.8	5.3	
$-\text{COOH}$	0.2	0.3	0.6	1.0	1.3
$-\text{COO}^-$	1.1	2.1	4.2		
	0.35	0.5	0.75	1.5	2
$-\text{Cl}$	0.003	0.006	0.015	0.06	(0.1)
$-\text{CN}$	0.015	0.02	0.065	0.22	(0.3)

Example 18.4

Estimate the moisture content of nylon 6,6 at 25 °C and a relative humidity of 0.7. The crystallinity is 70%.

Solution

The structural unit is



From Table 18.14, which gives data for amorphous polymers, it is evident that the sorptive capacity of the CH_2 groups may be neglected. So what remains is two CONH groups per structural unit with a molar water content (at a relative humidity of 0.7) of $2 \times 0.75 = 1.5$ mole/structural unit.

The molar weight of the structural unit is 226.3, so that 1.5×18 g water is absorbed on 226.3 g of polymer or 12 g per 100 g. Taking the crystallinity into account and using Eq. (18.15) we get for the solubility of the (semi-) crystalline polymer:

$$0.3 \times 12 = 3.6 \text{ g per 100 g of semi-crystalline polymer.}$$

This is in good agreement with the experimental value (4 g water/100 g of polymer).

Example 18.5

Estimate the values of α and $S(298)$ nylon 6,6 at 25 °C with the aid of Table 18.14 and the results of Example 18.4. The densities of water and of amorphous nylon 6,6 at 25 °C are 0.997 and $1.07 \text{ cm}^3/\text{g}$, respectively. The water pressure at 25 °C is 23.756 mm Hg = $23.756/7.5 \times 10^{-3} = 3167 \text{ Pa}$

Solution

From Table 18.14 and Example 18.4 it follows for the absorbed amount of water at various pressures:

p (Pa)	950	1584	2217	2851	3168
C (cm^3 water/ cm^3 amorphous nylon)	5.97	8.53	12.80	25.61	34.14
$10^3/p$	1.053	0.631	0.451	0.351	0.315
$1/C$	0.168	0.117	0.078	0.039	0.029

It follows for Eq. (18.49): $\frac{1}{C} = \frac{1}{S(298)p} + \alpha = \frac{185}{p} - 0.0175$ (correlation coefficient = 0.94)

So that $\alpha = -0.0175$ and $S(298) = 5.4 \times 10^{-3} \text{ cm}^3 \text{ water}/(\text{cm}^3 \text{ amorphous nylon} \cdot \text{Pa})$.

According to Eq. (18.12b) $\log S(298) = -7.0 + 0.0123 \times 373 = -2.41$, or $S(298) = 3.9 \times 10^{-3}$, which is in reasonable agreement with the previously calculated value.

Also the diffusivity of water in polymers is highly dependent on the polymer–water interaction. When a polymer contains many hydrogen-bonding groups (cellulose, poly(vinyl alcohol), proteins, etc., and to a lesser extent synthetic polyamides) the diffusivity increases with the water content. This is explained by the strong localisation of the initially sorbed water over a limited number of sites, whereas at higher water contents the polymer

matrix will swell and the sorbed water will be more and more mobile. As a good approximation the following expression can be used:

$$\log D = \log D_{w=0} + 0.08w \quad (18.50)$$

where w = water content in weight per cent.

Compared with the nonhydrophilic polymers the diffusivity as such is greatly retarded by the strong interaction forces: instead of Eqs. (18.18a) and (18.18b) one now finds the relationship for water in hydrophilic polymers

$$\log D_o \approx \frac{0.001E_D}{R} - 11 \quad (18.51)$$

where D is expressed in m^2/s and E_D in J/mol . This is a factor of 100 to 1000 lower than Eqs. (18.18a) and (18.18b) show.

The less hydrophilic polymers such as polyethers and polymethacrylates form the other extreme. Here the diffusivity markedly decreases with increasing water content. This is explained by the increasing "clustering" of water in the polymer (at polar "centres" or in micro cavities) so as to render part of the water comparatively immobile. In this case the influence of water can be approximated by the expression:

$$\log D = \log D_{w=0} - 0.08w \quad (18.52)$$

Furthermore the relationship between D_o and E_D is the same as for other simple gases.

The third case is that of really hydrophobic polymers, such as polyolefins and certain polyesters. Here the solubility is very low (thermodynamically "ideal" behaviour) and the diffusivity is independent of the water content. Water vapour then diffuses in exactly the same way as the other simple gases.

It will be clear that the diffusive transport (permeability) of water in and through polymers is of extreme importance, since all our clothes are made of polymeric materials and water vapour transport is one of the principal factors of physiological comfort.

18.3.5. Diffusion of organic vapours

The diffusion behaviour of organic vapours is much more complicated than that of simple gases. Normally the interaction is much stronger, so that the diffusion coefficient becomes dependent on the concentration of the penetrant:

$$D = D_{c=0}f(c) \quad (18.53)$$

Empirical equations for $f(c)$ are:

$$\left. \begin{array}{l} f(c) = \exp(\alpha c) \quad c = \text{concentration} \\ f(c) = \exp(\beta\varphi) \quad \varphi = \text{volume fraction of penetrant} \\ f(c) = \exp(\gamma a) \quad a = \text{activity} \end{array} \right\} \quad (18.54)$$

α , β and γ are temperature-dependent constants.

Usually the concentration dependence of D is reduced as the temperature is raised. The general equation for D then becomes:

$$D = D_o \exp[-E_{D,o}/(RT)]f(c) \quad (18.55)$$

If for a small temperature range a mean activation energy E_D is defined by

$$D = D_o \exp[-E_D/(RT)]$$

we get from the last two equations:

$$E_D = E_{D,o} - R \frac{\partial \ln f(c)}{\partial (1/T)} \quad (18.56)$$

So the apparent activation energy is also concentration-dependent! If $f(c)$ is a monotonically increasing function, E_D will decrease continuously with increasing c . If $f(c)$ is a monotonically decreasing function, E_D increases continuously with c . For the diffusion of benzene in natural rubber the apparent activation energy decreases from 48 kJ/mol at $c = 0$ to 35 kJ/mol at a volume fraction of 0.08. $E_{D,0}$ shows a discontinuity at transition temperatures.

For organic vapours the correlation $E_D \propto \sigma_x^2$, i.e. Eq. (18.17), which was found for simple gases, cannot be used any longer. Zhurkov and Ryskin (1954) and Duda and Vrentas (1968) correlated the energy of activation E_D with the molar volume of the diffusing molecules (V_D). Their results are reproduced in Fig. 18.11 and show that there is a linear correlation between E_D and V_D , the molar volume of the diffusing molecule, at very low concentrations of the diffusive (where the polymer does not show any swelling):

$$E_D/R(\text{in K}) = 1.93 \times 10^5 V_D (\text{nm}^3/\text{mol}) \quad (18.57)$$

18.3.6. Diffusion of liquids

Diffusion coefficients of organic liquids in rubber have been determined by Southern and Thomas (1967), who followed the kinetics of mass uptake of a rubber sheet immersed in the liquid. Anomalies in the mass uptake-time relation were found and are due to stresses set up in the sheet during swelling and to their variation as swelling proceeds. These anomalies could be eliminated by the use of specimens constrained laterally by bonding to metal plates, which maintains boundary conditions constant during swelling. At liquid concentrations used (up to volume fractions of 0.8 for the best swelling agents!) the diffusion coefficient was shown to depend on the liquid viscosity rather than on the compatibility of rubber and liquid. Fig. 18.12 shows the relationship found, which might have a more general significance.

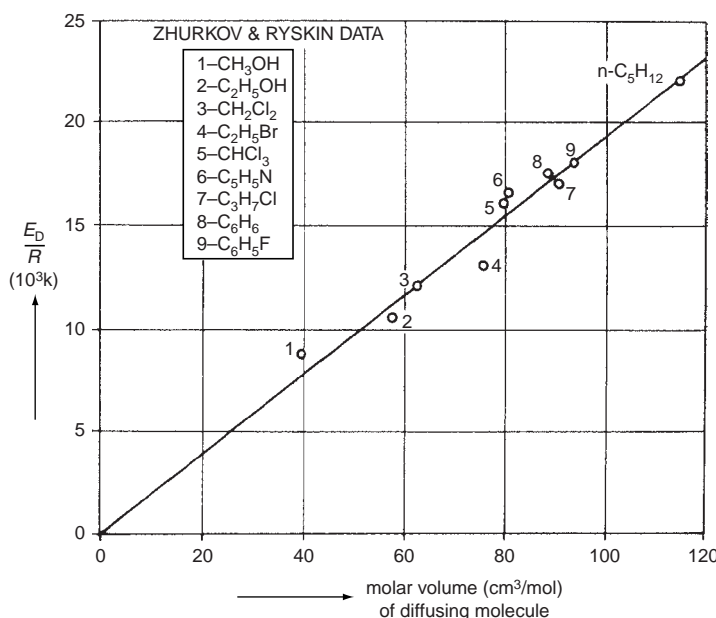


FIG. 18.11 Correlation of activation energy for diffusion in polystyrene with molar volume for temperature range $T_g < T$.

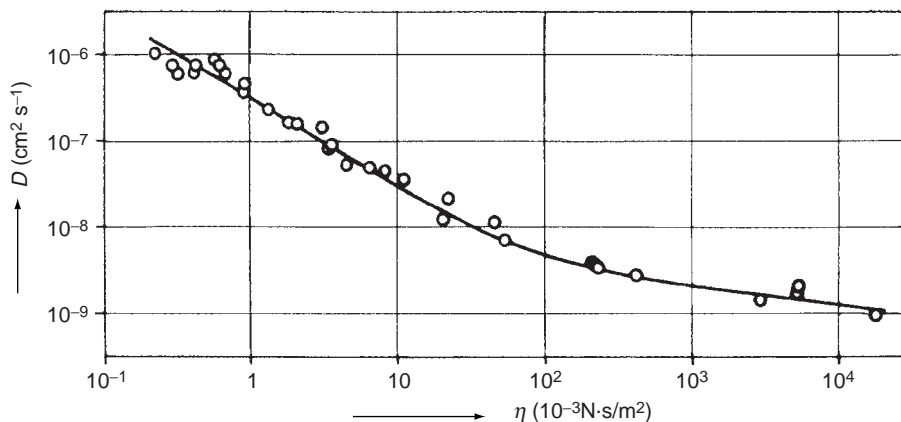


FIG. 18.12 Relation between diffusion coefficient D and liquid viscosity η for various liquids in natural rubber at 25 °C (after Southern and Thomas, 1967).

18.3.7. Self-diffusion

Self-diffusion is the exchange of molecules in a homogeneous material by a kind of internal flow. It has a direct bearing on *tackiness*, which depends on interpretation by diffusion of polymer molecules at the interface. This effect is well known in elastomers.

Bueche et al. (1952) derived that the coefficient for self-diffusion of poly(n-butyl acrylate) is inversely proportional to the bulk viscosity of this polymer. Also in the natural rubber (polysoprene) diffusion system a clear connection appears to exist between diffusion coefficient and bulk viscosity. In general the following expression may be used as a good approximation:

$$D\eta = CkT \quad (18.58)$$

where C is a constant.

For vinyl polymers C may be expressed as (Ferry, 1980; Doi and Edwards, 1986):

$$C = \frac{\rho N_{AV}}{36} \frac{\langle r^2 \rangle}{M} = \frac{\rho N_{AV}}{36} \frac{\langle r^2 \rangle}{2N M_0} \quad (18.59)$$

where $2N$ is the number of backbone C-atoms in the polymer molecule and M_0 the molecular weight of the monomeric unit.

From calculations presented in Table 18.15 it follows that for vinyl polymers the constant C may be approximated by $5 \times 10^7 \text{ m}^{-1}$, when D is expressed in m^2/s and η in Ns/m^2 .

TABLE 18.15 The constant C in $D\eta = CkT$ for some vinyl polymers

vinyl polymer	$(\langle r^2 \rangle / N)^{1/2} (\text{nm})^a$	$\rho (\text{kg}/\text{m}^3)$	$M_0 (\text{kg}/\text{mol})$	$C (\text{nm}^{-1})$
Polyethylene	0.385	850	0.028	0.151
Poly(vinyl chloride)	0.402	1400	0.0625	0.121
Poly(methyl methacrylate)	0.457	1170	0.100	0.082
Poly(vinyl acetate)	0.462	1190	0.086	0.099
Polystyrene	0.507	1050	0.104	0.087

^a see Flory (1969).

The energy of activation for self-diffusion of polymers is almost exactly equal to that of viscous flow, as was demonstrated by Bueche et al. Van Amerongen (1964) suggested that the activation energy for self-diffusion of low-molecular-weight material increases with molecular weight, levelling off above a molecular weight corresponding to that of a polymer chain section capable of making independent diffusion jumps. The limiting value would be the same as that of the activation energy for viscous flow.

18.3.8. General description of polymer–penetrant system

Hopfenberg and Frisch (1969) succeeded in describing all observed behavioural features for a given polymer–penetrant system in a diagram of temperature versus penetrant activity, which seems to be of general significance for amorphous polymers. It is reproduced in Fig. 18.13.

Concentration-independent diffusion only occurs at low temperatures and/or low penetrant “activities”. At high penetrant activities over a range of temperatures well below T_g the transport of penetrant into the polymer is accompanied by solvent crazing or cracking: the osmotic stresses produced by the penetrant are sufficiently large to cause local fracture of the material.

Between these two extremes there are a series of transitions. The so-called “Case II” transport (Alfrey et al., 1966) or “partial penetrant stress controlled transport” is characterised by an activation energy, which increases with the penetrant activity. It is a highly activated process (80–200 kJ/mol) and is confined to temperatures in the vicinity of and below the effective T_g of the system (dashed line in Fig. 18.13).

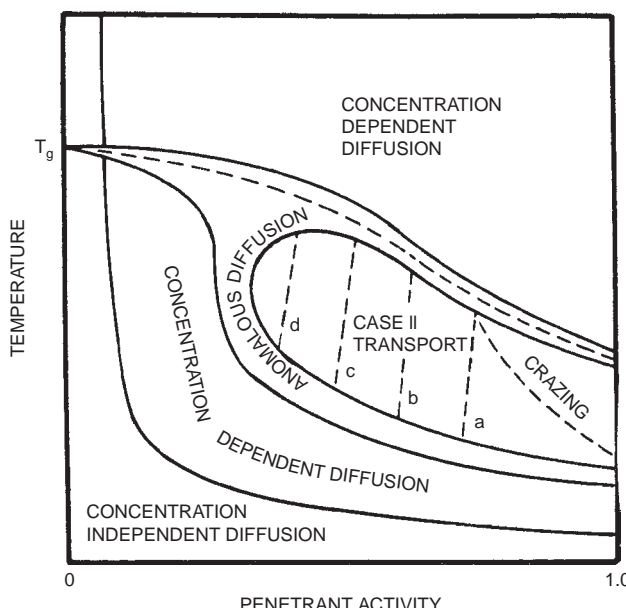


FIG. 18.13 Transport features in the various regions of the temperature–penetrant activity plane. Lines a, b, c, d are lines of constant activation energy. $E_{act(a)} > E_{act(b)} > E_{act(c)} > E_{act(d)}$ (after Hopfenberg and Frisch, 1969).

Case-II diffusion is a non-Fickian diffusion (Crank, 1956, Chap. 11), which is usually observed in glassy polymers subjected to penetration of low-molecular weight penetrants. It is an anomalous diffusion phenomenon in polymeric materials. The normal Fickian case-I diffusion is described by the diffusion coefficient and a scaling of position with $t^{1/2}$. Case-II diffusion is the result of plasticizing of the polymer by the penetrant. If the glass transition temperature of the penetrated polymer has decreased to the temperature of consideration, then the concentration profile becomes a sharp front that advances linearly with time. Ahead of this front the concentration of penetrant is still very low. Case-II diffusion has been intensively investigated experimentally and theoretically (see, e.g. Yaneva et al., 2005). Various microscopic and phenomenological models have been proposed to explain the observed features. Among the most popular are the models by Thomas and Windle (1978–1982) and of Rossi et al. (1993–1997), which was extended by Qian and Taylor (2000).

The region of “Case II sorption (relaxation-controlled transport) is separated from the Fickian diffusion region by a region where both relaxation and diffusion mechanisms are operative, giving rise to diffusion anomalies; time-dependent or anomalous diffusion.

Next to it is the concentration-dependent Fickian diffusion zone, which is characteristic of many small organic molecules of moderate to high activity at temperatures above or sufficiently below the effective T_g of the system.

Vrentas and Duda did outstanding work in the 1970s and 1980s. For this we have to refer to their contribution in the Encyclopaedia of Polymer Science and Engineering (1986) and their papers since 1976. They made use of the *Deborah-number*, introduced by Reiner, but defined in their special way:

$$De_D = \frac{\tau_m}{\tau_D} = \frac{\text{characteristic time of the fluid}}{\text{characteristic time of diffusion}} \quad (18.60)$$

As an illustration one of their diagrams is reproduced here (see Fig. 18.14).

They also found (1986) that there are at least two Fickian regions for polymer solvent diffusion, which can be observed by varying the time, scale, keeping the other parameters (T , c and M) constant. A low-frequency region is a viscous Fickian diffusion region, and a high-frequency region is a rubber like elastic Fickian diffusion region.

18.4. DISSOLUTION OF POLYMERS AS A CASE OF PERMEATION

The first phase of the process of polymer dissolution is the penetration of solvent molecules into the polymer structure. This results in a *quasi-induction period*, i.e. the time necessary to build up a swollen surface layer. The relationship between this “swelling time” τ_{sw} and the thickness of the swollen surface layer δ is:

$$\tau_{sw} = \frac{\delta^2}{6\bar{D}} \quad (18.61)$$

where \bar{D} is the average diffusion coefficient of the penetrating molecule.

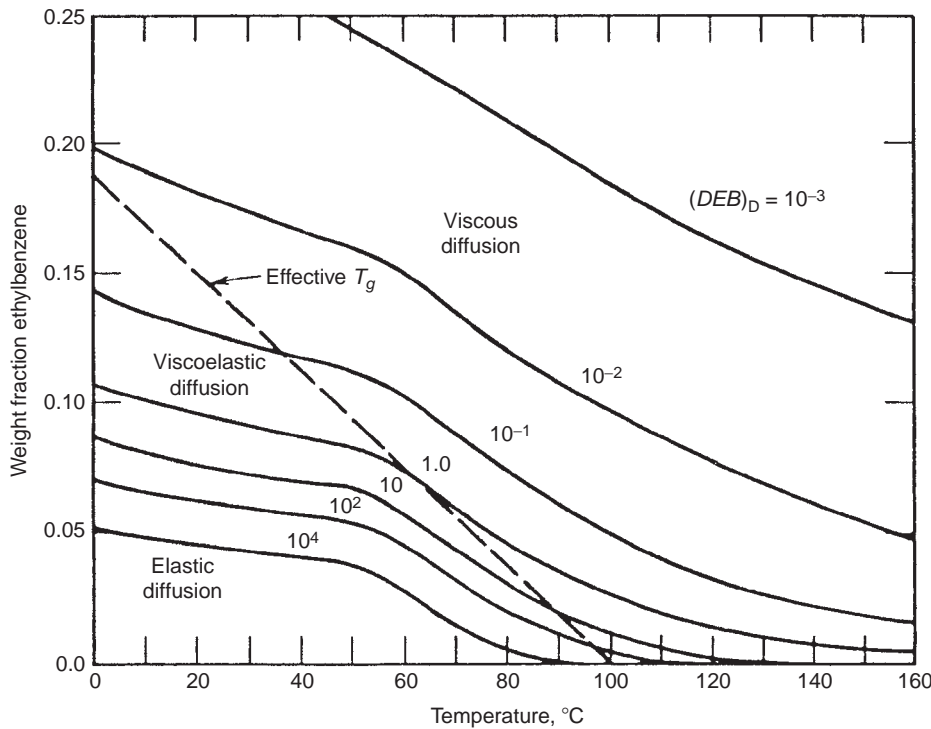


FIG. 18.14 Deborah number diagram for ethylbenzene-polystyrene system with $M = 3 \times 10^5$ and $L = 10^{-3}$ cm.

After this quasi-induction period a *steady state* may develop. During this steady state the volume-diffusion fluxes of the solvent and of the polymer will be equal. Then the *rate of dissolution* will be:

$$\dot{s} = \frac{\bar{D}}{\delta} \Delta \varphi_s \quad (18.62)$$

where φ_s is the volume fraction of the solvent and $\Delta \varphi_s$ is the total gradient in solvent concentration expressed in volume fractions) between liquid and polymer surface. If the dissolution takes place in pure solvent, $\Delta \varphi_s$ is unity, so that Eq. (18.62) becomes:

$$\dot{s} = \frac{\bar{D}}{\delta} \quad (18.63)$$

18.4.1. The diffusion layer

According to Ueberreiter (1968) the integral surface layer (δ) on glassy polymers is composed of four sub layers:

- δ_1 = The *hydrodynamic liquid layer*, which surrounds every solid in a moving liquid
- δ_2 = The *gel layer*, which contains swollen polymer material in a rubber-like state
- δ_3 = The *solid swollen layer*, in which the polymer is in the glassy state
- δ_4 = The *solid infiltration layer*, i.e. the channels and holes in the polymer filled with solvent molecules

Fig. 18.15 gives an impression of the size of these sub layers and of the polymer concentration in them. Quantitatively, δ_1 and δ_2 are by far the most important sub layers. It is

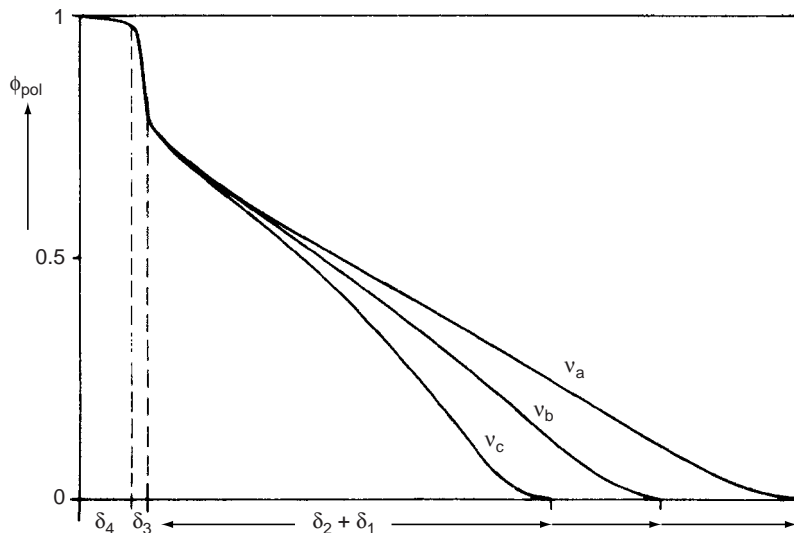


FIG. 18.15 Polymer concentration in the surface layer vs. layer thickness δ ; δ_4 = infiltration layer; δ_3 = solid swollen layer; $\delta_2 + \delta_1$ = gel and liquid layer; v_{a-c} = frequency of the stirrer. After Ueberreiter (1968).

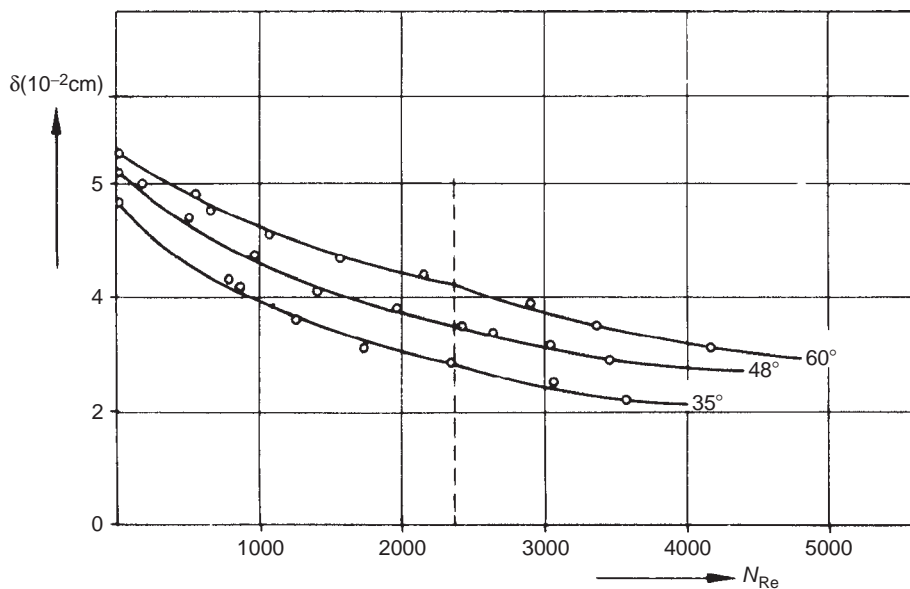


FIG. 18.16 Thickness of surface layer δ vs. Reynolds number. Temperatures of dissolution are indicated (Ueberreiter and Kirchner, 1965).

obvious that the thickness of the surface layer (δ) will be influenced by the degree of turbulence in the liquid. Since the latter is characterised by the Reynolds number ($Re = vL\rho/\eta$), one may expect a correlation between δ and Re . This has been found indeed, as is shown in Fig. 18.16. Below the glass transition temperature the influence of the temperature on δ follows the relation:

$$\delta = \delta_0 \exp(-A/T) \quad (18.64)$$

which indicates a dependence of the stability of the gel layer on the viscosity within it. The value of A is of the order of 1000 K. It shows that δ increases with temperature!

Finally, as might be expected, δ is dependent on the molecular weight of the polymer. In the normal range of molecular weights a relationship of the form

$$\delta = kM^{1/2}$$

has been found. For molecular weights higher than 6×10^5 g/mol, δ increases rapidly, possibly due to increasing entanglement of the macromolecules.

The overall expression for δ (integral surface layer) for polymers of the "normal" molecular weight range becomes:

$$\delta(\text{mm}) \approx 0.035M^{1/2} \frac{\exp(-A/T)}{1 + 0.35 \times 10^{-3}\text{Re}} \quad (18.65)$$

where M is expressed in g/mol. δ itself is of the order of 10^{-2} – 10^{-1} cm at usual temperatures and molecular weights.

Asmussen and Ueberreiter (1962) showed that the quantity

$$\frac{\text{layer thickness}(\delta)}{\text{coil diameter of polymer molecule } \langle r^2 \rangle^{1/2}} \quad (18.66)$$

is nearly constant and at room temperature approximately equal to 1.2×10^4 .

According to Chap. 9

$$\langle r^2 \rangle^{1/2} = \alpha M^{1/2} (K_\Theta / \Phi_0)^{1/3}$$

where $\Phi_0 \approx 2.5 \times 10^{23}$ mol⁻¹.

18.4.2. Diffusivity

Earlier (Sect. 18.3.6) we have shown that the diffusion coefficient of liquid penetrants appears to be determined by the viscosity of the solvent (at room temperature) as a measure of molecular size. This conclusion is confirmed by experiments of Ueberreiter (1965) on plasticizers where s and δ were measured simultaneously and \overline{D} could be calculated from Eq. (18.63).

18.4.3. Types of dissolution

Ueberreiter (1968) demonstrated that the state of a polymer influences the type of dissolution to a great extent.

If an amorphous polymer is dissolved at a sufficiently high temperature, viz. higher than the "flow temperature" (which is the limit of the rubbery state), the surface layer will consist of δ_1 only: the dissolution process is reduced to a simple mixing of two liquids.

If the polymer is in its pseudo-rubber-elastic state, the surface layer will contain δ_1 and δ_2 . Solvent molecules are able to penetrate faster into the polymer matrix than the macromolecules can be disentangled and transported into the solution.

Most of the amorphous polymers are dissolved when they are in the glassy solid state. In this case the surface layer is "fully developed". The solid state of the polymer permits the existence of all four layers. The gel layer δ_2 is very important because it heals the cracks and holes, which have been created by the penetrating front of dissolving macromolecules.

In some cases dissolution without a gel layer is found, especially at low temperatures. It appears that dissolution by stress cracking is the cause of this phenomenon. Cracks are observed which run into the polymer matrix and combine to form small blocks of the polymer, which leave the surface in a kind of eruption process. Large amounts of stored stress energy, frozen in the glass transition interval and concentrated along the wider

channels and hole systems, seem to be responsible for this process. In the extreme case of the original sub layers only δ_1 remains. In this process no induction period exists.

Different from the dissolution of amorphous polymers is that of semi-crystalline ones. Dissolution of these polymers is much more difficult than that in the glassy state, as the enthalpy of melting has to be supplied by the solvent. Many solvents, which are able to dissolve tactic but glassy polymers, are unable to dissolve the same polymer in the crystalline state. Asmussen et al. (1965) have found that the velocity of dissolution of crystalline polymers as a function of temperature closely resembles the velocity of crystallisation versus temperature curves. Polymers formed at the highest rate of growth also dissolve at the highest rate.

Example 18.6

Estimate the rate of dissolution of polystyrene in toluene at 35 °C at (a) a very low Reynolds number ($Re \approx 0$) and (b) a Reynolds number of 1000.

The molecular weight of polystyrene is 150,000; the diffusivity of toluene in polystyrene at 35 °C is about $1.5 \times 10^{-10} \text{ m}^2/\text{s}$.

Solution

We apply Eq. (18.65)

(a) at $Re \approx 0$:

$$\delta(\text{mm}) \approx 0.035(150,000)^{1/2} \exp(-1000/308) = 0.53 \text{ mm}$$

(b) at $Re = 1000$:

$$\delta(\text{mm}) \approx 0.035(150,000)^{1/2} \frac{0.0388}{1 + 0.35} = 0.39 \text{ mm}$$

We check this value with Eq. (18.66).

From Chap. 9 we know that K_Θ of polystyrene is $80 \text{ mm}^3 \text{ mol}^{1/2}/\text{g}^{3/2}$. So

$$\langle r^2 \rangle^{1/2} = \alpha M^{1/2} \left(\frac{K_\Theta}{2.5 \times 10^{23}} \right)^{1/3} = \alpha 150,000^{1/2} \left(\frac{80}{2.5 \times 10^{23}} \right)^{1/3} = 2.65 \times 10^{-5} \alpha \text{ mm}$$

Since $\alpha \approx 1.4$, we get

$$\delta \approx 1.2 \times 10^4 \langle r^2 \rangle^{1/2} = 1.2 \times 10^4 \times 1.4 \times 2.65 \times 10^{-5} \approx 0.45 \text{ mm (at } 25^\circ\text{C)}$$

in good agreement.

The rate of dissolution is

$$\dot{s} = \frac{\overline{D}}{\delta} = \frac{1.5 \times 10^{-4} \text{ mm}^2/\text{s}}{0.525 \text{ mm}} \approx 3 \times 10^{-4} \text{ mm/s} \quad \text{at } Re \approx 0$$

Ueberreiter and Kirchner (1965) measured a value of $5 \times 10^{-4} \text{ mm/s}$. The agreement may be considered fair.

At $Re = 1000$

$$\dot{s} = \frac{\overline{D}}{\delta} = \frac{1.5 \times 10^4}{0.039} \approx 4 \times 10^{-4} \text{ mm/s}$$

BIBLIOGRAPHY

General references

- Barer RM "Diffusion in and Through Solids", Cambridge University Press, London, 1941; 2nd Ed, 1951.
- Bicerano J, "Prediction of Polymer Properties", Marcel Dekker, New York, 3rd Ed, 2002, Chap. 15.
- Combellick WA, "Barrier Polymers" in Mark HF, Bikales NM, Overberger CG, and Menges G (Eds) "Encyclopaedia of Polymer Science and Engineering", Wiley, New York, Vol. 2, 2nd Ed, 1984, pp 176–192.
- Comyn J (Ed), "Polymer Permeability", Elsevier Applied Science Publishers, London, 1985.
- Crank J "The Mathematics of Diffusion", Clarendon Press, Oxford, 2nd Ed, 1990.
- Crank J and Park GS (Eds), "Diffusion in Polymers", Academic Press, London, New York, 1968.
- Fox D, Labes MM and Weissberger A (Eds), "Physics and Chemistry of the Organic Solid State", Interscience, New York, 1967.
- Haward RN (Ed) "The Physics of Glassy Polymers", Applied Science Publishers, London, 1973.
- Haward RN and Young RJ, "The Physics of Glassy Polymers", Chapman & Hall, London 2nd Ed, 1997.
- Hopfenberg HB (Ed) "Permeability of Plastic Films and Coatings to Gases, Vapours and Liquids", Plenum Press, New York, 1974.
- Koros WJ and Hellums MW, "Transport Properties", in Mark HF, Bikales NM, Overberger CG and Menges G (Eds) "Encyclopaedia of Polymer Science and Engineering", Wiley, New York, Supplement Vol., 2nd Ed, 1986, pp 724–802.
- Meares P, "Polymers: Structure and Bulk Properties", Van Nostrand, London, 1965.
- Pae KD, Morrow DR and Chen Y (Eds), "Advances in Polymer Science and Engineering", Plenum Press, New York, 1972.
- Stern SA, Krishnakumar B and Nadakatti SM, "Permeability of Polymers to Gases and Vapours", in Mark JE (Ed), "Physical Properties of Polymers Handbook", AIP Press, Woodbury, NY, 1996, Chap. 50.
- Stern SA and Fried JR "Permeability of Polymers to Gases and Vapours", in Mark JE (Ed), "Physical Properties of Polymers Handbook", Springer, 2nd Ed, 2007, Chap. 61.
- Sweeting OJ (Ed) "Science and Technology of Polymer Films", Wiley, New York, 1971.
- Ueberreiter K, "Advances in Chemistry Series" 48 (1965) 35.
- Vrentas JS and Duda JL, "Diffusion", in Mark HF, Bikales NM and Overberger CG (Eds), "Encyclopaedia of Polymer Science and Engineering", Vol 5, 2nd Ed, 1986 Wiley, New York, pp 26–68.
- Stern SA, "Polymers for Gas Separations: the Next Decade", J Membrane Sci 94 (1994) 1–65.

Special references

- Atkins PW and De Paula J, "Physical Chemistry", Oxford University Press, Oxford, 8th Ed, 2006.
- Alfrey T, Gurnee EF and Lloyd WG, J Polymer Sci C12 (1966) 249.
- Asmussen F and Ueberreiter K, J Polymer Sci 57 (1962) 199, Kolloid-Z 185 (1962) 1.
- Asmussen F, Ueberreiter K and Naumann Hin, Diplomarbeit, Fr Univ Berlin, 1965.
- Barbari TA, Koros WJ and Paul DR, J Polym Sci, Phys Ed 26 (1988) 709 and 729.
- Barer RM, Barrie JA and Slater J, J Polym Sci 27 (1958) 177.
- Barret RM, J Membrane Sci 18 (1984) 25.
- Barrie JA "Water in Polymers" in "Diffusion in Polymers" (1968) (see General references), Chap. 8, pp 259–314.
- Bueche F, J Chem Phys 20 (1952) 1959; 22 (1954) 603.
- Bueche F, "Physical Properties of Polymers", Interscience, New York, 1954.
- Bueche F, Cashin WM and Debye P, J Chem Phys 20 (1952) 1956.
- Chern RT, Sheu FR, Jia L, Stannett VT and Hopfenberg HB, J Membrane Sci 35 (1987) 103.
- Doi M and Edwards SF, "The Theory of Polymer Dynamics", Clarendon Press, Oxford, 1986.
- Duda JL and Vrentas JS, J Polym Sci A2, 6 (1968) 675.
- Duda JL, Vrentas JS, Ju ST and Liu HT, "Prediction of Diffusion Coefficients for Polymer–Solvent Systems", AIChE J 26 (1982) 279.
- Ferry JD, "Viscoelastic Properties of Polymers", Wiley, New York, 3rd Ed, 1980.
- Flory PJ, "Statistical Mechanics of Chain Molecules", Wiley, New York, 1969.
- Friedman A and Rossi G, Macromolecules 30 (1997) 153.
- Frisch HL, Polym Lett 1 (1963) 581.
- Fujita H, Kishimoto A and Matsumoto K, Trans Faraday Soc 54 (1958) 40; 56 (1960) 424.
- Fujita H, "Diffusion of Organic Vapours in Polymers above the Glass Temperature", in "Diffusion in Polymers" (see Gen Ref) (1968), Chap. 3, pp 75–106.
- Hopfenberg HB and Frisch HL, Polym Lett 7 (1969) 405.
- Koros WJ, Paul DR and Rocha AA, J Polym Sci, Phys Ed 14 (1976) 687.
- Koros WJ, Chan AH and Paul DR, J Membrane Sci 2 (1977) 165.

- Koros WJ and Paul DR, J Polym Sci, Phys Ed 16 (1978) 1947.
Koros WJ, Smith GN and Stannett VT, J Appl Polym Sci 26 (1981) 159.
Meares P, J Am Chem Soc 76 (1954) 3415; Trans Faraday Soc 53 (1957) 101; 54 (1958) 40.
Michaels AS and Bixler HJ, J Polym Sci 50 (1961) 393 and 50 (1961) 413.
Michaels AS, Vieth WR and Barrie JA, J Appl Phys 34 (1963) 1 and 13.
Paul DR, J Polym Sci A2 (1969) 1811.
Paul DR and Koros WJ, J Polym Sci, Phys Ed 14 (1976) 675.
Paul DR, Ber Bunsen Ges 83 (1979) 294.
Petropoulis JH, J Polym Sci A2, 8 (1970) 1797.
Qian T and Taylor PL, Polymer 41 (2000) 7159.
Raucher D and Sefcik MD, ACS Symp Series 223 (1983) 111, Polymer Preprints 24(l) (March 1983) 85–88.
Rogers CE, Meyer JA, Stannett VT and Szwarc M, Tappi 39 (1956) 741.
Rogers CE, in "Physics and Chemistry of the Organic Solid State" Fox . (Eds), 1965, Chap. 6 (see General reference).
Rogers CE in Comyn J (Ed), "Polymer Permeability", 1985, Chap. 2 (see General reference).
Rossi G and Mazich KA, Phys Rev E 48 (1993) 1182.
Rossi G, Pincus PA and De Gennes PG, Europhys Lett 32 (1995) 391.
Sada E, Kumazawa H et al., Ind Eng Chem 26 (1987) 433 and J Membrane Sci 37 (1988) 165.
Salame M, Polym Eng Sci 26 (1986) 1543.
Salame M, 1987, Personal Communication to DW van Krevelen.
Southern E and Thomas AG, Trans Faraday Soc 63 (1967) 1913.
Stannett VT and Szwarc M, J Polym Sci 16 (1955) 89.
Stannett VT, "Diffusion of Simple Gases", in "Diffusion in Polymers", 1968, Chap. 2 (see General references), pp 41–74.
Steiner K, Lucas KJ and Ueberreiter K, Kolloid-Z 214 (1966) 23.
Thomas NL and Windle AM, Polymer 19 (1978) 255; 21 (1980) 613; 22 (1981) 627; 23 (1982) 529.
Ueberreiter K, "The Solution Process", in Crank J and Park GS (Eds), "Diffusion in Polymers" 1968, pp 220–258 (see General references).
Ueberreiter K and Kirchner P, Makromol Chem 87 (1965) 32.
Van Amerongen GJ, J Appl Phys 17 (1946) 972; J Polym Sci 2 (1947) 381; 5 (1950) 307; Rubber Chem Technol 37 (1964) 1065.
Van Krevelen DW, "Properties of Polymers" 1st Ed, 1972, p 290.
Vieth WR and Sladek KJ, J Coll Sci 20 (1965) 1014.
Vieth WR, Howell JM and Hsieh JH, J Membrane Sci 1 (1976) 177.
Vieth WR and Eilenberg JA, J Appl Polym Sci 16 (1972) 945.
Vrentas JS, and Duda JL, "Molecular Diffusion in Polymer Solutions", AIChE J 25 (1979) 1–24.
Vrentas IS, Duda JL and Huang WJ, "Regions of Fickian Diffusion in Polymer–Solvent Systems", Macromolecules 19 (1986) 1718.
Yaneva J, Dünweg B and Milchev A, J Chem Phys 122 (2005) 4105.
Zhurkov SN and Ryskin GY, J Techn Phys (USSR) 24 (1954) 797.

CHAPTER 19

Crystallisation and Recrystallisation

Crystallisation of polymers depends on the possibilities of nucleation and growth. The structural regularity of the polymer has a profound influence on both. Interesting correlations were found for estimating the rate of spherulitic crystallisation. Besides this normal mode of bulk crystallisation, other modes are frequently observed: induced crystallisation by pressure and stress and extended chain crystallisation. The latter mode occurs under special conditions for flexible chain polymers, but is the normal mode for rigid chain polymers. All modes of crystallisation are correlated with the structure of the polymer chain and with the two main transition temperatures, T_g and T_m .

19.1. CRYSTALLINITY, NUCLEATION AND GROWTH

Most pure substances have a definite melting temperature below which the change from a random liquid structure to a well ordered, periodic crystalline structure can occur; this transformation is called *crystallisation*; the reverse process is called *melting*.

Crystallisation is also possible from solutions; the reverse process is called *dissolving*.

Melts of high-molecular substances have a high viscosity, which increases rapidly on cooling. Only polymers with rather regular molecular chains are able to crystallise fast enough from a melt, notwithstanding the high viscosity. Many polymers solidify into glassy solids.

Crystallisation from a solution largely depends on the rate of cooling and on the rate of change in solubility connected with it. Again, the polymers with a regular molecular chain without side groups crystallise fast.

19.1.1. Crystallinity

Since polymers cannot be completely crystalline (i.e. cannot have a perfectly regular crystal lattice) the concept "crystallinity" has been introduced. The meaning of this concept is still disputed (see Chap. 2). According to the original micellar theory of polymer crystallisation the polymeric material consists of numerous small crystallites (ordered regions) randomly distributed and linked by intervening amorphous areas. The polymeric molecules are part of several crystallites and of amorphous regions.

TABLE 19.1 Definitions of crystallinity (x_c) (after Kavesh and Schultz, 1969)

Based on	Definition
Specific volume (v)	$x_c = \frac{V_a - V}{V_a - V_c}$
Specific heat (c_p)	$x_c = \frac{c_p^a - c_p}{c_p^a - c_p^c}$
Specific enthalpy (h)	$x_c = \frac{h_a - h}{h_a - h_c}$
Specific enthalpy of fusion (Δh_m)	$x_c = \frac{\Delta h_m}{\Delta h_m^c}$
Infrared mass extinction coefficient (ε) of characteristic vibrational mode	$x_c = \frac{\varepsilon_\lambda}{\varepsilon_\lambda^{(c)}} = 1 - \frac{\varepsilon_\lambda}{\varepsilon_\lambda^{(a)}}$
X-ray scattering intensity (I = area under selected peak)	$x_c = \frac{I_c}{I_c + I_a} \approx 1 - \frac{I_a}{I_{a,melt}}$
Nuclear magnetic resonance	$\frac{x_c}{1 - x_c} = \frac{\text{area of broad component}}{\text{area of narrow component}}$

Many polymeric solids consist largely of folded chain lamellae and that the breadth of X-ray diffraction lines is caused by the crystallite size distribution and by the disorder within the lamella.

The several definitions of the fraction crystallinity (x_c) are presented in Table 19.1. A critical discussion of meaning and measurement of crystallinity in polymers was given by Kavesh and Schultz (1969).

It is understandable that the various methods of determination of crystallinity may lead to somewhat different figures for the same polymer.

19.1.2. Nucleation and growth

There is a striking resemblance between Permeation (Chap. 18) and Crystallisation. Just as Permeability is the product of Solubility and Diffusivity ($P = SD$), the rate of crystallisation is the product of Nucleability (or probability of Nucleation, also called "nucleation factor") and Transportability (Self-diffusivity of chains or chain fragments, also called "transport factor"). This statement is valid as well for the primary nucleation in melt or solution, as for the growth of the crystallites (which is a repeated sequence of surface nucleation and surface growth).

The general theory of phase transition by crystallisation was developed by Gibbs, and later extended by Becker and Döring (1935), Avrami (1939/1941), Turnbull and Fisher (1949) and Hoffman et al. (1958/1966). The theory is based on the assumption that in super-cooled melts there occur fluctuations leading to the formation of a new phase. The phase transformation begins with the appearance of a number of very small particles of the new phase (*nucleation*).

For very small particles the decrease in free energy due to phase transition is exceeded by the increase in interfacial free energy. So the possible growth of new particles depends on the ratio of surface area to volume. There is a *critical size* separating those particles whose free energy of formation increases during growth from those whose energy

decreases. So the small particles will tend to re-dissolve and the larger ones will tend to grow. A particle that has just the critical size, acts as a *nucleus for growth*.

As a model of the nucleus in polymer crystallisation one often takes a rectangular prism. A breakthrough in this respect was the discovery and exploration of *polymer single crystals* (Schlesinger (1953) and Keller (1957)) which are indeed small prisms, platelets of polymeric chains, *folded back and forth* in a direction perpendicular to the basal plane (see Fig. 19.1)

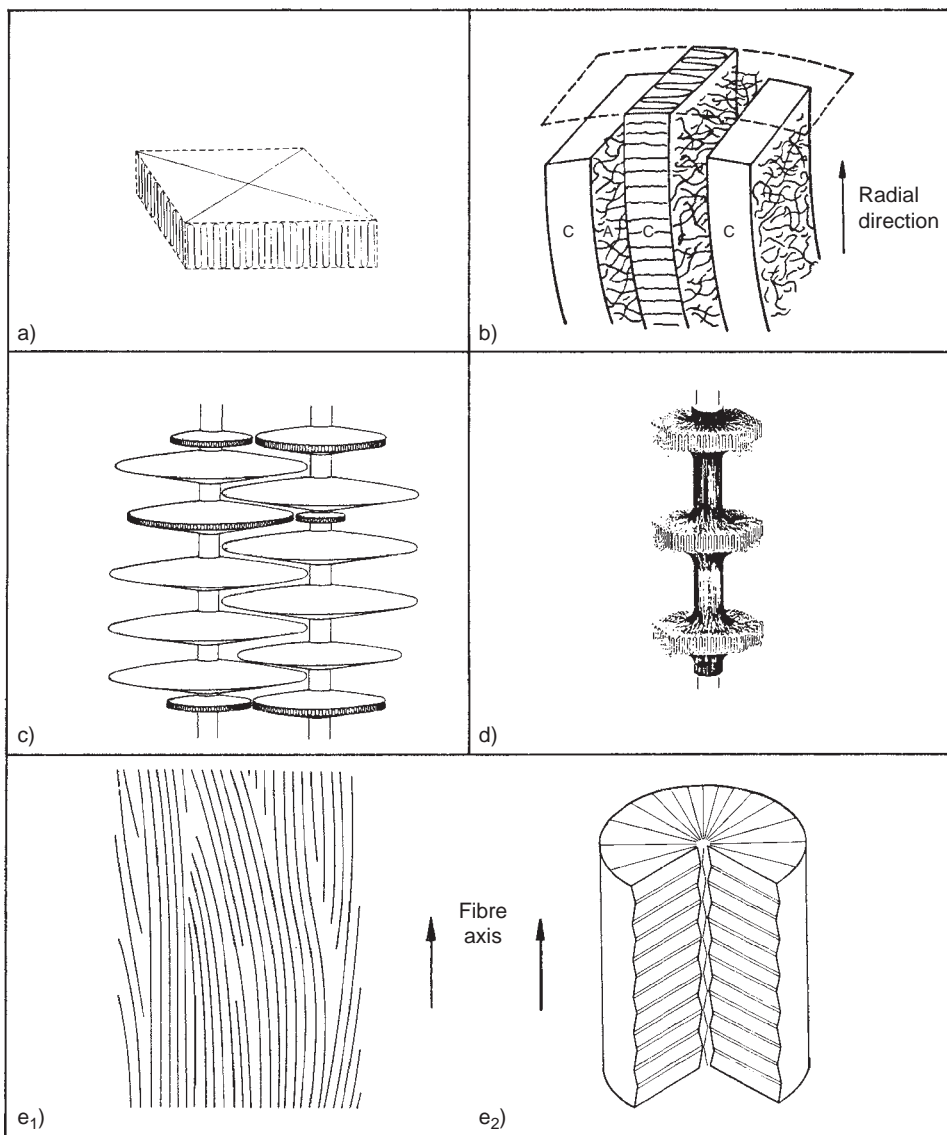


FIG. 19.1 Morphological models of some polymeric crystalline structures. (A) Model of a single crystal structure with macromolecules within the crystal (Keller, 1957). (B) Model of part of a spherulite (Van Antwerpen, 1971) A, Amorphous regions; C, Crystalline regions; lamellae of folded chains. (C) Model of high pressure crystallised polyethylene (Ward, 1985). (E) Model of a shish kebab structure (Pennings et al., 1970). (E) Model of paracrystalline structure of extended chains (aramid fibre). (E1) lengthwise section (Northolt, 1984). (E2) cross section (Dobb, 1985).

It is now generally accepted that folding is universal for spontaneous, free crystallisation of flexible polymer chains. It was first of all found in crystallisation from very dilute solutions, but it is beyond doubt now, that also *spherulites*, the normal mode of crystallisation from the melt, are aggregates of platelike crystallites with folded chains, pervaded with amorphous material. “*Extended chain crystallisation*” only occurs under very special conditions in the case of flexible chains; for rigid polymer chains it is the natural mode (“*rigid rod-crystallisation*”: from the melt in case of thermotropic polymers, and from solution in case of the lyotropic liquid-crystalline polymers; both of them show nematic ordering in the liquid state).

Table 19.2 gives a survey of the morphology of polymer crystallisation. The survey is self-explanatory; it demonstrates an almost continuous transition from the pure folded chain to the pure extended-chain crystallite.

We shall now discuss, successively, the four main modes of polymer crystallisation:

- a. The spontaneous, *spherulitic*, crystallisation of flexible polymeric molecules under quasi-isotropic conditions.
- b. The “*induced*” crystallisation of flexible polymeric chains in fields of force, mainly by application of stress.
- c. The “*extended chain*” crystallisation of *flexible* polymer molecules.
- d. The “*extended chain*” crystallisation of *semi-rigid* polymer molecules.

19.2. SPHERULITIC CRYSTALLISATION OF POLYMERS FROM THE MELT

The following subjects will, in succession, be discussed:

1. The overall rate of crystallisation
2. The nucleation
3. The rate of growth
4. A unified theory of crystallisation processes

19.2.1. Overall rate of crystallisation

The overall rate of crystallisation of a super-cooled liquid is determined by the two factors mentioned: the rate of formation of nuclei (above the critical size) and the rate of growth of such nuclei to the final crystalline aggregates.

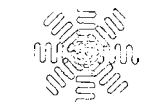
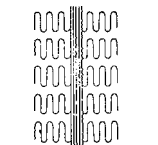
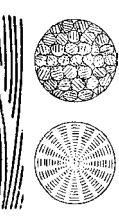
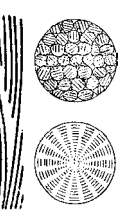
When a polymer sample cools down from the molten state to the temperature of measurement, crystallisation is very slow at first. After an “induction” period the process speeds up to a maximum rate and slows down again as it approaches the final equilibrium state.

Most polymers crystallise at measurable rates over a range of temperatures that is characteristic of each polymer. It may extend from about 30 °C above the glass temperature (T_g) to about 10 °C below the melting point (T_m).

The rate of crystallisation increases as the temperature decreases below T_m , reaching a maximum at T_k , and decreases again when the temperature is lowered still further.

There is hardly a class of materials in which bulk properties are as kinetically determined as in that of the macromolecules. The consequences of the nature of nucleation and that of growth are so persistent that virtually no amount of subsequent annealing can eliminate their effects.

TABLE 19.2 Morphology of crystallites in polymers (Van Krevelen, 1978)

Type of polymer chain	Conformation in melt/solution	Mode of crystallisation	Basic sub-structure of crystallites	Micro-structure		Illustration of characteristic features
				Conditions of formation	Type	
Flexible	Random coil	Free (spontaneous)	Lamellae made up of folded chains	Very dilute quiescent solution	Single crystals	
				Quiescent melt	Spherulites	
	Partly oriented or partly ordered (disentangled) coils	Induced by pressure, flow, stress, etc.	Hybrid structure made up of thin core of extended chains and matrix of Lamellae	Stirred very dilute solution	Shish kebab fibrils	
				Melt- or solution-spinning and drawing	Row nucleated crystallites	
Rigid	Liquid crystals of rigid rods	Mainly spontaneous	Microfibrils made up of rigid rodlets	Gel-spinning followed by ultradrawing	Extended chain microfibrils	
						
				Solution-spinning with gas gap and drawing	Para-crystalline microfibrils	

The usual procedure in studying the rate of crystallisation is to cool the polymer sample quickly from the molten state to the temperature of measurement and then measure the development of crystallinity at constant temperature (isothermal crystallisation).

When the crystallisation gives rise to well-defined spherulites visible under a microscope it is sometimes possible to follow simultaneously the rate of formation of the nuclei and their rate of growth into spherulites (in μm per min). Since growing spherulites soon interfere with one another's development, measurements are confined to early stages in the crystallisation.

If nucleation and growth cannot be studied independently, the overall conversion of amorphous into crystalline polymer may be followed with the aid of any technique giving a measure of the degree of crystallinity. For instance, the specific volume may be followed by enclosing the crystallising sample in a dilatometer. It is customary to define the overall rate of crystallisation at a given temperature as the inverse of the time needed to attain one-half of the final crystallinity ($t_{1/2}^{-1}$).

According to Avrami (1939–1941) the progress of the isothermal crystallisation can be expressed by the equation:

$$x(t) = 1 - \exp(-Kt^n) \quad (19.1)$$

where $x(t)$ is the fraction of material transformed (into the spherulitic state) at time t . K and n are constants.

Eq. (19.1) may also be written as

$$\ln \{-\ln [1 - x(t)]\} = n \ln t + \ln K \quad (19.2)$$

so that the constants n and K may be obtained by plotting $\ln \{-\ln [1 - x(t)]\}$ vs. $\ln t$. The volume fraction $x(t)$ may be obtained from dilatometer measurements in the following way. The relation between the total volume and the volume of the crystalline fraction is

$$V = V_c + V_a = V_c + \frac{m_a}{\rho_a} = V_c + \frac{m - m_c}{\rho_a} = V_c + \frac{m - V_c \rho_c}{\rho_a} = \frac{m}{\rho_a} - V_c \left(\frac{\rho_c}{\rho_a} - 1 \right) \quad (19.3)$$

where m , m_a and m_c are total mass, mass of amorphous fraction and mass of crystalline fraction, respectively; ρ_a and ρ_c are the densities of amorphous and crystalline fraction, respectively and V , V_a and V_c total volume, volume of amorphous fraction and volume of the crystalline fraction, respectively. The original volume is equal to $V_o = m_a / \rho_a$, so that the time dependent volume decrease $\Delta V(t)$ is equal to

$$V_o - V(t) = \Delta V(t) = V_c(t) \left(\frac{\rho_c}{\rho_a} - 1 \right) \text{ and } (\Delta V)_\infty = V_o - V_\infty = \frac{m}{\rho_a} - \frac{m}{\rho_c} \quad (19.4)$$

Accordingly, the fraction of crystalline material is

$$x(t) = \frac{\Delta V(t)}{(\Delta V)_\infty} \quad (19.5)$$

The Avrami-equation may now be expressed as

$$\ln \left\{ -\ln \left[1 - \frac{\Delta V(t)}{(\Delta V)_\infty} \right] \right\} = n \ln t + \ln K \quad (19.6)$$

The constant K contains nucleation and growth parameters; n is an integer whose value depends on the mechanism of nucleation and on the form of crystal growth. The

TABLE 19.3 Constants n and K of Avrami equation

Form of growth	Type of nucleation			
	Predetermined (constant number of nuclei per cm)		Spontaneous (sporadic) (constant nucleation rate)	
n	K	n	K	
Spherulitic (spheres)	3	$\frac{4}{3}\pi v^3 N \rho^*$	4	$\frac{1}{3}\pi v^3 J \rho^*$
Discoid (platelets)	2	$\pi b v^2 N \rho^*$	3	$\frac{1}{3}\pi b v^2 J \rho^*$
Fibrillar (rodlets)	1	$f v N \rho^*$	2	$\frac{1}{2} f v J \rho^*$

b = thickness of platelet; f = cross section of rodlet; ρ^* = relative density ρ_c/ρ ; N = number of nuclei per unit volume; J = rate of nucleation per unit volume; v = rate of crystal growth.

numerical value of K is directly connected with the overall rate of crystallisation $t_{1/2}^{-1}$, by means of the following equation:

$$K = \left(t_{1/2}^{-1} \right)^n \ln 2 \approx 0.7 \left(t_{1/2}^{-1} \right)^n \quad (19.7)$$

Theoretical values of n and K are summarised in Table 19.3.

Khanna and Taylor (1988) pointed out that the following expression would give a better description of the experimental data:

$$x(t) = 1 - \exp [-(Kt)^n] \quad (19.1a)$$

According to Marangoni (1998), however, their modification is largely arbitrary and creates dependence between the Avrami constant K and the Avrami exponent n, without providing a theoretical justification (see also Foubert et al., 2003). From a curve-fitting point of view, no advantages exist in using the modified over the original form of the Avrami model. The order of a polynomial fit to crystallisation data is not equivalent to the Avrami exponent. The use of turbidity measurements for the quantitative characterisation of crystallisation kinetics is not valid.

19.2.2. Nucleation

For polymeric molecules the temperature interval just below the equilibrium melting temperature is a metastable zone in which nuclei do not form at a detectable rate, but in which crystals, once nucleated, can grow. Below this metastable temperature zone nuclei may form spontaneously, either homogeneously or heterogeneously, but as the substance cools further, a high-viscosity zone is reached where again the formation of nuclei is inhibited and growth does not take place at a detectable rate. Both nucleation and growth show maxima in their rates, because at higher temperatures the driving force (supersaturation) decreases and at lower temperatures the rate of mass transfer is strongly decreased by the high viscosity. Homogeneous nucleation followed by growth of crystallites can only occur in the temperature range where the two curves overlap. The metastable zone of undercooling (supersaturation) is supposed to be due to the greater solubility of microscopic embryonic crystallites as compared with macroscopic crystals and, hence, to the fact that primary, spontaneous nucleation requires higher activation energy than growth.

It is very difficult to investigate the homogeneous nucleation, because heterogeneities, which are inevitably present in polymeric melts, greatly promote the (heterogeneous) nucleation.

The nucleation of many polymers is found to be highly dependent on their thermal history. It is affected by the conditions of any previous crystallisation as well as by the melting temperature and the time spent in the molten state. Tiny regions of a high degree of order, often stabilised by heterogeneities, may persist in a melt for a long time (resistant nuclei) and will act as predetermined nuclei for recrystallisation on cooling. The number and size of the nuclei that remain in the melt depend upon three factors: (a) temperature of any previous crystallisation; (b) temperature of the melt; (c) melting time.

In the special case of a very slowly crystallising polymer interesting effects have been observed (Boon, 1966; Boon et al., 1968). On severe super-cooling, "induced" nuclei are created which may grow into effective nuclei at higher temperatures. The crystallisation of a severely super-cooled polymer is completely governed by these induced nuclei, because they outnumber the resistant nuclei by some orders of magnitude. Purifying the polymer can decrease the number of these induced nuclei. When cooled polymers are heated to temperatures just above the melting point, the induced nuclei are destroyed and only the resistant nuclei, which are few in number, remain.

19.2.2.1. The critical size of nuclei

In homogeneous crystallisation, i.e. a crystallisation process where no heterogeneous nuclei are present, nuclei has to be formed before crystallisation starts. In a primary step a few molecules pack together to form a nucleus. If it happens to be that this nucleus is large enough, it will grow. If on the other hand, it is too small, it will dissolve again. The critical size depends on a combined action of surface energy and heat of crystallisation. For spherical nuclei with radius r the difference in Gibbs energy per unit volume between crystal and liquid is equal to

$$\Delta G = -\frac{4}{3}\pi r^3 \Delta G_v + 4\pi r^2 \gamma \quad (19.8)$$

where the first term on the right hand side of Eq. (19.8) is equal to the decrease of the Gibbs energy due to crystallisation and the second term to the increase of the Gibbs energy due to formation of a boundary. The dependence of ΔG on the radius of the nucleus is schematically shown in Fig. 19.2: ΔG first increase with increasing radius, because the surface energy is larger than the heat of crystallisation. A nucleus of this radius is unstable, because for growth energy is needed, and accordingly it will melt again. A maximum is obtained, after which the heat of crystallisation wins it from the surface energy. A nucleus with radius on the right hand side of the maximum is stable, because upon growing energy is released. The critical radius is the radius of the maximum, where $dG/dr = 0$:

$$-4\pi r^2 \Delta G_v + 8\pi r \gamma = 0 \quad (19.9)$$

Consequently the radius of a critical spherical nucleus is equal to

$$r_{\text{crit}} = \frac{2\gamma}{\Delta G_v} \quad (19.10)$$

At the melting point T_m it holds $\Delta G = \Delta H - T_m \Delta S = 0$, and therefore at temperature T we have

$$\Delta G = \Delta H - T \Delta S = \Delta H - T \frac{\Delta H}{T_m} = \Delta H \frac{T_m - T}{T_m} \quad (19.11)$$

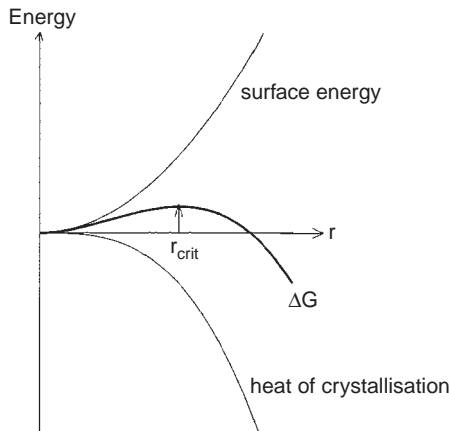


FIG. 19.2 Schematic representation of change in energy in the formation of spherical nuclei during polymer crystallisation. The total energy is the difference of the surface energy, $4\pi r^2 \gamma$ and the heat of crystallisation, $\frac{4}{3}\pi r^3 \Delta H_v$. Nuclei with $r < r_{\text{crit}}$ are unstable and will disappear; nuclei with $r > r_{\text{crit}}$ are stable and will grow to crystallites.

Accordingly we find for the critical spherical nucleus

$$r_{\text{crit}} = \frac{2\gamma}{\Delta G_v} = \frac{2\gamma T_m}{\Delta H_v(T_m - T)} \quad (19.12)$$

It follows that the rate of nucleation is zero at the melting temperature. With decreasing temperature the critical size is smaller, which means that smaller nuclei become stable. For that reason more nuclei will be formed at lower temperatures, and thus the nucleation rate is larger at stronger undercooling.

19.2.2.2. The number of nuclei N

Boon (1966/1968) investigated the kinetics of crystallisation of isotactic polystyrene. This polymer is extremely interesting as a model substance for crystallisation work. Its rate of growth is so low that the crystallisation can be studied in the whole region from T_g to T_m . Due to the low growth rate the fundamental processes of nucleation and growth can be studied almost separately.

Boon determined the number of nuclei in the two extreme cases:

- Starting from a super-heated melt and quenching to the crystallisation temperature
- Starting from the solid state and heating to the crystallisation temperature

His results are presented in Fig. 19.3.

After heating above T_m for some time the number of nuclei is extremely small ($N < 10^5 \text{ cm}^{-3}$). By quenching the number increases, attaining a maximum at T_g ($N > 10^{12} \text{ cm}^{-3}$). By heating from T_g to higher temperatures the number of nuclei diminishes, reaching very low values at the melting point.

Generally speaking we may say that for all crystallising polymers the number of nuclei will be of the following order of magnitude:

starting from the melt and quenched to T_k : $\approx 3 \times 10^6 \text{ cm}^{-3}$; starting from the quenched solid state ($T < T_g$) and heated to T_k : $3 \times 10^{11} \text{ cm}^{-3}$. N will of course determine the maximum size of the spherulites after conversion of the whole melt into crystalline material.

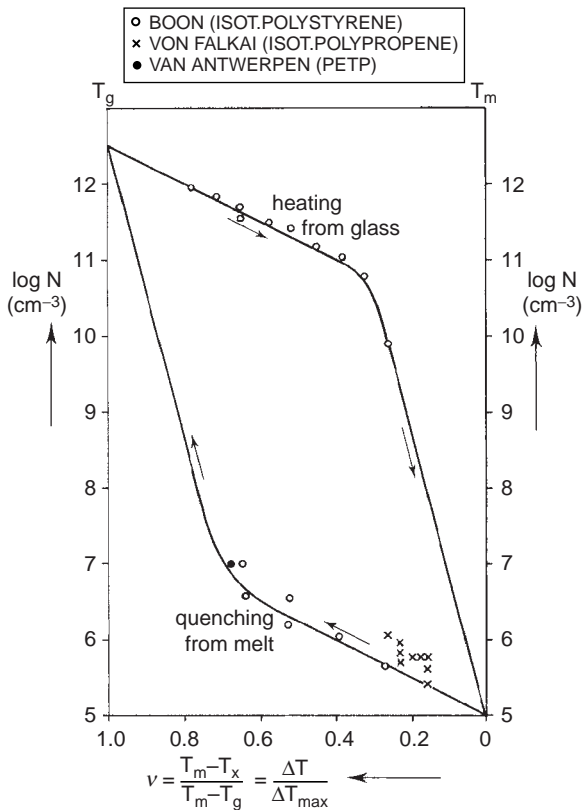


FIG. 19.3 Boon's data as a function of the dimensionless parameter $v = (T_m - T_x)/(T_m - T_g)$, the "relative undercooling" (T_x = crystallisation temperature). In this master-form the graph also fits with the data of Von Falkai (1960) for isotactic polypropene and with those of Van Antwerpen (1971, 1972) on PETP.

It can easily be seen that

$$\frac{4}{3}\pi\bar{R}_{\max}^3N = x_c \quad (19.13)$$

so that, if $x_c \approx 1$

$$\bar{R}_{\max} N^{1/3} \approx 0.62 \quad (19.14)$$

Theoretical expression for the rate of nucleation (see, e.g. Wunderlich, 1976 and Boon, 1966)

The theoretical basic equation for nucleation reads as follows:

$$\dot{N} = \dot{N}_0 \exp [-E_{sd}/(RT)] \exp [-\Delta G_n^*/(k_B T)] \quad (19.15)$$

where \dot{N} = rate of nucleation; \dot{N}_0 = is a constant for the zero-conditions (formally equal to the rate of nucleation for E and $\Delta G^* = 0$); E_{sd} = activation energy of transport (self-diffusion) (J/mol); ΔG_n^* = Gibbs free energy of formation of a nucleus of *critical size* (J).

The theory gives for ΔG_n^* (Turnbull et al., 1949, 1950):

$$\Delta G_n^*/(k_B T) = \frac{32\gamma_{||}^2\gamma_{\perp}T_m^4}{k_B T(\Delta H_m)^2 T^2(\Delta T)^2} \approx \frac{32\gamma_{||}^2\gamma_{\perp}T_m^2}{k_B T(\Delta H_m)^2(\Delta T)^2} \quad (19.16)$$

and for $E_{sd}/(RT)$:

$$\frac{E_{sd}}{RT} = \frac{C_1}{R(C_2 + T - T_g)} = \frac{C_1^*}{C_2 + T - T_g} \quad (19.17)$$

based on the viscosity relation of Williams, Landel and Ferry (WLF) (see Chap. 13).

In these equations:

$\gamma_{||}$ = free interfacial energy parallel to chain direction ($N/m = J/m^2$)

γ_{\perp} = free interfacial energy perpendicular to chain direction ($N/m = J/m^2$)

ΔH_m = heat of melting (fusion) (J/m^3)

$\Delta T = T_m - T$ = undercooling (K)

T = crystallisation temperature (K)

C_1 = constant = 17.2 kJ/mol (so-called standard value, but characteristic for every polymer)

C_2 = constant = 51.6 K (so-called standard value, but characteristic for every polymer)

C_1^* = constant = 2070 K (so-called standard value, but characteristic for every polymer)

The equations quoted here have a restricted value due to generalisations and idealised assumptions.

19.2.3. Rate of growth

In unstrained (quasi-isotropic) crystallisation processes the crystallisation starts from a number of point-nuclei, and progresses in all directions at an equal linear velocity (v). In the case of isothermal crystallisation the radius of the crystallised regions increases by an equal amount per unit of time ($v = \text{constant}$). The rate of growth is very much dependent, however, on the temperature of crystallisation.

At the melting point (T_m) and at the glass transition point (T_g) its value is nearly zero; in the intermediate region a maximum (v_{max}) is observed at a temperature T_k . *Gandica and Magill* (1972) have derived a master curve, valid for all “normal” polymers, in which the ratio v/v_{max} is plotted vs. a dimensionless crystallisation temperature:

$$\Theta = \frac{T - T_{\infty}}{T_m - T_{\infty}} \text{ where } T_{\infty} \approx T_g - 50$$

This master curve is shown in Fig. 19.4. The top of the curve is reached at $\Theta \approx 0.635$, corresponding roughly with the empirical relationship:

$$T_k \approx 0.5(T_m + T_g) \quad (19.18)$$

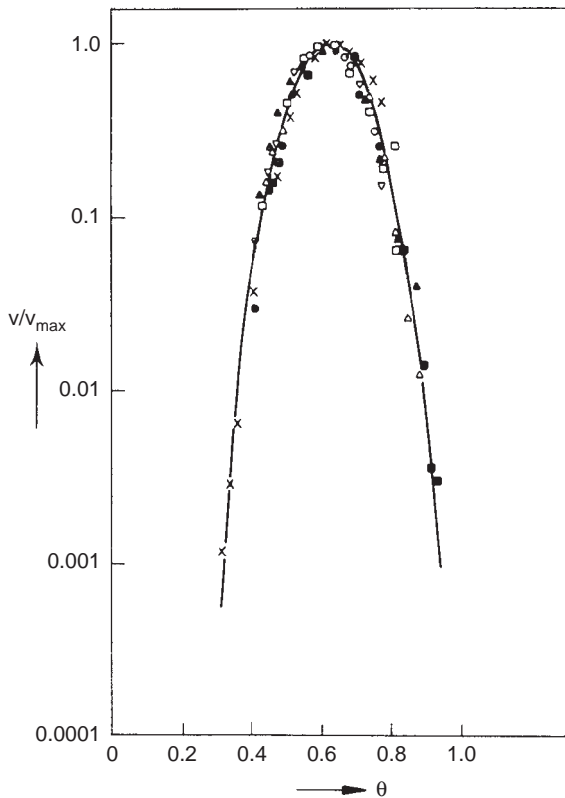


FIG. 19.4 Dimensionless master curve of the rate of growth, suggested by Gandica and Magill (1972).

19.2.3.1. Theoretical expression for the growth rate

The basic equation for growth is analogous to that of nucleation:

$$v = v_o \exp\left(-\frac{E_D}{RT}\right) \exp\left(-\frac{\Delta W^*}{k_B T}\right) \quad (19.19)$$

where E_D is the activation energy for the (diffusive) transport process at the interface (J/mol); ΔW^* is the free energy of formation of a surface nucleus of critical size (J).

Hoffman (1958, 1966) proposed the following particular relations for the growth rate (see also Suzuki and Kovacs, 1970):

$$\frac{E_D}{RT} = \frac{C_1^*}{C_2 + T - T_g} \text{ (WLF formulation)} \quad (19.20)$$

$$\frac{\Delta W^*}{kT} = \frac{4b_o \gamma_{||} \gamma_{\perp} T_m}{R \Delta h_m T \Delta T} = \frac{C_3 T_m}{T(T_m - T)} \quad (19.21)$$

where b_o = thickness of the chain molecules (m); $\gamma_{||}$ = interfacial free energy (per unit area) parallel to the chain (N/m or J/m²); γ_{\perp} = interfacial free energy (per unit area) perpendicular to the chain (N/m or J/m²); Δh_m = heat of melting per unit volume (J/mol);

T_m = equilibrium melting point (K); C_1^* , C_2 and C_3 are “constants” with the following values $C_1^* \approx 2070$ K; $C_2 \approx 51.6$ K; $C_3 \approx 265$ K.

A great amount of work has been done in this field, often leading to very complicated equations. Close examination of this kind of theories, however, reveals that they incorporate a major incorrectness, resulting from over-idealised assumptions and invalid generalisations, as Binsbergen (1970) has shown. The only certain fact is that the work factor has the general form:

$$\frac{W^*}{k_B T} \approx \frac{C}{T} \frac{T_m}{T_m - T} \quad (19.22)$$

and that C is a characteristic constant for every polymer that contains the ratio: surface energy of the nucleus/lattice energy of the crystal. For a number of polymers investigated the average value is $C \approx 265$ K.

Hoffman supposed that E_D was not a constant, but that the diffusive transport in a melt could be described by a WLF function, in the same way as visco-elastic deformations in a glassy polymer melt *near* T_g may be described by it.

He therefore posed:

$$\frac{E_D}{RT} \approx \frac{C_1}{R(C_2 + T - T_g)}$$

where $C_1 \approx 17.2$ kJ/mol (or $C_1/R = 2700$ K) and $C_2 \approx 51.6$ K, so that the final expression for the growth rate becomes:

$$v \approx 10^7 \exp\left[-\frac{C_1}{R(C_2 + T - T_g)}\right] \exp\left[-\frac{C_3 T_m}{T(T_m - T)}\right] \text{ nm/s} \quad (19.23)$$

This equation has been widely used although the validity of applying the WLF equation to spherulitic growth rate is merely a repetitive assertion (Hoffman et al., 1959; Hoffman and Weeks, 1962), not involving any direct proof of substantiation, as Mandelkern has stated.

Mandelkern et al. (1968) have *proved that the WLF formulation*, which has had an outstanding success in explaining the segmental mobility and flow properties of completely amorphous polymers, is *not applicable to the transport process involved in the growth of spherulites in melts of semi-crystalline polymers*. Rather, a temperature-independent energy of activation, specific to a given polymer and dependent on its glass temperature, suffices to explain the experimental data now available. Mandelkern’s equation reads:

$$\frac{v}{v_o} = \exp\left(-\frac{E_D}{RT}\right) \exp\left[-\frac{C_3 T_m^o}{T(T_m^o - T)}\right] \quad (19.24)$$

where v_o = a universal constant for semi-crystalline polymers: $v_o \approx 10^{12}$ nm/s; E_D = an activation energy for transport (J/mol); T_m^o = an “effective” melting point (K). Generally T_m^o is in the neighbourhood of the crystalline melting temperature as given in the literature, although it may show deviations of more than 10 °C; $C_3 = 265$ K.

In the undercooled melt far from T_g , E_D is constant for a given polymer. Mandelkern determined activation energies for a series of polymers and found that E_D for different polymers increases monotonically with T_g , in first approximation. Table 19.4 gives a survey of the data. Mandelkern stated that E_D increases “monotonically” with T_g . This correlation

TABLE 19.4 Survey of Mandelkern's data on crystallisation

Polymer	T_m° (K)	T_m (K)	E_D (kJ/mol)	T_g (K)	T_g/T_m
Polyethylene	419	414	29.3	195	0.47
Polypropylene	438	456	50.2	264	0.58
Polybutene (isot.)	407	415	44.4	249	0.60
Polystyrene (isot.)	527	513	84.6	373	0.72
Poly(chlorotrifluoroethylene)	499	491	59.4	325	0.67
Polyoxymethylene	456	456	41.0	191	0.42
Poly(ethylene oxide)	347	339	23.0	206	0.61
Poly(tetramethyleneoxide)	462	453	56.1	193	0.42
Poly(propylene oxide)	354	348	40.6	201	0.57
Poly(decamethylene sebacate)	356	358	12.6	—	—
Poly(decamethylene terephthalate)	418	411	46.5	268	0.65
Nylon 6	505	502	56.5	330	0.65
Nylon 5,6	541	531	61.1	318	0.62
Nylon 6,6	553	540	64.5	330	0.61
Nylon 9,6	529	515	56.9	—	—
Nylon 6,10	516	499	53.6	323	0.65

Conversion factor: 1 kJ/mol = 0.24 kcal/mol.

shows much scatter, however. Van Krevelen (1975) found that the following expression is a good approximation of Mandelkern's data:

$$\frac{E_D}{R} \approx \frac{5.3T_m^2}{T_m - T_g} \quad (19.25)$$

The present author found that the expression

$$\frac{E_D}{R} = 23T_g \quad (19.25a)$$

is also a good approximation of Mandelkern's data (both have a correlation coefficient equal to 0.989). Fig. 19.5 shows these functions, together with the experimental data.

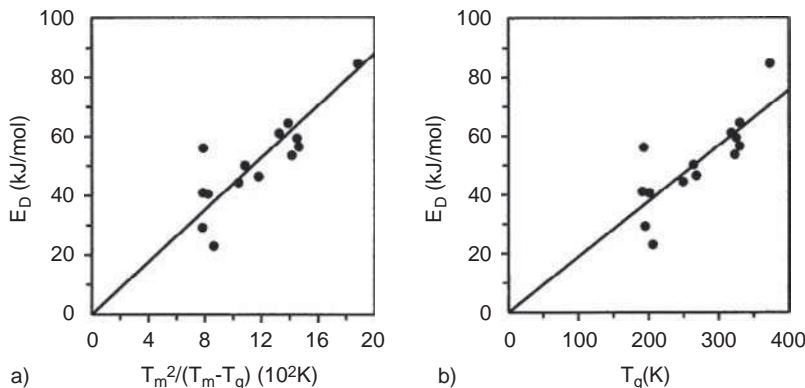


FIG. 19.5 Correlation for the activation energy for transport; (A) according to Van Krevelen (1975); (B) according to Te Nijenhuis.

19.2.3.2. A semi-empirical expression for the growth rate

Substitution of Eq. (19.25) into Eq. (19.24) gives:

$$\ln \frac{v}{v_o} \approx -\frac{T_m}{T} \left(\frac{5.3T_m}{T_m - T_g} + \frac{265}{T_m - T} \right) \quad \text{or} \quad \log \frac{v}{v_o} \approx -\frac{T_m}{T} \left(\frac{2.3T_m}{T_m - T_g} + \frac{115}{T_m - T} \right)$$

where $v_o \approx 10^{12} \text{ nm/s}$

(19.26)

whereas substitution of Eq. (19.25a) into Eq. (19.24) gives:

$$\ln \frac{v}{v_o} \approx -\frac{T_m}{T} \left(\frac{23T_g}{T_m} + \frac{265}{T_m - T} \right) \quad \text{or} \quad \log \frac{v}{v_o} \approx -\frac{T_m}{T} \left(\frac{10T_g}{T_m} + \frac{115}{T_m - T} \right)$$

where $v_o \approx 10^{12} \text{ nm/s}$

(19.26a)

Steiner et al. (1966), Magill (1967) and Van Antwerpen and Van Krevelen (1972) found that at low to moderate molecular weights the value of v_o is dependent on the molecular weight according to an equation of the following form:

$$v_o = a + b/M_n$$

In order to obtain a universal correlation for the linear growth rate in the full temperature region between T_g and T_m written in dimensionless variables, we introduce the variables

$$\xi = T_m/T \quad \text{and} \quad \delta = T_g/T_m$$

After substitution of these variables in Eqs. (19.26) or (19.26a) and (19.23), using $C_1/R = 2700$, $C_2 = 51.6$ and $C_3 = 265$, and some rearrangement, we obtain:

for $T \geq T_k$, Mandelkern type

$$\text{From Eq.(19.16)} : \log v = \log v_o - \frac{2.3\xi}{1-\delta} - \frac{115}{T_m} \frac{\xi^2}{\xi - 1} \quad (19.27)$$

or

$$\text{From Eq.(19.16a)} : \log v = \log v_o - 10\xi\delta - \frac{115}{T_m} \frac{\xi^2}{\xi - 1} \quad (19.27a)$$

for $T \ll T_k$, Hoffman type

$$\text{From Eq.(19.13)} : \log v = \log v_o - \frac{895\xi}{51.6\xi + T_m(1-\delta\xi)} - \frac{115}{T_m} \frac{\xi^2}{\xi - 1} \quad (19.28)$$

So for the lower temperature region a Hoffman-type equation, and for the higher temperature region a modified Mandelkern-type equation is recommended.

Fig. 19.6 presents these equations in a graphical form. For $T > T_k$ Eqs. (19.26) and (19.26a) can be used, as long as $\delta = T_g/T_m$ lies in between 0.4 and 0.75. In this region the

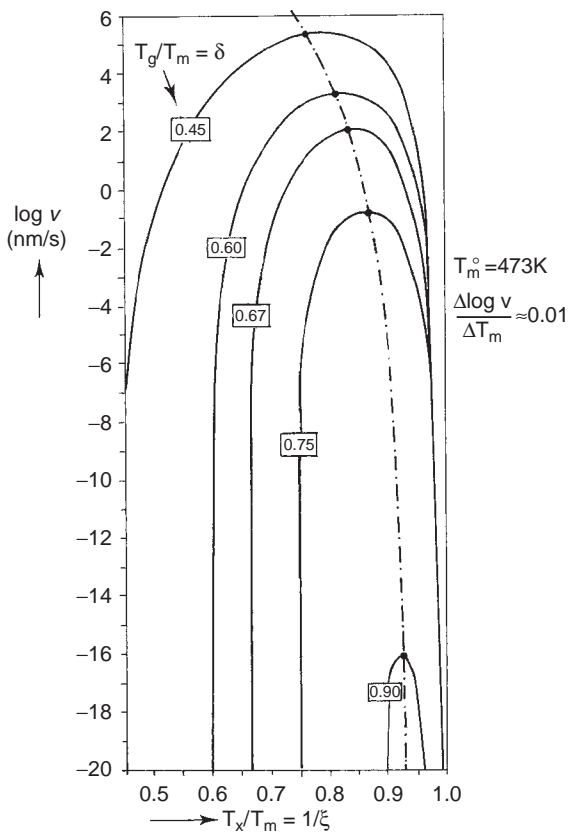


FIG. 19.6 Master curve of the rate of growth of spherulites as a function of the dimensionless parameters T_x/T_m and T_g/T_m (Van Krevelen, 1978).

values of $10 \delta \xi$ and $\xi/(1-\delta)$ are approximately equal (difference less than 12%). In fact for the polymers mentioned in Table 19.4 δ lies in between 0.42 and 0.72. In Fig. 19.6 for $T \ll T_k$ Eq. (19.28) was used. For the region $T < T_k$ the curves were drawn in such a way that a smooth curve was obtained. As a fixed standard value for T_m necessary to represent the equations in a two-dimensional graph, the value 473 K was chosen. For every 10 °C that T_m is higher or lower, $\log v$ will be about 0.1 higher or lower than given in the graph.

Fig. 19.6 enables us to predict the value of v under experimental conditions for all "normal" polymers. Eqs. (19.27) and (19.28) and Fig. 19.6 lead to some useful conclusions which are graphically represented in Fig. 19.7:

- The maximum rate of spherulite growth is a straightforward function of the ratio T_g/T_m . For the "average polymer" with T_g/T_m between 0.6 and 0.675 the maximum rate of growth is between 10^2 and 10^3 nm/s.
- The temperature of maximum crystallisation rate is also determined by T_g/T_m . For the average polymer, $T_{\max} = T_k$ equals $0.83 T_m$ in every good agreement with calculations by Okui (1987).
- The attainable degree of crystallisation depends to a great extent on the maximum rate of crystallisation and is therefore also determined by T_g/T_m . The average crystallisable polymer is also to attain a crystallinity between 0.45 and 0.6; only the very regular polymers with smooth chains without side groups or side chains, such as polymethylene

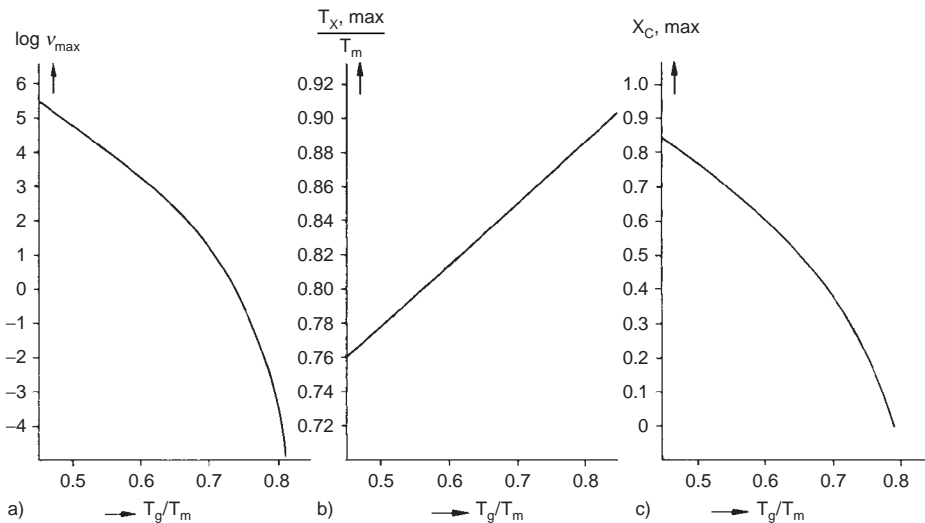


FIG. 19.7 The three main parameters of spherulitic crystallisation.

and poly(methylene oxide) are able to attain a substantially higher crystallinity. According to Bicerano (2002) $x_{c,\max}$ correlates with T_g/T_m . It generally increases with increasing T_m/T_g or decreasing T_g/T_m . An equation that describes this behaviour, but only in the T_g/T_m range from 0.35 to 0.79 is

$$x_{c,\max} = -13.475(T_g/T_m)^3 + 19.664(T_g/T_m)^2 - 10.898T_g/T_m + 2.987 \quad (19.29)$$

This is illustrated in Fig. 19.8. He explains the lower and upper limit in the following way. In practice, T_g/T_m is not less than 0.4 for any known polymer for which melt crystallisation data are currently available, so that the lower limit (0.35) of the validity of Eq. (19.26a) has not been reached. The upper limit (0.79) suggests that if T_m is not sufficiently large $x_{c,\max}$ will be zero. The reason is that the polymer will not have enough driving force for crystallisation and it will be amorphous, at least over the relatively short time periods used in typical crystallisation kinetic studies.

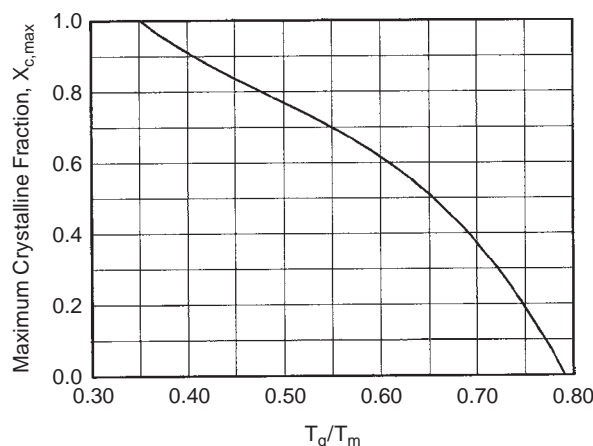


FIG. 19.8 Relationship between maximum crystalline fraction, $x_{c,\max}$, under isothermal quiescent crystallisation and the ratio T_g/T_m . According to Eq. (19.29); Bicerano, 2002.

As a further illustration, Table 19.5 shows for a number of well-investigated polymers (mainly the same ones as used by Mandelkern), the comparison between experimental and predicted values of the three main crystallisation parameters: v_{\max} , T_{\max} and $x_{c,\max}$.

Example 19.1

Estimate for isotactic polystyrene:

- The temperature of maximum crystallisation velocity
- The linear growth rate at this temperature
- The probable (maximum) degree of crystallinity

Solution

- Two methods of estimation are available: Eq. (19.18) and Fig. 19.7B.

Using equation (19.18) and putting $T_g = 373$ K and $T_m = 513$ K we get:

$$T_k = 0.5(513 + 373) = 443 \text{ K}$$

Using Fig. 19.7B with the value $T_g/T_m = 373/513 = 0.725$, we find $T_{x,\max}/T_m = 0.86$, so $T_{x,\max} = 0.86 \times 513 = 441$ K.

Both values are in good agreement with the experimental value found by Boon (1966): $T_{\max} = 449$ K

- Applying Eq. (19.26), with $T = T_{x,\max} (= T_k) = (\text{av.}) 442$ K, we find (with $\log v_o = 12$):

$$\log v_{\max} = 12 - \frac{2.3 \times 513}{442} \left(\frac{513}{513 - 373} + \frac{50}{513 - 442} \right) = 12 - 11.7 = 0.3$$

We can also apply Fig. 19.7A and find for $T_g/T_m = 0.727$: $\log v_{\max} = 0.5$.

The average value is $\log v_{\max} = 0.4$; so $v = 2.5 \text{ nm/s}$. This is in fair agreement with the experimental value of Boon, viz. 4.2 nm/s .

- Applying Fig. 19.7C, we find $x_{c,\max} = 0.3$, in very good agreement with Boon's experimental value, 0.34

Using Bicerano's Eq. (19.29) with $T_g/T_m = 0.727$ we find $x_{c,\max} = 0.28$, which also follows from Fig. 19.8; it is in fair agreement with Boon's results.

19.2.3.3. Practical conclusions

19.2.3.3.1. Influencing the spherulitic crystallisation From Eq. (19.2) and Table 19.3 the following expression for the overall rate of three-dimensional crystallisation can be derived:

$$t_{1/2}^{-1} = 1.8N^{1/3}v \quad (19.30)$$

Both N and v are important.

We have seen that N is mainly determined by the thermal programme. Just undercooling a melt gives N -values of about $3 \times 10^6 \text{ cm}^{-3}$. Quenching to room temperature and heating up gives values of N of the order of $3 \times 10^{11} \text{ cm}^{-3}$. For $N^{1/3}$ this gives a range from $1.5 \times 10^4 \text{ m}^{-1}$ to $7 \times 10^5 \text{ m}^{-1}$.

TABLE 19.5 Comparison of experimental and estimated (predicted) data in polymer crystallisation

Polymer	T_m (K)	T_g/T_m (-)	$T_{x,max}/T_m$ (-)	$T_{x,max} (=T_k)$ (K)		$\log v_{max}$ (nm/s)		$x_{c,max}$ (-)	
	Exp.	Exp.	Pred.	Exp.	Pred.	Exp.	Pred.	Exp.	Pred.
Polyethylene (linear)	414	0.475	0.77	—	319	4.92	5.1	0.80	0.80
Polypropene (isot.)	445	0.575	0.805	—	350	2.5	3.6	0.63	0.66
Poly(1-butene) (isot.)	380	0.63	0.825	—	318	2.2	2.9	0.50	0.55
Polystyrene (isot.)	513	0.725	0.86	449	442	0.6	0.8	0.34	0.32
Poly(chlorotrifluoro-ethylene)	500	0.62	0.834	—	418	2.65	2.9	0.70	0.57
Polyisoprene (cis)	300	0.67	0.84	248	251	—	1.9	0.45	0.47
Poly(methylene oxide)	400	0.54	0.79	—	318	3.5	4.2	—	0.72
Poly(ethylene oxide)	340	0.665	0.84	—	286	—	2.1	—	0.47
Poly(propylene oxide)	340	0.62	0.83	290	282	2.9	2.9	—	0.53
Polycarbonate	545	0.745	0.87	—	482	-0.8	-0.7	0.25	0.21
Poly(ethylene terephthalate)	548	0.63	0.835	459	466	2.1	2.8	0.5	0.54
Nylon 66	545	0.59	0.81	420	440	4.3	3.5	0.70	0.63
Nylon 6	496	0.675	0.84	413	418	3.5	1.9	0.5	0.45

The rate of growth is more important than the number of nuclei. According to Eqs. (19.27) and (19.28) it depends on:

- The ratio $T/T_m (=1/\xi)$
- The ratio $T_g/T_m (=δ)$
- The absolute value of T_m
- The absolute value of v_o

The growth rate shows a maximum at $T_k \approx 0.825 T_m$. This therefore is the “optimum temperature” for a rapid crystallisation. T_g/T_m and T_m are determined by the constitution of the polymer and cannot be influenced by process parameters. The parameter v_o may be influenced by the average molecular weight and by the addition of nucleation agents. So the practical way to influence the “free” crystallisation of polymers is by choosing:

- The right temperature programme for an optimal nucleation (c.q. quenching and reheating)
- The optimum crystallisation temperature for a rapid growth rate
- An optimal nucleation agent in order to increase the temperature-independent factor

19.2.3.3.2. Properties of semi-crystalline spherulitic polymers Since plastic materials are brittle when they consist of large spherulites, it is a great advantage if the spherulites are as small as possible. For this reason N must be large, and therefore undercooling by quenching must be deep and fast. The optimum conditions are obtained if quenching is followed by reheating to T_k with thorough crystallisation. In processes like vacuum-forming this can easily be done. Quantitative data on the correlation between spherulite size and (mechanical) properties are scarce. Sharpless (1966) mentions some data on the influence on the yield stress in nylon 66. They are given in Table 19.6.

19.2.4. Aspects of structure formation in processing

This subject has been treated extensively during the last 25 years at the Johannes Kepler University in Linz (Austria). More recent reviews on this subject were published by Eder et al. (1997), Janeschitz-Kriegl Eder et al. (2005) and Janeschitz-Krlegl (2007). A monograph of the latter author is in preparation (2008).

In the previous edition of “Properties of Polymers” (1990) one already finds a key picture to this research efforts. It describes the progress of crystallisation in a hot polymer melt after being brought into contact with a cold wall of invariable temperature (Fig. 19.9). The uppermost curve gives the course of the boundary between the still liquid and the

TABLE 19.6 Yield points of nylon 66

Spherulite size (d) (μ)	Yield stress P_Y	
	10^3 p.s.i	10^6 (N/m ²)
50	10.25	72
10	11.8	83
5	12.7	89
3	14.7	98

In equation: $P_y/P_{y,max} = 1 - 0.18 \log (2.86\mu)$

(19.31)

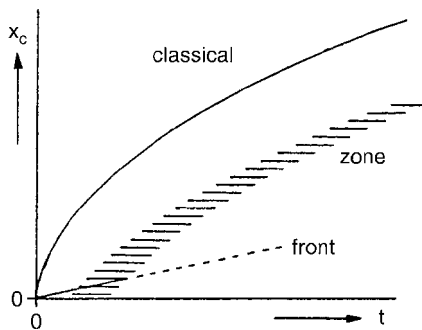


FIG. 19.9 Schematic presentation of the progress of crystallisation into a semi-infinite body quenched at zero time at the plane $x = 0$: x_c = distance at which crystallisation occurs, t = time.

solidified material according to the well-known Stefan theory (1889), which is valid for an infinite speed of crystallisation. However, semi-crystalline polymers crystallise rather slowly. Near the wall one finds a growth front, which moves according to the speed of the surface crystallisation at the wall temperature. After some time this growth front is superseded by a diffuse zone, for which nuclei are responsible, which come up in the interior of the fluid as this fluid is progressively undercooled. As the temporary temperatures always increase with the distance from the wall, the number density of nuclei decreases with this distance. As a result the size of crystalline entities (mostly spherulites) increases with this distance. They get more space for their growth. And the outward shape of the zone can only be calculated, if the number density of nuclei is known as a function of temperature. For some polypropylenes this number density could be determined as a function of temperature. As explained below, these nuclei are of the athermal type, so that their number density does not depend on time. In a temperature range from 130 to 85 °C these number densities are shown on the left side of Fig. 19.10, which is taken from a paper by Janeschitz-Kriegl et al. (2003). In the course of this investigation the fluid samples were rapidly quenched to a series of decreasing temperatures. After the termination of the quench the spherulites grow at a slow pace. Finally they were counted in cross-sections. Fortunately, there is no sporadic nucleation in quiescent polymer melts, so that all spherulites reach the same size, as they start growing simultaneously. The origin of the nuclei is based on local alignments of varying quality. This fact explains, why they are athermal. The lower the orderliness of these alignments is, the lower is the temperature of activation. Interestingly enough, in i-PP the said number density increases by about five decades, when the temperature is changed from 130 to 85 °C. A similar result has already been found earlier by Boon et al. (1968) for a sample of isotactic polystyrene, as shown in Fig. 19.3.

In addition, Fig. 19.10 shows another result, which is surprising. In fact, Fig. 19.10 is a three dimensional plot. The temperature axis is on the left side. The equilibrium melting point of i-PP is at 212 °C (Marrand et al., 1998). For its incorporation in the graph the length of the temperature axis should have been doubled. One can guess, how low the number density of nuclei is closer to the equilibrium melting point. On the right side one finds the axis giving the specific mechanical work, as applied to the sample during short term shearing or stretching. One notices that in a temperature range between 140 and 160 °C these flow treatments cause increases of the number density of nuclei, which are comparable with the one caused by quenches to low temperatures. (For the action of flow see also Tribout et al. (1996).)

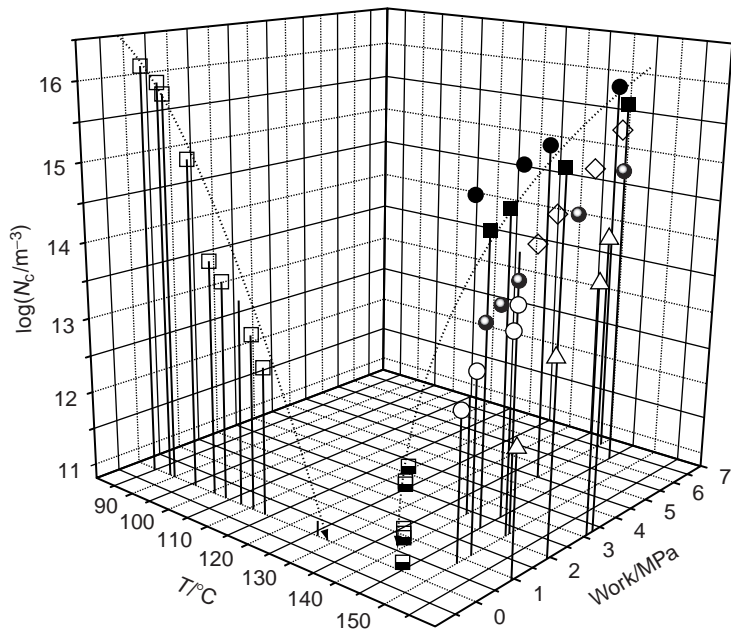


FIG. 19.10 Three-dimensional plot of the logarithm of the number density of nuclei vs. crystallisation temperature and specific mechanical work, as applied to a sample of industrial polypropylene. From Janeschitz-Kriegl et al. (2003). Courtesy Springer Verlag.

The influence of flow can be explained, if one assumes that nuclei, which are dormant in a quiescent melt, are transformed by the action of this flow. This has been argued by Janeschitz-Kriegl and Ratajski (2005). In fact, the dormant nuclei must have the shape of fringe micelles, which are oriented and “ironed” by the flow. It is also interesting to note that those transformed nuclei already have a lengthy appearance. Thread-like precursors (“shishs”), which cause oriented structures (shish-kebabs), only appear as soon as the length of the said nuclei surpasses the mutual distance between their centres. But this distance decreases rapidly with increasing specific work (increasing shearing time).

At this point it should be mentioned that supportive papers on the origin and on the remarkable stability of the formed (lengthy) athermal nuclei have been published by the research groups under the leaderships of Julia A. Kornfield (2006) in Pasadena and of Giancarlo Alfonso (2005) in Genova. Finally, another result of the research group at Linz University should be presented. For this purpose Fig. 19.11 is reproduced. This figure should advance an understanding of the contrast between the behaviour of metals and of glass forming minerals. In many respects this figure should be self-explanatory. Only a few hints would suffice. On top one finds a time scale giving the range of times τ_{cr} which are required for a solidification by crystallisation at the proper temperatures. This scale spans over so many decades that the other important time scale for the thermal equilibration time τ_{th} (the “cooling time”), becomes almost irrelevant. In fact, this latter scale spans only over four decades. One notices that the behaviour of crystallising polymers lies between that of metals and glass forming minerals. So far this fact has not been noticed. From the point of view of solidification HDPE behaves almost like a metal, whereas PET behaves (in the absence of flow) almost like a glass forming mineral. Surprisingly, in spite of the high thermal conductivity of metals, their enormous crystallisation speed wins the

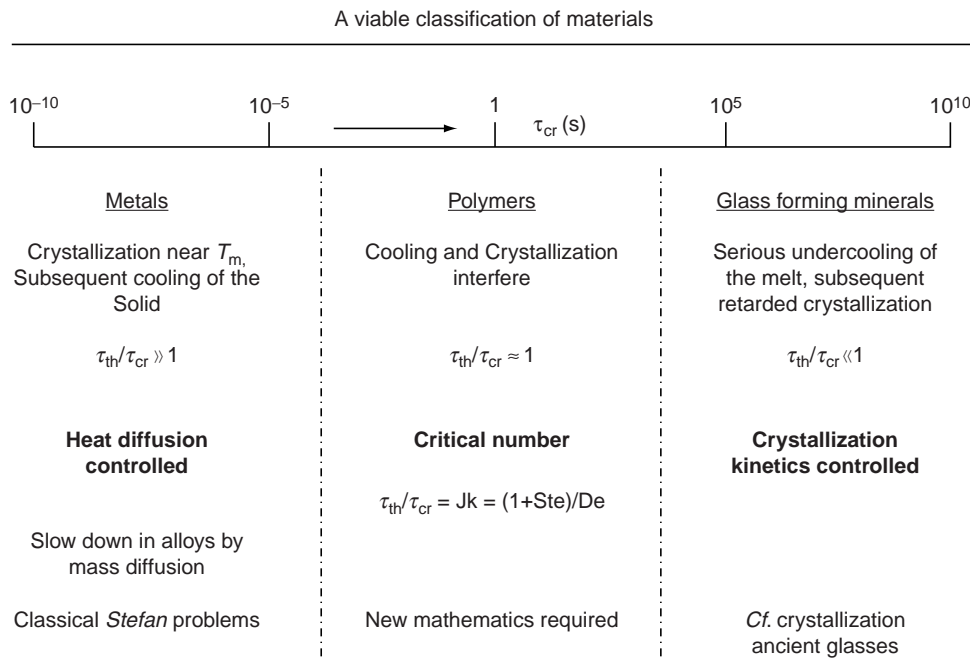


FIG. 19.11 A viable classification of materials. After Janeschitz-Kriegl et al. (2005).

game for the slower, i.e. the heat diffusion controlled processes. The dimensionless numbers in this figure are Ste , the well-known Stefan number, (Eq. (3.8)) and $\text{De} = \tau_{\text{cr}} a / d^2$, which is a third way of defining a Deborah number, with a being the heat diffusivity and d the thickness of the considered slab. (Other), similar definitions of De are found in Chaps. 2 and 3 and in Eq. (18.60)).

Fig. 19.11 shows that the treatment of the solidification of polymers is the most demanding undertaking. The required theoretical basis has been developed by Schneider et al. (1988) and developed further by Eder (see the above reviews). With the aid of the latter author a mathematical expression could be found for the process classification number Jk , i.e. the *Janeschitz-Kriegl number*, as has been called by Astarita (1987) The said mathematical expression reads

$$\text{Jk} = \frac{\tau_{\text{th}}}{\tau_{\text{cr}}} = \frac{1 + \text{Ste}}{\text{De}} = \frac{(1 + \text{Ste})d^2}{a\tau_{\text{cr}}} = \frac{(1 + \text{Ste})d^2}{a} \times 1.63v_{\text{max}}N_{\text{max}}^{1/3} \quad (19.32)$$

where τ_{th} = time needed for thermal equilibration = $1 + \text{Ste}$; τ_{cr} = time needed by the crystallisation process = $[1.63v_{\text{max}}N_{\text{max}}^{1/3}]^{-1}$; $\text{Ste} = \Delta H_{\text{cr}}/[C_p(T_f - T_s)]$; ΔH_{cr} = latent heat corresponding with the final degree of crystallinity; C_p = averaged specific heat; T_f = starting temperature of the fluid; T_s = final temperature of the solid; d = thickness of the sample; a = heat diffusivity of the sample, as averaged over the states of aggregation; v_{max} = maximum growth speed (see Fig. 19.4); N_{max} = number density of nuclei at the temperature of the maximum growth speed.

It goes without saying that also the growth speeds as functions of temperature were determined in Linz for a number of the rather fast crystallising industrial polymers (see the mentioned reviews.)

19.3. INDUCED CRYSTALLISATION OF FLEXIBLE POLYMERIC MOLECULES BY PRESSURE AND STRESS

In practice, many fabrication processes take place under non-isothermal, non-quiescent and high-pressure conditions. Mechanical deformation and pressure can enhance the crystallisation as well as the crystal morphology, by aligning the polymer chains. This leads to pressure-induced crystallisation and to flow-induced or stress-induced crystallisation, which in fact is the basis for fibre melt-spinning (see Sect. 19.4.1)

19.3.1. Pressure-induced crystallisation

Important investigations in this field have been made by Wunderlich (1964/1972) and Basset (1973/1974). The effect of high pressure on the crystallisation process is threefold:

1. A high pressure enhances the formation of crystal modifications with packing that are as dense as possible. Since extended chains have denser packing than folded chains, an increase of pressure is favourable for chain extension.
2. A high pressure raises the temperature of melting. For large pressure variations the change in the melting temperature is given by the Simon equation

$$P - P^{\circ} = a \left[\left(\frac{T_m}{T_m^{\circ}} \right)^c - 1 \right] \quad (19.33)$$

where the symbol \circ indicates the standard condition (atmospheric pressure).

For polyethylene the values of the constants in this formula are: $T_m^{\circ} = 409\text{ K}(136^\circ\text{C})$, $a \approx 3\text{ kbar}$, $c \approx 4.5$. Fig. 19.12 is a graphical representation (T_m in $^\circ\text{C}$) of this equation, which is fully confirmed by the experiments of Osugi and Hara (1966). It is obvious that the *melting region* may be raised by about $100\text{ }^\circ\text{C}$ at pressures of about 5 kbar or $20\text{ }^\circ\text{C/kbar}$. For the pressure dependence of T_g of aliphatic polymers was also found approximately $20\text{ }^\circ\text{C/kbar}$ (see Chap. 6).

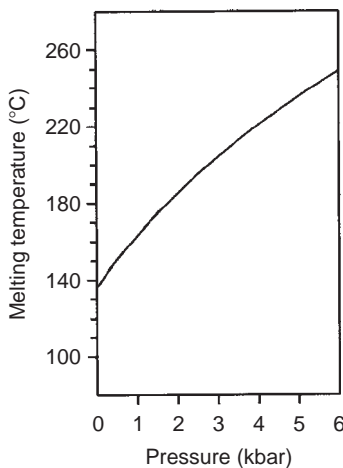


FIG. 19.12 Melting temperature of polyethylene as a function of pressure according to Osugi and Hara (1966).

3. It is a well-known fact that the *length of folds* in crystal lamellae increases with temperature. Since the melting temperature (=solidification temperature) goes up as a result of the high pressure, also the fold length will increase (with the full molecular chain length as the limit).

Of course the three effects are interrelated. From theoretical concepts as well as from experimental data it is obvious that crystallisation with extended chains over a length of, say $> 10^{-7}$ m only takes place if the annealing temperature is in the melting region of extended chain crystals.

Pressure crystallisation is a rather slow process; most authors report "annealing times" of several hours or even days.

There has been much confusion about the mechanism of formation of extended chains. The most probable conception is that formation direct from the melt is the dominant mechanism; unfolding and subsequent lamella-thickening may also take place, especially at lower temperatures and long annealing times.

Some authors have reported that fractionation of chain molecules according to their chain length occurs during pressure crystallisation. Crystals with fully extended molecules of uniform molecular mass (or about 10,000 g/mol) have been observed.

19.3.2. Structure and high-pressure crystallisation

Most of the pressure crystallisation research has been done on polyethylene. Pressures of 3 kbar or higher are required to obtain crystallite thicknesses of 10^{-7} m. Some other polymers have a much stronger tendency towards extended chain formation. Poly(chloro trifluoro)ethylene shows this effect at about 1 kbar; poly(tetrafluoro)ethene already at about 0.3 kbar.

There exists a relation between the tendency towards extended chain crystallisation and the melting point dependence on pressure.

Since

$$\frac{dT_m}{dP} = T_m^o \frac{\Delta V_m}{\Delta H_m} = \kappa \quad (19.34)$$

a close relationship may be expected between κ and the minimum pressure required to form extended chains $> 10^{-7}$ m in the crystal. From Table 19.7 it follows that this is the case indeed.

$$P_{(>100\text{nm})}^{\min} \approx 60\kappa^{-1} \quad (19.35)$$

The mechanical properties of pressure-crystallised polymers are disappointing, indeed they are very poor! The main disadvantage of pressure crystallisation is that it results in a quasi-isotropic brittle product, a mosaic of randomly oriented crystallites without much interconnection.

Wunderlich (1964) reports that his polyethylene materials were so brittle that they could be easily powdered in a mortar.

TABLE 19.7 Correlation between κ and $P_{(>100\text{nm})}^{\min}$

Polymer	κ (K/kbar)	$P_{(>100\text{nm})}^{\min}$ (kbar)
PE	25	~3
Nylon	15–40	~2?
PCTFE	65	~1
PTFE	140	~0.3

19.4. CRYSTALLISATION PHENOMENA IN UNIAXIAL DRAWING: FIBRE SPINNING

19.4.1. Melt spinning, stress-induced crystallisation

Stress-induced crystallisation is accomplished by spinning processes, followed by drawing of the spun elements, just by drawing of the spun filaments or by spinning with high-speed winding,

19.4.1.1. Axially oriented crystallisation by “drawing” of spun filaments

If an isotropic polymer is subjected to an imposed external stress at a suitable temperature (usually just above the glass-transition temperature) it undergoes a structural rearrangement called *orientation*.

In semi-crystalline polymers this rearrangement is so drastic that it may be called stress-induced crystallisation or recrystallisation.

Uniaxial orientation is of the utmost importance in the production of man-made fibres, since it provides the required mechanical properties and the necessary dimensional stability. The drawing process is usually carried out in two steps, for instance by guiding the yarns over three pairs of rolls. Pair 1 should be approximately at the glass transition temperature to initiate necking (abrupt thinning leading to a strong increase of orientation and some crystallisation). Pair 2 is at intermediate speed and temperature and pair 3 is held just below the melting temperature. The overall draw ratio depends on the pre-orientation during spinning and may be up to 6.

By rapid cooling-down of the filament – under stress – the obtained orientation is frozen in, combined with a very fast fibrillar crystallisation or recrystallisation.

We have considered the consequences of this phenomenon on the mechanicals properties already in Sect. 13.6.

19.4.1.1.1. Properties The influence of orientation on the properties is usually studied by investigating a so-called *drawing series*, i.e. a series of yarns drawn with different draw ratios.

Fig. 19.11A,B presents, as an example, data of drawing series of nylon 6 and polyester filaments (Van der Meer, 1970). The additional data for the polyester (polyethylene terephthalate) are given in Table 19.8 by stretching the Young modulus increases by a factor 8 and the tensile strength by a factor 5.5 (Fig. 19.13).

19.4.1.1.2. Morphology Some polymers, like PETP, are spun in a nearly amorphous state or show a low degree of crystallinity. In other polymers, such as nylon, the undrawn material is already semi-crystalline. In the latter case the impact of extension energy must be sufficient to (partly) “melt” the folded chain blocks (lamellae); in all cases non-oriented material has to be converted into oriented crystalline material. In order to obtain high-tenacity yarns, the draw ratio must be high enough to transform a fraction of the chains in more or less extended state.

An interesting model of the possible structure of semi-crystalline yarns is that given by Prevorsek and Kwon (1976) and shown in Fig. 19.14.

It consists of fibrils with a definite long period and thickness, consisting of crystallites characterised by a height of about 5 nm and a thickness of the order of 6 nm. Prevorsek supposes that along the fibrils a number of extended “tie molecules” are present, this number being responsible for the strength; at higher draw ratios the fraction of taut tie molecules increases.

TABLE 19.8 Stretch series of poly(ethylene terephthalate) yarns (data from Van der Meer, 1970)

	Draw ratio (λ)					
	1	2.77	3.08	3.56	4.09	4.49
Density (ρ) (20 °C) (g/cm ³)	1.3383	1.3694	1.3775	1.3804	1.3813	1.3841
Crystallinity (x_c) (%)	3	22	37	40	41	43
Birefringence (Δn) (20 °C)	0.0068	0.1061	0.1126	0.1288	0.1368	0.1420
Tensile strength (σ_{\max}) (cN/tex)	11.8	23.5	32.1	43.0	51.6	64.5
Elongation at break (%)	(450)	55	39	27	11.5	7.3
Young modulus (GPa)						
E' at 9370 Hz	(2.7)	8.3	12.3	17.4	20.2	22.9
E' at 5 Hz	2.6	7.8	11.5	14.9	18.0	19.9
Loss factor $\tan \delta$	4	0.20	0.165	0.155	0.135	0.12
T_g (dynamic) (°C)	71	72	83	85	90	89
T_d (damping peak) (°C)	84	107	118	124	128	131
ΔT_g (width of $\tan \delta$ -peak at in flection points)	10	39	43	45	50	55

The concept "Tie molecules" was introduced by Peterlin (1973), see Chap. 2. Tie molecules are part of chains or bundles of chains extending from one crystallite (or plate or lamella) to another; in fibres they even constitute the core of the stretched filament. They concentrate and distribute stresses throughout the material and are therefore particularly important for the mechanical properties of semi-crystalline polymers. Small amounts of taut tie molecules may give a tremendous increase in strength and a decrease in brittleness of polymeric materials.

19.4.1.2. Spinning with high-speed winding

In particular, polymers with a moderate rate of crystallisation exhibit a very strong dependence of their physical structure on the rate of extension during spinning, i.e. on the winding speed. Polyethylene terephthalate, PETP, is a good example. At spinning speeds below 35 m/s the yarn as spun is nearly amorphous, whereas when spun at speeds of more than 60 m/s and a winding speed after drawing of about 120 m/s, it contains well-developed crystallites of closely packed molecules. Fig. 19.15 presents the density, the sonic modulus (Young's modulus measured at a frequency of 10 kHz) and the crystallinity as a function of winding speed. These data were obtained by Huisman and Heuvel (1978).

Residence times of the real drawing are extremely short: some milliseconds; compared with the normal half-time of crystallisation ($t_{1/2}$ of the order of 50 s) it is clear that the crystallisation process during spinning with high-speed winding is many decades faster than that in the isotropic melt.

Fig. 19.15D presents the size of the crystallites, as obtained by X-ray analysis, as a function of winding speed.

It is to be expected that (with respect to orientation) not only the winding speed but also the molecular weight, the temperature, the way of cooling and other parameters will influence the crystalline structure.

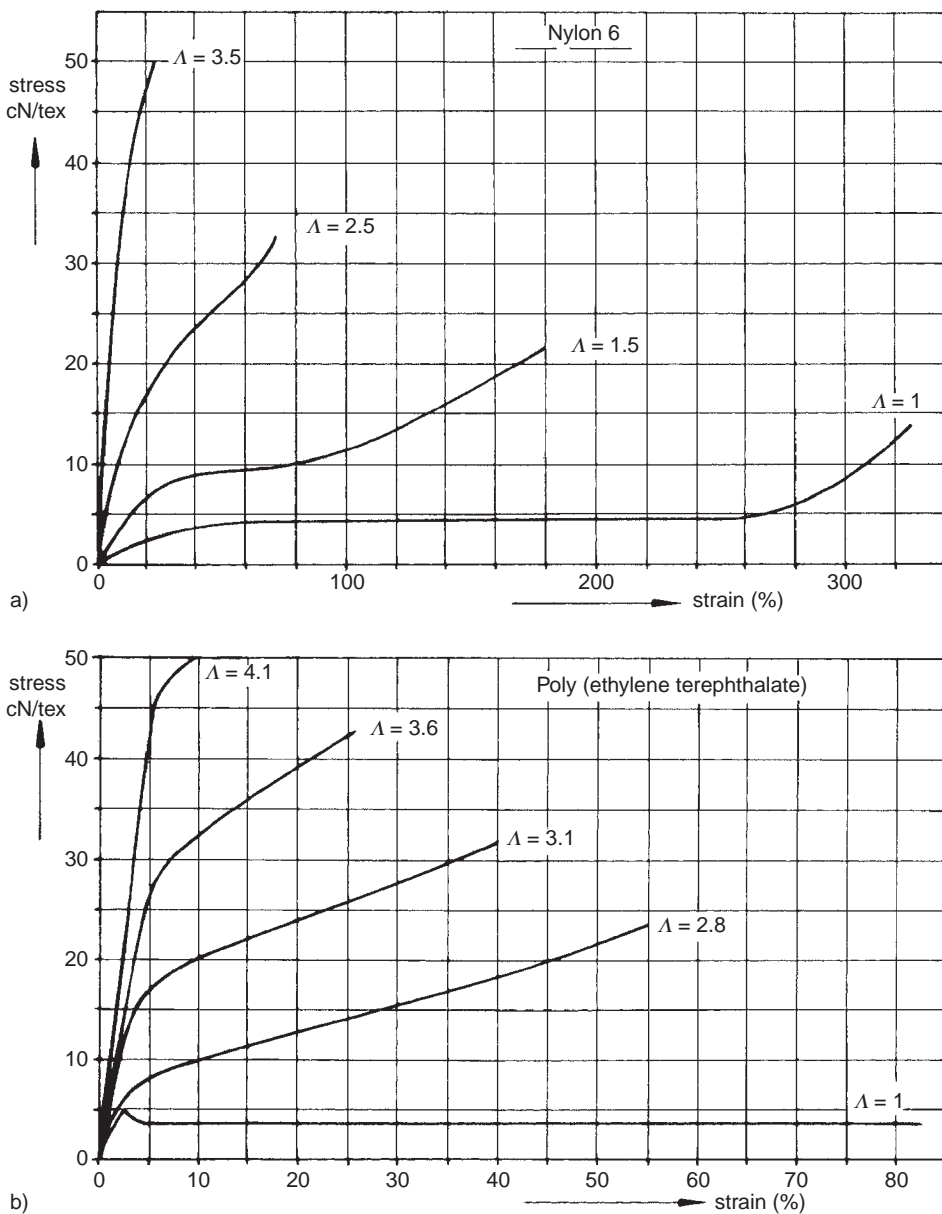


FIG. 19.13 Stress-strain diagram. After Van der Meer (1970).

19.4.2. Gel-spinning

Until the 1970s there was a substantial gap between the theoretical modulus of polymer chains and the practical stiffness achieved in the existing processes. Since then the fibres made by extended chain crystallisation have bridged this gap. Solution spun fibres of high molecular linear polyethylene have been prepared with a Young modulus (at low temperature) of 90% of the theoretical value. Tables 19.9 and 19.10 illustrate the whole extent of elastic moduli in the various materials.

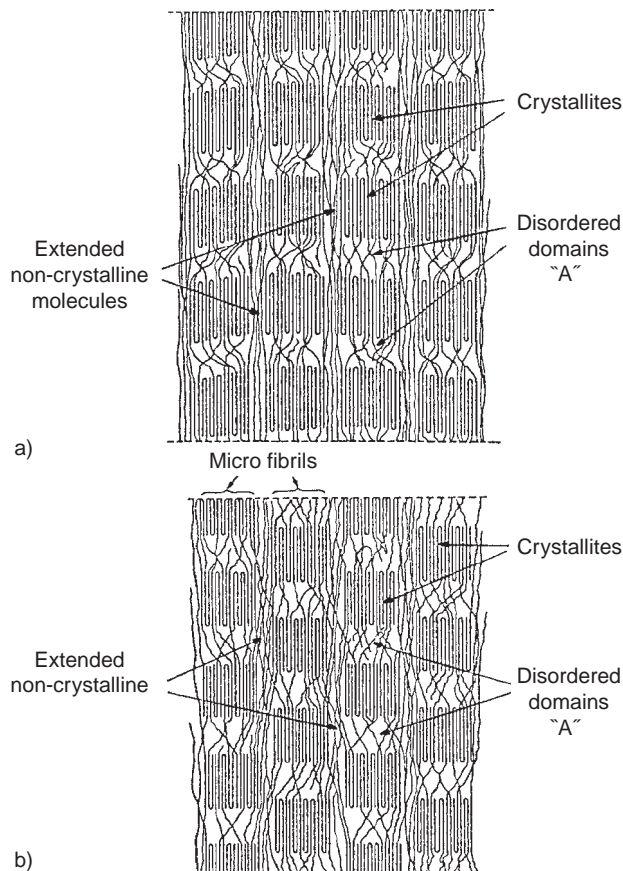


FIG. 19.14 Structure model of (A) nylon fibres; (B) PETP fibres (fibre axis vertical) as suggested by Prevorsek and Kwon (1976).

This development started with an observation of Pennings and Kiel (1965) that, when dilute solutions of polyethylene were cooled under conditions of continuous stirring, very fine fibres were precipitated on the stirrer. These fibres had a remarkable morphology: a fine central core of extended CH₂-chains, with an outer sheath of folded chain material. Electron microscopy revealed a beautiful “shish kebab” structure (see Fig. 19.16). Shish kebabs have also been observed in experiments without any stirring. For example, by washing polyethylene powder with xylene (Jamet and Perret, 1973) and by crystallising nylon 4 from a glycerol/water mixture (Sakaoku et al., 1968).

A further breakthrough was achieved by Zwijnenburg and Pennings in the early 1970s (1973, 1976, 1978, 1979) with the discovery that ultra-high modulus polyethylene fibres could be produced by growth of fibrillar polyethylene crystals, drawn directly out of a very dilute (0.5%) polyethylene solution at high crystallisation temperatures. The technique was to induce extension forces by rotating a cylindrical rotor within a cylindrical stator, with the polyethylene solution in the slit between the two cylinders. The macro-fibre then grew onto an identical seed crystal attached to a thin wire which left the vessel through a small pipe and was then wound continuously at low speeds (20 cm/min) onto

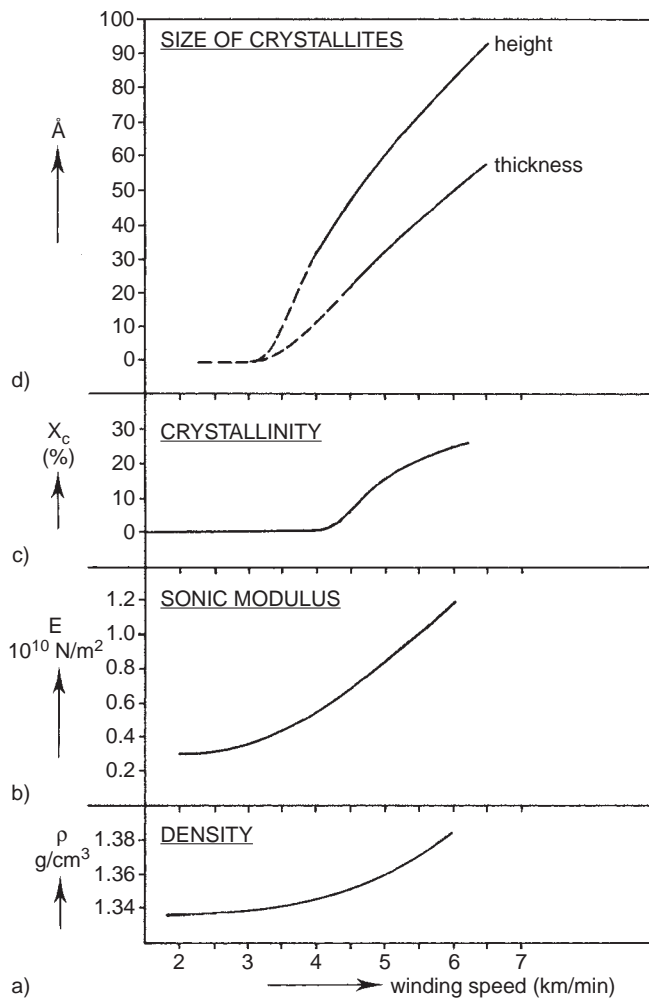


FIG. 19.15 Physical constants of PETP yarns wound at various speeds Data of Huisman and Heuvel (1978).

TABLE 19.9 Elastic moduli of some materials

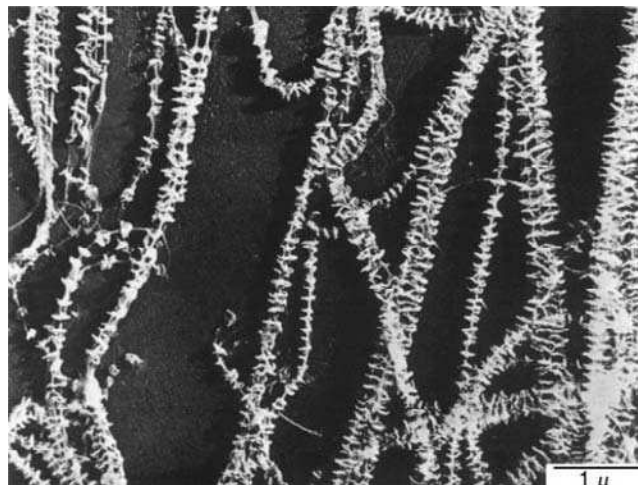
	Class of materials	E-value (GPa)
Polymers	<i>Elastomers</i> (rubbers)	0.001
	<i>Soft plastics</i> (e.g. low density PE)	0.2
	<i>Isotropic hard plastics</i>	
	{ Amorphous	{ Glassy 2.5–3
	{ Semi-crystalline	{ Cross-linked 2.5–5
		{ $T_g < 275$ K 1–3
		{ $T_g > 325$ K 3
	<i>Conventional fibres</i> (nylon, PETP)	5–15 ^a
	“ <i>Extended chain</i> ” fibres	
	{ Extended zig-zag chains	250 ^a
	{ Extended helical chains	ca 50 ^a
Inorganics	<i>Ceramics</i>	30–70
	<i>Glass</i>	60–100
	<i>Steel</i>	200
	<i>Whiskers</i>	1000–2000

^a In direction of orientation.

TABLE 19.10 Modulus and strength of ultradrawn conventional polymers

		Polymer					
		PE (linear)	PP	PMO	PVA	PAN	(Nylon)
Tensile modulus E (GPa)	Theoretical ^a	250	49	53	250	250	173
	Experimental:						
	Gel spun and ultradrawn	130–220	36	35	70	27	Not possible
	Melt/solution spun and drawn	10–20	5–10	–	(10)	5–10	5–15
	Melt/solution crystallised	<2	1.5	–	–	–	1.9
Tensile Strength σ_{\max} (GPa)	Theoretical ^a	25	–	–	(25)	(25)	17
	Experimental:						
	Gel spun and ultradrawn	2.6–3.5	1	1	2.3	1.5	not possible
	Melt/solution spun and drawn	0.5	0.5	–	(1)	0.2	0.9
	Melt/solution crystallised	0.025	0.05	0.065	–	–	0.08

^a See Treloar (1960), Sakurada et al. (1966–70), Britton et al. (1976) and Northolt et al. (1974–86).

**FIG. 19.16** Electron micrograph of polyethylene “shish kebabs”. From Pennings et al. (1970).

a take-up roll. Fibres were obtained directly with a strength of 3.0 GPa and a modulus of 100 GPa. However, due to the low spinning speeds and the very dilute solutions, this was not an attractive industrial process.

The next major development was the “gel-spinning” by Smith and Lemstra (1979), where a “gel fibre” is first produced by spinning a dilute solution of very high molecular weight polyethylene into cold water; after drying this “gel fibre” is drawn in a hot oven at

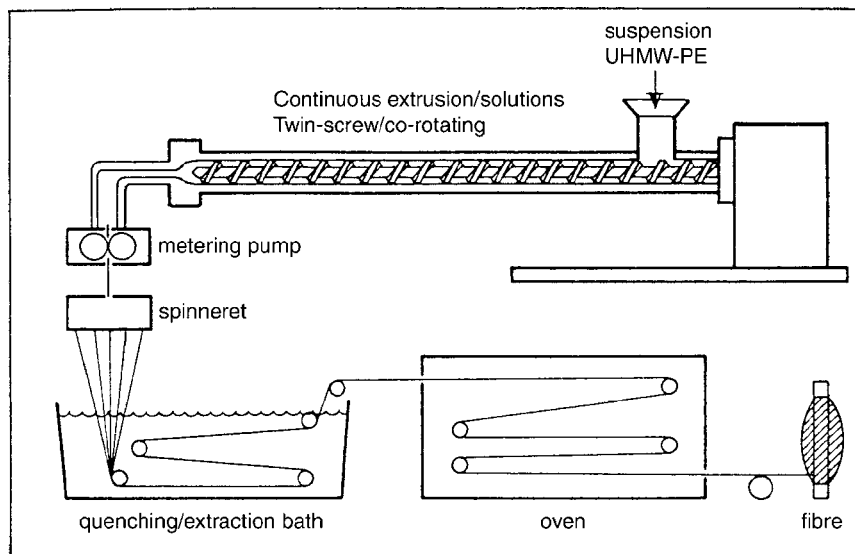


FIG. 19.17 Experimental set-up for the continuous production of HP-PE fibres. After Lemstra et al. (1987).

about 120 °C. Out of this discovery the technical gel-spinning process was born (Fig. 19.17). For successful gel-spinning/ultra-drawing two requirements must be fulfilled:

- The molecular weight must be very high ($M_w > 10^6$).
- The individual molecular coils must be almost dis-entangled, in order to make the subsequent ultradrawing possible (no constraints); the reason is that dis-entangled coils crystallise on quenching into very regular folded-chain clusters (possibly with "adjacent re-entry" of the chains), which can easily be unfolded on drawing (Smith and Lemstra, 1985/1987).

19.4.2.1. Some basic considerations

In extended chain crystallisation the chain molecules are extended prior to crystallisation, or during recrystallisation. Chain extension as such requires a considerable stretching force in order to balance the entropic retracting force of the chains. It is necessary that the extension time is of the same order as the relaxation time of the chains. This means that the following relationships should hold:

$$\dot{\varepsilon}\tau \approx 1, \text{ for tensile stretch and } \dot{\gamma}\tau \approx 1, \text{ for shear}$$

where $\dot{\varepsilon}$ = rate of elongation; $\dot{\gamma}$ = rate of shear and τ = relaxation time. The relaxation time of polymer melts is of the order of 10^{-3} s. According to Bueche the relaxation time (at low rate of deformation) is:

$$\tau_0 = \frac{6 \eta_0 M}{\pi^2 \rho R T} \quad (19.36)$$

Chain extension under the influence of stretch or shear is therefore a function of molecular weight.

McHugh (1975) has calculated the amount of extension as a function of deformation rate and molecular weight in polymer solutions. His results are presented in Fig. 19.18. They illustrate the enormous difference between shear and stretch. *Stretch forces are far more conducive to chain extension and hence to fibrous nucleation than shear forces.*

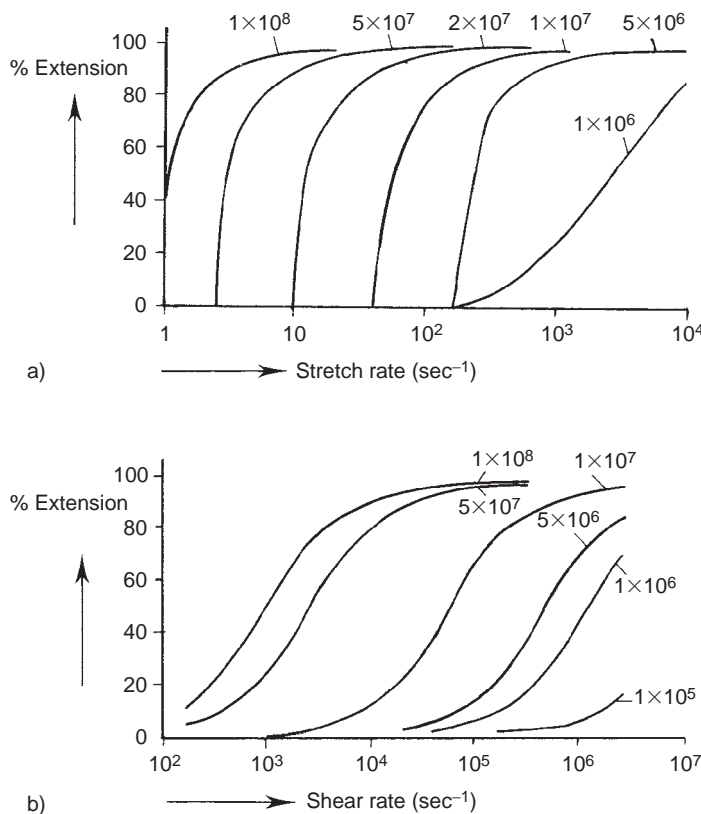


FIG. 19.18 Percentage extension of a polymer solution caused by different deformations (at 100 °C); parameter: M . (A) as a function of the stretch rate (for various molar masses) (B) as a function of the shear rate (for various molecular masses). Calculations by McHugh (1975).

It is clear that the extension must be maintained until the melt has solidified by crystallisation. For spherulitic crystallisation this would require residence times of 0.5–50 s (0.5 s for PE and 50 s for PETP), which excludes normal spherulitic crystallisation for most polymers, since only fractions of seconds are available in practice. *It is therefore fortunate that another type of crystallisation, that of the microfibrillar crystallite, is the dominant mode.* This is due to the fact that under tension *threadlike nucleation* is favoured.

Kobayashi and Nagasawa (1970) calculated the acceleration of nucleation by means of simple elongation in the ideal case where there is no relaxation after elongation. They found that the nucleation and hence the crystallisation may be orders of magnitude higher than in spherulitic crystallisation.

Axtell and Haworth (1994) showed that rheology, and in particular elongational deformation plays a key role. Ziabicki (1999, 2000) laid a theoretical basis of the role of enhancing the nucleation of crystallisation.

19.4.2.2. Properties of gel-spun yarns

The difference in drawing behaviour between conventional melt-extruded polymers and ultra-drawable gel-spun polymers is indeed striking (see Fig. 19.19, curves a and b respectively). There is an interesting correlation between the initial concentration of the

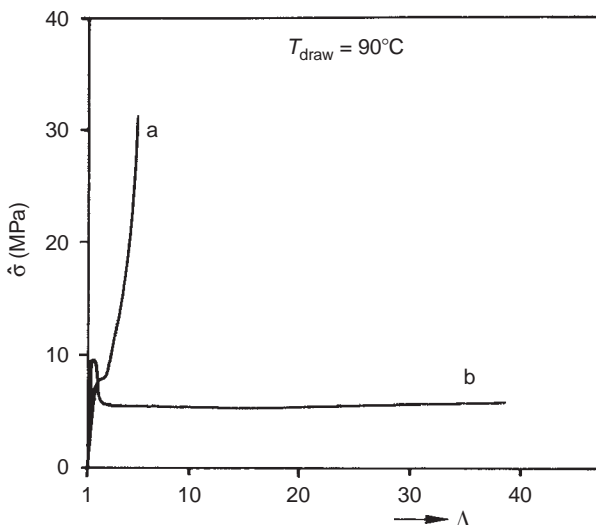


FIG. 19.19 Nominal stress σ ($=F/A_0$) vs. draw ratio Λ ($=l/l_0$) of Hostalen Gur 412, recorded at 90°C at constant cross-head speed of 100 mm/min: (A) melt-crystallised; (B) solution-spun/extracted. After Lemstra and Kirschbaum, (1985); Courtesy of Butterworths & Co.

polymer (Hostalene, i.e. high molecular weight polyethylene) in its solvent and the attainable draw ratio:

$$\Lambda_{\max} = C\varphi^{-1/2} \quad (19.37)$$

where φ = polymer volume fraction; C = a “constant”, still depending on the temperature of drawing; it varies from 7.5 at 130°C to 3.75 at 90°C .

It is interesting to note that Smook et al. (1990) found for flexible polymers a convicting relationship between Λ_{\max} and the cohesive energy

$$\Lambda_{\max}^2 = A \exp\left(-\frac{E_{\text{coh}}}{RT_d}\right) \quad (19.38)$$

where E_{coh} = cohesive energy (J/mol) (see Table 7.4); T_d = drawing temperature (K); A = constant, equal to 1.3×10^5 .

Accordingly,

$$\ln \Lambda_{\max} = 5.89 - [E_{\text{coh}}/(RT_d)]^{0.5} \quad (19.39)$$

This relationship is, for a number of flexible polymers, demonstrated in Fig. 19.20.

Fig. 19.21 shows, for the spun Hostalene fibres, the relationships between modulus and strength, both as functions of draw ratio. The Young modulus proves to be a nearly linear function of the draw ratio:

$$E(\text{GPa}) = 2.85\Lambda_{\max} \quad (19.40)$$

Such a relationship has also been found for PA6 fibres by Smook et al. (1990). These authors also showed that the Young modulus increases with molecular weight.

Combination of Eq. (19.40) with Eq. (19.38) leads for Hostalen to

$$E \approx 10^3 \left[\exp\left(-\frac{E_{\text{coh}}}{RT_d}\right) \right]^{1/2} \quad (19.41)$$

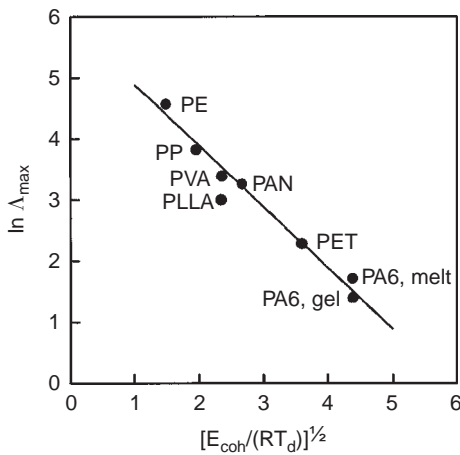


FIG. 19.20 Maximum draw ratio vs. cohesive energy contribution for a series of flexible chain polymers, After Smook et al. (1990).

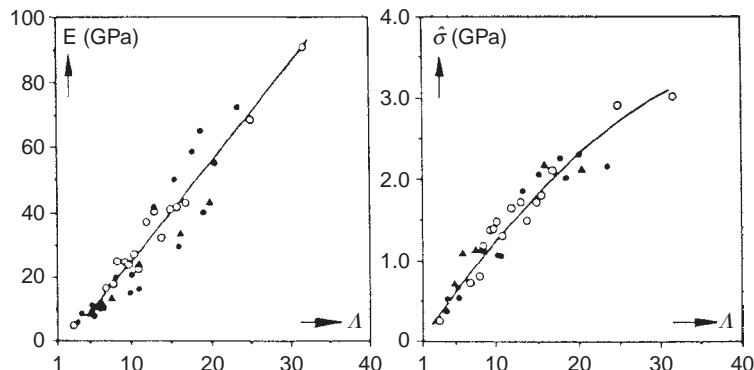


FIG. 19.21 Effectiveness of drawing gel-filaments: (○) “wet” filaments (90% residual solvent); (●) partly dried filaments (6% residual solvent); $\hat{\sigma} = \sigma_{\max}$ (▲) dried (extracted) filaments; drawing performed single-stage at 120 °C. After Lemstra et al. (1987).

Because E_{coh} is proportional to the solubility parameter δ , the conclusion might be that $\ln E_{coh}$ of spun fibres is proportional to their solubility parameter.

The simple relationship, not to be compared with Eq. (13.171), between tensile strength and modulus has a well-known empirical form:

$$\sigma_{\max} = 0.15E^{2/3} \quad (19.42)$$

It is reproduced in Fig. 19.22. (An even better curve fit is $\sigma_{\max}=0.055E-0.00025E^2$; this curve fit is more in agreement with the clearly recognisable decrease of slope at high values of σ_{\max} and E). In comparing this Eq. (19.42) with Eq. (13.171) and Fig. 13.102, it would result in a value for β of approximately 0.095. In comparison with Eq. (13.134) for low modulus polymers, the coefficient in Eq. (19.42) is a factor of 5 larger.

19.4.2.3. Restrictions

Heating above the melting temperature for a short time (about one minute) destroys the ultra-drawability of gel-spun polymers; the extended chains then retract to folded chains. This is also the reason that the maximum use temperature is about 40 °C below the melt temperature.

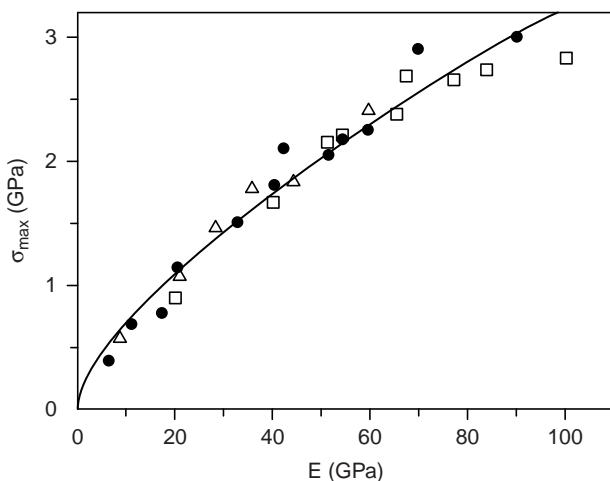


FIG. 19.22 Tensile strength vs. Young's modulus for high-molecular-weight polyethylene ($M_n = 200 \times 10^3$, $M_w = 1.5 \times 10^3$): (□) surface grown, Zwijnenburg and Pennings; (●) solution spun-drawn wet; (△) solution spun/drawn dried. Smith et al. (1982); Courtesy of John Wiley & Sons, Inc.). The drawn line corresponds to Eq. (19.42).

In order to be usable for ultra-drawing the polymer should have smooth chains, without large side groups or hydrogen-bonding groups and with as few entanglements as possible. For a limited number of polymers ultra-drawing has proved possible and successful: poly(ethylene) (linear!), poly(propylene), poly(oxy-methylene), poly (vinyl alcohol) and poly(acrylonitrile). Gel-spun PE is in industrial production. Also polyketon (POK or PECO, i.e. an alternating copolymer of C=O and CH₂=CH₂) can be gel-spun from a resorcinol containing solution (Maat et al., 1990, 1996) to obtain strong fibres. It seems that aqueous metal salt solutions (e.g. CaCl₂ and ZnCl₂) can also be used as spinning solutions for POK (Morita et al., 2004).

Table 19.10 gives a survey of the main properties of gel spun yarns in comparison with spun-drawn yarns and melt-crystallised specimens of the same polymers.

For an interesting review concerning gel-spinning the reader is referred to the paper by Van Dingenen (2001).

19.4.3. Other techniques for extended chain crystallisation of flexible polymers

19.4.3.1. “Super-drawing” of spun treads or films

As mentioned before, the conventional drawing process leads to the well-known fibrillar structure, which still contains a majority of folded chains (Fig. 19.14). In drawing above the “natural” draw ratio further unfolding takes place. Such a process at very high draw ratios must be conducted with the utmost care since critical concentrations of stress on the folded chain surface of the crystal blocks must be avoided: they lead to fracture. The super-drawing can be carried out in one and two stages.

The two-stage super-drawing consists of a normal fast drawing process as a first stage, followed by a second stage: a slow drawing process to very high draw ratios.

Sheehan and Cole (1964) drew polypropylene at a speed of 2 cm/s in a glycerol bath of 135 °C and obtained draw ratios up to 50 resulting in a modulus of about 15 GPa (30% of the theoretical value).

Spectacular results have been obtained with two-stage drawing of polyoxymethylene by *Clark and Scott* (1974). In the first stage the polymer is drawn to the natural draw ratio of about 7. The second stage takes place at a very low velocity (50% elongation per minute) up to an ultimate draw ratio of about 20. The optimum temperature for the second step is about 30 °C below the standard melting point. A modulus of 35 GPa, about 70% of the theoretical value has been obtained in this way. The drawn material did not show folded chain periodicity anymore.

Another striking example concerns the polymer poly(p-xylylene) (PPX). It is obtained by condensation at room temperature of the gaseous monomer. A clear foil may be obtained in that way. The melting point of PPX is 427 °C and it crystallises immediately after polymerisation, so that entanglement cannot be formed. *Van der Werff and Pennings* (1988, 1991) have shown that hot drawing of such a material at 420 °C yields a material with a tensile strength of 3 GPa and a tensile modulus of 100 GPa.

Very high draw ratios can also be obtained by extremely careful one-stage drawing. *Capaccio and Ward* (1973, 1975) obtained with polyethylene draw ratios up to 30, and moduli up to 70 GPa have been reported.

19.4.3.2. Hydrostatic extrusion, ram extrusion and die drawing

These techniques can only be mentioned here. *Ward* and co-workers and *Porter* and co-workers were especially active in these fields. For an interesting review the reader is referred to the paper by *Weedon* (2001).

19.4.4. LC-spinning: extended chain crystallisation of rigid macromolecules

A completely different approach to polymer crystallisation in extended-chain conformation became possible with the coming of a new class of polymers: the para–para type aromatic polymers. These polymers possess inherently rigid molecular chains in an extended conformation (Preston, 1975; Magat, 1980; Northolt, 1974, 1980, 1985; Dobb, 1985). Theoretically they should give rise to high orientation in fibre form without the necessity of subjecting the as spun filaments to the conventional drawing process.

The difficulty with these polymers is that they usually do not melt without heavy thermal degradation and can hardly be dissolved. If melting or dissolving would be successful an extreme viscosity of the melt or solution above the clearing temperature had to be expected.

Fortunately such systems exhibit the unusual property to be able to form liquid-crystalline liquids under certain conditions (of molecular mass, temperature, nature of solvent, concentration, etc.; the liquid-crystalline liquid obtained is mostly of the nematic type. As already described in Chap. 2, two types of semi-rigid polymers can be distinguished:

- a. The *lyotropic* liquid-crystalline type (see also Chap. 16). The most important representatives are PpPTA (Twaron® and Kevlar®), PBO (Zylon®), PIPD or M5 and cellulose. These polymers are spun from solutions in unconventional solvents (see Fig. 19.23).
- b. The *thermotropic* liquid-crystalline type (see also Chap. 15). The most representative polymers of this type are the *Arylates* or fully aromatic polyesters, e.g. Vectran® (see Chap. 15). These are melt-spun.

Hearle (2001) has presented an excellent review of these high performance fibres.

One of the semi-rigid polymer fibres, which is now produced on a big scale is Poly (p-Phenylene Terephthal Amide); we shall discuss this product in some more detail.

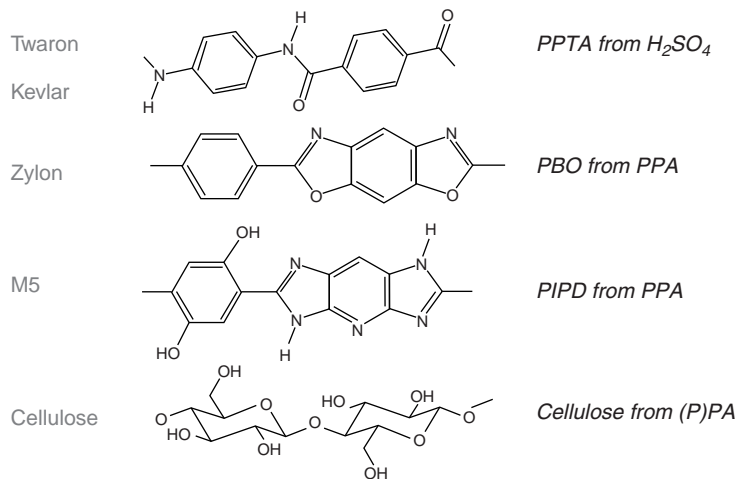


FIG. 19.23 Spinning solutions of the most representative lyotropic LC polymers; PPA=polyphosphoric acid; the first three polymers spun into water as a coagulation liquid, whereas cellulose is spun into acetone. After Picken et al. (2001).

19.4.4.1. PpPTA

This polymer is spun from a solution in pure (100%) sulphuric acid. A typical, but too simple phase diagram for the PpPTA-sulphuric acid/water system is shown in Fig. 19.24 (also shown as Fig. 16.27). It shows that the solution is solid at sulphuric acid/water ratio smaller than approximately 0.95; liquid solutions are obtained at high sulphuric acid contents: at low polymer concentrations isotropic solutions are obtained whereas at higher polymer concentrations the solutions are anisotropic. It is clear that for solution spinning almost pure sulphuric acid or even oleum (i.e. H_2SO_4

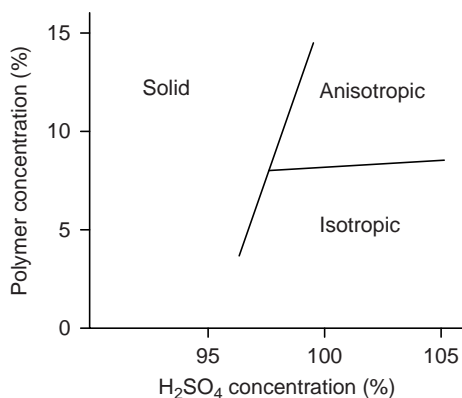


FIG. 19.24 A typical phase diagram for poly (p-phenylene terephthalamide) showing percentage polymer plotted against percentage sulphuric acid in water; >100% sulphuric acid is obtained by adding SO_3 (this is called oleum). After Dobb (1985).

$+ \text{SO}_3$) is needed. Much more details about the phase diagram of PpPTA and $\text{H}_2\text{SO}_4/\text{H}_2\text{O}$ is found in a paper by Rommel and Förster (1994).

In this system the viscosity of an isotropic solution increases with increasing polymer concentration (as expected), but eventually reaches a point where an anisotropic phase separates. As more polymer is added, the viscosity actually decreases very markedly. Such liquid-crystalline dopes of appropriate concentration form highly ordered domains of extended polymer chains which – during flow through a spinneret and subsequently during air gap drawing – are aligned and lead to a product of very high orientation. Typical optimum conditions in the PPTA– H_2SO_4 system are the following:

Solvent: 99.8% sulphuric acid

Polymer concentration: 18–22%

Spinning temperature: 70–90 °C

Dopes like these exhibit mesomorphic behaviour; they are solid at room temperature, but at higher temperature become less viscous and show optical anisotropy. If heated further, the clearing temperature (T_{cl}) is reached at which a phase transformation takes place from an anisotropic solution to an isotropic solution. With increasing polymer concentration both T_a and the melting point of the dope (T_m^d) increase. Fibres of the highest quality (tenacity) are obtained by spinning at temperatures between T_m^d and T_a , but as low as possible. The spun filament is solidified in a coagulating bath, preferably at temperatures below 5 °C.

For satisfactory fibre production it is essential that an inert layer (of gas or a non-coagulating liquid) separates the face of the spinneret from the coagulating bath, in order to separate the spinning temperature and the coagulation temperature. The spin-stretch factor (= ratio of fibre velocity at the end of the coagulating bath to the jet velocity in the spinneret capillary) may vary between 1 and 14 (breaking stretch). After washing and drying a subsequent heat treatment might be important.

19.4.4.2. Properties

The mechanical properties of paracrystalline aramides and other high-performance polymeric fibres are shown in Table 19.11. In comparison some other fibres are mentioned in this table (see also Sect. 13.6). Aramide fibres display a very high refractivity (refractive index and strong birefringence: $n_{//} \approx 2.2$, $n_{\perp} \approx 1.6$).

There is overwhelming evidence that the aramide fibres possess a radially oriented system of crystalline supramolecular structure (see Fig. 19.1). The background of the properties, the filament structure, has been studied by Northolt et al. (1974–2005), Baltussen et al. (1996–2001), Picken et al. (2001), Sikkema et al. (2001, 2003), Dobb (1977–1985) and others. The aramid fibres (and the “rigid” extended chain fibres in general) are exceptional insofar as they were – with the rubbers – the first polymer fibres whose experimental stress-strain curve can very well be described by a consistent theory.

Northolt and Van der Hout (1985) originally derived theoretical (and experimentally confirmed) expressions for the modulus and the elastic stress–strain relation for aramids and similar fibres.

At the present time (2008) a general description is available for polymer fibres, due to the development by Northolt and Baltussen (see papers from 1995 to 2005) of the

TABLE 19.11 Physical properties of para-crystalline fibres in comparison with other reinforcing materials

Properties	Paracrystalline fibres												Conventional spun/drawn fibres		Inorganic filaments		
	Aramid		Carbon		Arom. polyester	PBO Zylon	PIPD M5	Cellulose ^a		POK ^b Carilon	Gel-spun PE	PA-6	PETP	E-glass	Steel		
	HM	HS	HM	HS				I	II								
Modulus E and E/ρ (specif.)	Tensile (GPa)	130	65	400	230	75	280	330	110	55	50	150–220	5–15	10–20	75	200	
	Do., theor. ^c (GPa)	240	240	960	960	(250)	500	550	136	88		250	170	137	69–138	208	
	Tensile (specific) (MPa/(kg m ⁻³))	90	45	300	150	35	180	195	71	58	200	7	10	20	26		
Strength σ_{\max} and σ_{\max}/ρ (specif.)	Tensile (GPa)	3.0	4	2.3	3.1	2.9	5.8	5.0		1.7	3.8	3.5	0.8	1	2.1	2.8	
	Do., theor. ^c (GPa)	21	21	4	5.7							25	28	17	11	11	
	Tenacity (MPa/(kg m ⁻³))	2.1	2–3	1.2	2–3	2.1	3.7	2.9		1.2	3.0	3.5	0.8	0.75	0.8	0.35	
	Compression (GPa)	0.5	0.5	1.5	2.5		0.4	1.6		0.8 ^d			0.7	0.1	0.5	2.4	
σ_{\max}/ρ (specif.)	Do. (specific) (MPa/(kg/m))	0.17	0.2	0.86	1.3		0.25	0.95		0.55			0.07	0.07	0.19	0.31	
Other physical properties	Density (g/cm ³)	1.44	1.44	1.90	1.74	1.40	1.56	1.70	1.55 ^d	1.52 ^d	1.3	1.0	1.1	1.38	2.6	7.8	
	Max. working temp.(°C)	200	250	600	500	150	300	300	200	200	150	60	120	120	350	300	
	T _m (°C)	480	480	3600	3600	305						258	135	220	260	700	1400
	T _d (°C)	480	480	3600	3600	400						390	350	380			
	Brittleness (test result)	+	+	–	–	+						+	+	+	–	+	

^a Cellulose I = native fibre; Cellulose II = regenerated (or man-made) fibre.

^b From: B.J. Lommerts (1994).

^c See Treloar (1960), Sakurada et al. (1966/1970), Britton et al. (1976) and Northolt et al. (1974–1986).

^d From: P.H. Hermans (1949).

so-called *continuous chain model*, which is able to describe the tensile deformation properties of well-oriented polymer fibres properly. Some results for initial modulus and deformation are

$$S_{\text{in}}^{\text{F}} = \frac{1}{E_{\text{in}}^{\text{F}}} = \frac{1}{e_{\text{ch}}} + \frac{\langle \sin^2 \Theta \rangle_{\text{E}}}{2g_{\text{d}}} \quad (19.43)$$

$$\varepsilon^{\text{F}} = e_{\text{ch}} + \varepsilon_{\text{sh}} = \frac{\sigma^{\text{F}} \langle \cos^2 \theta \rangle}{e_{\text{ch}}} + \frac{\langle \cos \theta \rangle - \langle \cos \Theta \rangle}{\langle \cos \Theta \rangle} \quad (19.44)$$

where e_{ch} and ε_{ch} are the chain modulus and chain deformation, respectively, g_{d} the modulus for shear between the chains and $\langle \sin^2 \Theta \rangle$ the initial orientation distribution parameter and θ and Θ the orientation angles in the deformed and undeformed state, respectively. This model has been rather extensively described in Sect. 13.6.

BIBLIOGRAPHY

General references

- Blumstein A, "Polymer Liquid Crystals", Plenum Press, New York, 1985.
 Ciferri A and Ward IM (Eds), "Ultra-high Modulus Polymers", Applied Science Publishers, London, 1978.
 Ciferri A, Krigbaum WR and Meyer RB (Eds), "Polymer Liquid Crystals", Academic Press, New York, 1982.
 Dosiére M (Ed), "Crystallization of Polymers", Kluwer, Dordrecht, 1993.
 Geil PH, "Polymer Single Crystals", Interscience, New York, 1963.
 Gibbs JW, "Collected Works", Longmans, New York, Vol. 1, p 94, 1928.
 Hearle JWS (Ed), "High-performance Fibres", The Textile Institute and Woodhead Publishing Ltd, Abington, Cambridge, UK, 2001.
 Keller A, "Growth and Perfection of Crystals", Wiley, New York, 1958.
 Mandelkern L, "Crystallization of Polymers", McGraw-Hill, New York, 1964.
 Miller RL (Ed), "Flow Induced Crystallization in Polymer Systems", Gordon and Breach, New York, 1977.
 Morton WE, and Hearle JWS, "Physical Properties of Textile Fibres", The Textile Institute and Butter-worth, London, 1962.
 Northolt MG and Sikkema DJ, "Lyotropic Main Chain Liquid Crystal Polymers", Adv Polym Sci 98 (1990) 115.
 Patki R, Mezghani K and Phillips PJ, "Crystallization Kinetics of Polymers" in Mark JE (Ed), "Physical Properties of Polymers Handbook", Springer, Berlin, 2nd Ed, 2007, Chap. 39.
 Sanchez IC, "Modern Theories of Polymer Crystallization", J Macromol Sci C; Rev Macromol Chem 10 (1974) 114–148 (772 refs).
 Sharples A, "Introduction to Polymer Crystallization", Edw Arnold, London, 1966.
 Stuart HA, "Die Physik der Hochpolymeren", Springer, Berlin, Vol. IV, 1956.
 Ueberreiter K, "Kristallisieren, Kristallzustand und Schmelzen" in "Struktur und physikalisches Verhalten der Kunststoffe" (Nitsche und Wolf, Eds), Springer, Berlin, Vol. I, 1962.
 Uhlmann DR and Chalmers B, "Energetics of Nucleation", Ind Eng Chem 57 (1965) 19.
 Volmer M, "Kinetic der Phasenbildung", Steinkopf, Dresden, Leipzig, 1939.
 Ward IM (Ed), "Mechanical Properties of Solid Polymers", Wiley, London, 2nd Ed, 1983.
 Ward IM (Ed), "Developments in Oriented Polymers", Elsevier Applied Science Publishers, London, Vol. 2, 1987.
 Watt W and Perov BV, "Strong Fibres", North Holland, Amsterdam, 1985.
 Wunderlich B, "Macromolecular Physics", Academic Press, New York, "Crystal Structure", Vol. I, 1973; "Crystal Nucleation and Growth", Vol. 2, 1976; "Crystal Melting", Vol. 3, 1980.
 Zachariades AE and Porter RS (Eds.), "The Strength and Stiffness of Polymers", Marcel Dekker, New York, 1983.
 Ziabicki AE and Kawai H (Eds), "High-speed Fibre Spinning", Wiley, New York, 1985.

Special references

- Andrews RD, J Appl Phys 25 (1954) 1223.
 Astarita G and Kenny JM, Chem Eng Com 53 (1987) 69.

- Avrami M, J Chem Phys; 7 (1939) 1103; 8 (1940) 212; 9 (1941) 177.
- Axtell FH and Haworth B, "Plastics, Rubber and Composites Processing and Applications", 92 (2000) 127.
- Azzurri F and Alfonso G, Macromolecules 38 (2005) 1723.
- Baltussen JJM, "Tensile Deformation of Polymer Fibres", PhD Thesis, Delft, 1996.
- Baltussen JJM and Northolt MG, Polym Bull 36 (1996) 125.
- Baltussen JJM and Northolt MG, J Rheol 41 (1997) 575.
- Baltussen JJM and Northolt MG, Polymer 42 (2001) 3835.
- Basset DC and Carder DR, Phil Mag 28 (1973) 513, 535.
- Basset DC and Turner B, Phil Mag 29 (1974) 925.
- Becker R, Ann Physik 32 (1938) 128.
- Becker R and Döring W, Ann Physik 24 (1935) 719; 32 (1938) 128.
- Bicerano J, "Prediction of Polymer Properties", Marcel Dekker, New York, 3rd Ed, 2002, Chap. 6.
- Binsbergen FL, Kolloid Zeitschrift 237 (1970) 289; 238 (1970) 389.
- Boerstoel H, "Liquid Crystalline Solutions of Cellulose in Phosphoric Acid", Doctoral Thesis Groningen, 1998.
- Boerstoel H, Maatman H, Westerink JB and Koenders BM, Polymer 42 (2001) 7371.
- Boon J, PhD Thesis Delft University of Technology, 1966.
- Boon J, Challa G and Van Krevelen DW, J Polym Sci A2, 6 (1968) 1791, 1835.
- Britton RN, Jakeways R and Ward IM, J Mater Sci 11 (1976) 2057.
- Capaccio G, Pol Eng Sci 15 (1975) 219; Polymer 16 (1975) 239, 469.
- Capaccio G and Ward IM, Nature 243 (1973) 143.
- Clark ES, in "Structure and Properties of Polymer Films", Lenz RW and Stein RS (Eds) Plenum Press, New York 1973.
- Clark ES and Scott LW, Polym Eng Sci 14 (1974) 682.
- Dobb MG, Johnson DJ and Saville BP, J Polym Sci (Pol Symp) 58 (1977) 237; Polymer 20 (1979) 1284; Polymer 22 (1981) 960.
- Dobb MG, in Watt and Perov (Eds), "Strong Fibres" Watt W and Perov BV, "Strong Fibres", North Holland, Amsterdam, pp 673–704, 1985 (see General references).
- Eder G and Janeschitz-Kriegl H, Mater Sci Technol 18 (1997) 269.
- Foubert I, Dewettinck K and Vanrolleghem PA, Trends Food Sci Technol 14 (2003) 79.
- Frank FC, Keller A and Mackley MR, Polymer 12 (1971) 467.
- Gandica A and Magill JH, Polymer 13 (1972) 595.
- Gornick F and Hoffman JD, "Nucleation in Polymers", Ind Eng Chem 58 (1966) 41.
- Hermans PH, "Physics and Chemistry of Cellulose Fibres", Elsevier, Amsterdam, 1949.
- Herwig HU, Internal Report Akzo Research & Engineering NV (1970).
- Hoffman JD, J Chem Phys 28 (1958) 1192; SPE Trans 4 (1964) 315; Ind Eng Chem 58 (1966) 41.
- Hoffman JD and Weeks JJ, J Chem Phys 37 (1962) 1723; 42 (1965) 4301.
- Hoffman JD, Weeks JJ and Murphey WM, J Res NBS 63A (1959) 67.
- Huisman R and Heuvel HM, J Appl Polym Sci 22 (1978) 943 and 2229.
- Janeschitz-Kriegl H, Monath für Chem 138 (2007) 138 (in English).
- Janeschitz-Kriegl H, Monatshafte für Chemie 138 (2007) 327 (in English).
- Janeschitz-Kriegl H, "Processing of Semi-crystalline Polymers: Fundamentals of Structure Formation", in preparation.
- Janeschitz-Kriegl H and Ratajski E, Polymer 46 (2005) 3856.
- Janeschitz-Kriegl H, Ratajski E and Stadlbauer M, Rheol Acta 42 (2003) 355.
- Janeschitz-Kriegl H, Eder G, Stadlbauer M and Ratajski E, Monatsh Chem 136 (2005) 136.
- Janeschitz-Kriegl H, Eder G, Stadlbauer M and Ratajski E, Monatshefte für Chemie 136 (2005) 1119 (in English).
- Jamet M and Perret R, CR Acad Sci Ser C 277 (1973) 941.
- Kavesh S and Schultz JM, Polym Eng Sci 9 (1969) 5.
- Keller A, Phil Mag 2 (1957) 1171.
- Keller A and Mackley MR, Polymer 14 (1973) 16.
- Keller A and Mackley MR, Pure Appl Chem 39 (1974) 195.
- Khanna YP and Taylor TJ, Polym Eng Sci 28 (1988) 1042.
- Kobayashi K and Nagasawa T, J Macromol Sci; Phys B4 (1970) 331–45.
- Lemstra PJ and Kirschbaum R, Polymer 26 (1985) 1372.
- Lemstra PJ and Smith P, Brit Polym J 12 (1980) 212.
- Lemstra PJ, Kirschbaum R, Ohta T, and Yasuda H, in Ward IM, "Developments in Oriented Polymers", Vol. 2, pp 39–77, 1987 (see General references).
- Lemstra PJ, Van Aerle PJ and Bastiaansen CWN, Polymer J 19 (1987) 85.
- Lommerts BJ, "Structure development in polyketone and polyalcohol fibers", PhD Thesis, Groningen (1994).
- Maat HT, Cloos PJ, Van der Werff H and Lommerts BJ, European Patent WO 90/14453 (1990) and US Patent 5,555,218 (1996).
- Maddock BH, SPE J 15 (1959) 383.

- Magat EE, Phil Trans Roy Soc Ser A 294 (1980) 463.
- Magill JH, Polymer 2 (1961) 221; Polymer 3 (1962) 43; J Appl Phys 35 (1964) 3249; J Polym Sci A-2, 5, (1967) 89.
- Mandelkern L, Jain NL and Kim H, J Polym Sci A-2, 6 (1968) 165.
- Marangoni A, J Am Oil Chem Soc 75 (1998) 1465.
- Marrand H, Xu J and Srinivas S, Macromolecules 31 (1998) 8219.
- McHugh AJ, J Appl Polym Sci 19 (1975) 125.
- Morita T, Taniguchi R, Matsuo T and Kato J, J Appl Polym Sci 92 (2004) 1183.
- Morita T, Taniguchi R and Kato J, J Appl Polym Sci 94 (2004) 446.
- Northolt MG, Eur Polym J 10 (1974) 799; Polymer 21 (1980) 1199; J Mater Sci 16 (1981) 2025; Ned Tijdschr Natuurk A50 (1984) 48.
- Northolt MG, in Kleintjes LA and Lemstra PJ (Eds) "Integration of Fundamental Polymer Science and Technology" Elsevier Applied Science Publishers, 1986, p 567 Northolt MG, J Mater Sci 16 (1981) Letters, 2025.
- Northolt MG and Baltussen JJM, J Appl Polym Sci 83 (2002) 508.
- Northolt MG and De Vries H, Angew Makromol Chem 133 (1985) 183.
- Northolt MG and Van Aartsen JJ, J Polym Sci, Polym Lett Ed 11 (1973) 333; J Polym Sci, Polym Symp 38 (1977) 283.
- Northolt MG, and Van der Hout R, Polymer 26 (1985) 310.
- Northolt MG, Kroon-Batenburg LMJ and Kroon J, Polym Commun 27 (1986) 290.
- Northolt MG, Roos A and Kampschreur JH, J Polym Sci B, Phys 27 (1989) 1107.
- Northolt MG, Baltussen JJM and Schaffers-Korff B, Polymer 36 (1995) 3485.
- Northolt MG, Boerstoel H, Maatman H, Huisman R, Veurink J and Elzerman H, Polymer 42 (2001) 8249.
- Northolt MG, Sikkema DJ, Zegers HC and Klop EA, Fire Mater 26 (2002) 169.
- Northolt MG, Den Decker P, Picken SJ, Baltussen JJM and Schlatmann R, Adv Polym Sci 178 (2005) 1.
- Okui N, Polym J 19 (1987) 1309.
- Olsen AP, Fagan RC and Kornfield JA, Macromolecules 39 (2006) 8419.
- Osugi J and Hara H, Rev Phys Chem Jpn 36 (1966) 28.
- Pennings AJ, J Phys Chem Solids, Suppl 1 (1967) 389.
- Pennings AJ and Meihuizen KE, in Ciferri and Ward (Eds), (see General references) "Ultra-high Modulus Polymers", p 117, 1979.
- Pennings AJ and Kiel AM, Kolloid Z 205 (1965) 160.
- Pennings AJ, Van der Mark J and Booy H, Kolloid Z 236 (1970) 99.
- Pennings AJ, Van der Mark J and Kiel AM, Kolloid Z 237 (1970) 336.
- Pennings AJ, Schouten C and Kiel AM, J Polym Sci C 38 (1972) 167.
- Pennings AJ, Zwijnenburg A and Lageveen R, Kolloid Z 251 (1973) 500.
- Peterlin A, Polym Sci Technol 1973 no 1, 253; J Macromol Sci, Phys B8 (1-2) (1973) 83; J Mater Sci 6 (1973) 490; Polym Eng Sci 17 (1977) 183.
- Peterlin A, in Zachariades and Porter (Eds) "The Strength and Stiffness of Polymers" (see General references) pp 93–127, 1983.
- Picken SJ, Boerstoel H and Northolt MG, "Processing Rigid Polymers to High Performance Fibres" in "Encyclopaedia of Materials: Science and Technology", Elsevier, Amsterdam, 2001.
- Preston I, Polym Eng Sci 15 (1975) 199.
- Prevorsek DC and Kwon YD, J Macromol Sci, Phys B 12 (4) (1976) 447–485.
- Rommel H and Förster G, Macromolecules 27 (1994) 4570.
- Sakaoku K, Clark HG and Peterlin A, J Polym Sci A2, 6 (1968) 1035.
- Sakurada J and Kaji K, J Polym Sci C 31 (1970) 57.
- Sakurada J, Ito T and Nakamae K, J Polym Sci C 15 (1966) 75.
- Schlesinger W and Leeper HM, J Polym Sci 11 (1953) 203.
- Schneider W, Köppel A and Berger J, Int Polym Proc 2 (1988) 151.
- Sheehan WC and Cole TB, J Appl Polym Sci 8 (1964) 2359.
- Sikkema DJ, "Manmade Fibers One Hundred Years: Polymers and Polymer Design". J Appl Polym Sci 83 (2001) 484.
- Sikkema DJ, Northolt MG and Pourdeyhimi B, MRS Bull 28 (2003) 579.
- Smith P and Lemstra PJ, Makromol Chem 180 (1979) 2983; Polymer 21 (1980) 1341; Br Polym J 12 (1980) 212; J Mater Sci 15 (1980) 505; Colloid Polym Sci 258 (1980) 891.
- Smith P and Lemstra PJ, J Polym Sci, Polym Phys Ed 19 (1981) 1007.
- Smith P, Lemstra PJ, Kalb B and Pennings AJ, Polym Bull 1 (1979) 733.
- Smith P, Lemstra PJ and Booy HC, J Polym Sci Phys Ed 19 (1981) 877.
- Smith P, Lemstra PJ and Pijpers AJ, J Pol Sci Phys Ed 20 (1982) 2229.
- Smith P, Lemstra PJ, Pijpers AJ and Kiel AM, Colloid Polym Sci 259 (1981) 1070.
- Smith P, Chanzy HD and Rotzinger BP, Polym Comm 26 (1985) 257.
- Smook J, Vos GJH and Doppert HL, J Appl Polym Sci, 41 (1990) 105.
- Stefan J, Sitzungsberichte (Math Naturw) Akad Wissensch Wien, 98 (1889) 473 and 965.

- Stein RS and Tobolsky AV, Textile Res J 18 (1948) 201, 302.
- Steiner K, Lucas KJ and Ueberreiter K, Kolloid Z 214 (1966) 23.
- Suzuki T and Kovacs AJ, Polym J 1 (1970) 82.
- Treloar LRG, Polym 1 (1960) 95.
- Tribout C, Monasse B and Haudin J-M, Colloid Polym Sci 274 (1996) 197.
- Turnbull D and Fisher JC, J Chem Phys 17 (1949) 71.
- Van Antwerpen F, PhD Thesis, Delft University of Technology, 1971.
- Van Antwerpen F and Van Krevelen DW, J Polym Sci: Polym Phys 10 (1972) 2409, 2423.
- Van der Meer SJ, PhD Thesis Delft University of Technology, 1970.
- Van der Werff H, PhD Thesis Groningen, 1991.
- Van der Werff H and Pennings AJ, Polym Bull 19 (1988) 587.
- Van Dingenen JLJ, "Gel-spun high-performance polyethylene fibres", in Hearle JWS (Ed), "High-performance Fibres", The Textile Institute and Woodhead Publishing Ltd, Abington, Cambridge, 2001, Chap. 3.
- Van Krevelen DW, (1975); published in "Properties of Polymers", 2nd Ed, 1976, Elsevier, Amsterdam, p 432.
- Van Krevelen DW, Chimia 32(8) (1978) 279–294.
- Van Krevelen DW and Hoftyzer PJ, Angew Makromol Chem 52 (1976) 101.
- Von Falkai B, Makromol Chem 41 (1960) 86.
- Ward IM, Adv Polym Sci 70 (1985) 3.
- Ward IM, in Kleintjes LA and Lemstra PJ (Eds) "Integration of Polymer Science and Technology", Elsevier Applied Science, London, pp 550–565, 1988, ("Recent Progress in the development of High-modulus flexible Polymers").
- Weedon G, "Solid State Extrusion High Molecular Weight Polyethylene Fibres", in Hearle JWS (Ed) "High-performance Fibres", The Textile Institute and Woodhead Publishing Ltd, Abington, Cambridge, UK,, , 2001, Chap. 4.5.
- Wunderlich B, Pure Van der Werff Appl Chem 31 (1972) 49.
- Wunderlich B, Angew Chem 80 (1968) 1009.
- Wunderlich B and Arakawa T, J Polym Sci A 2 (1964) 3697.
- Wunderlich B, Grüner CL and Bopp RC, J Polym Sci A 2, 7 (1969) 2099.
- Ziabicki A, Colloid Polym Sci 277 (1999) 752.
- Ziabicki A, Polimery 45 (2000) 520 and 581.
- Zwijnenburg A, PhD Thesis, Groningen, 1978.
- Zwijnenburg A and Pennings AJ, Colloid Polym Sci 254 (1976) 868.
- Zwijnenburg A and Pennings AJ, J Polym Sci, Pol Lett, 14 (1979) 539.
- Janeschitz-Kriegl H, Monatshafte für Chemie 138 (2007) 327 (in English).
- Janeschitz-Kriegl H and Ratajski E, Polymer 46 (2005) 3856.
- Janeschitz-Kriegl H, Ratajski E and Stadlbauer M, Rheol Acta 42 (2003) 355.
- Janeschitz-Kriegl H, Eder G, Stadlbauer M and Ratajski E, Monatshefte für Chemie 136 (2005) 1119 (in English).

PART **V**

PROPERTIES DETERMINING THE CHEMICAL STABILITY AND BREAKDOWN OF POLYMERS

*"And what I wanted to do was,
I wanted to explore problems and areas
where we didn't have answers.
We didn't even know the right questions to ask"*

Donald Johanson, 1943

This page intentionally left blank

CHAPTER 20

Thermochemical Properties

In this chapter it will be demonstrated that the *free enthalpy of reactions* can be calculated by means of additive group contributions.

20.1. THERMODYNAMICS AND KINETICS

All polymers are formed and changed by chemical reactions.

Chemical Reaction Science has two domains: *chemical thermodynamics*, dealing with equilibrium states, and *chemical kinetics*, dealing with reaction rates.

Thermodynamic potentials constitute the driving forces causing every natural process to proceed in the direction of its eventual state of equilibrium. Thermodynamics therefore determines whether a reaction is possible or not.

Whether or not a reaction in principle can proceed, depends on the thermodynamics, in particular on the free enthalpy,

$$G = H - TS \quad (20.1)$$

The reaction: *Monomer* \rightarrow *Polymer* can in principle proceed only if

$$\begin{aligned} G_{\text{polymer}} - G_{\text{monomer}} &= \Delta G = \Delta H - T\Delta S \\ &= H_{\text{polymer}} - H_{\text{monomer}} - T(S_{\text{polymer}} - S_{\text{monomer}}) < 0 \end{aligned} \quad (20.2)$$

In Fig. 20.1 the free enthalpy is sketched for polymer and monomer as a function of temperature. It shows that the free enthalpy decreases with increasing temperature due to the term $-TS$. Moreover the slope will be more negative with increasing temperature, because

$$\left(\frac{\partial G}{\partial T}\right)_p = -S < 0 \quad (20.3)$$

The entropy of a polymer is in general smaller than that of its monomer, which means that the slope of the free enthalpy of the polymer vs. temperature is less negative than that of the monomer. The result is that at some temperature both lines in Fig. 20.1 will cross each other. Below that temperature the free enthalpy of the polymer is smaller than the free

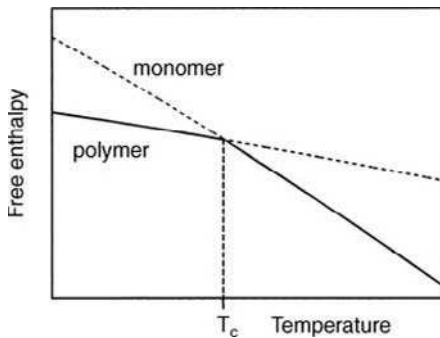


FIG. 20.1 Free enthalpy as a function of temperature for a polymer and for its monomer. The full line refers to the stable state.

enthalpy of the monomer; above this temperature it is the other way round. Accordingly below this temperature polymerisation can proceed in principle, whereas above this temperature the polymer is unstable and thus will depolymerise. This temperature is called the *ceiling temperature* and it is equal to

$$T_c = \frac{\Delta H}{\Delta S} \quad (20.4)$$

In view of thermodynamics the ceiling temperature looks like a melting point. Below and above this temperature the system consists of 100% polymer and of 100% monomer, respectively. This is shown in Fig. 20.2. If, however, the polymer is soluble in its monomer, then the free enthalpy of mixing also plays a role and the result will be that the “melting point” is not as sharp as shown: there will be a gradual change (i.e. the dashed line) from 100% polymer to 100% monomer. The ceiling temperature is in this case defined as the temperature where the amount of monomer equals the amount of polymer (i.e. at 50%) and equal to (see, e.g. Ivin, 2000):

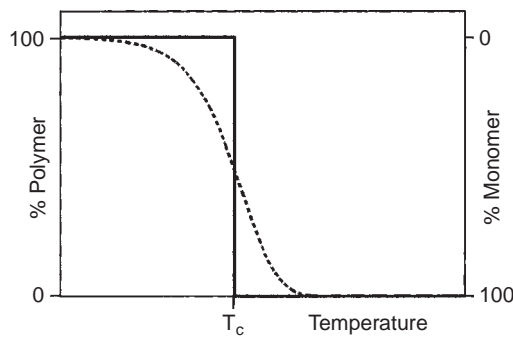


FIG. 20.2 The “melting point” of a polymer that is whether (full line) or not mixed on molecular scale with its monomer (dashed line).

$$T_c = \frac{\Delta H}{\Delta S + k_p \ln[M]} \quad (20.5)$$

where k_p is the rate constant for propagation.

In very special cases the entropy of the polymer is larger than the entropy of the monomer. If, moreover, the reaction is endothermic, so that both ΔH and ΔS are negative, then there is a minimum temperature, where above polymerisation will proceed; below this temperature the monomer is stable. In such a special case the critical temperature is called the *floor temperature*. An example is the polymerisation of crystalline sulphur.

Whether or not a reaction will actually proceed depends on kinetic factors. A certain amount of activation energy and activation entropy is necessary to keep up practically any reaction. However, in many of the cases in which a reaction is thermodynamically feasible it has also proved possible to find a catalyst, active and selective enough to realise this reaction. A classical example is the polymerisation of ethylene, either under high pressure with radical initiators or at low pressure with Ziegler-type catalysts.

Thermodynamics determines the possibility, kinetics the actuality of the conversion.

The *equilibrium constant* K_{eq} is connected with thermodynamic data, viz. the enthalpy of reaction ΔH° and the entropy of reaction ΔS° .

$$-RT \ln K_{eq} = \Delta H^\circ - T\Delta S^\circ = \Delta G^\circ \quad (20.6)$$

where ΔG° is the so-called standard “free” enthalpy change of the reaction. Expression (20.6) can be written in a well-known form (*Van't Hoff equation*):

$$\ln K_{eq} = -\frac{\Delta G^\circ}{RT} - \frac{\Delta H^\circ}{RT} + \frac{\Delta S^\circ}{R} \quad (20.7)$$

which describes the temperature dependence of the equilibrium constant.

Analogous to the Van't Hoff equation for equilibria is the *Arrhenius equation* for the reaction rate constant:

$$\ln k = -\frac{E_{act}}{RT} + \ln A \quad (20.8)$$

where E_{act} is the activation energy and A is a constant (“frequency factor”). Transition state theories formulate Eq. (20.8) in a form analogous to (20.7):

$$\ln k = -\frac{\Delta H_o^*}{RT} + \frac{\Delta S_o^*}{R} + \ln \frac{k_B T}{h} \quad (20.9)$$

where ΔH_o^* is the enthalpy of activation, ΔS_o^* is the entropy of activation, while k_B and h are the constants of Boltzmann and Planck respectively. Fig. 20.3 shows the interrelation of ΔH° and ΔH_o^* (or E_{act}).

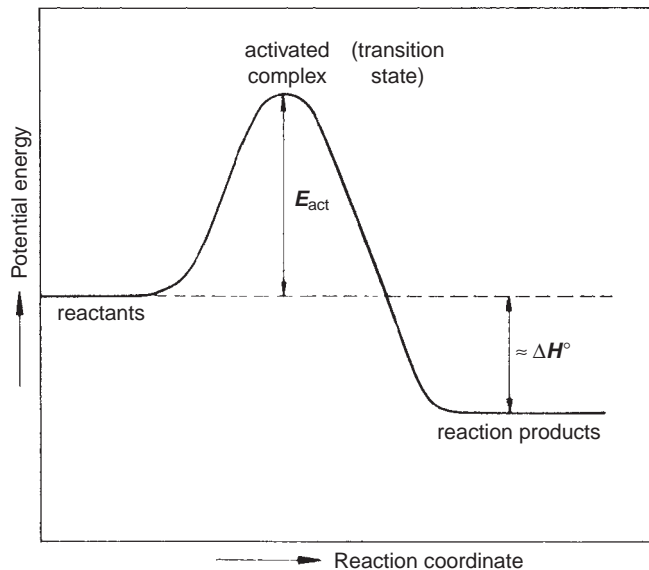


FIG. 20.3 Activation energy and heat of reaction in a reaction system.

If the same reaction is studied with different catalysts or if analogous reactions are compared, it is usually found that the quantities E_{act} and A of the Arrhenius equations are interrelated. An increase in E_{act} is then “compensated” by an increase in A according to the equation:

$$\ln A = \frac{E_{\text{act}}}{RT_R} + \ln B \quad (20.10)$$

where T_R is a characteristic constant with the dimension of temperature (the “*isokinetic temperature*”). Substitution in (20.8) then gives:

$$\ln k = -\frac{E_{\text{act}}}{R} \left(\frac{1}{T} - \frac{1}{T_R} \right) + \ln B \quad (20.11)$$

This is the generalised Arrhenius equation for families of related reactions.

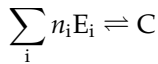
Eq. (20.10) is the mathematical form of the “*compensation effect*”, already mentioned in the treatment of diffusion constants, in Chap. 18.

Since chemical thermodynamics and chemical kinetics are vast domains of science, we will select some special topics, viz. calculation of free enthalpies of reactions from group contributions and thermodynamics of free radical formation.

20.2. CALCULATION OF THE FREE ENTHALPY OF REACTION FROM GROUP CONTRIBUTIONS

Unfortunately, the application of chemical thermodynamics is often handicapped by a lack of sufficient data. In these cases it is important to have a simple method for calculating these data, if only by approximation.

Given the reaction of formation of a compound C from its composing elements E_i



the equilibrium of this reaction at a given temperature is described by the equilibrium constant K_f :

$$K_f = \frac{[C]}{\prod_i [E]^n_i} \quad (20.12)$$

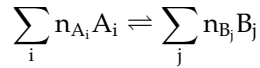
where Π means a product of concentrations.

Thermodynamics provides the relation between the equilibrium constant and the free enthalpy of formation (ΔG_f°)

$$\Delta G_f^\circ = -RT \ln K_f \quad (20.13)$$

From (20.12) it follows that the equilibrium mentioned is shifted to the right if K_f increases and to the left if K_f decreases. It also follows, from Eq. (20.13), that the equilibrium lies on the right (reaction products) for negative values of ΔG_f° and to the left (reactants) for positive values of ΔG_f° . Hence, the actual value of ΔG_f° is a quantitative measure of the stability of a compound, with respect to its elements.

For any arbitrary chemical reaction



the equilibrium at a given temperature is determined by the constant:

$$K_{eq} = \frac{\prod_j [B_j]^{n_{B_j}}}{\prod_i [A_i]^{n_{A_i}}} \quad (20.14)$$

The equilibrium constant K_{eq} is related to the change in free enthalpy caused by the reaction

$$\Delta G^\circ = -RT \ln K_{eq} \quad (20.15)$$

This change of free enthalpy may also be written as a difference in free enthalpies of formation of the compounds considered:

$$\Delta G^\circ = \sum_j n_{B_j} \Delta G_{fB_j}^\circ - \sum_i n_{A_i} \Delta G_{fA_i}^\circ \quad (20.16)$$

Therefore, if the free enthalpies of formation of the compounds participating in any reaction are known, it is possible to calculate the position of the equilibrium of this reaction.

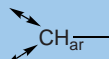
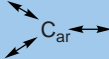
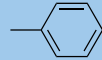
From the preceding it follows that it is of great practical importance, for polymerisation as well as for degradation and substitution reactions, to know the numerical value of the free enthalpy of formation.

Only a very small part of the overwhelming number of known organic compounds have been examined for their thermodynamic behaviour. Hence it is obvious that methods have been sought to calculate these data.

Theoretically it is possible to calculate thermodynamical data by means of statistical mechanical methods. However, these are laborious and moreover the (empirical!) spectroscopic data required to this end are usually lacking.

Also in this case the use of group contributions provides a powerful tool. Developments in this direction were made by Anderson et al. (1944), Bremner and Thomas (1948), Souders et al. (1949) and by Franklin 1949). The most elaborate system of group contributions was developed by Van Krevelen and Chermin (1951). A somewhat simplified version of this system is given in Table 20.1¹.

TABLE 20.1 Free enthalpy of formation of some small molecules and related group contributions to the free enthalpy of formation of large molecules

Group	$\Delta G_f^\circ(T)$ (J/mol)	Group	$\Delta G_f^\circ(T)$ (J/mol)
CH_4	$-79,000 + 92.5 T$	H_2O	$-243,000 + 48.2 T$
$-\text{CH}_3$	$-46,000 + 95 T$	$-\text{OH}$	$-176,000 + 50 T$
$-\text{CH}_2-$	$-22,000 + 102 T$	$-\text{O}-$	$-120,000 + 70 T$
$>\text{CH}-$	$-2,700 + 120 T$	$\text{H}_2\text{C}=\text{O}$	$-118,000 + 26 T$
$>\text{C}<$	$20,000 + 140 T$	$-\text{HC}=\text{O}$	$-125,000 + 26 T$
$=\text{CH}_2$	$23,000 + 30 T$	$>\text{C}=\text{O}$	$-132,000 + 40 T$
$=\text{CH}-$	$38,000 + 38 T$	HCOOH	$-381,000 + 100 T$
$=\text{C}<$	$50,000 + 50 T$	$-\text{COOH}$	$-393,000 + 118 T$
$=\text{C}=$	$147,000 - 20 T$	$-\text{COO}-$	$-337,000 + 116 T$
$\equiv\text{CH}$	$112,500 - 32.5 T$	NH_3	$-48,000 + 107 T$
$\equiv\text{C}<$	$115,000 - 25 T$	$-\text{NH}_2$	$11,500 + 102.5 T$
	$12,500 + 26 T$	$-\text{NH}-$	$58,000 + 120 T$
	$25,000 + 38 T$	$>\text{N}-$	$97,000 + 150 T$
	$21,000 + 21.5 T$		$69,000 + 50 T$
	$75,000 + 156 T$	H_2S	$-25,000 - 30 T$
		$-\text{SH}$	$13,000 - 33 T$
		$-\text{S}-$	$40,000 - 24 T$
			$60,000 - 60 T$
	$87,000 + 167 T$	$-\text{S}-\text{S}-$	$46,000 - 28 T$
		$>\text{S}=\text{O}$	$-63,000 + 63 T$
	$100,000 + 180 T$	$-\text{SO}_2-$	$-282,000 + 152 T$
		$-\text{NO}_2$	$-41,500 + 143 T$
		$-\text{ONO}$	$-21,000 + 130 T$
HF	$-270,000 - 6 T$	$-\text{ONO}_2$	$-88,000 + 213 T$
$-F$	$-195,000 - 6 T$	3-ring	$100,000 - 122 T$

(continued)

¹ The data for sulphur, bromine and iodine compounds in Table 20.1 are different from the data in the original paper. In Table 20.1 the elements in their stable form at 25 °C and 1 bar are taken as reference states, as is usual in thermodynamics; in the original publication $\text{S}_2(\text{g})$, $\text{Br}_2(\text{g})$ and $\text{I}_2(\text{g})$ were taken as reference state.

Table 20.1 (continued)

Group	$\Delta G_f^\circ(T)$ (J/mol)	Group	$\Delta G_f^\circ(T)$ (J/mol)
HCl	-93,000 - 9 T	4-ring	100,000 - 110 T
-Cl	-49,000 - 9 T	5-ring	20,000 - 100 T
HBr	50,000 - 14 T	6-ring	-3,000 - 70 T
-Br	-14,000 - 14 T	Conjugation of double bonds	
HI	12,000 - 41 T	<i>cis-trans</i> Conversion	-18,000 + 16 T
-I	40,000 - 41 T		-6,000 + 7 T
HCN	130,000 - 34.5 T		
-CN	123,000 - 28.5 T		
C ₃ O ₂	-92,000 - 59 T	N ₂ O	81,000 + 75 T
CO	-111,000 - 90 T	NO	90,500 - 13 T
CO ₂	-394,500 - 2 T	NO ₂	33,000 + 63 T
COCl ₂	-221,000 + 47 T	HNO ₃	-130,000 + 208 T
COS	-140,000 - 85 T	NOCl	53,000 + 48 T
CS ₂	-111,500 - 152 T	N ₂ H ₄	92,000 + 223 T
S ₂ (g)	130,000 - 164 T	Br ₂ (g)	31,000 - 93 T
SO ₂	-300,000 + 0 T	I ₂ (g)	63,000 - 144 T
SO ₃	-400,000 + 95 T	(CN) ₂	310,000 - 44 T
SOC ₂	-215,000 + 59 T	H ₂ O ₂	-138,000 + 108 T
SO ₂ Cl ₂	-360,000 + 158 T	O ₃	142,000 + 70 T

Enthalpy of formation of large molecules.

20.2.1. Group contributions

In the system of Van Krevelen and Chermin the free enthalpy of formation is calculated from group contributions, with some corrections due to structural influences:

$$\Delta G_f^\circ = \sum_{\text{component groups}}^{\text{contributions of}} + \sum_{\text{corrections}}^{\text{structural}} \quad (20.17)$$

The group contributions are considered to be linear functions of the temperature:

$$\Delta G_{f,\text{group}}^\circ = \mathbf{A} + \mathbf{B}T \quad (20.18)$$

This assumption is based on an argumentation by Scheffer (1945, 1958). Eq. (20.18) shows a strong similarity to the general thermodynamic equation:

$$\Delta G = \Delta H - T\Delta S \quad (20.19)$$

If Eqs. (20.18) and (20.19) are compared it follows that **A** has the dimension of a heat of formation and **B** that of an entropy of formation. According to Ulich (1930):

$$\begin{aligned} \mathbf{A} &\approx \Delta H_f^\circ(298) \\ \mathbf{B} &\approx -\Delta S_f^\circ(298) \end{aligned} \quad (20.20)$$

It is not possible to describe accurately the temperature dependence of the free enthalpy of formation by the simple Eq. (20.18) over a very large temperature interval, by it is sufficiently accurate in the temperature interval of 300–600 K.

All group contributions and structural corrections are based on experimental data of Rossini et al. (1953), the free enthalpies of formation calculated agree with the literature values within 3 kJ. For non-hydrocarbons the accuracy is less good and deviations up to 12 kJ may occur.

All values for the free enthalpy of formation are as a rule standardised for the ideal gaseous state of 1 (bar), (Standard State; this ideal state is called *fugacity*). This also holds for the group contributions given.

The fugacity f is the pressure value needed at a given temperature to make the properties of a non-ideal gas satisfy the equation for an ideal gas, i.e. $f = \gamma p$, where γ is the fugacity coefficient and p is the pressure. For an ideal gas $\gamma = 1$.

Example 20.1

Estimate the free enthalpy of formation of gaseous 1,3-butadiene and of the (imaginary) gaseous polybutadiene.

Solution

The structural units are:

monomer: $\text{CH}_2=\text{CH}-\text{CH}=\text{CH}_2$
and

polymer: $-\text{CH}_2-\text{CH}=\text{CH}-\text{CH}_2-$

For the monomer we calculate

$$\begin{array}{rcl} 2(=\text{CH}_2) & 46,000 + 60 T \\ 2(=\text{CH}-) & 76,000 + 76 T \\ \text{conjugation} & -18,000 + 16 T \\ \hline & 104,000 + 152 T \end{array}$$

At 300 K this becomes: 149,600 J/mol; the literature value is 152,900. At 600 K we calculate: 195,200; the literature value is 197,800 (this leads to a temperature coefficient of 141 instead of 152).

For the (imaginary) gaseous polymer unit we calculate:

$$\begin{array}{rcl} 2(-\text{CH}_2-) & -44,000 + 204 T \\ 2(=\text{CH}-) & 76,000 + 76 T \\ \hline & 32,000 + 280 T \end{array}$$

The molar free enthalpy of polymerisation will be:

$$\Delta G = 32,000 + 280T - (104,000 + 152T) = -72,000 + 128T = \Delta H - T\Delta S$$

So that $\Delta H = -72,000 \text{ J/mol}$ and $\Delta S = -128 \text{ J/(mol K)}$.

The literature value for $\Delta H_{gg}(\text{pol})$ is -73,000 (Polymer Handbook) which is in excellent agreement with our calculation. Thermodynamically the polymerisation is possible at temperatures below

$$\frac{-72,000}{-128} = 562 \text{ K (290 }^\circ\text{C)}.$$

So the ceiling temperature of the polymerisation of $\text{CH}_2=\text{CH}-\text{CH}=\text{CH}_2$ to polybutadiene (1,4) is 290 °C.

20.2.2. Corrections for other physical states

If the reactants or the reaction products are not in the (ideal) gaseous state, but in a condensed state (the latter is always true for polymers), corrections have to be made (see Dainton and Ivin, 1950).

The corrections are clearly visualised by means of the diagrams of enthalpy and entropy levels, as shown in Fig. 20.4 for polymerisation reactions. The equations to be used can easily be deduced from these diagrams and are summarised in Table 20.2.

The experimental data available to deduce these correction factors are extremely scarce.

The following empirical rules of thumb may be used for the corrections to be made for polymerisation reactions:

$$\Delta G_{ga}^{\circ} \approx \Delta G_{gg}^{\circ} - 7,000 + 15T \quad (20.21)$$

$$\Delta G_{gc}^{\circ} \approx \Delta G_{gg}^{\circ} - 17,000 + 40T \quad (20.22)$$

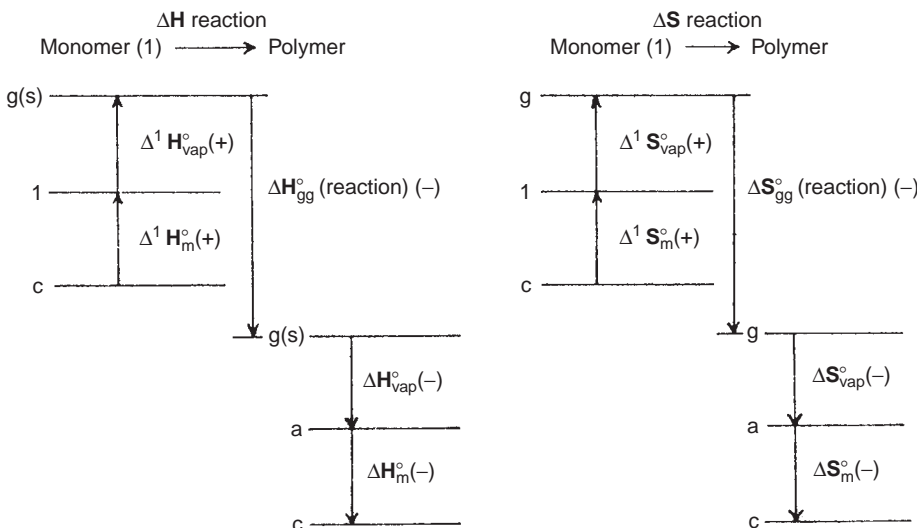


FIG. 20.4 Enthalpy and entropy levels of monomer and polymer in different physical states. Symbols: g = gaseous; l = liquid; a = amorphous; c = crystalline; s = dissolved; vap = vaporisation (condensation); m = melting (crystallisation); \circ = standard state (25°C , 1 bar).

TABLE 20.2 ΔH° - and ΔS° -corrections for the non-gaseous state

$\Delta H_{\text{polymerisation}}^{\circ}$	$\Delta S_{\text{polymerisation}}^{\circ}$
$\Delta H_{ga}^{\circ} = \Delta H_{gg}^{\circ} - \Delta H_{vap}^{\circ}$	$\Delta S_{ga}^{\circ} = \Delta S_{gg}^{\circ} - \Delta S_{vap}^{\circ}$
$\Delta H_{gc}^{\circ} = \Delta H_{gg}^{\circ} - \Delta H_{vap}^{\circ} - \Delta H_m^{\circ}$	$\Delta S_{gc}^{\circ} = \Delta S_{gg}^{\circ} - \Delta S_{vap}^{\circ} - \Delta S_m^{\circ}$
$\Delta H_{la}^{\circ} = \Delta H_{gg}^{\circ} + \Delta^1 H_{vap}^{\circ} - \Delta H_{vap}^{\circ}$	$\Delta S_{la}^{\circ} = \Delta S_{gg}^{\circ} + \Delta^1 S_{vap}^{\circ} - \Delta S_{vap}^{\circ}$
$\Delta H_{lc}^{\circ} = \Delta H_{gg}^{\circ} + \Delta^1 H_{vap}^{\circ} - \Delta H_{vap}^{\circ} - \Delta H_m^{\circ}$	$\Delta S_{lc}^{\circ} = \Delta S_{gg}^{\circ} + \Delta^1 S_{vap}^{\circ} - \Delta S_{vap}^{\circ} - \Delta S_m^{\circ}$
$\Delta H_{cc}^{\circ} = \Delta H_{gg}^{\circ} + \Delta^1 H_{vap}^{\circ} - \Delta H_{vap}^{\circ} + \Delta^1 H_m^{\circ} - \Delta H_m^{\circ}$	$\Delta S_{cc}^{\circ} = \Delta S_{gg}^{\circ} + \Delta^1 S_{vap}^{\circ} - \Delta S_{vap}^{\circ} + \Delta^1 S_m^{\circ} - \Delta S_m^{\circ}$

Notation: ΔH_{xy}° means: standard molar heat effect when monomer in state x is transformed into polymer in state y . ΔS_{xy}° means: standard molar entropy change, when monomer in state x is transformed into polymer in state y .

$$\Delta G_{la}^o \approx \Delta G_{gg}^o - 40T \quad (20.23)$$

$$\Delta G_{lc}^o \approx \Delta G_{gg}^o + 8,000 - 30T \quad (20.24)$$

$$\Delta G_{cc}^o \approx \Delta G_{gg}^o - 40T \quad (20.25)$$

where the symbol ΔG_{xy}^o means the molar free enthalpy change when a monomer in state x is transformed into a polymer in state y.

Example 20.2

Estimate the free enthalpy of polymerisation of 1,3-butadiene to polybutadiene (1:4) when the monomer is in the liquid state and the polymer is in the amorphous solid state.

Solution

From Example 20.1 we derive:

$$\Delta G_{gg}^o(\text{pol}) = -72,000 + 128T$$

Eq. (20.23) gives

$$\Delta G_{la}^o \approx \Delta G_{gg}^o - 40T$$

so that

$$\Delta G_{la}^o \approx -72,000 + 88T$$

or

$$\Delta H_{la}^o \approx -72,000 \text{ J/mol} \quad \text{and} \quad \Delta S_{la}^o \approx -88 \text{ J/(mol K)}$$

The literature value (Polymer Handbook) is:

$$\Delta H_{la}^o = -73,000 \text{ J/mol} \quad \text{and} \quad \Delta S_{la}^o = -88.8 \text{ J/(mol K)}.$$

so that the agreement is excellent.

20.3. THERMODYNAMICS OF FREE RADICALS

Many polymerisation and polymer degradation reactions proceed by radical mechanisms. Therefore it is important to know the thermodynamical data of free radicals in comparison with the bonded groups.

For the simple radicals these data are known from studies of flame reactions. Furthermore the dissociation energies of chemical bonds have been determined by thermochemical measurements. Table 20.3 provides the full information on these bond dissociation energies.

Finally, it is empirically known that the entropy change of simple bond breaking reactions is about 160 entropy units, so that the entropy change per free radical formed is about 80 entropy units (for atoms the latter value is about 40 e.u.).

By means of these empirical data it is possible to estimate the free enthalpy of radicals. These data are summarised in Table 20.4 for those radicals that are of interest in polymer chemistry (see Sawada, 1969).

TABLE 20.3 X-Y bond dissociation energies (kJ/mol)

H	F	Cl	Br	I	CH ₃	-CH ₂ -C(C)	$\begin{array}{c} \text{(C)} \\ \\ \text{-C-H} \\ \\ \text{(C)} \end{array}$	$\begin{array}{c} \text{(C)} \\ \\ \text{-C-C(C)} \\ \\ \text{(C)} \end{array}$	$\text{-CH}_2\text{-}\text{C}_6\text{H}_5$	-CH=CH ₂	-C≡CH	-CF ₃	-CCl ₃	-OH	-O-(C)	-CH=O	O=C-(C)	$\begin{array}{c} \text{O} \\ \\ \text{-C-O-} \\ \\ \text{(C)} \end{array}$	$\begin{array}{c} \text{O} \\ \\ \text{-C-O-} \\ \\ \text{(C)} \end{array}$	-NH ₂	-NH-(C)	(CH ₃) ₂ C(C)	-CN	-SH	-S-(C)					
432	566	128	363	296	436	111	394	381	469	335	436	507	444	402	499	427	365	360	354	469	432	385	360	377	369	H				
	159	251	235	218	453	444	440	427	524	377			541	444	247											F				
		239	218	208	352	339	339	331	419	285	360		356	306		205		344							272	Cl				
				180	293	289	285	264	335	214			293	226			281								Br					
				149	235	222	222	210	272	168	230		226				214								I					
					369	356	348	335	427	302	377	419	419		381	335	314	344			331		461		CH ₃					
						337	327	314	381	260	377	457		381	335	297	323		327							-CH ₂ -C(C)				
							318	306	348	230	356	432		385	339				323							(CH ₃) ₂ C(C)				
								293	327		339			381	327				323							(CH ₃) ₂ C(C)				
									432	323	423	499		469	423	377			419			545				-C ₆ H ₅				
										197	293			323		210	264	230		272			398				-CH ₂ -C ₆ H ₅			
										423												507				-CH=CH ₂				
											461															-C≡CH				
											406															-CF ₃				
												365														-OCF ₃				
													214		419	427										-OH				
														142													-O-(C)			
															251	251	247		377								-CH=O			
																251			411								O=C-(C)			
																	126									-C(=O)O-				
																		155									-NH ₂			
																			176									(CH ₃) ₂ C(C)		
																				608								-CN		
																					126								-SH	
																						264								-S-(C)

NB. The dissociation energy is lowered if the dissociating bond is in conjugation with a π-electron system.

System	Decrease of bond dissociation energy
C=C	≈67
C ₆ H ₅	≈67
>C=O	≈42

TABLE 20.4 Free enthalpies of free radicals and radical groups

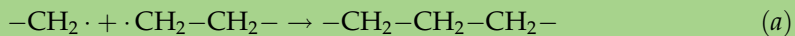
Radical or radical group	$\Delta G^\circ (T) (\text{J/mol})$
H	218,000 – 49.4 T
F	80,000 – 57 T
Cl	121,000 – 54 T
Br	112,000 – 99 T
I	107,000 – 112 T
CH ₃	134,000 + 9 T
CH ₂ –	142,000 – 4 T
CH<	150,000 + 38 T
.C\backslash	159,000 + 63 T
OH	38,000 – 6 T
O–	33,500 – 8 T
.C=O	21,000 – 42 T
.OC=O	-11,000 + 42 T
.HNC=O	17,000 + 42 T
CN	460,000 – 63 T
O–O–	31,500

Example 20.3

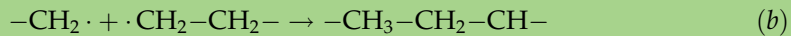
As an illustration of its use, we shall estimate the thermodynamic preference for two mechanisms of inter-radical reactions, viz. recombination and disproportionation. (This is of importance in Chaps. 21 and 22)

Solution

The reactions are:



or



From the group contributions can be calculated
for reaction (a)

$$\begin{aligned} \Delta G^\circ &= \Delta G^\circ(-\text{CH}_2-) - 2\Delta G^\circ(-\text{CH}_2) = (-44,000 + 204T) - (284,000 - 8T) \\ &= -328,000 + 212T \end{aligned}$$

for reaction (b)

$$\begin{aligned}
 \Delta G^\circ &= \Delta G^\circ(-\text{CH}_3) + \Delta G^\circ(\text{CH}_2=) + \Delta G^\circ(=\text{CH}-) - 2\Delta G^\circ(-\text{CH}_2\cdot) - \Delta G^\circ(-\text{CH}_2-) \\
 &= (-46,000 + 95T + 23,000 + 30T + 38,000 + 38T) \\
 &\quad -(284,000 - 8T - 22,000 + 102T) \\
 &= -247,000 + 69T
 \end{aligned}$$

so that the free enthalpy difference between the two reactions is:

$$\Delta(\Delta G^\circ) = -81,000 + 143 T \text{ so that } \Delta(\Delta G^\circ) = 0 \text{ at } 567 \text{ K}$$

So above 567 K = 294 °C disproportionation is preferred, below 567 K recombination.

BIBLIOGRAPHY

General references

Chemical thermodynamics

- De Nevers N, "Physical and Chemical Equilibrium for Chemical Engineers", Wiley, New York, 2002.
 De Voe H, "Thermodynamics and Chemistry", Prentice Hall, Upper Saddle River, 2001.
 Janz GJ, "Estimation of Thermodynamic Properties of Organic Compounds", Academic Press, New York, 1967.
 Kaufman M, "Principles of Thermodynamics", Dekker, New York, 2002.
 Klotz IM, "Chemical Thermodynamics", Wiley, New York, 2000.
 Levor T, "Chemical Thermodynamics", Blackwell Science, Oxford, 1999.
 Lewis GN and Randall M, "Thermodynamics", Rev by Pitzer KS and Brewer L, McGraw-Hill, New York, 2nd Ed, 1961.
 Parks GS and Huffman HM, "The Free Energies of Some Organic Compounds", Chem Cat Co, New York, 1932.
 Reid RC, Prausnitz JM and Sherwood TK, "The Properties of Gases and Liquids", McGraw-Hill, New York, 4th Ed, 1987.
 Rossini FD, "Chemical Thermodynamics", Wiley, New York, 1950.
 Rossini FD et al., "Selected Values of Chemical Thermodynamic Properties", Natl Bur Standards Circ 500, US Printing Office, Washington, 1952.
 Rossini FD et al., "Selected Values of Physical and Thermodynamic Properties of Hydrocarbons and Related Compounds", Carnegie Press, Pittsburgh, 1953.
 Schottky, in Gemeinschaft mit Ulich H, und Wagner C, "Thermodynamik", Springer, Berlin, 1973 (Facsimile Edition of Springer, Berlin, 1930).
 Stull DR, Westrum EF and Sinke GC, "The Chemical Thermodynamics of Organic Compounds", Wiley, New York, 1969.
 Wunderlich B, Cheng SZD and Loufakis K, "Thermodynamic Properties of Polymers", in Mark HF, Bikales NM, Overberger CG, Menges G and Kroschwitz JI (Eds), "Encyclopaedia of Polymer Science and Engineering", Wiley, New York, Vol. 16, 1989, pp 767-807.

Thermodynamics of polymerisation

- Busfield WK, "Heats and Entropies of Polymerization, Ceiling Temperatures and Equilibrium Monomer Concentrations, and Polymerizability of Heterocyclic Compounds", in Brandrup J and Immergut EH et al. (Eds), "Polymer Handbook", Wiley, New York, 4th Ed, 2005, Part II.
 Ivin KJ, "Heats and Entropies of Polymerization, Ceiling Temperatures and Equilibrium Monomer Concentrations", in "Polymer Handbook", Brandrup J and Immergut EH (Eds), Interscience, New York, 2nd Ed, 1975, Part II pp 421-450.
 Sawada H, "Thermodynamics of Polymerization", J Macromol Sci, Revs Macromol Chem C3 (1969) 313-396; C5 (1970) 151-174; C7 (1972) 161-187; C8 (1972) 236-287.

Chemical kinetics

- Bamford CH and Tipper CFH (Eds), "Comprehensive Kinetics", Elsevier, Amsterdam, 1969.
 Billing GD and Mikkelsen KV, "Introduction to Molecular Dynamics and Chemical Kinetics", Wiley, New York, 1996.
 Boudart M, "Kinetics of Chemical Processes", Prentice-Hall, Englewood, NJ, 1968.
 Burnett GM, "Mechanism of Polymer Reactions", Interscience, New York, 1954.

- Espenson JH, "Chemical Kinetics and Reaction Mechanisms", McGraw-Hill, New York, 1995.
Fransisco JS, Steinfeld JI and Hase WL, "Chemical Kinetics and Dynamics", Prentice Hall, Englewood Cliffs, 1989.
Glasstone S, Laidler KJ and Eyring H, "The Theory of Rate Processes", McGraw-Hill, New York, 1941.
Kuhn H and Dieter HD, "Principles of Physical Chemistry", Wiley, Chichester, 2000.
Lefler JE and Grunwald E, "Rates and Equilibria of Chemical Reactions", Wiley, New York, 1963.
Masel RI, "Chemical Kinetics and Catalysis", Wiley New York, 2001.
Missen RW, Mims CA and Saville BA, "Introduction to Chemical Reaction Engineering and Kinetics", Wiley, New York, 1999.

Bond strength and formation free radicals

- Franklin JL, "Prediction of Rates of Chemical Reactions Involving Free Radicals", Brit Chem Eng 7 (1962) 340.
Mortimer CT, "Reaction Heats and Bond Strengths", Pergamon Press, London, 1962.

Special references

- Anderson JW, Beyer GH and Watson KM, Natl Petr News 36R (1944) 476.
Bremner JGM and Thomas GD, Trans Faraday Soc 44 (1948) 230.
Dainton FS and Ivin KJ, Trans Faraday Soc 46 (1950) 331.
Franklin JL, Ind Eng Chem 41 (1949) 1070.
Ivin KJ, J Polym Sci, Part A, Polym Chem, 38 (2000) 2137.
Scheffer FEC, "Toepassing van de Thermodynamica op Chemische Processen", Waltman, Delft, 1945; Diepen, GAM, 2nd Ed, 1958.
Souders M, Matthews CS and Hurd CO, Ind Eng Chem 41 (1949) 1037.
Ulich H, "Chemische Thermodynamik", Dresden, Leipzig, 1930.
Van Krevelen DW and Chermin HAG, Chem Eng Sci 1(2) (1951) 66; 1(5) (1952) 238.

CHAPTER 21

Thermal Decomposition

The heat resistance of a polymer may be characterised by its temperatures of "initial" and of "half" decomposition. The latter quantity is determined by the chemical structure of the polymer and can be estimated by means of an additive quantity: the molar thermal decomposition function. The amount of char formed on pyrolysis can be estimated by means of another additive quantity: the molar char-forming tendency.

21.1. INTRODUCTION

Polymer degradation is a change in the properties – tensile strength, colour, shape, etc. – of a polymer or polymer based product under the influence of one or more environmental factors such as heat, light or chemicals. In a finished product such a change is to be prevented or delayed. On the other hand, however, the degradation process can be useful from the view points of understanding the structure of a polymer or recycling/reusing the polymer waste to prevent or reduce environmental pollution.

The way in which a polymer degrades under the influence of thermal energy in an inert atmosphere is determined, on the one hand, by the chemical structure of the polymer itself, on the other hand by the presence of traces of unstable structures (impurities or additions).

Thermal degradation does not occur until the temperature is so high that primary chemical bonds are separated. It begins typically at temperatures around 150–200 °C and the rate of degradation increases as the temperature increases. Pioneering work in this field was done by Madorsky and Straus (1954–1961), who found that some polymers (poly (methyl methacrylate), poly(α -methylstyrene) and poly (tetrafluoroethylene)) mainly form back their monomers upon heating, while others (like polyethylene) yield a great many decomposition products.

The types of polymer degradation can be divided into three general categories: *chain depolymerisation*, *random scission* and *substituent reactions*.

21.2. THERMAL DEGRADATION

For many polymers thermal degradation is characterised by the breaking of the weakest bond and is consequently determined by a bond dissociation energy. Since the change in entropy is of the same order of magnitude in almost all dissociation reactions, it may be

assumed that also the activation entropy will be approximately the same. This means that, in principle, the bond dissociation energy determines the phenomenon. So it may be expected that the temperature at which the same degree of conversion is reached will be virtually proportional to this bond dissociation energy. The numerical values of the bond dissociation energy are given in Chap. 20 (Table 20.3).

Table 21.1 summarises the most important data about the thermal degradation of polymers; these data are mainly taken from Madorsky and Strauss and from Korshak et al. (1968, 1971) and Arnold (1979).

In Fig. 21.1 the dissociation energy of the weakest bond of the same polymers, supplemented with the data of a number of radical initiators (peroxides and azo compounds) is plotted against the most characteristic index of the heat resistance, viz. the temperature of "half decomposition" ($T_{d,1/2}$). The relationship is evident, though not sufficiently accurate for a reliable estimate of $T_{d,1/2}$.

TABLE 21.1 Thermal Degradation of Polymers (I)

Polymer	$T_{d,o}$ (K)	$T_{d,1/2}$ (K)	$T_{d,1/2}/T_{d,o}$	E_{act} (kJ/mol)	Monomer yield (%)	k at 350 °C (%/min)	Char yield (%)
Poly(methylene)	660	687	1.04	300	0	4×10^{-3}	0
Poly(ethylene) (branched)	653	677	1.04	264	0	8×10^{-3}	0
Poly(propylene)	593	660	1.12	243	0	7×10^{-2}	0
Poly(isobutylene)	–	621	–	205	20	2.7	0
Poly(styrene)	600	637	1.06	230	~50	0.25	0
Poly(<i>m</i> -methyl styrene)	–	631	–	234	45	0.90	0
Poly(α -methyl styrene)	–	559	–	230	>95	228	0
Poly(vinyl fluoride)	623	663	1.06	–	–	–	–
Poly(vinyl chloride)	443	543	1.23	134	0	170	22
Poly(trifluoro ethylene)	673	685	1.02	222	~1	2×10^{-2}	–
Poly(chloro-trifluoro ethylene)	–	653	–	239	27	4×10^{-2}	–
Poly(tetrafluoro ethylene)	–	782	–	339	>95	2×10^{-6}	0
Poly(vinyl cyclohexane)	–	642	–	205	0.1	0.45	0
Poly(vinyl alcohol)	493	547	1.11	–	0	–	7
Poly(vinyl acetate)	–	542	–	–	0	–	–
Poly(acrylonitril)	563	723	1.28	–	–	–	15
Poly(methyl acrylate)	–	601	–	–	0	10	0
Poly(methyl methacrylate)	553	610	1.10	218	95	5.2	0
Poly(butadiene)	553	680	1.23	260	2	2×10^{-2}	0
Poly(isoprene)	543	596	1.10	250	–	–	0
Poly(<i>p</i> -phenylene)	> 900	> 925	–	–	0	–	85
Poly(benzyl)	–	703	–	209	0	6×10^{-3}	–
Poly(<i>p</i> -xylylene) = poly (<i>p</i> -phenylene-ethylene)	–	715	–	306	0	2×10^{-3}	–

(continued)

TABLE 21.1 (continued)

Polymer	$T_{d,o}$ (K)	$T_{d,1/2}$ (K)	$T_{d,1/2}/T_{d,o}$	E_{act} (kJ/mol)	Monomer yield (%)	k at 350 °C (%/min)	Char yield (%)
Poly(ethylene oxide)	—	618	—	193	0	2.1	0
Poly(propylene oxide)	—	586	—	147	1	5/20	0
Poly(2,6-dimethyl p-phenylene oxide)	723	753	1.04	—	0	—	25
Poly(ethylene terephthalate)	653	723	1.11	—	0	—	17
Poly(dian terephthalate)	673	~750	~1.11	—	0	—	20
Poly(dian carbonate)	675	~750	~1.11	117?	0	—	30
Poly(hexamethylene adipamide)	623	693	-1.11	—	—	—	0
Poly(ϵ -caproamide) (Nylon 6)	623	703	1.13	180	—	—	0
Poly(p-phenylene terephthalamide)	~720	~800	~1.11	—	—	—	~40
Poly (pyromellitide) (Kapton)	723	~840	~1.16	—	—	—	70
Poly(m-phenylene 2,5-oxadiazole)	683	~800	1.17	—	—	—	30
Cellulose	500	600	1.200	210	—	—	7

21.2.1. Phenomenology of the thermal decomposition

The process of thermal decomposition or pyrolysis is characterised by a number of experimental indicators:

- The temperature of initial decomposition ($T_{d,o}$). This is the temperature at which the loss of weight during heating is just measurable (inclination point of the loss of weight/temperature curve).
- The temperature of half decomposition ($T_{d,1/2}$). This is the temperature at which the loss of weight during pyrolysis (at a constant rate of temperature rise) reaches 50% of its final value.
- The temperature of the maximum rate of decomposition ($T_{d,max}$), measured as the rate of loss of weight (at a standardised rate of temperature rise).
- The average energy of activation ($E_{act,d}$), determined from the temperature dependence of the rate of loss of weight.
- The amount of char residue at the end of the pyrolysis (at a standard temperature, normally 900 °C).

These indicators, especially the characteristic temperatures, are dependent on the rate of heating (rise of temperature) applied during the pyrolysis (normally about 3 K/min or 5×10^{-2} K/s). At increasing rate of heating the characteristic temperature shifts to a higher value.

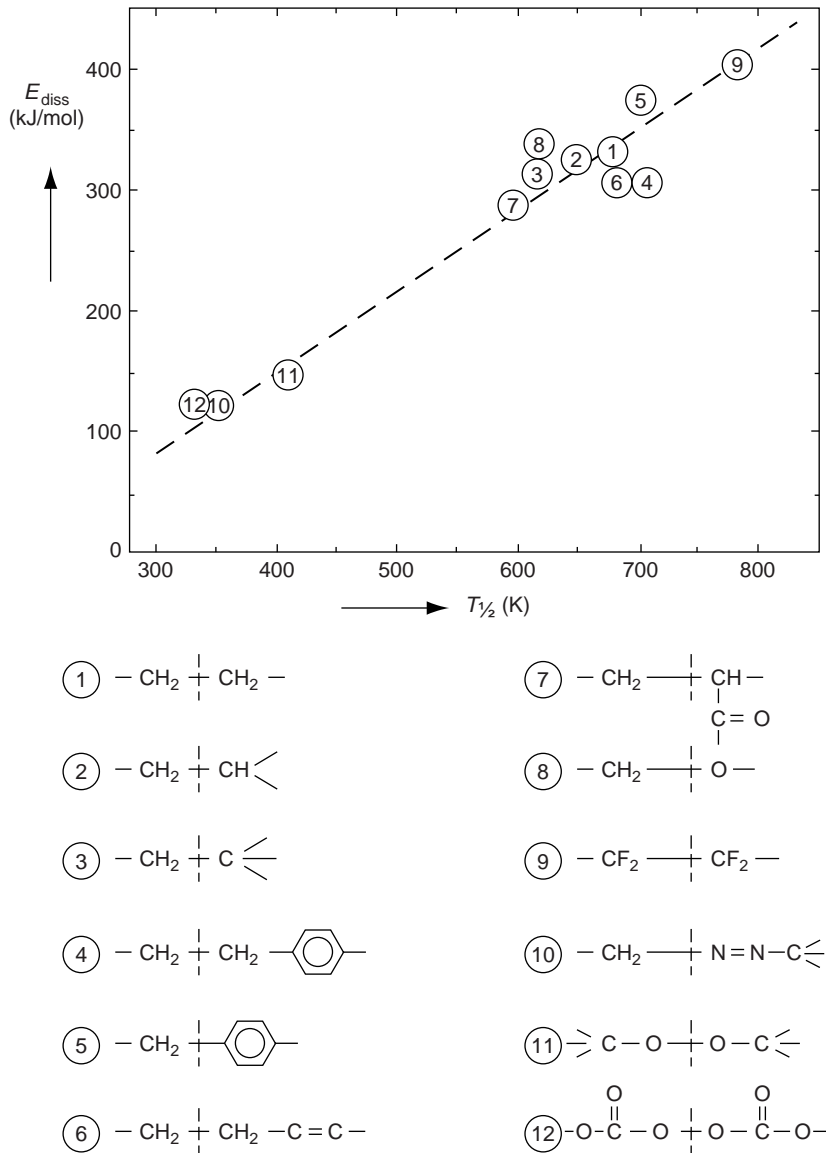


FIG. 21.1 Correlation between temperatures of half decomposition and dissociation energy of weakest bond.

Table 21.1 shows measured values of the main indices. They appear to be interrelated:

$$T_{d,1/2}/T_{d,o} \approx 1.13 \pm 0.07 \quad (21.1)$$

$$T_{d,max} \approx T_{d,1/2} \quad (21.2)$$

$$E_{act,d} \approx AT_{d,1/2} - 423 \quad (21.3)$$

where $A \approx 1 \text{ kJ}/(\text{mol K})$

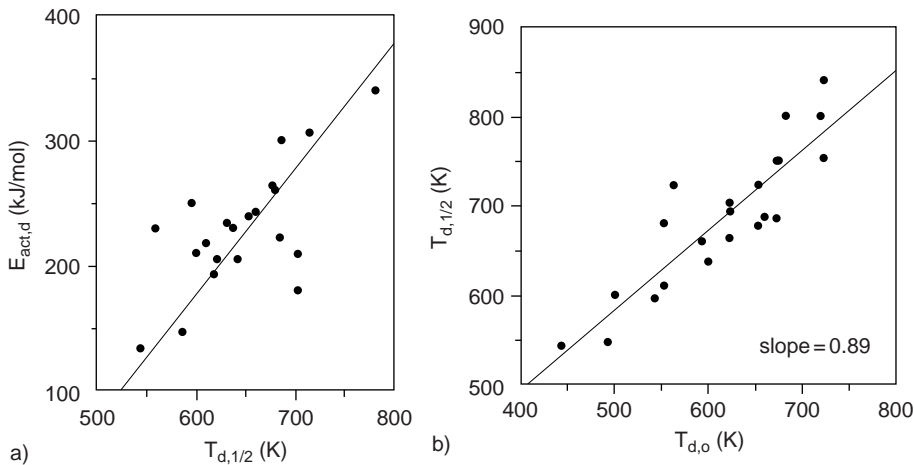


FIG. 21.2 Relationships between (A) the activation energy of decomposition, $E_{act,d}$ and the characteristic decomposition temperature $T_{d,1/2}$ and (B) the characteristic decomposition temperature $T_{d,1/2}$ and the temperature of initial decomposition $T_{d,o}$.

The latter relationship is shown in Fig. 21.2A; it is not very accurate, partially because $E_{act,d}$ proves to vary in a number of cases during the pyrolysis (least squares fit leads to $E_{act,d} = 0.6T_{d,1/2} - 149$ with $cc = 0.68$). The relation between $T_{d,1/2}$ and $T_{d,o}$ is shown in Fig. 21.2B.

The amount of char residue will be subject of a separate discussion.

21.2.2. An additive molar function for the thermal decomposition: $\mathbf{Y}_{d,1/2}$

Van Krevelen (1987) found that the relationship between the chemical structure of polymers and their characteristic temperature of decomposition, $T_{d,1/2}$, may be approached in the same way as we have got to know for other characteristic temperatures, viz. T_g and T_m . The product $M \cdot T_{d,1/2}$ (M =molecular weight of monomer) proves to have additive properties:

$$MT_{d,1/2} \equiv \mathbf{Y}_{d,1/2} = \sum_i N_i \mathbf{Y}_{d,1/2,i} \quad (21.4)$$

Table 21.2 gives the group contributions for this additive function, which is coined: *Molar Thermal Decomposition Function*. The analogy of $\mathbf{Y}_{d,1/2}$ with \mathbf{Y}_g and \mathbf{Y}_m is striking indeed: also in the increments of $\mathbf{Y}_{d,1/2}$, an important effect for conjugation of π -electrons is found, resulting in two or three numerical values of the contributions of the same group, as conjugation with a neighbouring group is absent, one-sided or two-sided. The same is true for the effect of bulky groups. Table 21.3 gives the comparison of the experimental and calculated values of $T_{d,1/2}$ for the series of polymers mentioned in Table 21.1. The agreement is satisfactory.

21.2.3. The overall mechanism of the thermal decomposition

As mentioned earlier, there are three types of thermal decomposition: chain depolymerisation, random decomposition and degradation by substituents reactions.

TABLE 21.2 Group contributions to $\{Y_{d,1/2}\}$ (K kg/mol)

Group	$(Y_{d,1/2})_i$	Group	$(Y_{d,1/2})_i$
$-\text{CH}_2-$	9.5		$\begin{cases} 44 \\ 52 \\ 65 \end{cases}$
$-\text{CH}(\text{CH}_3)-$	18.5		$\begin{cases} 54 \\ 62 \\ 75 \end{cases}$
$-\text{CH}(\text{C}_6\text{H}_{11})-$	60		
$-\text{CH}(\text{C}_6\text{H}_5)-$	56.5		82
$-\text{CH}(\text{COOCH}_3)-$	42.5		
$-\text{CH}(\text{OCOCH}_3)-$	37.5		87
$-\text{C}(\text{CH}_3)_2-$	$\begin{cases} 25.5 \\ 30 \\ 35 \end{cases}$		93
$-\text{C}(\text{CH}_3\text{C}_6\text{H}_5)-$	56		
$-\text{C}(\text{CH}_3)(\text{COOCH}_3)-$	51		83
$-\text{CHF}-$	18		
$-\text{CHCl}-$	23.5		111
$-\text{CH}(\text{CN})-$	28		
$-\text{CH}(\text{OH})-$	14		103
$-\text{CF}_2-$	38.5		
$-\text{CFCl}-$	(39)		119
$-\text{CCl}_2-$	39		
$-\text{CH}=\text{CH}-$	18		135
		$-\text{O}-$	8
		$-\text{NH}-$	16
$-\text{HC}=\overset{\text{CH}_3}{\text{C}}-$	21.5	$-\text{S}-$	(33)

(continued)

TABLE 21.2 (continued)

Group	$(Y_{d,1/2})_i$	Group		$(Y_{d,1/2})_i$
	{ 14 20 26	Benzoxazole		110
	{ 20 25	Benzthiazole		125
	{ 30 37	Benzimidazole		105
	(30)	Quinoxaline		100
	32.5			
	(40)	Phthalimide		(150)
	(60)	Diimidazo-benzene		130
	(50)			
1,3,4-Oxadiazole	50	Pyromellit-imide		200
1,3,4-Thiadiazole	60	Tetra-azapryrene		185
1,2,4-Triazole	(60)	Benzo-imido-pyrrolone		190

Chain depolymerisation is the successive release of monomer units from a chain end or at a weak link, which is essentially the reverse of chain polymerisation; it is often called *depropagation* or *unzipping*. This depolymerisation begins at the ceiling temperature. A “weak link” may be a chain defect, such as an initiator fragment, a peroxide or an ether linkage arising as impurities from polymerisation in the presence of oxygen.

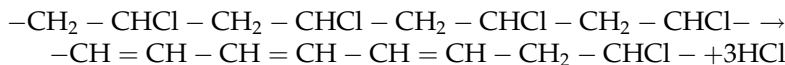
TABLE 21.3 Thermal degradation of polymers (II)

Polymer	$T_{d,1/2}$ exp. (K)	M (g/mol)	$\Upsilon_{d,1/2}$		$T_{d,1/2}$ calc. (K)
			Exp. (Kkg/mol)	Calc.	
Poly(methylene)	687	14	9.6	9.5	680
Poly(ethylene) (branched)	677	28	19	19	680
Poly(propylene)	660	42	28	28	665
Poly(isobutylene)	621	56	35	35	625
Poly(styrene)	637	104	66	66	630
Poly(m-methyl styrene)	631	118	75	75.5	640
Poly(α -methyl styrene)	559	118	66	65.5	555
Poly(vinyl fluoride)	663	46	30	27.5	600
Poly(vinyl chloride)	543	62.5	34	33	530
Poly(trifluoro ethylene)	682	82	56	56.5	690
Poly(chloro-trifluoro ethylene)	653	116.5	76	77.5	600
Poly(tetrafluoro ethylene)	782	100	78	77	770
Poly(vinyl cyclohexane)	642	110	70	69.5	630
Poly(vinyl alcohol)	547	44	24	23.5	535
Poly(vinyl acetate)	542	86	47	47	545
Poly(acrylonitril)	723	53	38	37.5	708
Poly(methyl acrylate)	601	86	52	52	605
Poly(methyl methacrylate)	610	100	61	60.5	605
Poly(butadiene)	680	54	37	37	688
Poly(isoprene)	596	68	40	41	605
Poly(p-phenylene)	925	76	70	75	985
Poly(benzyl)	703	90	64	63.5	705
Poly(p-xylylene) = poly(p-phenylene ethylene)	715	104	74.5	72	695
Poly(ethylene oxide)	618	44	27	27	615
Poly(propylene oxide)	586	58	33	33.5	578
Poly(2,6-dimethyl p-phenylene oxide)	753	120	90	90	750
Poly(ethylene terephthalate)	723	192	139	138	720
Poly(dian terephthalate)	(750)	358	268	262	735
Poly(dian carbonate)	(750)	254	190	173	683
Poly(hexamethylene adipamide)	693	226	156	160	635
Poly(ϵ -caproamide) (Nylon 6)	703	113	79	80	635
Poly(p-phenylene terephthalamide)	800	238	190	189	798
Poly(pyromellitide) (Kapton)	840	382	320	316	830
Poly(m-phenylene 2,5-oxadiazole)	800	144	115	115	720
Cellulose	600	162	98	—	—

depolymerisation is characterised by a) the major product is monomer, b) the decrease of degree of polymerisation is initially negligible, and accordingly the mechanical properties do not deteriorate fast and c) the rate of depolymerisation gradually decreases (Welsh, 1996). A well-known example is the crackle of Poly(methyl methacrylate) due to explosion of liberated monomer, when a sample is held close to a burning candle. The easy depolymerisation of Poly(oxy methylene) is prevented by end capping the polymer with the aid of vinyl acetate.

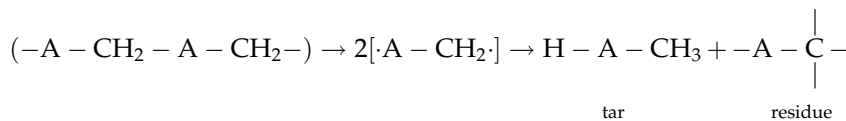
Random degradation occurs by chain rupture at random points along the chain, giving a disperse mixture of fragments which are usually large compared with the monomer unit. Random scission is characterised by a) the major products are typically fragments with molecular weights up to several hundreds (monomers, dimers, trimers, etc.), b) the decrease of molecular weight is initially appreciable, and accordingly the mechanical properties deteriorate rather fast and c) the rate of degradation is initially rapid and approaches a maximum (Welsh, 1996). Typical examples are Polyethylene and Polypropylene. Random scission may be considered as the reverse of polycondensation reactions where all kinds of oligomers react with each other to increase the molecular weight of the polymer. These two types of thermal degradation may occur separately or in combination; the latter case is rather normal. Chain depolymerisation is often the dominant degradation process in vinyl polymers, whereas the degradation of condensation polymers is mainly due to random chain rupture.

Degradation by substituent reactions occurs by modification or elimination of substituents attached to the polymer backbone. Accordingly volatile products are not monomers, but, e.g. hydrogen chloride in the case of Poly(vinyl chloride). This polymer undergoes degradation reactions in oxygen free circumstances, e.g. during extrusion, at processing temperatures of 200 °C, where it loses HCl quite easily, under the formation of polymer backbones with conjugated double bonds, e.g. as:



Accordingly, the degree of polymerisation of the degraded polymer is not decreased, but a deeply red to violet coloured PVC material is obtained

The overall mechanism of *thermal decomposition* or *pyrolysis* of polymers has been studied by Wolfs et al. (1959, 1960). They used polymers in which the link between the structural units (CH_2 bridges) was radioactive, so that the course of decomposition could be traced by radioactivity measurements in gas and residue, together with chemical and elementary analysis. In all cases the thermal degradation is a free radical reaction. The basic mechanism of pyrolysis is sketched in Fig. 21.3. In the first stage of pyrolysis (<550 °C) a disproportionation takes place. Part of the decomposing material is enriched in hydrogen and evaporated as tar and primary gas, the rest forming the primary char. In the second phase (>550 °C) the primary char is further decomposed, i.e. mainly dehydrogenated, forming the secondary gas and final char. During the disproportionation reaction, hydrogen atoms of the aliphatic parts of the structural units are "shifted" to "saturate" part of the aromatic radicals, as is visualised by the simplified scheme:



where A is an aromatic nucleus.

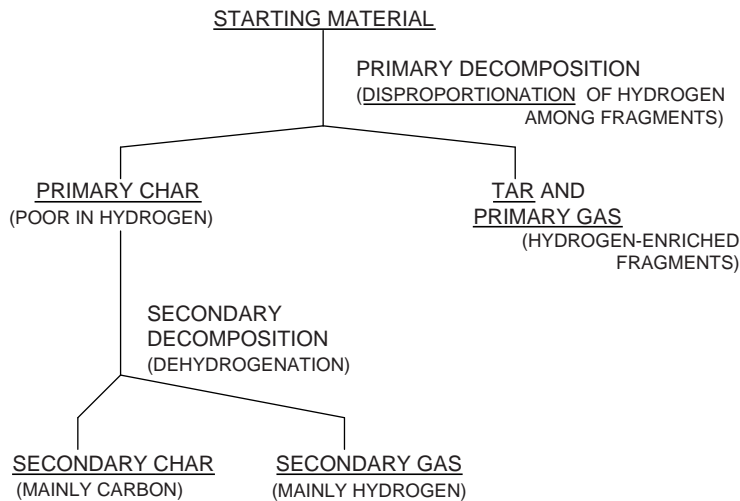


FIG. 21.3 Basic mechanism of pyrolysis.

The hydrogen shift during disproportionation is highly influenced by the nature of the structural groups. Groups which are capable of reacting with H atoms of the aromatic nucleus give rise to post-condensation (cross-linking); this occurs if the aromatic nucleus also contains --OH or $=\text{O}$ groups. The char residue then is higher than in the case of non-substituted aromatic units. On the other hand, if the aromatic nucleus contains alkyl groups, the alkyl hydrogen may act as an extra source of hydrogen atoms; the formation of tar is enhanced in this case.

21.3. CHAR FORMATION

21.3.1. An additive molar function for the char-forming tendency: c_{ft}

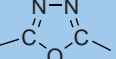
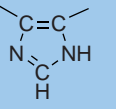
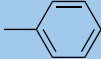
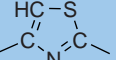
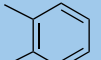
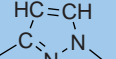
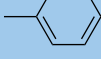
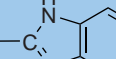
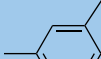
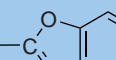
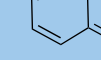
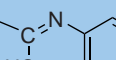
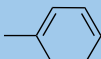
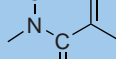
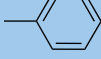
The results of pyrolysis experiments with nearly 100 polymers enabled Van Krevelen (1975) to quantify the *char-forming tendency*, defined as the amount of char per structural unit divided by 12 (the atomic weight of carbon), i.e. the amount of C equivalents in the char per structural units of polymer.

This char-forming tendency proved to be an additive quantity. Each structural group in principle contributes to the char residue in its own characteristic way. Aliphatic groups, connected to aromatic nuclei, show a negative char-forming tendency, since they supply hydrogen for the disproportionation reaction ("H shift"). Table 21.4 gives the char-forming tendency (C_{FT}) of the different structural groups.

The use of the additive molar C_{FT} function is restricted to polymers exempt from halogen. Halogen atoms are in-built soot formers (and consequently in-built flame retardants in the presence of oxygen) engaged in secondary reactions, thus influencing the char formation markedly.

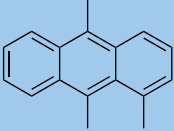
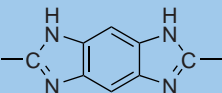
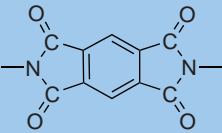
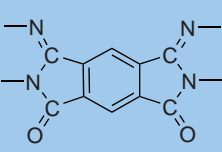
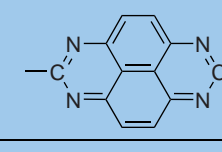
We want to emphasise that the char-forming tendency is a statistical concept. The fact that the phenyl group has a C_{FT} value of 1 C equivalent means that on the average only one out of six phenyl groups in the polymer goes into the residue (five going into the tar and gas).

TABLE 21.4 Group contributions to char formation

Group	Contribution to residue per structural unit C _{FT}	Do. in C-equiv	Group	Contribution to residue per structural unit C _{FT}	Do. in C-equiv
"All" aliphatic groups	0	0		12	1
-CHOH- (exception)	4	1/3		36	3
	12	1		42	3½
	24	2		42	3½
	36	3		84	7
	48	4		84	7
	60	5		108	9
	72	6		132	11
	96	8			
	60	5			
	72	6			
	120	10			

(continued)

TABLE 21.4 (*continued*)

Group	Contribution to residue per structural unit C_{FT}	Do. in C-equiv	Group	Contribution to residue per structural unit C_{FT}	Do. in C-equiv
	168	14		120	10
Correction due to disproportioning (H-shift):				144	12
>CH ₂ and >CH-CH ₂ -	-12	-1		120	10
-CH ₃	-18	-1½		180	15
>C(CH ₃) ₂	-36	-3			
-CH(CH ₃) ₃	-48	-4			

If the benzene ring contains four side groups (i.e. if four hydrogen atoms are substituted), all the rings land in the residue. If the benzene group contains two side groups, the amount going into residue depends on the distance between the side groups: if ortho, meta or para hydrogen atoms are substituted, the C_{FT} values are 2, 3 or 4 C equivalents, respectively. By means of the group contributions to the char-forming tendency, the *char residue* on pyrolysis can be estimated:

$$CR(\text{in weight\%}) = \frac{\sum_i (C_{FT})_i}{M} 1200 \quad (21.5)$$

The standard deviation from the experimental values for the polymers investigated is 3.5%. Fig. 21.4 shows the CR values experimentally found and calculated by means of Table 21.4. The agreement is satisfactory.

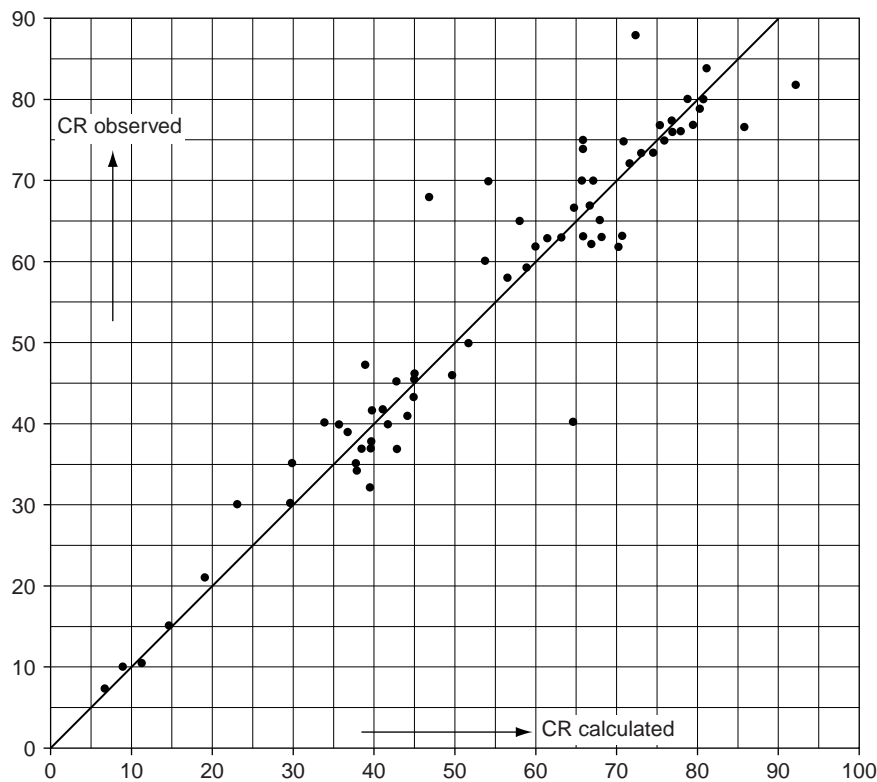


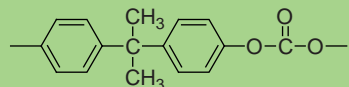
FIG. 21.4 Calculated versus observed CR-values.

Example 21.1

Estimate the char residue on pyrolysis of polycarbonate.

Solution

The structural unit of polycarbonate is:



The molecular weight per unit is 254.3

The following group contributions may be taken from Table 21.4:

Groups	C_{FT}
2 p-C ₆ H ₄ -	8
-C(CH ₃) ₂ -	-3
-O-	0
-O-CO-	0
	5

So the char residue will amount to $5 \times 12 = 60$ g per structural unit.

This is $\frac{60}{254.3} \times 100\% = 24\%$

This is in agreement with the experimental value (24%).

21.4. KINETICS OF THERMAL DEGRADATION

Random thermal degradation can usually be described as a first-order reaction (loss of weight as a parameter) if the decomposition products are volatile. For the mathematical treatment we refer to Van Krevelen et al. (1951), Reich (1963, 1967) and Broido (1969).

Chain depolymerisation has been extensively studied (Simha and Wall, 1952). The two factors that are important for the course of the depolymerisation are:

- (1) The reactivity of depropagating radical
- (2) The availability of a reactive hydrogen atom for chain transfer

All polymers containing α -hydrogen (such as polyacrylates, polyolefins, etc.) give poor yields of monomer; conversely, polymethacrylates and poly(α -methyl styrenes) give high yields of monomer, due to the blocking of chain transfer by the α -methyl group. Poly(tetrafluoroethylene) gives high yields of monomer because the strong C-F bonds are resistant to transfer reactions.

Also this type of degradation can be described by an overall quasi-first-order reaction, but the kinetic scheme may be complicated. Besides the rate constant two other parameters can be obtained by kinetic analysis:

$$\text{the transfer constant} = k_{\text{tr}} = \frac{\text{probability of transfer}}{\text{probability of initiation}}$$

$$\text{the kinetic chain length} = \Lambda_{\text{kin}} = \frac{\text{probability of propagation}}{\text{probability of (termination + transfer)}}$$

For polyethylene $\Lambda_{\text{kin}} \approx 0$ (no monomer produced); for poly(methyl methacrylate) $\Lambda_{\text{kin}} \approx 200$ (nearly 100% monomer produced).

BIBLIOGRAPHY

General references

- Arnold C, "Stability of High -Temperature Polymers", J Polym Sci: Macromol Rev, 14 (1979) 265–378.
 Behr E, "Hochtemperaturbeständige Kunststoffe", Carl Hanser, Munich, 1969.
 Beyler CL and Hirschler MM, "Thermal Decomposition of Polymers", in DeNenno PJ (Ed), "SFPE Handbook of Fire Protection Engineering", NFPA, Quincy, Ma, 3rd Ed, 2002, Chap. 7.
 Bicerano J, "Prediction of Polymer Properties", "Thermal Stability", Marcel Dekker, New York, 3rd Ed, 2002, Chap. 16.
 Conley RT (Ed), "Thermal Stability of Polymers", Marcel Dekker, New York, 1970.
 Jellinek HHG (Ed), "Aspects of Degradation and Stabilization of Polymers", Elsevier, Amsterdam, 1978.
 Grassie N, "Chemistry of High Polymer Degradation Processes", Interscience, New York, 1956.
 Grassie N, in Mark HF (Ed) "Encyclopaedia of Polymer Science and Technology", Wiley, New York, 1966, Vol. 4, p 647.
 Grassie N and Scott G, "Polymer Degradation and Stabilization", Cambridge University Press, Cambridge, 1985, pp 1–99.
 Hamid SH, "Handbook of Polymer Degradation", Marcel Dekker, New York, 2nd Ed, 2000.
 Hergenrother PM, "Heat Resistant Polymers", in Mark HF, Bikales NM, Overberger CG, Menges G and Kroschwitz JI, Eds "Encyclopaedia of Polymer Science and Engineering", Wiley, New York, 2nd Ed, 1987, Vol. 7, pp 639–665.
 Korshak VV, "The Chemical Structure and Thermal Characteristics of Polymers", (Translation), Israel Program for Scientific Translations, Jerusalem, 1971.
 Kuleznev VN and Shershnev VA, "Thermal Degradation and Stability", in "The Chemistry and Physics of Polymers", Translated from the Russian by Leib, G, Mir Publishers, Moscow, 1990, Chap. 15.
 Madorsky SL, "Thermal Degradation of Organic Polymers", Interscience, New York, 1964.
 Madorsky SL and Straus S, "High Temperature Resistance and Thermal Degradation of Polymers", SCI Monograph 13 (1961) 60–74.

- Rodriguez F, "Degradation and Stabilization of Polymer Systems", in his monography "Principles of Polymer Systems", Hemisphere Publishing Corporation, New York, 5th Ed, 2003, Chap. 11.
- Van Krevelen DW, "Group Contribution Techniques for Correlating Polymer Properties and Chemical Structure", in Bicerano J (Ed) "Computational Modelling of Polymers", Marcel Dekker, New York, 1992, Chap. 1.
- Vasile C, "Degradation and Decomposition", in Vasile C (Ed), "Handbook of Polyolefins", Marcel Dekker, New York, 2nd Ed, 2000, Chap. 17.
- Voigt J, "Die Stabilisierung der Kunststoffe gegen Licht und Wärme", Springer, Berlin, 1966.
- Welsh WJ, "Thermal-Oxidative Stability and Degradation of Polymers", in Mark JE (Ed), "Physical Properties of Polymers Handbook", AIP Press, Woodbury, NY, 1996, Chap. 43.
- Zaikov GE, Russ Chem Revs 44 (1975) 833.

Special references

- Broido A, J Polym Sci A2, 7 (1969) 1761.
- Drozdov A, Model Simul Mater Sci Eng, 12 (2004) 575.
- Korshak VV and Vinogradova SV, Russian Chem Ser 37 (1968) 11.
- Madorsky SL and Straus S, J Res Natl Bur Stand 53 (1954) 361; 55 (1955) 223; 63A (1959) 261.
- Manrin LE, Macromolecules 21 (1988) 528; 22 (1989) 2673.
- Reich L, Macromol Chem 105 (1967) 223.
- Reich L and Levi DW, Makromol Chem 66 (1963) 102.
- Simha R and Wall LA, J Phys Chem 56 (1952) 707.
- Van Krevelen DW, "Coal", Elsevier, Amsterdam, 1961, Chaps.25 and 26, 2nd Pr 1981.
- Van Krevelen DW, Polymer 16 (1975) 615.
- Van Krevelen DW (1987), Unpublished Results.
- Van Krevelen DW, Van Heerden C and Huntjens FJ, Fuel 30 (1951) 253.
- Welsh WJ, "Thermal-Oxidative Stability and Degradation of Polymers", in Mark JE (Ed), "Physical Properties of Polymers Handbook", AIP Press, Woodbury, NY, 1996, Chap. 43.
- Wolfs PMJ, PhD Thesis, Delft University of Technology, 1959.
- Wolfs PMJ, Van Krevelen DW and Waterman HI, Brennstoff Chemie 40 (1959) 155, 189, 215, 241, 314, 342, 371; Fuel 39 (1960) 25.
- Zeng WR, Li SF and Chow WK, J Fire Sci, 20 (2002) 401.

This page intentionally left blank

CHAPTER **22**

Chemical Degradation

Degradation of polymers by chemical reactions is a typical constitutive property. No methods for numerical estimations exist in this field. Only qualitative prediction is possible.

The rate of chemical degradation can often be measured by means of physical quantities, e.g. stress relaxation measurements.

22.1. INTRODUCTION

A polymer may be degraded by chemical changes due to reaction with components in the environment. The most important of these degrading reagents is oxygen. Oxidation may be induced and accelerated by radiation (photo-oxidation) or by thermal energy (thermal oxidation).

Besides the oxidative degradation, also other forms of chemical degradation play a part, the most important of which is the hydrolytic degradation.

22.2. DEGRADATION UNDER THE INFLUENCE OF LIGHT

Of the electromagnetic energy emitted by the sun only a small portion reaches the earth's surface, namely, rays with a wavelength above 290 nm. X-rays are absorbed in the outermost part of the atmosphere and UV rays with wavelengths up to 290 nm in the ozone atmosphere. Although the total intensity is subject to wide variations according to geographical and atmospheric conditions, the overall composition of sunlight is practically constant.

In photochemical degradation the energy of activation is supplied by sunlight. Most ordinary chemical reactions involve energies of activation between 60 and 270 kJ/mol. This is energetically equivalent to radiation of wavelengths between 2000 and 440 nm. The energies required to break single covalent bonds range, with few exceptions, from 165 to 420 kJ/mol, which corresponds to radiation of wavelengths from 720 to 280 nm (see Fig. 22.1). This means that the radiation in the near ultraviolet region (300–400 nm) is sufficiently energetic to break most single covalent bonds, except strong bonds such as C–H and O–H.

Only the part of the radiation that is actually absorbed by the material can become chemically active. Most pure, organic synthetic polymers (polyethylene, polypropylene,

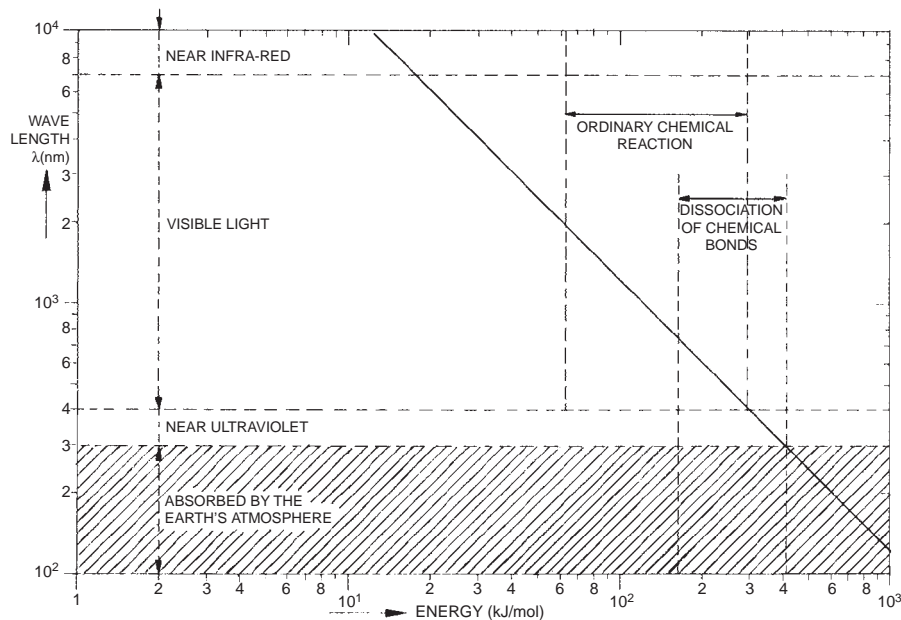


FIG. 22.1 Energy equivalence of light waves.

poly(vinyl chloride), polystyrene, etc.) do not absorb at wavelengths longer than 300 nm owing to their ideal structure, and hence should not be affected by sunlight. However, these polymers often do degrade when subjected to sunlight and this has been attributed to the presence of small amounts of impurities or structural defects, which absorb light and initiate the degradation. Much of the absorbed light energy is usually dissipated by either radiationless processes (rotations and vibrations) or by secondary emission (fluorescence).

Although the exact nature of the impurities or structural defects responsible for the photosensitivity is not known with certainty, it is generally accepted that these impurities are various types of carbonyl groups (ketones, aldehydes) and also peroxides. The primary chain rupture or radical formation in the various photochemical processes is often followed by embrittlement due to cross-linking, but secondary reactions, especially in the presence of oxygen, cause further degradation of the polymer. Mechanical properties, such as tensile strength, elongation and impact strength, may deteriorate drastically. Coloured degradation products are often developed. Surface crazing can also be a sign of UV-induced degradation.

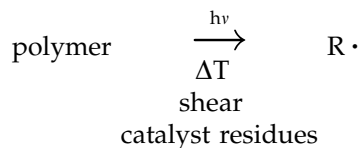
Some polymers show discolouration as well as reduction of the mechanical properties (e.g. aromatic polyesters, aromatic polyamides, polycarbonate, polyurethanes, poly(phenylene oxide, polysulphone), others show only a deterioration of the mechanical properties (polypropylene, cotton) or mainly yellowing (wool, poly(vinyl chloride)). This degradation may be less pronounced when an ultraviolet absorber is incorporated into the polymer. The role of the UV-absorbers (usually o-hydroxybenzophenones or o-hydroxyphenylbenzotriazoles) is to absorb the radiation in the 300–400 nm region and dissipate the energy in a manner harmless to the material to be protected. UV-protection of polymers can be well achieved by the use of additives (e.g. nickel chelates) that, by a transfer of excitation energy, are capable of quenching electronically excited states of impurities (e.g. carbonyl groups) present in the polymer (e.g. polypropylene).

22.3. OXIDATIVE DEGRADATION

At normal temperature polymers generally react so slowly with oxygen that the oxidation only becomes apparent after a long time. For instance, if polystyrene is stored in air in the dark for a few years, the UV spectrum does not change perceptibly. On the other hand, if UV light under similar conditions irradiates the same polymer for 12 days, there appear strong bands in the spectrum. The same applies to other polymers such as polyethylene and natural rubber.

Therefore, in essence the problem is not the oxidizability as such, but the synergistic action of factors like electromagnetic radiation and thermal energy on the oxidation. By the action of these factors on the polymer free radicals are formed, which together with oxygen initiate a chain reaction. Hence most oxidation reactions are of an autocatalytic nature.

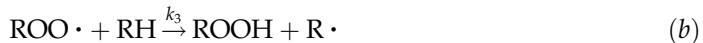
If the oxidation is induced by light, the phenomenon is called photo-oxidation. If the oxidation is induced by purely thermal factors, the term thermal oxidation is used. In photo-oxidation a radical is formed by absorption of $h\nu$ and in thermal oxidation by ΔT , shear or even by residues of the polymerisation catalysts:



22.4. PHOTO-OXIDATION

The most thoroughly investigated oxidative degradation is that of natural rubber. In 1943 Farmer and Sundralingham found that in the photochemical oxidation of this polymer a hydroperoxide is formed, the number of double bonds in the chain remaining constant. The oxygen was found to act on an activated methylene group, not on a double bond, as had previously been assumed.

Later the mechanism of the rubber oxidation was studied extensively by Bolland and coworkers (1946–1950), who mainly used model substances. In his first publication Bolland proposed the following mechanism for the propagation reaction:

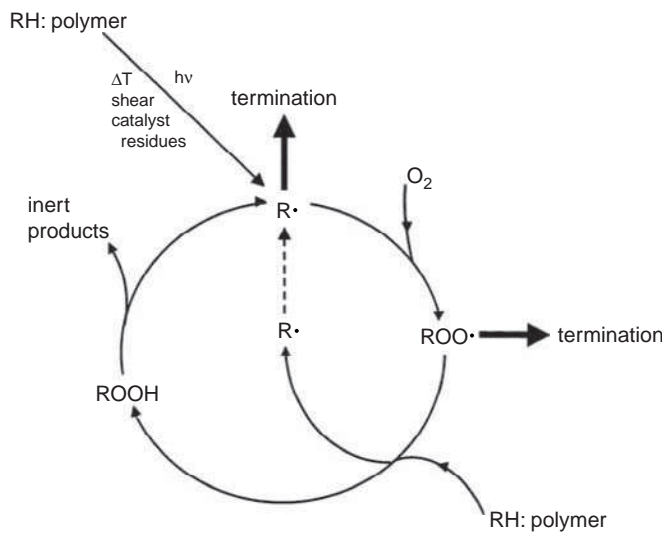


where RH is the polyolefin, R· a radical obtained by abstraction of hydrogen in the allyl position and the ROO· the peroxy radical obtained by addition of oxygen to this radical. According to Bolland, the initiation process is the production of R· or RO₂· radicals by the decomposition of the peroxide ROOH. To conform with the results of the decomposition experiments this reaction must be of second order:



The reaction chains are terminated by the combination of allyl and peroxy radicals:





SCHEME 22.1 Schematic presentation of cyclical oxidation process according to the mechanism presented by Bolland (1946).

This reaction scheme is presented in Scheme 22.1, where $h\nu$ is the source of the formation of radicals (other ways of initiation of autoxidation are also mentioned in the Scheme: high temperature, shear or the presence of residues of polymerisation catalysts). The cyclical chain length v of the oxidation chain is given by

$$v = \frac{k_2}{\sqrt{k_1 k_6}} \frac{[RH]}{[ROOH]} \varphi(p) \quad (22.1)$$

where $\varphi(p)$ is a function of oxygen pressure. According to Bolland, assuming $\varphi(p) = 1$, the cyclical chain length is of the order of 50–100 at a temperature of 45 °C (Fig. 22.2).

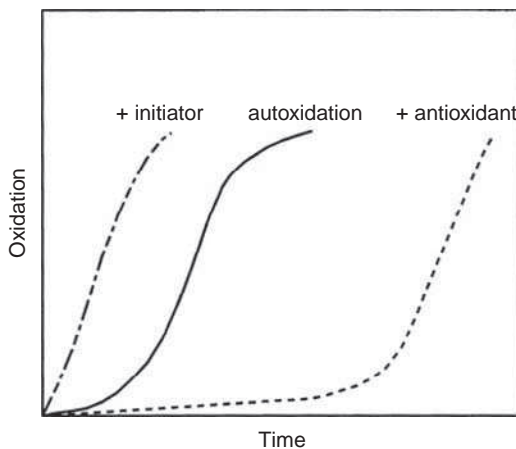


FIG. 22.2 Generalised scheme for autoxidation as such, in the presence of an initiator or in the presence of an anti-oxidant.

Nowadays the autocatalytic nature of the reaction is thought to be due to the decomposition of the hydroperoxides (Denisov, 2000; Al-Malaika, 2003):



followed by:



The hydroperoxides also give rise to secondary reactions in which coloured resinous products are formed (via carbonyl compounds).

Stabilisation to photo-oxidation can be achieved by the use of suitable UV absorbers in combination (synergistic action) with antioxidants (AH) which are capable of preventing reactions (a) and (b):



22.5. THERMAL OXIDATION

Especially above room temperature many polymers degrade in an air atmosphere by oxidation that is not light-induced (heat ageing). A number of polymers already show a deterioration of the mechanical properties after heating for some days at about 100 °C and even at lower temperatures (e.g. polyethylene, polypropylene, poly(oxy methylene) and poly(ethylene sulphide)).

The rate of oxidation can be determined by measuring the oxygen uptake at a certain temperature. Such measurements have shown that the oxidation at 140 °C of low-density polyethylene increases exponentially after an induction period of 2 h. It can be concluded from this result that the thermal oxidation, like photo-oxidation, is caused by autoxidation, the difference merely being that the radical formation from the hydro peroxide is now activated by heat.

The primary reaction can be a direct reaction with oxygen



The thermal oxidation can be inhibited by antioxidants as before: Eqs. (j), (k) and (l).

22.6. EFFECTS OF OXIDATION DEGRADATION

The principal effects of oxidative degradation of polymers are the decay of good mechanical properties (strength, elongation, resilience, etc.) and discolouration (mainly yellowing).

The behaviour of polymers may vary widely. A polymer may be resistant to mechanical decay but not to colour decay, or the reverse. Often the two go together. Table 22.1 gives a survey of these effects for the different polymer families in the case of photo-degradation.

TABLE 22.1 Photo-degradation of polymers

Polymer	Mechanical properties	Discoloration (yellowing)
Poly(methyl methacrylate)	0	0
Polyacrylonitrile	0	0
Cotton	1	+
Rayon	1	1
Polyoxymethylene	1	1
Polyethylene	2	0
Poly(vinyl chloride)	0	2
Qiana® (=Nylon fibre)	2	1
Terlenka	2	1
Nylon 6	1	2
Polystyrene	1	2
Polypropylene	4	0
Polycarbonate	2	2
Wool	1	3
Polyurethanes	1	3
Polysulphone	3	4
Poly(2,6-dimethylphenylene oxide)	3	4
Poly(2,6-diphenylphenylene oxide)	3	4

Meaning of symbols: +, improvement; 0, no change; 1, slight deterioration; 2, moderate deterioration; 3, strong deterioration; 4, very strong deterioration.

22.7. STABILISATION

The oxidative degradation of a polymer can be retarded or even practically prevented by addition of stabilisers. The following types of stabilisers may be used:

a. *UV absorbers*

A good UV absorber absorbs much UV light but no visible light. It should dissipate the absorbed energy in a harmless manner by transforming the energy into heat.

Other requirements are: compatibility with the polymer, non-volatility, light fastness, heat stability and, for textiles, also resistance to washing and dry cleaning.

The optimum effect of a UV absorber in a polymer film can be calculated from the absorbancy of the UV absorber and the thickness of the film. Such calculations show that the effect of UV absorbers is small in thin films and in yarns.

b. *Antioxidants*

The degradation of polymers is mostly promoted by autoxidation. The propagation of autoxidation can be inhibited by antioxidants (e.g. hindered phenols and amines).

c. *Quenchers*

A quencher induces harmless dissipation of the energy of photo-excited states. The only quenchers applied in the polymer field are nickel compounds in the case of polyolefins.

A worthwhile survey of this field was given by De Jonge and Hope (1980).

d. Hindered Amine Light Stabilisers (HALS)

Hindered Amine Light Stabilisers were introduced in the 1970s (Gugumus, 1975). They are derivatives of 2,2,6,6-tetramethyl piperidine. These extremely efficient stabilisers do not absorb UV radiation, but act to inhibit degradation of the polymer. They have the advantage that they react with the chain radicals R·, RO· and ROO· and with the hydroperoxide ROOH as well. Moreover, their extremely high efficiency and longevity are due to a cyclic process wherein the HALS are regenerated rather than consumed during the stabilisation process. The mechanism of hindered amine stabilisers against thermo-oxidation appears to be complex and is not fully understood (Step et al., 1994). Overviews are given by Gugumus (2000), by Ye and King III (2006) and by King III et al. (2007).

22.8. HYDROLYTIC DEGRADATION

Hydrolytic degradation plays a part if hydrolysis is the potential key reaction in the breaking of bonds, as in polyesters and polycarbonates. Attack by water may be rapid if the temperature is sufficiently high; attack by acids depends on acid strength and temperature. Degradation under the influence of basic substances depends very much on the penetration of the agent; ammonia and amines may cause much greater degradation than substances like caustic soda, which mainly attack the surface. The amorphous regions are attacked first and the most rapidly, but crystalline regions are not free from attack.

22.9. STRESS RELAXATION AS A MEASURE OF CHEMICAL DEGRADATION

Stress relaxation occurs when a molecular chain carrying a load breaks. This occurs, e.g., during the oxidation of rubbers. When a stretched chain segment breaks, it returns to a relaxed state. Only stretched chains carry the load, and a load on a broken chain in a network cannot be shifted to other chains. It may be assumed that the rate at which stretched network chains are broken is proportional to the total number of chains (n) carrying the load:

$$-\frac{dn}{dt} = kn \quad (22.2)$$

From the theory of rubber elasticity one can then derive in a simple way that:

$$\frac{\sigma}{\sigma_0} = \frac{\sigma(t)}{\sigma_0} = e^{-kt} \quad (22.3)$$

This expression is of the same shape as that of stress relaxation of viscoelastic materials (Chap. 13). By analogy 1/k is called the "relaxation time" (τ). Since chemical reactions normally satisfy an Arrhenius type of equation in their temperature dependence, the variation of relaxation time with temperature may be expressed as follows:

$$\ln \tau = \ln \frac{1}{k} = \ln A + \frac{E_{act}}{RT} \quad (22.4)$$

where E_{act} is the activation energy of the chemical reaction. A typical value of E_{act} is 125 kJ/mol for the oxidative degradation of rubbers.

BIBLIOGRAPHY

General references

- Al-Malaika S, "Oxidative Degradation and Stabilisation of Polymers", Intern Mater Rev 48 (2003) 165.
- Conley RT (Ed), "Thermal Stability of Polymers", Marcel Dekker, New York, 1970.
- Grassie N, "Chemistry of High Polymer Degradation Processes", Interscience, New York, 1956.
- Grassie N and Scott G, "Polymer Degradation and Stabilisation", Cambridge University Press, Cambridge, 1985; Paperback Ed 1988.
- Emmanuel NM and Buchenko AL, "Chemical Physics of Polymer Degradation and Stabilization", VNU, Utrecht, 1987.
- Guillet J "Polymer Photophysics and Photochemistry", Cambridge University Press, Cambridge, 1985.
- Hamid SH (Ed), "Handbook of Polymer Degradation", Marcel Dekker, New York, 2nd Ed, 2000.
- Jellinek HHG, "Degradation of Vinyl Polymers", Academic Press, New York, 1955.
- Jellinek HHG (Ed), "Aspects of Degradation and Stabilization of Polymers", Elsevier, Amsterdam, 1978.
- Kolodovych V and Welsh WJ, "Thermal Oxidative Stability and Degradation of Polymers", in Mark JE (Ed), "Physical Properties of Polymers Handbook", Springer, 2nd Ed, 2007, Chap. 54.
- Kuleznev VN and Shershnev VA, "Thermal Degradation and Stability", in "The Chemistry and Physics of Polymers", Translated from the Russian by Leib, G, Mir Publishers, Moscow, 1990, Chap. 15.
- Neimann MB (Ed), "Aging and Stabilization of Polymers", Consultants Bureau, New York, 1965.
- Reich L and Stivala SS, "Autoxidation of Hydrocarbons and Polymers", Marcel Dekker, New York, 1969.
- Reich L and Stivala SS, "Elements of Polymer Degradation", McGraw-Hill, New York, 1971.
- Rodriguez F, "Degradation and Stabilization of Polymer Systems", in "Principles of Polymer Systems", Taylor and Francis, New York, 5th Ed, 2003, Chap. 11.
- Scott G, "Atmospheric Oxidation and Antioxidants", Elsevier, Amsterdam, 1965.
- Vasile C, "Degradation and Decomposition", in Vasile C (Ed), "Handbook of Polyolefins", Marcel Dekker, New York, 2nd Ed, 2000, Chap. 11.
- Zaikov GE, Russ Chem Revs 44 (1975) 833.

Special references

- Bergen RL, SPF Journal 20 (1964) 630.
- Bolland JL, Proc Roy Soc (London) A 186 (1946) 218.
- Bolland JL et al., Trans Faraday Soc 42 (1946) 236, 244; 43 (1947) 201; 44 (1948) 669; 45 (1949) 93; 46 (1950) 358.
- De Jonge I and Hope P, in Scott G (Ed), "Developments in Polymer Stabilization", 3, Applied Science Publishers (Elsevier), London, 1980, pp 21–54.
- Denisov ET, "Polymer Oxidation and Antioxidant Action", in Hamid SH (Ed), "Handbook of Polymer Degradation", Marcel Dekker, New York, 2nd Ed, 2000, Chap. 9.
- Farmer EH and Sundralingham A, J Chem Soc (1943) 125.
- Gugumus FL, Kunstst Plast 22 (1975) 11.
- Gugumus FL, Caout Plast 558 (1976) 67.
- Gugumus FL, "Polyolefin Stabilization: From Single Stabilizers to Complex Systems", in Hamid SH (Ed) "Handbook of Polymer Degradation", Marcel Dekker, New York, 2nd Ed, 2000, Chap. 1.
- King III RE, Lelli N and Solera P, "Overview of Recent Developments in the UV Stabilization of Polyolefins", Paper presented at the Additives 2007 Conference, January 22–24, 2007, San Antonio TX.
- Step EN, Turro NJ, Gande ME and Klemchuk PP, Macromolecules 27 (1994) 2529.
- Ye Y and King III RE, "Additives for Polyolefin Film Products: an Overview of Chemistry and Effects", www.tappi.org/content/enewsletters/eplace/2006/06PLA04.pdf.
- Zeng WR, Li SF and Chow WK, J Fire Sci 20 (2002) 401.

PART **VI**

POLYMER PROPERTIES AS AN INTEGRAL CONCEPT

*“The point is not to take the world’s opinion as a guiding star,
but to go one’s way in life and working unerringly,
neither depressed by failure nor seduced by applause”*

Gustav Mahler, 1860–1911

This page intentionally left blank

CHAPTER 23

Intrinsic Properties in Retrospect

23.1. INTRODUCTION

In the preceding 22 chapters many important intrinsic properties have been discussed. They depend in essence on two really fundamental characteristics of polymers (Chap. 2): the chemical structure of their repeating units and their molecular-weight-distribution pattern. The latter is of major importance for those cases where the molecular translational mobility is developed, i.e. for polymer properties in melts and solutions.

We have shown that the molecular structure is reflected in all the properties; ample use has been made of the empirical fact that many intrinsic quantities or combinations of quantities, if related to the structural molar unit, have additive properties, so that these quantities can be estimated in a simple manner from empirically derived group contributions or increments.

We repeat what has been said in Chap. 1: *reliable experimental data are always to be preferred to values obtained by an estimation method*. But in many cases they are not available; then estimation methods are of great value.

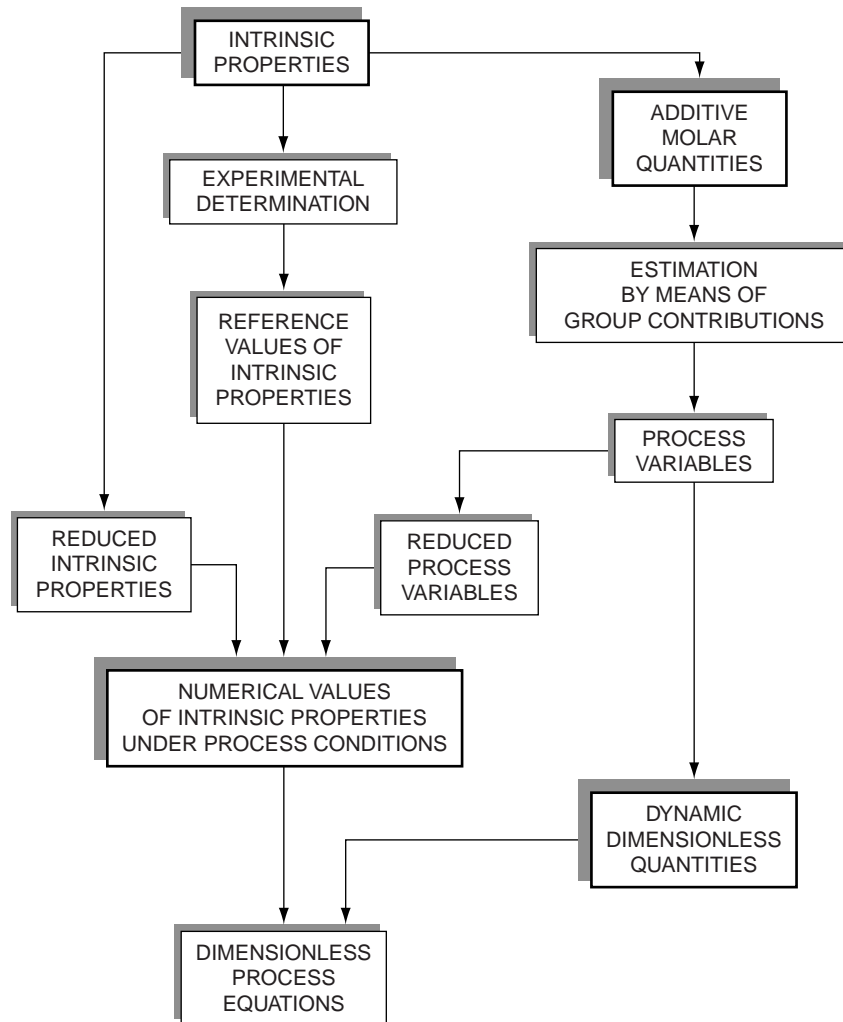
There is one additional virtue of our estimation method: if a predicted value shows a serious discrepancy with a measured one, there possibly is a theoretical problem. In this way the semi-empirical estimation method may also give incentives to theoretical scientists.

The philosophy of this book is clearly represented in Fig. 23.1. Of practical significance are the numerical values of intrinsic properties under the prescribed experimental conditions. For this purpose one needs *reference values* under standard conditions and their *dependence* on certain variables, such as time, temperature, pressure and concentration.

The reference values may be estimated by means of additive molar quantities; often the values at 298 K and atmospheric pressure are used as such. Division of an intrinsic quantity by its reference value gives the reduced, dimensionless, intrinsic quantity.

The reduced intrinsic quantities in turn are functions of dimensionless process variables. If these functional correlations are known, every value of the required intrinsic quantity under arbitrary experimental conditions can be estimated. In this procedure the systems of dynamic dimensionless quantities may be of great help.

Finally the process equations may be formulated in dimensionless form.

**FIG. 23.1** Relationships of intrinsic properties.

23.2. REFERENCE VALUES OF INTRINSIC PROPERTIES EXPRESSED AS A FUNCTION OF ADDITIVE QUANTITIES

In retrospect we shall give a summary of all additive relationships that have been found. We use the sequence followed in this book (T. = table, Eq. = equation).

1. Volumetric and calorimetric intrinsic properties (Chaps. 4 and 5)

specific volume	$v = \frac{V}{M}$	T.4.2 & 4.10
density	$\rho = \frac{M}{V}$	T.4.10

specific expansivity	$e = \frac{E}{M}$	Eq.(4.29) & (4.30)
thermal expansion coefficient	$\alpha = \frac{E}{V}$	Eq.(4.9)
specific heat	$c_p = \frac{C_p}{M}$	T.5.1
specific entropy of fusion	$\Delta s_m = \frac{\Delta S_m}{M}$	T.5.7

2. *Other thermo physical properties* (Chap. 6–9)

crystalline melting temperature	$T_m = \frac{Y_m}{M}$	T.6.8–6.10, 6.12, 6.19. & 6.15
glass transition temperature	$T_g = \frac{Y_g}{M}$	T.6.1–6.3 & 6.19
cohesive energy density	$e_{coh} = \frac{E_{coh}}{V}$	T.7.1
solubility parameter	$\delta = \frac{F}{V}$	T.7.3 & 7.10–7.12
surface tension	$\gamma = \left(\frac{P_s}{V} \right)^4$	T.8.1
unperturbed viscosity coefficient	$K_\Theta \left(\frac{[\eta]_\Theta}{M^{1/2}} \right) = \left(\frac{J + 4.2Z}{M} \right)^2$	T.9.3

3. *Optical and other electromagnetic properties* (Chaps. 10–12)

refraction index	$n = \left[\frac{1 + 2 \frac{R_{LL}}{V}}{1 - \frac{R_{LL}}{V}} \right]^{1/2} = 1 + \frac{R_{GD}}{V} = \frac{R_V}{M}$	T.10.4
specific refractive index increment	$\frac{dn}{dc} = \frac{V}{M} \left(\frac{R_V}{M} - n_s \right)$	T.10.4
dielectric constant!	$\epsilon = \frac{1 + 2 \frac{P_{LL}}{V}}{1 - \frac{P_{LL}}{V}} = \frac{P_V}{M}$	T.11.1
magnetic susceptibility	$\chi = \frac{X}{M}$	T.12.3

4. *Mechanical and rheological properties* (Chaps. 13–16)

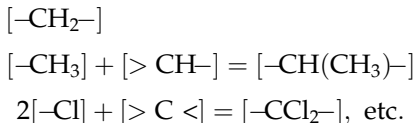
longitudinal sound velocity	$u_{long} = \left(\frac{U_R}{V} \right)^3 \left(\frac{3(1-v)}{1+v} \right)^{1/2}$	T.14.4
transversal sound velocity	$u_{shear} = \left(\frac{U_H}{V} \right)^3$	T.14.4

specific shear modulus	$\frac{G}{\rho} = \left(\frac{\mathbf{U}_H}{\mathbf{V}} \right)^6$	T.14.4
specific bulk modulus	$\frac{K}{\rho} = \left(\frac{\mathbf{U}_R}{\mathbf{V}} \right)^6$	T.14.4
activation energy of viscous flow	$E_\eta(\infty) = \left(\frac{\mathbf{H}_\eta}{\mathbf{M}} \right)^3$	T.15.7
5. Thermo chemical properties (Chaps. 20–22)		
molar free enthalpy of formation	$\Delta G_f^o = A + BT$	T.20.1
temperature of “half” decomposition	$T_{d,1/2} = \frac{Y_{d,1/2}}{M}$	T.21.2
carbon residue on pyrolysis(%)	$CR = \frac{C_{FT}}{M} \times 1200$	T.21.4

In Part VII, Table IX, a comprehensive tabulation of numerical group contributions to the different additive quantities is given. The table contains the data needed for calculating the reference values of the intrinsic properties.

23.3. EFFECT OF STRUCTURAL GROUPS ON PROPERTIES

The degree to which properties are influenced by characteristic groups can best be assessed as follows. All groups can be combined as to form exclusively bivalent units, e.g.



From the additive quantities of these bivalent groups one can calculate the properties of a *hypothetical* polymer entirely consisting of these bivalent groups. In this way one finds the surface tension, solubility parameter, refractive index, etc., of this hypothetical polymer and consequently, of the constituting bivalent group. Thus a clear numerical insight is gained into the quantitative influence of the group on the properties.

In Fig. 23.2 this has been done for a number of important quantities.

With some audacity one may say that Fig. 23.2 reflects the “spectra” of the properties; by way of the additive quantities the composite “colour” of a substance (the “average value”) is as it were split up into spectral lines, the system of additive quantities functioning as prism or grating.

23.4. DEPENDENCE OF INTRINSIC PROPERTIES ON PROCESS VARIABLES

23.4.1. Dimensionless expressions for temperature dependence

Every intrinsic quantity can be made dimensionless by dividing it by its value in the reference state. The reduced quantity obtained in this way can be expressed as a dimensionless function of a reduced temperature.

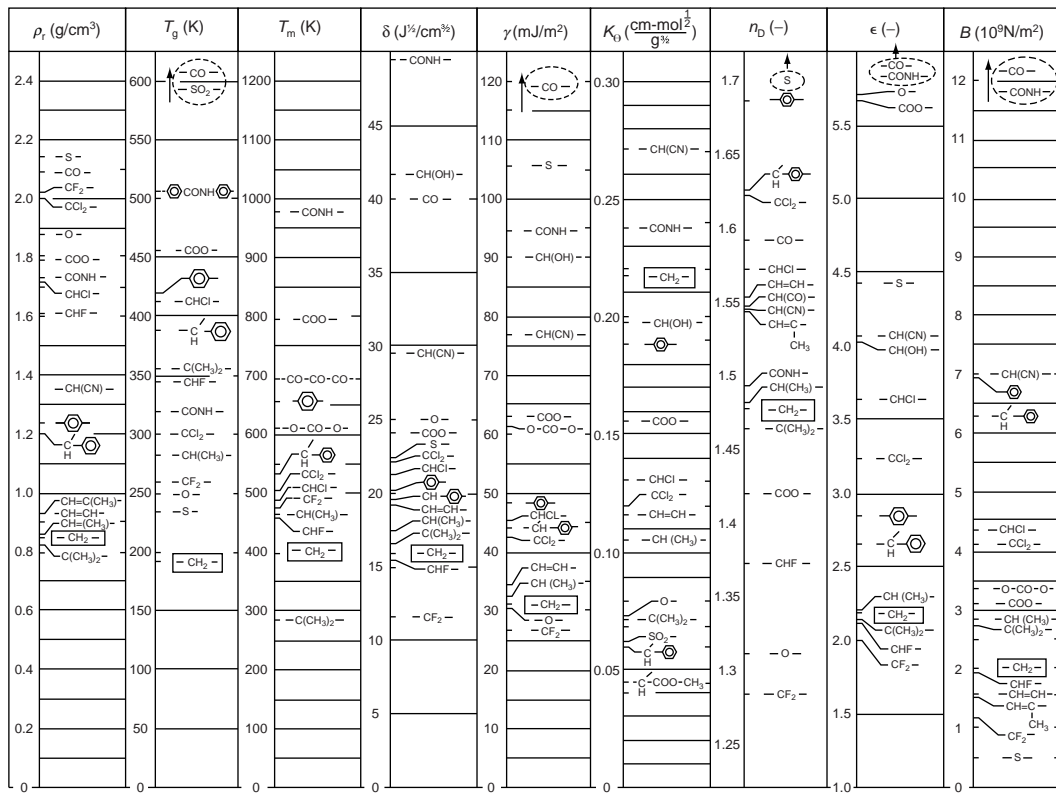


FIG. 23.2 Effect of structural groups on properties.

The temperature dependence of “non-activated” processes differs from that of “activated” processes. In the latter the temperature dependence is in essence determined by an activation energy that determines the probability of the process.

a. *Non-activated processes.* These are found in thermal expansion and related phenomena. The general expression has the following form:

$$\frac{A(T)}{A_R} = 1 + \frac{B}{A_R} (T - T_R)$$

A may be a volume, a specific heat, etc.; B is an expansion property; B/A_R usually is nearly constant. As an example, the molar volume in the glassy state was expressed (Chap. 4) as:

$$\frac{V_g(T)}{V_g(298)} = 1 + \frac{E_g}{V_g(298)} (T - 298) = 1 + 0.29 \times 10^{-3} (T - 298) = 0.914 + 0.29 \times 10^{-3} T$$

b. *Activated processes.* These are found in all rate phenomena. The general expression is:

$$\frac{A(T)}{A_R} = \exp \left[\frac{E_{act}}{R} \left(\frac{1}{T} - \frac{1}{T_R} \right) \right]$$

The ratio E_{act}/R has the dimension of a temperature. Sometimes it is related to characteristic temperatures that play a part in the process. We have, for instance, seen that in the shift factor of relaxation processes (Chap. 13) the following correlation is valid:

$$\frac{E_{\text{act}}}{R} \approx \frac{T_m T_R}{T_m - T_R}$$

In the crystallisation phenomena we have found (Chap. 19):

$$\frac{E_{\text{act}}}{R} \approx \frac{5.3 \times T_m^2}{T_m - T_g}$$

23.4.2. Dimensionless expressions for time dependence

Many reduced intrinsic quantities are correlated with a reduced time quantity; usually the expression can be written in the following form:

$$-\log \frac{A(t)}{A_R} = f(t/t_R)$$

The reference time may be an arbitrarily chosen time, but normally it is connected with the nature of the phenomenon observed. In these cases the reference time has a very specific meaning:

Phenomenon	Characteristic reference time	Chapter
Relaxation phenomena ("natural" time)	$\frac{\eta}{G} (= \tau)$	15
Heat transfer	$\frac{L^2 c_p \rho}{\lambda}$	17
Diffusion phenomena	$\frac{L^2}{D}$	18
Crystallisation	$\frac{1}{vN^{1/3}} (\approx t_{1/2})$	19
Effluence	$\frac{\eta}{\Delta p}$	
Sedimentation	$\frac{\eta}{g \rho L}$	
Centrifugation	$\frac{\eta}{\rho \omega^2 L^2}$	
Surface levelling	$\frac{\eta L}{\gamma}$	

The last-mentioned characteristic time plays a part in coating processes, e.g. formation of films and paint levelling (L is a characteristic length).

23.4.3. Dimensionless expressions for concentration dependence

In Chaps. 9, 16 and 18 we have met expressions for the concentration dependence of intrinsic properties. They have the general form:

$$\frac{A(c)}{A_o} = f(Bc)$$

B in this case is a quantity with the dimension c^{-1} .

Again we may distinguish between non-activated and activated processes.

- a. *Non-activated processes*. Here the expression has the form:

$$\frac{A(c)}{A_o} = 1 + f(Bc) \approx 1 + Bc + \dots$$

We have seen (Chap. 16) that the Huggins equation for the viscosity of a dilute solution has this form; it can be expressed in the following way:

$$\frac{\eta_{\text{red}}}{[\eta]} = 1 + k_H[\eta]c$$

Analogous equations have been found for the osmotic pressure, the diffusion coefficient and the sedimentation coefficient (Chap. 16).

- b. *Activated processes*, i.e. phenomena that are controlled by an activation energy barrier. Here the equation takes the form:

$$\frac{A(c)}{A_o} = \exp(Bc)$$

We met this case in Chap. 18 for the penetration of vapours into polymers.

23.4.4. (Dimensionless) Power functions

We have met power functions in many preceding chapters. They all have the form:

$$Y = aX^z$$

or the reduced form (more general, since dimensionless):

$$\frac{Y}{Y_o} = A \left(\frac{X}{X_o} \right)^z$$

z is called the “universal” exponent, whereas a and A are constants, varying with the nature of the material type. This kind of functions plays an important role in De Gennes’ scaling concepts (see Chap. 9).

In Table-form we give here a short survey:

Chapter	Y	X	z
8	$K = 1/\kappa$	γ	$3/2$
	$\delta = e_{\text{coh}}^{1/2}$	$\gamma/V^{1/3}$	$3/7$
9	$[\eta]$	M	$a \approx 2/3$
	$[\eta]_\Theta$	M	$\frac{1}{2}$
	$s_{(o)}$	M	$(2 - a)/3$
	$D_{(o)}$	M	$-(a + 1)/3$
	$\langle r^2 \rangle^{1/2}$	M	$(a + 1)/3 \approx 3/5$
13	σ_{\max}	E	$\gamma_3 - 0.8$
15	M_{cr}	K_Θ	-2
	σ_{sh}	$\dot{\gamma}$	$0.2 - 1$
16	η	$(c^{3/2}M)$	3.4
18	E_D	d	2
19	$\ln[1 - x_c(t)]$	t	$1 - 4$
	Avrami-eq.		

23.5. OUTLOOK

In Fig. 23.1 the relevance of the intrinsic properties and their relations to process equations have been outlined.

In the following Chaps. 24–27 the most important process and product properties will be discussed along the lines sketched in Chap. 3.

Processing properties are mostly determined in specific standard tests; often they are the result of model experiments. In the scientific analysis of these model experiments the dimensionless process equations can be of considerable help.

By processing, the material receives “added” properties, desired as well as undesired ones. It is the combination of the intrinsic properties with the added properties which determines the product or article properties, often in a very complex and still obscure way.

Fig. 23.3 illustrates the interrelations between the different types of properties.

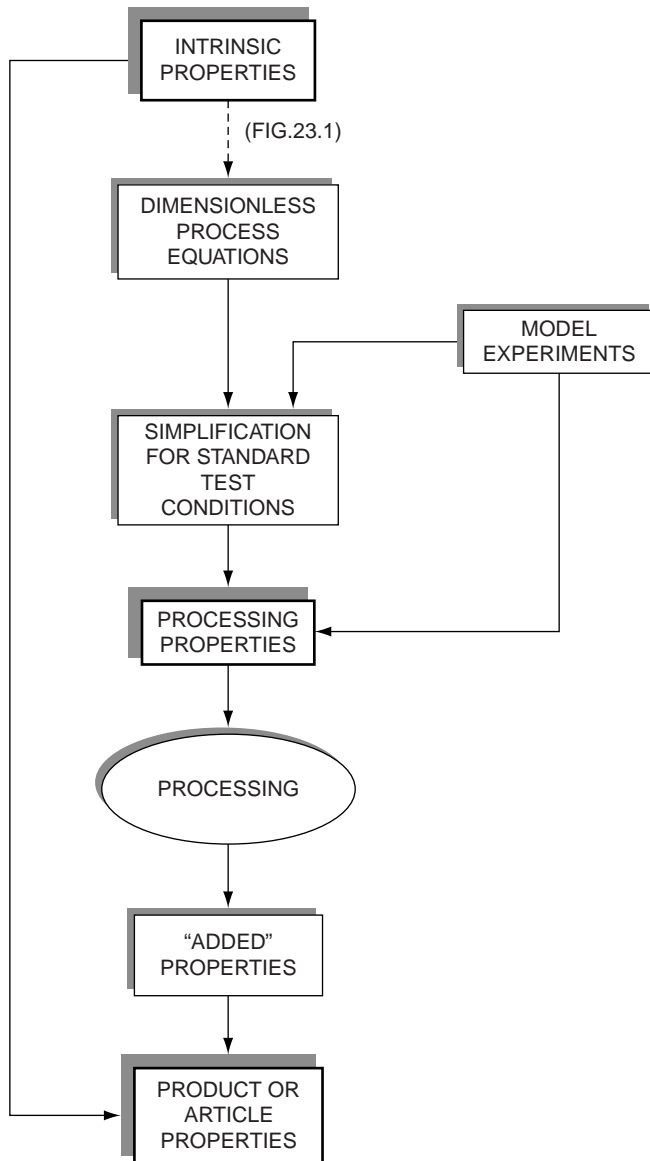


FIG. 23.3 Importance of intrinsic properties with respect to processing and product (article) properties.

This page intentionally left blank

CHAPTER 24

Processing Properties

Most of the common polymers are processed by a treatment in the molten state, followed by cooling. Dimensionless groups may be derived which control these processing steps.

Criteria of *extrudability*, *mouldability*, *spinnability* and *stretchability* as used in practice are described (melt index, spiral length, mouldability index, melt strength, ultimate thread length, etc.). These criteria are based on the dimensionless parameters (numerics) of the processes.

24.1. CLASSIFICATION OF PROCESSES

The aim of polymer processing is to convert the polymer, usually in the form of powder or granules, into a more useful form. Usually the change involved is largely physical, although in some conversion processes chemical reactions play a part.

The variety of conversion processes is very large (see Fig. 3.2):

- (1) One class of processes involves *simple extrusion*; by using different dies it is possible to make sheets, tubes, monofil, other special shapes and also plastic-coated wires.
- (2) Another class consists of *extrusion immediately followed by an additional stage*. This includes blow moulding, film blowing, quenched film forming, fibre spinning, and extrusion coating.
- (3) The third large class involves the processes of *moulding* (injection and compression moulding).
- (4) The fourth class is a miscellaneous collection of *shaping processes*, such as vacuum forming, calendering, rotation casting, and foaming.

As we have remarked in Chap. 3, the common features of all these processes may be summarised under four headings:

- (a) Mixing, melting and homogenisation (*transportation and conditioning*)
- (b) Transport and extrusion (*transportation and conditioning*)
- (c) Drawing and blowing (*forming proper*)
- (d) Cooling and finishing (*setting*)

The rheological conditions of these processing techniques are different. The shear rates, for instance, show enormous differences, as will be clear from the following survey (Table 24.1).

TABLE 24.1 Processing conditions

Operation	Shear rate (s^{-1})
Calendering (rubber)	<50
Mixing rollers (rubber)	50–500
Banbury mixer (rubber)	500–1000
Extrusion of pipes	10–1000
Extrusion of film	10–1000
Extrusion of cable	10–1000
Extrusion of filaments	1000–100,000
Injection moulding	1000–100,000

Each processing technique has to fulfil certain requirements of economy. Often the most economic (i.e. the cheapest) method is the worst from the technological point of view. Commercial processing is always a compromise between the best quality and the lowest cost.

Three questions of particular importance claim attention:

1. The processability (and reprocessability) of the polymer as such
2. The controllability of the processing
3. The influence of the processing on the ultimate properties of the product

Constancy of the processing conditions is essential for quality. This applies first of all to the uniformity and constancy of the starting material. Equally important, however, is the constancy of processing itself. To achieve quality control, the speed of the operations is a critical factor. The filling of dies, for instance, should take place rapidly. In the case of highly crystalline materials also the cooling should proceed rapidly, to prevent the formation of large spherulites. For glassy polymers, annealing is mostly beneficial (stress relaxation), for crystalline plastics it is mostly harmful (growth of secondary crystallites). The constancy of the processing should also be analysed by careful *checking* of the product, which can be done by *control tests*. Measurements of the strength perpendicular and parallel to the direction of flow are essential to evaluate the *orientation sensitivity* of a material.

In this chapter we shall discuss some important unit operations as far as the processing properties are concerned, viz. extrusion, injection moulding, spinning and stretching.

24.2. SOME IMPORTANT PROCESSING PROPERTIES

24.2.1. Extrudability

In the extrusion process a polymer melt is *continuously* forced through a die shaped to give the final object after cooling. In the extruder the polymer is propelled along a screw through sections of high temperature and pressure where it is compacted and melted. A wide variety of shapes can be made by extrusion: rods, tubes, hoses, sheets, films and filaments.

Shear viscosity (η) is the most important intrinsic property determining extrudability. Since the apparent viscosity is highly dependent on temperature and shear stress (hence on pressure gradient), these variables, together with the extruder geometry, determine the output of the extruder.

According to the considerations in Chap. 3 the most important dimensionless quantities in extrusion will be

$$\frac{\Delta p D}{\eta v}, \frac{D}{L} \text{ and } \frac{\eta}{\eta_0}$$

where Δp is the pressure drop, v is the average linear velocity of the melt (directly connected with the flow rate), D and L are characteristic diameter and length dimensions, η is the shear viscosity and η_0 the viscosity at zero shear rate.

In order to assess the extrudability of a polymer two practical tests are applied: the melt flow index test and the flow rate test at various pressures (and temperatures).

24.2.1.1. Melt flow index (MI)

The melt (flow) index has become a widely recognised criterion in the appraisal of extrudability of thermoplastic materials, especially polyolefins. It is standardised as the weight of polymer (polyolefin) extruded in 10 min at a constant temperature (190°C) through a tubular die of specified diameter (0.0825 in. = 2.2 mm) when a standard weight (2.160 kg) is placed on the driving piston (ASTM D 1238).

Although commonly used, the melt flow index is not beyond criticism (see also Chap. 15).

First, the rate of shear, which is not linear with the shearing stress due to the non-Newtonian behaviour, varies with the different types of polymer. The processability of different polymers with an equal value of the MI may therefore differ widely. An illustration of this behaviour is given in Fig. 15.14. Furthermore the standard temperature (190°C) was chosen for polyethylenes; for other thermoplastics it is often less suitable. Finally, the deformation of the polymer melt under the given stress is also dependent on time, and in the measurements of the melt index no corrections are allowed for entrance and exit abnormalities in the flow behaviour. The corrections would be expected to vary for polymers of different flow characteristics. The length-diameter ratio of the melt indexer is too small to obtain a uniform flow pattern.

Nevertheless, due to its relative simplicity, the melt flow index is one of the most popular parameters in the plastics industry, especially for polyethylenes. Here the melt index is a good indicator of the most suitable (end) use. Table 24.2 gives some data. A melt flow index of 1.0 corresponds to a melt viscosity of about $1.5 \times 10^4 \text{ N s/m}^2$ ($= 1.5 \times 10^5 \text{ poises}$)

Busse (1967) gives the following relationship between melt flow index and inherent viscosity:

$$(MI) \propto \eta_{inh}^{-4.9} \quad (24.1)$$

From this it follows that:

$$(MI) \propto [\eta]^{-4.9} \propto (M_v)^{-3.5} \propto \eta_0^{-1} \quad (24.2)$$

where η_0 is the melt viscosity at zero shear rate.

Boenig (1966) gives a similar correlation (for polyethylenes) between melt index and melt viscosity (at 190°C):

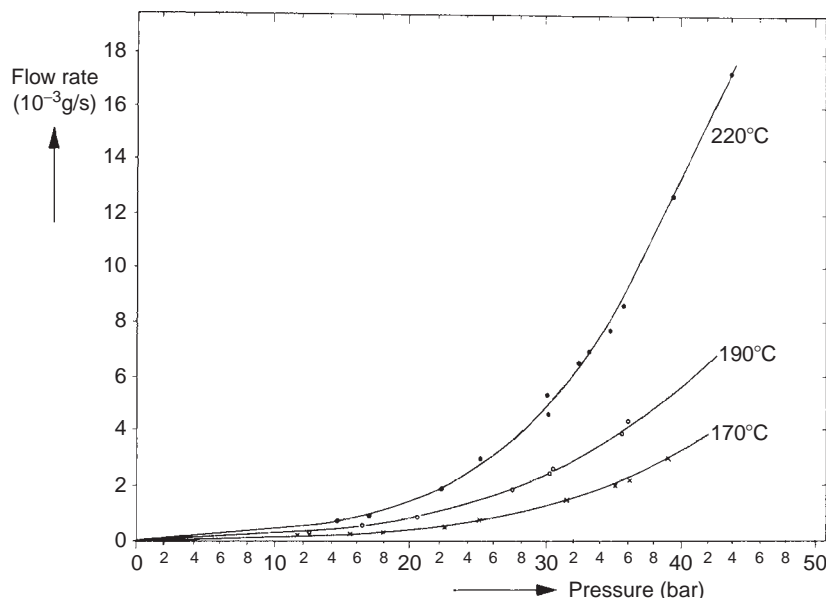
$$\log(MI) = \text{const} - \log \eta_0 \quad (24.3)$$

24.2.1.2. Melt flow rate diagram

A more informative test is the measurement of the melt flow rate at varying temperature and pressure (Fig. 24.1).

TABLE 24.2 Melt flow index values

Unit process	Product	Melt flow index required
Extrusion	Pipes	<0.1
	Sheets, bottles	0.1–0.5
	Thin tubes	0.1–0.5
	Wire, cable	0.1–1
	Thin sheets	0.5–1
	Monofilaments (rope)	0.5–1
	Multifilaments	≈1
	Bottles (high glass)	1–2
Injection moulding	Film	9–15
	Moulded articles	1–2
Coating	Thin-walled articles	3–6
	Coated paper	9–15
Vacuum forming	Articles	0.2–0.5

**FIG. 24.1** Melt flow rate of polypropylene at different temperatures. Capillary $d = 1.05$ mm, L/d ratio = 4.75 (after Vinogradov and Malkin, 1966).

The results of this test may be generalised by plotting $\frac{32Q\eta_0}{\pi D^3}$ ($= \dot{\gamma}\eta_0$) versus $\frac{\Delta p}{4L/D}$ ($= \sigma_{sh,w}$) (Fig. 24.2, data from Vinogradov and Malkin, 1966), where Q is the volume flow rate, d the diameter of the circular capillary, L its length, $\dot{\gamma}$ the shear rate and $\sigma_{sh,w}$ the shear stress at the wall. From this figure the influence of pressure and geometry of the apparatus on the flow rate can be derived if the $\eta_0 - T$ relationship is known.

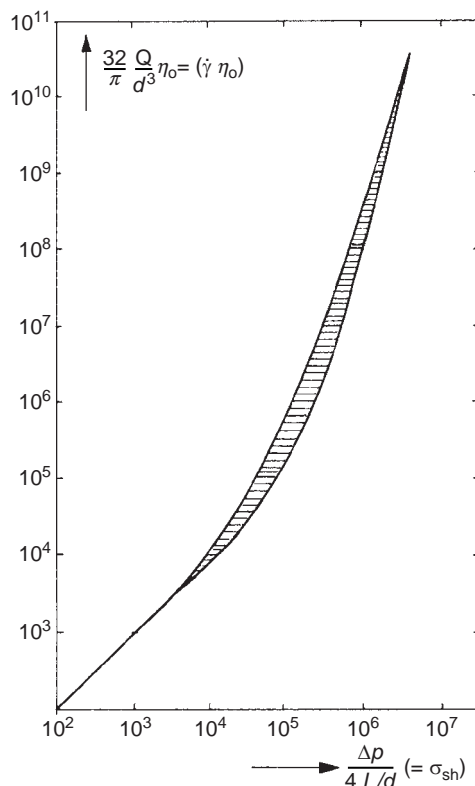


FIG. 24.2 Generalised melt flow rate diagram for commercial polymers (after Vinogradov and Malkin, 1966).

24.2.1.3. Die swell

The phenomenon of post-extrusion swelling or “ballooning” has been discussed in Chap. 15. It is related to the so-called Barus effect, according to which the diameter of polymer extrudates is larger than the capillary diameter when the melt is forced through an orifice. All materials with any degree of melt elasticity display this effect. The origin of the effect is related to the elastico-viscous nature of polymer melts, thus to $N_1 = T_{11} - T_{22}$.

Die swell is dependent upon the L/D ratio of the die. The phenomenon is a limiting factor in the drive to reduce moulding cycles, since the conditions which lead to excess swelling lead also to quality deficiencies in appearance, form and properties of the extrudate. In order to control the swelling the temperature of the melt can be increased, which causes a decrease in relaxation time. A long tapered die has also been found to reduce post-swelling.

On the basis of the melt viscosity and viscoelasticity discussed in Chap. 15 the amount of die swell under processing conditions can be estimated.

24.2.2. Mouldability

During moulding a polymer melt is *discontinuously* extruded and immediately cooled in a mould of the desired shape.

Mouldability depends on the polymer and the process conditions, of which the rheological and thermal properties of the polymer as well as the geometry and the temperature and pressure conditions of the (test) mould are the most important.

Dimensional analysis (see Chap. 3) shows that the following dimensionless quantities must be expected to determine the process:

$$\frac{\Delta p D}{\eta v}, \frac{c_p \rho v D}{\lambda} \left(= \frac{\Delta H}{\Delta T} \frac{\rho v D}{\lambda} \right), \frac{L}{D} \quad \text{and} \quad \frac{\eta}{\eta_0}$$

where λ is the thermal conductivity and ΔH the change in heat content over a temperature change ΔT .

A well-known type of (purely empirical) processability characteristic is the *moulding area diagram* (Fig. 24.3). In the moulding area diagram the limits of pressure and temperature are indicated for the processing of a defined polymer in a given moulding press. The maximum temperature is determined by (visible) decomposition, the lower temperature limits by the development of too high viscosity and melt elasticity. The higher-pressure limits are given by the start of "flashing": the polymer is then pressed through the clearance between the parts of the mould; the lower pressure limits are determined by "short shots", incompletely filling the mould.

It is clear that this diagram as such gives very little information of a general nature and is completely dependent on the accidental combination of material, machine and die. Therefore other criteria have been developed which are of a more general value and are based on the intrinsic polymer properties and the processing variables.

For estimation of the processability of a moulding polymer melt, the pressure to fill a standard mould has to be measured. Furches and Kachin (1989) have compared the results of several rheological tests often used to evaluate injection moulding polymer melts.

24.2.2.1. Spiral flow length

A widely used test for mouldability evaluation is the *spiral flow test* (Fig. 24.4). In this test the mould has the form of a spiral; the polymer melt flows into this mould under pressure and freezes in the spiral, the length of the polymer spiral being the test result. Mould geometry, temperature and pressure are standardised.

Holmes et al. (1966) made an engineering analysis of the test and found that the ultimate length of the spiral is a function of two groups of variables, one describing the

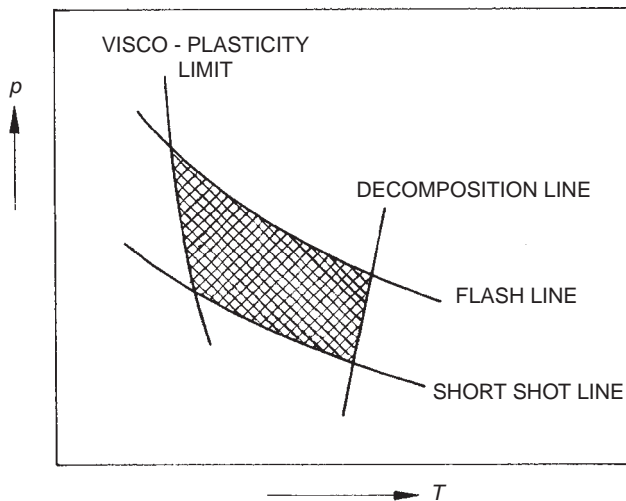


FIG. 24.3 Moulding area diagram.

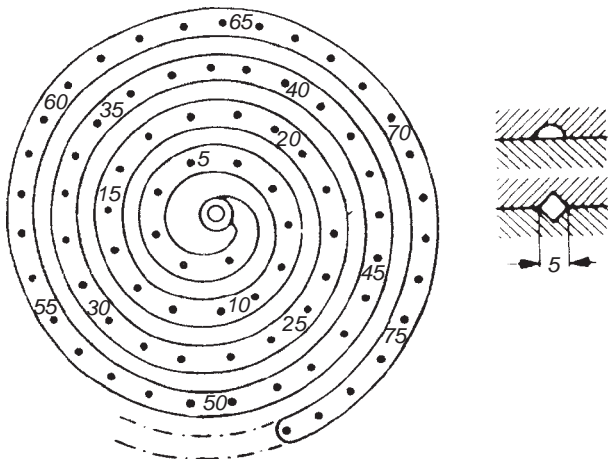


FIG. 24.4 The spiral flow test. The inlet cone is in the middle of the spiral.

process conditions ($\Delta p D^2 / \Delta T$), the other being representative of the polymer's rheological and thermal properties ($\rho \Delta H / (\lambda \eta)$). The following dimensionless relationship was obtained:

$$\left(\frac{L}{D}\right)^2 = C \left(\frac{\Delta p D^2}{\Delta T}\right) \left(\frac{\rho \Delta H}{\lambda \eta}\right) = C \left(\frac{\Delta p D}{\eta v}\right) \left(\frac{\Delta H \rho v D}{\Delta T \lambda}\right) \quad (24.4)$$

In this equation L = spiral length; D = effective diameter, characteristic of the channel cross section; ΔT = temperature difference between melt and channel wall; Δp = pressure drop; ρ = density of the solid polymer; λ = heat conductivity of the solid polymer; η = viscosity of the melt; ΔH = enthalpy difference between melt and solid.

The constant C in Eq. (24.4) is determined by the geometry of the cross section. Eq. (24.4) indeed contains the product of the dimensionless quantities predicted (Chap. 3).

In their analysis Holmes et al. demonstrated that the spiral length is limited by heat transfer (see Fig. 24.5). The fluid entering the cavity solidifies upon contact with the wall, resulting in a reduced cross section for flow. This freezing on the wall continues until the solid layers meet in the centre of the channel, stopping the flow. In the tip of the spiral a core of liquid is left which freezes after the flow has stopped. This core solidifies stress-free and is optically isotropic, whereas the rest of the spiral solidifies under stress and is birefringent.

If during the experiment the plunger is withdrawn, eliminating the pressure difference before the heat transfer has resulted in flow stoppage, the spiral length becomes shorter.

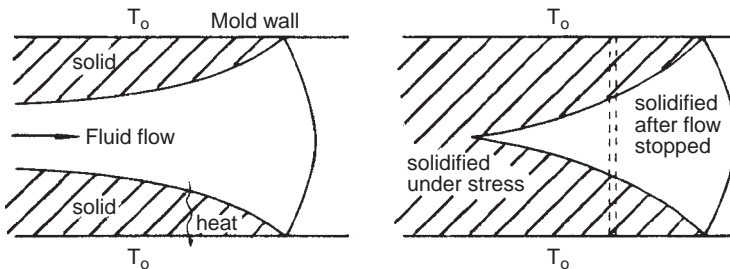


FIG. 24.5 Flow and solidification in mould channel.

By varying the "plunger forward time" Holmes et al. were able to determine the time necessary to just obtain the maximum value of L ; this time was called *freeze-off time* (t_f). The following approximate relation was found:

$$t_f \approx C' \frac{\Delta H \rho D^2}{\Delta T \lambda} = f \left(\frac{T_{\text{solidif}} - T_{\text{mould}}}{T - T_{\text{mould}}} \right) \quad (24.5)$$

In this equation pressure and viscosity do not appear because they are factors related to the flow but not to the heat transfer. This analysis clearly shows the significance of dimensionless quantities to polymer processing.

Richardson (1985) obtained, on the basis of an analytical model of the flow in a cooled spiral mould of rectangular cross section at fixed wall temperature, for the flow length

$$L = Ch \left[\frac{h^2}{\alpha} \left(\frac{\Delta p}{K} \right)^{1/n} \right]^{n/(1+n)}$$

where L = flow length; h = smaller dimension of a rectangular spiral mould; α = thermal diffusivity; K = power-law constant; n = power-law index; C = constant of order 0.1.

Since the thermal diffusivity is much less sensitive to molecular weight distribution than the viscosity, it is the high shear rate viscosity that is the governing property.

Experimental results yield values of L corresponding to values of C between 0.2 and 0.4 (Dealy and Wissbrun, 1990, General references, Chap. 15).

Fritch (1986) gives the following advice regarding flow length testing:

1. Stick to one machine and mould
2. Keep the hydraulic pressure constant
3. Melt temperature is more important than mould temperature, but a single temperature is not adequate
4. Injection rate influences the shear rate in the mould and a single value is not adequate

Scaling up, however, a single spiral mould test is not possible. Therefore, Fritch recommends that test should be carried out at three melt temperatures and three injection rates for a total of nine tests, in such a way that they cover melt temperature and mould flow rate in commercial processing.

24.2.2.2. Mouldability index

The mouldability index is the length of the elongated flow path that is filled before solidification of the injected molten polymer composition at specified moulding conditions, i.e., volumetric injection rate, mould temperature, polymer melt temperature. The mouldability index of the moulding compositions of this invention is characterised by spiral flow.

Weir (1963) defined the mouldability index, α_{STV} (the index STV stands for shear-temperature-viscosity), as follows:

$$\alpha_{\text{STV}} = \frac{10^9}{\eta} \frac{\frac{\partial \ln \eta}{\partial \ln \dot{\gamma}}}{\frac{\partial \ln \eta}{\partial (1/T)}} \approx \frac{10^9 |n - 1|}{\eta E_\eta / R} \left(\frac{m^2}{N s K} \right) \quad (24.6)$$

where α_{STV} = mouldability index [$m^2 (N s K)^{-1}$]; η_o = apparent melt viscosity at low shear rates ($\approx 10 s^{-1}$); $\dot{\gamma}$ = shear rate; n = exponent in the power law expression for non-Newtonian viscosity (see Chap. 15); E_η = activation energy of viscous flow (see Chap. 15).

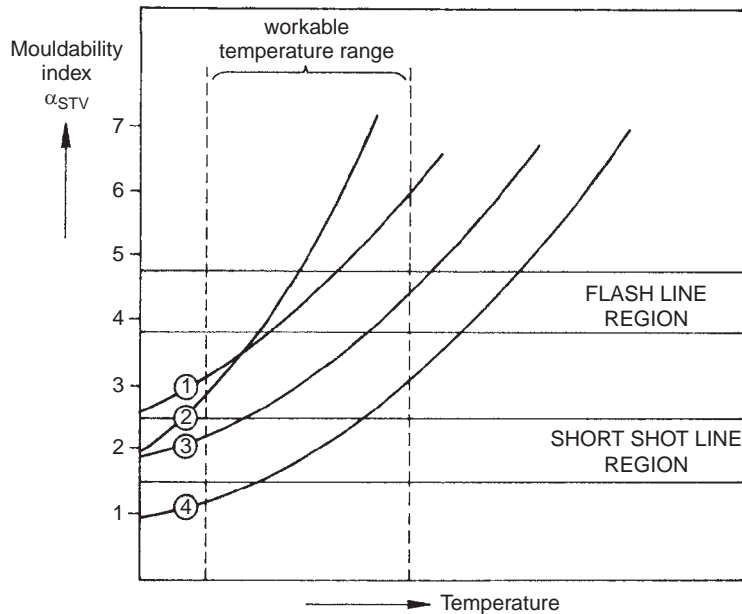


FIG. 24.6 Evaluation of four different polypropylenes by means of their mouldability index (after Weir et al., 1963).

Weir et al. (1963) have shown that for a series of polypropylenes there is a significant relation between α_{STV} and the spiral length (in the spiral flow test).

They also demonstrated that minimum cycle times are obtained at α_{STV} -values between 2 and 2.5. Boundary temperatures are found at $\alpha_{STV} \approx 2$ for "short shot" and at $\alpha_{STV} \approx 4.5$ for flashing (Fig. 24.6).

Consequently, evaluation and selection of polymers is possible by determining the α_{STV} vs. T relation from the $\eta = f(\dot{\gamma}, T, M)$ relationship (see Chap. 15). Then the working constraints, i.e. the temperature range, can be adapted to the critical T -values (see Fig. 24.6).

For a number of other polymers Deeley and Terinzi (1965) have confirmed that there is an unambiguous relation between α_{STV} and the spiral length, which indeed permits a good polymer selection. This does not mean that the mouldability index is beyond criticism. It is found, for instance, that the critical values mentioned do not apply to high-melting aromatic thermoplastics.

Nevertheless, the mouldability index is a valuable criterion, which provides a rational basis for the construction of the moulding area diagram.

24.2.2.3. Control testing of processing conditions on moulded samples

In moulding operations both the size and the shape of the products are determined by the rather complicated thermal and mechanical history of the material. Due to viscoelastic stress relaxation, post-moulding cure and after-crystallisation, slow changes may occur after moulding, which may be promoted by the (high) temperature during use. Factors such as moulding pressure, temperature (and their variations), injection speed, etc., have a profound effect. The pressure in the mould is probably the most important variable; it is not only needed for flow but also for the compensation of shrinkage.

It has been found that moulding conditions can affect almost every property of moulded parts. Among the properties affected are *impact strength*, *crack resistance*, and

appearance features such as *sink marks* and *voids*, *weld lines*, *clear spots*, *delamination* and *skinning*, *inhomogeneous pigment dispersion*, and *warping*.

The appearance of the article is one of the obvious criteria in evaluating the quality of processing. Measurements of gloss, clarity, etc., may help to quantify the assessment. But while appearance is an important aspect, it does not give us sufficient quantitative information about processing. Sometimes a better appearance may even mean less good mechanical properties!

One of the most important aspects of the processing conditions during moulding is the *orientation* in the mould. Van Leeuwen (1965) describes a special test mould developed for studying these orientation effects (see Fig. 24.7). The moulded object consists of two flat plates with a common runner. The plates can be tested as a whole, e.g. for falling-weight impact or for birefringence. Also, specimens may be cut out in two mutually perpendicular directions, e.g. for tensile impact and for "reversion" on heating.

The so-called *reversion test* is carried out by heating specimens floating on talcum powder to above the glass transition temperature. Reversion is then defined as follows:

$$\text{length reversion} = \frac{L_o}{L} - 1$$

$$\text{width inversion} = 1 - \frac{W_o}{W}$$

where L_o and W_o are the original length and width and L and W the same parameters after the revision test.

No unique relationship between width and length revision has been found (Paschke, 1967). The revision runs parallel with birefringence up to a limiting value. Van Leeuwen showed that a distinct relationship exists between the drop weight impact strength and the birefringence; the impact strength is very sensitive to orientation. A less satisfactory correlation with reversion was found.

Test programs like the one described here permit an increase of the information in the moulding area diagram. Fig. 24.8 gives Van Leeuwen's data for rubber-modified

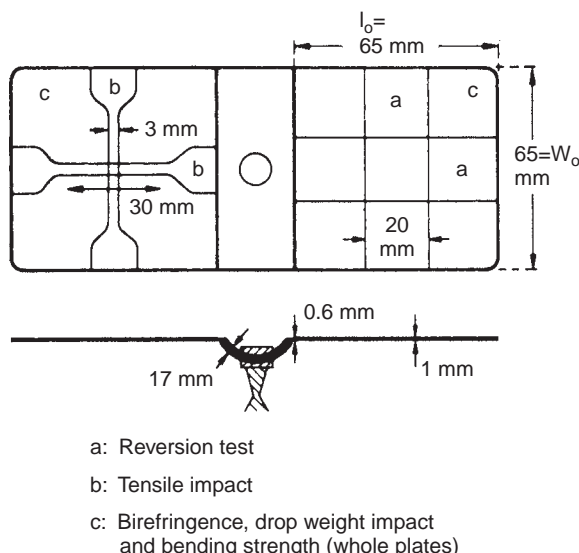


FIG. 24.7 Test mould for orientation.

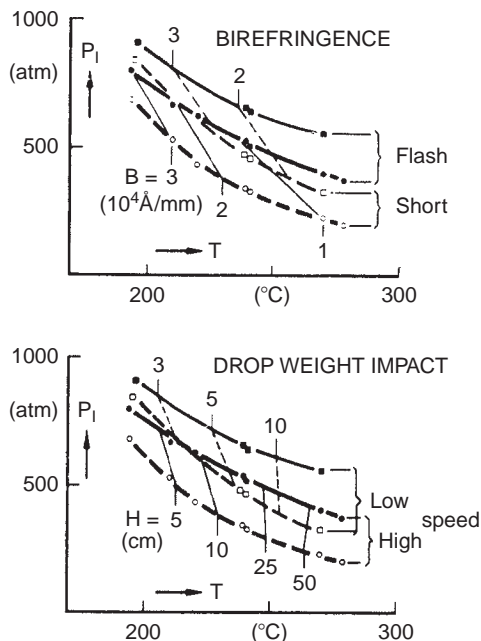


FIG. 24.8 Moulding diagrams for PS-R.

polystyrenes. Curves of constant birefringence and constant impact strength have been drawn at two different injection speeds, for both short shot and flash. In the upper diagram birefringence was used as a criterion of quality, in the lower one impact strength. It makes a significant difference which of the two criteria is used. A *high temperature and a high injection speed appear to be favourable for impact strength (a measure of brittleness and internal stresses)*. As to birefringence (as a measure of potential reversion and warping), moulding near the flash condition gives better results than marginal mould filling.

It is obvious that (apart from processing conditions) the degree of warping, the reversion and the impact strength are also determined by intrinsic properties of the polymer. Goppel and Van der Vegt (1966) showed that the first two effects increase with molecular mass and with broader molecular mass distribution. On the other hand, the impact strength increases with molecular mass and with narrower molecular mass distribution.

In conclusion, it may be said that the degree of orientation (and therefore the tendency to deformation under the influence of temperature and time) and the resistance to impact will be dependent partly on material properties and partly on process conditions.

24.2.3. Spinnability

Spinnability is the ability of a polymer to be transformed into long continuous solid threads by a *melt-spinning* process. Therefore a spinnable polymer must conform to three requirements:

1. The polymer should be thermally and chemically stable under the spinning conditions, that is, at a temperature sufficiently high to permit flow through a nozzle
2. The liquid thread produced should remain intact at least until it has solidified
3. The thread should be highly extendable during the process

Spinnability, although a necessary prerequisite for fibre formation, by no means guarantees that the polymer will be suitable as a fibre.

One of the earliest conventional methods for the assessment of spinnability was the "pulling rod" test: drawing a thread from the melt by means of a glass rod. Of course this very simple and convenient method is qualitative, since the drawing speed and the heat transfer are not controlled. Yet the thread length gives an immediate impression of the spinnability.

The first requirement of spinnability, thermal stability, has been discussed in Chap. 21. The other two requirements are closely related with the flow stability of fluid jets.

24.2.3.1. Stability of fluid threads in melt spinning

There is extensive literature on the stability of liquid jets. Lord Rayleigh discussed this subject as early as 1878, while the first quantitative description of the disintegration of a liquid jet was given by Weber (1931). A general survey of the stability of jets of Newtonian liquids with constant velocity (constant diameter) was already given by Ohnesorge (1936). Even with the two restrictions mentioned the phenomenon is rather complicated because, depending on the velocity, four regions can be distinguished in which different mechanisms of disintegration prevail. In the order of increasing velocity these regions are:

1. Formation of separate drops
2. Formation of a liquid thread, which eventually disintegrates by the formation of successive beadlike swellings and contractions along the length of the thread (symmetrical drop break-up)
3. Formation of a liquid thread which assumes the shape of a wave before disintegration (transverse wave break-up)
4. Direct atomisation

A complete description of this theory will not be given here. The most important fact is that under the conditions mentioned, the stability of a liquid jet is determined by two dimensionless groups:

$$\text{Re} = \frac{\rho v D}{\eta} \text{ and } \text{We} = \frac{\rho v^2 D}{\gamma}$$

where v = velocity of jet; D = diameter of jet; ρ = density; η = viscosity; γ = surface tension.

In the second region of disintegration, which is the most important for viscous liquids, the stability criterion is

$$\frac{L_{\max}}{D} = 12(\text{We}^{1/2} + 3\text{We}/\text{Re}) \quad (24.7)$$

where L_{\max} = maximum stable jet length.

In many cases, this equation can be simplified to ($v\eta/\gamma \gg 1$):

$$\frac{L_{\max}}{D} = 36 \frac{v\eta}{\gamma} \quad (24.8)$$

Under actual melt-spinning conditions, the situation is far more complicated as the velocity always increases (D decreases), while the fluid generally does not show Newtonian behaviour. Moreover, the temperature decreases, so that the physical properties change in the course of the process.

Stability conditions for a jet showing increasing velocity, but having a constant temperature and Newtonian behaviour, have been derived by Ziabicki and Takserman-Krozer (1964). Their formula has no direct practical use, however, as it contains the amplitude of the original distortion as a parameter; this quantity is generally not known. But also in this treatment the stability is largely determined by the dimensionless group $v\eta/\gamma$.

The stability of melt spinning under non-isothermal conditions and for non-Newtonian fluids has been discussed by Pearson and Shah (1972, 1974). Their results cannot be summarised in a few words, but again the quantity $v\eta/\gamma$ plays an important part.

In most cases a sufficient stability criterion is that Eq. (24.8) is satisfied over the whole spinning zone.

Table 24.3 shows an application of the stability criterion to three different types of melt. Completely different values are calculated for the ratio $v\eta/\gamma$. It is an empirical fact that glass can be spun whereas metals cannot. Table 24.3 shows that impractically high velocities would be necessary to stabilise a jet of liquid metal, i.e. in satisfying Eq. (24.8). Spinning of metals such as steel is possible in gaseous atmospheres where a reaction takes place on the surface of the metal jet (Monsanto, 1972).

Another conclusion is that the high viscosity of polymer melts is an important requirement for their spinnability.

24.2.3.2. Self-stabilising effects in polymer spinning

A number of incorrect opinions about the stability of melt spinning have been expressed in the past. Nitschmann and Schrade (1948) suggested that an increase of the extensional viscosity with increasing extension rate was essential for spinnability. As was stated in Chap. 15, the underlying supposition is incorrect, as in many cases the extensional viscosity does not increase during extension, or at least decreases again at high extensional rates.

It is also incorrect to assume that the increase of viscosity due to the decrease of temperature during the spinning process is essential for the stability. Nevertheless, both factors mentioned may have a very favourable effect on the process since they promote the stability: the process becomes "self-stabilising" by them.

The reverse may also be true, however, as the viscosity may decrease with increasing rate of deformation. This subject has been discussed by Pearson and Shah (1974).

Another effect of the variation of the extensional viscosity is the maximum extensibility. For polymers like high-density polyethylene, the rapid increase of the extensional viscosity during the spinning process limits the obtainable spin-draw ratio that is the ratio between the winding velocity and the velocity in the orifice. Examples can be found in an article of Han and Lamonte (1972).

TABLE 24.3 Application of stability criterion to different types of melt

Melt	η (Ns/m ²)	γ (N/m)	η/γ (s/m)
Metal	0.02	0.4	0.05
Glass	100	0.3	300
Polymer	10^4	0.025	4×10^5

24.2.3.3. Melt strength

Liquid jet instability is only one possible cause of thread fracture during melt spinning. The order breaking mechanism is cohesive fracture. The importance of this phenomenon has been stressed by Ziabicki and Takserman-Krozer (1964).

For *isothermal* deformation of Newtonian fluids, Ziabicki and Takserman-Krozer derived the formula:

$$L_{\max} = \frac{1}{\xi} \ln[(2e_{\text{coh}}E)^{1/2}/(3\eta v_o \xi)] \quad (24.9)$$

where L_{\max} = maximum length of jet; $\xi = d \ln v / dx$; e_{coh} = cohesive energy density; E = modulus of elasticity; η = viscosity; v_o = initial velocity.

Because

$$\frac{d \ln v}{dx} = \frac{1}{v} \frac{dv}{dx} = \frac{\dot{\epsilon}}{v} = \frac{\sigma}{\eta_e v} \rightarrow \text{for Newtonian liquids } \frac{\sigma}{3\eta v}$$

it follows that for extensional deformation of Newtonian liquids, due to a constant tensile force, the following expression holds:

$$\xi = \frac{\sigma_o}{3\eta v_o} \quad (24.10)$$

where σ_o = initial tensile stress.

Example 24.1

The application of Eq. (24.9) may be elucidated by a numerical example. For the quantities involved, the following order of magnitude may be assumed

$$\left. \begin{array}{l} \sigma_o = 10^4 \text{ N/m}^2 \\ \eta = 2 \times 10^4 \text{ Ns/m}^2 \\ v_o = 0.02 \text{ m/s} \end{array} \right\} \xi = 8 \text{ m}^{-1}$$

$$e_{\text{coh}} = 3 \times 10^8 \text{ J/m}^3$$

$$E = 3 \times 10^4 \text{ N/m}^2$$

Substitution of these data in Eq. (24.9) gives: $L_{\max} = 0.7 \text{ m}$

This is an order of magnitude that will permit spinning under normal conditions. A relatively small variation in the magnitude of the parameters involved, however, may lead to cohesive fracture.

A rapid method for determining the *melt strength* has been developed by Busse (1967). He extruded a polymer melt through a standard orifice at a given temperature and a standard rate. The thread obtained was taken up on a pulley with variable speed. During a test the take-up speed was gradually increased until the thread broke, while the tension was recorded as a function of time.

Different polymers showed considerable differences both in melt strength and in maximum extension ratio. For a given polymer, the melt strength increased with the melt viscosity (decreasing temperature).

This test may be useful for a rapid comparison of a number of polymers. A theoretical interpretation of the results is almost impossible, however, because temperature and stress history of the polymer are completely undefined.

24.2.4. Stretchability

Stretchability denotes the suitability of a polymer in the solid state (amorphous or semi-crystalline) to be stretched in one direction (occasionally in two directions). Of course, this processing step only serves a useful purpose in a specimen with a large aspect (i.e. length to diameter) ratio (fibres, films, sheets). The purpose of this operation generally is to achieve an improvement of mechanical properties, especially in the direction of stretching.

Although some operations in the plastics industry, such as calendering, could be described as stretching processes, the most important application of stretching is usually called *drawing* (of fibres and films).

There exists extensive literature on the drawing of synthetic polymers, of which only very broad outlines can be given here.

A phenomenon often encountered in drawing is *necking*, which may be described as a discontinuity in the reduction of the diameter of the specimen in the direction of stretching. The name "neck" has been chosen because in fibres the shape of this discontinuity often shows some similarity with the neck of a bottle.

Considère gave a criterion of the appearance of a discontinuity during stretching already in 1885. If a cylindrical body is subjected to a force F , the local mean tensile stress in an arbitrary cross section (area A) is

$$\sigma = F/A$$

For constant density

$$\frac{A_o}{A} = \frac{l}{l_o} \equiv \Lambda$$

where A_o = original area; l = length of a small part; l_o = original length of this part; Λ = local draw ratio.

Combination of the above equations gives:

$$\sigma = \frac{F}{A_o} \Lambda$$

So for constant F , σ is proportional to Λ . The straight lines in Figs. 24.9 and 24.10 represent this expression. The deformation mechanics of the polymer, however, do not allow arbitrary combinations of σ and Λ .

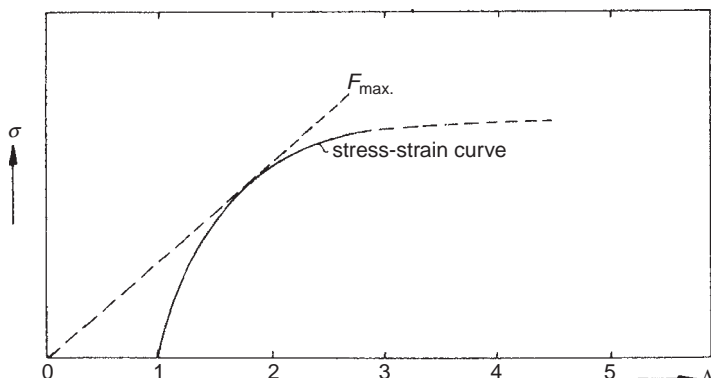


FIG. 24.9 Considère plot for a material without strain hardening.

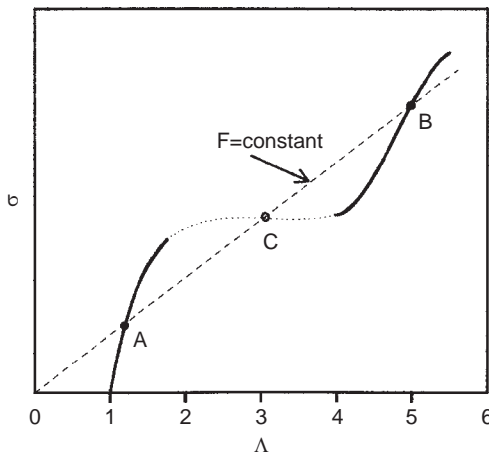


FIG. 24.10 Considère plot for a material with strain hardening.

If the stress-strain curve of a given material has a shape as sketched in Fig. 24.9, the tensile force in a drawing experiment can be increased to a maximum value F_{\max} . This force corresponds to the tangent to the curve from the origin. A further increase of the tensile force causes breakage of the specimen.

A number of materials, however, show stress-strain curves of the shape sketched in Fig. 24.10. After the normal convex first part, the stress-strain curve shows an inversion point, after which the stress increases rapidly with strain. This phenomenon is sometimes called "strain hardening". In this case, a straight line through the origin can intersect the stress-strain curve at two points A and B. This means that only the intersection points A and B are possible conditions. The intermediate intersection point C is unstable. So in this case two parts of the specimen, e.g. a fibre, with different draw ratios and, hence, different cross sections can coexist. If the fibre is stretched, part of the material with a cross section of point A is converted into material with a cross section of point B. In contrast, in Chap. 13 the Considère plot is defined as the *tangent line* on the true stress-strain curve.

These considerations lead to a criterion of the stretchability of a material: *the stress-strain curve should show an inversion point (strain hardening)*. This is not a sufficient criterion, however, as under some experimental conditions these materials simply break on extension.

The second criterion is that the material should have sufficient molecular mobility to withstand a rapid reduction in diameter. The nature of the molecular mobility that permits drawing depends on the structure of the material. As a general rule, semi-crystalline polymers are drawn at temperatures from somewhat below the melting point, down to the glass transition temperature, while amorphous polymers are drawn at temperatures in the neighbourhood of the glass transition temperature. In this connection it should be mentioned that at high rates of deformation the temperature of the fibre can be considerably higher than the temperature of the surroundings.

The drawing of semi-crystalline polymers is a very complicated morphological phenomenon. According to Peterlin (1971) and Wada (1971) at least three stages can be distinguished:

1. Plastic deformation of the original semi-crystalline structure
2. Transformation of this structure into a fibre structure by a mechanism called "micro-necking"
3. Plastic deformation of the fibre structure

Macroscopically, a sharp neck can generally be observed.

In the drawing of amorphous polymers, the structural changes involved principally result in an increasing degree of orientation, followed or not by partial crystallisation.

As was described by Marshall and Thompson (1954) and by Müller and Binder (1962), drawing of amorphous polymers may involve two different molecular mechanisms. At a given rate of deformation of a given polymer there exists a transition temperature in the neighbourhood of the glass transition temperature, below which drawing takes place with the formation of a rather sharp neck. Above the transition temperature, there is a more gradual decrease in diameter. The transition temperature increases with the rate of deformation. Marshall and Thompson introduced the names *cold drawing* and *hot drawing* for these phenomena. For poly(ethylene terephthalate), for instance, the transition temperature is about 80 °C for low rates of deformation, as used in a tensile test. But the transition temperature can exceed 100 °C under the high rates of deformation used in technical yarn drawing apparatus.

A confirmation of these phenomena has been given by Spruiell et al. (1972).

That cold drawing and hot drawing involve different deformation mechanisms can be concluded from the accompanying changes in physical properties. The increase of birefringence with draw ratio, for instance, is different for cold drawing from that for hot drawing. Hot drawing is the type of deformation that already occurs during the spinning process. After the spinning process, synthetic fibres are generally subjected to a cold-drawing process, followed or not by annealing.

An interesting example of the difference in drawing behaviour between amorphous and crystalline yarn is the drawing of crystalline poly(ethylene terephthalate). It is often stated that crystalline PETP cannot be drawn. It is true that the material breaks if drawn at a temperature of 80 °C, which is a drawing temperature normal for the amorphous polymer. Mitsuishi and Domae (1965), however, were able to draw crystalline PETP to a draw ratio of 5.5 at a temperature of 180 °C.

A quantity often used in the description of drawing phenomena is the *natural draw ratio*. As can be seen in Fig. 24.10, simple drawing of a material with the given stress-strain curve results in a fixed draw ratio corresponding to point B on the curve. This is called the natural draw ratio.

The natural draw ratio is not constant, but dependent on experimental conditions: temperature, rate of deformation, etc. Nevertheless, the order of magnitude of the natural draw ratio gives an indication of the stretchability of a given material. Very broadly speaking, the polymers can be divided into three categories:

1. Typically amorphous polymers, such as polystyrene and polysulphone; they generally show a weak strain-hardening effect and their natural draw ratios are about 1.5–2.5
2. Polymers with a certain degree of crystallinity in the drawn state; to this group belong the important synthetic fibres like polyesters and polyamides with natural draw ratios of about 4–5
3. The typically high-crystalline polymers, such as polyethylene and polypropylene; here high natural draw ratios (5–10) are found; in combination with gel-spinning they may be as high as 50

In principle, a simple bench-drawing test may be used to obtain an impression of the stretchability and of the natural draw ratio of a given polymer. However, as the rate of deformation in the bench test is appreciably lower than under technical drawing conditions, testing should be done below the technical drawing temperature. An impression of the order of magnitude of this temperature difference may be obtained by application of the Williams–Landel–Ferry equation (see Chap. 13). The temperature difference may be more than 20 °C.

To summarise: the stretchability of a polymer depends on the occurrence of strain hardening. It is limited to a temperature region where the polymer shows a specific magnitude of molecular mobility.

24.3. IMPLEMENTATION OF PROCESSING RESEARCH

In order to bridge the gap between research data and the behaviour of products in actual practice, systematic application research has to be carried out. Fig. 24.11 shows what this means.

Usually so-called *simulation experiments* are carried out first. As regards *processing*, these simulation experiments should approach practice as closely as possible. It stands to reason that the conditions applied in *testing* should also correspond closely to those in practice.

The simulation experiments are followed by systematic *processing experiments* on a *model machine*, which should be a small, well-equipped production machine. This gives data that are still closer to practice, because they have been obtained under practically equal, though carefully watched, circumstances.

Practice itself will afterwards supply the *feed back information*, which may even be more important. It will be clear that the practical knowledge of the process engineer is essential here. Mostly, however, this knowledge has no background in the research data available. In the introduction of new plastics, but also in the technical applications of existing material this may be a strongly limiting factor. In this connection, a scientific analysis of processing practice is very important.

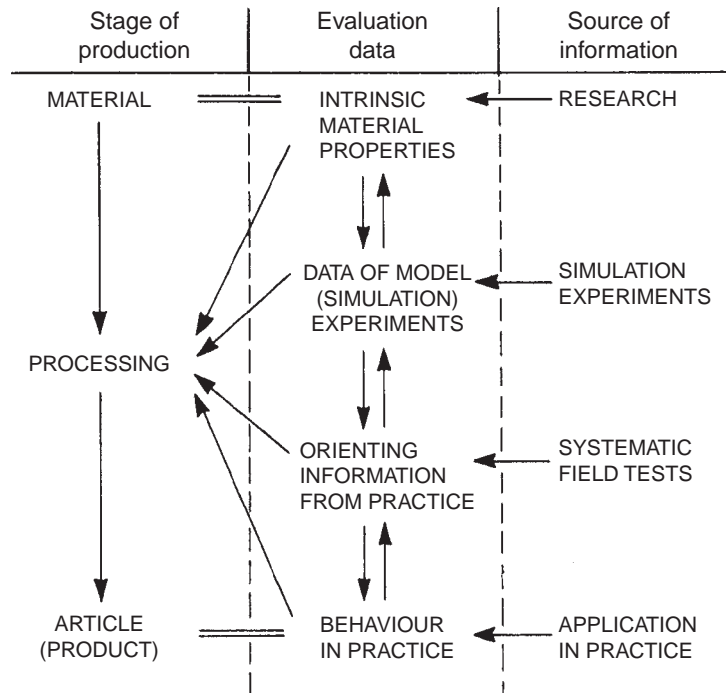


FIG. 24.11 Application research (Van Krevelen, 1967).

BIBLIOGRAPHY

General references

- Astarita G and Nicolais L (Eds), "Polymer Processing and Properties", Plenum Press, New York, 1984.
- Becker WE (Ed), "Reaction Injection Molding", Van Nostrand Reinhold, New York, 1979.
- Bird RB, Armstrong RC and Hassager O, "Dynamics of Polymeric Liquids", Wiley, New York, 2 Vols, 2nd Ed, 1987.
- Brown I, "Injection Molding of Plastic Compounds", McGraw-Hill, New York, 1979.
- Brydson JA, "Flow Properties of Polymer Melts", Iliffe Books Ltd, London, 2nd Ed, 1981.
- Crawford RJ, "Plastics Engineering", Pergamon Press, Elmsford, 1981.
- Dealy JM and Wissbrun KF, "Melt Rheology and its Role in Plastics Processing", Van Nostrand Reinhold, New York, 1990.
- Dubois JH and Pribble WI (Eds), "Plastic Mold Engineering Handbook", Van Nostrand Reinhold Co, New York, 3rd Ed, 1978.
- Dym IB, "Injection Molds and Molding, A Practical Manual", Van Nostrand Reinhold Co, New York, 1979.
- Elden RA and Swan AD, "Calendering of Plastics", Iliffe Books Ltd, London, 1971.
- Fisher EG and Chard ED, "Blow Molding of Plastics", Iliffe Books Ltd, London, 1971.
- Fisher EG and Whitfield EC, "Extrusion of Plastics", Wiley, New York, 1976.
- Frados J, Ed "Plastics Engineering Handbook of the Society of the Plastics Industry", Van Nostrand Reinhold Co, New York, 1976.
- Furches BJ and Kachin GA, SPE Tech Papers 35 (1989) 1663.
- Han CHD, "Multiphase Flow in Polymer Processing", Academic Press, New York, 1981.
- Holmes-Walker WA, "Polymer Conversion", Applied Science Publishers, London, 1975.
- Kobayashi A, "Machining of Plastics", McGraw-Hill, New York, 1967.
- Kresta JF, "Reaction Injection Molding", ACS Symp Ser 270, Washington DC, 1985.
- Levy S, "Plastics Extrusion Technology Handbook", Industrial Press, New York, 1981.
- Manson JA and Sperling LH, "Polymer Blends and Composites", Heyden, London, Plenum Press, 1976.
- Martelli FG, "Twin Screw Extruders: A Basic Understanding", Van Nostrand Reinhold Co, New York, 1983.
- Martin ER, "Injection Moulding of Plastics", Iliffe Books Ltd, London, 1964.
- McKelvy JM, "Polymer Processing", Wiley, New York, 1962.
- Ogorkiewicz RM (Ed) "Engineering Properties of Thermoplastics", Wiley Interscience, New York, 1970.
- Pearson JRA, "Mechanical Principles of Polymer Melt Processing", Pergamon Press, Oxford, 1966.
- Pearson JRA, "Mechanics of Polymer Processing", Elsevier Applied Science Publishers, London, 1985.
- Piau J-M and Agassant J-F (Eds), "Rheology for Polymer Melt Processing", Rheology Series, Vol. 5, Elsevier, Amsterdam, 1996.
- Pye RGW, "Injection Mould Design", Iliffe Books Ltd, London, 1968.
- Rauwendaal C, "Polymer Extrusion", Hanser, Munich, 1986.
- Rohn LR, "Analytical Polymer Rheology; Structure-Processing-Property Relationships", Carl Hanser Verlag, Munich, 1995.
- Rubin II, "Injection Molding Theory and Practice", Wiley, New York, 1972.
- Tadmor Z and Klein L, "Engineering Principles of Plasticating Extrusion", Van Nostrand, New York, 1970.
- Tadmor Z and Gogos CG, "Principles of Polymer Processing", Wiley, New York, 1979.
- Tess RW and Poehlein GW (Eds), "Applied Polymer Science", ACS Symp Ser, No 285, Washington ACS, 2nd Ed, 1985.
- Thiel A, "Principles of Vacuum Forming", Iliffe Books Ltd, London, 1965.
- Thorne JL, "Plastics Process Engineering", Marcel Dekker, New York, 1979.
- Weir CI, "Introduction to Injection Molding", Soc Plastics Eng, Brookfield Center, CO, 1975.

Special references

- ASTM D 1238-70 "Measuring Flow Rates of Thermoplastics by Extrusion Plastometer".
- Boenig HV, "Polyolefins", Elsevier, Amsterdam, 1966, Chap. 8, p 262.
- Busse WF, J Polymer Sci A2, 5 (1967) 1219 and 1261.
- Considère A, Ann Ponts Chaussées 6 (1885) 9.
- Deeley CW and Terinzi JF, Modern Plastics 42 (1965) 111.
- Fritch LW, Plastics Engineering 42, no 6 (June) (1986) 41; SPE Tech Papers 32 (1986) 1663.
- Goppel JM and Van der Vegt AK, "Processing Polymers to Products", Proc Intermit Congress, Amsterdam (1966), 't Raedthuys, Utrecht, 1967, p 177.
- Han CD and Lamonte RR, Trans Soc Rheol 16 (1972) 447.
- Holmes DB, Esselink BP and Beek WJ, "Processing Polymers to Products", Proc International Congress, Amsterdam (1966), 't Raedthuys, Utrecht, 1967, p 131.

- Marshall I and Thompson AB, Proc Royal Soc (London), A 221 (1954) 541; J Appl Chem 4 (1954) 145.
Mitsubishi Y and Domae H, Sen-i Gakkaishi 21 (1965) 258.
Monsanto CO, US Patent 3, 645, 657 (1972).
Müller FH and Binder G, Kolloid-Z 183 (1962) 120.
Nitschmann IT and Schrade J, Helv Chim Acta 31 (1948) 297.
Ohnesorge W, Z Angew Math Mech 16 (1936) 355.
Paschke E, "Processing Polymers to Products", Proc International Congress, Amsterdam (1966), 't Raedhuys, Utrecht, 1967, p 123; see also Kunststoffe 57 (1967) 645.
Pearson JRA and Shah YT, Ind Eng Chem Fund 11 (1972) 145; 13 (1974) 134.
Peterlin A, J Mater Sci 6 (1971) 490.
Powell PC, "Processing Methods and Properties of Thermoplastic Melts", in Ogorkiewicz RM (Ed), "Thermoplastics", Wiley, London, 1974, Chap. 11.
Rayleigh, Strutt JW Lord, Proc London Math Soc 10 (1878) 7.
Richardson SM, Rheol Acta 24 (1985) 509.
Spruiell JE, McCord DE and Beuerlein RA, Trans Soc Rheol 16 (1972) 535.
Van der Vegt AK Trans Plastics Inst 32 (1964) 165.
Van Krevelen DW, "Processing Polymers to Products", Proc International Congress, Amsterdam (1966), 't Raedhuys, Utrecht, 1967.
Van Leeuwen J, Kunststoffe 55 (1965) 491; "Processing Polymers to Products", Proc International Congress, Amsterdam (1966), 't Raedhuys, Utrecht, 1967, p 40.
Vinogradov GV and Malkin AYA, Kolloid-Z 191 (1963) 1; J Polym Sci A2, 2 (1964) 2357; A2, 4 (1966) 137.
Wada Y, J Appl Polym Sci 15 (1971) 183.
Weber C, Z Angew Math Mech 11 (1931) 136.
Weir FE, SPE Trans (1963) 32.
Weir FE, Doyle ME and Norton DG, SPE Trans (1963) 37.
Ziabicki A and Takserman-Krozer R, Kolloid-Z 198 (1964) 60; 199 (1964) 9.

CHAPTER 25

Product Properties (I): Mechanical Behaviour and Failure

Product (article) properties are in principle determined by combinations of intrinsic and “added” properties. However, the correlations between these basic properties and the (more or less subjectively defined) product properties are often complex and only partly understood. They are “system-related”.

None of the mechanical product properties can be estimated directly from additive quantities. There exist, however, several quantitative relationships that connect the mechanical product properties with intrinsic mechanical properties.

25.1. INTRODUCTION

Product or article properties (also called *end-use properties*) are very complex. They depend not only on the material of which the product or article is made, but also – and mainly – on the system of which the article forms part: product properties are “*system related*”.

Friction, abrasion and wear, for instance, are – mathematically – “operators” of a system, i.e. they depend on the parameters of a system, such as the geometry of the surface, the temperature, the load, the relative velocities, the composition of the environmental atmosphere, etc. The operational character of wear, for example, depends on the physicochemical interaction of surfaces and on *their* interaction with the lubricant and the atmosphere.

As far as the article itself is concerned, the product or article properties are in principle determined by combinations of intrinsic and “added” properties; the latter are obtained by processing. However, the correlations between these basic material properties and the more or less subjectively defined article properties have often been only partly investigated or are not yet fully understood.

It is, of course, impossible to give a general survey of product properties: every article has to be considered in its specific application as part of a system. So in this chapter *we shall give only some general lines of approach*.

The mechanical product properties are characteristic parameters for mechanical behaviour and failure under use conditions. They can roughly be divided into two categories, viz.:

- a. Properties connected with *high stress levels* and *short periods*
 - b. Properties connected with *low stress levels* and *long periods*
- Table 25.1 gives a classification of the mechanical end use properties

TABLE 25.1 Mechanical end use properties

Class	Short-term behaviour	Long-term behaviour
<i>Deformation properties</i>	<i>Stiffness</i>	<i>Creep</i>
	Stress-strain behaviour	Uniaxial and flexural deformation
	Modulus Yield stress	Creep behaviour
<i>Durability properties</i> Bulk	<i>Toughness</i>	<i>Endurance</i>
	Ductile and brittle fracture	Creep rupture
	Stress and elongation at break	Crazing (and cracking)
Surface	Impact strength	Flexural resistance Fatigue failure at cyclic stress
	<i>Hardness</i>	<i>Friction and Wear</i>
	Scratch resistance Indentation hardness	Coefficient of friction Abrasion resistance

25.2. FAILURE MECHANISMS IN POLYMERS

The behaviour of linear polymers depends largely on the temperature and the stress state; e.g. the response in tension may differ markedly from that in compression.

In Chaps. 13 and 15 we have already discussed several mechanisms of failure, so that we may confine ourselves to a short summary. This will be based on a very clear survey by Bin Ahmad and Ashby (1988).

At temperatures well below the glass transition temperature (T_g) the polymer responds in an almost linear-elastic manner and may fail by *brittle fracture*; the elastic elongation is only a few percent and the catastrophic failure occurs suddenly, although it is probably initiated by localised yielding or crazing. Shear band yielding and crazing are competing mechanisms; both are favoured by localisation of plastic strain and common in all polymers exhibiting strain-softening characteristics. Environmental conditions determine which mechanism dominates. Crazing may, e.g. be suppressed by compressive stresses and be favoured by certain environmental factors (vapours and liquids).

By increase of the temperature the mode of failure is changed from brittle fracture to ductile fracture, characterised by the appearance of a yield point prior to fracture, and sometimes by indications of necking.

A further temperature rise leads to necking, with the possibility of cold drawing; the latter phenomenon is dependent on the stability of the neck, and is governed by the level of adiabatic heating and strain hardening. In this case the extensions can be very large.

Finally, at a still higher temperature the polymer starts to deform homogeneously by viscous flow. For amorphous polymers the stress levels are very low in this case.

Each mechanism has a characteristic range of temperature and strain rate, in which it is dominant.

A survey of the load-deformation curves for linear polymers at different temperatures is given in Fig. 25.1A. Each mechanism is further illustrated by a schematic diagram (Figs. 25.1B–E). The mathematical equations for the different mechanisms were given in the Chaps. 13–15. Based on the respective equations Ahmad and Ashby designed *Failure Mechanism Maps*. The most important of these are reproduced here as Fig. 25.2A–D.

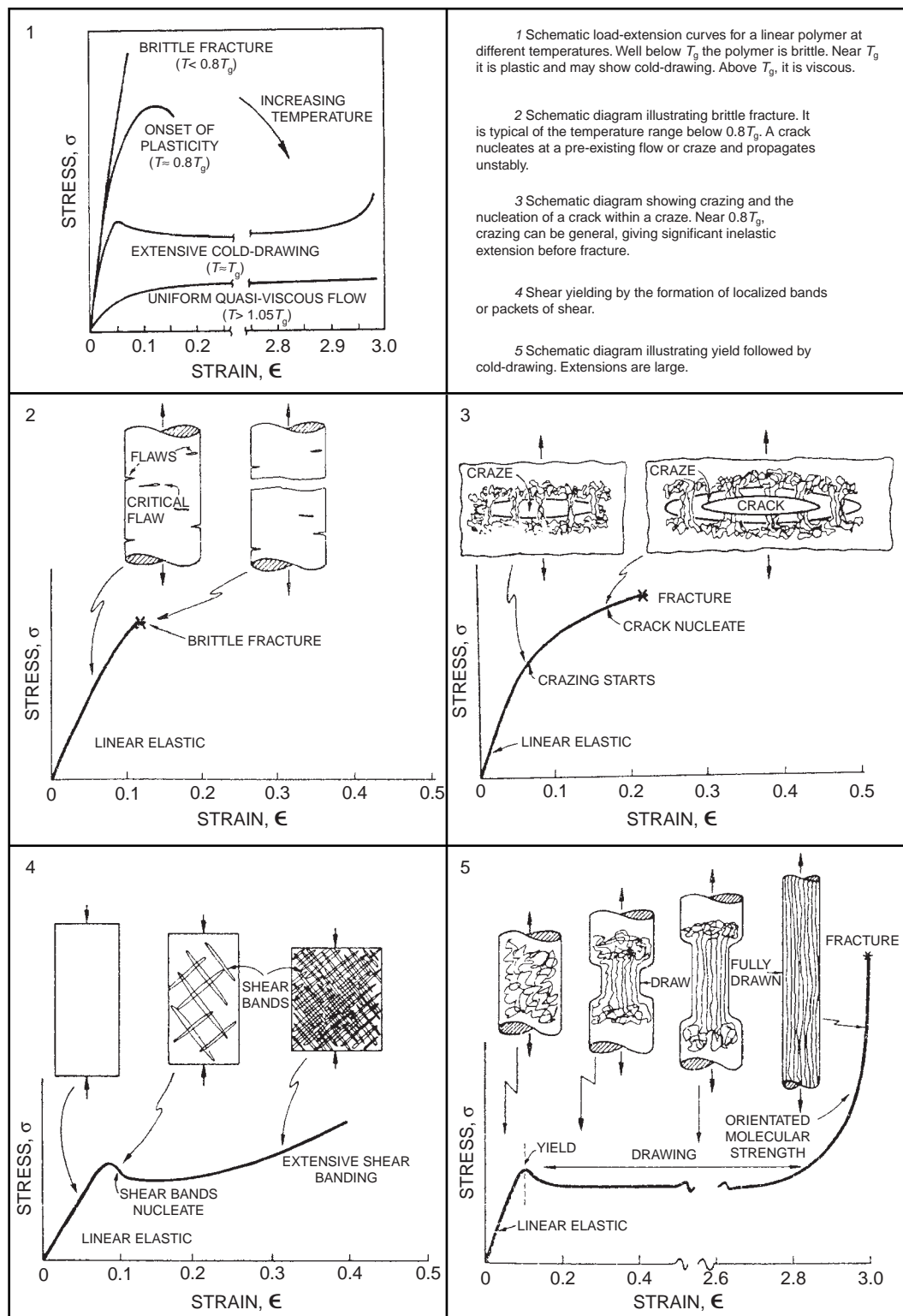


FIG. 25.1 Failure mechanisms in polymers. From Bin Ahmad and Ashby (1988); Courtesy of Chapman and Hall.

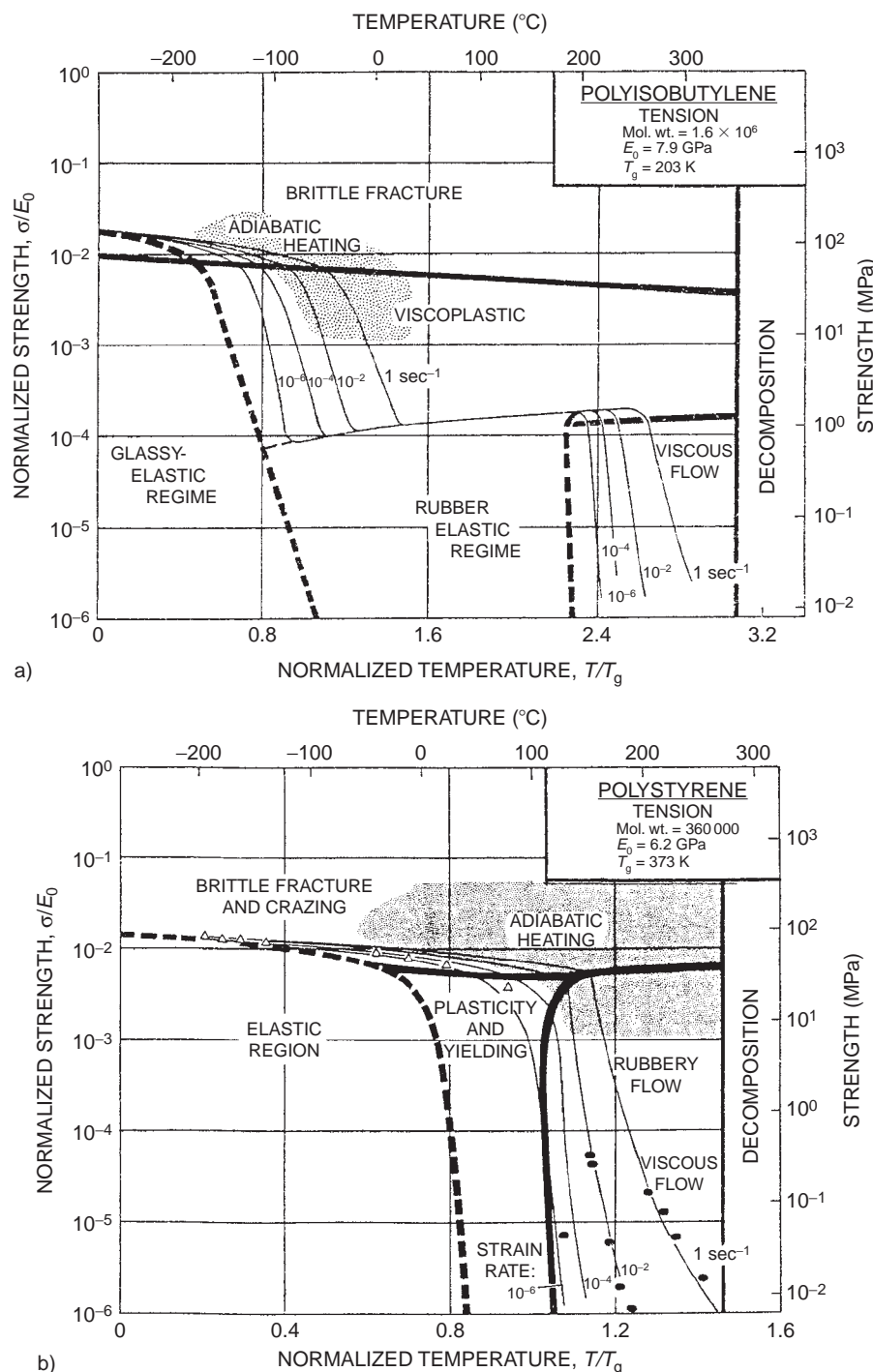
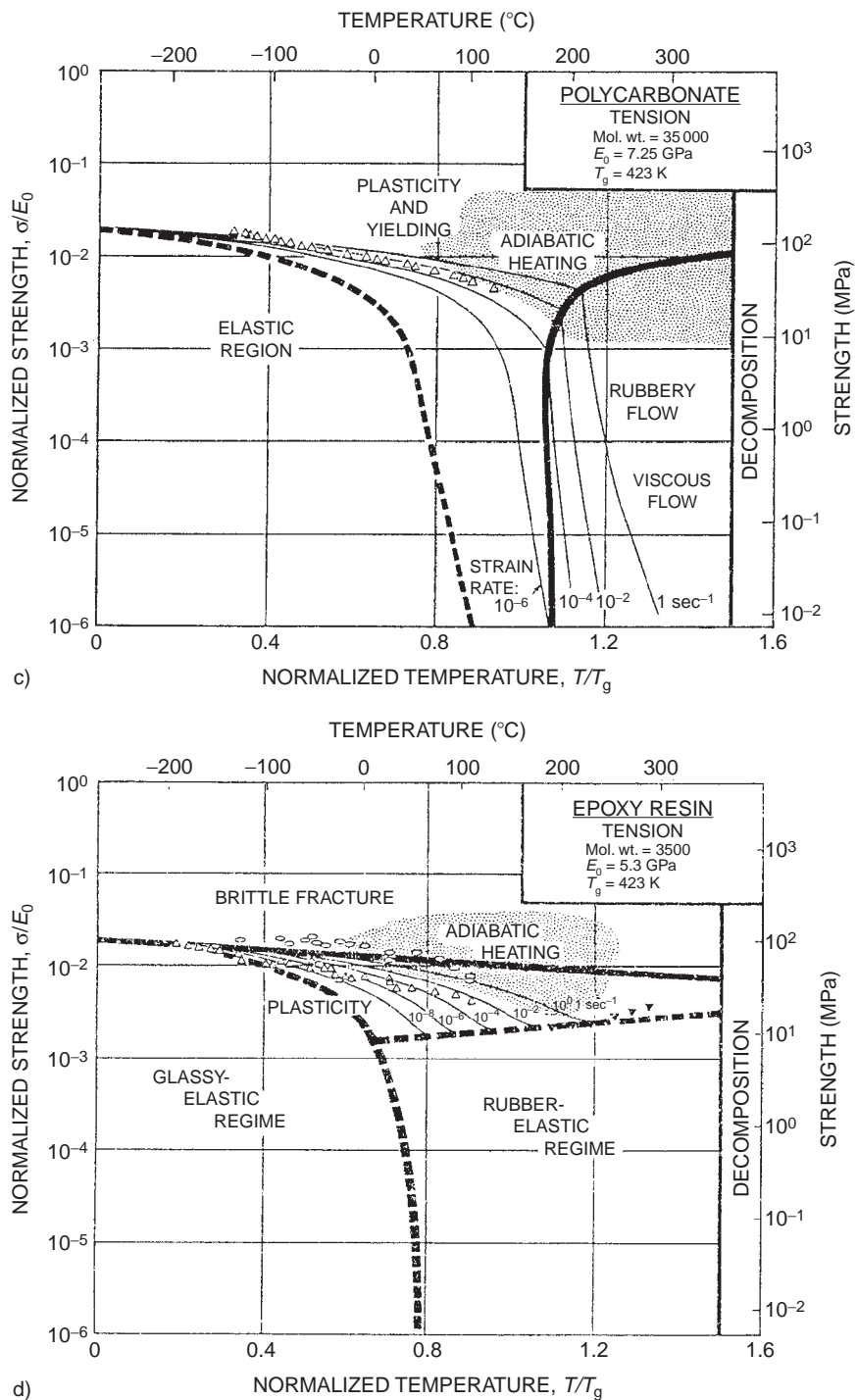


FIG. 25.2 Failure maps of representative polymers. From Bin Ahmad and Ashby (1988); Courtesy of Chapman and Hall.

**FIG. 25.2** (continued)

In these maps the strength (common, σ_{\max} and normalised, σ_{\max}/E_0) is plotted versus the temperature (common, $^{\circ}\text{C}$, and normalised, T/T_g); the diagram obtained is thus subdivided into fields in which a single mechanism will allow failure at a lower stress than any other; these fields represent a regime:

- (a) The regime of brittle fracture
- (b) The regime of visco-plastic yielding
- (c) The regime of flow
- (d) The rubber-elastic regime
- (e) The regime of cold drawing (adiabatic heating)

The field boundaries (the heavy lines) are the loci of points at which two mechanisms have equal failure strength.

Superimposed on these fields are contours of constant strain rate, $\dot{\varepsilon}$. The heavy broken lines correspond to the contour at a strain rate of 10^{-12} s^{-1} . The region of cold drawing by adiabatic heating is shown as a shaded zone, bounded by the conditions of adiabatic heating:

$$\left[\frac{\sigma_{d,\max}/E_0 \geq 2 \times 10^{-3}}{\dot{\varepsilon} \geq 10^{-3} \text{ s}^{-1}} \right] \quad (25.1)$$

Four representative polymers were chosen: polyisobutylene, polystyrene, polycarbonate and epoxy resin. PIB is a polymer with a very low T_g and shows all regimes; PS has a "normal" T_g and lacks a rubber-elastic regime; PC has a high T_g and does not exhibit brittle fracture at tension; EP, as a cross-linked polymer, does not flow on heating. From the maps one immediately sees how the polymer will behave at a certain temperature and stress, i.e. which failure mechanism will prevail. The four maps are valid for *tension*. Bin Ahmad and Ashby also designed maps for the case of compression. In the latter case the diagram is qualitatively identical with the exception of the fact that in the compressive behaviour the brittle fracture regime is absent; instead plastic yielding with shear bands will be observed. Quantitatively the curves will show a small shift upwards, viz. by a factor of about 2, so in the logarithm 0.3.

25.3. DEFORMATION PROPERTIES

Polymers are used in many applications where substantial loads have to be carried. A good designer tries to ensure that a given article will not break, deflect or deform, bearing in mind the economic penalties of over-design. Considerable quantities of design data are nowadays available, making major contributions to the resolution of many design problems. But these data can only resolve part of the problems, since many of them are extremely complicated and defy rigorous or even approximate analysis.

The most serious obstacle in the design of plastic articles is the influence of stress concentrations, *which should therefore be reduced to a minimum*.

In the category of deformation properties the phenomena of stress-strain behaviour, modulus and yield, stress relaxation and creep have been discussed already in Chap. 13. Here we want to give special attention to the long-term deformation properties. For a good design we need sufficiently reliable creep data (or stress-strain curves as a function of time and temperature).

25.3.1. Uniaxial deformation under constant load

The usual design procedure is to couple a specific value of design stress with a conventional stress or strain analysis of the assumed structural idealisation. The uniaxial deformation behaviour is of special importance in thin-walled pipes, circular tanks and comparable systems under simple stress.

We confine ourselves here to cylindrical tanks as an example. For free-standing liquid storage tanks the following formula applies to the design stress σ_D :

$$\sigma_D(\text{at } \varepsilon = 1\%) \geq \frac{pR}{d\mu} \left(\approx \frac{g\rho HR}{d} \mu \right) \quad (25.2)$$

where p is the hydrostatic pressure, R the radius and d the wall thickness of the tank, H the height of liquid above the base of the tank, and μ a shape factor of the order of 1.

If one knows σ as a function of ε , t and T , or the Young's modulus as a function of t and T , then the geometrical data can be calculated, e.g. the wall thickness at a given tank capacity.

Example 25.1

What is the minimum wall thickness of a cylindrical tank, 5 m in height, 1.5 m in radius, made of polypropylene and capable of storing aqueous solutions for a year, if the allowed maximum design strain is 1%.

Solution

The modulus of polypropylene at room temperature (100 s creep modulus) is 15×10^8 N/m² (see Chap. 13, Table 13.11). Applying Eq. (13.126) we find

$$\log \frac{E_R}{E} = \log \frac{1.5 \times 10^9}{E} \approx 0.08 \log \frac{t}{t_R} \approx 0.08 \log \frac{3.16 \times 10^7}{10^2}$$

$$1 \text{ year} = 3.16 \times 10^7 \text{ s}$$

$$\text{This gives } E = 5.5 \times 10^8 \text{ N/m}^2$$

$$\text{so that } \sigma_D = E\varepsilon = 5.5 \times 10^8 \times 10^{-2} \geq \frac{9.81 \times 1000 \times 5 \times 1.5 \times \mu}{d}, \mu \approx 1$$

$$\text{or } d \geq \frac{7.4 \times 10^4}{5.5 \times 10^6} \mu \approx 13.5 \times 10^{-3} \text{ m} = 13.5 \text{ mm}$$

So the wall thickness has to be at least 13.5 mm.

25.3.2. Flexural deformation under constant load

Again, reliable creep modulus data have to be available in order to apply the deflection equations. Tables 25.2 and 25.3 (see also Fig. 25.3) give the expressions for the deflections and torsional deformations of bars. By means of these equations the modulus of engineering materials may be determined from deflection and torsion experiments. The reader is also referred to, e.g. Ferry (1980), McCrum et al. (1997), Whorlow (1992) and Te Nijenhuis (1980, 2007).

In practice the strain involved in the flexure of beams and struts is normally small; a practical limit of 0.5% has been suggested

TABLE 25.2 Summary of flexural formulas (after Schmitz and Brown (1965–1969), Vol. 2, p. 329)

Sample geometry	Type of support	Type of loading	Maximum tensile stress σ_{\max}	Modulus ^a E	Strain ^a ϵ
Rectangular beam of width b and thickness d	To simple supports at distance L	Single concentrated load P at midpoint $L/2$	$\frac{3PL}{2bd^2}$	$\frac{PL^3}{4bd^3y}$	$\frac{6dy}{L^2}$
Rectangular beam of width b and thickness d	Two simple supports at distance L	Two equal loads $P/2$ at 1/3 points $L/3$ and $2L/3$	$\frac{PL}{bd^2}$	$\frac{23PL^3}{108bd^3y}$	$\frac{108dy}{23L^2}$
Rectangular beam of width b and thickness d	Two simple supports at distance L	Two equal loads $P/2$ at 1/4 points $L/4$ and $3L/4$	$\frac{3PL}{4bd^2}$	$\frac{11PL^3}{64bd^3y}$	$\frac{48dy}{11L^2}$
Rectangular beam of width b and thickness d	Fixed cantilever	Single concentrated load at free end	$\frac{6PL}{bd^2}$	$\frac{4PL}{bd^3y}$	$\frac{3dy}{2L^2}$
Rod of diameter D	Two simple supports at distance L	Single concentrated load at midpoint	$\frac{8PL}{\pi D^3}$	$\frac{4PL^3}{3\pi D^4y}$	$\frac{6Dy}{L^2}$
Rod of diameter D	Fixed cantilever	Single concentrated load at free end	$\frac{32PL}{\pi D^3}$	$\frac{64PL}{3\pi D^4y}$	$\frac{3Dy}{2L^2}$
Tube of outside diameter D and inside diameter d	Two simple supports at distance L	Single concentrated load at midpoint	$\frac{8PLD}{\pi(D^4 - d^4)}$	$\frac{4PL^3}{3\pi(D^4 - d^4)y}$	$\frac{6Dy}{L^2}$

^a Note: y = maximum beam deflection in all cases.

TABLE 25.3 Summary of torsion formulas

Bar cross section	Shear modulus G (static)	G' (dynamic) at forced resonance
Circular	$\frac{2T_M L}{\pi r^4 \theta}$	$\frac{2LI\omega_{\text{res}}^2}{\pi r^4}$
Equilateral triangle	$\frac{26T_M L}{b^4 \theta}$	$\frac{26LI\omega_{\text{res}}^2}{b^4}$
Square	$\frac{7.11T_M L}{d^4 \theta}$	$\frac{7.11LI\omega_{\text{res}}^2}{d^4}$
Rectangular	$\frac{16T_M L}{\mu bd^3 \theta}$	$\frac{16LI\omega_{\text{res}}^2}{\mu bd^3}$
Circular tube ^a	$\frac{2T_M L}{\pi(r_1^4 - r_2^4)\theta}$	$\frac{2LI\omega_{\text{res}}^2}{\pi(r_1^4 - r_2^4)}$

^aFor thin tubes: $r_1^4 - r_2^4 = (r_1^2 + r_2^2)(r_1 + r_2)(r_1 - r_2) \approx 2r^2 2r \Delta r = 4r^3 \Delta r$.

Nomenclature	Value of shape factor	
	b/d ratio	μ
L = Length of straight bar (m)	1.0	2.25
b = Width or side (m)	2.0	3.66
d = Diameter or thickness (m)	3.0	4.21
r = Radius (m)	5.0	4.66
μ = Shape factor	10	5.0
T_M = Torque (torsion couple) = moment of force F (N m)	20	5.17
θ = Angle of twist (rad)	50	5.27
I = Moment of inertia of the oscillatory system (N m s^2)	100	5.30
ω_{res} = angular frequency (rad/s) at forced resonance	∞	5.53

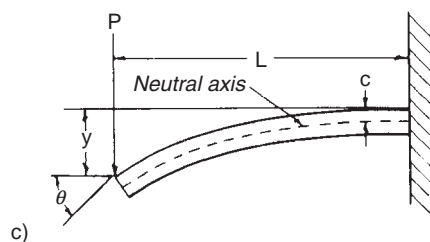
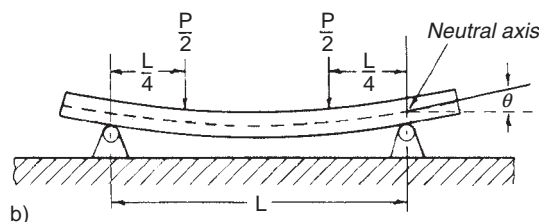
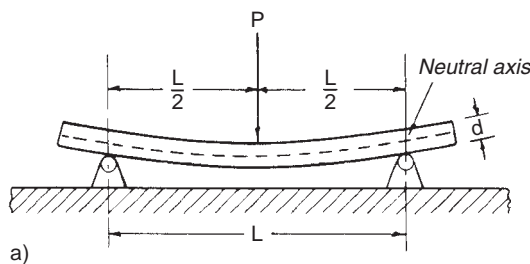


FIG. 25.3 Simple beam loaded at: (A) midspan; (B) one-quarter points; (C) cantilever beam loaded at free end (reproduced from Schmitz and Brown (1965–1969), Vol. 2, p. 323).

Example 25.2

Estimate the deflection after 1 year at 25 °C at the free end of a nylon cantilever beam, 150 mm long, 10 mm wide and 12 mm thick, when it is subjected to a constant load of 2.5 N at the free end. Make the calculation for the following cases:

- nylon 66 in equilibrium with a dry atmosphere;
- ditto at 65% relative humidity (RH);
- for glass-reinforced nylon (dry);
- for glass-reinforced nylon under water (RH = 100%);
- estimate also the maximum fibre strain in the beam.

The following data for 100 s creep modulus are known:

$$\text{Nylon 66: } E(298 \text{ K}, 100 \text{ s}) \approx [25 - 20(\text{RH}/100)] \times 10^8 \text{ N/m}^2$$

$$\text{Nylon 66, glass fibre reinforced: } E(298 \text{ K}, 100 \text{ s}) \approx [100 - 55(\text{RH}/100)] \times 10^8 \text{ N/m}^2$$

Solution

The following expression is available for the deflection (see Table 25.2):

$$y = \frac{4PL^3}{bd^3E}$$

So the deflection is:

$$y = \frac{4 \times 2.5 \times (150 \times 10^{-3})^3}{10 \times 10^{-3} \times (12 \times 10^{-3})^3 \times E} = \frac{1.95 \times 10^6}{E} \quad (\text{y in m, if } E \text{ in N/m}^2)$$

The equation for the modulus of nylon (see Chap. 13, Eq. (13.126)) is:

$$\log \frac{E_R}{E} \approx 0.1 \log \frac{t}{t_R} \approx 0.1 \log \frac{3.16 \times 10^7}{10^2} \text{ or } E \approx \frac{E_R}{3.55}$$

The following values for E_R have to be substituted:

Dry nylon	$E_R \approx 25 \times 10^8 \text{ N/m}^2$	so $E \approx 7.1 \times 10^8$
nylon 65% RH	$E_R \approx 12 \times 10^8 \text{ N/m}^2$	so $E \approx 3.4 \times 10^8$
glass-reinforced nylon	$E_R \approx 100 \times 10^8 \text{ N/m}^2$	so $E \approx 28 \times 10^8$
glass-reinforced nylon, wet	$E_R \approx 45 \times 10^8 \text{ N/m}^2$	so $E \approx 12.6 \times 10^8$

The maximum tensile stress in the beam is

$$\sigma_{\max} = \frac{6PL}{bd^2} = \frac{6 \times 2.5 \times 150}{10 \times 10^{-3} \times (12 \times 10^{-3})^2} \approx 1.57 \text{ MN/m}^2$$

$$\text{The maximum fibre strain is } \varepsilon_{\max} \approx \frac{1.57 \times 10^6}{E}$$

This leads to the following values:

Sample	y (mm)	ε_{\max} (%)
nylon, dry	2.39	0.18
nylon, 65% RH	5.74	0.46
nylon, dry, glass-reinf.	0.70	0.056
nylon, wet, glass-reinf.	1.55	0.12

25.4. TOUGHNESS AND ENDURANCE

The phenomena of ductile and brittle fracture and of ultimate stress and elongation have been discussed in Chap. 13.

The ultimate stress is very much time-dependent, as may be understood from the viscoelastic behaviour of polymers. At very high velocities there is, even in ductile materials, a change from ductile to brittle fracture.

25.4.1. Impact strength

Impact strength is the resistance to breakage under high-velocity impact conditions. This property is of great practical importance, but extremely difficult to define in scientific terms.

Many impact tests measure the energy required to break a standard sample under certain specified conditions. The most widely used tests are the *Izod test* (pendulum-type instrument with notched sample, which is struck on the free end), the *Charpy test* (pendulum-type instrument with sample supported at the two ends and struck in the middle), the *falling-weight test* (standard ball dropped from known height), and the *high-speed stress-strain test*.

The impact strength is temperature-dependent; near the glass temperature the impact strength of glassy polymers increases dramatically with temperature. Secondary transitions play an important role-, a polymer with a strong low-temperature secondary transition in the glassy state is nearly always much tougher than a polymer which has no such transition.

Crystalline polymers have high impact strengths if their glass transition temperature is well below the test temperature. With increasing crystallinity and especially with increasing size of the spherulites the impact strength decreases.

The impact strength of thermosetting polymers varies little with temperature over a wide range.

25.4.2. The Izod test

In this test a failing weighted pendulum strikes a rectangular bar specimen, mounted vertically by being clamped at the lower end; the specimen is usually notched, the notch dimensions being specified. Commonly used standard conditions are:

bar: width 12.7 mm: thickness ~3.5 mm.
notch: V-shaped; depth 2.5 mm; tip radius 0.25 mm.
pendulum velocity at strike: 3.4 m/s.
location of strike: notch side; 22 mm above notch.
temperature: 23 °C.

The height to which the pendulum breaks through is recorded; it gives the energy loss at the impact.

The result of the test is expressed in several ways:

- a. In units of energy per standard width of sample (J)
- b. In units of energy per unit of width of notch, so in J/m or ft.lb/inch
- c. In units of energy per cross-sectional area fractured, so in kJ/m²

Interconversion of these values is possible to a certain extent. To convert a value expressed in kJ/m^2 into J/m it has to be multiplied by about 13.

Values in ft lb/in into J/m a multiplication factor of 53.4 has to be used.

The Izod impact strength values are useful in giving a rough ranking of materials for quality control purposes, since the tests are simple and quick to carry out. The test is hardly of any use for design calculations for plastic parts. Neither has the test any physical base.

The Izod impact strength of a number of common polymers at room temperature is listed in Table 25.4. Plotted versus the modulus at room temperature, as is shown in Fig. 25.4 it gives a rough correlation for first estimations.

Some polymers show large deviations. Polycarbonate (nr. 17) is an extremely tough polymer, with a high modulus; polyethylene ld. (nr. 1) and poly(tetrafluoroethylene) (nr 8) combine a high impact strength with a low modulus. The other polymers are spread around the drawn line.

The only physical quantity which shows a rather simple correlation with the Izod impact strength is T_β , the temperature of the β -relaxation, i.e. the first secondary transition temperature below the glass transition. This correlation is shown in Fig. 25.5. The drawn line corresponds to the equation:

$$\text{Iz} = 4000/(T_\beta - 140) \quad (\text{J/m}) \quad (25.3)$$

It expresses that Iz is very high for polymers whose T_β lies in the neighbourhood of 140 K, as long as they are in the solid state. The approximation is especially good for typically amorphous polymers.

25.4.3. Crazing

Brittle fracture is normally preceded by crazing, i.e. a running crack is preceded by a zone of crazed material (see Chap. 13, Fig. 13.81). Like cracks, crazes in isotropic materials grow at right angles to the principal tensile stress and only propagate if the stress at their tip exceeds a certain value. The craze can be described as an "open cell foam" with voids of the order of 10–20 nm in diameter and centre-to-centre distances of 50–100 nm.

Crazes usually form under tensile stress when a critical strain is surpassed; they do not occur under compressive stress; applying hydrostatic pressure during tensile deformation can even inhibit their development. Crazes always nucleate preferentially at points of triaxial stress concentration. It is the dilatational strain which initiates crazes and cracks.

As already remarked in Chap. 13, craze formation is now considered to be a mode of plastic deformation peculiar to glassy polymers (or to glassy regions in the polymer) that is competitive with shear ductility in reducing stress. The strength of specimens that are crazed completely through their cross-sections is a manifestation of the degree of residual mechanical integrity of the polymer in the craze. Craze formation appears to be a plastic deformation in the tensile stress direction without lateral contraction.

In this respect the behaviour of vulcanised natural rubber, pre-oriented above T_g and rapidly quenched, is interesting (Natarajan and Reed, 1972). At temperatures immediately below T_g necking can be observed. At slightly lower temperatures the material becomes brittle. But as the temperature is further reduced a new region of ductility is found, the plastic deformation now taking place by cavitations, beginning as narrow crazes but developing by lateral growth of the craze to give homogeneous voiding over a large volume.

TABLE 25.4 Data on impact strength, hardness, friction and abrasion

Polymer	Izod impact strength (J/m)	Rockwell hardness		Ball indentation hardness (10 ⁷ N/m ²)	Shore D hardness	Friction coefficient (–)	Abrasion resistance (ASTM- D1044) (Taber)	Abrasion loss factor (DIN 53516) (mg)	Polymer ref. nr. in figures (cf. Table 13.12)
		T _β (K)	R scale						
Polyethylene (low d.)	700	(150)	(10)	1.35	59	(0.5)			1
Polyethylene (high d.)	130	(150)	40	5.35	71	0.23		2	2
Polypropylene	80	165	100	7.25	74	0.67			3
Polystyrene	28	280	(125)	75	11	0.38	640		5
Poly(vinyl chloride)	43	245	115	60	11.5	0.50			6
Poly(chlorotritfluoroethylene)	~200	–	110	7.0	74	0.56	160		7
Poly(tetrafluoroethylene)	160	160	85	3.1	66	0.10	470		8
Poly(methyl methacrylate)	27	300	125	95	17.2	85	0.4		9
Polyoxymethylene	80	180	120	94	14.0	80	20		10
Polyphenylene oxide	390	(155)							11
Polyphenylene sulfide	75	(260)							12
Poly(ethylene terephthalate)	70	250	120	106	12.0	0.25	3		13
Nylon 6,6	110	230	114	(70)	7.25	75	0.36	25	15
Nylon 6	(25)	–	85		6.25	72	0.39	8	16
Poly(bisphenol carbonate)	800	155	118	78	9.75	75	0.25	10	17
Polysulfone	85	175							18
Polyimide	50								19
Cellulose acetate	120	–	100	25	4.3	0.55			20
Phenol formaldehyde resin	~20	–	125		(19)	82	0.61	60	21
Melamine formaldehyde resin	~20	–	130		>17	90			21a
Unsaturated polyester resin	~20	–	125	75	17	82			22
Epoxy resin	(75)				20				23
Polyetherketone	85	210							24
Polybenzthiazole	70	–							25

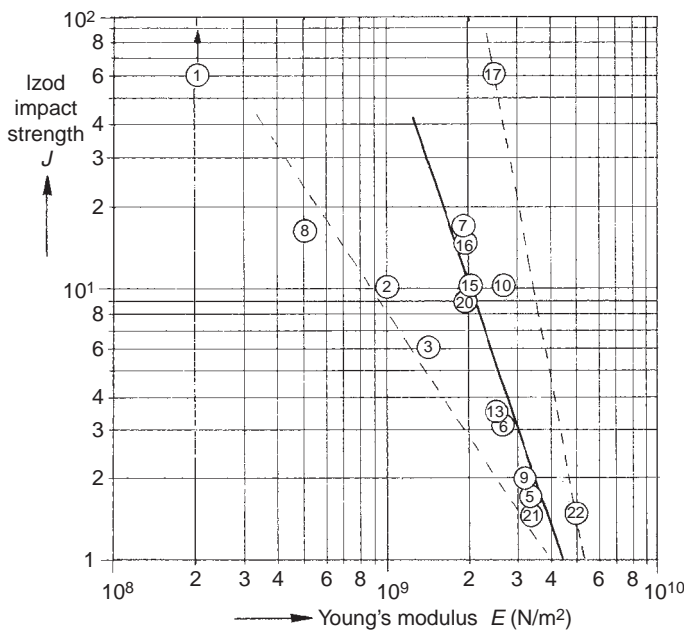


FIG. 25.4 Correlation between impact strength and modulus (See Tables 13.12 and 25.4 for reference numbers).

25.4.4. Fatigue resistance

Failure and decay of mechanical properties after repeated applications of stress or strain are known as fatigue. Generally the "fatigue life" is defined as the number of cycles of deformation required to bring about rupture (see also Chap. 13).

Many types of fatigue tester are used (flexing beams, rotating beams, constant amplitude of cyclic stress or strain, constant rate of increase in amplitude of stress or strain, etc.).

The results are reported as the number of cycles to failure versus the stress level used. The limiting stress below which the material will "never" fail is called the *fatigue* or *endurance limit*; for many polymers this fatigue limit is about one-third of the static tensile strength. A typical curve for a polymer is clearly shown in Fig. 25.6. In this case the fatigue limit is approximately 12 MN/m². Hence, if the stress amplitude decreases below 12 MN/m², the polymer will "never" fail. In practice it is important to design constructions subjected to vibrations in such a way that the maximum stresses to which they are subjected are below the fatigue limit rather than below the static tensile strength.

Also in this case there is a kind of temperature-time equivalence; the fatigue life of a polymer is generally reduced by an increase of temperature. The temperature-dependence can usually be expressed by:

$$\log t_{\text{fat}} = A + \frac{B}{T} \quad (25.4)$$

Mechanical damping is important in the fatigue life determination. High damping (in the neighbourhood of a transition temperature) may be largely responsible for the fatigue

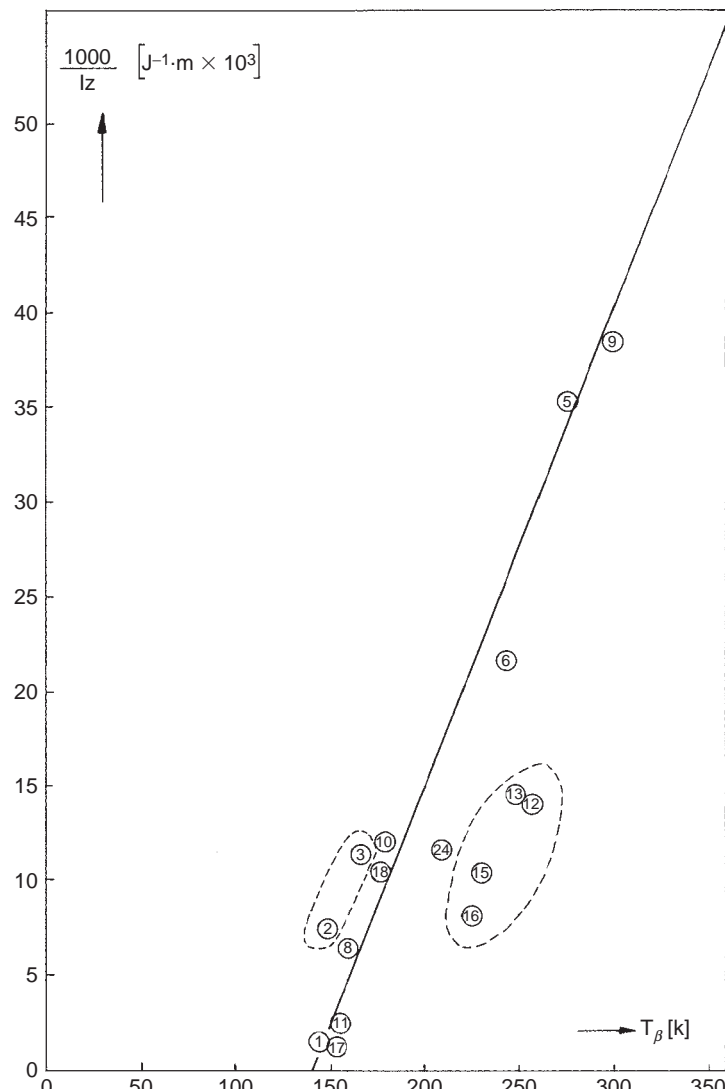


FIG. 25.5 Correlation between the Izod Impact Strength and T_β (the temperature of the β -relaxation, i.e. the second order transition temperature, directly below the glass transition temperature). For reference numbers see Tables 13.12 and 25.4. The deviating polymers have a strongly developed crystallinity.

failure, due to heat build-up. On the other hand damping is favourable, since without damping resonance vibrations may cause failure.

Very little is known about the effect of molecular structure on fatigue life.

25.4.5. Creep rupture

Creep tests are normally carried out with small loads, so that the sample does not break. If the loads approach the breaking strength, rupture will occur after some time. The following expression has been derived both theoretically and experimentally (Coleman, 1956):

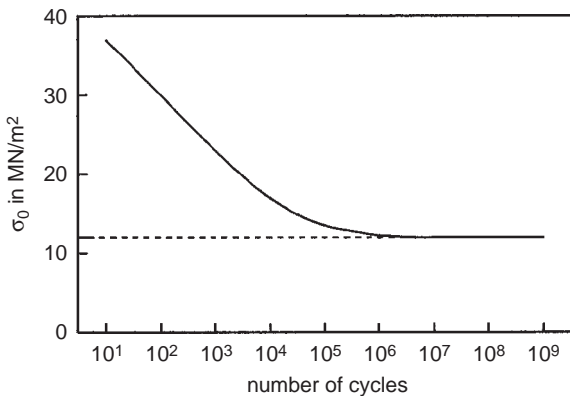


FIG. 25.6 Stress amplitude vs. fatigue lifetime in number of stress cycles.

$$\ln t_{\text{br}} = A + \frac{E_{\text{act}} - B\sigma}{RT} \quad (25.5)$$

where t_{br} is the time required for creep rupture, or is the applied stress, E_{act} is the energy of activation of the fracture process, A and B are constants. Eq. (25.5) shows that the applied stress lowers the activation energy E_{act} to a value $E_{\text{act}} - B\sigma$.

25.4.6. Compressive failure

In many applications materials are subjected to compressive stresses. The macroscopic phenomena of collapse under an axial compression are the well-known *shear and kink bands*. In polymers they are caused by the buckling of chains, accompanied by changes in the chain conformation. The resistance against buckling is expressed by the yield strength under axial compression, $\sigma_{c,\text{max}}$. Northolt (1981) found a relationship between $\sigma_{c,\text{max}}$ and T_g :

$$\log \sigma_{c,\text{max}} = 1.85T_g - 2.75 \quad (25.6)$$

or approximately

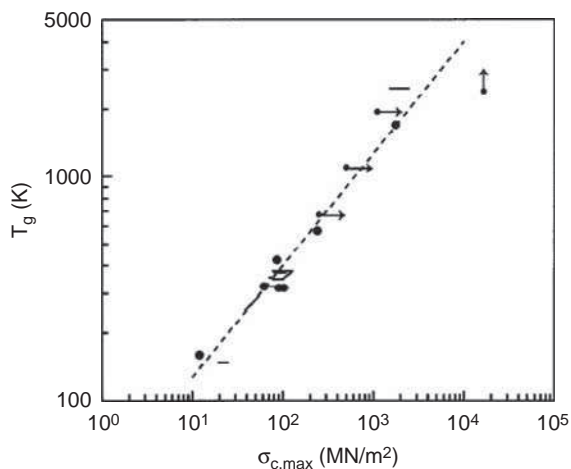
$$\sigma_{c,\text{max}} \propto T_g^2 \quad (25.5a)$$

Such a relationship is not surprising; according to molecular interpretations the glass transition of polymers is a relaxation process originating in large-scale vibrations of chain segments. As in buckling, large changes in chain conformation will take place. This empirical correlation holds not only for polymers, but also even for materials such as carbon fibre, glass, fused quartz and diamond: see Table 25.5 and Fig. 25.7, where the dashed line corresponds to Eq. (25.5a).

According to Van der Zwaag and Kampschoer (1988) a very simple test may be used to determine the compressive strength of a filament, viz. the "elastica" test of Sinclair (1950). A filament is wound into a single loop, which is then gradually contracted. During the contraction the length of the two axes, c and a , are measured using an optical microscope. For a uniformly deforming fibre the c/a ratio has a constant value of 1.34. At the onset of compressive failure the value of the c/a ratio increases: kink bands at the top of the loop act as plastic hinges. Using simple elastic bending beam theory, the following equation for the compressive strength could be derived

TABLE 25.5 Compressive strength $\sigma_{c,\max}$ Young's modulus E and T_g of various materials

Material	T_g (K)	E (GPa)	$\sigma_{c,\max}$ (MPa)
Polyethylene	148	8.5	19–25
Polypropylene	253–293	9.6	38–55
Polystyrene	373	3.5	79–110
Polyacrylonitril	378	7	76–130
Polymethylmethacrylate	353–373	3	103–124
Polycarbonate	423	—	86
Polyethyleneterephthalate	348	19.5	76–103
Polytetramethyleneterephthalate	323	—	59–100
Nylon 6	318	5	90
Nylon 66	318	5	103
Polyamide-imide	573		241
Poly-p-phenyleneterephthalamide	673	100	>250
Polyvinyl chloride	353	5	69–76
Polyvinylidenefluoride	323	—	62
Polychlorotrifluoroethylene	318	1.3	51–64
Polytetrafluoroethylene	160	0.4	12
Carbon fibre	2470	800	1500–2500
Graphite	3500	1000	
Silicon carbide fibre	1700	200	1765
E-glass fibre	1100	70	>500
Fused quartz	1940	72	>1100
Diamond	>2400	1160	16,500

**FIG. 25.7** Relationship between glass transition temperature and compressive strength, where the data of Table 25.5 are used. The dashed line corresponds to Eq. (25.5a): $T_g = 40\sigma_{c,\max}^{0.5}$ or $\sigma_{c,\max} = 6.25 \times 10^{-4}T_g^2$.

$$\sigma_{c,\max} = 1.34 \frac{Ed}{c_{cr}} \quad (25.7)$$

where E = elastic modulus, d = fibre diameter and c_{cr} = length of c -axis at which the c/a ratio starts to deviate from the elastic value.

Van der Zwaag and Kampschoer proved that *no simple relation exists between compressive and tensile strength*; for a wide range of tensile stresses the compressive strength remained

surprisingly constant in the aramid fibres investigated. On the other hand there is a relationship between compressive strength and modulus:

$$\sigma_{c,\max} \approx 7 \times 10^{-2} E^{1/2} \quad (25.8)$$

where $\sigma_{c,\max}$ and E are both expressed in GPa.

Obviously the value of $\sigma_{c,\max}$ depends on the combined effect of the bending stiffness and the lateral cohesive binding forces. For carbon fibres both are very high, for extended-chain polyethylene filaments the lateral binding forces are weak, for aramid fibres both are relatively strong. For all refractory fibres (silica, carbon) both bending stiffness and lateral cohesion are very strong, but compressive failure means *complete* failure, whereas in organic fibres only a fraction of the tensile strength is lost (in the case of aramids about 10%) due to the presence of kink bands.

According to the data in Table 25.5 and to Eq. (25.6) the compressive strength of filaments of refractory materials such as carbon and silicon carbide have compressive strengths about 10 times as large as those of organic fibres. This would seem to be a serious restriction to the use of organic polymers such as aramids in their application in composites. For most of the applications this restriction is of minor importance, however, since long before $\sigma_{c,\max}$ is reached, instability in the construction will occur. The resistance of a column or a panel under pressure is proportional to the product of a load coefficient and a material efficiency criterion:

$$\text{Resistance} \propto [P^m/L^n][E^p/\rho] \quad (25.9)$$

The values of the exponents are:

	m	n	p
Columns	1/2	2	1/2
Panels	2/3	5/3	1/3

Whereas the compressive strengths of carbon and aramid differ by a factor 10, the material efficiency criterion of the composite differs less than 20%.

25.5. HARDNESS

Two categories of hardness definitions can be distinguished:

- (a) The scratch resistance
- (b) The indentation hardness

25.5.1. Scratch resistance

The oldest criterion for scratch resistance, the Mohs scale of hardness was originally devised in 1812. It is still used to classify the various minerals and consists of a list so selected and arranged that each mineral is able to scratch the ones preceding in the list shown in Table 25.6.

The Mohs scale is useful for defining the scratch resistance of plastics relative to those things with which the plastic may come in contact during its service life. It is of limited value, however, for differentiating between the scratch resistance of the various plastics, since practically all of them, including both the thermosetting and the thermoplastic types,

TABLE 25.6 Mohs' scale of hardness

Hardness number	Mineral	Hardness number	Mineral
1	Talc	6	Orthoclase
2	Gypsum	7	Quartz
3	Calcite	8	Topaz
4	Fluorite	9	Corundum
5	Apatite	10	Diamond

are in the range of 2–3 Mohs. Many of the materials with which the plastic will come in contact during service are higher than 3 on the Mohs scale.

In examining new polymers, the hardness may be estimated by using one's fingernail (Mohs 2), a brass scribe (Mohs 3), a knife blade (Mohs 4), or a piece of glass (Mohs 5).

The relative scratch resistance of two polymers may be readily determined by scratching the surface of one with the corner of the other.

The scratch resistance of rigid polymers is related to abrasion. In general, for rigid polymers scratch resistance runs parallel with modulus. Cross-linked rubber shows a high scratch resistance, however, which is due to easy deformation combined with complete resilience.

25.5.2. Indentation hardness

Indentation hardness is a very common determination in materials testing. In this test a very hard indenter (a hard steel sphere in the *Brinell test*, a diamond pyramid in the *Vickers test*) is pressed under a load into the surface of the material.

The mechanism of the indentation process has been clearly defined by Tabor (1947). When a ball presses on a metal surface, the material deforms elastically. As the load increases, the stresses soon exceed the elastic limit and plastic flow starts. By increasing the load still further the material directly beneath the penetrator becomes completely plastic. On release of the load there is an amount of elastic recovery.

From the theory of the stress field around the indenter it follows that almost two thirds of the mean pressure is in the form of a hydrostatic component and therefore plays no part in producing plastic flow. Thus as an approximation

$$p_y = \frac{W}{A} \approx 3\sigma_y \quad (25.10)$$

where W = load applied; A = surface area under indentation; σ_y = uniaxial yield stress of the material; p_y = pressure at which plastic flow starts.

So the yield stress of a material may be determined by a hardness measurement.

The original theory of the Brinell hardness test was developed by Hertz (1881) and revised by Timoshenko (1934, 1970); their treatment was based on the elasticity theory.

Starting from Tabor's concepts of plastic deformation and analysing the recovery process after the load release in terms of the elastic concepts, Baer et al. (1961) derived the following formula:

$$\frac{W}{E} \approx 3(d_1 - d_2)(d_1 D)^{1/2} \quad (25.11)$$

where W = load applied; E = Young's modulus; d_1 = indentation depth; $d_1 - d_2$ = distance of recovery; D = diameter of penetrator (ball).

By measuring the initial distance of indentation and the distance of recovery the modulus E can be determined.

The hardness is defined as:

$$\frac{W}{\pi D d_1} = H_p \quad (25.12)$$

Since $Dd \propto A$ (area under indentation) and σ_y is closely related to the modulus ($\sigma_y \propto E^n$), combination of Eqs. (25.10) and (25.12) gives the following proportionality for a standard load and a standard indenter

$$H_p \propto E^n \quad (25.13)$$

Table 25.4 gives some values for polymers investigated. Fig. 25.8 shows that Eq. (25.13) is approximately confirmed. The empirical expression is:

$$H_p \approx 10E^{3/4} \quad (25.14)$$

(H_p and E both expressed in N/m^2).

For very soft materials such as elastomers (rubbers) other hardness testers are used, the so-called *Shore Hardness testers*. As indenting body a steel pencil is used in the form of a truncated cone (Shore A and C) or of a rounded cone (Shore D). With a certain force exerted by a spring the pencil is pressed into the material and the indentation depth is measured on a scale ranging from 0 to 100.

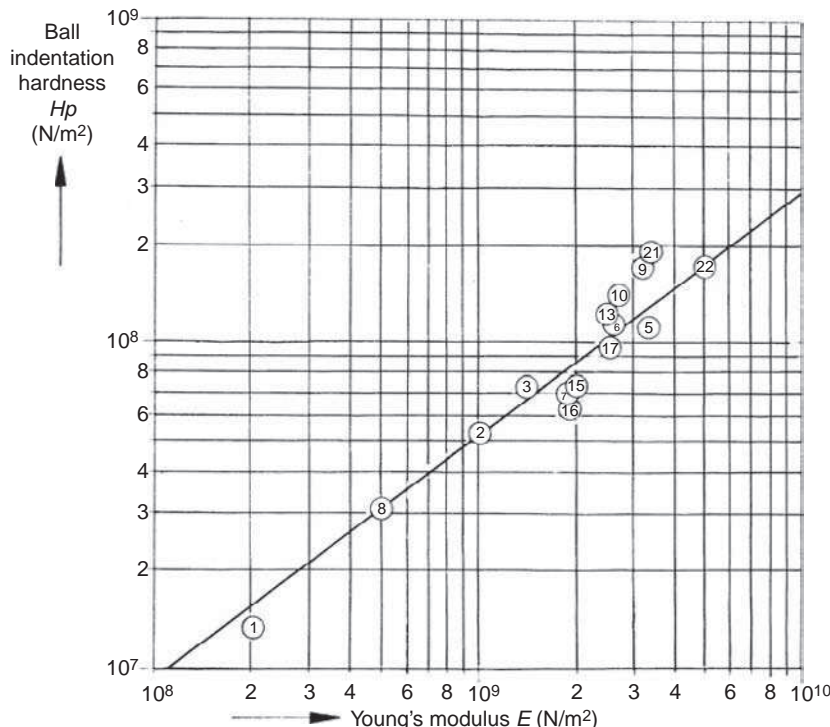


FIG. 25.8 Correlation between indentation hardness and modulus (see Tables 13.12 and 25.4 for reference numbers).

25.5.3. Correlation between the hardness tests

Between the different hardness tests a rather good correlation exists. Fig. 25.9 shows this for hard materials, Table 25.7 for soft materials.

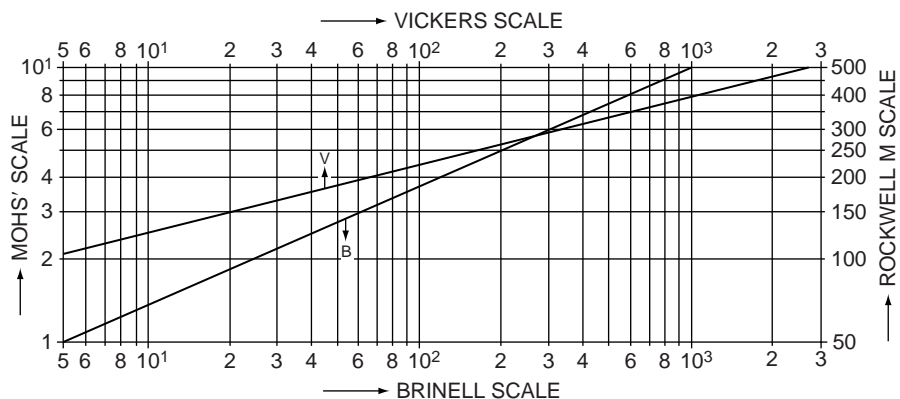


FIG. 25.9 Hardness scales for hard materials.

TABLE 25.7 Comparative hardness scales for soft materials

Hardness scale							
Mohs	Brinell	Rockwell		Shore			Types of product
		M	$\alpha (\approx R)$	D	C	A ($\approx IRHD$)	
2	25	100					Hard plastics
	16	80					
	12	70	100	90			
	10	65	97	86			
	9	63	96	83			Moderately hard plastics
	8	60	93	80			
	7	57	90	77			
	6	54	88	74			
	5	50	85	70			
	4	45		65	95		
1	3	40	(50)	60	93	98	Soft plastics
	2	32		55	89	96	
	1.5	28		50	80	94	
	1	23		42	70	90	
	0.8	20		38	65	88	Rubbers
	0.6	17		35	57	85	
	0.5	15		30	50	80	
				25	43	75	
				20	36	70	
				15	27	60	
				12	21	50	
				10	18	40	
				8	15	30	
				6.5	11	20	
				4	8	10	

25.6. FRICTION AND WEAR

25.6.1. Friction

The coefficient of friction μ is defined as the ratio of the tangential force F to the normal load W when the surface of a material is moved relative to another surface

$$\mu = \frac{F}{W} \quad (25.15)$$

The coefficient of friction is by no means a constant, since it still depends on the load, the contact area, the surface structure, the velocity of sliding, the temperature and, above all, on lubricants.

Of the intrinsic properties the molecular adhesion the softening temperature and the relative hardness of the two materials are the most important. Friction is high when molecular adhesion is high: therefore friction of a material with itself is usually higher than that with a dissimilar material.

According to the studies of Bowden and Tabor (1954) friction is a complex summation of different factors:

1. Internal friction, caused by mechanical damping
2. Surface shear friction, i.e. shearing of the junction where the surfaces are in intimate contact; the extreme form of this shearing is ploughing of the harder material into the softer

25.6.1.1. Internal friction

This type of friction is most important in cyclic processes like rolling friction and automobile tires. Mechanical damping and delayed recovery cause dissipation of energy; consequently, rolling friction and mechanical damping are well correlated. For a hard ball rolling on a plastic surface the following expression was found by Flom (1961):

$$\mu = 0.115 \left(\frac{G''}{G'} \right) \left(\frac{W}{G' r^2} \right)^{1/2} \quad (25.16)$$

where W = load on the rolling ball of radius r ; G' = storage modulus of polymer surface on which the ball is rolling; G'' = loss modulus of polymer surface on which the ball is rolling; G''/G' = dissipation factor = $\tan \delta$.

Eq. (25.16) clearly demonstrates that rolling friction is large if $G''/G' = \tan \delta$ is large; so friction will be large in transition regions.

25.6.1.2. Surface friction

Even the smoothest surfaces are rough on a sub-microscopic scale. The contacting surfaces touch each other on the relatively few points only. Sliding of one surface over the other produces large forces at the contact points. In many cases plastic deformation will occur; junctions will be welded together, so that shearing can take place even below the surface of the softer material. Sliding will cause periodic rupture of temporary junctions formed.

If shearing is the largest factor in friction, the coefficient of friction is roughly determined by

$$\mu_{sh} = \frac{\sigma_{sh,max}}{p_y} \quad (25.17)$$

where $\sigma_{sh,max}$ is the shear strength of the softer material and p_y is the yield pressure of the softer material.

The yield pressure p_y is related to the modulus:

$$p_y \propto E^n. \quad (25.18)$$

In the extreme case where the asperities of the harder material plough grooves into the softer material, strong abrasion and wear will occur. Since polymers are relatively soft materials, this "ploughing" term in the total friction may be important.

25.6.2. Slip-stick motion

If the static friction is greater than the kinetic friction, slip-stick motion may be the result. In rigid plastics the kinetic friction coefficient is normally lower than the static coefficient, in elastomers the reverse applies. At high velocities it is sometimes difficult to separate the effects of velocity and temperature.

25.6.3. Abrasion

Abrasion is closely related to friction, especially the "ploughing component" of the frictional force; it is, of course, also closely related to the scratch resistance. Zapp (1955) found that the abrasion loss was proportional to the kinetic coefficient of friction and to the dynamic modulus, and inversely proportional to the tensile strength. One of the well-known abrasion testers is the Taber Abraser (ASTM D 1044 and 1300).

Table 25.4 gives a survey of the coefficients of friction of a number of plastics together with the relative abrasion losses.

25.7. THE MECHANICAL SHORTCOMINGS OF HOMOGENEOUS MATERIALS AND THE NEED FOR COMPOSITES

Almost all homogeneous materials have their inherent shortcomings in mechanical respect. When they are stiff and sufficiently hard (ceramics and heavily cross-linked polymers) they are mostly brittle and hardly processible; when they are ductile and well-processible, they are not stiff and hard enough.

By combination of materials it proved possible to attain a situation in which "the whole is more than the sum of its parts". Composites were a need in the evolution of engineering materials. The simplest combination is of course that of only two materials, where one is acting as a reinforcement, the other as the matrix. Often a combination of more than two materials is needed, e.g. with two reinforcing materials, one complementing the other (e.g. the combination aramid/carbon fibres and extended-PE /carbon fibres).

It is almost paradoxical that in the history of mankind composite materials were earlier used than their "homogeneous" rivals. The earliest "engineering materials" were bone, wood and clay. Wood is a composite of matrix lignin and a cellulosic reinforcement; bone is a natural composite where fibres of hydroxyapatite reinforce the collagen matrix; and the oldest building material was adobe: clay as a matrix, reinforced by vegetable fibres. After the industrial revolution other composites were added: reinforced rubber, reinforced concrete, reinforced asphalt, etc.

The difference between the old composites and the modern is, that in the latter ones mostly new materials are used; often materials which did not yet exist in, e.g. the 1950s.

In principle any isotropic material can be reinforced; the combination of the materials has to meet the requirement that the reinforcing material has to be stiffer, stronger or tougher than the matrix; furthermore there has to be a very good adhesion between the components. In a composite the reinforcement has to carry the stresses to which the composite material is subjected; the matrix has to distribute the stresses. By means of a good distribution of the reinforcement the latter blocks the propagation of cracks, which mostly start at the outer surface, and would lead to rupture of the whole object if no blockade were present. By optimum reinforcement the strength of a matrix material can be improved to the tenfold, albeit in one direction.

The secret of the success of a good composite is based on the fact that in its construction one exploits a number of apparent paradoxes, found in homogenous solid materials.

First of all there is the apparent paradox, formulated by Zwicky (1929):

- (I) All solid materials have strengths (far) lower than theoretically possible
Secondly there are the three apparent paradoxes, discovered by Griffith (1920) for the solid state in filament form:
- (II) All solid materials are stronger in filament form than in bulk
- (III) The thinner a filament, the stronger it is per unit of cross-section; this means that an equal weight of thin filaments is stronger than a single thick one
- (IV) The measured strength of a filament is higher, the shorter the distance between the fastening clamps

All four apparent paradoxes find their logical explanation in the fact that no homogeneous material is without imperfections, either on its surface or in its bulk volume.

Surface imperfections are often caused by damaging; they are the most important source of cracks that are propagated throughout the material under influence of external or internal stresses. Volume imperfections are all kinds of structural disorder, such as dislocations in metals and crystalline polymers and chain ends in all polymers.

Under tension all imperfections generate deformations, which if propagated, end either catastrophically or more gradually in break.

Filaments normally possess less imperfections than bulky objects and the smaller the clamp distance the smaller their role in strength measurements. So in filaments the disadvantages of homogeneous materials are partly or even largely removed. If the adhesion between the materials is good, the situation is as if the clamp distance is reduced to zero; the filament strength is then optimum.

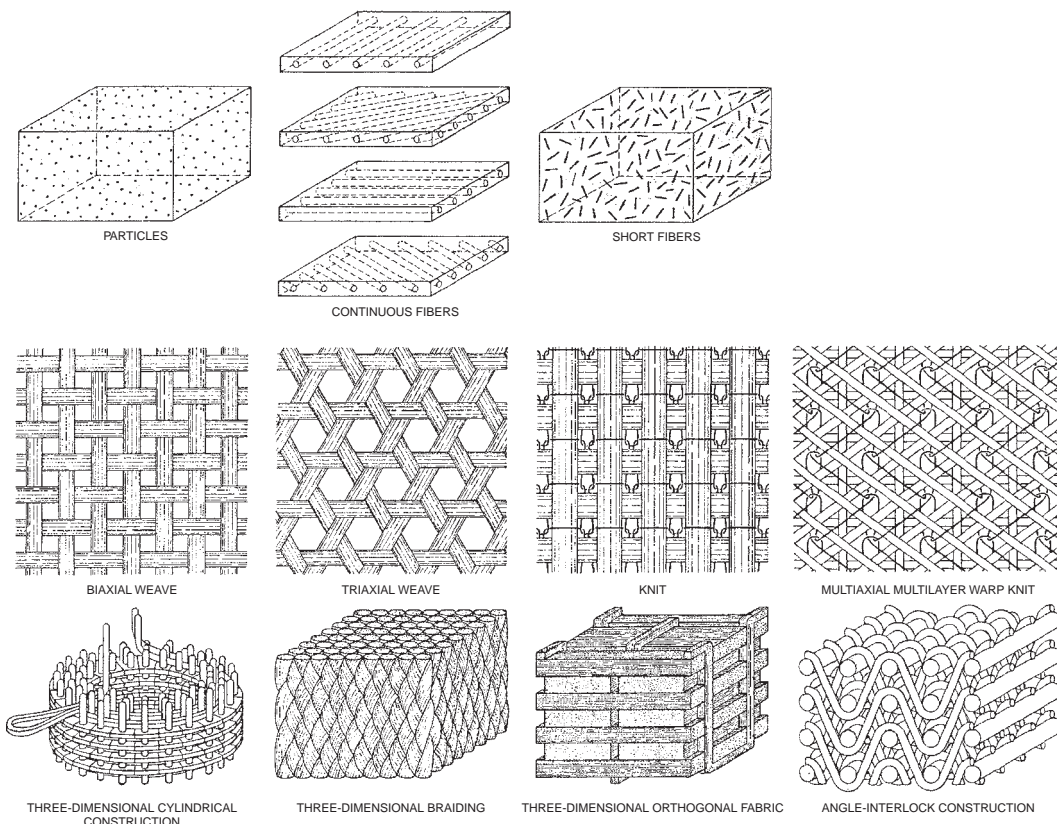
If the filaments are unidirectional oriented the strength of the composite is of the order of that of the filament; it may be tenfold the strength of the matrix. A composite may be stronger than a metal in one direction. With a three-dimensional woven or knitted reinforcing network it may be stronger than metals in all directions. The adhesion between the components is crucial.

The most important polymeric matrices are: linear and cross-linked polyesters, epoxy resins and linear and cross-linked polyimides; the most important reinforcements are: high-performance polymeric fibres and filaments (for polymeric composites), filaments of refractory metals and inorganic materials (E-glass, Al_2O_3 , B, BN, SiC and Carbon) and whiskers (fibrillar single crystals of Al_2O_3 , B_4C , WC, SiC and C, exclusively for reinforcement of metals).

A classification system for composites, based on the morphology of their reinforcement, was developed by Van Krevelen (1984). In a somewhat modified form it is reproduced as Table 25.8 and illustrated by Fig. 25.10.

TABLE 25.8 Classification of composites based on their reinforcement morphology

Reinforcing geometry		Examples
Corpuscular or Particulate	Particles	Impact-resistant plastics Filled plastics and rubbers “Cermets” (ceramics reinforced metals)
	Flakes	Mica-reinforced plastics
Fibrillar	Short fibres	Glass reinforced plastics
	Long filaments	Reinforced columns and panels Pre-stressed concrete
Laminar or Laminate	Fabrics and non-wovens	Fabric-reinforced plastics Reinforced plastic tubes and hoses Reinforced tires and conveyor belts
	Foils and sheets	Laminated glass Laminated plastics “Clad” metals
		Not yet commercial
Three-dimensional constructions		

**FIG. 25.10** Reinforcing geometries of composites (from Chou et al., 1986, Courtesy Scientific American).

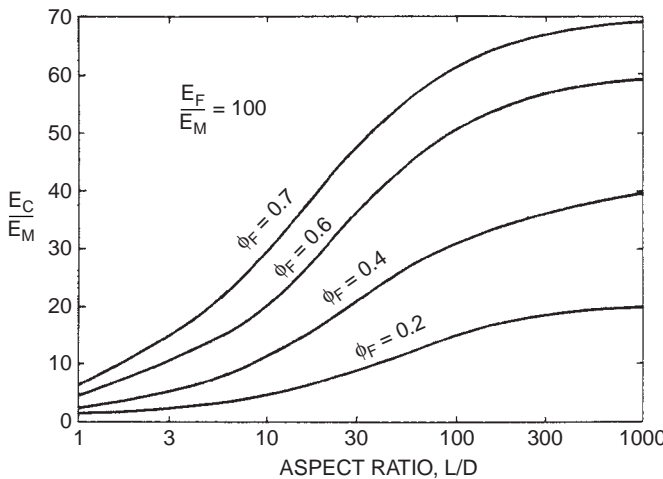


FIG. 25.11 Graphical representation of the Halpin–Tsai equation for the representative case $E_F/E_M \approx 100$.

In simple cases the mechanical properties of composites can be estimated.

For unidirectional reinforced composites (by means of continuous filaments) the following formulae may be used:

$$E_C/E_M \approx \varphi_F(E_F/E_M) \quad (25.19)$$

$$\sigma_{C,\max}/\sigma_{M,\max} \approx \varphi_F \cdot (\sigma_{F,\max}/\sigma_{M,\max}) \quad (25.20)$$

where E = modulus of elasticity; σ_{\max} tenacity (strength); φ = volume fraction of filaments and the subscripts have the following significance: C = composite; M = matrix; F = reinforcing fibre. For quasi-isotropic short-fibre reinforced plastics the *Halpin–Tsai equation* is a good approximation:

$$\frac{E_C}{E_M} = \frac{1 + AB\varphi_F}{1 - B\varphi_F} \quad (25.21)$$

where the symbols used have the same significance as above and $A = 2 \times$ aspect ratio = $2 L/D$ = ratio of fibre length/fibre radius

$$B = \frac{E_F/E_M - 1}{E_F/E_M - A} \quad (25.22)$$

The graphical reproduction of the expression is given in Fig. 25.11.

BIBLIOGRAPHY

General references

- Bowden FP and Tabor D, "The Friction and Lubrication of Solids", Clarendon Press, Oxford, 1954.
- Brostow W, "Einstieg in die moderne Werkstoff-wissenschaft", Carl Hanser, Munchen, 1985.
- Bucknall CB, "Toughened Plastics", Applied Science Publishers (Elsevier), London, 1977.
- Chou TW and Ko FK, "Textile Structural Composites", Elsevier, Amsterdam, 1989.
- Kausch HH, Hassel JA and Jaffee RJ (Eds), "Deformation and Fracture of High Polymers", Plenum Press, New York, 1973.
- Kinloch AJ and Young RJ, "Fracture Behaviour of Polymers", Elsevier Applied Science Publishers, London, 1983.
- Kragelskii LV, "Friction and Wear", Butterworth, London, 1965.

- Ku PM (Ed) "Interdisciplinary Approach to Friction and Wear", NASA SP-181, US Government Printing Office, Washington, DC, 1968.
- Laeis W, "Einführung in die Werkstoffkunde der Kunststoffe", Carl Hanser, München, 1972.
- Nielsen LE, "Mechanical Properties of Polymers", Reinhold, New York, 1962.
- Nielsen LE, "Mechanical Properties of Polymers and Composites", 2 Vols, Marcel Dekker, New York, 1974.
- Ogorkiewicz RM (Ed), "Thermoplastics, Properties and Design", Wiley Interscience, London, 1974.
- Ogorkiewicz RM (Ed), "Engineering Properties of Thermoplastics", Wiley Interscience, London, 1970.
- Rabinowicz E, "Friction and Wear of Materials", Wiley, New York, 1974.
- Roff WJ and Scott JR, "Fibres, Films, Plastics and Rubbers", Butterworths, London, 1971.
- Rosen B (Ed), "Fracture Processes in Polymeric Solids", Interscience, New York, 1964.
- Schmitz JV and Brown WE (Eds), "Testing of Polymers", 4 Vols, Interscience, New York, pp 1965–1969.
- Timoshenko S, "Theory of Elasticity", McGraw-Hill, New York, 1934; 3rd Ed, 1970.

Special references

- Baer E, Maier RE and Peterson RN, SPE J 17 (1961) 1203.
- Bin Ahmad Z and Ashby MF, J Mater Sci 23 (1988) 2037.
- Chou TW, McCullough RL and Pipes RB, Sci Am, 255 (1986) Nr 4, 167–176.
- Coleman BD, J Polym Sci 20 (1956) 447; Textile Res J 27 (1957) 393; 28 (1958) 393, 891.
- Ferry JD, "Viscoelastic Properties of Polymers", Wiley, New York, 3rd Ed, 1980.
- Flom DG, J Appl Phys 32 (1961) 1426.
- Griffith AA, Phil Trans Roy Soc (London) A221 (1920) 163.
- Halpin JC, J Composite Mater 3 (1969) 732.
- Hertz H, J Reine Angew Mathem 92 (1881) 156.
- McCrumb NG, Buckley CP and Bucknall CB, "Principles of Polymer Engineering", Oxford University press, Oxford, 2nd Ed, 1997.
- Natarajan R and Reed PE, J Polym Sci A2, 10 (1972) 585.
- Northolt MG, J Mater Sci 16 (1981)-Letters, 2025.
- Sinclair D, J Appl Phys 21 (1950) 380.
- Smith TL, J Appl Phys 35 (1964) 27.
- Tabor D, Proc Roy Soc (London) 192 (1947) 247.
- Te Nijenhuis K, "Viscoelastic Polymeric Fluids" in Tropea C, Yarin AL and Foss JF (Eds) "Handbook of Experimental Fluid Mechanics", Springer, Berlin, 2007, Chap. 9.1.
- Te Nijenhuis K, "Survey of Measurement Techniques for the Determination of the Dynamic Moduli", in Astarita G, Marrucci G and Nicolais L (Eds) "Rheology", Plenum Publishing Company, New York, Vol 1, 1980.
- Tsai SW, US Govt Rept AD 834851, 1968.
- Vander Zwaag S and Kampschoer G, in Lemstra PJ and Kleintjens LA (Eds) "Integration of Fundamental Polymer Science and Technology", 2, Elsevier Applied Science, London, 1988.
- Van Krevelen DW, Kautschuk + Gummi-Kunststoffe 37 (1984) 295.
- Whorlow R, "Rheological Techniques", Ellis Horwood, Chichester, 2nd Ed, 1992, pp 545–47.
- Zapp RL, Rubber World 133 (1955) 59.
- Zwicky F, Proc Nat Acad Sci (USA) 15 (1929) 253, 816.

This page intentionally left blank

CHAPTER **26**

Product Properties (II): Environmental Behaviour and Failure

The environmental product properties comprise the heat stability, flammability and resistance to organic solvents and detergents.

The *heat stability* is closely related to the transition and decomposition temperatures, i.e. to intrinsic properties.

The *degree of flammability* of a polymeric material may be predicted from its chemical structure. One of the most valuable criteria in fire research, the so-called limiting oxygen index (LOI) may be estimated either from the specific heat of combustion or from the amount of char residue on pyrolysis. Since both quantities can be determined if the chemical structure is known, also the LOI can be estimated. An approximate assessment of the LOI value direct from the elementary composition of the polymer is also possible.

The *environmental decay* of polymers in liquids is primarily dependent on the solubility parameters of polymer and liquid and on the hydrogen bond interaction between polymer and liquid.

26.1. INTRODUCTION

The properties which determine the “environmental behaviour” of polymers after processing into final products may be divided into three categories: the thermal end use properties, the flammability, and the properties determining the resistance of polymers to decay in liquids.

26.2. THERMAL END USE PROPERTIES

26.2.1. Heat stability

By heat stability is exclusively understood the stability (or retention) of properties (weight, strength, insulating capacity, etc.) under the influence of heat. The melting point or the decomposition temperature invariably forms the upper limit; the “use temperature” may be appreciably lower.

All intrinsic properties are influenced by temperature; these relationships have been treated in the relevant chapters of this book. Especially the influence of temperature on the

mechanical properties proved to be of great importance (Chaps. 13 and 25). Sometimes the expression "maximum continuous use temperature" is found. It is rather vaguely defined but gives a certain impression of heat stability, especially in comparison with the glass transition, melting point or decomposition temperature. Table 26.1 gives some values.

26.2.2. Heat distortion

The heat distortion test is similar to a creep test, except that the temperature is increased at a uniform rate rather than being kept constant. At the softening or heat distortion temperature the polymer begins to deform at a rapid rate over a narrow temperature interval. In the heat distortion test ISO-HDT-A or ISO-HDT-B a standard bar is loaded

TABLE 26.1 Heat stability of polymers

Polymer	Ultimate end-use temperature range in 200 h (°C)	Ultimate end-use temperature range in 1000 days (°C)
Poly(vinyl chloride)	60–90	60
Polystyrene	60–90	60
Polyisoprene	60–90	60–80
Poly(meth)acrylates	70–100	60–80
Polyolefins	70–100	60–90
Polyamides	100–150	80–100
Linear polyurethanes	130–180	70–110
Unsaturated polyurethanes	130–220	80–110
Epoxy resins	140–250	80–130
Cross-linked polyurethanes	150–250	100–130
Polycarbonate	140	100–135
Linear polyester (PETP)	140–200	100–135
Cross-linked arom. polyester	180–250	120–150
Poly(phenylene oxide) (PPO)	160–180	130–150
Polysulphone	160–180	140–160
Fluor elastomers	200–260	130–170
Siloxane elastomers	200–280	130–180
Polyester imides	200–280	150–180
Polyamide imide	200–280	150–180
Silcone resins	200–300	150–200
Polyfluorocarbons	230–300	150–220
Diphenyloxide resins	230–300	180–220
Aromatic polyamides	250–300	180–230
Polyimides	300–350	180–250
Polyphenylene sulfide	300–350	200–230
Polyether ketones	300–350	200–240
Poly(tetrafluoroethylene)	300–350	180–250
Polybenzimidazole	350–400	250–300

with a constant bending force (maximum bending stress is for ISO-A 1.8 MPa and for ISO-B 0.45 MPa). The temperature is increased gradually with a rate of 2 °C per minute and the temperature at a specific bending (0.32 mm) is detected. This softening temperature is called the heat distortion temperature (HDT). In fact this experiment determines the temperature where the Young modulus E is lowered to a level of 1000 MPa (ISO-A) or 250 MPa (ISO-B). The heat distortion behaviour for amorphous polymers, semi-crystalline polymers and thermo-sets is quite different, as depicted in Fig. 26.1:

- For amorphous polymers, where in the neighbourhood of the glass transition temperature the Young modulus decreases fast with increasing temperature, both HDTs are only a little lower than the glass transition temperature and accordingly the difference between both HDTs is small (e.g. 2–15 °C)
- For semi-crystalline polymers, where the Young modulus decreases slowly with increasing temperature, both HDTs are much higher than the glass transition temperature and the difference between both HDTs is large (e.g. 15–100 °C)
- For thermo-sets the Young modulus does in general not decrease far enough for a determination of the ISO-B heat distortion temperature

Another standard heat distortion test is the Vicat test where a flat-ended needle (diameter 1 mm) penetrates to the depth of 1 mm under a specific load of 50 N (Vicat A) or 10 N (Vicat B). It will be clear that the penetration depth is again determined by the Young modulus, although in a much more complicated way than in the bending test. A rough estimate yields Vicat softening temperatures where $E \approx 1000$ MPa (Vicat A) or $E \approx 200$ MPa (Vicat B).

The difference in softening temperatures for amorphous and semi-crystalline polymers becomes also clear from Fig. 13.3, where the Young moduli of amorphous and of semi-crystalline polystyrene are illustrated. For amorphous polystyrene the two HDTs appear to be 92 and 97 °C and for the semi-crystalline polystyrene 99 and 114 °C. It has to be mentioned, however, that the curves in Fig. 13.3 are the so-called 10 s moduli, i.e. measured after 10 s of stress relaxation, every point at a specific temperature. The measurements in the softening experiments are not in agreement with the determination of the standard Young modulus.

In Table 26.2 values of softening temperatures of some polymers are shown. It is clear from this table that the softening points for polystyrene are different from those determined from Fig. 13.3. In this table also glass fibre filled polymers are incorporated.

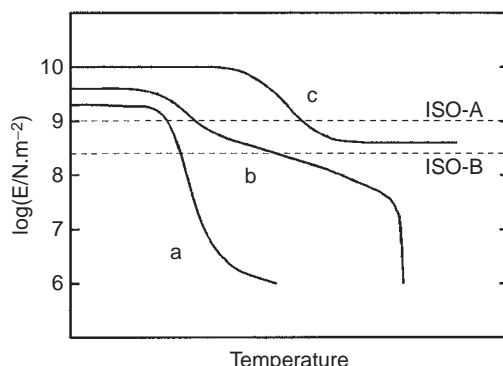


FIG. 26.1 Schematic view of the ISO-A and ISO-B softening temperatures and the Young moduli as functions of temperature for (A) amorphous polymers, (B) semi-crystalline polymers and (C) thermo-sets.

TABLE 26.2 Softening points in °C of amorphous and semi-crystalline polymers; $\Delta T = \text{Vicat-B} - \text{ISO-A}$

Polymer	T_g	T_m	ISO-A	ISO-B	Vicat-B	ΔT
<i>Amorphous</i>						
PVC	87		70		85	15
PS	95		85	96	90	5
SAN	105		85	95	100	15
ABS	105		95	98	100	5
ASA	100		95		85	-10
PMMA	110		105	113	125	20
PC	150		135	145	145	10
PC + glass fibres	150		145		155	10
PSU	190		175	185		
PI	400		>250			
<i>Semi-crystalline</i>						
LDPE	-120	110	35	45	55	20
HDPE	-120	130	45	70	75	30
PP	-15	170	60	100	105	45
PA 6	50	223	95	190	200	105
PA + glass fibres	50	223	190	210	200	
PA 6,6	50	260	90	220	230	140
PA 6,6 + glass fibres	50	260	245	255		
PA 11	45	175	70		170	100
PA 12		175	70		170	100
POM	-50	175	115	150	165	50
PETP	75	260	80	105	170	90
PETP + glass fibres	75	260	235	250	240	
PBTP	70	210	60	170	180	120
PBTP + glass fibres	70	210	205	215	205	
PPS	85	290	135			
PTFE	126	327	55	135	110	55
PVDF	-40	170	92		130	38

Adding glass fibres does not increase glass and melting temperature, but it does change to Young modulus to higher values. The result is that the softening temperatures are raised.

Frozen-in stresses due to molecular orientation may also be measured by this technique, since oriented polymers shrink rapidly above the softening temperature. Non-homogeneously oriented parts cause deformations.

The polymer will only shrink if the applied stress is less than the frozen-in stress. If the external stress is greater than the internal stress, the sample will never shrink. Therefore distortion curves at different applied stresses are useful in the study of oriented polymer samples (e.g. drawn fibres) and the effect of heat treatments.

26.3. FLAMMABILITY AND COMBUSTION OF POLYMERS

Flammability is the ease with which a substance will ignite, causing fire or combustion. Combustion or burning of solid polymers is a complicated process involving physical and chemical phenomena that are only partially understood (Nelson, 2002). It is a sequence of

exothermic reactions between fuel and antioxidant accompanied by the production of heat or both heat and light in the form of either a glow or flames. Nelson et al. have studied the combustion process of polymers intensively, and the interested reader is referred to their papers, ranging at least from the years 1995 till 2005. Furthermore Tewarson's contribution (General references, 2007) is worthwhile to study.

Most organic materials will burn and produce gasses and smoke when subjected to a flame. They will degrade at high temperatures into volatile and gaseous products. For combustion to take place three components are necessary and these components form the fire triangle as shown in Fig. 26.2 (Zeus Industrial Products, Inc., 2005). Removing any one of the components will prevent or extinguish fire. These components are fuel, oxygen and ignition source. Fuel is the source of fire. In most cases the fuel does not itself burn (except if it is a gas) but the volatile combustibles that are produced by heat. Oxygen is the basic component of combustion and ignition is needed to heat up the fuel sufficiently to generate volatiles.

The actual process of combustion for organic materials follows roughly six separate stages, as schematically shown in Fig. 26.3 (Zeus Industrial Products, Inc., 2005):

- (a) Primary thermal: the ignition source heats the bulk material to create a rise in temperature
- (b) Primary chemical: the heated material starts to degrade
- (c) Polymer decomposition: the material starts to rapidly degrade into a range of lower molecular weight decomposition products
- (d) Ignition: the combustible gases, in the presence of sufficient oxygen and the ignition source, ignite to start combustion
- (e) Combustion: the burning gases produce combustion at or near the surface of the organic material and the process can become self-sustaining if it produces sufficient energy
- (f) Flame propagation: depending on the organic material, the combustion stage produces charred surface layers and flames, which can propagate, and can be accompanied by the emission of smoke and toxic gases

What happens in broad outline when a material burns is schematically indicated in Fig. 26.4. Fundamentally there are two consecutive chemical processes: *decomposition* and *combustion*, connected by *ignition* and *thermal feedback*. Primarily the material

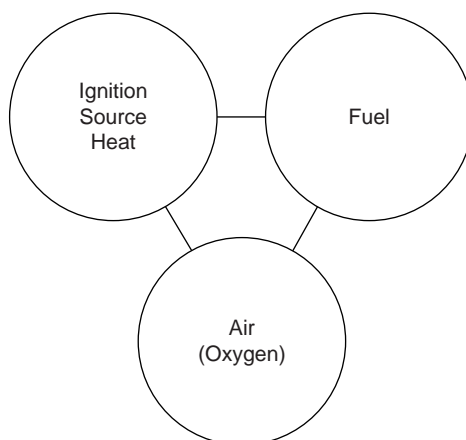
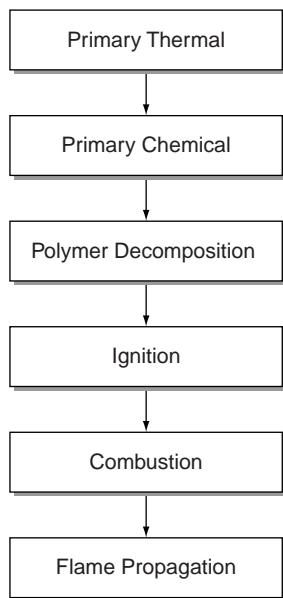
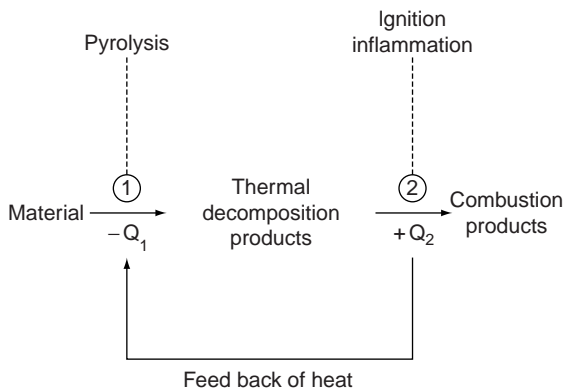


FIG. 26.2 The fire triangle.

**FIG. 26.3** The combustion process.**FIG. 26.4** Consecutive reactions during burning.

decomposes (pyrolysis), which normally *requires* heat. The decomposition products are combusted, which involves generation of heat. This heat of combustion is (partly) used to support the decomposition. An *ignition mechanism is essential*. Of great importance are the heat effects, Q_1 and Q_2 , as well as the available area, A , of exchange of heat and matter.

To be fire resistant, a material should have a low Q_2 value and a low A value; another possibility is that the material contains elements which, on decomposition, form combustion inhibitors (Cl- and Br-containing polymers). Q_2 will be low if only small amounts of combustible gases develop in the pyrolysis, for instance, because the material chars considerably and mainly splits off carbon dioxide and water. The *residue of pyrolysis* or the sum of the residue and the weight of carbon dioxide and water formed by pyrolysis may be used as a rough measure of non-flammability.

Although the term "polymer flammability" is widely used, it has no intrinsic scientific meaning; it depends on the physical state of the product in which it appears and on the

particular fire scenario that is considered. Accordingly, the number of empirical fire tests is numerous. Many of them make use of Bunsen burner. A major step forward in the systematic quantification of the flammability of organic materials was the development of the "Cone Calorimeter" in the 1980s at the US National Bureau of Standards (Babrauskas, 1982, 1984, 1993, 2006 and Babrauskas and Parker, 1986). The Cone Calorimeter is used to determine the following principal fire properties: rate of heat release per unit area, cumulative heat released, effective heat of combustion, time to ignition, mass loss rate, and total mass loss, as well as smoke obscuration. Other important determinations are the ease of ignition, the rate of flame spread, the time-to-ignition, the toxicity of combustion gases and the amount of smoke generated. It is usually assumed in polymer combustion models and in the analysis of experimental data, that gaseous kinetics occur on a faster timescale than the degradation kinetics. The rate of heat release is therefore controlled by the rate of flow of volatiles into the flame and not by gaseous kinetics (Nelson, 2002).

26.3.1. The limiting oxygen index

Oxygen index methods describe the tendency of a material to sustain a flame. The quintessential feature of oxygen-index methods is that a sample is burnt within a controlled atmosphere. The standard method is to ignite the top of the sample, using a gas flame which is withdrawn once ignition has occurred, and to find the lowest oxygen concentration in an upward flowing mixture of oxygen and nitrogen which just supports sustained burning (Nelson, 2002).

The LOI was introduced by Fenimore and Martin (1966). It is also called critical oxygen index (COI) or Oxygen Index (OI) and it is defined as the minimum fraction of oxygen in a mixture of oxygen and nitrogen that will just support combustion (after ignition). The test is performed under standardised conditions, at 25 °C. In their initial description of the LOI technique they reported that LOI values are constant at linear flow rates of 3–10 cm/s. The current standard method for LOI determinations specifies linear flow rates of 4 ± 1 cm/s. Table 26.3 gives the LOI value of some polymeric materials. More data are found in Tewarson (2007). Air contains approximately 21% oxygen and therefore any material

TABLE 26.3 Oxygen indices of Polymers

Polymer	LOI	Polymer	LOI
Polyformaldehyde	0.15	Wool	0.25
Poly(ethylene oxide)	0.15	Polycarbonate	0.27
Poly(methyl methacrylate)	0.17	Nomex®	0.285
Polyacrylonitrile	0.18	PPO®	0.29
Polyethylene	0.18	Polysulphone	0.30
Polypropylene	0.18	Phenol-formaldehyde resin	0.35
Polyisoprene	0.185	Polyether-ether ketone	0.35
Polybutadiene	0.185	Neoprene®	0.40
Polystyrene	0.185	Polybenzimidazole	0.415
Cellulose	0.19	Poly(vinyl chloride)	0.42
Poly(ethylene terephthalate)	0.21	Poly(vinylidene fluoride)	0.44
Poly(vinyl alcohol)	0.22	Polyphenylene sulfide	0.44
Nylon 66	0.23	Poly(vinylidene chloride)	0.60
Penton®	0.23	Carbon	0.60
		Poly(tetrafluoroethylene) (Teflon®)	0.95

with an LOI of less than 0.21 will probably support burning in an open-air situation. In the LOI test a candle-like sample is supported in a vertical glass column and a slow stream of oxygen/nitrogen mix is fed into the glass column. The sample is ignited with a flame and burns downward into unheated material. The oxygen/nitrogen ratio can be varied and the test records the minimum concentration of oxygen (as a percentage) that will just support combustion. The LOI test is a basic property of the material but tells nothing about how the material will react during burning in an open atmosphere (Zeus Industry Products, Inc., 2005).

A material must be considered flammable as long as the LOI value is smaller than 0.26. Later investigations (e.g. Hendrix et al., 1973) have shown that the LOI value is dependent on the weight, construction, moisture content and purity of the sample, on the temperature of the testing environment, and on the size and construction of the sample holder. Yet under standardised conditions the method is very precise, highly reproducible and applicable to a wide variety of materials (plastics, films, textiles, etc.). It is a most valuable test in fire research, although it cannot be considered as a replacement for all existing fire test methods. For instance, it cannot be used for assessing glow and flow (droplet) factors. The specific advantage of the LOI Test is that it gives numerical results and generally shows linear relationships to the flame-retardant level, whereas the other assessment tests, like, e.g. the Tunnel Test, Underwriters Laboratory (UL94), the Horizontal Burning Test (94HB) and the Vertical Burning Test (94V) do not.

Since the flammability of materials increases with the ambient temperature, the LOI may be expected to decrease with increasing temperature. Johnson (1974) derived a quantitative experimental expression for LOI-retention as a function of temperature. Fig. 26.5 illustrates this. The LOI value decreases by the $3/2$ power of temperature, which indicates that diffusion processes are more important than chemical activation of pyrolysis. From Fig. 26.5 the temperature can be derived at which any given LOI, measured at room temperature, will be reduced to 0.21. This will be the temperature at which the flammability of a material with a given LOI will permit candle-like burning in ordinary air. The result is given in Fig. 26.6.

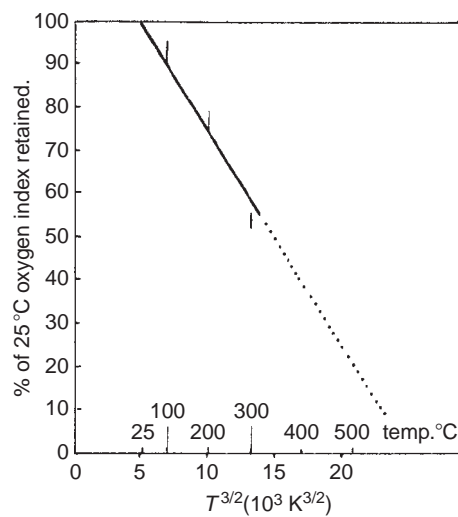


FIG. 26.5 Effect of temperature on limiting oxygen index (after Johnson, 1974).

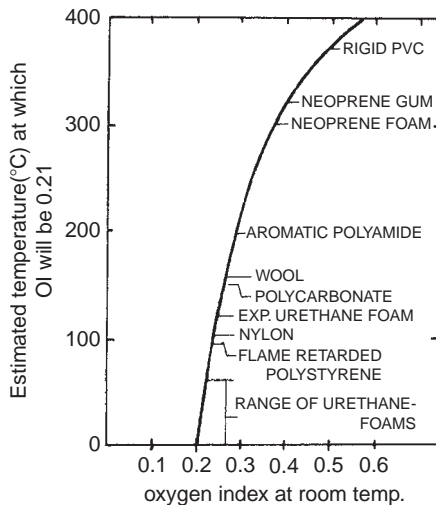


FIG. 26.6 Temperature for candle-like burning in air (after Johnson, 1974).

26.3.2. Relationships between LOI and parameters of the combustion process

Two interesting relationships have been found between the LOI and the parameters of the combustion process.

26.3.2.1. LOI and heat of combustion

It is not surprising that a relationship exists between the heat evolved during combustion and the LOI, the more so as ΔH_{comb} is closely correlated with the oxygen demand during combustion.

The molar heat of combustion can be calculated from the difference between the heat of formation of the carbon dioxide and water formed by complete combustion and the heat of formation of the substance combusted. The data for this calculation are provided in Chap. 20.

Much easier is the application of a simple rule, viz.

$$\Delta H_{\text{comb}} = \Delta(O_2) \times 435 \text{ kJ/mol} \quad (26.1)$$

where $\Delta(O_2)$ is the number of oxygen molecules needed for complete combustion of the structural unit (*molar oxygen demand*).

If we divide ΔH_{comb} by \mathbf{M} , we obtain Δh_{comb} , the specific heat of combustion.

$$\Delta h_{\text{comb}} = \frac{\Delta(O_2)}{\mathbf{M}} \times 435 \quad (26.2)$$

Table 26.4 shows how well Δh_{comb} is predicted by Eq. (26.2).

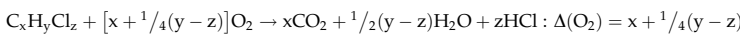
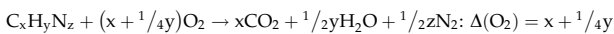
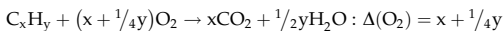
According to Johnson (1974) the LOI values of many common materials can be reasonably well predicted by the expression, provided the atomic C/O ratio is larger than 6:

$$\text{LOI} = \frac{8000}{\Delta h_{\text{comb}}} \quad (26.3)$$

where Δh_{comb} is the *specific heat of combustion* in J/g.

TABLE 26.4 Specific heat of combustion of some polymers; comparison of calculation values

Polymer	Elementary composition of structural unit	M	$\Delta(O_2)$	Δh_{comb} (kJ/g)	
				Calc.	Exp.
Polyformaldehyde	CH ₂ O	30.0	1.0	14.5	16.7
Poly(methyl methacrylate)	C ₅ H ₈ O ₂	100.1	6.0	26.1	—
Polyacrylonitrile	C ₃ H ₃ N	53.1	3.75	30.8	30.6
Polyethylene	C ₂ H ₄	28.1	3.0	46.3	46.5
Polypropylene	C ₃ H ₆	42.1	4.5	46.5	46.5
Polyisoprene	C ₅ H ₈	68.1	7.0	44.7	44.9
Polybutadiene	C ₄ H ₆	54.1	5.5	44.2	45.2
Polystyrene	C ₈ H ₈	104.1	10.0	41.7	41.5
Cellulose	C ₆ H ₁₀ O ₅	162.2	6.0	16.1	16.7
Poly(ethylene terephthalate)	C ₁₀ H ₈ O ₄	192.2	10.0	22.7	22.2
Poly(vinyl alcohol)	C ₂ H ₄ O	44.1	2.5	24.7	25.1
Nylon 66	C ₁₂ H ₂₂ O ₂ N ₂	226.3	16.5	31.7	31.4
Polycarbonate	C ₁₆ H ₁₄ O ₃	254.3	18.0	30.8	31.0
Nomex®	C ₁₄ H ₁₀ O ₂ N ₂	238.3	15.5	28.3	28.7
Polychloroprene (Neoprene®)	C ₄ H ₅ Cl	88.5	5.0	24.5	24.3
Poly(vinyl chloride)	C ₂ H ₃ Cl	62.5	2.5	17.5	18.0
Poly(vinylidene chloride)	C ₂ H ₂ Cl ₂	97.0	2.0	9.0	10.45



Combination of Eqs. (26.2) and (26.3) gives:

$$LOI = 0.184 \times \frac{M}{10\Delta(O_2)} \quad (26.4)$$

Fig. 26.7 shows the LOI values in comparison with the drawn line calculated according to Eq. (26.3). It is clear that not only oxygen-rich polymers show large deviations, but also nitrogen-rich polymers such as polyacrylonitrile. Materials poor in hydrogen, such as carbon chars, graphite, etc., deviate as well. As a rule one may say that if the atomic C/O ratio or the C/N ratio is smaller than 6, the material is more flammable than is predicted by Eq. (26.4). If the C/H ratio is larger than about 1.5, the material will be less flammable than is predicted by Eq. (26.4). Halogen-containing polymers fit more or less into the scheme if their C/O and C/H ratios are appropriate.

26.3.2.2. LOI and the char residue on pyrolysis

Pyrolysis being the first step in the combustion process of polymers, one may expect a relationship between LOI and the parameters of pyrolysis.

An interesting correlation, *for halogen-free polymers only*, between LOI and *char residue* (CR) on pyrolysis was found by Van Krevelen (1974):

$$LOI = \frac{17.5 + 0.4CR}{100} \quad (26.5)$$

where CR is expressed as a weight percentage. Fig. 26.8 shows the relationship for a number of polymers.

Since the char residue on pyrolysis can be estimated by means of group contributions (see Chap. 21), also the value of LOI may be estimated by means of Eq. (26.5).

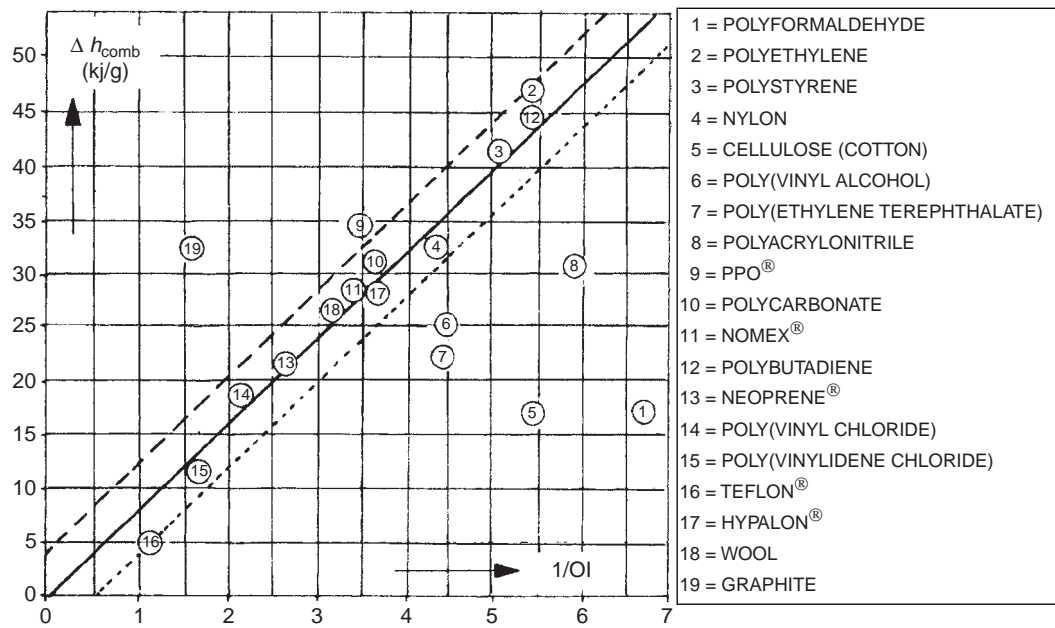


FIG. 26.7 Heat of combustion vs reciprocal limiting oxygen index (after Johnson, 1974).

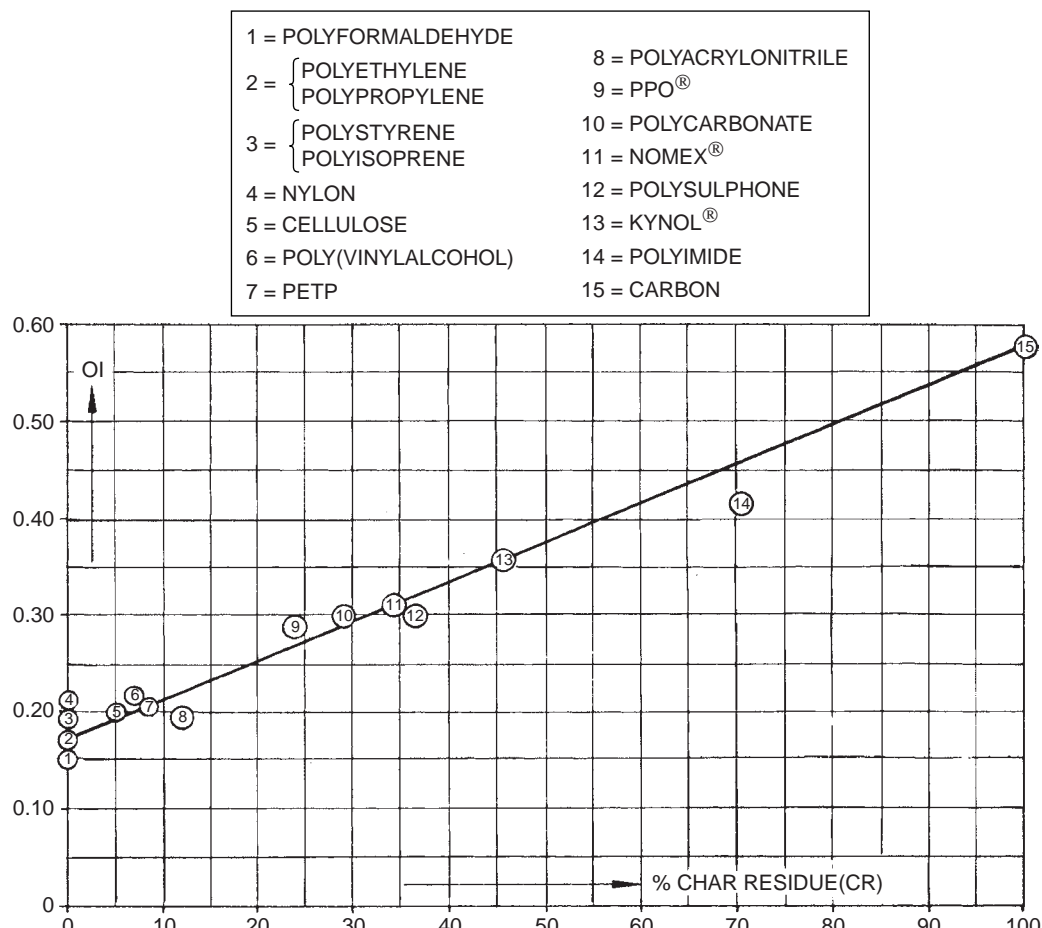


FIG. 26.8 Correlation between LOI and CR.

26.3.3. Limiting oxygen index and elementary composition

Since the heat of combustion of a material and its char residue can be calculated from its elementary structure, it seemed logical to ascertain whether there is a direct relation between the LOI and the elementary composition. Van Krevelen and Hoflyzer (1974) succeeded in finding such a relationship by using the following composition parameter (CP) (see also Van Krevelen, 1977):

$$CP = \frac{H}{C} - 0.65 \left(\frac{F}{C} \right)^{1/3} - 1.1 \left(\frac{Cl}{C} \right)^{1/3} \quad (26.6)$$

where H/C, F/C and Cl/C are the atomic ratios of the respective elements in the polymer composition. *The presence of oxygen and/or nitrogen in the elementary structure does not influence the composition parameter.*

For the LOI the following correlations could be derived:

$$\text{For } CP \geq 1 : LOI \approx 0.175 \quad (26.7a)$$

$$\text{For } CP \leq 1 : LOI \approx 0.60 - 0.425 CP \quad (26.7b)$$

The equations give fairly good results for many polymers, as is shown in Fig. 26.9.

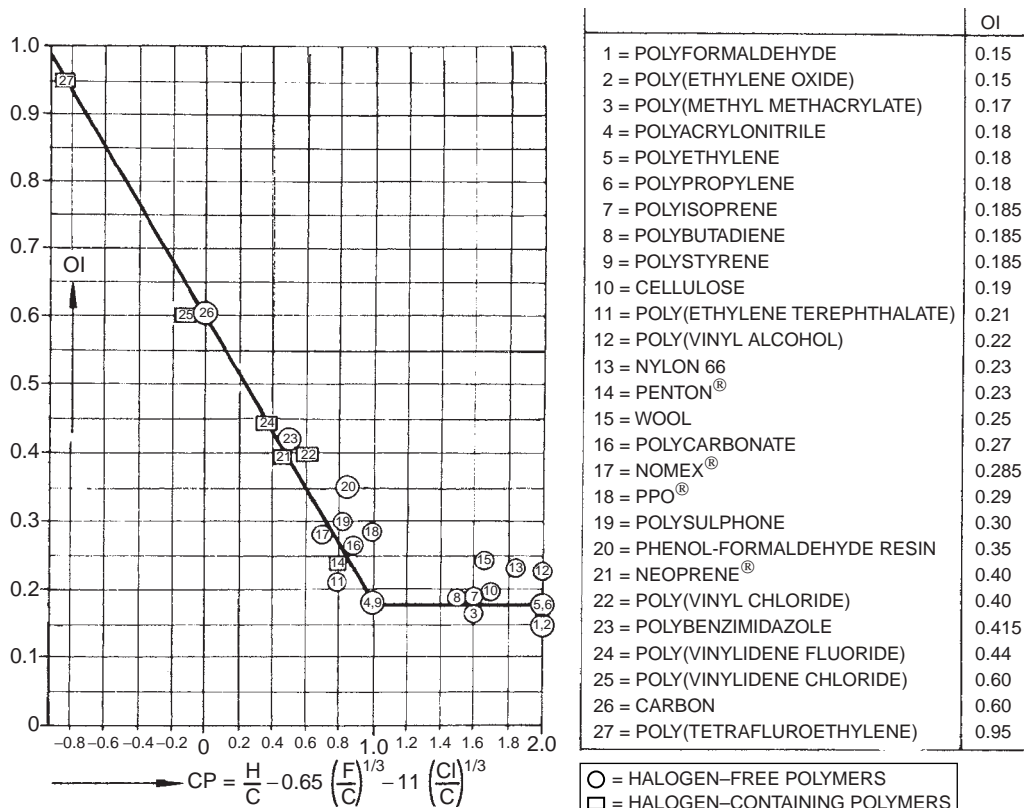


FIG. 26.9 Correlation between limiting oxygen index and elementary composition.

26.3.4. Estimation of the limiting oxygen index

We now have three relations that – with some limitations – enable us to make an estimation of the LOI:

1. $\text{LOI} = \frac{8000}{\Delta h_{\text{comb}}} \approx 0.184 \frac{\mathbf{M}}{10\Delta(\text{O}_2)}$ (valid if C/O and C/N < 6 and C/H > 1.5)
2. $\text{LOI} = \frac{1}{100}(17.5 + 0.4 \text{ CR})$ (for halogen-free polymers only)
3. $\text{LOI} \approx 0.60 - 0.425 \text{ CP}$ for $\text{CP} \leq 1$
 $\text{LOI} \approx 0.175$ for $\text{CP} \geq 1$

where CP is defined by Eq. (26.6).

Table 26.5 shows the results of LOI estimation by these three relations in comparison with the experimental values. It is probably wise to use every one of these estimation methods, and take the average value.

TABLE 26.5 Comparison of experimental and calculated LOI values

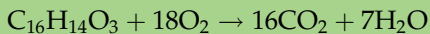
Polymer	LOI Exp.	LOI calculated from		
		CR	Δh_{comb}	CP
Polyformaldehyde	0.15	0.175	–	0.175
Poly(ethylene oxide)	0.15	0.175	–	0.175
Poly(methyl methacrylate)	0.17	0.175	–	0.175
Polyacrylonitrile	0.18	0.175	0.26	0.175
Polyethylene	0.18	0.175	0.17	0.175
Polypropylene	0.18	0.175	0.17	0.175
Polyisoprene	0.185	0.175	0.18	0.175
Polybutadiene	0.185	0.175	0.18	0.175
Polystyrene	0.185	0.175	0.19	0.175
Cellulose	0.19	0.195	–	0.175
Poly(ethylene terephthalate)	0.21	0.205	–	0.26
Poly(vinyl alcohol)	0.22	0.21	–	0.175
Nylon 66	0.23	0.175	0.25	0.175
Penton®	0.23	–	0.44	0.27
Wool	0.25	0.195	0.30	0.175
Polycarbonate	0.27	0.27	0.26	0.23
Nomex®	0.285	0.295	0.28	0.295
PPO®	0.29	0.295	0.23	0.175
Polysulphone	0.30	0.315	0.26	0.255
Phenol-formaldehyde resin	0.35	0.355	0.25	0.235
Neoprene®	0.40	–	0.34	0.36
Polybenzimidazole	0.415	0.445	(0.25)	0.39
Poly(vinyl chloride)	0.42	–	0.45	0.34
Poly(vinylidene fluoride)	0.44	–	0.59	0.45
Poly(vinylidene chloride)	0.60	–	(0.8)	0.64
Carbon (graphite)	0.60	0.575	–	0.60
Poly(tetrafluoroethylene) (Teflon®)	0.95	–	0.95	0.95

Example 26.1

Estimate the specific heat of combustion of polycarbonate and its limiting oxygen index by means of Eq. (26.3).

Solution

The elemental formula of polycarbonate is $C_{16}H_{14}O_3$ ($M = 254.3$), so that the combustion equation reads:



The molar oxygen, $\Delta(O_2)$ demand is 18. For the specific heat of combustion, Eq. (26.2), we get:

$$\Delta h_{\text{comb}} = \frac{\Delta(O_2) \times 435}{254.3} = \frac{7830}{254.3} = 30.8 \text{ kJ/g}$$

The experimental value is 30.9, so there is an excellent agreement. The C/O ratio of polycarbonate is $16/3 = 5.35$. So Eq. (26.3) may be applied. We find

$$\text{LOI} = \frac{8000}{30,800} = 0.26$$

The experimental values mentioned in the literature vary from 0.25 to 0.28 with a most probable value of 0.27

Example 26.2

Estimate the char residue on pyrolysis of polycarbonate and its limiting oxygen index.

Solution

In Example (21.1) we have already estimated the char-forming tendency and the char residue of polycarbonate. A CR value of 24% was found.

By means of Eq. (26.5) we calculate the LOI value:

$$\text{LOI} = \frac{17.5 + 0.4 \times 24}{100} = \frac{17.5 + 9.6}{100} = 0.27$$

This is in excellent agreement with the experimental value (0.27).

Example 26.3

Estimate the limiting oxygen index of polycarbonate from its chemical composition.

Solution

From the elementary formula $C_{16}H_{14}O_3$ the H/C value of $14/16 = 0.875$ is derived. Since the polymer does not contain halogen, also the CP value is 0.875. So Eq. (26.7b) gives $\text{LOI} \approx 0.60 - 0.425 \times 0.875 \approx 0.23$.

26.3.5. Flame-retardant additives

Flame-retardant additives are often used to make polymers more fire resistant. Already in ancient times flame-retardants were applied: during the siege of Piraeus in 83BC wooden assault towers were treated with an alum solution; in 1638 Sabatini's book "*The risk of fire in theatres*" was published, where the preparation of flame-retardant coulisses is described and Montgolfier impregnated his hot-air balloons with alum ("Technische Winkler Prins Encyclopedie", Deel 2, Elsevier, Amsterdam, 1976, in Dutch).

Worldwide 1.2×10^6 tons of flame-retardants were applied in products, (see BBC Research) with a value of almost 2×10^9 US\$. It is expected that this will be increased up to 3×10^9 US\$ in 2008. The biggest part concerned in 2005 Alumina-trihydrate (43%), followed by bromated chemicals (21%) and organo-phosphor chemicals (14%) (Statistics of SRI International, Zürich, 2005). Many of them are also based on synergisms of these compounds with nitrogen and/or antimony. Hoke (1973) gave a handy classification scheme which is reproduced in Fig. 26.10 , while Table 26.6 gives the average concentrations required to render the common polymers self-extinguishing.

Flame-retardants may be based on different functions:

- They may reduce the area of contact between the material and oxygen, either by mechanical sealing or by splitting off non-combustible gases which temporarily seal the surface from the air. Mechanical sealing may be caused by chain decomposition under influence of the flame-retardant that produces a thinner liquid that may drip (cooling effect) or form a film of foam (sealing effect).
- They may influence the pyrolysis, e.g. by "steering" the polymer decomposition, promoting char formation and/or formation of non-combustible gases such as carbon dioxide and water vapour.
- They may undergo endothermic reactions, physically and chemically as well (so-called *heat sinks*).

They may influence the combustion by disturbing the ignition or the combustion mechanism itself, e.g. by capturing OH radicals. For instance, as in the following reaction scheme:

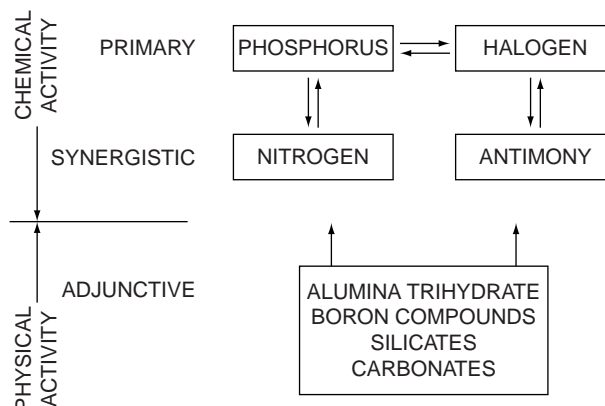
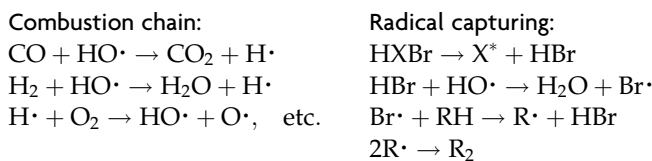


FIG. 26.10 Classification of flame-retardants (after Hoke, 1973).

TABLE 26.6 Average requirements for fire-retardant elements to render common polymers self-extinguishing (Lyons, 1970)

Polymer	% P	% Cl	% Br	% P + % Cl	% P + % Br	% Sb ₄ O ₆ + % Cl	% Sb ₄ O ₆ + % Br
Cellulose	2.5–3.5	>24	—	—	1 + 9	12–15 + 9–12	—
Polyolefins	5	40	20	2.5 + 9	0.5 + 7	5 + 8	3 + 6
Poly(vinyl chloride)	2–4	40	—	NA	—	5–15% Sb ₄ O ₆	—
Polyacrylates	5	20	16	2 + 4	1 + 3	—	7 + 5
Polyacrylonitrile	5	10–15	10–12	1–2 + 10–12	1–2 + 5–10	2 + 8	2 + 6
Polystyrene	—	10–15	4–5	0.5 + 5	0.2 + 3	7 + 7–8	7 + 7–8
Acrylonitrile–butadiene–styrene	—	23	3	—	—	5 + 7	—
Urethane	1.5	18–20	12–14	1 + 10–15	0.5 + 4–7	4 + 4	2.5 + 2.5
Polyester	5	25	12–15	1 + 15–20	2 + 6	2 + 16–18	2 + 8–9
Nylon	3.5	3.5–7	—	—	—	10 + 6	—
Epoxies	5–6	26–30	13–15	2 + 6	2 + 5	—	3 + 5
Phenolics	6	16	—	—	—	—	—

Very often a linear relationship between the limiting oxygen index and the concentration of the flame-retardant additive is observed:

$$\text{LOI} = (\text{LOI})_0 + K(\text{FR}) \quad (26.8)$$

where K is a constant of the order of 0.005 and (FR) is the flame-retardant additive concentration (% by weight) (see Van Krevelen, 1977).

26.3.6. Examples of flame-retardants

26.3.6.1. Brominated flame-retardants

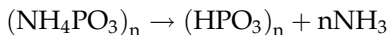
Brominated flame-retardants are produced in approximately 70 variants, each with its own specific properties. Chemically the following groups may be distinguished:

- (a) Poly-bromated diphenyl ethers, or PBDE (among which are Octa-, Deca- and Penta-DBE)
- (b) Poly-bromated biphenyls, or PBB
- (c) Bromated cyclic hydrocarbons

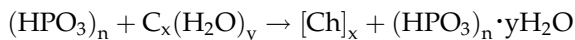
In 1978 the poly-chlorobifenylyls (PCBs) flame-retardants were overreached by the bromated flame-retardants as the most important flame-retardants. They are used in the protection of electronic apparatuses, clothing and furniture. They have the advantage that the start of a fire is retarded and that they have an inhibition effect on the extension of fire.

26.3.6.2. Phosphoric compounds

Phosphoric acid esters, ammonium phosphate and other inorganic phosphates react at a fire to poly-phosphoric acids and meta-phosphoric acids that form an oxygen-blocking layer. As an example:



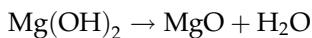
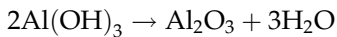
Ammonia is split off at a temperature above 250 °C and phosphoric acid is formed, that forms a oxygen-blocking layer together with the generated soot layer (represented by "Ch") by dehydration of alcohols:



Phosphoric compounds are frequently used. Their advantage is that they can exert a radical trapping mechanism through reactions with halogen radicals (Mascia, 1974).

26.3.6.3. Metal hydroxides

Metal hydroxides will be converted into metal oxide and water, where the water molecules dilute the oxygen concentration around the burning material. Moreover, the reaction is endothermic, so that heat is withdrawn from the fire (a heat sink) and the metal oxide forms an inflammable layer on the organic material. Reactions are:



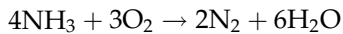
Aluminium oxide is the most representative of this kind of flame-retardants.

26.3.6.4. Antimony oxide

The use of this flame-retardant is based on the generation of gaseous halogen-antimony compounds that prevent the contact between oxygen and the burning material. Antimony oxide offers virtually no flame retardation by itself since it melts at temperatures above the ignition temperature of most polymers and therefore cannot afford fire protection. In mixtures with halogen compounds however, it can form antimony chlorides and oxy-chlorides, which are gaseous at the ignition temperature and will dilute the combustible gases. These compounds act also as radical capturer so that the radical reactions that occur during a fire are retarded. This flame-retardant is used frequently with poly(vinyl chloride) with its many chlorine atoms (Mascia, 1974).

26.3.6.5. Intumescing agents

The application of these agents is based on the generation of an oxygen-blocking foam layer. The most representative is melamine and its salts. An example is polyphosphates together with melamine and a carbon supplier. At fire gaseous product are generated like carbon dioxide and ammonia. Ammonium phosphate splits ammonia under generation of phosphoric acid that reacts with organic material to form soot. Melamine decomposes into ammonia that together with ammonia from ammonium phosphate reacts with oxygen to form nitrogen and water. This blows up the soot to a cross-linked foam layer:



26.3.7. Smoke formation

Smoke generation may be a serious factor in a fire.

Normally polymer structures containing aliphatic backbones are low in smoke-generating character and are generally not self-extinguishing. Additives to such systems to achieve flame-retardancy often enhances smoke generation! Polymers with aromatic side groups such as polystyrene have a considerable tendency to generate smoke.

Polymers with an aromatic group in the main chain, however, such as polysulphones, polycarbonates and poly(phenylene oxides) proved to be intermediate in their smoke generation, possibly due to their considerable charring tendency. Also the unexpected drop in smoke density observed when poly(vinyl chloride) is partially chlorinated may be attributed to the high char yield. Einhorn et al. (1968) concluded that smoke development decreases with increasing amount of chlorine- and phosphorus-containing additives, and with increasing cross-link density.

Gross et al. (1967) and Imhof and Stueben (1973) developed a smoke density index (D_m) based on the maximum specific optical density, ranging from 0 to 1000. High D_m values are found for polymers with LOI values between 0.18 and 0.30.

26.4. ENVIRONMENTAL DECAY OF POLYMERS

Environmental stress cracking or corrosion (ESC) is the phenomenon that materials fail, in the presence of relatively inert chemical agents (liquids or gasses) and/or radiation, at much lower stresses, than in their absence, under the formation of many little cracks. We distinguish real chemical corrosion and stress corrosion, each with its own characteristics.

- (a) *Real chemical corrosion* takes place also in the absence of mechanical stresses; the environment acts simply corrosive by cross-linking or chain fracture and the result is that the material brittles. Subjection to relatively small stresses may be sufficient for failure of the material. Examples are the sensitivity of polymers for UV and oxygen that are going on without mechanical loading of the material.
- (b) *Stress corrosion* that only takes place in a corrosive environment, if at the same time the material is subjected to mechanical stresses; internal stresses due to polymer processing may be already sufficient.

A sharp boundary between (a) and (b) is not always clear.

Stress corrosion can be subdivided in chemical and physical corrosion:

- (b1) *Corrosion due to cooperation of chemical reactions and mechanical stresses*

Under the influence of stresses chemical reactions take place leading to chain fracture. Examples are

- The ozone sensitivity of natural rubber under mechanical stresses: double bonds are broken; an example is found in, e.g. laboratories where glass tubes are connected with rubber hoses: at the connection where the rubber is subjected to stresses, in the long run little tears are formed.
- The acid and base sensitivity of condensation polymers whether or not under stress, e.g. polycarbonate, polyesters, polyamides and polysilanes; under influence of acid or base the condensation bonds are hydrolysed under the cooperative action of mechanical stresses and the environment. A striking example is shown in Fig. 26.11, where the strength retention of PpPTA fibres is plotted versus pH after an exposure of 3 months at room temperature (Van den Heuvel and Klop). The hydrolysis of the polyamide is acid or alkali catalysed, in particular below pH = 3 and above pH = 9.

- (b2) *Corrosion due to cooperation of physical interactions and mechanical stresses*

The environment that causes this kind of corrosion is often rather inert: the polymer does not dissolve or swell, but there is some diffusion of liquid or gas, in particular at the surface. If the diffusion rate is small localised plasticization is possible and subsequently deformation is caused by the stresses. This leads to increased plasticization and to the formation of crazes and even of cracks.

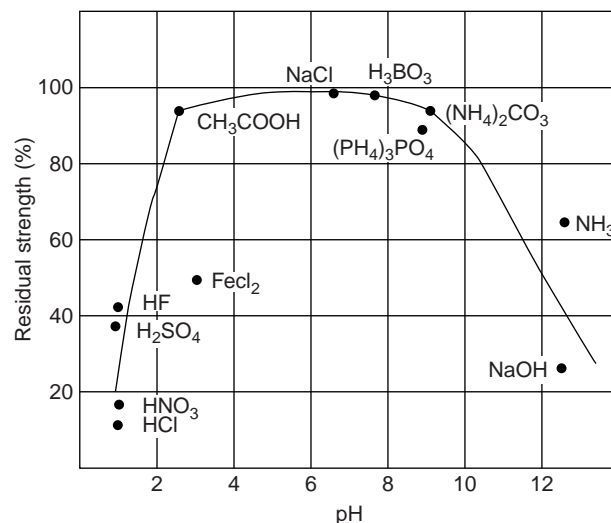


FIG. 26.11 Critical corrosion stress as a function of pH (after Van den Heuvel and Klop, 2002).

26.4.1. Characteristics of stress corrosion

There are many special characteristics of stress corrosion:

- Cracks are created at the surface and they extend in a direction perpendicular to the direction of the stress, just like the cracks schematically shown in Fig. 13.80
- The stress needed to create cracks is small compared to normal loading
- A minimum stress σ_c is needed, below which no ESC takes place
- σ_c is a function of temperature T_c , up to a critical temperature T_c^* in a way as schematically shown in Fig. 26.12
- T_c^* depends on the kind of corrosive agent (liquid or gas) and decreases with decreasing solvent quality
- The time t_f needed to create cracks is a function of several parameters:
 - t_f decreases with increasing stress
 - t_f decreases with decreasing solvent quality
 - t_f decreases with increasing temperature
 - t_f increases strongly with the molar mass of the polymer

The remainder of this section on environmental decay of polymers is devoted to the physical interaction between polymer and environment. This is what in general is called "*environmental stress cracking*", which thus is only one part of the story.

26.4.2. Physical environmental stress cracking

While a given polymer may be quite resistant to some organic liquids and it may be attacked more or less severely by others. The effect of organic liquids on polymers can take several forms:

- a. dissolution
- b. swelling
- c. environmental stress cracking
- d. environmental crazing

Solubility and swelling have already been discussed in Chap. 7.

In *environmental stress cracking* the material fails by breaking when exposed to mechanical stress in the presence of organic liquids or wetting agents (soap solutions, etc.). A well-known example is the action of carbon tetrachloride in polycarbonate: a little drop of this liquid on a strip of this polymer causes a very fast cracking upon a little bending of the strip.

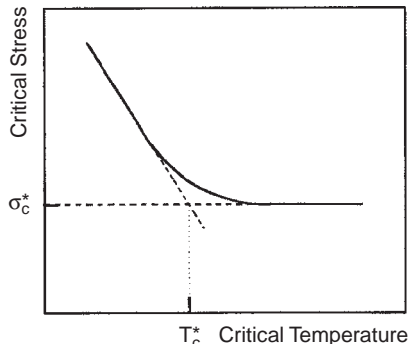


FIG. 26.12 Schematic view of critical stress for environmental stress cracking as a function of critical temperature.

In *environmental crazing* the specimen fails by the development of a multitude of very fine cracks in the presence of an organic liquid or its vapour. This phenomenon may manifest itself even without the presence of mechanical stress: the internal stresses, always present in plastic specimens, can be sufficient.

The phenomena of stress cracking and crazing in the presence of a wide variety of organic liquids occur in both amorphous and semi-crystalline materials. They can lead to catastrophic failure at stresses far below the tensile strength and the critical stress for crazing of the materials tested in air. Especially solvent crazing may be regarded as an inherent material weakness of glassy polymers; in semi-crystalline polymers the problem is somewhat less serious.

It is not always possible to distinguish clearly between the phenomena a. to d., as they are dependent on the way the experiment is performed, on the time scale, the molecular weight of the polymer, etc. So the same polymer–solvent combination may be classed into different categories by different investigators.

26.4.3. Mechanism of solvent cracking and solvent crazing

Dissolution, swelling and solvent cracking are closely related phenomena. The initial action of an aggressive agent is to swell the polymer. The resulting lowering of the T_g causes a reduction of the stress required to initiate plastic flow at a given temperature. Whether dissolving or cracking will dominate is determined by the rate of solvent penetration on one hand and the rate of crack formation on the other. These phenomena are dependent on a number of properties of polymer and solvent and on the applied stress.

The phenomenon of solvent crazing cannot be explained from swelling, as many liquids that cause crazing do not show any swelling effect. Some authors assumed that the effect was caused by a lowering of the surface energy of the polymer in the presence of a solvent. Andrews and Bevan (1972) calculated values for the minimum surface energy of poly(methyl methacrylate) in different solvents that caused crazing. From work of Kambour et al. (1973), however, doubts raised about the surface energy hypothesis. Although the last word has not been said in this matter, the effect of crazing solvents must probably be attributed to plasticization. This means that crazing agents, although present in minute concentrations, lower the stress level at which void propagation takes place.

According to MacNulty (1974), failure by solvent crazing occurs by brittle fracture, even when the failure is slow. Always a small liquid penetration zone appears to initiate the break.

26.4.4. Prediction of solvent cracking and solvent crazing

The foregoing considerations about the mechanism of solvent cracking and solvent crazing suggest that the solubility parameter difference, as a quantitative measure of the interaction between polymer and solvent, will play an important part in these phenomena.

This is confirmed already in the 1960s in an investigation by Bernier and Kambour (1968) into the effect of different solvents on poly(dimethylphenylene oxide). (In this investigation, liquids thought to interact via hydrogen bonding were left out of consideration.) The authors demonstrated that the *critical strain* plotted against the solubility parameter of the solvent shows a minimum, while the equilibrium solubility against the solubility parameter shows a maximum at the same value (see Figs. 26.12 and 26.13. It may be assumed that at the minimum critical strain (maximum solubility) the solubility parameter of the polymer δ_P equals that of the solvent δ_S . Small differences between δ_P and δ_S give rise to solvent cracking; larger differences are attended with solvent crazing (Fig. 26.14).

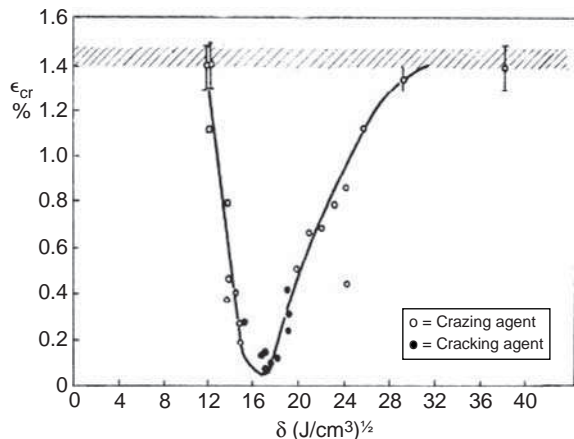


FIG. 26.13 Critical strain of poly(2,6-dimethyl-1,4-phenylene oxide) vs. solubility parameter δ of crazing and cracking liquids. Minimum in ϵ_{cr} occurs at δ equal to that of the polymer. Band at top indicates critical strain of polymer in air (Bernier and Kambour, 1968; reproduced by permission of the American Chemical Society).

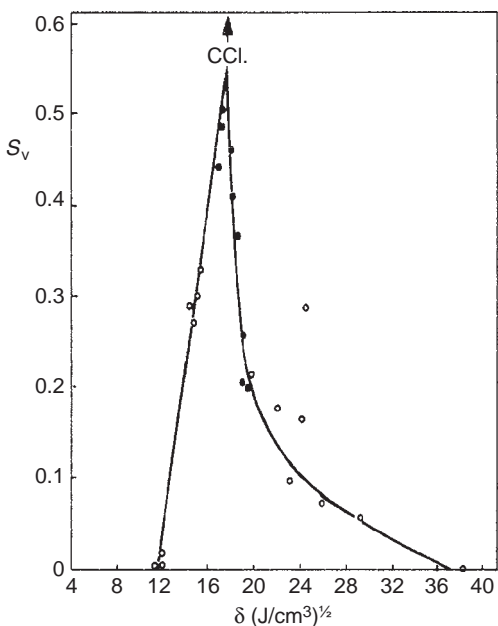


FIG. 26.14 Equilibrium solubilities of crazing fluids in poly(2,6-dimethyl-1,4-phenylene oxide) (Bernier and Kambour, 1968; reproduced by permission of the American Chemical Society).

26.4.5. Classification of environmental stress cracking liquids

As has already been discussed in Chap. 7 the enthalpy and entropy of mixing determine the dissolution of a polymer in a liquid:

$$\Delta G_m = \Delta H_m - T\Delta S_m < 0 \quad (26.9)$$

The entropy of mixing is in general positive so that the enthalpy of mixing may be positive but not too much. Hildebrand and Scott (1950) suggested the following expression

$$\Delta H_m = V\varphi_1\varphi_2(\delta_S - \delta_P)^2 \quad (26.10)$$

where δ_S and δ_P are the solubility parameter of solvent and polymer, respectively (see also Chap. 7).

Concerning environmental corrosion we have the following classification:

- (a) Solvents: the solubility parameter of the liquid differs only slightly of that of the polymer:

$$|\delta_S - \delta_P| < 6(\text{MJ/m}^3)^{1/2} \quad \text{or} \quad |\delta_S - \delta_P| < |\delta_S - \delta_P|_c \quad (26.11a)$$

- (b) Liquids where the polymer does not dissolve in, but only swells in:

$$|\delta_S - \delta_P| > 6(\text{MJ/m}^3)^{1/2} \quad \text{or} \quad |\delta_S - \delta_P| > |\delta_S - \delta_P|_c \quad (26.11b)$$

- (b1) Liquids that cause cracks without appreciable stresses:

$$0 < ||\delta_S - \delta_P| - |\delta_S - \delta_P|_c| \ll 1, \quad \text{e.g. } 6 < |\delta_S - \delta_P| < 6.4(\text{MJ/m}^3)^{1/2} \quad (26.11c)$$

- (b2) Liquids that cause crazes at not too big stresses:

$$0 < ||\delta_S - \delta_P| - |\delta_S - \delta_P|_c| < 1, \quad \text{e.g. } 6.4 < |\delta_S - \delta_P| < 8(\text{MJ/m}^3)^{1/2} \quad (26.11d)$$

- (b3) Liquids that cause crazes only if the stress are big:

$$1 < ||\delta_S - \delta_P| - |\delta_S - \delta_P|_c|, \quad \text{e.g. } |\delta_S - \delta_P| > 8(\text{MJ/m}^3)^{1/2} \quad (26.11e)$$

These ranges are schematically shown in Fig. 26.15 in a one-dimensional plot.

This picture becomes more complicated, however, if liquids that can participate in hydrogen bonding are taken into account. This is schematically shown in a two-dimensional plot in Fig. 26.16. Experiments were published by Vincent and Raha (1972) for poly(methyl methacrylate), poly(vinyl chloride) and polysulphone. They plotted their results as a function of solubility parameter and hydrogen-bonding parameter. Their graphs are reproduced in Fig. 26.17. In each graph a solubility region is indicated as the closed area, where the plus sign in the centre shows both parameters of the polymer. The solvents that cause cracking are near the periphery of the solubility region, the crazing solvents at a greater distance. Qualitatively their results are in agreement with the schematic view in Fig. 26.16.

So attempts to correlate solvent cracking and solvent crazing with solvent properties lead to the same conclusion as was drawn in Chap. 7 for the solubility of polymers, viz. that besides the solubility parameter at least one other solvent property must be taken into account. The method proposed by Vincent and Raha is one of several possible two-dimensional correlation methods.

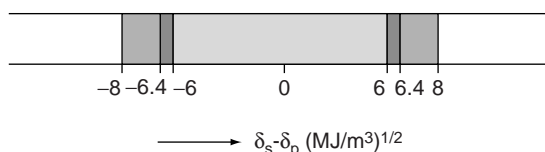


FIG. 26.15 Schematic view of the various kinds of environmental causing liquids shown as function of the differences in solubility parameters of polymer and liquid.

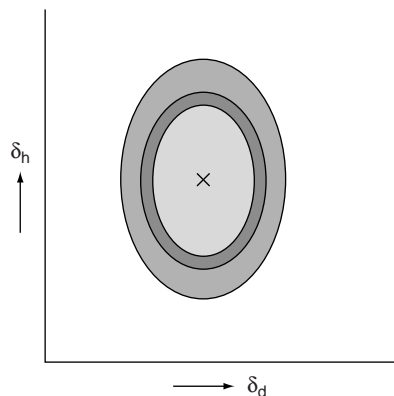


FIG. 26.16 The same kind of view as Fig. 26.15, but now two-dimensionally plotted as functions of the solubility parameter δ_d and the hydrogen bonding parameter δ_h . The cross in the closed areas depicts the parameters of the polymer.

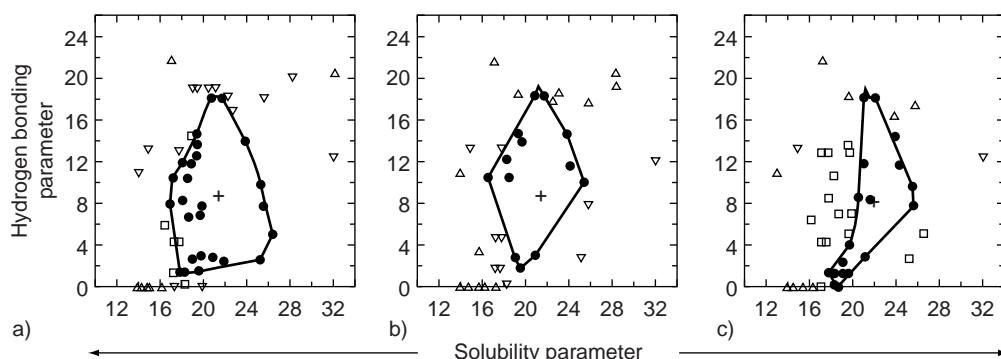


FIG. 26.17 Plot of data of Vincent and Raha (1972). Parameters in $(\text{MJ}/\text{m}^3)^{1/2}$. Solvents (●), cracking agents (□), low-strain crazing agents (▽) and high-strain crazing agents (△) for (A) PMMA, (B) for PVC and (C) for polysulphone. The plus signs in the centre of the closed areas depict the parameters for the actual polymers (reproduced by permission of the publishers, IPC Business Press Ltd.).

It was demonstrated in Chap. 7 that solubility data could effectively be represented in a $\delta_v - \delta_h$ diagram, where $\delta_v = \sqrt{\delta_d^2 + \delta_p^2}$ and δ_d , δ_p and δ_h are the solubility parameter components according to Hansen representing disperse forces, polar forces and hydrogen bonding, respectively.

A good correlation is obtained if the results of Vincent and Raha are plotted in a $\delta_v - \delta_h$ diagram. The results for the three polymers can be made to coincide if $\delta_{vS} - \delta_{vP}$ and $\delta_{hS} - \delta_{hP}$ are used as parameters, where the capital subscripts S and P denote solvent and polymer. The difficulty in this approach is that the solubility parameter components of the polymers are not readily available. For poly(methyl methacrylate) and poly(vinyl chloride), values of δ_v and δ_h , as determined by Hansen (1969) have been mentioned in Chap. 7; these values are used here. For polysulphone the values of δ_v and δ_h have been chosen in such a way that a good correlation was obtained. The solubility parameter components used are mentioned in Table 26.7.

The data of Vincent and Raha for the three polymers mentioned have been plotted in Fig. 26.18. Additional experimental data on polysulphone by Henry (1974) and MacNulty (1974) proved to be in good agreement with those of Vincent and Raha.

TABLE 26.7 Solubility parameter components of sonic polymers ($MJ^{1/2}/m^{3/2}$)

Polymer	δ_v	δ_h
Poly(vinyl chloride)	21.3	7.2
Poly(methyl methacrylate)	21.4	8.6
Polysulphone	22.0	8.0

There is a small zone near the centre ($\delta_{vS} \approx \delta_{vP}$; $\delta_{hS} \approx \delta_{hP}$), where all solvents dissolve the polymer. At a large distance from the centre, crazing is generally found. In the intermediate zone, the main phenomenon is solvent cracking, although dissolving, swelling or crazing are observed with some solvents.

In principle, Fig. 26.18 permits the prediction of solvent behaviour. The essential difficulty is the choice of proper values of the solubility parameter components δ_{vP} and δ_{hP} for a given polymer. A fair estimation is possible by means of the methods of Hoftyzer-van Krevelen and of Hoy, described in Chap. 7 (see in particular Eq. (7.25)). An experimental check remains desirable in all cases.

26.4.6. Life of a polymer in a liquid environment

Table 26.8 gives a survey of the parameters influencing the time to failure and the effects of environment on polymers. Ways to reduce the effects are to be found in the use of the parameters. Several attempts have been made to quantitatively predict the lifetime of

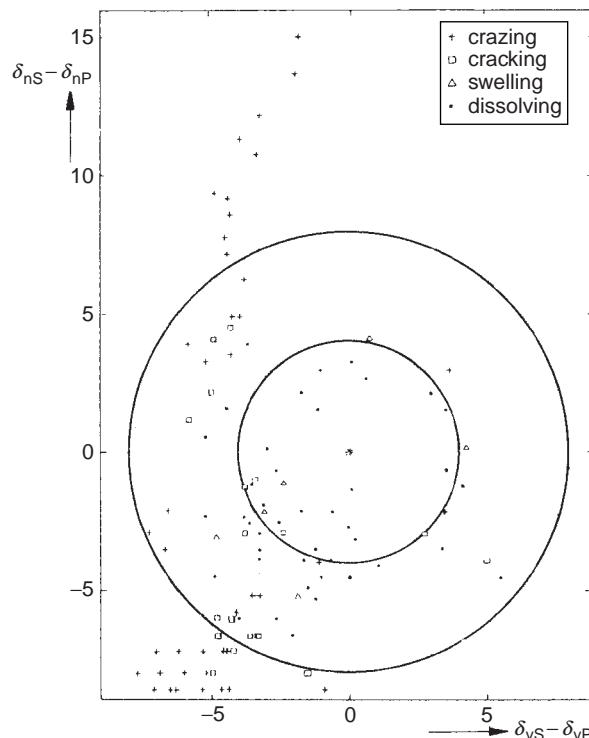
**FIG. 26.18** Generalised plot of data of Vincent and Raha (1972).

TABLE 26.8 Parameters and effects of environment

Parameters	Effects
Stress and strain	Dissolution
Nature of environment	Softening
Temperature	Stress-cracking
Molecular weight	Embrittlement
Molecular architecture	Chemical degradation
Crystallinity	Photochemical degradation
Orientation	Biological degradation

TABLE 26.9 Environmental shift factors

Polymer	Hexane = 1	Shift factor for isopropyl alcohol
Acrylonitrile–butadiene–styrene copolymer		120
Poly(vinyl chloride)		0.08
Polycarbonate		3
Styrene–acrylonitrile copolymer		1500

polymers in different liquid environments. Suezawa et al. (1963) showed that lifetimes under load in different liquids can be fitted to a master curve and that, in addition to stress also the environment can be considered a reduced variable.

Fulmer (1967) demonstrated that for a specific polymer every environment (liquid) shows a constant shift factor versus another environment. Next to his own experiments on (filled) polyethylene he used data obtained by Bergen (1964) in creep investigations. Table 26.9 lists some of these environmental shift factors for different polymers in two liquids. Comparative data for other polymer–liquid combinations are scarce.

BIBLIOGRAPHY

General references

- Bradley LN, "Flame and Combustion Phenomena", Methuen, London, 1969.
- Cullis CF and Hirschler MM, "The Combustion of Organic Polymers", Clarendon Press, Oxford, 1981.
- Davis A and Sims D, "Weathering of Polymers", Applied Scientific Publishers (Elsevier), London, 1983.
- Einhorn IN, "Fire Retardance of Polymeric Materials", J Macromol Sci, Revs Polymer Technol D1 (2) (1971) 113–184.
- Haward RN (Ed), "The Physics of Glassy Polymers", Applied Science Publishers, London 1973.
- Haward RN and Young RL (Eds), "The Physics of Glassy Polymers", Chapman and Hall, London, 2nd Ed, 1997.
- Hawkins W (Ed) "Polymer Stabilization", Wiley-Interscience, New York, 1972.
- Hawkins WL, "Polymer Degradation and Stabilization", Springer, Berlin, 1984.
- Hilado CJ, "Flammability Handbook for Plastics", Technomic Publications, Stamford TC, 1969.
- Korshak VV, "The Chemical Structure and Thermal Characteristics of Polymers", Israel Program for Scient Transl, Jerusalem, 1971.
- Lyons JW, "The Chemistry and Uses of Fire Retardants", Wiley Interscience, New York, 1970.

Queen Mary College, "Smoke from Burning Plastics", A Micro-Symposium organised by the Industrial Materials Research unit on February 22, 1973. Queen Mary College, University of London, 1973; with papers of Berman AM, Scott KA, Smith DA et al.

Tewarson A, "Flammability" in Mark JE (Ed), "Physical Properties of Polymers Handbook", Springer, Berlin, 2nd Ed, 2007, Chap. 53.

Thiery P, "Fire Proofing", Elsevier, Amsterdam, 1970.

Special references

Andrews EH and Bevan L, Polymer 13 (1972) 337.

Babrauskas V, "Development of the Cone Calorimeter" (NBSIR 82-2611), [US] Natl Bur Stand, 1982.

Babrauskas V, Fire Mater 8 (1984) 81.

Babrauskas V, "Ten Years of Heat Release Research with the Cone Calorimeter", in Hasemi Y (Ed) "Heat Release and Fire Hazard", Vol I, pp III-1 to III-8, Building Research Institute, Tsukuba, Japan, 1993.

Babrauskas V, an updated version of the previous reference: "Ten Years of Heat Release Research with the Cone Calorimeter" Fire Science and Technology, Inc., 2006.

Babrauskas V and Parker WJ, "Ignitability Measurements with the Cone Calorimeter", (NBSIR 86-3445), [US] Natl Bur Stand, 1986.

Bergen RL, SPE J 20 (1964) 630.

Bernier GA and Kambour RP, Macromolecules 1 (1968) 393.

Emmons HW, J Heat Transfer 95 (1973) (2) 145.

Einhorn IN, Mickelson RW, Shah B and Craig R, J Cell Plast 4 (1968) 188.

Fenimore CP and Martin FJ, Modern Plastics 44 (1966) 141; Combustion Flame 10 (1966).

Fulmer GE, Polym Eng Sci 7 (1967) 280.

Gross D, Loftus JJ and Robertson AF, ASTM STP-422 (1967) 166.

Hansen CM, Ind Eng Chem Prod Res Dev 8 (1969) 2.

Hendrix JF, Drake GL and Reeves WA, (J Am Assoc) Textile Chemist Colourist 5 (1973) 144.

Henry LF, Polym Eng Sci 14 (1974) 167.

Hoke CHE, Soc Plast Eng Techn Pap 19 (1973) 548; SPE J 29 (1973) (5) 36.

Imhof LG and Stueben KC, Polym Eng Sci 13 (1973) 146.

Johnson PR, J Appl Polym Sci IS (1974) 491.

Kambour RP, Gruner CL and Romagosa EE, J Polym Sci, Polym Phys Ed 11 (1973) 1879.

MacNulty BJ, Br Polym J 6 (1974) 39.

Mascia L, "The Role of Additives in Plastics", Edward Arnold Publishers Ltd, London, 1974.

Nametz RC, "Flame Retarding Synthetic Textile Fibres", Ind Eng Chem 62 (1970) 41-53.

Nelson MI, Proc Roy Soc Lond A 454 (1998) 789.

Nelson MI, Comb Theory Model 5 (2001) 59 and Comb Sci Tech 167 (2001) 83.

Nelson MI, <http://www.uow.edu.au/~mnelson/review.dir/polymer.html>, 29th January 2002.

Nelson MI, Brindley J and McIntosh AC, Fire Safety J 24 (1995) 107; Math Comp Model 24 (1996) 39; Comb Sci Tech 113/114 (1996) 221; Polym Degrad Stab 54 (1996) 255 and Fire Safety J 28 (1997) 67.

Nelson MI, Sidhu HS, Weber RO and Mercer GN, ANZIAM J 43 (2001) 105.

Nelson MI, Balakrishnan E and Chen XD, Trans ICE 81 Part B (2003) 375.

Suezawa Y, Hojo H, Ideda T and Okamura Y, Mater Res Stand 3 (1963) 550.

Vincent PI and Raha S, Polymer 13 (1972) 283.

Van den Heuvel CJM and Klop EA, "High-Performance Fibers – A Bird's eye View of their Structure, Properties and Applications", paper presented at the "9th Twaron Symposium", Königswinter, Germany, 24/25 April, 2002.

Van Krevelen DW, "New Developments in the Field of Flame-Resistant Fibres", Angew Makromol Chem 22 (1972) 133-158.

Van Krevelen DW, "Correlation between Flame Resistance and Chemical Structure of Polymers", Paper No IV 5-2, IUPAC Conference on Macromolecules, Madrid, 1974; Polymer 16 (1975) 615.

Van Krevelen DW, J Appl Polym Sci, Appl Polym Symp 31 (1977) 269-292.

Van Krevelen DW and Hoffyzer PJ, Unpublished results, 1974.

This page intentionally left blank

CHAPTER 27

An Illustrative Example of End use Properties: Article Properties of Textile Products

There is no category of products made from polymeric materials in which the article properties play such a predominant role – and are so varied – as in textile products; therefore the emphasis in this last chapter is on textile applications.

An integral method of evaluating polymeric materials for specific end uses is given: the so-called *profile method*.

27.1. INTRODUCTION

Textile articles are more or less unique by the wide and varied range of product properties which prove to be important. This is the reason why this product category will be discussed in more detail.

As described in Chap. 3, the article properties can be distinguished into three groups:

- (a) The aesthetic properties
- (b) The use or performance properties
- (c) The maintenance or care properties

In this order the article properties of textile products will be discussed.

27.2. AESTHETIC PROPERTIES

In this category belong the properties that determine the reactions (*perceptions*) of the senses: the eye (colour, lustre, covering power, appearance), and the tactile sense, viz. the tactile corpuscles of the skin (handle). While the aesthetic properties are influenced by the intrinsic properties, they depend much more on the “added” properties, that is to say on those obtained during processing, as is clearly shown in Table 27.1. The correlation of the aesthetic properties with the intrinsic and added properties is very complex and only partly understood. As matters stand at present, they are more qualitative than quantitative. The main aesthetic properties are considered below.

TABLE 27.1 General correlation of aesthetic properties with intrinsic and added properties

Properties	Whiteness and colour	Lustre and gloss	Covering power	Handle and drape
<i>Intrinsic properties</i>				
Chemical structure	×			
Physical morphology	×	×	×	
Thermal stability	×			
Bending modulus				×
Stress relaxation				×
<i>Added properties</i>				
Fibre and yarn fineness		×	××	×
Fibre cross-section		××		×
Fibre microstructure	×	××	×	×
Fibre and yarn surface				×
Yarn construction		×	××	××
Fabric construction		××	××	××
Fabric finish (heat treatment)	×			××

× = statistically significant; ×× = (very) important.

27.2.1. Colour and whiteness

Colour is very important, but it normally is an added property; it is obtained by a dyeing process. Brilliant colours are the most popular but the most difficult to obtain. They can be realised only if the polymer itself is water-white (colourless). It is necessary that the whiteness is also maintained during processing and after treatment; yellowing of the polymer as such severely affects the appearance of the coloured product.

Whether a polymer can be suitably coloured depends on:

- The chemical structure of the polymer; functional groups determine which class or pigments or dyestuffs is preferable. Basic dyestuffs lead to the highest brilliance but the colour often has a poor fastness. In acrylic fibres basic dyestuffs are more brilliant and much faster than in other polymeric fibres, such as polyesters.
- The fine structure of the polymer; a smooth compact fibre, for instance, is more favourable than a micro porous structure (although with regard to accessibility or ease of dyeing the reverse is true).
- The whiteness of the polymer. Whiteness means that the spectrum of the polymer shows no absorption bands in the visual part.

27.2.2. Lustre and gloss

Lustre is the integral effect of reflection and diffraction. The larger the size of the reflecting areas, the more pronounced the reflection (glittering). This is the reason why the morphology of the fibre, and its cross-section, play a dominating part in textiles. A silky lustre is highly appreciated. Combination of lustre and colour may produce very special effects (gold, copper, silver lustre, etc.).

27.2.3. Covering power

While transparency is preferred in polymeric films, the covering power is an important factor in textiles.

Unlike the transparency of fibres, the transparency of fabrics is strongly reduced by light diffraction and lustre: *the transparency of a fabric is almost entirely determined by the morphology of the fibre and by the construction of yarn and fabric. Pigments and dyes exert additional influence.*

For films and paper there are standard methods for measuring the transparency; such standards are not yet available for fabrics.

27.2.4. Handle and drape

In the evaluation of a textile product the handle and drape, both subjective quantities, play an important part.

Handle may be defined as a subjective tactile evaluation of the textile quality.

Howorth (1958, 1964) concluded that three fundamental cloth properties determine the handle, viz. *stiffness*, *softness* and *bulkiness* (thickness per unit weight). It appears that the effect of the yarn and fabric construction on these properties is at least as great as the effect of the differences resulting from the nature of the polymer.

The *stiffness* of a fabric can be objectively determined as the average of the flexural rigidities (in warp and weft direction). These depend on the shear modulus and the coefficient of friction; both are influenced by swelling and, therefore by humidity.

The *softness* of a textile material is presumably built up of two components: the smoothness of the fibre and the smoothness of the fabric; the latter is determined by the fabric construction and the yarn structure (bulkiness, etc.).

In regard to *bulkiness*, we distinguish between the bulkiness of a fabric and that of a yarn (thickness per unit weight). Yarns having a higher bulkiness will give fabrics with a better handle and drape, a higher covering power and greater comfort.

The influence of the intrinsic polymer properties on the yarn bulkiness is relatively small (low density and high stiffness are favourable) in contrast with that of the fibre, yarn and cloth constructions. Hence the significance of texturing (crimping) processes, which impart a greater bulkiness (crimp) to the compact filament yarn.

Drape is a visual quality characteristic, referring to the degree to which a fabric falls into folds under the influence of gravity. Paper and film have a very poor drape; fabrics generally have a drape varying from acceptable to excellent. In knitted fabrics the drapability is generally quite sufficient; for woven articles a proper drape can usually be realised by choosing a suitable weave and finish treatment. The drape of non-woven presents problems because of the stiffness produced by the bonding of fibres and filaments.

Drape is determined by the same basic quantities as handle. Both handle and drape are strongly influenced by the cloth construction and the after-treatment (finish) of the article. The chemical structure of the polymer has a secondary influence.

27.3. USE OR PERFORMANCE PROPERTIES

Most of the use properties have to do with comfort or with the retention of desired properties (colour, shape, appearance, etc.). Also this category of properties is much more dependent on added properties than on the intrinsic ones. Again, the correlations are of a complex nature and are qualitative rather than quantitative. Table 27.2 shows the interdependence. In the following, the use properties will be discussed in some detail.

27.3.1. Thermal comfort

Thermal comfort exists if the human body is in thermal equilibrium with its environment, implying a constant temperature of the body. Comfort is mainly determined by the construction of a garment, in particular by its thermal *insulation* and by *moisture transfer*.

TABLE 27.2 General correlation of use (performance) properties with intrinsic and added properties

Intrinsic/added properties	Use (performance) properties							
	Thermal comfort	Mechanical comfort	Shape retention (wrinkle fastness)	Retention of surface appearance (wear fastness)	Colour fastness	Soiling resistance	Resistance to static charging	Resistance to fatigue
<i>Intrinsic properties</i>								
Chemical structure	×				×	×	×	×
Physical morphology		×		×	×			×
Transition regions		xx						xx
Surface energy	×					×	×	
Moisture absorption	×		xx				xx	
Light fastness						×		
Thermal stability			×			×		
Stress-strain pattern	×	×		×				
Stress relaxation			×					
Creep		xx						
Young's modulus	×	×		×				
Mechanical damping					×			xx
Elastic recovery		×	×					
Torsion relaxation		×	×					
Bending modulus		×	×					
Lateral strength				×				
<i>Added properties</i>								
Fibre and yarn fineness	×							
Fibre micro structure	×					×		
Fibre and yarn friction				xx				xx
Yarn construction	xx	xx	xx	xx			xx	
Fabric construction	xx	xx	xx	xx			xx	
Heat treatment ("finish")	×	×	xx		×	xx	xx	

× = statistically significant; xx = (very) important.

This means that – save in exceptional circumstances – the nature of the textile fibre is less material than the fabric construction.

Heat insulation is *mainly determined by the construction of the fabric*, is proportional to its thickness, and decreases with increasing air velocity (wind).

Moisture may be transferred via three mechanisms:

- (1) *Water vapour permeation*, which is inversely proportional to thickness and increases with air velocity
- (2) *Capillary moisture transfer*, which increases with the *wetability*, and therefore depends on *interfacial tension*
- (3) *Moisture transfer through fibres*, which increases with the *moisture absorption*. Of these mechanisms the water vapour permeation seems to be the most important

TABLE 27.3 Average comfort data of textile articles

Textile product	Thickness (mm)	Weight (kg/m ²)	Air permeation (m ³ /(m ² s))	Heat permeability coefficient, a (J/(m ² s K)) ^a	Water vapour permeability coefficient, b (g/(s bar))	a/b
Lingerie	0.8	0.17	55	17.5	0.58	30
Linings	0.15	0.11	10	22	0.65	34
Shirting	0.30	0.11	10–100	21.5	0.70	31
Pullovers	2.0	0.4	50	12.5	0.44	29
Suiting	0.75	0.25	5–50	18.5	0.57	32
Overcoating	1.5	0.4	15	14	0.45	31
Work clothing	0.8	0.17	50	17.5	0.58	30

^aIn clothing physiology a thermal resistance coefficient, the *Clo*, is often used: 1 Clo = 0.155 m² s K/J.

In steady states, where the heat production of the human body is practically in equilibrium with the heat loss, discomfort is nevertheless felt if about 25% of the skin is moistured by perspiration.

Comfort is felt if the heat insulation and the water vapour permeability agree with the key values in Table 27.3, which are based on experience. Since the ratios of the heat and water vapour permeability coefficients do not differ much, it suffices to assess one of them.

27.3.2. Mechanical comfort

A distinction may be made between:

- a. Comfort in the sense that there is no tight fitting: the garment shows a reversible stretch corresponding to the *movements* of the body
- b. Comfort derived from ready adaptation to the *shape* of the body; here the *resilience* of the fabric is important

The *cloth elasticity*, determined by the fabric construction, is the principal factor. Knitted fabrics may have a recoverable stretch of 200–300%, while woven fabrics cannot have more than about 25%.

The *yarn elasticity* plays a *minor* role, unless the elasticity of the yarn is very low or very high (high-elastic false twist yarns, elastomeric yarns).

27.3.3. Shape retention

Shape retention is a factor in almost all articles made from polymeric materials (cf. warping of plastic articles, deformation of films, etc.). In textiles the lack of shape retention is reflected in the sagging of curtains, the bagging of trousers, etc. Shape retention is determined by the viscoelastic properties of the polymer, especially under the influence of moisture: plastic deformation and creep are highly undesirable, whereas resilience is favourable.

Special forms of shape retention are wrinkle recovery and pleat and crease retention.

27.3.3.1. Wrinkle recovery (wrinkle fastness)

By wrinkling is understood any fabric deformation resulting from the formation of folds that is not immediately and completely reversible.

The wrinkling behaviour of textile fabrics is determined not only by factors such as cloth construction, yarn construction, yarn fineness, friction, but also by the viscoelastic behaviour of the yarn (Rawling et al., 1956; Van der Meer, 1970). As a result, wrinkling is dependent on humidity, temperature and load. On the basis of results obtained with many different textile materials we may assume that the wrinkling of textile fabrics is much worse within "transition" ranges than beyond these ranges. A purely amorphous polymer has a transition range around the glass transition temperature (T_g). In highly crystalline polymers we find such a range around the crystalline melting point (melt transition). Partly crystalline polymers (i.e. nearly all the polymers used for textiles) have transition ranges both around the T_g and the T_m .

The properties of yarns made from partly crystalline polymers are dependent, among other factors, on the degree of crystallisation and the nature of the crystalline ranges. As a result, measurements on model yarns, etc., of factors such as T_g , T_m and loss factor as a function of temperature, are not nearly sufficient to serve as a basis for making predictions concerning the wrinkling of textiles. However, it seems likely that for a good wrinkling behaviour the transition ranges of the material must lie outside the range of temperatures to which it is subjected during use, i.e. roughly outside the temperature range of 0–100 °C. For a polymer this means a T_g in water above 100 °C or a T_g in air below 0 °C. In pressing and ironing, when we do want clear, irreversible deformations (smoothing, sharp creases or pleats), a transition range will have to be passed, and the treatment will have to take place as much as possible within a dispersion range. For polymers with a high T_g the transition range around T_g can be used. For hydrophilic materials this range can be shifted to lower temperatures by means of water (ironing of cotton, wool, rayon, using steam). If the amorphous material is in the rubbery state, excessive shrinking or sticking occurs in the transition range around the T_g . Ironing and pressing of these materials is impossible or very critical. For partly crystalline material with a low T_g (below 0 °C), ironing and pressing will have to be carried out in the transition range around the crystalline melting point. This, too, may be risky.

It seems probable that information on wrinkling can be obtained not only from the *loss factor* but also from the curve of the *modulus of elasticity as a function of temperature in air and water*. In this connection it has to be ascertained whether the deformation in wrinkling is imposed or determined by the load. If the latter is true, the modulus of elasticity will be an important parameter.

27.3.3.2. Pleat and crease retention

Pleat and crease retention may be defined as the spontaneous reversal to the original state of a purposely made pleat or crease after it has temporarily faded through wear or washing. This property very much resembles that of wrinkle recovery, both having in common that there is always a return to a specially imposed shape, whether flat or pleated. The pleat is made under conditions in which the material is soft, that is at an elevated temperature and – if desired – in the presence of water or steam. Subsequent crystallisation of the fibre will then restore the desired shape, which is so fixed that it is very difficult to remove at a lower temperature, or even in water. Only during use, for instance during washing, if the temperature rises to above the softening temperature (in water!) will the pleat more or less disappear, depending on the degree of deformation imposed and on the duration.

It may be concluded that shape retention, wrinkle recovery and pleat and crease retention depend on well-known viscoelastic properties: the existence of a transition range, stress relaxation, creep and permanent deformation, and a possible resilience by a change in external conditions.

27.3.4. Retention of surface appearance

The degradation of surface appearance is generally connected with wear, but in the case of textiles it has also secondary effects like "fluffing" and "pilling". In *plastics* the surface appearance is mainly determined by scratching. *Scratch hardness* is the main parameter. In textiles the coefficient of friction is the main factor.

27.3.4.1. Resistance to wear

Loss by wear is dependent on the coefficient of friction, the stiffness, the resilience and the degree of brittleness. In order to assess the resistance to wear it has to be ascertained whether this property is in equilibrium with other properties, e.g. colour fastness and shape retention. If the durability is determined by the resistance to wear, the aesthetic and use properties must remain virtually constant during the life of the product.

A high wear resistance is a special advantage if it permits a lower weight per unit product.

27.3.4.2. Fluffing and pilling

Since fluffs (or hairiness) and fibre balls (pills) have an unfavourable influence on the appearance of the fabric, their formation must be avoided. Hairiness precedes the formation of pills: whether it gives rise to pilling depends on the number and length of the protruding fibres or filament ends per unit surface area.

Among the fibre properties, the lateral strength (double loop strength) and the bending abrasion resistance are the decisive factors. But more important than the intrinsic properties are the yarn and fabric constructions. Pilling decreases with decreasing filament fineness, increasing fibre length, increasing twist, and increasing fabric density.

This whole complex of parameters is normally assessed in a pilling tester, e.g. Baird's Random Tumble Pilling Tester (Baird et al., 1956). In this test various specimens are compared with a standard by counting the pills per unit area or by determining the weight per unit area.

27.3.5. Colour fastness

A good colour fastness implies that the colour is maintained under different conditions (rubbing, washing, exposure to sunlight, seawater, etc.). Colour fastness has many aspects, but it is sufficient to mention the three main groups: *light fastness*, *wet fastness* (washing, seawater, sweat, cleaning liquids), and *heat* (sublimation) *fastness*.

Light fastness is mainly determined by the nature of polymer and dyestuff and by the interaction between the two. Additives like pigments and stabilisers (antioxidants) are important. The better the light fastness of the polymer, the greater the chance that it will have a good colour fastness.

The wet fastness is determined by the bond strength between polymer and dyestuff, and therefore by the presence of specific functional groups in the polymer.

The heat (sublimation) fastness increases with the bond strength between polymer and dyestuff and with the sublimation temperature of the dyestuff.

27.3.6. Resistance to soiling

The soiling tendency of textiles can only be determined properly by means of actual wear and wash tests.

Two factors have direct impact:

- a. The affinity of the polymer for fatty substances; this affinity is determined by the relation between the solubility parameters of polymer and soiling substance.
- b. The roughness of the yarn surface; a rough yarn surface may mechanically take up finely dispersed soil, which can hardly be removed by washing.

Static charging may play a role, since a charged surface (yarn, cloth) attracts oppositely charged dust particles.

27.3.7. Resistance to static charging

The background of static charging has been discussed in Chap. 11. In general a strongly hydrophilic material will cause no static charging, in contrast with a hydrophobic material. In the latter, static charging can be largely suppressed by antistatic agents.

27.3.8. Resistance to fatigue

Fatigue is the decay of mechanical properties after repeated application of stress and strain. Fatigue tests give information about the ability of a material to resist the development of cracks or crazes resulting from a large number of deformation cycles.

Fatigue resistance is a major factor in industrial applications of textile materials (conveyor belts, automobile tyres, etc.). The fatigue resistance depends on the viscoelastic properties (mechanical damping) of the material, but equally on the soundness of bonds between the surfaces or interfaces.

In composite materials, such as tyres (reinforced with tensile canvas) and other reinforced materials, the adhesion between the two phases is of prime importance: poor adhesion may induce fatigue failure.

The main variable in the fatigue test is the *fatigue life* as a function of the total number of cycles. Generally, the fatigue life is reduced by an increase of temperature. Therefore mechanical damping is so important: high damping may raise the temperature. In polymers of which the strength decreases rapidly with increasing temperature, high damping may be largely responsible for fatigue failure.

27.4. MAINTENANCE OR CARE PROPERTIES

This aspect will only be briefly discussed. The general correlations are shown in Table 27.4. The main properties in the category are:

27.4.1. Washability

- a. *Resistance to washing*. This is measured by the loss of strength after 10, 20 or 50 washes. Mechanical dispersion (transition) regions and environmental degradation are important.
- b. *Clean ability by washing*. Cleanability may be defined as the degree to which dirt and stains can be removed. This property is dependent on the *nature of the polymer* and that of the dirt, and on the detergent used (surface energy); furthermore it is determined by the geometrical structure of the fabric and the yarn construction. It is clear that also the washing method and the temperature have a great influence.

TABLE 27.4 General correlation of maintenance properties with intrinsic and added properties

Intrinsic/added properties	Maintenance properties					
	Washability	Quick drying	Wrinkle – free drying	Shrinkage	Pressability	Suitability for dry cleaning
<i>Intrinsic properties</i>						
Chemical structure	×	×	×			×
Physical morphology					×	×
Transition regions	×		×			×
Moisture absorption		××	×	×		
Light fastness	×					
Thermal stability					×	
Solubility parameter	×					××
Surface energy	××					
Stress relaxation	×		×		×	
Creep	×		×	×	×	
Elastic recovery	×					
Torsion relaxation			×		×	
Bending modulus			×		×	
<i>Added properties</i>						
Yarn construction	××	×	×	××	×	
Fabric construction	××	×	×	××		×
Heat treatment (finish)	×		×	××		

× = statistically significant; ×× = (very) important.

- c. *Shrinkage resistance during washing.* This property, which is mainly dependent on the chemical structure of the polymer, has long been in the centre of attention. Interest has somewhat diminished following the development of anti-shrink finish treatments and stabilisation. The distance between washing temperature and glass rubber transition temperature has a great effect on the property.

27.4.2. Dryability

- a. *Quick drying.* The rate of drying is determined by the cloth construction, the swelling value of the fibre (on moisture uptake), and the bulkiness of the yarn.
- b. *Wrinkle-free drying.* Shape retention in the washing process is an adequate expression for this property. It has already been discussed under Sect. 27.3.

27.4.3. Pressability (Ironability)

The ease of ironing (pressing) depends on the relative positions of glass transition temperature and heat distortion or decomposition temperature. Also the influence of moisture on T_f is very important.

27.4.4. Suitability for dry-cleaning

This property is closely connected with the solubility parameters of polymer and dry-cleaning agent. Furthermore the dry-cleaning temperature should be outside a mechanical dispersion (transition) region of the polymer, since otherwise deformation may occur.

27.5. INTEGRAL EVALUATION OF FIBRE POLYMERS, FIBRES AND YARNS BY THE CRITERIA MENTIONED (PROFILE METHOD)

The potential market for a polymer is primarily determined by its suitability for application in various fields. For a simple and rapid study of this qualitative aspect a selection method was developed which is referred to as *the profile method*. This method compares the properties required for the end product with those of the starting materials.

The *qualitative demands* made on the end product can be established by a study of consumer requirements. In an ideal situation the degree of importance would have to be established quantitatively, for instance as the *d-function* (desirability). By means of such a d-function the importance of the various properties can be measured and, consequently, also the influence of a change in one of the properties on the overall desirability. For practical reasons (practicability, time) the requirements to be satisfied by the end product in various applications usually are not indicated as d-functions, but are simple *rated* as *unimportant*, *important* and *very important*. This procedure is based on the results of consumer studies and gives the *desirability profile for the application*. Also the article properties obtained by suitable processing form a profile, viz. the product profile.

The article properties are rated by experts, partly on the basis of quantitative measurements of intrinsic properties, partly on the basis of their experience.

By *comparison of the product profile with the desirability profile*, the strong and weak points of the product are immediately visible. By comparison of a starting material with materials that have already penetrated into a particular end use, the product's chances of capturing a market share by its qualitative aspects can be assessed.

Although the system is not perfect, it has been found to provide useful indications about the question in what applications the properties of some starting material are used to the best advantage and whether this starting material stands a chance in competition with other starting materials.

In Fig. 27.1 an example is given of the position of wool and textured polyester in a well-defined application: sweaters. Almost the only points in favour of wool are its appearance and comfort; textured polyester does not score such high marks in these properties, but its care properties are considerably better than those of wool.

Textured polyester has mainly penetrated into a consumer category where, in addition to appearance, special value is attached to ease of care properties (middle price class).

Woollen articles are particularly dominant in the higher price bracket, where greater demands are made on the appearance; the ease of care properties only play a minor role (dry-cleaning instead of domestic laundering).

The wool industry has introduced a system of attaching the wool market exclusively to shrink-free and washable woollen sweaters. By the special treatment carried out to realise these properties it has been possible to reduce one of the greatest disadvantages of wool relative to synthetic fibres: its lack of shrink fastness.

In the same way any product may be rated for a specific end use of which the desirability profile can be designed.

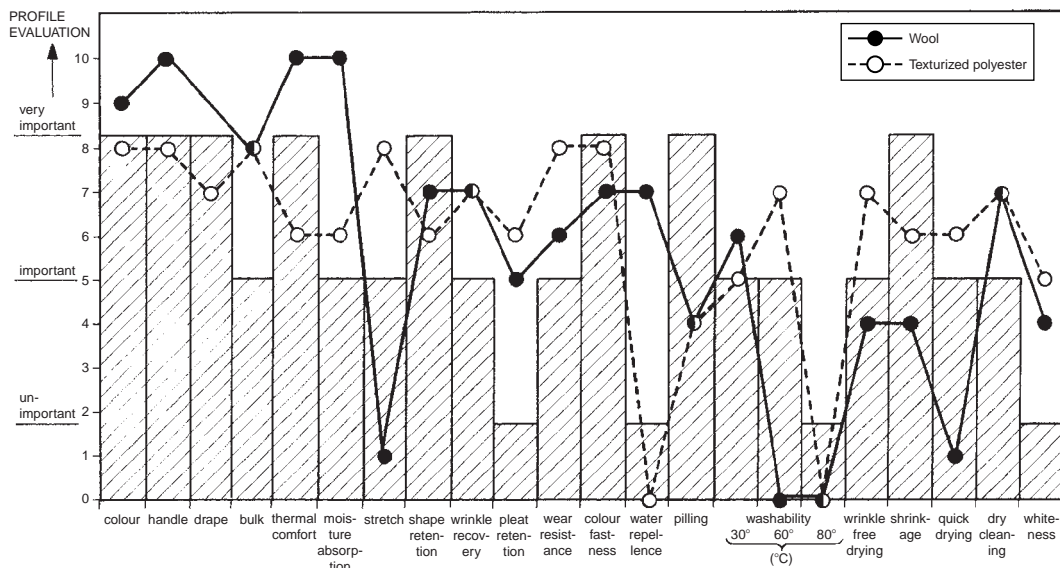


FIG. 27.1 Desirability profile (blocks) for a certain application (sweaters) compared with the product profile (lines) of wool and polyester.

BIBLIOGRAPHY

General references

- Cook JG, "Handbook of Textile Fibers", 2 Vols, Watford, Harrow, 5th Ed, 1984.
 "Encyclopedia of Textiles", Prentice-Hall, Inc., Englewood Cliffs, New Jersey, 1960.
 Fourt L and Hollies NRS, "Clothing, Comfort and Function", Marcel Dekker, New York, 1970.
 Happie F (Ed), "Applied Fibre Science", 3 Vols, Academic Press, London, 1978.
 Hearle JWS, Grosberg P and Backer S, "Structural Mechanics of Fibers, Yarns and Fabrics", Wiley Interscience, New York, 1969.
 Kaswell ER, "Textile Fibers, Yarns and Fabrics", Reinhold Publishers Corp, New York, 1953.
 Lewin M and Sello SB (Eds), "Handbook of Fiber Science and Technology", Marcel Dekker, New York, 1983–1984.
 Mark HF, Atlas SM and Cernia E (Eds), "Man-made Fibers; Science and Technology", 3 Vols, Interscience, New York, 1967.
 Moncrieff RW, "Man-made Fibres", Heywood Books, London, 5th Ed, 1970.
 Renbourn ET, "Materials and Clothing in Health and Disease", HK Lewis & Co, London, 1972.

Special references

- Baird EM, Legere LE and Stanley HE, Text Res J 26 (1956) 731.
 Howorth WS, J Textile Inst 55 (1964) T 251.
 Howorth WS and Oliver PH, J Textile Inst 49 (1958) T 540.
 Rawling GD, Stanley HE and Wilkinson PR, Text Res J 26 (1956) 974.
 Tippets EA, Text Res J 37 (1967) 527.
 Van der Meer SJ, "Dynamic Mechanical Properties and Permanent Deformation of Yarns, Cords and Fabrics", PhD Thesis, Delft University of Technology, 1970.

This page intentionally left blank

PART **VII**

COMPREHENSIVE TABLES

*"Facts and theories are different things,
Not rungs in a hierarchy of increasing certainty.*

Facts are the world's data.

Theories are structures of ideas that explain and interpret facts.

Facts do not go away

When scientists debate rival theories to explain them."

Stephen Jay Gould, 1941–2002

This page intentionally left blank

TABLE I International system of units (SI)

1. Basic SI units					
Physical quantity		Unit		Symbol	
Length		Meter		m	
Mass		Kilogram		kg	
Time		Second		s	
Plane angle		Radian		rad	
Solid angle		Steradian		sr	
Electric current		Ampere		A	
Thermodynamic temperature		Kelvin		K	
Amount of substance		Mole		mol	
Luminous intensity		Candela		cd	

2. Decimal fractions and multiples					
Fraction	Prefix	Symbol	Multiple	Prefix	Symbol
10^{-1}	deci	d	10	deca	da
10^{-2}	centi	c	10^2	hecto	h
10^{-3}	milli	m	10^3	kilo	k
10^{-6}	micro	μ	10^6	mega	M
10^{-9}	nano	n	10^9	giga	G
10^{-12}	pico	p	10^{12}	tera	T
10^{-15}	femto	f	10^{15}	peta	P
10^{-18}	atto	a	10^{18}	exa	E

3. Derived SI units (examples)		
Physical quantity	Unit	Definition
Area (surface)	Square meter	m^2
Volume	Cubic meter	m^3
Velocity	Meter per second	$m\ s^{-1}$
Angular velocity	Radian per second	$rad\ s^{-1}$
Acceleration	Meter per square second	$m\ s^{-2}$
Wave number	Reciprocal meter	m^{-1}
Density	Kilogram per cubic meter	$kg\ m^{-3}$
Mass concentration	Kilogram per cubic meter	$kg\ m^{-3}$
Molar concentration	Mol per cubic meter	$mol\ m^{-3}$
Intensity of electric current	Ampere per square meter	$A\ m^{-2}$
Luminance	Candela per square meter	$cd\ m^{-2}$

N.B. $kg\ m^{-3}$ may be written as kg/m^3 , etc.

(continued)

TABLE I (*continued*)

3a. Derived SI units with special names and symbols, common derived units			
Physical quantity	Unit	Symbol	Definition
Frequency	Hertz	Hz	s^{-1}
Energy	Joule	J	$kg\ m^2\ s^{-2}$
Force	Newton	N	$kg\ m\ s^{-2} = J\ m^{-1}$
Pressure	Pascal	Pa	$kg\ m^{-1}\ s^{-2} = N\ m^{-2}$
Power	Watt	W	$kg\ m^{-2}\ s^{-3} = J\ s^{-1}$
Electric charge	Coulomb	C	A s
Electric potential difference	Volt	V	$kg\ m^2\ s^{-3}\ A^{-1} = J\ A^{-1}\ s^{-1}$
Electric resistance	Ohm	Ω	$kg\ m^2\ s^{-3}\ A^{-2} = V\ A^{-1}$
Electric conductance	Siemens	S	$kg^{-1}\ m^{-2}\ s^3\ A^2 = \Omega^{-1}$
Electric capacitance	Farad	F	$A^2\ s^4\ kg^{-1}\ m^{-2} = A\ s\ V^{-1}$
Magnetic flux	Weber	Wb	$kg\ m^2\ s^{-2}\ A^{-1} = V\ s$
Inductance	Henry	H	$Wb\ A^{-1} = kg\ m^2\ s^{-2}\ A^{-2}$ $= V\ A^{-1}\ s$
Magnetic flux density (magnetic induction) (magnetic field)	Tesla	T	$kg\ s^{-2}\ A^{-1} = V\ s\ m^{-2}$

3b. Derived SI units formed by combination of (1) and (3a) (examples)		
Physical quantity	Unit	Definition
Moment of force	Newton meter	$N\ m$
Surface tension	Newton per meter	$N\ m^{-1}$
Dynamic viscosity	Newton second per square meter	$N\ s\ m^{-2}$
Thermal conductivity	Watt per meter per kelvin	$W\ m^{-1}\ K^{-1}$
Molar energy	Joule per mol	$J\ mol^{-1}$
Electric field strength	Volt per meter	$V\ m^{-1}$

TABLE II Survey of conversion factors

Quantity		Expressed in (units)		Multiplication factor	Expressed in S.I.
Name	Symbol	Name	Symbol		
<i>1. Space and time</i>					
Length or	l, L	Kilometer	km	10^3	m
Width	b	Centimeter	cm	10^{-2}	
Height	h	Millimeter	mm	10^{-3}	
Thickness	d, δ	Micron	μm	10^{-6}	
Radius	r	Nanometer	nm	10^{-9}	
Diameter	$d(D)$	Ångstrom	Å	10^{-10}	
Path length	s	Inch	in	0.0254	
Wavelength	λ	Foot	ft	0.3048	
		Yard	yd	0.9144	
		Mile	mile	1.609×10^3	
		Nautical mile	n mile	1.852×10^3	
		Astronomical unit		1.496×10^{11}	
		Fathom		1.829	
		League (British nautical)		5.559×10^3	
		League (statute)		4.828×10^3	
		Light year		9.461×10^{15}	
		Rod		5.029	
		Mil		2.54×10^{-5}	
Area (surface)	$A, (S)$	Hectare	ha	10^4	m^2
		Are	a	10^2	
		Square centimeter	cm^2	10^{-4}	
		Square millimeter	mm^2	10^{-6}	
		Square Ångstrom	\AA^2	10^{-20}	
		Square inch	in^2	0.645×10^{-3}	
		Square foot	ft^2	9.29×10^{-2}	
		Square yard	yd^2	0.836	
		Acre	acre	4.047×10^3	
		Square mile	mile^2	2.590×10^6	
		Barn		1.0×10^{-28}	

(continued)

TABLE II (continued)

Quantity		Expressed in (units)			Multiplication factor	Expressed in S.I.
Name	Symbol	Name	Symbol			
Volume	V	Cubic decimeter	dm^3	10^{-3}	10^{-3}	m^3
		Cubic centimeter	cm^3	10^{-6}		
		Liter	l	10^{-3}		
		Deciliter	dl	10^{-4}		
		Milliliter	ml	10^{-6}		
		Cubic inch	in^3	1.639×10^{-5}		2.832×10^{-2}
		Cubic foot	ft^3	1.639×10^{-5}		
		Cubic yard	yd^3	0.765		
		Barrel (US)	barrel	0.159		
		Gallon (US)	gal (US)	3.785×10^{-3}		
		Gallon (UK)	gal (UK)	4.546×10^{-3}		
		Bushel		3.524×10^{-2}		
		Dram (U.S. fluid)		3.697×10^{-6}		
		Gill (U.S.)		1.183×10^{-4}		
		Peck (U.S.)		8.810×10^{-3}		
		Pint (U.S. dry)		5.506×10^{-4}		
		Pint (U.S. liquid)		4.732×10^{-4}		
		Quart (U.S. dry)		1.101×10^{-3}		
		Quart (U.S. liquid)		9.464×10^{-4}		
Angle	$\alpha, \beta, \delta, \theta, \varphi$	Radian	rad	1	1.745×10^{-2}	rad
		Degree ($= 2\pi/360$ rad)	1°	1.745×10^{-2}		
		Minute ($= 1/60^\circ$)	$1'$	2.91×10^{-4}		
		Second ($= 1/60'$)	$1''$	4.85×10^{-6}		
Time	t, τ, θ	Year	a	3.16×10^7	3.16×10^7	s
		Month	month	2.63×10^6		
		Day	d	8.64×10^4		
		Hour	h	3.6×10^3		
		Minute	min	0.6×10^2		

Frequency	$v, \omega (=2\pi v)$	Cycles per minute Cycles per hour	c/min c/h	0.6×10^2 3.6×10^3	$\text{Hz} = \text{s}^{-1}$ (hertz)
Velocity	$v(u)$	Kilometers per hour Foot per minute Foot per second Mile per hour Knot	km/h ft/min ft/s mile/h kn	0.278 5.08×10^{-3} 0.3048 0.4470 0.514	m/s
Volumetric flow (rate) density	v	Cub foot per square foot sec = foot per second	$\text{ft}^3/(\text{ft}^2 \text{ s}) = \text{ft/s}$	0.3048	m/s
Acceleration	a, g	Foot per square second Gal (Galileo)	ft/s^2	0.3048, 1.0×10^{-2}	m/s^2
Volumetric flow rate	Φ	Liter per second Liter per minute Cubic meter per minute Cubic meter per hour Cubic foot per second Cubic foot per hour Cubic foot per minute Barrel (US) per day Gallon (US) per minute Gallon (UK) per minute	l/s l/min m^3/min m^3/h ft^3/s ft^3/h cfm barrel/d gal (US)/min gal (UK)/min	10^{-3} 1.667×10^{-5} 1.667×10^{-2} 0.2778×10^{-3} 2.832×10^{-2} 7.87×10^{-6} 4.72×10^{-4} 1.840×10^{-6} 6.31×10^{-5} 7.58×10^{-5}	m^3/s
2. Mechanics					
Mass	m	Ton Gram Milligram Microgram Carat Grain	t g mg μg CD gr	10^3 10^{-3} 10^{-6} 10^{-9} 2×10^{-4} 6.48×10^{-5}	kg

(continued)

TABLE II (continued)

Quantity		Expressed in (units)		Multiplication factor	Expressed in S.I.
Name	Symbol	Name	Symbol		
		Ounce (avoirdupois)	oz	2.83×10^{-2}	
		Pound (avoirdupois)	lb	0.4536	
		Stone	st	6.35	
		Slug	slug	14.5939	
		Hundred weight (UK)	cwt	50.8	
		Short hundred weight	sh cwt	45.36	
		Short ton (US)	sh tn	0.907×10^3	
		Long ton (UK)	ton	1.016×10^3	
		Dram (apothecaries)		3.888×10^{-3}	kg
		Dram (avoirdupois)		1.772×10^{-3}	
		Ounce (troy)		3.110×10^{-2}	
		Pound (troy)		0.3732	
		Pennyweight		1.555×10^{-3}	
		Quintal		1.0×10^2	
Density (mass density) ρ		Gram per cubic centimeter	g/cm ³	10^3	kg/m ³
		Grain per cubic foot	gr/ft ³	2.288×10^{-3}	
		Pound per cubic foot	lb/ft ³	16.02	
		Pound per cubic inch	lb/in ³	2.768×10^4	
		Pound per gallon (US)	lb/gal	0.120×10^3	
Specific volume	$v = 1/\rho$	Cubic centimeter per gram	cm ³ /g	10^{-3}	m ³ /kg
		Cubic foot per pound	ft ³ /lb	6.24×10^{-2}	
Fineness (linear density of yarns and fibres)	Td	Denier	den = g/9 km	0.111	tex =
		Tex	tex = g/km	1	10^{-6} kg/m
		Decitex	dtex = g/10 km	0.1	
Mass flow rate (production capacity)	Φ_m	Kilogram per hour	kg/h	2.778×10^{-4}	kg/s
		Ton per day	t/d	1.157×10^{-2}	
		Ton per month	t/mth	3.79×10^{-4}	

		Ton per year	t/a	3.17×10^{-5}	kg/s
		Pound per minute	lb/min	7.56×10^{-3}	
		Short ton per day	shtn/d	1.050×10^{-2}	
		(long) Ton per day	ton/d	1.176×10^{-2}	
Mass flow density	φ_m	Kilogram per sq meter p. h	kg/(m ² h)	2.778×10^{-4}	kg/(m ² s)
		Pound per square foot p. min	lb/(ft ² min)	8.14×10^{-2}	
Force or weight	$F (W)(P)$	Dyne	dyn (=g cm/s ²)	10^{-5}	N (newton)
		Gram-force	gf	9.81×10^{-3}	(= kg m/s ²)
		Kilogram-force	kgf	9.81	
		Ton-force	tf	9.81×10^3	
		Poundal	pdl	0.1383	
		Pound force	lbf	4.448	
		Kip	kip (klb)	4.448×10^3	
		Impact strength (Izod, notched)	ft lbs/in	53.4	J/m = N
Specific weight (force per unit volume)	γ	Gram-force per cubic cm	gf/cm ³	9.81×10^3	N/m ²
		Pound-force per cubic foot	lbf/ft ³	157.1	
Moment of force or bending moment; torque moment of a couple	$M (S)$	Dyne centimeter	dyn cm	10^{-7}	N m
		Kilogram force meter	kgf m	9.81	(N m = J)
		Foot poundal	ft pdl	4.214×10^{-2}	
		Pound-force foot	lbf ft	1.356	
Moment of inertia	I	Gram square centimeter	g cm ²	10^{-7}	kg m ²
		Pound foot squared	lb ft ²	4.214×10^{-2}	
Second moment of area	(axial) I_a (polar) I_p	Inch to the fourth	in ⁴	4.162×10^{-7}	m ⁴
Section modulus (moment of resistance)	$Z(W)$	Inch cubed	in ³	1.639×10^{-5}	m ³

(continued)

TABLE II (continued)

Quantity		Expressed in (units)		Multiplication factor	Expressed in S.I.
Name	Symbol	Name	Symbol		
Force per unit surface		Dyne per square centimeter	dyn/cm ²	10 ⁻¹	N/m ² = Pa (pascal)
Pressure	<i>p</i>	Kilogram-force per sq. meter	kgf/m ²	9.81	
Normal stress	σ	Technical atmosphere	at	9.81 × 10 ⁴	
Shear stress	σ_{sh}	Atmosphere	atm	1.013 × 10 ⁵	(N/m ² = J/m ³ = Pa)
Modulus		Kilogram-force per sq. mm	kgf/mm ²	9.81 × 10 ⁶	N/m ² = Pa
Young's or elasticity modulus	<i>E</i>	Millimeter mercury (torr)	mmHg (torr)	133.3	
Rigidity or shear modulus	<i>G</i>	Millimeter water	mmH ₂ O	9.81	
Bulk modulus or compression modulus	<i>K, B</i>	Bar (= 10 ⁶ dyn/cm ²)	bar	10 ⁵	
		Poundal per square foot	pdl/ft ²	1.488	
		Pound-force per square foot	lbf/ ft ²	47.88	
		Pound-force per square inch	lbf/ m ²	6.894 × 10 ³	
		Inch of water	in H ₂ O	2.491 × 10 ²	
		Foot of water	ft H ₂ O	2.989 × 10 ³	
		Inch of mercury	in Hg	3.386 × 10 ³	
Specific strength of yarns and fibres		Gram-force per denier	gf/den	0.0883	N/tex
		Rupture kilometer	Rkm	0.981 × 10 ⁻²	
		Centi-newton per tex	cN/tex	10 ⁻²	
		Gram-force per tex	gf/tex	0.981 × 10 ⁻²	
		Gram-force per decitex	gf/dtex	0.0981	
Tensile stress in yarns and fibres	σ	Newton per tex	N/tex	10 ⁶ ρ	N/m ²
		Gram-force per tex	gf/tex	0.981 × 10 ⁴ ρ	(ρ = density in kg/m ³)
		Gram-force per denier	gf/den	0.883 × 10 ⁵ ρ	
Stiffness factor		Kilogram-force centimeter squared	kgf cm ²	9.81 × 10 ⁻⁴	N m ²

Surface tension	γ, σ	Dyne per centimeter Pound-force per foot	dyn/cm lbf/ft	10^{-3} 14.59	N/m (N/m = J/m ²)
Viscosity (dynamic)	η	Poise Centipoise Kilogram-force sec per sq. meter Kilogram-force hour per sq. meter Poundal second per sq. foot Pound-force sec per sq. foot Pound-force sec per sq. inch	$P = \text{dyn s}/\text{cm}^2$ cP kgf s/m ² kgf h/m ² pdl s/ft ² lbf s/ft ² lbf s/in ²	10^{-1} 10^{-3} 9.81 3.531×10^4 1.488 47.88 6.90×10^3	N s/m ²
Kinematic viscosity	ν	Square centimeter per second	cm ² /s	10^{-4}	m ² /s
Diffusion coefficient	D	Square meter per hour	m ² /h	2.778×10^{-4}	
Thermal diffusivity	a	Stokes Centistokes Square inch per second Square foot per second	S = cm ² /s cS = cm ² /100 s in ² /s ft ² s	10^{-4} 10^{-6} 0.645×10^{-3} 9.29×10^{-2}	
Energy or Work	E W, A	Erg (= dyne cm) Kilogram-force meter	dyn cm kgf m	10^{-7} 9.81	J (Joule)
Potential energy	E_p	Foot poundal	ft pdl	4.21×10^{-2}	(J = Nm)
Kinetic energy	E_k	Foot pound-force Liter atmosphere Cubic foot atmosphere Horse power hour Kilowatt hour Kilocalorie Calorie British thermal unit Electron volt	ft lbf 1 atm ft ³ atm hph kWh kcal cal Btu eV	1.356 1.013×10^2 2.869×10^3 2.685×10^6 3.60×10^6 4.19×10^3 4.19 1.055×10^3 1.602×10^{-19}	= W s)
Power	P	Erg per second Kilogram-force meter per sec Horse power (UK) Horse power (metric) Foot pound-force per second Foot poundal per second	erg/s kgf. m/s hp hp ft lbf/s ft pdl/s	10^{-7} 9.81 7.46×10^2 7.36×10^2 1.356 4.214×10^{-2}	W (watt) (W = J/s)

(continued)

TABLE II (continued)

Quantity		Expressed in (units)		Multiplication factor	Expressed in S.I.
Name	Symbol	Name	Symbol		
<i>3. General thermodynamics</i>					
Temperature	T	Degree centigrade	$^{\circ}\text{C} = \text{K} - 273.15$	1	K
		Degree fahrenheit	$^{\circ}\text{F} = 1.8\text{K} - 459.67$	0.55555	(kelvin)
Energy or Heat quantity	E Q	Erg (= dyne. cm) Liter atmosphere	dyn cm 1 atm	10^{-7} 1.013×10^2	J (joule)
Internal energy	U	Cubic foot atmosphere	ft ³ atm	2.869×10^2	(J = Nm)
Enthalpy	H	Calorie	cal	4.19	= W s)
Free energy	F	Kilocalorie	kcal	4.19×10^3	
Free enthalpy	G	British thermal unit	Btu	1.055×10^3	
Latent heat	L	Therm	Btu $\times 10^5$	1.055×10^8	
Specific energy					
Sp. internal energy	u	Calorie per gram	cal/g	4.19×10^3	J/kg
Specific enthalpy	h	Br. therm. unit per pound	Btu/1b	2.326×10^3	
Sp. free energy	f				
Sp. free enthalpy	g				
Sp. latent heat	l				
Heat capacity	C	Kilocalorie per $^{\circ}\text{C}$	kcal/ $^{\circ}\text{C}$	4.19×10^3	J/K
Entropy	S	Calorie per $^{\circ}\text{C}$	cal/ $^{\circ}\text{C}$	4.19	
		Br. therm. Unit p. degree			
		Fahrenheit	Btu/ $^{\circ}\text{F}$	1.90×10^3	
Specific heat capacity	c	Calorie p. gram degree Centigrade	cal/(g $^{\circ}\text{C}$)	4.19×10^3	J/(kg K)
Specific entropy	s	Brit. therm. unit per pound degree	Btu/(1b $^{\circ}\text{F}$)	4.19×10^3	
		Fahrenheit			

Heat flow (power)	Φ_h	Erg per second	erg/s	10^{-7}	W
		Kilocalorie per hour	kcal/h	1.163	(watt)
		Calorie per second	cal/s	4.19	(W = J/s)
		Br. therm. unit per second	Btu/s	1.055×10^3	
		Br. therm. unit per hour	Btu/h	0.293	
Heat flow density	φ_h	Calorie p. sq. centimeter p. sec	cal/(cm ² s)	4.19×10^4	W/m ²
		Kilocalorie p. sq meter p. hour	kcal/(m ² h)	1.163	
		Brit. therm. unit p. sq. foot sec	Btu/(ft ² s)	1.136×10^4	
		Brit. therm. unit p. sq. foot hour	Btu/(ft ² h)	3.16	
Thermal conductivity	$\lambda (k)$	Calorie per centimeter second degree Centigrade	cal/(cm s °C)	4.19×10^2	J/(m s)
		Kilocalorie per meter hour degree Centigrade	kcal/(m h °C)	1.163	= W/(m K)
		British thermal unit per hour foot degree Fahrenheit	Btu/(ft h °F)	1.73	
		British thermal unit inch per hour square foot degree F	Btu in/(ft ² h °F)	0.144	
		British thermal unit per second square foot degree F	Btu/(ft s °F)	6.23×10^3	
Overall coefficient of heat transfer	U, K	Calorie per square centimeter second degree Centigrade	cal/(cm ² s °C)	4.19×10^4	J/(m ² s K)= W/(m ² K)
Heat transfer coefficient	h	Kilocalorie per square meter hour degree Centigrade	kcal/(m ² s °C)	1.163	
		British thermal unit per hour square foot degree Fahrenheit	Btu/(ft ² h °F)	5.68	
		British thermal unit per second square foot degree F	Btu/(ft ² s °F)	2.044×10^4	
Concentration	c	Gram per liter	g/l	1	kg/m ³
		Gram per deciliter	g/dl	10	
		Gram per cubic centimeter	g/cm ³	10^3	
		Grain per cubic foot	gr/ft ³	0.2288×10^{-2}	
		Pound per cubic foot	lb/ft ³	16.02	

(continued)

TABLE II (continued)

Quantity		Expressed in (units)		Multiplication factor	Expressed in S.I.
Name	Symbol	Name	Symbol		
<i>4. Chemical thermodynamics</i>					
Amount of substance	<i>n</i>	Grammole	mol	1	mol
Concentration	<i>c</i>	Molarity	mol/l	10^3	mol/m ³
		–	mol/100 g solvent	10	mol/kg solvent
		Molality	mol/1000 g solvent	1	mol/kg solvent
Molecular energy	(E)	Calorie per mole	cal/mol	4.19	J/mol
		Electron volt per molecule	eV/molecule	0.965×10^5	
		Erg per molecule	erg/molecule	6.022×10^{16}	
		Wave number	cm ⁻¹	11.96	
Molecular entropy	(S)	Calorie per (mol.K)	(Thomson)	4.184	J/(mol K) = Cl (Clausius)
<i>5. Optics</i>					
Stress optical coefficient	<i>C</i>	Brewster	$\equiv 10^{-13} \text{ cm}^2/\text{dyne}$	10^{-12}	m ² /N
Hydrogen bonding number	<i>Δv</i>	Gordy \equiv shift of 10 wave numbers in spectroscopic OD absorption band			
<i>6. Electricity and magnetism</i>					
Electric current (flow rate)	<i>I</i> (<i>i</i>)	Electrostatic cgs unit	cm ^{3/2} g ^{1/2} /s ²	3.333×10^{-10}	A (ampere)
		Electromagnetic cgs unit	cm ^{1/2} g ^{1/2} /s	10	
Quantity of electricity (Electric charge)	<i>Q</i> (<i>e</i>)	Electrostatic cgs unit	cm ^{3/2} g ^{1/2} /s	3.333×10^{-10}	C (coulomb)
		Electromagnetic cgs unit	cm ^{1/2} g ^{1/2}	10	= A s
Electric field strength	<i>F</i> (<i>E</i>)	Electrostatic cgs unit	g ^{1/2} /(cm ^{1/2} s)	3.00×10^4	V/m =
		Electromagnetic cgs unit	cm ^{1/2} g ^{1/2} /s ²	10^{-6}	N/(A s)

Potential	V	Electrostatic cgs unit	$\text{cm}^{1/2} \text{g}^{1/2}/\text{s}$	3.00×10^2	V (volt)
Electric motive force	(E)	Electromagnetic cgs unit	$\text{cm}^{3/2} \text{g}^{1/2}/\text{s}^2$	10^{-8}	= N m/(A s)
Resistance	R	Electrostatic cgs unit	s/cm	9.00×10^{11}	Ω (ohm)
		Electromagnetic cgs unit	cm/s	10^{-9}	= V/A
Specific resistance	ρ	Electromagnetic cgs unit	cm^2/s	10^{-11}	Ω m
		Ohm centimeter	$\Omega \text{ cm}$	10^{-2}	
Conductance		Electrostatic cgs unit	cm/s	0.11×10^{-11}	S (siemens)
		Electromagnetic cgs unit	s/cm	10^9	= 1/ Ω
Electric conductivity	γ	Electromagnetic cgs unit	$\text{s}/(\Omega \text{ cm})$	10^{11}	$1/(\Omega \text{ m})$
Power	P	Electromagnetic cgs unit	$\text{cm}^2 \text{g}/\text{s}^3$	10^{-7}	W (watt) = V A
Energy	E	Electromagnetic cgs unit	$\text{cm}^2 \text{g}/\text{s}^2$	10^{-7}	J (= joule) = W s
Capacitance	C	Electrostatic cgs unit	cm	1.11×10^{-12}	F (farad)
		Electromagnetic cgs unit	s^2/cm	10^9	= A s/V
Inductance	L	Electromagnetic cgs unit	cm	10^{-9}	H (henry) = V s/A
Electric displacement	D	Electrostatic cgs unit	$\text{g}^{1/2}/(\text{cm}^{1/2} \text{s})$	2.653×10^{-7}	$\text{A s}/\text{m}^2$
		Electromagnetic cgs unit	$\text{g}^{1/2}/\text{cm}^{3/2}$	7.958×10^3	= C/m ²
Electric moment	M	Electrostatic cgs unit	$\text{cm}^{5/2} \text{g}^{1/2}/\text{s}$	3.333×10^{-12}	A s m = C m
		Electromagnetic cgs unit	$\text{cm}^{3/2} \text{g}^{1/2}$	0.1000	
		Debye = 10^{-18} esu cm	$\text{cm}^{5/2} \text{g}^{1/2}/\text{s}$	3.333×10^{-30}	
Electrization		Electrostatic cgs unit	$\text{g}^{1/2}/(\text{cm}^{1/2} \text{s})$	3.333×10^{-6}	$\text{A s m}/\text{m}^3$
Electric polarizability	α	Electrostatic cgs unit	cm^3	1.11×10^{-16}	$\text{A s m}/(\text{V}/\text{m})$
Electric susceptibility	χ_e	Dimensionless number		1	number
Magnetic flux	Φ	Maxwell	$\text{cm}^{3/2} \text{g}^{1/2}/\text{s}$	10^{-8}	V s = Wb (= Weber)

(continued)

TABLE II (continued)

Quantity		Expressed in (units)		Multiplication factor	Expressed in S.I.
Name	Symbol	Name	Symbol		
Magnetic field strength	H	Oerstedt		$g^{1/2}/(cm^{1/2} s)$	$A/m = N/(V s)$
Magnetic induction	B	Gauss		$g^{1/2}/(cm^{1/2} s)$	$V s/m^2$
Magnetic moment	$\mu(\beta)$	Gauss cubic centimeter		$cm^{5/2} g^{1/2}/s$	$V s m (= Tesla)$
Magnetization	M	Gauss		$g^{1/2}/(cm^{1/2} s)$	$V s m/m^3$
Magnetic susceptibility	χ	Dimensionless number			
Hall-constant		Electromagnetic cgs unit		$cm^{5/2}/g^{1/2}$	$m^3/(A s)$
<i>7. Luminous radiation</i>					
Luminous intensity	I_v	Candela		cd	cd (= candela)
Illuminance	E_v	Lux		lx	
		Lambert		la	3.183×10^3
Luminous flux	φ_v	Lumen		lm	cd sr
Energy	Q_v	Lumen second		lm s	$lm s (\approx J)$
<i>8. X-ray radiation</i>					
Radiation dose	—	Röntgen		ro	2.58×10^{-4} C/kg
<i>9. Radioactivity</i>					
Radioactivity (desintegrations/s)	—	Becquerel		Bq	
		Curie		Ci	3.7×10^{10}
Radiation dose		Sievert		Sv	
		Rem		rem	10^{-2}
Absorbed dose		Gray		Gy	
		Rad		rd	10^{-2}

TABLE III Values of some fundamental constants

For each constant the standard deviation uncertainty in the least significant digits is given in parentheses*

Quantity	Symbol	Value
Permeability of vacuum	μ_0	$4\pi \times 10^{-7} \text{ H m}^{-1}$ (exactly)
Speed of light in vacuum	c_0	$299\,792\,458 \text{ m s}^{-1}$ (exactly)
Permittivity of vacuum	$\epsilon_0 = 1/(\mu_0 c_0^2)$	$8.854\,187\,817 \times 10^{-12} \text{ F m}^{-1}$
Planck constant	h	$6.626\,068\,96 (33) \times 10^{-34} \text{ J s}$
	$\hbar = h/(2\pi)$	$1.054\,571\,628 (53) \times 10^{-34} \text{ J s}$
Elementary charge	e	$1.602\,176\,487 (40) \times 10^{-19} \text{ C}$
Electron rest mass	m_e	$9.109\,382\,15 (45) \times 10^{-31} \text{ kg}$
Proton rest mass	m_p	$1.672\,621\,637 (83) \times 10^{-27} \text{ kg}$
Neutron rest mass	m_n	$1.674\,927\,211 (84) \times 10^{-27} \text{ kg}$
Atomic mass constant (unified atomic mass unit)	$m_u = 1 \text{ u}$	$1.660\,538\,782 (83) \times 10^{-27} \text{ kg}$
Avogadro constant	L, N_A	$6.022\,141\,79 (30) \times 10^{23} \text{ mol}^{-1}$
Boltzmann constant	k_B	$1.380\,6504 (24) \times 10^{-23} \text{ J K}^{-1}$
Molar gas constant	R	$8.314\,472 (15) \text{ J K}^{-1} \text{ mol}^{-1}$
Faraday constant	F	$9.648\,533\,99 (24) \times 10^4 \text{ C mol}^{-1}$
Zero of the Celsius scale		273.15 K (exactly)
Molar volume, ideal gas, $p = 100 \text{ kPa}, T = 273.15 \text{ K}$		$22.711\,981 (40) \text{ l mol}^{-1}$
Standard atmosphere	atm	$101,325 \text{ Pa}$ (exactly)
Fine structure constant	$\alpha = \mu_0 e^2 c / (2\hbar)$	$7.297\,352\,5376 (50) \times 10^{-3}$
	α^{-1}	$137.035\,999\,679 (94)$
Bohr radius	$a_0 = 4\pi\epsilon_0\hbar^2 / (m_e e^2)$	$5.291\,772\,0859 (36) \times 10^{-11} \text{ m}$
Hartree energy	$E_h = \hbar^2 / (m_e a_0^2)$	$4.359\,743\,94 (22) \times 10^{-18} \text{ J}$
Rydberg constant	$R_\infty = E_h / (2\hbar)$	$1.097\,373\,156\,8527 (73) \times 10^7 \text{ m}^{-1}$
Bohr magneton	$\mu_B = e\hbar / (2m_e)$	$9.274\,00915 (23) \times 10^{-24} \text{ J T}^{-1}$
Electron magnetic moment	μ_e	$9.284\,763\,77 (23) \times 10^{-24} \text{ J T}^{-1}$
Landé g factor for free electron	$g_e = 2\mu_0 / \mu_B$	$2.002\,319\,304\,3622 (15)$
Nuclear magneton	$\mu_N = (m_e / m_p)\mu_B$	$5.050\,783\,24 (13) \times 10^{-27} \text{ J T}^{-1}$
Proton magnetic moment	μ_p	$1.410\,606\,662 (37) \times 10^{-26} \text{ J T}^{-1}$
Proton magnetogyric ratio	γ_p	$2.675\,222\,099 (70) \times 10^8 \text{ s}^{-1} \text{ T}^{-1}$
Magnetic moment of protons in H_2O , μ'_p	μ_p / μ_B	$1.520\,993\,129 (17) \times 10^{-3}$
Proton resonance frequency per field in H_2O	$\gamma_p' / (2\pi)$	$42.576\,375 (13) \text{ MHz T}^{-1}$
Stefan–Boltzmann constant	$\sigma = 2\pi^5 k_B^4 / (15h^3 c^2)$	$5.670\,400 (40) \times 10^{-8} \text{ W m}^{-2} \text{ K}^{-4}$
First radiation constant	$c_1 = 2\pi hc^2$	$3.741\,771\,18 (19) \times 10^{-16} \text{ W m}^2$
Second radiation constant	$c_2 = hc / k_B$	$1.438\,7752 (25) \times 10^{-2} \text{ m K}$
Gravitational constant	G	$6.674\,28 (67) \times 10^{-11} \text{ m}^3 \text{ kg}^{-1} \text{ s}^{-2}$
Standard acceleration of free fall	g_n	$9.806\,65 \text{ m s}^{-2}$ (exactly)
<i>Accurate values of common mathematical constants</i>		
Ratio of circumference to diameter of a circle	π	$3.141\,592\,653\,59$
Base of natural logarithms	e	$2.718\,281\,828\,46$
Natural logarithm of 10	$\ln 10$	$2.302\,585\,092\,99$

*Most values from The NIST Reference on Constants and Uncertainty; The Physics Laboratory of NIST, December 2003

TABLE IV Physical constants of the most important solvents

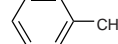
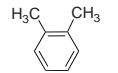
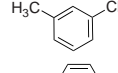
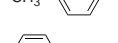
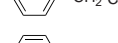
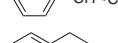
Temperature 20°C except if other value is mentioned

Name	Formula	<i>M</i>	<i>ρ</i>	<i>V</i>	<i>T_b</i>	<i>T_m</i>	<i>η</i>	<i>γ</i>	<i>n_D</i>
		g/mol	g/cm ³	cm ³ /mol	°C	°C	(25°C) mPas	10 ⁻³ N/m	
<i>Hydrocarbons</i>									
Hexane	CH ₃ –(CH ₂) ₄ –CH ₃	86.17	0.660	130.5	69	−94	0.29	18.43	1.3754
Heptane	CH ₃ –(CH ₂) ₅ –CH ₃	100.21	0.684	146.6	98	−91	0.39	20.30	1.386
Octane	CH ₃ –(CH ₂) ₆ –CH ₃	114.23	0.703	162.6	126	−57	0.51	21.14	1.396
Cyclohexane		84.16	0.779	108.0	81	7	0.90	25.5	1.4290
Benzene		78.11	0.879	88.9	80	6	0.60	28.85	1.5011
Methylbenzene (toluene)		92.13	0.867	106.3	111	−95	0.55	28.5	1.4969
1,2-Dimethylbenzene (o-xylene)		106.16	0.880	120.6	144	−27/−29	0.77	30.10	1.5055
1,3-Dimethylbenzene (m-xylene)		106.16	0.864	122.8	139	−47/−54	0.58	28.9	1.4972
1,4-Dimethylbenzene (p-xylene)		106.16	0.861	123.2	138	13	0.61	28.37	1.4958
Ethylbenzene		106.16	0.867	122.4	134–136	−93/94	0.64	29.20	1.4983
Ethenylbenzene (styrene)		104.14	0.907	114.7	146	−31	0.70	32.3	1.5434
1,2,3,4-Tetrahydronaphthalene (Tetralin)		132.20	0.870/0.971	136.1/152.0	207	−30	2.0	35.46	1.5391
Decahydronaphthalene (Decalin)		138.25	0.870/0.996	154.3/158.9	186/195	−43/−31	2.1/3.4	29.9/ 31.2	1.470/ 1.482

<i>Hydrocarbons, halogenated</i>										
Dichloromethane (methylene chloride)	CH ₂ Cl ₂	84.94	1.336	63.6	40	-97	0.42	26.52	1.4237	
Trichloromethane (chloroform)	CHCl ₃	119.39	1.499	79.7	58/62	-64	0.54	27.14	1.4464	
Tetrachloromethane (carbon tetrachloride)	CCl ₄	153.84	1.595	96.5	77	-21/-29	0.88	26.95	1.4631	
Chloroethane (ethyl chloride)	CH ₃ -CH ₂ Cl	64.52	0.88	73.3	12	-139	~0.27	~19.5	(1.3738)	
1,2-Dichloroethane (ethylene chloride)	CH ₂ Cl-CH ₂ Cl	98.97	1.257	78.7	84	-35	(0.73)	24.15	1.4443	
1,1-Dichloroethane (ethylidene chloride)	CHCl ₂ -CH ₃	98.97	1.174	84.3	57	-97	0.47	24.75	1.416	
1,1,2-Trichloroethane	CHCl ₂ -CH ₂ Cl	133.42	1.443	92.5	114	-37	0.11	33.75	1.4715	
1,1,1-Trichloroethane	CCl ₃ CH ₃	133.42	1.325	100.7	74	-31	0.80	25.56	1.4379	
1,1,2,2-Tetrachloroethane	CHCl ₂ -CHCl ₂	167.86	1.600	104.9	146	(-36)/-44	(1.75)	35.6	1.493	
1-Chloropropane (n-propyl chloride)	CH ₃ -CH ₂ -CH ₂ Cl	78.54	0.890	88.2	45/47	-123	(0.35)	21.78	1.386	
1-Chlorobutane (n-butyl chloride)	CH ₃ -(CH ₂) ₂ -CH ₂ Cl	92.57	0.884	104.7	78	-123	0.43	23.75	1.400	
Chlorobenzene		112.56	1.107	101.7	132	-45/(-55)	(0.80)	33.56	1.5248	
Bromobenzene		157.02	1.499	104.7	155/156	-31	(0.99)	36.5	1.5598	
1-Bromonaphthalene		207.07	1.488	139.2	281	0/6	4.52	44.19	1.6580	
1,1,2 Trichloro-1,2,2-trifluoroethane (freon 113)	CFCl ₂ -CF ₂ Cl	187.38	(1.564)	119.8	48	-36	(0.71)	17.75	1.3557	
<i>Ethers</i>										
Ethoxyethane (diethyl ether)	CH ₃ -CH ₂ -O-CH ₂ -CH ₃	74.12	0.714	103.9	35	-116	0.22	17.01	1.3497	
1-Propoxypropane (dipropyl ether)	C ₃ H ₇ -O-C ₃ H ₇	102.18	0.736/0.749	136.9/138.8	90	-123	(0.38)	20.53	1.3805	
2-Isopropoxypropane (diisopropyl ether)		102.17	0.726	140.7	68/69	-60/-86	0.38	17.34	1.367	

(continued)

TABLE IV (continued)

Name	Formula	ϵ	μ	$\Delta\nu$	δ	δ_d	δ_p	δ_h	δ_a	δ_v
		debye	gordy				(MJ/m ³) ^{1/2}			
<i>Hydrocarbons</i>										
Hexane	CH ₃ -(CH ₂) ₄ -CH ₃	1.89	0/0.08	0	14.8/14.9	14.8	0	0	0	14.8
Heptane	CH ₃ -(CH ₂) ₅ -CH ₃	1.92	0.0	0	15.2	15.2	0	0	0	15.2
Octane	CH ₃ -(CH ₂) ₆ -CH ₃	1.95	0	-	15.6	15.6	0	0	0	15.6
Cyclohexane		2.02	0/1.78	0	16.7	16.7	0	0	0	16.7
Benzene		2.28	0/1.56	0	18.5/18.8	17.6/18.5	1.0	2.0	2.3/6.4	17.6/18.5
Methylbenzene (toluene)		2.38	0.43	4.2/4.5	18.2/18.3	17.3/18.1	1.4	2.0	2.5/6.0	17.3/18.1
1,2-Dimethylbenzene (o-xylene)		2.57	0.44/0.62	4.5	18.4	16.8/17.6	1.0	1.0	5.3/7.4	16.9/17.7
1,3-Dimethylbenzene (m-xylene)		2.37	0.30/0.46	4.5	18.0	16.7/17.4	1.0	1.0	4.8/6.8	16.7/17.5
1,4-Dimethylbenzene (p-xylene)		2.27	0.23	4.5	17.9/18.0	16.6/17.3	1.0	1.0	4.7/6.8	16.7/17.3
Ethylbenzene		2.41	0.35/0.58	1.5/4.2	17.9/18.0	16.7/17.8	0.6	1.4	1.6/1.8	16.7/17.8
Ethenylbenzene (styrene)		2.43	0/0.56	1.5	18.0/19.0	16.8/18.6	1.0	4.1	4.2/9.0	16.9/18.6
1,2,3,4-Tetrahydronaphthalene (Tetralin)		2.77	0.49/0.67	-	19.5	19.1/19.2	2.0	2.9	3.1/3.5	19.3/19.4
Decahydronaphthalene (Decaline)		-	-	-	18.4	18.4	0	0	0	18.4

Hydrocarbons, halogenated

Dichloromethane (methylene chloride)	CH_2Cl_2	9.08	1.47/1.9	1.5	19.9	17.4/18.2	6.4	6.1	8.8/10.4	18.6/19.3
Trichloromethane (chloroform)	CHCl_3	4.81	1.0/1.55	1.2/1.5	18.9/19.0	17.7/18.1	3.1	5.7	5.2/6.6	18.0/18.4
Tetrachloromethane (carbon tetrachloride)	CCl_4	2.24	0	0	17.7	16.1/17.7	0.0	0.0	0/8.3	16.1/17.7
Chloroethane (ethyl chloride)	$\text{CH}_3\text{CH}_2\text{Cl}$	9.45	2.04	—	17.4	16.3	—	—	6.1	—
1,2-Dichloroethane (ethylene chloride)	$\text{CH}_2\text{Cl}-\text{CH}_2\text{Cl}$	10.65	1.1/2.94	1.5	20.0/20.1	17.4/18.8	5.3	4.1	6.7/10.0	18.2/19.6
1,1-Dichloroethane (ethylidene chloride)	CH_3CHCl_2	10.15	1.97/2.63	—	18.3	16.8	—	—	8.2	—
1,1,2-Trichloroethane	$\text{CH}_2\text{Cl}-\text{CHCl}_2$	—	1.15/1.55	1.5	19.7/20.8	18.3	—	—	10.0	—
1,1,1-Trichloroethane	CCl_3-CH_3	7.53	0.88/2.03	—	17.5	16.6/16.9	4.3	2.0	4.8/5.5	17.2/17.4
1,1,2,2-Tetrachloroethane	$\text{CHCl}_2-\text{CHCl}_2$	8.20	1.29/2.00	~1.5	19.9/20.2	18.7	—	—	7.3	—
1-Chloropropane (n-propyl chloride)	$\text{CH}_3\text{CH}_2-\text{CH}_2\text{Cl}$	7.7	1.83/2.06	—	17.4	15.9	—	—	7.2	—
1-Chlorobutane (n-butyl chloride)	$\text{CH}_3-(\text{CH}_2)_2-\text{CH}_2\text{Cl}$	—	1.90/2.13	—	17.3	16.1/16.3	5.5	2.1	5.9/6.4	17.0/17.2
Chlorobenzene		5.71	1.58/1.75	1.5/2.7	19.5/19.6	18.8/19.0	4.3	2.1	4.8/5.6	19.3/19.5
Bromobenzene		5.4	1.36/1.79	0	21.7	20.5	5.5	4.1	6.9	20.3
1-Bromonaphthalene		5.12	1.29/1.59	—	21.0	18.8/20.4	3.1	4.1	5.1/9.3	19.0/20.6
1,1,2-Trichloro-1,2,2-trifluoroethane (freon 113)	$\text{CFCl}_2-\text{CF}_2\text{Cl}$	(2.41)	—	—	14.8	14.5	1.6	0	1.6	14.8

Ethers

Ethoxyethane (diethyl ether)	$\text{CH}_3\text{CH}_2-\text{O}-\text{CH}_2-\text{CH}_3$	4.33/4.34	1.15/1.30	13.0	15.2/15.6	14.4	2.9	5.1	5.9	14.7
1-Propoxyp propane (dipropyl ether)	$\text{C}_3\text{H}_7-\text{O}-\text{C}_3\text{H}_7$	(3.39)	1.3	11.7	14.1	—	—	—	—	—
2-Isopropoxyp propane (diisopropyl ether)	$\begin{matrix} \text{CH}_3 & & \text{CH}_3 \\ & -\text{CH}-\text{O}- & \text{CH}-\text{CH}_3 \\ & \text{CH}_3 & \end{matrix}$	3.88	1.13/1.26	12.3	14.4	13.7	—	—	4.4	—

(continued)

TABLE IV (continued)

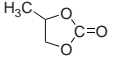
Name	Formula	<i>M</i>	ρ	\mathbf{V}	T_b	T_m	η	γ	n_D
		g/mol	g/cm ³	cm ³ /mol	°C	°C	(25°C) mPas	10 ⁻³ N/m	
<i>Ethers (continued)</i>									
1-Butoxybutane (dibutyl ether)	C ₄ H ₉ —O—C ₄ H ₉	130.23	0.769	169.3	142	−95/(−98)	~0.63	~22.9	1.3992
Dimethoxymethane (methylal)	CH ₃ —O—CH ₂ —O—CH ₃	76.09	0.856	88.9	44	−105	(0.33)	21.12	1.3534
Methoxybenzene (anisole)		108.13	0.995	108.6	155	−37	(1.32)	(36.18)	1.515
1,4-Epoxybutane (tetrahydrofuran)		72.10	0.888	81.2	64/66	−65/−109	0.36	26.4	1.4091
p-Dioxane		88.10	1.035	85.1	102	(9/13)	1.2	36.9	1.4232
1,4-Epoxy-1,3-butadiene (furan)		68.07	0.937	72.7	31	−86	0.36	24.10	1.4216
2,2'-Dichlorodiethyl ether	CH ₂ Cl—CH ₂ —O—CH ₂ —CH ₂ Cl	143.02	1.222	117.0	178	−50	2.14	37.6	1.4575
1-Chloro-2,3-epoxypropane (epichlorohydrin)		92.53	1.180	78.4	117	−26	1.03/~1.05	37.00	1.4420
<i>Esters</i>									
Ethyl formate	HCO—O—C ₂ H ₅	74.08	0.924	80.2	54	−81	(0.40)	23.6	1.3598
Propyl formate	HCO—O—C ₃ H ₇	88.10	0.901	97.8	81	−93	(0.46)	24.5	1.3771
Methyl acetate	CH ₃ —CO—O—CH ₃	74.08	0.934	79.3	57	−98	0.36	24.6	1.3594
Ethyl acetate	CH ₃ —CO—O—C ₂ H ₅	88.10	0.901	97.8	77	−84	0.44	23.9	1.3722
Propyl acetate	CH ₃ —CO—O—C ₃ H ₇	102.13	0.887	115.1	102	−93	0.55	24.3	1.382
Isopropyl acetate	CH ₃ —CO—O—CH(CH ₃) ₂	102.13	0.873	116.9	89	−73	~0.47	22.10	1.375

Butyl acetate	$\text{CH}_3\text{-CO-O-(CH}_2)_3\text{-CH}_3$	116.16	0.882	131.7	(124/126)	-77	0.69	~24.8/27.6	1.3951
Isobutyl acetate	$\text{CH}_3\text{-CO-O-CH}_2\text{-CH(CH}_3)_2$	116.16	0.871	133.3	115/117	-99	0.65	23.7	1.388
Amyl acetate	$\text{CH}_3\text{-CO-O-(CH}_2)_4\text{-CH}_3$	130.18	0.875	148.7	145/149	-79	0.86	25.68/25.8	1.4028
Isoamyl acetate	$\text{CH}_3\text{-CO-O-(CH}_2)_2\text{-CH(CH}_3)_2$	130.18	0.867/ 0.872	149.3/ 150.1	138/143	-79	0.79	24.62	1.403
Ethyl lactate	$\text{CH}_3\text{-CHOH-CO-O-C}_2\text{H}_5$	118.13	1.031	114.6	150/154	-25	2.44	29.9	1.412
Butyl lactate	$\text{CH}_3\text{-CHOH-CO-O-C}_4\text{H}_9$	146.18	0.968	151.0	160/190	-43	3.18	30.6	1.4217
2-Ethoxyethyl acetate (cellosolve acetate)	$\text{CH}_3\text{-CO-O-(CH}_2)_2\text{-O-C}_2\text{H}_5$	132.16	0.973	135.8	156	-62	1.03/1.21	31.8	1.4023
Diethylene glycol, monoethyl ether, acetate (carbitol acetate)	$\text{H}_3\text{C}-\overset{\text{O}}{\underset{\text{O}}{\text{C}}}-\text{O-(CH}_2)_2\text{-O-(CH}_2)_2\text{-O-C}_2\text{H}_5$	176.21	1.009	174.6	218	-25	(2.8)	-	1.4213
1,2-Ethanediol, carbonate (ethylene carbonate)		88.06	1.334	66.0	238	36	-	-	1.426
1,2-Propanediol, carbonate (propylene carbonate)		102.09	1.201	85.0	242	-49	2.8	40.5	1.4209
<i>Ketones and aldehydes</i>									
2-Propanone (acetone)	$\text{CH}_3\text{-CO-CH}_3$	58.08	0.792	73.3	57	-95	0.32	23.70	1.3589
2-Butanone (methyl ethyl ketone)	$\text{CH}_3\text{-CO-C}_2\text{H}_5$	72.10	0.805	89.6	80	-86	(0.42)	~24.3	1.3807
3-Pentanone (diethyl ketone)	$\text{C}_2\text{H}_5\text{-CO-C}_2\text{H}_5$	86.13	0.816	105.6	103	-42	0.44	~24.8/25.26	1.3939
2-Pentanone (methyl propyl ketone)	$\text{CH}_3\text{-CO-C}_3\text{H}_7$	86.13	0.812	106.1	102	-78	0.47	25.2	1.3895

(continued)

TABLE IV (continued)

Name	Formula	ϵ	μ	$\Delta\nu$	δ	δ_d	δ_p	δ_h	δ_a	δ_v
		debye	gordy				(MJ/m ³) ^{1/2}			
<i>Ethers (continued)</i>										
1-Butoxybutane (dibutyl ether)	C ₄ H ₉ -O-C ₄ H ₉	3.08	1.09/1.26	11.0	14.5/15.9	15.2	-	-	4.5	-
Dimethoxymethane (methylal)	CH ₃ -O-CH ₂ -O-CH ₃	2.65	0.67/1.14	-	17.4	~15.1	~1.8	~8.6	8.8	~15.2
Methoxybenzene (anisole)		(4.33)	1.25/1.4	7.0	~19.5/20.3	~17.8	~4.1	~6.8	~7.9	~18.3
1,4-Epoxybutane (tetrahydrofuran)		(7.58)	1.48/1.84	12.0	19.5	16.8/18.9	5.7	8.0	4.7/9.8	17.8/19.8
p-Dioxane		2.21	0/0.49	9.7/14.6	19.9/~20.5	17.5/~19.1	~1.8	~7.4	~7.6/9.5	~17.6/~19.1
1,4-Epoxy-1,3-butadiene (furan)		2.95	0.63/0.72	-	18.6/18.7	17.3/17.8	1.8	5.3	5.6/6.9	17.4/17.9
2,2'-Dichlorodiethyl ether	CH ₂ Cl-CH ₂ -O-CH ₂ -CH ₂ Cl	(38)	2.36/2.60	8.4	~21.1/212	17.2-~18.3	~9.0	~3.1	~9.5/12.2	19.5/~20.9
1-Chloro-2,3-epoxypropane (epichlorohydrine)		23/26	1.8	10.4	21.9	19.0	10.2	3.7	10.9	21.6
<i>Esters</i>										
Ethyl formate	HCO-O-C ₂ H ₅	7.16/9.10	1.94/2.01	8.4	18.7	15.5	7.2	7.6	10.6	17.1
Propyl formate	HCO-O-C ₃ H ₇	7.72	1.91	-	19.6	15.0	-	-	12.5	-
Methyl acetate	CH ₃ -CO-O-CH ₃	6.68	1.45/1.75	8.4	18.7	15.5	7.2	7.6	10.6	17.1
Ethyl acetate	CH ₃ -CO-O-C ₂ H ₅	6.02	1.76/2.05	8.4	18.6	15.2	5.3	9.2	10.6	16.1
Propyl acetate	CH ₃ -CO-O-C ₃ H ₇	5.60/6.00	1.79/1.91	8.5/8.6	17.9/18.0	15.6	-	-	8.8	-
Isopropyl acetate	CH ₃ -CO-O-CH(CH ₃) ₂	-	1.83/1.89	8.5/8.6	17.2/17.6	14.4/14.9	4.5	8.2	9.4/9.6	15.1/15.6

Butyl acetate	$\text{CH}_3\text{-CO-O-(CH}_2)_3\text{-CH}_3$	5.01	1.82/1.9	8.8	17.3/17.4	15.7	3.7	6.4	7.3	16.1
Isobutyl acetate	$\text{CH}_3\text{-CO-O-CH}_2\text{-CH(CH}_3)_2$	5.29	1.87/1.89	8.7/8.8	17.0/17.2	15.1	3.7	7.6	8.4	15.5
Amyl acetate	$\text{CH}_3\text{-CO-O-(CH}_2)_4\text{-CH}_3$	4.75	1.72/1.93	8.2/9.0	17.1	15.3	3.1	7.0	8.2	15.6
Isoamyl acetate	$\text{CH}_3\text{-CO-O-(CH}_2)_2\text{-CH(CH}_3)_2$	(4.63)	1.76/1.86	—	17.0	15.3	3.1	7.0	7.6	15.6
Ethyl lactate	$\text{CH}_3\text{-CHOH-CO-O-C}_2\text{H}_5$,	13.1	1.9/2.34	7.0	20.5/21.6	16.0	7.6	12.5	14.6	17.7
Butyl lactate	$\text{CH}_3\text{-CHOH-CO-O-C}_4\text{H}_9$	—	1.9/2.4	7.0	19.2/19.8	15.7	6.6	10.2	12.2	17.0
2-Ethoxyethyl acetate (cellosolve acetate)	$\text{CH}_3\text{-CO-O-(CH}_2)_2\text{-O-C}_2\text{H}_5$	(7.57)	2.24/2.32	10.1	19.7	15.9	4.7	10.6	11.5	16.6
Diethylene glycol, monoethyl ether, acetate (carbitol acetate)	$\text{H}_3\text{C}-\overset{\text{O}}{\underset{\text{O}}{\text{C}}}-\text{O}-(\text{CH}_2)_2-\overset{\text{O}}{\underset{\text{O-C}_2\text{H}_5}{\text{C}}}-\text{O}-\text{C}_2\text{H}_5$	—	1.8	9.4	17.4/19.3	16.2	—	—	10.5	—
1,2-Ethanediol, carbonate (ethylene carbonate)		(89.6)	1.0/4.91	4.9	29.6/30.9	19.5/22.2	21.7	5.1	21.5/23.3	29.1/31.1
1,2-Propanediol, carbonate (propylene carbonate)		—	1.0/4.98	4.9	27.2	20.1	18.0	4.1	18.4	27.0
<i>Ketones and aldehydes</i>										
2-Propanone (acetone)	$\text{CH}_3\text{-CO-CH}_3$	20.70/21	2.86/2.9	9.7/12.5	20.0/20.5	15.5	10.4	7.0	12.6	18.7
2-Butanone (methyl ethyl ketone)	$\text{CH}_3\text{-CO-C}_2\text{H}_5$	15.45/18.51	2.5/3.41	7.7/10.5	19.0	15.9	9.0	5.1	10.4	18.3
3-Pentanone (diethyl ketone)	$\text{C}_2\text{H}_5\text{-CO-C}_2\text{H}_5$	17.00	2.5/2.82	7.7	18.0/18.1	15.7	—	—	9.5	—
2-Pentanone (methyl propyl ketone)	$\text{CH}_3\text{-CO-C}_3\text{H}_7$	15.45	2.5/2.74	8.0	18.3	15.8	—	—	9.2	—

(continued)

TABLE IV (continued)

Name	Formula	<i>M</i>	<i>ρ</i>	<i>V</i>	<i>T_b</i>	<i>T_m</i>	<i>η</i>	<i>γ</i>	<i>n_D</i>
		g/mol	g/cm ³	cm ³ /mol	°C	°C	(25°C) mPas	10 ⁻³ N/m	
<i>Ketones and aldehydes (continued)</i>									
2-Hexanone (methyl butyl ketone)	CH ₃ —CO—C ₄ H ₉	100.16	0.808/0.812	123.4/123.9	127	−57	0.58	25.2	1.395
4-Methyl-2-pentanone (methyl isobutyl ketone)	CH ₃ —CO—CH ₂ —CH(CH ₃) ₂	100.16	0.802	124.9	115/119	−85	0.54/0.57	23.64	1.394
2,6-Dimethyl-4-heptanone (diisobutyl ketone)	[CH(CH ₃) ₂ —CH ₂] ₂ —C=O	142.24	0.806	176.4	165/168	42	1.0	—	1.412
4-Methyl-3-penten-2-one (mesityl oxide)	(CH ₃) ₂ C=CH—CO—CH ₃	98.14	0.854	114.9	129/(131)	−59	0.88	—	1.442
Cyclohexanone		98.14	0.948/0.998	98.4/103.5 (155)/157	−16/−32	(1.80)	34.50	1.4507	
4-Hydroxybutanoic acid, lactone (butyrolactone)		86.09	(1.129)	76.3	206	−44	1.7	—	1.434
Methyl phenyl ketone (acetophenone)		120.14	1.026	117.1	202	20	1.62	39.8	1.5342
3,5,5-Trimethyl)-2-cyclohexen-1-one (isophorone)		138.20	0.923	149.7	215	−8	(2.62)	—	1.4789
Ethanal (acetaldehyde)	CH ₃ —CH=O	44.05	0.783	56.3	21	−124	0.22	21.2	1.3316
Butanal (butyraldehyde)	CH ₃ —(CH ₂) ₂ —CH=O	72.10	0.817	88.3	76	−99	(0.46)	29.9	1.3791
Benzencarbonal (benzaldehyde)		106.12	(1.050)	101.0	180	−26/−57	1.39	40.04	1.5463

<i>Alcohols</i>									
Methanol	CH ₃ OH	32.04	0.792	40.4	65	-98	0.55	22.61	1.3312
Ethanol	C ₂ H ₅ OH	46.07	0.789	58.4	(78)/79	-115/-117	1.08	22.75	1.3624
1-Propanol	CH ₃ (CH ₂) ₂ OH	60.09	0.780/0.804	74.7/77.1	97/(98)	-127	1.91/2.02	23.78	1.3854
2-Propanol (isopropyl alcohol)	CH ₃ -CHOH-CH ₃	60.09	0.785	76.5	82	-90	~1.9	21.7	1.3776
1-Butanol	CH ₃ (CH ₂) ₃ OH	74.12	0.810	91.5	118	(-88)/-90	2.46/2.60	24.6	1.3993
2-Methyl-1-propanol (isobutyl alcohol)	CH(CH ₃) ₂ -CH ₂ OH	74.12	0.801	92.5	106/108	-108	3.24/3.9	23.0	1.3968
2-Butanol (sec.-butyl alcohol)	CH ₃ -CHOH-C ₂ H ₅	74.12	0.808	91.7	100	-89	~3.1	23.47	1.397
1-Pentanol (amyl alcohol)	CH ₃ (CH ₂) ₄ OH	88.15	0.814	108.2	138	-79	3.19/3.35	25.6	1.4099
Cyclohexanol		100.16	0.962	104.0	162	22/25	56.2	33.91	1.4656
Phenol		94.11	1.072	87.8	182	41	(12.7)	40.9	1.5509
3-Methylphenol (m-cresol)		108.13	1.034	104.6	203	11/12	(20.8)	(38.01)	1.5398
Phenyl methanol (benzyl alcohol)		108.13	1.050	103.0	205	-15	(5.8)	39.0	1.5396
1,2-Ethanediol (ethylene glycol)	CH ₂ OH-CH ₂ OH	62.07	1.109/1.116	55.6/56.0	198/200	(-12)/-17	17.4	47.7	1.4274
1,2-Propanediol (propylene glycol)	CH ₃ -CHOH-CH ₂ OH	76.09	1.040	73.2	189	-60	~30/43	~36.8/40.1	1.431
1,3-Butanediol (butylene glycol)	CH ₃ -CHOH-CH ₂ -CH ₂ OH	90.12	1.005	89.7	204	<-50	98.3/110	37.8	1.441
1,2,3-Propanetriol (glycerol)	CH ₂ OH-CHOH-CH ₂ OH	92.09	1.260	73.1	290	18	945/954	63.4	1.4729
2-Methoxy ethanol (methyl cellosolve)	CH ₃ -O-CH ₂ -CH ₂ OH	76.09	0.966	78.8	124	-85	1.60	35	1.400
2-Ethoxyethanol (ethyl cellosolve)	CH ₃ -CH ₂ -O-CH ₂ -CH ₂ OH	90.12	0.930/0.931	96.8/97.0	135	-90	1.85	28.2/32	1.405

(continued)

TABLE IV (continued)

Name	Formula	ϵ	μ	$\Delta\nu$	δ	δ_d	δ_p	δ_h	δ_a	δ_v
		debye	gordy				(MJ/m ³) ^{1/2}			
<i>Ketones and aldehydes (continued)</i>										
2-Hexanone (methyl butyl ketone)	CH ₃ -CO-C ₄ H ₉	12.2	2.5/2.75	8.4	17.4/17.7	15.9	—	—	7.7	—
4-Methyl-2-pentanone (methyl isobutylketone)	CH ₃ -CO-CH ₂ -CH(CH ₃) ₂	13.11	2.7	7.7/10.5	17.2/17.5	15.3	6.1	4.1	8.5	16.5
2,6-Dimethyl-4-heptanone (diisobutyl ketone)	[(CH ₃) ₂ CH-CH ₂] ₂ C=O	—	2.66/2.7	8.4/9.8	16.0/16.7	15.9	3.7	4.1	5.4	16.3
4-Methyl-3-penten-2-one (mesityl oxide)	(CH ₃) ₂ C=CH-CO-CH ₃	—	2.79/ 3.28	9.7/12.0	18.4/18.8	16.3	7.2	6.1	9.4	17.8
Cyclohexanone		18.3	2.7/3.08	11.7/13.7	19.0/20.2	17.7	8.4	5.1	9.8	19.6
4-Hydroxybutanoic acid, lactone (butyrolactone)		39	2.7/4.15	9.7	26.1/31.7	19.0/ 20.1	16.6	7.4	16.8/18.1	25.2/ 26.1
Methyl phenyl ketone (acetophenone)		17.39	2.60/3.4	7.7	19.8	17.5/ 18.5	8.6	3.7	7.1/9.4	19.5/ 20.4
3,5,5-Trimethyl-2-cyclohexen-1-one (isophorone)		—	3.99	14.9	19.9	16.6	8.2	7.4	11.0	18.5
Ethanal (acetaldehyde)	CH ₃ -CH=O	21.8	2.55	—	20.2	14.7	8.0	11.3	13.9	16.8
Butanal (butyraldehyde)	CH ₃ -(CH ₂) ₂ -CH=O	13.4	2.45/ 2.74	11.7	17.1	14.7	5.3	7.0	8.7	15.6
Benzencarbonal (benzaldehyde)		16/17.8	2.72/ 2.99	8.4	19.2/21.3	18.2/ 18.7	8.6	5.3	10.1/10.2	20.2/ 20.6

<i>Alcohols</i>										
Methanol	CH ₃ -OH	33.62	1.7/1.71	18.7/19.8	29.2/29.7	15.2	12.3	22.3	25.4	19.5
Ethanol	C ₂ H ₅ -OH	24.3	1.7/1.73	17.7/18.7	26.0/26.5	15.8	8.8	19.5	21.4	18.1
1-Propanol	CH ₃ (CH ₂) ₂ -OH	20.1	1.54/ 3.09	16.5/18.7	24.4/24.5	15.9	6.8	17.4	18.6	17.2
2-Propanol (isopropyl alcohol)	(CH ₃) ₂ CH-OH	13.8/ 18.3	1.48/ 1.80	16.7	23.6	15.8	6.1	16.4	17.5	16.9
1-Butanol	CH ₃ -(CH ₂) ₃ -OH	17.8	1.7/1.81	18.0/18.7	23.1/23.3	16.0	5.7	15.8	16.8	17.0
2-Methyl-1-propanol (isobutyl alcohol)	(CH ₃) ₂ CH-CH ₂ -OH	17.7	1.42/ 2.96	17.9	22.9	15.2	5.7	16.0	17.0	16.2
2-Butanol (sec.-butyl alcohol)	CH ₃ -CHOH-C ₂ H ₅	15.8	1.66	17.5	22.2	15.8	-	-	15.6	-
1-Pentanol (amyl alcohol)	CH ₃ -(CH ₂) ₄ -OH	13.9	0.89/1.8	18.2	21.7	16.0	4.5	13.9	14.7	16.6
Cyclohexanol		15.0	1.3/1.9	16.5/18.7	22.4/23.3	17.4	4.1	13.5	14.2	17.9
Phenol		(9.78)	1.48/ 1.55	7.0	24.1	18.0	5.9	14.9	16.4	19.0
3-Methylphenol (m-cresol)		11.8	1.55/ 2.39	-	22.7	18.1/ 19.4	5.1	12.9	12.0/13.9	18.8/ 20.0
Phenyl methanol (benzyl alcohol)		13.1	1.67/ 1.79	18.7	23.8	18.4	6.3	13.7	15.1	19.5
1,2-Ethanediol (ethylene glycol)	CH ₂ OH-CH ₂ OH	34/37.7	2.20/ 4.87	20.6	29.1/33.4	16.9	11.1	26.0	28.7	20.2
1,2-Propanediol (propylene glycol)	CH ₃ -CHOH-CH ₂ OH	32.0	2.2/3.63	20.0	30.3	16.9	9.4	23.3	25.1	19.3
1,3-Butanediol (butylene glycol)	CH ₃ -CHOH-CH ₂ -CH ₂ OH	-	-	-	29.0	16.6	10.0	21.5	23.8	19.4
1,2,3-Propanetriol (glycerol)	CH ₂ OH-CHOH-CH ₂ OH	42.5	~2.3/4.21	~22.0	33.8/43.2	17.3	12.1	29.3	39.5	21.1
2-Methoxyethanol (methyl cellosolve)	CH ₃ -O-CH ₂ -CH ₂ OH	(16.93)	2.06/ 2.22 2.24	-	24.7	16.2	9.2	16.4	17.0	18.6
2-Ethoxyethanol (ethyl cellosolve)	C ₂ H ₅ -O-CH ₂ -CH ₂ OH	(29.6)	2.10/ 2.24	15.7	24.3	16.1	9.2	14.3	17.5	18.5

(continued)

TABLE IV (continued)

Name	Formula	<i>M</i>	<i>ρ</i>	<i>V</i>	<i>T_b</i>	<i>T_m</i>	<i>η</i>	<i>γ</i>	<i>n_D</i>
		g/mol	g/cm ³	cm ³ /mol	°C	°C	(25 °C) mPas	10 ⁻³ N/m	
<i>Akohols (continued)</i>									
2-Butoxyethanol (butyl cellosolve)	CH ₃ -(CH ₂) ₃ -O-CH ₂ -CH ₂ OH	118.17	0.903	130.9	171	—	3.15	31.5	1.4198
4-Hydroxy-4-methyl-2-pentanone (diacetone alcohol)	CH ₃ -CO-CH ₂ -C(CH ₃) ₂ -OH	116.16	0.938	123.8	164/166	-44/-57	(2.9)	31.0	1.4235
<i>Acids</i>									
Formic acid	HCOOH	46.03	1.220	37.7	101	8	1.97	37.6	1.3714
Acetic acid	CH ₃ -COOH	60.05	1.049	57.2	118	17	1.16	27.8	1.3718
Butyric acid	CH ₃ -(CH ₂) ₂ -COOH	88.10	0.959	91.9	163	-5/-8	1.57	26.8	1.3991
Acetic acid anhydride	CH ₃ -CO-O-CO-CH ₃	102.09	1.082	94.4	140	-73	(0.78)/(0.91)	32.7	1.3904
<i>Nitrogen compounds</i>									
1-Aminopropane (propylamine)	CH ₃ -(CH ₂) ₂ -NH ₂	59.11	0.719	82.2	49	-83	0.35	22.4	1.386
Diethylamine	C ₂ H ₅ -NH-C ₂ H ₅	73.14	0.707	103.5	56	(-39)/-50	0.35/0.37	(20.63)	1.3854
Aminobenzene (aniline)		93.12	1.022	91.1	184	-6	3.71	42.9/44.1	1.5863
2-Aminoethanol (ethanolamine)	H ₂ N-CH ₂ -CH ₂ OH	61.08	1.018	60.0	172	11	19.35	48.89	1.452
Nitromethane	CH ₃ -NO ₂	61.04	1.130	54.0	101	-29	0.62	36.82	1.380
Nitroethane	C ₂ H ₅ -NO ₂	75.07	1.052	71.4	115	<-50/-90	0.64	32.2	1.3901
Nitrobenzene		123.11	1.204	102.3	211	6	(2.03)	43.9	1.5529
Ethanenitrile (acetonitrile)	CH ₃ -CN	41.05	0.783	52.4	82	-41/-44	0.35	29.30	1.3460
Methanamide (formamide)	O=CH-NH ₂	45.04	1.134	39.7	211	3	3.30	58.2	1.4453

Dimethylformamide	O=CH-N(CH ₃) ₂	73.09	0.949	77.0	153	-58	0.80	36.76/~38	1.427
Dimethylacetamide	CH ₃ -CO-N(CH ₃) ₂	87.12	(0.937)	93.0	166	-20	~0.92	~34	1.4384
1,1,3,3-Tetramethylurea	(CH ₃) ₂ N-CO-N(CH ₃) ₂	116.16	(0.969)	119.9	177	-1	-	-	1.4493
Pyridine (azine)		79.10	0.982	80.5	115	-42	0.88	38.0	1.5092
Morpholine		87.12	1.0	87.1	126/130	-3	(1.79/2.37)	37.63	1.4542
2-Pyrrolidone		85.10	1.116	76.3	245/(251)	25	13.3	-	1.486
N-Methyl-2-Pyrrolidone		99.13	(1.028)	96.4	202	-16/-24	1.67	41.83	1.4680
<i>Sulphur compounds</i>									
Dimethyl sulphide	CH ₃ -S-CH ₃	62.13	0.846	73.5	38	-83	0.28	24.48	1.4353
Diethyl sulphide	C ₂ H ₅ -S-C ₂ H ₅	90.18	0.837	107.7	92	-102	0.42	25.2	1.442
Carbon disulphide	CS ₂	76.13	1.263	60.3	46	-109/-112	(0.36)	32.33	1.6295
Dimethyl sulphoxide	CH ₃ -SO-CH ₃	78.13	1.102	71.0	189	19	2.0	43.54	1.476
<i>Other substances</i>									
Triethyl phosphate	(C ₂ H ₅) ₃ PO ₄	182.16	1.069	170.5	216	-56	-	(30.61)	1.4067
Hexamethyl phosphoramide	[(CH ₃) ₂ N] ₃ P=O	179.20	1.027	174.5	233	7	(3.47)	33.8	1.4588
Water	H ₂ O	18.02	0.998	18.0	100	0	0.89	72.75	1.3333

(continued)

TABLE IV (continued)

Name	Formula	ϵ	μ	$\Delta\nu$	δ	δ_d	δ_p	δ_h	δ_a	δ_v
		debye	gordy				$(\text{MJ}/\text{m}^3)^{1/2}$			
<i>Alcohols (continued)</i>										
2-Butoxyethanol (butyl cellosolve)	$\text{CH}_3-(\text{CH}_2)_3-\text{O}-\text{CH}_2-\text{CH}_2\text{OH}$	(9.30)	2.10	13.0	21.0	15.9	6.4	12.1	13.7	17.1
4-Hydroxy-4-methyl-2-pentanone (diacetone alcohol)	$\text{CH}_3-\text{CO}-\text{CH}_2-\text{C}(\text{CH}_3)_2-\text{OH}$	(18.2)	2.5/3.24	13.6/ 16.3	18.8/20.8	15.7	8.2	10.9	13.5	17.7
<i>Acids</i>										
Formic acid	HCOOH	58.5	1.20/ 2.09	—	24.9/25.0	~14.3/15.3	~11.9	~16.6	19.8/20.4	~18.6/19.4
Acetic acid	CH_3-COOH	6.15	0.38/ 1.92	20.0	~18.8/21.4	~14.5/16.6	~8.0	~13.5	~13.2/15.7	~16.6/18.4
Butyric acid	$\text{CH}_3-(\text{CH}_2)_2-\text{COOH}$	2.97	0/1.9	—	~18.8/23.1	~14.9/16.3	~4.1	~10.6	~11.4/16.3	~15.5/16.8
Acetic acid anhydride	$\text{CH}_3-\text{CO}-\text{O}-\text{CO}-\text{CH}_3$	20.7	2.7/3.15	—	21.3/22.2	15.4/16.0	11.1	9.6	14.7/15.1	18.9/19.5
<i>Nitrogen compounds</i>										
1-Aminopropane (propylamine)	$\text{CH}_3-(\text{CH}_2)_2-\text{NH}_2$	5.31	1.17/ 1.39	—	19.7	17.0	4.9	8.6	9.8	17.7
Diethylamine	$\text{C}_2\text{H}_5-\text{NH}-\text{C}_2\text{H}_5$	(3.58)	0.91/ 1.21	—	16.3	14.9	2.3	6.1	6.5	15.1
Aminobenzene (aniline)		6.89/7	1.5/1.56	18.1	22.6/24.2	19.5	5.1	10.2	11.4	20.2
2-Aminoethanol (ethanolamine)	$\text{H}_2\text{N}-\text{CH}_2-\text{CH}_2\text{OH}$	(37.72)	2.59	—	31.7	17.1	15.6	21.3	26.4	23.1
Nitromethane	CH_3-NO_2	38.57	2.83/ 4.39	2.5	25.1/26.0	15.8/16.4	18.8	5.1	19.0/19.5	24.6/25.0
Nitroethane	$\text{C}_2\text{H}_5-\text{NO}_2$	28.0	3.22/ 3.70	2.5	22.7	16.0/16.6	15.6	4.5	15.5/16.2	22.3/22.8
Nitrobenzene		35.74/36	3.93/4.3	2.8	20.5/21.9	17.6/19.9	12.3	4.1	8.7/13.0	21.5/23.4
Ethanenitrile (acetonitrile)	CH_3-CN	37	3.08/ 4.01	5.7/ 6.3	24.1/24.5	15.4/16.2	18.0	6.1	18.0/19.0	23.7/24.2
Methanamide (formamide)	$\text{O}=\text{CH}-\text{NH}_2$	109	3.25/ 3.86	—	36.7	17.2	26.2	19.0	32.4	31.3

Dimethylformamide	O=CH-N(CH ₃) ₂	(26.6/ 36.71)	2.0/3.86	11/7/ 18.9	24.9	17.4	13.7	11.3	17.8	22.2
Dimethylacetamide	CH ₃ -CO-N(CH ₃) ₂	(37.78)	2.0/3.81	12.3	22.1/22.8	16.8	11.5	10.2	15.4	20.3
1,1,3,3-Tetramethylurea	(CH ₃) ₂ N-CO-N(CH ₃) ₂	23.06	3.28/ 3.92	-	21.7	16.8	8.2	11.1	13.8	18.7
Pyridine (azine)		12.3	1.96/ 2.43	18.1	21.7/21.9	18.9/20.1	8.8	5.9	8.3/10.6	20.9/21.9
Morpholine		7.33	1.49/ 1.75	-	21.5	18.2/18.8	4.9	9.2	10.4/11.7	18.9/19.5
2-Pyrrolidone		-	2.3/3.79	-	28.4	19.5	17.4	11.3	20.7	26.1
N-methyl-2-Pyrrolidone		(32.0)	4.04/ 4.12	-	22.9	17.9	12.3	7.2	14.2	21.7
<i>Sulphur compounds</i>										
Dimethyl sulphide	CH ₃ -S-CH ₃	6.2	1.41/ 1.50	-	18.4	17.6	-	-	5.9	-
Diethyl sulphide	C ₂ H ₅ -S-C ₂ H ₅	(5.72)	1.52/ 1.62	-	17.3	16.0/16.9	3.1	2.1	3.7/6.7	16.3/17.2
Carbon disulphide	CS ₂	(2.64)	0/0.49	0	20.4/20.5	16.2/20.4	0	0	0/12.3	16.2/20.4
Dimethyl sulphoxide	CH ₃ -SO-CH ₃	(46.68)	3.9	7.7	26.5/26.7	18.4/19.3	16.4	10.2	18.1/19.3	24.7/25.3
<i>Other substances</i>										
Triethyl phosphate	(C ₂ H ₅) ₃ PO ₄	-	2.84/ 3.10	11.7	22.3	16.8	11.5	9.2	14.7	20.3
Hexamethyl phosphoramide	[(CH ₃) ₂ N] ₃ P=O	30	5.54	-	23.3	18.4	8.6	11.3	14.2	20.3
Water	H ₂ O	80.37	1.82/ 1.85	39.0	47.9/48.1	~12.3/14.3	~31.3	~34.2	~45.9// 46.4	~16.4/16.8

TABLE V Physical properties of the most important polymers

Polymers	Physical properties							
	M g/mol	ρ_a g/cm ³	ρ_c g/cm ³	e_g $10^{-4} \text{ cm}^3 \text{ g}^{-1} \text{ K}^{-1}$	e_l	c_p^s $\text{J g}^{-1} \text{ K}^{-1}$	c_p^l $\text{J g}^{-1} \text{ K}^{-1}$	ΔH_m kJ/mol
<i>Polyolefines</i>								
Polyethylene	28.1	0.85	1.00	2.4/3.6	7.5/9.6	1.55/1.76	2.26	8.22
Polypropylene	42.1	0.85	0.95	2.2/(4.4)	5.5/9.4	1.62/1.78	2.13	8.70
Poly(1-butene)	56.1	0.86	0.94	3.8	8.8	1.55/1.76	2.13	7.00
Poly(3-methyl-1-butene)	70.1	<0.90	0.93					17.3
Poly(1-pentene)	70.1	0.85	0.92		9.2			
Poly(4-methyl-1-pentene)	84.2	0.838	0.915	3.83	7.61	1.67		9.96
Poly(1-hexene)	84.2	0.86	0.91					
Poly(5-methyl-1-hexene)	98.2		0.84					
Poly(1-octadecene)	252.5	0.86	0.95					
Polyisobutylene	56.1	0.84	0.94	1.6/2.0	5.6/6.9	1.67	1.95	12.0
1,2-Poly(1,3-butadiene) (iso)	54.1		>0.96					
1,2-Poly(1,3-butadiene) (syndio)	54.1	<0.92	0.963					
<i>Polystyrenes</i>								
Polystyrene	104.1	1.05	1.13	1.7/2.6	4.3/6.5	1.23	1.71	10.0
Poly(α -methylstyrene)	118.2	1.065						
Poly(2-methylstyrene)	118.2	1.027	1.07	2.6	5.3			
Poly(4-methylstyrene)	118.2	1.04						
Poly(4-methoxystyrene)	134.2		>1.12					
Poly(4-phenylstyrene)	180.2							
Poly(3-phenyl-1-propene)	118.2	1.046	>1.052					
Poly(2-chlorostyrene)	138.6	<1.25						
Poly(4-chlorostyrene)	138.6							
<i>Polyhalo-olefines</i>								
Poly(vinyl fluoride)	46.0	<1.37	1.44					7.5
Poly(vinyl chloride)	62.5	1.385	1.52	1.1/2.1	4.2/5.2	0.95	~1.21	11.0
Poly(vinyl bromide)	107.0							
Poly(vinylidene fluoride)	64.0	1.74	2.00	1.2	2.1/4.6			6.70
Poly(vinylidene chloride)	97.0	1.66	1.95	1.2	5.7			0.86
Poly(tetrafluoroethylene) (Teflon)	100.0	2.00	2.35	(1.3)/3.0	4.8	0.96	0.96	8.20
Poly(chlorotrifluoroethylene)	116.5	1.92	2.19	1.0/1.5	2.0/3.5	0.92		5.02

Poly(vinyl cyclopentane)	96.2	<0.965	0.986				
Poly(vinyl cyclohexane)	110.2	0.95	0.982				
Poly(α -vinyl naphthalene)	154.2		1.12				
Poly(vinyl alcohol)	44.1	1.26	1.35	3.0		1.30/1.51	6.9/7.0
Poly(vinyl methyl ether)	58.1	<1.03	1.175				
Poly(vinyl ethyl ether)	72.1	0.94	>0.97				
Poly(vinyl propyl ether)	86.1	<0.94					
Poly(vinyl isopropyl ether)	86.1	0.924	>0.93				
Poly(vinyl butyl ether)	100.2	<0.927	0.944				
Poly(vinyl isobutyl ether)	100.2	0.93	0.94				
Poly(vinyl sec.-butyl ether)	100.2	0.92	0.956				
Poly(vinyl tert.-butyl ether)	100.2		0.978				
Poly(vinyl hexyl ether)	128.2	0.925	>0.925				
Poly(vinyl octyl ether)	156.3	0.914	>0.91				
Poly(vinyl methyl ketone)	70.1	1.12	1.216				
Poly(methyl isopropenyl ketone)	84.1	1.12/1.15	1.15/1.17				
Poly(vinyl formate)	72.1	<1.35	1.49				
Poly(vinyl acetate)	86.1	1.19	1.34	1.8/2.4	5.0/6.0	1.34/1.47	1.97
Poly(vinyl propionate)	100.1	1.02					
Poly(vinyl chloroacetate)	120.5	1.45		1.3	3.4		
Poly(vinyl trifluoroacetate)	140.1		1.633				~7.5
Poly(vinyl benzoate)	148.2						
Poly(2-vinyl pyridine)	105.1						
Poly(vinyl pyrrolidone)	111.1	1.25					
Poly(vinyl carbazole)	193.2	<1.19/1.2	0.988				
<i>Polyacrylates</i>							
Poly(acrylic acid)	72.1						
Poly(methyl acrylate)	86.1	1.22		1.8/2.7	4.6/5.6	1.34	1.80
Poly(ethyl acrylate)	100.1	1.12		2.8	6.1	1.45	1.80
Poly(propyl acrylate)	114.1	<1.08	>1.18				
Poly(isopropyl acrylate)	114.1		1.08/1.18	2.2/2.6	6.1/6.3		5.9
Poly(butyl acrylate)	128.2	1.00/1.09		2.6	6.0	1.64	1.82
Poly(isobutyl acrylate)	128.2	<1.05	1.24				
Poly(sec.-butyl acrylate)	128.2	<1.05	1.06	2.75	6.1		
Poly(tert.-butyl acrylate)	128.2	1.00	1.04/>1.08				

(continued)

TABLE V (continued)

Polymers	Physical properties							
	T_g K	T_m K	δ $J^{1/2}/cm^{3/2}$	γ mN/m	n	ϵ	λ_a $J s^{-1} m^{-1} K^{-1}$	λ_c $cm^3 mol^{1/2} g^{-3/2}$
<i>Polyolefines</i>								
Polyethylene	195(150/253)	414.6	15.8/17.1	31/36	1.49/1.52	2.3	(0.16)/(0.48)	(0.74) 0.20/0.26
Polypropylene	260	460.7	16.6/18.8	29/34	1.49	2.2	(0.09)/(0.22)	0.120/0.182
Poly(1-butene)	249	411.2		34	1.5125			0.105/0.123
Poly(3-methyl-1-butene)	<323	573/583						
Poly(1-pentene)	233	403.2						0.113/0.120
Poly(4-methyl-1-pentene)	303	523.2		25	1.459/1.465	2.1		
Poly(1-hexene)	223	321						
poly(5-methyl-1-hexene)	<259	383/403						
Poly(1-octadecene)	<328	341/353			1.471/1.507			
Polyisobutylene	200	317	16.0/16.6	27/34	1.508		0.123/0.130	0.085/0.115
1,2-Poly(1,3-butadiene) (iso)	208	398						
1,2-Poly(1,3-butadiene) (syndio)		428						
<i>Polystyrenes</i>								
Polystyrene	373	516.2	17.4/19.0	27/43	1.591	2.55	0.131/0.142	(0.110) 0.067/0.100
Pols(α -methylstyrene)	441			36				0.064/0.084
Poly(2-methylstyrene)	409	633			1.5874			
Poly(4-methylstyrene)	380							0.066/0.070
Poly(4-methoxystyrene)	~362	511			1.5967			0.062
Poly(4-phenylstyrene)	434							
Poly(3-phenyl-1-propene)	333	503/513						
Poly(2-chlorostyrene)	392		18.2	42	1.6098	2.6		
Poly(4-chlorostyrene)	406					2.6	0.116	0.050
<i>Polyhalo-olefins</i>								
Poly(vinyl fluoride)	314	503.2		28/37				
Poly(vinyl chloride)	354	546	19.2/22.1	26/42	1.539	2.8/3.05	0.16/0.17	0.095/0.335
Poly(vinyl bromide)	373		19.6					0.040
Poly(vinylidene fluoride)	212	483.2		25/33	1.42	8/13	0.13	
Poly(vinylidene chloride)	255	463	20.3/25.0	40	1.60/1.63	2.85		
Poly(tetrafluoroethylene) (Teflon)	200	605	12.7	16/22	1.35/1.38	2.1	(0.25)	
Poly(chlorotrifluoroethylene)	325	493	14.7/16.2	31	1.39/1.43	2.3/2.8	(0.14)/0.25	

Poly(vinyl cyclopentane)	<348	565						
Poly(vinyl cyclohexane)	<363	575/656						
Poly(α -methyl naphthalene)	408/435	633						
Poly(vinyl alcohol)	343/372	521	25.8/29.1	37	1.5	8/12		0.160/0.300
Poly(vinyl methyl ether)	242/260	417/423		29	1.467			
Poly(vinyl ethyl ether)	231/254	359		36	1.4540			
Poly(vinyl propyl ether)		349						
Poly(vinyl isopropyl ether)	270	464						
Poly(vinyl butyl ether)	220	337			1.4563			
Poly(vinyl isobutyl ether)	246/255	443			1.4507			
Poly(vinyl sec.-butyl ether)	253	443			1.4740			
Poly(vinyl tert.-butyl ether)	361	533						
Poly(vinyl hexyl ether)	196/223				1.4591			
Poly(vinyl octyl ether)	194				1.4613			
Poly(vinyl methyl ketone)		443			1.50			
Poly(methyl isopropenyl ketone)	353/387	473/513			1.5200			
Poly(vinyl formate)	304/310				1.4757			
Poly(vinyl acetate)	304		19.1/22.6	36/37	1.467	3.25	0.159	0.078/0.110
Poly(vinyl propionate)	283		18.0/18.5		1.4665			
Poly(vinyl chloroacetate)	304				1.513			
Poly(vinyl trifluoroacetate)	319	448			1.375			
Poly(vinyl benzoate)	341				1.5775			0.062
Poly(2-vinyl pyridine)	377	488						0.082
Poly(vinyl pyrrolidone)	418/448				1.53			0.074/0.090
Poly(vinyl carbazole)	473/481				1.683		0.126/0.155	0.074/0.076
<i>Polyacrylates</i>								
Poly(acrylic acid)	379		29/35	1.527				0.076/0.165
Poly(methyl acrylate)	279		19.8/21.3	41	1.479	4.4/5.5		0.054/0.081
Poly(ethyl acrylate)	249		19.2	35	1.4685			0.090
Poly(propyl acrylate)	229	388/435	18.4					
Poly(isopropyl acrylate)	262/284	389/453						
Poly(butyl acrylate)	218	320	18.0/18.5	28	1.466			
Poly(isobutyl acrylate)	249	354	18.4/22.5					
Poly(sec.-butyl acrylate)	250/256	403						
Poly(tert.-butyl acrylate)	313/316	466/473						

(continued)

TABLE V (continued)

Polymers	M g/mol	Physical properties					
		ρ_a g/cm ³	ρ_c g/cm ³	e_g $10^{-4} \text{ cm}^3 \text{ g}^{-1} \text{ K}^{-1}$	e_l	c_p^s J g ⁻¹ K ⁻¹	c_p^l J g ⁻¹ K ⁻¹
<i>Polymethacrylates</i>							
Poly(methacrylic acid)	86.1					1.05/1.30	
Poly(methyl methacrylate)	100.1	1.17	1.23	1.2/2.3	5.2/5.4	1.37	~1.80
Poly(ethyl methacrylate)	114.1	1.119	1.19	2.75	5.40/5.7	1.49	
Poly(propyl methacrylate)	128.2	1.08		3.2	5.7		
Poly(isopropyl methacrylate)	128.2	1.033		2.0/2.4	6.2		
Poly(butyl methacrylate)	142.2	1.055			6.1	1.68	1.84
Poly(isobutyl methacrylate)	142.2	1.045		2.4	6.0		
Poly(sec.-butyl methacrylate)	142.2	1.052		3.3	6.3		
Poly(tert.-butyl methacrylate)	142.2	1.02		2.7	7.0		
Poly(2-ethylbutyl methacrylate)	170.2	1.040			5.76		
Poly(hexyl methacrylate)	170.2	1.01			6.3/6.6		
Poly(octyl methacrylate)	198.3	0.971			5.8		
Poly(dodecyl methacrylate)	254.4	0.929		3.8	6.8		
Poly(octadecyl methacrylate)	338.6		>0.97				
Poly(phenyl methacrylate)	162.2	1.21		1.3	4.4		
Poly(benzyl methacrylate)	176.2	1.179		1.45	4.2		
Poly(cyclohexyl methacrylate)	168.2	1.098		2.7	5.4		
<i>Other polyacrylics</i>							
Poly(methyl chloroacrylate)	120.5	1.41/1.49					
Polyacrylonitrile	53.1	1.184	1.27/1.54	1.4/(1.6)	2.9/(3.1)	1.26	4.9/5.2
Polymethacrylonitrile	67.1	1.10	1.134				
Polyacrylamide	71.1	1.302					
Poly(N-isopropylacrylamide)	113.2	1.03/1.07	1.118				
<i>Polydienes</i>							
Poly(1,3-butadiene)(cis)	54.1		1.01			1.84	9.20
Poly(1,3-butadiene)(trans)	54.1		1.02			2.39	7.50
Poly(1,3-butadiene)(mixt)	54.1	0.892		2.0	6.4/7.7	1.65	
Poly(1,3-pentadiene)(trans)	68.1	0.89	0.98				
Poly(2-methyl-1,3-butadiene)(cis)	68.1	0.908	1.00	2.0	6.0/7.4		8.7
Poly(2-methyl-1,3-butadiene)(trans)	68.1	0.904	1.05		8.3		12.8
Poly(2-methyl-1,3-butadiene)(mixt.)	68.1				1.59	1.91	

Poly(2-tert.-butyl-1,3-butadiene)(cis)	110.2	<0.88	0.906					
Poly(2-chloro-1,3-butadiene)(trans)	88.5		1.09/1.66					
Poly(2-chloro-1,3-butadiene)(mixt.)	88.5	1.243	1.356		4.2/5.0			8.4
<i>Polyoxides (Polyethers)</i>								
Poly(methylene oxide)	30.0	1.25	1.54	1.8		~1.42	~2.09	9.79
Poly(ethylene oxide)	44.1	1.125	1.28		6.4	~1.26	2.05	8.67
Poly(tetramethylene oxide)	72.1	0.98	1.18		6.9	1.65	2.07	14.4
Poly(ethylene formal)	74.1		1.325/1.414			1.29	1.84	16.7
Poly(tetramethylene formal)	102.1		1.234			1.41	1.90	14.0/14.7
Polyacetaldehyde	44.1	1.071	1.14	2.1	6.3			
Poly(propylene oxide)	58.1	1.00	1.10/1.21		7.2	~1.423	1.917	8.4
Poly(hexene oxide)	100.2	<0.92	>0.97					
Poly(octene oxide)	128.2	<0.94	>0.97					
Poly(trans-2-butene oxide)	72.1	<1.01	1.099					
Poly(styrene oxide)	120.1	1.15	>1.18					
Poly(3-methoxypropylene oxide)	88.1	<1.095						
Poly(3-butoxypropylene oxide)	130.2	<0.982						
Poly(3-hexaoxypropylene oxide)	158.2	<0.966						
Poly(3-phenoxypropylene oxide)	150.2	<1.21	1.305					
Poly(3-chloropropylene oxide)	92.5	1.37	1.461		5.6			
Poly[2,2-bis(chloromethyl) trimethylene-3-oxide] (Penton)	155.0	1.39	1.47		3.2	0.96		32
Poly(2,6-dimethyl-1,4-phenylene ether) (PPE)	120.1	1.07	1.31			1.23	1.76	5.95
Poly(2,6-diphenyl-1,4-phenylene ether) (Tenax, P30)	244.3	<1.15		1.3				
<i>Polysulphides</i>								
Poly(propylene sulphide)	74.1	<1.10	>1.21/1.234					
Poly(phenylene sulphide)	108.2	<1.34	1.44					
<i>Polyesters</i>								
Poly(glycolic acid)	58.0	1.60	1.70					
Poly(ethylene succinate)	144.1	1.175	1.358	3.16	4.0		11.1	
Poly(ethylene adipate)	172.2	<1.183/1.221	1.25/1.45		5.9		15.9/21.0	
Poly(tetramethylene adipate)	200.2	<1.019					50.7	
Poly(ethylene azelate)	214.3		1.17/1.22					

(continued)

TABLE V (continued)

Polymers	Physical properties							
	T_g	T_m	δ	γ	n	ε	λ_a	λ_c
	K	K	J ^{1/2} /cm ^{3/2}	mN/m			J s ⁻¹ m ⁻¹ K ⁻¹	cm ³ mol ^{1/2} g ^{-3/2}
<i>Polymethacrylates</i>								
Poly(methacrylic acid)	501							0.066
Poly(methyl methacrylate)	378	433/473	18.6/26.4	27/44	1.490	2.6/3.7	0.15/0.20	0.042/0.090
Poly(ethyl methacrylate)	338		18.3	33	1.485	2.7/3.4		0.047
Poly(propyl methacrylate)	308/316				1.484	3.1		
Poly(isopropyl methacrylate)	300/354				1.552	3.0		
Poly(butyl methacrylate)	293		17.8/18.4		1.483	2.5/3.1		0.030/0.038
Poly(isobutyl methacrylate)	326		16.8/21.5		1.477			
Poly(sec.-butyl methacrylate)	333							
Poly(tert.-butyl methacrylate)	280/387	377/438	17.0		1.4638			
Poly(2-ethylbutyl methacrylate)	284							0.035
Polyl(hexyl methacrylate)	256/268				1.4813			0.042
Poly(octyl methacrylate)	253							0.030
Poly(dodecyl methacrylate)	208/218	239			1.4740			0.032/0.035
Poly(octadecyl methacrylate)		309						
Poly(phenyl methacrylate)	378/393				1.5706/1.7515			
Poly(benzyl methacrylate)	327		20.3		1.5679			
Poly(cyclohexyl methacrylate)	324/377				1.5065			0.034
<i>Other polyacrylics</i>								
Poly(methyl chloroacrylate)	416				1.517	3.4		
Polyacrylonitrile	378	591	25.6/31.5	44	1.514	3.1/4.2		0.225
Polymethacrylonitrile	393	523	21.9		1.52			0.220
Polyacrylamide	438			35/40				0.260
Poly(N-isopropylacrylamide)	358/403	473	21.9					
<i>Polydienes</i>								
Poly(1,3-butadiene)(cis)	171	284.7	17.6	32	1.516			0.145/0.185
Poly(1,3-butadiene)(trans)	190	415		31				0.200
Poly(1,3-butadiene)(mixt.)	188/215		17.0		1.518			
Poly(1,3-pentadiene)(trans)	213	368						
Poly(2-methyl-1,3-butadiene)(cis)	200	301.2	16.2/17.2	31	1.520			0.119/0.130
Poly(2-methyl-1,3-butadiene)(trans)	205/220	347		30				0.230
Poly(2-methyl-1,3-butadiene)(mixt.)	225					2.4	0.134	

Poly(2-tert. Butyl-1,3-butadiene)(cis)	298	379			1.506				
Poly(2 chloro-1,3-butadiene)(trans)	225	353/388	16.8/18.8						
Poly(2-chloro-1,3-butadiene)(mixt.)	228	316	16.8/19.0	38/44	1.158		0.19		0.095/0.135
<i>Polyoxides (Polyethers)</i>									
Poly(methylene oxide)	190	457.2	20.9/22.5	29/38	1.510	3.1/3.6	(0.16)/(0.42)	(0.62)	0.130/0.380
Poly(ethylene oxide)	206	342		43	1.4563/1.54	4.5			0.100/0.230
Poly(tetramethylene oxide)	189	330	17.0/17.5	32					0.180/0.33
Poly(ethylene formal)	209	328/347							0.200
Poly(tetramethylene formal)	189	296							
Polyacetaldehyde	243	438							
Poly(propylene oxide)	198	348	15.3/20.3	32	1.450/1.457	4.9			0.108/0.125
Poly(hexene oxide)	204	345							
Poly(octene oxide)	255	347			1.469				
Poly(trans-2-butene oxide)	277	387							
Poly(styrene oxide)	312	413/452							
Poly(3-methoxypropylene oxide)	211	330			1.463				
Poly(3-butoxypropylene oxide)	194	300			1.458				
Poly(3-hexoxypropylene oxide)	188	317			1.459				
Poly(3-phenoxypropylene oxide)	315	485							
Poly(3-chloropropylene oxide)		390/408	19.2						
Poly[2,2-bis(chloromethyl) trimethylene-3-oxide] (Penton)	281	353/459				3.0			
Poly(2,6-dimethyl-1,4-phenylene ether) (PPE)	483	580	19.0		1.575	2.6			
Poly(2,6-diphenyl-1,4-phenylene ether) (Tenax, P30)	500	730/770	19.6		1.64/1.68	2.8			
<i>Polysulphides</i>									
Poly(propylene sulphide)	221/236	313/326			1.596				
Poly(phenylene sulphide)	360	630				3.1	(0.29)		
<i>Polyesters</i>									
Poly(glycolic acid)	318	506							
Poly(ethylene succinate)	272	379			1.4744	5.0/5.5			
Poly(ethylene adipate)	203/233	320/338	~19.4			5.2			
Poly(tetramethylene adipate)	205	328.8				3.1			
Poly(ethylene azelate)	228	319				3.95			

(continued)

TABLE V (continued)

Polymers	M g/mol	Physical properties					
		ρ_a g/cm ³	ρ_c g/cm ³	e_g $10^{-4} \text{ cm}^3 \text{ g}^{-1} \text{ K}^{-1}$	e_l	c_p^s J g ⁻¹ K ⁻¹	c_p^l J g ⁻¹ K ⁻¹
<i>Polyesters (continued)</i>							
Poly(ethylene sebacate)	228.3	1.04/1.11	1.083/1.21	1.96	3.6/6.9		1.93/2.05
Poly(decamethylene adipate)	284.4		1.16		7.3		15.9/45.6
Poly(decamethylene sebacate)	340.5		1.13		7.5		30.2/56.5
Poly(α,α -dimethylpropiolactone)	100.1	1.097	1.23				14.9
Poly(para-hydroxybenzoate) (Ekonol)	120.1	<1.44	>1.48				
Poly(ethylene oxybenzoate) (A-tell)	164.2	<1.34				2.2	10.5
Poly(ethylene isophthalate)	192.2	1.34	>1.38	2.0	3.8/5.3		
Poly(ethylene terephthalate)	192.2	1.335	1.46/1.52	1.4/2.4	6.0/7.4	1.13	1.55
Poly(tetramethylene isophthalate)	220.2	1.268	<1.309				42.3
Poly(tetramethylene terephthalate)	220.2		<1.08	2.9		1.8	(10.6)/31/32
Poly(hexamethylene terephthalate)	248.3		1.146				33.5/35.6
Poly(decamethylene terephthalate)	304.4		1.012/1.022		5.3		43.5/48.6
Poly(1,4-cyclohexane dimethylene terephthalate) (trans)	274.3	1.19	1.265				
Poly(ethylene-1,5-naphthalate)	242.2	<1.37		1.56	3.43		
Poly(ethylene-2,6-naphthalate)	242.2	<1.33	>1.35	1.41	4.86		
Poly(1,4-cyclohexylidene dimethylene terephthalate) (Kodel) (cis)	274.3	1.21	1.303				
Poly(1,4-cyclohexylidene dimethylene terephthalate) (Kodel) (trans)	274.3	1.19	1.265				
<i>Polyamides</i>							
Poly(4-aminobutyric acid) (nylon 4)	85.1	<1.25	1.34/1.37				
Poly(6-aminohexanoic acid) (nylon 6)	113.2	1.084	1.23	2.7	5.6	1.47/1.59	2.13/2.47
Poly(7-aminoheptanoic acid) (nylon 7)	127.2	<1.095	1.21	3.5		>1.67/1.84	
Poly(8-aminoctanoic acid) (nylon 8)	141.2	1.04		3.1			

Poly(9-aminononanoic acid) (nylon 9)	155.2	<1.052	>1.066	3.6				
Poly(10-aminodecanoic acid) (nylon 10)	169.3	<1.032	1.109	3.5				
Poly(11-aminoundecanoic acid) (nylon 11)	183.3	1.01	1.12/1.23	3.6			41.4	
Poly(12-aminododecanoic acid) (nylon 12)	197.3	0.99		3.8	0.71		16.7	
Poly(hexamethylene adipamide) (nylon 6,6)	226.3	1.07	1.24		1.47		67.9	
Poly(heptamethylene pimelamide) (nylon 7,7)	254.4	<1.06	1.108					
Poly(octamethylene suberamide)(nylon 8,8)	282.4	<1.09						
Poly(hexamethylene sebacamide) (nylon 6,10)	282.4	1.04	1.19		1.59	2.18	30.6/58.6	
Poly(nonamethylene azelamide)(nylon 9,9)	310.5	<1.043						
Poly(decamethylene azelamide)(nylon 10,9)	324.5	<1.044		6.6			36.2/68.2	
Pol(decamethylene sebacamide) (nylon 10,10)	338.5	<1.032	>1.063	6.7			32.7/51.1	
Poly[bis(4-aminocyclohexyl)methane-1,10 - decanedicarboxamide](Qiana) (trans)	404.6	1.034	1.040		2.8		12	
Poly(m-xylylene adipamide)	246.3	<1.22	1.22/1.251					
Poly(p-xylylene sebacamide)	302.4	<1.14	1.169					
Poly(2,2,2-trimethylhexamethylene terephthalamide)	288.4	1.12			1.47			
Poly(piperazine sebacamide)	252.4			5.9			26.0/26.4	
Poly(metaphenylenе isophthalamide) (Nomex)	238.2	<1.33	>1.36	0.45		1.42		
Poly(p-phenylene terephthalamide) (Kevlar, Twaron)	238.2		1.48					
<hr/>								
<i>Poly carbonates</i>								
Poly[methane bis(4-phenyl)carbonate]	226.2	1.24	1.303					
Poly[1,1-ethane bis(4-phenyl)carbonate]	240.3		>1.22					
Poly[2,2-propene bis(4-phenyl)carbonate]	254.3	1.20	1.31	2.4/2.9	4.8/5.9	1.19	1.61	33.5
Poly[1,1-butane bis(4-phenyl)carbonate]	268.3		>1.17					
Poly[1,1-(2-methyl propane)bis(4-phenyl) carbonate]	268.3		>1.18					
Poly[2,2-butane bis(4-phenyl)carbonate]	268.3	<1.18						

(continued)

TABLE V (continued)

Polymers	Physical properties							
	T_g	T_m	δ	γ	n	ε	λ_a	λ_c
	K	K	J ^{1/2} /cm ^{3/2}	mN/m		J s ⁻¹ m ⁻¹ K ⁻¹		cm ³ mol ^{1/2} g ^{-3/2}
<i>Polyesters (continued)</i>								
Poly(ethylene sebacate)	243	356.2				4.1		
Poly(decamethylene adipate)	217	343/355						
Poly(decamethylene sebacate)		344/358				3.35		0.220
Poly(α , ω -dimethyl(propiolactone)	258/315	513						
Poly(para-hydroxybenzoate) (Ekonol)	>420	590/>770				3.3/3.8	0.75	
Poly(ethylene oxybenzoate) (A-tell)	355	475/500						
Poly(ethylene isophthalate)	324	416/513						
Poly(ethylene terephthalate)	342	553	19.8/21.9	40/43	1.64	2.9/3.2	0.22	(0.28) 0.15/020
Poly(tetramethylene isophthalate)		426						
Poly(tetramethylene terephthalate)	295/353	505				3.1		
Poly(hexamethylene terephthalate)	264/318	427/434						
Poly(decamethylene terephthalate)	268/298	396/411						
Poly(1,4-cyclohexane dimethylene terephthalate)(trans)	365	591						
Poly(ethylene-1,5-naphthalate)	344	503						
Poly(ethylene-2,6-naphthalate)	386/453	533/541						
Poly(1,4-cyclohexylidene dimethylene terephthalate) (Kodel) (cis)		530						
Poly(1,4-cyclohexylidene dimethylene terephthalate) (Kodel) (trans)	365	590						
<i>Polyamides</i>								
Poly(4-aminobutyric acid) (nylon 4)		523/538						
Poly(6-aminohexanoic acid) (nylon 6)	313	533	22.5	40/47	1.53	4.2/4.5		0.190/0.230
Poly(7-aminoheptanoic acid)(nylon 7)	325/335	490/506						
Poly(8-aminoctanoic acid)(nylon 8)	324	458/482	26.0					
Poly(9-aminononanoic acid)(nylon 9)	324	467/482						
Poly(10-aminodecanoic acid)(nylon 10)	316	450/465						
Poly(11-aminoundecanoic acid)(nylon 11)	319	455/493		33/43		3.7		

Poly(12-aminododecanoic acid)(nylon 12)	310	452			2.8/3.6	(0.24/0.35)		
Poly(hexamethylene adipamide) (nylon 6,6)	323	553	27.8	42/46	1.475/1.580	3.8/4.3		0.190/0.250
Poly(heptamethylene pimelamide (nylon 7,7)		469/487		43				
Poly(octamethylene suberamide) (nylon 8,8)		478/498		34				
Poly(hexamethylene sebacamide) (nylon 6,10)	303/323	488/506			1.475/1.565	3.5		
Poly(nonamethylene azelamide) (nylon 9,9)		450		36				
Poly(decamethylene azelamide) (nylon 10,9)		487						
Poly(decamethylene sebacamide) (nylon 10,10)	319/333	469/489		32		3.4/3.8		
Poly[bis(4-aminocyclohexyl)methane-1, 10-decanedicarboxamide](Qiana) (trans)	408/420	(548)/581						
Poly(m-xylylene adipamide)	363	518						
Poly(p-xylylene sebacamide)	388	541/573						
Pol(2,2,2-trimethylhexamethylene terephthalamide)					1.566	3.1/3.5	(0.21)	
Poly(piperazine sebacamide)	355	455						
Poly(m-phenylene isophthalamide)(Nomex)	545	660/700						
Poly(p-phenylene terephthalamide)(Kevlar)	580/620	770/870						
<i>Polycarbonates</i>								
Poly[methane bis(4-phenyl)carbonate]	393/420	513/573						
Poly[1,1-ethane bis(4-phenyl)carbonate]	403	468			1.5937	2.9		
Poly[2,2-propane bis(4-phenyl)carbonate]	418	608.2	20.3	35/45	1.585	2.6/3.0	0.19/0.24	0.180/0.277
Poly[1,1-butane bis(4-phenyl)carbonate]	396	443			1.5792	3.3		
Poly[1,1-(2-methyl propane) bis(4-phenyl) carbonate]	422	453			1.5702	2.3		
Poly[2,2-butane bis(4-phenyl)carbonate]	407	495			1.5827	3.1		

(continued)

TABLE V (continued)

Polymers	Physical properties						
	M	ρ_a	ρ_c	e_g	e_l	c_p^s	c_p^l
	g/mol	g/cm ³	g/cm ³	$10^{-4} \text{ cm}^3 \text{ g}^{-1} \text{ K}^{-1}$	$\text{J g}^{-1} \text{ K}^{-1}$	$\text{J g}^{-1} \text{ K}^{-1}$	kJ/mol
<i>Polycarbonates (continued)</i>							
Poly[2,2-pentane bis(4-phenyl)carbonate]	282.3			>1.13			
Poly[4,4-heptane bis(4-phenyl)carbonate]	310.4			>1.16			
Poly[1,1-(1-phenylethane)bis(4-phenyl)carbonate]	316.3			>1.21			
Poly[diphenylmethane bis(4-phenyl)carbonate]	378.4	<1.27					
Poly[1,1-cyclopentane bis(4-phenyl)carbonate]	280.3			>1.21			
Poly[1,1-cyclohexane bis(4-phenyl)carbonate]	294.3			>1.20			
Poly[thio bis(4-phenyl)carbonate]	244.3	1.355		1.500			
Poly[2,2-propane bis {4-(2-methyl)phenyl} carbonate]	282.3			>1.22			
Poly[2,2-propane bis {(4-(2-chlorophenyl)} carbonate]	323.2			>1.32			
Poly[2,2-propane bis {(4-(2,6-dichlorophenyl)} carbonate]	392.1			>1.42			
Poly[2,2-propane bis {(4-(2,6-dibromophenyl)} carbonate]	569.9			>1.91			
Poly[1,1-cyclohexane bis {(4-(2,6-dichlorophenyl)} carbonate]	432.1			>1.38			
<i>Other polymers</i>							
Poly(p-xylene)	104.1	1.05/1.10		1.08/125			10.0/16.5
Poly(chloro-p-xylene)	138.6	<1.28					
Poly($\alpha,\alpha,\alpha',\alpha'$ -tetrafluoro-p-xylylene)	176.1	<1.506		>1.597			
Poly(4,4'-tetramethylene dioxydibenzoic anhydride)	312.3	<1.266		>1.301			
Poly[4,4'-isopropylidene diphenoxy di(4-phenylene) sulphone] (polysulphone)	442.5	<1.24			1.35		
Poly[N,N'(p,p'-oxydiphenylene)-pyromellitimide] (Kapton)	382.3	1.42	(1.42)			1.51	
Poly(dimethylsiloxane)	74.1	0.98	1.07	2.7/3.2	9.14		1.47/1.59 2.6

See further Table VI.

Polymers	Physical properties							
	T_g	T_m	δ	γ	n	ε	λ_a	λ_c
	K	K	J ^{1/2} /cm ^{3/2}	m N/m			J s ⁻¹ m ⁻¹ K ⁻¹	cm ³ mol ^{1/2} g ^{-3/2}
<i>Polycarbonates (continued)</i>								
Poly[2,2-pentane bis(4-phenyl)carbonate]	410	493			1.5745			
Poly[4,4-heptane bis(4-phenyl)carbonate]	421	473			1.5602			
Poly[1,1-(1-phenylethane)bis(4-phenyl)carbonate]	449/463	503			1.6130			
Poly[diphenylmethane bis(4-phenyl)carbonate]	394	503			1.6539			
Poly[1,1-cyclopentane bis(4-phenyl)carbonate]	440	523			1.5993			
Poly[1,1-cyclohexane bis(4-phenyl)carbonate]	446	533			1.5900	2.6		
Poly[thio bis(4-phenyl)carbonate]	383	513						
Poly[2,2-propane bis {4-(2-methyl)phenyl}carbonate]	368/418	443			1.5783			
Poly[2,2-propane bis {(4-(2-chlorophenyl)}	420	483			1.5900			
carbonate]								
Poly[2,2-propane bis {(4-(2,6-dichlorophenyl)}	453/493	533			1.6056			
carbonate]								
Poly[2,2-propane bis {(4-(2,6-dibromophenyl)}	430	533			1.6147			
carbonate]								
Poly[1,1-cyclohexane bis {(4-(2,6-dichlorophenyl)}	446	543			1.5858			
carbonate]								
<i>Other polymers</i>								
Poly(p-xylylene)	333/353	700			1.669	2.65		
Poly(chloro-p-xylylene)	353/373	552/572			1.629	3.0		
Poly($\alpha,\alpha,\alpha',\alpha'$ -tetrafluoro-p-xylylene)	363	~773				2.35		
Poly(4,4'-tetramethylene dioxydibenzoic anhydride)	348	477						
Poly[4,4'-isopropylidene diphenoxy di(4-phenylene) sulphone] (polysulphone)	463/468	570	20.3		1.633	3.1	0.26	0.45
Poly[N,N'(p,p'-oxydiphenylene)-pyromellitimide] (Kapton)	600/660	770				3.5		
Poly(dimethylsiloxane)	150	234/244	14.9/15.6	20/24	1.4035/1.43	0.13/0.163	0.070/0.106	

See further Table VI.

TABLE VI Published data of "high performance" polymers

Generic name	Code symbol	Supposed structural formula	Trade name
Polyphenylene sulfide	PPS		Ryton® Fortron® Tedor® Supec®
Polysulfones	PES		{ Victrex® PES Ultrason®/E
	PS		Radel®
			{ Udel® Ultrason®/S
Polyketones	PEK		{ Victrex® PEK Ultrapek®
	PEEK		{ Victrex® PEEK Hostatec®
	PEKK		PEKK Kadel®
	PECO		Carilon
Polyarylates	PAR		Ekonol®
			{ Ardel® D100 Kodel®
			Durel® Arylon® 401
Liquid crystal Polymers (LCP's)	LCP		Vectra®
			Xydar® Ultrax®
			HX 4101 X7G Rodrun®

Manufacturer	T_g (°C)	T_m (°C)	HDT (°C)	Max			IZOD			ρ g/cm³	M g/mol	OI
				C.U.T. (°C)	E (GPa)	σ_{\max} (GPa)	ε_{\max} (%)	Impact (J/m)				
Phillips Petr. Hoechst/Celanese	85	275	266	240?	4.2	0.079	≥2	75 (16)	1.36	108	44	
	90	285	270			0.150		1	80			
ICI BASF	222		203	180	2.6	0.084	40	84		1.37	232	
	220		205	180	2.6	0.084		90		1.37		
Amoco	290		204		2.1	0.007	35			1.29	400	
Amoco BASF	190	(297)	174	166	2.6	0.070	50	69		1.27	442	
	182	(290)		150						1.37		
ICI BASF	161	367	300	260	3.8	0.100		85			196	
	145	324	395	250	3.7	0.092	50	83		1.3	288	35
ICI Hoechst	162											
	165	384		4.5	0.100	4				1.3	300	40
Amoco		326	260									
Shell	258		150	50	3.8					1.3	42	
-	(400)										120	
Amoco	177										358	
Eastman	173										358	
Hoechst/Celanese									1.2		26	
DuPont		160		2	68		288					
Hoechst/Celanese	280	230		10.5	140	3.0	50					
Amoco	280	270		10.5		4.9	50					
(Orig Dartco)												
BASF				~12.0			~40				48	
DuPont	275											
Eastman												
Unitica	175					4						

(continued)

TABLE VI (*continued*)

Generic name	Code symbol	Supposed structural formula	Trade name
Poly-aramides (ARAMIDS)	PPTA		{ Kevlar® Twaron®
Poly-amide-imides	PAI		Torlon®
Poly-imides	PEI		Ultem®
	PI		Larc®
			Avimid® K111
			Eymid®
			Kapton®
Polybenzo-bisoxazole	PBO		Zylon
Poly-benz-imidazoles	PBI		Celazole®
	PIPID		M5
Poly-phenyl-quinoxaline	PPQ		—
<i>For comparison:</i>			
Epoxy (phenoxy-) resin	EP		EP 3501
Polycarbonate	PC		{ Makrolon® Lexan®

Abbreviations: HDT = Heat distortion temperature; C.U.T = Continuous use temperature.

TABLE VII Code symbols for the most important polymers

ABS	Acrylonitrile-butadiene-styrene copolymer
AMMA	Acrylonitrile-methyl methacrylate copolymer
ASA	Acrylic ester-styrene-acrylonitrile copolymer
BR	Polybutadiene rubber
CA	Cellulose acetate
CAB	Cellulose acetobutyrate
CAP	Cellulose acetopropionate
CBR	Chloro-butadiene rubber
CF	Cresol formaldehyde
CMC	Carboxymethyl cellulose
CN	Cellulose nitrate
CP	Cellulose propionate
CPE	Chlorinated polyethylene
CPVC	Chlorinated poly(vinyl chloride)
CS	Casein resin
EC	Ethyl cellulose
EP	Epoxide resin
EPR	Ethylene-propylene rubber
EPTR	Ethylene-propylene terpolymer rubber
ETFE	Ethylene-tetrafluoroethylene copolymer
EU	Polyether-urethane
EVA	Ethylene-vinyl acetate copolymer
HD-PE	High-density polyethylene
IBR	Isobutylene rubber, Butyl rubber
IR	Isoprene rubber
LD-PE	Low-density polyethylene
MBS	Methyl methacrylate–butadiene–styrene copolymer
MF	Melamin-formaldehyde resin
NBR	Acrylonitrile–butadiene rubber
NCR	Acrylonitrile–chloroprene rubber
NR	Natural rubber
PA	Polyamide
PA 6	Polycaprolactam
PA 6,6	Poly(hexamethylene adipamide)
PA 6,10	Poly(hexamethylene sebacamide)
PA 11	Polyamide of 11-aminoundecanoic acid
PA 12	Polylaurolactam
PAA	Poly(acrylic acid)
PAI	Poly-amide-imide
PAN	Polyacrylonitril
PAR	Polyarylate
PARA	Polyaryl-amide
PAS(U)	Polyaryl sulfone
PAT	Poly-aminotriazole
PATR	Polyalkylene terephthalate thermoplastic rubber

(continued)

TABLE VII (*continued*)

PB	Poly(n.butylene)
PBI	Poly(benzimidazole)
PBMA	Poly(n.butyl methacrylate)
PBO	Poly(benzoxazole)
PBT(H)	Poly(benzthiazole)
PBTP	Poly(butylene glycol terephthalate)
PC	Polycarbonate
PCHMA	Poly(cyclohexyl methacrylate)
PCTFE	Poly(chloro-trifluoro ethylene)
PDAP	Poly(diallyl phthalate)
PDMS	Poly(dimethyl siloxane)
PE	Polyethylene
PEHD	High density polyethylene
PELD	Low density polyethylene
PEMD	Medium density polyethylene
PEC	Chlorinated polyethylene
PEEK	Poly-ether-ether ketone
PEG	poly(ethylene glycol)
PEI	Poly-ether-imide
PEK	Poly-ether ketone
PEN	Poly(ethylene-2,6-naphthalene dicarboxylate)
PEO	Poly(ethylene oxide)
PES	Poly-ether sulfone
PET	Poly(ethylene terephthalate)
PF	Phenol formaldehyde resin
PI	Polyimide
PIB	Polyisobutylene
PMA	Poly(methyl acrylate)
PMMA	Poly(methyl methacrylate)
PMI	Poly(methacryl imide)
PMP	Poly(methylpentene)
POB	Poly(hydroxy-benzoate)
POM	Polyoxymethylene = polyacetal = polyformaldehyde
PP	Polypropylene
PPE	Poly (2,6-dimethyl-1,4-phenylene ether) = Poly(phenylene oxide)
PPP	Polyparaphenylenne
PPPE	Poly(2,6-diphenyl-1,4-phenylene ether)
PPQ	Poly(phenyl quinoxaline)
PPS	Polyphenylene sulfide, polysulfide
PPSU	Polyphenylene sulfone
PS	Polystyrene
PSU	Polysulfone
PTFE	Poly(tetrafluoroethylene)
PTMT	Poly(tetramethylene terephthalate)
PU	Polyurethane
PUR	Polyurethane rubber

(continued)

TABLE VII (*continued*)

PVA(L)	Poly(vinyl alcohol)
PVAC	Poly(vinyl acetate)
PVB	Poly(vinyl butyral)
PVC	Poly(vinyl chloride)
PVCA	Vinyl chloride-vinyl acetate copolymer
PVDC	Poly(vinylidene chloride)
PVDF	Poly(vinylidene fluoride)
PVF	Poly(vinyl fluoride)
PVFM	Poly(vinyl formal)
PVK	Poly(vinyl carbazole)
PVP	Poly(N-vinyl pyrrolidone)
PY	Unsaturated polyester resin
RF	Resorcinol - formaldehyde resin
RP	Reinforced plastic
SAN	Styrene-acrylonitrile copolymer
SB	Styrene-butadiene copolymer
SBR	Styrene-butadiene rubber
SI	Silicone rubber
SIR	Styrene-isoprene rubber
SMS	Styrene- α -methylstyrene copolymer
TR	Thiokol rubber = Polyethylene sulfide
U(R)E	Polyurethane rubber, ether type
U(R)ES	Polyurethane rubber, ester type
UF	Urea-formaldehyde resin
UP	Unsaturated polyester resin
UR	Polyurethane rubber
VC/E	Vinyl chloride/ethylene copolymer
VC/E/MA	Vinyl chloride/ethylene/methyl acrylate terpolymer
VC/E/VAC	Vinyl chloride/ethylene/vinyl acetate terpolymer
VC/MA	Vinyl chloride/methylene acrylate copolymer
VC/MMA	Vinyl chloride/methyl methacrylate copolymer
VC/VAC	Vinyl chloride/vinyl acetate copolymer
VC/VDC	Vinyl chloride/vinylidene chloride copolymer

TABLE VIII Trade names and generic names

Trade or brand name	Product	Manufacturer
Abson	ABS polymers	Goodrich
Aclar	Polychlorotrifluoroethylene	Allied
Acilan	Polyacrylonitrile	Chemstrand
Acrylite	Poly(methyl methacrylate)	American Cyanamid
Adiprene	Polyether-based polyurethane (elastomer)	Du Pont
Akulon	Nylon plastic	DSM
Alathon	Polyethylene	Du Pont
Alkathene	Polyethylene resins	Imperial Chemical Industries
Amberlite	Ion-exchange resins	Rohm & Haas
Ameripol	Polyethylene	Goodrich-Gulf
Antron	Nylon fiber	Du Pont
Araldite	Epoxy resins	Ciba
Ardel	Polyarylate	Union Carbide
Ardil	Protein fiber	Imperial Chemical Industries
Arnel	Cellulose triacetate	Celanese
Arnite	Polyethylene terephthalate	DSM
Arnitel	Thermoplastic elastomer	DSM
Bakelite	Phenol-formaldehyde	Union Carbide
Cadon	Styrene-maleic acid copolymer, impact	Monsanto
Caprolan	Nylon 6 (polycaprolactam)	Allied
Carbowax	Polyethylene glycols	Union Carbide
Cariflex I	cis-1,4-Polyisoprene	Shell
Carilon	Ethylene-carbon monoxide altern. Copolymer	Shell
Carina	Polyvinyl chloride	Shell
Carinex	Polystyrene	Shell
Celanese	Aromatic polyester	Vectran
Celcon	Acetal copolymer	Celanese
Celluloid	Plasticized cellulose	Celanese
Chemigum	Polyester-based polyurethane (elastomer)	Goodyear
Collodion	Solution of cellulose nitrate	Generic name
Corfam	Poromeric film	Du Pont
Creslan	Acrylonitrile-vinyl ester	American Cyanamid
Cycolac	Acrylonitrile-butadiene-styrene terpolymer ABS	Borg-Warner
Cymac	Thermoplastic molding materials	American Cyanamid
Cymel	Melamine molding compound	American Cyanamid
Dacron	Polyester fiber	Du Pont
Darvan	Vinylidene cyanide-vinyl acetate copolymer	Celanese
Delrin	Acetal polymer	Du Pont
Desmodur	Isocyanates for polyurethane foam	Bayer
Desmopan	Polyurethanes	Bayer
Desmophen	Polyesters and polyethers for polyurethanes	Bayer

(continued)

TABLE VIII (*continued*)

Trade or brand name	Product	Manufacturer
Dowex	Ion-exchange resins	Dow
Durethan	Nylon 6	Bayer
Durethan U	Polyurethanes	Bayer
Durethane	Polyethylene film	Sinclair-Koppers
Dylan	Polyethylene resins	Sinclair-Koppers
Dyneema	Super-strong polyethylene fiber	DSM/Toyoba
Dynel	Acrylonitrile-vinyl chloride copolymer	Union Carbide
Elvacite	Methyl, ethyl, butyl methacrylate polymers and copolymers	Du Pont
Elvanol	Poly(vinyl alcohol) resins	Du Pont
Elvax	Poly(ethylene-co-vinyl acetate)	Du Pont
Epikote	Epoxy resins	Shell
Estane	Polyester-based polyurethane (elastomer)	Goodrich
Fluon	Polytetrafluoroethylene	Imperial Chemical Industries,
Fluon	PTFE powders and dispersions	Imperial Chemical Industries,
Fluorel	Poly(vinylidene fluoride)	Minnesota Mining and Mfg
Formica	Thermosetting laminates	Formica
Forticel	Cellulose propionate	Celanese
Fortiflex	Polyethylene	Celanese
Fortisan	Saponified cellulose acetate	Celanese
Fortrel	Polyester fiber	Fiber Industries
Galalith	Casein Plastics	Generic name
Geon	Poly(vinyl chloride)	Goodrich
Grilon	Nylon 6,12 copolymer	Emser Industries
Halar	Ethylene chlorotrifluoroethylene copolymer	Allied
Halon	Polytetrafluoroethylene	Allied
Herculon	Polypropylene	Hercules
Hi-Fax	Polyethylene	Hercules
Hostaflon C2	Polychlorotrifluoroethylene	Hoechst
Hostaflon TF	Polytetrafluoroethylene	Hoechst
Hostalen	Polyethylene	Hoechst
Hycar	Butadiene acrylonitrile copolymer	Goodrich
Hydropol	Hydrogenated polybutadiene	Phillips Petroleum
Hylene	Organic isocyanates	Du Pont
Hypalon	Chlorosulfonated polyethylene	Du Pont
Kapton	Polyimide	Du Pont
Kel-F	Trifluorochloroethylene resins	Minnesota Mining & Mfg
Keltan	Ethylene-propylene-diene terpolymer	DSM

(continued)

TABLE VIII (*continued*)

Trade or brand name	Product	Manufacturer
Kevlar	Poly(p-phenylene terephthalamide)	Du Pont
Kodel	Polyester fibers	Eastman Kodak
Kollidon	Poly(vinyl pyrrolidone)	General Aniline & Film
Kralastic	ABS	Uniroyal
Kraton	Butadiene block copolymers	Shell
Kynar	Poly(vinylidene fluoride)	Pennwalt
Leguval	Polyester resins	Bayer
Lekutherm	Epoxy resins	Bayer
Lexan	Polycarbonate	General Electric
Lycra	Polyurethane (fiber)	Du Pont
Lucite	Poly(methyl methacrylate)	Du Pont
Lustran	ABS	Monsanto
Lustrex	Polystyrene	Monsanto
Lutonal	Poly(vinyl ethers)	Badische
Luvican	Poly(vinyl carbazole)	Badische
Lycra	Spandex fibers	Du Pont
Makrolon	Polycarbonate	Bayer
Marbon	Polystrene and copolymers	Borg-Warner
Marlex	Polyolefin resins	Phillips Petroleum
Melinex	Poly(ethylene terephthalate)	Imperial Chemical Industries
Melurac	Melamine-urea resins	American Cyanamid
Merlon	Polycarbonate	Mobay
Moltopren	Polyurethane foam	Bayer
Mondur	Organic isocyanates	Mobay
Moplen	Polypropylene	Montecatini
Mowilith	Poly(vinyl acetate)	Hoechst
Mowiol	Poly(vinyl alcohol)	Hoechst
Mowital	Poly(vinyl butyral)	Hoechst
Multron	Polyesters	Mobay
Mylar	Polyester film	Du Pont
M5	Polydiimidazole	Magellan Systems, Du Pont
Natsyn	cis-1,4 Polyisoprene	Goodyear
Neoprene	Polychloroprene	Du Pont
Nomex	Poly(m-phenylene isophthalate)	Du Pont
Nordel	Ethylene-propylene	Du Pont
Noryl	Poly(phenylene oxide)-polystyrene blend	General Electric
Novodur	ABS polymers	Bayer
Nylon	Polyamides	Du Pont
Oppanol	Polyisobutylene	Badische
Orlon	Acrylic fiber	Du Pont
Parylene	Polyxylene	Union Carbide

(continued)

TABLE VIII (*continued*)

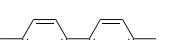
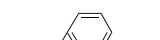
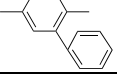
Trade or brand name	Product	Manufacturer
Penton	Chlorinated polyether resins	Hercules
Perbunan N	Butadiene-acrylonitrile copolymers	Bayer
Perlon	Polyurethane filament	Bayer
Perspex	Acrylic resins	Imperial Chemical Industries
Phenoxy	Polyhydroxy ether of bisphenol A	Union Carbide
Philprene	Styrene-butadiene rubber	Phillips Petroleum
Plaskon	Alkyd, diallyl phthalate	Allied
Plexiglas	Poly(methyl methacrylate)	Rohm & Haas
Pliofilm	Rubber hydrochloride	Goodyear
Plioflex	Poly(vinyl chloride)	Goodyear
Pliolite	Cyclised rubber	Goodyear
Pliovic	Poly(vinyl chloride)	Goodyear
Pluronic	Block polyether diols	Wyandotte
Polymin	Polyethylene-imine	Badische
Polyox	Poly(ethylene oxide)	Union Carbide
Polysizer	Poly(vinyl alcohol)	Showa
Polyviol	Poly(vinyl alcohol)	Wacker
PPE	Poly(phenylene ether)oxide	Hercules,
Prevex	Poly(phenylene ether)	Borg Warner
Profax	Polypropylene	Hercules
Propathene	Polypropylene	Imperial Chemical Industries, Du Pont
Quiana	Poly(<i>bis-p</i> -aminocyclohexylmethane dodecamide)	
Radel	Poly(aryl sulfone)	Union Carbide
Rilsan	Nylon 11	Aquitaine-Organico
Rynite	Poly(ethylene terephthalate) (glass reinforced)	Du Pont
Ryton	Poly(phenylene sulfide)	Phillips Petroleum
Saflex	Poly(vinyl butyral)	Monsanto
Santolite	Sulfonamide resin	Monsanto
Saran	Poly(vinylidene chloride)	Dow
Silastic	Silicone material	Dow Corning
Silastomer	Silicones	Midland Silicones
Solvic	Poly(vinyl chloride)	Solvay
Spandex	Polyurethane filaments	Du Pont
Spectra	Super-strong polyethylene fiber	Allied fibers
Stamylan	Polyethylene	DSM
Stanyl	Nylon 4,6	DSM
Styron	Polystyrene	Dow
Surlyn	Ionomer resins	Du Pont
Sylgard	Silicone casting resins	Dow Corning
Technora	Aromatic copolyamide	Teijin
Tedlar	Poly(vinyl fluoride)	Du Pont

(continued)

TABLE VIII (*continued*)

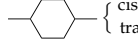
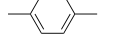
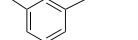
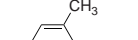
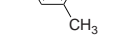
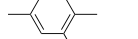
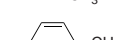
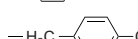
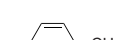
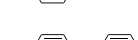
Trade or brand name	Product	Manufacturer
Teflon	Fluorocarbon resins	Du Pont
Teflon FEP	Tetrafluoroethylenehexafluoropropylene copolymer	Du Pont Teflon
Teflon TFE	Polytetrafluoroethylene	Du Pont
Tefzel	Tetrafluoroethylene-ethylene copolymer	Du Pont
Tenite	Polyethylene, Polypropylene and copolymers	Eastman
Tenite	Poly(ethylene terephthalate)	Eastman
Tenite	Cellulose-esters	Eastman
Terylene	Polyester fiber	ICI
Thiokol	Polyethylene sulfide	Thiokol
Torlon	Polyamide-imide	Amoco
Twaron	Poly(p-phenylene terephthalamide)	Teijin
Tygon	Poly(vinyl chloride) and copolymers	U.S. Stoneware
Tyvek	Spun-bonded polyolefin	Du Pont
Udel	Polysulfone	Union Carbide
Uformite	Urea resins	Rohm & Haas
Ultem	Polyether-imide	General Electric
Ultramid	Nylons	Badische
Valox	Poly(butylene terephthalate)	General Electric
Verel	Modacrylic staple fibers	Eastman
Versamid	Polyamide resins	General Mills
Vespel	Polymellitimide	Du Pont
Vestamid	Nylon 12	Hüls
Vestolit	Poly(vinyl chloride)	Hüls
Vestyron	Polystyrene	Hüls
Vibrathene	Polyurethane prepolymers	Uniroyal
Victrex	Poly(ether sulfone)	ICI
Vinylite	Poly(vinyl chloride co-vinyl acetate)	Union Carbide
Vinyon	Poly(vinyl chloride co-acrylonitrile)	Union Carbide
Vistanex	Polyisobutylene	Enjay
Vitel	Polyester resins	Goodyear
Viton	Copolymer of vinylidene fluoride and hexafluoropropylene	Du Pont
Vulcaprene	Polyurethane	Imperial Chemical Industries, Mobay
Vulkollan	Urethane elastomer	General Electric
Xenoy	Poly(butylene terephthalate)-polycarbonate blend	Toyoba
Zylon	Polybenzoxazole	Du Pont
Zytel	Nylon	

TABLE IX Survey of group contributions in additive molar quantities

Group	Z	M	V_a	V_w	C_p^s	C_p^l	ΔS_m	Y_g	Y_m	E_{coh}	F_{small}	P_s
	g/mol	cm ³ /mol	cm ³ /mol	J/mol K	J/mol K	J/mol K	g K/mol × 10 ⁻³	J/mol	(J cm ³) ^{1/2} /mol			
<i>Bifunctional hydrocarbon groups</i>												
-CH ₂ -	1	14.03	16.37	10.23	25.35	30.4	(9) ²	2.7 ⁴	5.7 ⁷	4190	272	39.0
-CH(CH ₃) ₃ - (s,as)	1	28.05	32.7	20.45	46.5	57.85	9.0	8.0	13.0	10,060	495	78.0
-CH(C ₆ H ₅)-	1	82.14	82	53.28	110.8	147.5		30.7		(24,000)	1430	208.3
-CH(C ₆ H ₁₁)-	1	96.17	101	63.58	121.2	173.9		41.3			1680	244.9
-CH(C ₆ H ₅)-	1	90.12	84	52.62	101.2	144.15	9.5	36.1	48	31,420	1561	211.9
-C(CH ₃) ₂ -	1	42.08	49	30.67	68.0	81.2	19 ³	8.5/26 ⁵	12.1/39 ⁵	13,700	686	117.0
-C(CH ₃)(C ₆ H ₅)-	1	104.14	100.5	62.84	122.7	167.5		51	54	35,060	1752	250.9
-CH=CH- { cis trans }	2	26.04	27	16.94	37.3	42.8	12.5 0	3.8 7.4	8.0 11	10,200	454	67.0
-CH=C(CH ₃)- { cis trans }	2	40.06	42.8	27.16	60.05	74.22	0.1 16	8.1 9.1	10 13	14,500	(704)	106.0
-C≡C-	2	24.02	25	16.1						71,600	435	56.0
-Cyclohexyl- { cis trans }	4	82.14	86	53.34	103.2	147.5		19 27	31 45		1410	205.9
<i>Monofunctional hydrocarbon groups</i>												
	4	76.09	65.5	43.32	78.8	113.1	(5)	29/41 ⁶	38/56 ⁶	25,140	1346	172.9
	3	76.09	69	43.32	78.8	113.1		25/34 ⁶	31/42 ⁶	(26,000)	1346	172.9
	2	76.09	65.5	43.32	78.8	113.1					1346	172.9
	4	104.14	104	65.62	126.8	166.8	5	54	(67)	(40,000)	1900	250.9
	4	90.12	87	54.47	102.75	140.1		35	(45)		(1600)	211.9
	5	90.12	80	53.55	104.15	143.5				29,330	1618	211.9
-H ₂ C- 	6	104.14	97	63.78	129.5	173.9		25	47	33,520	1890	250.9
	9	166.21	150	96.87	182.95	256.6		65	85	54,470	2964	384.8
	8	152.18	134	86.64	157.6	226.2		70	99	50,280	2692	345.8
	4	228.22	208	130	236	339	10	118	173	(92,500)	4000	518.7

(continued)

TABLE IX (continued)

Group	J	R _{LL}	R _{GD}	P _{LL}	X	U _R	U _H	H _η	ΔG _f ⁰	Y _{d,1/2}
	$\frac{g^{1/4}}{cm^{3/2}/mol^{3/4}}$	cm^3/mol	cm^3/mol	cm^3/mol	$10^{-6} cm^3/mol$ (cgs)	$cm^{10/3}/(s^{1/3} mol)$	$cm^{10/3}/(s^{1/3} mol)$	(g/mol) ^{1/3}	$J/mol \times 10^{-3}$	g K/mol
<i>Bifunctional hydrocarbon groups</i>										
-CH ₂ -	2.35	4.65	7.83	4.65	11.35	880	675	420	- 22,000 + 102 T	9.3
-CH(CH ₃)- (s,as)	4.7	9.26	15.62	9.26	23.5	1875	1650	1060	- 48,700 + 215 T	18.5
-CH(C ₅ H ₅)-		25.65	43.77	(25.65)	63.5	(4600)			- 73,400 + 548 T	
-CH(C ₆ H ₁₁)-	11.15	30.30	51.75						- 118,400 + 680 T	60
-CH(C ₆ H ₅)-	19.4	29.03	50.97	29.12	62	4900	4050	3600	84,300 + 287 T	56.5
-C(CH ₃) ₂ -	7.1	13.87	23.36	13.86	36	2850	2350	1620	-72,000 + 330 T	25.5/35 ^b
-C(CH ₃)(C ₆ H ₅)-	21.8	33.44	58.41	33/72	74.5	6100			61,000 + 402 T	56
-CH=CH- { cis trans }	0.5	8.88	15.50	8.9	13.2	1400			76,000 + 76 T	18
-CH=C(CH ₃)- { cis trans }	2.9	13.49	23.24		25.6	2150			42,000 + 183 T	21.5
-C≡C-					14	1240			36,000 + 190 T	
	8.0	25.70	44.00						230,000 - 50 T	
									- 96,400 + 578 T	
									- 102,400 + 585 T	
	16.3	25.03	44.8	25.0	50	4100	3300	3200	100,000 + 180 T	54/75 ^b
		25.00	44.7		50	4050	3100		100,000 + 180 T	44/65 ^b
	24.72	44.2			50				100,000 + 180 T	
	34.8	61.0			75	6100	4800		33,000 + 394 T	82
	29.9	52.7			63				66,500 + 287 T	
	18.65	29.53	52.06	29.65	61	4980			78,000 + 282 T	
	21.0	34.03	59.32	34.3	73	5860			56,000 + 384 T	7.3
	34.95	54.56	96.9	54.65	111	9080			178,000 + 462 T	(114)
	32.6	50.06	89.6	50.0	100	8200			200,000 + 360 T	122
	74.9	134.0			152	12650			299,000 - 538 T	93

(continued)

TABLE IX (continued)

Group	Z	M	V_a	V_w	C_p^s	C_p^l	ΔS_m	Y_g	Y_m	E_{coh}	F_{small}	P_s
		g/mol	cm ³ /mol	cm ³ /mol	J/mol K	J/mol K	J/mol K	g K/mol × 10 ⁻³	J/mol	(J cm ³) ^{1/2} mol		
<i>Other hydrocarbon groups (continued)</i>												
-CH ₃	0	15.03	23	13.67	30.9	36.9			9,640	438	56.1	
-C ₂ H ₅	0	29.06	38.5	23.90	56.25	67.3			13,830	710	95.1	
-nC ₃ H ₇	0	43.09	55.5	34.13	81.6	97.7			18,020	982	134.1	
-iC ₃ H ₇	0	43.09	55.5	34.12	77.4	94.75			19,700	933	134.1	
-tC ₄ H ₉	0	57.11	74	44.34	99.0	118.1			23,340	1124	173.1	
>CH-	1	13.02	10.8	6.78	15.9	20.95	0.6		420	57	21.9	
>C<	1	12.01	5.32	3.33	6.2	7.4			-5580	-190	4.8	
=CH ₂	0	14.01		11.94	22.6	21.8				389	50.6	
=CH-	1	13.02	13.8	8.47	18.65	21.8			5100	227	33.5	
=C<	1	12.01	8.0	5.01	10.5	15.9			(-240)	39	16.4	
=C=	1	12.01		6.96						266	28.0	
-CH=C<	2	25.03	21	13.48	29.15	37.3			4860		49.9	
≡CH	0	13.02		11.55						356	45.1	
≡C-	1	12.01		8.05						227	28.0	
>C=C< { cis	2	24.02	(12.24)	10.02	21.0	31.8			(-480)	78	32.8	
trans											34.5	
CH _{ar} -	1	13.02		8.06	15.4	22.2						
→C _{ar} -	1	12.01		5.54	8.55	12.2					17.4	
—Cyclohexyl	0	69.12		46.56	95.2	126.55				1370	186.4	
—Cycloheptyl	0	83.15		56.79	105.6	152.95				1620	223.0	
—Benzyl	0	77.10	64.65	45.84	85.6	123.2			31,000	1504	190.0	
—4-Methylbenzyl	4	74.08		38.28	65.0	93.0			(970)		138.7	
—4-Ethylbenzyl	4	75.08		40.80	71.85	103.2			(1160)		155.8	
<i>Bifunctional oxygen containing groups</i>												
-O-	1	16.00	(8)	3.71/[5.8] ^l	16.8	35.6	6	4	13.5 ⁸	6290	143	20.0
>C=O { alif	1	28.01	13.6	8.5	(18.5)	11.7	(0)	11.5	15.5	(17,500)	563	(48)
arom			18.5	11.7				28	29			
-O-CO- { general	2	44.01	24.6	15.2/[17.0] ^l	(46)	65.0	4	12.5/15 ⁶	30 ⁸	13,410	634	64.8
acrylic			21.0									
-O-CO-O-	3	60.01	31	18.9/[23.0] ^l	(63)		(0)	20	(30) ⁸	(18,000)	775	84.8
-OC-O-CO-	3	72.02	(40)	(27)	(63)	(114)	(0)	22	35 ⁸	40,000	1160	(113)
-CH(OH)-	1	30.03	23	14.82	32.6	65.75		13	21			59.0
-CH(COOH)-	1	58.04			(65.6)	119.85						103.8
-CH(HC=O)-	1	42.14		21.92								(87)
—COO-	6	120.10	86.0	58.52	(124.8)	178.1	(58)			38,550	1980	237.7
-O-CH ₂ -O-	3	46.03	33.45	17.63	58.95	101.6		10.7	32.7	16,770	558	79.0

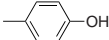
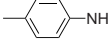
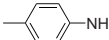
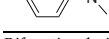
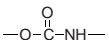
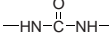
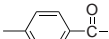
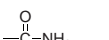
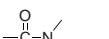
(continued)

TABLE IX (continued)

Group	J	R _{LL}	R _{GD}	P _{LL}	X	U _R	U _H	H _η	ΔG _f ⁰	Y _{d,1/2}
	g ^{1/4} cm ^{3/2} / mol ^{3/4}	cm ³ /mol	cm ³ /mol	cm ³ / mol	10 ⁻⁶ cm ³ / mol	cm ^{10/3} / (s ^{1/3} mol)	cm ^{10/3} / (s ^{1/3} mol)	(g/mol) (J/mol) ^{1/3}	J/mol × 10 ⁻³	g K/mol
<i>Other hydrocarbon groups (continued)</i>										
-CH ₃	3.55	5.64	8.82	5.64	14.5	1400	1130	810	-46,000 + 95 T	
-C ₂ H ₅	5.9	10.29	16.65	10.29	25.85	2280			-68,000 + 197 T	
-nC ₃ H ₇	8.25	14.94	24.48	14.94	37.2	3160		3350	-90,000 + 199 T	
-iC ₃ H ₇	8.25	14.90	24.44	14.90	38	3250			-94,700 + 310 T	
-tC ₄ H ₉	10.65	19.51	32.18	19.50	50.5	4250			-118,000 + 425 T	
>CH-	1.15	3.62	6.80	3.62	9	460	370	250	-2,700 + 120 T	
>C<	0	2.58	5.72	2.58	7	40	35	0	20,000 + 140 T	
=CH ₂		5.47	8.78		9				23,000 + 30 T	
=CH-	0.25	4.44	7.75		6.6	745	600	380	38,000 + 38 T	
=C<	-0.9	3.41	6.67		4.5	255	200	0	50,000 + 50 T	
=C=		4.23	7.62						147,000 - 20 T	
-CH=C<	-0.65	7.85	14.42		11.1	750			88,000 + 88 T	
≡CH						9			112,500 - 32.5 T	
≡C-						7			115,000 - 25 T	
>C=C< { cis	-1.8	6.81	13.34		9	100			100,000 + 100 T	
trans						9.2	830	665	94,000 + 107 T	
—CH _{ar} —									12,500 + 26 T	
—C _{ar} —						7	400	320	25,000 + 38 T	
—Cyclopentyl		22.0	36.97						-70,700 + 428 T	
—Cyclohexyl	10.0	26.69	44.95						-115,700 + 560 T	
—Biphenyl	18.25	25.51	44.63	25.5	53	5000	4000		87,000 + 167 T	
—Phenyl-phenyl		23.85	44.72		46.4	3300	2600		125,000 + 204 T	
—Phenyl-phenyl		24.4	44.76		48.6	3700	2590		112,500 + 192 T	
<i>Bifunctional oxygen containing groups</i>										
-O-	0.1	1.59/1.77 ⁹	2.75/2.96 ⁹	5.2	5	400	300	480	-120,000 + 70 T	8
>C=O	(9)	4.53/5.09 ¹⁰	7.91/8.82 ¹⁰	(10)	6.5	875	600		-132,000 + 40 T	14/26 ⁶
-O-CO-{ general	9.0	6.21/	10.47/							
acrylic	6.4	6.71 ¹¹	11.31 ¹¹	15	14	1225	900	1450	-337,000 + 116 T	20/25 ⁶
-O-CO-O-	(27.5)	7.75 ¹²	13.12/13.39 ¹²	22	19	1575	1200	3150		(30)
-OC-O-CO-		(10.7)	(18.4)	(25)	18	(2150)				(50)
-CH(OH)-	(9.15)	6.07	10.75	(10)	16.5	1050			-178,700 + 170 T	14
-CH(COOH)-	9.15	10.83	18.79		28				-395,700 + 238 T	
-CH(HC=O)-		9.45	16.43		17.4				-127,700 + 146 T	
—C ₆ H ₄ -COO—	25.3	31.74	56.1	40	64	5350			-237,000 + 296 T	
-O-CH ₂ -O-	2.55	7.93	13.45	15.05	21.35	1680			-262,000 + 242 T	

(continued)

TABLE IX (*continued*)

Group	Z	M	V_a	V_w	C_p^s	C_p^l	ΔS_m	Y_g	Y_m	E_{coh}	F_{small}	P_s
		g/mol	cm ³ /mol	cm ³ /mol	J/mol K	J/mol K	J/mol K	g K/mol × 10 ⁻³	J/mol	(J·cm ³) ^{1/2} /mol		
<i>Other oxygen containing groups</i>												
—OH	0	17.01		8.04	17.0	44.8						37.1
 —OH	0	93.10		51.36	95.8	157.9						210.0
—CH=O	0	29.01		15.14								(65)
—COOH	0	45.02			(50)	98.9						81.9
<i>Bifunctional nitrogen containing groups</i>												
—NH—	1	15.02	12.8	8.08	14.25	(31.8)	7	18				29.6
—CH(CN)—	1	39.04		21.48	(40.6)				25,420	896		(86)
—CH(NH ₂)—	1	29.04		17.32	36.55							68.6
 —NH—	5	91.11		(51.4)	93.05	(144.9)						202.5
<i>Other nitrogen-containing groups</i>												
—NH ₂	0	16.02		10.54	20.95							46.7
>N—	1	14.01		4.33	17.1	(44.0)						12.5
 N _{ar}	1	14.01										
—C≡N	0	26.02		14.7	(25)				25,000	839		63.7
 —NH ₂	0	92.12		53.86	99.75							219.6
 —N—	5	90.10		47.65	95.9	(157.1)						185.4
<i>Bifunctional nitrogen and oxygen containing groups</i>												
 —C(=O)NH—	2	43.03	(25)	19.56/[18.1] ¹	(38/54)	(90.1)	2	15/30 ⁶	45/60 ^{6,8}	60,760	(1160)	(78)
 —O—C(=O)NH—	3	59.03	(30)	(23)	(58)			20	(43.5) ⁸	(26,500)	(1200)	(94)
 —HN—C(=O)NH—	3	58.04	(30)	(27.6)	(50)		0	20	(60) ⁸	(35,000)	(1500)	(107)
—CH(NO ₂)—	1	59.03		23.58	57.5							960
 —C(=O)NH—	6	119.12		62.88	(116.8/132.8)	(203.2)		(7.0)	98	85,900		
<i>Other nitrogen and oxygen containing groups</i>												
 —C(=O)NH ₂	0	44.03		(22.2)								
 —C(=O)N—	2	42.02		(16.0)								
—NO ₂	0	46.01		16.8	41.9							900

(continued)

TABLE IX (continued)

Group	J	R_{LL}	R_{GD}	P_{LL}	X	U_R	U_H	H_n	ΔG_f⁰	Y_{d1/2}
	$\text{g}^{1/4}/\text{cm}^{3/2}/\text{mol}^{3/4}$	cm^3/mol	cm^3/mol	10^{-6}	$\text{cm}^{10/3}/(\text{s}^{1/3}\text{ mol})$	$\text{cm}^{10/3}/(\text{s}^{1/3}\text{ mol})$	(g/mol)	$\text{J}/\text{mol} \times 10^{-3}$	g/K/mol	
<i>Other oxygen containing groups</i>										
-OH	(8)	2.45/ 2.55 ¹³	3.85/ 4.13 ¹³	(6)	7.5	630	500		-17,6000 + 50 T	
	(24.3)	27.30	48.33	(45)	57.5	4700			- 76,000 + 230 T	
-CH=O		5.83	9.63		8.4				-125,000 + 26 T	
-COOH	8.0	7.21	11.99		19				-393,000 + 118 T	
<i>Bifunctional nitrogen-containing groups</i>										
-NH-		3.59	6.29		9	875	800		58,000 + 120 T	16
-CH(CN)-	(16.15)	9.14	15.88	14.6	20				120,000 + 91.5 T	28
-CH(NH ₂)-		7.97	14.05		21				8,800 + 222.5 T	
		29.56	53.48		59				158,000 + 300 T	
<i>Other nitrogen-containing groups</i>										
-NH ₂		4.36	7.25		12				11,500 + 102.5 T	
>N-		2.80	5.70		6	65	50		97,000 + 150 T	
					12				69,000 + 50 T	
-C≡N	(15)	5.53	9.08	11	11	1400	1150		123,000 - 28.5 T	
		29.92	53.2		62				111,500 + 282.5 T	
		29.08	53.5		56	4200			197,000 + 330 T	
<i>Bifunctional nitrogen- and oxygen containing groups</i>										
	12.6	7.23	15.15	30	14	1750	1400	1650	-74,000 + 160 T	30/ 37 ⁶
	(25)		(16.9)		20	(2100)			-279,000 - 240 T	32.5
			(20.5)		(27)	(2000)			-16,000 + 280 T	(40)
-CH(NO ₂)-		10.28	17.81						-44,200 + 263 T	
	28.9	33.5	62.9	55	64	5800				
<i>Other nitrogen- and oxygen containing groups</i>										
	(23)				17					
	(8)				11	(1000)				
-NO ₂		6.66	11.01						-41,500 + 143 T	

(continued)

TABLE IX (*continued*)

	Z	M	V_a	V_w	C_p^s	C_p^l	ΔS_m	Y_g	Y_m	E_{coh}	F_{small}	P_s
Group		g/mol	cm ³ /mol	cm ³ /mol	J/mol K	J/mol K	J/mol K	g K/mol × 10 ⁻³	J/mol	(J·cm ³) ^{1/2} /mol		
<i>Bifunctional sulphur containing groups</i>												
-S-	1	32.06	17.3	10.8	24.05	44.8	2	8	22.5 ⁸	8800	460	48.2
-SS-	2	64.12	36	22.7	(48.1)	(89.6)		16	30	(17,600)	(920)	(96.4)
-SO ₂ -	1	64.06	32.5	20.3	(50)		(0)	32/40 ⁶	56/66 ⁶			
-S-CH ₂ -S-	3	78.15	46.45	31.8	73.45	120.0				21,790	1192	135.4
<i>Other sulphur-containing groups</i>												
-SH	0	33.07		14.81	46.8	52.4				644		65.3
<i>Bifunctional halogen containing groups</i>												
-CHF-	1	32.02	19.85	13.0	(37.0)	(41.95)	5	12.4	17.4	4890	(307)	47.6
-CF ₂ -	1	50.01	24.75	15.3	(49.0)	(49.4)	7	10.5	25.5	3360	(310)	56.2
-CHCl-	1	48.48	28.25	19.0	42.7	(60.75)	10.2	19.4	27.5	13,410	609	76.2
-CCl ₂ -	1	82.92	41.55	27.8	60.4	(87.0)	11	22.0	29	20,400	914	113.4
-CH=CCl-	2	60.49	41	25.72	56.25	(77.1)	9.6	15.2	32	17,850	818	104.2
-CFCl-	1	66.47	33.15	21.57	(54.7)	(68.2)	(9)	28	32	11,880	(612)	84.8
-CHBr-	1	92.93		21.4	41.9					15,920	753	89.9
-CBr ₂ -	1	171.84		32.5	58.8					25,420	1202	140.8
-CHI-	1	139.93		27.1	38.0						927	112.9
-Cl ₂ -	1	265.83		44.0	51.0						1550	186.8
<i>Other halogen containing groups</i>												
-F	0	19.00	10.0	6.0	(21.4)	(21.0)				4470	(250)	25.7
-CF ₃	0	69.01	34.75	21.33	(70.4)	(70.4)				7830	(560)	81.9
-CHF ₂	0	51.02	29.85	18.8	(58.4)	(62.95)				9360	(557)	73.3
-CH ₂ F	0	33.03	26.45	16.2	(46.75)	(51.4)				8660	(522)	64.7
-Cl	0	35.46	18.4	12.2	27.1	(39.8)				12,990	552	54.3
-CCl ₃	0	118.38	59.95	(40)	87.5	(126.8)				33,390	1344	167.7
-CHCl ₂	0	83.93	46.65	31.3	69.8	(100.55)				26,400	1121	130.5
-CH ₂ Cl	0	49.48	34.85	22.5	52.45	(70.2)				17,180	824	93.3
	0	111.55	79.8	55.3	105.9	(152.9)				38,130	1898	227.2
-Br	0	79.92		14.6	26.3					15,500	696	68.0
-CBr ₃	0	251.76		(47.1)	85.1					40,920	1898	208.8
-CHBr ₂	0	172.85		36.0	68.					31,420	1449	157.9
-CH ₂ Br	0	93.94		24.8	51.65					19,690	968	107.0
-I	0	126.91		20.4	22.4						870	91.0
-Cl ₃	0	392.74		(64.4)	73.4						2420	277.8
-CHI ₂	0	266.84		47.5	60.4						1797	203.9
-CH ₂ I	0	140.94		30.6	47.75						1142	130.0

Significance of annotations in Table IX:

1. Between square brackets (in **V_w**-columns): **V_w**-values of Slonimskii et al. (1970).
2. The ΔS_m -value is 9.9 in carbon main chains; -1.6 in carbon side chains; ≈8.5 in hetero-chains.
3. The ΔS_m -value is 19 in polyisobutylene; between two aromatic rings it may be as high as 58.
4. The Y_g -value is 2.7 in main chains; in hydrogen-bonded hetero-chains it is 4.3; for side chains see equations 6.6/8.
5. The lower Y_g -value of 8.5 is valid for polyisobutylene only; the higher value is the maximum for strong steric hindrance, e.g. between two aromatic ring-systems.
6. The lower Y_g -value is for non-conjugated groups; the higher values are for groups with maximum conjugation.
7. The general value for CH₂-sequences larger than 6 is 5.7; for smaller CH₂-sequences in main chains, see Table 6.10; for side chains use Eqs. (6.22)/(6.24).
8. The odd-even effect in hetero-chains makes a correction necessary; use Table 6.12.
- 9-12. In general the lower values are valid for the group between 2 CH₂-groups; the higher values are valid for the group, if it is attached to an aromatic ring.

TABLE IX (continued)

Group	J	R _{LL}	R _{GD}	P _{LL}	X	U _R	U _H	H _η	ΔG _f ⁰	Y _{d1/2}
	g ^{1/4} cm ^{3/2} /mol ^{3/4}	cm ³ /mol	cm ³ /mol	cm ³ /mol	10 ⁻⁶ cm ³ /mol	cm ^{10/3} /(s ^{1/3} mol)	cm ^{10/3} /(s ^{1/3} mol)	(g/mol)/(J/mol) ^{1/3}	J/mol × 10 ⁻³	g K/mol
<i>Bifunctional sulphur containing groups</i>										
-S-	8.07	14.44		8	16	550	(440)		40,000 – 24 T	(3.3)
-S-S-	16.17	29.27		16	(32)				46,000 – 28 T	
-SO ₂ -	(12)					1250	1000		-282,000 + 152 T	(50)
-S-CH ₂ -S-	20.8	36.71		21	43				58,000 + 54 T	
<i>Other sulphur-containing groups</i>										
-SH	8.79/9.27 ¹⁴	15.14/15.66 ¹⁴			18				13,000 – 33 T	
<i>Bifunctional halogen containing groups</i>										
-CHF-	4.51	7.68		(5.42)	15.6	(950)			-197,700 + 114 T	18
-CF ₂ -	4.38	7.12		6.25	20.2	(1100)	900		-370,000 + 128 T	38.5
-CHCl-	13.4	9.64	16.71	13.7	27.5	1725	1450	2330	-51,700 + 111 T	23.5
-CCl ₂ -	24.5	14.63	25.54	17.7	44	2350			-78,000 + 122 T	39
-CH=CCl-	11.6	13.87	24.33		29.6	1900			39,000 + 79 T	
-CFCI-		9.50	16.3	(13.9)	32.1	(1700)			-224,000 + 125 T	39
-CHBr-	(12.15)	12.57	22.06		36.5				-16,000 + 106 T	
-CBr ₂ -	(22)	20.49	36.24		62				-8,000 + 112 T	
-CHI-	17.52	31.80			52				37,300 + 79 T	
-Cl ₂ -	30.38	55.72			93				100,000 + 58 T	
<i>Other halogen containing groups</i>										
-F	0.90 ¹⁵	0.70/0.88 ¹⁵	(1.8)	6.6	(530)	(400)			-195,000 – 6 T	
-CF ₃	5.27	7.83		25	(1550)				-565,000 + 122 T	
-CHF ₂	5.41	8.20			22.2	(1450)			-392,700 + 108 T	
-CH ₂ F	5.55	8.71	(6.45)	18.0	(1380)				-217,000 + 96 T	
-Cl	12.25	5.93/6.05 ¹⁶	9.84/10.07 ¹⁶	(9.5)	18.5	1265	(1000)	2080	-49,000 – 9 T	
-CCl ₃	36.75	20.7	35.93		60	3500			-127,000 + 113 T	
-CHCl ₂	25.65	15.7	26.94		46	2750			100,000 + 102 T	
-CH ₂ Cl	14.6	10.7	17.90	(14.15)	30	2030			-71,000 + 93 T	
 -Cl	28.55	30.63	53.62	(34.5)	68.5	5250			51,000 + 171 T	
-Br	(11)	8.90/9.03 ⁷	15.15/15.29 ¹⁷		27.5	1300	1000		-14,000 – 14 T	
-CBr ₃	(33)	29.3	51.2		89.5				-22,000 + 98 T	
-CHBr ₂	(23.15)	21.4	37.10		64				-30,700 + 92 T	
-CH ₂ Br	(13.35)	13.5	22.98		39				-36,000 + 88 T	
-I		13.90	25.0		43				40,000 – 41 T	
-CI ₃		44.3	80.7		136				140,000 + 17 T	
-CHI ₂		31.4	56.8		95				77,300 – 38 T	
-CH ₂ I		18.5	32.83		54				18,000 + 61 T	

9. 1.59 and 2.96 for methyl ethers; 1.63 and 2.75 for acetals; 1.64 and 2.81 for higher ethers; 1.77 and 2.84 for groups attached to benzene ring.

10. 4.79 and 8.42 for methyl ketones; 4.53 and 7.91 for higher ketones; 5.09 and 8.82 for groups attached to benzene ring.

11. 6.24 and 10.76 for methyl esters; 6.38 and 10.94 for ethyl ethers; 6.21 and 10.47 for higher esters; 6.71 and 11.31 for groups attached to benzene ring; 6.31 and 10.87 for acetates.

12. 7.75 and 13.39 for methyl carbonates; 7.74 and 13.12 for higher carbonates.

13–17. The higher values are those of tertiary groups.

13. 2.55 and 4.13 for primary alcohols; 2.46 and 3.96 for secondary alcohols; 2.45 and 3.85 for tertiary alcohols.

14. 8.85 and 15.22 for primary, 8.79 and 15.14 for secondary, and 9.27 and 15.66 for tertiary thioalcohols.

15. 0.90 and 0.88 for mono-, 0.90 and 0.70 for per-substituted F.

16. 6.05 and 10.07 for primary, 6.02 and 9.91 for secondary, and 5.93 and 9.84 for tertiary Cl-atoms.

17. 8.90 and 15.15 for primary, 8.96 and 15.26 for secondary, and 9.03 and 15.29 for tertiary Br-atoms.

This page intentionally left blank

INDEXATION

*"Whenever I found out anything remarkable,
I have thought it my duty to put down my discovery on paper,
so that all ingenious people might be informed thereof."*

Anthonie van Leeuwenhoek, 1632–1723

This page intentionally left blank

SYMBOL INDEX

		Used in Chapter
a	Constant	General
a	Activity	18
a	Exponent of the Mark–Houwink equation	2, 7, 9, 6
a	Surface per unit volume	3
a	Lattice spacing	13
a	1/2 Crack length	13
a	Long semi-axis of an ellipse	13
a	Long side in slit rheometer	15
a	Pressure constant in Van der Waals isotherm	18
a_{cr}	1/2 Critical crack length	13
a_p	Persistence length	9
a_P	WLF pressure–temperature shift factor	13
a_{PT}	WLF combined time–pressure–temperature shift factor	13
a_{STV}	Weir mouldability index	24
a_T	WLF time–temperature shift factor	13
A	Constant	General
A	Area	General
A	atomic weight	3
A	Kuhn length/statistical chain length	9
A	Original area	24
A_o	Value of A for zero concentration	23
A_R	Reference value of A	23
A_2	Second virial coefficient	9, 10
b	Constant	General
b	Bond angle factor	9
b	Short side in slit rheometer	15
b	Short semi-axis of an ellipse	18
b	Volume constant in Van der Waals equation	18
b	Langmuir activity coefficient	18
b	Thickness, width	9, 25
b_o	Thickness of chain molecules	19
b_T	Shift factor in Eq. (13.140)	13
B	Constant	General
B	Interaction parameter	9
\mathbf{B}	Bulk modulus	4, 13, 23
B	Extrudate swell ratio/die swell	15
B	Magnetic flux density	12
B	Finger deformation tensor	13
B^{-1}	Reciprocal Finger deformation tensor/Cauchy deformation tensor	13
B_o	Reducing parameter	4

B_{loc}	Local magnetic flux density in Eqs. (12.21) and (12.22)	12
B_o	Magnetic field strength	12
B_R	Magnetic field strength corresponding to the resonance frequency of nucleus	12
c	Concentration	General
c_o	Original concentration	18
c_∞	Final concentration	18
\tilde{c}	Reduced concentration	16
c^*	Critical concentration	9
c_x, c_{cr}	Ditto, in Rudin equations	9, 16
c_p	Specific heat capacity at constant pressure	General
c_p^a	Specific heat capacity of amorphous polymer	19
c_p^c	Specific heat capacity of crystalline polymer	19
c_p^l	Specific heat capacity of liquid polymer	5
c_p^s	Specific heat capacity of solid polymer	5
c_v	Specific heat capacity at constant volume	5, 13, 17
c_1^g, c_2^g	Constants in WLF equation with T_g as reference temperature	13
c_1^o, c_2^o	Constants in WLF equation with T_o as reference temperature	13
c_1^S, c_2^S	Constants in WLF equation with T_S as reference temperature	15
C	Constant	General
CR	Char residue (% by weight)	3, 21, 23, 26
C_o	Constant in Eq. (13.37)	13
C_p	Molar heat capacity at constant pressure	General
C_p^l	Molar heat capacity of liquid polymer	5, 6
C_p^s	Molar heat capacity of solid polymer	5, 6
C_v	Molar heat capacity at constant volume	5, 13
C_{FT}	Molar char formation tendency	3, 21, 23
C_H^s	Saturation capacity in "holes"	18
C_e	Constant in Eq. (13.155)	13
C_Λ	Constant in Eq. (13.152)	13
C_σ	Stress optical coefficient	10, 15
C_2	Constant in sorption and transport equations	18
C_1^*	Constant, approximately equal to 2070 K	19
d	Diameter, thickness, depth, distance	13, 15, 18, 24, 25
d_1	Indentation depth	25
d_{iso}	Diameter of a thread in the isotropic state	14
D	Diameter of cylindrical rod	18
D	Diameter	25
D	Diffusivity	3, 9, 16, 18, 23
D	Distance	13
D	Electric flux density/electric displacement/electric induction	12
D_a	Diffusivity of amorphous polymer	18

D_D	Diffusivity of dispersed component	18
D_H	Diffusivity in "holes"	18
D_m	Smoke density index	26
D_o	Limiting diffusion coefficient	9, 16
D_o	Reference value of diffusivity	18
\bar{D}	Average diffusion coefficient	19
e	Correction factor in Eq. (15.A3)	15
e	Electric charge	3
e	Specific thermal expansivity	3, 4, 23
e_c	Thermal expansivity of a crystal	4
e_{ch}	Tensile modulus parallel to chain axis	18
e_\perp	Tensile modulus perpendicular to chain axis	18
e_{coh}	Cohesive energy density	General
e_g	Thermal expansivity of a glass	4
e_1	Thermal expansivity of a liquid	4, 7
E	Energy content	12
E	Extinctivity (attenuation coefficient)	10
E	Electric field	12
E	Modulus of elasticity (Young's modulus)	General
E_{act}	Activation energy	General
E_c	Tensile modulus of crystalline polymer	13
E_d	Contribution of dispersion forces to the cohesive energy	7
E_D	Activation energy of diffusion	18, 19
$E_{D,o}$	Value of E_D for zero concentration	18
E_{Dg}	Activation energy of diffusion in the glassy state	18
E_{diss}	Bond dissociation energy	21
E_{Dr}	Activation energy of diffusion in the rubbery state	18
E^F	Young's modulus of fibre	13
E_g	Tensile modulus of glassy polymer	13
E_h	Contribution of the hydrogen bonding forces to the cohesive energy	7
E_{in}	Initial Young's modulus	13
E_{iso}	Value of E for isotropic material	13
E_L	Local electric field	12
E_{max}	Maximum value of tensile modulus	13
E_M	Maxwell spring constant in Burgers' element	13
E_p	Contribution of the polar forces to the cohesive energy	7
E_p	Activation energy of permeability	18
E_R	Reference value of E	13, 25
E_{rl}	Relaxation modulus	13
E_{sd}	Activation energy for transport (self diffusion)	19
E_{subl}	Sublimation energy/lattice energy	13
E_{VK}	Voigt–Kelvin spring constant in Burgers' element	13
E_η	Activation energy for viscous flow	15, 16, 24
$E_{\eta(\infty)}$	Value of E_η for $T \gg T_g$	3, 15, 16, 23
E_o	Initial value of E	13
E_o	Newtonian value of E	15
E^*	Complex tensile modulus	13

$ E^* $	Absolute value of E^*	13
E'	Real component of E^*	13
E''	Imaginary component of E^*	13
ϵ	Molar thermal expansivity	3, 4, 13, 23
ϵ_c	Molar thermal expansivity of crystalline polymer	4
ϵ_{coh}	Molar cohesive energy	General
ϵ_g	Molar thermal expansivity of a glass	4, 23
ϵ_l	Molar thermal expansivity of a liquid	4, 7
f	Cross section of rodlet	19
f	Force per unit volume	3
f	Free volume fraction	13
f_c	Free volume fraction at concentration c	16
$f_{c,s}$	Degree of surface crystallinity	8
f_{el}	Electric field per unit volume	3
f_g	Free volume fraction at T_g	13
f_H	Fraction of unrelaxed volume in the glassy state	16
f_p	Fractional volume of pure polymer	16
F	Force	13, 24, 25
F	Dimensionless ratio D_H/D_o	8
F	Correction factor in surface energy equations	8
F_{max}	Maximum force	24
F	Additive function	3
F	Molar attraction function	3, 7, 23
F_d	Dispersion component of the molar attraction function	7
F_p	Polar component of the molar attraction function	7
g	Gravitational acceleration	3, 23, 25
g	Splitting factor	12
g	Correlation factor	11
g	Shear modulus parallel to symmetry axis	13, 19
g_d	Shear modulus of domain surrounding a chain segment	13
g_e	Gyromagnetic ratio of electron/spectroscopic splitting factor	12
g_N	Dimensionless constant	12
G	Shear modulus (rigidity)	13, 14, 15, 23
G	Molar loss area	14
G_c	Rigidity of crystalline polymer	13
G_g	Rigidity of glassy polymer	13
G_i	Constant in Eq. (15.58)	15
G_r	Shear modulus of the rubbery plateau	13
G_R	Reference value of G	13
G_{sc}	Rigidity of semi-crystalline polymer	13
G_o	Newtonian shear modulus	15, 16
G_C	Work done per unit area of crack surface creation	13
G_{IC}	Work done per unit area of crack surface creation due to tensile stress	13
G_{IIC}	Work done per unit area of crack surface creation due to sliding stress	13

G_{IIC}	Work done per unit area of crack surface creation due to tearing	13
G^*	Complex shear modulus	13, 15, 25
$ G^* $	Absolute value of complex shear modulus	13, 15
G'	Real component of complex shear modulus	13, 15, 25
G''	Imaginary component of complex shear modulus	13, 15, 25
$[G']_R$	Reduced storage modulus	16
$[G''']_R$	Reduced loss modulus	16
ΔG	Free enthalpy change	20
ΔG_M	Free energy of mixing	7
ΔG_o	Standard free enthalpy change of reaction	20
ΔG_f^o	Standard free enthalpy of formation	3, 20, 23
ΔG_{xy}^o	Standard molar free enthalpy difference when a monomer in state x is transformed into a polymer in state y	20
ΔG_n^*	Free enthalpy (Gibbs free energy) of formation of nucleus of critical size	19
h	Planck's constant	12, 20
h	Heat transfer coefficient	3
h	Height	4
h	Specific enthalpy	19
h_a	Specific enthalpy of amorphous polymer	19
h_c	Specific enthalpy of amorphous polymer	19
Δh_{comb}	Specific enthalpy of combustion	26
Δh_m	Specific enthalpy of fusion	19
Δh_M	Specific enthalpy of mixing	7
Δh_m^c	Specific enthalpy of fusion of crystalline polymer	19
H	Magnetic field strength	12
H_p	Indentation hardness	25
H_R	Reference magnetic field strength	12
H_o	Unshielded magnetic field strength	12
H_o^o	Cohesive energy at 0 K (after Bondi)	7
ΔH	Change in heat content	24
ΔH_{comb}	Heat of combustion	26
ΔH_m	enthalpy of mixing	7
ΔH_s	Heat of solution	18
ΔH_{sg}	Heat of solution for a glassy polymer	18
ΔH_{sr}	Heat of solution for a rubbery polymer	18
$\Delta H_{1/2}$	Line width at half height	12
H	Magnetic field intensity	12
H	Molar enthalpy	5
H_c	Molar enthalpy of crystalline substance	5
H_l	Molar enthalpy of liquid	5
H_η	Molar viscosity-temperature function	3, 15, 23
ΔH_f^o	Standard enthalpy of formation	20
ΔH_m	Molar enthalpy of fusion	5, 6, 7, 13, 19
ΔH_{vap}	Molar enthalpy of evaporation	3, 7
ΔH^o	Standard enthalpy of reaction	20

ΔH_{xy}^o	Standard molar enthalpy difference when monomer in state x is transformed into polymer in state y	20
ΔH_o^*	Standard enthalpy of activation	20
i	$\sqrt{(-1)}$	General
i_θ	Intensity of light per unit volume at angle θ	10
I	Ionic strength	9
I	Intensity of light	10, 19
I	Impact strength	14, 25
I	Moment of inertia	25
I	Nuclear spin quantum number	12
I	Orbital angular momentum	12
I_a	Intensity of radiation for amorphous polymer	19
I_c	Intensity of radiation for crystalline polymer	19
I_z	Component of spin angular momentum in the direction of magnetic field	12
Iz	Izod impact strength	25
$j(t)$	Time dependent compliance of domain surrounding chain segment	13
J^*	Complex shear compliance	13
$ J^* $	Absolute value of complex shear compliance	13
J'	Real component of complex shear compliance	13
J''	Imaginary component of complex shear compliance	13
J	Transport flux	18
J_e	Equilibrium shear compliance	15
J_e^0	Elastic shear compliance	15
J	Molar intrinsic viscosity function	3, 9
k	Constant	General
k	Reaction rate constant	3, 20, 22
k	Extinction index = n''	10
k_B	Boltzmann constant	10, 11, 19, 20
k_D	Concentration coefficient of diffusion	16
k_e	Constant	8
k_H	Huggins constant	16, 23
k_I	Rate constant of first order reaction	3
k_K	Kraemer constant	16
k_m	Mass transfer coefficient	3
k_s	Constant	8
k_s	Concentration coefficient of sedimentation	16
k_{tr}	Transfer constant	21
K	Constant	12, 13
K'	constant	12, 13
K	Mark-Houwink constant	9, 16
K	Absorption index	10

K	Bulk modulus (compression modulus)	3, 13, 14, 25
K	Constant in Eqs. (16.28)–(16.31)	16
K	Dimensionless ratio $C_H^s b/S$	18
K	Slope	18
K_C	Critical stress energy factor in crack formation	13
K_{IC}	Critical stress energy factor in crack formation due to tensile stress	13
K_D	Constant in Eq. (9.73)	9
K_{cr1}	Constant in Eq. (6.13)	6
K_{eq}	Equilibrium constant	3, 20
K_f	Equilibrium constant of formation reaction	20
K_g	Constant in Eqs. (6.10) and (6.11)	6
K_r	Constant in Eq. (9.16)	9
K_s	Constant in Eq. (9.69)	9
K_Θ	Unperturbed viscosity coefficient	3, 9, 15, 19, 23
l	Bond length	4, 9
l	Length (per unit volume)	3, 10
L	(characteristic) Length	General
L	Crack length	13
L	length of rod	16
L	Constant in Eq. (17.7) of the order of 5×10^{-11} m	17
L	Average free path length	17
L	Membrane thickness	18
L	Spiral length	24
L	Projection length of a chain onto the fibre axis at tensile stress	13
L_o	Projection length of a chain onto the fibre axis in unloaded state	13
L_{ch}	Contour length of polymer molecule	9
L_{eff}	Effective flow length	15
L_{max}	Maximum length	24
L_o	Original length	13, 15, 24
LA	Loss area	14
LCP	Liquid crystal polymer	General
LOI	Limiting oxygen index	26
m	Constant	14
m	Mass	18
m_e	Mass of electron	12
m_H	Mass of proton	12
m_I	Magnetic quantum number	12
M	Magnetization	12
M	Molar mass (molecular weight)	General
\mathbf{M}	Molar mass per structural unit	General
M_b	Molar mass of branched polymer	9
M_c	Molar mass between cross-links	13
M_{cr}	Critical molar mass	9, 13, 15, 16
M_e	Molar mass between entanglements	13

M_l	Molar mass of linear polymer	9
M_u	Molecular mass of the "interacting unit"	7
M_{crl}	Molecular mass of the polymer segment between cross-links	6, 13
M_n	Number-average molecular mass	2, 3, 13
M_v	Viscosity-average molecular mass	2, 9, 24
M_w	Weight-average molecular mass	2, 3, 10, 15
M_z	z-Average molecular mass	2
M_{z+1}	($z + 1$)-average molar mass	15
MI	Melt index	24
MMD	Molar mass distribution	2
MWD	Molecular weight distribution	2
n	Constant	General
n	Number	General
n	Index of refraction	3, 10, 11, 13, 23
n	Ostwald–de Waele constant	15, 24
n_D	Refractive index in sodium light	10, 11, 23
n_{iso}	Refractive index of isotropic material	14
n_p	Number of particles	9
n_p	Refractive index of polymer	10
n_s	Refractive index of solvent	10, 23
n_ϕ	Number of phenylene groups per structural unit	6
\bar{n}	Average index of refraction	10
n^*	Complex refractive index	11
n'	Real part of complex refractive index = n = index of refraction	10
n''	Imaginary part of complex refractive index = k = extinction index	10
$n_{//}$	Refractive index in parallel direction	10
n_{\perp}	Refractive index in perpendicular direction	10
n_{crl}	Number of backbone atoms between cross-links	6
Δn	Birefringence	10, 11, 15
N	Number	General
N	Number of nuclei per unit volume	19, 23
N_{Av}	Avogadro number	General
N_1	First normal stress difference	13, 15, 16
N_2	Second normal stress difference	13, 15, 16
\dot{N}	Rate of nucleation	19
OI	Oxygen index	26
p	Constant	16
p	Pressure	General
p	Parameter defined by Eq. (18.17)	18
p_y	Yield pressure	25
\tilde{p}	Reduced pressure	4
P	Polarisation	11
P	Permeability	18
P_{at}	Atomic polarisation	11

P_c	Buckling load	25
P_{dip}	Dipole polarisation	11
P_{el}	Electronic polarisation	11
$P(0)$	Reduced intensity of scattered light	10
P_o	Initial value of P	2
P^*	Complex driving force	2
P^*	Standard permeability	18
\mathbf{P}	Molar dielectric polarization	3, 11
\mathbf{P}_{LL}	Molar dielectric polarization according to Lorentz and Lorenz	11, 23
\mathbf{P}_s	Parachor	3, 4, 8, 23
\mathbf{P}_{so}	Reference value of \mathbf{P}_s	3
\mathbf{P}_v	Molar dielectric polarization according to Vogel	11, 23
P_2	Order parameter/Hermans' orientation function	13, 15
q	Heat production rate per unit volume	3
q	Temperature coefficient of density	4
q	(constant) Shear rate	10, 13, 15, 16
q	Wave number($= 2\pi/\lambda$)	10
q	Cooling rate	13
q_e	(constant) Rate of elongation	13, 15, 16
Q	Distribution factor ($= M_w/M_n$)	2, 15, 29
Q'	Distribution factor ($= M_z/M_w$)	2
Q	Amount of heat	5, 13, 26
Q	Volume flow rate	15
r	Ratio	General
r	Radius	General
r	Reaction rate per unit volume	3
r	End-to-end distance of polymer chain	9, 19
r	Reflectance	10
r_{crit}	Radius of critical spherical nucleus	19
r_i, r_o, r_{av}	Inner, outer and average radii of slit in Couette cylinders	15
r_{max}	End-to-end distance of fully extended polymer chain	9
r_o	Ideal specular reflectance	10
r_p	Reflectance coefficient of p-polarised light	10
r_s	Reflectance coefficient of s-polarised light	10
r_{sr}	Specular reflectance of rough surface	10
R	Gas constant	General
R	Response	2
R	Atomic radius	4
R	Volume resistivity	11
R	Resilience	13
R_G	Radius of gyration	9, 10
R_{Go}	Unperturbed radius of gyration	9, 15
R_{max}	Maximum radius of spherulites	19
R_0	Rayleigh's ratio	10
R_o	Initial value of response R	2
R^*	Complex response	2

R_p	Reflectance of p-polarised light	10
R_s	Reflectance of s-polarised light	10
R	Molar refraction	3, 10
R_{GD}	Molar refraction according to Gladstone and Dale	3, 10, 23
R_{LL}	Molar refraction according to Lorentz and Lorenz	3, 10, 11, 23
R_v	Molar refraction according to Vogel	3, 10, 11, 23
s	Weight factor	6
s	Sedimentation coefficient	9, 16
s	Skeletal factor	9
s	Scaling factor of permachor	18
s_o	Limiting sedimentation coefficient	9, 16
s_g	Pressure coefficient of T g	6
\dot{s}	Rate of dissolution	19
Δs_m	Specific entropy of fusion	3, 23
S	Response coefficient	2
S	Entropy	5
S	Molar entropy	5
S	Spreading coefficient	8
S	Distance from centre of gravity	9
S	Tensile compliance	13
S	Solubility	18
S_a	Solubility of amorphous polymer	18
S_{in}	Initial tensile compliance	13
S_o	Reference value of S	2, 18
S_2	Second moment defined in Eq. (12.31)	12
S^*	Complex response coefficient	2
$ S^* $	Absolute value of complex response coefficient	2
S'	Real component of the response coefficient	2
S''	Imaginary component of the response coefficient	2
S_o	Initial value of S	13
S^*	Complex tensile compliance	13
$ S^* $	Absolute value of complex tensile compliance	13
S'	Real component of complex tensile compliance	13
S''	Imaginary component of complex tensile compliance	13
ΔS	Entropy change	20
ΔS_M	Entropy of mixing	7
ΔS_o^*	Standard entropy of activation	20
ΔS_m	Entropy of fusion	3, 5, 6, 7, 23
ΔS^o	Standard entropy of activation	20
ΔS_{xy}^o	Standard molar entropy difference when monomer in state x is transformed into polymer in state y	20
t	Time	General
t_{br}	Time-to break	13, 25
t_f	Freeze-off time	24
t_{fat}	Fatigue life	25
t_R	Reference time	13, 23, 25
t_{res}	Residence time	3

t_s	Flow time of solvent	9
t_o	Oscillation period	25
$t_{1/2}$	Time of half conversion	19, 23
T	Temperature	General
T	Torque	25
T	Magnetic relaxation time	12
T	Stress tensor	13
T_b	Boiling point	7, 18
T_c	Ceiling temperature	20
T_{cl}	Clearing temperature	16
T_{cr}	Critical temperature	7, 18
T_d	Temperature of damping peak	13, 14
$T_{d,1/2}$	Temperature of half decomposition	21
T_g	Glass–rubber transition temperature	General
$T_{g(L)}$	Lower glass transition temperature	6
$T_{g(U)}$	Upper glass transition temperature	6
$T_{g,n}$	Transition temperature glass/nematic	6
$T_{g,s}$	Transition temperature glass/smectic	6
T_{gP}	Glass transition temperature of polymer	16
T_{gS}	Glass transition temperature of solvent	16
T_i	Clearance temperature of LCPs	6
T_{ij}	i,j Component of stress tensor	13
T_k	Crystal disordering temperature in LCPs	6
T_k	Temperature of maximum crystal growth	19
T_{ll}	Liquid–liquid relaxation temperature	6
T_m	Crystalline melting point	General
T_m^o	“Effective” melting point	19
T_{mS}	Melting point of solvent	16
T_r	Reduced temperature: $(T - \Theta)/\Theta$	9
T_p	Transmittance of p-polarised light	10
T_s	Transmittance of s-polarised light	10
T_R	Reference temperature	13, 15, 18, 20, 23
T_R	Trotou ratio = η_e/η	13, 15, 16
T_S	Standard temperature	15
T_{tr}	Second order transition temperature	6
$T_{s,i}$	Transition temperature smectic/isotropic	6
T_α	Temperature of α -transition	6
$T_{\alpha c}$	Premelting transition temperature	6
T_β	Transition temperature of β -relaxation	6
T_o	Reducing parameter	4
T_o	Wall temperature	24
$T_{1/2}$	Characteristic temperature for half conversion	21
T_∞	Characteristic temperature at which polymer chain segmental transport tends to zero	19
\tilde{T}	Reduced temperature	4
T_1	Spin-lattice relaxation time/longitudinal relaxation time	12
T_{1G}	Rotating frame relaxation time	12
T_2	Spin-spin relaxation time/transverse relaxation time	12
T_{CP}	Cross polarisation relaxation time	12

u	Sound velocity	13, 17
u_B	Bulk velocity of sound	13, 14
u_{ext}	Velocity of propagation of extensional waves	13, 14
u_L	Longitudinal sound velocity	3, 13, 17, 23
u_{sh}	Velocity of propagation of transverse waves	13, 14
U	Non-uniformity index ($= Q-1$)	2
U	Internal energy	5, 7
U^*	Complex disturbance	10
U_o	Amplitude of disturbance	10
U_R	Rao function or molar sound velocity function	3, 13, 17, 23
U_H	Hartmann function or molar shear sound velocity	13, 14
ΔU_{vap}	Energy of evaporation	7
v	Specific volume	General
v	Velocity	General
v	Rate of crystal growth	19, 23
v_o	Reference value of v	19, 24
v_o	Reducing parameter of v	4
v_1	Velocity in x_1 direction	15
v_a	Specific volume of amorphous polymer	19
v_c	Specific volume of crystalline polymer	19
v_h	Hydrodynamic volume per particle	9
v_{\max}	Maximum rate of growth	General
v_w	Velocity at the wall	15
V	Volume general	16
V_{act}	Activation volume	13
V_{cr}	Critical volume	18
V_D	Molar volume of diffusing molecule	18
V_R	Retention volume	2
V_s	Parameter with additive properties	6
V_{solv}	Volume of a solvated polymer molecule	16
V	Molar volume per structural unit general	6
V_a	Molar volume of amorphous polymer	4
V_c	Molar volume of crystalline polymer	4
V_g	Molar volume of glassy amorphous polymer	4, 23, 24
V_1	Molar volume of organic liquids	4, 8, 21
V_r	Molar volume of rubbery amorphous polymer	4
V_s	Molar volume of solid	8
V_S	Molar volume of solvent	4
V_{sc}	Molar volume of semi-crystalline polymer	4 12
V_w	Van der Waals volume	4, 7, 12
V_o	Reference value of V	3, 13, 12
$V^o(0)$	Zero point molar volume	4
ΔV_g	Excess molar volume of glassy amorphous polymer	4 12
ΔV_{g0}	Value of ΔV_g at 0 K	4
ΔV_m	Melting expansion	4

w	Weight fraction of molecules	2
w	Weight factor	3
w	Water content	18
W	Weight, load	General
W	Heat stored per unit volume during sinusoidal deformation	13
W	Width	24
W_{adh}	Work of adhesion	8
W_{coh}	Work of cohesion	8
W_o	Original width	24
ΔW^*	Work required to form a crystal nucleus	19
x	Degree of polymerisation	General
x	Length coordinate	3, 9, 15, 18, 24
x	Fraction of material	19
x_c	Degree of crystallinity	General
x_{crl}	Degree of cross-linking	6
X	Property	General
X	Molar magnetic susceptibility	3, 12, 23
y	Maximum beam deflection	25
$Y_{d,1/2}$	Molar thermal decomposition function	3, 21
Y_g	Molar glass transition function	3, 23
Y_m	Molar melt transition function	3, 6, 23
z_{crl}	Average number of cross-links per structural unit	13
Z	Number of backbone atoms per structural unit	6, 9, 19
Z_{cr}	Critical value of the number of chain atoms in the polymer molecule	15
α	Coefficient of thermal expansion	General
α	Relative position of $-\text{CH}_2-$ to functional group	6
α	Molecular aggregation number	7
α	Expansion factor	9, 19
α	Molecular polarisability	10, 11
α'	Molecular polarisability volume	10, 11
α	First order hyper-polarisability tensor	11
α	Sonic absorption coefficient	14
α	Half angle of natural convergence	15
α	Exponent e.g. In Eq. (16.21)	16
α	Coefficient, constant	18
α_c	Coefficient of thermal expansion of crystalline polymer	4
α_d	Molecular distortional polarisation	10
α_f	Coefficient of thermal expansion of free volume	13
α_g	Coefficient of thermal expansion of glassy polymer	4, 6, 16
α_{gP}	Expansion coefficient of polymer below T_g	16

α_{gS}	Expansion coefficient of solvent below T_g	16
α_h	Hydrodynamic expansion factor	9
$\alpha_{h,cr}$	Hydrodynamic expansion factor at $M = M_{cr}$	9
α_i	Degree of ionization	9
α_l	Coefficient of thermal expansion of liquid polymer	4, 6, 16
α_L	Longitudinal sonic absorption coefficient	14
α_{IP}	Expansion coefficient of polymer above T_g	16
α_{IS}	Expansion coefficient of solvent above T_g	16
α_s	Molecular orientational polarisability	16
α_{sh}	Shear sonic absorption coefficient	14
α_{STV}	Mouldability index	24
$\alpha_{//}$	Polarisability parallel to the direction of the chain	10
α_{\perp}	Polarisability perpendicular to the direction of the chain	10
β	Linear coefficient of thermal expansion	4
β	Relative position of $-CH_2-$ to functional group	6
$\pmb{\beta}$	Second order hyper-polarisability tensor	11
β	Critical or maximum strain value	13
β	Constant	18
β	Angle between rods	16
β	Degree of bulkiness of a side group	19
β	Constant in Eqs. (16.42)–(16.46)	16
β	Half angle of natural convergence	15
β_B	Bohr magneton	12
β_f	Compressibility of free volume	13
β_N	Nuclear magneton	12
β_p	Pressure dependence of viscosity	15
β_T	Temperature dependence of viscosity	15
γ	Surface tension	General
γ	Relative position of $-CH_2-$ to functional group	6
γ	Exponent introduced by De Gennes	9
$\pmb{\gamma}$	Third order hyper-polarisability tensor	11
γ	Magneto-gyric ratio	12
γ	Constant	18
γ	Shear deformation	13, 15
γ	Shift factor	16
γ_{cr}	Critical surface tension of wetting	8
γ_c	Elastic shear deformation	15
γ_l	Surface tension of liquid	8
γ_l^d	Dispersion component of surface tension of liquid	8
γ_l^h	Hydrogen bonding component of surface tension of liquid	8
γ_{rec}	Recoverable shear	13
γ_s	Surface tension of a solid	8
γ_s^d	Dispersion component of surface tension of a solid	8
γ_s^a	"Polar" component of surface tension of a solid	8
γ_{sl}	Interfacial tension between liquid and solid	8
γ_{sv}	Surface tension of the solid in equilibrium with the saturated vapour pressure of the liquid	8
γ^d	Dispersion component of the surface tension	8

γ^a	"Polar" component of the surface tension	8
γ^{AB}	Surface tension due to Lewis acid-base interactions	8
γ^D	Surface tension due to Debye interactions	8
γ^K	Surface tension due to Keesom interactions	8
γ^L	Surface tension due to London interactions	8
γ^{LW}	Surface tension due to Lifschitz–Van der Waals interactions	8
γ^+	Surface tension due to electron-acceptor interactions	8
γ^-	Surface tension due to electron-donor interactions	8
γ_o	Amplitude of the imposed dynamic shear	15
γ_o	Reference value of surface tension	3
γ_{12}	Interfacial tension	8
$\gamma_{//}$	Interfacial free energy per unit area parallel to the chain	19
γ_{\perp}	Interfacial free energy per unit area perpendicular to the chain	19
$\dot{\gamma}$	Shear rate	3, 9, 15, 24
$\dot{\gamma}_N$	Shear rate of a Newtonian fluid	15
δ	Loss angle	2, 11, 13, 25
δ	Relative position of $-\text{CH}_2-$ to functional group.	6
δ	Chemical shift	12
δ	Layer thickness	18, 19
δ	Solubility parameter	3, 7, 8, 11, 23
δ_a	Contribution of polar and hydrogen bonding forces to the solubility parameter	7
δ_d	Contribution of dispersion forces to the solubility parameter	7, 26
δ_{dP}	Dispersion force component for the polymer	7, 9
δ_{dS}	Dispersion force component for the solvent	7, 9
δ_E	Loss angle in dynamic tensile deformation	13
δ_G	Loss angle in dynamic shear deformation	13
δ_h	Contribution of hydrogen bonding to the solubility parameter	7, 26
δ_{hP}	Hydrogen bonding component for the polymer	9, 26
δ_{hs}	Hydrogen bonding component for the solvent	9, 26
δ_p	Contribution of polar forces to the solubility parameter	7, 26
δ_P	Solubility parameter of a polymer	7, 9, 26
δ_{pP}	Polar component for the polymer	7, 9
δ_{ps}	Polar component for the solvent	7, 9
δ_s	Solubility parameter of a solvent	7, 9, 26
δ_v	Contribution of dispersion and polar forces to the solubility parameter	7, 26
δ_{vP}	Dispersion and polar force component for the polymer	9, 26
δ_{vs}	Dispersion and polar force component for the solvent	9, 26
δ_o	Reference value of surface layer thickness	19
ΔT	Lydersen constant of liquid	7
$\Delta_T^{(P)}$	Lydersen–Hoy constant for polymers	7
ϵ	Dielectric constant (permittivity)	3, 11, 23
ϵ	Exponent in Eq. (9.31)	9
ϵ	Swelling factor	9, 16
ϵ	Tensile strain, elongation	13, 14, 15, 25

ε	Potential energy constant	13
ε	Infrared mass extinction coefficient	19
$\dot{\varepsilon}$	Rate of elongation or extension	13
δ_{br}	Elongation at break	13
ε_c	Elastic part of the tensile deformation	13, 15
ε_{ch}	Strain of chain segment	13
ε_{cr}	Critical strain	26
ε_{\max}	Maximum tensile deformation	13, 15, 25
ε_n	Nominal strain	13
ε_s	Static or relaxed dielectric constant	11
ε_{tr}	True strain	13
ε_v	Viscous part of tensile deformation	13
ε_λ	Mass extinction coefficient at given wavelength	10, 19
$\varepsilon_\lambda^{(a)}$	Mass extinction coefficient of amorphous polymer	19
$\varepsilon_\lambda^{(c)}$	Mass extinction coefficient of crystalline polymer	19
ε^F	Fibre strain	13
ε_0	Vacuum permittivity	11
ε_o	Maximum amplitude of dynamic tensile deformation	13
ε_o	Imposed strain	13
ε_o	Swelling at infinite dilution	16
ε_∞	Non-relaxed dielectric constant	11
ε^*	Complex electric inductive capacity	11
ε^*	Complex tensile deformation	13
ε'	Real component of ε^*	11, 13
ε''	Imaginary component of ε^*	11, 13
ε/k_B	Lennard Jones temperature	18
η	Shear viscosity	General
$\eta^+(t)$	Transient viscosity	13
η_{cr}	Viscosity at critical molecular weight	15
η_e	Extensional or elongational viscosity	13, 15, 16
η_{eo}	Extensional viscosity under Newtonian conditions	15
η_e^*	Complex extensional viscosity	13
η_e'	Real component of complex extensional viscosity	13
η_e''	Imaginary component of complex extensional viscosity,	13
η_{inh}	Inherent viscosity	9, 24
η_M	Maxwell dashpot constant in Burgers' element	13
η_{MP}	Viscosity at melt fracture	15
η_P	Viscosity of polymer	16
η_P^*	Viscosity of undiluted polymer	16
η_{red}	Reduced viscosity	9, 23
η_{rel}	Relative viscosity	9
η_S	Viscosity of solvent	9, 16
η_{sp}	Specific viscosity	9, 16
η_o	Newtonian viscosity	15, 16, 24
η_{VK}	Voigt-Kelvin dashpot constant in Burgers' element	13
η_∞	Second Newtonian viscosity	16
$\tilde{\eta}$	Reduced viscosity	16

$[\eta]$	Limiting viscosity number (intrinsic viscosity)	2, 9, 16, 23, 24
$[\eta]_b$	Limiting viscosity number of branched polymer	9
$[\eta]_{cr}$	Limiting viscosity number at the critical molecular weight	9
$[\eta]_l$	Limiting viscosity number of linear polymer	9
$[\eta]_R$	Reference value of the limiting viscosity number	9
$[\eta]_{rod}$	Rod limiting viscosity number of rod-like molecules	9
$[\eta]_\Theta$	Limiting viscosity number of Θ -solution	3, 9, 23
η^*	Complex shear viscosity	13, 15
$ \eta^* $	Absolute value of the complex shear viscosity	13, 15
η'	Real component of complex shear viscosity	13
η''	Imaginary component of complex shear viscosity	13
θ	Angle	General
θ	Angle between chain axis and fibre axis under tensile stress	13
θ	Function in Eqs. (16.53)–(16.55)	16
θ_B	Polarising angle (Brewster angle)	10
θ_{crit}	Critical angle of incidence where $\theta_t = \pi/2$ rad	10
θ_i	Angle of incidence	10
θ_r	Angle of refraction	10
θ_t	Angle of transmission	10
Θ	Time lag	18
Θ	Angle between chain axis and fibre axis in unloaded state	13
Θ_F	Flory-temperature/theta temperature	7
Θ_M	Formal time constant	15, 16
Θ_{sw}	Swelling time	19
$\Delta\Theta$	Angle between cone and plate	15
κ	Compressibility	General
κ_g	Compressibility of glassy polymer	6, 13
κ_l	Compressibility of liquid polymer	6, 13
λ	Thermal conductivity	3, 17, 23, 24
λ	Structural correction factor	12
λ	Wavelength	10, 22
λ	Lamé constant ($= K - \frac{2}{3}G$)	13
λ_a	Thermal conductivity of amorphous polymer	17
λ_c	Thermal conductivity of crystalline polymer	17
λ_{iso}	Thermal conductivity of isotropic material	14
λ_{or}	Thermal conductivity of oriented material	14
λ_o	Wavelength of light in vacuum	10
$\lambda_{//}$	Thermal conductivity in chain direction	14
λ_{\perp}	Thermal conductivity perpendicular to chain direction	14
Λ	Logarithmic decrement	13
Λ	Extension ratio	13, 24
Λ	Constant in Eq. (17.4)	17
Λ_{br}	Extension ratio at break	13
Λ_{kin}	Kinetic chain length	21
Λ_{max}	Maximum extension ratio	9

Λ_{tot}	Total extension ratio	13
Λ_o	Initial extension ratio	13
μ	Dipole moment	7, 11
μ	Magnetic inductive capacity (magnetic permeability)	10
μ	Magnetic permeability = $\mu_0\mu_r$	12
μ	Magnetic dipole moment	12
μ	Lamé constant (= G)	13
μ	Coefficient of friction	25
μ	Shape factor	25
μ_m	Orientation of the spin magnetic moment	12
μ_0	Magnetic permeability of vacuum	12
μ_r	Relative magnetic susceptibility	12
μ_{sh}	Coefficient of shearing friction	25
μ_z	Component of magnetic dipole moment in the direction of magnetic field	12
v	Frequency	General
v	Kinematic viscosity	3
v	Poisson ratio	3, 15, 17, 23, 25
v	De Gennes exponent	9
v	Resonance frequency	12
v	Ratio $(T_m - T)/(T_m - T_g)$	19
v_e	Number of elastically active network chains in a rubber	13
v_L	Larmor frequency	12
v_r	Resonance frequency, numerically equal to Larmor frequency	12
Δv	Hydrogen bonding number	7
ξ	Size of blob (molecular subunit)	9
ξ	Deformation gradient	24
π	Specific permachor	3, 19
π	Internal pressure	7
π_{eq}	Equilibrium spreading pressure	8
Π	Molar permachor of Salame	3, 18
Π	Osmotic pressure	10
Π	Universal parameter of Askadskii	10
ρ	Density	General
ρ	Radius of curvature	13
ρ_a	Density of amorphous polymer	4, 17
ρ_c	Density of crystalline polymer	4, 17, 19
ρ_g	Density of glassy amorphous polymer	4
ρ_p	Density of polymer	10
ρ_r	Density of rubbery amorphous polymer	4
ρ_R	Density at reference temperature	13
ρ_{sc}	Density of semi-crystalline polymer	4
ρ^*	Relative density	19

σ	Tensile stress	General
σ	Stiffness factor	9
σ	Turbidity or scattering coefficient	10
σ	Average surface roughness	10
σ	Screening or shielding constant	12
σ	True stress	13
σ	Lennard-Jones temperature	18
σ_{br}	Stress-at-break, tenacity	13
σ_c	Compressive stress	25
$\sigma_{c,\text{max}}$	Yield strength under axial compression	25
σ_D	Design stress	25
σ_e	Elastic component of stress	13
σ_{el}	Specific conductivity	10
σ_{eng}	Engineering stress	13
σ^F	Tensile stress parallel to fibre axis	13
σ_{Gr}	Griffith strength	13
σ_{max}	Maximum tensile stress	13, 25
σ_M	Mooney stress	13
σ_{sh}	Shear stress	3, 13, 15, 24, 25
$\sigma_{\text{sh},o}$	Amplitude of dynamic shear stress	13
$\sigma_{\text{sh},N}$	Shear stress of a Newtonian fluid	15
σ_{th}	Theoretical strength	13
σ_X	Collision diameter of molecule X	18
σ_v	Viscous component of stress	13
σ_y	Yield stress	13, 25
σ_o	Amplitude of dynamic tensile stress	13
σ_o	Imposed creep stress	13
σ_o	Initial tensile stress	22, 24
σ^*	Complex tensile stress	13
τ	Relaxation time	2, 3, 13, 22, 23
τ	Turbidity	10
τ	Characteristic shear time	15
τ_{cr}	Time needed for thermal equilibration	19
τ_{th}	Time needed by the crystallization process	19
τ_{ret}	Retardation time	13
τ_e	Characteristic extension time	15
τ_{eo}	Characteristic extension time under Newtonian conditions	15
τ_o	Characteristic shear time under Newtonian conditions	3, 15, 16
τ_o	Tortuosity of crystallites	18
ϕ	Volume fraction	7, 9, 16, 18
ϕ_o	Ditto, at its initial value	13
$\phi(r)$	Lennard Jones interaction energy	18
ϕ_e	Fractional excess volume	4
ϕ_f	Free volume fraction	15
ϕ_g	Free volume fraction at glass transition temperature	15
ϕ_P	Volume fraction of polymer	16, 19
ϕ_S	Volume fraction of solvent	16, 19

ϕ_{solv}	Volume fraction of the solvated polymer	16
ϕ^*	Critical concentration	16
Φ	Work function, contact potential	11
Φ	Ratio of liquid and solid molar volumes in Eqs. (8.7)–(8.10)	8
Φ	Constant in Eq. (9.22)	9
Φ_o	Constant in Eq. (9.29)	9, 19
χ	Magnetic susceptibility	3, 12, 23
χ	Thermodynamic interaction parameter	7
χ	Extinction angle	15
χ_m	Molar magnetic susceptibility (or shortly susceptibility)	12
χ_e	Electric susceptibility	11
$\chi_e^{(1)}$	Electric susceptibility tensor	11
$\chi_e^{(2)}$	First-order electric susceptibility tensor	11
$\chi_e^{(2)}$	Second-order electric susceptibility tensor	11
$\chi_e^{(3)}$	Third-order electric susceptibility tensor	11
χ_g	Mass magnetic susceptibility	12
χ_H	Interaction parameter defined in Eq. (7.11)	7
χ_v	Volume magnetic susceptibility	12
ψ	Specific damping capacity or internal friction	13
Ψ_1	First normal stress coefficient	13, 15, 16
$\Psi_{1,0}$	First normal stress coefficient at zero shear rate	13, 15, 16
Ψ_2	Second normal stress coefficient	13, 15, 16
$\Psi_{2,0}$	Second normal stress coefficient at zero shear rate	13, 15, 16
$\Psi_1^+(t)$	Transient first normal stress coefficient	13
ω	Angular frequency = $2\pi\nu$	General
ω	Constant in Eq. (7.26), i.e. Specific volume at $p = 0$ and $T = 0$	7
ω_L	Larmor angular frequency	12
Ω	Residual volume	4
Ω	Rotational or angular velocity	15
<i>Dimensionless numbers</i>		
Bm	Bingham number	3
Bo	Bodenstein number	3
Da	Damkohler number	3
De	Deborah number	2, 3, 18, 19
Fa	Fanning number	3
Fo	Fourier number	3
Jk	Janeschitz-Kriegl number	3, 19
Le	Lewis number	3
Ma	Mach number	3
Me	Merkel number	3
Mf	Melt fracture number	15
Nu	Nusselt number	3

Pe	Péclet number	3
Po	Poiseuille number	3
Pr	Prandtl number	3
Re	Reynolds number	3, 19, 24
Sc	Schmidt number	3
Sh	Sherwood number	3
Ste	Stefan number	3, 19
St	Stanton number	3
We	Weber number	3, 24
Wg	Weissenberg number	3, 15

This page intentionally left blank

AUTHOR INDEX

Note: Page numbers in italics denote author names in Bibliography.

A

- Acierno, D., 587, 595, 596, 643, 644
Adam, G., 151, 187, 244, 595
Adamse, J.W.C., 554, 557, 558, 559, 595
Aharoni, S.M., 146, 187, 635, 636, 643
Alfonso, G., 724, 744
Alfrey, T., 42, 171, 187, 500, 695, 701
Allen, G., 46, 99, 107, 108, 225, 226
Allen, V.R., 535, 596
Al-Malaika, S., 783, 786
Altenburg, K., 46
Altgelt, K.H., 46
Anderson, J.W., 366, 754, 762
Andrade, da Costa E.N., 537, 595, 603, 608
Andreeva, L.N., 306, 318
Andrew, E.R., 375, 381
Andrews, E.H., 461, 500, 867, 873
Andrews, R.D., 302, 318, 501
Angad, Gaur, H., 378
Angus, W.R., 357, 381
Armstrong, R.C., 547, 595, 597
Arnett, R.L., 107, 579
Arnold, P.A., 202, 226, 764
Asada, T., 581, 582, 583, 597, 639
Ashby, M.F., 820, 821, 822, 824, 845
Askadskii, A.A., 4, 5, 73, 107, 108, 302, 303, 317, 318
Asmussen, F., 699, 700, 701
Astarita, G., 595, 725, 743
Atkins, P.W., 352, 380, 658, 701
Avrami, M., 704, 708, 709, 744, 796
Axtell, F.H., 735, 744

B

- Babrauskas, V., 853, 873
Baer, E., 837, 845
Bagley, E.B., 208, 226, 595
Baird, E.M., 881, 885
Balazs, C.F., 450, 503
Ballman, R.L., 502, 579, 596
Ballou, J.W., 388, 505, 508, 522
Baltá-Calleja, F.J., 360, 381
Baltussen, J.J.M., 483, 484, 489, 490–1, 493, 494, 498, 500, 501, 502, 744, 745, 741
Barbari, T.A., 684, 687, 688, 689, 701
Barnes, H.A., 526, 568, 569, 595, 630, 634, 643
Barnet, F.R., 390, 460, 503
Barnett, S.M., 579, 595
Barrales-Rienda, J.M., 360, 381
Barrer, R.M., 682, 687, 701
Barrie, I.T., 594, 595
Barrie, J.A., 690, 701, 702

- Barton, J.M., 130, 187
Bartos, O., 579, 595
Basset, D.C., 726, 744
Batchinski, A.J., 537, 595
Batzer, H., 130, 149, 188
Bauwens, J.C., 464, 501
Bauwens-Crowet, C., 464, 501
Bayer, O., 41
Beaman, R.G., 167, 187
Beckmann, P., 317
Beck, R.H., 317, 444
Becker, R., 130, 187, 704, 744
Bedwell, M.F., 360, 381
Beekmans, F., 582, 583, 587, 595
Bekkedahl, N., 380, 501
Benbow, J.J., 578–9, 580, 595, 596
Bennett, H.E., 317, 318
Benoit, H., 274, 284
Beret, S., 102, 107
Bergen, R.L., 786, 872, 873
Berger, J., 149, 187, 745
Bernier, G.A., 7, 868, 869, 873
Berry, G.C., 535, 595
Bertola, V., 580, 595, 597
Berzelius, J.J., 64
Bestul, A.B., 125, 127
Bevan, L., 867, 873
Bhatnagar, S.S., 357, 381
Bianchi, U., 151, 187
Bicerano, J., 5, 127, 146, 147, 148, 149, 187, 202, 244, 283, 317, 352, 521, 652, 701, 719, 744, 776, 777
Biltz, W., 76, 107
Bin, Ahmad, Z., 820, 822, 824, 845
Binder, G., 815, 818
Binsbergen, F.L., 715, 744
Bird, R.B., 595, 597, 629, 643, 817
Bitter, F., 357, 381
Bixler, H.J., 661, 663, 702
Black, W.B., 390, 501
Blagrove, R.J., 21, 46
Bland, D.R., 325, 326, 354
Beerbower, A., 205, 210, 226
Blanks, R.F., 203, 226
Blokland, R., 404, 501
Boenig, H.V., 801, 817
Boerstoel, H., 495, 501, 502, 635, 636, 643, 644, 744, 745
Boger, D.V., 526, 578, 595, 631
Bolland, J.L., 781, 782, 786
Bondi, A., 4, 5, 64, 66, 72, 73, 76, 90, 100, 107, 119, 123, 127, 226, 643
Boon, J., 710, 711, 712, 720, 723, 744
Bowden, F.P., 840, 844

- Bower, D.I., 320, 339, 341, 352, 353, 380
 Boyd, B.H., 99, 108
 Boyd, R.H., 327, 352
 Boyer, R.F., 90, 91, 100, 107, 108, 132, 167, 168, 170,
 173, 187, 381, 426, 603, 644
 Brandrup, J., 3, 5, 107, 127, 187, 225, 226, 244, 283, 318,
 322, 352, 604, 643, 761
 Braun, G., 611, 643
 Bredas, J.L., 341, 353, 354
 Breitmaier, E., 370, 380, 382
 Bremner, J.G.M., 754, 762
 Breuer, H., 150, 187
 Bristow, G.M., 203, 226
 Britton, R.N., 733, 744
 Broersma, S., 357, 381
 Broido, A., 776, 777
 Brostow, W., 36, 46, 844
 Brown, W.E., 826, 845
 Brügging, W., 183, 187, 879
 Brydson, J.A., 187, 579, 580, 595, 817
 Bu, H.S., 117
 Buckley, C.P., 398, 399, 472, 500, 506, 521, 845
 Bucknall, C.B., 398, 399, 472, 500, 844, 845
 Bueche, F., 90, 99, 107, 187, 188, 283, 534, 548, 556, 561,
 595, 613, 643, 644, 694, 695, 701, 734
 Bunn, C.W., 64, 66, 167–8, 187, 191, 192, 226, 500
 Burchard, W., 21, 46
 Burghardt, W.R., 583, 584, 585, 596, 641, 643
 Burke, J., 210, 225
 Burrell, H., 205, 226
 Busse, W.F., 801, 812, 817
- C**
- Cabrera, B., 357, 381
 Cao, M.Y., 117, 127
 Capaccio, G., 739, 744
 Carreau, P.J., 547, 596, 625, 643
 Cassidy, P.E., 243, 244
 Chance, R.R., 300, 341, 353, 354, 478, 881, 884
 Chang, M.C.O., 518, 519, 522
 Chang, S.S., 125, 127
 Chee, K.K., 24, 46, 203, 210, 226
 Chen, S.-A., 208, 226
 Cheng, S.Z.D., 117, 127, 761
 Chermin, H.A.G., 64, 67, 754, 755, 762
 Chern, R.T., 688, 701
 Chou, T.W., 843, 844, 845
 Chu, B.J., 21, 46
 Clark, E.S., 739, 744
 Clasen, C., 276, 283
 Clausius, R., 64, 66, 320, 321, 322, 323, 622, 900
 Clegg, D.W., 592–3, 596
 Clegg, P.L., 573, 596
 Coates, J., 513, 522, 646, 653
 Coehn, A., 333, 354
 Cogswell, F.N., 545, 574, 577, 581, 583–5, 594, 596
 Cohen, R.E., 547, 597
 Cole, K.S., 326, 327, 329, 354
 Cole, R.H., 326, 327, 329, 354
 Cole, T.B., 738, 745
 Coleman, B.D., 550, 833, 845
 Collins, E.A., 24, 46
 Collyer, A.A., 587, 596, 634, 635, 643, 644
 Cornelissen, J., 539, 596
 Corradini, P., 11, 45, 47
 Cote, J.A., 563, 596
 Cotton, J.P., 24, 46
 Cotts, D.B., 327, 353
 Cowan, B., 380
 Cowan, D.O., 337, 338, 342, 343, 353
 Cowie, J.M.G., 146, 187
 Cox, W.P., 553, 596
 Crank, J., 425, 696, 701, 702
 Cross, M.M., 547, 596, 643
 Crowley, J.D., 205, 226
 Cruikshank, J.H., 357, 381
 Czechowski, G., 586, 588, 596
- D**
- Dainton, F.S., 111, 123, 127, 757, 762
 Dale, T.P., 61, 64, 66, 290–1, 292, 318
 Dann, J.R., 235, 244
 Daoud, M., 271, 283, 284
 Darby, J.R., 331, 354
 Darby, R., 24, 354
 Dautzenberg, H., 276, 283
 Davies, H., 317, 318
 Davis, H.G., 76, 77, 78, 107
 Debye, P., 66, 116, 308, 318, 354, 701
 Dee, G.T., 237, 244
 Deeley, C.W., 807, 817
 De Gennes, P.G., 266–72, 279, 283, 284, 518, 522, 580,
 595, 596, 702, 795
 De Jonge, I., 785, 786
 Delmas, G., 203, 227
 Demus, D., 36, 46
 Denisov, E.T., 783, 786
 Denys, K.F.J., 592, 596
 De Paula, J., 380, 658, 701
 Deutsch, K., 380, 407, 501
 De Vries, H., 307, 318, 483–4, 486, 501, 502, 745
 De Waele, A., 546, 596
 Di Benedetto, A.T., 149, 226
 Diehl, P., 371, 382
 Dillon, R.E., 548, 597
 Di Marzio, E.A., 148, 151, 187
 Dinter, R., 545, 596
 Dobb, M.G., 635, 643, 705, 739, 740, 741, 744
 Doi, M., 283, 585, 595, 635, 643, 701
 Domae, H., 815, 818
 Doolittle, A.K., 537, 596, 621
 Doppert, H.L., 640, 641, 643, 745
 Dorfman, J.G., 357, 358, 380
 Döring, W., 294
 Dorsey, N.E., 101, 107
 Doty, P., 276, 284
 Dreval, V.Y.E., 615, 643, 644
 Duda, J.L., 693, 696, 701, 702

Dunkel, M., 191, 192, 198, 226
 Dunlop, A.N., 24, 46

E

Eder, G., 722, 725, 744, 746
 Edwards, S.F., 283, 635, 643, 701
 Ehrenfest, P., 150, 151, 152, 187
 Eiermann, K., 501, 646–50, 653
 Einhorn, I.N., 864, 872, 873
 Einstein, A., 116, 251, 602
 Eisele, U., 403, 443, 501
 Eisenberg, H., 275, 276, 283, 284
 Eisenlohr, F., 61, 292, 318
 Elias, H.G., 21, 45, 211, 225, 283
 Engel, F.V.A., 55, 66
 Epstein, A.J., 348, 353, 354
 Ernst, R.R., 366, 380
 Everage, A.E., 579, 596
 Exner, O., 66, 77, 78, 107
 Eyring, H., 421, 464–7, 500, 537, 595, 596, 762

F

Fahlenbrach, H., 357, 381
 Farmer, E.H., 781, 786
 Farquharson, J., 357, 381
 Fedors, R.F., 77, 78, 107, 191, 192, 195, 198, 226, 475,
 477, 501, 502
 Fenimore, C.P., 853, 873
 Ferguson, J., 631, 632, 633, 644
 Ferrari, A.G., 579, 596
 Ferry, J.D., 409, 442, 444, 445, 447, 452, 500, 503, 507,
 521, 547, 595, 596, 597, 611, 620–4, 643, 644, 694,
 701, 713, 813, 815, 825, 845
 Fetter, L.J., 247, 283, 284
 Fillers, R.W., 447, 448, 501
 Finger, F.L., 402, 403
 Finkelmann, H., 36, 47, 175, 187
 Finn, A., 291, 318
 Fisher, J.C., 704, 746
 Fixman, M., 252, 263, 265, 284
 Flom, D.G., 840, 845
 Flory, P.J., 18, 22, 103, 146, 167, 187, 201, 202, 211, 214,
 225, 246, 249, 283, 272, 273, 274, 401, 500, 501,
 608, 638, 682
 Ford, T.F., 602, 643
 Fortune, L.R., 99, 107
 Foster, G.N., 224, 226
 Fouquet, I., 709, 744
 Fowkes, F.M., 235, 239–40, 244
 Fox, H.W., 232, 233, 244
 Fox, R.B., 236, 244
 Fox, T.G., 146, 149, 187, 211, 226, 534, 535,
 539, 595, 596
 Frank, F.C., 390, 501, 587–8
 Franken, P.A., 349, 354
 Franklin, J.L., 66, 754, 762
 Franse, M.W.C.P., 177, 187, 642, 643
 Frensdorff, H.K., 390, 501
 Frisch, H.L., 221, 225, 284, 674, 695, 701

Fritch, L.W., 806, 817
 Fröhlich, H., 324, 353, 421
 Fuller, G.G., 583, 585, 596, 641
 Fulmer, G.E., 872, 873
 Fuoss, R.M., 275, 284
 Furches, B.J., 804, 817

G

Gandica, A., 713, 714, 744
 Gee, D.R., 111, 123, 128
 Gee, G., 151, 187, 226, 401, 501
 Gibbs, J.H., 148, 151, 187
 Gibbs, J.W., 202, 704, 710, 712, 743
 Giddings, J.C., 21, 47
 Gilmore, G.D., 103, 108, 222, 223, 227
 Girifalco, L.A., 233, 239, 244
 Gladstone, J.H., 61, 64, 290–2, 318
 Gligo, N., 605, 607, 644
 Goedhart, D.J., 47, 292, 309, 318
 Goldbach, G., 430–1, 501
 Good, R.J., 239, 244
 Goppel, J.M., 809, 817
 Gordy, W., 205, 226
 Gortemaker, F.H., 553, 554, 596
 Gotsis, A.D., 583–5, 596
 Gottlieb, S., 76–8, 107
 Graessley, W.W., 24, 47, 188, 284, 548, 563, 595, 596,
 627–9, 643
 Gray, F.W., 357, 381
 Gray, G., 36
 Grebowicz, J., 172, 187, 188
 Greet, R.J., 537, 596
 Gregory, D.R., 544, 564, 596
 Greiner, R., 427, 501
 Griffith, A.A., 455, 473, 474, 475, 501, 842, 845
 Griskey, R.G., 126, 128, 226
 Gross, D., 864, 873
 Grunberg, L., 230, 244
 Grüneisen, E., 391, 393, 501
 Guggenheim, E.A., 237, 244
 Gugumus, F.L., 785, 786
 Gurnee, E.F., 171, 187, 701
 Guskey, S.M., 585, 596
 Guth, E., 41, 401, 502, 505–506, 522

H

Haberditz, W., 357, 358, 380
 Hadden, S.T., 77, 108
 Hadley, D.W., 455, 464, 465, 501
 Halpin, J.C., 844, 845
 Han, C.D., 557, 558, 559, 574–5, 596, 817
 Hands, D., 646, 653
 Hansen, C.M., 205–208, 210, 212, 215, 218, 219, 226,
 870, 873
 Haque, M.A., 103–105, 107
 Hara, H., 726, 745
 Harrison, E.K., 76, 77, 107
 Hartmann, B., 103–105, 107, 376, 377, 388, 391, 394,
 502, 506–508, 510–12, 514–15, 521, 522

- Havriliak, S.J., 329
 Havriliak, Jr., S., 329
 Hawker, C.J., 40, 47
 Haworth, B., 735, 744
 Hayes, R.A., 130, 187, 191, 192, 197, 198, 226
 Hazell, E.A., 462, 503
 Hazleton, R.L., 627, 628, 643
 Hearle, J.W.S., 46, 307, 318, 322, 353, 500, 743, 746, 885
 Heckert, W.W., 481, 502
 Heeger, A.J., 44, 337, 344, 345, 353, 354
 Heijboer, J., 421–5, 502
 Heinze, H.D., 149, 187
 Heitz, W., 183, 187
 Hellwege, K.H., 545, 596, 646, 653
 Hendrix, J.F., 854, 873
 Henry, L.F., 208, 226, 355, 870, 873, 890, 901
 Hermann, K., 29, 47
 Hermans, J.J., 276, 277, 284, 479–80, 492, 608, 643
 Hermans, P.H., 500, 502, 742, 744
 Hertz, H., 502, 837, 845
 Herwig, H.U., 485, 488, 502, 744
 Heusch, R., 611, 612, 615, 644
 Heuvel, H.M., 729, 732, 744
 Hiatt, G.D., 454, 501
 Hildebrand, J.H., 189, 201, 205, 210, 226, 230, 244, 868–9
 Hill, W.K., 357, 381
 Hoarau, J., 360, 381
 Hoernschemeyer, D., 208, 226
 Hoffman, J.D., 704, 714, 715, 717, 744
 Hoftyzer, P.J., 47, 64, 67, 77, 108, 188, 132, 191, 192, 197, 198, 212, 213, 215, 216, 218, 219, 226, 227, 253, 256, 284, 392, 400, 503, 539, 541, 542, 597, 617, 643, 746, 858, 871, 873
 Hoke, C.H.E., 861, 873
 Holmes, D.B., 804, 805–806, 817
 Holzmüller, W., 46, 545, 596
 Hope, P., 785, 786
 Hopfenberg, H.B., 695, 701
 Horiguchi, H., 329, 354
 Hornak, J.P., 373, 380
 Hosemann, R., 31, 32, 47, 381
 Houwink, R., 18, 221, 250, 252, 255–7, 261, 263, 265, 273–4, 276, 278, 280, 284, 503, 601–603, 619
 Howells, E.R., 579, 596
 Howorth, W.S., 877, 885
 Hoy, K.L., 191, 194, 197, 198, 212, 216–19, 227, 871
 Huang, C.J., 110, 128
 Hudson, N.E., 596, 631, 632, 633, 644
 Huggins, M.L., 47, 65, 66, 77, 78, 107, 201, 202, 273, 292, 318, 600–601, 603, 604, 618, 644, 681, 682, 795
 Huisman, R., 502, 644, 729, 732, 744, 745
 Huntjens, F.J., 149, 187, 777
 Huppler, J.D., 629, 644
 Hutton, J.F., 526, 568, 595, 634, 643
- I**
- Imhof, L.G., 864, 873
 Immergut, E.H., 5, 107, 127, 187, 225, 226, 244, 283, 318, 352, 322, 604, 643, 761
- J**
- Iovleva, M.M., 636, 644
 Ito, Y., 626, 644
 Ivin, K.J., 750, 757, 761, 762
- K**
- Jabarlin, S.A., 316, 318
 Jacobson, S., 350, 354
 Jadzyn, J., 586, 588, 596
 James, D.F., 568, 596, 631, 632, 644
 James, H.M., 401, 502
 Jamet, M., 744
 Janeschitz-Kriegl, H., 57, 300, 303, 305, 317, 318, 551–2, 554, 572, 595, 596, 621, 644, 722–5, 744, 746
 Jannink, G., 271, 283, 284
 Jansen, J.C., 175, 177, 188
 Jarvis, N.L., 236, 244
 Jarzynski, J., 507, 513, 522
 Jenckel, E., 611, 615, 644
 Jenekhe, S.A., 338, 354
 Jin, S., 590, 596
 Johnson, A.J., 110, 128
 Johnson, M.F., 605, 644
 Johnson, P.R., 854, 855, 857, 873
 Jones, D.M., 633
 Jones, L.D., 110, 128
 Jones, T.E.R., 596, 631, 632
- L**
- Kachin, G.A., 804, 817
 Kamal, H.R., 222, 227
 Kambour, R.P., 615, 616, 644, 867, 868, 873
 Kaminsky, W., 43
 Kampschoer, G., 834, 835, 845
 Kampschreuer, J.H., 489, 502, 745
 Kampschulte, U., 183, 187
 Kanig, G., 149, 188
 Karasz, F.E., 147, 148, 188, 353
 Kardos, A., 646, 653
 Katz, J.R., 41
 Kauzmann, W., 151, 188
 Kavesh, S., 704, 744
 Keller, A., 29, 32, 47, 705, 743, 744
 Keller, F., 370, 382
 Kelley, F.N., 188, 611, 615, 644
 Kevorkian, R., 111, 123, 128
 Khanna, Y.P., 709, 744
 Kiel, A.M., 731, 745
 Kilb, R.W., 273, 284
 King, III, R.E., 283, 785
 Kirchner, P., 698, 700, 702
 Kirkland, J.J., 21, 46, 47
 Kirschbaum, R., 736, 744
 Kirshenbaum, L., 99, 107
 Kissi, N.E., 578, 596
 Kiss, G., 639, 640, 644
 Klaase, P.T.A., 350, 353
 Klinkenberg, A., 57, 66
 Klop, E.A., 502, 745, 865, 873
 Knappe, W., 596, 646, 652, 653

- Knight, G.J., 147, 169, 188
 Kobayashi, K., 735, 744
 Koenhen, D.M., 207, 227
 Kogut, J., 266, 284
 Koppelman, J., 411, 502
 Kornfield, J.A., 724, 745
 Koros, W.J., 682, 684, 686–9, 701, 702
 Korshak, V.V., 764, 776, 777, 872
 Kothonaraman, H., 152, 188
 Kovacs, A.J., 151, 188, 430, 502, 611, 643, 714, 746
 Kraemer, E.O., 22, 600, 644
 Kratky, O., 248, 284, 479, 502
 Kreibich, U.T., 130, 149, 188
 Krigbaum, W.R., 42, 46, 187, 252, 284, 743
 Kuhn, W., 247–8, 284, 401, 502
 Kulicke, W-M., 276, 283
 Kurata, M., 246, 284
 Kurtz, S.S., 77, 78, 107
 Kwon, Y.D., 34, 47, 728, 731, 745

L

- Lacombe, R.H., 103, 107
 Lamb, P., 578–80, 595, 596
 Lamble, J.H., 302, 318
 Lammers, M., 636, 644
 Lamonte, R.R., 811, 817
 Landel, R.F., 475, 477, 501, 502, 503, 597, 713, 815
 Landi, P., 350, 354
 Larson, R.G., 572, 585, 587, 595, 597, 643, 644
 Laun, H.M., 570, 571, 572, 596, 597, 631
 Leaderman, H., 442, 502
 Le Bas, G., 76, 107
 Lee, L.H., 169, 235, 244
 Lee, W.A., 130, 187, 188, 230
 Leeper, H.M., 29, 47, 745
 Lehmann, O., 34, 47
 Lemstra, P.J., 318, 733, 734, 736, 737, 744,
 745, 746, 845
 Lenz, R.W., 180, 187, 188, 222, 227
 Leuchs, O., 29, 30, 47
 Levan, N.T., 222, 227
 Levy, G.C., 370, 380, 381
 Lewis, O.G., 3, 5, 107
 Li, K., 77, 78, 107
 Lin, K.F., 77, 78, 107, 191, 192, 227
 Lindeman, L.R., 627, 628, 643
 Lindemann, F.A., 117, 128
 Lipkin, M.R., 77, 78, 107
 Litt, M., 538, 596
 Liu, F., 327, 352
 Lodge, A.S., 548, 552, 570, 595
 Lommerts, B.J., 742, 744
 Looyenga, H., 61–2, 66, 292, 318
 Lorentz, H.A., 61, 66, 291, 318, 321
 Lorenz, L.V., 66, 291–2, 321, 324
 Loshaek, S., 149, 187, 188, 539, 596
 Lowe, I.J., 226, 375, 382
 Lydersen, A.L., 216, 227
 Lyons, P.F., 353, 618–19, 862

M

- Maat, H.T., 738, 744
 McArdle, C.B., 36, 46
 McCrum, N.G., 187, 353, 398, 399, 424, 426, 465, 466,
 472, 500, 521, 825, 845
 MacDiarmid, A.G., 337, 341, 344–6, 353, 354
 McGowan, J.C., 230, 244, 392, 502, 545, 594, 596
 McHugh, A.J., 734, 735, 745
 McLoughlin, J.R., 433, 502
 MacNulty, B.J., 867, 870, 873
 Macosko, C.W., 569, 595, 644
 Madorsky, S.L., 763, 764, 776, 777
 Maeda, Y., 505–506, 522
 Magat, E.E., 739, 745
 Magat, M., 203, 227
 Magda, J.J., 640, 641, 644
 Magill, J.H., 537, 596, 713, 714, 717, 744, 745
 Maier, W., 638, 644
 Maklakov, A.J., 360, 381
 Malcolm, G.N., 99, 107
 Mandel, M., 276, 279, 283, 284
 Mandelkern, L., 715, 717, 720, 743, 745
 Marangoni, A., 709, 745
 Marcinčin, C.T., 130, 188
 Mark, H., 47, 250, 284, 502
 Mark, H.F., 5, 18, 41, 127, 283, 284, 382, 521, 652, 701,
 761, 776, 885
 Mark, I.T., 502
 Mark, J.E., 3, 5, 127, 187, 188, 225, 226, 244, 283, 284,
 317, 339, 340, 346, 353, 354, 381, 382, 500, 502,
 521, 652, 701, 743, 777, 786, 873
 Marrand, H., 723, 745
 Marrucci, G., 639, 644, 845
 Marshall, I., 815, 818
 Martin, E.R., 817, 853
 Marvin, R.S., 412, 502
 Mascia, L., 863, 864, 873
 Mason, P., 405, 502, 595
 Mason, W.P., 505, 521, 522
 Mathews, A.P., 76, 107
 Matvyeyev, Yu, I., 5
 Maxwell, J.C., 52, 66, 299, 319, 412–18, 420, 432, 505,
 546, 548, 549, 560, 569, 570
 Meier, G., 36, 46
 Meissner, J., 556, 565–8, 573, 596, 597
 Melia, T.P., 111, 123, 127, 128
 Mendelson, R.A., 24, 47, 557
 Merz, E.H., 553, 596
 Metzger, A.P., 24, 46
 Meulenbroek, B., 580, 595, 597
 Michaels, A.S., 661, 663, 669, 702
 Mills, N.J., 24, 47, 557, 597
 Mitra, N.G., 357, 381
 Mitsuishi, Y., 815, 818
 Moldenaers, P., 597, 634, 639, 640, 641, 644
 Mooney, M., 402–404, 502
 Mooy, H.H., 57, 66
 Morton, W.E., 307, 318, 322, 353, 500, 743
 Mosotti, O.F., 64, 67, 320–3, 354

Moynihan, C.T., 152, 188
 Müller, F.H., 354, 815
 Mumford, S.A., 231, 244
 Münstedt, H., 567, 570, 571, 597

N

Nagasawa, M., 276, 283, 644
 Nagasawa, T., 735, 744
 Napper, D.H., 211, 227
 Natarajan, R., 830, 845
 Natta, G., 11, 47
 Nelson, G.L., 370, 380
 Nelson, M.I., 850–1, 853, 873
 Nernst, W., 117, 128
 Ngai, K.L., 147, 187, 188, 500
 Nielsen, L.E., 148, 149, 188, 388, 500, 845
 Nissan, A.H., 230, 244
 Nitschmann, I.T., 811, 818
 Nolle, A.W., 505, 522
 Northolt, M.G., 483, 484, 486, 489–500, 501, 502, 503,
 635, 644, 705, 733, 739, 741, 742, 743, 744, 745,
 834, 845
 Nutting, P., 436, 502

O

Odijk, T., 279, 284
 Odriozola, M.A., 585, 596
 Ogorkiewicz, R.M., 401, 450, 500, 597, 817, 818, 845
 Ohnesorge, W., 810, 818
 Okui, N., 718, 745
 Oliver, P.H., 631, 885
 Ono, S., 754
 Onogi, S., 581–3, 605, 639, 644
 Onsager, L., 637, 638, 644
 Oosawa, F., 276, 283
 Orwoll, R.A., 103, 107, 202, 226
 Ostwald, Wo., 546, 597
 Osugi, J., 726, 745
 Oth, A., 276, 284
 Ovchinnikov, A., 356, 381
 Owen, M.J., 235, 240, 244
 Owens, D.K., 239, 240, 243, 244
 Oyanagi, Y., 621, 623, 644

P

Pake, G.E., 374, 382
 Pals, D.T.F., 277, 284
 Pan, R., 117, 127, 340, 482, 733, 737
 Panzer, J., 235, 244
 Parker, W.J., 853, 873
 Pascal, P., 64, 67, 357–8, 381, 673, 890, 896
 Paschke, E., 808, 818
 Passaglia, E., 111, 123, 128
 Patterson, D., 203, 227
 Paul, D.R., 684, 686, 687, 689, 701, 702
 Pauling, L., 72, 107
 Pearson, J.R.A., 811, 817, 818
 Pederson, K.O., 280, 284

Pennings, A.J., 705, 731, 733, 738, 739, 745, 746
 Perepechko, II., 506, 522
 Perret, R., 731, 744
 Peterlin, A., 33, 34, 47, 745, 818, 729, 814
 Pethrick, R.A., 107, 187, 318, 506, 522
 Pezzin, G., 605, 611, 613, 644
 Phillips, J.W.C., 231, 244
 Piau, J.-M., 578, 596, 817
 Picken, S.J., 187, 502, 586, 587, 588, 597, 636, 638, 640,
 641, 643, 644, 740, 745
 Plazek, D.J., 147, 187, 500
 Platzek, P., 479, 502
 Platzer, N.A.J., 37, 46
 Pockels, F., 349, 351, 353
 Pohl, R.W., 297, 318
 Porod, G., 248, 284
 Porter, R.S., 97, 108, 501, 564, 597, 639, 640,
 644, 739, 743
 Porteus, J.O., 317, 318
 Pouyet, J., 275, 276, 284
 Powell, P.C., 547, 577, 578, 594, 597, 818
 Prasad, P.N., 36, 46, 354
 Prausnitz, J.M., 5, 102, 107, 127, 226, 227, 761, 203
 Preston, I., 739, 745
 Prevorsek, D.C., 34, 47, 728, 731, 745
 Ptitsyn, O.B., 152, 188

Q

Qian, C., 202, 227
 Qian, T., 696, 702
 Quach, A., 102, 107
 Quayle, O.R., 231, 244

R

Rabinowitz, S., 464, 465, 502
 Raha, S., 869, 870, 871, 873
 Rákoš, M., 360, 381
 Ratajski, E., 724, 744, 746
 Raucher, D., 687, 702
 Rawling, G.D., 880, 885
 Read, B.E., 187, 426, 500, 521
 Reck, B., 182, 188
 Reddish, W., 407, 501
 Redlich, O., 119, 128
 Reed, P.E., 830, 845
 Rehage, G., 130, 131, 150–2, 175, 187, 188, 430, 431, 501
 Reich, L., 776, 777, 786
 Reid, R.C., 3, 4, 5, 127, 227, 761
 Reiner, M., 427, 595, 596, 696
 Reinitzer, F., 34, 47
 Reyes, Z., 327, 353
 Reynolds, J.R., 55, 56, 59, 353, 580, 655, 698, 700
 Rheineck, A.E., 77, 75, 107, 191, 192, 227
 Rice, S.A., 276, 283
 Richardson, S.M., 806, 818
 Richter, L., 36, 46
 Ringsdorf, H., 36, 47, 101, 102, 188
 Rivlin, R.S., 402–404, 502
 Robertson, R.E., 99, 107

- Rodriguez, F., 46, 619, 644, 777, 786
 Roe, R.-J., 234, 235, 244
 Rogers, C.E., 674, 681, 682, 689, 702
 Romanov, A., 130, 188
 Rommel, H., 741, 745
 Roos, A., 489, 502, 745
 Rossi, G., 696, 701, 702
 Rossini, F.D., 107, 756, 761
 Roth, S., 341, 344, 347, 353, 354
 Rottink, J.B.H., 589, 597
 Rouse, P.E., 561, 619–21
 Rubinstein, M., 276, 283
 Rudd, J.F., 302, 318
 Rudin, A., 24, 46, 272, 284, 600, 602, 603, 605, 644
 Rusch, K.C., 444, 502
 Ryskin, G.Y., 693, 702
- S**
- Sada, E., 687, 688, 702
 Saechtling, H., 3, 5
 Saeda, S., 24, 47, 563, 597
 Sagalaev, G.V., 223, 227
 Sakai, M., 629, 630, 644
 Sakai, T., 601, 644
 Sakaoku, K., 731, 745
 Sakiaades, B.C., 513, 522
 Sakurada, I., 390, 502
 Sakurada, J., 733, 742, 745
 Salame, M., 64, 676–80, 702
 Sanchez, I.C., 103, 107, 743
 Satoh, S., 64, 110–12, 128
 Sauer, B.B., 237, 244
 Saunders, D.W., 305, 318
 Saupe, A., 638, 644
 Sauteray, R., 360, 381
 Sawada, H., 758, 761
 Scatchard, G., 189, 227
 Scheffer, F.E.C., 755, 762
 Schiesinger, W., 29, 47
 Schimpf, M.E., 21, 47
 Schlesinger, W., 705, 745
 Schlichter, W.P., 421, 502
 Schmidt, H.W., 56, 183, 187
 Schmieder, K., 149, 187, 354, 502
 Schmitz, J.V., 826, 827, 845
 Schneider, B., 374, 382
 Schneider, W., 725, 745
 Schnell, G., 149, 187
 Schoenhorn, H., 235, 244
 Schon, J.H., 340, 354
 Schoorl, N., 291, 292, 318
 Schulz, N., 202, 226
 Schultz, J.M., 18, 704, 744
 Schuyer, J., 64, 67, 388, 390, 460, 502, 522, 506, 514
 Schwarzl, F.R., 410, 427, 452, 500, 501, 502, 503
 Scott, L.W., 739, 744
 Scott, R.L., 203, 226, 227, 230, 244, 868
 Sefcik, M.D., 687, 702
 Segal, L., 24, 46, 47, 596
- Seitz, J.T., 187, 450, 503
 Selwood, P.W., 360, 380, 381
 Sessler, G.M., 353
 Shah, B.H., 24, 47
 Shah, Y.T., 811, 818
 Shamov, L., 390, 460, 503
 Shashoua, J., 333, 354
 Shaw, R., 64, 67, 110–12, 128
 Sheehan, W.C., 738, 745
 Sherwood, Th K., 3, 5, 59, 127, 227, 761
 Shibaev, V.P., 35, 46, 187, 354
 Shida, M.J., 46, 563, 596
 Shishido, S., 626, 644
 Shore, J.D., 597, 831, 838, 839
 Sikkema, D.J., 483, 486, 502, 503, 741, 743, 745
 Silverman, J., 388, 522
 Simha, R., 77, 90, 91, 100, 102, 103, 107, 108, 608, 644, 776, 777
 Simmens, S., 307, 318
 Simon, F.E., 151, 188
 Sinclair, D., 834, 845
 Sinha, M., 506, 521
 Slichter, W.P., 374, 381
 Slonimskii, G.L., 72, 73, 108
 Slothers, J.B., 370, 381
 Smirnova, V.N., 636, 644
 Smith, P., 733, 734, 738, 744, 745
 Smith, R.P., 223, 227
 Smith, ThL., 475, 476, 503
 Smolders, C.A., 207, 227
 Smook, J., 736, 737, 745
 Snape, C.E., 376, 382
 Sokolova, T.S., 608, 644
 Somcynsky, T., 103, 108
 Souders, M., 754, 762
 Southern, E., 693, 694, 702
 Spencer, R.S., 90, 100, 103, 107, 108, 222, 223, 227, 548, 597
 Sperling, L.H., 518, 519, 521, 522
 Spevacek, J., 374
 Spizzichino, A., 317
 Spriggs, T.W., 546, 597
 Spruiell, J.E., 815, 818
 Stanford, S.C., 205, 226
 Stannett, V.T., 665, 674, 701, 702
 Starkweather, H.W., 99, 108, 121, 128
 Staudinger, H., 8, 46, 47, 250
 Staverman, A.J., 130, 160, 188, 410, 502, 503
 Stefan, J., 56, 723, 725, 745
 Stein, R.S., 316, 317, 318, 470, 501, 503, 744, 746
 Steiner, K., 717, 702, 746
 Step, E.N., 785, 786
 Stille, J.K., 184, 188
 Stockmayer, W.H., 246, 252, 255, 263, 265, 273, 284
 Strathdee, G.B., 602, 603, 605, 644
 Stratton, R.A., 555, 563, 597
 Straus, S., 763, 776, 777
 Strauss, U.P., 275, 284, 764
 Streeter, D.J., 603, 644
 Strella, S., 333, 334, 354

- Struik, L.C.E., 33, 47, 188, 431, 433, 434, 436–42, 501, 503
 Stueben, K.C., 864, 873
 Suezawa, Y., 872, 873
 Sugden, S., 64, 67, 76, 108, 231, 234, 244, 513
 Sun, S.F., 21, 47, 284
 Sundararajan, P.R., 211, 226
 Sundralingham, A., 781, 786
 Suzuki, T. L.W., 714, 746
 Svedberg, T., 280, 284
 Szwarc, M., 674, 702

T

- Tabor, D., 455, 503, 837, 840, 844, 845
 Tager, A.A., 618, 643, 644
 Tait, P.G., 101–103, 108
 Takeda, M., 329, 354
 Takserman-Krozer, R., 811, 812, 818
 Tanford, C., 226, 308, 318, 643
 Tanner, R.I., 575, 597
 Tatevskii, V.M., 77, 108
 Taylor, P.L., 696, 702
 Taylor, T.J., 709, 744
 Te Nijenhuis, K., 409, 446, 501, 503, 528, 530, 548, 572, 574, 585, 590, 595, 597, 631, 632, 643, 644, 825, 845
 Terhune, R.W., 349, 354
 Terinzi, J.F., 807, 817
 Tewarson, A., 853, 873
 Thackray, G., 466, 502
 Thakur, M., 338, 354
 Thomas, A.G., 693, 694, 702
 Thomas, D.A., 518, 522
 Thomas, D.P., 24, 47, 557, 558, 559
 Thomas, G.D., 754
 Thomas, N.L., 696, 762
 Thompson, A.B., 815, 818
 Tibbetts, S.J., 338, 354
 Timmermans, J., 76, 108
 Timoshenko, S., 837, 845
 Tobolsky, A.V., 90, 99, 107, 108, 391, 393, 397, 433, 442, 443, 479, 501, 502, 503, 618, 619, 644, 746
 Tokita, N., 388, 503
 Tonelli, A.E., 284, 362, 381
 Tordella, J.P., 573, 579, 597
 Torrance, J.B., 356, 381
 Traube, J., 64, 67, 76, 77, 78, 108, 217
 Treloar, L.R.G., 390, 401, 501, 503, 733, 742, 746
 Tribout, C., 723, 746
 Tsai, S.W., 844, 845
 Tschoegl, N.W., 447, 448, 501
 Tsvetkov, V.N., 306, 318
 Tung, L.H., 22, 46
 Turnbull, D., 704, 713, 746

U

- Ueberreiter, K., 149, 188, 697–700, 701, 702, 743, 746
 Ulich, H., 755, 761, 762
 Utracki, L., 608, 644

V

- Vaidyanathan, V.I., 357, 381
 Van Amerongen, G.J., 660, 661, 662, 695, 702
 Van Benschop, H.J., 631, 644
 Van den Heuvel, C.J.M., 865, 873
 Van der Hout, R., 489, 502, 741, 745
 Van der Meer, S.J., 388, 485, 503, 728–30, 746, 880, 885
 Van der Vegt, A.K., 470–1, 561, 563, 597, 817, 818
 Van der Werff, H., 739, 744, 746
 Van der Zwaag, S., 834, 835
 Van Dingenen, J.L.J., 738, 746
 Van Krevelen, D.W., 22, 24, 46, 64, 65, 67, 77, 101, 108, 132, 188, 191, 197, 198, 212–13, 226, 227, 284, 392, 617, 707, 716
 Van Leeuwen, J., 808, 818
 Van Nes, K., 61, 66, 67, 108
 Van Oss, C.J., 242, 244
 Van Saarloos, W., 580, 597
 Van Turnhout, J., 330, 331, 353
 Van Westen, H.A., 61, 66, 77, 108
 Vermant, J., 583, 597, 644
 Vieth, W.R., 682, 702
 Vincent, P.I., 461, 463, 467, 468, 869–71, 873
 Vinogradov, G.V., 305, 318, 556, 595, 597, 619, 644, 802, 803, 818
 Voeks, J.F., 225, 227
 Vogel, A., 61, 291, 292, 318
 Voigt, J., 325, 412–16, 436, 777
 Volkenshtein, M.V., 152, 188
 Von Falkai, B., 712, 746
 Von Helmholtz, H., 55, 67
 Vrentas, J.S., 693, 696, 701, 702
 Vrij, A., 103, 107

W

- Wada, Y., 503, 505, 522, 814, 818
 Wagner, M.H., 573, 597
 Wales, J.L.S., 24, 47, 300, 305, 318, 595
 Walker, L.M., 583, 597, 639, 644
 Wall, L.A., 776, 777
 Walters, K., 526, 568, 569, 578, 595, 631–4, 643, 644
 Warburton Hall, H., 462, 503
 Ward, I.M., 455, 464, 465, 489, 502, 503, 705, 739, 743, 744, 745, 746
 Warfield, R.W., 103, 107, 117, 118, 128, 368, 390, 396, 460, 501, 503
 Waterman, H.I., 422, 539, 596, 777
 Watson, J.P., 203
 Watson, W.F., 203, 226
 Weber, C., 810, 818
 Weber, M., 55, 67
 Weedon, G., 739, 746
 Weeks, J.J., 596, 715
 Welsh, W.J., 771, 777, 786
 Weir, F.E., 806, 807, 818
 Weissenberg, K., 526, 531, 556, 580, 597
 Wendt, R.C., 239, 240, 244
 Westover, R.F., 545, 597

Weyland, H.G., 64, 67, 130, 484, 503
 Whorlow, R., 501, 825, 845
 Wibaut, J.P., 292, 318
 Wilbourn, A.H., 425, 503
 Williams, D.J., 36, 46
 Williams, G., 187, 353, 426, 500, 521
 Williams, H.L., 24, 46
 Williams, M.L., 421, 442, 444, 503, 538, 597
 Wilson, C.W., 360, 374, 381, 382
 Wilson, K.G., 266, 267, 284
 Winding, C.C., 454, 501, 568, 728–9, 732, 811
 Windle, A.M., 696, 702
 Winter, H.H., 585, 596
 Wissbrun, K.F., 584–5, 596, 806, 817
 Wolf, B.A., 202, 226
 Wolf, K.A., 149, 187, 502
 Wolstenholme, A.J., 130, 188
 Woodbridge, D.B., 357, 381
 Wu, H.F., 499, 503
 Wu, S., 234, 235, 237, 238, 240, 244
 Wübbenhörst, M., 328
 Wunderlich, B., 32, 46, 47, 110, 114, 116, 117, 121, 123,
 127, 128, 152, 172, 188, 426, 712, 726, 727, 743,
 746, 761

Y

Yaneva, J., 696, 702
 Yano, O., 424, 503
 Yasuda, K., 547, 597, 625, 644
 Yau, W.W., 21, 46, 47
 Ye, Y., 560, 785, 786
 Young, J., 292, 318
 Young, R.L., 425, 426, 431, 500, 872

Z

Zapp, R.L., 841, 845
 Zentel, R., 181, 188
 Zhurkov, S.N., 693, 702
 Ziabicki, A.E., 735, 743, 811, 812
 Ziegler, K., 751
 Zimm, B.H., 272, 273, 284, 309, 310, 318
 Zisman, W.A., 232, 233, 234, 235, 244
 Zoller, P., 102, 123, 146, 166, 188
 Zwicky, F., 842, 845
 Zwijnenburg, A., 731, 738, 745, 746

This page intentionally left blank

SUBJECT INDEX

A

Abbe refractometer, 298
Abrasion, 841
 loss factor, 831
 resistance, 831, 881
Absorption, 313
 coefficient, 288
 index, 313
Absorptivity, 288
Acceleration of nucleation, 735
Acoustic
 properties, 505
 wave, 506, 507–508
Activation energy
 of the shift factor, 450
 for transport, 715, 716
 of viscous flow, 792
 volume, 464, 465, 466
Added properties, 797
Additive
 group contributions, 61
 molar functions, 60
 classification, 62
 properties, 60
Additivity, 4
Aesthetic properties, 52, 875
Affinity coefficient, 682
Aging time, 440
Alternating copolymers, 15, 16
Amorphous phase, 32
Andrade's equation, 603, 608
Angle, Brewster, 298
 contact, 232
 phase, 39
Angular frequency, 409
Angular velocity, 280, 527, 528
Anisotropy, 289
Antioxidants, 83, 784, 881
Apparent activation energy of permeation, 656
Apparent paradoxes, Griffith, 842
 Zwicky, 842
Apparent shear rate, 591, 592
Application(s)
 research, 816
 of solubility parameter diagrams, 221
Approach and objective, 3
Aramidés, 140
Arc resistance, 352
Arrhenius equation, 751
Article properties, 819
 of textile products, 875

Arylates, 140
Aspect ratio, 844
Atomic contributions, 61
Atomic and structural contributions to the parachor, 231
Attainable degree of crystallisation, 718–19
Attenuation, 288, 341
Autoxidation, 782, 783, 784
Average energy of activation, 765

B

Ball indentation hardness, 831, 838
Ballooning, 803
Band and line narrowing, 378
Band theory of electronic conduction, 335, 336
Barrier performance, 656
Barus effect, 526, 803
Basic mechanism of pyrolysis, 771, 772
Basic polymers, 137, 138, 153, 157, 178, 180
Basic volume ratios, 95
Bead-spring model, 619, 620
Beta-relaxation, 172
Biaxial extensional flow, 533
Biaxial shear, 533
Bingham number, 59
Binodal, 211, 212
Bipolarons, 341, 343
Birefringence, 289, 299–300, 304, 307, 479
 of drawn fibres, 307
 flow, 299, 300, 554
 form, 300
 intrinsic, 300
 as a measure of potential reversion and warping, 809
 stress, 300
Blobs, 270–1
Block copolymers, 16
Bodenstein number, 59
Bohr magneton, 379
Boiling point, 661
Bond
 dissociation energy, 759, 763–4
 strength and formation free radicals, 490, 881
Bondi rule, 100
Boyer/Spencer rule, 100
Boyle point branched polymers, 247, 657
Branching point, 274
Breaking of the weakest bond, 763–4
Brewster angle, 298
Brinell test, 837
Brittle fracture, 821

- Brittleness, 455
 Brittle temperature, 461, 467–9
 Bulk/Bulkiness, 877
 compliance, 385
 modulus, 385, 395, 396, 405
 Burgers model, 413
- C**
- Calculation of the free enthalpy of reaction from group contributions, 752
 Calorimetric properties, 109
 Capacity
 electric inductive, 287, 326
 heat, 109, 117
 magnetic inductive, 287, 355
 Capillary moisture transfer, 878
 Carbon residue on pyrolysis (%), 792
 Carreau model, 547
 Case I &II, diffusion, 696
 Case II
 sorption, 696
 transport, 695
 Catalog of group contributions, 61
 Categories of
 dimensionless groups, 55
 physical quantities, 54
 Causes of band and line broadening, 368, 375
 Ceiling temperature, 750
 Chain
 depolymerisation, 763, 767, 769, 771, 776
 modulus, 490
 Characteristic of
 absorption bands, 314
 extension time, 734
 shear time, 734
 Char extension, 754
 Charge-injection doping, 341, 345
 Charpy test, 829
 Char residue on pyrolysis, 774, 775, 856
 Chemical degradation, 779
 Chemical n-doping, 338, 341
 Chemical p-doping, 341
 Chemical shift anisotropy, 376
 Chemical shift, proton, 369
 ^{13}C , 367
 Chemical structure, 7
 Chiral, 35, 172
 Chirality of polarised light, 289
 Chronological development of commercial polymers, 44
 Circular anisotropy, 289
 Clarity, 313, 316
 Classification of
 composites, 843
 multiple component polymer systems, 36
 polymeric on the basis of mechanical behaviour, 29
 polymeric liquid crystals, 36
 processes, 799
 sorption isotherms, 681
- Clausius
 Clapeyron equation, 662
 Mosotti relation, 320, 321, 323
 Cloth elasticity, 879
 Clustering, 690, 692
 Coating, 794
 Code symbols for polymers, 938
 Coefficient
 absorption, 288
 diffusion, 604
 extinction, 288
 friction, 831, 841
 permeation, 673
 sedimentation, 604
 stress-optical, 303, 305
 thermal expansion, 97, 223, 791
 Cohesive energy, 189, 190
 density, 189, 190, 791
 Cohesive properties, 189
 Coiled chains and blobs, 270
 Cold drawing, 478, 821
 Cole–Cole plot, 326, 327, 329
 Coleman–Markovitz relationship, 550
 Colligative properties, 57
 Collision diameter of the gas, 669
 Colour
 fastness, 881
 and whiteness, 745
 Comb polymers, 132, 153
 Compensation effect, 667, 668, 752
 Complex modulus, 551
 Compliance(s), 325, 383
 bulk, 385
 creep, 415, 416
 shear, 385
 tensile, 385
 Composite structure of fibres, 33
 Composition parameter, 858
 Comprehensive tables, 858
 Compressibility, 224, 385
 Compressional waves, 390–1
 Compression (bulk) modulus, 514
 Compressive failure, 834
 Compressive strength, 835
 Concept
 of additive group contributions, 4
 “polymer properties”, 49
 “property”, 49
 Conductive polymers, 44
 Conductivity, 319, 332, 333
 electrical, 335
 thermal, 645
 Conductors, 333, 338
 Cone Calorimeter, 853
 Cone and plate rheometer, 533, 554, 580, 584
 Configurations, 8, 11, 15
 Conformations, 8
 Coni-cylindrical flow, 593
 Connectivity index, 117
 Considère

- Considère (*Continued*)
 construction, 462, 463
 plot, 813, 814
- Constant K and the exponent a of the Mark–Houwink equation, 255
- Constitutive properties, 60
- Contact angle, 232
- Continuous chain model, 489–90
- Continuous wave NMR, 365
- Contour length, 247, 490
- Controllability, 800
- Control testing of processing conditions, 807
- Convergent flow, 533, 578
- Conversion factors, 891
- Copolymers, 11–16, 37, 170
 alternating, 15, 16
 block, 16
 graft, 16
 random, 15, 16
- Correction of Rabinowitsch, 591
- Correlation
 between dielectric constant and solubility parameter, 331
 between electric resistivity and dielectric constant, 337
 of heat conductivity with crystallinity and density, 650
 between impact strength (brittleness) and critical molecular mass (M_{cr}), 536
 between impact strength and modulus, 832
 between indentation hardness and modulus, 838
 between Izod impact strength and T_g , 833
 of non-Newtonian shear data, 556
 between oxygen index and elementary composition, 853
 of permeability data, 674
 between the various molar volumes, 87
- Corresponding states principle, 608
- Cotton–Mouton effect, 299
- Couette
 flow, 527, 528, 529
 geometry, 527
- Counter-ions, 275, 276
- Coupling constants, 371
- Covalent atomic radii, 73
- Covering power, 876–7
- Cox–Merz relationship, 553
- C_p/C_v relationships, 117
- Cracking, 221, 866, 868
 solvent, 867
- Crack-tip, 455
- Crank-shaft mechanism, 425
- Crazing, 456, 820
 solvent, 867
- Creep, 405, 406
 compliance, 415, 416
 failure, 470–1
 rupture, 833–4
- Critical concentration, 279, 605
- Critical molecular mass, 146, 400, 534, 536, 537
- Critical Oxygen Index (COI), 853
- Critical size, 704–705
- Critical spherical nucleus, 710, 711
- Critical strain, 867, 868
- Critical stress energy factor, 474
- Critical surface tension of wetting, 232
- Critical temperature, 655
- Cross-linked polymers, 29
- Cross-linking, 148
- Cross model, 731
- Cross polarisation, 376, 377
- Crystallinity, 728, 732, 815
- Crystallites/Crystallisation, 690, 725
 of rigid macromolecules, 739
- Cyclical chain length, 782
- D**
- Damköhler number, 59
- Damping behaviour, 518
- Dangling ends, 400, 402
- Deborah number, 39, 696, 697, 725
- Debye
 dispersion relation, 326
 equation, 326
 forces, 242
 model, 326, 327
 relaxation, 325
- Decibel, 507
- Decimal fractions and multiples, 889
- Definition of molecular mass averages, 17
- Deformation
 flexural, 825
 plastic, 830
 polarisation, 325
 properties, 824
 uniaxial, 825
- De Gennes
 reptation model, 518
 scaling concepts, 795
- Degradation
 chemical, 779
 hydrolytic, 779, 785
 oxidative, 781
 photochemical, 779
 thermal, 763, 764
- Degree of
 crystallinity, 720, 728, 815
 ionisation, 275, 276, 278
- Dendrimers, 43
- Density, 790, 791
- Depolarisation, 38, 329
- Depropagation, 769
- Derived SI units, 889, 890
- Desirability, 884, 885
 profile for the application, 884
- Determination of the full molecular mass distribution, 19
- Diamagnetic, 355
- Dichroism, 289

- Die drawing, 739
 Dielectric, 321
 constant, 287, 321, 791
 loss, 326
 polarisation, 321
 relaxation, 38, 325
 strength, 345
 Die swell, 564, 573, 803
 Diffuse crystallisation zone, 723
 Diffusion/Diffusivity, 280, 663
 coefficient, 663
 of gases, 665
 layer, 697
 of liquids, 693
 of organic vapours, 692
 at room temperature, 668
 of simple gases in polymers, 666
 Dilatational waves, 506
 Dilute polymer solutions, 600
 Dimensionless
 groups of quantities, 55, 565
 process variables, 789
 Dipolar forces, 242
 Dipole moment, 323, 324
 Discotic, 35
 Disentangles, 707
 Dislocations, 29–31
 Dispersion
 curves, 332
 forces, 205
 Disproportionation, 771
 Dissipation factor, 330
 Dissociation energy of the weakest bond, 764
 Dissolution of polymers, 696
 Distortional waves, 506
 Distribution of molecular mass, 17
 Ditonic system, 66
 Doolittle equation, 621
 n-doping, 338
 p-doping, 338
 Doped conjugated organic polymers, 335
 Double refraction, 289
 Drape, 877
 Drawing, 813, 814
 cold, 478, 815
 hot, 815
 of spun filaments, 728
 Draw ratio, 478
 Driving force, 38, 39
 Drop weight impact strength, 808
 Dryability, 883
 Dry-cleaning, 884
 Dual-mode
 model, 682, 685, 687, 689
 of permeation, 685
 sorption and mobility data, 688
 Dual sorption model, 682
 Ductility, 455–6, 830
 Dullness, 313
 Dynamic laser-light scattering, 20
 Dynamic light scattering (DLS)dissipation) factor, 327, 840
 Dynamic mechanical measurements, 407
 Dynamic modulus, 451, 508
 Dynamic network of blobs, 279
 Dynamic or absolute system of units, 53
 Dynamic shear viscosity, 410
 Dynamictensile viscosity, 410
 Dynamic transitions, 418
- E**
- Ease of care properties, 884
 Effective flow length, 591
 Effect of
 structural groups on properties, 792
 temperature on oxygen index, 853
 temperature on viscosity, 538, 609
 Ehrenfest equations, 150, 152
 Einstein equations, 602
 for suspensions, 251
 Elastica test of Sinclair, 834
 melt, 316
 Elastic effects in polymer melts, 578
 Elastic moduli of some materials, 732
 Elastic parameters, 383, 386, 391
 Elastic shear deformation, 500, 531
 Elastic shear quantities, 556
 Electret, 329, 331
 Electrical conductivity, 319, 335, 337, 339
 Electrical properties, 319
 Electric displacement, 348
 Electric field, 351
 Electric flux density, 348
 Electric inductive capacity, 287, 319, 326
 Electric permittivity, 287
 Electric susceptibility, 348, 349
 Electrochemical
 n-doping, 341
 p-doping, 341
 Electron acceptor, 333
 parameter, 242
 Electron donor, 333, 337
 parameter, 242
 Electron spin resonance (ESR), 359, 379
 Electrophorus, 329
 Electrostatic interaction, 275
 Elliptic anisotropy, 289
 Ellis model, 547
 Elongation/Elongational, 459
 at break, 454, 475
 flow, 532, 585
 rate, 459
 viscosity, 585
 at yield, 457
 Emeraldine, 344
 End-to-end distances, 246, 248
 End groups, 7, 8
 End of pyrolysis, 765

- Endurance, 820, 829
 End use properties, 819, 847
Energy
 activation, 421, 537, 609, 656, 693
 cohesive, 190, 191
 of diffusion, 656
 dissociation, 764
 equivalence of light waves, 780
 interfacial, 229, 713
 internal, 190
 surface, 229, 230, 232
Entanglements, 29
Enthalpy/Entropy
 elasticity, 402
 as a function of temperature, 123
 of melting of various polymers, 120
 of mixing, 201
Environmental behaviour and failure, 847
Environmental decay in liquids, 864
Environmental shift factors, 872
Equations
 of conservation, 58
 Hartmann–Haque, 103
 Spencer–Dillon, 548
 of state, 103, 222, 223
 Tait, 101
Equilibrium
 constant, 751, 753
 spreading pressure, 230
 swelling, 190
Even/odd effect, 161, 186
Exaltation, 136
Excess volume of the glassy state, 94
Expansion
 coefficient, 246
 factor, 249
Experimental determination of the molecular mass
 average, 19
Expressions
 for concentration dependence, 795
 for temperature dependence, 792
 for time dependence, 794
Extended
 chain crystallisation, 706, 727, 730
 tie molecules, 728
Extensional deformation of polymer solutions,
 630
Extensional flow, 530, 532
Extensional viscosity, 565
Extensional viscosity of polymer melts, 564
Extensional wave, 390
Extensive quantities, 54
Extinction
 coefficient, 288
 index, 287
Extinctivity, 288
Extrudability, 800
Extrusion, 801
Eyring model, 465
- F**
- Factors influencing the value
 of T_g , 145
 of T_m , 166
Failure
 envelope, 475
 maps, 822
 mechanism
 maps, 820
 in polymers, 820
Falling weight
 impact, 808
 test, 829
Fanning number, 59
Fano flow, 632
Faraday–Verdet effect, 299
Fatigue, 832
 failure, 469
 life, 832
 limit, 832
 resistance, 832
 tester, 832
Feed back information, 816
Ferromagnetic, 355
 polymers, 356
Fiber-reinforced polymer systems, 38
Fickian diffusion, 665
Fick's law, 663, 684
Field flow fractionation, 20
Filled polymers, 38
First normal stress
 coefficient, 545
 difference, 640
First-order transition, 27, 152
Flame-retardant additives, 861
Flammability, 847
Flashing, 804
Flash line region, 807
Flexibility of a chain molecule, 246
Flexible polymer molecules, 706
Flexural deformation under constant load, 825
Flexural formulas, 826
Flexural rigidity, 877
Floor temperature, 751
Flory–Huggins
 interaction parameter, 273
 lattice theory, 201
Flow
 birefringence, 299, 300, 554
 convergent, 533, 578
 Poiseuille, 529
 simple shear, 528, 531
 unstable, 578
Fluctuating density, 288
Fluffing, 881
Folded chains, 705, 706
 blocks, 728
 lamellae, 704

Ford equation for the viscosity of a suspension, 602
 Form birefringence, 300
 Formula of Seitz and Balazs, 450
 Fourier
 number, 59
 transform, 361
 Fourier Transform Infrared Spectroscopy, 313
 Fractional free volume, 666
 Fraction amorphous, 679
 Fractionation of chain molecules according to their
 chain length, 727
 Fracture mechanics, 472
 Free enthalpy of formation, 753, 754
 Freely jointed chain model, 247
 Free-rotation model, 246
 Free surface energy, 229
 Free volume fraction, 537
 Freeze-off time, 806
 Freezing-in process, 151
 Frequency
 doubling, 349
 factor, 751
 Frequently used combinations of groups, 141
 Fresnel's relationship, 297
 Friction, 840
 coefficient, 831
 Fringed micelle model, 29
 Fugacity, 756
 coefficient, 756
 Functional structural groups, 129
 Fundamental quantities of mass and volume, 72
 Fundamental viscoelastic phenomena, 406

G

Gas-polymer-matrix model, 687
 Gaussian or random-flight statistics, 246
 Gel layer, 697
 Gel-permeation chromatography (GPC), 19
 Gel-spinning, 730
 Gel-spun yarns, 735
 General correlation of
 aesthetic properties, 876
 maintenance properties, 883
 use (performance) properties, 878
 General description of polymer-penetrant system,
 695
 General expressions, 97
 for the interfacial tension, 239
 Generalised curve for the thermal conductivity, 648
 Generalised failure envelope, 464
 Generalised form of WLF equation, 538
 Generalised melt flow rate diagram, 801
 Generalised stress-strain relationship, 488
 Generalised tensile stress-strain curve, 453, 454
 Generalised ultimate parameters of an elastomer, 476
 Glass-rubber transition, 26, 130
 temperature, 26

Glass transition
 and compressive strength, 835
 temperature, 167, 426, 611, 669, 791
 of plasticizer (solvent), 611
 polymer solutions, 611
 Glittering, 876
 Graft copolymers, 16
 Griffith's
 equation, 474
 model, 473
 Group contributions/Group increments, molar
 attraction, 191
 char formation/forming tendency, 763, 773
 function, 4, 61
 to molar cohesive energy, 190, 197
 dielectric polarisation, 332
 elastic wave velocity (Rao and Hartmann
 functions), 515
 entropy of melting, 122
 free energy of formation, 704–705
 glass transition, 132
 for combi-groups, 141, 142
 heat capacity, 110
 intrinsic viscosity, 253
 loss area in acoustic waves, 507–508
 mass of structural unit, 73
 melt transition, 153
 for combi-groups, 163
 number of backbone atoms per structural unit,
 63, 253
 optical refraction, 290
 parachor, 231
 permachor, 678
 refraction (Gladstone–Dale, Lorentz–Lorenz,
 Vogel), 292
 thermal decomposition, 767
 Van der Waals volume, 74, 75
 viscosity–temperature function, 543
 volume in amorphous state, 86
 in crystalline state, 85, 86
 in glassy state, 80, 82
 in rubbery state, 77, 79
 to zero-point molar volume, 76
 Group-contribution technique, 4
 Grow rate, 714
 Growth, 703, 704
 Grüneisen
 rule, 391
 Tobolsky rule, 391
 Gyromagnetic ratio, 379

H

H shift, 772
 Hagen–Poiseuille law, 591
 Handle, 747
 indentation, 456, 837
 Mohs, 836–7

- Handle (*Continued*)
 Rockwell, 831
 Shore, 831, 838
- Hardness scales
 for hard and soft materials, 839
- Hartmann
 function, 391
- Hahn condition, 376
- Haque equation, 103
- Heat
 capacities, 109, 117
 of polymers, 112
 of combustion, 852
 distortion, 848
 temperature, 848–9
 fastness, 784
 stability, 847, 848
 transfer coefficient, 645
- Helix conformation, 279
- Hencky strain, 565, 568
- Henry's law, 658, 681
- Hermans' function, 480
 orientation function, 586
- Heterochain polymers, 11, 14
- Heterogeneity, 289
- Heterogeneous nucleation, 710
- Highly crystalline polymers, 647
- High performance polymers, 842
- High power decoupling, 376
- High-pressure crystallisation, 727
- High-resolution NMR, 361, 368
- High-speed stress-strain test, 829
- Hindered Amine Light Stabilisers, 785
- Hoffman-type equation, 717
- Holes, 682, 684
- Homochain polymers, 11, 12
- Homogeneous nucleation, 710
- Homo-polymer, 7
- Hooke
 element, 412
 model, 413
- Horizontal Burning Test, 854
- Hot drawing, 815
- Hoy's system for estimation of the solubility parameter and its components, 217
- Huggins
 constant, 600, 601
 equation, 600
- Hydrodynamic
 expansion factor, 251
 liquid layer, 697
 volume, 251
- Hydrogen bonding, 205
 number, 205
 parameter, 869
 tendency, 206
- Hydrolytic degradation, 785
- Hydroperoxides, 783
- Hydrophilic materials, 880
- Hydroplastics, 29
- Hydrostatic compression, 385
- Hydrostatic extrusion, 739
- Hydrostatic pressure, 384
- Hyper-polarisability, 351
 tensor, 351
- Hysteresis in V-T-diagram, 427
- I**
- Ignition, 352
- Immersion technique, 507
- Immobilisation, 682
- Impact
 resistant polymer systems, 38
 strength, 780
- Imperfections, 842
- Increase at the glass transition, 117
- Increments, 4, 137
see also Group contributions/Group increments, molar
- Indentation hardness, 455, 831
- Induced crystallisation, 726, 728
- Induction
 forces, 242
 period, 706, 783
- Inflammation, 852
- Influence
 of entanglements, 625
 on viscosity, 626
 of functional groups on the $Y_m(\text{CH}_2)$ increment, 158, 159
 of orientation on the properties, 728
 of procesing on the ultimate properties, 800
 of symmetry, 186
- Infrared
 absorption, 313
 spectroscopy, 313
- Infra-sonic frequency, 505
- Inherent viscosity, 250
- Initial compliance, 491, 495
- Initial modulus, 485, 490
- Injection moulding, 800
- Inorganic filaments, 742
- Insulators, 335
- Intensive quantities, 54
- Interaction parameter, 201
- Inter-atomic distance, 73
- Interfacial energy properties, 229
- Interfacial free energy, 704–705
- Interfacial tension, 227
 between liquid and solid, 230
 between a solid and a liquid, 232
- Intermolecular interaction, 60
 by hydrogen bonding, 139
- Internal energy, 190
- Internal friction, 464, 840
- Internal pressure, 222, 225, 230
- International System of Units (SI), 53, 889

- Inter-relations of elastic parameters, 386
 Interrelationships
 between static and dynamic viscoelastic functions, 452
 between transport quantities, 281
 Intramolecular blends, 37
 Intramolecular interactions, 60, 140
 Intrinsic birefringence, 300
 Intrinsic flow birefringence, 304
 Intrinsic numerics, 56, 684
 Intrinsic properties, 49, 50, 789
 Intrinsic viscosity, 245, 249, 251
 Intumescing agents, 864
 Ionic strength, 275
 Ironability, 883
 Iso-ionic dilution, 276
 Isokinetic temperature, 752
 Isotherm according to Brunauer, Emmett and Teller, 681
 Izod
 impact strength, 830, 831
 test, 829–30
- K**
- Keesom forces, 242
 Kelley–Bueche equation, 611
 Kerr effect, 299, 349
 Kinetic(s)
 chain length, 776
 of thermal degradation, 776
 Kraemer
 constant, 600
 equation, 600
 Krigbaum equation, 252
 Kuhn-length, 247
- L**
- Lambert's
 law, 288
 relationship, 288, 313
 Lamé constants, 386
 Lamellar structures, 31
 Larmor
 frequency, 362
 precession, 362
 Latent heat of fusion (crystallisation), 118
 Layer thickness, 698, 699
 Length of folds in crystal lamellae, 727
 Lennard-Jones
 equation, 658
 scaling factors, 658
 temperature, 658, 661, 662, 663
 Leslie–Ericksen theory, 585, 587, 641
 Leuco-emeraldine, 345, 346
 Lewis
 acid-base polar interactions, 242
 number, 56
 Lifschitz–Van der Waals (LW) interactions, 242
- Light
 fastness, 784, 878
 refraction, 290
 scattering, 308, 404
 Limiting Oxygen Index (LOI), 486
 Limiting viscosity number, 245, 249, 250
 under Θ -conditions, 253
 Linear coefficient of thermal expansion, 89
 Linear density, 488
 Linear non-thermoplastic polymers, 28
 Linear thermoplastic semicrystalline polymers, 29
 Liquid crystalline polymers, 35, 38, 176, 177, 350,
 581, 582, 634
 melts, 581
 Liquid–liquid relaxation, 171
 Local mode relaxation, 170
 Lodge's constitutive equation, 548
 Logarithmic
 decrement, 397
 viscosity number, 250
 London forces, 242
 Longitudinal absorption, 511, 513
 Longitudinal sound velocity, 791
 Longitudinal speed, 505
 Longitudinal waves, 390, 506
 Long-range order, 25
 Long-term
 behaviour, 820
 creep, 415
 stiffness, 25
 Lorentz–Lorenz relation, 321
 Loss
 area, 505
 factor, 326
 modulus, 408–409
 tangent, 326
 Lower critical solution temperature (LCST), 211
 Lower glass transition, 171
 Lustre, 317
 and gloss, 876
 Lyons–Tobolsky equation, 618
 Lyotropic, 35
 Lyotropic liquid-crystalline type, 739
- M**
- McGowan rule, 392
 Mach number, 56
 Macroconformations, 31, 32
 Macro-ions, 275
 Macromolecules, 7
 Magic-angle spinning, 375
 Magnetic critical phenomena, 266
 Magnetic dipole moment, 362
 Magnetic energy levels, 365, 366
 Magnetic field, 299
 intensity, 355
 strength, 355

- Magnetic flux density, 355
 Magnetic induction, 355
 Magnetic inductive capacity, 287, 355
 Magnetic permeability, 287
 Magnetic properties, 355
 Magnetic resonance, 359
 high resolution, 362, 368
 wide line, 361, 373, 374
 Magnetic susceptibility, 355–9, 791
 Magnetic tricritical phenomena, 266, 267
 Magnetisation, 902
 Magnetogyric ratio, 362, 366
 Magneto-optic effect, 299
 Maier–Saupe mean field theory, 638
 Main parameters of spherulitic crystallization, 703
 Maintenance or care properties, 51, 882
 Mandelkern's equation, 715
 type equation, 717
 Mark–Houwink
 constant, K, 603
 equation, 252, 255
 exponent a , 256
 Mass magnetic susceptibility, 356
 Mass transfer in polymeric systems, 655
 Master curve, 713
 of creep compliance, 416
 of the rate of growth of spherulites, 718
 for $\eta_{cr}(T)$, 541
 Matrix, 841
 model, 687
 Maximum extension ratio, 812
 Maximum rate of spherulite growth, 718
 Maxwell
 element, 412, 413
 model, 413, 415, 418
 relationship, 319
 Wiechert model, 414, 417
 Measurement techniques of the elastic moduli, 388
 Mechanical behaviour and failure, 819
 Mechanical comfort, 879
 Mechanical properties of
 solid polymers, 383
 various materials, 389
 Melt/Melting, 167, 700
 elasticity, 316
 expansion, 97
 flow index, 801, 802
 flow rate diagram, 801
 fracture, 578
 number, 579
 strength, 799, 812
 Merkel number, 59
 Mesogenic groups, 34
 in the main chain, 177
 side-chain, 179
 Mesogenic polymers, 172
 see also Liquid crystalline polymers
 Mesophases, 34, 172
 see also Liquid crystalline polymers
 Metallocene refraction, 43
 Method(s)
 of band and line narrowing in the NMR spectroscopy, 378
 for expressing the additivity, 61
 of reduced parameters, 609
 Micro-voids, 666, 681
 Miesowicz viscosities, 586–8
 Mode of fracture deformation, 474
 Mode I, II, III, 474
 Models of viscoelastic behaviours, 412
 Modes of deformation, 526
 Modulus, 396
 bulk, 395, 405, 447, 514
 complex, 410, 418
 dynamic, 451
 loss, 408
 shear, 384, 400, 489
 and strength of ultradrawn polymers, 733
 tensile, 385, 401, 432, 458
 Young's, 385
 Mohs' scale of hardness, 837
 Moisture absorption, 878
 and transport, 689–90
 Moisture transfer, 877–8
 Molar attraction
 component group contributions, 214
 constant, 191
 Molar elastic wave functions, 383, 391
 Molar free enthalpy of formation, 792
 Molar functions, classification, 62
 Molar heat
 capacity at constant pressure, 109
 capacity at constant volume, 109
 capacity of solid and liquid polymers at 25°C, 110
 of sorption, 656
 Molar loss area, 519
 Molar magnetic susceptibility, 63, 356
 Molar mass, 73
 Molar oxygen demand, 855
 Molar permachor, 678, 679
 Molar polarisation, 320, 321
 Molar quantities, 54
 Molar refraction, 291–2
 Molar thermal decomposition function, 763, 767
 Molar thermal expansivity, 89
 Molar viscosity–temperature function, 543
 Molar volume (s)
 of crystalline polymers at 298 K, 80
 of fully crystalline polymers at 25°C, 84
 as a function of temperature, 97
 as a function of the Van der Waals volume, 81
 of glassy amorphous polymers at 25°C, 82
 of glassy amorphous polymers, 80
 of organic liquids, 78
 of rubbery amorphous polymers, 79
 of semi-crystalline polymers, 85
 Molar water content of polymers, 690
 Molecular aggregation number, 216–17
 Molecular asymmetry, 167
 Molecular composite, 37

- Molecular dimensions, 246
 Molecular lattice fitting, 159
 Molecular mass, 17
 critical, 54, 146, 400, 537
 determination, 19
 distribution, 7, 17, 19, 23
 number-average, 17
 viscosity average, 17
 weight-average, 18
 z-average, 18
 Molecular polarisability, 320
 Monodomain, 583
 Mooney engineering stress, 403, 404
 Mooney–Rivlin equation, 402, 403
 Mooney stress, 402
 Morphology/Morphological, 29, 706
 in crystallites, 707
 models, 705
 Mouldability, 799
 index, 799, 806
 Moulding, 799
 area diagram, 804, 807
 Multi angle laser light scattering (SEC/MALLS), 16
 Multiple-component polymer systems, 36, 38
 Multiplet structure, 368
- N**
- Natural draw ratio, 738
 Nature of the glass transition, 151
 Neck/Necking, 463, 728, 813
 zones, 33
 Nematic, 35, 175, 176
 Network
 of intermolecular hydrogen bonds, 139
 polymers, 16
 structure, 148
 Newton/Newtonian
 element, 412
 model, 412
 viscosity, 554
 New viscosity–temperature relationship, 539
 NLO phenomena, 351
 NMR spectroscopy, 375
 Nomenclature of solution viscosity, 250
 Nominal
 strain, 386
 stress, 736
 Non-Fickian diffusion, 696
 Non-functional structural groups, 129
 Non-linear optics, 347
 Non-Newtonian viscosity, 554
 Non-redox doping, 345
 Non-relaxed dielectric constant, 325
 Normal
 force pump, 526
 stress, 529
 coefficient, 526
 difference, 526
 Northolt's equations for well-oriented fibers, 498
- Nuclear magnetic resonance (NMR) spectroscopy, 361, 367, 374
 Nuclear magneton, 364
 Nuclear quadrupole
 moment, 361
 resonance, 361
 Nucleation, 703, 708, 709
 factor, 704
 predetermined, 709
 spontaneous (sporadic), 709
 Number
 average molecular mass, 17
 of nuclei, 711
 of repeating units per effective chain segment, 217
 Numerics, 55
 Nusselt number, 56, 59
 Nutting's formula, 436
- O**
- Odd–even effect, 159
 Onsager rigid-rod model, 637
 Opaque material, 288
 Opaqueness, 313, 316
 Open siphon flow, 526
 Optical activity, 289, 299
 Optical appearance properties, 313, 316
 Optical properties, 287
 Optical rotation, 299
 Orbital angular momentum, 363
 Ordering parameters, 152
 Orientation, 478, 741
 distribution parameter, 479
 parameter, 492
 polarisation, 322
 process, 33
 sensitivity, 800
 Oriented fibres, 478
 Origin of aging, 439
 Osmotic second virial coefficient, 272
 Ostwald–De Waele
 constant, 494
 equation, 546
 Overall
 mechanism of the thermal decomposition, 767
 rate of crystallisation, 706, 708
 Oxidative degradation, 781
 Oxygen index (OI), 853
 and elementary composition, 858
 of polymers, 853
 test, 853
- P**
- Packing, 71
 Parachor, 229
 Paracrystalline
 fibres, 742
 structure, 705
 Paracrystallinity model, 31, 32

- Parallel plates, 527
- Parallel polarised light, 299
- Paramagnetic, 355
- Padox of Kauzmann, 151
- Partially immobilising sorption, 682
- Partly oriented yarns, 483
- Péclet number, 56, 59
- P-electron conjugation, 140, 161, 183
- Penetrant, 655
- Performance properties, 52
- Permachor, 676
- Permeability, 656, 673, 676
 - coefficient, 656
 - magnetic, 287
 - of polymers, 675
- Permeation
 - coefficient, 673
 - of a more complex nature, 681
 - of simple gases, 656
- Permittivity, 319
- Pernigraniline, 339
- Peroxy radicals, 781
- Perpendicular-polarised light, 299
- Persistence length, 248
- Phase transitions, 25
 - of the first order, 123
- Phenomenology of the thermal decomposition, 765
- Phonon model, 646
- Photochemical degradation, 779
- Photo-doping, 341
- Photooxidation, 781, 783
- Physical ageing, 438
- Physical constants of solvents, 904
- Physical data of simple gases, 657, 658
- Physical properties of polymers, 920
- Physical quantity, 52
- Pilling, 881
 - tester, 881
- Planar extensional flow, 533
- Plane
 - strain, 475
 - stress, 474
- Plastic
 - deformation, 814
 - flow, 837
- Plasticizer, 150
- Pleat and crease retention, 879
- Pleochroism, 289
- Ploughing, 841
- Plunger forward time, 806
- Pockels-effect, 349
- Poiseuille
 - flow, 591
 - number, 59
- Poisson ratio, 383
- Polar forces, 205
- Polarisation, 319
 - flux density, 348
- Polaron, 341
- Polydispersity index Q, 21
- Polydomain, 582
- Polyelectrolytes, 274
 - solution, 275
- Polymer
 - adhesion, 242
 - branched, 16, 273
 - comb, 178, 180
 - cross-linked, 29
 - heterochain, 11, 14
 - homochain, 11, 12
 - liquid crystals, 308
 - network, 16–17
 - rigidity, 400
 - self-reinforcing, 37
 - solvent interaction parameter, 203
 - structure, 8, 303
- Polymeric alloys, 37
 - liquid crystals, 34
 - matrices, 842, *see* Liquid crystalline polymers
- Polysalt, 275
- Power functions, 795
- Power-law
 - equation, 605
 - method, 607
- Practical unit system, 53
- Prandtl number, 56
- Predictions, 3
 - of solvent behaviour, 871
 - of viscosity as a function of shear rate, 561
- Premelting transition (T_{xc}), 171
- Pressure
 - coefficient of viscosity, 544, 545
 - hydrostatic, 385
 - induced crystallisation, 726
 - internal, 222, 223, 225
 - temperature superposition, 442
 - yield, 840
- Primary char, 771
- Primary gas, 771
- Principal solid state ^{13}C NMR techniques, 337
- Pristine, 337–8
- Processability, 800
- Processing
 - conditions, 800
 - properties, 49, 50, 796, 797
- Product or article properties, 49, 796, 797
 - profile, 884
 - method, 884
 - properties, 819, 847
- Properties
 - added, 52, 797
 - aesthetic, 52, 875
 - article, 819
 - colligative, 57
 - deformation, 824
 - end-use, 819
 - intrinsic, 49, 50, 792, 795
 - system-related, 819
 - use, 52, 821
 - of very dilute solutions, 245

- Proton chemical shifts, 369
 Pseudo ideal state, 247
 Pulling rod, 810
 Pulsed Fourier Transform NMR, 361
 Pulsed NMR, 365
 Pure shear flow, 533
 Pyrolysis, 765
- Q**
- Quantities
 extensive, 54
 intensive, 54
 molar, 54
 physical, 52
 specific, 54
 Quasi-induction period, 696
 Quasi second-order transition, 130
 Quenching, 712, 722
- R**
- Radius of gyration, 249, 309
 Ram extrusion, 739
 Random
 coil, 29
 statistics, 246
 copolymers, 15
 degradation, 771
 scission, 763, 771
 walk necklace model, 247
 Rao-function, 391, 513, 514
 Rate
 constant, 38
 of cooling, 703
 of crystallisation, 706, 708
 dependence of ultimate strength, 459
 of dissolution, 697
 of elongation, 459, 734
 of growth, 706, 708
 of loss of weight, 765
 of shear, 275
 Rayleigh's ratio, 308
 Real polymer chain, 247
 Recommended values for group contributions to standard molar volume, 87
 Recoverable shear, 531, 551
 Recoverable shear strain, 551
 Recrystallisation, 703
 Rectilinear flow, 527
 Redox doping, 341
 Reduced
 intrinsic quantities, 794
 Mark-Houwink equation, 261
 viscosity, 250
 Reference
 time, 794
 values, 789
 of intrinsic properties, 790
 Refinements of the solubility parameter concept, 205
 Reflectance, 297
 coefficient, 297
- Reflection, 297
 of light, 297
 Refraction, molar, 291
 Refractive index, 287, 741
 increment, 309
 Regions of viscoelastic behaviour, 398
 Reinforcements/Reinforcing, 841
 geometries of composites, 843
 material, 842
 Relation/Relationship
 between dielectric constant and optical quantities, 331
 between dielectric polarisability and optical dispersion, 331
 between diffusion coefficient and liquid viscosity, 694
 Relationship of Dupre, 242
 the permeation parameters, 674
 Relation of williams, Landel and Ferry, 713
 the elastic moduli, 387
 glass transition temperature and melting point of polymer, 161
 maximum elongation and Poission ratio, 458
 morphology and rheology, 584
 T_g, T_m and other transition temperatures, 170
 Relative
 magnetic susceptibility, 355
 scratch resistance, 837
 viscosity, 250
 Relaxation
 phenomena, 38, 331
 time, 39, 414, 424, 734
 time spectrum, 432
 Relaxed dielectric constant, 325
 Repeating units (structural units), 7
 Reptation
 model, 271
 movements, 279
 Residue of pyrolysis, 852
 Resilience, 412
 Resistance
 arc, 352
 fatigue, 832
 scratch, 836
 static charging, 878
 wear, 881, 885
 Resonance, 161
 Response, 39
 coefficient, 39
 Retardation time, 417
 Retention of surface appearance, 881
 Reversion, 808
 test, 808
 Reynolds number, 580, 655, 698
 Rheological behaviour
 of isotropic versus anisotropic melts, 582
 isotropic versus anisotropic solutions, 642
 Rheological constitutive equation, 386
 Rheological properties of polymer solutions, 459

- Rheological quantities, 548
 Rigidity, 400
 Rigid rodocrystallisation, 706
 Rod climbing effect, 526
 Rod-like molecules, 252
 Rod-like polymer molecules, 274
 Rod-shaped particle, 276
 Rubber elasticity, 401
 Rubbery plateau, 400
 Rudin equations, 272
 Rudin–Strathdee equation, 602
 Rules of thumb for substituting an H-atom by a group X, 182
- S**
- Saturation capacity, 681
 Scaling factor, 676
 Scattering, 316
 coefficient, 288
 crystallisation, 719
 of polymers from the melt, 706
 of light, 308
 of particles, 288
 Schmidt number, 56
 Scratch resistance, 836
 Second Newtonian flow region, 564
 Second normal
 stress coefficient, 531
 stress difference, 531
 Second-order
 susceptibility, 350
 transition, 26, 149
 Second virial coefficient, 309
 Sedimentation, 280
 coefficient, 604
 Segmental anisotropy, 304, 306
 Self-avoiding walks, 269
 Self-diffusion, 694
 Self-reinforcing polymers, 37
 Self-stabilising effects in polymer spinning, 811
 Semi-conductors, 336
 Semi-empirical approach, 4
 Semi-rigid polymer molecules, 706
 Series aggregate model, 486
 Shape retention, 879
 Shaping processes, 799
 Shear, 384
 absorption, 511
 biaxial, 533
 compliance, 385
 critical, 579, 580
 ductility, 456
 moduli of polymers, 392
 modulus, 383, 492
 rate, 627, 800
 simple, 384, 526
 speed, 506
 stress, 465
 viscosity, 525
 waves, 388, 506
- Sherwood number, 56, 59
 Shielding constant, 368
 Shift factor, 443
 Shish kebab structure, 705, 731
 Shore D hardness, 831
 Shore hardness testers, 838
 Short-range order, 25
 Short shots, 804
 line region, 807
 Short-term behaviour, 820
 Short-time stiffness, 25
 Side chain effects, 184
 Significance of the shift factor, 450
 Silky lustre, 876
 Simha/Boyer rule, 100
 Similarities and differences between Y_g and Y_m , 183
 Simple
 extension, 526
 shear, 385, 527
 flow, 528
 Simulation experiments, 816
 Single crystals, 25, 705, 707
 Size-exclusive chromatography (SEC), 16
 Skeletal factor, 246
 Slip-stick motion, 841
 Small angle neutron scattering (SANS), 245
 Smectic, 35, 172
 Smith failure envelope, 475
 Smoke formation, 864
 Snellius law, 291, 297
 Softness, 877
 Soiling, 881
 Solid
 infiltration layer, 671
 state NMR, 361, 376
 swollen layer, 697, 698
 Solitons, 339
 Solubility/Solubilities, 189, 201, 659, 662
 circles, 210
 of crazing fluids, 868
 of gases
 in polymers, 659
 in rubber, 661
 limits, 211
 of lyotropic liquid crystal polymers, 634
 parameter, 189, 190, 200, 867, 884
 and Θ -temperatures, 213
 components, 212
 of simple gases in polymers, 660
 Solvent(s)
 cracking, 867
 crazing, 867
 rigid-rod aromatic polymers, 221–2
 Sonic absorption, 517
 Sonic waves, 505
 Sorption
 behaviour according to Henry's law, 681
 energy, 662
 isotherm according to Langmuir, 681
 isotherm of Flory–Huggins, 681

- Sound
 - absorption, 505, 506
 - propagation, 506
 - speed, 506
 - velocity, 506, 514
- Spacers, 177
- Specific bulk modulus, 792
- Specific conductivity, 287
- Specific damping capacity, 411
- Specific entropy of fusion, 791
- Specific expansivity, 791
- Specific heat, 791
- Specific heat capacity at constant pressure, 109
- Specific heat capacity at constant volume, 109
- Specific heat as a function of temperature, 111
- Specific permachor, 676
- Specific quantities, 54
- Specific refraction, 291
- Specific refractive index increment, 791
- Specific shear modulus, 792
- Specific tenacity
 - versus initial specific modulus, 482
 - versus specific dynamic tensile modulus, 482
- Specific thermal expansivity, 89
- Specific viscosity, 250
- Specific volume, 790
- Spectroscopic splitting factor, 379
- Specular reflectance, 316–17
- Spencer–Dillon equation, 548
- Spencer–Gilmore equation, 103
- Spherulite/Spherulites/Spherulitic, 31, 707, 708
- Spin
 - angular momentum, 363–4
 - draw ratio, 811
 - lattice relaxation time T_1 , 374
 - stretch factor, 741
- Spinnability/Spinning, 809
 - with high-speed winding, 728
- Spinodal, 211
- Spin–spin
 - coupling, 368
 - interactions, 370
 - relaxation, 372
 - time T_2 , 374, 376
- Spiral flow length, 804
- Spiral flow test, 805
- Spiral length, 799
- Spreading
 - coefficient, 232
 - pressure, 230
- Spriggs' truncated power law model, 546
- Stabilisers, 784
- Stability of fluid threads in melt spinning, 810
- Standard molar volumes at room
 - temperature, 76
- Stanton number, 59
- Static charging, 882
- Static electrification, 333
- Staudinger index, 250
- Steady state, 697
- Stefan number, 56
- Steric hindrance, 162, 183, 292
- Stiffness, 395, 730
 - factor, 246
- Stockmayer–Fixman equation, 252
- Storage modulus, 408
- Strain, 414
 - at break, 480
 - hardening, 814
- Stress
 - birefringence, 300
 - components in simple shear, 530
 - induced crystallisation, 726, 728
 - multipliers, 455
 - optical coefficients, 300, 301, 303, 305
 - overshoot, 546
 - relaxation, 432, 433
 - as a measure of chemical degradation, 785
 - strain behaviour of drawn yarns, 484
 - strain curves, 454, 461, 480
 - strain diagram, 453
 - tensor, 402, 409
 - vector, 529, 530
- Stretchability, 813
- Stretch rate, 735
- Structural/Structure
 - composites, 38
 - groups, 8, 9
 - interaction effects, 161
 - isomer effects, 184
 - model of fibres, 731
- Struik's rules, 437
- Substituent reactions, 763, 771
- Superconductivity, 340–1
- Superconductors, 336
- Supercooled liquid, 151
- Super-cooling, 710
- Super-drawing, 738
- Supersaturation, 709
- Surface
 - energy, 230
 - solid polymers, 234
 - of liquids and melts, 230
 - entropy, 237
 - friction, 840
 - imperfections, 842
 - tension, 229, 791
 - of liquid, 229
 - of solid, 229, 234
- Survey
 - of additive molar functions, 62
 - of group contributions in additive molar quantities, 946
- Susceptibility tensor, 349
- Swelling
 - behaviour, 221
 - factor, 272
 - ratio, 577
- Symbol index, 957
- Systematic processing experiments, 816
- System of dimensionless groups, 59

T

Taber abraser, 841
 Tacticity, 147, 167
 Tait equation, 101
 Telechelic polymers, 8
 Telescopic flow, 528
 Temperature
 coefficient of density, 89
 dependence of solubility, 203
 dependence of viscosity, 537
 Flory, 211, 214
 glass transition, 611, 808
 of half decomposition, 765
 of initial decomposition, 765
 isokinetic, 752
 of maximum crystallisation rate, 718
 of the maximum rate of decomposition, 765
 melting, 709, 711
 ranges of strong ageing, 439
 transition, 170, 383
 Tenacity, 480
 Tensile
 compliance, 383
 creep, 438
 modulus, 457, 458, 489
 strength, 457
 correlated with modulus, 458
 Tension, 455
 Test mould, 803
 for orientation, 808
 Theory of Gibbs and Di-Marcio, 151
 Thermal
 comfort, 877
 conductivity, 645
 decomposition, 763
 degradation, 763
 of polymers, 764
 diffusivity, 806
 end use properties, 847
 expansion, 89
 coefficient, 223, 791
 model of polymers, 90
 expansivity of polymers, 92
 feedback, 851–2
 history, 176
 insulation, 877
 Thermally stimulated discharge (TSD), 329
 oxidation, 779, 781, 783
 Thermochemical properties, 749
 Thermodynamics of free radicals, 758
 Thermoplastic(s), 29
 elastomers, 37
 Thermotropic, 35
 liquid-crystalline type, 739
 liquid crystal polymers, 172
 Thermotropy, 176
 Theta
 solvent, 246
 temperature, 247
 Tie molecules, 34, 729

Time

dependent effects, 368
 domain NMR, 361
 to failure in a liquid environment, 871
 lag, 665, 684
 temperature equivalence (superposition) principle, 447
 Tobolski–Bueche rule, 99
 Torsion/Torsional
 flow, 529
 formulas, 827
 rigidity, 384
 Tortuosity, 679
 Toughness, 829
 Trade names and generic names of polymers, 941
 Transformations of 1st and 2nd order, 131
 Transient
 behaviour, 585
 viscosity, 568
 Transition
 glass–rubber, 26, 27, 130
 (“leathery”) region, 396
 premelting, 171
 second-order, 26, 150
 temperatures, 129, 392
 Translucent/Translucence, 316
 material, 289
 Transmission of light, 289
 Transmittance, 316
 Transparent/Transparency, 316, 876
 material, 291
 Transport
 factor, 704
 properties in dilute polymer solutions, 604
 Transportability, 704
 Transversal sound velocity, 791
 Transverse waves, 506
 Tresca yield criterion, 455
 Triboelectric series, 333
 Triboelectric series of polymers, 334
 Trouton’s
 law, 657
 ratio, 569
 True strain, 386
 Turbidity, 288, 308
 Two-stage super-drawing, 738
 Types
 of mesophases, 35
 of molar properties, 57
 Typology
 of polymers, 7
 of properties, 49

U

Ultimate
 electrical properties, 352
 elongation, 480, 483
 mechanical properties, 453, 457
 strength, 454, 455
 Ultradrawing, 734

Ultra-sonic frequency, 505
 orientation, 478, 728
 Ultraviolet absorber, 780
 Uniaxial
 deformation under constant load, 825
 extension, 385
 flow, 569
 flow, 532
 Unified theory of crystallisation processes, 706
 Unit of a physical quantity, 53
 Unperturbed random-coil macromolecule, 248
 Unperturbed state, 246
 Unperturbed viscosity coefficient, 791
 Unstable flow, 578
 Unzipping, 769
 Upper critical solution temperature (UCST), 211
 Upper glass transition, 171
 Use or performance properties, 877
 UV absorbers, 784

V

Vacuum forming, 799
 Values of fundamental constants, 903
 Values of increments in Hoy's system (1985) for the molar attraction function, 217
 Van der Waals'
 law, 657
 radius, 72
 volumes of structural units and structural groups, 73
 VanKrevelen-Hoftijzer viscosity-temperature relationship, 539
 Van't Hoff equation, 751
 Velocities of sound waves, 390
 Velocity gradient, 526
 Vertical Burning Test, 854
 Vicat softening temperature, 849
 Vickers hardness test, 837
 Viscoelasticity, 405
 Viscoelastic properties of polymer solutions, 619
 Viscosity
 average molecular mass, 18
 of concentrated polymer solutions, 599, 605
 extensional, 564
 as a function of shear rate, 545
 inherent, 250
 intrinsic, 245, 249, 253
 limiting, 249, 250, 253, 255
 Newtonian, 533
 number, 245
 of polymer solutions, 547
 ratio, 250
 reduced, 250
 relative, 250
 shear, 525
 specific, 250, 618
 temperature gradient, 645
 Vitrification process, 151
 Voigt element, 416
 Voigt model, 413, 415, 436

Volume
 imperfections, 842
 magnetic susceptibility, 355
 relaxation, 80
 resistivity, 336
 retardation, 427
 temperature diagram of a liquid crystal polymer, 175
 Volumetric properties, 71
 Von Mises yield criterion, 455

W

Wagner's constitutive equation, 572
 Warping, 808
 Washability, 882
 Water sorption, 690
 Wave number, 288
 Wear, 819
 Weber number, 59
 Wedge-flow, 574
 Weight-average molecular mass, 18
 Weissenberg effect, 526
 number, 57, 556
 Wet fastness, 881
 Wide-line NMR, 368, 373, 374
 WLF
 equation, 421
 formulation, 714, 715
 function, 715
 shift factor, 421
 Work
 factor, 715
 function, 334
 hardening, 454, 455
 Wormlike chain model, 248
 Wrinkle
 fastness, 879–80
 recovery, 879–80

X

X-ray diffraction, 479

Y

Yarn elasticity, 879
 Yarns wound at various speeds, 732
 Yasuda, Armstrong Cohen model, 547
 Y_g and Y_m increments of some important mesogenic and linking functional groups, 179
 Yield/Yielding, 455, 463
 behaviour, 462
 point, 462
 stress, 455
 Young's modulus, 401

Z

Z-average molecular mass, 18
 Zero point molar volume, 76
 Zimm plot, 310